FAA CENTER OF EXCELLENCE FOR ALTERNATIVE JET FUELS & ENVIRONMENT

Annual Technical Report
2016

For the period

October 1, 2015 - September 30, 2016

Boston University
Georgia Institute of Technology
Massachusetts Institute of Technology
Missouri University of Science and Technology
Oregon State University
Pennsylvania State University
Purdue University
Stanford University
University of Dayton
University of Hawaii
University of Illinois
University of North Carolina
University of Pennsylvania
University of Tennessee
University of Washington
Washington State University

This work was funded by the US Federal Aviation Administration (FAA) Office of Environment and Energy as a part of ASCENT Project AJFE under FAA Award Number 13-C. Any opinions, findings, and conclusions or recommendations expressed in this material are those of the authors and do not necessarily reflect the views of the FAA or other ASCENT Sponsors.

Table of Contents

Overview

This report covers the period October 1, 2015 through September 30, 2016. The Center was established by the authority of FAA solicitation 13-C-AJFE-Solicitation. During that time the ASCENT team launched a new website, which can be viewed at https://ascent.aero/. The next meeting will be held September 26 - 27, 2017 at the Embassy Suites in Alexandria, Virginia.

Over the last year, the ASCENT team has made great strides in research, outreach, and education. The team's success includes the following:

- **54 research projects.**

The projects can be divided into five categories: tools, operations, noise, emissions, and alternative fuels. See the project category descriptions for more detail on each category and a summary of the active projects. Funding for these projects comes from the FAA in partnership with Transport Canada.

- **119 publications, reports, and presentations by the ASCENT team.**

Each project report includes a list of publications, reports, and presentations published between October 1, 2015 and September 30, 2016. A comprehensive list of the publications, reports, and presentations is available in the publications index on page 670.

- **117 opportunities for students to participate in aviation research with the ASCENT team.**

Each project report includes the names and roles of the graduate and undergraduate students in the investigator's research. Students are selected by the investigators to participate in this research.

- **70 industry partners involved in ASCENT.**

ASCENT's industry partners play an important role in the Center. The 59 members of the ASCENT Advisory Board provide insight into the view of stakeholders, provide advice on the activities and priorities of the Center's co-directors, and ensure research will have practical application. The committee does not influence FAA policy. Industry partners also play a direct role in some of the research projects, providing resources and expertise to the project investigators.

Leadership

Dr. Michael Wolcott
Center Director and Technical Lead for Alternative Jet Fuels Research
Washington State University
(509) 335-6392
wolcott@wsu.edu

Dr. R. John Hansman
Center Co-Director and Technical Lead for Environmental Research
Massachusetts Institute of Technology
(617) 253-2271
rjhans@mit.edu

Dr. John Gardner
Industry and Stakeholder Liaison
Washington State University
(206) 448-1330
gardnerj@wsu.edu

Dr. John Holladay
Federal Research Laboratories and Agency Liaison
john.holladay@pnnl.gov

Dr. James Hileman
Chief Scientific and Technical Advisor for Environment and Energy
Office of Environment and Energy
Federal Aviation Administration
james.hileman@faa.gov

Research Topics

Research projects within ASCENT are divided into five categories: tools, operations, noise, emissions, and alternative fuels.

Tools

Research within the tools category involves researching current systems to understand the short- and long-term effects of new technologies. The ASCENT ream is working to develop tools to model and assess new and existing aircraft technology.

Projects include:

- 010 - Aircraft Technology Modeling and Assessment
- 011 - Rapid Fleet-wide Environmental Assessment Capability
- 035 - Airline Flight Data Examination to Improve Flight Performance Modeling
- 036 - Parametric Uncertainty Assessment for AEDT 2b
- 037 - CLEEN II Technology Modeling and Assessment
- 045 - Takeoff/Climb Analysis to Support AEDT APM Development
- 046 - Surface Analysis to Support AEDT APM Development

Operations

Research within the operations category involves improving aviation operations to reduce negative impacts on local communities, the environment, and the economy. The ASCENT team is working to develop efficient gate-to-gate aircraft operations, develop evaluation tools for aircraft performance, and explore new operations procedures.

Projects include:

- 015 - Cruise Altitude and Speed Optimization
- 016 - Airport Surface Movement Optimization
- 023 - Analytical Approach for Quantifying Noise from Advanced Operational Procedures

Noise

Research within the noise category involves researching noise pollution caused by the aviation industry. The ASCENT team is working to understand the impact of noise pollution on health, create tools for analyzing aircraft noise, understand how specific variables impact noise, and conduct outreach and education about aircraft noise reduction.

Projects include:

- 003 - Cardiovascular Disease and Aircraft Noise Exposure
- 004 - Estimate of Noise Level Reduction
- 005 - Noise Emission and Propagation Modeling
- 006 - Rotorcraft Noise Abatement Operating Conditions Modeling
- 007 - Civil, Supersonic Over Flight, Sonic Boom (Noise) Standards Development
- 008 - Noise Outreach
- 017 - Pilot Study on Aircraft Noise and Sleep Disturbance
- 023 - Analytical Approach for Quantifying Noise from Advanced Operational Procedures
- 038 - Rotorcraft Noise Abatement Procedures Development
- 040 - Quantifying Uncertainties in Predicting Aircraft Noise in Real-world Situations
- 041 - Identification of Noise Acceptance Onset for Noise Certification Standards of Supersonic Airplane
- 042 - Acoustical Mode of Mach Cut-off
- 043 - Noise Power Distance Re-Evaluation

Emissions

Research within the emissions category focuses on reducing emissions from the aviation industry. The ASCENT team is working to analyze data and improve models to better understand the effect of airplane emissions, create and refine analysis techniques, and understand how policy changes could affect emissions.

Projects include:

- 002 - Ambient Conditions Corrections for Non-Volatile PM Emissions Measurements
- 013 - Micro-Physical Modeling & Analysis of ACCESS 2 Aviation Exhaust Observations
- 014 - Analysis to Support the Development of an Aircraft CO2 Standard
- 018 - Health Impacts Quantification for Aviation Air Quality Tools
- 019 - Development of Aviation Air Quality Tools for Airport-Specific Impact Assessment: Air Quality Modeling
- 020 - Development of NAS wide and Global Rapid Aviation Air Quality
- 021 - Improving Climate Policy Analysis Tools
- 022 - Evaluation of FAA Climate Tools
- 024 - Emissions Data Analysis for CLEEN, ACCESS, and Other Recent Tests
- 039 - Naphthalene Removal Assessment
- 048 - Analysis to Support Development of an Engine nvPM Emissions Standards

Alternative Fuels

Research within the alternative fuels category addresses the challenges associated with the creation and accessibility of alternative fuels. The ASCENT team is working to improve the feasibility of renewable fuels, understand how alternative fuels will affect emissions, air quality, and performance, and create standards for alternative fuel certification.

Projects include:

- 001 - Alternative Jet Fuel Supply Chain Analysis
- 021 - Improving Climate Policy Analysis Tools
- 024 - Emissions Data Analysis for CLEEN, ACCESS, and Other Recent Tests
- 025 - National Jet Fuels Combustion Program – Area #1: Chemical Kinetics Combustion Experiments
- 026 - National Jet Fuels Combustion Program – Area #2: Chemical Kinetics Model Development and Evaluation
- 027 - National Jet Fuels Combustion Program – Area #3: Advanced Combustion Tests
- 028 - National Jet Fuels Combustion Program – Area #4: Combustion Model Development and Evaluation
- 029 - National Jet Fuels Combustion Program – Area #5: Atomization Tests and Models
- 030 - National Jet Fuels Combustion Program – Area #6: Referee Swirl-Stabilized Combustor Evaluation/Support
- 031 - Alternative Jet Fuels Test and Evaluation
- 032 - Worldwide LCA of GHG Emissions from Petroleum Jet Fuel
- 033 - Alternative Fuels Test Database Library
- 034 - National Jet Fuels Combustion Program – Area #7: Overall Program Integration and Analysis

Project 001(A) Alternative Jet Fuel Supply Chain Analysis

Washington State University

Project Lead Investigator

Michael P. Wolcott
Regents Professor
Department of Civil & Environmental Engineering
Washington State University
PO Box 642910
Pullman, WA 99164-2910
509-335-6392
wolcott@wsu.edu

University Participants

Washington State University

- P.I.(s): Michael P. Wolcott, Regents Professor; Michael Gaffney, Director, DGSS; Manuel Garcia-Perez, Associate Professor; and Xiao Zhang, Associate Professor
- FAA Award Number: 13-C-AJFE-WaSU-010
- Period of Performance August 1st, 2016 to July 31, 2017
- Task(s):
    - WSU 1. Design cases– Garcia-Perez, Zhang
    - WSU 2. Evaluation of the most promising bio-refinery concepts for AJF production. Garcia-Perez, Zhang
    - WSU 3. Supplement and maintain the current inventory of bio-refinery infrastructure identified in the conversion design cases that are useful for production of AJF Wolcott
    - WSU 4. Community Social Asset Assessment Gaffney
    - WSU 5. Refine and deploy the facility siting tools for determining regional demand and potential conversion sites to be used in regional analyses. Wolcott
    - WSU 6. Refinery to Wing Stakeholder Assessment. Gaffney
    - WSU 7. Supply Chain analysis. Wolcott-Garcia-Perez
    - WSU 8. Analytical support for regional CAAFI and USDA jet fuel project. Wolcott

Project Funding Level

$274,999 FAA funding and $274,999 matching funds. Source of matching funds are $270,000 Washington State University salary contributions.

Investigation Team

- Michael Wolcott, Project Director/Principal Investigator
- Michael Gaffney, Co-Project Director/Co-Principal Investigator
- Manuel Garcia-Perez, Co-project Director/Co-Principal Investigator
- Paul Smith, Faculty
- Season Hoard, Faculty
- John Snyder, Faculty
- Kristin Brandt, Staff Engineer
- Natalie Martinkus, Staff Engineer
- Sarah Dossey, Staff Engineer

Postdoctoral (100 %)

- Dane Carmenzid, Graduate Student

- Lina Pilar Martinez Valencia, Graduate Student
- Tanzil Abid Hossain, Graduate Student
- Daniel Mueller, Graduate Student

Collaborating Researchers

- Burton English, University of Tennessee
- Kristin C. Lewis, Volpe

Project Overview

As part of an effort to realize an "aviation system in which air traffic will move safely, swiftly efficiently, and seamlessly around the globe", the Federal Aviation Administration (FAA) has set a series of goals and supporting outcomes, strategies, and performance metrics (Hileman et al 2013). The goal entitled, "Sustaining our Future" outlines a number of strategies that are collectively aimed at reducing the environmental and energy impacts of the aviation system. To achieve this goal, the FAA set an aspirational goal of aviation utilizing 1 billion gallons of AJF by the year 2018. This goal was created from an economic, emissions, and overall feasibility perspective (Richard 2010, Staples et al. 2014).

Current approaches to supply chain analysis for AJF optimizes transportation logistics of feedstocks to refinery and refinery to wing (Bond et al 2014). One of the largest barriers to large scale production of all bio-fuels is the high capital cost of greenfield facilities translating to risk in the investment community (Huber et al 2007). The capital cost of cellulosic ethanol plants range from $ 10-13/gal capacity (Hileman and Stratton, 2014). The additional process steps required to convert the intermediate to a drop in AJF could increase this cost to over $ 25/gal capacity (Hileman 2014).

The realities of these initial commercialization efforts into second-generation biofuel have led to studies that envision alternate conversion scenarios including transitioning existing facilities (Brown 2013). Gevo is employing retrofit strategies of corn ethanol plants for producing isobuthanol, a potential intermediate for the alcohol-to-jet process of producing iso-paraffinic kerosene (Pearlson 2011, Pearlson et al 2013). Research to envision scenarios to achieve the FAA aspirational goal of AJF consumption relied upon "switching" scenarios where existing and planned capacity would be used for producing the drop-in fuel (Malina et al 2012). All of these approaches require identifying existing industrial assets to target for future AJF production. Siting becomes, not just an exercise of optimizing feedstock transportation, but aligning this critical factor with a host of existing infrastructure, markets within regions with the proper social capital for developing this new industry (Seber et al 2014, Henrich et al 2007).

Up to now all the AJF supply chain analyses published have been limited to standalone jet fuel production technologies that do not generate bio-products. The potential techno-economic and environmental benefits of using existing industrial infrastructure and the production of co-product on the development of jet fuel production scenarios has to be considered in future studies.

This project is part of a series of activities to evaluate regional jet fuel supply chains and to estimate the potential of the U.S. to produce alternative jet fuels. In previous years we created the tools to conduct such analyses. At WSU several design cases for alternative jet fuels (Alcohol to Het (ATJ), Hydrotreated Depolymerizes Cellulosic Jet (HDCJ), Direct Sugars to Hydrocarbons (DSHC), Synthetic kerosene and Synthetic Aromatic Kerosene (SK&SAK), Catalytic Hydrothermolysis (CH) and Synthesized Kerosene-containing Aromatics (FT-SKA) and some of the technologies forming our infrastructure (pulp and paper mills, sugarcane mills, dry corn ethanol plants, petroleum refineries) were created as well as data bases of the existing infrastructure. This information is being used in supply chain analyses. Our goal is to identify supply chains that could allow U.S. achieve alternative jet fuels production as close as possible to its potential. The technical results obtained by the regional teams will be analyzed in conjunction with the studies on social attitudes to create recommendations on how we best catalyze the creation of jet fuel supply chains.

Task WSU 1. Design cases

Washington State University

Objective(s)

Continue refining and improving the design cases developed for six standalone alternative jet fuel (AJF) production technologies (Alcohol to Jet (ATJ), Hydrotreated Depolymerized Cellulosic Jet (HDCJ), Direct Sugars to Hydrocarbons (DSHC), Synthetic kerosene and Synthetic Aromatic Kerosene (SK&SAK), Catalytic Hydrothermolysis (CH) and Synthesized Kerosene-containing Aromatics (FT-SKA) and existing infrastructure (sugarcane, pulp and paper, corn ethanol and petroleum refineries) that could help with the growth of this industry;

Research Approach

Background: The design cases developed for AJFs and for existing industrial infrastructure, are being used in the development of supply chains and on the identification of synergisms that could eventually lead to the construction of integrated systems of AJF production that take advantage of the infrastructure in a given region. Analysis of the location of existing infrastructure showed that the United States can be divided in regions dominant biomass of the region. So, we believe that a viable approach to evaluate the synergism between the AJF pathways, the existing infrastructure and the co-products is to generate advanced bio-refinery concepts around the Petroleum Refineries Pulp and Paper Mills Sugar Cane Mills, Corn Ethanol Mills and to compare the biorefinery concepts developed for each of these technologies to decide the most promising ones. The most promising bio-refinery concepts for the synergistic production of AJFs and co-products with these industries will then be used in the supply chain analyses.

Standalone design case reports are generated by conducting reviews of research related to each in academic literature and public information available from commercial interests developing the technology. The reports are meant to detail the processes involved in each conversion pathway and outline the technology readiness and particular barriers to implementation. Publically available information on the commercial processes and research literature will provide the foundation of information later used in modeling efforts. Where detailed process engineering information is lacking, new models will be built to estimate the parameters needed to complete assessments such as techno-economic modeling, lifecycle analysis, and supply chain modeling. Aspen Plus is primarily used to generate process models and details including mass balances, energy balances, energy requirements, and equipment size and cost. These results will also aim to provide the basis for comparative analysis between design cases, identifying key advantages and markets for each technology.

Each design case will have the following components: (1) Feedstock requirement (Availability and feedstock composition) (2) Flow diagram of technology (3) Companies commercializing the technology (level of maturity) (4) Current location of units in the United States (In case of an existing technology it will be the inventory of units that could be retrofitted) (5) Literature review on papers reporting data relevant to the operation of the technology (operating conditions, type of reactor used, catalysts, yield of products) (6) Properties of Jet fuel produced (7) Identification of potential intermediates (bio-oil, sugars, densified feedstock); current and potential uses of wastes and effluents; and co-products (biochemicals, carbon, etc.) that can be obtained from the technology

We continued refining the design cases developed for six standalone AJF technologies (Alcohol to Jet (ATJ), Hydrotreated Depolymerized Cellulosic Jet (HDCJ), Direct Sugars to Hydrocarbons (DSHC), Synthetic kerosene and Synthetic Aromatic Kerosene (SK&SAK), Catalytic Hydrothermolysis (CH) and Synthesized Kerosene-containing Aromatics (FT-SKA) and for four important industries (sugarcane, pulp and paper, corn ethanol and petroleum refineries). We received the comments from internal reviewers, and from most industrial reviewers, we are now addressing the comments and recommendations received. Our plan is to submit the final report in the summer 2017. This year we will start developing the design cases for targeted co-products that could improve the economic viability of AJFs. Because lignin utilization alternatives is a problem for all the AJF production concepts using biochemical pathways, we propose to build design cases (a literature review, mass and energy balances and technoeconomic analyses) for three lignin utilization strategies (1) Oxidative depolymerization of biorefinery lignin to valuable chemicals (phenolics and dicarboxylates) (2) Modification of biorefinery lignin for additive and adhesive applications and (3) Synthesize renewable materials from biorefinery lignin.

Responsible: Manuel Garcia-Perez, Xiao Zhang and Michael Wolcott

Milestone(s)

Literature search complete for all pathways and design cases. Draft design cases complete for all pathways and design cases. Internal reports reviewed by team members and external reviewers. We are currently updating the design cases and addressing the comments received from the reviewers.

We are currently building the design cases for targeted co-products from lignin.

Major Accomplishments

Models were developed for the main AJF production technologies and for relevant technologies that can be used as baseline for the synthesis of bio-refinery concepts. The methodology for these models are providing data to form a baseline for comparative analysis with other design cases. Key process variations have been identified in several design cases and have been modeled to determine their effects on process economics and viability, as well as to identify the key barrier toward commercialization in complete biorefinery concepts.

Data generated from the design cases were also supplied to A01 partners to assist with supply chain, lifecycle analysis, and techno-economic models by improving the conversion and cost figures database values. Evaluations of the effects of process variations on the chemical properties of products generated are being used to provide insight into the challenges that will be faced when blending that the AJFs into commercial jet fuel.

Most of the design cases have been reviewed by external reviewers and we are currently addressing their comments and updating the final reports.

Publications

None - Task in Progress

Outreach Efforts

None – Task in Progress

Awards

None – Task in Progress

Student Involvement

Several graduate (Scott Geleynse, Mond Guo, Carlos Alvarez Vasco, Ruoshui Ma, Jonathan Pulgarin-Leon and Tanzil Hossain) and undergraduate students participated in the creation, editing and updating of the design cases for standalone AJF technologies, for relevant existing infrastructure and for co-products from lignin.

Plans for Next Period

Publication of design cases for standalone AJF production technologies and for relevant infrastructure. Complete the first draft design case for co-products from lignin

Task WSU 2. Evaluation of the most promising bio-refinery concepts for AJF production

Washington State University

Objective(s)

Evaluation of most promising bio-refinery concepts for AJF production. Evaluation of co-products opportunities and synergisms of AJF pathways with existing infrastructure to overcome some of the barriers to produce 1 billion gallons of alternative jet fuel by 2018. Use design cases of existing infrastructure, AJF production technology and co-products

identified to generate new bio-refinery concepts for Petroleum Refineries, Pulp and Paper Mills, Sugarcane Mills and dry corn mills. Use technoeconomic and life cycle assessment to identify the most promising bio-refinery concepts that could be implemented as part of the supply chain analysis. Understand the major technical gaps towards commercialization of each of the bio-refinery concepts proposed.

Research Approach

Background: In this task we are using the design cases of existing infrastructure, AJF production technology and co-products identified to generate new bio-refinery concepts for Petroleum Refineries, Pulp and Paper Mills, Sugarcane Mills and dry corn mills. Each of the bio-refinery concepts proposed is being evaluated. The results from this effort will allow us to identify and select the most commercially feasible bio-refinery concepts. Major technical gaps/barriers toward commercialization of each of the bio-refinery concepts will also be revealed from the results of this study.

Integration of process technologies through a similar approach to the standalone design cases is assessed. Further evaluation of integration concepts will be developed by pairing standalone cases with these opportunities to evaluate the economic and environmental advantage of the integration approaches. During this period we conducted detailed analyses of alcohol to jet conversion (ATJ) and integration with pulp mill operations. We have also investigated the potential of lignin co-products contribution to the overall process economy.

A dry grind corn ethanol mill (DGCEM) with a capacity of 80 million gallons of ethanol per year (MGY) was studied in order to evaluate potential biorefinery scenarios for AJF production. Five alternative jet fuel (AJF) technologies were studied: Virent's BioForming, alcohol to jet (ATJ), direct sugar hydrocarbon (DSHC), fast pyrolysis (FP) and Fischer-Tropsch (FT). A standardized methodology was adopted to evaluate twelve integration scenarios between DGCEM and AJF technologies in terms of minimum fuel selling price (MFSP) and greenhouse gas (GHG) emission. The total alternative jet fuel production capacity ranged from 25 MGY to 50 MGY. Eight scenarios resulted in cost reduction opportunities in capital expenditure (CAPEX) and operational expenditure (OPEX) leading to reduced MFSPs in the range of 6% to 29%. Four scenarios resulted in negative GHG emission. A performance evaluation revealed that integration scenario of fast pyrolysis provided the better results in cost and GHG emission reduction. We are currently conducting similar analyses for a Corn ethanol plant and petroleum refineries.

Major Accomplishments

Economic models and Life Cycle Assessments were used to support the selection of the most promising bio-refinery concepts that make use of our existing infrastructure for AJF production. Modeling project have been underway for the Pulp and Paper and Corn Ethanol integration cases and have been applied to evaluate integration potential, particularly with the Alcohol to Het design one. These efforts are leading to two publications on integration strategies (Pulp and Paper, Corn Ethanol) currently in progress.

Publications

Three publications are in Progress:

(1) Evaluation of the Alcohol to Jet Process
(2) Pulp and paper Integration Strategies for AJF Production
(3) Corn Ethanol Mill Integration Strategies for AJF Production

Outreach Efforts

Pulp Mill Process Integration and Repurposing for Bio-catalytic Alcohol to Jet Fuel Production" Senthil Subramaniam,252nd American Chemical Society, August 20-25, 2016, Philadelphia
Evaluation of Alcohol-to-Jet (ATJ) Conversion Technology for Renewable Jet Fuel, Scott Geleynse at the 2016 Annual Meeting for the American Institute of Chemical Engineers in San Francisco. November 16, 2016
Integration of Renewable Jet Fuel Production with the Pulp Industry through Alcohol Conversion, Scott Geleynse at the 2016 Annual Meeting for the American Institute of Chemical Engineers in San Francisco. November 17, 2016

Techno-Economic Modeling of Lignin to Vanillic Acid Production, Kitana Kaiphanliam at the 2016 Annual Meeting for the American Institute of Chemical Engineers in San Francisco. November 17, 2016
Alternative Jet Fuel Production in Integrated Biorefineries Using Existing Dry Corn Mill: Cost Reduction Opportunities. Abid Hossain Tanzil, Manuel Garcia-Perez, Xiao Zhang, Michael Wolcott.

Awards

None

Student Involvement

Graduate students Scott Geleynse, Senthil Subramaniam, Mond Guo, Carlos Alvarez-Vaso, Abid Tanzil Houssain, Lina Martinez Valencia and Ruoshui Ma have received trained working in this project. An undergraduate student, Kitana Kaiphanliam, funded under an NSF REU grant assisted with building techno-economic models for co-products production scenarios.

Plans for Next Period

Next period Dr. Garcia-Perez's team will focus on the potential cost reductions if alternative jet fuels are integrated with a petroleum refinery and a sugarcane mill. Further work into developing design cases will focus on new technologies and the integration of co-products into biorefinery concepts. Hydrothermal liquefaction, a thermochemical conversion process under significant research at Pacific Northwest National Laboratory, has been identified as a new technology potentially nearing commercial readiness and should be evaluated as a standalone design case. Co-products are alternative chemical products that can be produced alongside AJF that provide additional value in other markets or as a higher-priced commodity. Development of co-product strategies can change the economic outlook for conversion pathways by improving process economics and thus reducing the minimum fuel selling price. As with integration with existing infrastructure, co-product integration is likely a necessary component particularly of early projects which do not follow "nth plant" economics.

Task WSU 3. Supplement and Maintain the Current Inventory of Biorefinery Infrastructure Identified in the Conversion Design Cases that are useful for Production of AJF.

Washington State University

Objective(s)

Specifically, this task requires annual evaluation of the database to add or eliminate new and close facilities in each category so that the geospatially specific assets are current with reality.

Research Approach

Background: Utilizing existing infrastructure assets is key to retrofit approaches to developing the industry. But to differentiate between the relative value of different options, the specific assets must be valued with respect to their potential use within a conversion pathway. Regional databases of industrial assets that might be utilized by a developing AJF industry, have been assessed on a national level. These baseline databases are compiled from a variety of sources that include industry associations, universities, and news outlets. These databases will be expanded, refined, and validated as the conversion design cases articulate additional needs for the regional analyses.

Milestone(s)

National databases are compiled, geolocated, validated and shared for biodiesel, corn ethanol, energy pellet, pulp & paper, and sugar mill production. We are evaluating the database to add or eliminate new and closed facilities in each category so that the geospatially specific assets are current with reality.

A regional supply chain analysis was completed for eastern Washington and western Montana using forest harvest residuals as the feedstock. This analysis included market fuel demand, potential siting assets and feedstock availability. A

siting tool was developed to help determine if the most economical site was a greenfield, co-location or conversion of an existing facility. This tool includes the impact of operating costs including electricity rate, natural gas rate and delivered feedstock cost. Capital costs are included by applying a factored approach to estimating capital costs and accounts for infrastructure that would be included at an existing facility such as service facilities, equipment costs, buildings and yard improvements. The siting tool combines the operating and capital cost components in a cost-weighted equation. The results of the equation allow for quantitative comparison of multiple locations based on both operating and capital costs.

Major Accomplishments

The national databases have been compiled, validated, and shared with the A01 teams. All of the metadata is complete for use in the regional analyses

Publications

None – these are shared assets for later analyses

Outreach Efforts

Wolcott, M., Martinkus, N., Brandt, K., Garcia-Perez, M., Zhang, X. *Alternative Jet Fuel Supply Chain Analysis ASCENT 1: Northwest Supply Chains. Aviation Sustainability Center (ASCENT) Meeting,* April, Washington D.C.
Wolcott, M., Lewis, K., Brandt, K., Camenzind, D., Martinkus, N., Dossey, S. *Analysis of 2030 Jet Fuel Demand and Supply Chain Assets of Multiple Biojet Feedstocks* [poster]. Aviation Sustainability Center (ASCENT) Meeting, September, Washington D.C.

Awards

None – these are shared assets for later analyses

Student Involvement

Dane Camenzind, Master's student in Civil Engineering, validated the operating status of previously identified production facilities, compiled and geolocated MSW incinerators and landfill gas to energy facilities and worked to assemble and update all county level feedstock information.
Natalie Martinkus, pH.D. candidate in Civil Engineering (degree completed), developed the siting decision matrix as a portion of her dissertation.

Plans for Next Period

Additional refinements will be completed for the siting tool. GIS analysis will be completed after tool is finalized.We plan to continue the annual evaluation of the database to add or eliminate new and close facilities in each category so that the geospatially specific assets are current with reality.

Task WSU 4. Continue work on social asset decision tools developed in Phase 1 for plant siting (Community Asset & Attribute Model—CAAM) through additional statistical testing and case study validation. Extend application to full NARA region and another US region (e.g. MASBI or Chesapeake). Prepare for extension nationally & replication for select EU countries.

Washington State University

Objective(s)

Continue work on social asset decision tools developed in Phase 1 for plant siting (Community Asset & Attribute Model—CAAM) through additional statistical testing and case study validation. Extend application to full NARA region and another US region (MASBI). Prepare for extension nationally & replication for Canada, and select EU countries.

Research Approach

Based on key measures of collective action, creativity, and health, WSU has developed and refined a Community Asset and Attribute Model (CAAM). This quantitative tool was initially applied to the NARA region. It will subsequently be refined, re-weighted, re-calibrated, and applied to the US Midwest region and then made available nationally. Social Assets, the weighted measures of a community's capacity for collective action and adaptation to change, have been aggregated at the county level for the entire US. These measures have been used to assess social capacity for biorefinery siting, and were recently combined with biogeophysical analysis to identify former paper mill facilities that could most effectively be retrofitted to support a biorefinery in the Pacific Northwest.. Social capacity measures include indicators of social capital, creative leadership, and human capital, which are currently being validated through ground-truthing analysis to assess their role in the success or failure of biofuel related projects in both the NARA and BANNER regions.

Milestone(s)

The validated CAAM model based on county-level comparative rankings on Social, Human and Cultural Capitals is tested and available for use.

Major Accomplishments

The refined CAAM model has been combined with biogeophysical analysis to rank and select pulp mills in the Pacific Northwest region with the necessary combination of biogeophyscial and social assets to support retrofitting into a biorefinery. This analysis has led to an invited presentation at the Northwest Wood Based Biofuels Coproducts Conference in Seattle WA, and an R&R (currently re-submitted) for a manuscript submitted to Biomass and Bioenergy. A manuscript on the refined CAAM has been developed, and has been submitted to Politics and Life Sciences.

Publications

Peer-reviewed journal publications:

Martinkus, N. Rijkhoff, S.A.M., Hoard, S.A., Shi, W., Smith, P., Gaffney, M., & Wolcott, M. (submitted, R&R). Biorefinery Site Selection Using a Stepwise Biogeophysical and Social Analysis Approach. *Biomass and Bioenergy.*
Rijkhoff, S.A.M., Hoard, S., Gaffney, M., Smith, P. (submitted). Communities Ready for Takeoff: Integrating Social Assets for Biofuel Site-selection Modeling. *Politics and Life Sciences.*

Outreach Efforts

Martinkus, N., Rijkhoff, S., **Hoard, S.,** Shi, W., Smith, P., M. Gaffney. *A Stepwise Biogeophysical and Social Analysis to Approach Site Selection of Biorefineries,* Northwest Wood Based Biofuels Coproducts Conference, May, Seattle, WA.
Mueller, D., **Hoard, S.,** Sanders, C., Gaffney, M., P. Smith. *Strategic Applications of the Community Assets and Attribute Model* [poster]. Aviation Sustainability Center (ASCENT) Meeting, September, Washington D.C.

Awards

None

Student Involvement

Daniel Mueller, Ph.D. candidate in political science at WSU and research assistant on this project, will continue validation efforts for the CAAM and help develop measurements for political capital.

Kelli Roemer, Master's student of natural resources at the University of Idaho, is continuing validation work of the CAAM as part of her thesis work.

Plans for Next Period

Subsequent development of the CAAM will include inclusion of political capital through aggregation of national data on local and national elections at the county level, and development of alternative measures of creativity that rely on publically available indicators. Plans are currently underway to extend the research to Canada.

Task WSU 5. Refine and deploy the facility siting tools for determining regional demand and potential conversion sites to be used in regional analyses.

Washington State University

Objective(s)

Refine and deploy the facility siting tools for determining regional demand and potential conversion sites to be used in regional analyses.

Research Approach

Building on two iterations of the CAAM model developed under the NARA project, the ASCENT applications for this subtask include substituting original data for previously-used aggregated sources, statistically testing and validating the model, refining the comparative benchmarks used to establish county-level ratings on the three community capitals (Social, Human, Cultural) previously incorporated into the model, and collecting case study information for use in further validation of the model's efficacy. The research remains focused on refining a model which is based on readily available national datasets (aggregated at the county level) which can be used to conduct a preliminary assessment of community characteristics for three (Cultural, Social, Human) of the seven "Community Capitals" framework. (Emery, Mary and Cornelia Flora. 2006. "Spiraling Up: Mapping Community Transformation with the Community Capitals Framework." Journal of the Community Development Society, Vol. 37, p. 22.) which informs the NARA project.

This year we are working on the development of readiness level tools for regional projects. In the past year, we have integrated the factored TEA analysis approach into facility siting analysis to weigh the value of retrofitting or colocating biorefinery assets. This approach was demonstrated on a cellulosic Alcohol-to-Jet supply chain in the Pacific Northwest. In the upcoming year, we will demonstrate the tool for supply chain and siting analysis for the alternative jet fuel production using FOGs converted from HEFA in the same region.

Milestone(s)

CAAM v.3.0 statistically analyzed and validated. We are currently developing readiness level tools for regional projects

Major Accomplishments

During this reporting period, further research and validation of The CAAM has been conducted. Further validation and refinement has included incorporating standard deviation comparisons in an effort to more easily illustrate where cases fall on rankings for each asset (community capital) compared to the defined regional average, and beginning development of gradation measurement of capital comparative status through incorporation of standard deviations to examine distance from regional averages and impacts on development and implementation success. The CAAM model with reported standard deviations was combined with biogeophysical analysis and presented at the Northwest Wood Based Biofuels Coproducts Conference, and a manuscript has been submitted to Biomass and Bioenergy. Suitable case study sites have been identified for ground truthing, which will lead to further validation and refinement of the model. National datasets on voting trends in local and national elections have been acquired, aggregated at the county-level and will be added to the model to include a fourth important community capital – political capital.

Publications
None

Outreach Efforts
None

Awards

None

Student Involvement

Daniel Mueller, Ph.D. candidate in Political Science, now holds a funded Research Assistant appointment working on this project, and has been primarily responsible for acquisition of new primary data, further validation of the model, and the (continuing) development of the fourth iteration of the CAAM.

Kelli Roemer, Master's student of natural resources at the University of Idaho, is continuing validation work of the CAAM as part of her thesis work.

Plans for Next Period

In the next year, a new iteration of the CAAM will be fully developed, validated, and applied in the NARA and BANNER regions, with expansion to the Midwest region. This model will be based upon: (1) Addition of new data to support addition of the fourth Political Capital to the model through ground truthing, case study analysis, and addition of National voting datasets at the county-level. (2) Development of more refined measurement of capital comparative ranking beyond dichotomous outperform/under perform ratings using standard deviations to examine distance from regional average and impact on successful development and implementation. (3) Alternative Creative Vitality aggregate measure developed from alternative primary source data in order to support updated, and more robust analyses and modelling. (4) Final validation, after statistical confirmation, using selected case studies to confirm the efficacy of the model.

The Fourth CAAM will be available for use nationally, allowing comparison of counties against defined regional norms on Cultural, Social, Human, and Political Capital scales that have been statistically tested and validated through triangulated testing with external data.

Task WSU 6. Refinery to Wing Stakeholder
Washington State University

This is a shared task lead by Penn State University. The reporting is provided in Award No. 13-C-AJFE-PSU-002.

Objective(s)

Complete assessment of key aviation fuel supply chain stakeholder perceptions regarding the conditions necessary for the adoption and diffusion of AJF in the NARA region. Assess perceptions in another US MASBI region

Research Approach

The team will collect primary data via interviews and surveys to better understand the awareness, opinions, and perspectives of key aviation fuel supply chain stakeholders regarding to the potential impacts and key success factors for an economically viable biojet fuel production industry in the NARA and US Midwest region. These aviation fuel supply chain stakeholders include airport management, FBOs, other aviation fuel handlers, relevant airlines, and CAAFI personnel. Databases of regional aviation fuel supply chain stakeholders will include airport management, FBOs, fuel resellers, terminal and pipeline operators, and the airlines. This effort will be conducted jointly with Volpe where appropriate. Data

collection to assess aviation fuel supply chain stakeholder opinions, awareness, and perceptions regarding factors impacting the adoption and diffusion of AJF in the NARA region has been completed. Data collection through interviews with aviation stakeholders in the US Midwest region is currently underway, and a national survey of aviation management is being developed and will be fielded in early 2017 after consultation with CAAFI.

Milestone(s)

Assessment in the Pacific Northwest region of stakeholder perceptions using interviews and a survey of airport management have been completed, resulting in one published paper and a manuscript currently in progress.

Major Accomplishments

The team has completed stakeholder assessment interviews and surveys in the Pacific Northwest NARA region and has published a paper on interview results from this region. A second manuscript is currently in progress detailing the survey results from stakeholders in the same region. Interview contacts in the Midwest have been established and a first round of interview requests has been sent out.

Publications

Smith, P.M., Gaffney, M.J., Shi, W., Hoard, S., Ibarrola Armendariz, I., Mueller, D.W., 2017. Drivers and Barriers to the Adoption and Diffusion of Sustainable Jet Fuel (SFJ) in the U.S. Pacific Northwest. *Journal of Air Transport Management, 58*, 113-124.

Outreach Efforts

Mueller, D. **Hoard, S.,** Smith, P. Sanders, C., M. Gaffney. *Airport Management Perceptions of Aviation Biofuels in the Pacific Northwest* [poster]. Aviation Sustainability Center (ASCENT) Meeting, April, Alexandria, VA.

Smith, P., Gaffney, M., Shi, W., **Hoard, S.,** Ibarrola Armendariz, I., D.M. Mueller. *Aviation Fuel Supply Chain Stakeholder Perceptions in the PNW,* Aviation Sustainability Center (ASCENT) Meeting, April, Alexandria, VA.

Mueller, D., **Hoard, S.,** Smith, P., Sanders, C., M. Gaffney. *Stakeholder Perceptions of Aviation Biofuels in the PNW,* Northwest Wood Based Biofuels Coproducts Conference, May, Seattle, WA.

Smith, P., Gaffney, M., Shi, W., **Hoard, S.,** Ibarrola Armendariz, I., D.M. Mueller. *Aviation Fuel Supply Chain Stakeholder Perceptions in the PNW,* Northwest Wood Based Biofuels Coproducts Conference, May, Seattle, WA.

Awards

None

Student Involvement

Daniel Mueller, Ph.D. candidate in political science at WSU and research assistant on this project, has aided in writing and publishing NARA interview results and is currently involved in the interview process for the Midwest, gathering contact information, aiding in question development, and contacting potential interviewees.

Joseph Rogachevsky, Master's student in BioRenewable Systems (BRS), has aided in gathering contact information for interviews and has contacted stakeholders to set up interviews.

Plans for Next Period

The next year will see the completion of the stakeholder assessment in the Midwest, with the team continuing to gather contact information of stakeholders in the region. A national survey is also being developed, and will be sent out to aviation management stakeholders throughout the country. Plans are currently underway to replicate the research in Canada.

Task WSU 7. Supply Chain Analysis

Washington State University-Volpe

Objective(s)

Use the design cases developed in previous years for standalone alternative jet fuel production technologies to estimate production volumes and breakeven price for all the facilities identified by the Volpe Center. This effort will continue towards the continual refinement of the FAA aspirational jet fuel production goal.

Research Approach

Our team will use the design cases developed in previous years for standalone alternative jet fuel production technologies to estimate production volumes and breakeven price for all the facilities identified by the Volpe Center. Our expectation is that Volpe will provide us with a list of potential facilities, their throughput capacity, price of the feedstock at the gate and we will estimate the capital investment, operational costs and beakeven cost for each of the facilities.

Milestone(s)

Our team has been providing Volpe with information that will allow them to use the design cases developed in previous years for standalone alternative jet fuel production technologies to estimate production volumes and breakeven price.

Major Accomplishments

The team is in contact with Volpe to support them in the Supply chain analyses.

Publications

None

Outreach Efforts

None

Awards

None

Student Involvement

A graduate student (Lina Martinez) is receiving training (taking courses) to contribute in this task.

Plans for Next Period

Participate in the development of supply chain analysis tasks.

Task WSU 8. Analytical Support for regional CAAFI and USDA jet fuel project

Washington State University

Objective(s)

Develop a readiness level tool to assess the status of regional alternative jet production projects. In addition, use the supply chain and standalone design cases to support the USDA BANR project in TEA and supply chain analysis. This

regional CAP project focuses on the use of softwood forest salvage feedstock for fuels via a catalyzed pyrolysis conversion pathway.

Research Approach

We will develop readiness level tools for regional projects to assess their status of developing fuel project and assist in understanding critical missing components. This tool, will take similar form and approaches to the CAAFI Feedstock and Fuel Readiness Levels and will be used to assist CAAFI in understanding the stage of development for projects of interest and assess critical gaps. In addition, we will assist the regional USDA BANR team in deploying TEA and Supply Chain analysis to their project. This effort is structured around using softwood forest salvage feedstock with a thermochemical conversion process to produce fuels and coproducts.

Milestone(s)

We are progressing on the use of the supply chain and standalone design cases to support the USDA BANR project in TEA and supply chain analysis.

Major Accomplishments

In contact with the USDA BANR project.

Publications

None

Outreach Efforts

None

Awards

None

Student Involvement

None

Plans for Next Period

To work with the USDA BANR team in TEA and supply chain analyses.

References

Bond JQ, Upadhye AA, Olcay H, Tompsett GA, Jae J, Xing R, Alonso DM, Wang D, Zhang T, Kumar R, Foster A, Sen SM, Maravalias CT, 13 R, Barret SR, Lobo R, Wayman CE, Dumesic JA, Huber GW. (2014). Production of renewable jet fuel range alkanes and commodity chemicals from integrated catalytic processing of biomass. Energy Environ. Sci, 7:1500.

Brown, N. (2013). FAA Alternative Jet Fuel Activities. Overview. Presented to: CLEEN Consortium, November 20, 2013.

Henrich E. (2007). The status of FZK concept of biomass gasification. 2nd European Summer School on Renewable Motor Fuels. Warsaw, Poland 29-31, August 2007.

Hileman JI, De la Rosa-Blanco E, Bonnefoy PA, Carter NA: The carbón dioxide challenge facing aviation. (2013). Progress in Aerospace Sciences. 63:84-95.

Hileman, J. I., and R. W. Stratton. (2014). "Alternative jet fuel feasibility." Transport Policy, 34:52-62.

Hileman J. (2013). Overview of FAA Alternative Jet Fuel Activities. Presentation to the Biomass R&D Technical Advisory Committee, Washington DC, August 14, 2013.

Huber GW, Corma A. (2007). Synergies between Bio- and Oil Refineries for the Production of Fuels from Biomass. Angewandte Chemie. 46(38):7184-7201.

Malina R. (2012). HEFA and F-T jet fuel cost analyses. Laboratory for Aviation and the Environment. MIT, Nov 27, 2012.

Pearlson MN. (2011). A Techno-economic and Environmental Assessment of Hydroprocessed Renewable Distillate Fuels. MSc Thesis in Technology and Policy, MIT.

Pearlson M, Wollersheim C, Hileman J. (2013). A techno-economic review of hydroprocessed renewable esters and fatty acids for het fuel production. Biofuels, Bioproducts and Biorefining, 7(1):89-96.

Richard TL: Challenges in Scaling Up Biofuels Infrastructure. (2010). Science, 329:793.
Seber G, Malina R, Pearlson MN, Olcay H, Hileman JI, Barret SRH. (2014). Environmental and Economic Assessment of Producing hydroprocessed jet and diesel fuel from waste oil and tallow. Biomass and Bioenergy 67:108-118.
Spath P, Aden A, Eggeman M, Ringer B, Wallace B, Jechura J. (2005). Biomass to Hydrogen Production detailed Design and Economic Utilizing the Battelle Columbus Laboratory Indirectly Heated Gasifier. Technical Report NREL/TP-510-37408.
Staples MD, Malina R, Olcay H, Pearlson MN, Hileman JI, Boies A, Barrett SRH. (2014). Lifecycle greenhouse gas footprint and minium selling price of renewable diesel and jet fuel from fermentation and advanced fermentation technologies. Energy & Environmental Science, 7:1545.

Project 001(B) Alternative Jet Fuel Supply Chain Analysis-Tropical Region Analysis

University of Hawaii

Project Lead Investigator

University of Hawaii Lead:
Scott Q. Turn
Researcher
Hawaii Natural Energy Institute
University of Hawaii
1680 East-West Rd., POST 109; Honolulu, HI 96822
(808) 956-2346
sturn@hawaii.edu

University Participants

University of Hawaii

- P.I.(s): Scott Q. Turn, Researcher
- **FAA Award Number: 13-C-AJFE-UH, Amendment 005**
- Period of Performance: 10/1/15 to 9/30/16
- Task(s):
    1. Informing Regional Supply Chains
    2. Identification of Supply Chain Barriers in the Hawaiian Islands

University of Hawaii

- P.I.(s): Scott Q. Turn, Researcher
- **FAA Award Number: 13-C-AJFE-UH, Amendment 007**
- Period of Performance: 10/1/16 to 9/30/17
- Task(s):
    1. Informing Regional Supply Chains
    2. Support of Indonesian Alternative Jet Fuel Supply Initiatives

Project Funding Level

Under **FAA Award Number 13-C-AJFE-UH, Amendment 005**, the Alternative Jet Fuel Supply Chain Analysis-Tropical Region Analysis project received $75,000 in funding from the FAA and cost share funding of $75,000 from the State of Hawaii.

Under **FAA Award Number 13-C-AJFE-UH, Amendment 007**, the Alternative Jet Fuel Supply Chain Analysis-Tropical Region Analysis project received $100,000 in funding from the FAA and cost share funding of $75,000 from the State of Hawaii and $25,000 of in-kind cost match in the form of salary support for Scott Turn from the University of Hawaii.

Investigation Team

Lead:
Scott Turn – University of Hawaii

Other Lead Personnel:
Tim Rials and Burt English (UT Co-PIs)
Manuel Garcia-Perez (WSU Co-PI)
Kristin Lewis (Volpe PI)

Michael Wolcott (WSU PI)

UH Investigation Team:
Under **FAA Award Number 13-C-AJFE-UH, Amendment 005**, Task 1 and Task 2 includes
Dr. Scott Turn, Researcher, Hawaii Natural Energy Institute, UH
Dr. Trevor Morgan, Assistant Researcher, Hawaii Natural Energy Institute, UH
Dr. Richard Ogoshi, Assistant Researcher, Department of Tropical Plant and Soil Sciences, UH
Dr. Adel H. Youkhana, Junior Researcher, Department of Tropical Plant and Soil Sciences, UH

Under **FAA Award Number 13-C-AJFE-UH, Amendment 007**, Task 1 and Task 2 includes:
Dr. Scott Turn, Researcher, Hawaii Natural Energy Institute, UH
Dr. Trevor Morgan, Assistant Researcher, Hawaii Natural Energy Institute, UH
Dr. Richard Ogoshi, Assistant Researcher, Department of Tropical Plant and Soil Sciences, UH

Project Overview

Under **FAA Award Number 13-C-AJFE-UH, Amendment 005**, the research effort has two objectives. The first objective is to develop information on regional supply chains for use in creating scenarios of future alternative jet fuel production in tropical regions. Outputs from this project may be used as inputs to regional supply chain analyses being developed by the FAA and Volpe Center. The second objective is to identify the key barriers in regional supply chains that must be overcome to produce significant quantities of alternative jet fuel in the Hawaiian Islands and similar tropical regions.

The **FAA Award Number 13-C-AJFE-UH, Amendment 005** project goals are to:

- Review and summarize:
  - the available literature on biomass feedstocks for the tropics,
  - the available literature on pretreatment and conversion technologies for tropical biomass feedstocks,
  - the available literature on geographic information systems data sets available for assessment of alternative jet fuel production systems in the tropics.
- Identify alternative jet fuel supply chain barriers in the Hawaiian islands

Under **FAA Award Number 13-C-AJFE-UH, Amendment 007**, the research effort has two objectives. The first objective is to develop information on regional supply chains for use in creating scenarios of future alternative jet fuel production in tropical regions. Outputs from this project may be used as inputs to regional supply chain analyses being developed by the FAA and Volpe Center. Included in this objective is the development of fundamental property data for tropical biomass resources to support supply chain analysis. The second objective is to support the Memorandum of Understanding between the Federal Aviation Administration (FAA) and Indonesian Directorate General of Civil Aviation (DGCA) to promote developing and using sustainable, alternative aviation fuels.

The **FAA Award Number 13-C-AJFE-UH, Amendment 007** project goals are to:

- Support the Volpe Center and Commercial Aviation Alternative Fuels Initiative (CAAFI) Farm to Fly 2.0 supply chain analysis.
- Use GIS-based estimates of fiber crop production potential to develop preliminary technical production estimates of jet fuel in Hawaii.
- Develop fundamental property data for tropical biomass resources.
- Transmit data and analysis results to other ASCENT Project 1 researchers to support improvement of existing tools and best practices.
- Support Indonesian alternative jet fuel supply initiatives

13-C-AJFE-UH, Amendment 005 Task 1: Informing Regional Supply Chains

University of Hawaii

Objective(s)

Task 1, Activity 1. Review the archival literature and assemble relevant citations for the tropical crops/feedstocks for alternative jet fuel production.

Task 1, Activity 2. Review the archival literature and assemble relevant citations for pretreatment and conversion technology options and experience with potential tropical feedstock materials.

Task 1, Activity 3. Review the archival literature and assemble relevant citations for GIS biofuel production system analyses elsewhere in the tropics

Research Approach

Task 1, Activity 1. The archival literature will be reviewed to construct an updated database of relevant citations for the tropical crops identified in section 8; new potential energy crops will be identified and added to the database. Available information on agronomic practices, crop rotations, and harvest techniques will be included. The database will be shared with and serve as a resource for the Project 1 team and Volpe Center analyses of regional supply chains.

Task 1, Activity 2. A database of relevant pretreatment and conversion technology options and experience with potential tropical feedstock materials will be assembled from the archival literature and from existing Project 1 team shared resources. Of particular interest are inventories of material and energy flows associated with the pretreatment and conversion unit operations, fundamental to the design of sustainable systems and the underlying analysis. Pairings of pretreatment and conversion technology options provide the starting point for evaluation of tropical biorefineries that can be integrated into ASCENT Project 1 team and Volpe Center activities.

Task 1, Activity 3. GIS tools that are currently available to support tropical supply chain analysis will be reviewed and revised as needed to conform to Project 1 team working standards. Literature review of published GIS biofuel production system analyses elsewhere in the tropics will be conducted and a database assembled. Repositories of GIS data layers typically needed in regional supply chain analysis maintained by institutions elsewhere in the tropics will be surveyed and compiled into a report. The existing GIS analyses and the database of GIS analyses for the tropics will serve as a resources for Project 1 Team and Volpe Center analyses of regional supply chains.

Milestone(s)

Include a description of any and all milestones reached in this research according to previously indicated timelines.
Task 1, Activity 1: Identify target list of databases to search for relevant literature.
Task 1, Activity 1: Interim report summarizing progress on literature search.
Task 1, Activity 2: Identify target list of databases to search for relevant literature.
Task 1, Activity 2: Interim report summarizing progress on literature search.
Task 1, Activity 3: Identify target list of databases to search for relevant literature.
Task 1, Activity 3: Interim report summarizing progress on literature search.

Major Accomplishments

None – Task in progress

Publications

None – Task in progress

Outreach Efforts

None – Task in progress

Awards

None – Task in progress

Student Involvement

None

Plans for Next Period

Reports for each of the three literature review activities have been drafted and will be finalized in the coming year. The reports will be merged into a publication on options for alternative jet fuel production in the tropics.

13-C-AJFE-UH, Amendment 005 Task 2: Identification of Supply Chain Barriers in the Hawaiian Islands

University of Hawaii

Objective(s)

Identify the key barriers in regional supply chains that must be overcome to produce significant quantities of alternative jet fuel in the Hawaiian Islands and similar tropical regions.

Research Approach

UH developed the Hawaii Bioenergy Master Plan for the State of Hawaii [1]. Completed in 2009, UH was tasked with determining whether Hawaii had the capability to produce 20% of land transportation fuels and 20% of electricity from biobased resources. Toward this end, the plan included assessments of (1) land and water resources that could support biomass feedstock production, (2) potential biomass resources and their availabilities, (3) technology requirements, (4) infrastructure requirements to support logistics, (5) economic impacts, (6) environmental impacts, (7) availability of human capital, (8) permitting requirements, and (9) limitations to developing complete value chains for biomass based energy systems. In keeping with the stakeholder driven development of the Hawaii Bioenergy Master Plan, barriers to development of regional supply chains for ASCENT will be identified by interacting with key stakeholder groups. Green Initiative for Fuels Transition Pacific (GIFTPAC) meetings are held quarterly and are attended by biofuel development interests in Hawaii including representatives of large landowners, producers of first generation biofuels, petroleum refiners, electric utilities, the State Energy Office, U.S. Pacific Command, biofuel entrepreneurs, county government officials, and the University of Hawaii. Additional stakeholders are invited as necessary to fill information and value chain gaps. These meetings are excellent opportunities to receive stakeholder input, identify barriers to supply chain development, and organize data collection efforts that span supply chain participants.

Milestone(s)

Task 2: Introduce activities at next regularly scheduled GIFTPAC meeting after contract executed.
Task 2: Interim report outlining two tropical supply chain scenarios developed in consultation with Project 1 team, and with input from GIFTPAC participants.

Major Accomplishments

None – Task in progress

Publications

None – Task in progress

Outreach Efforts

Task objectives were introduced to stakeholders at the Green Initiative Fuels Pacific meeting on April 8, 2016 and a facilitated stakeholder meeting was held on September 21, 2016, to aid in identifying alternative jet fuel production barriers.

Awards

None

Student Involvement

None

Plans for Next Period

A report on barriers to alternative jet fuel production based on stakeholder meetings has been drafted and will be finalized in the coming year.

13-C-AJFE-UH, Amendment 007 Task 1: Informing Regional Supply Chains

University of Hawaii

Objective(s)

Task 1, Activity 1. Support Volpe Center and Commercial Aviation Alternative Fuels Initiative (CAAFI) Farm to Fly 2.0 supply chain analysis.
Task 1, Activity 2. Use GIS-based estimates of fiber crop production potential to develop preliminary technical production estimates of jet fuel in Hawaii.
Task 1, Activity 3. Develop fundamental property data for tropical biomass resources.
Task 1, Activity 4. Transmit data and analysis results to support improvement of existing tools (e.g. POLISYS).

Research Approach

Task1 Activities 1 and 4 will be coordinated with the respective cooperating organizations through discussions to identify support points and data gaps. These are anticipated to align with work carried forward from Amendment 005 activities related to supply chain analyses in Hawaii and elsewhere in the tropics but is also open to respond to immediate needs as they are identified.

Task 1, Activity 2 will rely on GIS layers for fiber crop production potential that are based on soil type, rainfall patterns, irrigation availability, slope, elevation, land use zoning, and land owner classification. Using this as a basis, fiber yield projections based on available crop models will be implemented and alternative jet fuel (AJF) production will be estimated. This activity will also provide guidance for locating AJF production sites and a basis for estimating supporting logistic requirements.

Task 1, Activity 3 will focus on identifying and filling data gaps related to AJF feedstock materials and conversion processes. Examples of potential activities undertaken as part of this subtask include (i) identifying higher value compounds present in tropical oil seeds that could provide co-product price support for AJF production, (ii) determining physical and chemical property data for tropical candidate feedstocks, and (iii) logistics data related to feedstock handling, port/harbor capacity, or harvesting time and motion studies.

Milestone(s)

Task 1, Activity 1: Identify target opportunities to augment POLYSYS, AFTOT, and conversion modules
Task 1, Activity 2: Review previously developed GIS information layers for tropical fiber crops and identify updating requirements
Task 1, Activities 1 & 4: Status report on provision of data to other ASCENT 1 researchers (e.g. POLYSIS and AFTOT)
Task 1, Activity 2: Preliminary estimates of AJF technical potential in Hawaii based on previously developed GIS information layers
Task 1, Activity 3: Status report on biomass resources in Hawaii

Major Accomplishments

None – Task in progress

Publications

None – Task in progress

Outreach Efforts

None – Task in progress

Awards

None

Student Involvement

None

Plans for Next Period

Next steps for this task will include activities to accomplish the following:
Task 1, Activity 1. Support Volpe Center and Commercial Aviation Alternative Fuels Initiative (CAAFI) Farm to Fly 2.0 supply chain analysis.
Task 1, Activity 2. Use GIS-based estimates of fiber crop production potential to develop preliminary technical production estimates of jet fuel in Hawaii.
Task 1, Activity 3. Develop fundamental property data for tropical biomass resources.
Task 1, Activity 4. Transmit data and analysis results to support improvement of existing tools (e.g. POLISYS).

13-C-AJFE-UH, Amendment 007 Task 2: Support of Indonesian Alternative Jet Fuel Supply Initiatives

University of Hawaii

Objective(s)

The objective of Task 2 is to support the Memorandum of Understanding between the Federal Aviation Administration (FAA) and Indonesian Directorate General of Civil Aviation (DGCA) to promote developing and using sustainable, alternative aviation fuels.

Research Approach

This task will support the Memorandum of Understanding between the Federal Aviation Administration (FAA) and Indonesian Directorate General of Civil Aviation (DGCA) to promote development and use of sustainable, alternative aviation fuels. This will begin with working with the FAA to establish points of contact to coordinate efforts with Indonesian counterparts. The Indonesian Aviation Biofuels and Renewable Energy Task Force (ABRETF) membership includes Universitas Indonesia, Institut Teknologi Bandung, and Universitas Padjadjaran. A prioritized list of tasks will be developed in consultation with Indonesian counterparts and data required to inform sustainability and supply analyses and potential sources of information will be identified. This could include data collection on Indonesian jet fuel use and resources for alternative jet fuel production, airport locations and annual and monthly jet fuel consumption patterns. Characterization of sustainable biomass resources with potential for use in producing alternative jet fuel supplies could include developing preliminary GIS mapping information of their locations and distributions and preliminary estimates of their technical potentials.

Milestone(s)

Preliminary report on Indonesian project element 1 (e.g. airport and jet fuel consumption patterns)
Status report on project element 2 (e.g. targeted biomass resources in Indonesia)
Status report on project element 3 (e.g.data required to inform sustainability analyses and potential sources of information for Indonesian alternative jet fuel production options)

Major Accomplishments

None – Task in progress

Publications

None – Task in progress

Outreach Efforts

None – Task in progress

Awards

None

Student Involvement

None

Plans for Next Period

Plans for the next period include working with the FAA to establish points of contact to coordinate efforts with Indonesian counterparts to meet project objectives.

Project 001(C) Alternative Jet Fuel Supply Chain Analysis

Purdue University

Project Lead Investigator

Wallace E. Tyner
James and Lois Ackerman Professor
Department of Agricultural Economics
Purdue University
403 West State Street
West Lafayette, IN 47907-2056
765-494-0199
wtyner@purdue.edu

University Participants

Purdue University

- Wallace E. Tyner, James and Lois Ackerman Professor
- FAA Award Number: 13-C-AJFE-PU
- Period of Performance: July 14, 2014 – August 31, 2017
- Task(s):

1. **Lead: Tyner; supported by post doc and graduate students)** – Develop stochastic techno-economic models for relevant pathways and identify key stochastic variables to be modeled for assessing risk in conversion pathways. This work will lead to our capability to compare pathways, their expected economic cost plus the inherent uncertainty in each pathway.
2. **Lead: Tyner; supported by Taheripour and Malina (MIT))** – Work with the CAEP/AFTF life cycle assessment committee (WP3) on issues such as system boundaries, induced land use change, LCA methodology, and pathway GHG emissions assessment.
3. **Lead**: **Tyner; supported by Taheripour** – Work with the CAEP/AFTF market based measures group to develop a methodology for applying market based measures for an aviation biofuels system.
4. **Lead: Tyner; supported by Taheripour and post doc** – Develop a new version of the GTAP-BIO model capable of handling land use changes on the intensive margin and of balancing extensive and intensive margin changes.

Project Funding Level

Amendment 3 - $250,000, Amendment 6 - $110,000, Amendment 10 - $230,000, Amendment 15 - $373,750.
Current cost sharing is from Oliver Wyman

Investigation Team

Wallace E. Tyner – PI – James and Lois Ackerman Professor
Farzad Taheripour – Research Associate Professor – involved in several aspects of the project, but especially life cycle analysis and land use change
David Cui – post doc, GTAP-BIO model modifications and simulations
Xin Zhao – PhD student Purdue University – stochastic techno-economic analysis and GTAP ILUC analysis
Elspeth McGarvey – MS student, Purdue University - stochastic techno-economic analysis
Guolin Yao – PhD student Purdue University - stochastic techno-economic analysis
Luis Pena Levano – PhD student Purdue University – GTAP-BIO intensification

Project Overview

This project has four main components. First is advancement of stochastic techno-economic analysis for aviation biofuel pathways. Second is life cycle and production potential analysis of alternative aviation biofuel pathways in coordination

with ICAO-AFTF. The third component also involves working with ICAO-AFTF but on the market based measures activity. This component includes life cycle analysis issues such as co-product allocation and land use change. The fourth component involves developing a new version of GTAP-BIO that does a better job of handling intensification in estimating land use change. Historical data suggests that changes at the intensive margin have been quite important in some regions over the past decade.

Task 1

Purdue University

Objective(s)

Develop stochastic techno-economic models for relevant pathways and identify key stochastic variables to be modeled for assessing risk in conversion pathways. This work will lead to our capability to compare pathways, their expected economic cost, plus the inherent uncertainty in each pathway.

Research Approach

For each pathway being evaluated, we develop a stochastic model that covers the entire pathway so that it can be used for both techno-economic and life cycle analysis. Over this period, we have evaluated alcohol to jet and the Catalytic Hydrothermolosis (CH) process. We have also developed some new approaches to stochastic TEA.

Milestone(s)

The alcohol to jet paper was presented at the annual meetings of the US Association of Energy Economics:
Yao, Guolin, Mark D. Staples, Robert Malina, and Wallace E. Tyner. "Stochastic Techno-economic Analysis of Alcohol-to-Jet Fuel Production." Paper presented at the annual meetings of the U.S. Association of Energy Economics, Pittsburg, PA, October 25-28, 2015.
The research also has been submitted to a journal.

Two other papers on quantifying stochastic TEA were published. See publications below.

Major Accomplishments

We had two presentations at the USAEE meetings in 2015 plus two published journal papers in 2015/16 and a poster at the ASCENT meeting in March 2015.

Publications

Zhao, Xin, Tristin R. Brown, and Wallace E. Tyner. "Stochastic techno-economic evaluation of cellulosic biofuel pathways." *Bioresource Technology* 198 (2015), pp.755-763.

Zhao, Xin, Guolin Yao, and Wallace E. Tyner. "Quantifying breakeven price distributions in stochastic techno-economic analysis." *Applied Energy* 183 (2016) 318-326.

Outreach Efforts

Tyner made a presentation on stochastic TEA for aviation biofuels at the DOE workshop on aviation biofuels in Macon, GA
He also made a presentation for a NAS committee on aviation biofuels.

Awards

Tyner was named a fellow of the American Association for the Advancement of Science (AAAS) to be awarded in February 2017 at the AAAS meetings in Boston.
Tyner was named one of the top 100 people in the Advanced Bioeconomy by *Biofuels Digest*.

Student Involvement

Xin Zhao – PhD student, Purdue University

Guolin Yao – PhD student, Purdue University
Elspeth McGarvey – MS student, Purdue University
The students have worked on the stochastic techno-economic analysis.

Plans for Next Period
We will continue stochastic TEA, with the next pathway to be completed being the Catalytic Hydrothermolosis (CH) process.

Task 2
Purdue University

Objective(s)
Work with the CAEP/AFTF life cycle assessment committee (WP3) on issues such as system boundaries, induced land use change, LCA methodology, and pathway GHG emissions assessment.

Research Approach
There are many varied assignments and pieces under this task. For life cycle analysis, working with other team members, we use standard approaches for consequential LCA. For system boundaries, we have investigated the consequences of different approaches to defining system boundaries. For estimating induced land use change, we use the GTAP model and have modified it to improve land allocation at the extensive and intensive margins (see task 4).

Milestone(s)
Tyner participated in the AFTF meetings in Montreal in October 2015 and June 2016. He has been involved in many of the tasks and document preparation for the meetings. In Montreal, he gave presentations on the improvements in induced land use change modeling and the work plan for the ILUC sub-group.

Major Accomplishments
The ILUC work plan has been approved by AFTF. Tyner is now co-lead of the ILUC task with Brad Saville of the University of Toronto.

Publications
de Carvalho Macedo, I., Andre M. Nassar, Annette L. Cowie, Joaquim E.A. Seabra, Luisa Marelli, Martina Otto, Michael Q. Wang, and Wallace E. Tyner. Greenhouse Gas Emissions from Bioenergy (chapter 17), in Bioenergy and Sustainability: bridging the gaps, G.M. Souza, et al., Editors. 2015, Scientific Committee on Problems of the Environment (SCOPE): Paris. p. 582-616.

Outreach Efforts
N/A

Awards
See awards under Task 1

Student Involvement
Xin Zhao has been involved in the AFTF ILUC work

Plans for Next Period
In the next period, we will be doing test simulations for multiple aviation biofuel pathways and regions. The basic objectives are to determine if there are significant regional differences for any given pathway and to determine the extent to which emissions change as the size of test shocks increase.
Following the February AFTF meeting, additional GTAP simulations will be accomplished.

Also, beginning in 2017, there will be collaborative work with the International Institute for Applied Systems Analysis on comparing model results from their GLOBIOM model with GTAP_BIO.

Task 3

Purdue University

Objective(s)

Work with the CAEP/AFTF market based measures group to develop a methodology for applying market based measures for an aviation biofuels system.

Research Approach

We have not worked much on this task, as tasks 1, 2, and 4 were deemed to be more urgent. We have begun working some with the policy sub-group in AFTF.

Milestone(s)

Major Accomplishments

Most of the accomplishments under this task are in the form of work progress of ICAO/CAEP/AFTF. The group is making significant progress under the leadership of James Hileman and Maria del Mar Rica Jimenez.

Publications

none

Outreach Efforts

N/A

Awards

See task 1.

Student Involvement

No graduate students are involved in this task.

Plans for Next Period

This task in not included in the 2016-17 statement of work.

Task 4

Purdue University

Objective(s)

Develop a new version of the GTAP-BIO model capable of handling land use changes on the intensive margin and of balancing extensive and intensive margin changes.

Research Approach

We began the research by examining the changes in cropland cover and harvested area around the world. If the changes in harvested area are roughly equal to changes in cropland cover, then all the land use change is at the extensive margin. However, if the changes in harvested area are greater than the changes in cropland cover, then there has been intensification (e.g., double cropping) in that region. Using FAO data we estimated the changes over the period 2003-13 by region. We then made changes in the GTAP-BIO by introducing an intensification parameter that varies by region. We then calibrated the values for this parameter by region from the historical data. Finally, test simulations were done to determine how well the results matched historic data.

Milestone(s)

The modeling changes and preliminary results were presented at the June 2016 AFTF meeting in Montreal.

Major Accomplishments
Improving GTAP-BIO to do a better job on intensification and the extensive/intensive margin was a major accomplishment. Also, we updated the GTAP data base from 2004 to 2011.

Publications
Taheripour, F., Cui, H., & Tyner, W. E. (2016). An Exploration of Agricultural Land use Change at the Intensive and Extensive Margins: Implications for Biofuels Induced Land Use Change. In Z. Qin, U. Mishra, & A. Hastings (Eds.), Bioenergy and Land Use Change: American Geophysical Union (Wiley)

This work also has been submitted to a journal.

Outreach Efforts
Tyner gave a presentation on this research at the DOE Aviation Biofuels workshop in Macon, GA.

Awards
See task 1.

Student Involvement
Luis Pena Levano was involved in this research.

Plans for Next Period
We continue to refine some aspects of the model and parameters. We will be using the model to do test simulations for the February 2017 AFTF meeting in Montreal and also for simulations for the June meeting in Washington, DC.

ASCENT 001(D) Alternative Jet Fuel Supply Chain Analysis of the Mid-Atlantic

Project Lead Investigator

Investigating Team:

- Leads: Katherine Y. Zipp – PSU

Other Lead Personnel:

- Tom Richard – PSU, Caroline E. Clifford – PSU, Lara Fowler – PSU, Michael P. Wolcott – WSU, Manuel Garcia-Perez – WSU, Tim Rials – UT, Burt English – UT, Kristin Lewis – Volpe

Penn State Lead:

Katherine Y. Zipp
Assistant Professor of Environmental and Resource Economics
Department of Agricultural Economics, Sociology, and Education
The Pennsylvania State University
112-F Armsby
University Park, PA 16802
814.863.8247
kyz1@psu.edu

University Participants

Penn State University: Project Title "Alternative Jet Fuel Supply Chain Analysis of the Mid-Atlantic".

Project Co-Director: Katherine Y. Zipp (PSU)
Other researchers: Tom Richard – PSU, Caroline E. Clifford – PSU, Lara Fowler – PSU

FAA Award Number: FAA Cooperative Agreement No. 13-C-AJFE-PSU, Amendment 028

Period of Performance: August 1, 2016 – July 31, 2017

Task(s):

1.5.1 (Lead: Richard; supported by Zipp, Rials, and English) – Delineate the sustainability impacts associated with various feedstock choices (switchgrass, oilseeds and winter grasses) including land-use effects for the mid-Atlantic region, including the Chesapeake Bay watershed.

1.5.2 (Lead: Zipp, supported by Richard and Lewis) - Evaluate the supply chains associated with switchgrass, oilseeds and winter grasses for the mid-Atlantic region.

3.3.1 (Lead: Clifford; supported by Garcia-Perez) - Report on preprocessing requirements and refinery insertion points for various bio-oil and biomass feeds.

3.3.3 (Lead: Garcia-Perez, supported by Clifford) – Simulate satellite biomass-to-liquid processing (e.g. gasification/F-T catalysis, pyrolysis, hydrothermal liquefaction or vegetable oil processing)

7.1.4 (Lead: Richard, supported by Wolcott) - Updated Data Management Plan and Status Report

8.1 (Lead: Zipp, supported by Fowler, and Richard) - Analysis of ecosystem service valuation, law and policy drivers, and potential policy design of water quality improvements associated with perennial grasses and cover crops.

Project Funding Level

- FAA Funding: $200,000.
- Matching:
  - Penn State - $200,000
- Total Funding: $400,000

Investigation Team

1.5.1 (Lead: Richard; supported by Zipp, Rials, and English) – Delineate the sustainability impacts associated with various feedstock choices (switchgrass, oilseeds and winter grasses) including land-use effects for the mid-Atlantic region, including the Chesapeake Bay watershed.

1.5.2 (Lead: Zipp, supported by Richard and Lewis) - Evaluate the supply chains associated with switchgrass, oilseeds and winter grasses for the mid-Atlantic region.

3.3.1 (Lead: Clifford; supported by Garcia-Perez) - Report on preprocessing requirements and refinery insertion points for various bio-oil and biomass feeds.

3.3.3 (Lead: Garcia-Perez, supported by Clifford) – Simulate satellite biomass-to-liquid processing (e.g. gasification/F-T catalysis, pyrolysis, hydrothermal liquefaction or vegetable oil processing)

7.1.4 (Lead: Richard, supported by Wolcott) - Updated Data Management Plan and Status Report

8.1 (Lead: Zipp, supported by Fowler, and Richard) - Analysis of ecosystem service valuation, law and policy drivers, and potential policy design of water quality improvements associated with perennial grasses and cover crops.

Project Overview

1.5.1 Delineate sustainability impacts associated with various feedstocks, including land use effects for mid-Atlantic region/Chesapeake Bay watershed. Includes subtasks addressing erosion and sediment delivery and water quality.

1.5.2 Evaluate the supply chains associated with switchgrass, oilseeds and winter grasses for the mid-Atlantic region.

3.3.1 Report on preprocessing requirements and refinery insertion points for various bio-oil and biomass feeds.

3.3.3 Simulate satellite biomass-to-liquid processing (e.g. gasification/F-T catalysis, pyrolysis, hydrothermal liquefaction or vegetable oil processing)

7.1.4 Updated Data Management Plan and Status Report

8.1 Analysis of ecosystem service valuation, law and policy drivers, and potential policy design of water quality improvements associated with perennial grasses and cover crops. Includes subtasks 8.1.1, a literature review, and 8.1.2, a report analyzing Chesapeake Bay opportunities as a co-product market opportunity.

Task 1.5

Penn State

Objective(s)

Evaluate the supply chains associated with switchgrass, oilseeds and winter grasses for the mid-Atlantic region.

Research Approach

Determine the price-supply curves to determine crop acreages at different price points. This task is informed by our new Task 8.1, and will apply the UT estimates of erosion, sediment, and water quality impacts for perennial grasses and cover

crops in the Chesapeake Bay region. This objective will also leverage ongoing work by the USDA funded NorthEast Woody/warmseason Biomass (NEWBio) Consortium to evaluate sustainability impacts of switchgrass and winter rye. See Task 8.1 for a description of the returns to biomass needed to induce conversion.

Milestone(s)

Determined the returns needed to induce farmers to convert to switchgrass. This is the first step to estimate the price-supply curves.

Major Accomplishments

Economic model to motivate land use conversion has been developed and demonstrated at ASCENT and CAAFI meetings

Publications

NA

Outreach Efforts

NA

Awards

NA

Student Involvement

One graduate student is a major contributor to this project, drafting both the literature review, and the coding to estimate our model.

Plans for Next Period

Future work will use these boundaries to determine the price-supply curves for perennial grasses and winter cover crops.

References

See Task 8.1

Task 3.3

Penn State and Washington State

Objective(s)

Evaluate commercial options for biofuel intermediates insertion into petroleum refineries for conversion to AJF.

Research Approach

Using an extensive literature review, PSU identified and evaluated commercial biomass feedstocks and bio-based intermediates that could be inserted in a refinery or be converted to alternative jet fuel with minimal processing. The evaluation considered bio-based liquids at three insertion points: 1) “bio-crude” introduced at the front of the refinery for crude processing with petroleum, 2) refinery-ready liquids inserted after crude processing and utilizing conversion and/or finishing unit operations to upgrade the bio-based liquids into fuels, and 3) blend-ready fuels that are inserted during blending to upgrade low-value refinery streams, improve specifications, and take advantage of blending, storage and distribution capacity. Unit operations and process opportunities and constraints were assessed for a range of bio-based liquids relevant to alternative jet fuels.

Milestone(s)

A draft of the first literature report was completed in July 2015 and shared with Delta Airlines in October 2015. The report was posted in 2016 for the group. Currently we are working on report focused on oxygen removal of bio-based fuels and intermediates.

Major Accomplishments

The accomplishments of this task (Task 3.3) will provide the project and stakeholders with a clearer understanding of the options, pros and cons of integrating bio-based feedstocks in a conventional petroleum refinery. Our hope is that Delta will implement one or more of these options for a demonstration at their refinery. This report is the basis for the project work in the coming year. Oxygen in biomass intermediates may discourage petroleum-refining facilities from pursuing the use of intermediates, so how to remove the oxygen is critical. We are working on a literature review of how to remove oxygen using conventional processes and catalysts as well as suggesting alternative catalysts.

Publications

A Technical Report was developed for discussion with Delta Airlines. We have written a publication on this material that will be submitted in the next couple of months.

Outreach Efforts

Results and recommendations from the Literature Review were communicated to Delta Airlines in October 2015. We have also initiated discussions with Rich Altman of the Commercial Aviation Alternative Fuels Initiative (CAAFI) and the Farm to Fly 2 (F2F2) program. Rich is working with the University of Virginia on distribution systems of alternative fuels to airports in the greater Washington DC area. We had an introductory teleconference with that group in September 2015 had a face-to-face meeting with that group in Virginia in October 2015. We are currently working on a publication to submit in early 2017 to the journal Energy and Fuels.

Awards

NA

Student Involvement

NA

Plans for Next Period

Delta Airlines has not been involved with the AJF aspect in the last year. In recent conversations with Delta, we have learned that Delta is involved again; further discussions with Delta will continue.

References

See technical report.

Task 7.1

Penn State and Washington State and ORNL

Objective(s)

Update Data Management Plan and provide status report.

Research Approach

The primary goal of this task is to develop a common framework that facilitates transparent and open data access for supply chain model intercomparison and improvement, specifically targeting the needs and opportunities of the AJF sector. This effort requires coordination of all team members, many of whom have independent models and datasets, some of which are proprietary. The team will develop a consensus approach to data use and model access and then establish appropriate agreements and documentation. The participating DOE labs have extensive experience with this activity in other applications, including with Dr. Richard and other university team members working on regional biofuel projects funded by DOE and USDA. Expanding these efforts to include alternative aviation fuel supply chains will allow

intercomparison and improvement of supply chain models and increase the confidence of the aviation sector in model predictions.

Milestone(s)
Our goal this year was to have multi-institutional participation in the data management system. That milestone was exceeded, although not all PIs are participating.

Major Accomplishments
Several actions toward implementation of the Data Management plan have been accomplished. PIs and students working on the project have reviewed signed the Data Use Agreement document and the Data Use Acknowledgement document, file naming conventions and meta data documentation have been developed, and over 2200 files have been uploaded into the system. Most of these files are journal articles, but 70 of the files are datasets that have been classified and logged in our Common Data needs document for internal data sharing and eventual public release.

Publications
None

Outreach Efforts
NA

Awards
NA

Student Involvement
NA

Plans for Next Period
Continue to encourage participation.

Task 8.1
Penn State

Objective(s)
Analysis of Ecosystem service valuation and policy design of water quality improvements associated with perennial grasses and cover crops. Includes subtasks 8.1.1 (Literature review) and 8.1.2 (Report analyzing Chesapeake Bay opportunities as a co-product market opportunity.

Research Approach

We develop a land use conversion contract model following the general land conversion model by (Song, Zhao, & Swinton, 2011), while also incorporating subsidies in the form of payments for ecosystem services and incentive compatibility constraints. Specifically, we expand the model by considering that the potential payoff for farmers who choose to initiate land use conversion and adopt biofuel crops consists of not only the monetary values of crop outputs, but also a one-time lump-sum payment and subsidies that are depended on the consequential environmental benefits. The one-time lump-sum welfare transfer (denoted as T_{cs}) includes monetary compensation as well as technological assistance from government agencies to offset any fixed costs that farmers might incur if they convert their cropland from a corn-soybean rotation (denoted as *c*) to biofuel crops such as switchgrass (denoted as *s*). For simplicity, consider that $\{c, s\}$ is the only set of crop choices for a risk-neutral farmer with a unit of cropland, and any one-time land use conversion from *i* to *j* would incur a lump-sum cost $C_{ij}, i, j \in \{c, s\}$. Hence, it is necessary that $T_{cs} \geq C_{cs}$ holds for any conversion from *c* to *s* in order for farmers to participate.

The farmer's payoff consisted of two components. First, the monetary values of crop *i* outputs in period *t* is denoted by $\pi_i(t)$ which follows a stochastic process with evolution of a general form (Song et al., 2011), as follows:

(1) $$d\pi_i(t) = \theta_i(\pi_i, t)dt + \sigma_i(\pi_i, t)d\varepsilon_i,\ i \in \{c, s\}$$

where the drift term $\theta_i(\pi_i, t)$and variance $\sigma_i(\pi_i, t)$ are observable nonrandom functions, and $d\varepsilon_i$ is the increment of a Wiener process[1] which assumes that farmers would be able to learn about and predict future returns in each new period based on information updated in previous period. The correlation coefficient between *c* and *s* is denoted as ρ, such that $\mathrm{E}[d\varepsilon_c d\varepsilon_s] = \rho dt$. Farmers' expected present value payoff from crop returns on land use *i* at period *t* is denoted $V^i\big(\pi_c(t), \pi_s(t)\big)$, which depends on the distribution of future returns of both land uses and farmers make decisions between keeping land use *i* or convert it into alternative *j* (Song et al., 2011), as:

(2) $$V^i\big(\pi_c(t), \pi_s(t)\big) = max\begin{Bmatrix}\pi_i(t)dt + e^{-rdt}EV^i[\pi_c(t+dt) \times \pi_s(t+dt)],\\ V^j\big(\pi_c(t), \pi_s(t)\big) - C_{ij}\end{Bmatrix}$$

Second, farmers who agree to convert land use from corn-soybean to switchgrass (thus a $c \to s$ process) can receive, by the end of each period *t* of this particular conversion process, a subsidy from government agencies based on the generated environmental values. Switchgrass and many other biofuels have the potential to provide a variety of environmental benefits such as soil nitrogen sequestration, water nutrient reduction, and biodiversity conservation. These benefits, although often not traded with market values, can be utilized by government agencies and regulators as a part of the efforts on environmental protection and ecosystem restoration. For simplicity, we denote the environmental performance level of land use alternative *i* as a stochastically continuous and twice differentiable function $\phi_i(e_t), i \in \{c, s\}$, such that:

$$\frac{d\phi_s(e_t)}{dt} > 0, \qquad \frac{d^2\phi_s(e_t)}{dt^2} \le 0$$
$$\frac{d\phi_c(e_t)}{dt} \le 0, \qquad \frac{d^2\phi_c(e_t)}{dt^2} \le 0$$

This restriction allows us to differentiate the environmental performance of the two land uses so that switchgrass would generate increasing environmental benefits, while corn would generate limited (but not necessarily negative) environmental benefits.

Suppose that $\phi_i(e_t)$ is observable to government agencies at the end of period *t*, and a subsidy is paid to farmers based on the perceived environmental performance level. Without loss of generality, we define a subsidy rate, m, as a per unit compensation rate paid to farmers according to the perceived environmental performance level at the end of period *t*. Hence, the total subsidies paid to farmers in each possible land use scenario in period *t* are as follows:

(3-1) grow corn in period $t-1$, and convert land use to switchgrass in period t:
$$-C_{cs} + T_{cs} + m\phi_s(e_t) = m\phi_s(e_t), \text{ since } T_{cs} = C_{cs}$$

(3-2) grow switchgrass in period $t-1$ and period t:
$$m\phi_s(e_t)$$

(3-3) grow corn in period $t-1$ and period t:
$$m\phi_c(e_t)$$

(3-4) grow switchgrass in period $t-1$, and convert land use to corn in period t:
$$-C_{sc} + m\phi_c(e_t)$$

Since we assume that $\phi_s(e_t)$ is increasing over time, it is necessary that the total subsidy paid to farmers of land use type *s* by government at the end of each period *t* is strictly higher than farmers of land use type *c*.

Hence, the optimal land use decision problem in Equation (2), for value functions V^i and $V^j, i, j \in \{c, s\}$, must satisfy the following conditions along with the IC and IR constraints:

[1] The Wiener pdf is $f_{W_t}(x) = \frac{1}{\sqrt{2\pi t}}\exp(-\frac{x^2}{2t})$, following normal distribution with zero mean and variance *t* at any fixed period *t*. The covariance between any *s* and *t* is $cov(W_s, W_t) = \min(s, t)$, and $corr(W_s, W_t) = \sqrt{\frac{\min(s,t)}{\max(s,t)}}$.

(4-1) $$LV^i\left(\pi_c(\mathrm{t}),\pi_s(\mathrm{t})\right) \geq 0, i,j \in \{c,s\}$$

where $LV^i\left(\pi_c(\mathrm{t}),\pi_s(\mathrm{t})\right)$ is the second order Taylor expansion of $V^i\left(\pi_c(\mathrm{t}),\pi_s(\mathrm{t})\right)$ by applying Ito's lemma, as:

$$LV^i\left(\pi_c(\mathrm{t}),\pi_s(\mathrm{t})\right) = \mathrm{r}V^i(\pi_c,\pi_s) - \pi_i(\mathrm{t}) - \sum_{p=c,s}\alpha_p\left(\pi_p,\mathrm{t}\right)\frac{\partial V^i}{\partial \pi_p} - \sum_{p=c,s}\frac{\sigma_p^2\left(\pi_p,\mathrm{t}\right)}{2}\frac{\partial^2 V^i}{\partial \pi_p \partial \pi_p}$$

$$-\rho\sigma_c(\pi_c,\mathrm{t})\sigma_s(\pi_s,\mathrm{t})\frac{\partial^2 V^i}{\partial \pi_c \partial \pi_s}$$

(4-2) $$V^i(\pi_c,\pi_s) \geq V^j(\pi_c,\pi_s) - C_{ij}, i,j \in \{c,s\}\ and\ i \neq j$$

(4-3) Either (4-1) or (4-2) holds with strict equality.

Parameter Calibration and Estimation

The model can be parameterized and solved by collocation using OSSOLVER (Fackler, 2008) and estimated with CompEcon package in Matlab (Miranda & Fackler, 2002). Value functions can be approximated using a linearized combination of a sequence of known basis functions, such as:

(5) $$\widehat{V^i}(\pi_c,\pi_s) = \sum_{j_c=1}^{n_c}\sum_{j_s=1}^{n_s} c_{j_c j_s}\,\psi_{j_c j_s}(\pi_c,\pi_s)$$

where $c_{j_c j_s}$ is obtained when the decision optimality conditions are satisfied. The optimal decision rule is determined by solving and evaluating the approximated value functions at $\{c,s\}$ as well as the return minus the conversion costs, and based on the results the best payoffs from converting are then compared with the best payoffs from not converting (Fackler, 2008).

The empirical method involves solving the parameters in the return equation and calibrating parameters in the value functions. Return from land use is assumed to follow stochastic processes, with unknown parameters including the drift term θ_i, variance σ_i and correlation between the two alternatives ρ, which can be re-parameterized by linearization approximation. Two stochastic processes are often used. If return follows geometric Brownian motion (GBM), the analytical representation is as follows:

(6) $$d\pi_i = \theta_i \pi_i dt + \sigma_i \pi_i d\varepsilon_i,\ i \in \{c,s\}$$

Discrete approximation of the inter-temporal return difference gives:

(7) $$\ln \pi_{i,t} - \ln \pi_{i,t-1} = \left(\theta_i - \frac{\sigma_i^2}{2}\right) + \sigma_i \varepsilon_i,\ i \in \{c,s\}$$

Denote $\alpha_i = \theta_i - \frac{\sigma_i^2}{2}$, then α_i, σ_i and ρ can be estimated by maximum likelihood estimates.

If the returns follow mean reversion (MR), the analytical representation is as follows:

(8) $$d\pi_i = \theta_i(\widetilde{\pi_\iota} - \pi_i)dt + \sigma_i \pi_i d\varepsilon_i,\ i \in \{c,s\}$$

where $\widetilde{\pi_\iota}$ is the historically observed average return of land use *i*, and θ_i here measures speed of reversion. Discrete approximation of the inter-temporal return difference gives:

(9) $$\frac{\pi_{i,t}-\pi_{i,t-1}}{\pi_{i,t-1}} = \theta_i\left(\widetilde{\pi_\iota} - \pi_{i,t-1}\right) + \sigma_i\varepsilon_i$$
$$= \theta_i\widetilde{\pi_\iota} - \theta_i\pi_{i,t-1} + \sigma_i\varepsilon_i, \qquad i \in \{c,s\}$$

Denote $\beta_{1i} = \theta_i\widetilde{\pi_\iota}$, $\beta_{2i} = -\theta_i$, , then β_{1i}, β_{2i}, σ_i and ρ can be estimated.

Parameters

Table 1: Parameter assumptions

			Source
Corn-soybean returns		$229/acre	(Song et al., 2011)
Switchgrass returns (approximation, calculated from data below)		$423/acre	(Song et al., 2011)
Switchgrass yield mean		5.35 tons/acre	
Switchgrass yield variance		0.20 tons/acre	
Maintenance costs year 2-10		$192/acre	
Transportation costs		$8/ton	(Babcock, Gassman, Jha, & Kling, 2007)
Ethanol yields from one ton of switchgrass		79 gallons	(Schmer, Vogel, Mitchell, & Perrin, 2008)
Ethanol price		$1.46/gallon	NE Govt. 2016 (http://www.neo.ne.gov/statshtml/66.html)
Ethanol conversion costs		$0.91/gallon	(DiPardo, 2000)
Price subsidy for switchgrass from USDA (one time subsidy)		$45/ton	(Song et al., 2011)
	Corn-soybean	Switchgrass	
Drift ($\hat{\theta}_i$)	0.018	0.026	
Variance ($\hat{\sigma}_i$)	0.198	0.294	
Correlation ($\hat{\rho}$)	-0.098		
Conversion costs ($100 per acre)			
Corn-soybean to switchgrass	Switchgrass to corn-soybean		
1.36	0.47		(Song et al., 2011)
Discount factor	0.08		(Song et al., 2011)
Subsidies to environmental benefits ($\$m$ per unit ϕ_i)			
To corn-soybean	To switchgrass		
$0	$100/acre		(Woodbury, Kemanian, Jacobson, & Langholtz, n.d.)

Preliminary Results

The preliminary results[2] are presented as conversion boundaries. If a farmer is growing corn-soybeans they will convert to growing switchgrass when annual returns to switchgrass are above the line b^{CS}. If a farmer is growing switchgrass they will convert to growing corn-soybeans when annual returns to corn-soybeans are greater than the line b^{SC}. Because of uncertainty, risk, and the option value (the value of continuing the current use and having the option of converting crops in the future when it is more profitable to do so) the annual returns to switchgrass have to be higher than the net present value (b^{CS}_{NPV}) of the annual returns to switchgrass to induce conversion.

Figure 1: Replicate of the baseline model in (Song et al., 2011)

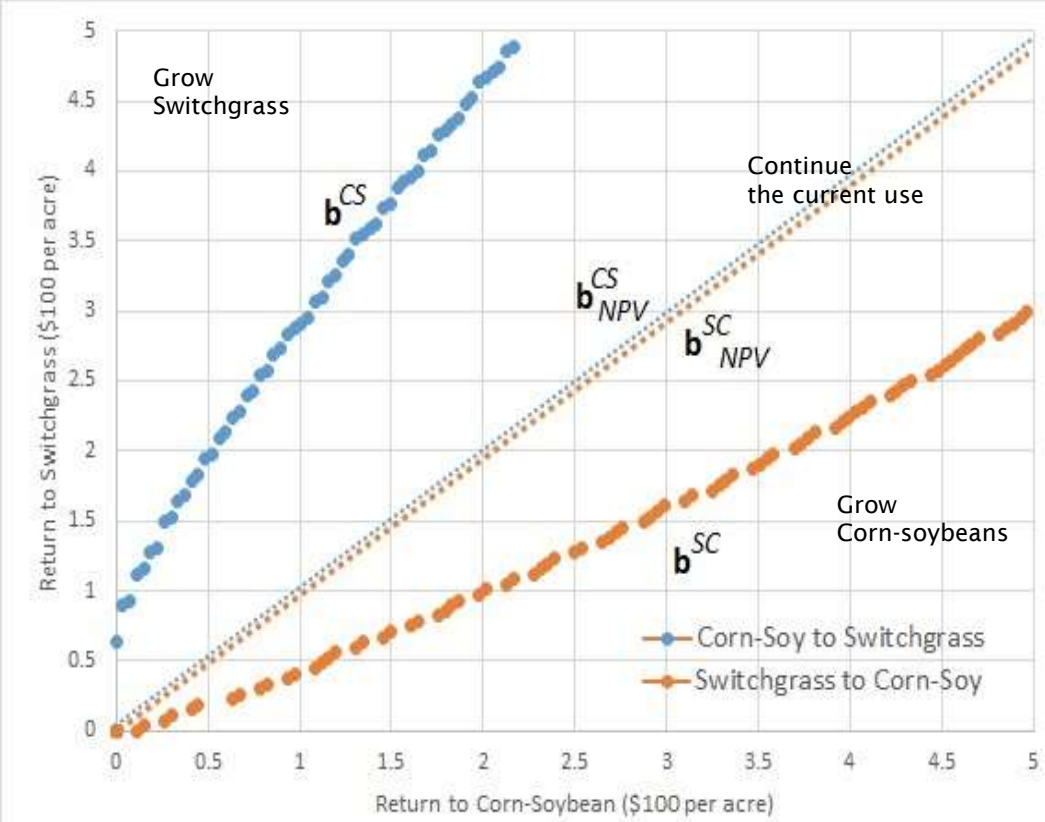

First, we replicated the baseline model in (Song et al., 2011). The optimality condition for conversion decisions are solved using Compecon toolbox (Miranda & Fackler, 2002) in MATLAB. The nodal points for the state variables (returns to corn-soybean and switchgrass, respectively) are evenly scattered over a revenue interval [0, 5] in hundred dollars ($100) in $1982. The output diagram shows the two boundaries in solid lines for conversions from corn-soybean to switchgrass (b^{cs}) and from switchgrass to corn-soybean (b^{sc}).

[2] These results are preliminary so please do not cite.

Figure 2: Subsidy to Switchgrass: $100 per acre from (Woodbury et al., n.d.)

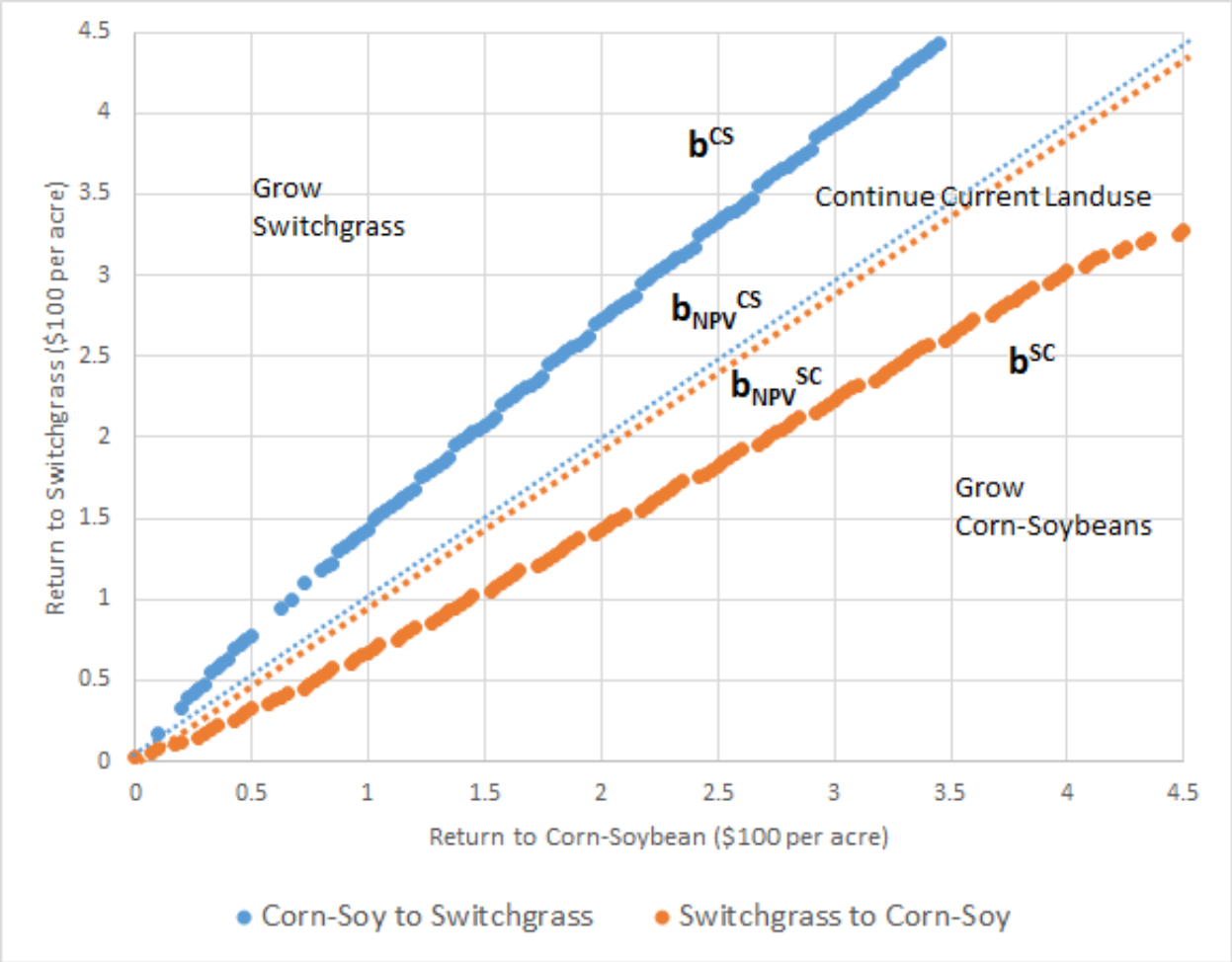

In this modification, we applied a subsidy of $100 per acre to farmers if the crops are converted from corn-soybean to switchgrass.

Converting all units to 2016$, without a government subsidy if farmers can earn $230/acre per year with a corn-soybean rotation and $337/acre per year with switchgrass, then they will not convert to switchgrass unless they can earn more than $512/acre per year. Uncertainty, risk, and the option value to convert in the future increase the minimum return from switchgrass needed to induce farmers to convert to switchgrass. With a $100/acre per year payment for ecosystem services (PES) subsidy, farmers would only need $399/acre per year returns to convert their land to switchgrass. Therefore, farmers do need more than the real annual returns to incentivize them to grow switchgrass but a $100/acre subsidy for ecosystem services reduces the uncertainty and risk and therefore reduces the returns need to convert by more than $100/acre.

Table 2: The real annual returns (Song et al. 2011) vs. the dynamically optimal conversion boundary

Subsidy to grow switchgrass	Real annual returns for corn-soybeans	Minimum return from switchgrass needed to convert from corn-soybean to switchgrass
$0/acre	$229/acre	$498/acre ($103/Mg, $5.74/GJ, $0.76/gallon)
$100/acre	$229/acre	$308/acre ($63/Mg, $3.55/GJ. $0.47/gallon)

Milestone(s)

A draft of a review of the ecosystem benefits of perennial grasses and winter cover crops (water quality improvements, soil improvements, and biodiversity improvements) has been started. A draft of a manuscript to estimate the effects of payments for ecosystem services (PES) subsidies on the willingness to convert to biomass has been started.

Publications

None

Outreach Efforts

NA

Awards

NA

Student Involvement

One graduate student is a major contributor to this project, drafting both the literature review, and the coding to estimate our model.

Plans for Next Period

The plans for next period include: (1) working with a law student or staff member to complete a law and policy review of optimal payments for the ecosystem services provided by biomass crops, (2) updating the assumptions of biomass yields and prices, (3) comparing other types of land use instead of corn-soybeans to include marginal lands, (4) collect data at a finer scale to be able to use the estimated conversion boundaries to simulate land conversion decisions and thus the supply of biomass.

References

Babcock, B. a, Gassman, P. W., Jha, M., & Kling, C. L. (2007). Adoption Subsidies and Environmental Impacts of Alternative Energy Crops. *Director*, *2600*(March), 15. Retrieved from http://publications.iowa.gov/5090/1/07bp50.pdf

DiPardo, J. (2000). Outlook for biomass ethanol production and demand. *… Eia. Doe. Gov/Oiaf/Analysis Paper/Pdf/Biomass …*, *0581*(May 1998), 1–14.

Duffy, M. D., & Nanhou, V. Y. (2002). Costs of producing switchgrass for biomass in southern Iowa. *Trends in New Crops and New Uses*, *1998*(November 1998), 267–275. Retrieved from http://www.hort.purdue.edu/newcrop/ncnu02/pdf/duffy-267.pdf

Fackler, P. L. (2008). Solving Optimal Switching Models. *Working Paper. North Carolina State University*. Retrieved from http://www4.ncsu.edu/unity/users/p/pfackler/www/ECG766/switch.pdf

Miranda, M. J., & Fackler, P. L. (2002). *Applied Computational Economics and Finance*. Cambridge: MIT Press.

Schmer, M. R., Vogel, K. P., Mitchell, R. B., & Perrin, R. K. (2008). Net energy of cellulosic ethanol from switchgrass. *Proceedings of the National Academy of Sciences*, *105*(2), 464–469. http://doi.org/10.1073/pnas.0704767105

Song, F., Zhao, J., & Swinton, S. M. (2011). Switching to Perennial Energy Crops Under Uncertainty and Costly Reversibility. *American Journal of Agricultural Economics*, *93*(3), 768–783. http://doi.org/10.1093/ajae/aar018

Tyner, W. E. (2010). The integration of energy and agricultural markets. *Agricultural Economics*, *41*(SUPPL. 1), 193–201. http://doi.org/10.1111/j.1574-0862.2010.00500.x

Woodbury, P., Kemanian, A., Jacobson, M., & Langholtz, M. (n.d.). Improving water quality in the Chesapeake Bay using payment for ecosystem services for perennial biomass production. *Biomass & Bioenergy*.

Project 001(E) Alternative Jet Fuel Supply Chain Analysis

University of Tennessee

Project Lead Investigator

Timothy Rials
Professor and Director
Center for Renewable Carbon
University of Tennessee
2506 Jacob Dr. Knoxville, TN 37996
865-946-1130
trials@utk.edu

University Participants

The University of Tennessee

- CO-PI: Burton C. English (Professor)
- FAA Award Number: 11712069
- Period of Performance: [August 1, 2016 to July, 31, 2017]
- Task(s):
    1. Develop a rotation based oil seed crop scenario and evaluate potential with POLYSYS
    2. Develop database on infrastructure and needs for Southeast
    3. Initiate aviation fuel supply chain study in the southeast
    4. Continue with sustainability work for both goals 1 and 4

Project Funding Level

FAA = 91,009
Match=69,444

Investigation Team

Tim Rials – Project Director(s)/Principal Investigator (PD/PI)
Burton C. English – Co-Principal Investigator (Co PD/PI)
Chris Clark – Faculty – Policy analysis
Lixia He – Other Professional – GAMS programmer
Kim Jensen – Faculty – By-product Markets
Dayton Lambert – Faculty – Rural Development
Jim Larson – Faculty – Production Economics
Ed Yu – Faculty -- Logistics
Evan Markel – Graduate Student

Project Overview

The University of Tennessee (UT) is responsible for generating the feedstock availability database for further analysis by the project team. Assessment work has been completed for forest residues and woody crops, and is advancing for agricultural crops (including cover/rotational crops). Also, sustainability information (environmental and socioeconomic) is underway to complete the Year 3 goals. Year 2 work will continue to tailor the feedstock database by incorporating pennycress as a winter cover crop providing an oil feedstock. POLYSYS and related models will be used to determine the

potential impact of this new scenario. Additionally, work will continue gathering information needed for a comprehensive supply chain analysis for the southeast region. This will involve identification of current infrastructure, as well as garnering stakeholder input on supply chain challenges through a structured workshop. This effort will produce an assessment report to establish the foundation for detailed analysis in subsequent project periods.

Task 1

University of Tennessee

Objective(s)

Develop a rotation based oil seed crop scenario and evaluate potential with POLYSYS
Conduct research on Pennycress and ran POLYSYS

Research Approach

Use POLYSYS to estimate the impact that a cover crop would have in meeting renewable fuel needs. Literature review was conducted on the agronomic features of pennycress and a rotation was developed. Yield and cost parameters were developed. POLYSYS was run using price ranging from $0.5 to $0.5/pound. To estimate yield impacts, monthly climate data 48 states and 344 climate divisions were collected from 2000 through 2014 The months of June, July and August are removed from the sample. Then the frequency of reaching the lower and upper bound temperature is calculated within each climate division and each year, for the months September through May. The frequencies are then aggregated over the years 2000 through 2014. Using the aggregated frequencies, we calculate the median number of times an upper or lower bound temperature is reached for each of the 344 climate divisions. This information is then disaggregated to the county level using a spatial union. Used median values range from zero to three over the sample. Median of one will imply a 25% yield reduction, a median of two will imply a 50% yield reduction, and a median of three will imply a 75% yield reduction. Estimated potential yields for each county in the 48 contiguous states using a base yield of 1500 pounds per acre.

Information on pennycress

- Large scale cultivation has not yet been undertaken for pennycress, thus management practices and stand establishment practices are still in research and development.
- Variety trials have been undertaken throughout the Midwest, particularly in Western Illinois, Minnesota, and Nebraska.
- A variety of planting methods have been tested, including drill, broadcast and aerial seeding.
- Aerial seeding over standing corn canopy or a broadcast with light incorporation after corn harvest has been successful.
- Aerial or broadcast seeding rates of 5lbs/acre have generated yields ranging from approximately 1400 lbs./acre to 2200 lbs./acre with an average yield of1800 lbs./acre.
- To establish a stand of pennycress ready for harvest in May-June to not interfere with soybean planting, aerial seeding over corn canopy may generate the best results.
- However, planting earlier than September 1st should be avoided, because if the plant flowers too early in winter months, survival rates are low.
- September planting dates should be identified by producers to ensure stand establishment. Phippen, John et al. (2010), conducted a study of five different September planting dates and found that seed oil content was not significantly different among the various planting dates.
- However, stand establishment declined as temperatures declined throughout the fall.
- Plants of the brassica family are susceptible to a fungus following an unusually wet spring. Insects and pests however, are not likely to pose a risk.
- The pennycress plant completes its life cycle in the spring when insects are emerging so insects do not pose a substantial risk.
- Pennycress is very cold tolerant and can grow in wide range of conditions. However, the plant is sensitive to high heat conditions.

- Pennycress has been known to survive very cold conditions with the ability to survive Canadian Prairie winters where temperatures can drop to negative 30 degrees Celsius. Sharma, Cram et al. (2007), found that Pennycress exhibits a higher freezing tolerance than its close relatives of Arabidopsis thaliana and Brassica napus (Canola).
- With a three week cold acclimation period, pennycress was freeze tolerant at -16.8 degrees Celsius or less than 2 degrees Fahrenheit.
- Temperatures above 85 degrees Fahrenheit pose a risk to pennycress and are found to have an impact on pod and seed numbers (Parker and Phippen 2012).
- Higher temperatures of 92 degrees Fahrenheit and above cause the plant to abort flowering (Sedbrook, Phippen et al. 2014).

Yield Variability

- Yields are not expected to be constant across varying geographic regions.
- The freeze tolerance and heat stress characteristics of pennycress imply a minimum and maximum range of temperatures of 20F to 930F for plant survival.
- However, heat exposure seems to pose the more significant risk and temperatures of 860F and above have a significant impact on pod and seed numbers.
- Therefore, we identify geographic regions across the United States which poses a risk to pennycress production yield, using a lower bound of 50F and upper bound of 880F.
- To identify those regions which pose a risk to pennycress we calculate the median number of times an upper or lower bound temperature is reached for each region

Outcome

Land use changes will occur when the production of one crop is incentivized with respect to others. Over the period of analysis, the average annual land use change was estimated for cotton (-18%) wheat (-17%), rice (-12%), oats (-11%) and grain sorghum (10%) with the corn/pennycress/soybean acreage increasing 13% (Table 1) resulting in a 5% increase in corn acreage and a 10% increase in soybean acreage. This change in acreage allowed a supply of Pennycress seed to be harvested on 25.8 million acres along with corn and soybeans. Prices also changed as production changed. The average change in production and prices are shown in Figure 1. For most crops an inverse relationship between price and production exists. Corns increase in production results in a decrease in price. The same is true for soybeans. Location of the pennycress production occurs largely in the western Corn Belt and Great Plains area (Figure 2). The above analysis was done when the pennycress price was set to $0.50 per pound. However, one important aspect might be what happens as price is reduced. Figure 5 contains a supply curve moving from $0.05 to $0.50 per pound. At five cents per pound, enough pennycress seed is harvested to produce over a billion gallons of aviation fuel. Increasing average realized net farm income $7.7 billion or 25%.

Conclusions and Next steps

It appears that pennycress is a potential feedstock for aviation fuel. The agronomic characteristics of the plant allow for it to be planted between corn and soybeans allowing for a farmer to get three crops over a two-year period if they use a corn/pennycress/soybean rotation. Cost will change as demand for pennycress oil increases. In this project pennycress price is varied between $0.05 and $0.50 per pound. Land does shift out of some crops and toward soybeans while corn acreage shifts are small in comparison. Production is predominately in the western corn belt and great plains though some production does occur in the pacific north west.

The next steps will involve analysis of other oil seed crops to evaluate their potential in developing an oil to aviation fuel market without impact

This project has shown that it is possible to produce enough pennycress feedstock to produce over 6 billion gallons of aviation fuel. Using POLYSYS, the potential of a corn/pennycress/soybean rotation is modeled and allowed to compete with traditional cropping systems. An analysis was conducted of runs from $0.05 to $0.50 per pound, Most of the potential is achieved at $0.20/pound. However, if the nation is to have 50% of the aviation fuel in alternative fuel, a single feedstock like pennycress will not meet the goal.

Table 1. Average Planted acres (Mil Ac)			
Crop	Without Pennycress	With PennyCress	% Change
Corn	79.6	84.5	6%
Grain Sorghum	5.1	4.6	-9%
Oats	0.9	0.8	-9%
Barley	2.6	2.4	-9%
Wheat	44.1	36.9	-16%
Soybeans	80.1	86.9	8%
Cotton	8.4	6.9	-18%
Rice	2.9	2.5	-13%
Hay	56.8	56.5	0
Pennycress	0.0	24.5[a]	NA[b]
Total All Crops	280.4	282.0	1%

[a] Acres already included in corn acres as a double crop

[b] Not Applicable

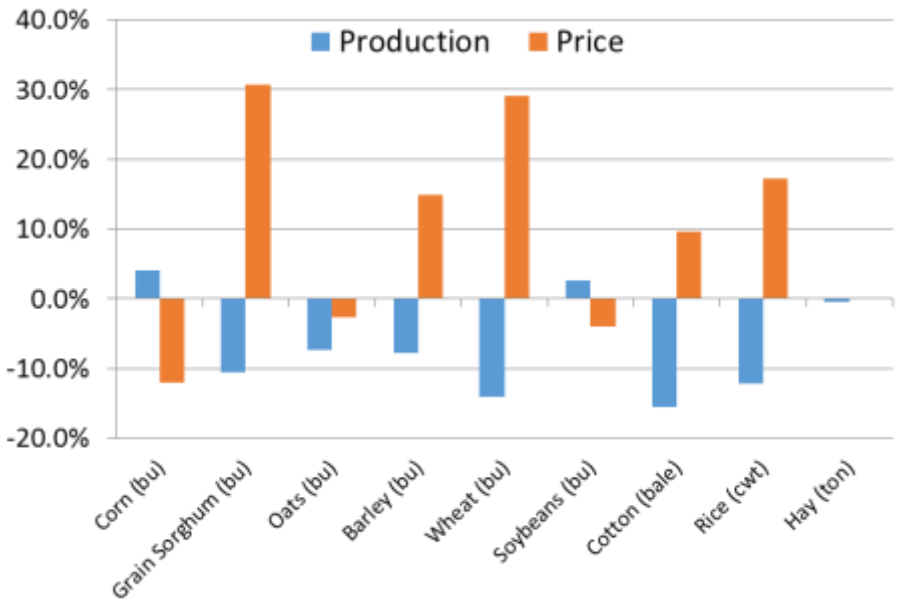

Figure 1. Land Use Changes : Pennycress Price = $0.20/pound

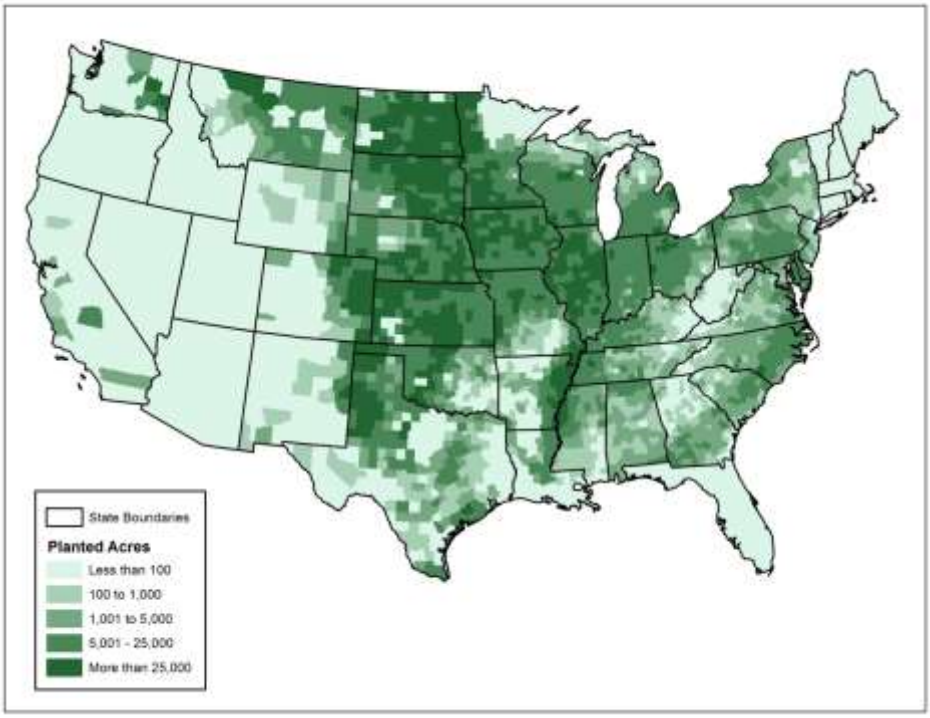

Figure 2. Locations where pennycress comes into solution

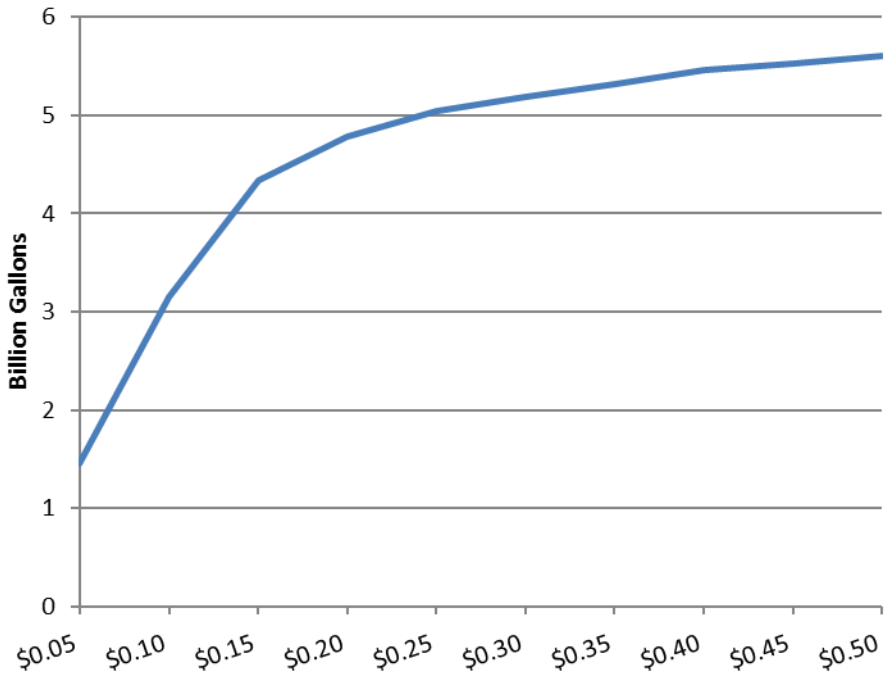

Figure 3. Pennycress supply curve

Task 2

University of Tennessee

Objective(s)

Develop information on other cover crops.

Research Approach

Conduct Literature review and determine how other cover crops might work in providing feedstock for renewable aviation fuel. PSU was contacted in September and a copy of a dissertation done on potential cover crops was provided. Crop selection began keeping it to a maximum of four. Crops selected included Camelina, Triticale, Winter Rye, and Oilseed Radish.

Plant characteristics are defined in figures 4 through 6

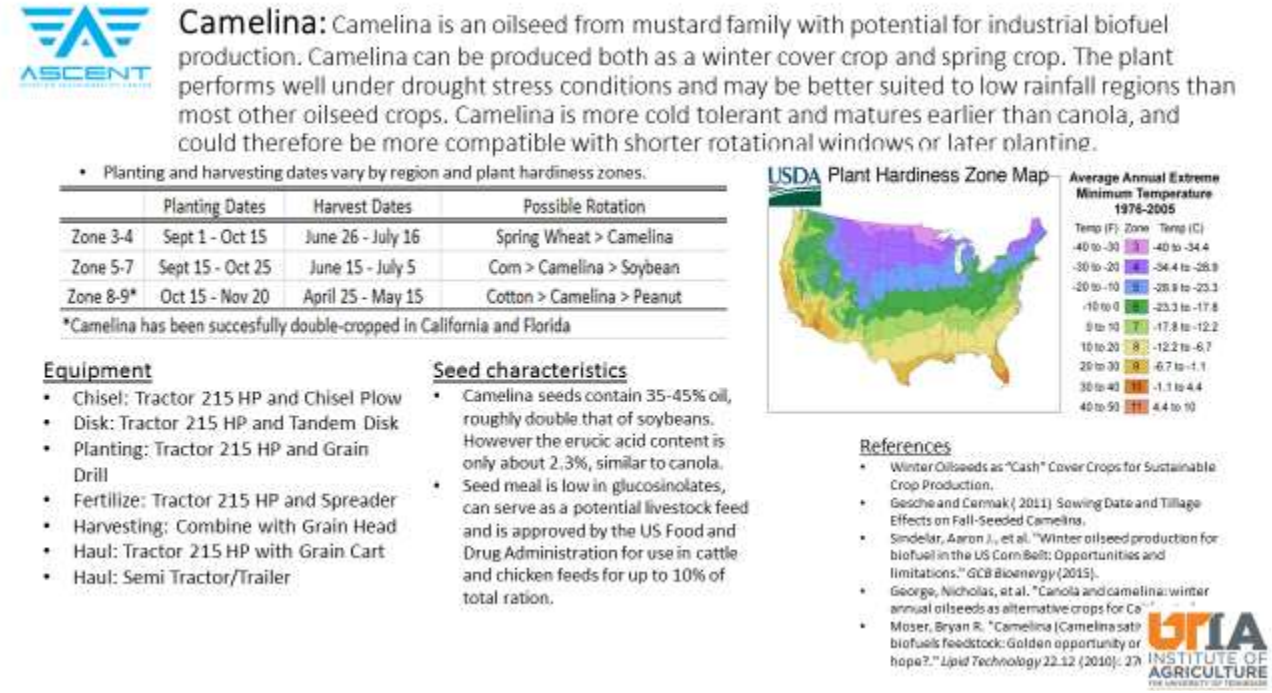

Figure 4. Information on Camelina

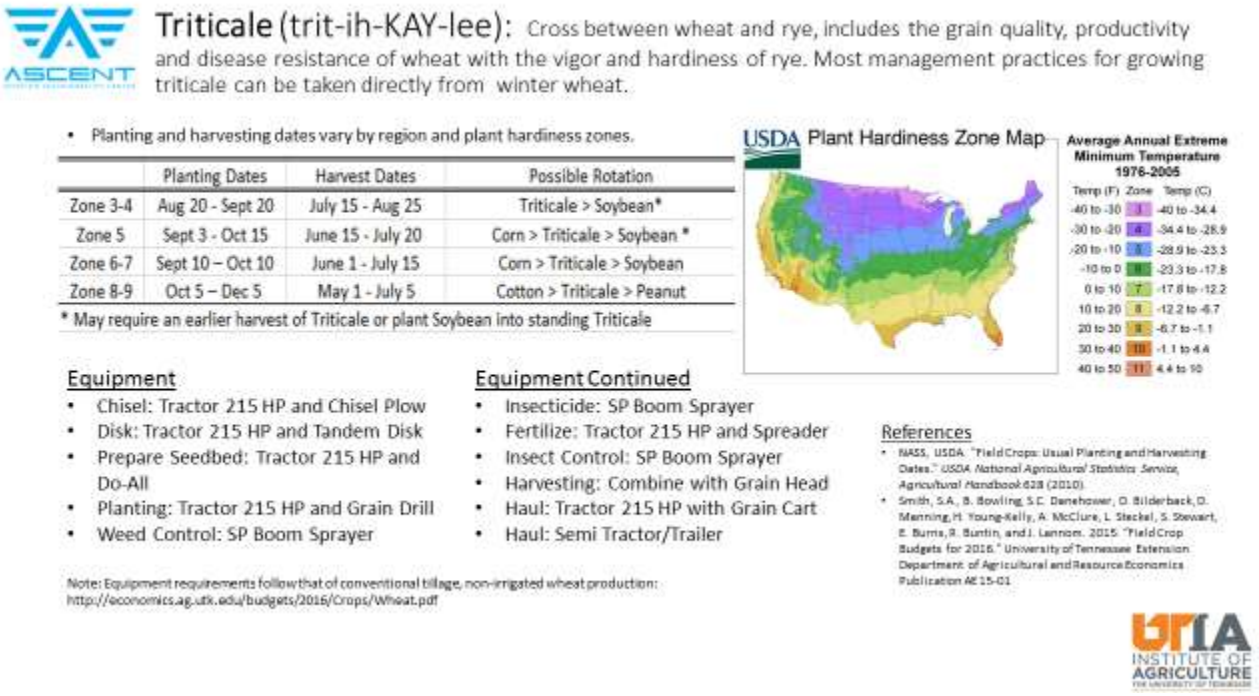

Triticale (trit-ih-KAY-lee): Cross between wheat and rye, includes the grain quality, productivity and disease resistance of wheat with the vigor and hardiness of rye. Most management practices for growing triticale can be taken directly from winter wheat.

- Planting and harvesting dates vary by region and plant hardiness zones.

	Planting Dates	Harvest Dates	Possible Rotation
Zone 3-4	Aug 20 - Sept 20	July 15 - Aug 25	Triticale > Soybean*
Zone 5	Sept 3 - Oct 15	June 15 - July 20	Corn > Triticale > Soybean *
Zone 6-7	Sept 10 – Oct 10	June 1 - July 15	Corn > Triticale > Soybean
Zone 8-9	Oct 5 – Dec 5	May 1 - July 5	Cotton > Triticale > Peanut

* May require an earlier harvest of Triticale or plant Soybean into standing Triticale

Equipment
- Chisel: Tractor 215 HP and Chisel Plow
- Disk: Tractor 215 HP and Tandem Disk
- Prepare Seedbed: Tractor 215 HP and Do-All
- Planting: Tractor 215 HP and Grain Drill
- Weed Control: SP Boom Sprayer

Equipment Continued
- Insecticide: SP Boom Sprayer
- Fertilize: Tractor 215 HP and Spreader
- Insect Control: SP Boom Sprayer
- Harvesting: Combine with Grain Head
- Haul: Tractor 215 HP with Grain Cart
- Haul: Semi Tractor/Trailer

Note: Equipment requirements follow that of conventional tillage, non-irrigated wheat production: http://economics.ag.utk.edu/budgets/2016/Crops/Wheat.pdf

References

- NASS, USDA. "Field Crops: Usual Planting and Harvesting Dates." *USDA National Agricultural Statistics Service, Agricultural Handbook* 628 (2010).
- Smith, S.A., B. Bowling, S.C. Danehower, D. Bilderback, D. Manning, H. Young-Kelly, A. McClure, L. Steckel, S. Stewart, E. Burns, R. Buntin, and J. Lannon. 2015. "Field Crop Budgets for 2016." University of Tennessee Extension Department of Agricultural and Resource Economics Publication AE 15-01

Figure 5. Information on Triticale

Winter Rye: Cereal Rye, (a.k.a. Winter Rye) holds significant promise as feedstock for cellulosic biofuels. Relative to other cover crop/double crop feedstocks, cereal rye has an extensive growing range, robust germination and establishment, frost tolerance and ability to accumulate large amounts of biomass during cool weather periods

- Planting and harvesting dates vary by region and plant hardiness zones.

	Planting Dates	Harvest Dates	Possible Rotation
Zone 3-4	Aug 15 - Sept 10	July 10 - Aug 20	Winter Rye > Soybean*
Zone 5	Aug 30 - Sept 26	June 30 - July 30	Corn > Winter Rye > Soybean*
Zone 6-7	Sept 3 - Oct 15	June 3 - July 2	Corn > Winter Rye > Soybean
Zone 8-9	Sept 20 - Nov 10	May 10 - June 20	Cotton > Winter Rye > Peanut

* Soybean planted into Rye by early June

Equipment
- Chisel: Tractor 215 HP and Chisel Plow
- Disk: Tractor 215 HP and Tandem Disk
- Prepare Seedbed: Tractor 215 HP and Do-All
- Planting: Tractor 215 HP and Grain Drill
- Weed Control: SP Boom Sprayer

Equipment Continued
- Insecticide: SP Boom Sprayer
- Fertilize: Tractor 215 HP and Spreader
- Insect Control: SP Boom Sprayer
- Harvesting: Combine with Grain Head
- Haul: Tractor 215 HP with Grain Cart
- Haul: Semi Tractor/Trailer

Note: Equipment requirements follow that of conventional tillage, non-irrigated wheat production: http://economics.ag.utk.edu/budgets/2016/Crops/Wheat.pdf

References

- North Dakota – Cover Crops Report 2015-2016. http://www.mccc.msu.edu/meetings/2016/2015%20State%20reports/2015%20MCCC%20report%20for%20North%20Dakota.pdf
- NASS, USDA. "Field Crops: Usual Planting and Harvesting Dates." *USDA National Agricultural Statistics Service, Agricultural Handbook* 628 (1997).

Figure 6. Infromation on Winter Rye

- Oilseed radish is of the Brassicaceae family, the mustard family of flowering plants. The family includes many plants of economic importance such as those of the genus Brassica, including cabbage, broccoli, kale, turnips, horseradish, radish, white mustard and others (EOE Brittanica 2015).
- Oilseed radish is composed of a taproot and several stemmed leafs which flower and produce oilseeds. The taproot can grow to 2 inches in diameter and up to 1 foot in length. This large taproot can break up and aerate the soil, alleviating soil compaction, which is why it is sometimes referred to as tillage radish (Weil, White, & Lawley, 2006).

Management:

- Oilseed radish establishes quickly and management is minimal. Seed harvest should be done when pods turn from green to yellow/brown. Seedpods do not readily shatter and require mechanical separation using stationary threshers with rollers to remove chaffy material (Novazio, 2007). However, large scale seed harvest is difficult. Using a combine to harvest seeds requires custom attachments (Jacobs, 2012b).

Region of Growth:

- Temperatures below 20 degrees F will damage or terminate the plant. Therefore, cover/feedstock production may be limited to regions with mild winters. The Mid-Atlantic and Southeast regions are likely to be suitable areas for growth as a feedstock (Weil et al 2006 & Chammoun 2013).

Potential as Feedstock

- Prior research has examined the potential of oilseed radish as a biodiesel feedstock. Extracted oil was converted to a fatty acid methyl ester (biodiesel) via transesterification.
- Chammoun, Geller, and Das (2013), find oilseed radish to have an oil yield and fatty acid profile similar to rapeseed. The authors also find that biodiesel from oilseed radish meets ASTM limits. However, the cold filter plugging point (CFPP) is determined to be 6 degrees Celsius, which may limit its fuel use in colder environments.

Invasiveness Potential:

- Oilseed radish is a non-native species. It is coded as an introduced species to the Lower 48 and Alaska within the USDA-NCRS PLANTS database. However, it is widely distributed throughout North America.
- Oilseed radish has potential to become weedy and invasive, although there are no restrictions on its use as a cover crop (Jacobs, 2012b).
- We decided that there was to much that was unknown about the harvest equipment for the oilseed radish.

Estimated Cost of Production

Costs per Acre			
cover crop	operating costs	fixed costs*	total costs of production
Triticale	108.59	44.02	152.61
Winter Rye	160.57	55.66	216.23
Pennycress	67.47	18.24	85.71
Camelina	61.44	46.22	107.66
*Does not include land ownership costs			

Task 3

University of Tennessee

Objective(s)

Develop database on infrastructure and needs for Southeast.

Research Approach

Collect spatial datasets that exist and initiate a southeast regional analysis. The Forest Sustainable and Economic Analysis Model (ForSEAM) is a linear programming model can be used to estimate forestland production over time, and its capacity to produce not only traditional forest products but also products of woody biomass to meet energy feedstock demand. It

solves and reports the quantity and types of woody biomass that can be available as energy feedstock with respect to certain marginal costs at the 305 Crop Report District (CRD) level of United States. This model can be divided into three major sections including supply, demand, and sustainability. The supply component includes general timber production activities for 305 production regions or crop reporting districts (CRD). Each region has a set of production activities defined by the U.S. Forest Service. These production activities include saw timber, pulpwood, and energy feedstock (woody biomass). Two sources of energy feedstock were considered in the model: logging residue generated from saw timber and pulpwood harvest activities; removal of whole pulpwood and un-merchantable trees. Demand component is based on six U.S. Forest Service Scenarios with estimates developed by the U.S. Forest Products Module (USFPM). The sustainability component insures that harvest in each region does not exceed annual growth, that roads have been constructed and forest tracts are located within mile of the roads, and that current year forest attributes reflect previous year's conventional wood product harvests and woody biomass as energy feedstock removals. Dynamic tracking of forest growth is incorporated into the analysis.

Spatial Datasets Collected

We have spatial information on airports, pipelines, and forest product mills. We have information also on forest residues at the POLYSYS region level. The forest residue data were generated for the Billion Ton 16 study using ForSEAM. ForSEAM is a forest model that can estimate the potential supply of forest residues, and trees harvested for biomass once traditional products are harvested. ORNL has developed procedures to downscale the supply curves developed by ForSEAM at the POLYSYS region level. These data are downloadable from ORNL

Task 4

University of Tennessee

Objective(s)

Initiate aviation fuel supply chain study in the southeast

Research Approach

Develop feedstock layers of alternative dedicated crops and develop an analysis with VOLPE's assistance.

Develop feedstock layers that have supply curves imbedded for each county.

Initiated feedstock layer development. We have layers for the yield and cost layers for the following feedstocks:

1. Corn Stover
2. Wheat Straw
3. Sorghum Residue
4. Oat Residue
5. Barley Residue
6. Pennycress,
7. Cotton Seed,
8. Trees – Supply curves for small and medium diameter natural pine, planted pine, lowland hardwood, upland hardwood, and mixed, and
9. Wood Residue that are available as a result of traditional harvests.

Task 5

University of Tennessee

Objective(s)

Continue with sustainability work for both goals 1 and 4]

Research Approach

Develop modules for POLYSYS that estimates changes in erosion, develop modules for POLYSYS that estimates changes in erosion, sediment Delivery, chemical purchases, and N and P application. This will be an export analysis for now. POLYSYS results will be placed in ACCESS and used to estimate changes in the parameters mentioned above.

Methodology Developed
Access has been used to estimate the parameters. Programming has commenced so that the system will be automated. The pennycress solution will be the initial trial of the system and should be completed by April.

Milestone(s)
Pennycress has been evaluated as a feedstock and a manuscript is being written.

Major Accomplishments
The potential of three additional cover crops have been identified and analysis for these will begin in April.

Publications
None

Outreach Efforts
Evan Markel, Chad Hellwinckel, and Burton C. English, 2016. Project 1: Pennycress to Aviation Fuel: Its Potential Impact on U.S. Agriculture. Poster presented at the Sept 27-28 annual ASCENT meeting, Washington D.C.

Evan Markel, Burton C. English, R. Jamey Menard, 2016. Project 1: Pennycress to Aviation Fuel: Its Impact on U.S. Agriculture and the Nation's Economy, Poster presented at the October CAAFE annual meeting, Washington D.C.

Burton C. English, Lixia He-Lambert, Evan Markel, and Tim Rials, 2016. Feedstock, presented at the semi-annual ASCENT meeting, Seattle, WA., March.

Burton C. English, Evan Markel, Umama Rahman, and Chad Hellwinckel, 2016. Cover Crop Potential as a Feedstock for Aviation Fuel, Webinar Dec. 6, 2016

Burton C. English, Edward Yu, Dayton Lambert, and James Larson, 2016. Determination of the Environmental Impact of Growing Feedstock for Aviation Fuel, Webinar Dec. 12 2016.

Awards
None

Student Involvement
Evan Markel – Ph D student, developed the Pennycress work, leading effort on gathering information on other cover crops.
Umama Rahman -- Worked on Camalina information

Plans for Next Period
I plan on continuing to work on the 4 objectives or tasks. These tasks wil provide information on impacts to the ag sector and to the environment. I also will continue to estimate the impacts to the economy in terms of GDP and employment opportunities. Finally, a techno-economic analysis of the feedstocks will be initiated so that important factors are identified that might impact the economic sustainability of the feedstock.

Project 001(F) Alternative Jet Fuel Supply Chain Analysis

Massachusetts Institute of Technology

Project Lead Investigators

PI: Prof. Steven Barrett
Associate Professor of Aeronautics and Astronautics
Finmeccanica Career Development Professor of Engineering
Director, Laboratory for Aviation and the Environment
Massachusetts Institute of Technology
77 Massachusetts Ave, Building 33-322, Cambridge, MA 02139
+1 (617) 452-2550
sbarrett@mit.edu

Co-PI: Dr. Robert Malina
Research Scientist
Associate Director, Laboratory for Aviation and the Environment
Department of Aeronautics and Astronautics
Massachusetts Institute of Technology
rmalina@mit.edu

University Participants

Massachusetts Institute of Technology

- P.I.: Professor Steven Barrett; Co-PI: Dr. Robert Malina
- FAA Award Number: 13-C-AJFE-MIT, Amendment No. 003, 012, 016, and 028
- Period of Performance: August 1, 2014 to August 31, 2017 (reporting here with the exception of FAA funding and cost share for October 1, 2015 to September 30, 2016)
- Task(s):
    1. Economic and environmental feasibility of alternative jet fuels derived from municipal solid waste (MSW)
    2. Future lifecycle GHG emissions from alternative jet fuel
    3. 2050 alternative jet fuel production potential and associated GHG emissions reductions
    4. LCA methodology development and default value calculation for ICAO global market-based measure
    5. Support of the US FAA at ICAO AFTF on development of sustainability criteria for alternative jet fuels and policy and feasibility assessment of ICAO climate change goals, including in person support at meetings of ICAO CAEP AFTF
    6. Long-term production and GHG emissions' reduction potential of alternative jet fuel in the US
    7. Economic and environmental assessment of alternative jet fuels accounting for the potential for technology maturation

Project Funding Level

$1,185,000 FAA funding and $1,185,000 matching funds. Sources of match are approximately $226,000 from MIT, plus 3rd party in-kind contributions of $326,000 from Byogy Renewables, Inc. and $633,000 from Oliver Wyman Group.

Investigation Team

Principal Investigator: Prof. Steven Barrett (MIT)
Co-Principal Investigator: Dr. Robert Malina (formerly MIT, now Hasselt University)
Co-Investigator: Dr. Raymond Speth (MIT)
Graduate Students: Mark Staples, Pooja Suresh, Cassandra Rosen, Timothy Galligan

Project Overview

The overall objectives for ASCENT Project 1 funding provided to MIT for the reporting period 10/1/2015 to 9/30/2016 are to derive information on regional supply chains to create scenarios for future alternative jet fuel production, identify the key supply chain-related obstacles that must be overcome to produce 1 billion gallons of alternative jet fuel by 2018, and to achieve an order of magnitude larger production in the longer term.
Following these overall objectives, the MIT's work on ASCENT Project 1 during AY 2015/2016, as defined in the ASCENT 2015-1 Grant Proposal Narrative, is focused on: developing long-run scenarios for future alternative jet fuel production and the associated savings in greenhouse gas (GHG) emissions attributable to global aviation for use at the International Civil Aviation Organization (ICAO); supporting the FAA in the development of a methodology for lifecycle CO_2 emissions of alternative jet fuels for use in the market based measures scheme currently under discussion at ICAO, and estimating the costs of producing alternative jet fuel using municipal solid waste (MSW) as a feedstock.

For AY 2016/2017, MIT's work under ASCENT Project 1 is defined in the ASCENT 2016-1 Grant Proposal Narrative as focusing on: supporting US participation in ICAO-CAEP AFTF to develop a methodology for the appropriate accounting of alternative fuels life cycle greenhouse gas (GHG) emissions in a global market-based measure; support FAA assessment of policy options for alternative jet fuels in the context of AFTF; build upon and extend previous work to estimate the economic production costs and lifecycle GHG benefits of alternative jet fuel production from MSW; assess the long-term potential for alternative jet fuel production in the US; and explore the time- and path-dependent characteristics of alternative jet fuel technologies, including the effects of learning-by-doing on production costs and environmental performance.

In order to capture work that occurred during the reporting period of this report (10/1/2015 to 9/30/2016) and overlaps with both funding periods, MIT's work under ASCENT 1 is described here under 7 categories:

1. AY 2015/2016 Task 1 & AY 2016/2017 Task 3 – Economic and environmental feasibility of alternative jet fuels derived from municipal solid waste (MSW);

2. AY 2015/2016 Task 2 – Future lifecycle GHG emissions from alternative jet fuel;

3. AY 2015/2016 Task 3 – 2050 alternative jet fuel production potential and associated GHG emissions reductions;

4. AY 2015/2016 Task 4 & AY 2016/2017 Task 1 - LCA methodology development and default value calculation for ICAO global market-based measure;

5. AY 2015/2016 Task 5 & AY 2016/2017 Tasks 2 and 6 – Support of the US FAA at ICAO AFTF on development of sustainability criteria for alternative jet fuels and policy and feasibility assessment of ICAO climate change goals, including in person support at meetings of ICAO CAEP AFTF;

6. AY 2016/2017 Task 4 - Long-term production and GHG emissions' reduction potential of alternative jet fuel in the US;

7. AY 2016/2017 Task 5 - Economic and environmental assessment of alternative jet fuels accounting for the potential for technology maturation

Because 11 of the 12 months of the reporting period correspond to AY 2015/2016, the bulk of this annual report focuses on work accomplished during that time. The plan to accomplish the tasks under ASCENT 1 for AY 2016/2017 is also summarized.

AY 2015/2016 Task 1 & AY 2016/2017 Task 3 – Economic and environmental feasibility of alternative jet fuels derived from municipal solid waste (MSW)

Massachusetts Institute of Technology

Objective(s)

For AY 2015/2016 Task 1, the objective of the funded work is to use material and energy balances for MSW-to-jet fuel production technologies in order to build a techno-economic model based on discounted cash flow rate of return (DCFROR) analysis. The model will be used to estimate the production costs and calculate minimum selling price (MSP) of MSW-derived jet fuels, as described more fully in Suresh (2016). Work during AY 2016/2017 for Task 3 builds on this and other work in order to assess the economic and environmental feasibility of MSW-to-jet production for additional conversion technologies and locations of fuel production.

Research Approach

Note that the economic assessment of MSW-to-jet fuel production technologies described here is a summary of the work contained in Suresh (2016).

Introduction

The economics of using MSW as an alternative jet fuel feedstock are potentially favorable as municipalities currently pay to dispose of MSW in landfills. This translates to a negative feedstock cost or source of revenue for MSW-derived jet fuels and may (partially) offset higher fuel production costs. Additionally, waste management infrastructure for collection and sorting of MSW already exists and can be utilized, reducing the net production costs.

At present, MSW-derived jet fuels have not been produced at an industrial scale because significant challenges remain to be resolved, primarily the heterogeneity of the feedstock (requiring expensive pretreatment) and the lack of maturity of the conversion technologies (low efficiency and yields). As a result of these remaining challenges, it is not yet known empirically how these technologies will develop and perform commercially. Therefore, this work considers three MSW-to-fuel conversion pathways that are better suited to the heterogeneity of MSW and currently show the most commercial promise: 1) conventional/plasma gasification followed by Fischer-Tropsch, 2) conventional/plasma gasification followed by catalytic synthesis and alcohol-to-jet, and 3) conventional/plasma gasification followed by gas fermentation and alcohol-to-jet. A sensitivity analysis is carried out using Monte Carlo simulations on the MSP results in order to quantify the effect of various economic assumptions and critical input parameters, such as feedstock composition, feedstock cost and feedstock-to-fuel conversion efficiency.

In AY 2016/2017, the resulting stochastic techno-economic model, as well as modeling tools developed in year 1 of ASCENT funding, are being used to assess the economic and environmental feasibility of additional MSW-to-jet conversion technologies and locations.

Methods

In order to calculate MSW-to-jet MSP, facility capital cost estimates are obtained from the literature for each pathway (Niziolek et al. 2015, Jones et al. 2009, Motycka 2013) and, in some cases, estimates are supplemented with additional capital costs of the processes that are not modeled in the particular studies. The additional capital costs for upgrading naphtha to gasoline are estimated from Niziolek et al (2015). The capital costs of the dehydration, oligomerization and hydroprocessing equipment necessary to convert ethanol to MD fuel are estimated from Staples et al (2014). Variable operating costs and sales revenues are calculated from the prices of gasoline, jet fuel, diesel, electric power and natural gas, and are based on historical and projected data. Fixed operating costs are estimated as a function of capital expenses. Insurance, local taxes, maintenance and contingency costs are estimated using heuristics from the petroleum refining industry from Gary et al (2007).

A stochastic assessment of MSP is carried out using Monte Carlo simulations, wherein parameters are randomly sampled from their probability distributions for 10,000 iterations of the model calculations. This translates the uncertainty in the input parameters to uncertainty in the results. Parameter uncertainty in this study stems primarily from data limitations. Uniform distributions are assigned when available data are considered equally likely. When data is available to estimate minimum and maximum bounds, as well as a most likely value, triangular or pert distributions are assigned. A second type of parameter uncertainty in this analysis is statistical uncertainty associated with availability of a large number of data samples, for example, availability of historical data for commodity prices. In this case, the uncertainty distributions are dictated by the samples, based on best fit using the Anderson-Darling test (Stephens 1974).

The uncertainty associated with the conversion efficiency of the pathway is captured by assigning probability distributions to the overall fuel yield (including MD fuels, gasoline and higher alcohols). The capital cost estimates from literature used for this analysis are based on empirical data or chemical engineering models that apply equipment factor estimates and cost all major equipment individually. The error associated with these estimates is typically assumed to be ±20% (Gary et al. 2007).

This work also applies Geometric Brownian motion (GBM) to capture uncertainty in fuel and energy prices. A normal distribution is fitted to the year-to-year price variations of the past 20 years from 1996 to 2015. This distribution is randomly sampled from in order to predict price deviations in future years.

Results

The median MSP results are 0.99, 1.78 and 1.20 $ per liter for FT, Plasma FT and ATJ MD fuels, respectively. Parameter uncertainty results in ranges of values that 95% of the Monte Carlo simulation results lie within: 0.72 – 1.28, 1.24 – 2.39 and 0.68 – 1.75 $ per liter for FT, Plasma FT, and ATJ MD fuels, respectively. These results, even at the lower bound, are above the approximate current US price of conventional middle distillate fuel of 0.50 $ per liter. The probability of achieving positive NPV for the project is calculated from the NPV results to be 14%, 0.1% and 7% for FT, Plasma FT, and ATJ MD fuels, respectively.

Capital costs and fixed operating expenses, which are a function of the capital costs, are the major cost contributors for all three pathways, making up 70-75% of total expenses. The net capital costs are highest for the Plasma FT MD pathway and the lowest for the ATJ MD pathway but when normalized to the MD fuel yield, the FT MD pathway has the lowest median capital cost per liter of $0.89/L.

The variable operating expenses attributable to water, catalysts, cleaning chemicals and disposal of wastes are only 2-3% of MSP for all three pathways. Comparison of the results indicates that revenues from the sale of gasoline, and of scrap metals and glass, vary among the three pathways due to technology-specific differences in conversion process product slates and plant feed capacities. The Plasma FT and ATJ MD pathways have higher co-product revenues from higher export of excess electricity and sale of higher alcohols. Non-energy co-products such as slag and construction aggregates contribute less than 3% to reducing the overall cost.

The majority of variance in the NPV results arises from uncertainty associated with fuel prices. Since the fuel yields are higher for the FT MD pathway, the total variance and standard deviation are also greater than that of the other two pathways. On the other hand, the MSP of the FT MD pathway has the lowest standard deviation (0.14 $/L) of the three pathways because calculation of the MSP divides the net costs over the fuel yield, thereby resulting in an inverse relationship.

The ATJ MD pathway has the least negative median NPV because the relative reduction of net capital costs outweighs other costs compared to the other two pathways. However, to achieve a positive NPV, the ATJ MD pathway requires a higher selling price for the fuel than the FT MD pathway, because the lower fuel yield implies that each unit of fuel needs to be sold at a higher price.

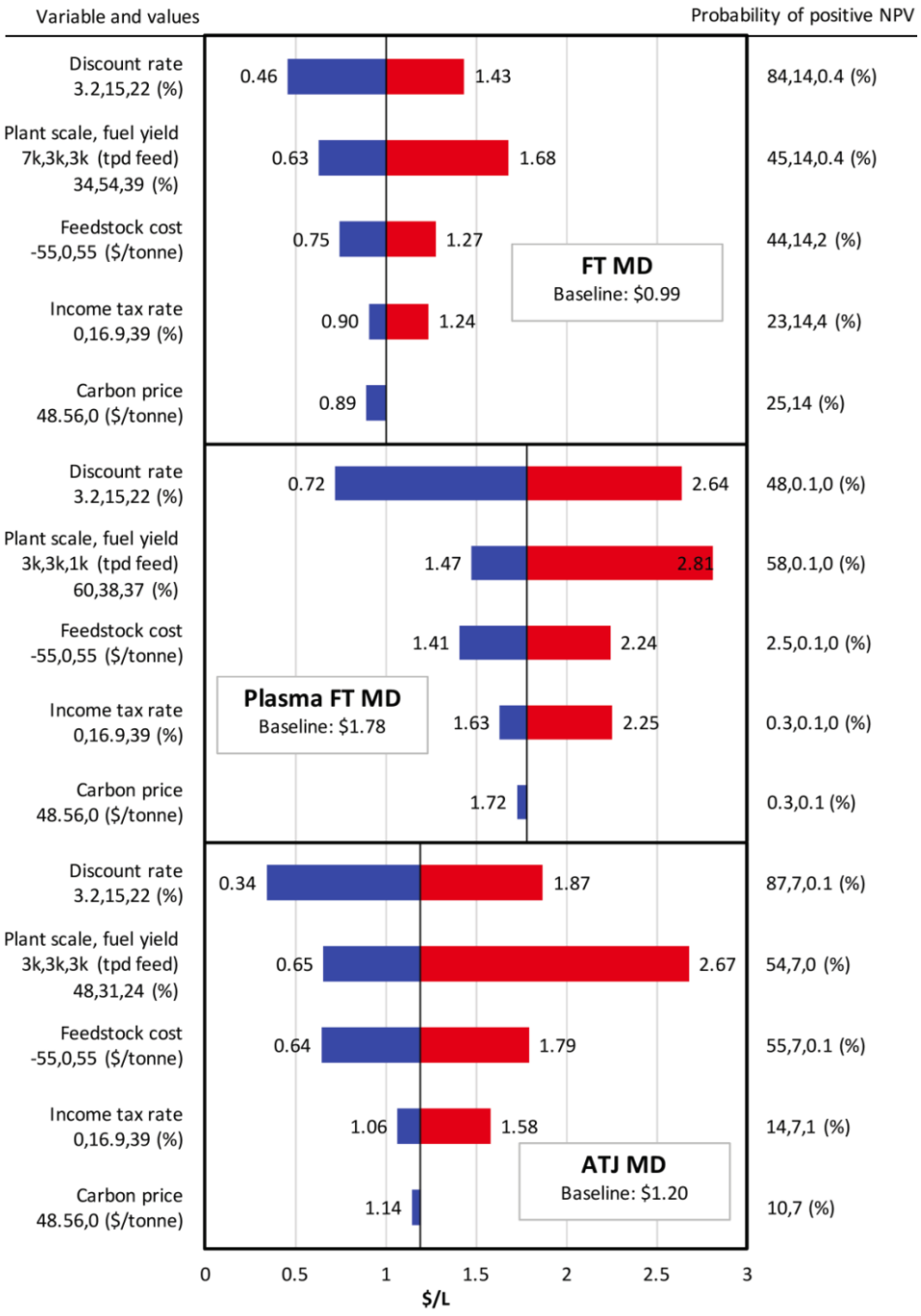

Figure 1: MSP sensitivity analysis showing the resultant median values. The variables and assumptions are listed on the left axis (low, baseline, high). On the right axis, the probability of positive NPV associated with each case (low, baseline, high) is listed.

Figure 1 presents the results of the sensitivity analysis for the MSP and NPV in terms of discount rate, income tax rate, feedstock cost, plant scale and associated technology parameters, and carbon pricing as an example of a policy driver. The discount rate, which is dictated by the rate of required return for equity and loan interest rate for debt, has the greatest impact on the results. At larger feed input capacities, economies of scale are achieved for the conversion technologies. At

the same feed capacity and level of capital investment, improvements in fuel yield increase the probability of positive NPV to greater than 50%. In the case of the FT MD pathway, at the same feed capacity, lower fuel yield (39%) and 8% higher capital costs than the baseline results in a decrease of the probability of positive NPV to 0.4%.

In order to quantify the impact of feedstock cost, 2013 US average landfill tipping fees are used [6]. In the discount rate and feedstock cost cases, the ATJ MD pathway demonstrates the lowest median MSPs ($0.34/L, $0.64/L) and highest probability of positive NPV (87%, 55%) compared to the other two pathways. Figure 1 also presents the results of implementing a carbon price of $48.56 (2014 dollars) based on the revised social cost of carbon guidance provided by the US Interagency Working Group on Social Cost of Carbon (2013).

Milestone(s)

This work was completed in May 2016, and is contained in Pooja Suresh's 2016 Master's thesis submitted to MIT. The thesis is also available as a lab report on the website of the Laboratory for Aviation and the Environment at MIT.

Major Accomplishments

During this period, the MSP of MSW-to-jet fuel production technologies, and the NPV of projects using these technologies, were estimated. A summary of the work is contained in Suresh (2016), and the models used to perform this analysis were documented such that they can be used in subsequent projects under ASCENT 1.

Publications

Peer-reviewed journal publications

P. Suresh, R. Malina, M. D. Staples, D. Blazy, M. N. Pearlson, S. R. H. Barrett "Lifecycle greenhouse gas emissions and costs of production of diesel and jet fuel from municipal solid waste," (*in preparation)*

Written reports

P. Suresh, "Environmental and economic assessment of transportation fuels from municipal solid waste," Master of Science thesis, Department of Aeronautics and Astronautics, Massachusetts Institute of Technology, 2016. Available online: http://lae.mit.edu/uploads/LAE_report_series/2016/LAE-2016-002-T.pdf

Outreach Efforts

None.

Awards

None.

Student Involvement

Pooja Suresh, Masters student at MIT's Department of Aeronautics and Astronautics, carried out the majority of this analysis, as it constituted her masters thesis. She graduated in June 2016, and now works at Boston Consulting Group in Toronto, Canada.

Mark Staples, PhD student at MIT's Institute for Data, Systems and Society, also assisted with this work. Mark finished his PhD at MIT in December, 2016.

Plans for Next Period

During AY 2016/2017, the economic and environmental feasibility of alternative jet fuels derived from MSW will be assessed for additional conversion technologies, as well as additional locations. This work will be carried out at Hasselt University under the leadership of Professor Robert Malina.

Work in year 1 and year 2 (as described here) of this project has led to the development of models to quantify the US-average costs of production and lifecycle GHG emissions of several thermochemical pathways for MSW conversion into liquid transportation fuels, accounting for parameter uncertainty through a Monte-Carlo Framework. In the current year,

the existing model is being extended to account for biochemical pathways that are currently in the process of being commercialized. Candidate pathways include:

- Hydrolysis and fermentation to alcohols, followed by alcohol to jet fuel conversion
- Gasification and gas fermentation to alcohols, followed by alcohol to jet fuel conversion
- Anaerobic digestion to biogas, followed by steam reforming and Fischer Tropsch or catalytic synthesis to jet fuel

This ongoing work uses the existing modeling capabilities for the gasification, alcohol-to-jet conversion, Fischer-Tropsch and catalytic synthesis steps, and will incorporate additional modules for hydrolysis, fermentation, anaerobic digestion and steam reforming. Since these pathways use only the biogenic proportion of MSW, they could be environmentally advantageous as they convert only the carbon proportion, which would have been released as methane in landfills, to biogenic carbon dioxide at the end of the life cycle. Biochemical processes also tend to be less capital-intensive but they require more feedstock pretreatment and have lower conversion yields. Though there is some existing literature on MSW-to-ethanol and MSW-to-energy biochemical pathways, a large research gap remains to be bridged in the area of evaluating the environmental and economic performance of MSW-to-jet biochemical pathways.

The model is currently tailored to calculate costs of production and GHG emissions as a US-average. However, the model is now being augmented to account for spatial variation, both within the United States, and for non-US locations. In terms of non-US analyses, a case-study on the economic and environmental viability of MSW to jet fuel production in Indonesia will be conducted. This work would also entail training Indonesian researchers in the use of life cycle emissions and economic modeling to help build modeling capacities in Indonesia, if requested by FAA. By doing so we will support FAA in its agreement with the Indonesian Directorate General of Civil Aviation (DGCA) to promote developing and using sustainable alternative aviation fuels.

J. H. Gary, G. E. Handwerk, and M. J. Kaiser, Petroleum Refining: Technology and Economics, 5 ed., Basel, Switzerland: Taylor & Francis, 2007.

S. B. Jones, Y. Zhu, and C. Valkenburg, "Municipal Solid Waste (MSW) to Liquid Fuels Synthesis, Volume 2: A Techno-economic Evaluation of the Production of Mixed Alcohols," Pacific Northwest National Laboratory PNNL-18482, 2009.

S. A. Motycka, "Techno Economic Analysis Of A Plasma Gasification Biomass To Liquids Plant " Doctor of Philosophy thesis, School of Engineering and Applied Sciences, George Washington University, 2013.

A. M. Niziolek, O. Onel, M. M. F. Hasan, and C. A. Floudas, "Municipal solid waste to liquid transportation fuels – Part II: Process synthesis and global optimization strategies," Computers & Chemical Engineering, vol. 74, pp. 184-203, 2015.

M. D. Staples, R. Malina, H. Olcay, M. N. Pearlson, J. I. Hileman, A. Boies, et al., "Lifecycle greenhouse gas footprint and minimum selling price of renewable diesel and jet fuel from fermentation and advanced fermentation production technologies," Energy & Environmental Science, vol. 7, p. 1545, 2014.

M. A. Stephens, "EDF Statistics for Goodness of Fit and Some Comparisons," Journal of the American Statistical Association, vol. 69, pp. 730-737, 1974.

P. Suresh, “Environmental and economic assessment of transportation fuels from municipal solid waste,” Master of Science thesis, Department of Aeronautics and Astronautics, Massachusetts Institute of Technology, 2016.

AY 2015/2016 Task 2 – Future lifecycle GHG emissions from alternative jet fuel

Massachusetts Institute of Technology

Objective(s)

In this task, lifecycle emissions studies for different alternative jet fuel production technologies were adjusted to year 2050 by, *inter alia*, using assumptions about efficiency improvements for different conversion pathways and by forecasting the GHG footprints of input requirements to 2050. The purpose of this analysis is to inform the ICAO CAEP AFTF decision-making process, by quantifying the potential for GHG emissions savings per unit of alternative jet fuel used in future years.

Research Approach

Introduction

In order to assess the range of potential GHG emissions from reductions from the use of alternative fuels in aviation to 2050, the ICAO CAEP AFTF agreed to 1) develop and use ranges for lifecycle GHG emissions for different types of alternative jet fuels, and 2) assess the potential availability of those fuels in the short- and long-run, where long-run is defined at 2050.

In order to carry out this work MIT developed a methodology to augment existing LCA studies to 2050, and to quantify the effects on the GHG emission intensity of these technology options for producing alternative jet fuels. The studies covered include a variety of feedstock (oily, starchy, sugary and lignocellulosic crops, crop and forestry residues, waste oils, microalgae and municipal solid waste) and three different feedstock-to-fuel conversion technologies: Hydroprocessed Esters and Fatty Acids (HEFA), Fischer-Tropsch (FT) and Advanced Fermentation (AF).

Methods

In order to capture the potential range of LCA values in 2050, low, baseline and high scenarios are defined for the major parameters considered. The parameters values that are identified that could change in future years and have an appreciable impact on lifecycle GHG emission, include:

- Agricultural productivity in terms of yield improvements, associated nutrient application rates and farming energy estimates
- Process efficiencies for both the pre-processing step (if any) and the fuel production process
- Emission factors of electricity and hydrogen energy inputs

Other lifecycle inputs and parameters such as transportation emission factors, herbicide/pesticide and other chemical inputs were found to have negligible impact on pathway GHG intensities overtime. Therefore, these parameters are not adjusted to 2050. The methodology uses energy allocation for allocating emissions among all co-products, including energy products, animal meals, chemicals, liquid fuel products and electricity at the process level and along the conversion process. This is consistent with AFTF's agreed upon LCA methodology. The LCA results include only the core lifecycle greenhouse gas emissions (CO_2, N_2O and CH_4 emissions in terms of gCO_2e/MJ_{fuel}). The results do not include land-use change.

The parameters listed above are varied for the existing LCA study scope described in Table 1, and 2050 results are generated by updating the models used for those studies.

Table 1: Feedstock, technology and geographical scope

Feedstock group	Feedstock	Technology	Geographical Scope	Analysis Year	MIT References
Vegetable oily crops	Soybean	HEFA	US	2015	Stratton et al. (2010)
	Rapeseed		UK, France/US		
	Oil palm fruit		Malaysia/US		
	Jatropha		India/US		
Starchy crops	Maize	AF	US	2014	Staples et al. (2014)
Sugary crops	Sugarcane		Brazil	2014	
Lignocellulosic energy crops	Switchgrass		US	2014	
		FT		2015	Stratton et al. (2010)
Energy, food crop and forestry residues	Corn stover		US	2015	
	Forest residue		US	2015	
Other	Tallow	HEFA	US	2012	Seber et al. (2014)
	Yellow grease			2012	
	Microalgae			2010	Carter (2012)
	MSW	FT		2016	Suresh (2016)

The GHG emissions attributable to the cultivation step in the lifecycle depend on nutrient use and cultivation energy, which are both a function of agricultural yields in future years. Therefore, projections of future agricultural yields are combined with projections of nutrient application rates and cultivation energy to 2050. An example of agricultural yield projections for soybean oil, from the Global Agro-ecological Zones model and United Nations FAOSTAT data, is given in Figure 2.

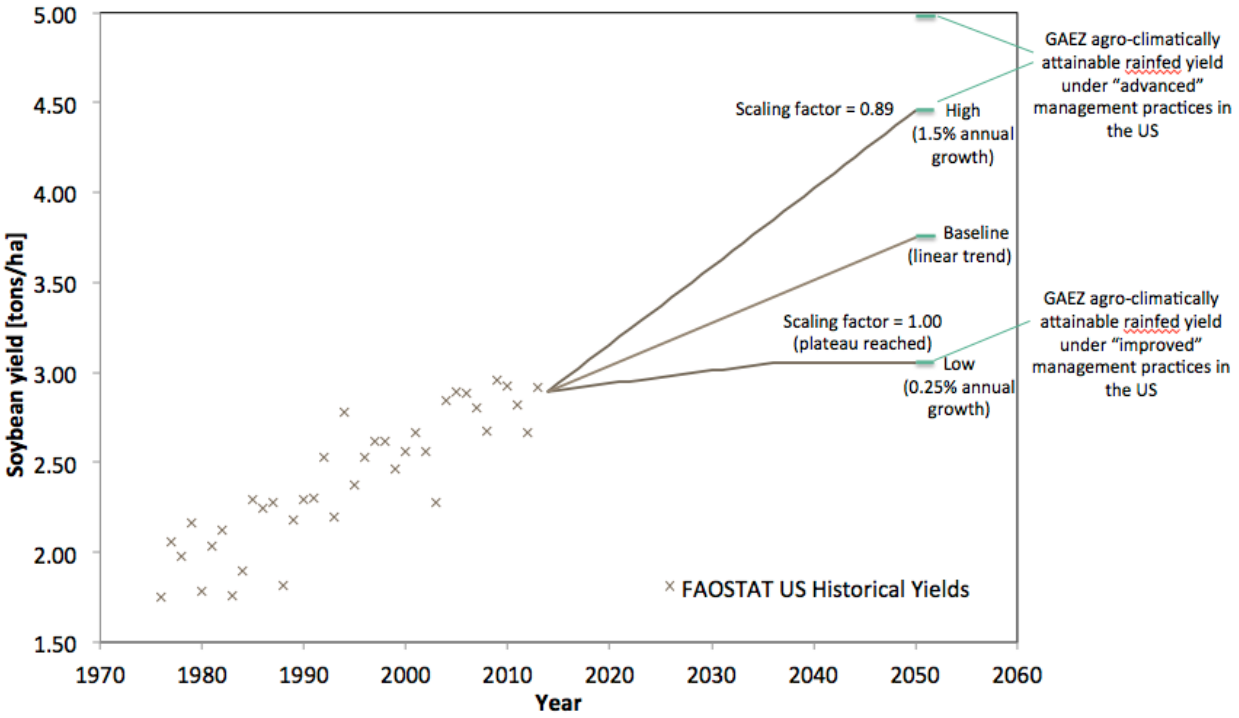

Figure 2: Historical and projected soybean yield in the US

Improvements in the lifecycle GHG emissions of alternative jet fuels could also potentially come from improvements in feedstock-to-fuel conversion efficiency. Therefore, this potential contribution to reductions in lifecycle GHG emissions is estimated by modeling the most efficient fuel production process described in the engineering literature. The references used to generate these results are given in Table 2.

Table 2: Feedstock-to-fuel conversion efficiency projections for 2050

Pathway	2050 feed to jet conversion efficiency	Improvement from existing baseline	Units	Key references
Soybean HEFA	21.79	0%	MJ jet/kg oil	Pearlson et al. (2013)
Rapeseed HEFA	21.79	0%	MJ jet/kg oil	
Jatropha HEFA	21.79	0%	MJ jet/kg oil	
Oil palm HEFA	21.79	0%	MJ jet/kg oil	
Tallow HEFA	21.79	0%	MJ jet/kg oil	
Yellow grease HEFA	21.79	0%	MJ jet/kg oil	
Microalgae HEFA	21.79	0%	MJ jet/kg oil	
Switchgrass FT	13.00	4%	% MJ jet/MJ biomass	Stratton et al. (2010)
Corn stover FT	13.00	4%	% MJ jet/MJ biomass	
Forest residue FT	13.00	4%	% MJ jet/MJ biomass	
MSW FT	14.80	NA	% MJ jet/MJ MSW	Niziolek et al. (2015)
Switchgrass AF	8.21	40%	MJ jet/kg dry biomass	Staples et al. (2014)
Maize AF	9.96	25%	MJ jet/kg grain (15.5% mst)	
Sugarcane AF	2.88	34%	MJ jet/kg sugarcane (50% mst)	

Finally, the results for 2050 also account for potential reductions in the emissions factors of electricity and hydrogen required for fuel production. The key references and resulting emissions factors are given in Table 3.

Table 3: 2050 projections for the emission factors of electricity and hydrogen

Energy inputs	Emission factors (gCO_2e/MJ)				Key references
	Current	2050 Low	2050 Baseline	2050 High	
US grid electricity mix	174.36	25.86	112.03	159.41	ETP (2014)
Brazil grid electricity mix	20.84	10.66	26.93	50.83	ETP (2014)
North American hydrogen mix	94.53	26.69	35.90	94.53	WETO – H_2 (2006) and ANL (2005)

Results

The methodology described above was implemented to calculated three 2050 lifecycle GHG values for the alternative jet fuel pathways of interest, and these results are shown in tabular format in Table 4, and graphical format in Figure 3.

Table 4: Final 2050 LCA projections for low, baseline and high scenarios

Feedstock group	Pathway	Current lifecycle GHG emissions (gCO_2e/MJ_{fuel})	2050 lifecycle GHG emissions projections (gCO_2e/MJ_{fuel})			Difference between the current and 2050 baseline values
			Low	Baseline	High	
Oily crops	Soybean HEFA	42.15	24.53	29.56	39.61	-29.9%
	Rapeseed HEFA	58.34	34.87	39.38	53.29	-32.5%
	Oil palm HEFA	39.09	21.92	26.08	35.93	-33.3%
	Jatropha HEFA	58.27	40.24	47.18	58.61	-19.0%
Starchy crops	Maize AF	52.20	21.30	27.80	31.30	-46.7%
Sugary crops	Sugarcane AF	10.70	3.50	3.80	4.20	-64.5%
Lignocellulosic energy crops	Switchgrass AF	37.40	12.80	18.40	25.90	-50.8%
	Switchgrass FT	19.38	9.81	16.34	24.95	-15.7%
Energy, food crop and forestry residues	Corn stover FT	13.82	10.89	12.00	17.49	-13.2%
	Forest residue FT	7.71	6.92	7.16	7.40	-7.1%
Other	Tallow HEFA	29.80	11.19	16.54	25.84	-44.5%
	Yellow grease HEFA	19.40	6.69	8.47	16.48	-56.3%
	Microalgae HEFA	68.08	11.07	27.00	39.78	-60.3%
	MSW FT	27.63	32.89	38.16	43.42	38.1%

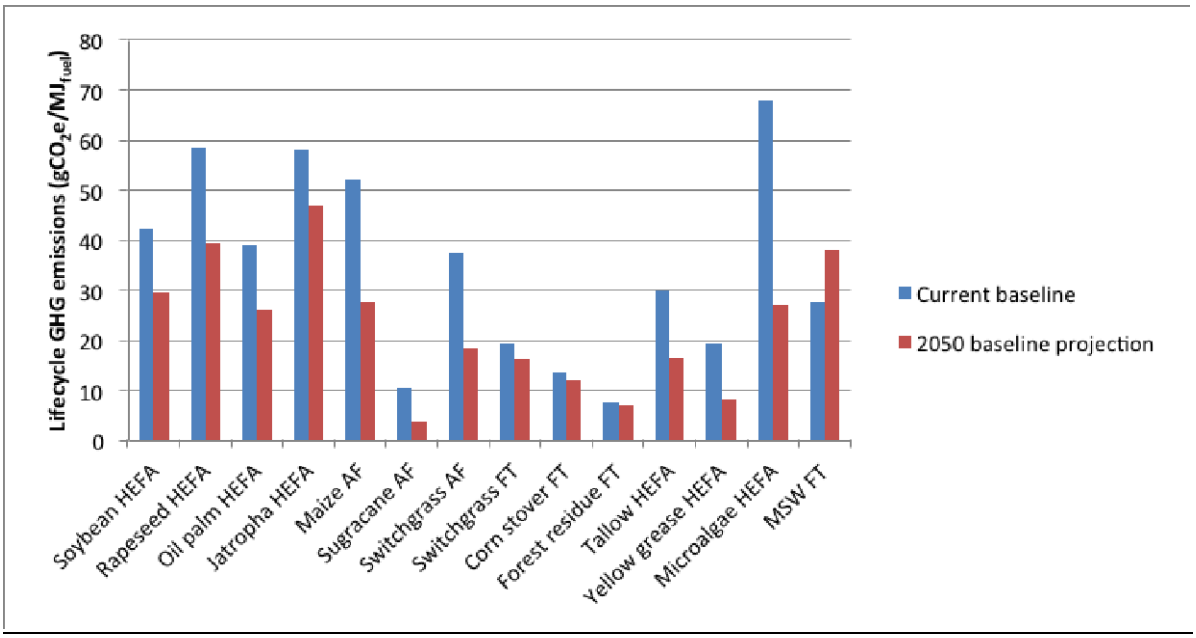

Figure 3: Final 2050 baseline LCA projections compared to the current baseline LCA values

The primary conclusions from this analysis are summarized by the following points:

- Adjustment of agricultural yields, nutrient application rates, and cultivation energy inputs to 2050 produces variations or approximately 2% for most of the crops studied. Maize, rapeseed and oil palm are the exceptions to this finding, with variations of 4 to 6 gCO_2e/MJ_{fuel} (~10%)
- In most of the cases investigated, adjusting the farming energy inputs only changed the LCA results by less than 4%.
- The greatest difference in LCA results is observed for the AF pathways, leading to reductions in LCA emissions of 6 to 20 gCO_2e/MJ_{fuel}
- Adjusting electricity emissions factors results in variations of 2-4% for all of the pathways except for those with high electricity requirements, such as maize AF, and tallow and microalgae HEFA.
- The impact of adjusting the hydrogen emission factor is significant, leading to reductions of 7-8 gCO_2e/MJ_{fuel} for the HEFA pathways.

Milestone(s)

This work began in the summer of 2015, and was completed in early October 2015. This compressed timeline was required in order to present the findings of this analysis to AFTF in the face-to-face meeting in Montreal.

Major Accomplishments

The major accomplishment of this work was to complete the analysis, have it reviewed and accepted by AFTF in October 2015, and then to use the resulting data in order to calculate the potential contribution of alternative jet fuels to GHG emissions reductions.

Publications

This work is carried out in support of an international negotiation. As such, the methodology and results have not be published in scientific journals or presented at conferences, in order to respect the sensitive nature of the negotiation. The

major publication associated with MIT's work on this project is the information paper (IP) presented to AFTF, and ultimately to CAEP in CAEP/10-IP/13 and CAEP/10-IP/14.

Outreach Efforts

This work was presented to other members of AFTF in teleconferences leading up to the October 2015 meeting of the group in Montreal, as well as in person to the member of AFTF at that meeting.

Awards

None.

Student Involvement

Pooja Suresh, Masters student at MIT's Department of Aeronautics and Astronautics, carried out the majority of this analysis, as it constituted her masters thesis. She graduated in June 2016, and now works at Boston Consulting Group in Toronto, Canada.

Mark Staples, PhD student at MIT's Institute for Data, Systems and Society, also assisted with this work. Mark finished his PhD at MIT in December 2016.

Plans for Next Period

There is no plan for this specific task in the next period. The data that was generated has been used for its purpose. If an updated assessment of how alternative jet fuel LCA values might change in future years is required in the context of AFTF or ICAO CAEP, this analysis could be used as a starting point.

References

Carter, N.A. (2012). Environmental and economic assessment of microalgae-derived jet fuel. Massachusetts Institute of Technology.

FAOSTAT historical yields (accessed 2015), Production quantities by country and crop 1993-2013, Food and Agriculture Organization of the United Nations Statistics Division.

GAEZ v3.0 Global Agro-ecological Zones (accessed 2015), IIASA, Laxenburg, Austria and Rome, Italy.

A. M. Niziolek, O. Onel, M. M. F. Hasan, and C. A. Floudas, "Municipal solid waste to liquid transportation fuels – Part II: Process synthesis and global optimization strategies," Computers & Chemical Engineering, vol. 74, pp. 184-203, 2015.

Pearlson, M., Wollersheim, C. & Hileman, J. (2013). A techno-economic review of hydroprocessed renewable esters and fatty acids for jet fuel production. Biofuels, Bioproducts and Biorefining 7 (1), pp.89-96.

Seber, G; Malina, R; Pearlson, M; Olcay, H; Hileman, J; Barrett, S. Environmental and economic assessment of producing hydroprocessed jet and diesel fuel from waste oils and tallow, Biomass and Bioenergy Vol. 67 (2014).

Staples, M; Malina, R; Olcay, H; Pearlson, M; Hileman, J; Boies, A; Barrett, S. Lifecycle Greenhouse Gas Footprint and Minimum Selling Price of Renewable Diesel and Jet Fuel from Fermentation and Advanced Fermentation Production Technologies, Energy and Environmental Science, 7, 1545 (2014).

Stratton, R; Wong, H; Hileman, J. Life Cycle Greenhouse Gas Emissions from Alternative Jet Fuels, PARTNER COE-2010-001, Partnership for AiR Transportation Noise and Emissions Reduction (PARTNER) (2010).

AY 2015/2016 Task 3 – 2050 alternative jet fuel production potential and associated GHG emissions reductions

Massachusetts Institute of Technology

Objective(s)

The objective of this task is to finalize estimates for bioenergy potential and jet fuel achievement in 2050, for the purposes of informing the ICAO CAEP AFTF process. This work was initiated in year 1. The scenario results for potentially available jet fuel volumes are combined with the 2050 lifecycle GHG emissions estimates for different feedstock to fuel pathways as described above. Overall, this yields a range of GHG emissions reductions from alternative jet fuel usage in 2050. Results were presented to CAEP in early 2016, and were used in the update to the ICAO-CAEP trends assessment.

Research Approach

Introduction

This task was to carry out analysis that supports AFTF's task to evaluate the range of potential GHG emissions reductions from the use of alternative jet fuels to 2050. The results were used as an input in CAEPs environmental trends assessment to 2050.

Methods

For this analysis, short-term is defined as 2020, and alternative jet availability is established for this from fuel producers' announcements and targets set by States. Six scenarios were developed for the short-term assessment, varying by the credibility requirements for inclusion of companies' production plans, and the consideration of green diesel as a potential future low-percentage blending opportunity with conventional jet fuel.

For the long-term, defined as 2050, alternative jet fuel availability is estimated by first calculating the primary bioenergy potential constrained by environmental and socio-economic factors; then estimating the proportion of bioenergy potential that could actually be achieved or produced; and finally by calculating the quantity of alternative jet that could be produced from the available bioenergy. 9 different feedstock types are considered (starchy crops; sugary crops; lignocellulosic crops; oily crops; agricultural residues; forestry residues; waste fats, oils and greases; microalgae; municipal solid waste (MSW)). Five different sets of assumptions for primary bioenergy potential, three sets for bioenergy achievement, and four sets of alternative jet achievement assumptions were developed, yielding a total of 60 different production scenarios. The quantity of potentially available alternative jet fuel also involves the calculation of emissions from direct land-use change (LUC) due to biomass feedstock cultivation.

In order to quantify the lifecycle GHG emissions associated with the production volumes, a database of existing LCA results for different feedstock-to-fuel technology combinations was developed. For the 2020 GHG intensities, existing study results were adapted to reflect allocation of emissions to co-products based on their energy-content, and the average emissions value of each bioenergy feedstock was calculated for all studies. The results described in the previous task were used to quantify lifecycle GHG emissions from alternative jet fuels in 2050.

Results

For 2020, the range of results for AJF production are between 56 kt/y to 6.5 Mt/y, corresponding to 0-2% of global aviation fuel demand in 2020. This corresponds to a reduction of lifecycle GHG emissions by 0-1.3% compared to only using petroleum-derived jet fuel, as shown in Figure 4. Among the different scenarios considered for 2020, emission reduction values increase assuming that green diesel could be used jet engines (in low blends up to 5%).

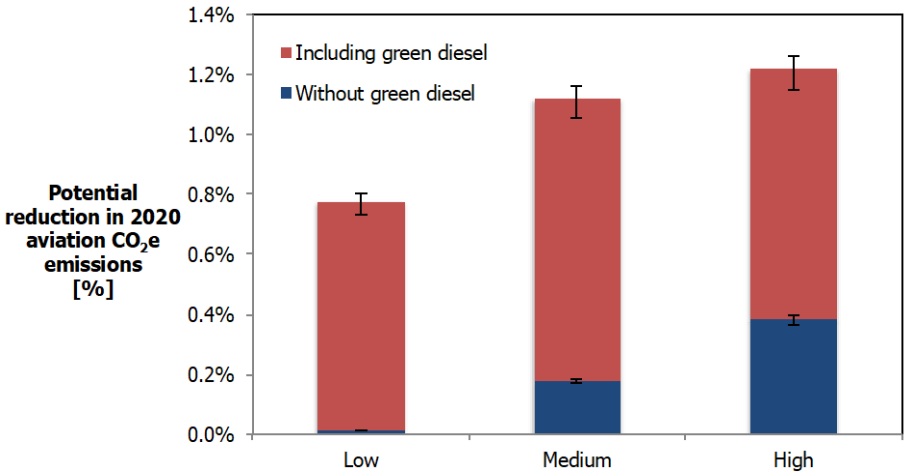

Figure 4: Potential reducton in 2020 aviation lifecycle GHG emissions, compared to the 100% petroleum-derived jet baseline. The variability bars reflect different fuel burn projections for 2020.

Emissions from LUC were calculated for each scenario in 2050, and were found to vary among scenarios from 1g to 20gCO_2e/MJ on average, depending on the mix of alternative jet fuel pathways produced. The average emissions from LUC associated with a certain mix of alternative jet fuels decreases, inter alia, as the share of feedstocks not requiring dedicated land conversion, such as wastes, residues, and MSW, increases. Overall, scenarios with higher alternative fuel production volumes tend to show higher emissions from LUC per unit of fuel produced, as AJF production becomes increasingly dependent on the conversion of additional land area for feedstock cultivation. This is shown in Figure 5.

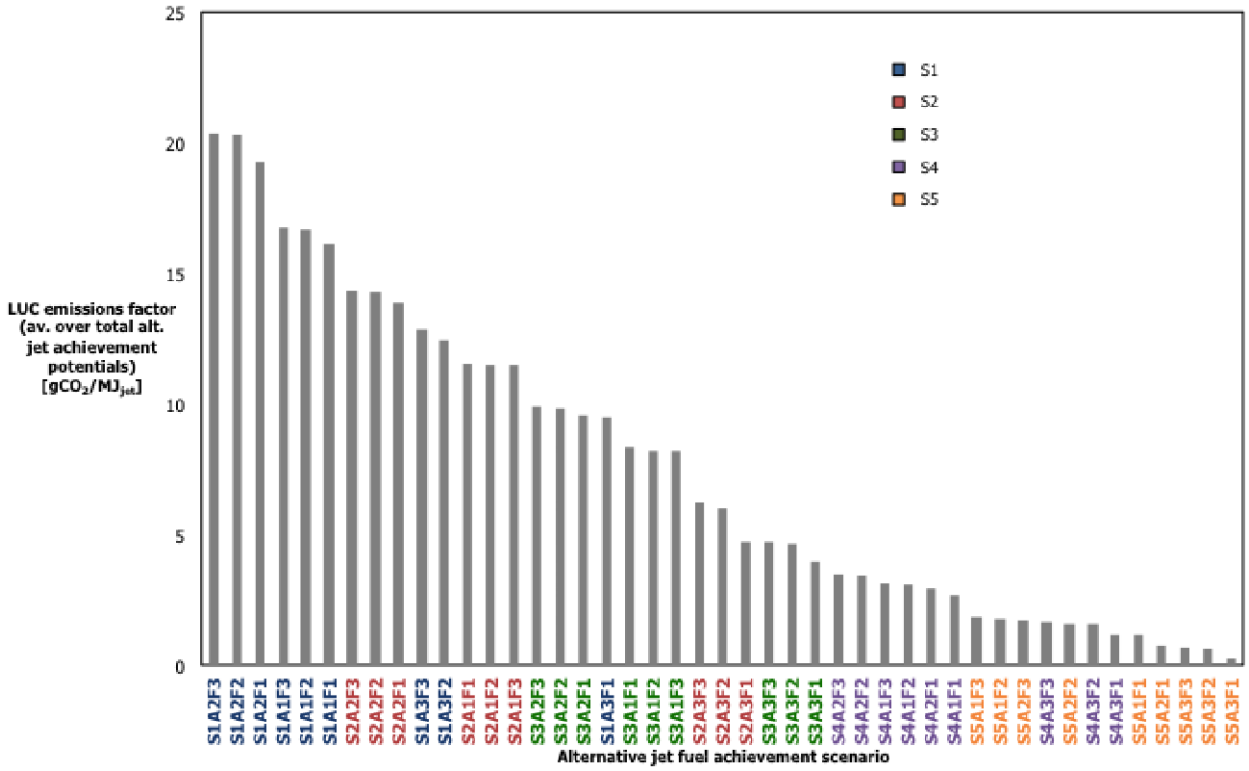

Figure 5: Allocated LUC emissions, averaged over total alternative jet fuel volumes, for each scenario and amortized over 25 years. Each label on the x-axis corresponds to a different alternative jet fuel achievement scenario.

Depending on the assumptions associated with different scenarios, alternative jet fuel production in 2050 could range from zero to 4.600 Mt per year, offsetting between 0-100% of the projected petroleum-derived jet fuel demand in 2050. This is shown in Figure 6. This translates into a reduction of total lifecycle GHG emissions reduction of between 0-63%. The range of potential GHG reductions is smaller than the fuel replacement range, as the alternative jet fuel mix in the different scenarios is associated with lifecycle GHG emissions of 31-64% of those of petroleum-derived jet fuel, on average.

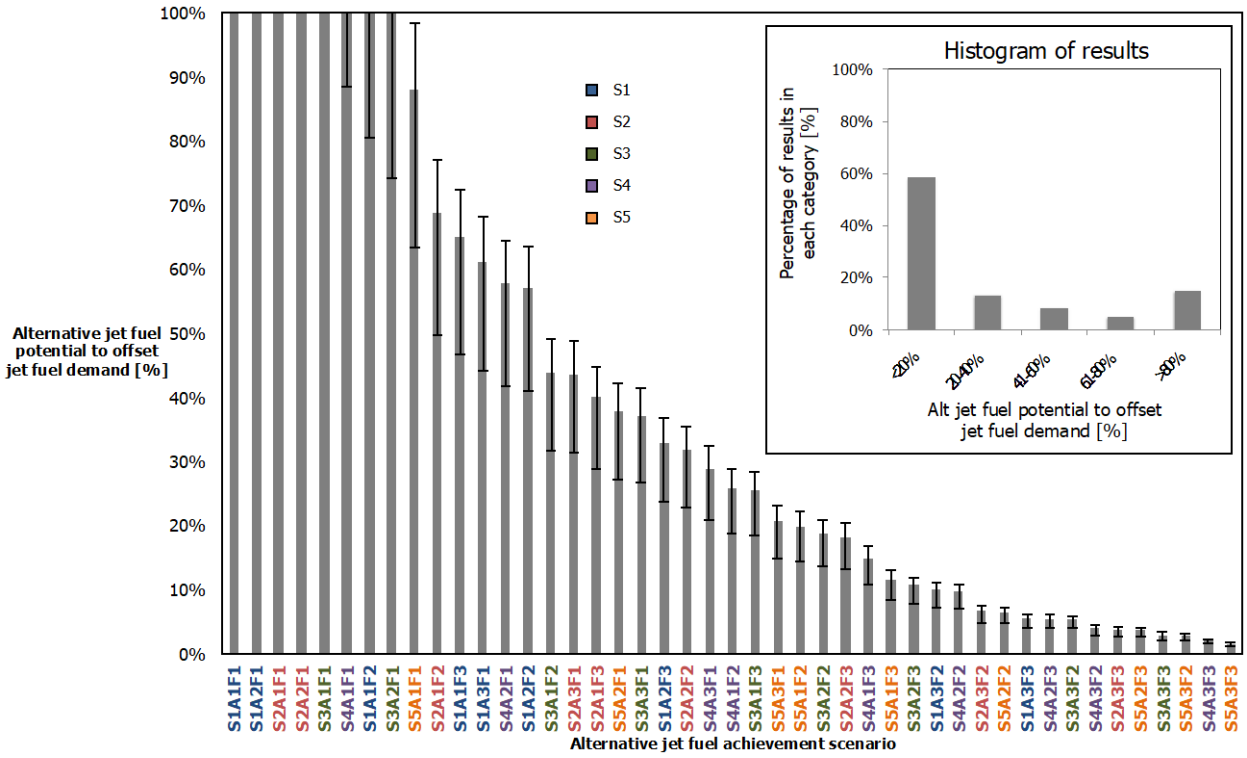

Figure 6: Percentage of 2050 jet fuel demand potentially satisfied by alternative jet, in decreasing size of offset potential. The whiskers indicate the change in percentage of potential offset due to the range of fuel burn projections.

The results indicate that the potential to reduce GHG emissions from aviation via the use of alternative jet fuel increases with assumptions that imply greater availability of alternative jet fuel. These assumptions include factors such as: larger agricultural yield increases; greater land availability; higher accepted rates of residue removal; increases in feedstock and fuel production efficiencies; reductions in GHG emissions from utilities; increased policy emphasis on bioenergy production relative to other land usages in general, and on alternative jet fuel production in particular; and other factors.

An "illustrative example" based on one specific scenario of 17% GHG emissions reduction with 220 Mt/yr of alternative fuel production in 2050 was further explored to assess the feasibility. The selected scenario assumes a mid-level of overall bioenergy potential, high actual achievement rates for this potential, equal policy-emphasis on all potential end-usages of bioenergy, and relatively low GHG intensity of alternative jet fuel produced in 2050. In addition, the conditions that would need to be in place in order for alternative jet fuel to potentially to yield particular levels of GHG reductions were also explored.

For example, a 2% reduction of lifecycle aviation GHG emissions would require a global production volume of alternative jet of about 30 Mt/yr in 2050. A 17% reduction in GHG emissions would entail alternative jet fuel production of approximately 220 Mt/yr in 2050. Under a linear growth assumption between 2020 and 2050, this would require approximately 70 biorefineries to be constructed every year (required capital investment of approximately $6B-$25B/yr) and exponential growth implies that 200-300 facilities will have to be built per year closer to 2050 (required jet-fuel specific capital investment of approximately less than $1B/yr to $2B/yr in 2025 and $30B-$110B/yr in 2050). These investments would cover the capital expenditure for the refineries and not the operational expenditures of the entire alternative fuel supply chain. (e.g. feedstock and utility costs).

For the highest modelled GHG emissions reduction under all scenarios assessed of 63%, approximately 870 Mt/yr of alternative jet fuel would need to be produced in 2050. In addition to the significant capital investment in biorefineries

required, this emissions reduction would require the realization of the highest assumed increases in agricultural productivity, the highest considered availability of land for feedstock cultivation, residue removal rates, conversion efficiency improvements, and significant reductions in the GHG emissions of utilities, as well as a strong market or policy emphasis on bioenergy in general, and alternative jet fuel in particular. The latter would entail large shares of the available bioenergy pool be devoted to producing alternative jet as opposed to other end uses such as transportation fuels or electricity and heat. These scenarios are shown in Table 5.

Table 5: Required fuel production volume in 2050, number of new 500 bpd facilities required annually, and range of annual capital investment required for different GHG emission reduction percentages.

Aviation GHG emissions reduction	Required AJF production volume in 2050 (Mt/yr)	Requirements under linear growth		Requirements under exponential growth	
		Number of new biorefineries/yr	Capital investment/yr	Number of new biorefineries/yr	Capital investment/yr
2%	30	10	$1B - $3B	<5 (2025) to 30 (2050)	<$1B - $2B (2025) to $3B - $10B (2050)
10%	130	40	$3B - $14B	<5 (2025) to 200 (2050)	<$1B - $2B (2025) to $15B - $60B (2050)
17%	220	70	$6B - $25B	<5 (2025) to 300 (2050)	<$1B - $2B (2025) to $30B - $110B (2050)
40%	570	170	$15B - $60B	<10 (2025) to 1000 (2050)	$1B - $3B (2025) to $80B - $330B (2050)
63%	870	260	$20B - $90B	<10 (2025) to 1600 (2050)	$1B - $3B (2025) to $130B - $550B (2050)
Average historical global ethanol and biodiesel production		Total annual volumes (Mt/yr)		10 (years 1975 - 2000) to 45 (2001 - 2011)	
		Number of new biorefineries/yr		5 (years 1975 - 2000) to 60 (2001 - 2011)	
Projection for average annual investment in petroleum refining in 2035				$55B	

This results of this analysis indicate that in order to achieve significant reduction in aviation GHG emissions by 2050, high capital investments are required and these might be feasible only if the investments begin in time and consistently grow over time, or if existing infrastructure can be leveraged to reduce the initially required capital investments. Comparison to the development in global ethanol and biodiesel production shows that the growth in alternative aviation fuel production would need to be on the order of recently observed growth of 5-15 Mt/yr in global biofuel production capacity to achieve a 10% and 17% emissions reduction by 2050, and would have to significantly exceed historical global biofuel production growth rates for total GHG emission reductions above 20%.

Milestone(s)
The major milestone of this work was presentation of final results to CAEP in February 2016.

Major Accomplishments
Completion of the task, such that AFTF could provide an estimate of the potential contribution of alternative jet fuels to reduction in CO_2 emissions from aviation. This result was included in the CAEP environmental trends assessment.

Publications
This work is carried out in support of an international negotiation. As such, the methodology and results have not be published in scientific journals or presented at conferences, in order to respect the sensitive nature of the negotiation. The analysis is summarized in information papers (IP) CAEP/10-IP/13 and CAEP/10-IP/14 presented to CAEP, and working paper (WP) CAEP/10-WP/44 presented to CAEP.

This element of the work of AFTF concluded with the CAEP 10 cycle in February 2016. However, MIT is currently drafting a journal article to publish these results. The journal to which it will be submitted has not yet been decided.

Outreach Efforts
The work described here was discussed at length during face-to-face meetings of AFTF in Montreal in October 2015 and June 2016. Between the meetings, a number of teleconferences were held to discuss methodological decisions and initial results with the other members of AFTF.

This work was also presented at the March 15, 2015 FAA AEE external tools call, and on the June 10, 2016 SOAP-Jet webinar.

Awards
None.

Student Involvement
Mark Staples was the primary developer of the 2050 fuel production assessment methodology. He drafted the iterations of the IP, prepared briefings for AFTF, and incorporated the requested and required changes. He also carried out the integration of the LCA and fuel production assessment analyses to generate final results, and drafted the IP that presents and explains the results. Mark completed his PhD at MIT in December 2016.

Pooja Suresh carried out the analysis of LCA values for alternative fuels in 2050. Her analysis involved calculating alternative jet fuel LCA results, taking into account changes in the technologies and process inputs to 2050. Pooja prepared briefings for the LCA analysis group during teleconferences, and face-to-face meetings. She graduated in June 2016, and now works at Boston Consulting Group in Toronto, Canada.

Plans for Next Period
The results of this analysis will continue to be used to inform the AFTF process in the coming period. For instance, these results will be used to quantify the effect of different policy decisions on the potential availability of alternative jet fuel.

In addition, MIT will draft and submit a journal paper documenting this work and its findings in the coming period.

AY 2015/2016 Task 4 & AY 2016/2017 Task 1 - LCA methodology development and default value calculation for ICAO global market-based measure

Massachusetts Institute of Technology

Objective(s)

The objectives of these tasks are two-fold. First, MIT is to help develop the core lifecycle assessment (LCA) methodology for the inclusion of alternative fuels in ICAO's global market-based measure. This entails developing recommendations for the choice of allocation rules, system boundary limits, the treatment of emissions from land-use change and sustainability requirements, as well as recommendations on the entity that shall conduct the actual calculations and the frequency of re-assessment of the calculations. The development of the proposal will be informed by calculations on the impact of methodological choices on CO_2 emissions attributed to alternative jet fuel.

Once the methodology has been agreed upon, it is to be used for the calculation of default LCA values to be applied to different feedstock-to-fuel technologies under GMBM.

Research Approach

Introduction

Over this reporting period, AFTF used the core LCA methodology developed previously for the fuel production assessment as a starting point. MIT summarized this methodology in a "Guidance Document" to be circulated amongst interested parties outside of AFTF, in order to solicit LCA data for the calculation of default values.

In addition, MIT carried out analyses to assess the appropriate level of aggregation for the calculation of default values. This involved examining the impact of feedstock, technology and regional aggregation on the accuracy of the calculated default values.

Summary of the LCA methodology as defined in the Guidance Document

The purpose of the guidance document is to describe the agreed upon LCA methodology for the calculation to default core values under GMBM, such that interested parties can submit data to aid in the calculation of these values. The requirements for data submitted to AFTF are also described.

Alternative jet fuel is defined as any fuel that generates lower carbon emissions than conventional kerosene on a lifecycle basis, and the LCA methodology only applied to the attributional emissions from alternative jet fuel. The system boundary of interest includes the full supply chain of AJF production and use, and shown in Figure 7.

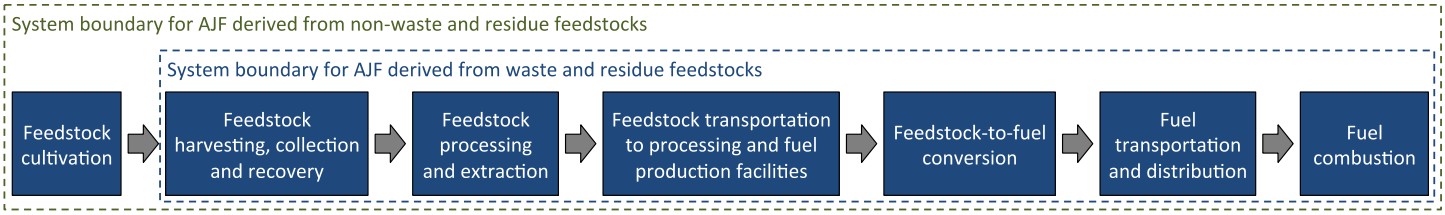

Figure 7: Alternative jet fuel lifecycle steps

The calculated LCA results include well-to-pump emissions of CH_4, N_2O and CO_2, and combustion CO_2 emissions. Emissions from on-going operational activities, as well as emissions from utility inputs are included, however emissions generated from one-time construction or manufacturing activities are not. Waste and residue feedstocks are assumed to generate zero GHG emissions during feedstock production. All results are expressed in 100-year global warming potential CO_2 equivalents. Energy allocation is used at all stages of the LCA, and the results are compared to a conventional jet fuel baseline of 89.0 gCO_2e/MJ_{jet}.

Criteria of submission of LCA data for consideration under GMBM

AFTF has limited capacity to assess submitted data and calculated LCA results. Therefore, the Guidance Document prepared by MIT contains a number of criteria in order to target the work of AFTF where it would be most fruitful.

Firstly, AFTF the pathways evaluated by AFTF should be likely to achieve commercial-scale production in the near-term. Therefore, a working list of feedstock-to-fuel pathways that are certified by ASTM and for which there are commercial entities planning to produce fuel is given in Table 6.

Table 6: Working list of the feedstock-to-fuel alternative jet fuel pathways for which default core LCA values will be established by AFTF by GMBM

Technology	Feedstock
Fischer-Tropsch (FT)	Agricultural residues
	Forestry residues
	Short rotation woody crops
	Herbaceous lignocellulosic energy crops
	Municipal solid waste
Hydroprocessed esters and fatty acids (HEFA)	Waste tallow
	Used cooking oil
	Corn oil
	Canola/rapeseed
	Soybean
	Palm oil
	Camelina
	Palm fatty acid distillate (pending data avail.)
	Jatropha
	Tall oil
Synthesized Iso-Paraffins (SIP) aka. direct sugar-to-hydrocarbon (DSHC)	Sugarbeet (pending data avail.)
	Sugarcane
Alcohol (iBuOH)-to-jet (ATJ)	Sugarcane
	Corn grain
	Herbaceous lignocellulosic energy crops
	Agricultural residues
	Forestry residues

The source of the submitted data also must be credible, such as a study published in a peer-reviewed journal, an appropriate state agency, or direct submission of a study carried out by a State agency, intergovernmental agency, non-profit or NGO, or private entity.

The data submitted to AFTF must also be transparent and replicable, and the data must be accessible such that the LCA values can be re-calculated and verified.

Aggregation analyses

In order to carry out the calculation of default core LCA values in line with the agreed upon methodology, AFTF will have to decide on the appropriate level of feedstock, conversion technology and geographical aggregation to consider. In order to support this decision, MIT has carried out a number of analyses to quantify the impact of differing levels of aggregation on

the LCA results. In preparation for the face-to-face meeting of AFTF in October 2016, an analysis of regional variation in lifecycle GHG emissions for a number of pathways was carried out. This was done by leveraging pathways that are already modeled in GREET, and augmenting the parameter values to better reflect LCA results of other world regions. These results are shown in Figure 8.

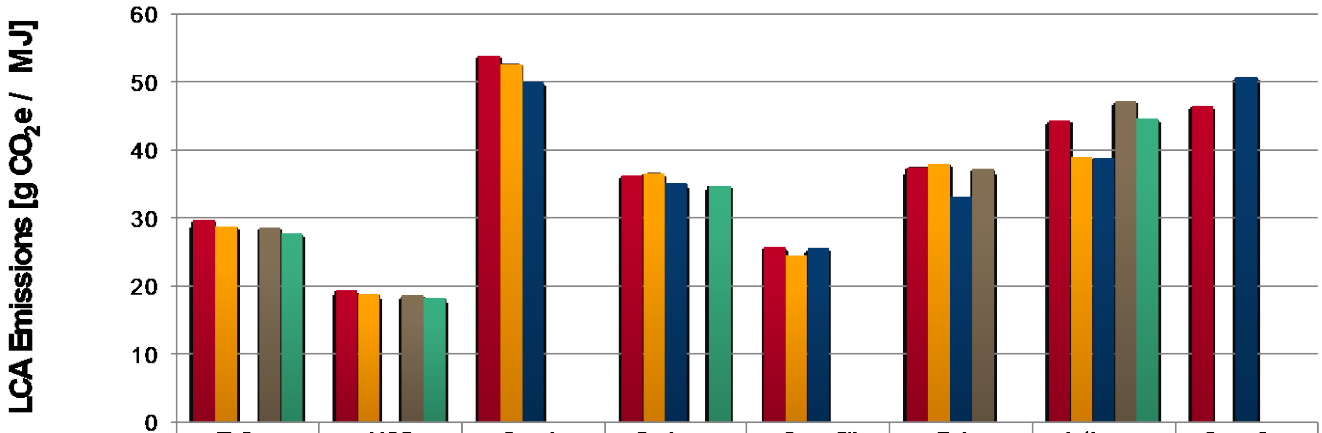

	Tallow	UCO	Canola	Soybean	Corn Oil	Palm	Jathropa	Camelina
USA	29.8	19.4	53.9	36.3	25.8	37.5	44.4	46.5
EU	28.8	18.9	52.7	36.6	24.5	38.0	38.9	
Canada			50.0	35.2	25.6	33.1	38.9	50.8
SE Asia	28.6	18.7				37.2	47.2	
Latin America	27.7	18.3		34.8			44.7	

Figure 8: Aggregation analysis results for regional variation

The findings indicate that regional variation may be less important than initially expected for many of the pathways

Milestone(s)

The major milestones of this task were presentation of the Guidance Document summarizing the agreed upon LCA methodology to AFTF in the fall of 2016, and the presentation of aggregation analyses to AFTF in May, June and September of 2016.

Major Accomplishments

By drafting and agreeing upon the Guidance Document described here, MIT has contributed to setting up AFTF for success in accomplishing the tasks it has been given by CAEP. The Guidance Document will be used to solicit LCA data from interested parties for the establishment of default values, and the aggregation analyses establish the reasoning for the level of resolution at which the default value calculation must be carried out.

Publications

This work is carried out in support of an international negotiation. As such, the methodology and results have not be published in scientific journals or presented at conferences, in order to respect the sensitive nature of the negotiation.

However, the work carried out by MIT in this reporting period is contained in the following AFTF papers: CAEP/11-AFTF/1-IP/14 and CAEP/11-AFTF/2-WP/2 include general information about the LCA task carried out by MIT, CAEP/11-AFTF/2-IP/4 summarizes the pathway aggregation study carried out by MIT, and CAEP/11-AFTF/2-IP/03 contains a draft of the Guidance Document put together by MIT.

Outreach Efforts

A preliminary version of this work was presented at the AFTF meeting Montreal in June 2016. In addition, the Guidance Document and aggregation analyses were presented via telecon to AFTF in September 2016, in preparation for the face-to-face meeting in Montreal in October 2016.

Awards

None.

Student Involvement

Mark Staples drafted the Guidance Document, presented it to AFTF members and made revisions as necessary. Mark also wrote the corresponding information papers. He completed his PhD at MIT in December 2016.

Cassandra Rosen carried out the aggregation analysis in co-operation with Argonne National Laboratory. Cassandra also presented the work and drafted the information paper. She is a continuing Masters student at MIT.

Plans for Next Period

For the next period, one of the main areas of work will be the development of an initial set of core default LCA emission values. In order to do this, we will make a proposal on the level of resolution of data to be used under AFTF, both geo-spatially and in terms of feedstock and technology groupings. In addition, we will develop an initial list of core LCA values to be brought forward to AFTF. Finally, we will work towards a proposal for a petition process, by which eligible entities could prove lower LCA values of a fuel under consideration.

In the coming period we will also assist Purdue University in the development of ILUC emission factors by, for example, providing input on scenario assumptions. We will also help in the development of an appropriate definition of carbon-hotspot areas, the usage of which would make the related aviation fuel ineligible for a credit under the GMBM.

AY 2015/2016 Task 5 & AY 2016/2017 Tasks 2 and 6 – Support of the US FAA at ICAO AFTF for development of sustainability criteria, policy and feasibility assessment of ICAO climate change goals, including in person support at meetings of ICAO CAEP AFTF

Massachusetts Institute of Technology

Objective(s)

The objective of this task is to support the US FAA's engagement with ICAO CAEP AFTF in a number of additional areas, including the development of sustainability criteria and policy and feasibility assessment of ICAO's climate change goals.

Research Approach

Alternative jet fuels might have to satisfy some sustainability considerations other than CO_2 reductions, which are to be defined by AFTF during CAEP/11. MIT will assist to identify the environmental, social and economic aspects that should be taken into account. In addition, we will contribute to this effort over the coming year by collaborating on a review and comparison of existing sustainability frameworks.

MIT will also contribute to the task group working on developing guidance for policies to encourage deployment of alternative jet fuels.

Finally, MIT will carry out an analysis to put international aviation emissions, including emissions from alternative jet fuels, into the context of international climate change goals. These goals may include keeping average global temperature change below some threshold, such as 2˚C, or a global carbon budget of 1,000 billion tonnes. This task is particularly relevant because, while alternative jet fuels may reduce aviation's contribution to climate change, the technologies may also shift some of the emissions burden to other sectors or industries, such as agriculture or fuel production. This is an important feedback that has not yet been considered for aviation in the context of global climate change targets.

Milestone(s)

These specific tasks fall under the work plan for AY 2016/2017. Therefore, the major milestones for this work will occur in the next period.

Major Accomplishments

These specific tasks fall under the work plan for AY 2016/2017. Therefore, the major accomplishments for this work will occur in the next period.

Publications

None.

Outreach Efforts

None.

Awards

None.

Student Involvement

This work will be carried out by Mark Staples and Cassandra Rosen. Mark completed his PhD at MIT in December 2016, but will continue working on this project as a post-doctoral researcher. Cassandra is a continuing masters student at MIT.

Plans for Next Period

Please see the task description above under "Research Approach".

AY 2016/2017 Task 4 – Long-term production and GHG emissions' reduction potential of alternative jet fuel in the US

Massachusetts Institute of Technology

Objective(s)

The objective of this task is to assess the long-term production potential of alternative jet fuel in the US.

Research Approach

This research will use a three step analysis that considers: the availability of primary bioenergy constrained by the physical limits of agro-climatic conditions, bio-productivity, environmental sustainability and socio-economic conditions; the proportion of potentially available bioenergy that could actually be produced on the basis of feedstock economics; and the proportion of produced bioenergy dedicated to the production of alternative jet fuels as opposed to other potential uses. This analysis will leverage the modeling framework developed for the Fuel Production Assessment carried out during CAEP/10. Whereas the previous modeling and analysis was carried for a global scope, the work carried out during the coming year will be focused on the US.

In addition to fuel volumes, this analysis will also provide a high-level estimate of the greenhouse gas (GHG) emissions reductions associated with different scenarios of alternative jet fuel deployment in the US context, including both attributional life cycle GHG emissions and emissions from land use change (LUC). The analysis will use an additional approach for the quantification of LUC emissions, meaning that all bioenergy feedstock cultivation is assumed to be additional to future projected land uses in the US, and therefore there are LUC emissions associated with all alternative jet fuels derived from cultivated energy crops. This was the method employed for the CAEP/10 AFTF Fuel Production Assessment, and the advantage of this approach is that it can be used to quantify the trade-off between increased alternative jet fuel volumes, and increased emissions from LUC.

Milestone(s)

This task falls under the work plan for AY 2016/2017. Therefore, the major milestones for this work will occur in the next period.

Major Accomplishments

These specific tasks fall under the work plan for AY 2016/2017. Therefore, the major accomplishments for this work will occur in the next period.

Publications

None.

Outreach Efforts

None.

Awards

None.

Student Involvement

This work will be carried out by Timothy Galligan. Timothy is a continuing masters student at MIT.

Plans for Next Period

Please see the task description above under "Research Approach".

AY 2016/2017 Task 5 – Economic and environmental assessment of alternative jet fuels accounting for the potential for technology maturation

Massachusetts Institute of Technology

Objective(s)

The objective of this task is to provide an assessment of the economic and environmental viability of alternative jet fuels, accounting for time- and path-dependency of technology maturation.

Research Approach

This is an important aspect to consider because a number of long-term trends suggest that the economic and environmental performance of alternative jet fuels, relative to petroleum-derived jet fuels, may change over time. For example, a growing proportion of non-conventional crude oil production is anticipated to be required to meet new demand for liquid fuels (ExxonMobil 2014), and jet derived from non-conventional crude oil has a higher GHG footprint than conventional petroleum-derived jet fuel: 19% and 39% higher for jet fuel derived from Canadian oil sands and oil shale, respectively (Stratton et al. 2011). As a result, alternative jet fuels' GHG footprint may become smaller relative to petroleum-derived jet fuels.

In addition, empirical data from the Brazilian sugarcane ethanol industry indicate that learning-curve effects contributed to a 29% reduction in cost for every doubling of cumulative production (Goldemberg et al. 2004), implying the potential for similar effects for analogous alternative jet fuel production processes. Some of these cost reductions are likely attributable to improved process efficiencies, which also imply the potential for improvements in life cycle GHG performance of alternative jet fuels as a function of cumulative fuel production.

In order to achieve these learning-curve effects some rate of alternative jet fuel production is required in order to accumulate experience, and this suggests endogeneity and path-dependence associated with the development and performance of alternative jet fuels production technologies. This research project will use a system dynamics modeling approach to quantify the changes in the environmental and economic performance of alternative jet fuels, taking into account the time- and path-dependence of technology development and maturation. This task will include an assessment of alternative jet fuel adoption rates and associated emissions impacts that are required to get from 2020 to 2050 estimates of alternative jet fuel use generated by AFTF under CAEP/10.

Milestone(s)

This task falls under the work plan for AY 2016/2017. Therefore, the major milestones for this work will occur in the next period.

Major Accomplishments

These specific tasks fall under the work plan for AY 2016/2017. Therefore, the major accomplishments for this work will occur in the next period.

Publications

None.

Outreach Efforts

None.

Awards

None.

Student Involvement

This work will be carried out by Mark Staples. Mark completed his PhD at MIT in December 2016, and will continue to work on this as a post-doctoral researcher.

Plans for Next Period

Please see the task description above under “Research Approach”.

References

ExxonMobil, "The outlook for energy: A view to 2040," Technical report 2014.

J. Goldemberg, S.T. Coelho, P.M. Nastari, and O. Lucon, "Ethanol learning curve - the Brazilian experience," Biomass and Bioenergy, vol. 26, pp. 301-304, 2004.

Stratton, R; Wong, H; Hileman, J. Quantifying Variability in Life Cycle Greenhouse Gas Inventories of Alternative Middle Distillate Transportation Fuels, in: Environmental Science & Technology, Vol. 45 (2011).

Project 002 Ambient Conditions Corrections for Non-Volatile PM Emissions Measurements

Missouri University of Science and Technology
Aerodyne Research Inc.

Project Lead Investigator

Philip D. Whitefield
Professor and Department Chair
Chemistry
Missouri University of Science and Technology
142 Schrenk Hall, 400 W 11th Street, Rolla, MO 65409
573-341-4420
pwhite@mst.edu

University Participants

Missouri University of Science and Technology

- P.I.(s): Philip D. Whitefield
- FAA Award Number: 13-C-AJFE-MST-002 (Amendments 002-009)
- Period of Performance: 9.18.14 to 9.30.17
- Task(s):
    - Task 1 Ambient conditions corrections for nv PM
    - Task 2
        - (a) NARS Upgrade for gaseous emissions and smoke number
        - (b) NARS Upgrade for Canadian electrical standards compliance
    - Task 3 - nv PM measurements at RR Indianapolis
    - Task 4 - nv PM measurements at P&W
    - Task 5 - nv PM measurements at the VARIANT 2 Campaign
    - Task 6 - nv PM measurements at Honeywell
    - Task 7 - Engine to Engine Variability and Derivation of Characteristic nvPM Emissions

Project Funding Level

$3,402,234.00
3rd Party In-kind Cost Share from Empa: $3,402,234.00

Investigation Team

Philip D. Whitefield PI
Donald E. Hagen Co-PI
Prem Lobo Co-PI
Richard Miake-Lye Co-PI
Max Trueblood Research Associate
Steven Achteberg Research Associate

Project Overview

The Society of Automotive Engineers (SAE) Aircraft Exhaust Emissions Measurement Committee (E-31) has published an Aerospace Information Report (AIR) 6241 detailing the sampling system for the measurement of non-volatile particulate matter (nvPM) from aircraft engines (SAE 2013). The system is designed to operate in parallel with existing International Civil Aviation Organization (ICAO) Annex 16 compliant combustion gas sampling systems used for emissions certification from aircraft engines captured by conventional (Annex 16) gas sampling rakes (ICAO, 2008). Based on the AIR 6241, ICAO has specified in Annex 16, Vol. II, a standardized nvPM measurement system for demonstrating compliance with the new CAEP/10 nvPM standard for gas turbine engines. The engine certification measurements of nvPM emissions will be performed using the Annex 16 compliant nvPM sampling system.

The Missouri University of Science and Technology (Missouri S&T) owns and operates an Annex 16 compliant mobile system to measure nvPM emissions from the exhaust of aircraft engines. The MST system based on past measurement campaigns and data inter-comparisons is the North American Reference System and is one of the three reference systems in the world. The other two reference systems are: a) The Swiss FOCA Measurement System; and b) The EASA SAMPLE System.

The nvPM system consists of three sections – collection, transfer, and measurement – connected in series (Figure 1). A description of each section is provided below.

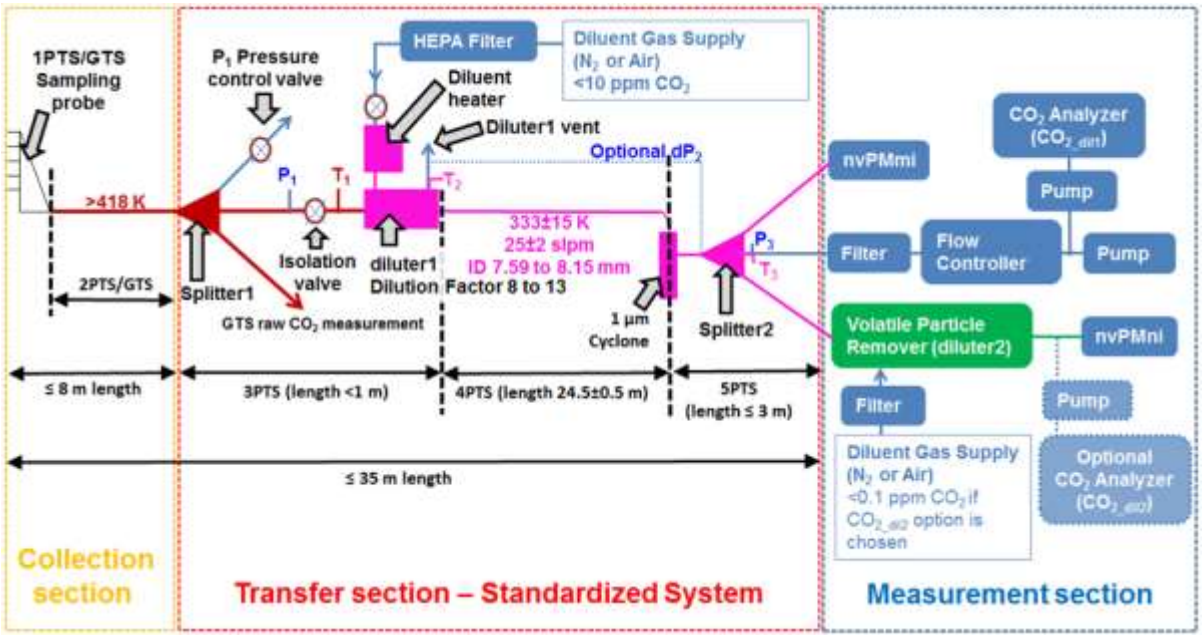

Figure 1: Components of an AIR6241 nvPM system

Collection section: The collection section consists of the probe rake system and up to 8m of stainless sample line heated to 160˚C.

Transfer section: The transfer section consists of a three way sample splitter, a PM sample eductor/dilutor, flow controllers, and sample line heater controllers The first sub-component of the transfer section is a three way sample splitter which divides the total exhaust gas sample from the rake into three flow streams. The first is the required flow of exhaust for the Annex 16 combustion gas sample. The second is the PM sample and the third is an excess flow dump line controlled with a pressure relief valve. The PM sample is diluted by a factor 8-13 with dry nitrogen (heated to 60˚C) by means of an eductor/dilutor. The diluted PM sample with a flow rate 25 ± 2 SLPM is transferred by an electrically heated, temperature controlled conductive, grounded, carbon loaded PTFE PM sample transfer line 25m in length, maintained at

60˚C to a 1µm cyclone and then a second three way splitter to direct the sample to the number and mass measurement devices in the measurement system.

Measurement section: The measurement section consists of a volatile particle remover and a particle number measurement device, a mass measurement device and a mass flow controller, pump and CO_2 detector as specified by AIR6241.

As part of evaluating the methodology and the robustness of the system described in AIR6241, the North American nvPM reference system has been deployed at several OEM facilities in North America (McCaldon, 2013; Lobo and Condevaux, 2014) as well as the SR Technics maintenance facility in Zurich, Switzerland (Lobo et al., 2015). These demonstration/inter-comparison studies served to provide information regarding the variability of the individual sampling and measurement systems. Additional testing at OEM facilities has also be conducted to acquire QL2 data on a set of engines identified to be representative of the commercial fleet for entry into the nvPM values database (Lobo and McKinney, 2014). Datasets from these initial measurement activities are being used by the ICAO Committee on Aviation Environmental Protection (CAEP) and their PM Task Group (PMTG) as they consider future aviation PM regulations. The data will be used by PMTG to develop a metric on which the regulation for nvPM emissions will be based.

Task 1: Ambient conditions corrections for nvPM

Missouri University of Science and Technology

Objective(s)

1. Conduct combustor rig testing to determine ambient condition corrections for non-volatile PM Emissions measurements
    - Perform combustor rig tests at GE Aviation facilities using an AIR6241 compliant Sampling System for the measurement of non-volatile PM (nvPM) emissions
    - Evaluate the influence of ambient conditions on PM production
    - Determine appropriate corrections to standard atmospheric conditions for aircraft nvPM

Research Approach

Missouri S&T and ARI will coordinate with GE Aviation to secure access to altitude test cells at which nvPM emissions can be acquired for varying ambient temperature, pressure, and relative humidity. To evaluate the effects of ambient conditions on PM production, a multi-sector combustor will be used as the PM emissions source.

Missouri S&T will work with GE Aviation to plan and prepare for the nvPM measurements in the altitude test cell. During the planning process, a detailed plan for the test will be developed in collaboration with the OEMs. The plan will include details of the sample extraction system, interfacing with the North American AIR6241 mobile reference system, simulating a range of ambient conditions for the test, measurement protocol, and data analysis. A site visit will also be undertaken as part of the planning process to have face-to-face discussions with the OEM facility engineers and technicians and also determine essential details regarding placement of sampling and measurement system, interfacing with existing probe-rake hardware, power and air requirements, etc.

After the test plan has been developed and approved, and a test window identified, Missouri S&T will begin preparation for deploying the system to the GE Aviation facility, including but not limited to, calibration of instruments, checkout of various system components, and preparing the system for transport. The nvPM system will be deployed alongside Annex 16 Volume II certification-grade gaseous and smoke measurement systems to obtain the full complement of gaseous and nvPM data.

The testing itself will be conducted in accordance with the test plan developed during the planning phase. Data for nvPM mass, number, and gaseous emissions and smoke number will be acquired for simulated ambient conditions spanning the full realistic parameter space using a multipoint probe similar to those used for gaseous emissions certification. The OEMs will be responsible for providing the probe system to be used for these tests. Following the test, the data will be analyzed and appropriate correlations will be developed for nvPM data acquired under different ambient conditions. A correction of nvPM data to standard atmospheric conditions will then be developed based on these correlations.

Milestone(s)

Testing scheduled for January/February 2017.

Major Accomplishments
Test plan completed and testing date scheduled for January 2017.

Publications
None.

Outreach Efforts
None.

Awards
None.

Student Involvement
None.

Plans for Next Period
Conduct test, analyze data and report findings.

Task 2:
(a) NARS Upgrade for gaseous emissions and smoke number
(b) NARS Upgrade for Canadian electrical standards compliance

Missouri University of Science and Technology

Objective(s) and Research Approach
Missouri S&T will procure a portable emissions cart designed for raw exhaust measurement for gaseous emissions such as NO/NOx, UHC, CO and CO_2. Figure 3 shows the portable unit and the analyzers available from California Analytical Instruments (CAI). OEMs such as GE, Pratt and Whitney, and Honeywell all use gaseous emissions analyzers manufactured by CAI during the emissions tests, including certification tests.

Figure 2: Portable emissions cart designed for raw exhaust measurement for engine gaseous emissions

Missouri S&T will also procure a smoke meter from Chell Instruments. Figure 4 shows a smoke meter manufactured by Chell Instruments. This smoke meter has also been used by Rolls-Royce, UK for emissions measurements.

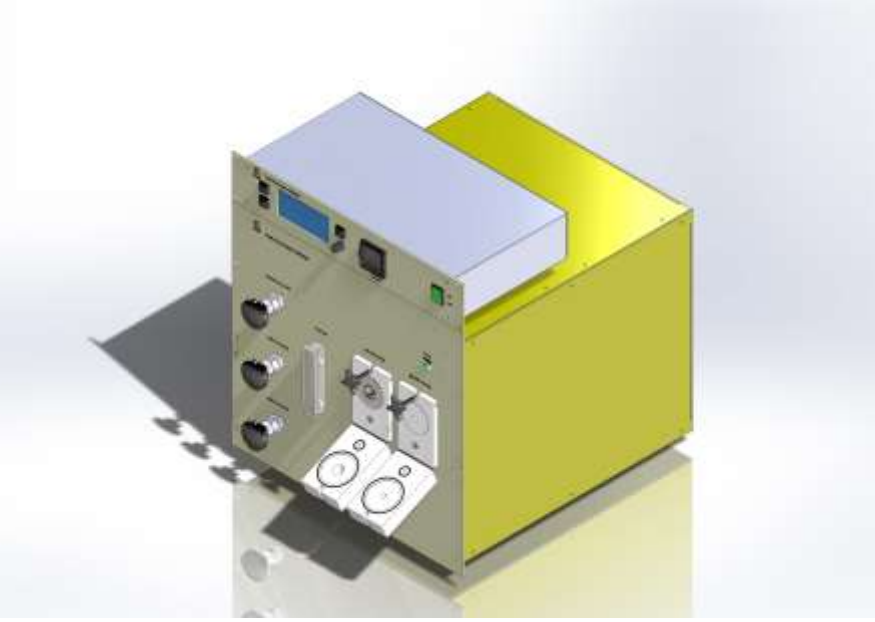

Figure 3: Smoke meter

The North American mobile reference system will need to comply with the Canadian electrical standards. To gain approval for use in Canada, the system must pass a field evaluation (FE) performed by a third party recognized by ESA. This field evaluation will take place on location at Missouri S&T, and will necessitate paid travel and time of an ESA recognized inspector. The field evaluation process follows CSA SPE-1000 standard, which requires three mandatory tests; these tests are non-destructive and ensure the electrical safety requirements meet CEC standards and the equipment can be operated safely. During the field evaluation process, the Missouri S&T team will be provided documentation of failures, and will be required to make modifications as necessary. Once modifications are complete, inspections will resume until the field evaluator is satisfied and the North American mobile reference system is deemed electrically safe according to ESA and CEC standards. It is projected that a minimum of three trips will be required by an ESA recognized inspector: initial inspection with the Missouri S&T team and electrician to identify necessary upgrades, follow-up inspections to critique and further guide the Missouri S&T team and electrician, and final inspection. Once deemed safe, a serialized FE label will be put on each individual piece of equipment.

Milestone(s)

Completed

Major Accomplishments

Upgrades were completed. The North American Reference System can now be used in Canada without any limitation.

Publications
None

Outreach Efforts
None.

Awards
None

Student Involvement
None.

Plans for Next Period
With these tasks being completed the NARS has been upgraded to include gaseous and smoke emissions measurement capabilities and has been certified as compliant for use in Canada.

Task 3: nvPM measurements at RR Indianapolis
Missouri University of Science and Technology

Objective(s)
To gather emissions data on a RR engine, an engine identified by PMTG for inclusion in their nvPM emissions database to develop a metric to regulate nvPM.

Research Approach
Missouri S&T will deploy the North American nvPM mobile reference system at an OEM facility (Rolls-Royce, Indianapolis, IN) to gather emissions data on the engine. This engine is a mixed turbo-fan engine and one that has been identified by PMTG for inclusion in their nvPM emissions database to develop a metric to regulate nvPM. The data from this test will also be valuable to the SAE E-31 committee as they draft a nvPM ARP.

Missouri S&T will work with Rolls-Royce to plan and prepare for the nvPM measurements. During the planning process, a detailed plan for the test will be developed in collaboration with Rolls-Royce. The plan will include details of the sample extraction system, interfacing with the North American nvPM mobile reference system, measurement protocol, and data analysis. Essential details regarding placement of sampling and measurement system, interfacing with existing probe-rake hardware, power and air requirements, etc. will also be discussed.

After the test plan has been developed and approved, and a test window identified, Missouri S&T will begin preparation for deploying the system to the Rolls-Royce facility in Indianapolis, including but not limited to, calibration of instruments, checkout of various system components, and preparing the system for transport. The nvPM system will be deployed alongside Annex 16 Volume II certification-grade gaseous and smoke measurement systems to obtain the full complement of gaseous and nvPM data.

The testing itself will be conducted in accordance with the test plan developed during the planning phase. Data for nvPM mass, number, and gaseous emissions and smoke number will be acquired for a range of engine power conditions, spanning the full realistic parameter space using a multipoint probe similar to those used for gaseous emissions certification. The OEMs will be responsible for providing the probe system to be used for these tests. Following the test, the data will be analyzed and reported.

Milestone(s)
Task completed

Major Accomplishments
Measurements and analysis completed. RR-Indy has provided the data to ICAO Committee on Aviation Environmental Protection for an LTO based nvPM mass and number standards.

Publications
None.

Outreach Efforts
This test afforded RR-Indy testing personnel to experience firsthand the deployment of the NARS for nvPM emissions characterization.

Awards
None.

Student Involvement
None.

Plans for Next Period
None.

Task 4: nvPM measurements at P&W
Missouri University of Science and Technology

Objective(s)
To gather emissions data on a P&W engine, an engine identified by PMTG for inclusion in their nvPM emissions database to develop a metric to regulate nvPM.

Research Approach
Missouri S&T will deploy the North American nvPM mobile reference system at an OEM facility (Pratt and Whitney) to gather emissions data on the P&W engine. This engine has been identified by PMTG for inclusion in their nvPM emissions database to develop a metric to regulate nvPM. The data from this test will also be valuable to the SAE E-31 committee as they draft a nvPM ARP.

Missouri S&T will work with P&W to plan and prepare for the nvPM measurements. During the planning process, a detailed plan for the test will be developed in collaboration with P&W. The plan will include details of the sample extraction system, interfacing with the North American nvPM mobile reference system, measurement protocol, and data analysis. Essential details regarding placement of sampling and measurement system, interfacing with existing probe-rake hardware, power and air requirements, etc. will also be discussed.

After the test plan has been developed and approved, and a test window identified, Missouri S&T will begin preparation for deploying the system to the P&W facility in Connecticut, including but not limited to, calibration of instruments, checkout of various system components, and preparing the system for transport. The nvPM system will be deployed alongside Annex 16 Volume II certification-grade gaseous and smoke measurement systems to obtain the full complement of gaseous and nvPM data.

The testing itself will be conducted in accordance with the test plan developed during the planning phase. Data for nvPM mass, number, and gaseous emissions and smoke number will be acquired for a range of engine power conditions, spanning the full realistic parameter space using a multipoint probe similar to those used for gaseous emissions certification. The OEMs will be responsible for providing the probe system to be used for these tests. Following the test, the data will be analyzed and reported.

Milestone(s)
Testing completed December 14, 2016. Data analysis underway.

Major Accomplishments
None.

Publications
None.

Outreach Efforts
None.

Awards
None.

Student Involvement
None.

Plans for Next Period
Complete data analysis and prepare report.

Plans for Next Period
None.

Task 5: nvPM measurements at the VARIANT 2 Campaign
Missouri University of Science and Technology

Objective(s)
a) Upgrade the measurement capability of the North American reference system to sample nvPM emission from mixed flow engines certified in the mixed flow configuration

b) Participate in the VAriable Response In Aircraft nvPM Testing (VARIAnT) 2 campaign

Research Approach
The VAriable Response In Aircraft nvPM Testing (VARIAnT) campaign was conducted in Aug/Sep 2014 to (1) better understand variability within a single measurement system versus the allowable range of operational parameters, (2) better understand variability between (two) measurement systems and (3) better define variability among instruments of the same and different types. The PM sources used during the study included a miniCAST burner and a small GE J-85 turbojet engine. The study concluded that the system specifications for the sampling system and number measurement instrument were sufficiently robust. In terms of the mass measurement instruments the LII was found to be consistently lower than the NIOSH 5040 EC concentration by ~20% while using the miniCAST as the source and ~40% on J-85 engine emissions.

A subsequent study – MANTRA (Mass Assessment of nvPM Technology Readiness for Aviation) was conducted during Dec 2014 – April 2015 to further explore the differences in mass concentration reported by LII to that of MSS and NIOSH using laboratory and gas turbine emission sources. The primary objective of this study was to investigate the calibration source criterion impact on differences observed between LII and MSS mass instruments when applied to aviation engine PM measurements. The data from this study is being processed and will be reported on during the SAE E-31 Annual meeting in June 2015.

The VAriable Response In Aircraft nvPM Testing (VARIAnT) 2 campaign is currently scheduled for August 17-31, 2015 with a primary goal to determine the performance of the LII (with new firmware) and MSS using both miniCAST and gas turbine exhaust. This campaign will attempt to reproduce selected results from the MANTRA study with respect to both instrument performance and calibration protocol.

Milestone(s)
Analysis complete.

Major Accomplishments

Analysis completed and reported to ASCENT advisory board.

Publications
None.

Outreach Efforts
None.

Awards
None.

Student Involvement
None.

Plans for Next Period
None.

Task 6: nvPM measurements at Honeywell
Missouri University of Science and Technology

Objective(s)
a) Conduct non-volatile PM Emissions measurements of a turbofan engine at Honeywell

b) Validate ambient condition corrections for non-volatile PM Emissions measurements

Research Approach
Missouri S&T will deploy the North American nvPM mobile reference system at the Honeywell facility (Phoenix/San Tan, AZ) to gather emissions data on a mixed turbofan engine that has been identified by PMTG for inclusion in their nvPM emissions database to develop a metric to regulate nvPM. The data from this test will also be valuable to the SAE E-31 committee as they draft a nvPM ARP.

Missouri S&T will work with Honeywell to plan and prepare for the nvPM measurements. During the planning process, a detailed plan for the test will be developed in collaboration with Honeywell. The plan will include details of the sample extraction system, interfacing with the North American nvPM mobile reference system, measurement protocol, and data analysis. Essential details regarding placement of sampling and measurement system, interfacing with existing probe-rake hardware, power and air requirements, etc. will also be discussed. Honeywell will deploy their nvPM system in parallel and the data obtained will be used to compare the performance of the Honeywell nvPM system with the North American mobile reference system.

After the test plan has been developed and approved, and a test window identified, Missouri S&T will begin preparation for deploying the system to the Honeywell facility in Arizona, including but not limited to, calibration of instruments, checkout of various system components, and preparing the system for transport. The nvPM system will be deployed alongside Annex 16 Volume II certification-grade gaseous and smoke measurement systems to obtain the full complement of gaseous and nvPM data. In addition to measurements of nvPM number and mass-based emissions, ancillary instruments will also be deployed to characterize the nvPM in terms of particle size and composition.

All testing will be conducted in accordance with the test plan developed during the planning phase. Data for nvPM mass, number, and gaseous emissions and smoke number will be acquired for a range of engine power conditions, spanning the full realistic parameter space using a multipoint probe similar to those used for gaseous emissions certification. Honeywell will be responsible for providing the probe system to be used for these tests. Following the test, the data will be analyzed and reported.

As part of the standard setting process, corrections for measured nvPM emissions at various ambient conditions, similar to those employed for gaseous species, will need to be developed. Missouri S&T is currently working with GE Aviation conduct an nvPM emissions measurement campaign in an altitude test cell to acquire data that will be used to develop first order ambient conditions corrections of nvPM number- and mass-based emissions. These first order corrections will need to be validated in subsequent test to evaluate its applicability to a range of turbofan engines. Such validation is planned during the engine tests scheduled for Honeywell. Missouri S&T will review the Honeywell data and data from other engines tests conducted over a wide range of ambient conditions to validate the methodology and the model developed in previous campaign with GE Aviation.

Milestone(s)
Analysis completed

Major Accomplishments
Analysis completed and reported to agencies participating in the NDA associated with this task. Honeywell has provided the data to ICAO Committee on Aviation Environmental Protection for an LTO based nvPM mass and number standards.

Publications
None.

Outreach Efforts
None.

Awards
None.

Student Involvement
None.

Plans for Next Period
None.

Task 7: Engine to Engine Variability and Derivation of Characteristic nvPM Emissions
Missouri University of Science and Technology

Objective(s)
a) Conduct non-volatile PM Emissions measurements of a large number of turbofan engines at Honeywell

b) Analyze the data acquired to assess the characteristic variability of these engines for nvPM emissions

Research Approach
Honeywell will deploy their nvPM and gaseous emissions measurement system. Honeywell will work with Missouri S&T to plan and prepare for the nvPM measurements. During the planning process, a detailed plan for the test will be developed. The plan will include details of the sample extraction system, measurement protocol, and data analysis. Essential details regarding placement of sampling and measurement system, interfacing with existing probe-rake hardware, power and air requirements, etc. will also be discussed.

After the test plan has been developed and approved, and a test window identified, the Honeywell nvPM measurement system will be setup at the engine test facility in Phoenix, AZ. All testing will be conducted in accordance with the test plan developed during the planning phase. Data for nvPM mass, number, and gaseous emissions will be acquired for a

range of engine power conditions, spanning the full realistic parameter space using a multipoint probe similar designed to sample engine exhaust from the core flow. Honeywell will be responsible for providing the probe system to be used for these tests.

Following the emissions measurement tests, all the data collected will be reduced and analyzed. The nvPM number- and mass-based emissions data for each engine at each engine operating condition will be compared. This dataset will then be used to assess the characteristic variability in nvPM emissions for this particular engine type.

Milestone(s)
None

Major Accomplishments
None

Publications
None.

Outreach Efforts
None.

Awards
None.

Student Involvement
None.

Plans for Next Period
None.

Project 003 Cardiovascular Disease and Aircraft Noise Exposure

Boston University

Project Lead Investigator

Junenette L. Peters
Assistant Professor
Department of Environmental Health
Boston University School of Public Health
715 Albany St., T4W, Boston, MA 02118
617-638-4679
petersj@bu.edu

University Participants

Boston University (BU)

- P.I.(s): Jonathan Levy (University PI); Junenette Peters (Project PI)

FAA Award Number: 13-C-AJFE-BU-002;

- Period of Performance: September 1, 2015 to August 31, 2016
- Task(s):
  1. Assign aircraft noise exposures over time to geocoded participant addresses.
  2. Link to existing roadway proximity / density exposure measures by geocoded participant addresses.
  3. Link to air pollution measures by geocoded participant addresses.
  4. Link to participant individual data.
  5. Develop approaches for determining quantitative estimates of historical noise exposures for time periods when Aviation Environmental Design Tool (AEDT) modeling data are not available.
  6. Explore the Atherosclerosis Risk in Communities (ARIC) Study cohort for combined or sensitivity analysis on noise and CVD.

Project Funding Level

Total Funding $200,000
Matching: $66,667
Source of Matching: Non-federal donor to the Women's Health Initiative (WHI) cohort

Investigation Team

Junenette Peters, PI, Boston University

Dr. Peters is responsible for directing all aspects of the proposed study, including study coordination, design and analysis plans, and organizing co-investigator meetings.

Jonathan Levy, Boston University

Dr. Levy will participate in the noise exposure assessment effort and provide expertise in the area of predictive modeling and air pollution.

Eric Whitsel, University of North Carolina at Chapel Hill

Dr. Whitsel's team will assign aircraft noise exposures to geocoded WHI cohorts' participant address coordinates. Dr. Whitsel will also provide expertise related to cardiovascular outcomes and the WHI. Eric is our WHI sponsor, which is required for obtaining WHI approval to conduct an ancillary study.

Gregory Wellenius, Brown University

Dr. Wellenius will assist with documentation of data from the Women's Health Initiative (WHI) based on previous experience working on air pollution and cardiovascular disease research in the cohorts.

Project Overview

Aircraft noise is a considerable source of stress among near-airport communities. Exposure has been associated with sleep disturbance, physiological responses and psychological reactions, with corresponding effects on blood pressure. However, the extent to which aircraft noise increases the risk of cardiovascular disease (CVD) has not been fully elucidated. Likewise, the role of CVD risk factors in mediating an association between noise and CVD has not been assessed. Additionally, exposure assessment that includes time-varying and spatially resolved noise exposures has not been systematically incorporated into previous epidemiological studies. This study proposes to evaluate the effects of aircraft noise exposure on CVD in the longitudinal Women's Health Initiative (WHI) study cohorts, in which over 160,000 women were recruited from 1993 to 1998 from 40 clinics in 24 states.

Task 1. Assign aircraft noise exposures over time to geocoded participant addresses.

Boston University

Objective

To intersect geocoded addresses available from 1993 to 2012 with noise surfaces obtained.

Research Approach

Dr. Whitsel at UNC will intersect geocoded addresses available from 1993 to 2012 with noise surfaces, which will be developed by spatially interpolating between point estimates from AEDT or predictive models following standard procedures developed by the Physical and Built Environment Scientific Interest Group (SIG) to safeguard confidentiality. Given the longitudinal nature of this study, noise exposures will be assigned reflecting specific residential addresses over time based on participant address histories.

Milestone

- Receive aircraft noise data for multiple airports and years in various metrics.
- Execute final Data and Materials Transfer and Use Agreement (DTMUA) with WHI Coordinating Center, FAA and BU.
- Receive documentation (metadata) for noise data modeling.
- Resolve concerns about differences in attributes and methods used to generate data by data modeling sources.
- Assign noise exposure to WHI participants over time.

Major Accomplishments

- We have received aircraft noise data for 90 airports for the years 2000, 2005 and 2010; metrics received include Day-Night Average Sound Level *(*DNL*)*, Equivalent Sound Level (Leq), Leq Day and Leq Night.
- Executed final DTMUA with WHI Coordinating Center, FAA and BU.
- We have linked WHI participants to 2000 DNL to identify the number of participants by region, airport and participant race/ethnicity.
- We received and reviewed draft noise modeling documentation (metadata).

Publications

None

Outreach Efforts

None

Awards

None

Student Involvement

None

Plans for Next Period

- Obtain final metadata on aircraft noise modeling.
- Resolve modeling differences by data source.
- Assign all noise exposure estimates to participants.

Task 2. Link to existing roadway proximity / density exposure measures by geocoded participant addresses.

Boston University

Objectives

The objective of this task is link with roadway proximity/density measures for geocoded participant addresses.

Research Approach

We will link to roadway proximity / density measures previously developed for the WHI, which have been estimated for primary highways (A1), primary roads (A2), and secondary and connecting roads (A3) at geocoded addresses of the WHI CT and OS participants, 1993-2012. The estimates are expressed as distances to the nearest roadway of a given type and summed roadway lengths of a given type, each within geocoded participant address-centric buffers of 100-500 meters. This road proximity exposure estimate is considered a surrogate for traffic noise and traffic-related air pollution.

Milestone(s)

- Linked road proximity exposure estimates.

Major Accomplishments

None

Publications

None

Outreach Efforts

None

Awards

None

Student Involvement

None

Plans for Next Period

To link road proximity exposure estimates to dataset of aircraft noise exposure assignments.

Task 3. Link to air pollution measures by geocoded participant addresses.

Boston University

Objective

To link air pollution exposure data for geocoded participant addresses.

Research Approach

Data will also be linked to air pollution exposure data from the ongoing ancillary study with WHI headed by Dr. Wellenius.

Milestone(s)

- Dataset with linked air pollution exposure data.

Major Accomplishments

None

Publications
None

Outreach Efforts
None

Awards
None

Student Involvement
None

Plans for Next Period
Link air pollution exposure data to dataset of aircraft noise exposure assignments.

Task 4. Link to participant individual data.

Boston University

Objective
To link to participant individual data.

Research Approach
Exposure estimates will be linked to WHI cohort data. Cohort data will be anticipated to include socio-demographic data (e.g., age, race/ethnicity, education); behavioral (e.g. physical activity/exercise, diet, smoking, alcohol consumption); other (e.g., hearing and hearing loss, sleep disturbance); and clinical (e.g., body mass index; lipids; blood pressures, hypertension; glucose, insulin, diabetes; heart rate and its variability; CVD and CVD mortality).

Milestone
- Dataset with linked participant individual data.

Major Accomplishments
None

Publications
None

Outreach Efforts
None

Awards
None

Student Involvement
None

Plans for Next Period
Link individual participant data to dataset of aircraft noise exposure assignments.

Task 5. Determine approaches for estimating historical noise exposures for time periods when Aviation Environmental Design Tool (AEDT) modeling data are not available.

Boston University

Objective

AEDT modeling is not be available for certain years including the baseline (recruitment) period (1993 to 1998). We will use linear interpolation to estimate noise exposure for missing years that lie between years with available AEDT modeling data for a given airport.

Milestone(s)

- Approaches for performing historical modeling pre-2000.
- Approaches for years not modeled post 2000.

Major Accomplishments

- Recently negotiated to receive AEDT modeled aircraft noise data for 1995.

Publications

None

Outreach Efforts

None

Awards

None

Student Involvement

None

Plans for Next Period

Develop plan to assign noise exposure for years between intervals 1995-2000, 2000-2005, 2005-2010.

Task 6. Explore the ARIC cohort for combined or sensitivity analysis on noise and CVD.

Boston University

Objective

The objective of this task is to explore cohorts with both men and women.

Research Approach

We will explore the ARIC cohort for combined analysis with the WHI or to perform sensitivity analysis to determine whether there are significant differences in the exposure-outcome relationship by gender. This task will include determining the number of participants in ARIC surrounding airports.

Milestone(s)

- Knowledge of other cohorts including the ARIC cohort
- Determining the number of participants in the other cohorts surrounding airports

Major Accomplishments

- Team has determined the number of ARIC participants surrounding airports. The number of participants surrounding airports is small (N=239), so the ARIC cohort will not be used for this research effort.
- However, the team was approached by researchers from the Nurses' Health Study (NHS), which also includes the Health Professional Follow-up Study (HPFS; cohort of men).
- We have developed a collaboration to begin work on noise-health research in the NHS and HPFS.
- We have determined the number of participants of NHS and HPFS surrounding airports.

Publications

None

Outreach Efforts
None

Awards
None

Student Involvement
None

Plans for Next Period
- Perform noise-health research in the NHS and HPFS cohorts.
- Research involving the WHI cohorts is now being funded by the National Institutes of Health (NIH) [August 2016 to June 2020].

References

[1]Federal Aviation Administration. Aviation Environmental Design Tool (AEDT). https://aedt.faa.gov/.

[2]Stewart PA, Vermeulen R, Coble JB, et al. The Diesel Exhaust in Miners Study: V. Evaluation of the Exposure Assessment Methods. *Ann Occup Hyg.* Mar 1 2012.

[3]Vermeulen R, Coble JB, Lubin JH, et al. The Diesel Exhaust in Miners Study: IV. Estimating historical exposures to diesel exhaust in underground non-metal mining facilities. *Ann Occup Hyg.* Oct 2010;54(7):774-788.

[4]Hart JE, Yanosky JD, Puett RC, et al. Spatial modeling of PM10 and NO2 in the continental United States, 1985-2000. *Environ Health Perspect.* Nov 2009;117(11):1690-1696.

[5]Yanosky JD, Paciorek CJ, Suh HH. Predicting chronic fine and coarse particulate exposures using spatiotemporal models for the Northeastern and Midwestern United States. *Environ Health Perspect.* Apr 2009;117(4):522-529.

[6]Davis ME, Hart JE, Laden F, Garshick E, Smith TJ. A retrospective assessment of occupational exposure to elemental carbon in the U.S. trucking industry. *Environ Health Perspect.* Jul 2011;119(7):997-1002.

[7]Davis ME, Laden F, Hart JE, Garshick E, Blicharz A, Smith TJ. Predicting changes in PM exposure over time at U.S. trucking terminals using structural equation modeling techniques. *J Occup Environ Hyg.* Jul 2009;6(7):396-403.

Project 004(A) Estimation of Noise Level Reduction

Georgia Institute of Technology
University of Nebraska - Lincoln

Team of Investigators

Georgia Institute of Technology (GT)
- P.I.(s): Kenneth Cunefare, Professor of Mechanical Engineering
  Javier Irizarry, Associate Professor of Building Construction

University of Nebraska – Lincoln (UNL)
- P.I.(s): Erica Ryherd, Associate Professor of Architectural Engineering

Student Involvement
Two primary graduate students assisted in this project. Multiple students from the GT College of Architecture and Building Construction Program assisted in the test house construction.

René Robért was the lead graduate research assistant on this project. He was involved in almost all aspects of the work. He conducted all of the field NLR measurements and was responsible for analyzing the differences in field-measured NLR results. René graduated with his Master's Degree in Mechanical Engineering from GT in December 2015.

Hyun Hong was a graduate research assistant who contributed to a portion of the project. He was involved in Task 2B: Compare Field Measurements and Model Simulations. He was responsible for generating the models in IBANA-Calc and comparing the results to René's field measured data. Hyun graduated with his PhD in Architectural Engineering from UNL in December 2015.

Project Overview

FAA Award Number: 13-C-AJFE-GIT-005

The specific goal of Project 4A was to better understand and improve the outdoor loudspeaker methods of estimating the noise level reduction (NLR) performance of buildings exposed to aircraft noise. Measurements and modeling were conducted on a test house located outdoors with a loudspeaker placed at an array of spatial positions to simulate angular coverage of aircraft flyover in both vertical and lateral directions. Results were used to evaluate and compare various NLR estimating approaches.

Project Summary

Task 1: Conduct Field NLR Study

Task 1A: Test House Construction, Iterations, and Deconstruction
A test house was constructed to allow for direct measurement of NLR outdoors under semi-controlled conditions. Subtasks included securing and preparing a construction site, estimating construction materials, material procurement, material delivery, student training, test house construction, and test house iterations. The test house was a single-room structure of approximately 90 ft^2. It was constructed to be typical of the mixed-humid climate region in Atlanta, GA, with fiber-cement siding, an asphalt-shingled roof, and a single hung vinyl window [1,2]. The test house was constructed on the GT campus in an open green space. Two construction iterations were implemented: a) window type, and b) window condition. For the window type iteration, two windows with differing acoustical performance were measured (STC 25 and STC 31). For the window condition iteration, three positions were measured (closed, ½ open, and fully open). The test house was deconstructed after acoustic NLR measurements (Task 1B) were completed.

Task 1B: Acoustic NLR Measurements

NLR was directly measured in accordance with industry best practices and ASTM E966 [3, 4]. To summarize, a loudspeaker was located outside of the test house playing pink noise, a standard noise reduction measurement signal. Sensors located both inside and outside the test house captured NLR performance data. Three instrumentation iterations were implemented: a) source vertical location, b) source horizontal location, and c) sensor location.

The vertical and horizontal location iterations were included to investigate an array of spatial positions that simulate angular coverage of real aircraft flyover in both vertical and lateral directions. Two mounting methods were used to achieve a range of vertical locations: i) tripod mounting (3.4' and 7'), and ii) lift mounting (15', 20', and 30'). The range of horizontal angles was achieved by moving the source along fixed radial and linear increments.

Three sensor locations were included: i) fixed near, ii) fixed flush, and iii) moving. In the fixed near method, microphones were placed at a distance from the exterior façade surface. In the fixed flush method, microphones were located flush to the exterior façade surface. In the moving method, the microphone was dynamically swept along a path. The moving method was identified as one commonly used by industry practitioners. Guidance was provided by Landrum & Brown on appropriate implementation of this method.

In total, 197 construction and instrumentation iterations were measured, using a combination of the following iteration variables:

- Source vertical location
  - 3.4', 7', 15', 20', 30'
- Source horizontal location
  - 0°, ±15°, +30°, -35°, ±45°, +60°, +75°
- Sensor location
  - fixed near, fixed flush, moving
- Window type
  - STC 25, STC 31
- Window condition
  - closed, ½ open, fully open

Task 2: Evaluate NLR Estimation Approaches

NLR estimation approaches were evaluated by: a) analyzing differences in field-measured NLR for the various construction and instrumentation iterations, and b) comparing a subset of the field-measured NLR to model simulations.

Task 2A: Analyze Differences in Field-Measured NLR Iterations

The field-measured NLR results were compiled and analyzed using Excel software. Averages, confidence intervals, and graphical inspection techniques were used to compare results across various combinations of iterations. Extensive analyses were conducted to analyze the differences in the 197 field-measured NLR iterations. Examples are shown below.

Repeatability and Reproducibility Analysis

An analysis of the repeatability and reproducibility of the three sensor iterations (fixed near, fixed flush, and moving) was conducted. The repeatability test compared the results of a single test configuration multiple times. It therefore revealed the within-test variability, or the ability of a specific test to be implemented multiple times with comparable results. The reproducibility test compared the results of different test configurations. It therefore revealed the between-test variability, or the ability for various test configurations (allowed within the standard) to yield comparable results.

The fixed flush method was found to be the most repeatable— that is, it provided the most precise results when implementing identical tests. The repeatability 95% confidence interval (CI) for the fixed flush method was calculated to be ±0.3 dB. However, it was determined that the moving method provided the most reproducible results with a 95% confidence interval (CI) of ±0.5 dB. Reproducibility is a better metric of precision as it is the precision for a procedure rather than a specific test; thus, it was concluded that the moving method was the most precise procedure.

Differences Across Iterations
The variation in NLR measurements caused by the source location was measured with a loudspeaker mounted on a tripod and man lift with an STC 25 window. With the loudspeaker mounted on a tripod and altered on the radial locations at an angle of incidence of 75˚, the NLR values decreased likely due to the side façade affecting the measurement of the front façade since the speaker was approaching grazing. The locations of the tripod were also varied linearly such that the source variations were on the same plane at an equal offset from the façade. These locations resulted in a measured NLR an average of 1 dB less than the average NLR measured for the radial locations. This was expected since the speaker was nearly forty feet away from the center of the façade for the loudspeaker at the 75˚ angle of incidence linear location. The average moving test across all angles of incidence was 1 dB less than the average measured by the fixed near and fixed flush methods.

The testing performed with the speaker mounted on the man lift was used to evaluate the vertical angle of incidence as well as the symmetry of the measurements, but no clear angular dependency was observed. It was determined that the measurements were not symmetric for the test house, as the NLR values were not consistently similar across either side of normal incidence. The lack of symmetry in NLR measurements is likely due to flanking paths present in the construction. Once again, the moving method measured NLR values about 1 dB less than the fixed flush method. When comparing the measurements between the tripod and lift testing, it was determined that the tripod mounted testing resulted in NLR values that were less than the lift mounted testing.

Testing was also completed with two construction iterations: the acoustic performance of the window and window condition. In addition to the testing performed with the STC 25 window, NLR of the test house with an STC 31 window was also measured. The changing of the window offered minimum changes in NLR. The minimal changes were likely due to flanking paths present in the walls of the test house. Application of expanding foam to minimize flanking paths resulted in an average increase of 3.4 dB NLR; however, there was still no clear angular dependency after applying the foam.

Task 2B: Compare Field Measurements and Model Simulations
A subset of iterations were modeled in composite sound transmission software (IBANA-Calc) and compared to the field-measured results. In total, 27 iterations were modeled, using the following iteration variables:

- Source vertical location
  - 3.4’, 7’, 15’, 30’
- Source horizontal location
  - 15°, 45°, 75°
- Sensor location
  - fixed near, fixed flush, moving
- Window type
  - STC 25, STC 31
- Window condition
  - closed, ½ open, fully open

The difference between measured and modeled predictions was calculated using two measures: a) $|\Delta NR|$, and b) $|\Delta TL|$. Both measures were averages of the differences between measured and modeled predictions across the frequency range 315 – 5000 Hz. The $|\Delta NR|$ was a direct measure of the difference between measured and modeled results. The $|\Delta TL|$ was found by accounting for the horizontal angle of incidence. Results showed that the difference between measured and modeled was less than 3-5 dB for approximately 57% of the iterations ($|\Delta NR|$) and 83% of the iterations ($|\Delta TL|$) depending on the metric evaluated.

Task 3: Synthesize Findings and Future Steps

A variety of NLR estimation approaches were compared and evaluated. Overall, changes in NLR were observed across all of the measurements, but the measurements did not exhibit consistent angular dependency. It is suggested to implement the moving method for NLR measurements with the loudspeaker test as it was the most reproducible. Future testing should examine the correction factor for the moving method, as the average NLR for the radial locations test with both windows and the lift mounted tests was at least 1 dB less than the fixed flush method. Additionally, correction factors should be considered when measuring NLR with a tripod mounted speaker rather than an elevated source or when altering the source locations linearly rather than radially. A set procedure to measure NLR with a loudspeaker would also be beneficial in reducing variations allowed currently.

Comparisons between the loudspeaker and aircraft flyover method should be examined further, including the overall accuracy of each method. Currently, the measurements do not appear to be similar due to the characteristics of the sources; a fixed point source and a time varying line source are used as equivalent methods of testing a spectrum dependent method. The artificial noise source method may be better suited to perform measurements to determine the acoustic performance of a building before and after modifications, as is stated as the primary goal of these measurements for the FAA in ASTM E966-10. In other words, the artificial noise method may be better suited for comparative rather than absolute measurements.

Task 4: Collaborations

The objective of Task 4 was to collaborate with others from ASCENT and industry to strengthen the overall project. The GT Team collaborated with the University of Washington (UW), the Pennsylvania State University (PSU), and Landrum & Brown on various aspects of the project.

The team collaborated with The University of Washington (UW) on their ASCENT Project 4B. The goal of their project was to investigate a new, phased array microphone method to measure NLR. Several telecons were held to share information and exchange ideas on Project 4A and 4B. In addition to the periodic telecons, all members listed above were copied on the monthly briefs submitted to the FAA.
Participants included:

- K. Cunefare, J. Irizarry, R. Robért (GT)
- E. Ryherd (UNL)
- R. Doughtery and M. Kurosaka (UW)
- V. Sparrow (PSU)
- H. He (FAA)

The team also collaborated with Landrum & Brown, including a site visit by Landrum & Brown to the GT test house in December 2014.

Task 5: Travel Associated with the Project

The objective of Task 5 was to conduct appropriate travel associated with the project to foster collaboration, feedback, and information dissemination. The team participated in ASCENT meetings. Additionally, project funds, cost-share, and other funds were used to partially support travel to professional conferences.

The team participated in the three bi-annual ASCENT meetings during the project period. The team prepared slides which were presented by E. Ryherd and R. Robert and feedback was solicited from the ASCENT attendees. This included:

- ASCENT Fall 2014 Advisory Committee Meeting; October 2014; Alexandria, VA
- ASCENT Winter 2015 Advisory Committee Meeting; March 2015; Alexandria, VA
- ASCENT Fall 2015 Advisory Committee Meeting; October; Seattle, WA

The Advisory Committee and other attendees at these meetings provided many useful suggestions and comments that were incorporated into the project. These discussions helped facilitate directions of P4A.

References

1. U.S. DOE (2004)"Introduction to building systems performance: Houses that work II", NREL/SR-550-345-85, *Building America*, http://www.nrel.gov
2. Building Science Corporation, "Building Profiles", *Enclosures That Work*, (2010). http://www.buildingscience.com
3. Landrum & Brown (2013), "Study of Noise Level Reduction (NLR) Variation," *FAA Technical Directive Memorandum 0017.*
4. ASTM E966-10 (2011): Standard guide for field measurements of airborne sound attenuation of building facades and façade elements, *ASTM International*.

Project 004(B) Estimation of Noise Level Reduction

University of Washington

Project Lead Investigator

Mitsuru Kurosaka
Professor
William E. Boeing Department of Aeronautics and Astronautics
University of Washington
Box 35-2400, Seattle, WA 98195-2400
206 685-2619
kurosaka@aa.washington.edu

University Participants

University of Washington

- P.I.: Mitsuru Kurosaka, Professor, William E. Boeing Department of Aeronautics and Astronautics
- FAA Award Number: 13-C-AJFE-UW-002, 003, and 004.
- Period of Performance: August 18, 2014 to December 23, 2015.
- Tasks:
    1. Construct an isotropic speaker and phased array of microphones
    2. Conduct tests of a test house by ASTM E 966-10 (speaker outside, microphone inside) and by the UW method (speaker inside, microphone outside). Compare the two results to demonstrate the validity of the UW method.

Project Funding Level

$60,000 from the FAA to the University of Washington.
Non-Federal cost share total $ 60,105 consisting of (a) in-kind share of $ 24,125 from the University of Washington, and (b) in-kind cost share of $35,980 from Optinav,1414 127th Pl, NE #106, Bellevue, WA .

Investigation Team

Mitsuru Kurosaka, ,P.I.,professor, Robert P.Dougherty, affiliate associate professor, Tessa L. Robinson, graduate student. Dan Ablog and Ben Turner, undergrads

Project Overview

To improve measurement & modeling technology for characterizing Noise Level Reduction (NLR) of houses.

Task: Estimate of Noise Level Reduction-Assessment of Phased Array of Microphones

University of Washington

Objective

The objective of this activity is to assess the use of phased array of microphones for Noise Level Reduction (NRL) measurements, which can potentially make an improvement on the current ASTM standards E 966-10.

Research Approach

For housing near the airports, the eligibility criteria for the FAA funded Residential Sound Insulation Program (RSIP) are twofold:(1) the exterior noise exceeds 65 dB Day-Night-Average-Sound Level (DNL) and (2) the interior noise exceeds 45 dB DNL. The interior noise is a difference between the exterior noise and the noise level reduction (NLR). The NLR measurement method is based on the ASTM E-966-10, ref. 1, which specifies in detail the use of an artificial sound source placed outside of the house and a set of microphones positioned both outside and inside of the house. The difference between the outside and inside microphone data forms the basis of NLR. The use of a speaker outside of the house, which emits high-intensity sound for a prolonged time, would disrupt and annoy the neighbors. To alleviate this drawback, the goal of the UW efforts is to place a speaker inside of the house and microphone outside, which is the reverse of the ASTM guides. The interior placing of the speaker could substantially reduce the sound level perceived outside of the house and lessen the disturbances to neighbors. From the reciprocity principle of acoustics, the NRL obtained by this reverse arrangement should be equivalent to the one from the conventional ASTM method.

1. **Construction of an isotropic speaker and phased array of microphones**

Strictly speaking, the reciprocity principle upon which the UW method based , is applicable for a simple source. Therefore, as an approximated point source, an isotropic speaker is constructed.

Fig. 1 (left) isotropic speaker inside the bedroom, (right) phased array of speakers outside.

The isotropic speaker is a quasi-spherical, where twelve 6.5 inch, 100 W ceiling loudspeakers (On-Q/Legrand) were mounted in 9 inch pentagons made of ¾ inch plywood. The resulting dodecahedron loudspeaker (Fig. 1, left) was driven with a Dayton Audio MA1240a Multi-Zone 12 Channel Amplifier that can provide up to 40 W per channel with potentially independent inputs and gain control. A General Radio 1382 random noise generator was connected to all of the amplifier inputs, after splitting into the left and right banks. The amplifier gains were all set to about 2/3 of maximum to prevent the smoke that was observed at full power due to evident overheating. The RMS output of the random noise generator was usually set to 2 V. For some runs, the power was reduced by 10 dB by reducing the amplifier input voltage to 0.63 V. Driving all of the loudspeakers was intended to produce an isotropic source. For some runs, the leads for the six loudspeakers on one side of the dodecahedron were disconnected to produce an anisotropic sound source, intended to have directivity that is more representative of a commonly available loudspeaker.
A phased array, Fig. 1 (right), using 24 Panasonic WM-61 electret microphones was constructed with three 1 m arms and logarithmic element spacing on each arm with the element spacing decreasing away from the center of the array. The minimum spacing was constrained by the 2 inch foam windscreens. The arms, with integral OptiNav 8-channel preamplifiers, are removable for transportation. Data were acquired at 48 kHz using a 24-bit MOTU 24I/O audio interface. Thirty seconds of data were record for each condition. Phased array processing was performed using OptiNav Beamform Interactive software. The algorithm used was Robust Asymptotic Functional Beamforming (RAFB). This is a new method that provides quantitative results and offers much lower sidelobes, and hence higher dynamic range, than conventional beamforming. Functional Beamforming, the predecessor of RAFB, is described in Refs. 2 & 3. The robust, asymptotic extension offers improved level accuracy.

2 Description of the field tests

Tests were conducted at a two-bedroom house located at UW Center for Sustainable Forestry at Pack Forest in the Mt. Rainier National Park. Two separate tests were performed: (1) November, 4-8, 2014, and (2) April, 16-17,2015. The façade element tested is the bedroom windows, and the test layout for the UW method is shown in Fig.2 (left). Measurements were made for the four incidence angles as shown. Selected results to be reported herein are for the 0˚ position.

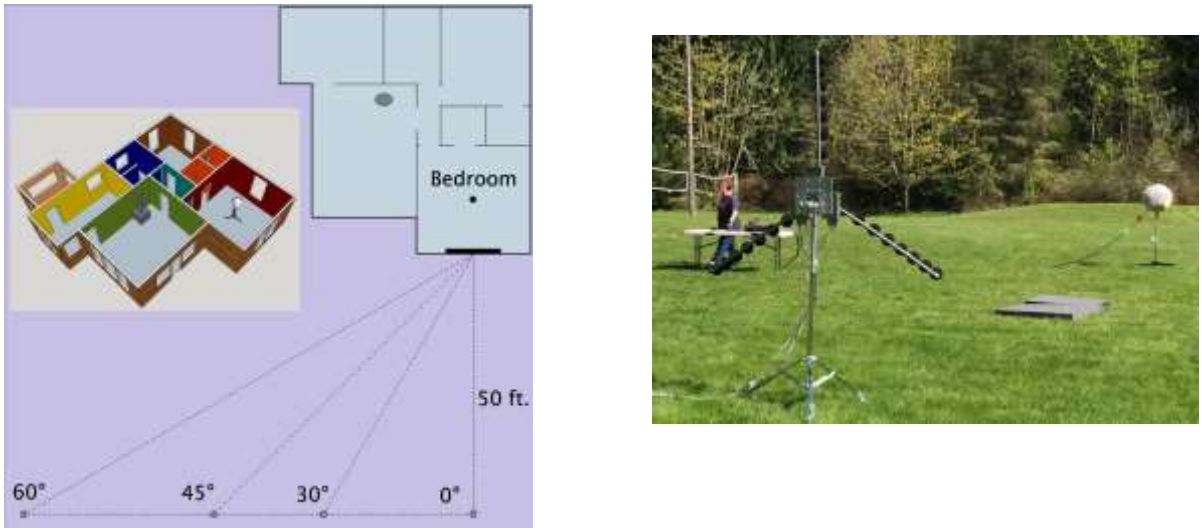

Fig. 2. (left)Test layout for the bedroom window, (right) free field calibration

The free-field test was conducted in an open field near the test house, Fig.2 (right), in accordance with ASTM E-966-10. The distance between the speaker and the microphones was 57ft. The ground reflection was removed using an analytical calculation involving the impedance of grass as given in Ref. 4. The bedroom windows were tested using both the ASTM and UW method. Some representative results obtained by the UW method are shown in Fig. 3, which displays Beamforming images at the 1/12 octave bands of 2114 and 4728 Hz; the bedroom left lower window was open, cracked, and shut. The open and cracked portion of the window are seen clearly in Fig. 3 (d) and (f). Figure 3 (c) shows that propagation thorough the window is important even when it is closed. It also shows the ground reflection and some radiation from parts of the house other than the bedroom.

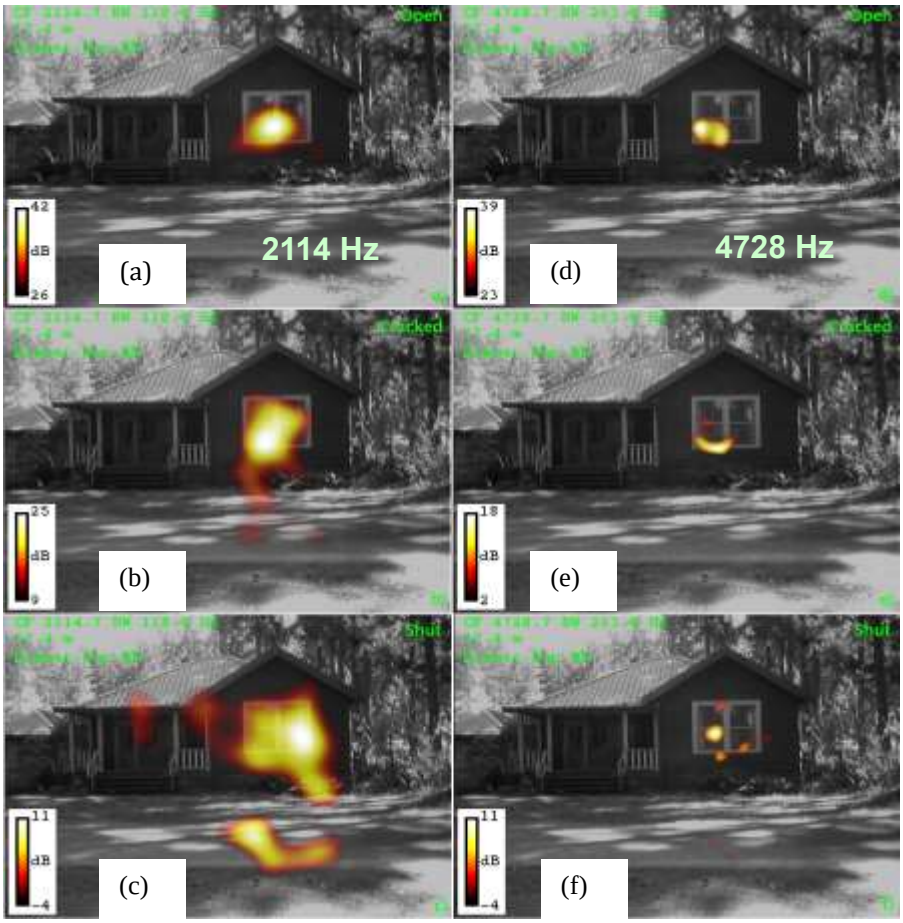

Left lower window fully open

Left lower window cracked open

All windows closed

Fig 3. Images obtained by the phased array of microphone placed outside (the UW method; (a) to (c) at 2114 Hz, (d) to(e) at 4728 Hz.

3. Comparison of the UW and ASTM method

The UW method rests on the reciprocity principle and its validation is shown in Fig. 4. The cases with the left window open and cracked are shown Fig. 4a, and the case with the window shut is given in Fig. 4b. For each window position, the ASTM spectrum, measured with the loudspeaker outside, and the UW, RAFB spectrum, measured with the loudspeaker in the bedroom and the array outside, generally match. This validates the fundamental approach of using reciprocity for the measurement. The agreement is not perfect. There are several factors that can potentially cause the ASTM and UW curves to differ. These include interfering noise, which varies between runs, the placement of the loudspeaker in the bedroom for the UW method in relation to the placement of the microphones in the bedroom for the ASTM method, and the details of the array processing algorithm.

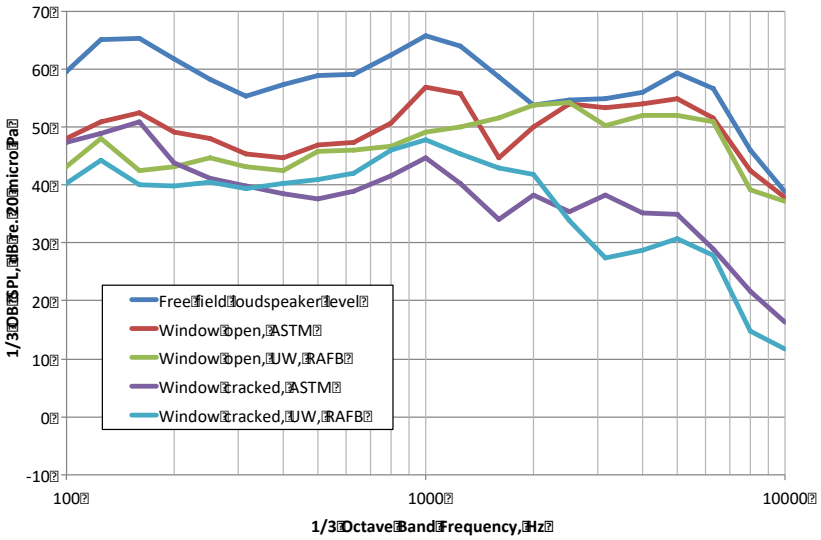

Fig. 4 a – Reciprocity check, window open and cracked.

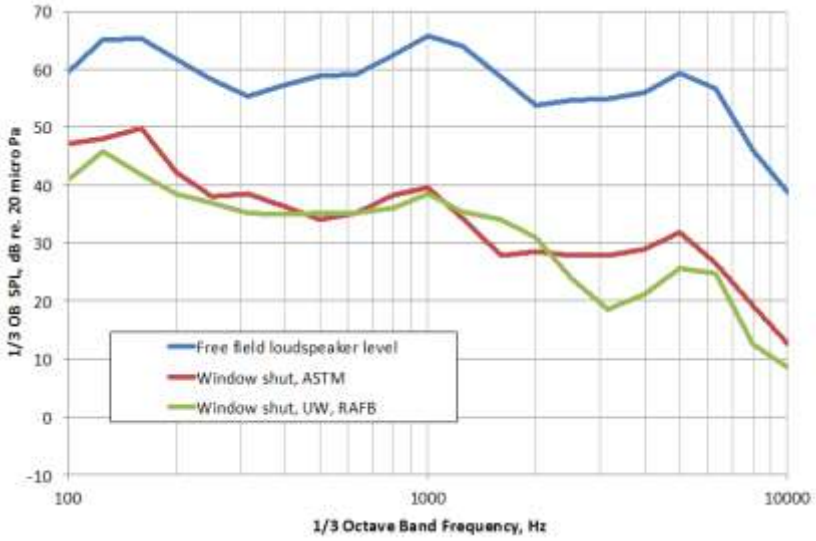

Fig. 4 b – Reciprocity check, window closed.

4. Noise Reduction Level

The 1/3 octave band noise reduction (NR) spectra are shown in Fig. 5. The noise level reduction values derived from the 1/3 OB values according to ASTM E1332-10a , ref. 5, are shown in the legend. The agreement between the NLR values from the ASTM and UW methods is perfect for the open window case. The UW method shows 1.06 dB less noise reduction for the window cracked and 2.82 more reduction for the window shut case. The UW method shows higher NR than ASTM for the window shut case at both high and low frequency. The low frequency difference carries more weight in the computation of the NLR because the NLR formula is more sensitive to changes in smaller NR values than larger ones. Starting with the UW NR spectrum and replacing the NR values for frequencies above 2 kHz with the ASTM NR values, the NLR estimate for the window shut case would drop from 23.79 dB to 23.58 dB. Alternatively, replacing the UW NR values with the ASTM NR values for frequencies below 400 Hz, the NLR for window-shut would become 20.98 dB, matching the observed ASTM result of 20.97 dB. The accuracy of the UW NR values for frequencies below

400 Hz is constrained by the size of the array tested. An array with longer arms would produce more reliable results. More loudspeaker power at low frequency would also improve the results by reducing the reliance on the beamforming at low frequency.

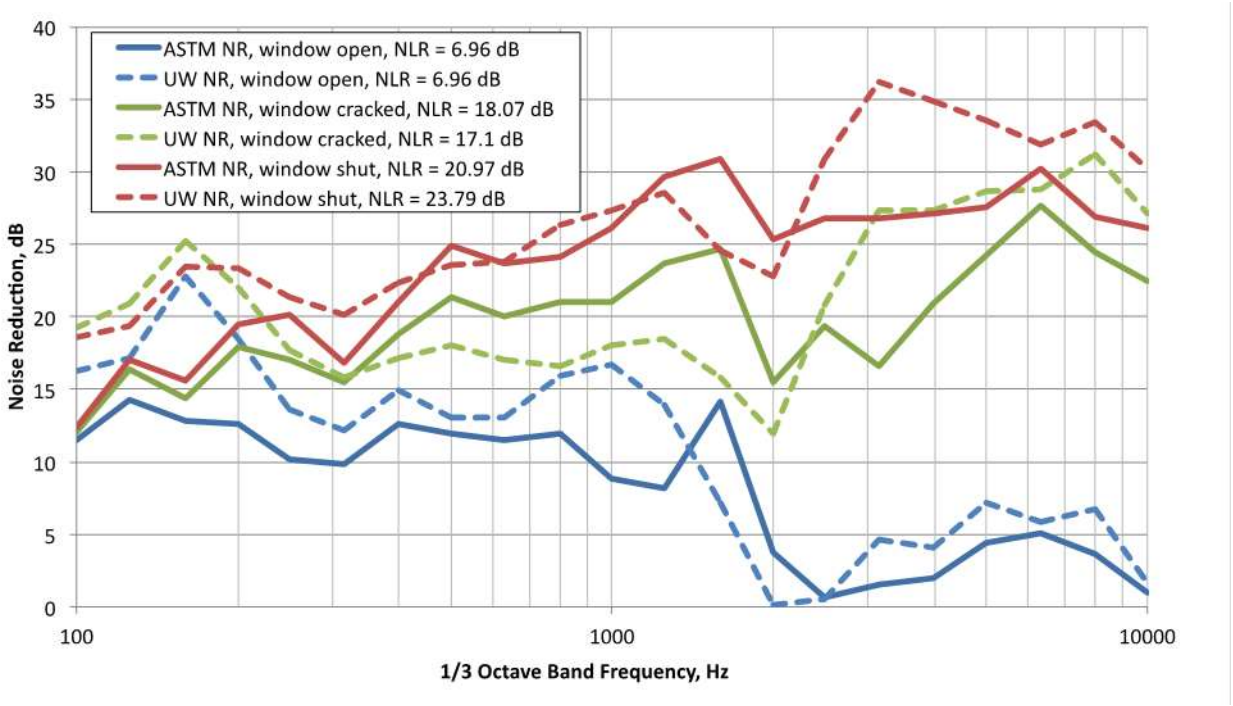

Fig. 5. Noise Level Reduction for several window conditions and measurement methods

References

1. ASTM E 966-10 "Standard Guide for Field Measurements of Airborne Sound Attenuation of Building Façade and Façade Elements", (2011)

2. R.P. Dougherty, "Functional Beamforming", Berlin Beamforming Conference, BeBeC 2011, (2014)

3. R.P. Dougherty, "Functional Beamforming for Aeroacoustic Source Distributions", AIAA Paper 2014-3066, (2014)

4. T.F.W. Embleton, J.E. Piercy, and N. Olson, "Outdoor sound propagation of ground of finite impedance", *J. Acoust. Soc. of Am.*, **59**(2). (1976)

5. ASTM E1332-10a "Classification for Rating Outdoor-Indoor Sound Attenuation", (2014)

Milestone(s)

All tasks were successfully completed with minor variations in the milestones

Major Accomplishments

The validity of the reciprocal measurement technique, the UW method, is proven. The combination of the phased array and the advanced beamforming technique more than compensates for the noise floor disadvantage of moving the microphones outside in the upper part of the frequency range. At low frequency, the ASTM method has higher dynamic range than the UW method with the tested array, processing technique, and indoor and outdoor

background noise. The UW method requires further development to be effective at low frequency. Changes that would improve the low frequency performance include use of a larger phased array and a loudspeaker with more low frequency output. The array technique provides detailed images of the portions of the house that transmit sound.

Publications

"Improved Method for Estimating Noise Level Reduction of Residential Houses", by R. P. Dougherty, T.L. Robinson, and M. Kurosaka, INTER-NOISE and NOISE-CON Congress and Conference Proceedings, InterNoise15, San Francisco, CA, pp. 2063-2074.

Outreach Efforts

Presented a poster and made a table top demonstration at the 'Research+Industry' symposium held at the Mary Gates Hall, UW, on November 21, 2014, and hosted by the William E. Boeing Department of Aeronautics and Astronautics.

Awards

None

Student Involvement

(a) Tessa L. Robinson, a graduate student and supported as a RA by this project for Autumn quarter 2014, and participated in the construction of the isotropic speaker and two field tests.
(b) Dan Ablog and Ben Turner, undergrads, who volunteered to participate in the field tests.

Plans for Next Period

None

Project 005 Noise Emission and Propagation Modeling

Pennsylvania State University
Purdue University

Project Lead Investigator

Victor W. Sparrow
Director and Professor of Acoustics
Graduate Program in Acoustics
Penn State
201 Applied Science Bldg.
University Park, PA 16802
+1 (814) 865-6364
vws1@psu.edu

University Participants

Pennsylvania State University

- P.I.: Victor W. Sparrow, Professor of Acoustics
- FAA Award Number: 13-C-AJFE-PSU, amendments 005, 015, 029.
- Period of Performance: August 18, 2014 to December 31, 2017.
- Task(s):
    1. Assess applicability of meteorological reanalysis models for possible use in FAA noise tools
    2. Assess measurement data sets for noise propagation model validation

Purdue University

- P.I.(s): Kai Ming Li, Professor of Mechanical Engineering
- FAA Award Number: 13-C-AJFE-PU, amendments 002, 007, 009, 016
- Period of Performance: June 1, 2014 to June 2017.
    3. Extend model for fast moving sources

Project Funding Level

FAA funding to Penn State in 2014-2015 was $132K and in 2015-2015 was $110K. FAA funding to Purdue in 2014-2015 and 2015-2016 was $80K and $90K, respectively.

In-kind cost sharing from Vancouver Airport Authority received in October 2016 was $294,500 to Penn State and $294,500 to Purdue. The point of contact for this cost sharing is Mark Cheng, mark_cheng@yvr.ca . Project support is in the form of aircraft noise and trajectory data, meteorology data, and consulting on those datasets.

Investigation Team

Penn State

Victor W. Sparrow (PI)
Graduate Research Assistant Rachel Romond (meteorological reanalysis data investigation)
Graduate Research Assistant Manasi Biwalkar (measurement data sets for model validation investigation)

Purdue

Kai Ming Li (PI)
Graduate Research Assistant Bao Tong (moving source investigation)
Graduate Research Assistant Yiming Wang (moving source investigation)

Project Overview

The FAA has been funding research efforts in developing enhanced noise emission and propagation capabilities to better support environmental impact studies at both local and national levels. The main emphasis in the near and mid-term is to increase the Research Readiness Level (RRL) of the capabilities so that they can be further matured for implementation into the FAA tools. Validation of the modeling capabilities has been the central focus of the project. Via recent US-EU research collaboration, the field measurement database (BANOERAC) is becoming available for model validation. This database contains acoustic time history of flight events from various types of commercial aircraft during cruise, climb and descent phases of the flight. In addition the DISCOVER/AQ and Vancouver Airport Authority databases have already come on line for use in this and other FAA projects. These datasets make model validation possible. In addition the work will make existing models ready for simulating real weather conditions via proper treatment of the meteorological input parameters and to establish a common basis for comparing US and EU models.

Task 1 "Assess applicability of meteorological reanalysis models for possible use in FAA noise tools"

The Pennsylvania State University

Objective(s)

Determine if meteorological reanalysis datasets and corresponding input parameters are useful for aircraft noise propagation prediction and whether the same can be integrated into the AEDT noise analysis framework.

Research Approach [the first few subsections are repeated from the 2015 annual report, but included here as a convenience]

Introduction

AEDT's acoustic propagation algorithms currently assume a homogeneous and still propagation medium. This omits variable acoustic absorption and refraction (bending) of sound as the sound travels from the source to a receiver. Future versions of AEDT may be able to include refraction in sound propagation calculations by including the inhomogeneity of the medium. This would allow prediction of ranges of received sound level that would occur due to atmospheric effects. Currently available surface-based atmospheric models [Wilson, 2004] are not appropriate for analysis of flight operations because they rely on the theory of the atmospheric surface layer. The thickness of the surface layer changes throughout the day, but generally makes up the lowest ~300 m of the atmosphere. This constitutes less than 5% of the propagation path of sound emitted from a typical en-route aircraft and received on the ground.

To include the medium inhomogeneity at all altitudes relevant to en-route flight noise, accurate upper-air atmospheric data are required. The data source needs to have relatively high resolution, and needs to include all the atmospheric variables required to calculate an acoustic field. A perfectly realistic representation of the medium is not feasible in terms of both data availability and computational efficiency. It is necessary to find a compromise between a homogenous-atmosphere assumption and a perfect recreation of the atmosphere in all dimensions of time and space. The atmospheric data also need to be consistently collected and quality-controlled, represent an adequate spatial sampling of the propagation field, and be openly accessible. One type of data product that satisfies these criteria is meteorological reanalysis.

Reanalysis

Meteorological reanalysis is a process that incorporates measurements of the atmosphere into a long-term model of the earth's geologic-oceanic-atmospheric system to produce a 4-D representation of the atmosphere in space (latitude, longitude, and altitude) and time. In a global reanalysis, observations of the oceans and atmosphere are collected from around the world over an extended time span. These observations are fed into a physics-based model of the atmosphere in a detailed data assimilation process. Reanalysis incorporates many historical observations over an extended time period (years to decades) using a consistent oceanic-atmospheric model and data assimilation scheme. The model is run forward in time, and the calibration and settings/sensitivities of the model are periodically checked against the collected observations. The model is used to predict analysis states, which are best estimates of the state of the total atmosphere for a number of points in time over a distribution of spatial locations.

Currently, about a dozen state-of-the-art reanalysis products exist. They are conducted and maintained by different entities, and each use slightly different atmospheric models, data assimilation methods, analysis time spans, and spatial coverage and resolution. The appropriate choice of reanalysis product depends greatly on the intended use. We have investigated two of these current reanalysis products for possible use in representing the atmosphere in an aviation noise model. The two products are the NCDC/UCAR's Climate Forecast System Reanalysis (CFSR) [Saha, et al., 2010] and NASA's Modern-Era Retrospective Analysis for Research and Applications (MERRA) [NASA, 2012].

Both CFSR and MERRA provide analysis points every 6 hours from 1979 to the present, providing excellent temporal coverage and resolution. Both CFSR and MERRA provide global coverage at a geographic resolution better than 1 degree latitude by 1 degree longitude. Figure 5.1 shows the geographic coverage and resolution for CFSR over the continental United States. Both CFSR and MERRA have vertical coverage from the ground to well past the altitude required for analysis of en-route operations (up to approximately 48 km for CFSR and 65 km for MERRA). The vertical resolutions vary with altitude, but both products are similar, ranging from approximately 100 m (near the ground) to approximately 2 km (at an altitude of 20 km). In addition, both CFSR and MERRA contain the necessary data fields (ambient pressure, temperature, humidity, wind speed and wind direction) for calculation of the sound speed and acoustic absorption coefficient at altitude. CFSR contains additional data fields for temperature at the ground, humidity at 2 m, and wind speed at 10 m. CFSR was ultimately chosen for this proof-of-concept project because of these additional data fields and because of the accessibility of the data.

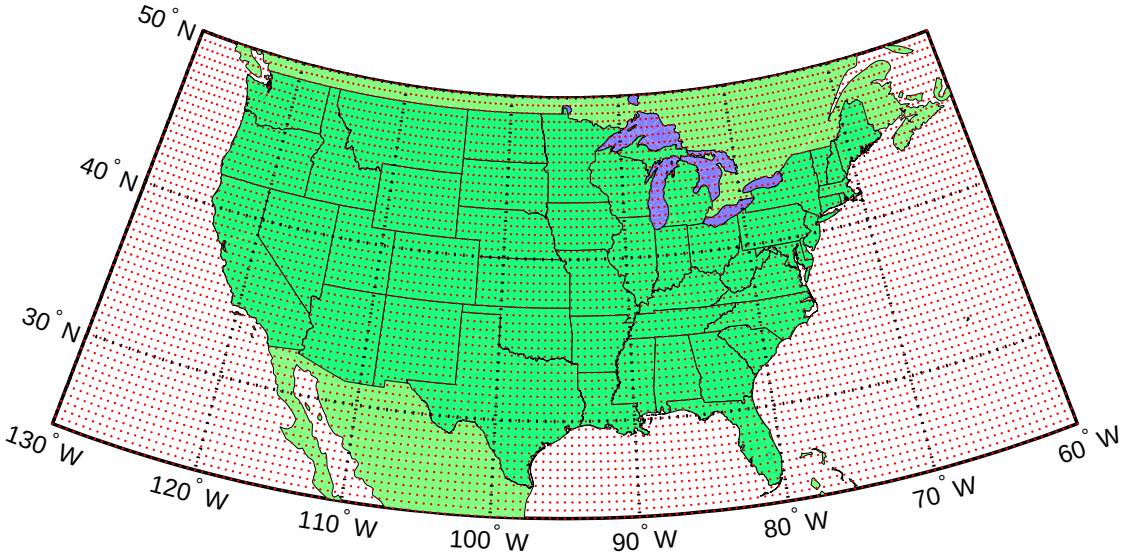

Figure 5.1: Geographic distribution and resolution of CFSR analysis points (in red) over the continental United States. Figure by R. Romond.

Long-Term Metrics

Historical atmospheric data could be used to improve the prediction of long-term average noise metrics by including the effects of meteorological conditions on acoustical propagation. Based on methods by previous researchers [Salomons, van den Berg & Brackenhoff, 1994; Heimann & Salomons, 2004], the statistics of occurrence of meteorological conditions can be used to weight the sound level predictions for certain propagation conditions before they are averaged to find long-term average sound level predictions. To do this, long-term periodic meteorological measurements can be grouped into a number of classes, while the average meteorological conditions of each class *k* is used to calculate the received sound

levels L_k that would occur under each condition. If each class k happens w_k% of the time, the long-term average level L_{eq} is the weighted average of each class level L_k, or

$$L_{eq} = 10\log_{10}\sum_{k=1}^{N} w_k 10^{L_k/10}$$

Upper Atmosphere

As previously mentioned, methods exist to include measured atmospheric data in acoustic propagation calculations. However, the methods are based on measurements made at or near the ground, and they rely on Monin-Obukhov similarity theory of the atmospheric boundary layer theory to extrapolate the values higher into the atmosphere. These methods have been validated for ground-to-ground sound propagation, but Monin-Obukhov similarity theory is only valid for the lowest ~300 m of the atmosphere [Wyngaard, 2010]. The existing methods would only be appropriate for aircraft ground operations such as taxiing and run-ups. They would not be appropriate for analysis of air-to-ground propagation where an aircraft is at altitude.

It would be preferable to include the full atmospheric profiles extracted from the reanalysis data. This ensures that the entire propagation space is represented, and that few assumptions are made about the state of the atmosphere. If necessary, the extracted profiles can be simplified and/or parameterized. This might increase processing efficiency because only the parameterization coefficients would be carried through the calculation (rather than the full profiles). Two possible methods are curve-fitting and layering.

In curve-fitting, a vertical profile is represented by a mathematical function where altitude z is the independent variable and the temperature, wind speed/direction, humidity, or ambient pressure is the dependent profile. Functions currently being considered are linear, logarithmic, log-linear, and polynomial. In layering the atmospheric profiles are split up into layers. Each layer can be homogeneous, or linear/logarithmic/log-linear. A spline fit would combine curve-fitting and layering, but care must be taken to ensure that the function isn't over-determined and includes spatial variations ("wiggles") that don't exist in the raw data. In either case, it is important to accurately represent the value at the ground, the gradient, and both the location and value of any inflection points.

Approach Utilized

Figure 5.2 shows the method currently utilized, developed in 2015, for including CFSR atmospheric reanalysis data in an acoustic propagation model. The raw data is downloaded from UCAR and pre-processed to select relevant data fields for the geographic area under consideration. The raw data .grb files contain one year of 6-hourly global data per file. The pre-processing routine selects the analysis location (out of the available locations shown in Figure 5.1) closest to the airfield. Then, vertical profiles of temperature (T), wind speed and direction (u), humidity (h), and ambient pressure (P) are extracted. Either single-time profiles are chosen, or the profiles are averaged over the applicable time period. The resulting atmospheric profiles are then converted to profiles of acoustic variables. Temperature and wind speed/direction profiles are converted to a sound speed profile c(z). Temperature, humidity, and ambient pressure profiles are converted to an acoustic absorption coefficient profile $\alpha(z)$. Finally, the calculated sound speed and absorption profiles are entered into an acoustic ray tracing program, along with source parameters and receiver grid information. The ray tracing program then calculates the received noise contour at the ground, taking into account the atmospheric conditions originally extracted from the CFSR data set.

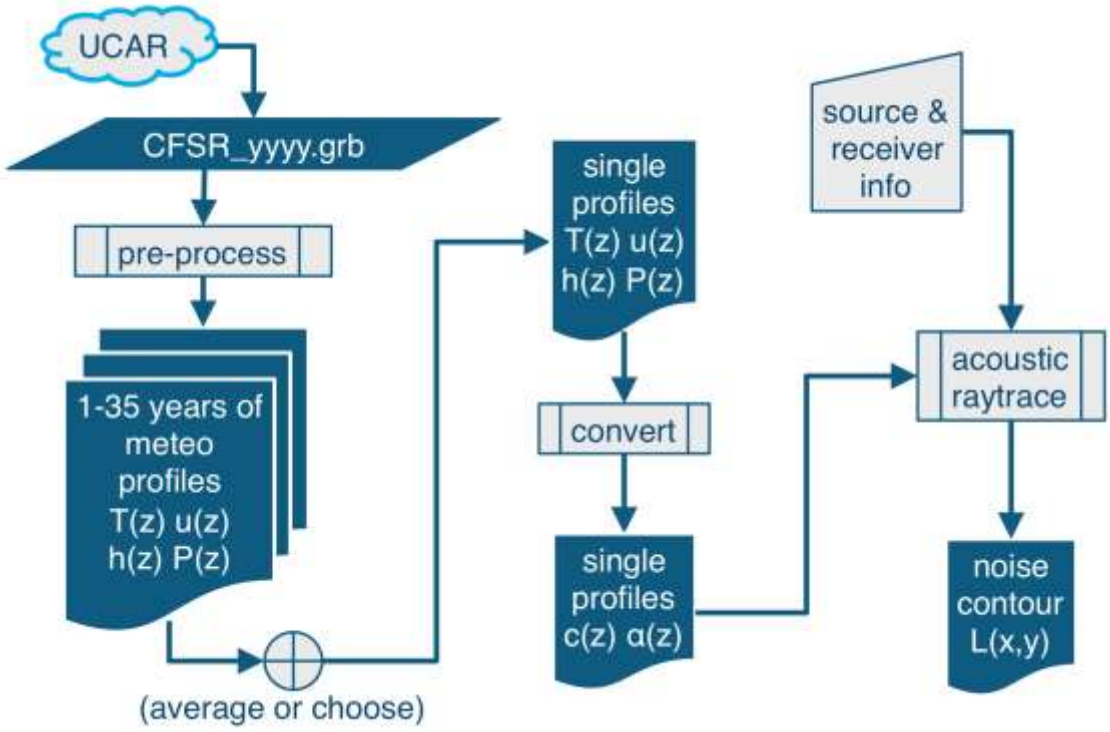

Figure 5.2: Current method for integrating CFSR atmospheric data into a noise model. The meteorological profile parameters are temperature (T), wind speed and direction (u), humidity (h), ambient pressure (P). The profiles required by the acoustic ray tracing program are sound speed (c) and acoustic absorption coefficient (α). The independent variable for each profile is altitude (z).

Comparison of temperature profiles

It is instructive to compare the temperature profile representation between a typical CFSR (stars) output versus other continuous profiles in Figure 5.3. These stars represent an annual average temperature profile close to the Pittsburgh, PA airport in 2010. One can see that the homogeneous temperature profile (used by AEDT), is the black vertical line in the figure, and it is way off except at the ground. The linear fit to the CFSR is the straight blue line, and it fares somewhat better. The ICAO standard atmosphere profile in red, or the 7th order polynomial fit of the ICAO standard atmosphere, still don't match the CFSR data (stars) quite closely as the green 8th order polynomial fit to the CFSR data. One take away is that almost any representation is better than the homogeneous atmosphere representation.

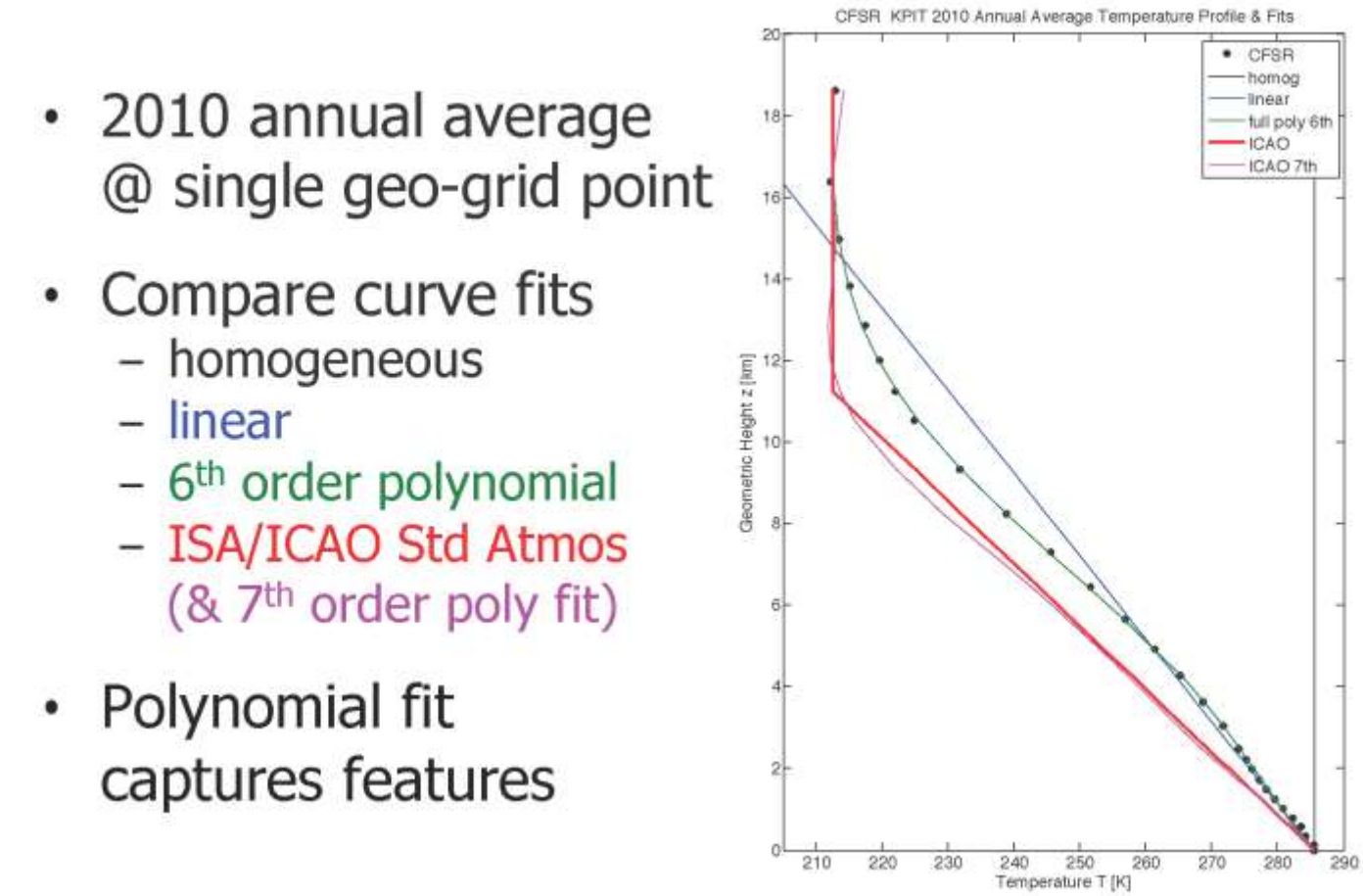

Figure 5.3: Comparison of temperature profiles (lines) with CFSR data (stars). The homogeneous profile uses the surface values. The linear (blue) and 6th order polynomial (green) approximate the CFSR data. For comparison the ICAO standard atmosphere (red) and a 7th order polynomial fit to it (purple) are also shown.

Humidity profile representations

Knowing the humidity profile is essential for accurate atmospheric absorption calculations as a part of a noise propagation prediction, the project team investigated a number of ways to represent humidity in a consistent way in conjunction with the CFSR reanalysis paradigm. Figure 5.4 shows both a single CFSR profile (left) as well as an annual average (right) for relative humidity. It is clear that one must go to a very high order polynomial to follow the CFSR data, even for the annual average. The relative humidity profile is not a well behaved function.

Alternatively the project team looked at specific humidity, and it turns out to be much better behaved as a function of height. Referring to Figure 5.5, the same CFSR data is shown as in Figure 5.4, but now the specific humidity is much easier to represent with a low-order polynomial. Specific humidity is the number of grams of water vapor in 1 kilogram of air, and unlike relative humidity, specific humidity does not depend on temperature or pressure. One notices from Figure 5.5 that the specific humidity continuously decreases with height and looks somewhat like an exponential decay. Specific humidity simply seems to be better suited for inclusion in noise propagation studies. It should be noted that the SAE AIR 5534 atmospheric absorption implemented in AEDT employs the specific humidity.

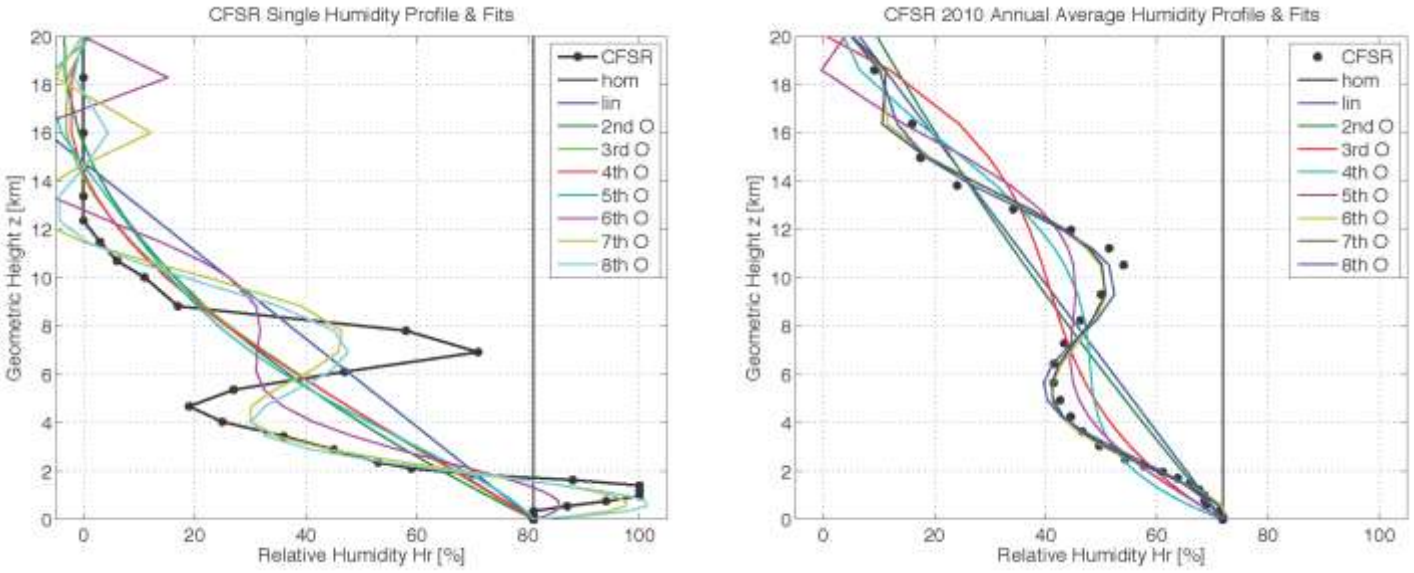

Figure 5.4: Relative humidity data from CFSR with polynomial fits. Left: a single profile sample. Right: annual averaged profile.

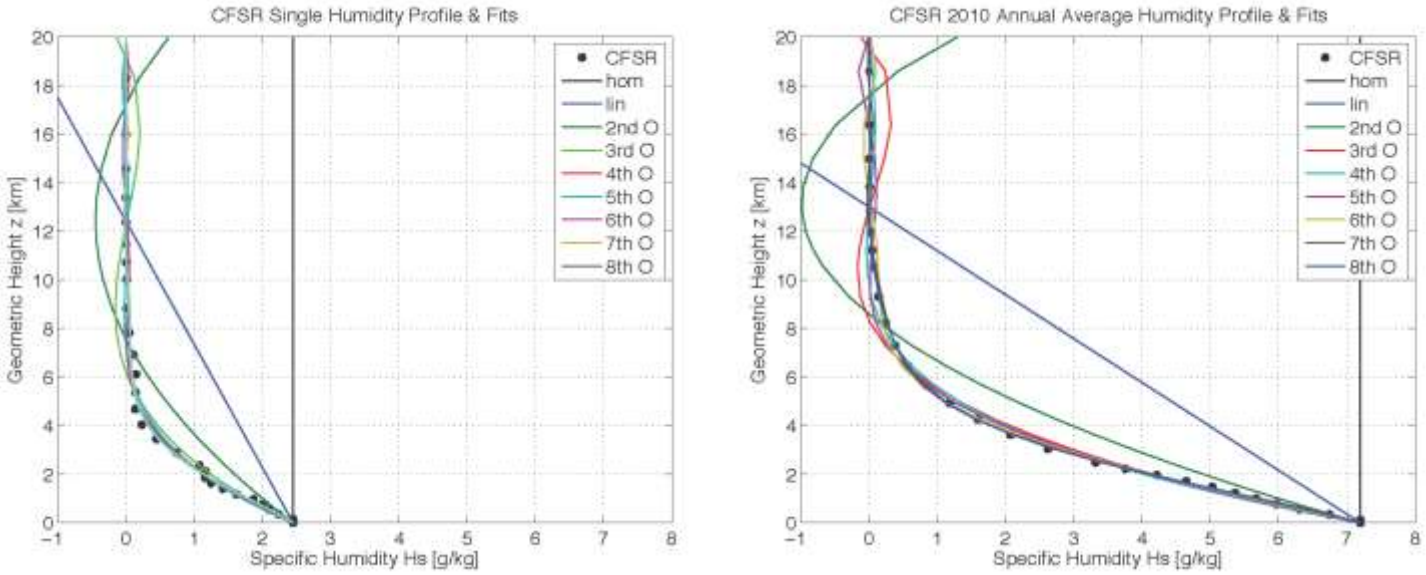

Figure 5.5: Specific humidity data from CFSR with polynomial fits. Left: a single profile sample. Right: annual averaged profile. (Compare with Figure 5.4.)

En-route sound pressure level differences on the ground due to different temperature and humidity profiles

At en-route altitudes, small differences in atmospheric absorption along the long propagation path make for large differences in sound levels on the ground. This is illustrated in Figure 5.6 showing sound pressure levels on the ground perpendicular to the direction of aircraft travel. The aircraft is flying steady at 275 m/s at a 10 km altitude. Four temperature profiles are shown with the different colors: black is the homogeneous atmosphere, blue is the linear fit to the CRFR temperatures, and green is the polynomial fit to the CFSR. The purple is the ICAO Standard Atmosphere temperature profile for comparison. The three line styles indicate the humidity used: dashed for dry air, thick/bold line for homogeneous humidity, and the thin line with dots is a polynomial fit to the CFSR humidity representation. One can quickly see that dry air (unrealistic) in the dashed lines leads to higher sound levels. The homogeneous temperature profile uses the surface value of temperature for all heights. It is seen that the homogenous temperature profile leads to substantially lower sound pressure levels (by 10 dB or more) than if a more reasonable temperature profile is included. Thus using a homogeneous temperature profile clearly is insufficient for making accurate predictions at en-route altitudes.

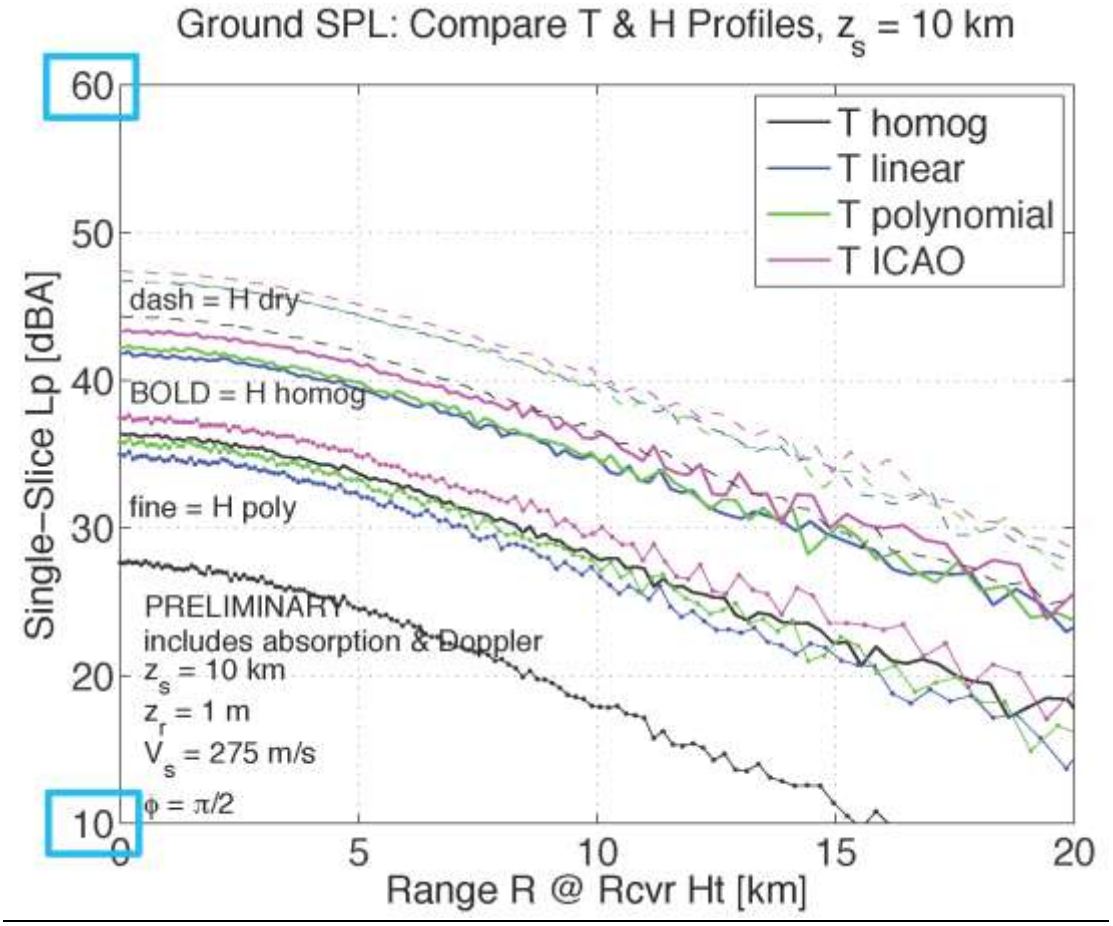

Figure 5.6: Sound pressure levels on the ground for a single steady flight at 10 km altitude, comparing different temperature and humidity representations. See text for additional details. The dashed lines show the dry air predictions yield unrealistically high levels, but the homogeneous temperature profile (using surface temperature values for all heights) gives fairly low levels for this scenario.

Milestone(s)
N/A

Major Accomplishments
The project team now recommends that specific humidity be implemented in all noise propagation models instead of relative humidity.

Publications
None.

Outreach Efforts
Presentation by Graduate Research Assistant Rachel Romond at 16 August 2016 FAA External Tools teleconference.

Awards
None.

Student Involvement
Graduate Research Assistant Rachel Romond has been the primary person working on this task. She is working toward a Spring 2017 or Summer 2017 graduation with her Ph.D. in Acoustics.

Plans for Next Period
In the next year R. Romond will finish her Ph.D. dissertation, leading to scholarly publications.

References

- Wilson, D.K., Ostashev, V.E. and Mungiole, M. (2004). "Categorization schemes for near-ground sound propagation," in *Proceedings of the International Congress on Acoustics*, Kyoto, Japan, pp. 361-364.
- Saha, S., et al. (2010), NCEP Climate Forecast System Reanalysis (CFSR) 6-hourly Products, January 1979 to December 2010, http://dx.doi.org/10.5065/D69K487J, Research Data Archive at the National Center for Atmospheric Research, Computational and Information Systems Laboratory, Boulder, CO. Accessed 27 Mar 2015
- NASA Global Modeling and Assimilation Office (2012). *File Specification for MERRA Products*. GMAO Office Note No. 1, Version 2.3, NASA Goddard Space Flight Center, Greenbelt, MD.
- Salomons, E.M., van den Berg, F.H.A, and Brackenhoff, H.E.A. (1994). "Long-term average sound transfer through the atmosphere: predictions based on meteorological statistics and numerical computations of sound propagation," in *Proceedings of the 6th International Symposium on Long Range Sound Propagation*, Ottawa, Canada, pp. 209-228.
- Heimann, D. and Salomons, E.M. (2004). "Testing meteorological classifications for the prediction of long-term average sound levels," in Applied Acoustics **65**(10), pp. 925-950.
- Wyngaard, J.C. (2010). *Turbulence in the Atmosphere* (Cambridge University Press). ISBN 978-0-512-88769-4.
- International Civil Aviation Organization (1993) Manual of the ICAO Standard Atmosphere - extended to 80 kilometres (262 500 feet), Third Edition, ICAO Doc 7488/3.

Task 2 "Assess measurement data sets for noise propagation model validation"
The Pennsylvania State University

Objective(s)

Begin examination of aircraft measurement databases and ascertain their applicability for validating aircraft noise prediction tools.

Research Approach

This was the first year that the aircraft noise measurement databases became available for use in ASCENT noise projects. Specifically the DISCOVER-AQ Acoustics data became available from Volpe in January 2016, and it took several weeks for the Penn State team to learn how to use SQL to access that data, and even longer to be able to access the data in AEDT 2b. In addition the Vancouver Airport Authority data became available in June 2016, near the end of the project period for this task. Nonetheless, this data made it possible for the Penn State team to gain valuable experience with these datasets.

For example Figure 5.7 shows a simple comparison between DISCOVER-AQ Acoustics event number 35 and straight line propagation with spherical spreading. The upper flowchart shows the simple propagation procedure used. The left plot shows a top-down view of the flight track for event 35 with the microphone SP1 clearly denoted. The right plot shows the difference between the calculated and measured sound pressure levels as a function of aircraft distance from the microphone SP1. The differences between measurement and prediction are surprisingly small over most, but not all, of the flight path. Going through this exercise was invaluable for Penn State Graduate Research Assistant Manasi Biwalkar who performed the work.

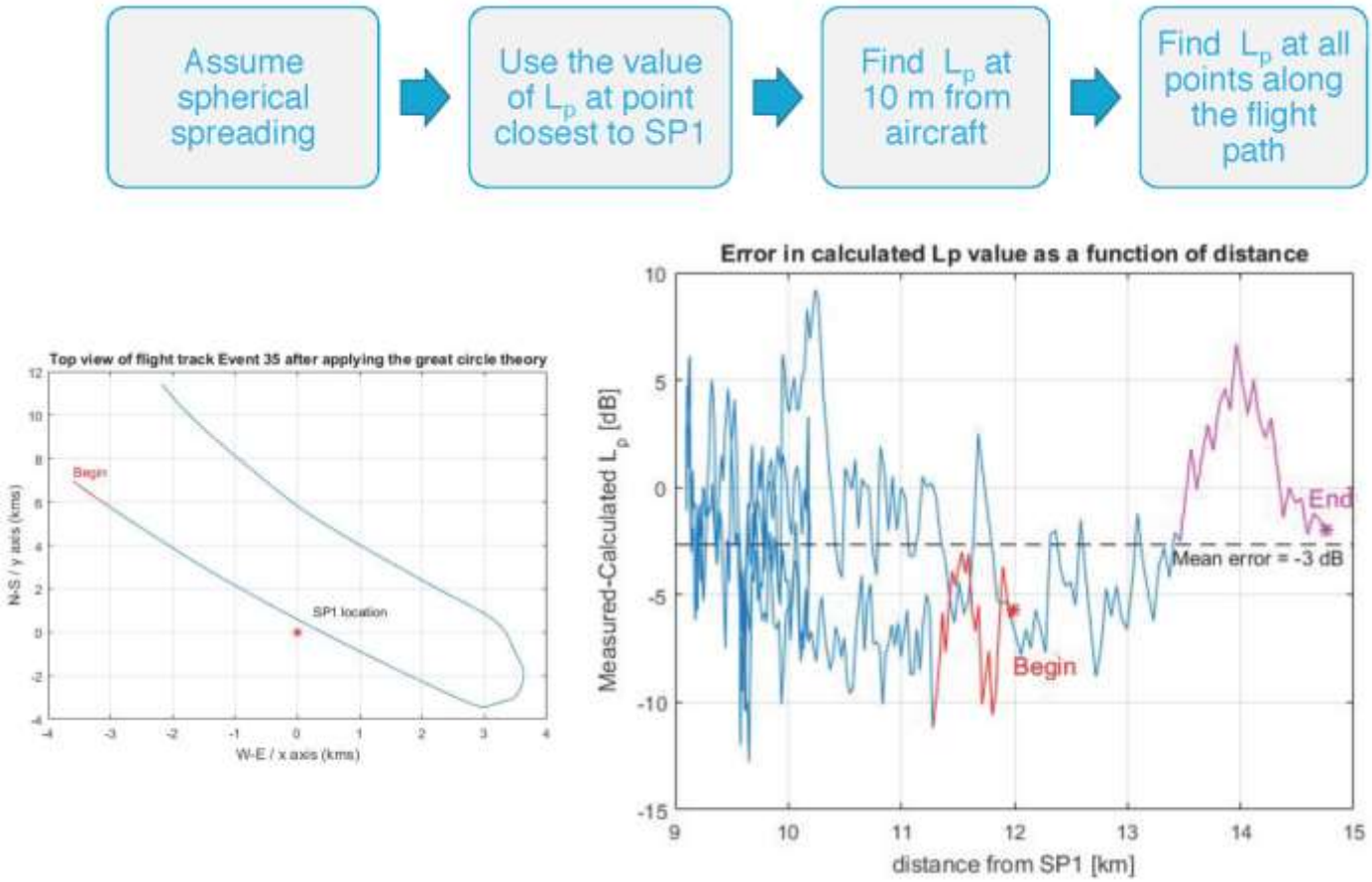

Figure 5.7: Comparison between measured and predicted sound pressure levels on the ground for DISCOVER-AQ Acoustics Event 35. Top: method of calculation. Left: top down view of aircraft trajectory and microphone location. Right: differences in sound pressure level as a function of distance from the microphone.

Another parallel activity in this task was continued discussions with the European Aviation Safety Agency (EASA) regarding the possible use of the BANOERAC data set. Although drawn out over many months due to legal proceedings, the discussions went well, and that avenue will be discussed further in the annual report for ASCENT Project 40. ASCENT Project 5 was no-cost extended to December 31, 2017 to ensure that a Penn State subcontract to ANOTEC Engineering of Motril, Spain would remain in place. ANOTEC has agreed to provide flight trajectory data for BANOERAC via the subcontract, once the data sharing agreement with EASA is in place.

Milestone(s)
N/A

Major Accomplishments
Data from both DISCOVER-AQ Acoustics and the Vancouver Airport Authority were received by the Penn State Team and data analysis began.

Publications
None.

Outreach Efforts
None.

Awards
None.

Student Involvement
Graduate Research Assistant Manasi Biwalkar was the primary person working on this task. She continues working on her M.S. degree in the Penn State Graduate Program in Acoustics.

Plans for Next Period
Continue the assessment of the noise measurement data sets in ASCENT Project 40.

References
E. Boeker, *et al.*, "Discover-AQ Acoustics Measurement and Data Report," DOT-VNTSC-FAA-15-09 (2015).
M. Cheng, *et al.,* Vancouver Airport Authority [Private Communication] (2016).
BANOERAC Project final report, Document ID PA074-5-0, ANOTEC Consulting S.L. (2009).

Task 3 "Investigate the convective amplification effects of fast moving sources"
Purdue University

Aircraft noise has been a concern for districts near airports and sometimes for noise sensitive areas away from airports such as regions in the vicinity of national parks. To better understand the aircraft noise, an accurate numerical model is needed to predict its impact on neighborhood communities.

Most of the previous models for the sound fields above a locally reacting ground are based on the assumption that the source is stationary.[1] The ground admittance is therefore constant for a given source frequency.[1] Extending this solution to a moving source, Buret et al[2] (see also Ref. [1]) derived an asymptotic solution assuming that the acoustical properties of the ground surface is only dependent on the source frequency. However, the Doppler effect causes a frequency shift as the source moving past a stationary receiver. Indeed, the wavelength of the harmonic source appears to be ‘compressed’ for an approaching source. It becomes ‘stretched’ for a receding source. The well-known Doppler effect has a detrimental effect on the sound waves reflected from a locally reacting ground because its specific normalized admittance will be modified due to the source motion. Ignoring such effect will inevitably introduce a significant error in the prediction of the sound fields, especially for a source traveling at high speeds and locating at low elevations above the

ground surface. In a recent study, Ochmann[3] used a simplified ground model and derived an alternative solution for a point source moving above a flat ground with varying admittance. On the other hand, Dragna and Blanc-Benon[4] considered the sound fields due to a line source moving above a locally reacting ground. They obtained a two-dimensional asymptotic solution analogous to those given in Ref. [1, 2] but their solution provides a correct interpretation of the frequency-dependent ground model.

In this report, we endeavor to extend Dragna and Blanc-Benon's model to three-dimensions, i.e. we consider a point source moving above a locally reacting ground. The Lorentz transform converts the moving source problem into a 'standard' monopole located at a stationary point in the Lorentz frame. Section 2 addresses the formulation and the asymptotic analysis for the sound field due to a moving source. A brief discussion of the radial-slice fast field formulation (FFP) will also be presented. In Section 3, we present the numerical validation of the asymptotic formula and the FFP solution. Finally, conclusion is offered in Section 4.

2. Theoretical analysis

Consider a point monopole source of unit strength moving at a constant speed $c_0 M$ at a constant height $z = z_s$ in the positive x-direction where c_0 is the sound speed and M is the Mach number. Suppose that, at time $t = 0$, the source and receiver are situated, respectively, at $r_s = (0, 0, z_s)$ and $r = (x, y, z)$. Figure 5.8 shows the geometrical configuration of the problem. The ground is located at the $z = 0$ plane. A similar method based on Dragna and Blanc-Benon[4] is used to include the varying admittance in the theoretical analysis for the three-dimensional sound fields.

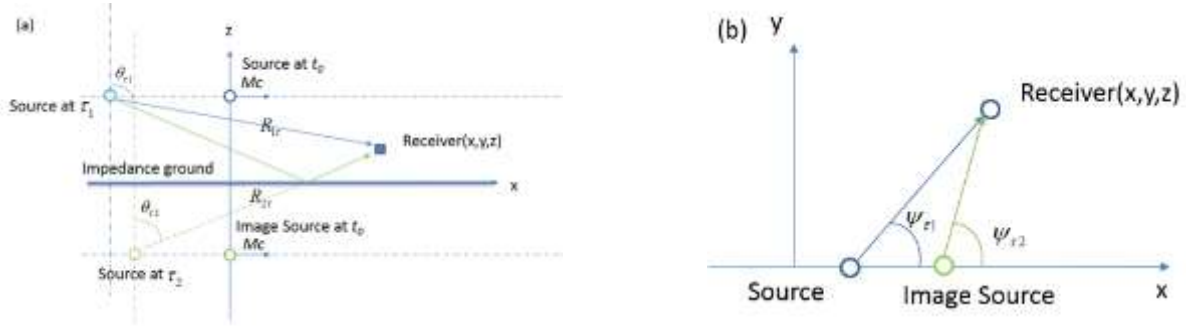

Figure 5.8: Schematic diagram to show the geometrical configuration of the problem with the source located at (0, 0, z_s) at $t = 0$. (a) Elevation, and (b) Plan view.

The governing wave equations for the source moving above a locally reacting plane is given by

$$\frac{\partial p}{\partial t} + \rho_0 c_0 \nabla \cdot \boldsymbol{u} = \rho_0 c_0^2 \delta(x - c_0 M t)\delta(y)\delta(z - z_s)e^{-i\omega_0 t} \quad (1)$$

$$\rho_0 \frac{\partial \boldsymbol{u}}{\partial t} + \nabla p = 0 \quad (2)$$

where p is acoustic pressure, $\boldsymbol{u} = (u_x, u_y, u_z)$ is the particle velocity, ω_0 is the angular frequency of the sound source and ρ_0 is the air density. The boundary condition at the ground surface, i.e. at $z = 0$, is specified by

$$\rho_0 c v_z(x, y, z = 0, t) + \int_{-\infty}^{+\infty} b(u)\, p(x, y, z = 0, t - u)du = 0 \quad (3)$$

where the impulse response $b(t)$ is determined by

$$\beta(\omega) = \int_{-\infty}^{+\infty} b(t)e^{i\omega t}dt \quad (4)$$

with $\beta(\omega)$ as the specific normalized admittance of the locally reacting ground, $\omega = 2\pi f$ and f is the source frequency.

We find it more convenient to use an acoustic potential ϕ which is defined as $p = -\rho \partial\phi/\partial t$ and $\boldsymbol{u} = \nabla \cdot \phi$. Using ϕ in Eqs. (1) and (3), we can show that

$$\Delta\phi - \frac{1}{c^2}\frac{\partial^2\phi}{\partial t^2} = \delta(x - cMt)\delta(y)\delta(z - z_s)e^{-i\omega_0 t} \quad . \quad (5)$$

$$\rho c \frac{\partial}{\partial z}\phi(x, y, z = 0, t) + \int_{-\infty}^{+\infty} b(u)\frac{\partial}{\partial t}\phi(x, y, z = 0, t - u)du = 0 \quad . \quad (6)$$

Applying the standard Lorentz transform:

$$x_L = \gamma^2(x - Mct), \quad y_L = \gamma y, \quad z_L = \gamma z,$$
$$t_L = \gamma^2(t - Mx/c),$$
$$\gamma = \left(1 - M^2\right)^{-\frac{1}{2}} \quad (7)$$

and introducing a two-dimensional Fourier transform, the wave equation in Eq. (5) can be reduced to a one-dimensional Helmholtz equation:

$$\frac{d^2\hat{\phi}}{dz_L^{\,2}} + \left(k_0^{\,2} - k_x^{\,2} - k_y^{\,2}\right)\hat{\phi} = \gamma^2\delta(z_L - z_{Ls}) \quad , \quad (8)$$

where the subscript *L* denotes the variables in the Lorentz space, ϕ_L and $\hat{\phi}$ form the Fourier transform pair:

$$\phi_L(x_L, y_L, z_L) = \frac{1}{4\pi^2}\int_{-\infty}^{+\infty}\int_{-\infty}^{+\infty}\hat{\phi}\left(k_x, k_y, z_L\right)e^{ik_x x_L + ik_y y_L}dk_x dk_y \quad , \quad (9)$$

$$\hat{\phi}\left(k_x, k_y, z_L\right) = \int_{-\infty}^{+\infty}\int_{-\infty}^{+\infty}\phi_L(x_L, y_L, z_L)e^{-i\left(k_x x_L + k_y y_L\right)}dxdy \quad . \quad (10)$$

The impedance boundary condition, Eq. (6), becomes

$$\frac{d\hat{\phi}}{dz_L}(k_x, k_y, z_L = 0) + i(k_0 + k_x M)\gamma\beta[(\omega_0 + k_x cM)\gamma^2]\hat{\phi}(k_x, k_y, z_L = 0) = 0 \quad (11)$$

It is tedious but straightforward to show that the solution for the velocity potential has a rather simple form as

$$\hat{\phi} = \frac{\gamma^2}{2ik_z}\left[e^{ik_z|z_L - z_{Ls}|} + R(k_x)e^{ik_z(z_L + z_{Ls})}\right] \quad , \quad (12)$$

where

$$R(k_x) = \frac{k_z - U}{k_z + U} = 1 - \frac{2U}{k_z + U} \quad , \quad (13)$$

$$U = (k_0 + Mk_x)\gamma\beta[(\omega_0 + c_0 Mk_x)\gamma^2] \quad , \quad (14)$$

$$k_z = +\sqrt{k^2 - k_x^2 - k_y^2} \quad . \quad (15)$$

Substitution of Eq. (12) into (9), we can obtain an integral representation of ϕ which can further be split into three terms. The first two terms can be identified as the Sommerfeld integrals for the direct and the image wave contribution. Consequently, the velocity potential ϕ becomes

$$\phi(x_L, y_L, z_L) = -\gamma^2 \frac{e^{ik_0 R_{1L}}}{4\pi R_{1L}} - \gamma^2 \frac{e^{ik_0 R_{2L}}}{4\pi R_{2L}} + I_\phi \quad (16)$$

where R_{1L} and R_{2L} are the direct distances measured from the source and its image to the receiver in the Lorentz frame. The third term of Eq. (16) is often referred as the diffraction integral given by

$$I_\phi = -\frac{1}{2\pi^2} \int_{-\infty}^{+\infty} \int_{-\infty}^{+\infty} \frac{\gamma^2}{ik_z} \frac{k_0 U}{k_z + k_0 U} e^{ik_x x_L + ik_y y_L + ik_{zL}(z+z_s)} dk_x dk_y \quad (17)$$

Changing the variables from the rectangular domain to their respective spherical-polar forms [i.e. (k_x, k_y, k_z) → (k_0, μ, ψ) and (x_L, y_L, z_L) → (R_{2L}, θ_L, ψ_L)]:

$$\begin{cases} k_x = k_0 \sin\mu\cos\psi; & k_y = k_0 \sin\mu\sin\psi; & k_z = k_0 \cos\mu \end{cases}, \quad (18)$$

$$\begin{cases} x_L = r_L \cos\psi_L; & y_L = r_L \sin\psi_L; & z_L = R_{2L}\cos\theta_L \end{cases}, \quad (19)$$

making use of the identity: $r_L = R_{2L}\sin\theta_L$ and the integral expression for the Bessel function,[5] we can simplify the diffraction integral as follows:

$$I_\phi = \frac{i\gamma^2}{4\pi} \int_{-\pi/2+i\infty}^{\pi/2-i\infty} \frac{\gamma D_L \beta(\omega_L)\sin\mu}{\cos\mu + \gamma D_L \beta(\omega_L)} H_0^{(1)}(k_0 r_L \sin\mu) e^{-ik_0 r_L \sin\mu} e^{ik_0 R_{2L}\cos(\mu-\theta_L)} d\mu \quad (20)$$

where ω_L and D_L are the modified frequency and the Doppler factor in the Lorentz frame:

$$\omega_L = \gamma^2 D_L \omega_0, \quad (21)$$

$$D_L(\mu) = 1 + M\sin\mu\cos\psi_L. \quad (22)$$

Figure 5.8(a) and 5.8 (b) show the schematic diagram for the corresponding polar and azimuthal angles, θ_L and ψ_L.

The acoustic pressure for the diffraction wave term can then be expressed by using Eq. (11) and noting

$$p = -\rho_0 \frac{\partial\phi}{\partial t} = -\rho_0\gamma^2 \frac{\partial\phi}{\partial t_L} + \rho_0 c_0 M\gamma^2 \frac{\partial\phi}{\partial x_L}. \quad (23)$$

In the Lorentz frame, the diffraction integral can then be written as

$$I_p = \frac{-\rho_0\omega_0\gamma^2}{4\pi} \int_{-\pi/2+i\infty}^{\pi/2-i\infty} \frac{\gamma D_L^2 \beta(\omega_L)\sin\mu}{\cos\mu + \gamma D_L \beta(\omega_L)} H_0^{(1)}(k_0 r \sin\mu) e^{ik_0 R_{2L}\cos\mu\cos\theta_L} d\mu \quad (24)$$

where the integration path starts at $-\pi/2 + i\infty$, moves through the points $-\pi/2$, $\pi/2$ and ending at $\pi/2 - i\infty$. In the special case of $M \to 0$ and $\gamma^2 \to 1$, the specific admittance of the ground surface is only dependent on the source frequency ω_0 which remains constant throughout the integration path.

A modified Miki model[6] is used to calculate the acoustical properties of the ground surface in which the normalized admittance is calculated by

$$\begin{cases} \beta(\omega) = \beta_\infty \tanh(-ik_c l) \\ \beta_\infty(\omega_L) = 1\Big/\left[1 + 0.459\left(i\sigma/\rho_0\omega_L\right)^{0.632}\right] \\ c_0 k_c(\omega_L) = \omega_L\left[1 + 0.643\left(i\sigma/\rho_0\omega_L\right)^{0.632}\right] \end{cases} \quad (25)$$

where σ is the effective flow resistivity and l is the layer thickness of the ground surface.

There is a pole in the integrand of Eq. (24) which gives rise to the surface wave pole contribution. The pole location, μ_p say, is determined by solving a non-linear equation:

$$\cos\mu_p + \gamma\left[1 + M\sin\mu_p\cos\psi_L\right]\beta(\omega_L) = 0 \quad (26)$$

where $\beta(\omega_L)$ is calculated by Eq. (25). The equation can be solved by means of the Newton-Raphson method.[7] Only the pole lies near the integration path is of interest in our problem, and the other poles have negligible effect on the total sound fields.

The diffraction integral, Eq. (24), cannot be evaluated analytically to yield an exact solution. However, it can be approximated asymptotically by the method of steepest descent. The details for approximating Eq. (24) can be found elsewhere[7] and the details will not be repeated here for brevity.

To present the analytic results for validation, it is more expedient to cast the formula in the emission time geometry. Here, the Doppler factor in the emission time τ (also known as the retarded time) is denoted by $D(\theta_\tau, \psi_\tau)$ where θ_τ and ψ_τ are the corresponding polar and azimuthal angles in the retarded time τ. Since $D(\theta_\tau, \psi_\tau) = D_L(\theta_L, \psi_L)$, it is possible to show that

$$D(\theta_\tau, \psi_\tau) = \frac{1}{1 - M\sin\theta_\tau\cos\psi_\tau} = \gamma^2\left(1 + M\sin\theta_L\cos\psi_L\right) \quad (27)$$

We can then specify the Doppler factors for the direct and reflected wave term as $D_{1\tau} = D(\theta_{\tau 1}, \psi_{\tau 1})$ and $D_{2\tau} = D(\theta_{\tau 2}, \psi_{\tau 2})$ where the subscripts 1 and 2 signify the corresponding parameters for the direct and reflected waves.

Substitution of Eq. (6) into Eq. (23), application of the inverse Lorentz transformation, and manipulation of the resulting equation yield the acoustic pressure in the emission time geometry:

$$p = p_d + p_i + I_p \quad (28)$$

where

$$p_d = -i\rho_0\omega_0 D_{1t}^2\left[1 - \frac{iD_{1\tau}M}{k_0 R_{1\tau}}(M - \cos\psi_{1\tau}\sin\theta_{1\tau})\right]e^{-i\omega_0 t}e^{ik_0 R_{1\tau}}/4\pi R_{1\tau}, \quad (29)$$

$$p_i = -i\rho_0\omega_0 D_{2\tau}^2\left[1 - \frac{iD_{2\tau}M}{k_0 R_{2\tau}}(M - \cos\psi_{2\tau}\sin\theta_{2\tau})\right]e^{-i\omega_0 t}e^{ik_0 R_{2\tau}}/4\pi R_{2\tau}. \quad (30)$$

The diffraction integral, i.e. the 3rd term of Eq. (28), can be evaluated asymptotically to give

$$I_p = -i\rho_0\omega_0 D_{2\tau}^2 e^{-i\omega_0 t}[V_{\theta\tau} - 1 + C(1 - V_{\theta\tau})F(w_a)]\frac{e^{ik_0 R_{2\tau}}}{4\pi R_{2\tau}} \quad (31)$$

where

$$V_{\theta\tau} = \frac{\cos\theta_{2\tau} - \beta(\omega_0 D_{2\tau})}{\cos\theta_{2\tau} + \beta(\omega_0 D_{2\tau})}, \quad (32)$$

$$C = \frac{r_\beta}{r_w}\frac{\sin\mu_p}{\sin\mu_p - \left.\frac{d\beta}{d\mu}\right|_{\mu=\mu_p}}\frac{1}{\sqrt{\sin\theta_L\sin\mu_p}}\frac{1 + M\cos\psi_L\sin\mu_p}{1 + M\cos\psi_L\sin\theta_L}, \quad (33)$$

$$F(w_a) = 1 + i\sqrt{\pi} w_a e^{-w_a^2} \operatorname{erfc}(-i w_a), \qquad (34)$$
$$w_a^2 = ikR_{2L}[1 - \cos(\mu_p - \theta_L)],$$

with μ_p as the solution of Eq. (26). The function $F(w_a)$ is often referred as the boundary loss factor and w_a is termed as the numerical distance. In a recent work,[8] C in Eq. (31) is approximated as 1. In the current study, a more accurate value for C is given in Eq. (33) where

$$r_\beta = -\cos\mu_p / [\gamma(1 + M\sin\theta_L \cos\psi_L)\beta(D_{2\tau}\omega_0)], \qquad (35)$$

$$r_\omega = w_a / w_\theta, \qquad (36)$$

and

$$\omega_\theta = \sqrt{ik_0 R_{2\tau} D_{2\tau}/2}\left[\cos\theta_{2\tau} + \beta(\omega_0 D_{2\tau})\right]. \qquad (37)$$

Substitution Eqs. (29), (30) and (31) into (28) and rearrangement of terms yield an analytical formula for the acoustic pressure of a moving source:

$$p = -i\rho_0\omega_0 e^{-i\omega_0 t}\left\{\Gamma_1 e^{ik_0 R_{1\tau}}/4\pi R_{1\tau} + \Gamma_2\left[V_{\theta\tau} - 1 + C(1 - V_{\theta\tau})F(w_a)\right]e^{ik_0 R_{2\tau}}/4\pi R_{2\tau}\right\} \qquad (38)$$

where Γ_i (i = 1, 2) is the convective source strength of the direct and reflected wave terms given by,

$$\Gamma_i = D_{i\tau}^2\left[1 - \frac{iD_{i\tau}M}{k_0 R_{i\tau}}(M - \cos\psi_{i\tau}\sin\theta_{i\tau})\right]. \qquad (39)$$

For an en-route aircraft, the boundary loss factor $F(w_a)$ is negligibly small. Furthermore, the second term in the convective source strength is small compared with the first term. Hence, the acoustic pressure above a locally-reacting ground may be simplified

$$p = \left(-i\rho_0\omega_0 e^{-i\omega_0 t}/4\pi\right)\left[D_{1\tau}^2 e^{ik_0 R_{1\tau}}/R_{1\tau} + V_{\theta\tau} D_{2\tau}^2 e^{ik_0 R_{2\tau}}/R_{2\tau}\right]. \qquad (40)$$

Equations (39) and (40) are the main results of the current study. They provide an extension to allow predictions of sound fields due to a moving point source.

To validate the asymptotic formulas, a radial-slice fast field program (FFP) has been developed which follows Wilson's formulation.[9] In his study, Wilson calculated an approximate numerical solution for the three-dimensional sound fields due to a moving point source. In particular, we apply the polar representation of the wave equation in the FFP.[10] The integration over the azimuthal angle is carried out by an asymptotic method. The computation in the azimuthal direction is then collapsed into an evaluation at a single angle corresponding to the direct line of sight between the source and receiver. Thus, the time-consuming two-dimensional integral can be reduced to a simpler one-dimensional integral. Using this radial-slice approach, we can obtain accurate numerical solutions for validating Eq. (38).

3. Result and comparison

In presenting the numerical results, we shall use Transmission Loss (TL) which is defined by

$$TL = 20\log_{10}\left|\frac{p}{\rho\omega_0/4\pi}\right|. \qquad (41)$$

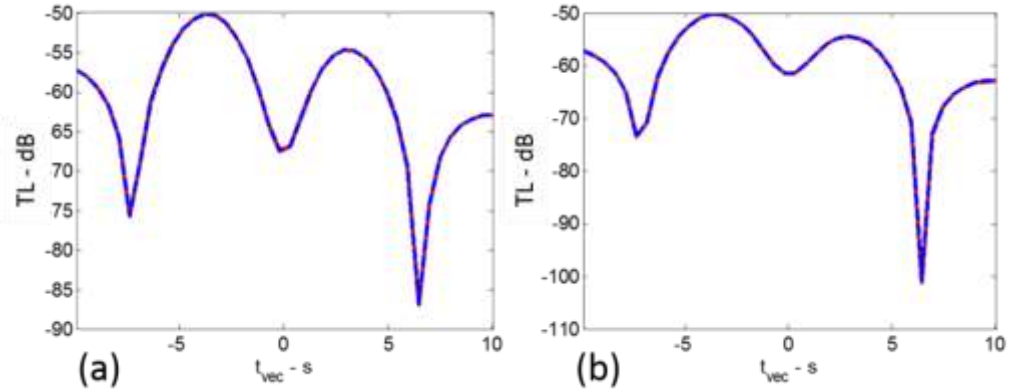

Figure 5.9: Asymptotic solution, Eq. (38) compare with the radial-slice FFP formulation. Blue line: FFP; Red dashed line: asymptotic solution, Eq. (38). The Miki one parameter model for hard-backed ground is used with the effective flow resistivity of 100 kPa sm^{-2} and a layer thickness of 0.01; The source, which has frequency of 300 Hz, moves with constant Mach number of 0.5 at height of 1000 m. The receiver is located at 1.2 m. The source passes through (0, *y,* 100) at t =0 with the off-set distance (a) y = 10 m; (b) y = 200 m.

It is the total sound field normalized with the free field sound pressure at 1 m from an equivalent stationary source. The Miki hard-back layered model is used to calculate the admittance of the ground surface. The parametric values of the effective flow resistivity (σ) of 100 kPa s m^{-2} and a layer thickness of 0.01 m are used in all numerical simulations presented in this paper. Figure 5.9(a), 5.9(b) and 5.10 show good agreements between the asymptotic solution, Eq. (38), and the radial-slice FFP solutions. In these plots, the source and receiver are located at 1000 m and 1.2 m respectively. The source moves with a Mach number of 0.5 and. The receiver is located at an offset distance of 10 m and 200 m for Figure 5.9(a) and 5.9(b) respectively. On the other hand, the offset distance is set at y = 0 in Figure 5.10, i.e. an overhead flight where the source is located directly above the receiver at t = 0. We see that these two prediction schemes agree in the majority of the time steps for $|t| > 0$ but the FFP results show significant fluctuations for the region near t = 0. Due to the assumption used, the FFP formulation cannot give accurate solutions at short horizontal range r in the region near t = 0. This numerical problem can be overcome by using a direct numerical integration scheme at the expense of longer computation times for each time step. We shall illustrate the accuracy in the use of the direct integration scheme in the following numerical simulations.

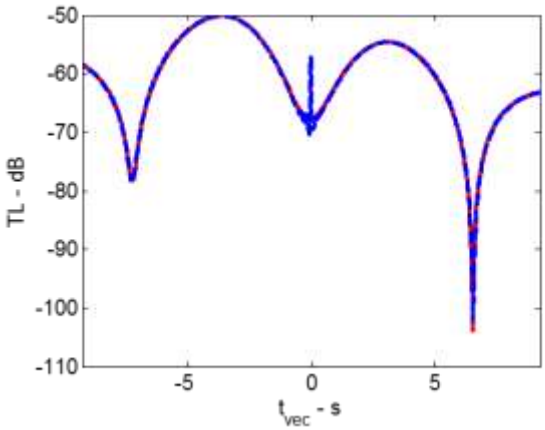

Figure 5.10: Asymptotic solution compare with radial-slice FFP formulation. Blue line: FFP solution; red dashed line: asymptotic solution. The same ground surface and geometry as Figure 5.8 are used except the offset distance, y = 0.

An assumption is often made on the admittance of the ground surface: it is evaluated at the source frequency which is kept constant for different time steps.[1,2] However, the well-known Doppler effect has caused a frequency shift for the moving source. In fact, the source frequency appears to be higher for an approaching source and this apparent frequency is lower when the source recedes. As a result, the apparent admittance of the ground surface varies at different time steps

for the source traversing past the receiver. This assumption leads to two approximations in the asymptotic formula. First, the pole location, μ_p, has been approximated by reducing Eq. (26) to

$$\cos\mu_p + \gamma^2\left[1+M\sin\mu_p\cos\psi_L\right]\beta(\omega_0) = 0 \quad . \quad (42)$$

Secondly, the factor C in Eq. (33) has been simplified to

$$C = \frac{r_\beta}{r_w}\frac{1}{\sqrt{\sin\theta_L\sin\mu_p}}\frac{1+M\cos\psi_L\sin\mu_p}{1+M\cos\psi_L\sin\theta_L} \quad , \quad (43)$$

because $\partial\beta/\partial\mu = 0$ as $\beta(\omega_0)$ is constant. These two approximations in Eq. (38) can lead to significant errors in calculating the diffraction integrals especially for the situations with high source speeds and low source heights.

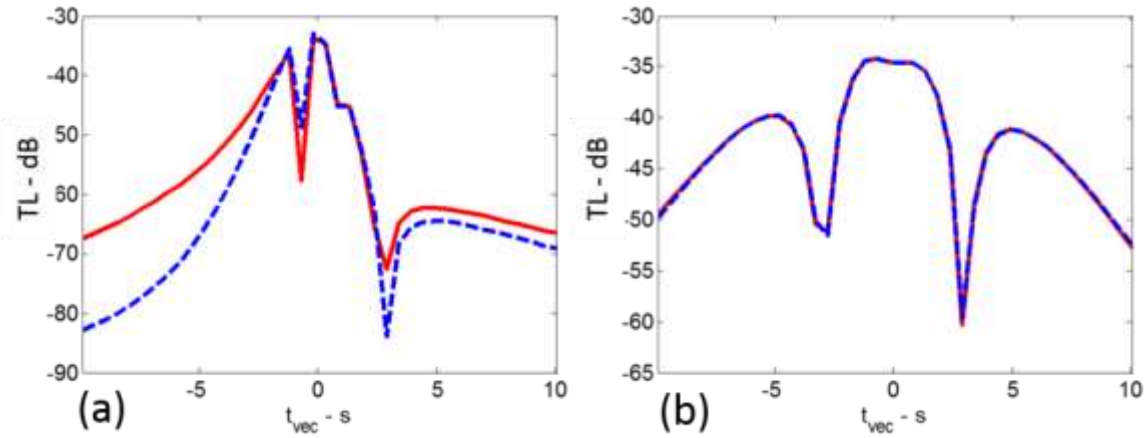

Figure 5.11: Comparison of asymptotic solutions for the model with a frequency-dependent admittance and a constant admittance at the source frequency. Red line: frequency-dependent model; Blue dashed line: constant admittance model. The same geometry, source frequency, and ground parameters as Figure 5.10 are used but the Mach number is (a) M = 0.5, and (b) M = 0.1.

To illustrate the impact of ignoring the Doppler effect on the apparent ground admittance, we display in Figure 5.11 the numerical results by using Eqs. (42) and (43) [instead of Eqs. (26) and (33)] in Eq. (38). In these two plots, the source has Mach numbers of 0.5 and 0.1 respectively. All other parameters are the same as Figure 5.10. As shown in Figure 5.11a (the left plot), there are significant errors in predicting the acoustic pressure especially when the source is located at longer ranges. On the other hand, the Doppler effect on the apparent admittance is insignificant if the source speed is low which is shown in Figure 5.11b (the right plot) with the Mach number of 0.1.

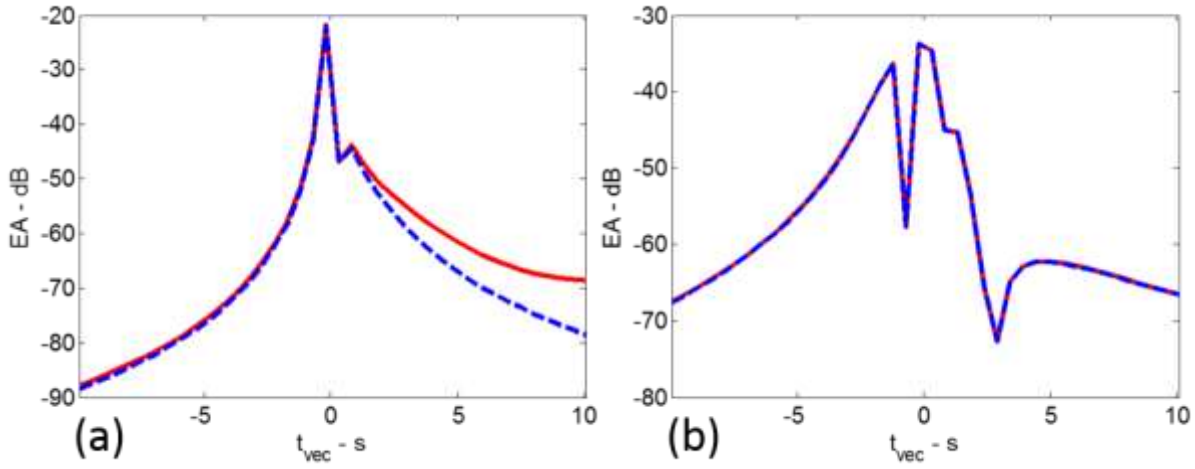

Figure 5.12: The importance of the ground wave term. Red line: direct integration scheme; Blue dashed line: asymptotic solution without the ground wave term, Eq. (40). Solid: asymptotic solution. The ground admittance and source frequency are the same as Figure 5.9. The receiver is located (0, 0, 1.2) The source travels at constant Mach number of 0.5. The source is located at (a) z_s = 10 m, and (b) z_s = 100 m.

We end this section by showing significance of the ground wave term by comparing the numerical solution obtained by the direct numerical integration scheme with the results predicted by Eq. (40). The same ground admittance model and source frequency as Figure 5.9 are used in the following numerical simulations. The receiver is located at (0, 0, 1.2) m. The source travels at a constant speed at a Mach number of 0.5. Two numerical simulations are presented in Figure 5.12 with source height at 10 m and 100 m. It can be seen that when the source is close to the ground, the ground wave term becomes important when the receiver is located at a long distance from the moving source, i.e. near-grazing propagation. In addition, there is no numerical instability for the direct numerical scheme (near the region of t = 0) as compared with the FFP solution shown in Figure 5.10.

4. Conclusion

A three-dimensional asymptotic formula for predicting the sound fields due to a source traveling at a constant speed above a locally reactive ground has been derived. Due to the Doppler effect, a frequency-dependent admittance model is required in order to give accurate numerical solutions. To validate the asymptotic formula, a three-dimensional radial-slice Fast Field Program (FFP) has also been implemented. Good agreements between the FFP solution and the asymptotic formula have confirmed the validity of these numerical solutions. Numerical simulations are also provided to investigate the validity of using various approximations[1,2] in earlier studies. Future work include the derivation of an asymptotic formula for the sound field caused by a source moving at a constant speed above a non-locally reacting ground.

Milestone(s)

N/A

Major Accomplishments

The project team now recommends that specific humidity be implemented in all noise propagation models instead of relative humidity.

Publications

None.

Outreach Efforts

Presentation by Graduate Research Assistant Yiming Wang at Noise Con 2016 at Providence RI.

Awards

N/A

Student Involvement

Graduate Research Assistant Bao Tong has been the primary person working on this task. Bao completed his PhD thesis in August 2015. Yiming Wang, who has just his preliminary exam, is currently a PhD student at Purdue. He has been working on this project since Summer 2015. A Master student Robert St. Claire spent the summer (work for a 6-credit self-study course) to work on the use of AEDT.

Plans for Next Period

Yiming Wang will aim to complete his preliminary within the next 2 years and aim to finish his Ph.D. dissertation in 2018. On the process of the research work, we aim to submit scholarly publications in refereed journals.

REFERENCES

K. Attenborough, K. M. Li, and K. Horoshenkov (2007). *Predicting outdoor sound*. Taylor & Francis, London and New York.
M. Buret, K. M. Li, and K. Attenborough (2006). "Optimizing of ground attenuation for moving sources," Applied Acoustics **67**, 135-156.
M. Ochmann (2013) "Exact solutions for sound radiation from a moving monopole above an impedance plane." The Journal of the Acoustical Society of America 133.4: 1911-1921.
D. Dragna and P. Blanc-Benon (2015). "Sound radiation by a moving line source above an impedance plane with frequency-dependent properties," Journal of Sound and Vibration **349**, 259-275.
M. Abramowitz and I. A. Stegun (1970). *Handbook of mathematical functions: with formulas, graphs, and mathematical tables*. 9th Ed. Dover Publication Inc., New York.
T. Komatsu (2008). "Improvement of the Delany-Bazley and Miki models for fibrous sound-absorbing materials," The Journal of the Acoustical Society of Japan **29**, 121-129.
K. M. Li and H. Tao (2014). "Heuristic approximations for sound fields produced by spherical waves incident on locally and non-locally reacting planar surfaces," The Journal of the Acoustical Society of America **135**, 58-66.
B. N. Tong and K. M. Li (2014). "Atmospheric effects on noise propagation from an en-route aircraft," In INTER-NOISE and NOISE-CON Congress and Conference Proceedings (Vol. 248, No. 1, pp. 656-663). Institute of Noise Control Engineering.
D. K. Wilson (1993). "Sound field computations in a stratified, moving medium," The Journal of the Acoustical Society of America **94**, 400-407.
B. N. Tong (2015). *Prediction and reduction of aircraft noise in outdoor environments*, PhD Thesis, School of Mechanical Engineering, Purdue University.

Project 006 Rotorcraft Noise Abatement Operating Conditions Modeling

The Pennsylvania State University
Continuum Dynamics, Inc.
Bell Helicopter Textron, Inc.
Sikorsky Aircraft Corporation

Project Lead Investigator

Kenneth S. Brentner
Professor of Aerospace Engineering]
Department of Aerospace Engineering
The Pennsylvania State University
233 Hammond Building, University Park, PA
(814)865-6433
ksbrentner@psu.edu

University Participants

The Pennsylvania State University

- P.I.: Kenneth S. Brentner, Professor of Aerospace Engineering
- FAA Award Number: 13-C_AJFE-PSU-006, Amendment No. 6
- Period of Performance: August 18, 2014 to January 31, 2016
- Task(s):
    1. Prediction system development
    2. Noise prediction system validation
    3. Noise predictions and noise mapping
    4. Flight test plan development
    5. Determination and development of data path to AEDT
    6. Selection and modeling of notional advanced technology rotorcraft
    7. Noise predictions and data preparation for AEDT

Project Funding Level

FAA: $250,326; In-Kind Match: (Continuum Dynamics, Inc: $112,500 to PSU and $75,000 to FAA; Bell Helicopter Textron, Inc.: $37,500; Sikorsky Aircraft Corporation: $37,500)

Investigation Team

Kenneth S. Brentner, PI, The Pennsylvania State University; acoustics predictions lead on all tasks.
Joseph F. Horn, Co-PI, The Pennsylvania State University; flight simulation lead supporting all tasks
Daniel A Wachspress, Co-PI, Continuum Dynamics, Inc.; responsible for rotor loads and wake integration and CHARM coupling, primarily involved in tasks 1-3, 6, and 7.
Yaowei Li, Graduate Research Assistant, The Pennsylvania State University; primary responsibility for coupling acoustic code into noise prediction system and acoustic predictions in tasks 1-3.
Willca Villafana, Graduate Research Assistant, The Pennsylvania State University; primary responsibility for model setup and acoustic predictions in tasks 3, 5-7.
Adam Thorsen, Graduate Research Assistant, The Pennsylvania State University; assisted in development of flight simulation code in task 1.
Umberto Saetti, Graduate Research Assistant, The Pennsylvania State University; assisted in flight simulation coupling and performing coupled simulations in tasks 2, 3, and 7.

Benjamin A Goldman, Industrial Partner, Bell Helicopter Textron, Inc.; support Bell 430 model setup and validation of the noise prediction system in task 1 and 2, provide feedback on all aspects of project, especially tasks 1-4.
Eric Jacobs, Industrial Partner, Sikorsky Aircraft Corporation; primary responsibility for flight test plan development in task 4, provide feedback on all aspects of project, especially tasks 3 and 4.

Project Overview

Rotorcraft noise consists of several components including rotor noise, engine noise, gearbox and transmission noise, etc. Rotor noise is typically the dominant component of rotorcraft noise that is heard by the community upon takeoff, landing, and along the flight path of the helicopter. Rotor noise is comprised of several different noise sources including thickness noise and loading noise (together typically referred to as rotational noise), blade-vortex-interaction (BVI) noise, high-speed-impulsive (HSI) noise, and broadband noise – with each noise source having its own unique directivity pattern around the helicopter. Furthermore, any aerodynamic interaction between rotors, interaction of the airframe wake and a rotor, or unsteady, time-dependent loading generated during maneuvers typically results in significant increases in loading noise. The combination of all the potential rotor noise sources makes prediction of rotorcraft noise quite complex, even though not all of the noise sources are present at any given time in the flight (e.g., BVI noise usually occurs during descent and HSI noise only occurs in high-speed forward flight).

The rotorcraft industry, universities, and government research labs have actively engaged in research activities since the late 1960's to understand rotorcraft noise generation mechanisms and mitigation techniques. Both first principles and semi-empirical prediction tools have been developed as a result of this research. This project will leverage that research and use tools developed by the research team to develop noise abatement flight procedures and a flight test plan to evaluate the effectiveness to those procedures. The noise prediction system will also be used to demonstrate its utility in predicting the noise from advance rotorcraft features and concepts.

OBJECTIVES

There are two main objectives for this project, described as follows:

(1) The first objective of this activity is to develop rotorcraft noise abatement procedures through computational and analytical modeling, and develop a comprehensive flight test plan to validate the effectiveness of resulting noise abatement flight procedures. This objective is addressed through the implementation of tasks 1-4 described below.

(2) The second objective is to use the computational and analytical modeling tools to demonstrate the ability to provide vehicle noise data for notional vehicles with advanced technology in a manner than can be used in the FAA Aviation Environmental Design Tool (AEDT). This objected is addressed in tasks 5-7described below.

The approach to developing rotorcraft noise abatement procedures requires the ability to compute the vehicle noise from the relevant noise sources in level flight, hover, takeoff, and approach. Emphasis will be given to the level flight conditions for conventional helicopters, but the tools coupled together will be able to predict the noise from tandem, tiltrotor, and compound rotorcraft as well. In normal civil operations only rotor noise is expected to be a significant source of community noise. For this reason, engine noise, and other noise sources that are important in the cabin are not planned for consideration. Furthermore, high-speed-impulsive (HSI) noise during high-speed forward flight should be avoided in civil operations; therefore, HSI noise will not be considered.

The approach planned to demonstrate computational and analytical modeling tools on advanced rotorcraft designs will leverage the work done for Objective 1 (tasks 1-3, described below). For this reason, the work on the second objective did not begin until approximately 6 months into the effort.

Task 1. Prediction System Development

The Pennsylvania State University

Objective(s)

The object of this task is to couple a flight simulator, rotor aerodynamics and wake computation, and a noise prediction code to form a noise prediction system that will be capable of predicting helicopter noise is various flight operations.

Research Approach

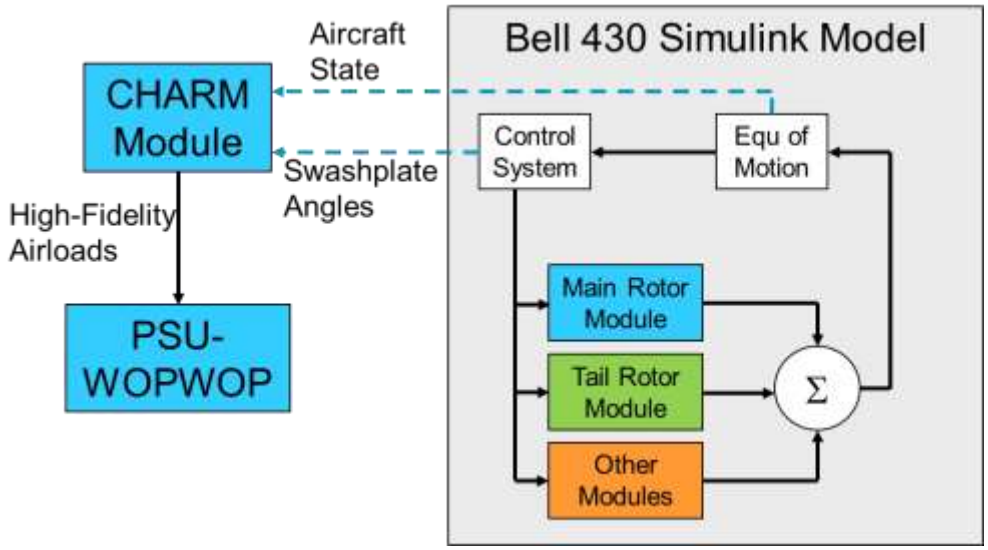

Figure 1.1 Integration Method 1 – CHARM de-coupled from flight simulator.

For this effort, the PSU-WOPWOP code will be used for noise prediction, and will be coupled with a MatLab flight simulator and CHARM (Comprehensive Hierarchical Aeromechanics Rotorcraft Model) to form a rotorcraft noise prediction system. Both CHARM and PSU-WOPWOP have previously been coupled (individually) to the flight simulation code GENHEL-PSU (which models helicopters similar to the Sikorsky UH-60); the three codes have not been coupled into a single noise prediction system. The first major task of this project is to update and enhance the coupling between the three codes. A newly developed flight simulation code will be used to compute the time-dependent flight state of the aircraft and initial blade loading and blade motion estimates. These results will be passed to the CHARM code (module) to predict the rotor wakes and resulting time-dependent blade loads. The loading output of these coupled codes will be input to PSU-WOPWOP to compute the noise during the helicopter flight operation.

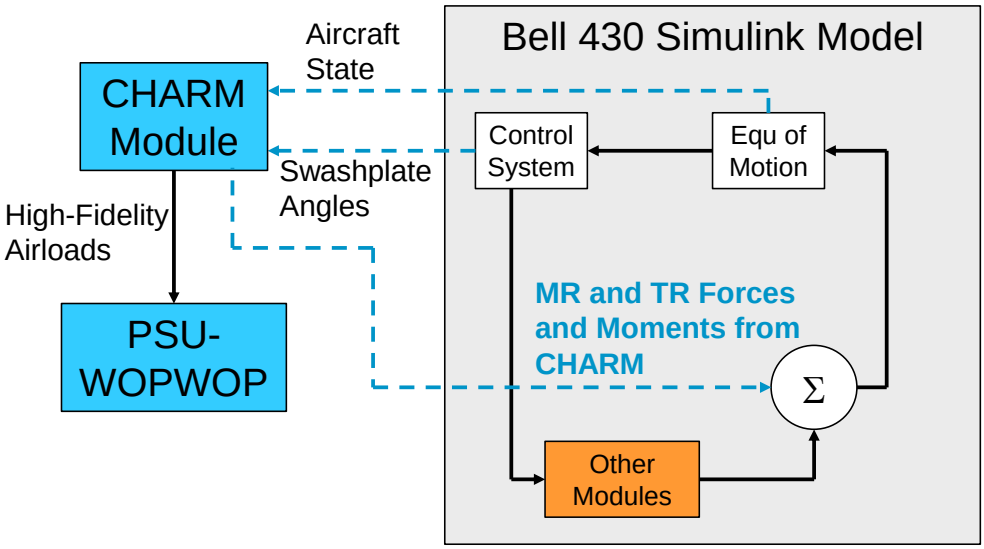

Figure 1.2. Integration Method 2 – CHARM fully coupled with flight simulator.

The coupling is time accurate because that is the normal operation mode of each of the codes. The initial coupling will include multiple rotors (main rotor/tail rotor) and noise computations for noise certification flight conditions and

microphone locations will be demonstrated. Two forms of coupling are used; the first (shown in Fig. 1.1) is a coupling in which the CHARM airloads computations are decoupled from the flight simulator. In this approach, the airloads and trim determined by the flight simulator may be different from those computed in CHARM and used in the noise prediction. To address this potential problem, a fully coupled approach was also developed (shown in Fig. 1.2).

The noise prediction system is anticipated to be sufficiently fast to predict the noise during an entire operation (several seconds at least) at a large number of observer locations so that noise contours on the ground can be predicted. The time accurate nature of the system will enable sweeps of control parameters to be evaluated to eliminate blade-vortex interaction (BVI) or other high noise conditions. This tool will enable the development and analysis of noise abatement flight procedures through relatively rapid computations.

The noise prediction system is envisioned to predict only rotor noise, but should be able to predict noise from helicopters, compound rotorcraft, and tiltrotors (i.e., the number and placement of rotors is not an issue). The system will be able to predict rotor noise in all normal operating flight conditions, ranging from hover (IGE or OGE), takeoff, level flight, approach, and maneuvering flight. Engine and related noise sources are not planned in this project.

Milestone(s)

The coupled noise prediction system was largely complete after the first 3 months, but as problems are encountered (i.e., software bugs), the system is corrected.

Major Accomplishments

The primary accomplishment of this task is the coupling of the three components (flight simulator, high fidelity rotor airloads and airwake (CHARM), and noise prediction (PSU-WOPWOP)) is new.

Another accomplishment was the development of the MatLab based flight simulation code (called HeloSim). This flight simulator is relatively simple because it does not need detailed rotor aerodynamics or wake models – the CHARM rotor module coupling provides higher fidelity loading to the flight simulator.

Publications

None

Outreach Efforts

None

Awards

None

Student Involvement

Adam Thorsen, Ph.D. student at PSU – provided limited support setting up MatLab based flight simulation tool.
Yaowei Li, M.S. student at PSU – primarily responsible for setting up and making acoustic predictions and analysis of acoustic data. He was also involved in developing the coupling between codes. Mr. Li graduated August 2015 and his plans after graduation unrelated to the project.

Plans for Next Period

This task of Project 6 is complete. Any software "bugs" found during the noise predictions in the other tasks will be corrected as required.

Task 2. Noise Prediction System Validation

The Pennsylvania State University

Objective(s)

This task will validate the noise prediction system to demonstrate that is sufficiently accurate to be used for the development and analysis of rotorcraft noise abatement flight procedures.

Research Approach

The noise prediction system will be validated through prediction of various flight conditions and comparison with recently acquired flight test data. NASA, Bell Helicopter, and the U.S. Army recently performed a maneuver acoustics flight test with the Bell 430 helicopter (Ref. 2.1). The data from this test provides an excellent opportunity to test the maneuver noise prediction system and demonstrate its accuracy, strengths and weaknesses. Data from this test is publicly available - and as a partner in this effort, Bell will be able to provide insight into the details of this flight test, which is very valuable in the validation effort. The primary goal of this validation is to characterize the accuracy of the system (with low to medium fidelity level), which will provide sufficiently short noise prediction times needed in noise abatement procedure development. It may also show "gaps" in the system that need to be addressed.

The noise prediction system predictions were compared to measurements from a cooperative flight test conducted by NASA, Bell Helicopter and the U.S. Army to characterize the steady state acoustics and measure the maneuver noise of a Bell Helicopter 430 aircraft (Refs. 2.1, 2.2). For the first validation comparison, a level flight "housekeeping condition" is modeled in which the aircraft was flown several times at nominally the same flight speed (80 kts) over the reference microphone. For this case the overall sound pressure level (OASPL), plotted as a function of distance along the flight path, has been compared to the noise prediction system results (shown in Fig. 2.1). In Fig. 2.1, the reference microphone is at $x = 0$ m and the distance on the x-axes indicates the position of the aircraft relative to the reference point. Figure 2.1(a) shows the OASPL levels as a function of where the helicopter is during the level flyover. The predicted noise is good agreement with the experimental data (the line colored lines) throughout the flyover. In Fig. 2.1(b), it is clear that each component of noise (thickness, loading, and broadband) is important when the frequency of the noise is considered – as it is in tone corrected perceived noise level (PNLT) measurements.

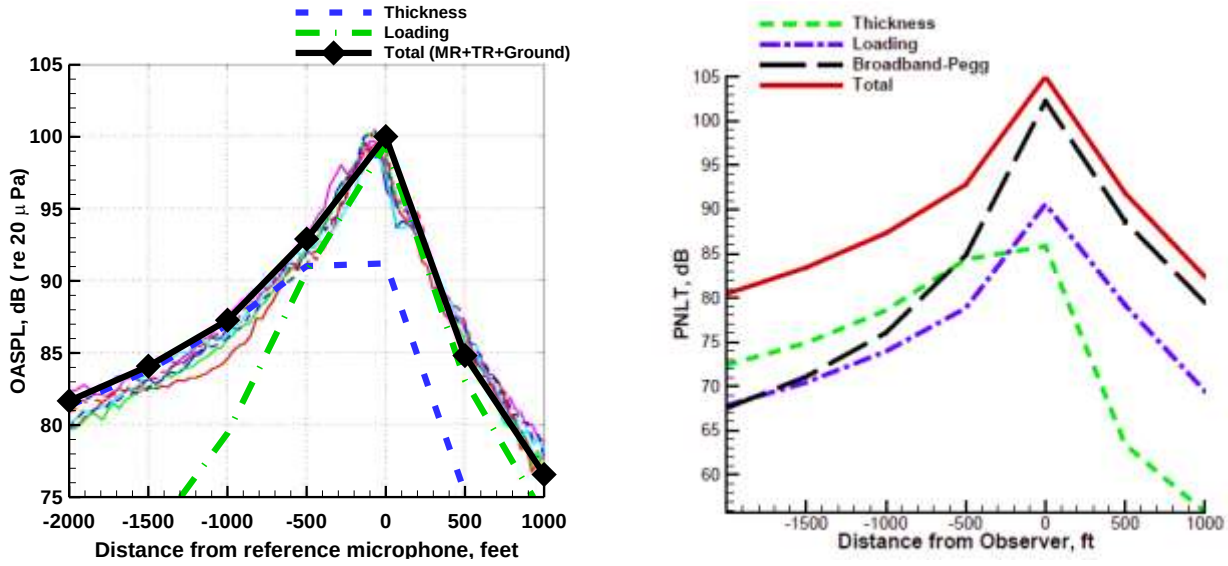

(a) OASPL (b) PNLT

Figure 2.1 OASPL and PNLT levels for 80 kts level flight "housekeeping" run. On the right in (a), the thin colored lines are the experimental data; in (b) the ground is not included in the prediction. (Note: In earlier presentations and reports, Fig. 2.1(a) did not include the ground plane and the agreement was not as good. This was changed when it was discovered that the effect of ground reflection was not removed from the flight test data as was previously thought.)

In Fig. 2.2, the acoustic pressure time history prediction during a mild BVI noise case is compared to measure data for the same condition. The primary character and levels are predicted reasonably well, but the BVI noise spikes are underpredicted. It is likely that a small change in predicted helicopter trim would adjust the BVI spikes substantially.

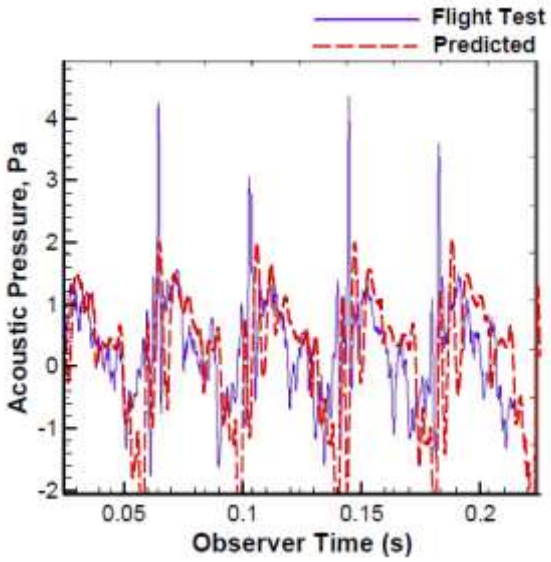

Figure 2.2 Acoustic pressure time history for 100 kts forward sped with 3-degree descent angle.

Milestone(s)

Completed validation of noise prediction system for level flight and descent (blade-vortex interaction) cases by comparison with flight test data for the Bell 430 helicopter.

Major Accomplishments

The validation of the noise prediction system in both level flight and a blade-vortex-interaction flight conditions is a significant achievement for the project. The agreement between the predicted and measured results is quite good for fidelity of these tools and it demonstrates that the tools are able to predict the significant physical noise sources that must be modified to achieve noise abatement. This validation enables the noise prediction system to be used for the other tasks in the project with a degree of confidence.

Publications

Li, Y.; Brentner, K.S.; Wachspress, D.A.; Horn, J.F.; Saetti, U.; and Sharma, K., "Tools for Development and Analysis of Rotorcraft Noise Abatement," proceedings of AHS "Sustainability 2015" conference, Montreal, Quebec, Canada, Sept 22-24, 2015, 10 pages.

Outreach Efforts

The validation effort summarized here was described to Juliet Page and David Senzig, both of VOLPE.

The validation effort was also highlighted in the conference presentation: Li, Y.; Brentner, K.S.; Wachspress, D.A.; Horn, J.F.; Saetti, U.; and Sharma, K., "Tools for Development and Analysis of Rotorcraft Noise Abatement," presented at AHS "Sustainability 2015," Montreal, Sept 22-24, 2015, (presented by K.S. Brentner).

Awards

None

Student Involvement

Yaowei Li, M.S. student at PSU – primarily responsible for setting up and making acoustic predictions and analysis of acoustic data. Mr. Li graduated August 2015 and his plans after graduation unrelated to the project.

Umberto Saetti, M.S. student at PSU – primarily responsible for flight simulation calculations and development and debugging of the coupling between the flight simulation code and the CHARM rotor module. Mr. Saetti graduated in August 2016, and is now pursuing a Ph.D. at PSU on another project.

Plans for Next Period

This validation effort is complete. No further work is currently planned for validation.

References

[2.1] Watts, M.E., Greenwood, E., Smith, C.D., Snider, R., and Conner, D. A., "Maneuver Acoustic Flight Test of the Bell 430 Helicopter Data Report," NASA/TM-2014-218266, May 2014.

[2.2] Snider, R., Samuels, T.O., Goldman, B., and Brentner K. S., "Full-Scale Rotorcraft Broadband Noise Prediction and its Relevance to Civil Noise Certification Criteria," Proceedings of American Helicopter Society 69th Annual Forum, Phoenix, Arizona, May 21–23, 2013.

Task 3. Noise Predictions and Noise Mapping

The Pennsylvania State University

Objective(s)

This object of this task is to examine several flight conditions, consider operational changes, and determine the impact on the noise levels. The goal of this task is to demonstrate how flight operations can reduce the noise.

Research Approach

In order to demonstrate the impact of noise abatement flight procedures, several simple parametric studies were performed. According to Helicopter Association International's "Fly Neighborly Guide", published report in 2007 (Ref. 3.1), the simplest way to reduce the rotorcraft noise during overflight is to increase the altitude and fly slower. To examine these common sense recommendations, the noise prediction system was used to predict the noise for various operating procedures. These predictions serve two purposes: 1) to develop further confidence that the noise prediction system captures the important noise characteristic of helicopters in various flight conditions; and 2) to provide detailed information that explain the mechanisms and directivity of noise changes (hopefully reductions) obtained through noise abatement flight procedures. Based on this guidance, the noise prediction system was used to predict the noise of the Bell 430 aircraft.

Impact of Altitude

The first case considered was level flyover with the Bell 430 helicopter flown with a velocity of 100 kts at different altitudes ranging from 150 m to 350 m in 50 m increments. This range of altitudes is arbitrary, but sufficient to demonstrate the powerful impact that distance makes in reducing noise. The aircraft weight and atmospheric conditions (standard sea level density and temperature) are held constant for each altitude. In Fig. 3.1, the PNLT is shown for locations directly below the flight path of the aircraft. In this figure, it is evident that distance plays an important role in the noise level – as was expected. The peak PNLT level is about 8 dB lower for the 350 m case than for the 150 m altitude.

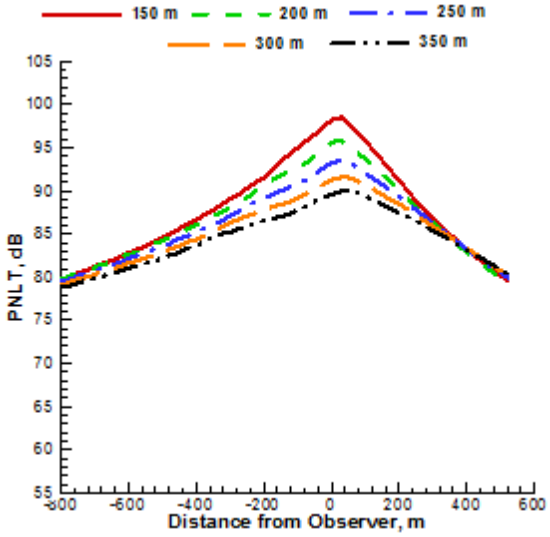

Figure 3.1 PNLT predictions for the Bell 430 helicopter with the aircraft at different flight altitudes.

While the behavior directly below the helicopter is what is expected – increased altitude decreases the noise level – this is not necessarily the case for observer locations to either side of the aircraft. Furthermore, the flight time over the observer is not included when considering the PNLT levels alone. To address these issues, the Effective Perceived Noise Levels (which are based on PNLT) were computed for an area below the aircraft (shown in Fig. 3.2). In Fig. 3.2(a), the EPNL levels are shown for a single altitude (150m) for approximately 1800m range and 700 m to either side of the flight path. The EPNL levels are highest directly under the aircraft, as would be expected. Notice that the EPNL levels do not vary with the x location because the helicopter is in level flight; thus a more quantitative examination of the results can be done by comparing the levels at the $x = 0$ positon for different lateral distances from the centerline (shown in Fig. 3.2(b)). Again in this figure, it is clear that as the altitude of the helicopter increases the noise levels decrease along the centerline. But at lateral distances greater than 300m (in this case), the noise levels are relatively unaffected and even increase slightly on the right side of the aircraft (advancing rotor side). Hence, even for a very straightforward approach to noise abatement, the results will not be the same at all observer positons.

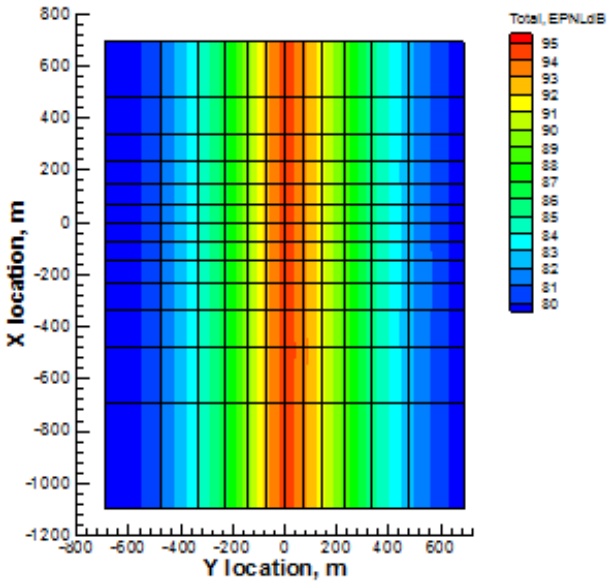

(a) EPNL contours, $V_H = 100$ kts, altitude =150m

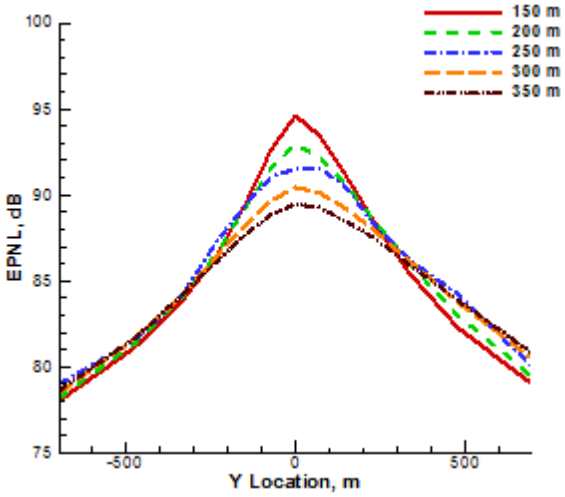

(b) EPNL at $x = 0$ plane, $-700 < y < 700$ m for various altitudes

Figure 3.2 Effective Perceived Noise Levels for Bell 430 helicopter flying at 100 kts at altitudes from 150m to 350 m.

Impact of Flight Speed

A similar comparison of EPNL levels was performed for the Bell 430 operating at forward speeds ranging from 60 kts to 140 kts in level flight at 150m (shown in Fig. 3.3). It is generally understood that flying slower will reduce the noise levels. The physics of the source noise mechanisms (in-plane noise in particular) indeed exhibit this behavior. Nevertheless, when the EPNL is considered, which takes into account the duration of the exposure as well as the level, the levels of EPNL do not change significantly below the helicopter even though the expected trend is seen away from the centerline (see Fig. 3.3). The reason for this is that while the noise level is lower for low speed (e.g., 60 kts), the exposure time is longer. Therefore, along the helicopter flight path the EPNL levels are essentially the same for the 60 kts and 140 kts cases.

Impact of Flight Path Angle

The Sound Exposure Level (SEL) contours were also computed for different descent and climb angle (from 6 deg. descent to 6 deg. climb). When the helicopter is not in level flight, the distance to the ground will be constantly changing and it has already been shown that increasing distance is an effective noise abatement strategy. Therefore, in these comparisons, the distance from the measurement plane is the same for $x = 0$ and either farther or closer to the plane otherwise. The comparison for 6 deg. and 3 deg. descent angle is shown in Fig. 3.4 (along with the level flight case as a reference). The SEL levels are significantly higher for the 6 deg. descent. For the uprange cases ($x < 0$) the impact of distance should be to reduce the level, but they are higher than the 3 deg. and level flight cases. In addition, it is clear at $x = 0$ that the levels are higher, yet the distance is the same here. Upon closer examination, the 6 deg. descent case has significantly more BVI than the 3 deg. descent case, and the level flight case does not have any BVI noise. Thus, it is clear that BVI should be avoided to have the lowest noise (and annoyance) levels.

In Fig. 3.5, the SEL contours for 6 deg. and 3 deg. climb are shown (along with a level flight case for reference). In this case, the change in SEL levels is primarily due to the distance the helicopter is above the measurement plane. This can be

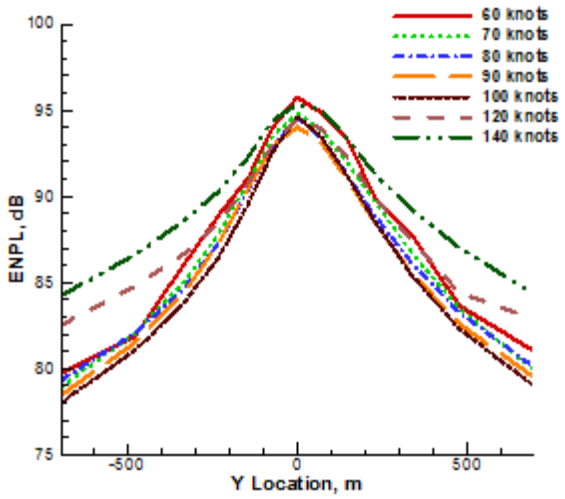

Figure 3.3 EPNL along $x = 0$ plane, $-700 \leq y \leq 700$ m for forward speeds ranging from 60 kts to 140 kts.

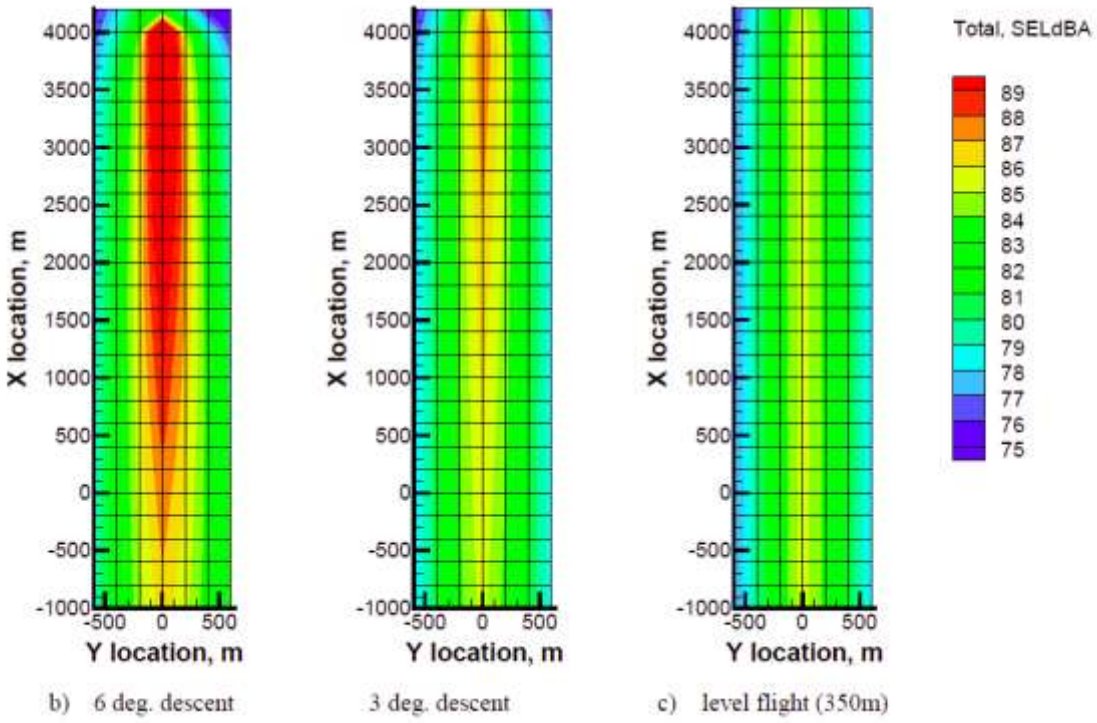

Figure 3.4 SEL contour plots for various descent angles.

seen by comparing the values at $x = 0$, which are essentially the same. Therefore, unlike the descent case where BVI noise was eliminated by changing the descent angle, there is no change in the physics in the climb case. Nevertheless, rapid climb is an effective means of increasing the distance and thereby reducing the noise.

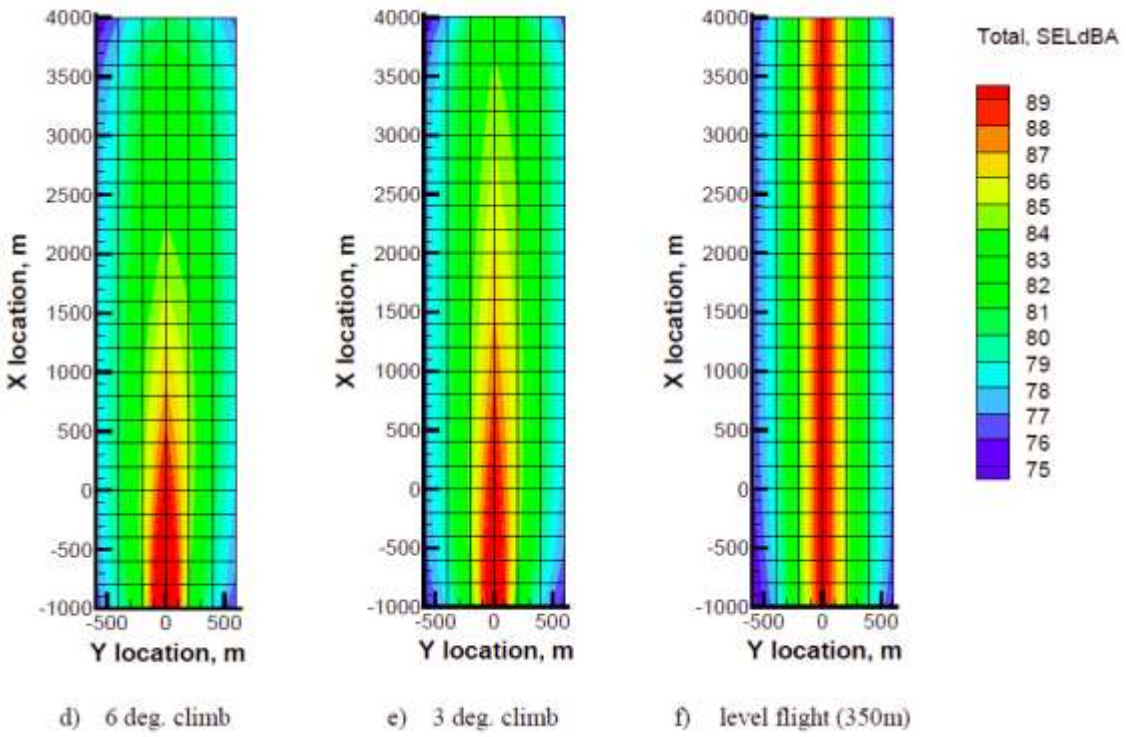

Figure 3.5 SEL contour plots for various climb angles.

Milestone(s)

Compute predicted noise for several operating scenarios. This milestone was met by the level flight, descent, and climb cases studied.

Major Accomplishments

This task has demonstrated the noise prediction system is able to show how different rotorcraft operations can reduce or increase the noise levels. Furthermore, the predictions have shown that even simple noise abatement strategies, like flying higher or flying slower, may provide noise reduction in some locations and yet result in increases in other locations. This task has demonstrated that to understand such complex changes it is important to have a physics-based noise prediction system so that a detailed investigation of the individual noise components and the noise directivity can be made.

Publications

Li, Y.; Brentner, K.S.; Wachspress, D.A.; Horn, J.F.; Saetti, U.; and Sharma, K., "Tools for Development and Analysis of Rotorcraft Noise Abatement," proceedings of AHS "Sustainability 2015" conference, Montreal, Quebec, Canada, Sept 22-24, 2015, 10 pages.

Outreach Efforts

The validation effort summarized here was described to Juliet Page and David Senzig, both of VOLPE.

The validation effort was also highlighted in the conference presentation: Li, Y.; Brentner, K.S.; Wachspress, D.A.; Horn, J.F.; Saetti, U.; and Sharma, K., "Tools for Development and Analysis of Rotorcraft Noise Abatement," presented at AHS "Sustainability 2015," Montreal, Sept 22-24, 2015, (presented by K.S. Brentner).

Awards

None

Student Involvement

Yaowei Li, M.S. student at PSU – primarily responsible for setting up and making acoustic predictions and analysis of acoustic data for Objective 1. He was also involved in developing the coupling between codes. Mr. Li graduated August 2015 and his plans after graduation unrelated to the project.

Umberto Saetti, M.S. student at PSU – primarily responsible for flight simulation calculations and development and debugging of the coupling between the flight simulation code and the CHARM rotor module. Mr. Saetti graduated August 2016, and is now pursuing a Ph.D. at PSU on another project.

Plans for Next Period

This task is complete. No additional work is planned, but if support is needed to finish the flight test plan development (task 4) then noise predictions could be made in support of that task.

References

[3.1] Fly Neighborly Guide, produced by the Helicopter Association International Fly Neighborly Committee, 2007. (http://www.rotor.org/portals/1/operations/Fly2007.pdf - accessed March 27, 2015)

Task 4. Flight Test Plan Development

The Pennsylvania State University

Objective(s)

This task will develop a draft flight test plan for evaluation of noise abatement procedures.

Research Approach

A draft test plan (or template) to test the effectiveness of various noise abatement procedures has been developed by our industrial partner Sikorsky Aircraft Corporation (Eric Jacobs). Eric has significant experience in flight testing and has Sikorsky has strong interest in participating in a proposed noise abatement flight test. The flight test plan will involve two phases of testing. Phase 1 will include noise characterization and model validation testing. This will provide the baseline to compare noise abatement procedures against and to determine if changes in the test plan are needed to take into account noise characteristics that may not be fully account for in the noise modeling. The Phase 2 plan will define the abatement procedures to be tested and the test conditions required to ensure the test is effective. The draft/template test plan has several "to be determined" items because the target aircraft and test site are not currently known, but are critical elements of such a plan. These items will likely not be determined until a specific test is planned (or at least proposed).

Milestone(s)

A flight test plan template has been developed for rotorcraft noise abatement procedure validation.

Major Accomplishments

An outline of the test plan and initial Phase 1 and Phase 2 plans has been drafted.

Publications

None

Outreach Efforts

None

Awards

None

Student Involvement

None

Plans for Next Period

The flight test plan development is complete and a draft/template flight test plan has been delivered to the FAA.

Task 5. Determination and Development of Data Path to AEDT

The Pennsylvania State University

Objective(s)

The object of this task is to develop the necessary noise prediction templates and post processing capabilities to generate noise with the rotorcraft noise prediction system developing in task 1 and generate the needed data, in the proper format, to be used in AEDT in lieu of manufacturer provided, or otherwise measured, data.

Research Approach

The first step is to determine the appropriate information that AEDT needs from the rotorcraft noise prediction system. This includes helicopter noise levels and directivity for various operating conditions and will likely need to be provided in some form of noise-power-distance (NPD) curves, spectral class data, etc. A different set of NPD data is required for each flight operational mode. The rotorcraft noise prediction system will have the advantage that for any given flight condition, the noise can be predicted in any direction (or on a sphere surrounding the vehicle). While such data is not currently used in AEDT, it can be used to determine if current and any advanced modeling in AEDT are capturing the nature of the helicopter noise sufficiently. Noise prediction templates will be developed to simplify the process of computing NPD and spectral class data. Ultimately the goal would be to set up the helicopter model in the rotorcraft noise prediction system, do some testing to make sure the setup is correct, and then submit a batch job and get out the data needed by AEDT.

Milestone(s)

Review input data requirements for AEDT and develop necessary post processing capabilities to provide any data or data format as needed. The work on this milestone is complete.

Major Accomplishments

The initial path for the work on this task was to provide data in format that can be used directly by AEDT. Upon consultation with Juliet Page (Volpe), it was decided that elements not currently included in the PSU noise prediction

system (i.e., ground reflections if the ground is not a hard plane, etc.) can be better handled by the tools that Volpe already has available. Therefore, the focus in this task is to compute the noise on hemispheres of the format the Volpe's software can use with their tools. Then atmospheric attenuation, atmospheric turbulence, and ground reflections can be performed in a manner consistent with Volpe's current toolset. Ultimately, this data is used to provide input to AEDT. It is important to point out that significantly more detail is provided (directivity, noise source identification, etc.) than is currently used by AEDT, but the ability to compute this data will provide AEDT developers tools to assess modeling choices and improve rotorcraft noise predictions.

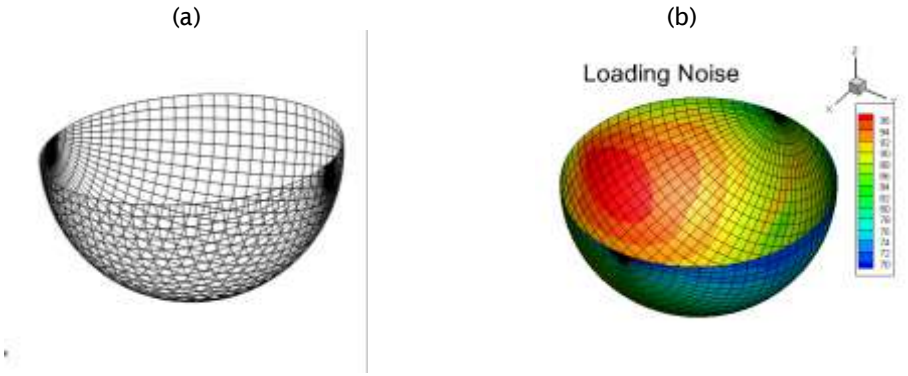

Figure 5.1 Typical hemisphere grid used to provide acoustic data that can be used by Volpe to provide data for AEDT. Positive *x*-axes is the direction of flight; Helicopter is located at the center of the sphere. (a) example hemisphere grid; (b) example noise computation plotted on the grid.

Publications

None

Outreach Efforts

We have interacted with Juliet Page, VOLPE, to help us understand the noise inputs requirements of AEDT.

Awards

None

Student Involvement

Willca Villafana, M.S. student at PSU – primarily responsible for acoustic work in Objective 2, i.e., prepared the noise prediction system to output the necessary data for input to AEDT. Mr. Villafana completed his M.S. degree work in August 2016 and graduated Dec 2016. He is now attending the von Karman Institute in Brussels, Belgium.

Plans for Next Period

This task is complete.

Task 6. Selection and Modeling of Notional Advanced Technology Rotorcraft

The Pennsylvania State University

Objective(s)

The objective of this task is to select a small number of advanced technology rotorcraft features to demonstrate how the noise prediction system can help assess the potential for new technology to impact rotorcraft noise abatement or how it may be assessed as part of the total air transportation system noise through modeling inputs for AEDT (before measured data would be available).

Research Approach

A limited number of notional rotorcraft with advanced technologies can be studied within the scope of this effort. Therefore, it is planned to select three new technologies that have a strong potential for noise reduction. These technologies will be integrated into notional rotorcraft, which in turn will be analyzed as representative cases. Ultimately the goal is to demonstrate that advanced technology rotorcraft could be studied within the context of AEDT and their noise impact/noise reduction could be assessed in the broader context provided by AEDT. For this demonstration, it was decided to pick a technology that would reduce BVI noise, which is a significant noise source upon approach.

Milestone(s)

Develop notional advanced rotorcraft configurations and build the necessary inputs for the rotor noise prediction system. This milestone is complete.

Major Accomplishments

A demonstration of the capability of the noise prediction system to predict the noise of an advanced technology rotorcraft for an advanced blade design known to reduce BVI noise (Figure 6.1)[6.1], Airbus Helicopter's "Blue Edge" blade. The concept behind this design is described in Ref. [6.2] as: "*With a standard blade, air coming off the end of the blade causes a vortex around the tip. Under certain flight conditions, the advancing blade then hits the vortex of the preceding blade. This causes a sudden change in the relative angle of attack and thus a change in pressure on the surface of the blade. This BVI causes the slapping sound ubiquitous to helicopter operations. With Blue Edge technology, the blade tip is swept forward, then aft. This causes the advancing blade tip to hit the previous blade's vortex at an oblique angle, reducing the noise level by 3 to 4 EPNdB.*" [6.2] This advanced technology blade design should be a good test of the noise prediction system.

Three main rotor blade configurations were selected to demonstrate the ability of the new analysis system to predict the reduction in BVI noise obtained using a Blue Edge-like planform. The three blade geometries were 1) conventional rectangular blades – nominally the current Bell 430 blade; 2) tapered blades, 3) Blue Edge-like planform with taper and forward/aft sweep. Figure 6.2 compares the tapered and Blue Edge-like planforms. No optimization of the tapered and Blue Edge-like planforms was performed to minimize noise. The Blue Edge-like planform forward/aft sweep schedule is roughly comparable to photographs of the Airbus Blue Edge blade, capturing the key feature of reducing the "parallel" nature of the BVI.

Figure 6.1. Blue Edge blade concept from Eurocopter (now Airbus Helicopters). [Ref. 6.1]

Figure 6.2. Tapered and Blue Edge-like planforms.

Publications

None

Outreach Efforts

None

Awards

None

Student Involvement

Willca Villafana, M.S. student at PSU – primarily responsible for acoustic work in Objective 2, i.e., prepared the noise prediction system to output the necessary data for input to AEDT. Mr. Villafana completed his M.S. degree work in August 2016 and graduated Dec 2016. He is now attending the von Karman Institute in Brussels, Belgium.

Umberto Saetti, M.S. student at PSU – primarily responsible for flight simulation calculations and development and debugging of the coupling between the flight simulation code and the CHARM rotor module. Mr. Saetti graduated August 2016, and is now pursuing a Ph.D. at PSU on another project.

Plans for Next Period

This task is complete.

References

[6.1] Paur, J. Eurocopter Moves One Step Closer To 'Whisper Mode'. 2010 Feb 25, 2010 [accessed 3/4/2016]; Available from: http://www.wired.com/2010/02/eurocopter-moves-one-step-closer-to-whisper-mode/
[6.2] Nelms, D. (2015). "New Eco-Friendly Bluecopter Unveiled," Vertiflite 61(5): pp. 26-28.

Task 7. Noise Predictions and Data Preparation for AEDT

The Pennsylvania State University

Objective(s)

The objective of this task is to demonstrate the new capability by preforming the complete set of noise predictions (for the advanced configurations selected in task 6) necessary to provide inputs to AEDT.

Research Approach

The notional rotorcraft, along with the Bell 430 (time permitting) will be analyzed in the rotorcraft noise prediction system for all the various operating conditions. The data identified in task 5 will be produced in the appropriate format. This data will be evaluated and analyzed with tools outside of AEDT to provide detailed information about the noise of the vehicles and to provide analysis of the data delivered at the end of this task.

Milestone(s)

Predict the noise from the advanced technology configurations, prepare the data for AEDT processing, and document the data and analysis. This milestone is complete.

Major Accomplishments

Three different rotor configurations were tested on the Bell 430 helicopter model in the noise prediction system: standard rectangular blades, tapered blades, and Blue Edge-like blades. Each of the configurations were tested in a high BVI noise condition with forward speed of 68 knots and 6-degree descent angle. First, the sound from the main rotor was predicted on a plane one-rotor radii below the main rotor. Figure 7.1 shows predictions of both the overall sound pressure level (OASPL) and the BVI sound pressure level (BVISPL) (harmonics 6-40 in blade passage frequency) for each configuration. The magnitude and directionality predicted is characteristic of the results seen for BVI-noise dominated descent flight conditions. The analysis predicts that the taper reduces the peak BVISPL by roughly 2dB and the Blue Edge-like planform further reduces the peak BVISPL by another 3dB for a total reduction of peak BVISPL of 5dB, thus capturing the documented benefit of the Blue Edge planform. Figure 7.2 shows the advancing-side BVI for the Blue Edge planform compared with a rectangular blade as predicted by the CHARM code. Notice in the figure that the tip vortex (the red curved line) is nearly parallel to the entire length of the blade for the rectangular blade (left), while the shape of the Blue Edge planform (right) results in an interaction that occurs over a wider range of rotor azimuth angles; hence, it is a much less impulsive interaction.

Figure 7.3 shows the acoustic pressure time histories for each of the main rotor planforms at a point located on the hemisphere at an azimuth of 125˚ and down 45˚ from the main rotor tip-path plane. Notice in the figure, for each blade geometry there are 4 very narrow and high amplitude pressure spikes (or group of spikes). These are the BVI from each of the four blades on the main rotor. The thickness and loading noise of the main rotor also occur approximate the same time, so they are difficult to see. Comparison of the three different rotor blade geometries shows how the BVI acoustic pressure spikes amplitude is greatly reduced for the case of the Blue Edge-like rotor. The tapered blade also has a small reduction in BVI spike amplitude, primarily seen on the positive part of the pressure spike. The other features, i.e., the tail rotor noise, is essentially unchanged.

The noise comparisons shown in this section demonstrate the utility of the flight simulation, high-fidelity wake, noise prediction system that has been developed here. Furthermore, design changes to reduce BVI noise – one of the more challenging components of the noise to predict – show the expected noise reduction trends.

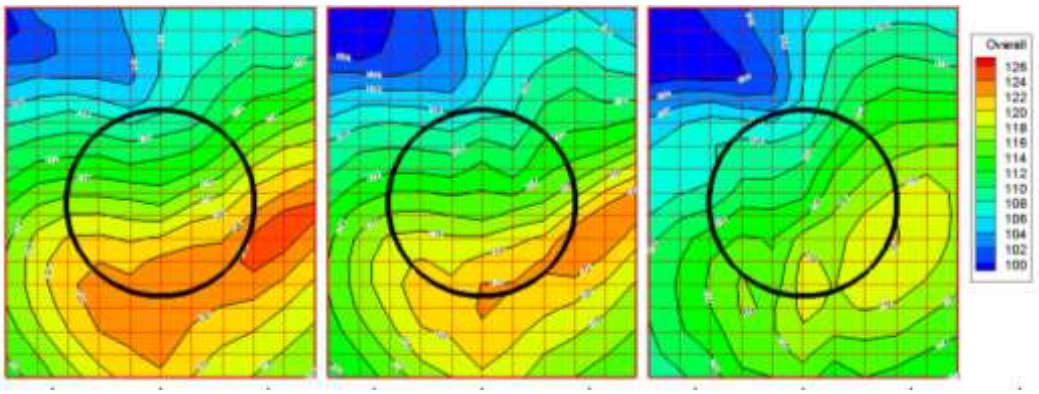

OASPL (harmonics 0 – 50 BPF)

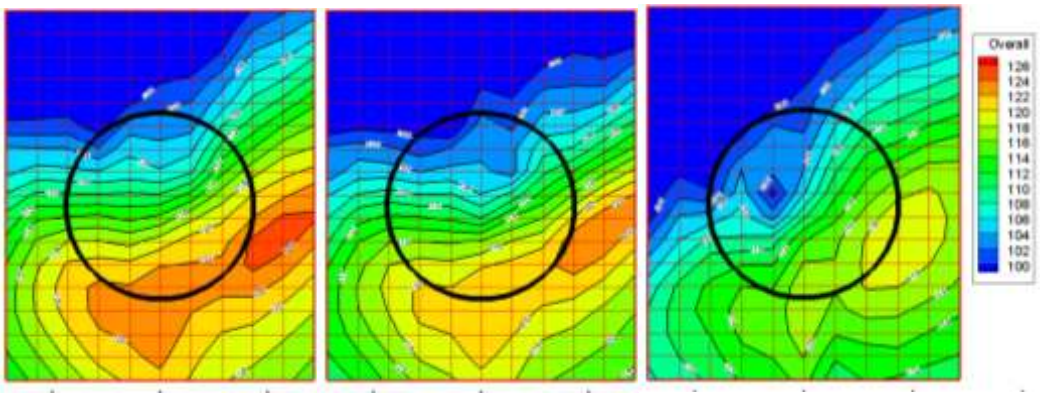

BVISPL (harmonics 6 – 40 BPF)

(a) RECTANGULAR (b) TAPERED (c) BLUE EDGE-like

Figure 7.1. CHARM/PSU-WOPWOP main rotor OASPL and BVISPL predictions one rotor radius beneath the nominal Bell 430 rotor for the three blade geometries; α_s=6° (back), μ=0.15 and C_T=.00143. The black circle represents the rotor tip – advancing side on the right.

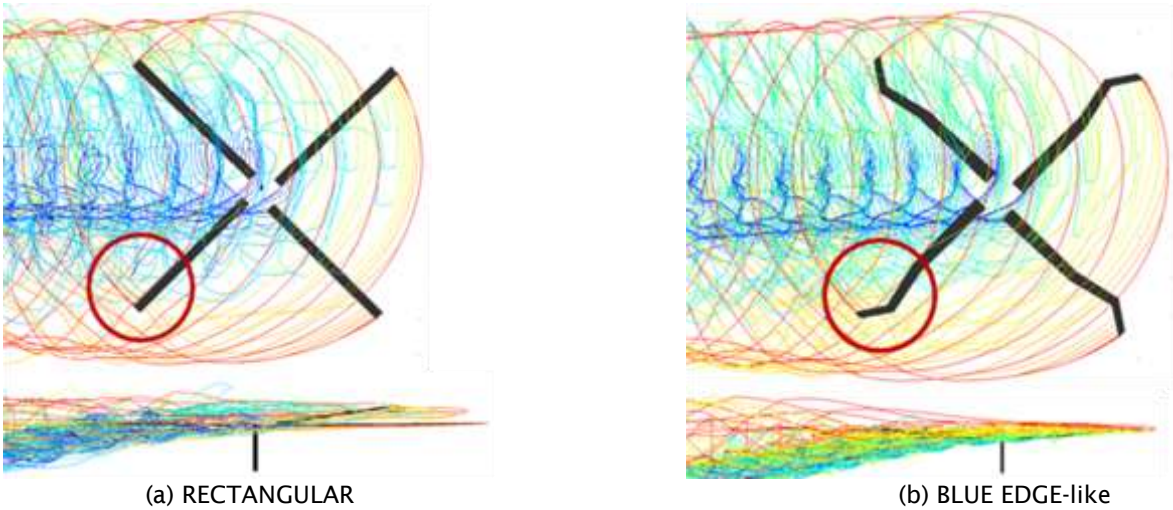

(a) RECTANGULAR (b) BLUE EDGE-like

Figure 7.2. BVI event as predicted by CHARM for the baseline RECTANGULAR blade and the BLUE EDGE blade.

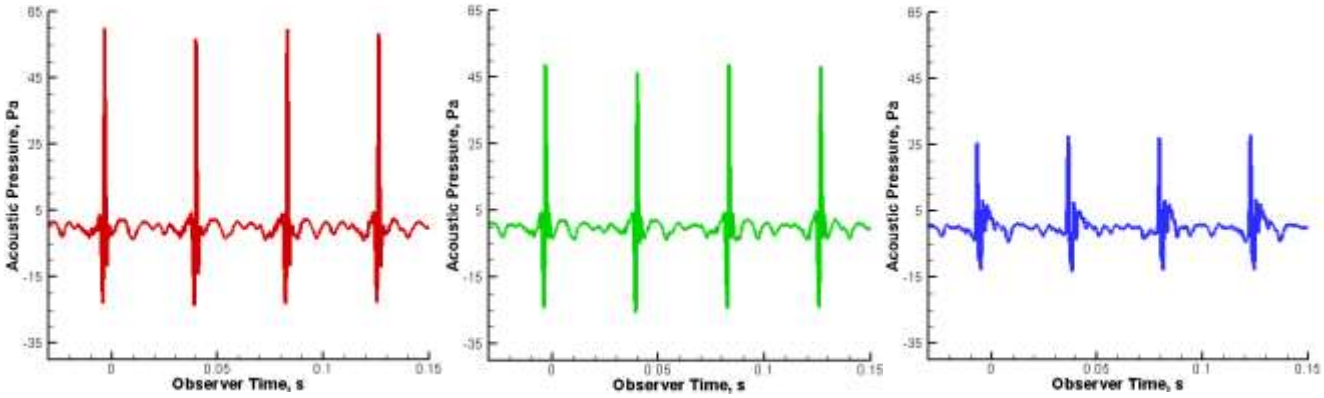

(a) RECTANGULAR (b) TAPERED (c) BLUE EDGE

Figure 7.3. Acoustic pressure time history at azimuth angle $\psi = 125$, elevation angle $\theta = -45\,°$ below the rotor plane, and radius of 30.48m from the helicopter c.g.

Publications

Saetti, U.; Horn, J.F.; Brentner, K.S.; Villafana, W.R.; and Wachspress, D.A., "Rotorcraft Simulations with Coupled Flight Dynamics, Free Wake, and Acoustics," proceedings of the 72nd AHS International Annual Forum and Technology Display, West Palm Beach, FL, May 17-19, 2016, 12 pages.

Outreach Efforts

None

Awards

None

Student Involvement

Willca Villafana, M.S. student at PSU – primarily responsible for acoustic work in Objective 2, i.e., preparing the noise prediction system to output the necessary data for input to AEDT. Work complete, graduation Dec 2016. Now attending the von Karman Institute in Brussels, Belgium.

Umberto Saetti, M.S. student at PSU – primarily responsible for flight simulation calculations and development and debugging of the coupling between the flight simulation code and the CHARM rotor module. Graduated August 2016, now pursuing a Ph.D. at PSU on another project.

Plans for Next Period

This task is complete.

Project 007 Civil, supersonic over-flight, sonic boom (noise) standards development

The Pennsylvania State University

University Members

Penn State Acoustics Program	Team Lead	Victor W. Sparrow
Penn State Applied Research Laboratory	Co-Principal Investigator	Kathleen K. Hodgdon

Advisory Committee Members

AERION: Jason Matisheck, Peter Sturdza, *et al.*
Boeing: Hao Shen, Bob Welge, *et al.*
Cessna: Kelly Laflin, *et al.*
Gulfstream: Robbie Cowart, Matthew Colmar, Brian Cook, Joe Gavin, *et al.*
Lockheed Martin: John Morgenstern, Tony Pilon, *et al.*
Volpe-The National Transportation Systems Center: Juliet Page, Bob Samiljan, et.al.
Wyle: Kevin Bradley, Chris Hobbs, *et al.*

Project Lead Investigator

Victor W. Sparrow
Director and Professor of Acoustics
Graduate Program in Acoustics
Penn State
201 Applied Science Bldg.
University Park, PA 16802
+1 (814) 865-6364
vws1@psu.edu

University Participants

The Pennsylvania State University

- P.I.: Vic Sparrow, Professor and Director, Graduate Program in Acoustics
- Researcher: Kathleen Hodgdon Research Associate
- FAA Award No.:13-C-AJFE-PSU Amendment 003, 013
- Period of Performance: August 4, 2014 to July 31, 2016
- Task(s):
  1. Study of Variability Effects

The Pennsylvania State University

- P.I.: Kathleen Hodgdon Research Associate
- Researcher: John Morgan R&D Engineer
- Researcher: Bernard Kozykowski
- FAA Award No.: 13-C-AJFE-PSU Amendments 004, 014, 026
- Period of Performance: August 4, 2014 to December 31, 2016
- Task(s):
  2. Community Instrumentation and Monitoring

Project Funding Level

This project supports the Civil Supersonics Overflight Sonic Boom (Noise) Standards Development through research conducted on multiple tasks at the Penn State University. FAA funding to Penn State in 2015-2016 was $200,000 comprised of $50K to Task 1 and $150K to Task 2.

In-kind cost sharing was provided by Gulfstream Aerospace Corporation in July 2016 to Penn State in excess of $200K. The point of contact for this cost sharing is Mr. Robbie Cowart, robbie.cowart@gulfstream.com . The Penn State Applied Research Laboratory also provided substantial in-kind cost share to Project 7.

Investigation Team

For 2015-2016 the investigation team included:
Penn State
Victor W. Sparrow (Co-PI) (Task 1)
Kathleen K. Hodgdon (Co-PI) (Task 2)
Researcher: John Morgan R&D Engineer (Task 2)
Researcher: Bernard Kozykowski R&D Engineer (Task 2)
ARL Graduate Research Assistant Will Doebler (Task 1: variability effects investigation)
ARL co-administered PSU Scholarship for Service undergraduate student Mitch Gold (Task 2: Community Monitoring)

Project Overview

Currently, the FAA is participating in ICAO CAEP effort to formulate new civil, supersonic aircraft sonic boom (noise) certification standard. To achieve this, CAEP Working Group 1 is addressing the sonic boom phenomenon, the signal acquisition and analysis of boom and making vibro-acoustical analyses and correlations with human response. This effort relies on extensive research being conducted to define the aircraft design and its performance. Equally important are ongoing efforts designed to better understand the subjective acoustical annoyance response for sonic boom levels that range from unacceptable to imperceptible. There are a number of areas that need to be addressed to support the standards setting process, but one of the primary ones is metrics validation and sensitivity studies for a wide range of boom levels.

The research tasks are designed to support FAA and NASA activities on supersonics and sonic boom research. As the research progresses, this may involve the support of testing, data acquisition and analyses, of field demonstrations, laboratory experiments or theoretical studies.

Task 1 Study of Variability Effects

The Pennsylvania State University

Objective

The objective of this activity is to continue research at The Pennsylvania State University in the ASCENT COE to complement the sonic boom standards development ongoing within the Committee for Aviation Environmental Protection's (CAEP) Working Group 1 (Noise Technical), Supersonics Standards Task Group (SSTG). This research will ensure that the behavior of the sonic boom metrics considered in the SSTG discussions are well-understood prior to down-selecting a finalized metric or metrics for use in possible sonic boom certification and/or rulemaking.

Research Approach

Similar to the work in 2015, various sonic boom noise metrics have been calculated for a number of sonic booms, primarily N-wave signatures. The newly computed metrics dataset utilized high-quality recordings from the Superboom Caustic Analysis and Measurement Program (SCAMP) [Page, *et al.,* 2013] and Farfield Investigation of No-Boom Thresholds (FaINT) [Cliatt, *et al.*, 2016] experiments conducted by NASA. With these signature datasets comprised of microphone measurements along substantial linear arrays, one can assess the waveform variability due to atmospheric turbulence influences across the arrays. Preferred boom events from these NASA datasets were then chosen after review of the flight conditions, flight objectives and actual waveforms generated in order to study only the non-focused, N-wave sonic boom signatures.

The sonic boom metrics chosen for application in the 2016 Project 7 studies are those described in a recent multi-author report describing a down-selection of appropriate sonic boom metrics [Loubeau, 2015], namely A-weighted sound exposure level, B-weighted sound exposure level, E-weighted sound exposure level, Steven's Mark VII perceived loudness, and NASA's Indoor Sonic Boom Annoyance Predictor. These metrics are abbreviated SEL_A, SEL_B, SEL_E, PL, and ISBAP.

Metrics robustness investigation

A major effort in Task 1 in 2016 was to investigate the robustness of sonic boom metrics to atmospheric absorption effects. It is well understood that the lowest altitudes of the atmosphere contain the planetary boundary layer, and that propagating through the atmospheric turbulence in that boundary layer distorts sonic boom signatures. N-wave sonic booms are prone to both spiking and rounding at both the front and back shocks comprising the signature, and the effect seems random. In the WG1 and SSTG discussions regarding picking an appropriate metric for use in certification, the question arose as to which of the metrics mentioned previously are the most robust with respect to turbulent distortion effects. That is, which metric is the least sensitive to turbulence effects.

After appropriate non-focused sonic boom signatures from the SCAMP dataset were identified, an effort was made to employ the Locey/Sparrow finite impulse response filters [Locey and Sparrow, 2007] to add turbulence to the measured data. Hence a number of turbulized sonic boom realizations were created from the clean signatures, and the above metrics were employed to see which metric had the smallest change in dB value caused by the effects of turbulence.

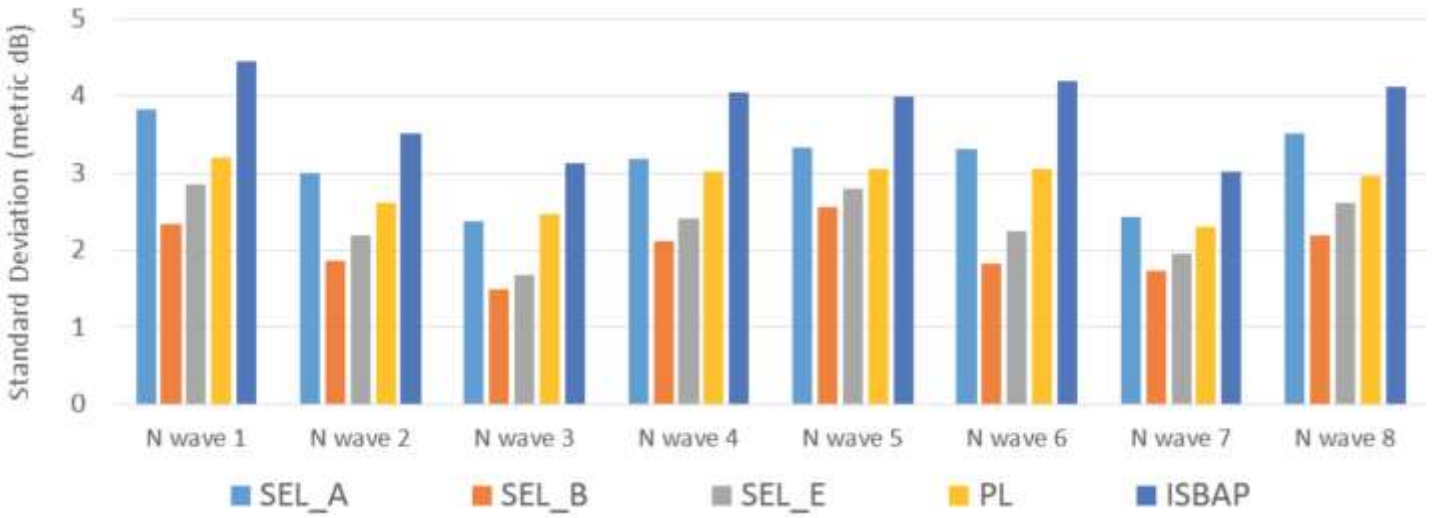

Figure 7.1. Influence of atmospheric turbulence on 8 N-wave sonic boom signatures for 5 different sonic boom metrics. Each bar shows the standard deviation in that metric in dB due to the turbulence effects. SEL_B shows the lowest SD (best, most robust) due to the turbulence effects. SEL_E is next best.

In Figure 7.1 it can be seen that for the 8 N-wave sonic booms selected, and the 10 turbulence filters available for producing the turbulence effects, that the SEL_B metric was the most robust (least sensitive), showing the smallest standard deviation in metric value. SEL_E showed the 2nd most robust characteristics. Not shown here, but an additional set of sonic boom waveforms, corresponding to low-boom signatures of an ASCENT industrial partner, were also carefully examined. In short, the industrial partner's low-boom sonic boom signatures were similarly affected by the atmospheric turbulence filters. For the low-boom signatures, SEL_B values were least affected by the simulated turbulence. The Penn State team is currently working on preparing a manuscript for submission to an archival journal to fully report these results.

Deturbing investigation

In 2016 the Penn State team also spent substantial time thinking about how to remove turbulence from ground-measured sonic boom signatures, a process referred to by some as "de-turbing". This is a lofty goal, and one that would be invaluable to the supersonics certification community.

The approach that Penn State took in 2016 focused on cross-correlation and averaging across a linear array of microphone measurements to remove the fine scale turbulence. This did work for the fine scales, but it did not work for the large scale turbulence which still required having the front shock and rear shocks be symmetric. That is OK for N-wave sonic booms, but this latter de-turbing method will not work for low-boom waveforms. Hence, additional work or alternative methods will be required. It was established, however, that for any de-turbing procedure that an estimation (or direct knowledge) of a clean sonic boom signature without turbulence is required. Essentially, you need to know your clean sonic boom waveform in advance in order to remove the turbulence from ground measured microphone data.

Some in WG1 and SSTG have suggested that the simplest thing one can do to measure clean sonic boom signatures is to suspend the microphone measuring equipment above the turbulence using balloons, sailplanes, motor gliders, or unmanned aerial vehicles. Such setups would be quite elaborate compared to today's typical practice of placing microphones on ground boards, so it seems that having a working de-turbing procedure would be very welcome.

Milestone(s)
N/A

Major Accomplishments
Project 7, task 1 showed that some sonic boom metrics are less sensitive to atmospheric turbulence than others. It was determined that B-weighted sound exposure level was the most robust metric out of several candidate metrics.

Publications
J. Palmer and V. Sparrow, “Measured N-wave sonic boom events and sensitivity in sonic boom metrics,” in *Recent Developments in Nonlinear Acoustics*, AIP Conf. Proc. **1685** 090012 (AIP, 2015), doi: 10.1063/1.4934478. (This conference publication describes the work performed in 2015 on Project 7 Task 1.)

Outreach Efforts
None.

Awards
V. Sparrow gave the 2016 Rayleigh Lecture to the American Society of Mechanical Engineers (ASME) Noise Control and Acoustics Division on November 15, 2016 at the 2016 International Mechanical Engineering Congress and Exposition in Phoenix, AZ. The title of the talk was "Two approaches to reduce the noise impact of overland civilian supersonic flight."

Student Involvement
William Doebler is the graduate research assistant funded by the Applied Research Laboratory on Project 7. He is currently working toward his Ph.D. at the Penn State Graduate Program in Acoustics.

Plans for Next Period
Project 7 Task 1 ended in July 2016. The work to support CAEP WG1 and SSTG will continue in ASCENT Project 41.

References
L. Cliatt, *et al.*, "Lateral cutoff analysis and results from NASA's farfield investigation of no-boom thresholds," NASA TM-2016-218850 (2016).
L. Locey and V. Sparrow, “Modeling atmospheric turbulence as a filter for sonic boom propagation,” Noise Control Eng. J. **55**(6) 495-503 (2007).
A. Loubeau, *et al.*, “A new evaluation of noise metrics for sonic booms using existing data,” in *Recent Developments in Nonlinear Acoustics*, AIP Conf. Proc. **1685** 090015 (AIP, 2015).

D. Maglieri, *et al.*, *Sonic Boom: Six Decades of Research* (NASA SP-2014-622, 2014), pp. 51-52.
J. Palmer and V. Sparrow, "Measured N-wave sonic boom events and sensitivity in sonic boom metrics," in *Recent Developments in Nonlinear Acoustics*, AIP Conf. Proc. **1685** 090012 (AIP, 2015), doi: 10.1063/1.4934478.
J. Page, C. Hobbs, E. Haering, D. Maglieri, R. Shupe, C. Hunting, J. Giannakis, S. Wiley, F. Houtas, "SCAMP: Focused sonic boom experiment execution and measurement data acquisition," AIAA paper 2013-0933, 51st AIAA Aerospace Sciences Meeting, Grapevine, TX, January 2013.

Task 2 Community Instrumentation and Monitoring

The Pennsylvania State University

Objective

The research is being conducted in anticipation of future low boom community field tests. The community instrumentation and monitoring task was undertaken to facilitate a pro-active approach to interacting with communities participating in future field tests.

Research Approach

The research includes the assessment of community noise impact and methods to assess public acceptability of low boom signatures. Aspects of this research include identifying cost effective methods to measure noise and to observe community response to noise impact by monitoring social media dynamics in the community during the field test.

Milestone(s)

Research was conducted in support of future NASA sponsored low boom community impact field tests which will support FAA in future certification and regulatory decisions. The development of cost effective noise monitors to augment existing field monitors was initiated, in an effort to optimize measurement requirements and minimize costs in future field tests. Social media monitoring tools were investigated, as a means to observe social dynamics and to provide insights into community perceptions of noise impact during the field tests.

Major Accomplishments

Social Media Monitoring Tools

The social media monitoring task is evaluating options that would allow researchers to observe the social dynamics in the overall community response during a low boom community field test. The intent is to observe community perspective on noise impact. By monitoring on line discussions we have the opportunity to identify concerns within the community related to the proposed or ongoing low boom community field test. The research team could then engage the community with targeted Outreach materials that address issues observed on posts to social media.

Social media monitoring tools are a soft sensor to observe community dynamics on population-centric media such as Facebook or Twitter. The use of a geographic based topic specific search of social media can be used to observe community dynamics. The search is dependent on users with the location feature enabled on the device that they are using to post. An article on PewInternet.org indicated that among adult social media users ages 18 and older, 30% say that at least one of their accounts is currently set up to include their location in their posts.[1] A fact sheet from the Pew Research Center provided the following chart on social media usage growth from 2005 to 2013 by age group.

[1] "Social Networking Fact Sheet." Pew Research Center Internet Science Tech RSS. N.p., 27 Dec. 2013. Web. 11 Mar. 2016. <http://www.pewinternet.org/fact-sheets/social-networking-fact-sheet/>.

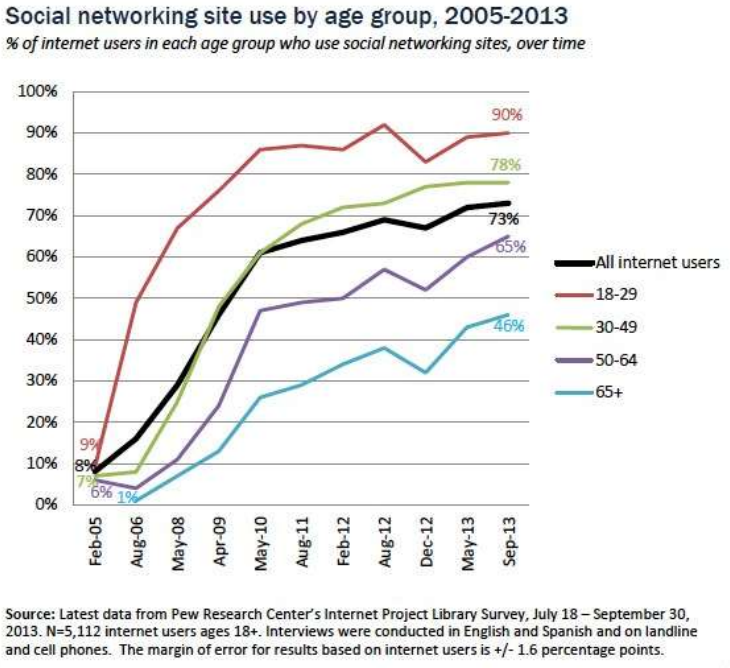

Figure 7.2. Social media site usage from 2005 -2013[2]

Figure 7.2 shows the growth of social media usage in the recent past, across all age groups. The use of social media monitoring affords the means to observe a community response to an event. The information will be used to draft news releases and outreach information. The social media observations are intended to inform the researchers of social climate and dynamics within community and are not considered to be subjective response test data.

We explored the use of the social media monitoring tool GeoFeedia, which excelled in visualization of the data analysis. However, the cost was $1000 per data set, which was too costly for this project, or for the real time support of the NASA field tests. We attempted to negotiate a reduced cost since it is for research purposes, but were not able to make that negotiation work. We are conducting tests of EchoSec, a social media monitoring tool that is $1068 per year, but has less archived data available, and different visualization of the data. The exploration of this tool's applicability in support of community response testing continues.

[2] "Social Networking Fact Sheet." Pew Research Center Internet Science Tech RSS. N.p., 27 Dec. 2013. Web. 11 Mar. 2016. <http://www.pewinternet.org/fact-sheets/social-networking-fact-sheet/>.

Figure 7.3. Snapshot of hits on boom comments using Echosec (https://www.echosec.net/)

The use of social media monitoring as a supplemental field research method affords a secondary means to observe a community response to an event, provided the biases and limitations of the approach are included with the observations.

Low Cost Noise Monitor (LCNM) Instrumentation

The team is designing a low cost noise monitor using commercial off the shelf (COTS) technology to measure low booms in support of future NASA low boom field tests. The purpose is to identify cost effective methods to measure noise in the community during the field test. The low cost noise monitor (LCNM) should be a self-powered weather proof rugged system. Several designs were considered, and component selection has been made and a prototype is in development. The LCNM design is mirroring, to the extent possible, the technical requirements that were used to develop the Sonic Boom Field Kits, or Sonic Boom Unattended Data Acquisition Systems (SBUDAS), briefly detailed below. The low cost noise monitors will be recording the same signals as the Field Kits. Some degradation in capabilities is expected in exchange for the reduction in cost. There is a desire to develop a lower cost monitor that can meet as many specifications as possible. The cost per unit should be on the order of $2K to $3K (if possible), maximum $5K, depending on the design and capabilities.

Signals:

- Outdoor sonic boom signatures (dynamic pressure)
- Time code for synchronization. GPS coordinates.
- Weather rugged recording mechanism

Existing High Fidelity Field Kit (SBUDAS) Sensors / Recording:

- Local Channel Count: 4 to 8 channels of A/D depending on the application
- Frequency range:
  - 1 Hz to 20 kHz (ICP mics). DC to 20 KHz (externally polarized mics).
  - Qualitative measures of signatures require a response that is flat from 0.1Hz-10KHz.
- Maximum pressure:
  - carpet boom measurements: < 1 psf (125 dB re 20 mPa)
  - focus boom measurements: < 10 psf (145 dB re 20 mPa)
- Dynamic Range: >104 dB / 24 bit
- Mic Noise Floor: <20 dBA due to mic (could be higher in focus boom config. due to NI dynamic range)

Several low cost options have been explored. A basic system is being investigated, with a single board computer, microphone, and batteries. Methods to acquire data for the entire duration of the test on remotely deployed systems are being investigated. The units are being design with a GPS receiver, similar to the one use in the SBUDAS field kits. The design is dependent on the addition cellular connectivity for remote triggering. Several designs were investigated considering the electrical power considerations, mechanical components, and the electrical data flow and data storage. The design includes two microphone channels that can be set with different dynamic ranges. This affords the ability to capture

low level signals with integrity, and affords a second microphone channel set with a higher dynamic range in case there is a focus boom. The overall design that was selected for implementation is reflected in the following schematic.

Low Cost Noise Monitor Chosen Design

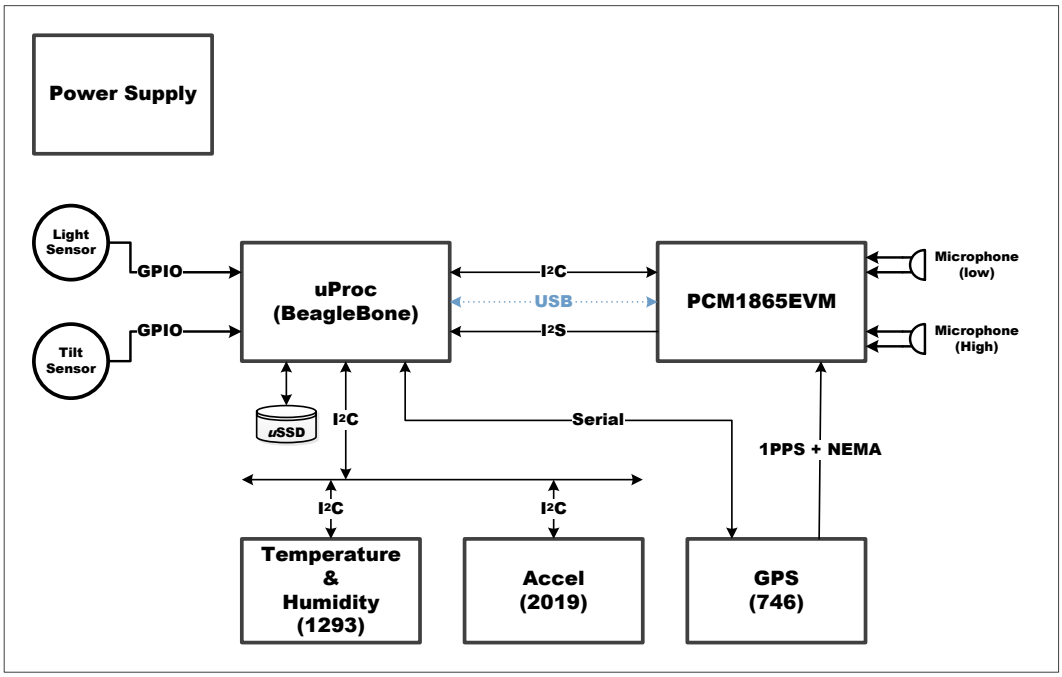

Figure 7.4.

The design includes an accelerometer channel, to allow the LCNM to have greater applicability for a wider range of noise monitoring projects, in addition to the support of the upcoming low boom field tests. Design selection was contingent on the availability of low cost parts for the monitor. Parts have been ordered and a proto-type will be developed and tested in a follow on effort. Field implementation of the LCNM requires development of software to facilitate the ability to readily download the field data.

Publications

None

Outreach Efforts

This research task supports NASA activities on supersonics and sonic boom research. The team has provided information to the NASA sponsored Waveforms Sonicboom Perception and Response Risk Reduction (WSPRRR) team. This NASA sponsored team consists of ASCENT Project 7 team members from Penn State, Volpe, Wyle and Gulfstream working with NASA team lead APS to formulate a test plan for future low boom community field tests.

Awards

None

Student Involvement

Mitch Gold is a PSU IST student working on the Social Medial Monitoring task. He is supported through the Federal Cyber Corps Scholarship for Service (SFS) program, which is offered and funded through the National Science Foundation (NSF) and the Department of Homeland Security (DHS). The PSU SFS program is administered through the College of Information Science and Technology and the Applied Research Lab. Because this appointment is funded externally, it does not count as cost share.

Plans for Next Period

The effort to expand the ability to observe the response within a community to a low boom field test led to the decision to also evaluate additional instrumentation and methods to document the noise impact across the community.

- The Research Instrumentation task will continue to assess the fidelity of lower cost noise monitors to optimize noise measurement requirements and minimize costs in future field tests.
- The Monitoring task will further evaluate social media as a means to observe social dynamics in the community that provide insights that afford the opportunity for subsequent Outreach.

References

"Social Networking Fact Sheet." Pew Research Center Internet Science Tech RSS. N.p., 27 Dec. 2013. Web. 11 Mar. 2016. <http://www.pewinternet.org/fact-sheets/social-networking-fact-sheet/>.

Project 008 Noise Outreach

The Pennsylvania State University

University Members

Penn State Applied Research Laboratory Team Lead	Kathleen Hodgdon
Penn State Institute for Energy and the Environment	Maurie Caitlin Kelly
Penn State Earth & Environmental Systems Institute	Bernd Haupt

Advisory Committee Members

Gulfstream Aerospace Corporation	Robbie Cowart
Port of Portland Sr. Noise Analyst	Jason Schwartz
Volpe National Transportation Systems Center	Juliet Page, Eric Boeker

Project Lead Investigator

Kathleen Hodgdon
Research Associate
Applied Research Laboratory
Pennsylvania State University
ARL North Atherton Street
P.O. Box 30 (Mail Stop 2210H)
State College PA 16804-0030
Phone: 814-865-2447
Email: kkh2@psu.edu

University Participants

Pennsylvania State University

- P.I.: Kathleen Hodgdon, Research Associate
- Researcher: Maurie Caitlin Kelly, Research Associate
- Researcher: Bernd Haupt, Senior Research Associate
- FAA Award No.:13-C-AJFE-PSU Amendments 16
- Period of Performance: July 31, 2016 to July 31, 2017
- Task(s):
  1. Stakeholders Interactions
  2. Content Development
  3. Site Navigation and Infrastructure Enhancement

Project Funding Level

This project supports the Outreach efforts at Penn State with $75K of FAA funds. Matching funds are anticipated to satisfy cost share on all tasks.

Investigation Team

For 2016-2017 the investigation team includes:
P.I.: Kathleen Hodgdon Research Associate
Researcher: Maurie Caitlin Kelly Research Associate
Researcher: Bernd Haupt Senior Research Associate

Project Overview

The Outreach project seeks to improve airport and community interactions by providing information and education on aviation noise topics. Outreach has been implemented through the NoiseQuest website and by direct interactions with stakeholders. NoiseQuest (NQ), located at www.noisequest.psu.edu, is an international resource that is designed to implement global education on aviation noise topics. The site presents outreach content and aviation noise information on a diverse set of topics. The PSU Outreach team has continued to expand and enhance the NoiseQuest website.

Outreach Goals:

1. Enhance global knowledge on aviation noise topics
2. Increase awareness and provide information to address aviation noise related issues
3. Interact with stakeholders to identify new content areas and current noise issues
4. Provide educational information in a format that is accessible to the general public
5. Present information on NoiseQuest in an easily navigated, user friendly context

Task 8.1: Stakeholders Interactions

Pennsylvania State University

Objectives

The objectives of this task includes: (1) interactive outreach to identify aviation noise programs; (2) obtain airport noise contour data from airport noise managers; and (3) gather contributions of content to be shared on the NoiseQuest site.

Research Approach

Interactive outreach with airport noise managers and community groups was conducted to: (1) identify concerns that could be addressed by expanded content topics; (2) identify successful programs and initiatives; and (3) request GIS noise contour data. The site user statistics are monitored to better inform the site development.

Milestones

We communicated with airport noise managers, stakeholders, and community organizations to identify updates for existing content and opportunities for new content development. We obtained GIS data to display airport noise contours on NQ Explorer from additional airports.

Major Accomplishments

We continue to interact with airport noise managers and community groups to identify topics of interest, successful implementations of outreach, or other approaches taken to resolve aviation noise issues. We investigated online feedback options for the site, but determined not to add the feature at this time. We had reservations since we would not be able to provide real-time monitoring of the comments and community members may post noise concerns to NQ instead of contacting local airport noise managers or the FAA's Noise Ombudsman. Jason Schwartz (ASCENT Advisory Committee Member), from the Port of Portland is an active team member. He has provided ideas and content topics as well as offering to interact with other airport noise managers on our behalf. We have contacted airport noise managers to obtain contours for NQ Explorer and we were successful in obtaining updated contours from Philadelphia International Airport. We also received data from the San Francisco International Airport, which consists of their 2014 Noise Exposure Map and the 5 year (2019) noise projections.

We interact with the National Organization to Insure a Sound-controlled Environment (N.O.I.S.E.) and they have shared their contact list for airport noise managers as well as provided ideas for content and the Spotlight section. Emily Tranter (N.O.I.S.E. National Coordinator) is working with us on identify content topics as well as programs to feature in the Spotlight section. We continue to encourage stakeholders to link their site to NoiseQuest. We continue to monitor our site statistics to gain insights on site usage (see Appendix 1 for Site Statistics).

Publications

Contents are published at www.noisequest.psu.edu.

Outreach Efforts

We interact with airport noise managers and community groups from across the country.

Awards
None

Student Involvement
None

Plans for Next Period
We will continue to monitor site statistics to determine site usage patterns. To promote greater site usage, we will work to get additional stakeholders to link to NoiseQuest and to provide recommendations for content.

Task 8.2: Content Development
Pennsylvania State University

Objectives
This task is focused on identifying and developing content that addresses aviation noise impact and outreach education.

Research Approach
The Outreach team seeks to identify content that presents updates on aviation noise research, addresses noise issues, or meets the educational outreach needs of aviation stakeholders on specific topics.

Milestones
The NoiseQuest team worked with a team of FAA managers to review the entire NoiseQuest site identifying areas for updated content. The team maintained existing site areas and added new content.

Major Accomplishments
A full site review was conducted by the NoiseQuest team working with FAA program managers. Edits were added to content in About Airports, Noise Basics and Noise Research and Community Tools. Topics reviewed included INM, AEDT, NextGen, PBN, general updates to noise models, air traffic control, metrics, and the glossary in community tools. We reviewed recommendations made by AEE managers and improved the readability of suggested edits so that the content reading level targeted approximately a 10th to 12th grade reading level before the final edits were uploaded to the site. Updated content was added to the "Noise Basics" and "Noise Models" section of the website. In addition, new content and edits to existing content were completed for the following webpages: Air Traffic Control, FAA Regulations, Continuous Descent, Spotlight on Noise, and Noise Effects. We are not adding content on historical noise contours at this time.

We are gathering additional materials to expand content on PBN and low boom noise impact. We are working with NASA and the NASA sponsored Waveforms Sonicboom Perception and Response Risk Reduction (WSPRRR) team to develop content on supersonics and low boom noise impact. This NASA sponsored team is developing a test plan for future low boom community field tests. The NASA WSPRRR team includes both ASCENT and NASA researchers, who can team with the NoiseQuest team to identify and develop the low boom content for the NoiseQuest site.

Working with PSU lawyers, we reviewed the site disclaimer language and left the current disclaimer in place. We can revisit this in the future if warranted. We updated the site to acknowledge contributions from both PARTNER and ASCENT researchers.

Publications
Site developed at www.noisequest.psu.edu

Outreach Efforts
We develop the Outreach content by reaching out to stakeholders for content ideas and development.

Awards

None

Student Involvement
None

Plans for Next Period
Content Development: The existing site content will be enhanced or expanded. New content topics will be identified and relevant features added to the site. Content is planned for, but not limited to, topics such as information on low boom noise, NextGen, and/or helicopter noise. Other topics will be identified based on stakeholder engagement.

Task 8.3: Site Navigation and Architecture Redesign and Development
Pennsylvania State University

Objectives
Efforts under this task maintain the site architecture and enhance site navigation.

Research Approach
To ensure that the site is accessible to the general public, the team works to assure that the information on NoiseQuest is presented in an easily navigated user-friendly format. This effort includes website management including backups, updates, and infrastructure enhancement.

Milestones
The entire site was reviewed and updates and new content were posted to the site. During the review, broken links were identified and addressed. Modifications to the NQ Explorer were investigated.

Major Accomplishments
The entire site was reviewed, resulting in updated and new content being added to NoiseQuest (see Task 8.2 for a list of topics). Methods to provide the opportunity for online user feedback on site content were discussed and a template for an online survey was devised. The decision was made to not add a feedback survey to the site at this time. The NQ website was migrated to new server in the Advanced CyberScience Infrastructure facility at Penn State. To monitor usage of the entire site, website statistics were moved to Google Analytics.

NoiseQuest has over 100 pages of content, each with multiple links. We continue to identify alternate links and materials for the site. Links changed by other sites are difficult to track, but we are working to identify and update broken links. Link checkers were run on all NQ pages and new links were updated.

We acquired and uploaded Geographic Information System (GIS) data to the NQ Mapper application for updated noise contours from Philadelphia International Airport and from San Francisco International Airport. The team identified display issues with the NQ Mapper application in the NQ Explorer, which were subsequently associated with a change in the Google Map's Application Programming Interface (API). This change in API affected the functionality of the NQ Explorer by interfering with the search and display of airports and the ability to view pop-up windows in the mapping interface. The team investigated options to revise the NQ Explorer and researched alternative options for the interface and a new basemap. These options included potentially utilizing the Environmental Systems Research Institute (ESRI) basemap and API, or alternatives such as Cesium. Options for ESRI were explored beyond the basemap and API. There is the potential for utilizing ESRIs ArcGIS Online (AGOL) as the basis for a new NQ Explorer. This would require that the airport database and noise contours stream via AGOL and a new application would be developed as an interface to the data. Limitations on pop-up windows and linking mechanisms may make this option unviable. The team also discussed options with the Cesium representatives. Cesium provides a 3D "map" so that users can visualize elevation and data together. Working with the Cesium representatives, the team investigated options to develop a test application in the Cesium environment.

Publications
None

Outreach Efforts
The team works to ensure that GIS data formats provided by airport noise managers are compatible with the site.

Awards
None

Student Involvement
None

Plans for Next Period
The team identified the need to upgrade the website to be device agnostic and user-friendly on all platforms simultaneously. The current website is accessible on multiple devices and browsers. However, navigation is not streamlined while accessing the site using small screened devices. The ongoing redesign of the site architecture will streamline the site's usability on a range of hardware (e.g., phones, tablets, touch-enabled laptops, etc.). We will also investigate options to redevelop the NQ Mapper in the NQ Explorer utilizing a new basemap provider to address issues with Google Map's API.

Appendix 1. NoiseQuest Annual Statistics 2016 vs 2015

30,000 Global Sessions in 2016 28,446 Global Sessions in 2015

NoiseQuest 2016 Annual Statistics		NoiseQuest 2015 Annual Statistics	
Page Title	Page views	Page Title	Page views
Total	57,643	Total	54,010
NoiseQuest: Noise Basics	12,402	NoiseQuest: Noise Basics	11,769
NoiseQuest: Community Tools	11,438	NoiseQuest: Community Tools	9,514
NoiseQuest: Noise Effects	10,545	NoiseQuest: Noise Effects	9,954
NoiseQuest: About Airports	7,337	NoiseQuest Home	6,584
NoiseQuest Home	6,591	NoiseQuest: About Airports	6,418
NoiseQuest: Sources of Noise	5,995	NoiseQuest: Sources of Noise	6,147
NoiseQuest: NQ Explorer	1,382	NoiseQuest: NQ Explorer	1,626
NoiseQuest: Research	939	NoiseQuest: Research	1,129
NoiseQuest	498	NoiseQuest	528
NoiseQuest: Spotlight	281	NoiseQuest: Spotlight	236

Monthly Trend in page views in 2016

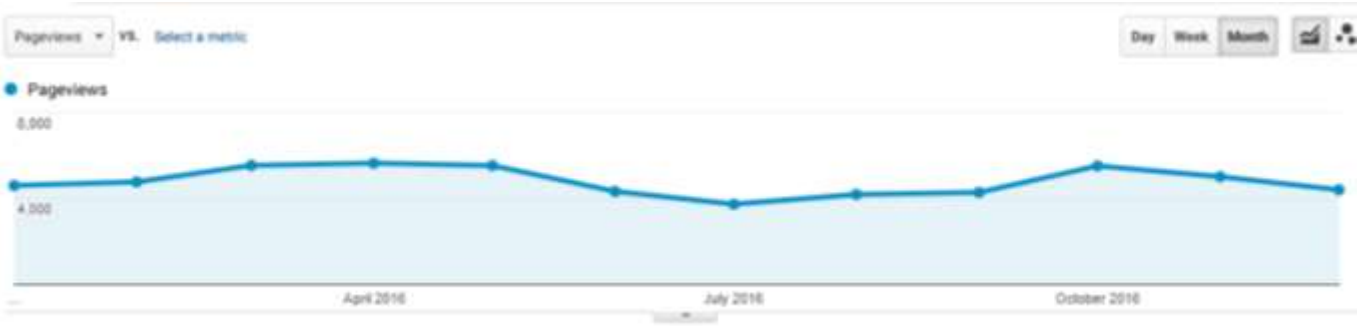

Project 010 Aircraft Technology Modeling and Assessment

Georgia Institute of Technology
Purdue University
Stanford University

Project Lead Investigator

Dimitri Mavris (PI)
Regents Professor
School of Aerospace Engineering
Georgia Institute of Technology
Mail Stop 0150
Atlanta, GA 30332-0150
Phone: 404-894-1557
Email: dimitri.mavris@ae.gatech.edu

Daniel DeLaurentis (PI)
Professor
School of Aeronautics and Astronautics
Purdue University
701 W. Stadium Ave
West Lafayette, IN 47907-2045
Phone: 765-494-0694
Email: ddelaure@purdue.edu

William Crossley (Co-PI)
Professor
School of Aeronautics and Astronautics
Purdue University
701 W. Stadium Ave
West Lafayette, IN 47907-2045
Phone: 765-496-2872
Email: crossley@purdue.edu

Juan J. Alonso (PI)
Professor
Department of Aeronautics & Astronautics
Stanford University
496 Lomita Mall, Durand Bldg. Room 252
Stanford, CA 94305-4035
Phone: 650-723-9954
Email: jjalonso@stanford.edu

University Participants

Georgia Institute of Technology
- P.I.(s): Dr. Dimitri Mavris (PI), Dr. Jimmy Tai (Co-PI)
- FAA Award Number: 13-C-AJFE-GIT-006
- Period of Performance: August 1, 2014 – August 31, 2017

Purdue University

- P.I.(s): Dr. Daniel DeLaurentis, Dr. William A. Crossley (Co-PI)
- FAA Award Number: 13-C-AJFE-PU-004
- Period of Performance: August 1, 2014 – May 31, 2017

Stanford University

- P.I.(s): Dr. Juan J. Alonso
- FAA Award Number: 13-C-AJFE-SU-004
- Period of Performance: August 1, 2014 – May 31, 2017

Project Funding Level

The project is funded at the following levels: Georgia Institute of Technology ($985,000); Purdue University ($209,969); Stanford University ($215,000). Cost share details for each university are below:

The Georgia Institute of Technology has agreed to a total of $985,000 in matching funds. This total includes salaries for the project director, research engineers, graduate research assistants and computing, financial and administrative support, including meeting arrangements. The institute has also agreed to provide tuition remission for the students paid for by state funds.

Purdue University provides matching support through salary support of the faculty PIs and through salary support and tuition and fee waivers for one of the graduate research assistants working on this project. While Purdue University provides the majority of the 1:1 cost share for ASCENT 10-Purdue, an in-kind matching contribution of just under $20,000 comes from a gift of the RDSwin-Pro aircraft design software from Conceptual Research Corp.

Stanford University has met or exceeded its matching funds contribution using a combination of elements. Firstly, Stanford University is cost sharing, through tuition reductions for the students working on this project for the entire period of performance. In addition, our partners at the International Council for Clean Transportation are providing in-kind cost-sharing for the remainder amount though internal and external efforts funded to better understand the impact of cruise speed reduction.

Investigation Team

Georgia Institute of Technology
Principal Investigator: Dimitri Mavris
Co-Investigator: Jimmy Tai
Technology Modeling Technical Lead: Christopher Perullo
Fleet Modeling Technical Lead: Holger Pfaender
Students: Matt Reilly, Braven Leung

Purdue University
Principal Investigator: Daniel DeLaurentis
Co-Investigator: William Crossley
Students: Kushal Moolchandani, Parithi Govindaraju, Nithin Kolencherry, Ogunsina Kolawole

Stanford University
Principal Investigator: Juan J. Alonso
Aircraft Modeling Technical Lead: Anil Variyar
The team also includes two additional graduate students that have been assisting with the technical work and the development of our aircraft optimization framework, SUAVE, Emilio Botero and Tim MacDonald.

Project Overview

Georgia Tech, Purdue, and Stanford partnered to investigate the impact of aircraft and vehicle technologies on future environmental impacts of aviation. This is a multi-step process involving the system assessment of FAA CLEEN program technologies by Georgia Tech, assessment of the impact of mission specification changes on public domain aircraft

performance by Stanford, and the impact of future fleet modeling assumptions on system wide fleet fuel burn and emissions by Purdue.

The research is conducted as a collaborative effort in order to leverage capabilities and knowledge available from the multiple entities that make up the ASCENT university partners and advisory committee. Georgia Tech has partnered with Purdue University and Stanford University to complete the following objectives.

The primary objective of this research project is to support the FAA in modeling and assessing the potential future evolution of the next generation aircraft fleet. Research under this project consists of three integrated focus areas: (1) Developing a set of harmonized fleet assumptions for use in future fleet assessments; (2) Modeling advanced aircraft technologies and advanced vehicles expected to enter the fleet through 2050; and (3) Performing vehicle and fleet level assessments based on input from the FAA and the results of (1) and (2).

Due to extensive experience assessing CLEEN I, Georgia Tech is the lead for all three objectives described above. Stanford and Purdue will support the objectives as shown in Table 1, listing the high-level division of responsibilities amongst the universities.

Table 1: University Contributions

Objectives		Georgia Tech	Stanford	Purdue
1	Harmonize Fleet Assumptions	Drive Process, coordinate industry, government participation, provide basis for discussion	Support assumptions definition, provide expert knowledge	Support assumptions definition, provide expert knowledge
2	Advanced Vehicle and Technology Modeling	CLEEN Boeing and GE proprietary technology modeling, additional public domain technology modeling, Provide tech models to SU and PU	Input into public domain technology modeling	N/A
3	Vehicle and Fleet Assessments	Perform vehicle and fleet level assessments for CLEEN technologies using GREAT/ANGIM	Provide trade factors for mission specification changes. Provide tech factors for any tech modeled in (2)	Sample problem demonstrating capabilities of FLEET

All three universities contributed to the development of harmonized fleet assessment assumptions. These assumptions formed the basis of both the proprietary and public domain modeling work currently being performed.

For the first year of this project Georgia Tech, independent of the two other universities, focused on finalizing the CLEEN I proprietary assessments due to existing non-disclosure agreements and detailed modeling knowledge acquired over the last four years. As part of this work Georgia Tech also performed CLEEN-specific analysis under objectives (2) and (3).

Stanford provided input based on its experience into applicable public domain technology modeling identified under objective (2) across the entire time horizon contemplated in this work. Stanford has also provided trade factors, resulting from redesign/resizing of all vehicle classes to account for changes in mission specification changes for a public domain mission analysis to be completed under objective (3). This task has helped to define the interfaces between Stanford's expertise with assessing mission specification changes and Georgia Tech and Purdue's expertise with fleet analysis.

Purdue has applied their FLEET tool under objective (3), using a subset of the fleet assumptions defined in objective (1) and public domain vehicle performance generated by Georgia Tech in prior years. This activity has demonstrated the capabilities of FLEET for assessment of fleet-level noise and emissions evolution as a result of new aircraft technologies and distinct operational scenarios.

Major Accomplishments

The following were the major tasks completed under this year of ASCENT Project 10:

Fleet Level Workshop Assumption Setting
Georgia Tech finalized technology development assumptions that can be used to drive fleet level predictions of key environmental metrics. These are called technology development roadmaps, which provide key information on technology impact, readiness, and estimated development time until entry into service. The technology roadmaps are intended to support modeling efforts and are tool agnostic.

Technology Level Workshop Assumption Setting
Final fleet assessment scenarios have been developed through the work of the team. These scenarios, presented in 0, provide a brief summary of the fleet assessment scenarios. The scenarios are descriptive, but tool agnostic. The defined fleet scenarios are intended to provide bounding cases on future U.S. fleet-wide performance to inform technology development and goal setting.

Demonstration of FLEET
Using FLEET, Purdue simulated a series of future aviation scenarios developed in discussion with the FAA, and using public domain Georgia Tech modeled N+1 and N+2 generation aircraft instead of the Purdue modeled aircraft in FLEET. The scenarios simulated include the "Aggressive minus CLEEN" scenario as specified in the CLEEN PARTNER Project 36 report, plus others that studied the impact of capacity constraints at airports and airline competition. With further studies, Purdue assessed the sensitivity of future aviation emissions to variations in fuel prices, market demand, and the dates of technology availability. Thus, Purdue has demonstrated FLEET capabilities to simulate a range of future aviation scenarios as well as its flexibility to handle different inputs.

Vehicle-Level Assessment of Mission Specification Changes
The group at Stanford University has focused on (a) the development of the necessary analysis and optimization capabilities within the Stanford University Aerospace Vehicle Environment (SUAVE) framework, (b) the development and validation (with publicly-available data) of model vehicles in each of the five ICAO/CAEP aircraft classes, and (c) a study of the fuel-burn-reduction opportunities afforded by decreases in cruise Mach number when re-designing (including airframe and engine) these aircraft. All redesigned vehicles have been validated and tested and have been done at current levels of technology and also at more advanced (N+1 and N+2 levels) levels of technology. These improved vehicles have been provided to the rest of the team, so that they can insert such vehicles in the fleet-level analyses done with the Georgia Tech GREAT and Purdue FLEET tools (section 0). The Stanford team has also supported the team's activities for the preparation and conduct of both the fleet-level and technology workshops.

Task 1: Developing Fleet Assumptions

Georgia Institute of Technology, Purdue University, and Stanford University

Objective(s)

In order to develop assumptions suitable for a forward-looking fleet level analysis that incorporates new vehicle technologies, it is necessary to forecast the future. However, most forecasts are extrapolations of the current status quo and current trends, which assume an undisturbed continuation of historical and recent developments. This type of forecasting is necessary and useful, but will miss any significant changes or disturbances to the current market environment. If one considers changes to the status quo or constraints that might prevent current trends to continue, a possibility space of overwhelming dimensionality opens up. This dimensionality makes it intractable to fully explore all possibilities.

Research Approach

Research Approach Overview
The approach taken here is to reduce the overwhelming dimensionality by selecting a small number of well-defined scenarios. The scenarios should encompass future states that are important for specific consideration of significant changes that could occur and also to bind some of the most important future outcomes that could conceivably occur. Therefore, the first goal of the workshop series was to define a range of scenarios to bound aviation's environmental impacts in the future and to examine the effects of aircraft technology on these impacts.

Due to the diverse expertise needed to come to consensus on a set of scenarios, two parallel workshop tracks were undertaken. The first track focused on fleet level trends and assumptions, including future demand and fleet evolution. A second track focused on the state and future of aircraft technologies that reduce fuel burn, emissions, and noise. The information gathered in both these focused workshop tracks is planned to be combined to fully define future bounding scenarios and assess the potential of aircraft technology to improve aviation's environmental impact. The fleet level trends are first discussed in Section 0, followed by the technology trending workshops in Section 0.

Fleet Workshops

Based on the Fleet Scenario Workshops that were conducted through Summer and Fall 2015, the team created a series of conclusions from the data obtained from the workshop participants. This includes prioritizations of the factors that describe a scenario as well as evaluations of some provided suggested example scenarios and scenarios that the participants were able to customize. This was then used by the team in the first half of 2016 to formulate a number of scenarios through a series of discussions. The final selection stands at twelve scenarios, which are shown in Table 2. The specific settings for each of the scenarios are colored by nominal (blue), low (purple), and high (orange). These values were outcomes of the Fleet Workshops and were obtained by analyzing the data that was collected from the participants.

	GDP Growth (%/year)	Energy Price ($/bbl)	Population Growth (%/year)	International Trade (%/year Asia)	Industry Competetiveness (cent/ASM)	Airport Noise Limitations (% airports noise limited in future)	Cost of CO2 Emissions ($/MT)
Current Trends "Best Guess"	2.8	77	0.58	4.3	12	25	21
Current Trends + High R&D	2.8	77	0.58	4.3	12	25	21
Current Trends + High R&D + Mission Spec.	2.8	77	0.58	4.3	12	25	21
Current Trends Frozen Tech - In-Production Only	2.8	77	0.58	4.3	12	25	21
Environmental "Bounds" - Low	1.8	181	0.45	3.3	12	95	85
Environmental "Bounds" - High	4	41	0.68	5.9	12	4	0
High Demand (Including Global) + High R&D	4	77	0.58	5.9	12	25	21
High Demand (Including Global) + Low R&D	4	77	0.58	5.9	12	25	21
Low Demand (Including Global) + High R&D	1.8	77	0.58	3.3	12	25	21
Low Demand (Including Global) + Low R&D	1.8	77	0.58	3.3	12	25	21
Very High Demand with Noise Limits - Low R&D	4	41	0.68	5.9	12	95	0
Very High Demand with Noise Limits - High R&D	4	41	0.68	5.9	12	95	0

TABLE 2: MATRIX OF SCENARIOS AND DEMAND AND ECONOMIC MODEL FACTORS

	Fleet Evolution Schedule	Aircraft Retirement	Production Capacity
Current Trends "Best Guess"	Nominal - Twin Aisle First in 2020s	Nominal	No Limits
Current Trends + High R&D	Nominal - Twin Aisle First in 2020s; Adjusted sequence if necessary for first application of new configuration/ architecture/ mission spec. change	Nominal	No Limits
Current Trends + High R&D + Mission Spec.	Nominal - Twin Aisle First in 2020s; Adjusted sequence if necessary for first application of new configuration/ architecture/ mission spec. change	Nominal	No Limits
Current Trends Frozen Tech - In-Production Only	Nominal - Twin Aisle First in 2020s	Nominal	No Limits
Environmental "Bounds" - Low	Nominal - Single Aisle First in 2020s	Early (relative to historical data)	No Limits
Environmental "Bounds" - High	Nominal - Twin Aisle First in 2020s	Late (relative to historical data)	Limits
High Demand (Including Global) + High R&D	Nominal - Twin Aisle First in 2020s	Nominal	No Limits
High Demand (Including Global) + Low R&D	Nominal - Twin Aisle First in 2020s	Nominal	No Limits
Low Demand (Including Global) + High R&D	Nominal - Twin Aisle First in 2020s	Nominal	No Limits
Low Demand (Including Global) + Low R&D	Nominal - Twin Aisle First in 2020s	Nominal	No Limits
Very High Demand with Noise Limits - Low R&D	Nominal - Twin Aisle First in 2020s	Late (relative to historical data)	Limits
Very High Demand with Noise Limits - High R&D	Nominal - Twin Aisle First in 2020s	Late (relative to historical data)	Limits

TABLE 3: MATRIX OF SCENARIOS AND FLEET EVOLUTION MODEL FACTORS

	Amount and Speed of Technology R&D Investment (relative)	TRL 9 Dates	Benefit Levels	Aircraft Configurations	Engine Architectures	Mission Specification Changes
Current Trends "Best Guess"	1.02	Medium	Medium	"Gen 1" Advanced High AR Wing Type 2035+ (check median gen 1 TRL 9 date response)	"Gen 1" as expected; "Gen 2" Open Rotor Type Benefits 2035+	None
Current Trends + High R&D	1.71	Early - Emphasis over benefit level	High	All 3 generations as responded in surveys, Gen 1 2025+, Gen 2/3 2035+	All 3 generations as responded in surveys, Gen 2/3 2035+	None
Current Trends + High R&D + Mission Spec.	1.71	Early - Emphasis over benefit level	High	All 3 generations as responded in surveys, Gen 1 2025+, Gen 2/3 2035+	All 3 generations as responded in surveys, Gen 2/3 2035+	3 generations. 2nd gen redesign for cruise speed reduction. Include range variants
Current Trends Frozen Tech - In-Production Only	0	N/A	N/A	None	None	None
Environmental "Bounds" - Low	1.71	Early - Emphasis over benefit level	High	All 3 generations as responded in surveys, Gen 1 2025+, Gen 2/3 2035+	All 3 generations as responded in surveys, Gen 2/3 2035+	3 generations. 2nd gen redesign for cruise speed reduction. Include range variants?
Environmental "Bounds" - High	0.52	Late	Low	None	None	None
High Demand (Including Global) + High R&D	1.71	Early - Emphasis over benefit level	High	All 3 generations as responded in surveys, Gen 1 2025+, Gen 2/3 2035+	All 3 generations as responded in surveys, Gen 2/3 2035+	3 generations. 2nd gen redesign for cruise speed reduction. Include range variants
High Demand (Including Global) + Low R&D	0.52	Late	Low	None	None	None
Low Demand (Including Global) + High R&D	1.71	Early - Emphasis over benefit level	High	All 3 generations as responded in surveys, Gen 1 2025+, Gen 2/3 2035+	All 3 generations as responded in surveys, Gen 2/3 2035+	3 generations. 2nd gen redesign for cruise speed reduction. Include range variants
Low Demand (Including Global) + Low R&D	0.52	Late	Low	None	None	None
Very High Demand with Noise Limits - Low R&D	0.52	Late	Low	None	None	None
Very High Demand with Noise Limits - High R&D	1.71	Early - Emphasis over benefit level	High	All 3 generations as responded in surveys, Gen 1 2025+, Gen 2/3 2035+	All 3 generations as responded in surveys, Gen 2/3 2035+	3 generations. 2nd gen redesign for cruise speed reduction. Include range variants

TABLE 4: MATRIX OF SCENARIOS AND AIRCRAFT TECHNOLOGY MODEL FACTORS

Technology Roadmapping Workshops Overview

The goal of the technology roadmapping workshops was to develop a range of scenarios bounding the possible future of technology, including their impacts and entry into service. This information was then used to model advanced aircraft technologies and advanced vehicles expected to enter the fleet through 2050. Technology Workshop 1 was held virtually on June 10th and 11th of 2015 to solicit feedback from government, industry, and academia on a wide range of aircraft technology topic areas. From the results, infographics were created that document the suggested scenarios including technology impact, time to entry into service, and examples of specific technologies. Technology Workshop 2 was followed

up by a virtual workshop held on February 16th of 2016 to evaluate the infographics and get a final consensus on the technology evolution scenarios. In addition to guiding the modelling of advanced aircraft, a publically available document will be prepared from the final infographics.

Attendees to the technology roadmapping workshops included representatives from: The U.S. Air Force, Booz Allen Hamilton, Boeing, Department of Transportation Volpe Center, Embraer, FAA Office of Environment and Energy, Georgia Tech, Honeywell, Lufthansa, Mitre, NASA, Pratt & Whitney, Purdue, Rolls-Royce, Stanford, Textron Aviation and Virginia Tech. The workshop was constructed to ask for information on examples of first, second, and third generation technologies. The first virtual workshop focused on airframe and operational technologies whereas the second focused on engine and operational technologies. Operational technologies were included in both workshops since they affect both aircraft and engine systems. As discussed during the workshop, participants were made aware that the final results of the survey would be published as aggregated data. Specific identifiers would be removed prior to publication other than a general list of organizations that participated. Participants were also made aware of the primary intent to use the data to quantify the potential aircraft and engine technology to meet the FAA's environmental goals.

In order to solicit meaningful feedback without asking for sensitive, proprietary information the Georgia Tech team constructed a survey that solicited information on technologies in the following areas:

- **Availability** – When will the technology be ready for entry into service (EIS)?
- **Applicability to subsystems and vehicle class** – Where on the aircraft/engine can the technology be applied? What sizes of aircraft are applicable? How does this change as the technology evolves?
- **Maturation Rate** – How quickly does each generation of a technology mature to technology readiness level (TRL)[1] 9?
- **Delineation between different generations of a technology** – How does the technology evolve as it matures over several product generations?
- **Primary impact areas** – What metrics on the aircraft are impacted by the technology?

Technology Roadmapping Survey 1 Format

A survey format was developed in Microsoft Excel to allow respondents to provide feedback in a structured manner that ensured consistency between responses and reduced the burden of filling out the survey. First, the survey was divided into multiple technology 'topic areas'. Broadly speaking, the technologies were classified into three distinct branches, *engine, airframe, and operational technologies.* Technologies were then further subdivided into technology areas as shown in Figure 1. Workshop participants were asked to provide information on three different generations of each technology area at the right-most level of the tree. It was left to workshop participants to define what constitutes a generational change in a technology area; however, as an example, the use of ceramic matrix composite (CMC) technology within an engine can be broken into different generations. A first generation application may involve the use of CMC on the turbine shroud and other static parts outside of the main flow path. Once more experience is gained with CMC; the material may be used in turbine vanes as a second generation application. Further development may enable the use of CMC on highly stressed rotating parts, such as turbine blades. Participants were asked to provide specific examples in each technology area to help baseline their opinion on delineations between technology generations.

[1] "Technology Readiness Levels (TRL) are a type of measurement system used to assess the maturity level of a particular technology. Each technology project is evaluated against the parameters for each technology level and is then assigned a TRL rating based on the projects progress. There are nine technology readiness levels. TRL 1 is the lowest and TRL 9 is the highest." - NASA

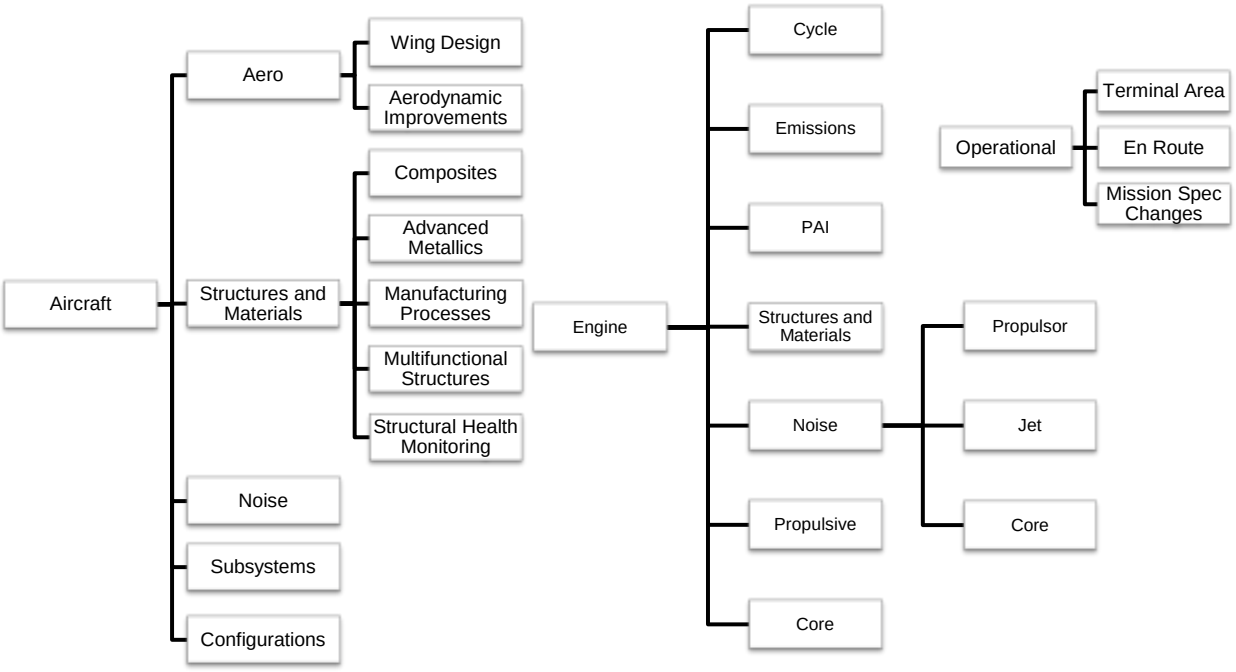

Figure 1: Technology Categorization

There are a few technology categories in Figure 1 which may require further explanation. Engine PAI for example stands for Propulsive Airframe Integration and relates to technologies such as boundary layer ingestion. Many of the technologies that affect Engine Propulsor Noise also affect Engine Jet Noise. Since this survey was mainly focused on turbofan powered aircraft, the major differentiator between the two is that any technology associated with fan noise is related to Engine Propulsor Noise, while technology associated to jet and shock noise is only related to Engine Jet Noise.

For each of the technology categories in Figure 1, a Microsoft Excel survey was constructed. Three generations of each category were placed on a single worksheet, all of which had a consistent structure, shown in Figure 2. The figure shows 1st generation wing design; however, all technology areas had a consistent structure, with the contents of each colored box adjusted accordingly.

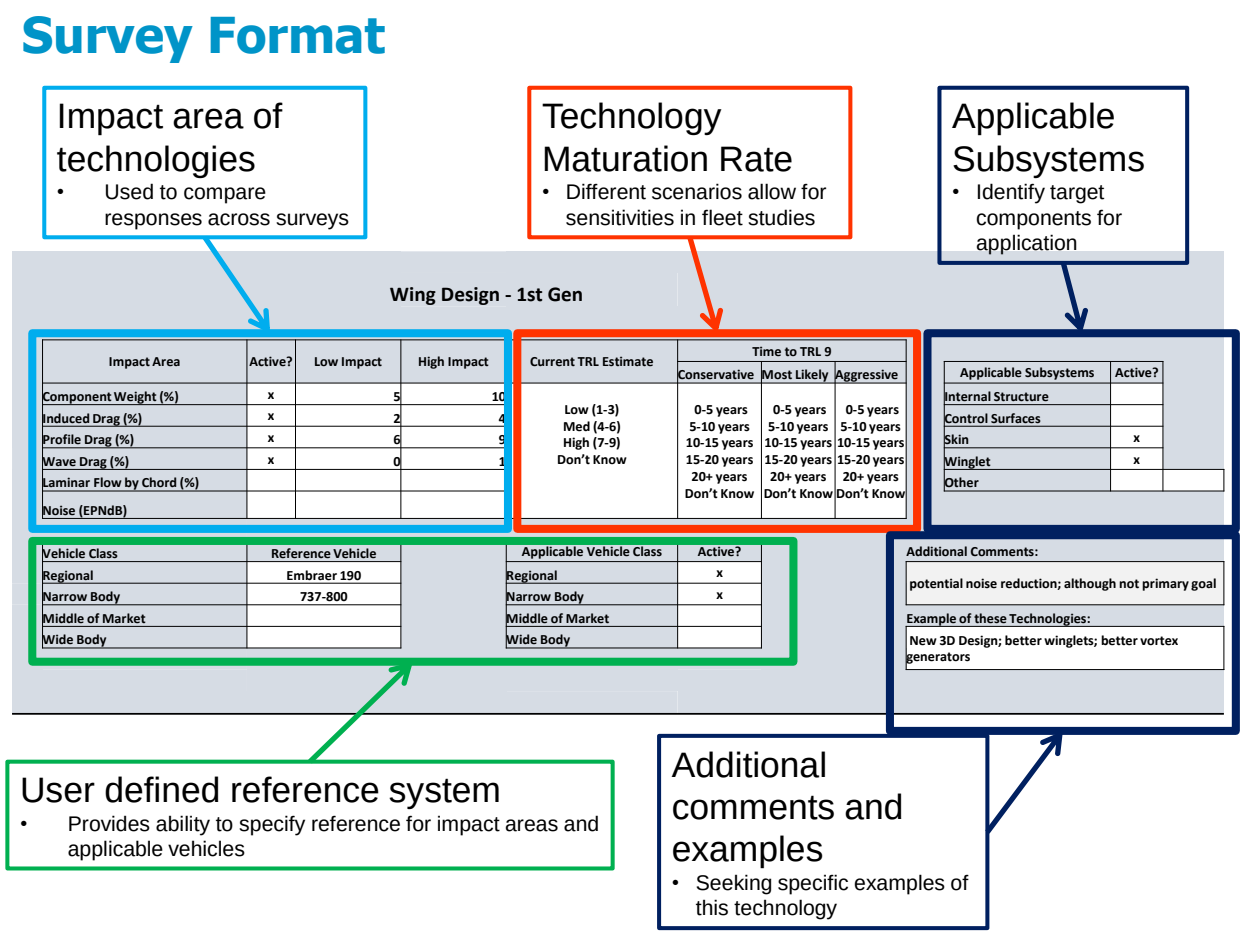

Figure 2: Technology Roadmapping Survey 1 Format

Working clockwise from the upper left of Figure 2, participants were asked for information on the impact of each generation within a technology category. The impact areas were chosen to be at an intermediate level of fidelity. For example, the wing design impacts were solicited as percent reductions from the current state of the art for weight, drag, laminar flow, and noise. Since multiple technologies could be included in a first generation wing design, participants were asked to list the total benefits for all technologies being considered. Moving to the right, the red box asked for the current TRL and estimated time to TRL 9. The current TRL estimate was grouped into low (TRL 1-3), medium (TRL 4-6), and high (TRL 7-9). This grouping was selected to allow for multiple technologies to be included in a generation, reduce the possibility of asking for sensitive data, and to account for some level of uncertainty in the technology development process. Under the time to TRL 9, responses were sought for three scenarios, a conservative, most likely, and aggressive technology progression. Possible responses were grouped into 5 year bins up through 20+ years. Moving to the upper right, applicable subsystems were listed for each technology area with check boxes that participants could easily select. On the lower left, participants were asked to provide a reference system which they used to estimate the reductions listed in the impact areas. Vehicle applicability was also requested to identify applicable size classes for the technology. Finally, write-in boxes were provided in the lower right to allow for any comments and concerns in addition to specific examples of technologies that should be classified within the provided technology area and generation.

Table 5 provides a complete listing of the impact areas and applicable subsystems Georgia Tech identified for each technology. Examples of each technology area were also provided to participants in order to help baseline responses.

Table 5: List of Impact Areas and Applicable Subsystems for Each Technology Category

Category	Examples	Impact Areas	Applicable Subsystems
Aircraft Wing Design	Adaptive Trailing Edge Gust/Maneuver Load Alleviation Hybrid Laminar Flow Control Spiroid Winglets	Component Weight (%) Induced Drag (%) Profile Drag (%) Wave Drag (%) Laminar Flow by Chord (%)	Internal Structure Control Surfaces Skin Winglet Design
Aircraft Aerodynamic Improvements	Drag reduction coatings Friction-reducing surface coatings Electro-magnetic technologies for drag reduction in cruise	Induced Drag (%) Profile Drag (%) Wave Drag (%) Laminar Flow by Chord (%)	Fuselage Wing Vertical Tail Horizontal Tail
Aircraft Composites	Damage Arresting Stitched Composites Damage Tolerant Laminates Tow Steered Fiber Composites Hybrid Nanocomposites	Component Weight (%) Reduction in Factor of Safety (%)	Fuselage Wing Vertical Tail Horizontal Tail
Aircraft Advanced Metallics	Functionally Graded Metallics Curvilinear Stiffened Metal Structures Advanced Superalloys Advanced Powder Metallurgy	Component Weight (%) Reduction in Factor of Safety (%)	Fuselage Wing Vertical Tail Horizontal Tail
Aircraft Manufacturing Processes	Ultrasonic Shot Peening Out-of-Autoclave Composite Fabrication Post-buckled Structures	Component Weight (%) Reduction in Factor of Safety (%)	Fuselage Wing Vertical Tail Horizontal Tail
Aircraft Multifunctional Structures	Primary Structure Joining Methodologies Unitized Metallic Structures	Component Weight (%) Reduction in Factor of Safety (%)	Fuselage Wing Vertical Tail Horizontal Tail
Aircraft Structural Health Monitoring	Wireless Integrated Strain Monitoring and Simulation System Fiber-optic Embedded Composites	Component Weight (%) Reduction in Factor of Safety (%)	Fuselage Wing Vertical Tail Horizontal Tail
Aircraft Noise	Continuous Moldline Link for Flaps Slat Inner Surface Acoustic Liner Over the Rotor Acoustic Treatment Landing Gear Integration	Approach Noise (EPNdB) Sideline Noise (EPNdB) Cutback Noise (EPNdB) Source Noise (dB)	Slats Flaps Landing Gear Wing/Tail

Category	Examples	Impact Areas	Applicable Subsystems
Aircraft Subsystems	Solid Oxide Fuel Cell Auxiliary Power Unit Hybrid Wing Ice Protection System Fly-by-Light Systems Lithium Batteries for Secondary Power	Component Weight (%) Fuel Burn (%) Drag (%) On board electrical energy consumption (%) On board pneumatic energy consumption (%) On board hydraulic energy consumption (%)	APU ECU Avionics and Control
Aircraft Configurations	Large-span aircraft (with or without truss- / strut-braced wings) Lifting fuselage (e.g., double bubble fuselage with conventional engine mounting) Integrated propulsion systems (boundary layer ingestion) Blended/Hybrid wing body (HWB)	Emissions (%) Fuel Burn (%) Noise (EPNdB)	Truss Braced Wing Double Bubble Hybrid Wing/Body
Engine Cycle	Direct Drive Cycle Geared Fan Cycle Open Rotor Cycle Hybrid Electric Pulse Detonation Core Engine Variable Core Cycle Technology	TSFC (%) Engine Weight (%) Noise (EPNdB) Emissions (%)	Direct Drive Geared Fan Open Rotor
Engine Emissions	Twin Annular Premixing Swirler (TAPS) Lean Direct Ingestion (LDI) Partially Evaporating Rapid Mixing Combustor (PERM) Lean Premixed Prevaporised Combustor (LPP)	NOx (%) UHC (%) nvPM (%)	
Engine Propulsion Airframe Integration	Low Interference Nacelle Natural Laminar Flow Fluidic Vaneless Thrust Reversers Short Inlet Engine placement	Interference Drag (%) Nacelle Drag (%) Component Weight (%) Noise Reduction (EPNdB)	Pylon Nacelle
Engine Structures and Material	Ceramic Matrix Composite (CMC) Nozzle Polymer Matrix Composite (PMC) Fan Case High Temperature Corrosion Coatings	Component Weight (%) Reduction in Factor of Safety (%)	Fan Compressor Turbine Nacelle

Category	Examples	Impact Areas	Applicable Subsystems
Engine Propulsor Noise	Fan Vertical Acoustic Splitter Noise Cancelling Stator Fluidic Injection Stator Sweep and Lean Variable Geometry Chevrons	Approach Noise (EPNdB) Sideline Noise (EPNdB) Cutback Noise (EPNdB) Source Noise (dB)	Treated Fan Forward Radiated Noise Treated Fan Aft Radiated Noise
Engine Jet Noise	Fan Vertical Acoustic Splitter Noise Cancelling Stator Fluidic Injection Stator Sweep and Lean Variable Geometry Chevrons	Approach Noise (EPNdB) Sideline Noise (EPNdB) Cutback Noise (EPNdB) Source Noise (dB)	Inner Stream Jet Noise Outer Stream Jet Noise Inner Stream Shock Noise Outer Stream Shock Noise
Engine Core Noise	Compressor Combustor Turbine	Approach Noise (EPNdB) Sideline Noise (EPNdB) Cutback Noise (EPNdB) Source Noise (dB)	Compressor Combustor Turbine
Engine Propulsive Efficiency	Variable Area Nozzle Boundary Layer Ingestion Variable Pitch Fan Ultra High Bypass Ratio Engines Contra-rotating Fan Engines	Propulsive Efficiency (%) Component Weight (%)	Inlet Propulsor Nacelle
Engine Thermal (Core) Efficiency	Tip Injection for Stability Enhancement System Intercooled Engine Heat Exchanger Installation Flow Control by Aspiration Active Tip Clearance Control	Thermal Efficiency (%) Component Weight (%)	Cooling HP Compressor HP Turbine Combustor Subsystems
Operations in the Terminal Area	Taxi Bot Controller Managed Spacing Combined Arrival and Departure Runway Scheduling (CADRS) Runway Configuration Management	Fuel Burn (%) Noise (EPNdB) Emissions (%)	Airport Operations Approach Takeoff/climb
Operations En Route	Operational Airspace Sectorization Integrated System (OASIS) Dynamic Weather Re-routing (DWR) Pair-wise Separation Management (PSM)	Fuel Burn (%) Noise (EPNdB) Emissions (%)	Aircraft in-flight Operation Dynamic Trajectory Re-Routing

Category	Examples	Impact Areas	Applicable Subsystems
Operations Mission Specification Changes	Cruise speed reduction (CSR) Range/payload design characteristics Maximum allowable span (see configurations) Take-off and landing field lengths	Fuel Burn (%) Noise (EPNdB), via weight reduction Emissions (%)	Design Range Design Mach Operational profile

In addition to the requested impact areas and example technologies, Georgia Tech provided examples of what may constitute a first, second, and third generation technology in each technology category. Participants were encouraged to modify according to their own knowledge and experience. A complete listing of the Georgia Tech provided examples of first, second, and third generation technologies in provided in Table 6.

Table 6: technology Generation Examples

Category	First Generation	Second Generation	Third Generation
Aircraft Wing Design	Winglet designs Variable wing camber designs	Active flow control NLF control HLF control	Active TS control Morphing wing
Aircraft Aerodynamic Improvements	Riblets Excrescence reduction	Shock bumps Active flow control	Discrete roughness elements (DRE)
Aircraft Composites	New composite fibers and matrix Optimized composite design solutions	Pre-form technology Efficient manufacturing processes Joining technologies	Self-reacting (adaptive) structures Nano-technologies
Aircraft Advanced Metallics	New alloys with targeted properties New design solutions	Tailored integral structures Bonding technology	Advanced assembly concepts Self-reacting (self-monitoring) structures
Aircraft Manufacturing Processes	Automated fiber placement layup Autoclave cure Fastener assembly	Advanced structural shapes Co-bonding/Paste bonding assembly 3D printed components	Major Aerostructures 3D Printed Advanced materials, resins, and stitching
Aircraft Multifunctional Structures	Multifunctional coatings	Morphing structures	Self-healing/self-repairing structures
Aircraft Structural Health Monitoring	Off-line sensor systems for maintenance benefits	On-line sensor systems for component weight and maintenance benefits	Fully integrated sensor systems for weight saving and maintenance benefits
Aircraft Noise	Fairing design Slat design Flap design	Flap treatment Slat treatment Landing gear treatment	Active flow control Plasma actuation
Aircraft Subsystems	Advanced fly-by-wire Lithium batteries for secondary power More electric aircraft	Proton exchange member fuel cells Fly-by-light	Solid acids as fuel cell Solid oxide fuel cell
Aircraft Configurations	Large Span / Trussed Braced Wing	Lifting fuselage Conventional engine mounting	Boundary layer ingestion Engines mounted above fuselage

Category	First Generation	Second Generation	Third Generation
Engine Cycle	Geared turbofan Advanced turbofan	Open rotor/unducted fan Counter-rotating fan	Adaptive cycle Pulse detonation Embedded distributed multi-fan
Engine Emissions	Twin annular premixing swirler RWL combustor	Lean direct injection Active combustion control Lightweight CMC liners	Ultra compact low-emission combustor
Engine Propulsion Airframe Integration	Reduced nacelle weight	Buried engines Boundary layer ingestion inlet	Adaptive/active flow control
Engine Structures and Material	CMC nozzle Advanced TBC coatings	Ubiquitous composites Advanced turbine superalloys	Advanced powder metallurgy disk Blisk and Bling concept
Engine Propulsor Noise	Rotor sweep/lean Rotor speed optimization VAN	Zero hub fan Soft vane Active stator	Over-the-rotor treatment Active blade tone control
Engine Jet Noise	Advanced long duct forced mixer Variable geometry chevrons	High frequency excitation Beveled nozzle	Fluidic injection Microjets
Engine Core Noise	Advanced core treatment	Bulk absorber materials 2 DOF/tailored absorbers	Low noise combustor
Engine Propulsive Efficiency	Variable fan nozzle Very high BPR fan Zero hub fan	Ultra high BPR fan Low FPR fan	Active distortion tolerant fan Embedded engines with inlet flow control
Engine Thermal (Core) Efficiency	Advanced combustor Advanced cooling technologies	Variable flow splits Ultra compact low-emission combustor Clearance control	Active film cooling Active flow control
Operations in the Terminal Area	Wake detection and prediction Taxi bot	Parameter driven aircraft separation standards and procedures	Integrated air/ground network for voice and data
Operations En Route	Aircraft-aircraft hazardous weather information sharing	Airborne collision avoidance Synthetic vision systems	Trajectory negotiation 4D Ts Delegated separation digital communications
Operations Mission Specification Changes	CSR on existing aircraft	Aircraft/engines redesigned for CSR Multi-range aircraft variants	Advanced configurations with mission spec changes Very large-span aircraft

Technology Roadmap Infographic Development

Following the first Technology Roadmapping Survey, a large dataset was collected. The results were combed through to identify any logical inconsistencies and gross outliers. For example, it was observed that for one of the respondents there were times when their Generation 2 and 3 impacts were less than their Generation 1 impacts. This respondent was contacted and it was found that they were giving their impacts relative to the previous generation. For example, their Generation 3 impact was the improvement from Generation 2. These responses were fixed, so that they were all relative to a 1995 baseline aircraft like the other responses.

The aim of the Technology Roadmap infographics was to effectively convey the range of impacts for each generation. An infographic was made for each of the 22 technology areas. Figure 3 provides a diagram of the initial infographic format

that was developed. On each infographic, a bar graph was included for each impact within that technology area. The high and low values from the responses were used to define the technology impact range for each generation. A nominal impact value was provided, which for the most part was computed as the average of the bounds of the range. The infographics also included examples of technologies broken into the generation they would be introduced. In addition, they had graphics that showed the range of responses for the "year to TRL 9" and "Current TRL" for each generation. Finally, at the bottom of the infographics was a matrix showing what respondents thought the applicable subsystems for that technology area's impacts were, for a given vehicle class and generation.

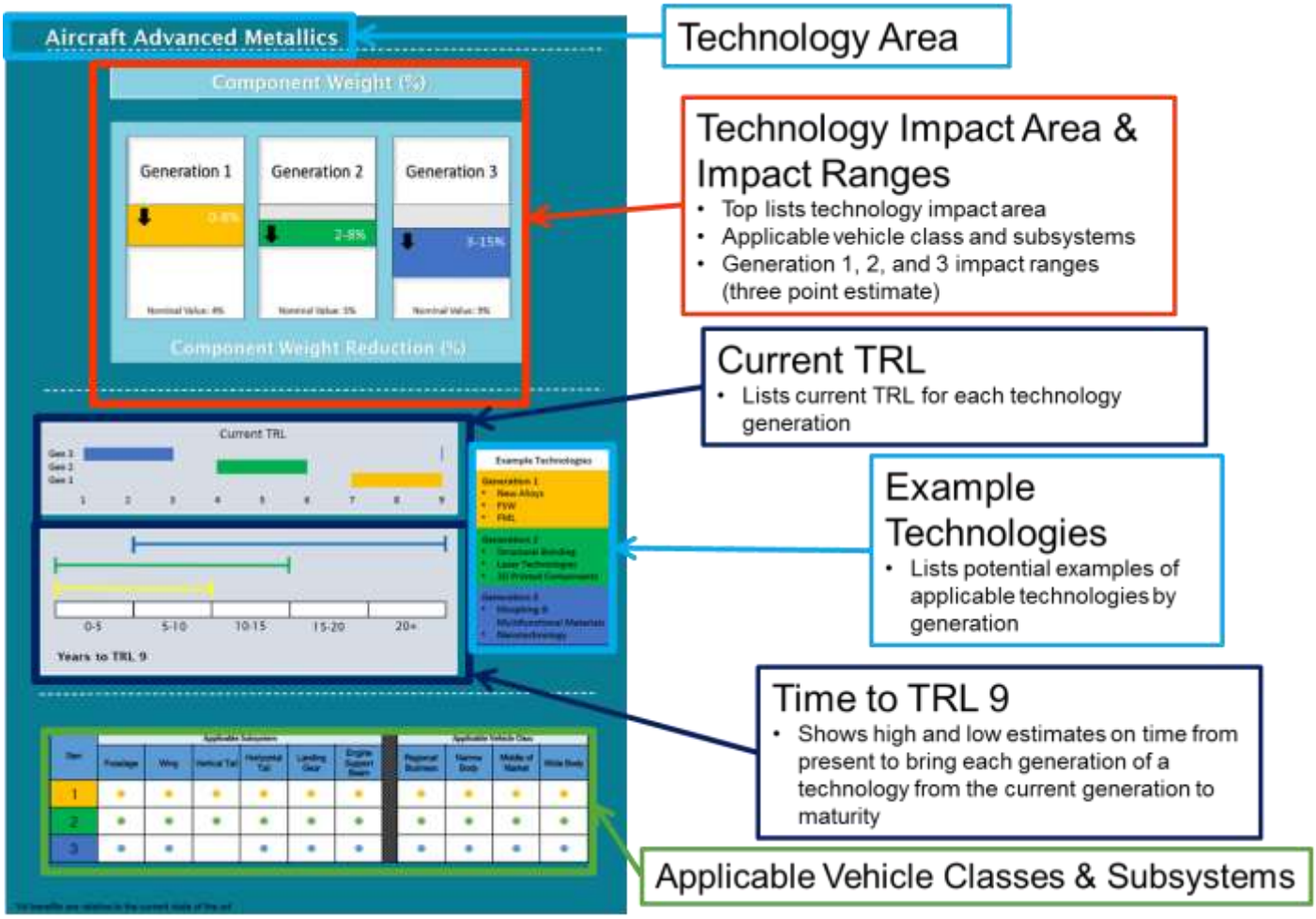

FIGURE 3: INITIAL TECHNOLOGY ROADMAP INFOGRAPHIC FORMAT PRESENTED AT TECHNOLOGY ROADMAPPING WORKSHOP 2.

Technology Roadmapping Survey 2 Format

The goal of the second Technology Roadmapping Workshop was to send participants the infographics to discuss and provide feedback on the range of responses given in the first workshops. Using the infographics kept the results anonymous, which helped avoid any bias and ensured participants were viewing the results objectively. As seen in Figure 4, the Technology Roadmapping Survey 2 format was straightforward. For each technology area, participants were asked to review the results one generation at a time. For a given generation, participants were first asked if there were any applicable vehicle classes, applicable subsystems, or example technologies that they thought should be added or removed. Then participants were asked to review the low, nominal, and high technology impact values for that generation. If participants believe an impact value needed to be changed they were asked to explain why. Similarly, for the Current TRL

and Time to TRL 9 participants were asked to review the range of values and explain any suggested changes. Throughout the survey participants were encouraged to leave answers blank if they felt they did not have the background to comment on a particular technology impact area.

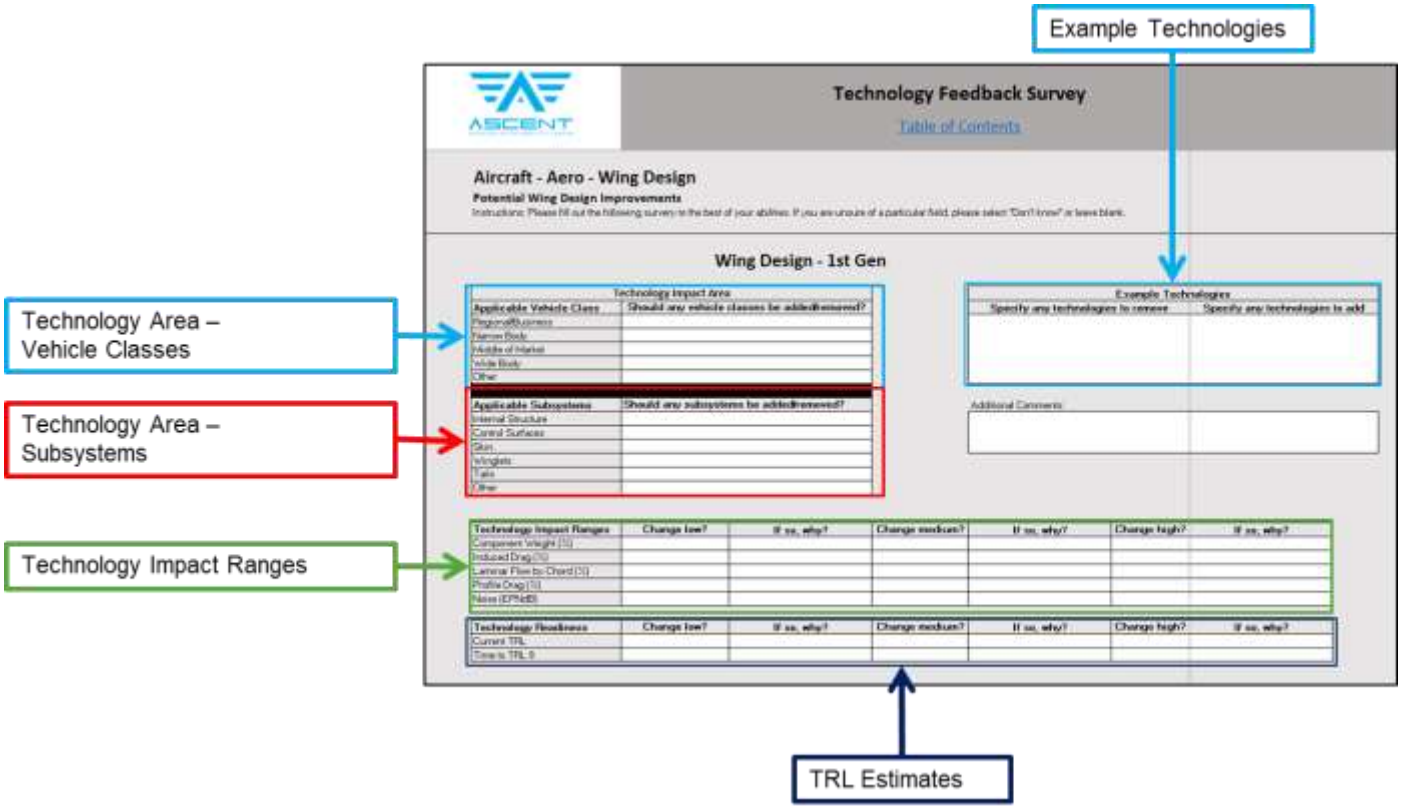

FIGURE 4: TECHNOLOGY ROADMAPPING SURVEY 2 FORMAT

Final Revisions to Technology Roadmap Infographics

Among the responses from the Technology Roadmapping Workshop 2 there was only one technology impact area where respondents felt the impact values should be significantly adjusted, namely Engine Emissions. For both improvement in Particulate Matter and Nitrogen Oxide emissions respondents felt the high values were too low and provided reasoning. They also noted studies to look at for adjusting the values.

Most comments were concerned with the example technologies given on the infographics. Participants either felt that a technology was under the wrong entry-into-service generation, or was not appropriate for the technology area it was assigned to. For example, additive manufacturing was originally listed as a Generation 1 technology for Engine Emissions. A respondent noted that, while it might be used on test stands, it would mostly not see use in production until Generation 2. Other comments focused on slight adjustments to the "Time to TRL 9" ranges. Overall, the survey feedback was generally showed agreement with the initial infographics. There was some confusion over the matrix at the bottom of the infographics. As seen in Figure 3, in the original infographics, on the left side of the matrix subsystems are listed. A dot was placed to indicate what generations the subsystem would be affected by improvements in the technology area. Separated on the right side of the matrix different vehicles were listed. Similar to the subsystems, a dot was placed to indicate the generations that a vehicle class would be affected by improvements in a technology area. The overwhelming response was that the matrix should really indicate what vehicle and what subsystems on that vehicle were affected by a technology area, instead of separating them. The culmination of these suggestions for the infographics can be seen in Figure 5 to Figure 26. These final infographics will be the basis for a document that will be made publically available on the results of this project.

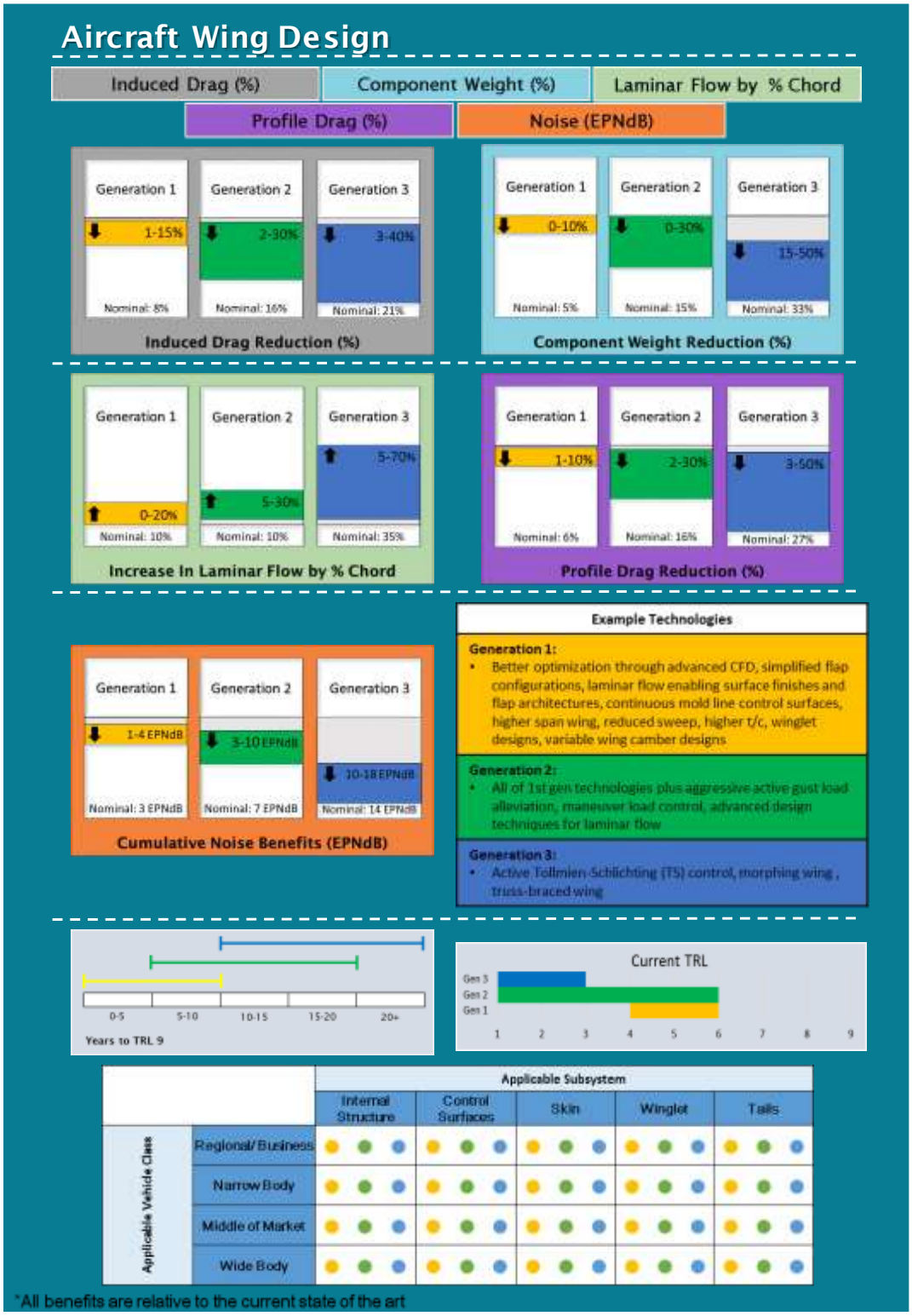

FIGURE 5. FINAL TECHNOLOGY ROADMAPS FOR AIRCRAFT WING DESIGN

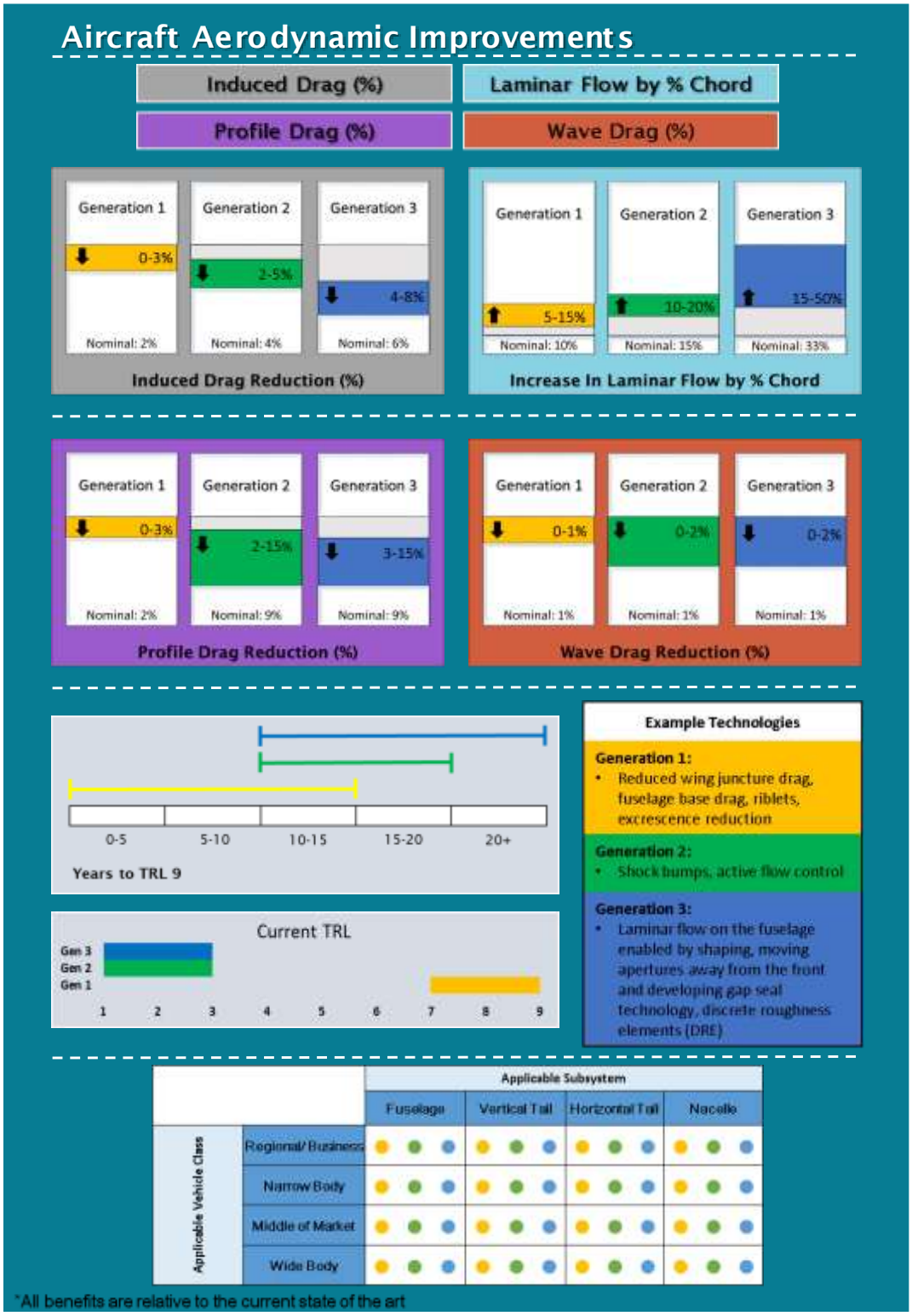

FIGURE 6. FINAL TECHNOLOGY ROADMAPS FOR AIRCRAFT AERODYNAMIC IMPROVEMENTS

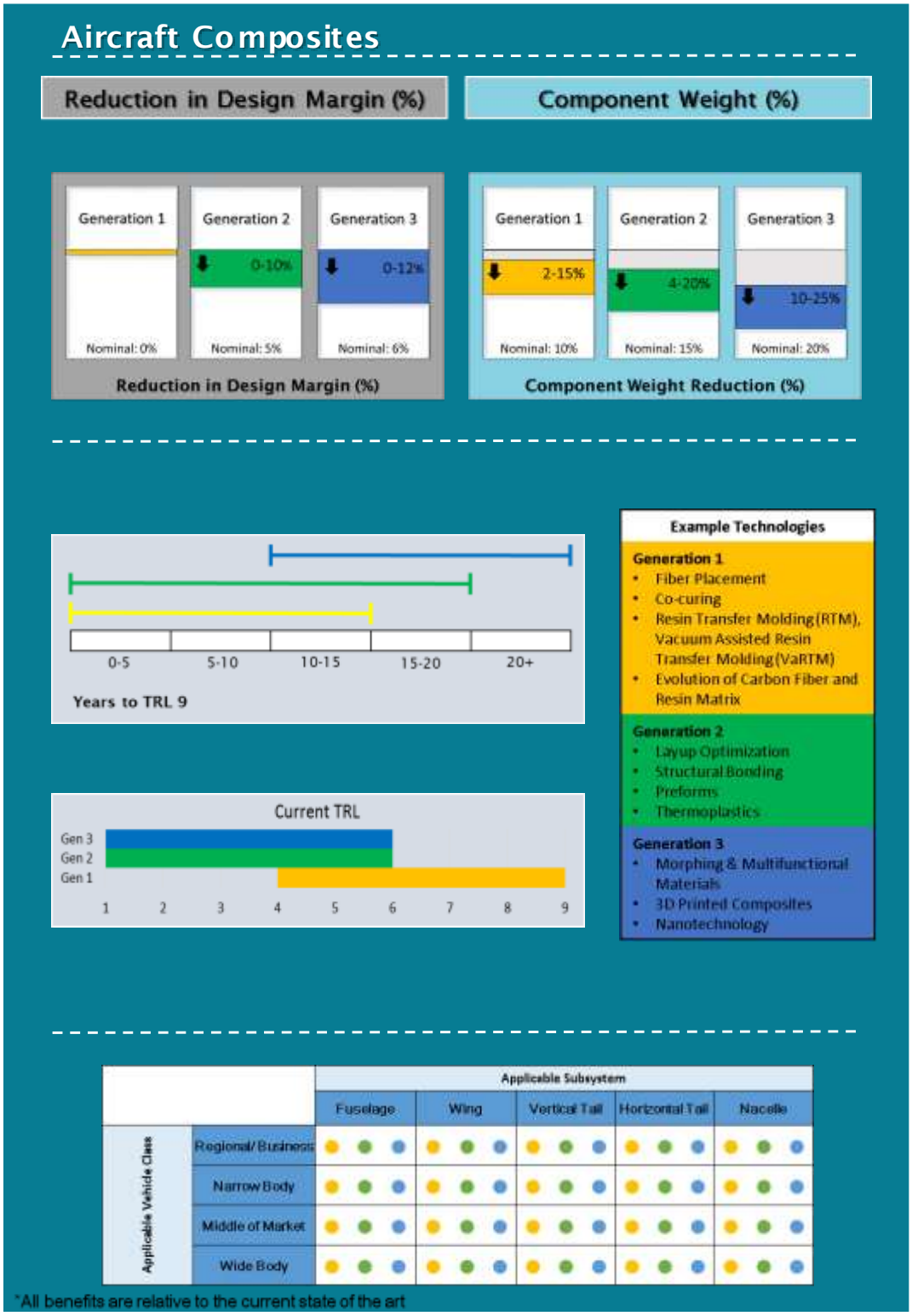

FIGURE 7. FINAL TECHNOLOGY ROADMAPS FOR AIRCRAFT COMPOSITES

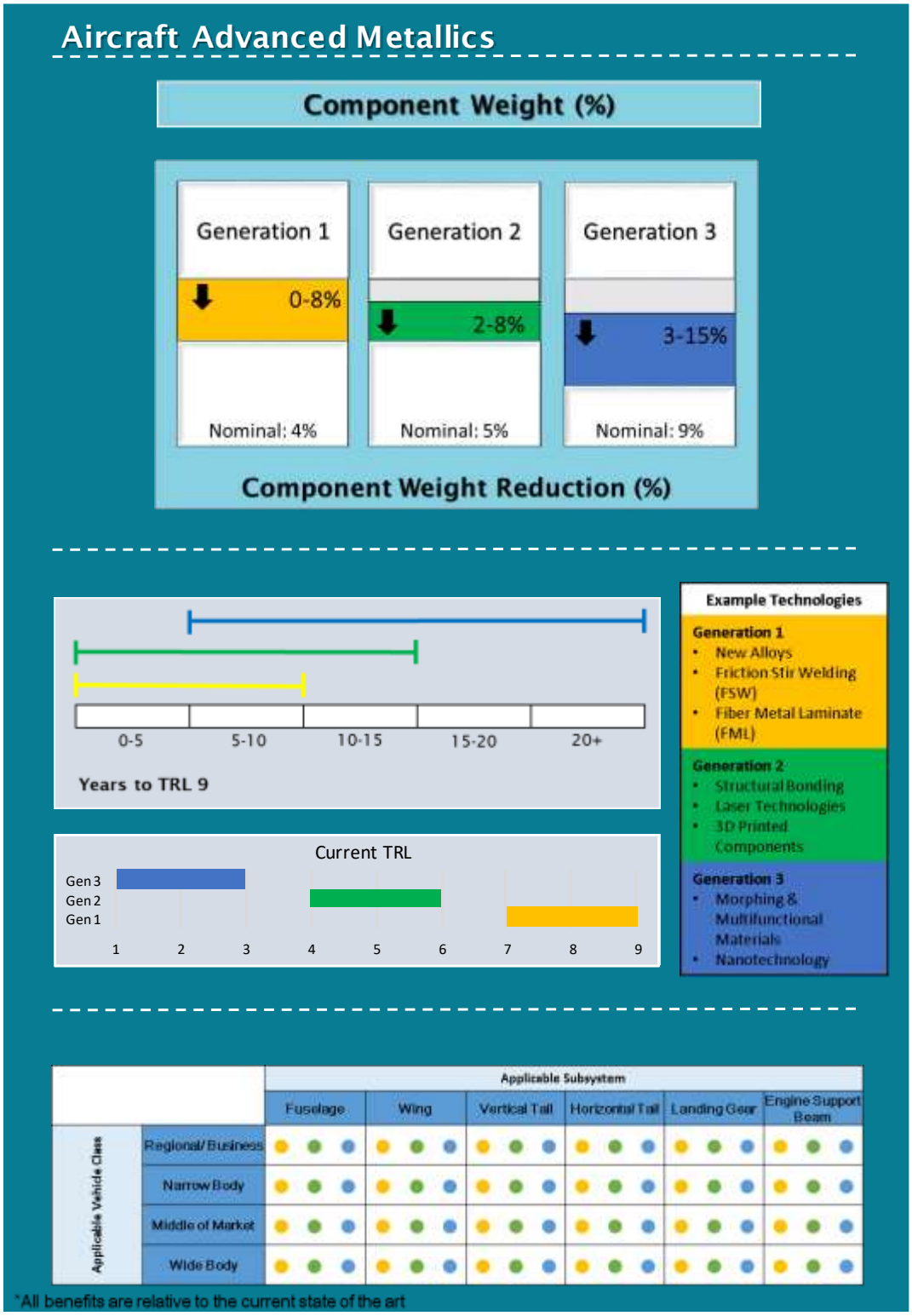

FIGURE 8. FINAL TECHNOLOGY ROADMAPS FOR AIRCRAFT ADVANCED METALLICS

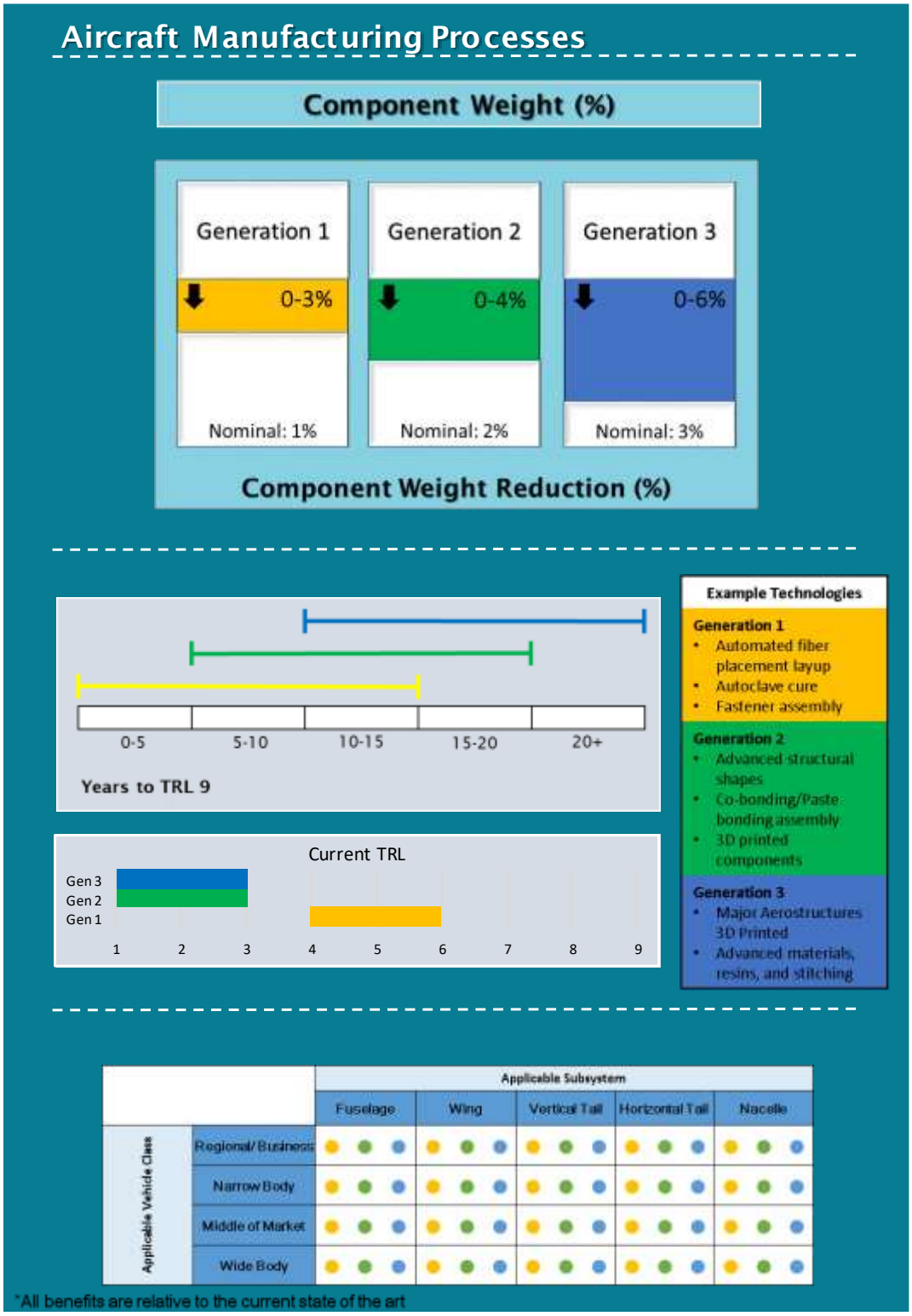

FIGURE 9. FINAL TECHNOLOGY ROADMAPS FOR AIRCRAFT MANUFACTURING PROCESSES

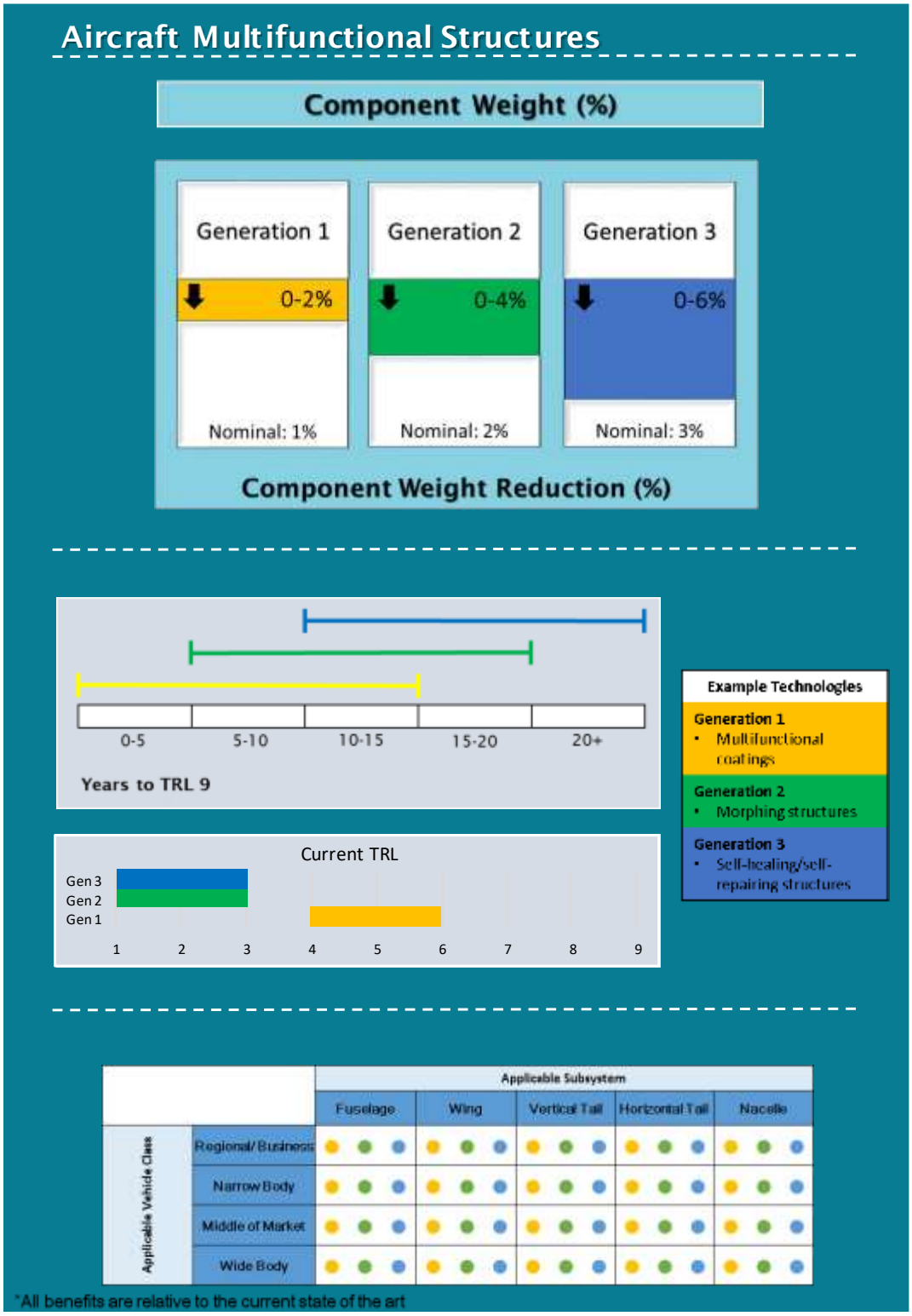

FIGURE 10. FINAL TECHNOLOGY ROADMAPS FOR AIRCRAFT MULTIFUNCTIONAL STRUCTURES

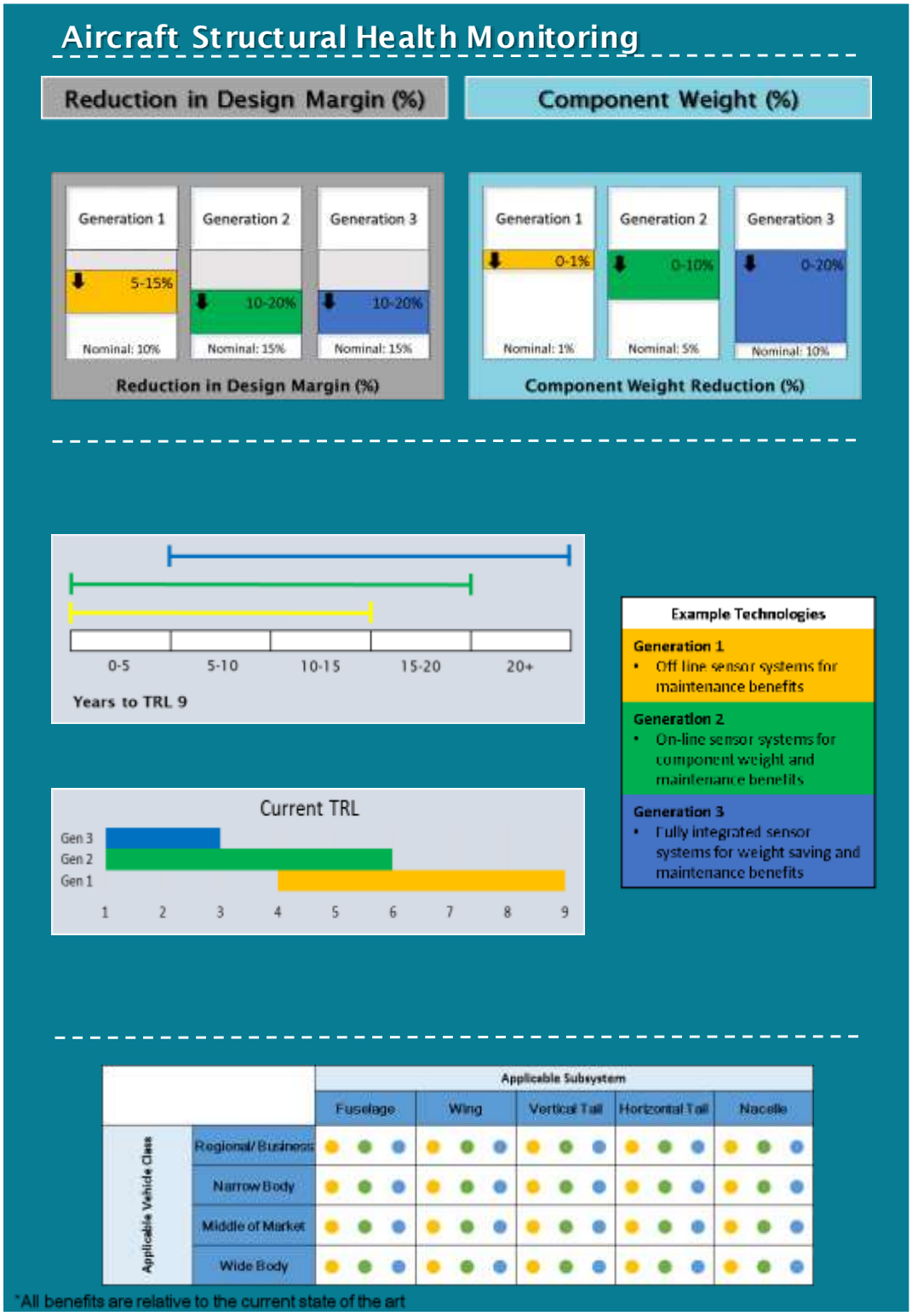

FIGURE 11. FINAL TECHNOLOGY ROADMAPS FOR AIRCRAFT STRUCTURAL HEALTH MONITORING

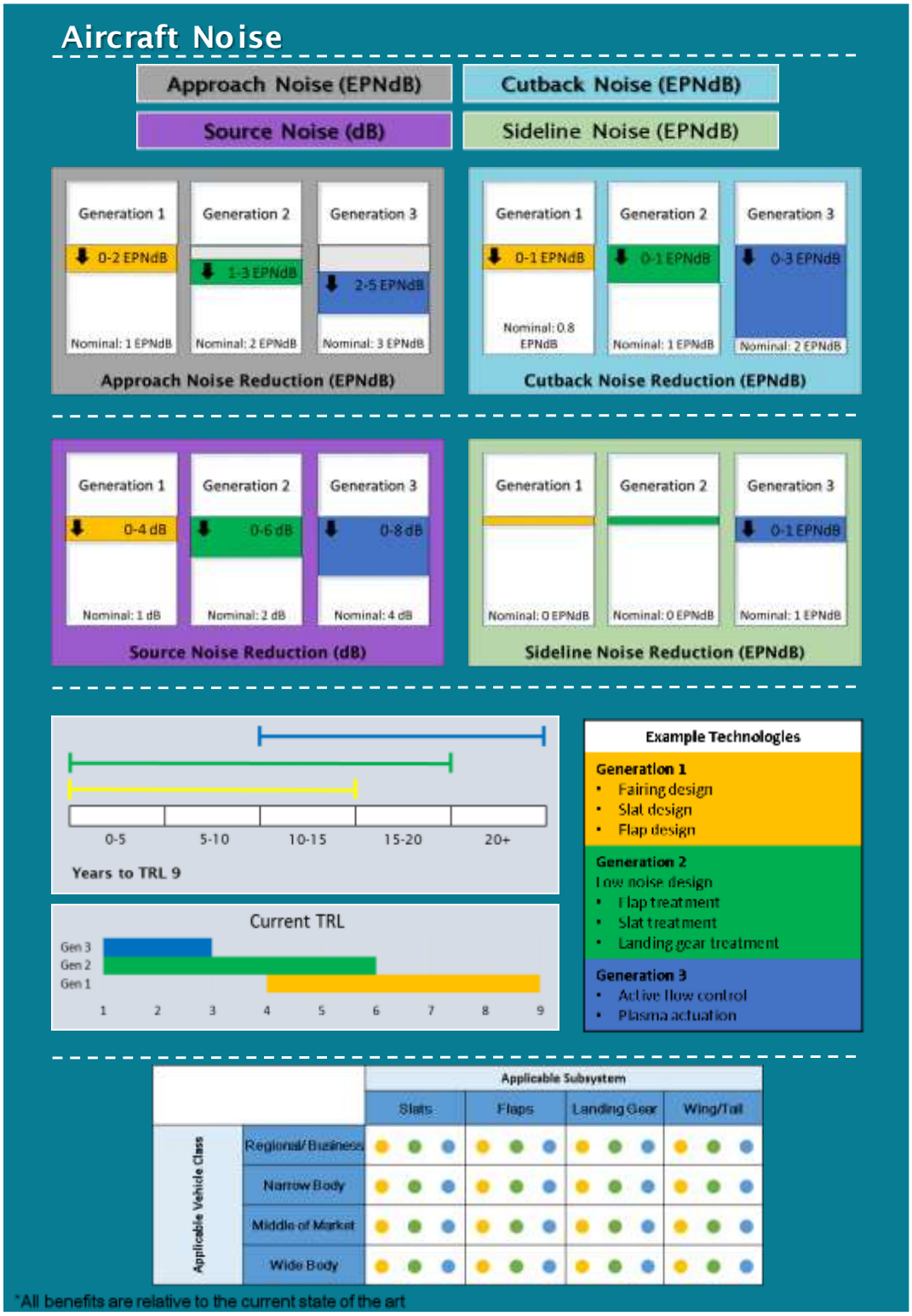

FIGURE 12. FINAL TECHNOLOGY ROADMAPS FOR AIRCRAFT NOISE

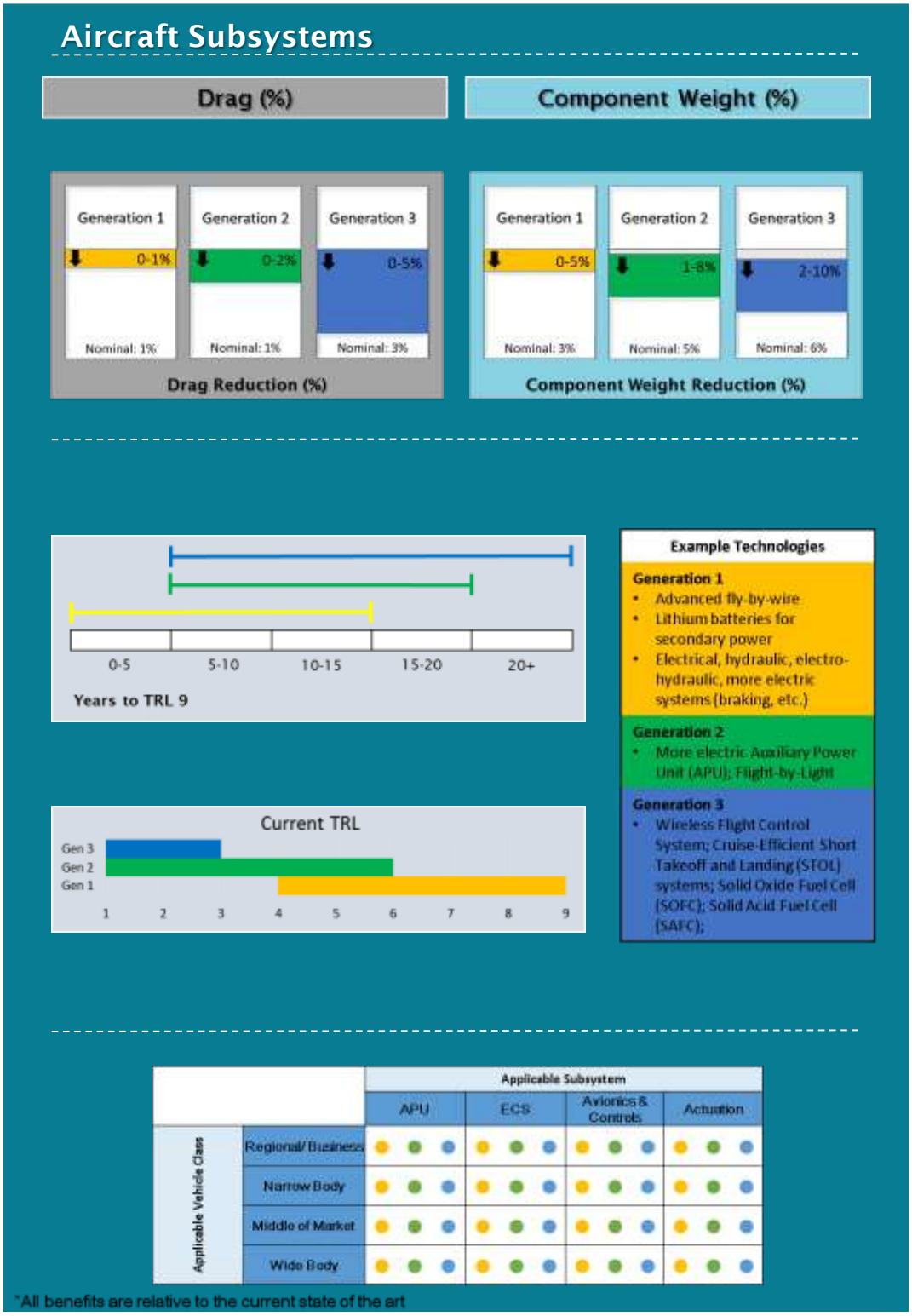

FIGURE 13. FINAL TECHNOLOGY ROADMAPS FOR AIRCRAFT SUBSYSTEMS

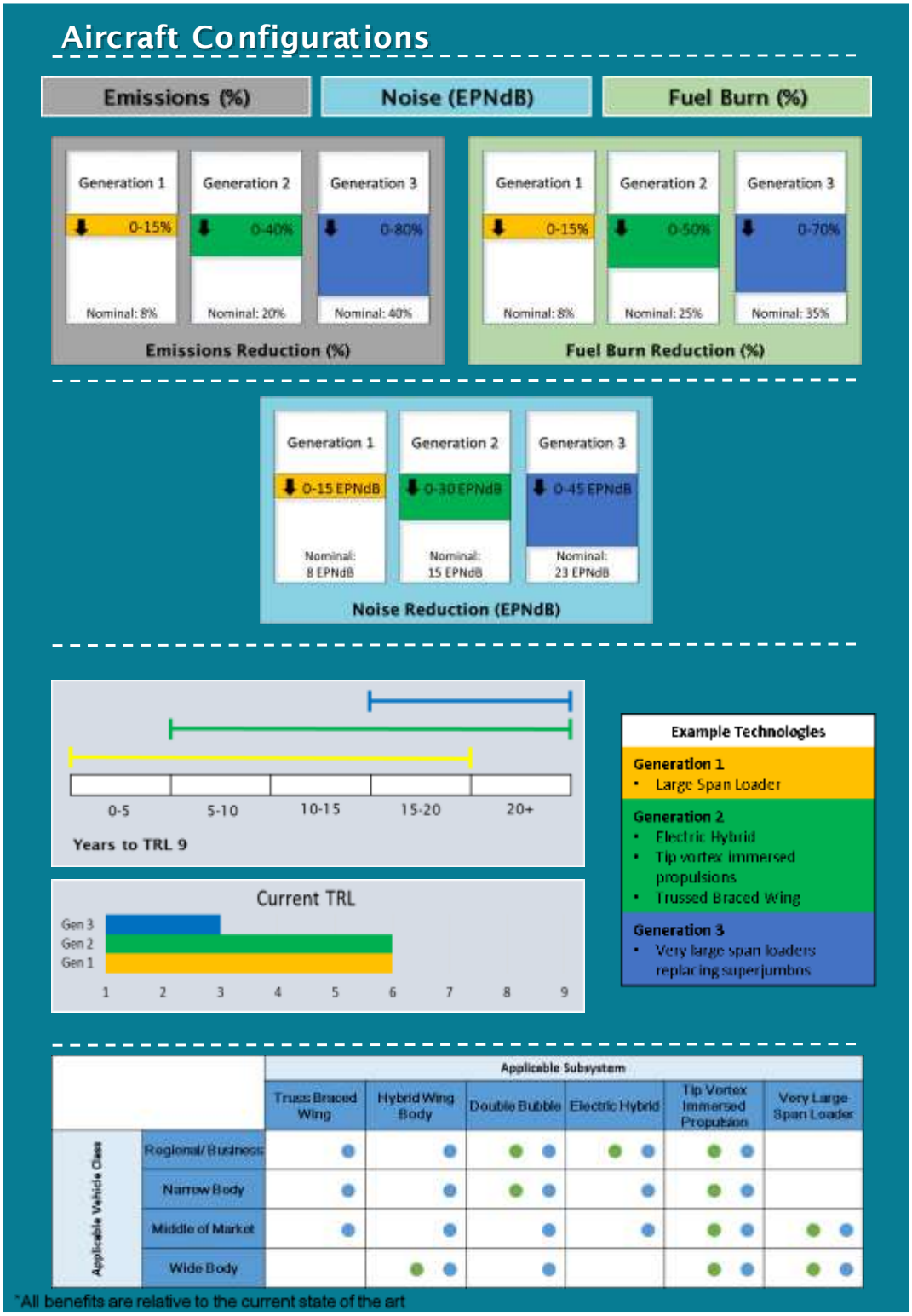

FIGURE 14. FINAL TECHNOLOGY ROADMAPS FOR AIRCRAFT CONFIGURATIONS

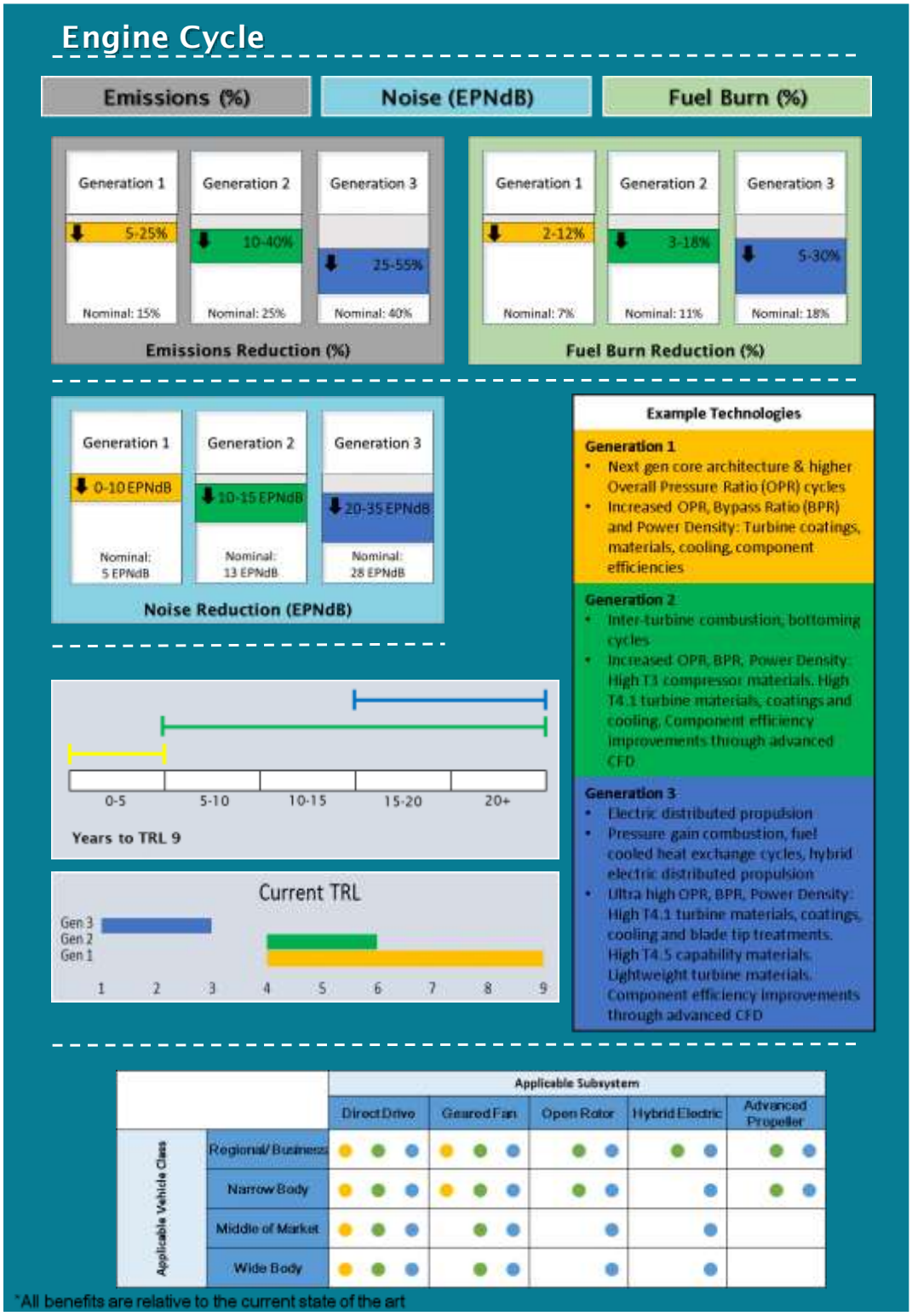

FIGURE 15. FINAL TECHNOLOGY ROADMAPS FOR ENGINE CYCLE

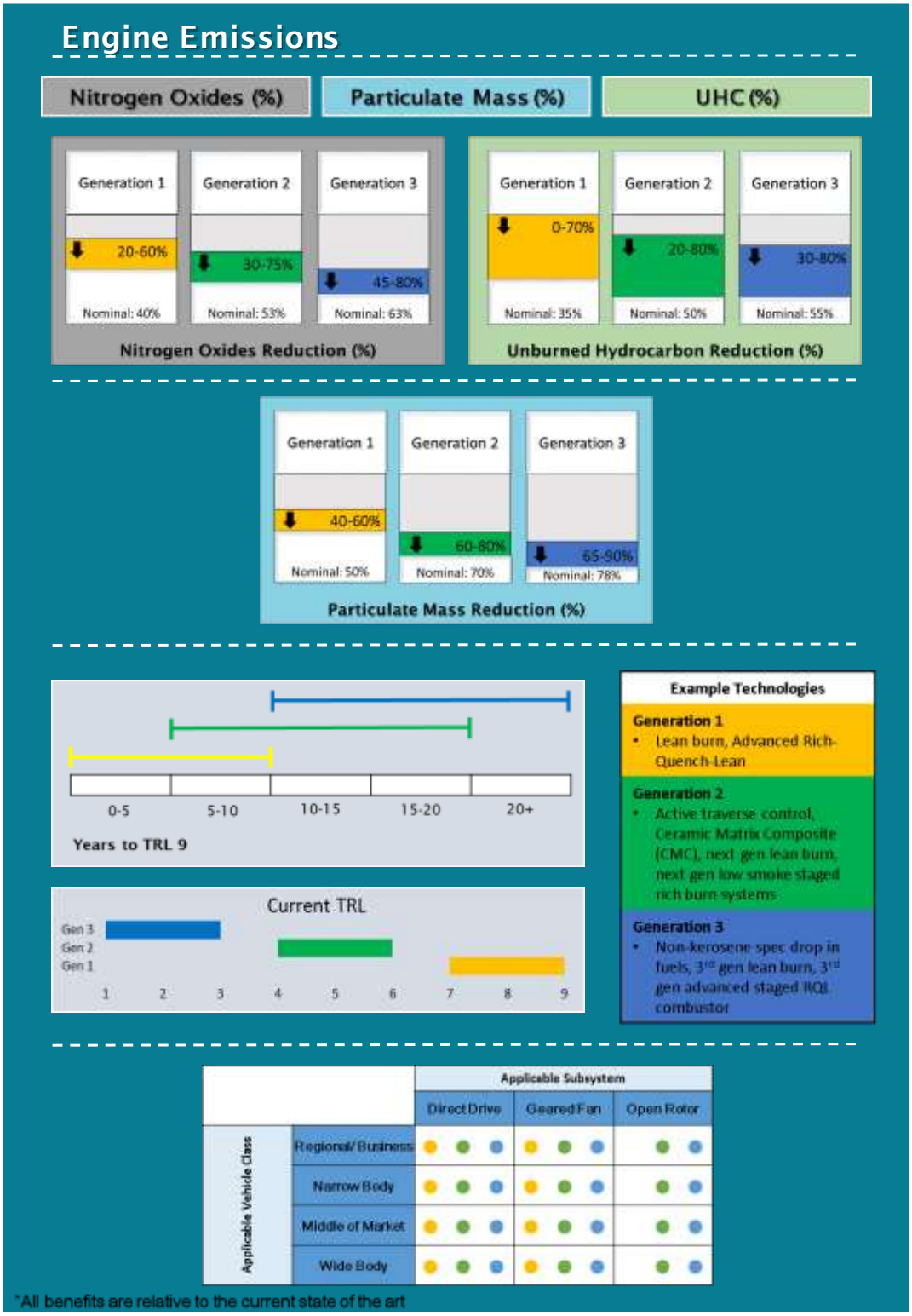

FIGURE 16. FINAL TECHNOLOGY ROADMAPS FOR ENGINE EMISSIONS

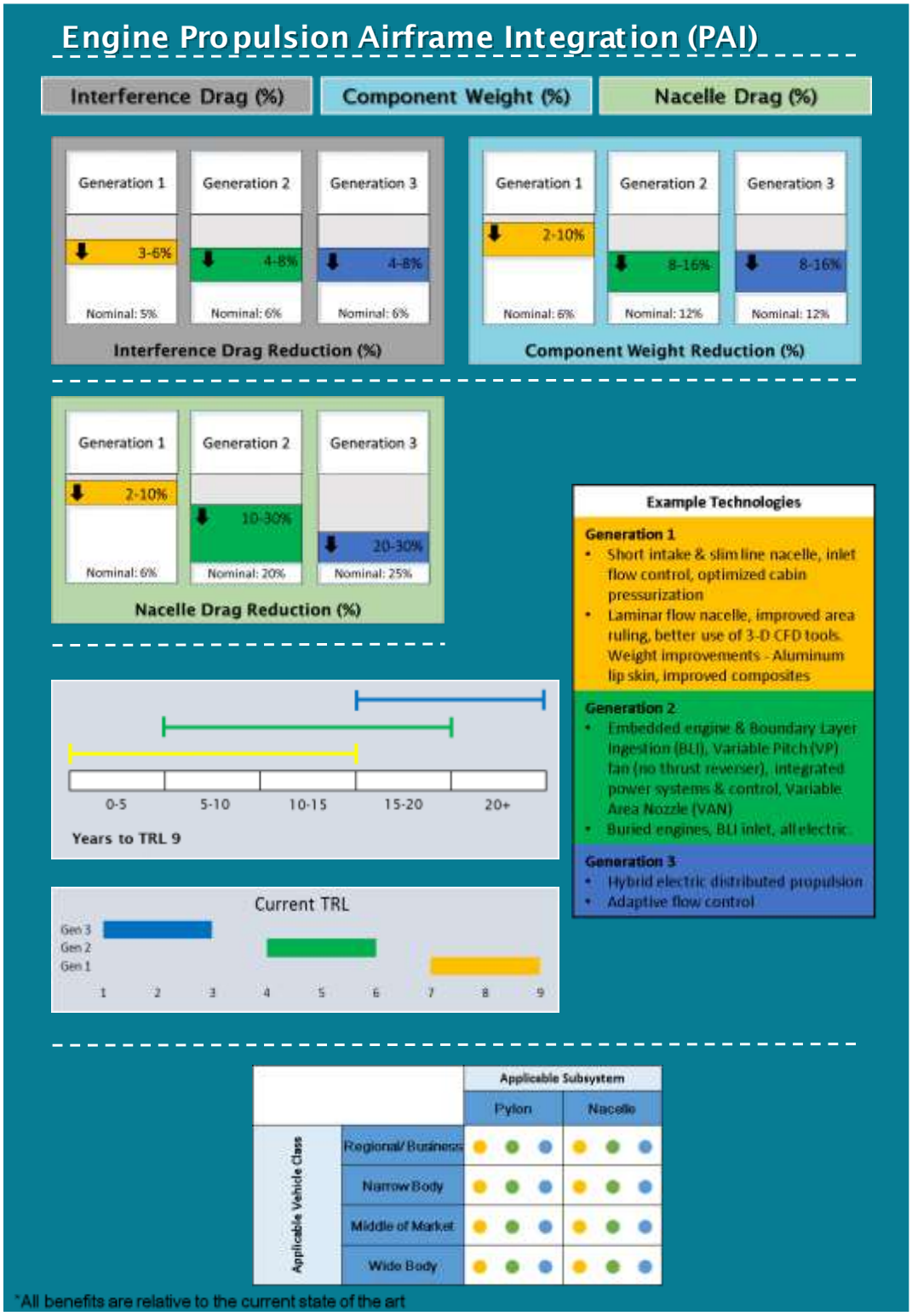

FIGURE 17. FINAL TECHNOLOGY ROADMAPS FOR ENGINE PAI

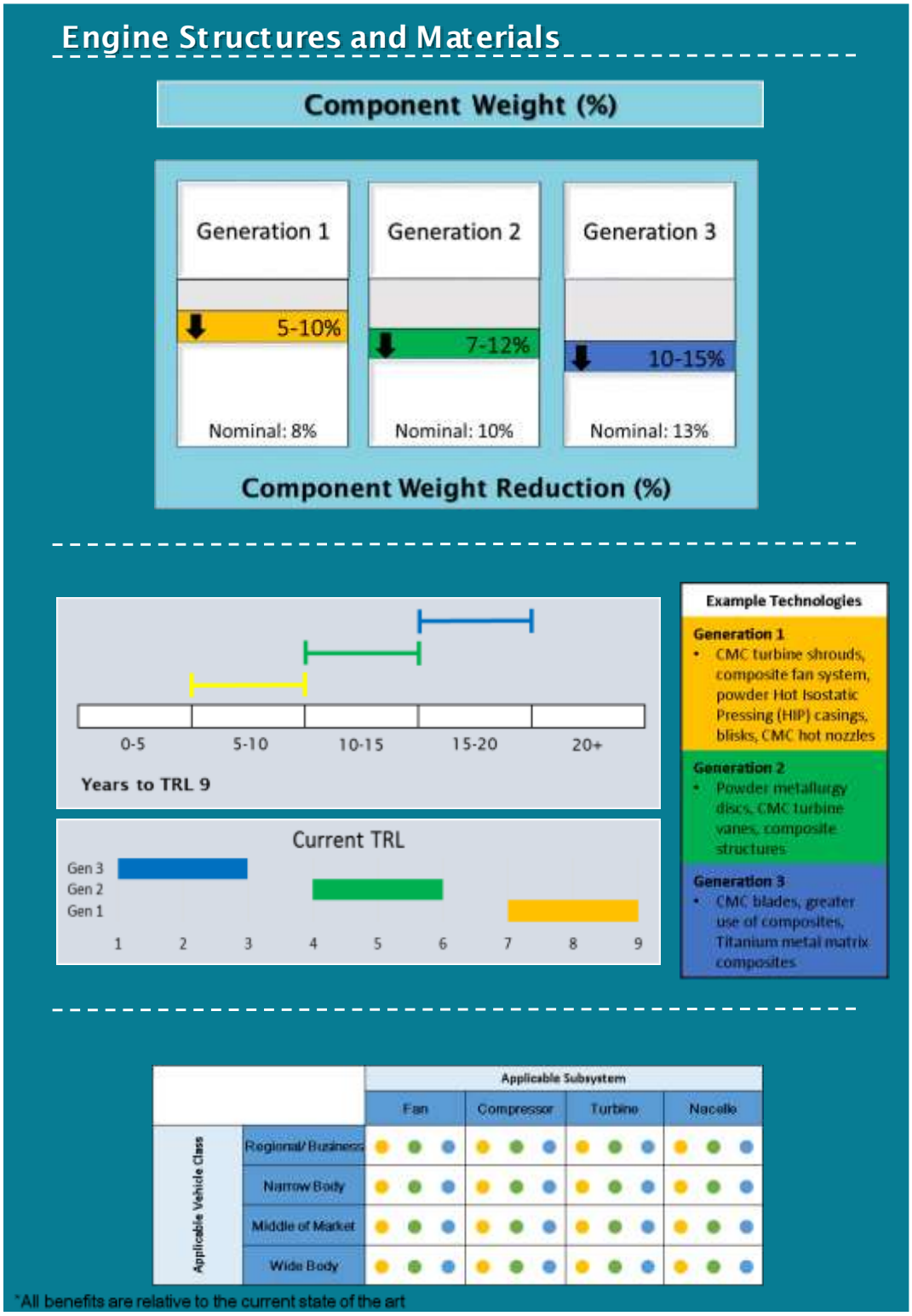

FIGURE 18. FINAL TECHNOLOGY ROADMAPS FOR ENGINE STRUCTURES AND MATERIALS

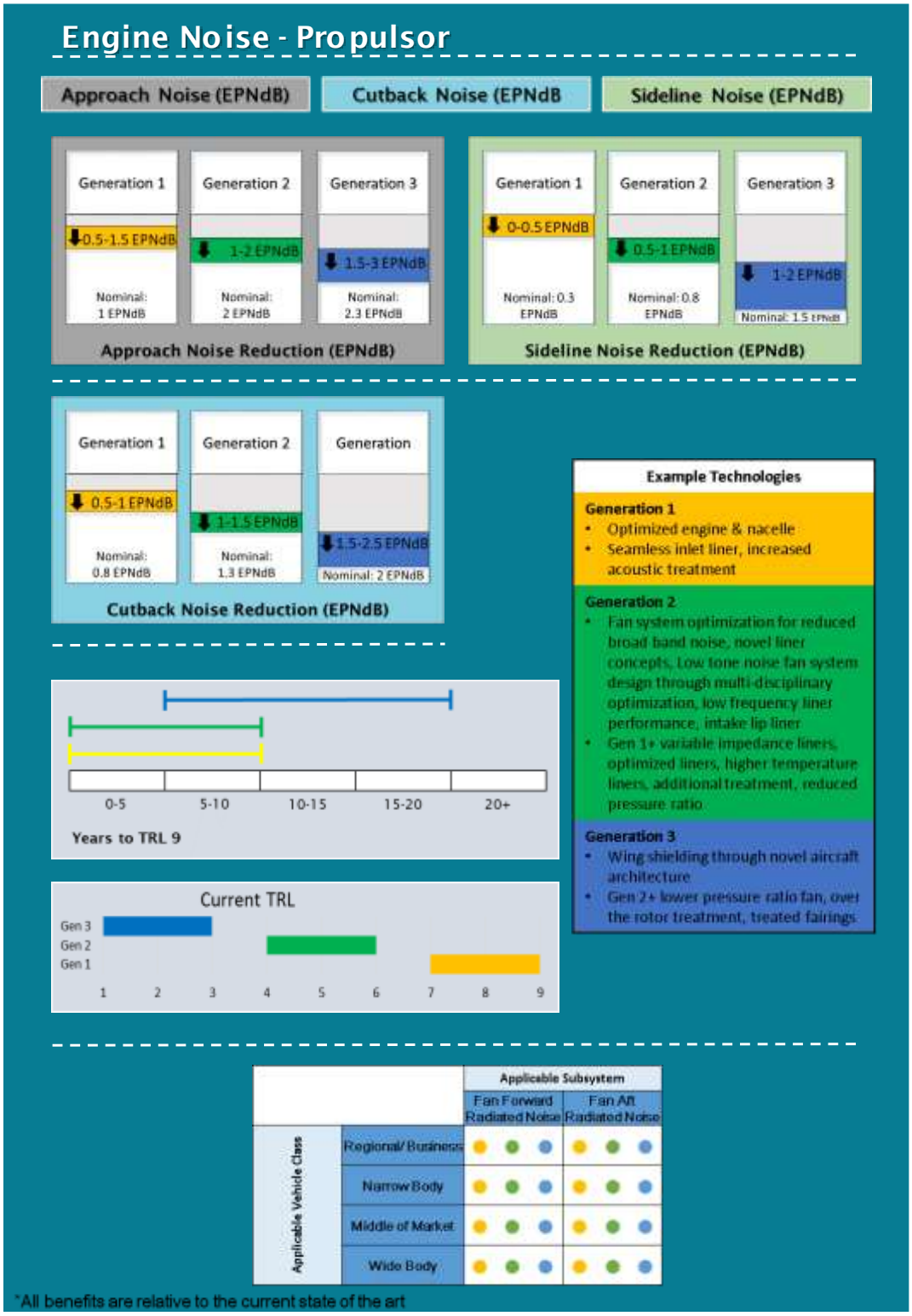

FIGURE 19. FINAL TECHNOLOGY ROADMAPS FOR ENGINE NOISE-PROPULSOR

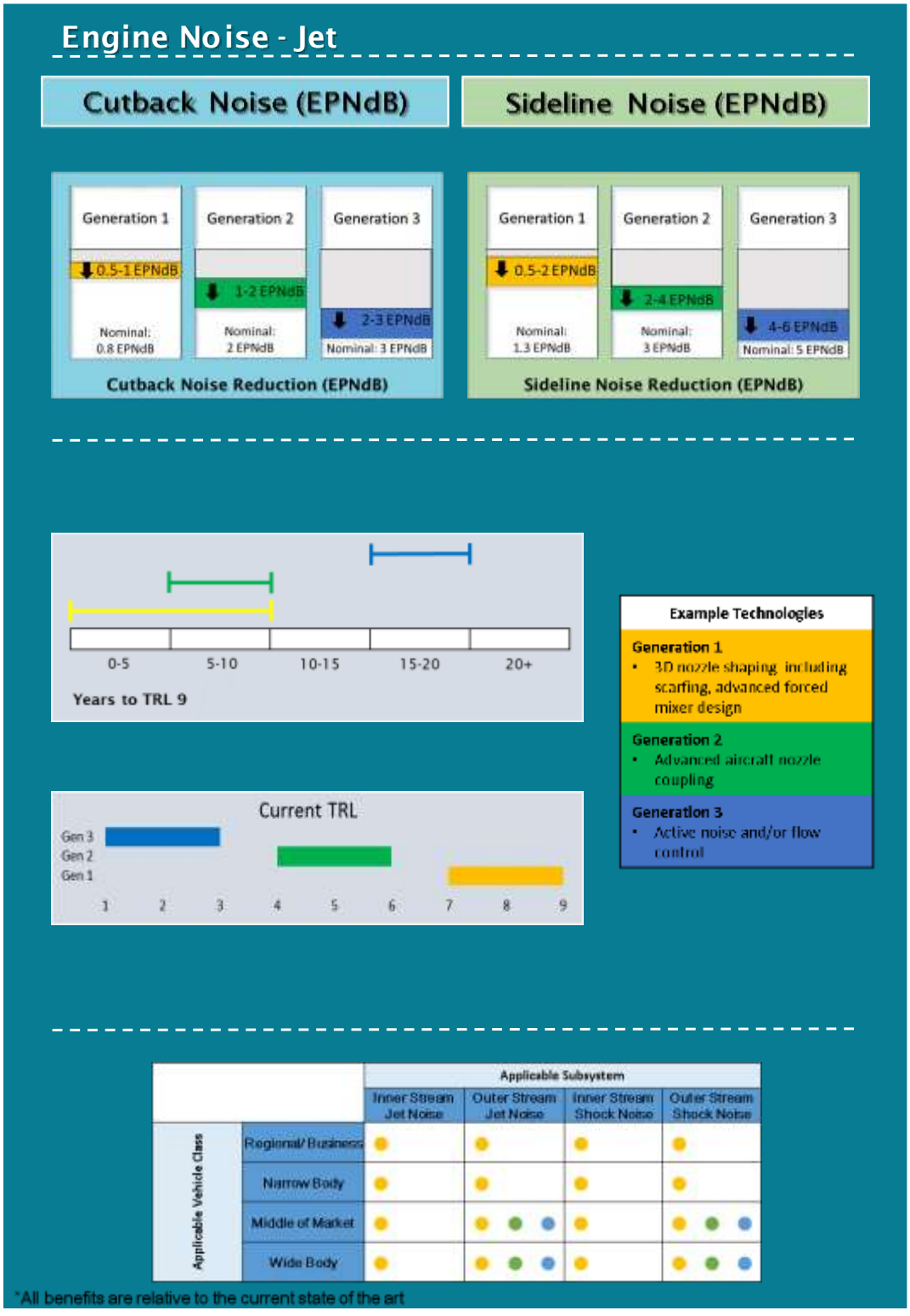

FIGURE 20. FINAL TECHNOLOGY ROADMAPS FOR ENGINE NOISE-JET

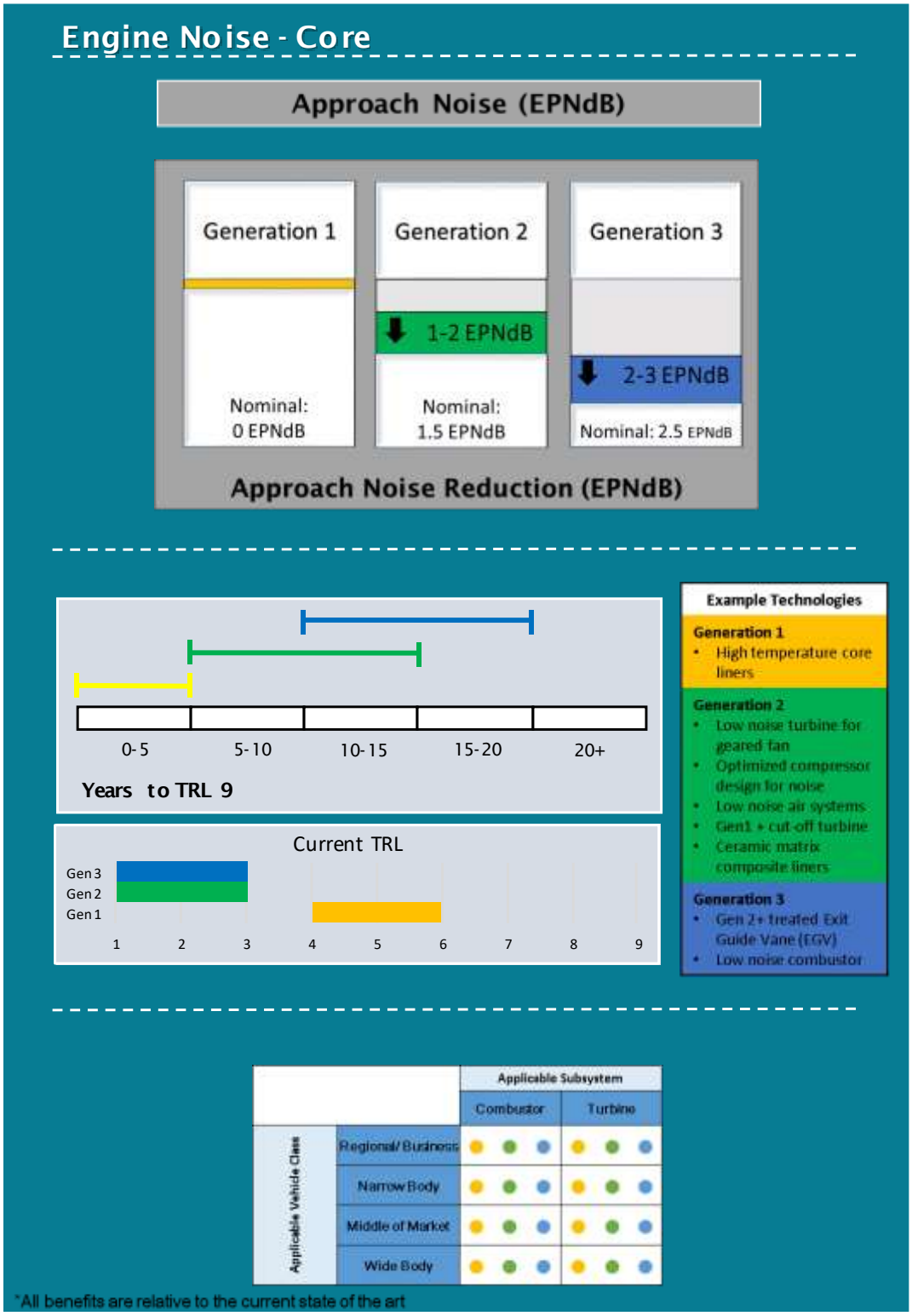

FIGURE 21. FINAL TECHNOLOGY ROADMAPS FOR ENGINE NOISE-CORE

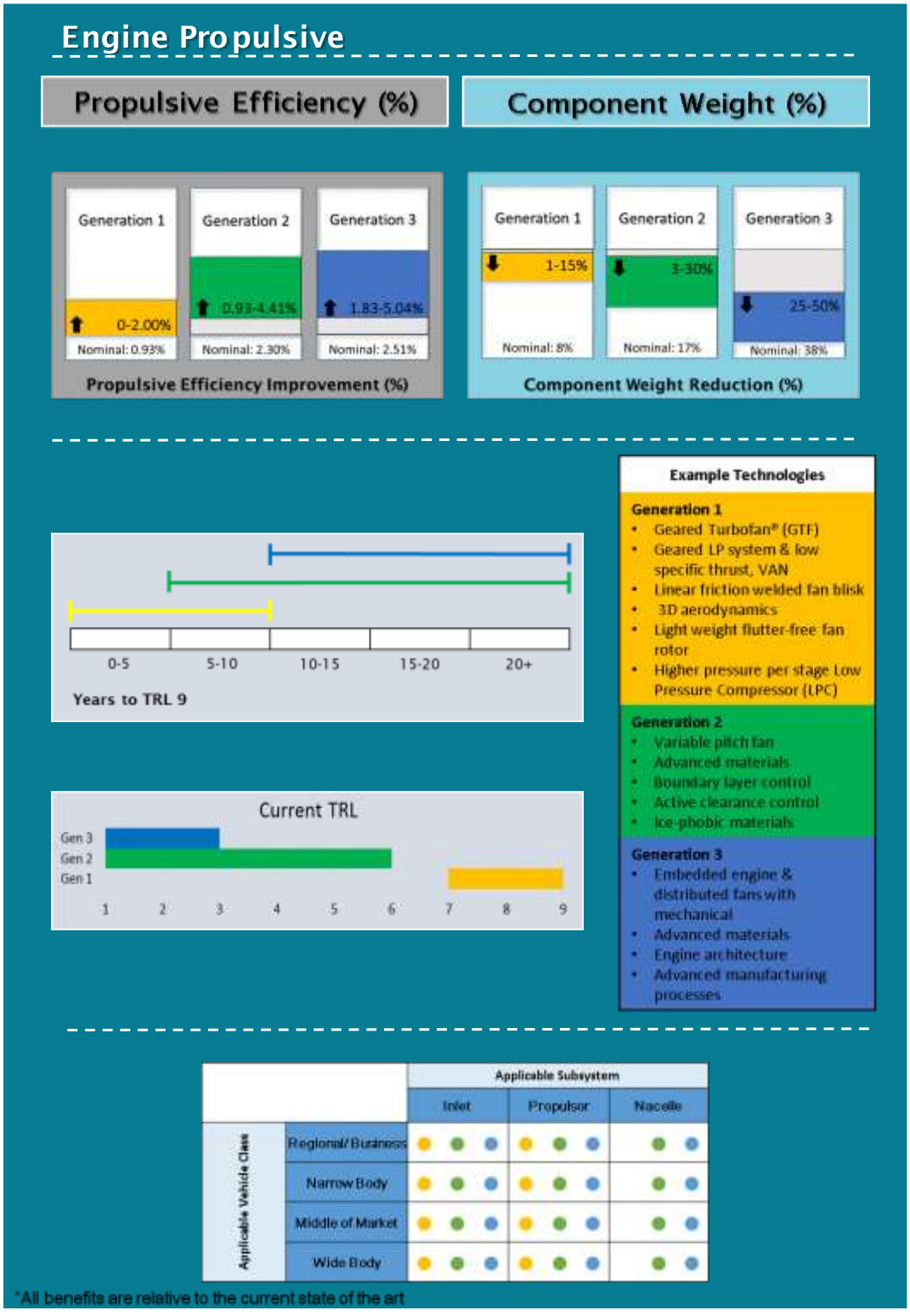

FIGURE 22. FINAL TECHNOLOGY ROADMAPS FOR ENGINE PROPULSIVE

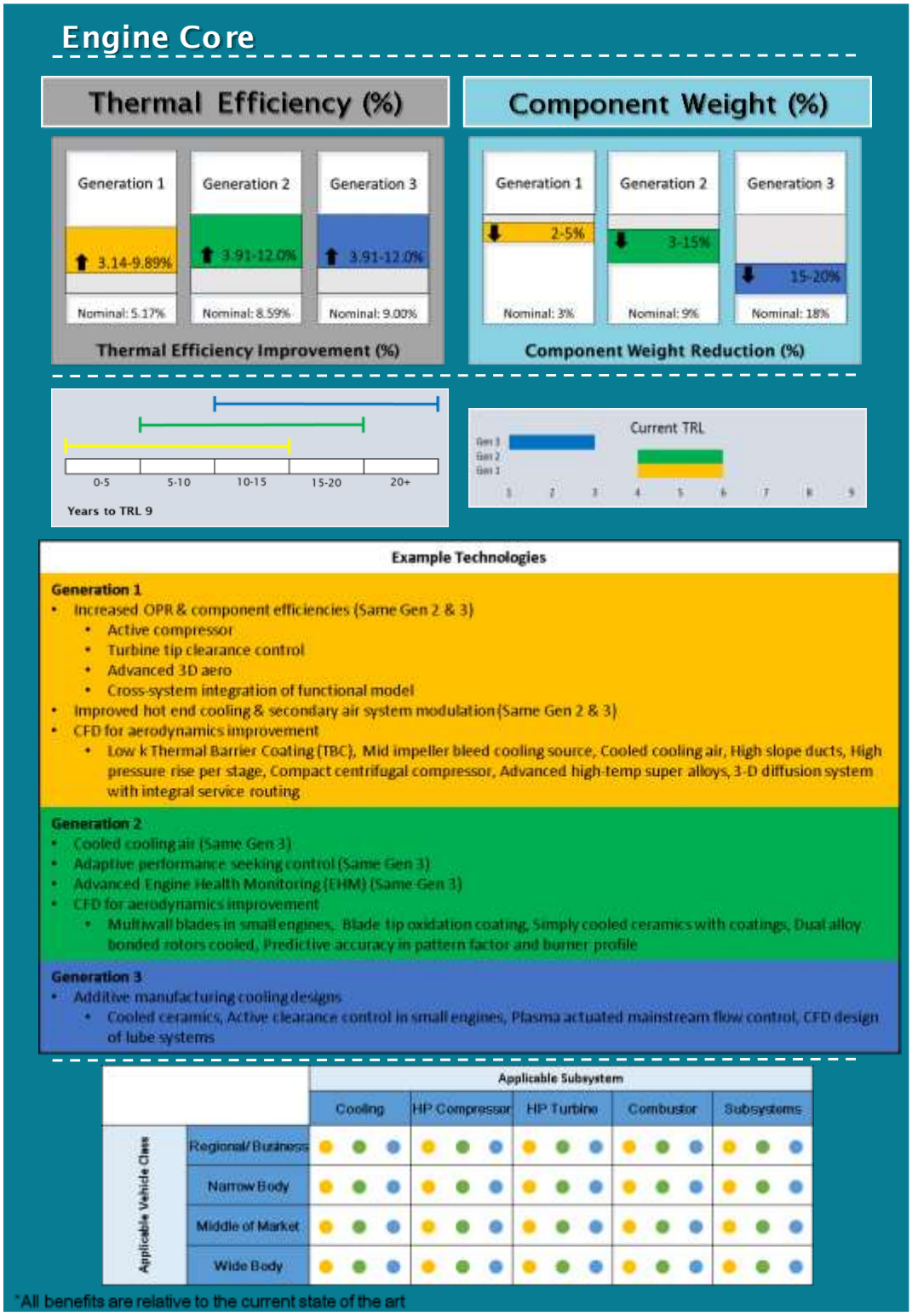

FIGURE 23. FINAL TECHNOLOGY ROADMAPS FOR ENGINE CORE

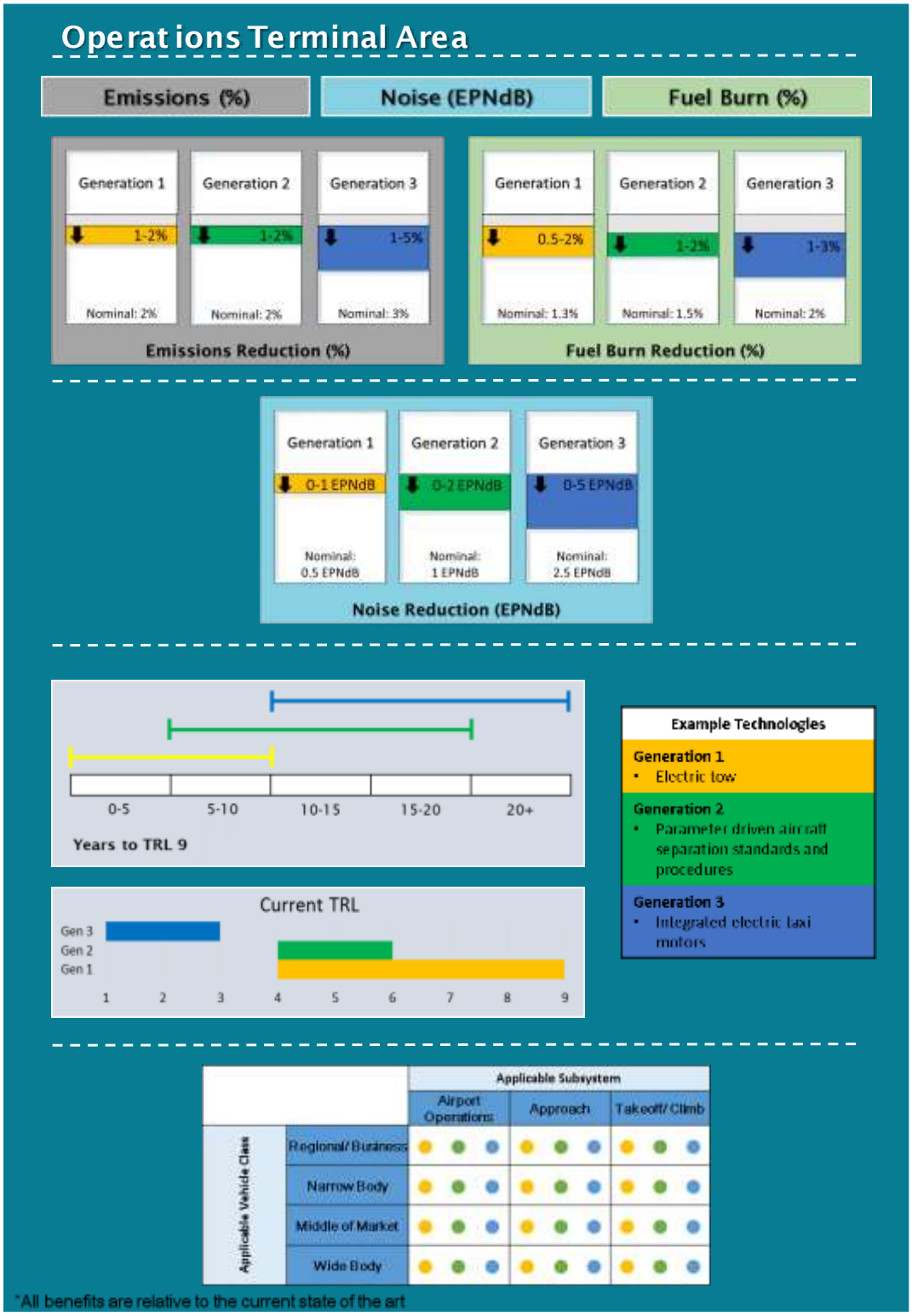

FIGURE 24. FINAL TECHNOLOGY ROADMAPS FOR OPERATIONS TERMINAL AREA

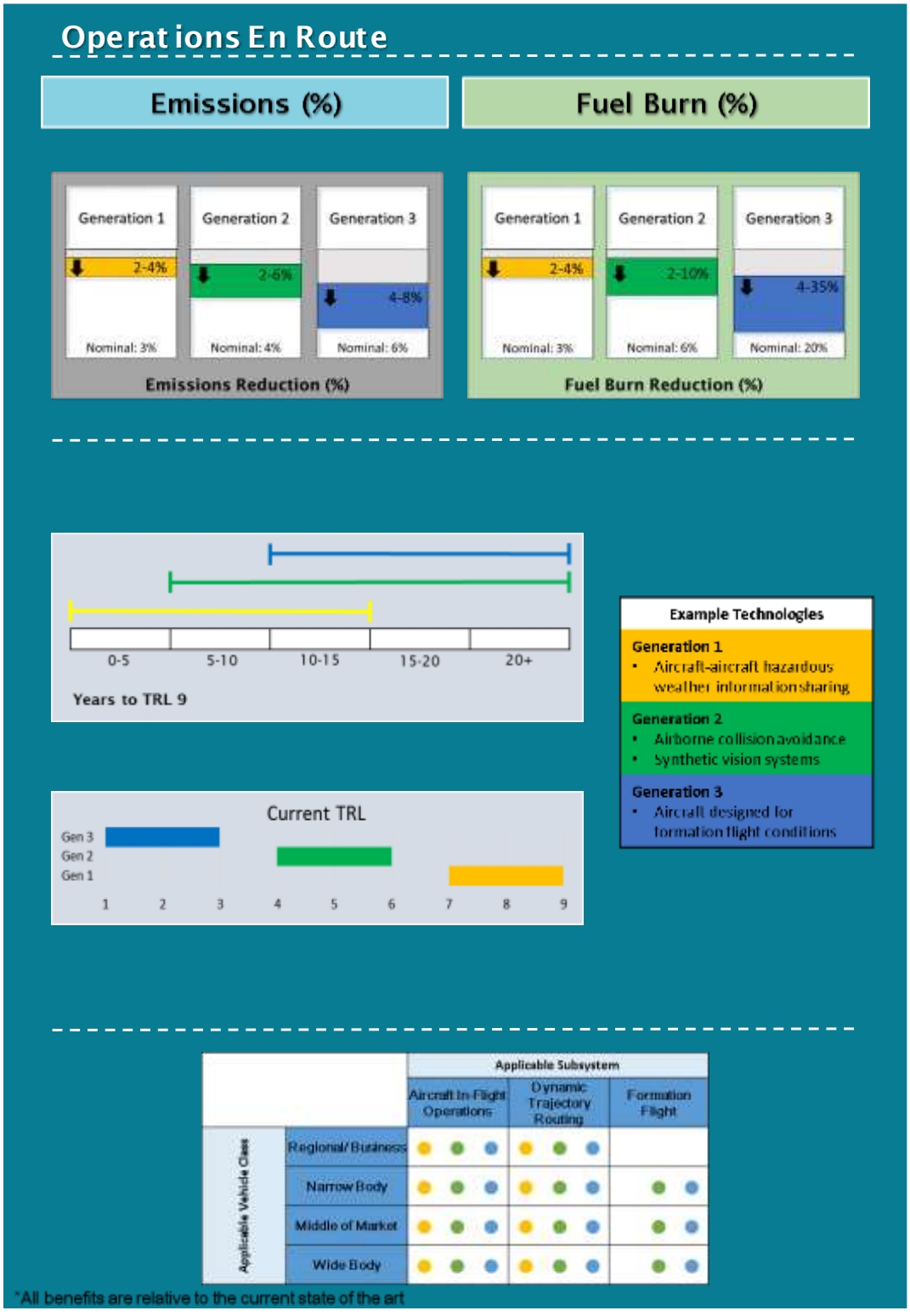

FIGURE 25. FINAL TECHNOLOGY ROADMAPS FOR OPERATIONS EN ROUTE

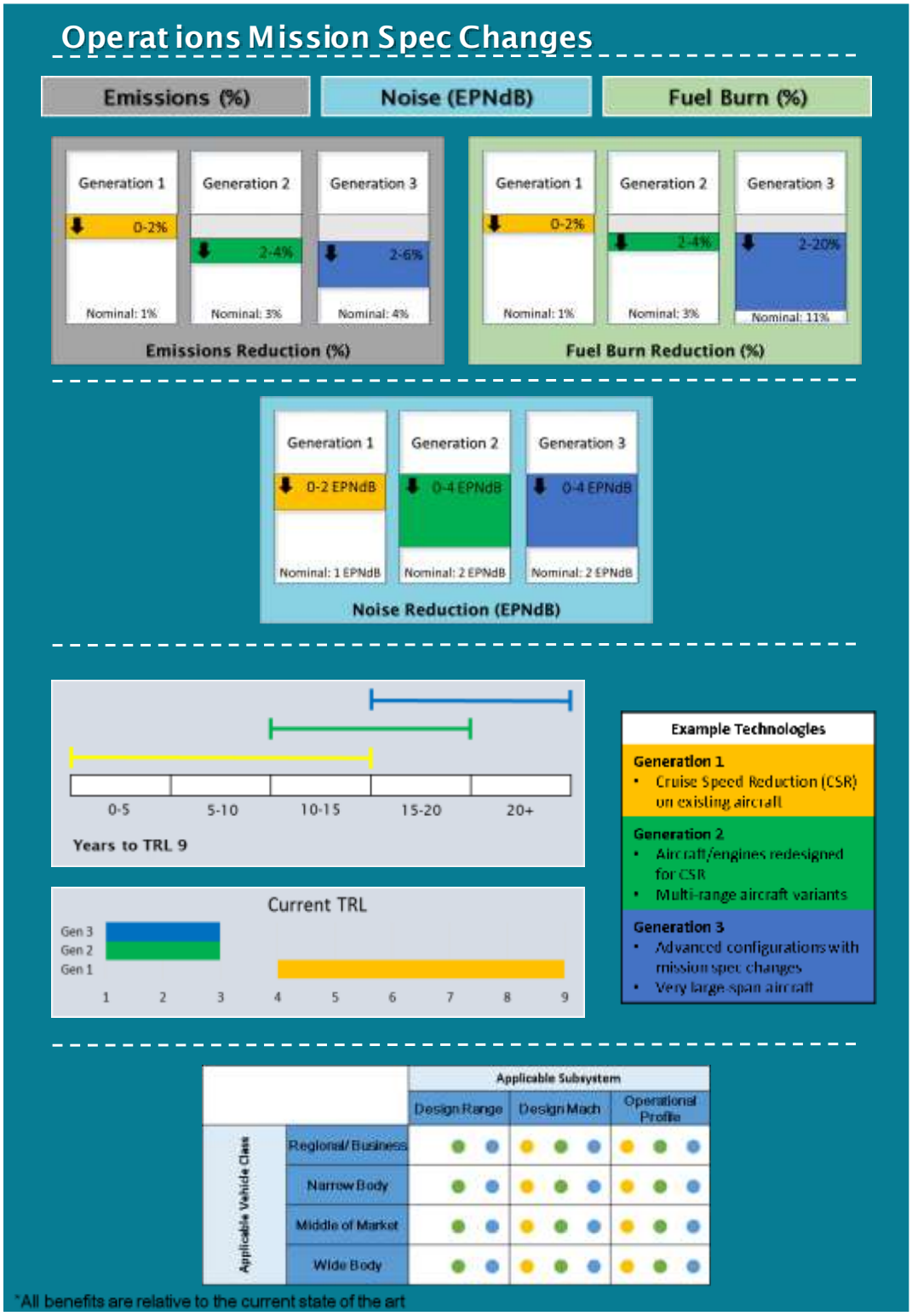

FIGURE 26. FINAL TECHNOLOGY ROADMAPS FOR OPERATION MISSION SPEC CHANGES

Milestones

Fleet Workshops
Based on the Fleet Scenario Workshops that were conducted through Summer and Fall 2015, the team created a series of conclusions from the data obtained from the workshop participants. This includes prioritizations of the factors that describe a scenario as well as evaluations of some provided suggested example scenarios and scenarios that the participants were able to customize. This was then used by the team in the first half of 2016 to formulate a number of scenarios through a series of discussions. These values were outcomes of the Fleet Workshops and were obtained by analyzing the data that was collected from the participants.

Technology Roadmapping Workshops
The first milestone for the Technology Roadmapping Workshops, following the 2015 Annual Report, was to finish review of the survey data and make initial infographic drafts for each technology area. This was accomplished by December 2016. The next milestone was the second Technology Roadmapping Workshop, held in January 2016. During the Workshop the infographics were presented to industry experts as a way to get feedback on the aggregate data from the first Technology Roadmapping Workshop surveys. Responses were asked to be sent back to Georgia Tech by the 8th of February 2016. The final milestone was reviewing the data from the latest responses and making final versions of the infographics. This was accomplished by March 2016. Slight modifications were made to Engine Propulsive and Engine Core infographics in July 2016, based on the results from Task 2.

Major Accomplishments

Fleet Workshops
The major accomplishment for the Fleet Workshops was to get input from experts across organizations and companies to provide feedback on what will be the major drivers that could shape the future of commercial aviation. The participants provided good feedback in terms of defining which descriptors are most important in describing potential future states of aviation as well as plausible settings for nominal, low, and high values. Additionally, participants provided feedback on a setoff provided scenarios as well as potential ideas for additional scenarios. This data was important in formulating a final set of recommended scenarios to be published and feeding into the other tasks.

Technology Roadmapping Workshops
The major accomplishment for the Technology Roadmapping Workshop was getting industry experts, across multiple companies and organizations, to provide meaningful feedback on the future of commercial aerospace. Attending both rounds of Workshops required participants to be committed. Clearly they saw the future benefits in the project results, which is what helped make the Workshops successful. The survey data was really the foundation for this project moving forward into Task 2 and 3. The data effected how he vehicle models were created and along with the scenarios.

Task 2: Modeling of Technologies and Advanced Configurations

Georgia Institute of Technology and Stanford University

Objective: Description of Advanced Vehicles Provided to Purdue and Stanford

In order to allow Stanford to assess the impacts of mission specification changes and for Purdue to exercise their FLEET tool, Georgia Tech provided both universities with a set of public domain Flight Optimization System (FLOPS) aircraft models from the 2014 CLEEN assessments performed under PARTNER Project 36 [1]. More specifically, the vehicles provided were from the assessment scenario named “Aggressive minus CLEEN” or AG-C. This scenario assumed an aggressive introduction of N+1 and N+2 technologies, including technologies currently under development or sponsorship of NASA. Since the scenario had all CLEEN technologies removed, Georgia Tech chose to use those models as advanced technology baselines that would allow Stanford and Purdue to carry out their respective tasks with a relatively common set of vehicle performance assumptions. Stanford used the FLOPS models to create corresponding versions in their vehicle modeling tool, SUAVE and Purdue used the FLOPS models directly within their FLEET tool. For more details on the usage of the models in SUAVE and FLEET please see Sections 0 and 0, respectively. For more details on the technologies included in the AG-C vehicle package, please see Reference [1].

Research Approach

Modeling of Technologies and Advanced Configurations Process Overview

The overarching goal was to create models of aircraft that showed improvements from a 1995 baseline vehicle, and matched the values participants had come up with during the Technology Roadmap survey. This was done for five standard vehicle classes. The final vehicle results were used during the fleet analysis by both Georgia Tech and Purdue. Further details on the Technology Roadmap Survey is provided in Section 0.The Environmental Design Space (EDS), developed by Georgia Tech, was used for creating these models. First, the variables within EDS that were applicable to the Technology Roadmap impacts were identified. Then it was determined how these EDS variables must be changed for the results to match the impacts. In most cases, there were EDS variables that related directly to impacts, but for some impacts a parametric study had to be performed. A Vehicle Timetable was created, using assumptions on when improved versions of different vehicle classes would enter the fleet. The spread of the "years to TRL 9" data from the Technology Roadmap survey were mapped to three different research and development (R&D) levels. For example, the maximum value for "years to TRL 9" for a given technology area generation was treated as a low R&D level scenario. This mapping was used to decide what year the three technology generations for each impact began, for each of the three different R&D levels. Using the Vehicle Timetable, the technology generations that were active during a vehicle generation could be determined for a given R&D level. This allowed vehicle models to then be created for different scenarios. As noted, these final vehicle models were then used as the basis for both Georgia Tech and Purdue's fleet analysis.

Identifying Applicable EDS Variables

Once the impact numbers from the Technology Workshop Survey data were finalized, the next step was to translate these impacts using variables native to the Environmental Design Space (EDS). EDS was the environment used by Georgia Tech to develop physics-based models of individual aircraft. Creating these models relies on the user providing values for a large number of variables that define both the physical and theoretical aspects of the aircraft. The team started with existing models Georgia Tech had previously developed that were representative of 1995 versions of each vehicle class. The variables of these baseline models were then systematically changed to model the effects of the impacts predicted by the Technology Workshop surveys. For each impact, a list was created of EDS variables that could potentially be changed to model that impact. EDS is based off of a number of NASA tools, including Numerical Propulsion System Simulation (NPSS), Weight Analysis of Turbine Engines (WATE++), and FLOPS. The manuals of these tools were also looked at to identify other variables that could be added to EDS that were currently being defaulted. The final list consisted of 89 EDS variables that would be used. The impacts for Operations Terminal Area, Operations En Route, and Operations Mission Spec Changes were not addressed since they are considered fleet level impacts. A list of the final EDS variable selections is provided in Table 7 broken down into the impacts for each technology area.

TABLE 7. MAPPING OF TECHNOLOGY ROADMAP IMPACTS TO EDS VARIABLES

IMPACT	METHOD FOR MODELING IN EDS
Aircraft Wing Design	
Induced Drag %	Lift dependent drag factor
Component Weight %	Total wing weight
Laminar Flow by % Chord	Percent LF on wing upper and lower surface
Profile Drag %	Lift independent drag factor
Noise EPNdB	Approach, Cutback, and Sideline Noise Suppression Factor on Trailing Edge Wing, Trailing Edge Flap, and Leading Edge Slats
Aircraft Aerodynamic Improvements	
Induced Drag %	Lift dependent drag factor
Laminar Flow by % Chord	Percent LF nacelle, fuselage, vertical tail, and horizontal tail upper and lower surfaces
Profile Drag %	
Wave Drag %	
Aircraft Composites	
Design Margin %	Empty Weight Margin
Component Weight %	Total wing, horizontal tail, vertical tail, and fuselage weight
Aircraft Advanced Metallics	
Component Weight %	Total wing, horizontal tail, vertical tail, fuselage, land gear main, and landing gear nose weight
Aircraft Manufacturing Processes	
Component Weight %	Total wing, horizontal tail, vertical tail, and fuselage weight

Impact	Method For Modeling In EDS
Aircraft Multifunctional Structures	
Component Weight %	Total wing, horizontal tail, vertical tail, and fuselage weight
Aircraft Structural Health Monitoring	
Design Margin %	Empty Weight Margin
Component Weight %	Total wing, horizontal tail, vertical tail, and fuselage weight
Aircraft Noise	
Approach Noise EPNdB	
Cutback Noise EPNdB	
Source Noise dB	Approach, Cutback, and Sideline Noise Suppression Factor on Main Landing Gear, Nose Landing Gear, Trailing Edge Horizontal Tail, and Trailing Edge Vertical Tail
Sideline Noise EPNdB	
Aircraft Subsystems	
Drag %	Lift independent drag factor
Component Weight %	Auxiliary power unit, Instrument Group, Hydraulics Group, Electrical Group, and Avionics Group Weight
Aircraft Configurations	
Emissions %	Percent NOx reduction
Fuel Burn %	
Noise EPNdB	
Engine Cycle	
Emissions %	Percent NOx reduction
Fuel Burn %	
Noise EPNdB	
Engine Emissions	
Nitrogen Oxides %	Percent NOx reduction
Pariculate Mass %	
UHC %	
Engine PAI	
Interference Drag %	
Component Weight %	Factor for bare engine weight to engine pod weight
Nacelle Drag %	SWETN
Engine Structures and Materials	
Component Weight %	Fan Containment Material density
Engine Noise - Propulsor	
Engine Approach Noise - Propulsor	Approach Noise Suppression Factor on Inlet and Fan Discharge Noise
Engine Cutback Noise Propulsor	Cutback Noise Suppression Factor on Inlet and Fan Discharge Noise
Engine Sideline Noise - Propulsor	Sideline Noise Suppression Factor on Inlet and Fan Discharge Noise
Engine Noise - Jet	
Cutback Noise EPNdB	Cutback Noise Suppression Factor on Jet Takeoff Noise
Sideline Noise EPNdB	Sideline Noise Suppression Factor on Jet Takeoff Noise
Engine Noise - Core	
Approach Noise EPNdB	Approach Noise Suppression Factor on Fan Discharge Noise
Engine Propulsive	
Propulsive Efficiency %	Improvement modeled adjusting FPR, Extraction ratio at Aero Design Point, HPT chargeable (exit) cooling effectiveness, HPT non-chargeable (inlet) cooling effectiveness, and Maximum T4 (set at Take Off)
Component Weight %	Weight of miscellaneous propulsion systems, Fan Blade Material Density, Fan Stator Material Density, Fan Case Material Density, Inlet Nacelle Material Density and Bypass Nozzle Weight
Engine Core	
Thermal Efficiency %	Improvement modeled adjusting FPR, LPCPR, HPCPR, HPT chargeable (exit) cooling effectiveness, and HPT non-chargeable (inlet) cooling effectiveness
Component Weight %	Material Density of Burner Liner and Blades, Stators, and Disks of HPC, LPC, HPT, and LPT

In a number of cases there were no EDS variables that could be tied directly to an impact. For example, observer effective perceived noise level (EPNL) impacts are not directly related to noise suppression factors. Changes in observer EPNL can only be observed after the model is run. To reconcile this, parametric studies were run to analyze how observer EPNL was

impacted by changing noise suppression factors related to wing design, propulsive, jet, and core noise. This is detailed further in Section 0. For Aircraft Noise, source noise impacts were provided in dB, which can be applied directly through noise suppression factors. By applying these suppression factors it was reasoned that the Aircraft Noise impacts for observer EPNL would be accounted for in terms of approach, sideline, and cutback.

Translating Impacts to EDS Variable Ranges

Once appropriate EDS variable had been chosen, the next major task was to determine how the impact values would be applied to the baseline values of the EDS variables. In some cases, it was seen that implementing stated impacts from the technology roadmaps could be done by simply adding, subtracting, or multiplying. In other cases, modeling the impacts required running a parametric study to determine the relationship between the EDS variable and impacts. After analyzing the EDS variables selected, 8 different categories of EDS variables were identified as presented in Table 8. A detailed description of the Technology Roadmap DOE Aggregator that was created to automate this process is given in Section 0. The Aggregator used the variable type that had been identified for each EDS variable to determine how to apply the impacts.

TABLE 8. HOW AN IMPACT IS APPLIED TO AN EDS VARIABLE DEPENDS ON THE VARIABLE TYPE

Variable Type	Description	Formula (K# Represents Individual Impact)
Scalar	Multiplicative	=Baseline*((1+K1/100)*(1+K2/100)*(1+K3/100)*…*(1+Ki/100))
Delta	Added together	=Baseline + (K1+K2+K3+…+Ki)
Noise	Combined on decibel scale	=Sum[(1*largest Ki) + (0.75 * 2nd largest Ki) + (0.5 * 3rd largest Ki) + (0.33 * 4th largest Ki)+ (0.16 * 5th largest Ki) + (0.08 * 6th largest Ki)….]
DeltaF	Added together as fraction/decimal	=Baseline + (K1+K2+K3+…+Ki)/100
Switch	Turns on or off from its baseline state if there is an impact	1 or 0
Absolute	Replaces baseline. Chosen based on parametric studies or must be set to zero	

Delta variables are typically percentages, so if the impact is a 74% increase, the new value for the EDS variable is 74 if the baseline value was zero. For DeltaF variables a 74% increase would be represented as 0.74, in other words its decimal form. For noise, in some cases the baseline suppression factor was non-zero, so when determining the new value the baseline was just treated as another one of the K-factors. In the case of jet, core, and propulsive noise the K-factors were chosen based off of a parametric study. The study found suppression factors that produced observer EPNL impact results close to those reported in the survey. This study is detailed further in Section 0. Using the EDS variables that were related to the increase in laminar flow impact required an additional step. First, the EDS variables related to the turbulent transition Reynolds number of different wing surfaces had to be set to zero.

Performing Sensitivity Checks On Benefit Ranges

For scalar and delta type EDS variables, a sensitivity study was run using the one-at-a-time method. This involved applying the Generation 3 maximum impact to a given EDS variable, while keeping all other EDS variables at their baseline values. A case was run for each EDS variable, for all five aircraft class models to see if the model would run at the limits of this projected future design space.

Results of Sensitivities

In addition to checking if an impact could actually be modeled, the sensitivities helped confirm that the right variable type had been identified for each EDS variable. The only EDS variable that posed a problem was PCT_NOx, which stands for "Percentage NOx reduction". The impacts for Engine Emissions Nitrogen Oxide Reduction, Engine Cycle Emissions Reduction, and Aircraft Configurations Emissions Reduction were all mapped to PCT_NOx. Since PCT_NOx was a DeltaF type variable the impacts would typically be added together. Unfortunately, the combination of the maximum values of these three impacts resulted in a NOx reduction value greater than 100%, which is not possible. It was decided that the

largest of these three impacts would be used as representative of all three when modeling the vehicles. This does not mean the same one of these impacts was always dominant. For example, for a vehicle modeled with all Generation 2 impacts, at a high technology level, the impact values for Engine Emissions, Engine Cycle, and Aircraft Configurations on PCT_NOx were 75%, 40%, and 40% respectively, so Engine Emissions dominated. For a high technology level vehicle with a Generation 2 Engine Emissions impact, and Generation 3 Engine Cycle and Aircraft Configurations impacts, the impact values on PCT_NOx were 75%, 40%, and 80% respectively, so Aircraft Configuration dominated instead.

Considerations for Noise and Engine Efficiency

Since observer EPNL and thermal and propulsive efficiency were output metrics of sizing, getting the correct impact values required first understanding the relationship between them and the EDS variables that affect them. This involved a full factorial approach to sensitivity analysis, where the effects of changing the multiple EDS variables together was looked at. The main parameters that could have be modified to improve propulsive efficiency were extraction ratio (Ext_Ratio), fan pressure ratio (FPR), and maximum burner exit temperature (T4max). Thermal efficiency could have been improved by increasing the overall pressure ratio (OPR) and modifying the worksplit between the low-pressure compressor ratio (LPCPR) and high-pressure compressor ratio (HPCPR). Note that OPR was not a direct EDS variable, but was the product of the EDS variables for LPCPR, HPCPR, and FPR. Both efficiencies could have also have been improved by decreasing the amount of cooling need by the engines using the EDS variables s_HPT_ChargeEff and s_HPT_NonChargeEff. For noise, increasing noise suppression factors could have continued to lower observer EPNL results, but with diminishing returns.

Conducting Parametric Studies for Engine Cycle Variables

As noted in Section 0, the propulsive and thermal efficiency were outputs of EDS, so they could not have be changed directly. In order to get the impacts reported in the workshop surveys, the engine cycle parameters that affect efficiency were changed. A parametric study was conducted for both thermal efficiency and propulsive efficiency. The goal was to first vary applicable cycle parameters over wide ranges to analyze trends in the efficiencies. From this analysis the team believed it would then be able to choose cycle parameters values to reach the low, nominal, and high efficiency values for each generation. These studies had to be repeated for each vehicle class, since the baseline models did not all have the same engines. The selected engine cycle parameters were then arranged as a look-up table that could be searched when constructing the EDS cases for the different technology scenarios that were modeled.

Thermal Efficiency Studies

The thermal efficiency sensitivity study was conducted by first increasing OPR by keeping FPR constant and increasing LPCPR and HPCPR, keeping the worksplit between the LPC and HPC constant. The worksplit was then modified to see the effects of shifting 20% more of the work to the LPC and then 20% more of the work to the HPC. The results of the first set of sensitivities for the Very Large Aircraft (VLA) are shown in Figure 27.

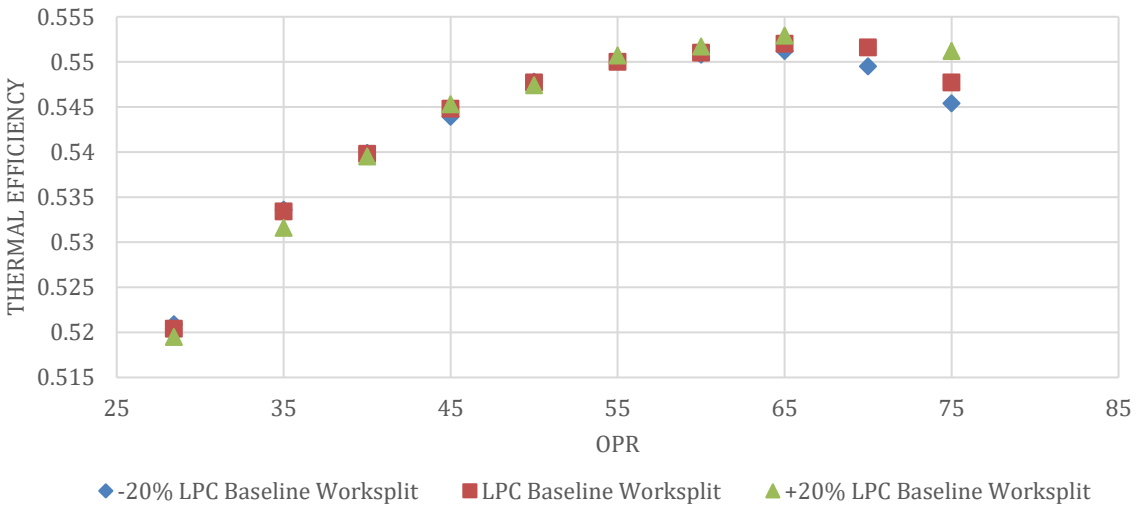

FIGURE 27. INITIAL RESULTS OF THERMAL EFFICIENCY STUDY FOR THE VLA

As can be seen this graph peaked at 55.2%, which was only a 6.2% relative percent increase from the baseline of 52%. The surveys expected a maximum relative percent increase of 30%, which in the case of the VLA would meant a thermal efficiency of 67.6%. An OPR of 75 was used as an aggressive upper limit for these studies. Note that for an OPR of 75 the theoretical maximum thermal efficiency for a gas turbine was calculated as 70.9%. Similar results were seen for the other four vehicles, where the relative thermal efficiency values were still far away from the maximum impacts reported in the surveys.

Further studies focused on the large twin-aisle (LTA) and single-aisle (SSA-LSA) aircraft models. The effects of decreasing the amount of cooling required by the high-pressure turbine (HPT) were looked at, lowering it until it was nearly zero. Changing FPR was also looked at using the same range of FPR values used during the initial propulsive efficiency studies. As previously noted, these studies used a full factorial approach. Therefore, if the FPR was changed, all cases that had been run with that previous FPR, changing OPR and cooling, were repeated. For the LTA the baseline thermal efficiency was 56.5% and from this process a maximum thermal efficiency of 60.4% was achieved, or a relative percent increase of 6.9%. For the SSA-LSA the baseline thermal efficiency was 49.5% and a maximum thermal efficiency of 54.2% was achieved, which translated to a relative percent change of 9.5%. These efforts began to call into question how reasonable the survey predictions were. As will be detailed further, it should be noted these maximum thermal efficiencies did not correspond the parameters to maximize propulsive efficiency.

Propulsive Efficiency Studies

The propulsive efficiency studies began by decreasing the FPR until it reached a hard lower limit of 1.25. In addition the extraction ratio was increased and decreased up to 20% of the baseline value. Presented in Figure 28 are the initial results of the study for the SSA-LSA. As can be seen there was a positive trend in propulsive efficiency between increasing extraction ratio and also decreasing FPR, but clearly there were diminishing returns.

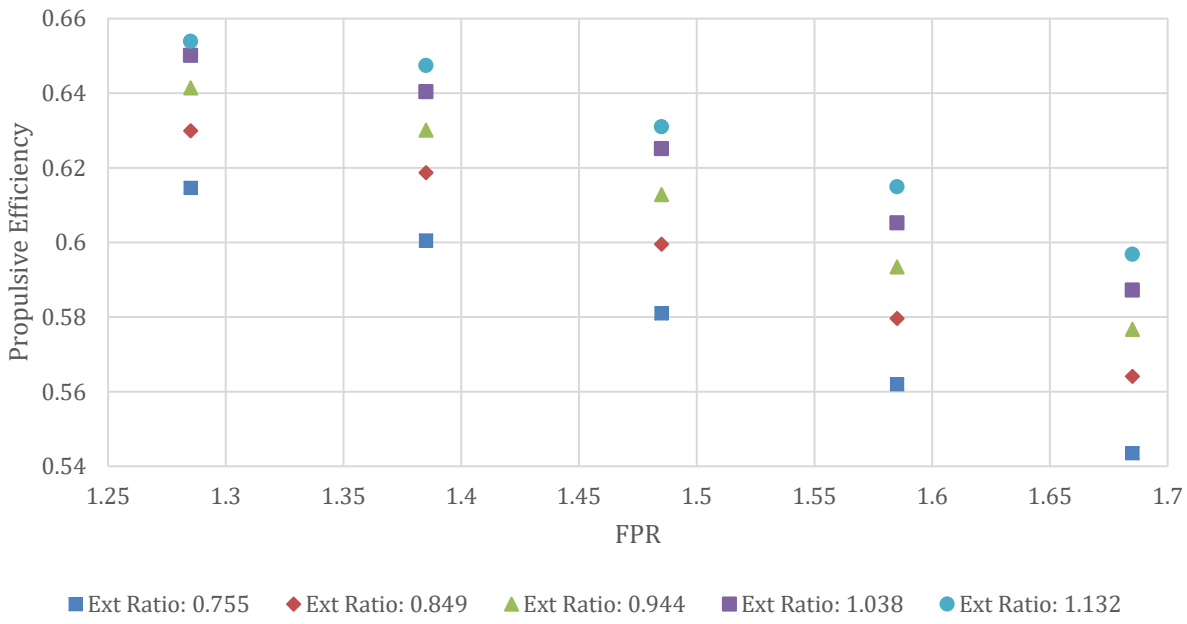

FIGURE 28. INITIAL PROPULSIVE EFFICIENCY SENSITIVITY STUDY RESULTS FOR THE SSA-LSA

The baseline propulsive efficiency for the SSA-LSA is 57.7% and the maximum propulsive efficiency reached in this study was 65.4%, which was only a relative change of 13.3%. This was below even the Generation 1 maximum impact gathered from the survey of 20%.

Similar to the thermal efficiency study, additional cases focused on the LTA and SSA-LSA, reducing the cooling required by the HPT until it was nearly zero. An additional EDS variable that was looked at for the propulsive efficiency study for the LTA was T4max, which was set at takeoff. It was increased from its baseline of 3450°R to as high as 3850°R, which was a highly optimistic prediction for future turbofan combustor exit temperatures. When analyzing an ideal fixed turbofan, the general trend is that increasing the burner exit temperature increases specific thrust, which causes propulsive efficiency to decrease and has no effect on thermal efficiency. Due to the dynamics of a real engine, the interrelation between OPR and T4 was seen to actually increase propulsive efficiency. Unfortunately, in this trade study it was also seen that it can cause thermal efficiency to decrease too, often with greater losses than the gains in propulsive efficiency. This further highlights the constant balancing act required to be performed by engine designers.

For the LTA the maximum propulsive efficiency achieved was 70.6%, which was a relative percent increase of 10.4% from the baseline. A maximum relative percent increase of 18.5% was achieved for the SSA-LSA. It was known that some companies have accounted for propulsive efficiency by dividing out the efficiency of the LPT. Doing this resulted in the maximum relative percentage change from the baseline becoming 11.3% and 18.9% for the LTA and SSA-LSA, respectively. Again these results were below even the maximum Generation 1 impact prediction of a 20% relative percent increase. In addition, the parameters to achieve these maximum propulsive efficiency increases did not correspond with the parameters to maximize thermal efficiency. This concern is best exemplified by Figure 29, which has the thermal efficiency of all the cases run for the LTA plotted against their propulsive efficiency with the LPT efficiency divided out. The figure shows a Pareto frontier, meaning there was a compromise occurring between propulsive and thermal efficiency.

Given the results of this study an alternative solution was proposed. The disparity between the survey and the trade study possibly could have been attributed to the fact that most industry experts spoke of engine improvements in terms of bypass ratio (BPR) and OPR instead of thermal and propulsive efficiency. A literature search was conducted to determine what academia and the aerospace industry believed OPR and BPR values would be over the next three generations for the five different aircraft classes that were modeled. The end goal was to then use those findings as a more credible basis for the engine cycle parameters. The infographics would then be updated based on the final results.

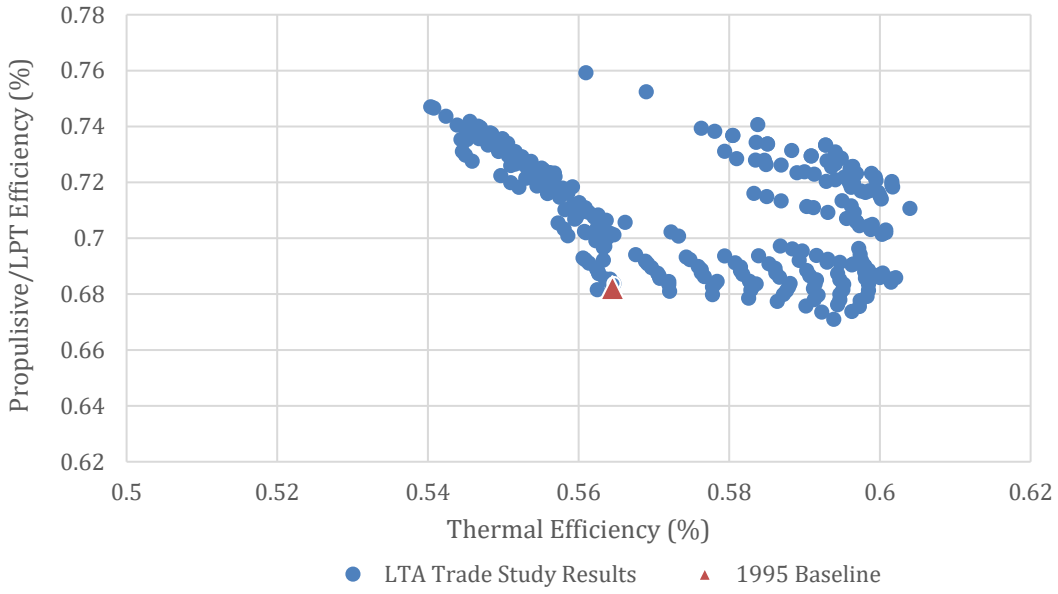

FIGURE 29. LTA EFFICIENCY TRADE STUDY RESULTS SHOWING PROPULSIVE EFFICIENCY WITH THE LPT EFFICIENCY DIVIDED OUT AGAINST THERMAL EFFICIENCY.

Generation 1 OPR & BPR Research

Generation 1 aircraft were viewed as those entering service in the near term, from 2015 to 2018. The Airbus A320neo, which entered service in January 2016, was a 189 passenger, single aisle jetliner [2]. Neo stands for new engine option, and customers are provided with the choice of either the Pratt & Whitney PW1100G Geared Turbofan (GTF) or the CFM International LEAP-1A turbofan. The A320neo was seen as a fair representation for the LSA. Pratt & Whitney's GTF is reported to have an HPCPR of 16:1 leading to an OPR of 50:1. The engine has a BPR of 12:1. The GE LEAP-1A first saw service on an A320neo in July 2016. It's purported to have a BPR of around 11:1, with a confirmed HPCPR of 22:1 and OPR of 40:1. The LEAP-1C will be powering the Comac C919, which is a narrow-body aircraft that will hold 156-168 seats, making it comparable to the SSA-LSA. The basic engine parameters for the LEAP-1C are the same as the LEAP-1A, it just has a slightly smaller fan causing it to have less thrust.

The Rolls Royce Trent XWB is a three-shaft turbofan currently seeing use on the Airbus A350 XWB, which holds between 250 and 440 passengers depending on the variant [3]. Together they entered commercial service in January 2015. The Trent XWB has a BPR of 9.6:1 and OPR of 50:1. Based on the large seat capacity range the Trent XWB was used as the basis for both LTA and VLA engine cycles.

The GE Passport is a regional and small business jet engine scheduled to first see service in 2018 on the Bombardier Global 7000 [4]. Development of the Passport benefitted greatly from the technology of the CFM International LEAP family of engines. Based on its FAA engine certificate data sheet, the Passport has a BPR of 5.6:1, OPR of 45:1 and HPCPR of 23:1 [5]. Georgia Tech already has Generation 1 regional jet (RJ) model that was used, which has a HPCPR of 22:1 and OPR of 47:1. The HPCPR for the Passport was used as a basis for the Generation 2 RJ engine.

Generation 2 OPR & BPR Research

Research for Generation 2 engine cycles focused on the 2020 to 2030 timeframe. Both the Vision 10 and 20 from Rolls Royce's Future Programmes gave good insight into the progression of turbofan technology [6]. The Advance family is an engine architecture that would enter service after 2020. The Advance3 the larger three-shaft version seen as the next evolution for Rolls Royce from the Trent XWB, and as a stepping stone towards future geared turbofans. It was chosen to represent the Generation 2 engine for the LTA with a BPR and OPR of over 11:1 and 60:1 respectively. The Advance2 is the two-shaft member of the family that would service aircraft in the 150 passenger market, making it an appropriate representation for the STA and SSA-LSA Generation 2 engines. The Advance2 is targeted to have a HPCPR of 22:1 and a

similar BPR to the Advance3. Since the LTA baseline is modeled with a two-shaft engine this HPCPR was also used for the LTA Generation 2 engine cycle.

The Boeing 777X is currently under development with the 777-9 variant slated to hold 400-425 passengers making it a comparable basis for the LTA [7, 8]. The 777X will be powered by GE Aviation's GE9X, which is approximated to achieve a BPR of 10:1, HPCPR of 27:1, and OPR of 60:1. Entry into service for the Boeing 777X is targeted for late 2019.

For Generation 2 Regional Jets there was limited quantitative information to be found. Based on historical trends, progress for RJ type aircraft tended to trail behind the larger aircraft classes due to space limitations. With this in mind the GE Passport HPCPR was used, but OPR was increased to be on par with the Trent XWB and BPR was also made more aggressive.

Generation 3 OPR & BPR Research
Rolls Royce's Vision 20 again provided some guidance when looking at Generation 3 engine cycles. The intention of the Advance3 is to be an intermediate step to the three-shaft, geared UltraFan™, as noted in Reference [6]. The current figures for this engine are a bypass ratio greater than 15:1 and OPR greater 70:1, with an entry into service beyond 2025. This engine was viewed as most applicable to the LTA. A large theme in discussions on Generation 3 powerplants was the diminishing gains in efficiency from increasing BPR. Most papers were focused on the implementation of open rotors or even alternative powerplants to gas turbines entirely. Without sufficient information it was decided that the Generation 2 cycle parameters would be reused for the other aircraft.

Identifying Appropriate FPR & Cooling Variables
Since BPR was an output parameter of engine sizing, the next step was to adjust the FPR and cooling required by the HPT to get within the range of the BPR values found, using the OPR and HPCPR values that were identified. After the FPR was found LPCPR was determined by dividing the OPR by the product of FPR and HPCPR. The engine cycle parameters chosen for every vehicle for every vehicle are presented in Table 9. The infographics values for propulsive and thermal efficiency were updated using final vehicles for each generation, with all impacts applied as presented in Section 0.

TABLE 9. ENGINE CYCLE PARAMETERS CHOSEN FOR EACH VEHICLE CLASS FOR EVERY GENERATION.

FPR					
Generation	**RJ**	**SSA-LSA**	**STA**	**LTA**	**VLA**
0	1.629	1.685	1.643	1.58	1.758
1	1.55	1.58	1.54	1.58	1.55
2	1.55	1.58	1.54	1.58	1.55
3	1.55	1.58	1.54	1.28	1.55
OPR					
Generation	**RJ**	**SSA-LSA**	**STA**	**LTA**	**VLA**
0	38.51	30.55	30.63	39.89	28.43
1	47.41	40	40	52	52
2	50	60	60	60	60
3	50	60	60	70	60

Selecting Noise Suppression Factors (Greg)

Approach to Sensitivities

Resulting Noise Suppression Factors

Technology Roadmap Design of Experiments (DOE) Aggregator
In order to generate the DOE tables for EDS for any combination of impacts from different generations, an easy to use dashboard interface was created in Excel. Having a DOE Aggregator helped avoid any potential mistakes from manually creating the DOE tables. The DOE Aggregator was also flexible enough to allow new impact values to be input, allowing this process to be repeated in the future with new surveys. The dashboard was created without the use of macros in order to allow ease of transfer across different organizations and machines.

Overall Layout of Technology Roadmap DOE Aggregator
A diagram of the overall flow of data through the DOE Aggregator is provided in Figure 30. On the Scenario Input sheet each row was a case. The user defined what the case's Technology Level and Vehicle Class was and what the Technology Generation was for each Technology Area. This case information then flowed into the Aggregator sheet, which used the information to look up what the impact values were in the Impact Mapping Sheet. It also found the correct values of the absolute type EDS variables from the Chosen Factors sheet. Impacts were aggregated for each variable according to their variable type. They were then passed on to the Case Construction sheet. The correct baseline EDS values were grabbed from the Baselines sheet based on what Vehicle Class was given for the case in the Scenario Input sheet. The impacts were then applied to these baselines, according to their variable type, or were replaced entirely if they were absolute type variables. Finally, from the Case Construction sheet cases were filtered into their correct vehicle DOE sheet. The baseline values for the EDS variables that were not modified were taken from the Baselines sheet to complete each DOE.

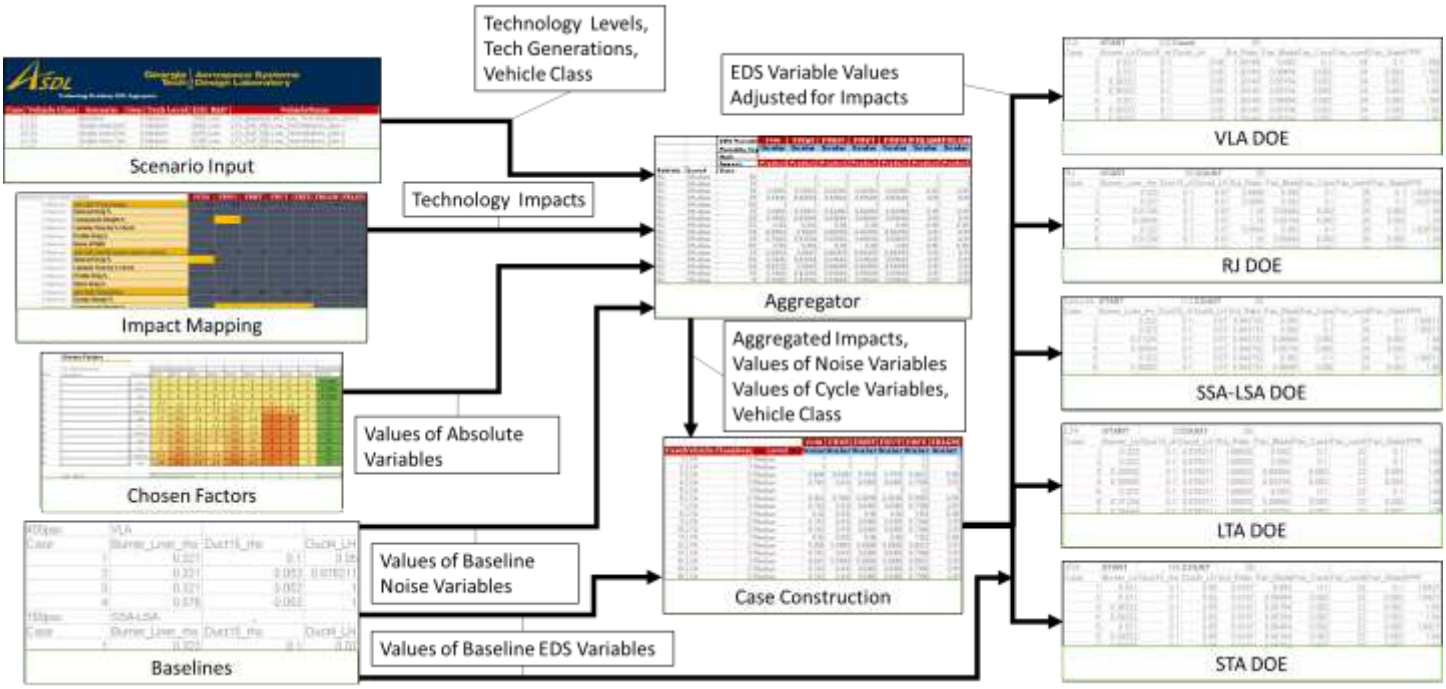

FIGURE 30. TECHNOLOGY ROADMAP DOE AGGREGATOR DATA FLOW

Scenario Input
The main interface was the Scenario Input sheet, as shown in Figure 31. Each row within the Scenario Input sheet defined a separate case. Cases were created based on the scenario timetables described in Section 0. The scenario timetables provided information specific to each vehicle class. The first column was simply the case number, which was used for

tracking purposes throughout the DOE Aggregator. The second column was where the user defined the Vehicle Class for each case, whether it was a VLA, RJ, SSA-LSA, LTA, or STA. The third column contained information on what scenario was being modeled, whether it was the baseline, twin-aisle vehicles entering the market first, or single-aisle vehicles entering the market first. This input did not affect DOE results, but was a reference to which scenario timetable the case was created from. Similarly, the fourth column, which gave the vehicle generation, was also a reference to the timetable. Vehicle generations ranged from 0 to 3. The fifth column was where the user defined the technology level. This referred to how great the technology's impact would turn out to be once it was fully developed. The user had the choice between Low, Medium, and High. Only a single overall technology level was chosen for each case and it effected what values are used from the Impact Mapping sheet. The entry-into-service (EIS) year for the vehicle was given the sixth column and was a reference from the scenario timetables. The seventh column was the R&D level, which can be Low, Medium, and High. R&D level was not used directly by the DOE Aggregator but was important when creating the cases, as described in Section 0. The technology generation for all 19 technology impact areas had to be defined in columns 9 through 27. These technology generations were chosen by the user based on the R&D level and "Years to TRL 9". This process is also described in Section 0. Note only three of the 19 impacts are shown Figure 31.


ASDL Georgia Tech Aerospace Systems Design Laboratory

Technology Roadmap DOE Aggregator

Case	Vehicle Class	Scenario	Gen	Tech Level	EIS	R&D	VehicleName	Aircraft Wing Design	Aircraft Aerodynamic Improvements	Aircraft Composites
1	LTA	Baseline	0	Medium	1995	Low	LTA_Baseline_RD-Low_Tech-Medium_Gen-0	0	0	0
2	LTA	Single-Aisle Firs	1	Medium	2020	Low	LTA_SAF_RD-Low_Tech-Medium_Gen-1	0	0	0
3	LTA	Single-Aisle Firs	2	Medium	2035	Low	LTA_SAF_RD-Low_Tech-Medium_Gen-2	2	2	2
4	LTA	Single-Aisle Firs	3	Medium	2100	Low	LTA_SAF_RD-Low_Tech-Medium_Gen-3	3	3	3
5	LTA	Twin-Aisle First	1	Medium	2020	Low	LTA_LAF_RD-Low_Tech-Medium_Gen-1	0	0	0
6	LTA	Twin-Aisle First	2	Medium	2030	Low	LTA_LAF_RD-Low_Tech-Medium_Gen-2	1	1	1
7	LTA	Twin-Aisle First	3	Medium	2045	Low	LTA_LAF_RD-Low_Tech-Medium_Gen-3	3	3	3
8	LTA	Single-Aisle Firs	1	Medium	2020	Medium	LTA_SAF_RD-Medium_Tech-Medium_Gen-1	1	0	0
9	LTA	Single-Aisle Firs	2	Medium	2035	Medium	LTA_SAF_RD-Medium_Tech-Medium_Gen-2	3	1	1

FIGURE 31. TECHNOLOGY ROADMAP DOE AGGREGATOR SCENARIO INPUT TAB

Impact Mapping

Impact Mapping was the sheet where the subcategories for all 19 vehicle impacts were mapped in a matrix to their appropriate EDS variables. Each subcategory had a value for all three generations for all three technology levels. The values of the subcategories, like Induced Drag % and Component Weight %, were summed in the rows labeled with the top-level impacts, like Aircraft Wing Design.

FIGURE 32. IMPACT MAPPING TAB IN TECHNOLOGY ROADMAP DOE AGGREGATOR

Aggregator

The Aggregator sheet was the first step in creating the DOE tables. Each row represented a case from the Scenario Input sheet. For each EDS variable identified, this sheet determined what impacts were related to it. For the subset of impacts related to the variable, the sheet then looked at the Scenario Input sheet to find what the Tech Level for the case was and what the generations were for the impacts in the subset. The sheet then looked at the Impact Mapping sheet for each

impact to find the value that was mapped to the EDS variable for that Technology level and Generation. The values for impacts in the subset were then combined based on what variable type the EDS variable was, as explained in Section 0 earlier.

An exception to that process was the EDS variables for the engine cycle related to thermal and propulsive efficiency. As discussed in Section 0, the values for FPR, Ext_Ratio, LPCPR, HPCPR, s_HPT_ChargeEff, and s_HPT_NonChargeEff were chosen based on a literature search on future engine cycles. Propulsive efficiency was a subcategory of Engine Propulsive and was largely a function of FPR and Ext_Ratio. Thermal Efficiency was a subcategory of Engine Core and was mainly a function of OPR (FPR, LPCPR, and HPCPR). Both were effected by s_HPT_ChargeEff, and s_HPT_NonChargeEff, which were related to the cooling required by the HPT. On the Scenario Input sheet the user had the option to choose different generations for Engine Propulsive and Engine Core. The mixing of engine cycle parameters from different generations though greatly increased the chance of the case failing. To account for this the Aggregator sheet used the lower of the generations between Engine Propulsive and Engine Core and the case's Technology Level and vehicle to look up the engine cycle parameters on the Chosen Factors sheet.

The EDS variables related to Engine Noise for the core, propulsor, and jet were also chosen like the values for the engine cycle, but were based entirely on a parametric study. Different generations were able to be entered for the core, propulsor, and jet engine noise without a problem. The Aggregator sheet then simply grabs the correct values from the Chosen Factors for the provided generation, vehicle and Technology Level. Combining noise variables was more involved than the other EDS variables. The Aggregator sheet had to determine the size order of the impacts, which included treating the baseline value as an impact. With the size order known the values were then combined following the rules in Table 8.

Case Construction
The Case Construction sheet first looked up the baseline value for the cases from the Baselines sheet based on what vehicle the case was using. The combined impacts from the Aggregator sheet were then taken and added to, multiplied by, or simply replaced the baseline value, depending on the EDS variable type. In the case of noise variables the baseline values were already needed by the Aggregator sheet when determining the new noise suppression factors, so these values were able to be put directly into place.

Baseline Vehicles
The Baselines sheet contained the baseline vehicles previously developed by Georgia Tech. For all five vehicle there were four cases. In all instances Case 1 was the baseline used since it represented a vehicle that entered into service in 1995. For future studies though the baseline could easily be transitioned to one of the other cases. The 1995 baseline for the RJ did not have a low pressure compressor (LPC), so the RJ Case 2 was modified to have values appropriate for a 1995 vehicle, but with a LPC. This modified case was then used as the RJ baseline moving forward.

Chosen Factors
The Chosen Factors sheet was where noise suppression factors, from the parametric study, and the engine cycle parameters, based on the literature review, were found. For a given generation and vehicle there was no difference in the engine cycle parameters for different Technology Levels, because there was not enough information found to base that differentiation on.

Vehicle DOEs
A design of experiments (DOE) table contained a row for each vehicle case and contained all the information that EDS needed to read in. Creating the DOE tables for each vehicle relied on all the cases for the same vehicle being together on the Scenario Input sheet. For each case the DOE sheet then went through all the EDS variables in the baseline EDS DOE table. If the EDS variable was one of the ones that had been modified, the DOE sheet obtained its new value from the Case Construction sheet. Otherwise it used the baseline value. Table 10 shows a subset of the final DOE sheet for the VLA, with only six of the over 300 EDS variables in a DOE shown. The "START" number 223 was the row in the Case Construction sheet where the VLA cases started, not the Scenario Input sheet case number. "Count" was the number of VLA cases counted in the Scenario Input sheet. The only manual step for the user was that the row formula had to be dragged down, or rows would be deleted so that the number of cases matched the "Count".

TABLE 10. SUBSET VIEW OF FINAL DOE TABLE FOR THE VLA FROM THE TECHNOLOGY ROADMAP DOE AGGREGATOR

VLA	START	223	Count	55		
Case	Burner_Liner_rho	Duct15_rho	Duct4_LH	Ext_Ratio	Fan_Blade_rho	Fan_Case_rho
1	0.321	0.1	0.05	1.30148	0.092	0.1
2	0.321	0.1	0.05	1.30148	0.08464	0.092
3	0.26322	0.1	0.05	1.30148	0.05704	0.062
4	0.26322	0.1	0.05	1.30148	0.05704	0.062

Using Technology Roadmap DOE Aggregator

In order to use the Technology Roadmap DOE Aggregator the most probable cases first had to be defined. Defining a case first involved assigning what scenario, vehicle class, and vehicle generation were being used. Using a vehicle replacement schedule the EIS year for the case vehicle could be determined. An R&D level was then chosen which, along with the "Year to TRL 9" data from the infographics, allowed the EIS year for the three generations of each technology area to be determined. The technology area EIS years were compared to the vehicle EIS year to identify what generation of each technology area were being used for that case. Finally, the case was assigned a technology level, which indicated how great the impacts of the technology areas would end up being. Cases were made for every combination of the two scenarios, five vehicle classes, three vehicle generations, three R&D levels, and three technology levels. Complete case definitions were inserted as a row in the Scenario Input sheet of the DOE Aggregator, which then created five DOEs separated into each vehicle class. These DOEs were then modeled using EDS.

Vehicle Timetable & Scenarios

With the capability provided by the Technology Roadmap DOE Aggregator over 800 billion different technology scenarios were able to be considered. To narrow down to the important ones first a replacement schedule was created. It identified the likely year for introduction of re-engined models, performance improvement packages, and new designs for each vehicle class from 2015 out to 2050. This replacement schedule was then used to assess what the entry into service (EIS) year would be for each vehicle class whether a twin-aisle or single-aisle vehicle was introduced first. The replacement schedule for the single-aisle first vehicle is shown in Figure 33 and the twin-aisle first vehicle is shown in Figure 34. For each of the 19 technology impact categories the "Years to TRL 9" was forecasted for the next three generations assuming a low, medium, or high R&D level, to get EIS dates for that technology. For a given R&D level, the EIS year of the generations for each vehicle was used to determine what the generation each technology impact would be on that vehicle based on the technology EIS years. Technology packages were made for all three vehicle generations for all five vehicles for all three R&D levels for both single-aisle and twin-aisle scenarios. This resulted in 90 cases. In addition, the surveys had provided the information to differentiate levels of technology effectiveness for each generation. Considering the three technology levels resulted in 180 cases worth investigating plus the 5 baselines if technology stayed frozen.

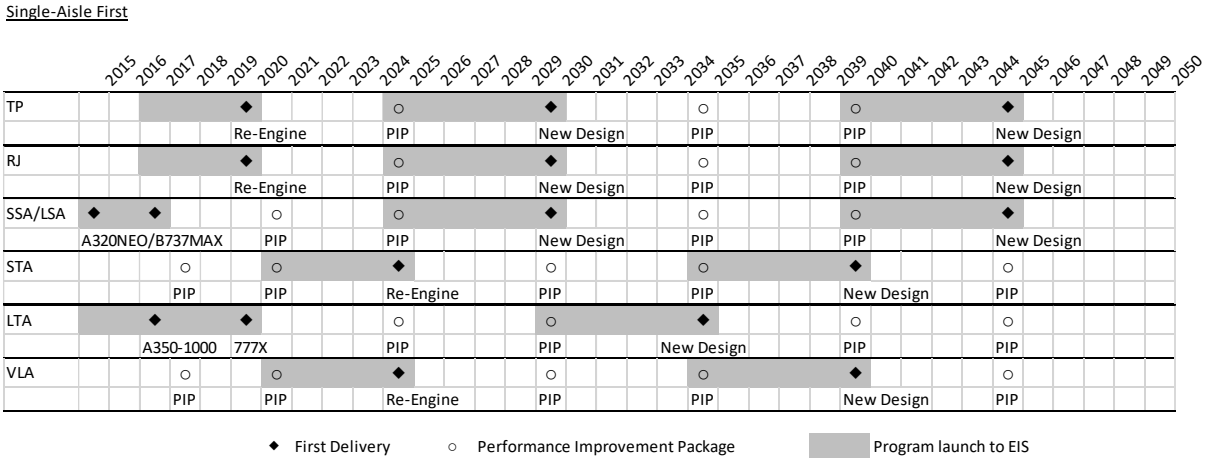

FIGURE 33. VEHICLE REPLACEMENT SCHEDULE FOR SINGLE-AISLE FIRST ASSUMPTION

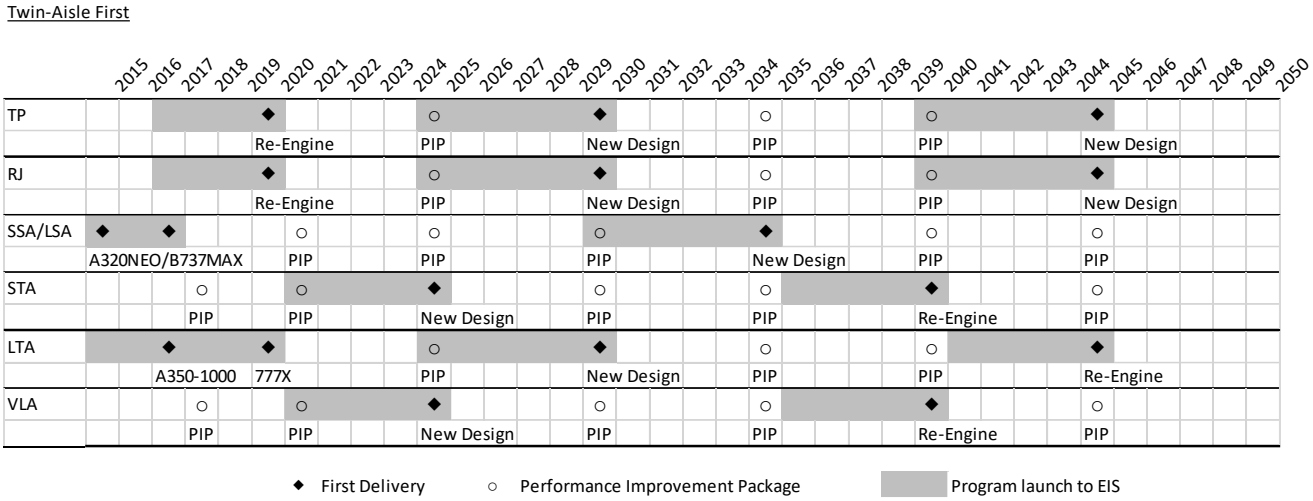

FIGURE 34. VEHICLE REPLACEMENT SCHEDULE FOR TWIN-AISLE FIRST ASSUMPTION

Vehicle Naming Convention & Identification

Each of the 185 cases was given a name based on its vehicle class, scenario, generation, technology level, and R&D level. The five vehicle size classes under investigation were the Regional Jet (RJ), Single-Aisle (SSA-LSA), and Small Twin Aisle (STA), Large Twin Aisle (LTA), and Very Large Aircraft (VLA). The passenger classes they corresponded to were 50, 150, 210, 300, and 400 passengers, respectively. Keep in mind when looking at the scenarios that the focus of using these five vehicles was on their passenger sizes, not their names. The scenario could be either the baseline, single-aisle first, or twin-aisle first. Single-aisle first and twin-aisle first were shortened to SAF and LAF in the vehicle name. Both the R&D and Tech Level were given intensities of either low, medium, or high. The final part of the name was what the vehicle generation was. This generation often varied from what the generation of technology impacts on the vehicle were. As an example, for a Generation 2 LTA, single-aisle first scenario, with a medium Tech Level and a high R&D Level, the vehicle name was LTA_SAF_RD-High_Tech-Medium_Gen-2.

Importing DOE Tables & Running EDS

Within the file-folder system for EDS were CSV files for each vehicle. The cases and heading were copied from the appropriate DOE sheets in the Technology Roadmap DOE Aggregator and then pasted as values into the CSV files. The 55 cases for each vehicle were then submitted to Condor, which was Georgia Tech's cluster computing network for running cases for different environments like EDS. A script was written to rename the AEDT files output by EDS to match the vehicle naming convention. These AEDT files were used for generating vehicle noise reports and also contained the information for moving forward to fleet level impact analysis. The script also placed the engine deck and flops files for each case in folders using the correct naming convention.

Vehicle Modeling Results

The main metrics from the vehicle results that were analyzed were fuel burn, emissions, and noise. Fuel burn was compared across vehicles by computing the percent reduction in the design block fuel relative to the appropriate baseline. Noise was compared by looking at the noise margin. Noise margin was the difference between the actual aircraft cumulative noise and the Stage 4 noise limit. For emissions only the reduction in nitric oxide relative to the CAEP/6 limit was compared. The CAEP/6 limit was given in terms of D_p/F_∞ which was the amount of grams of that emission, during the LTO-cycle, divided by the thrust rating of the engine. The CAEP/6 limit for an aircraft changed as a function of engine overall pressure ratio.

Fuel Burn

The fuel burn results for all the vehicles showed the trends that would be expected, with the same or greater fuel burn reduction as the generation and R&D level increased. The FLEET analysis made the assumption that all vehicles had at least a 15% improvement relative to their baseline vehicles. Any vehicles that did not meet this minimum improvement were modified to agree with this FLEET assumption. Figure 35 provides the final results for the Generation 1 vehicles assuming a

Single-Aisle First Scenario. Also overlaid on this bar graph were the high and low values for the NASA Subsonic Transport System Level Measures of Success. These were Near Term (2015-2025) desired technology benefits.

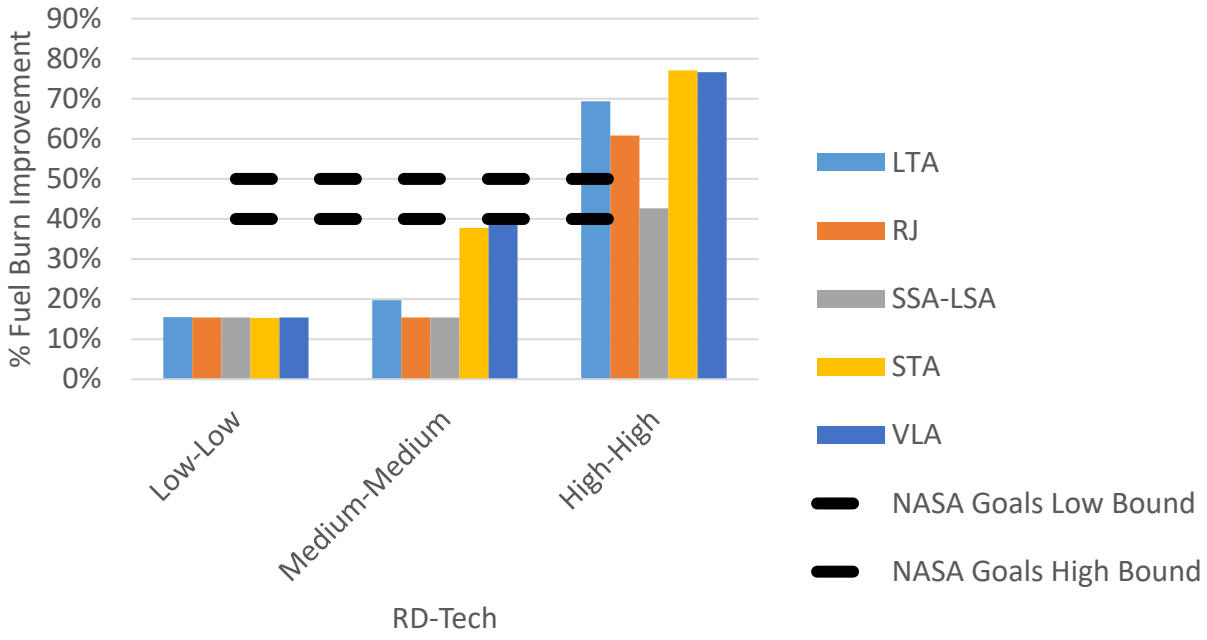

FIGURE 35. PERCENT REDUCTION IN FUEL BURN RELATIVE TO THE BASELINE FOR GENERATION 1 VEHICLES

1.1.1.1 Noise Margin

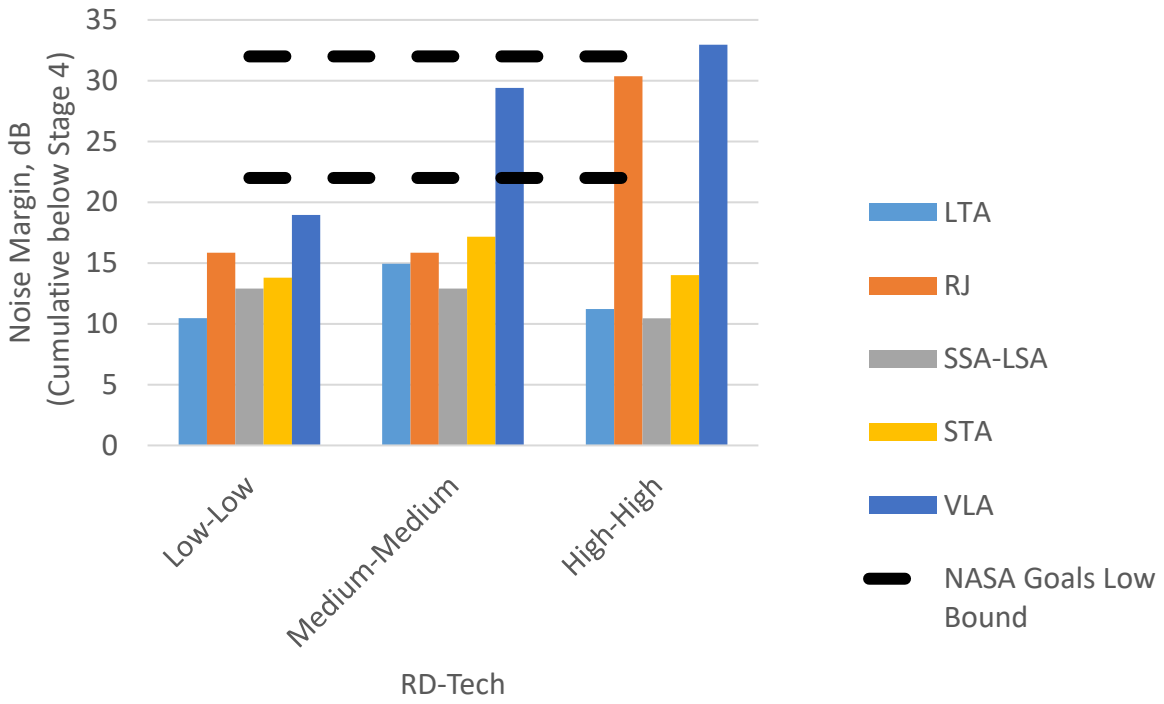

FIGURE 36. NOISE MARGIN RELATIVE TO STAGE 4 FOR GENERATION 1 VEHICLES

1.1.1.2 Nitric Oxide Emissions

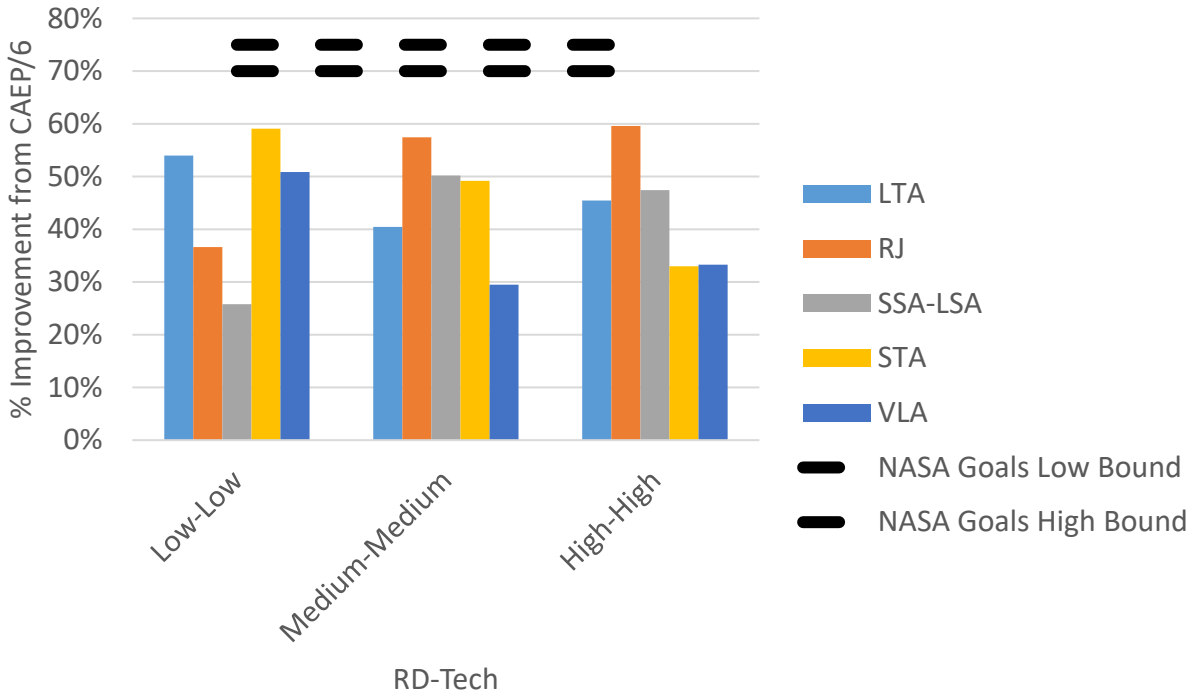

FIGURE 37. NITROUS OXIDE PERCENT IMPROVEMENT RELATIVE TO CAEP/6 FOR GENERATION 1 VEHICLES

Propulsive Efficiency

In order to update the propulsive efficiency improvement values on the Engine Propulsive infographic, a correlation between BPR and propulsive efficiency was used. The correlation was created by assuming a core velocity of 1660 ft/s and a flight speed of Mach 0.8 at 35,000 ft. It also assumed that, for that core velocity and a given BPR, the optimal jet velocity ratio to maximize propulsive efficiency was able to be achieved. Jet velocity ratio was the ratio between core velocity and bypass velocity. Propulsive efficiency could theoretically be derived as a relationship between bypass ratio, core jet velocity, freestream velocity, and velocity ratio, as given in Equation 1.

$$\eta_p = \frac{\left(u_c + BPR\left(\frac{u_c}{V_{ratio}}\right) - (1+BPR)u_o\right)u_o}{\left(\frac{u_c^2}{2}\right) + BPR\left[\left(\frac{1}{2}\right)\left(\frac{u_c^2}{V_{ratio}^2}\right)\right] - (1+BPR)\left(\frac{u_o^2}{2}\right)}$$

EQUATION 1

Using this relationship, and adjusting the jet velocity ratio to maximize propulsive efficiency, Figure 38 was created which plotted BPR against the theoretical peak propulsive efficiency. The BPR output by EDS for each case was used to determine what its propulsive efficiency would be based on this relation, assuming jet velocity was maximized. The propulsive efficiency for each case was compared to the propulsive efficiency for its respective 1995 baseline to determine what the percent improvement was. The low and high percent improvement values for each vehicle generation were found across all vehicle classes. The nominal values for each vehicle generation were then found as the average of the percent improvement values for that generation across all vehicle classes. The results were used to create the final Engine Propulsive infographic.

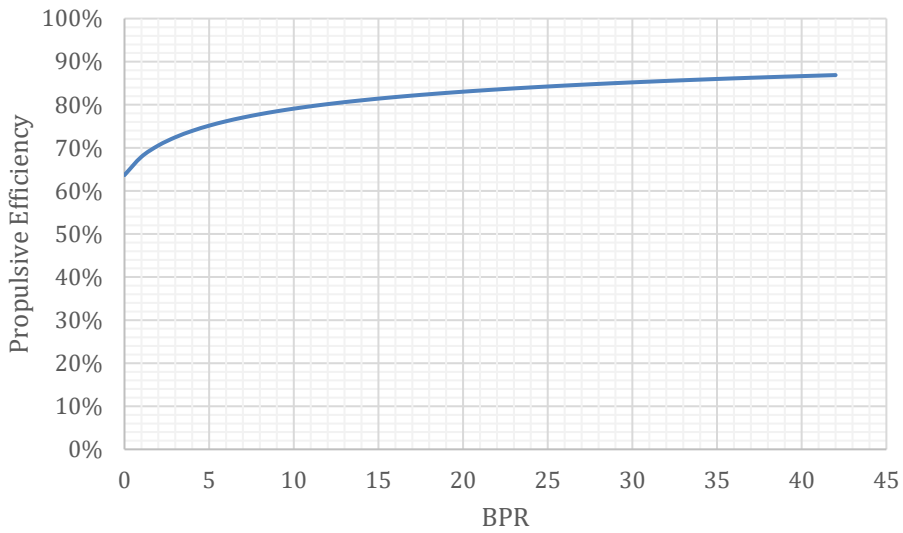

FIGURE 38. PLOT OF CORRELATION BETWEEN BPR AND PROPULSIVE EFFICIENCY

Thermal Efficiency

In order to update the thermal efficiency improvement values on the Engine Core infographic, Equation 2 was used which provides the theoretical thermal efficiency based on OPR and the heat capacity ratio. The thermal efficiency value was calculated for every case using an OPR that was the product of the HPCPR, LPCPR, and FPR values put into the DOE for that case. A heat capacity ratio of 1.4 was assumed. The thermal efficiency for each case was compared to the thermal efficiency for its appropriate 1995 baseline to determine what the percent improvement was. The minimum value for each vehicle generation was found as the lowest percent improvement for that vehicle generation, across all vehicle classes. Similarly, the maximum value was found as the highest value for that vehicle generation, across all vehicle classes. The nominal values were found by taking the average of thermal efficiency improvements for a given vehicle generation. These results were implemented in creating the final Engine Core infographic.

$$\eta_{thermal} = 1 - \frac{T_1}{T_2} = 1 - \frac{1}{OPR^{\frac{\gamma-1}{\gamma}}}$$

EQUATION 2

SUAVE Modeling of Public Domain EDS Technologies (Stanford)

Over the past few years, pressure to reduce the overall fuel consumption of the commercial aircraft fleet has been growing steadily. Expenses related to fuel are now one of the largest contributors to an airline's direct operating cost, even if the recent (2015-16) turn of events and global economic slowdown has substantially decreased the cost of fuel. As a result, many technological and operational changes are being considered to alleviate these issues. In this work, we begin to investigate the fuel burn impact of varying design mission specifications (e.g. payload, range, cruise Mach number, and allowable span) of tube-and-wing aircraft is studied. During the first two years of the effort, the Stanford team focused on aircraft and engine redesigns that consider the reduction of the aircraft cruise Mach number, but that leave all other mission requirements (cabin layout, range, payload, take-off and landing field lengths, etc.) unchanged. Representative aircraft from all ICAO (International Civil Aviation Organization) classes are chosen and redesigned for variations in the design cruise Mach number. The effects of improvements in aerodynamic, structural and propulsion technology expected over the next 20 years can also be taken into account in the context of technology scenarios for which the baseline aircraft could be redesigned. The work is done using a conceptual design environment developed at Stanford from scratch, the SUAVE environment, that represents all aspects of the design (including both the engine and the airframe) using an appropriate level of fidelity. Results from aircraft redesigns indicate that variations in design mission specifications for

existing technology aircraft can result in significant reductions in fuel burn that can be modeled using one of our team's fleet-level tools.

The following sections describe, in sequence, the improvements that the Stanford team has made to the capabilities and optimization framework in SUAVE under the sponsorship of ASCENT Project 10, the baseline vehicles for the various aircraft classes, the redesign process followed to come up with new vehicles that operate at reduced cruise Mach numbers, and a summary of preliminary / ongoing results that can be carried forward to fleet-level analyses.

SUAVE and Improvements to the Design Environment

At Stanford, we have devoted a considerable amount of effort to improve the SUAVE modelling characteristics (particularly in the off-design engine characteristics) and to create, test, and validate the optimization framework within SUAVE that enables the design of new aircraft capabilities with changed mission specifications. SUAVE is a conceptual level aircraft design environment that incorporates multiple information sources to analyze unconventional configurations. Developing the capability of producing credible conceptual level design conclusions for futuristic aircraft with advanced technologies is a primary directive for SUAVE. Many software tools for aircraft conceptual design rely upon empirical correlations and other handbook approximations. SUAVE proposes a way to design aircraft featuring advanced technologies by augmenting relevant correlations with physics-based methods.

SUAVE is constructed as a modular set of analysis tools written compactly and evaluated with minimal programming effort. Additional capabilities can be incorporated using extensible interfaces and prototyped with a top-level script. The flexibility of the environment allows the creation of arbitrary mission profiles, unconventional propulsion networks, and right-fidelity at right-time discipline analyses.

To date, SUAVE's analysis capabilities have been used to evaluate a wide variety of configurations including traditional commercial transports (of all sizes and speeds), as well as hybrid-electric commercial transports, supersonic vehicles, and even solar-electric unmanned aerial vehicles (UAVs) among others. Of particular interest to SUAVE is the capability to analyze advanced unconventional aircraft configurations, even if these are not the subject of the investigations in Project 10.

Previous work has shown SUAVE's capability to successfully analyze all these classes of aircraft. However, in order to understand the potential fuel burn reductions of redesigning aircraft with mission specification changes, SUAVE must be used to optimize such aerospace vehicles. During the course of Project 10 at Stanford University, we have conceptualized, developed, implemented, and tested a full optimization environment that works with all of SUAVE's analysis capabilities. In the context of optimization, SUAVE operates as a "black-box" function with multiple inputs and multiple outputs. Several convenient functions are provided to enable connecting the optimization packages to SUAVE more easily. Assuming an optimization algorithm is minimizing an objective subject to constraints by iteratively modifying input variables, SUAVE's code structure is general enough to be driven from a variety of optimization packages.

Several optimization studies have already been pursued. The primary example that has guided our development is the optimization of a Boeing 737-800 aircraft in multiple different scenarios. During the development and verification of the optimization framework, the Stanford team has also worked closely with colleagues at Embraer, who have also conducted their own verification studies (compared with their internal conceptual analysis tools) and who have ensured that the optimization problem formulations include all the necessary realistic constraints to be on par with typical industrial practice. Just as in the analysis capabilities, and beyond the canonical B737-800 problem, the optimization environment is being stress-tested with unconventional configurations on separate projects. The hope is that such additional tests will help our work in Project 10 to ensure that both the capabilities in SUAVE are as developed as possible, but that the robustness of the optimization procedures can allow for repeated redesigns in multiple different scenarios.

In the development of SUAVE, one of the major objectives was to build it flexible enough to interface with a multitude of different optimization packages. To adapt SUAVE to all the desired optimization programs, each optimization package must treat SUAVE as a "black-box" where the internal programs run cannot be modified. To formulate SUAVE as a black-box program, the engineer or scientist must specify what inputs need to be defined, how the inputs are connected to the vehicles and missions of interest, how vehicles and missions are connected, and what outputs are going to be returned. In addition, SUAVE allows design parameters, specified by the user, to map to their corresponding parameters inside the code. The general mathematical formulation can be written as a non-linear program:

$$\begin{aligned} \underset{\mathbf{x}}{\text{minimize}} \quad & f(\mathbf{x}) \\ \text{subject to} \quad & g_j(\mathbf{x}) = 0 \quad j \in \{1,...,l\} \\ & h_k(\mathbf{x}) < 0 \quad k \in \{1,...,m\} \\ & lb_i \leq x_i \leq ub_i, \; i \in \{1,...,n\} \\ & \mathbf{x} \in \mathbb{R}^n \end{aligned}$$

where **x** is a vector containing *n* design variables x_i, which are each bounded by lower and upper bounds lb_i and ub_i. The objective of interest is f(x), typically the fuel burn of the aircraft through an entire mission, including reserves. There are *l* equality constraints g(x) and *m* inequality constraints h(x), that must be satisfied by the re-designed aircraft. The design variables **x** are typically some subset of the inputs to SUAVE and wrapping functions are provided to enable translation between data dictionaries and design vectors.

When determining the inputs to SUAVE, the parts into which the inputs can be broken are: vehicle inputs, mission inputs, vehicle-mission connections, procedure, and variable setup. By determining what inputs are specified and what missions are performed, the engineer will define what type of problem is being analyzed. Part of the code inputs would be the design variables of interest, but others are just the information required to setup SUAVE to run the analyses.

Vehicle: Within the vehicle inputs, the designer must first choose what type or types of configurations SUAVE will study. Does the designer want to optimize a single aisle aircraft for a 1,000 nmi mission or a family of transoceanic aircraft sharing a common wing where one carries 300 passengers, one carries 350 passengers, and a third aircraft carries 425 passengers? Depending on the type of optimization desired, SUAVE needs to be configured to generate those results. Part of the code inputs is determining what fidelity level or levels will be used to analyze the configurations. A CFD code could have different inputs than a vortex lattice code or even handbook methods. Making sure the necessary data is provided to SUAVE for the desired analyses is the user's responsibility.

Mission: Beyond just looking at different vehicles over the same mission, we'd like for SUAVE to be able to run the same aircraft through different missions. Instead of optimizing the single aisle aircraft for a 1,000 nmi mission and not considering other missions, we could optimize over a 1,000 nmi mission, but add a constraint that the maximum range of the aircraft be 2,500 nmi. Just as we had to specify what parameters would define each vehicle, we must build the missions from the different segments available. For example, in the work the Stanford team has done in Project 10, we have ensured that the proper amount of reserve fuel is used. The reserve fuel is calculated by ensuring that the vehicle can fly a separate "reserve" mission at the end of the traditional mission.

Vehicle-Mission Connections: Once the vehicles and the missions the vehicles need to fly have been constructed, the connection between vehicles and missions needs to be specified. This can be done by creating different configurations of the same vehicle, maybe for takeoff and landing, where flaps are deployed, vehicle geometry has been modified, or specifying that only the 300 passenger aircraft will fly 8,200 nmi. This step tells SUAVE have aircraft-1 run missions 1, 2, 3 while aircraft-2 only does missions 1 and 3. It also specifies what results SUAVE will generate when the analysis is completed.

Procedure: The analysis of the problem requires a set of sequential actions to be performed. This is the procedure. A great example of this would be to resize the horizontal tail of the aircraft after a new wing area is selected by the optimization algorithm to keep the horizontal tail volume constant. Additionally, the types of missions are then set here such as a long-range mission and short field takeoff missions. Finally the constraints and objectives that require additional non-standard calculations can be performed as part of the procedure. An example of the non-standard constraints are fuel margins, which is fuel volume available in the vehicle minus the fuel used to run the mission.

Variable Setup: The optimization interface provides a concise way to define several important features of the optimization problem. Including variable names (or tags), the initial guess of the variable, the lower and upper bounds, how it should be scaled to yield favorable numerics within the optimizer, and finally its units. Using the information provided in a tabular structure like the one shown below, accepting input vectors becomes much simpler, enabling SUAVE to pattern across multiple optimization packages.

```
# [ tag , initial, [lb,ub], scaling, units ]
problem.inputs = [
    [ 'aspect_ratio'   ,  10.    , (   5.    ,   20.   ) ,   10. ,    Units.less],
    [ 'reference_area' , 125.    , (  70.    ,  200.   ) ,  125. , Units.meter**2],
    [ 'sweep'          ,  25.    , (   0.    ,   60.   ) ,   25. ,  Units.degrees],
    [ 'design_thrust'  , 24000.  , ( 10000.  , 35000.  ) , 24000. ,  Units.newton],
    [ 'wing_thickness' ,   0.11  , (   0.07  ,   0.20 ) ,     .11,    Units.less],
    [ 'MTOW'           , 79000.  , ( 60000.  ,100000.  ) , 79000. ,      Units.kg],
    [ 'MZFW'           , 59250.  , ( 30000.  ,100000.  ) , 59250. ,    Units.less],
]
```

Figure 39. Sample description of optimization problem design variables , bounds and units

Furthermore, within SUAVE we allow the design variable to be defined in any user preferred name and then "alias" it to the internal data structure name. For example, *aspect_ratio* above would be an alias of **problem.vehicle.wings.main_wing.aspect_ratio**. SUAVE uses a very verbose methodology, but if the engineer would like to use a different set of variable names, the functionality is in place. Outputs to be used for the objective function, constraints, and output characteristics of interest can also be defined in the same manner. This flexible naming convention also allows multiple parameters inside of SUAVE to be varied as one design variable in the optimization process. This capability reduces the number of variables and constraints since there are no longer multiple variables with constraints requiring that they be equal.

Code Outputs: After all the code inputs have been provided, and the desired vehicle characteristics, mission profiles, vehicle-mission connections and the SUAVE analysis structure are generated, results are produced. Not all of the code outputs are relevant to the optimization of interest. The code outputs might need to be post-processed to generate the actual result we care about for our problem. If we are trying to meet Stage 4 Noise levels, we care only about generating a cumulative total of 10 dB, not a matching certain levels at each condition. The objective function and constraints should be a subset of the final code outputs produced. Once these parameters have been generated, they can be fed to the optimization package for design studies to be completed.

Optimization

With a general interface in place, SUAVE can be incorporated into optimization packages. The flexibility of SUAVE and Python allow optimization with a variety of packages and algorithms. Throughout this section, a variety of optimization packages integrated with SUAVE, as well as various algorithms within these packages that have been applied to various design problems, are discussed.

VyPy: VyPy is a toolbox developed at the Stanford Aerospace Design Lab that exposes useful abstractions for optimization in the context of engineering. Similar to the concept from PyOpt, and serving as an inspiration for the SUAVE data structure, the top level interface is an optimization formulation, with variables, objectives and constraints. Unique to VyPy, these inputs can be defined in a tabular format or in an object oriented format. The problem is then run through a driver or several drivers that each implements an optimization algorithm. At the moment, interfaces for the following algorithms exist: SLSQP, BFGS, COBYLA, and CMA. The interfaces of these drivers have been expanded to permit consistent setup (for example by standardizing the name of common parameters and variable scaling) and consistent data output (like the presentation of the minimized objective and location). Another unique feature is that it handles data based on dictionaries instead of functions, which are especially useful in an engineering context where inputs and outputs are intuitively described with names instead of vector components.

PyOpt: PyOpt is a Python package containing a variety of nonlinear optimizers. The Sparse Nonlinear Optimizer (SNOPT) module, which relies on a Sequential Linear Programming algorithm and quasi-Newton methods, has been used within SUAVE for multiple optimization problems. The Sequence Least Squares Programming (SLSQP) algorithm, which is another quasi-Newton method, has also been used.

There are several more optimization algorithms in the PyOpt package, and all of them can be implemented easily in SUAVE by creating a base interface and attaching them to available SUAVE functions. The exact structure of the interface will depend on the chosen optimization algorithm and can be created based on existing PyOpt documentation.

Dakota: When determining what to expose to outside software and what to only use within SUAVE, Dakota (Design Analysis Kit for Optimization and Terascale Applications) guided this formulation. Dakota is an object-oriented framework developed by Sandia National Laboratories. Designed to work with high performance computers, Dakota together with SUAVE can expand the types of optimization aircraft designers' attempt. Dakota is constructed to connect easily with other "black-box" functions. The user defines the inputs Dakota can change and what results to expect just as the user in SUAVE specifies an input vehicle dictionary and creates an output data set with all the results of the analysis.

Dakota has both gradient and non-gradient based optimization capabilities. Some of the optimization algorithms available in Dakota include, Hasofer-Lind Rackwitz-Fissler (HL-RF), sequential quadratic programming (SQP) from NPSOL, and nonlinear interior-point (NIP) from OPT++.

In addition to optimization capabilities, Dakota combines stochastic expansion methods (such as Stochastic Collocation (SC) and Polynomial Chaos Expansion (PCE)), surrogate models, and Optimization Under Uncertainty (OUU) algorithms to expand the types of problems SUAVE can consider. These methods allow stochastic aircraft defining parameters to be considered as part of the optimization and vehicle analysis. Having the flexibility to deal with uncertainty in certain parameters gives designers the ability to see how certain parameter distributions will propagate through to the final vehicle. With this functionality, Dakota will not only be used as an optimization driver, but also as a tool to trade how certain design inputs can impact the final optimum aircraft.

SciPy: SUAVE is also capable of interfacing with SciPy. In this case, design variables must be inputted via a Python list. SciPy then calls a function designed to return an objective value, which unpacks the variables and interfaces it to a problem set up in SUAVE. Constraints may be handled by either the optimization algorithm, in which case they must be defined in the inputs file, or they must be handled by penalty functions included in the callable SUAVE file. The SciPy optimization package as of the time of writing includes a wide variety of optimization algorithms, including a Nelder-Mead simplex algorithm, SLSQP, and conjugate gradient methods, among others. However, the interface requirements, as well as handling of constraints vary from algorithm to algorithm. As a result, it is up to the user to appropriately ensure that the problem is well formulated.

Baseline to GT Vehicles

To capture the effect of the mission specification changes on the fleet wide fuel burn and emissions, aircraft from all the aircraft classes need to be modelled. For this study the CRJ900 is chosen for the Regional Jet, the B737-800 for the Single Aisle, the B767-300ER for the Small Twin Aisle, the B777-200ER for the Large Twin Aisle and the B747-400 for the very large aircraft. The baseline aircraft were modelled using SUAVE.

The baseline aircraft modelled in SUAVE were compared with the baseline aircraft modelled by GT. The geometric and propulsion parameters of the aircraft as well as the performance estimates including fuelburn, design and sea level static thrust are matched to ensure that the fuel burn of the redesigned aircraft computed using SUAVE can be modelled by GT using percentage changes. The fuel burn for a design mission provided by GT and offdesign missions are compared. It was observed the baseline fuel burn and the fuel burn variation with mission range match fairly well for the aircraft modelled by GT and Stanford for all but the B747-400. The level of agreement is within the expected differences that would be seen in similar analysis and conceptual design tools. This discrepancy will be investigated in detail and for the time being this aircraft is not redesigned for mission specification changes.

Mission Specification Change Modeling

The next step in this effort is the redesign of the baseline aircraft for mission specification changes. In this effort the Stanford team investigated the effect of cruise Mach reduction i.e. the baseline aircraft are redesigned for a reduced cruise Mach number. This results in aircraft that are significantly more fuel efficient than the baseline aircraft.

The aircraft redesign is posed as an optimization problem with the fuel burn for a design mission minimized for a lower cruise Mach number. For this study the optimization framework is made up of SUAVE linked up with a gradient based optimizer, SNOPT via PYOPT a python based optimization framework. The design variables and constraints used for this problem are shown below. The design variables used consist of the geometric parameters of the aircraft wing and the engine pressure and bypass ratios as well as the design thrust (which determines the engine size). The cruise altitude of the aircraft is also used as design parameter.

DESIGN VARIABLES:

- Main wing aspect ratio

- Main wing reference area
- Main wing sweep
- Main wing thickness to chord ratio
- Main wing taper
- Main wing root and tip twist
- Engine design thrust
- Low pressure compressor pressure ratio
- High pressure compressor pressure ratio
- Fan pressure ratio
- Bypass ratio
- Cruise altitude

The constraints used for this study are mainly feasibility constraints, a positivity constraint on the fuel burn, constraining the fuel margin (difference in the TOW and the sum of the OEW, payload and mission and reserves fuel) to be zero to ensure a feasible mission, a constraint on the wing span to match the baseline aircraft's span and constraining the takeoff field length, the pressure ratio at the combustor inlet and the fan diameter to be less than equal to the values on the baseline aircraft. These constraints ensure that the sizing/redesign of the aircraft is realistic and the aircraft is feasible.

CONSTRAINTS:

- Takeoff field length
- Fuelburn (positivity)
- Fuel balance : TOW – (OEW+payload+reserves+fuel burn)
- Wing span
- Combustor inlet pressure ratio
- Fan diameter

The reductions in the fuel burn for the 3 aircraft mentioned above is due to the fact that, as the cruise Mach number is reduced, the compressibility drag of the configuration is also reduced. This allows the wing to be unswept and the thickness to chord ratio of the wing increased, which can be seen in Table 5 where data for the B777-200ER is shown. In turn, this reduces the wing weight resulting in a reduction in induced drag. Thus the thrust requirements for the missions are much smaller. The consequence is a reduction in the design thrust of the aircraft resulting in smaller engine sizes. This allows the engines component pressure ratios and the bypass ratio to be changed while meeting the pressure ratio and the maximum allowable fan diameter constraints, and results in more efficient engines and thus further reduced fuel burn for the aircraft.

Table 11 : B737-800 fuel burn

Mno	Fuel burn (kg)
Baseline	16,616
0.76	12,417
0.72	12,587

Table 12 : CRJ-900 FUEL BURN

Mno	Fuel burn (kg)
Baseline	22,013
0.76	19,174
0.72	20,434

Table 13 : B767-300ER

Mno	Fuel burn
Baseline	69,067
0.76	69,331
0.72	70,939

Table 14 : B777-200ER FUELBURN AND DESIGN PARAMETERS VARIATION

AR	Sref (m2)	Sweep (deg)	Design Thrust(N)	t/c	MTOW(kg)	taper	lpc Pressure ratio	hpc pressure ratio	fan pressur e ratio	bypass ratio
8.6	427	31	73,000	0.1	66,280	0.182	1.26	20	1.58	8.2
8.8	418	26	40,000	0.13	57,760	0.1	1.46	21	1.62	7.2
8.6	426	19.43	40,000	0.13	57,940	0.1	1.5	21	1.51	8.64

Updates for work performed during year 2

Updates to Propulsion Analysis Module

It was observed that the initial results obtained from SUAVE did not match very well the baseline aircraft provided by Georgia Tech for some of the aircraft. The differences in the performance estimates were traced down to small but significant differences in the computation of the drag and the propulsion performance. The aerodynamic analysis routines were modified, especially the prediction of compressibility drag and induced drag, to be more accurate representations of the actual aircraft geometries.

The existing engine model in SUAVE, while predicting accurately the design performance of the turbofan engines, were seen to inaccurately predict the off-design performance of the engine (especially at very low Mach numbers). In order to fix the issue, two new turbofan analysis models were created and integrated into SUAVE.

The first propulsion model was an extension of the existing engine model in SUAVE. A more detailed off-design performance analysis module was implemented. This model used compressor and fan performance maps and Netwon (or damped Newton) iterations to converge the off-design mass flow residuals at the different engine positions. The engine performance estimates were then compared with data provided by Georgia tech and showed reasonable agreement (as shown in Figure 44).

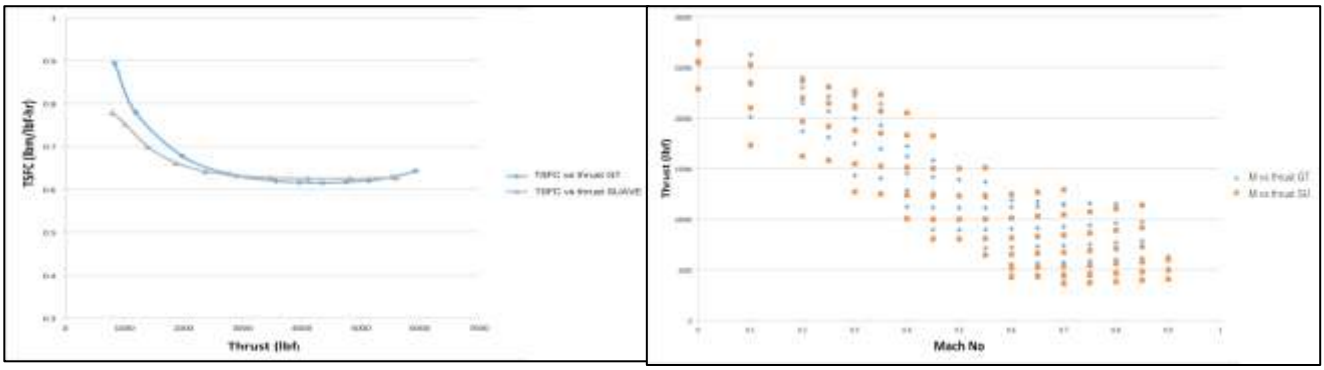

FIGURE 40 : COMPARISON OF OFF-DESIGN PROPULSION PERFORMANCE

A second engine model was created in order to interface with the EDS engine decks provided by GT. The engine deck provided contained the thrust, ram drag, specific fuel consumption and fuel flow rate for a set of Mach numbers, altitudes and throttle settings. The engine model reads in the engine deck. The parameters are stored as a database and interpolation models are created for thrust, ram drag and fuel flow rate with respect to the Mach number, altitude and the throttle setting. This ensures that when queried by the mission solver at different conditions, the engine model can provide performance estimates at conditions not specified in the deck by interpolating between the values.

Mission Specification Change Modeling

Once the updates to the propulsion model and the predictions of the baseline aircraft using the updated models were validated, the cruise Mach reduction cases were re-run.

Effect of cruise Mach reduction

As expected, redesigning the existing aircraft for reduced cruise Mach numbers resulted in low Mach variants that were more fuel efficient than the existing models. Figure 41 shows the percentage reduction in fuel burn for the baseline technology scenario for all five aircraft classes. It is observed that the percentage reduction in fuel burn is significantly larger (more than 10%) in the larger payload range aircraft (the B777 and B747). The smaller aircraft also show a reduction in fuel burn as cruise Mach number is reduced but the reduction are smaller in magnitude (closer to 5%). Some of the interesting design trends observed during this study are shown in Figure 42. We see that the redesigned aircraft in all 5 aircraft classes exhibit similar trends. The redesigned aircraft have a lower wing reference area compared to the baseline aircraft. This results in a reduction in wing weight and lower wing drag (parasite) contributing to the improvement in mission performance. The wings are also de-swept as the cruise Mach number is reduced until, for some cases, the lower bound of 5 degrees is met. Similarly the average thickness to chord ratio of the wings increases at lower cruise Mach numbers. These changes are permitted by the reduced effect of compressibility drag at lower cruise Mach numbers. The de-sweeping and increase in wing thickness results in a further reduction in wing weight. The reduction in wing weight and reduced fuel burn due to lower drag results in a reduction in the overall MTOW. This implies a reduction in the required lift and thus a reduction in the lift induced drag. A combination of the effect s described above result in the redesigned reduced Mach variants becoming much more efficient than the baseline (Mach) aircraft.

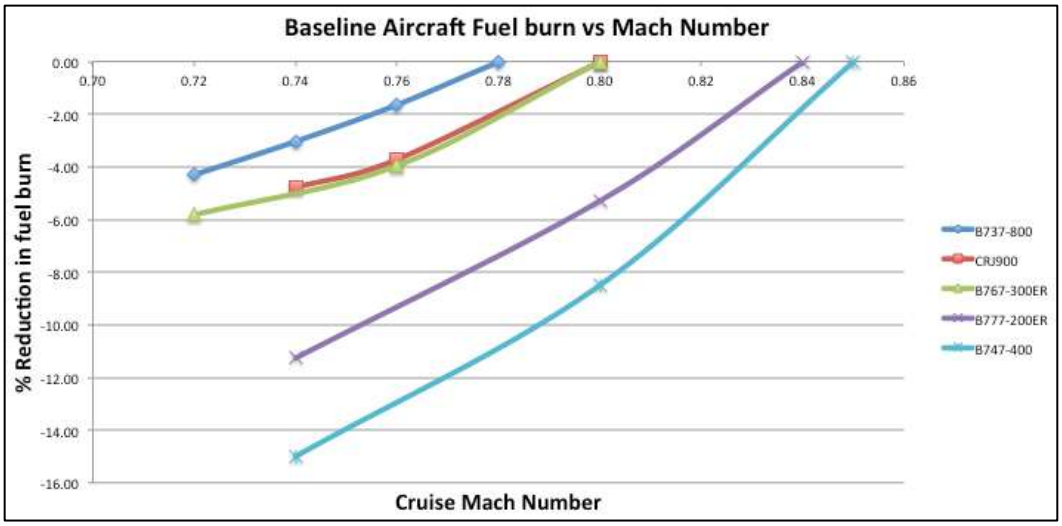

FIGURE 41: REDUCTION IN FUEL BURN WITH CRUISE MACH REDUCTION FOR ALL FIVE AIRCRAFT CLASSES FOR BASELINE TECHNOLOGY LEVELS

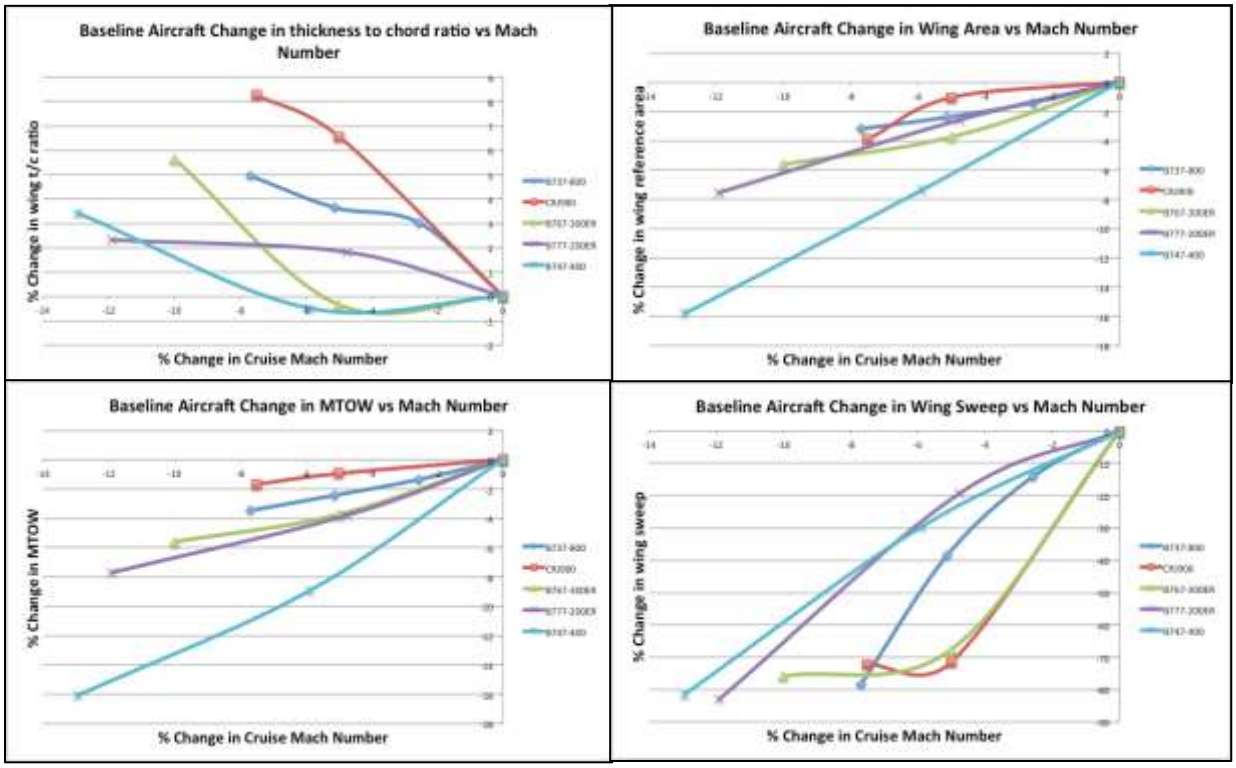

FIGURE 42 : CHANGE IN DESIGN VARIABLES WITH CRUISE MACH REDUCTION

Effect of Technology Variants

The results shown above were for the baseline technology scenario. However it is also important to study how cruise Mach reduction affects the higher technology variants. For this the technological baselines were modelled in SUAVE based on the corresponding EDS models provided by Georgia Tech. Then these aircraft were redesigned for reduced cruise Mach numbers. Figure 43 shows the effect of cruise Mach reduction on the fuel burn of the technology variants of the 5 aircraft classes for the baseline and two improved technology levels. For the higher technology derivatives, the results shown are with respect to the baseline Mach number at the corresponding technology level to isolate the effect of cruise Mach reduction. It is observed that for all 5 aircraft classes, cruise Mach reduction at the higher technology levels is as effective as the for the baseline technology levels.

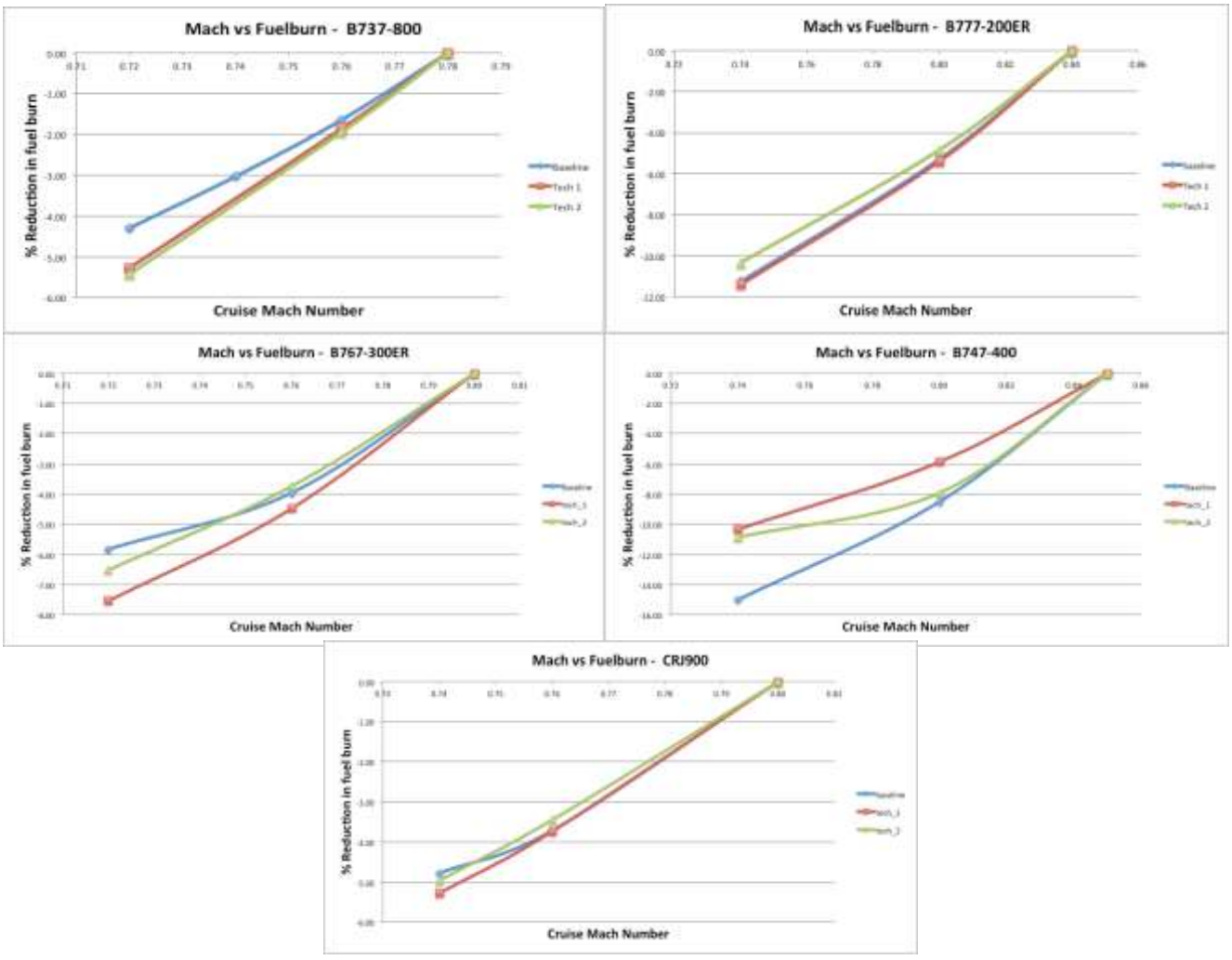

FIGURE 43 : EFFECT OF CRUISE MACH REDUCTION ON TECHNOLOGY VARIANTS

Off-design Performance over a mission

All the percentage reduction values shown above were for the design mission. However, once the aircraft (baseline and higher technology for all 5 classes) were re-designed for cruise Mach reduction, in order for Georgia Tech and Purdue teams to perform, fleet level analysis, the re-designed aircraft were flown for a set of off-design mission. The performance (fuel burn) of the aircraft for the off-design missions was compared to the performance of the baseline aircraft also flown for the same off-design missions. The results obtained are shown in Figure 44. Except for the second technology scenario for the CRJ900 (CRJ900 tech 2), most the other results show similar trends. The results in general indicate that at ranges significantly lower than the design range, the percentage reductions in fuel burn are not as high as at the higher ranges. However overall, the redesigned aircraft are more fuel efficient than the baseline aircraft for all the off-design missions. For the CRJ900 Tech 2 scenario also the redesigned aircraft are more fuel efficient for the off-design missions than the baseline aircraft. The percentage reductions however are different from the other aircraft and from the baseline and the Tech 1 scenario of the CRJ900 too. We are looking into this case in more detail to understand the reason for this behavior.

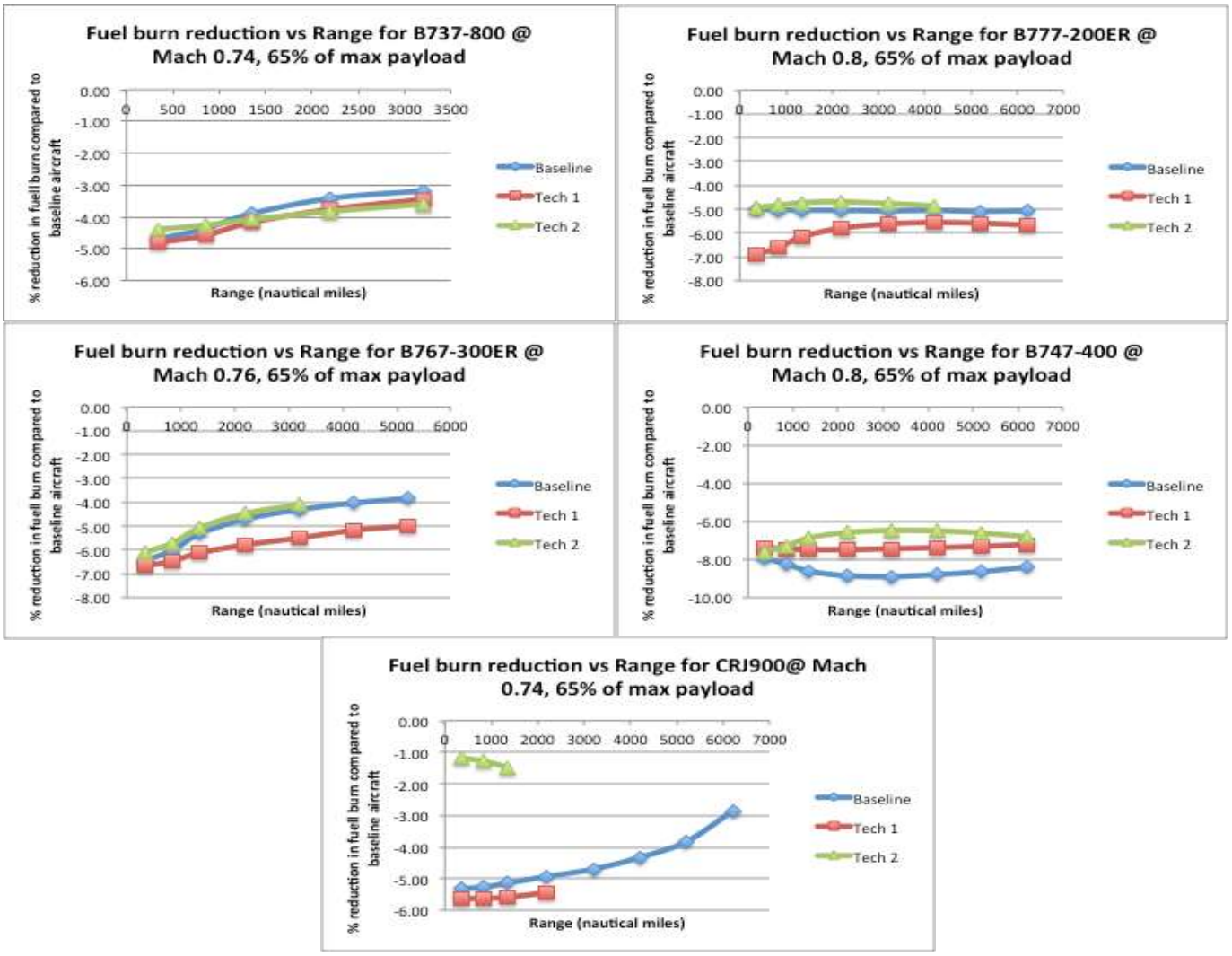

FIGURE 44 : OFFDESIGN PERFORMANCE COMPARISON WRT BASELINES

All of the results discussed in this section were compiled into the form of a series of improvement factors (multiplicative factors) that could be applied directly to the existing baseline aircraft models in GT's EDS and GREAT tools. Similar comments can be made about the FLEET tool used at Purdue. Using these performance factors for particular aircraft, flown distance, and payload, the actual fuel burn of the reduced cruise Mach number aircraft can be quantified. These fuel burn reductions can then be factored into the fleet-level calculations for the various scenarios that Project 10 is contemplating.

Milestones

Three major milestones were set for this task for Georgia Tech. First variables in EDS, the vehicle modeling environment used by Georgia Tech, had to be identified that could be changed to model the impacts from the Technology Roadmapping Workshop. Identifying and doing sensitivity testing on the majority of variables was completed by March 2016. Identifying EDS variable values for more difficult impacts, such as propulsive efficiency, was completed by July 2016. The second milestone was completing the Technology Roadmap DOE Aggregator. The Aggregator was built in Excel to automate the process of creating the inputs into EDS for all the future aircraft scenarios that were chosen to be modeled. The Aggregator was completed in July 2016. The final milestone was running the chosen vehicle scenarios, reviewing, and then compiling the results to be passed onto other project participants for the fleet analysis described in Task 3. This milestone was reached by mid-August 2016. All these milestones were met in accordance with the timeline that was projected following the 2015 Annual Report.

Major Accomplishments

The overall major accomplishment for this task was developing a variety of aircraft models for future scenarios for five different aircraft vehicle classes. Completing this task was pivotal to the progression of the project. These aircraft models are the basis for the fleet analysis performed by both Georgia Tech and Purdue University. As a result, they have a major impact on the findings of this project. Another major accomplishment was developing the process to move from the Technology Roadmapping Survey results to sizing and synthesizing aircraft and engine models. A logical set of steps had been hypothesized at the beginning of the project, but they were never carried out until this past year. As was described in the Research Approach in Section 0, a number of roadblocks were found along the way. In the end a way was found around them and the goals of the task were accomplished. Perhaps just as importantly, a sound process that can be followed in the future developed.

Task 3: Fleet Level Aircraft Technology Benefits Assessment

Georgia Institute of Technology, Purdue University

Objective: Fleet Level Technology Assessment

The fleet level aircraft technology benefit assessment at Georgia Tech will be performed using GREAT/ANGIM, which was developed at Georgia Tech for the purpose of the FAA seeking to complement the Aviation Environmental Design Tool (AEDT) with a lower fidelity screening tool capability that will allow for consideration of a large number of policy scenarios that could be quickly analyzed and reduced to a manageable set of scenarios for more focused, high fidelity analysis in AEDT. Georgia Tech has developed the Global and Regional Environmental Aviation Tradeoff (GREAT) tool, which provides a quick means of quantifying the impact of new technologies applied at the aircraft level to assess fleet-wide interdependencies on fuel burn and emissions. Noise and noise exposure are calculated through the Airport Noise Grid Interpolation Method (ANGIM). Designed to assess the system-wide impacts resulting from the implementation of vehicle-level technology improvements, the GREAT tool synthesizes forecasted operational activity growth, fleet composition evolution, and aircraft-level performance estimates to project fleet-level fuel burn and emissions over time. With its efficient computational algorithm, GREAT can be executed in batch mode to explore multiple scenarios and produce visualizations that highlight the relative contributions of various subsets of the fleet. ANGIM was developed in parallel with GREAT to enable rapid calculation of airport-level DNL contours. By leveraging SAE-AIR-1845 standards to pre-calculate a repository of single-event aircraft grids, ANGIM efficiently pairs airport flight schedules and runway layouts to rapidly produce airport-level DNL decibel grids with runtimes on the order of seconds per airport. Users can plot any contour level desired and measure contour areas and shapes. Population exposure counts can be quickly estimated by overlaying these DNL grids on airport-level population grids derived from 2010 Census-block data using a proportional area-weighted scheme. Recent research efforts have paired ANGIM with GREAT's schedule forecasting to produce similar visualizations of changes in contour areas and population exposure over time. Both GREAT and ANGIM are designed to accept EDS project aircraft as inputs. Both tools maintain flexibility to accept aircraft designs from other vehicle-level design tools as well, provided they adhere to established standards such as those presented in SAE-AIR-1845 and BADA documentation.

Research Approach

FLEET Sample Case (Purdue)

FLEET Overview

The Fleet-Level Environmental Evaluation Tool (FLEET) is a computational simulation tool developed to assess how aviation's fleet-level environmental impacts – in the form of CO_2, NO_x emissions and noise – evolve over time. Central to FLEET is an aircraft allocation model that represents airline operations and decision-making. Additionally, the tool has a system dynamics-inspired approach that mimics the economics of airline operations, models the airlines' decisions regarding retirement and acquisition of aircraft, and represents passenger demand growth in response to economic conditions. The overarching objective of FLEET is to enable an understanding of how variation in external factors such as market conditions, policy implementation, and technology availability will affect aviation environmental impacts into the future. The objective in exercising FLEET in this project period was to inform FAA and its partners about the workings of FLEET, its unique inputs and outputs, and a demonstration of its ability to compute estimates of emissions based on fleet level and technology scenarios [9,10,11,12,13,14,15,16].

While several studies exist that investigate either the environmental impact of aviation or the problem of aircraft allocation, these studies do not incorporate a simultaneous assessment of environmental impacts of aviation along with modeling of airline operations and an evolution of passenger demand and airline fleet mix and technology level. FLEET provides the ability to assess the impact of future aircraft concepts and technologies on fleet-wide environmental metrics while also considering economics and operational decisions of airlines and policy implementation. It goes beyond the aircraft-specific technological improvements, and its results reflect relationships between emissions, market demand, ticket prices, and aircraft fleet composition over a period of many years. Given the complexity of studying the aviation industry and the increasing importance being given to its environmental impact, the capabilities provided by FLEET, it is hoped, would help all stakeholders make informed decisions.

FLEET can be used for simulating a number of scenarios defined by setting values for various input parameters. FLEET groups available aircraft in four technology age categories:

1. Representative-in-class aircraft are the most flown aircraft in 2005 (base year for FLEET)
2. Best-in-class aircraft are the ones with most recent entry-in-service dates in 2005
3. New-in-class aircraft are either aircraft currently under development that will enter service in the future or concept aircraft that incorporate technology improvements expected in the future
4. Future-in-class aircraft are those aircraft expected to include another generation of technology improvements and therefore expected to enter in service a date further in the future

The aircraft within each technology age category further subdivide into six classes, based upon notional or typical seat capacity.

Description of Inherent Demand Model

The market demand model in FLEET is driven by economic growth in each continent and tries to represent two assumptions. First, a higher income per capita results in higher market demand, and second, there is an upper bound for number of trips per person because everyone has only 24 hours per day.

Based on the historical data from Airbus Company, which include trips per capita and GDP per capita in several countries, the model used hyperbolic tangent function to fit the historical data because of two reasons. The hyperbolic tangent function is analytic, and it asymptotically approaches an upper bound. Figure 45 shows the raw data and curve fitting results.

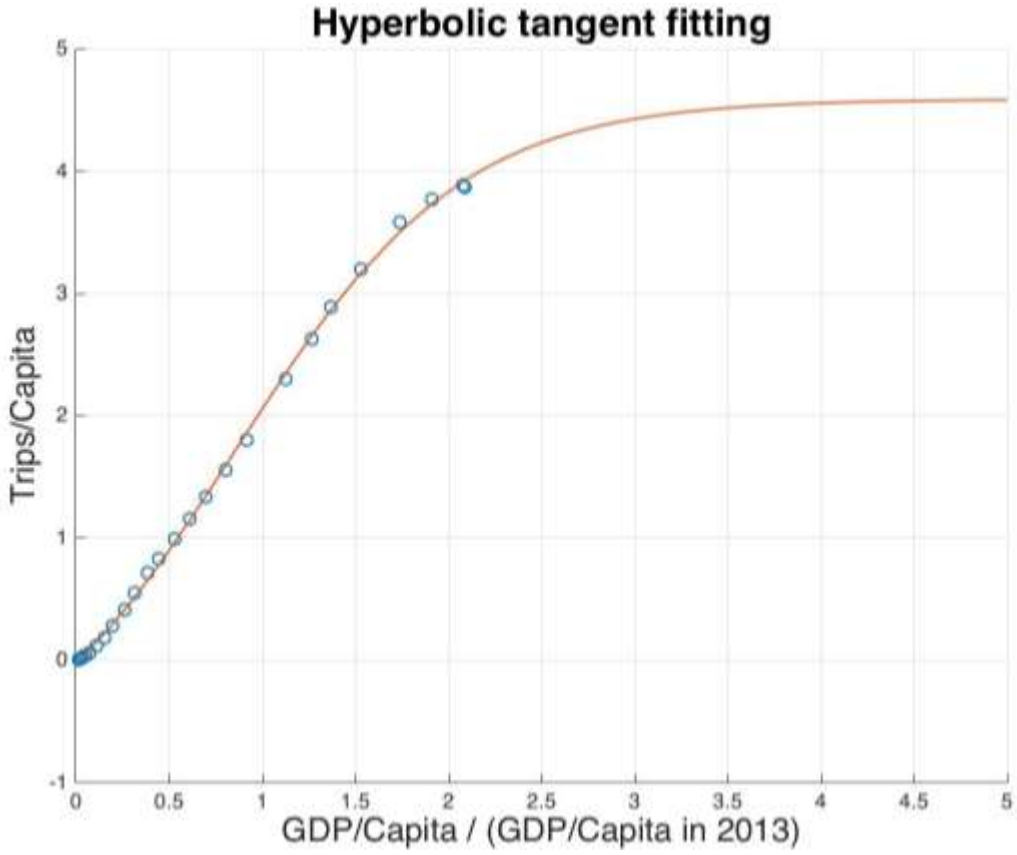

FIGURE 45: TRIPS PER CAPTIA, GDP PER CAPTIA AND CURVE-FITTING RESULT

Then, the demand growth rate in each continent in year n can be represented in Equation 3.

$$Dem_G^n = \frac{f'(GDP_C^n)GDP_C^n}{f(GDP_C^n)} \times \frac{GDP_G^n - Pop_G^n}{Pop_G^n + 1} + Pop_G^n$$

EQUATION 3

Dem_G^n shows the demand growth rate in year n, while $f(GDP_C^n)$ and $f'(GDP_C^n)$ represent the curve-fitting function and its first derivative, respectively. GDP_c^n and GDP_G^n show GDP per capita and GDP growth rate, while Pop_G^n represent population growth rate. Finally, the model used the GDP and the population in each continent in 2005 from World Bank as initial settings. And, according to the GDP growth rate and population growth rate historical data and predictions, it tracks the demand for each continent from 2005 to 2050 simulation year.

Description of exercised scenario setups

In the second project year, Purdue exercised FLEET with seven scenarios which were identified together with the ASCENT 10 Project partners. This activity also serves to identify enhancements necessary in FLEET to accommodate simulation of all the scenarios to be examined under ASCENT-10. The seven scenarios examined are:

A. Current Trends Frozen Technology
B. Current Trends Best Guess
C. Current Trends with High R&D

D. High Demand with High R&D
E. High Demand with Low R&D
F. Low Demand with High R&D
G. Low Demand with Low R&D

The "Current Trend Frozen Technology" scenario setup in FLEET is defined as follows:

- A network of 169 airports including U.S. domestic routes and international routes that either begin or end in the U.S.
- The annual gross domestic product (GDP) grows at a constant value of 4.3% in Asia, 4.2% in Latin America, 2.4% in Europe, and 2.8% for airports in the United States.
- The annual population growth rate at a constant value of 1.1% in Asia, 1.26% in Latin America, 0% in Europe, and 0.58% for the United States[17].
- Jet fuel prices grow according to the Energy Information Administration (EIA) reference fuel price case [17] and adjusted it to meet the ASCENT survey fuel price, $77/bbl, by 2050.
- Only the Representative-In-Class and Best-in-Class aircraft from Table 13 are included in the simulation. Aircraft from the Best-in-Class are produced until 2050. No New-in-Class or Future-in-Class aircraft are included in this scenario.

Table 15: Aircraft used in Simulation Studies

Aircraft Types in Study				
	Representative-in-Class	Best-in-Class	New-in-Class	Future-in-Class
SRJ	Canadair RJ200/RJ440	Embraer ERJ145		
RJ	Canadair RJ700	Canadair RJ900	GT Gen1 DD RJ (2020)	GT Gen2 DD RJ (2030)
SA	Boeing 737-300	Boeing 737-700	GT Gen1 DD SA (2017)	GT Gen2 DD SA (2035)
STA	Boeing 757-200	Boeing 737-800	GT Gen1 DD STA (2025)	GT Gen2 DD STA (2040)
LTA	Boeing 767-300ER	Airbus A330-200	GT Gen1 DD LTA (2020)	GT Gen2 DD LTA (2030)
LQ	Boeing 747-400	Boeing 777-200LR	GT Gen1 DD LQ (2025)	GT Gen2 DD LQ (2040)

In **Table 15**, the aircraft labeled as "GT Gen1 DD" are the Generation 1 aircraft modeled by Georgia Tech with a 'Direct Drive' engine. The 2nd Generation aircraft are labeled as "GT Gen2 DD". These include aircraft that belong to the following classes - regional jet (RJ), the single aisle (SA), the small twin aisle (STA), the large twin aisle (LTA), and the large quad (LQ). Based on the amount and speed of technology incorporated into aircraft, in each of the scenarios, the New-in-Class and Best-in-Class aircraft(in Table 13) models will vary.

The 'Current Trends Best Guess' and 'Current Trends with High R&D' scenarios, in addition to the 'Current Trend Frozen Technology' scenario setup, also incorporate the New-in-Class and Future-in-Class aircraft into their fleet mix. The High R&D case has higher speed and amount of technology investments accounted for in their aircraft development than the Best Guess case.

The 'High Demand with High R&D' and 'High Demand with Low R&D' scenarios assume a constant annual GDP growth rate of 5.9% for airports in Asia, 5.3% for airprots in Latin Ameirca, 4.2% for airports in Europe, and 4.0% for airports in America. The high R&D and low R&D case accounts for the rate of change and amount of investments in technology.

The 'Low Demand with High R&D' and 'Low Demand with Low R&D' scenarios use a constant annual GDP growth rate of 3.3% of airports in Asia 2.7% for airports in Latin America, 0.6% for airports in Europe, and 1.8% for airports in the United States.

Description of Results of the Scenario Runs with FLEET

The remainder of this section describes Purdue's representation of the "ASCENT 10 Project" scenario simulations using FLEET with the seven scenario setups aforementioned. The EIS dates of the Current Trend and High R&D and the corresponding aircraft modeled represents the GDP growth rate and EIS date setups for the other two scenarios. The purpose of the analysis is not to compare the quality of FLEET vs. Global and Regional Environmental Aviation Tradeoff (GREAT), but to understand the difference in results for the same scenario so the FAA can benefit from the different approaches to this difficult forecasting problem.

Figure 46 shows the normalized demand satisfied values for the results from simulations using the FLEET. Clearly, the demand increases to as much as 3.25 times the 2005 value by 2050. The passenger demand uses historical data for the years 2005 through 2014. After 2014, passenger demand changes as a function of two factors: the demand change due to economic factors, referred to as the "inherent demand growth", and the demand change due to passenger response to changes in ticket prices charged by the airlines, referred to as the "price-demand elasticity".

As mentioned earlier, in the current simulation, the GDP growth (inherent demand growth) is the major contributor to the total passenger demand growth (defined by the GDP growth rate evolution discussed in Section).

Table 16: Percent GDP Growth rates for each continent segregated by demand scenarios

Scenarios	North America	South America	Europe	Africa	Asia	Oceania
Current Trend	2.8%	4.2%	2.4%	2.8%	4.3%	2.8%
Low Demand	1.8%	2.7%	0.6%	1.8%	3.3%	1.8%
High Demand	4.0%	5.3%	4.2%	4.0%	5.9%	4.0%

Table 16 shows the percent GDP growth rate, for each continent and demand scenario in 2013, used to determine the evolution of the passenger demand growth rate throughout the simulation period. The initial population growth rates for all demand scenarios in 2013 were set to 0.58%, 1.26%, 0%, 2.6%, 1.10%, 1.10% for North America, South America, Europe, Africa, Asia, and Oceania respectively. Results from Current Trend Best Guess and Current Trend High R&D indicate that the normalized demand increases by a factor of 2.8 by 2050. In Low Demand scenarios, results show the normalized passenger demand in 2050 is about 2.5 times larger than the passenger demand by 2005. In High Demand scenarios, the passenger demand in 2005 increases by a factor of about 3.25 by 2050. The results reveal that GDP growth rate has a positive correlation with normalized passenger demand.

Both demand and CO_2 emissions values normalized to their respective 2005 values, and the normalization factors are the same for every scenario because in 2005 every scenario is identical in its setup. Results from the Current Trend Best Guess scenario and Low Demand Low R&D suggest that CO_2 emissions from US-related airline operations would increase by a factor of about 1.5 from their 2005 level by the year 2050, whereas results from the Low Demand High R&D and Current Trend High R&D scenarios suggest a decrease in CO_2 emissions by a factor of 0.65 and 0.95 respectively by 2050 (Figure 46). The CO_2 emissions for the High Demand High R&D, Current Trend Frozen Tech, and High Demand Low R&D increase by a factor of 1.08, 2.41, and 2.49 respectively by 2050. The GDP growth rates have a positive correlation with CO_2 emissions while R&D levels have a negative correlation with CO_2 emissions, as evidenced by the High Demand Low R&D and Low Demand High R&D scenarios. The technology improvements for airline fleets can reduce emission growths. Moreover, the lower demand can further decrease the number of aircraft operations and reduce emissions even further.

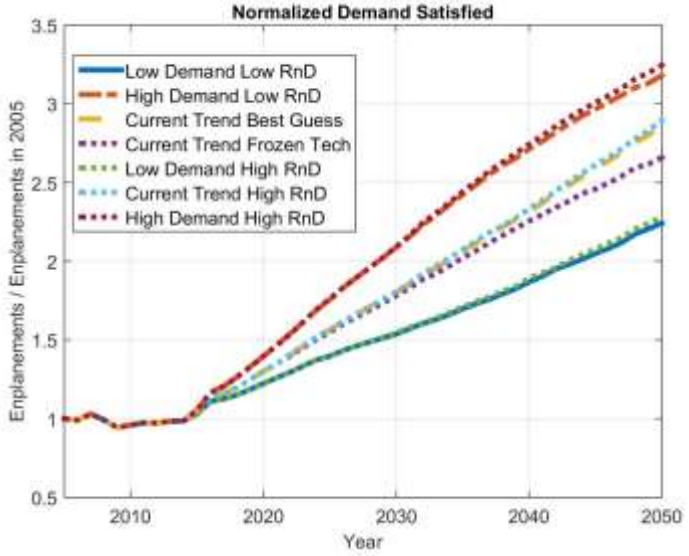

Figure 46: Normalized demand growth from 2005 to 2050

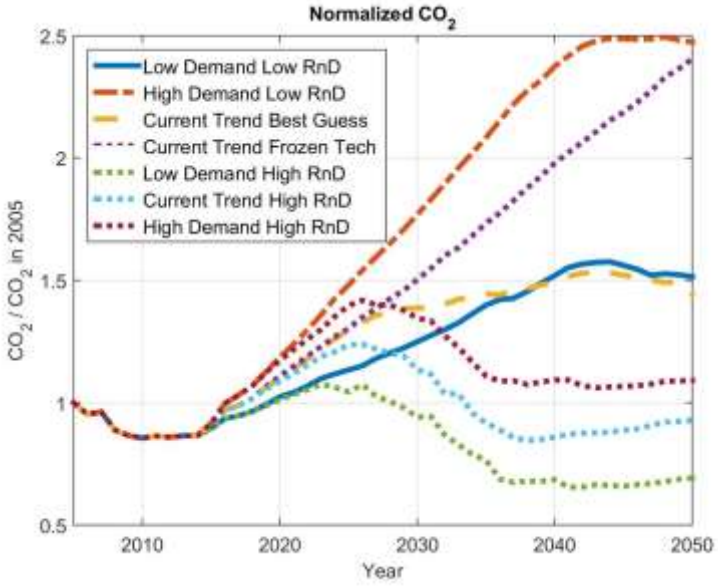

Figure 47: Normalized fleet-level emissions from 2005 to 2050

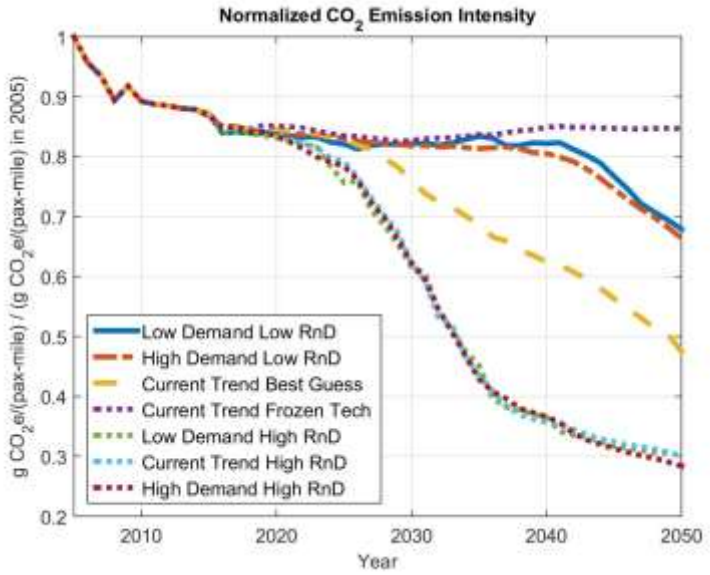

Figure 48: Normalized Fleet-level CO_2 Emission Intensity from 2005 to 2050

Figure 48 shows the CO_2 emission intensity (measured as CO_2 emission per passenger miles), normalized by the 2005 value, for all seven scenarios throughout the simulation period. The Current Trend High R&D and High Demand High R&D scenarios have the lowest emission intensities of 0.30 and 0.29 respectively by 2050. This suggests that the emission intensities in both scenarios reduced to 30% and 29% of their values in 2005 by 2050. The emission intensities in the Current Trend Buest Guess, High Demand Low R&D, and Low Demand High R&D scenarios reduced to 49%, 68.5%, and 69% of their respective values in 2005 by 2050. The Current Trend Frozen Tech scenario has the highest emission intensity of 0.85 times the value in 2005 by 2050. The evolution of the CO_2 emission intensities for all scenarios during the simulation period is dependent on the combined effect of variations in passenger demand and fleet utilization on the FLEET route network. Despite the decrease in emission intensities throughout the simulation, which indicates that the airline is operating more fuel efficient aircraft, the overall fleet-level emissions show an increasing trend due to the overwhelming demand growth in every scenario.

Figure 49 and **Figure 50** show the deployed fleet by aircraft class and type respectively, normalized by the values in 2005, for all seven scenarios in the FLEET study. Notably, the FLEET airline begins to operate a higher fraction of "GT N+2" Single Aisle (SA) future-in-class aircraft as this becomes available. Because this very efficient aircraft offer better economic returns and the retirements of representative and best-in-class class 1 aircraft create the demand for aircraft to satisfy the passenger demand, this leads to an "up-gauging" of the fleet on shorter routes. Furthermore, the airline flies very few trips using class 5 aircraft, primarily due to the class 6 Large Quad (LQ) aircraft, which has a capacity of 430 passengers, serving the relatively few long-range high-demand routes in the FLEET route network.

From **Figure 50**, for the High Demand scenarios (higher GDP growth rates in every continent), the number of aircraft deployed from 2005 to 2050 increases by a much larger multiple (as high as 2.75) than the number of aircraft deployed in Low Demand scenarios (factor of 1.5) over the same time period. From **Figure 48**, the significant change in CO_2 emission intensity trend slopes around the mid 2020s and 2030s in High R&D scenarios corresponds to the availability of New-in-Class and Future-in-Class aircraft. Additionally, the relatively constant trend in CO_2 emission intensity in the Current Trend Frozen Tech scenario after 2020 is primarily due to the lack of next-gen aircraft.

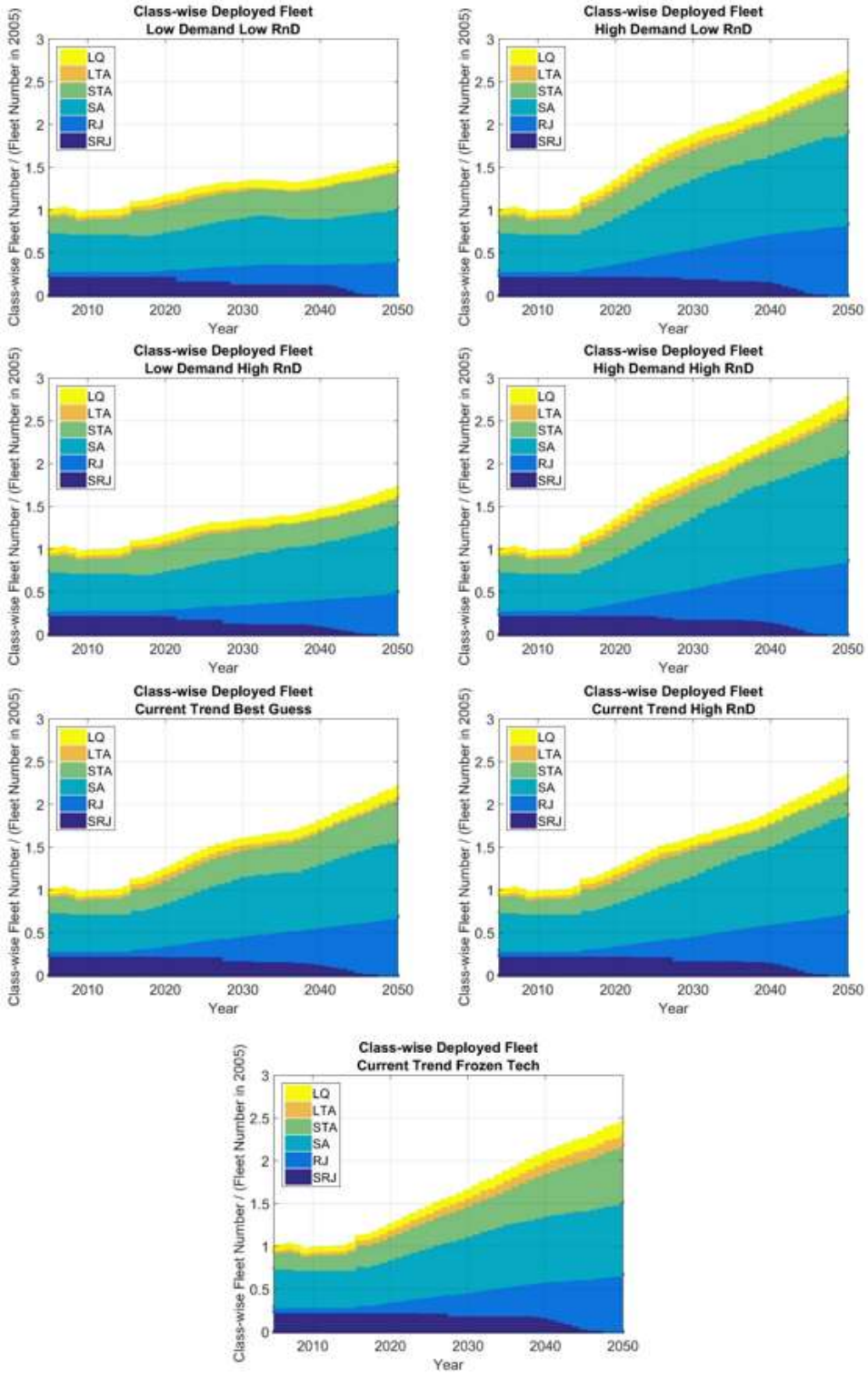

Figure 49: Normalized Deployed fleet by aircraft class (FLEET Run)

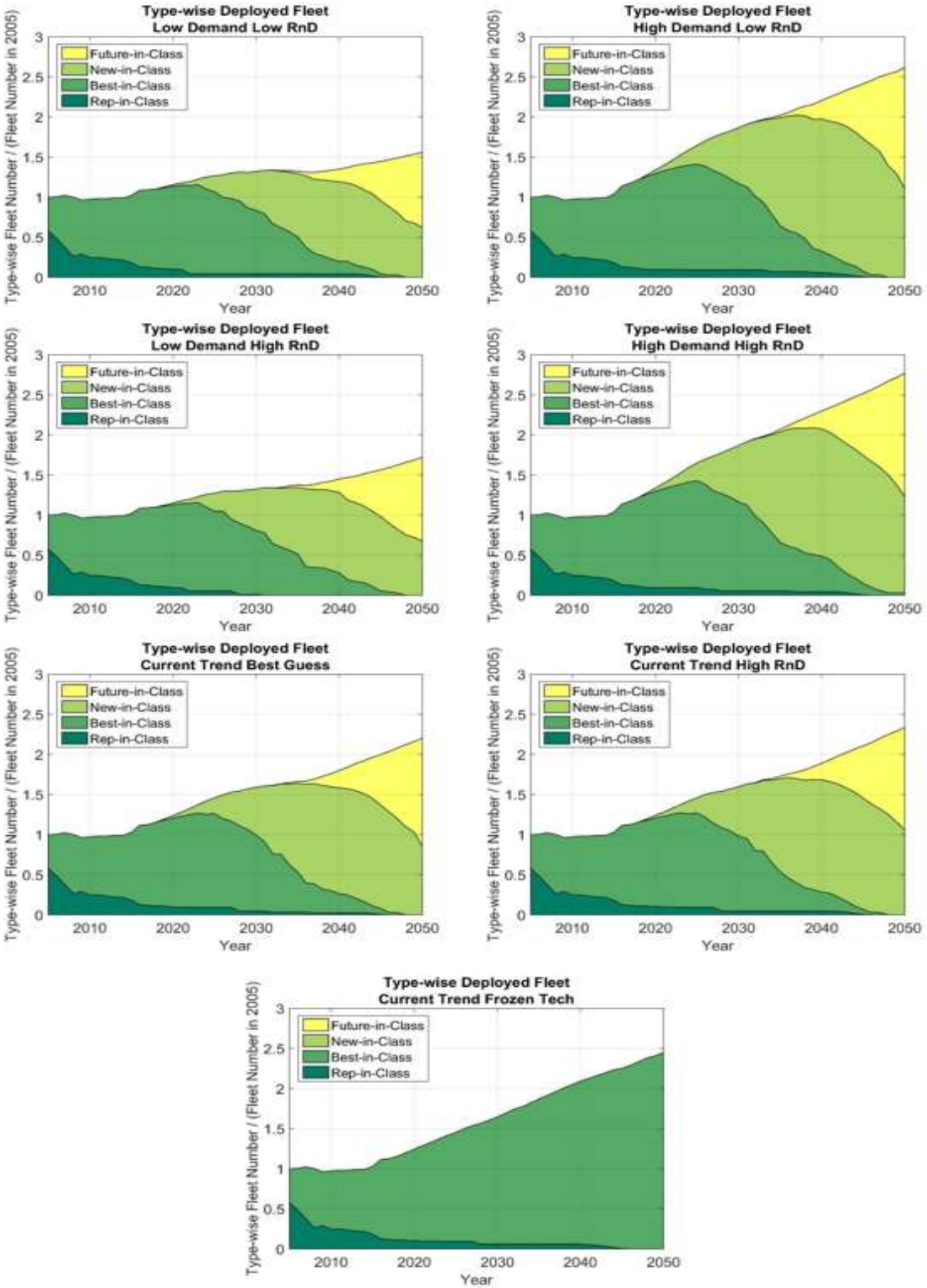

Figure 50: Normalized Deployed fleet by aircraft type (FLEET Run)

Comparison of aircraft types reveals that the airline retains some older aircraft for a longer duration; for instance, **Figure 50** shows that there are some representative-in-class aircraft still operating past 2040 and some best-in-class aircraft operating until 2050. **Figure 50** also shows a 10% - 25% larger fraction of future-in-class aircraft in the High R&D scenarios fleet when compared to Current Trends Best Guess Scenario. In Low Demand scenarios, the demand for aircraft to satisfy the increasing passenger demand is lower than Current Trend scenarios. Hence, airlines can acquire enough "newer" aircraft to replace their old generation aircraft, which results in a shorter fleet turn-over duration.

In summary, the Purdue team successfully demonstrated FLEET's capabilities for analyzing the scenarios developed by the ASCENT 10 Project partners. Current work involves resolving some of the remaining inconsistencies in scenario modeling assumptions and resulting metrics between FLEET and GREAT. The demonstrations in the past two years have shown that FLEET is capable of modeling scenarios developed by ASCENT 10 Project partners and provides some unique features that benefit the FAA in tackling challenging fleet-level emissions forecasting problems.

Mission Specification Trades (Stanford)

During this first portion of Project 10, the group at Stanford University has focused on (a) the development of the necessary analysis and optimization capabilities within the SUAVE framework, (b) the development and validation (with publicly-available data) of model vehicles in each of the five ICAO/CAEP aircraft classes, and (c) a preliminary study of the fuel-burn-reduction opportunities afforded by decreases in cruise Mach number when re-designing (including airframe and engine) these aircraft. The intent is to transfer the improved vehicles to the GT team, so that they can insert such vehicles in the fleet-level analyses done with GREAT. The Stanford team has also supported the team's activities for the preparation and conduct of both the fleet-level and technology workshops.

Publications

T. W. Lukaczyk, A. D. Wendorff, M. Colonno, E. Botero, T. D. Economon, J. J. Alonso, T. H. Orra, and C, Ilario, "SUAVE: An Open-Source Environment for Multi-Fidelity Conceptual Vehicle Design," 16th AIAA/ISSMO Multidisciplinary Analysis and Optimization Conference, doi:10.2514/6.2015-3087, June, 2015.

Outreach Efforts

Multiple interactions with government, industry, and academia have occurred during the course of the fleet and technology assumption setting workshops, described in Section 0 of this report.

Awards

None

Student Involvement

Of the Georgia Tech students, Benjamin Bitoun, Marcus Bakke, Ryan Donnan, and Arturo Santa-Ruiz, Marcus Bakke and Ryan Donnan have graduated and have been employed by Boeing and Pratt and Whitney, respectively. Current students include Matt Reilly and Braven Leung.

On the Stanford University side, Anil Variyar, Trent Lukaczyk, Emilio Botero, Tim MacDonald, and Ved Chirayath have participated in the work presented here, and the development of the SUAVE framework. Dr. Lukaczyk has recently completed his doctoral degree and has started a UAV company. Mr. Chirayath is completing his dissertation by the end of the calendar year (2015) and is currently working at the NASA Ames Research Center in the Earth Sciences division.

Both Purdue Graduate Research Assistants worked on this project for the entire first year of effort; both are still graduate students at Purdue.

Plans for Next Period

The team intends to finalize the fleet analysis by February 2017 and conclude the project shortly thereafter.

References

1 Mavris, D., Perullo, C., Pfaender, H., Tai, J., "Project 36, EDS Assessment of CLEEN Technologies: 21st Semiannual PARTNER Technical Status Report."
2 Pratt & Whitney's Geared Turbofan Growth Plan, Aviation Week, 1 July 2013, URL: http://aviationweek.com/awin/pratt-whitney-s-geared-turbofan-growth-plan [cited October 2016].
3 Trent XWB, Rolls-Royce, URL: http://www.rolls-royce.com/products-and-services/civil-aerospace/products/civil-large-engines/trent-xwb.aspx [cited October 2016].
4 GE Passport, GE Aviation, 2015, URL: http://www.geaviation.com/bga/engines/passport [cited October 2016].
5 GE Passport, U.S. Department of Transportation, 29 April 2016, URL: http://rgl.faa.gov/Regulatory_and_Guidance_Library/rgMakeModel.nsf/0/78ad2acef2ea44b986257fb00067591d/$FILE/E00091EN_Rev_0.pdf [cited October 2016].
6 Thomas, M., "Better Power for a Changing World," Royal Aeronautical Society, 11 February 2014, URL: http://aerosociety.com/Assets/Docs/Events/746/GBD_Propulsion_211014_RR_1.pdf [cited October 2016]
7 GE9X Commercial Aircraft Engine, GE Aviation, 2015, URL: http://www.geaviation.com/commercial/engines/ge9x [cited October 2016].
8 Perry, D., "Boeing Advances 777X Service Entry: Sources," FlightGlobal, 11 March 2016, URL: https://www.flightglobal.com/news/articles/boeing-advances-777x-service-entry-sources-423032/ [cited October 2016].
9 Tetzloff, I. and Crossley, W., "An Allocation Approach to Investigate New Aircraft Concepts and Technologies on Fleet-Level Metrics," 9th AIAA Aviation Technology, Integration, and Operations Conference (ATIO), Hilton Head, SC, 22 September 2009.
10 Zhao, J., Agusdinata, D.A., DeLaurentis, D., "System Dynamics Fleet Forecasting with Technology, Emission, and Noise Goals," 9th AIAA Aviation Technology, Integration, and Operations Conference (ATIO), Hilton Head, SC, 22 September 2009.
11 Zhao, J., Tetzloff, I.J., Tyagi, A., Dikshit, P., Mane, M., Agusdinata, D.A., Crossley W.A., DeLaurentis, D., "Assessing New Aircraft and Technology Impacts on Fleet-Wide Environmental Metrics Including Future Scenarios", AIAA 48th Aerospace Sciences Meeting, Orlando, Florida, Jan. 4-7, 2010.
12 Mane, M., Agusdinata, D.A., Crossley, W.A., and DeLaurentis, D.A., "Fleet-Wide Environmental Impacts of Future Aircraft Technologies", 10th AIAA Aviation Technology, Integration, and Operations Conference (ATIO), Fort Worth, TX, 18 September 2010.
13 Moolchandani, K. A., Agusdinata, D. B., Mane, M., Crossley, W. A., and DeLaurentis, D. A., "Impact of Development Rates of Future Aircraft Technologies on Fleet-wide Environmental Emissions," 11th AIAA Aviation Technology, Integration, and Operations Conference (ATIO), Virginia Beach, VA, 19 September 2011.
14 Moolchandani, K. A., Agusdinata, D. B., DeLaurentis, D. A., and Crossley, W. A., "Airline Competition in Duopoly Market and its Impact on Environmental Emissions," 12th AIAA Aviation Technology, Integration, and Operations Conference (ATIO), Indianapolis, IN, 17 September 2012.
15 Moolchandani, K. A., Agusdinata, D. B., DeLaurentis, D. A., and Crossley, W. A., "Developing Optimal Airline Fleets Under Environmental and Capacity Constraints," 28th International Congress of the Aeronautical Sciences (ICAS), Brisbane, Australia, 28 September 2012.
16 Moolchandani, K. A., Agusdinata, D. B., DeLaurentis, D. A., and Crossley, W. A., "Assessment of the Effect of Aircraft Technological Advancement on Aviation Environmental Impacts," AIAA 51st Aerospace Sciences Meeting, Grapevine (Dallas/Ft. Worth Region), Texas, Jan. 7-10, 2013.
17 U. S. Energy Information Administration, Annual Energy Outlook 2011, 2011, URL: www.eia.gov/forecasts/aeo/ [cited December 2012].
17 Population Reference Bureau, World Population Data Sheet 0213, 2016, URL: http://www.prb.org/Publications/Datasheets/2013/2013-world-population-data-sheet/world-map.aspx#table/world/population/2013 [cited December 2016].

Project 011(A) Rapid Fleet-Wide Environmental Assessment Capabilities

Georgia Institute of Technology

Project Lead Investigator

Prof. Dimitri Mavris
Professor Dimitri N. Mavris
Director
Aerospace Systems Design Laboratory
School of Aerospace Engineering
Georgia Institute of Technology
Phone: (404) 894-1557
Fax: (404) 894-6596
Email: dimitri.mavris@ae.gatech.edu

Dr. Michelle R. Kirby, Co-PI
Chief, Civil Aviation Research Division
Aerospace Systems Design Laboratory
School of Aerospace Engineering
Georgia Institute of Technology
Phone: (404) 385-2780
Fax: (404) 894-6596
Email: michelle.kirby@ae.gatech.edu

University Participants

Georgia Institute of Technology (GT)

- P.I.(s): Prof. Dimitri Mavris, Dr. Michelle R. Kirby (Co-PI)
- FAA Award Number: 13-C-AJFE-GIT, Amendment 024
- Period of Performance: August 1, 2015 to January 31, 2017

Project Funding Level

FAA funded amount is $50,000 for the period of performance of August 1, 2015 to January 31, 2017. The Georgia Institute of Technology has agreed to a total of $50,000 in matching funds. This total includes salaries for the project director, research engineers, graduate research assistants and computing, financial and administrative support. The institute has also agreed to provide equipment funds as well as tuition remission for the students paid for by state funds.

Investigation Team

Prof. Dimitri Mavris, Dr. Michelle Kirby, Dr. Don Lim, Dr. Yongchang Li, Dr. Holger Pfaender, and Dr. Matthew Levine. Graduate Students: Jung (Andy) Hyun, Evanthia Kallou. Undergraduates: Emily Glover and Jacob Jacob

Project Overview

This project focuses on continued development of ASDL's rapid fleet-wide environmental assessment capabilities that complement the FAA's Aviation Environmental Design Tool (AEDT) with a lower fidelity screening tool that allows for consideration of a large number of technology scenarios. These technology scenarios can be quickly analyzed and reduced to a manageable set of scenarios for more focused, high fidelity analysis in the environmental tools suite. The Global and Regional Environmental Assessment Tradeoff (GREAT) tool has been developed, validated, and utilized on several FAA and

NASA projects in the past that have assessed fleet-level fuel burn and emissions over time. This tool links official forecasts, origin-destination pair route scaling, and replacement schedules to comparatively evaluate multiple technology and policy scenarios. In recent years, GREAT has been linked to ASDL's Airport Noise Grid Integration Method (ANGIM) tool to automatically generate baseline and future year airport schedules. While ANGIM has been validated against the FAA's INM tool and the method has been peer reviewed and published in AIAA's Journal of Aircraft, ANGIM had never been formally validated against AEDT and official inventory studies. The goal of this project was to validate ANGIM against AEDT using the 2012 Goals and Target Benefit Assessment (GATBA) and determine possible improvements to the linked GREAT-ANGIM tool based on the results of this comparative study. After implementing these improvements, the GREAT-ANGIM tool shall be used to analyze a series of noise goal scenarios defined by FAA.

Task 1 – Validating ANGIM against AEDT using GATBA study

Georgia Institute of Technology

Objective(s)

Validate ANGIM's capability to measure contour area and population exposure for DNL-55dB, 60dB, and 65dB by comparing against an AEDT study that included three study scenarios: a 2012 baseline, a 2030 evolutionary technology scenario, and a 2030 aggressive technology scenario. It should be noted that these future technology scenarios use an equivalency approach to scale operations rather than considering specific technologies and unique Noise-Power-Distance curves for future aircraft types.

Research Approach

This task consisted of three primary subtasks. The first task focused on acquiring the GATBA scenarios from the FAA and executing them in AEDT. The second task required queries from the AEDT study databases to prepare input files of consistent schedules and vehicles for ANGIM. The first two tasks enabled the same scenarios to be executed in ANGIM in order to evaluate the uncertainty introduced by ANGIM's simplifying assumptions.

AEDT Runs of GATBA Scenarios

While the GATBA studies had been previously run by Volpe, Georgia Tech had to acquire these studies from Volpe and re-run them in AEDT 2b FP1, as the studies were incompatible with any other version of AEDT. For each study, Georgia Tech ran 3 different atmospheric absorption models (SAE-AIR-1845, SAE-ARP-866A, and SAE-ARP-5534) at a subset of five airports (KATL, KJFK, KMIA, KMDW, and KSAN). For all of these cases, the SAE-ARP-866A contours were greater than the SAE-AIR-1845 contours, and the SAE-ARP-5534 contours were slightly larger than the SAE-ARP-866A contours. This is a significant finding, because ANGIM assumes standard day conditions with the SAE-AIR-1845 atmospheric model. The standard day atmosphere assumption allows the aircraft level grids to be pre-computed for ANGIM, which is the most significant enabler of ANGIM's rapid formulation. The ANGIM-AEDT comparisons that followed were only compared for the SAE-AIR-1845 model. An additional 33 airports were run in AEDT using the SAE-AIR-1845 model.

For each scenario and each airport, operations by military, small general aviation, and old out of production aircraft with negligible operations were removed from these operational schedules. Georgia Tech also changed the grid dimensions from the original scenario because they were inconsistent from airport to airport, and occasionally the grid resolutions were too coarse. Guidance on acceptable grid resolutions are discussed in ECAC.CEAC Doc29[1], where the balance between interpolation errors introduced by coarse grid spacing and the increased computation time associated with more grid points are addressed. The document cites comparative studies that have shown a *maximum* value of 300 meters, or approximately 0.16-nautical miles, constitutes a good compromise between accuracy of the interpolated noise contours and computational times, yet some cases in the GATBA study used resolutions as coarse as 0.25-nautical miles. Georgia Tech came to similar conclusions years ago when establishing a standard grid resolution for ANGIM, Generic Airports, and Generic Vehicles. Given ANGIM's computational speed relative to AEDT, a finer grid-spacing of 0.08-nautical miles in each direction was chosen, and Georgia Tech has consistently used this resolution on all noise analyses. Thus, Georgia Tech modified the grid resolution in AEDT to match the grid resolution used in ANGIM. This lead to long computer runtimes for each AEDT airport and scenario.

[1] ECAC.CEAC Doc 29, Report on Standard Method of Computing Noise Contours Around Civil Airports, Vol. 2, 3rd ed., Technical Guide, Dec. 2005.

After running these cases in AEDT, contour area measurements and population exposure counts were collected for each scenario. It should be noted that Georgia Tech discovered a bug in AEDT's contouring algorithm that impacted AEDT's contour printing, contour area calculation, and population exposure counts. This bug was reported to Volpe, and once they were fixed the contours were regenerated. The combination of long computer runtimes and bug fixing increased the number of iterations and amount of time it took to complete this subtask.

Queries of AEDT Study Databases and Preparation of ANGIM Input Files
The first part of this subtask required a query to determine the full set of unique aircraft in the GATBA studies. The relevant AEDT coefficients that define each of these aircraft were extracted from the AEDT database version associated with the GATBA study. These collections of coefficients were saved as aircraft XML files to ensure consistency with the GATBA analysis. The aircraft XML files were used as inputs to ASDL's in house tool referred to as the AEDTTester. This tool uses AEDT source code including the Aircraft Performance Module (APM) and Aircraft Acoustics Module (AAM) to generate single aircraft Sound Exposure Level (SEL) grids for each unique departure stage-length and arrival procedure. ASDL has also developed a MATLAB based wrapper around the AEDTTester that allows it to be run in batch mode and collect all the necessary grids for use in ANGIM. The SEL grids generated for this ANGIM analysis assume standard day sea-level atmospheric conditions and straight ground tracks. Each of these assumptions enables pre-computation of aircraft-level half grids. ANGIM mirrors, translates, and rotates these grids into place and performs logarithmic addition to calculate airport-level DNL grids.

Once all of the grids were generated, the schedules for the relevant airports were extracted using SQL queries on the GATBA study database and formatted as necessary to be used with ANGIM. It should be noted that the GATBA studies included specific runway assignments for all operations, and the ANGIM flight schedules match these specific runway assignments.

Comparison of ANGIM and AEDT
Once the ANGIM files were prepared, running all three scenarios took less than one hour, compared to greater than 36 days to run similar cases in AEDT. Under the assumption of SAE-AIR-1845 atmospheric model and matching runway assignments, comparison of contour areas showed good agreement between ANGIM and AEDT, with most contour area comparisons within 5%. A few airports with extreme track divergence, particularly airports in the New York Metroplex (KEWR, KJFK, and KLGA) had larger contour area differences. These results suggest that the straight track assumption used by ANGIM is a good assumption at most airports, but a suggested improvement for ANGIM is an ability to include curved tracks at a select few airports. Depending on the number of track designs included, it may be feasible to add unique curved tracks for these few airports, although half-grids cannot be used for these turning tracks because the SEL noise grids will no longer be symmetric about the runway centerline.

More important than accuracy per airport is the ability of ANGIM to capture the trends for future scenarios relative to the baseline scenario. When evaluating the change in ANGIM contours per scenario versus the change in AEDT contours per scenario, the cumulative contour changes across all 38 airports in ANGIM was within 2.5% of the cumulative contour changes in AEDT.

When evaluating population exposure, a similar conclusion was reached. ANGIM was reasonably accurate compared to AEDT, but the few airports with significant diverging ground tracks were also associated with high density population dispersion around the airports. However, when 4 of the 38 airports (KEWR, KJFK, KLGA, and PHNL) were removed from the population comparison study, the cumulative population exposure counts were very close, as shown in Table 1. Similar results were observed for the two 2030 scenarios. This once again supports the conclusion that the straight track assumption is good for most airports, but modeling diverging tracks at a few airports could improve ANGIM's assessment capability.

The full validation study was compiled into a single Powerpoint presentation and provided to the FAA. The presentation includes AEDT-ANGIM contour overlay plots, contour area measurements, and population exposure counts for all 38 airports at every scenario.

Table 1. ANGIM-AEDT Cumulative Population Comparison for GATBA 2012 Scenario

	AEDT	ANGIM		
	Option 1	Option 1		
	Population Count	Population Count	Diff	Pct Diff
55	2405839.694	2534627.436	128788	5.35%
60	679404.4952	740265.7896	60861	8.96%
65	126028.5925	128587.242	2559	2.03%

Task 2 – Enhancement of ANGIM, AEDTTester, and GREAT Capabilities

Georgia Institute of Technology

Objective(s)

The lessons learned from the GATBA study have guided the recent enhancement of ASDL's complementary tools. This section is divided into three subsections, each focused on one of the following three tools: ANGIM, AEDTTester, and GREAT. Developments for each are currently ongoing.

Research Approach

While the validation of ANGIM was performed using a GATBA 2012 analysis, Georgia Tech and the FAA agreed that GREAT should use data from the FAA's most recent inventory analysis based on 2015 data. This dataset was acquired from the FAA and is currently being used to update Georgia Tech's tools.

Enhancements of ANGIM

One of the most significant lessons learned from the GATBA Analysis concerned the actual utilization of airport runways at each airport. Georgia Tech learned that many airports feature departure threshold displacements such that brake release points do not coincide with runway endpoints. ANGIM's runway configurations did not capture this threshold displacement, which resulted in a mismatch of AEDT and ANGIM contours. To accommodate these threshold displacements, Georgia Tech modified the runway configuration files and added a convention for enabling displacement thresholds.

Additionally, ANGIM contains a utilization factor method for distributing operations across the different runway endpoints in the event that runway assignments are not known a priori. In the past, Georgia Tech did not have knowledge or data of actual airport utilization, and so an equal utilization assumption was often used. The example GATBA studies and the more recently acquired 2015 noise inventory have shed much light on actual runway usage and shown that equal utilization is not a good assumption. In fact, many runways are used preferentially in one direction due to prevailing winds and traffic flows. Some runways are used preferentially as departure runways or approach runways. In response to this observation, ANGIM was enhanced to include unique approach and departure utilization factors. The values for these utilization factors were determined from queries on the airport schedules in the 2015 noise inventory, and a verification study was run at five representative airports (KMSP, KLAX, KORD, KSAN, and KSDF). This verification study compared ANGIM schedule with specific runway assignments versus the same ANGIM schedule using no specific runway assignments and instead leveraging the utilization factors. For most of the airports, this comparison was nearly exact. Slight runway preferences for certain aircraft types can lead to slight inaccuracies, but even in these cases the utilization factors greatly improve accuracy compare to the equal utilization assumption.

In response to this modification of the ANGIM method, new runway configuration files were created for all of the MAGENTA 95 airports using the 2015 noise inventory as the reference point. A team of undergraduate students conducting research for course credits were assigned the task of analyzing flight schedules to determine runway utilization factors for each runway endpoint, including threshold displacements. This enhancement will improve the ability to generate more accurate

contours, area measurements, and population exposure counts for ANGIM schedules automatically generated by GREAT, which lacks information on specific runway assignments of projected future operations.

Enhancements of AEDTTester
The original AEDTTester code was developed simultaneously with AEDT 2a. The code essentially mimics AEDT's database query methods by reading in user XML aircraft and flights files instead. The AEDTTester then calls actual AEDT methods including the APM and AAM models that are necessary for generating SEL noise grids. This code was not synced to changes and updates to AEDT, which is constantly releasing new versions and updates as it continues to be developed. In conjunction with other ASCENT projects being conducted at ASDL, Georgia Tech was given access to AEDT developer's source code through the TFS. The AEDTTester required updates to accommodate new updates that have been made since AEDT 2a. The current version of the AEDTTester is synced to the AEDT 2c official release.

One previous convention that was built into the AEDTTester was a straight ground track assumption for terminal area procedures. This coincided with the ANGIM assumption of straight ground tracks, and thus diverging tracks were not previously considered. The results of the GATBA comparison determined the need to include diverging ground tracks for a select subset of airports in order to improve accuracy. A derivative version of the AEDTTester was thus developed to allow for diverging ground tracks. This version of the AEDTTester will be used to expand ANGIM's library of pre-computed SEL grids for airport analysis to improve accuracy at a select few major airports.

Enhancements of GREAT
Each of the improvements to ANGIM and AEDTTester will enhance the integrated GREAT-ANGIM tool. Additionally, the linkage between GREAT and ANGIM has been enhanced to include out-of-production operations. This capability was requested by the FAA in order to perform scenario analyses to evaluate the noise implications of of various retirement rates. Initially, the GREAT enhancement was only designed to use representative vehicles for all out of production aircraft, similar to the generic vehicles used for in-production vehicles, which have been shown to provide good accuracy. The representative out-of-production vehicles, however, did not well approximate the fleet-level noise contributed by out of production vehicles. Modeling generic out-of-production vehicles is not worth the effort because there is no goal of improving these vehicles through technology infusion. Rather these vehicles will be phased out as they age or new policy restrictions are implemented. Efforts are ongoing to include all out of production vehicle grids for every airport in the MAGENTA 95 subset, but it is unclear how these additional grids may impact the integrated GREAT-ANGIM runtime.

Milestone(s)
GATBA Analysis comparing ANGIM and AEDT was completed and a detailed documentation of all airport comparisons was provided to the FAA. (Completed August 2016)

Integration of Enhancements to ANGIM, AEDTTester, and GREAT. (Targeted completion mid-January 2017)

Sample Noise Scenario and Transfer of Tool to FAA. (Targeted completion end of January 2017)

Major Accomplishments
Validated ANGIM against AEDT and showed straight ground track assumption is typically reasonable.

Updated airport configurations and utilization factors at all MAGENTA 95 airports.

Updated ANGIM to enable departure threshold displacements and unique approach/departure utilization factors.

Compiled an updated AEDTTester synced to AEDT 2c release and enabled diverging ground tracks for terminal procedures.

Publications
N/A

Outreach Efforts
Presentations at Spring and Fall ASCENT meetings.

Presentations of Results on Tools Teleconference in March and August.

Prepared detailed comparisons of every airport in GATBA analysis in Powerpoint file, available upon request.

Awards
N/A

Student Involvement
Jung (Andy) Hyun Kim – Graduate Research Assistant, Georgia Institute of Technology
- Aided SQL queries and airport schedule generation for ANGIM analysis

Evanthia Kallou – Graduate Research Assistant, Georgia Institute of Technology
- Trained on AEDT and helped collect AEDT GATBA contour areas and population exposure counts

Emily Glover – Undergraduate Research Assistant, Georgia Institute of Technology
- Analyzed airport schedules and collected runway utilization factors

Jacob Jacob – Undergraduate Research Assistant, Georgia Institute of Technology
- Analyzed airport schedules and collected runway utilization factors

Plans for Next Period

Task 1 – Validating ANGIM against AEDT using GATBA study
This task is complete, and no other action is necessary.

Task 2 – Enhancement of ANGIM, AEDTTester, and GREAT Capabilities
Enhancements to ANGIM and AEDTTester shall be integrated into GREAT. All out-of-production grids shall be added to the GREAT-ANGIM integrated tool, and a sample noise goal analysis shall be conducted.

Project 011(B) Development of Rapid Fleet-Wide Environmental Assessment Capability Using a Response Surface Modeling Approach

Massachusetts Institute of Technology

Project Lead Investigator

R. John Hansman
T. Wilson Professor of Aeronautics & Astronautics
Department of Aeronautics & Astronautics
MIT
Room 33-303
77 Massachusetts Ave
Cambridge, MA 02139
617-253-2271
rjhans@mit.edu

University Participants

Massachusetts Institute of Technology

- P.I.(s): R. John Hansman
- FAA Award Number: 13-C-AJFE-MIT, Amendment Nos. 006, 011, 014 and 023
- Period of Performance: Aug. 18, 2014 to Aug. 31, 2017
- Task(s):
    1. Develop Model Architecture
    2. Extend Existing Capabilities of TASOPT
    3. Develop Simplified Version of Surrogate Model (Fuel-Only)
    4. Develop Noise Modeling Approach
    5. Develop Multi-Output Surrogate Model
    6. Test the Multi-Output Rapid Assessment System on a Representative Sample Problem
    7. Develop Revolutionary Technology Evaluation Capability
    8. Coordination within FAA and Volpe

Project Funding Level

$670,000 FAA funding and $670,000 matching funds. Sources of match are approximately $279,000 from MIT, and $231,000 from Byogy Renewables, Inc., and $160,000 from Oliver Wyman Group.

Investigation Team

Prof R. John Hansman (PI)
Luke Jensen (Graduate Student)
Jacqueline Thomas (Graduate Student)

Project Overview

The objective of the research is to continue development of an analytical framework for evaluating the environmental impact of aviation. This framework uses rapid models for aircraft-level performance and noise, enabling broad scenario explorations and fast parametric analyses in environmental studies. Phase I of this research consisted of general analysis framework development, sample problem selection, and surrogate model development. The current phase of this research

has aimed to demonstrate the capability of the surrogate modeling approach on a multi-dimensional output space, with emphasis on system-level aviation noise sample problems.

Task 1: Develop Model Architecture

Objective(s)

In the first task, completed under Phase I of this research, the system architecture and general modeling framework have been developed. The set of potential scenario input variables and their forms are defined based on anticipated policy or technology impact questions. Some of these are discrete inputs, some are parametrically defined, and some are defined in standard forms such as the TAF or CAEP forecasts, retirement curves or reference initial conditions such as the 2010 COD flight database. In addition, the desired output space must be defined. This may include standard AEDT outputs such as fuel burn, CO2, NOX, Noise as well as the capability to define other impact parameters of interest. Based on the inputs and outputs, the general model framework has been defined. The working model includes the capability for multiple surrogate model response surfaces to interact in a hierarchical framework, depending on the complexity and scope of the problem at hand.
In Phase II of the project, the model framework will continue to be assessed to ensure that tradeoffs between computational speed and fidelity are appropriate for the chosen sample problem.

Research Approach

- Iteratively refine the inputs and interfaces between the modeling components in analysis architecture diagrams to ensure that the analysis architecture developed under Phase I are consistent with current modeling processes and objectives.

Major Accomplishments

- Selected gridded superposition approach for rapid modeling, allowing for flexible use of multiple noise and emissions models and scalable computation cost depending on desired fidelity

Task 2: Extend Existing Capabilities Of TASOPT

Objective(s)

In order to meet the project objectives, the capabilities of TASOPT has been extended under Phase I of this project. Aircraft-level noise modeling has been added to TASOPT as a post-processing module. This involves an interface with NASA's ANOPP noise modeling code. In Phase II of the project, flexibility will be added to the aircraft trajectory and performance assumptions to enable studies of the environmental impacts of operational changes.

Research Approach

- Collaborate with the TASOPT development team at MIT to ensure that TASOPT 2 and components of TASOPT 3 are consistent with the objectives of this project.
- Identify methods to incorporate high-lift devices and non-standard climb and descent profiles into TASOPT outputs.

Major Accomplishments

- Identified appropriate outputs and controls for TASOPT necessary for input to ANOPP (performance modeling, engine parameters, and aircraft mass estimation)

Task 3: Develop Simplified Version of Surrogate Model (Fuel-only)

Objective(s)

Under Phase I of the project, the model framework has been evaluated using a simplified version of the architecture. This results in a surrogate model with a single output variable (fuel burn) using TASOPT as the high-fidelity basis. This version can be rapidly implemented as it can build on the existing artificial neural network models developed by Yutko. The preliminary version will be validated against AEDT or other available data sets.

Research Approach

- Apply method developed by Yutko (2012) to a systemwide fuel consumption analysis using the same fleet and network assumptions that will be applied to noise modeling objectives.

Major Accomplishments

- Generated fuel results for a sample network using surrogate model version of TASOPT

Task 4: Develop Noise Modeling Approach

Objective(s)

Under Phase I of this project, options for surrogate noise models that can be used as the basis for rapid fleet-wide analysis were explored. An approach using an aircraft-level surrogate model for performance and noise has been identified as the most promising solution, with direct system-level calculation generated with a gridded superposition approach. The output of this task is a detailed noise modeling approach that falls under the general modeling framework conceptualized in Task 1. Under Phase II of this project, refinements to the surrogate noise modeling approach may be necessary based in practical implementation challenges.

Research Approach

- Identify methods to model flight operations in the vicinity of airports using representative trajectories based on historical radar data and published procedures
- Integrate schedule, fleet, and runway utilization data from external sources to allow calculation of noise contours at airports of interest
- Implement noise modeling of identified representative trajectories using multiple noise models: ANOPP and AEDT
- Track computational cost and implementation complexity for each noise modeling alternative

Major Accomplishments

- Developed profile generator for approach and departure thrust estimation
- Developed representative track identification method using historical radar data and published RNAV procedures
- Continued validation of ANOPP and AEDT noise results using FAA certification data and noise monitor measurements
- Integrated noise modeling capability from ANOPP and AEDT into a common flexible analysis architecture

Task 5: Develop Multi-output Surrogate Model

Objective(s)

This task will develop a multi-output version of the surrogate model that will include all of the key environmental outputs identified in Task 1, likely including Fuel Burn, NOx, and Noise. Noise related surfaces would be created using the method developed in Task 4.

Research Approach

- Implement fuel burn model using BADA and TASOPT

- Implement emissions modeling using emissions index approach using data available from ICAO
- Develop analysis workflow that integrates fuel and emissions calculation with noise analysis

Major Accomplishments

- Implemented emissions index method for emissions calculation
- Generated fuel and emissions results for sample problem developed under Task 6

Task 6: Test The Multi-output Rapid Assessment System On A Representative Scenario Evaluation Problem (Sample Problem)

Objective(s)

One or more representative evaluation problems will be defined and the multi-output version will be used to evaluate relevant scenarios for that problem. The rapid assessment results can be used to identify specific AEDT cases that will be run both to explore the problem of interest and also to validate the rapid assessment model.

Research Approach

- Identify single-airport sample problem that exercises the intended functionality of the analysis architecture
- Generate results for noise, fuel, and emissions for sample problem

Major Accomplishments

- Developed a capacity evolution scenario at DCA to guide further model development
- Developed DCA sample problem in detail (flight schedule, representative fleet types, runway utilization).
- Refined clustering method for trajectory generation in DCA sample problem
- Generated preliminary results for DCA sample problem

Task 7: Develop Revolutionary Technology Evaluation Capability

Objective(s)

Methods will be evaluated for modeling revolutionary technological advances that a simple extrapolated prediction framework would not capture. Both physics based models and historical case studies will be used to identify how historical or potential technologies could change the response surfaces. It is expected that it should be possible to identify standard ways in which the response surface changes. If this were correct, these insights would be used to define indicators of potential future capability that could be evaluated parametrically to explore potential future performance spaces.

Research Approach

- Use TASOPT to model novel aircraft geometries, configurations, and technology levels.
- Integrate TASOPT outputs with ANOPP to generate noise results for revolutionary technology evaluation.
- Evaluate impact of revolutionary technology in single-airport sample problem.

Major Accomplishments

- Developed method for upgauging aircraft in TASOPT and evaluating impact in terms of noise, fuel burn, and emissions
- Integrated upgauged aircraft in DCA sample problem to demonstrate analysis architecture
- Began development of noise modeling technique for advanced double-bubble aircraft concept

Task 8: Coordination Within FAA And Volpe

Objective(s)

The research team will be utilizing a number of tools within the FAA Tool Suite for which experts reside at FAA and Volpe, specifically AEDT. TASOPT has previously been connected with AEDT, and it may be useful to call on experts that have worked in this specific area.

Research Approach

- Regular communication and outreach as required to leverage noise modeling expertise and FAA/AEE and Volpe.

Major Accomplishments

- Built automated interface with AEDT 2b for certain single-airport noise modeling and logging of results.

Publications

None

Outreach Efforts

11/24/2016: Briefing at FAA Tools/Analysis Coordination Meeting
8/1/2016: Briefing to FAA Joint University Program research update meeting
8/5/2016: Briefing at FAA Tools/Analysis Coordination Meeting
In-person outreach and collaboration with TASOPT aircraft performance model development team at MIT
In-person outreach and collaboration with Volpe noise tool development team

Awards

None

Student Involvement

Graduate students have been involved in all aspects of this research and have been the key implementers.

Plans for Next Period

The next phase of this project will involve the development and analysis of additional multi-objective sample problems to demonstrate the flexibility and extensibility of the rapid environmental analysis framework. This phase will refine the relationship between local and system-level impacts, including stakeholder valuation and welfare changes that may result.

Project 013 Microphysical Modeling & Analysis of ACCESS 2 Aviation Exhaust Observations

Stanford University

Project Lead Investigator

Mark Z. Jacobson
Department of Civil and Environmental Engineering
Stanford University
473 Via Ortega, Room 397
Stanford University, Stanford, CA 94305-4020
Tel: 650-723-6386
jacobson@stanford.edu

University Participants

Stanford University

- P.I.(s): Mark Z. Jacobson, Sanjiva K. Lele
- FAA Award Number: 13-C-AJFE-SU-002, 13-C-AJFE-SU-012
- Period of Performance: 10/01/2014 – 9/30/2016

Project Funding Level

$200,000 from FAA funding

Project Overview

As the popularity of and global access to air travel expands, quantifying its impact on climate and air pollution becomes increasingly important. However, the spatial-temporal distribution of aircraft emissions and their byproducts spans many orders of magnitude, as contrail development begins within seconds, but can spread to the kilometer-scale and persist for hours. The wide range of spatial and temporal scales makes it difficult to obtain detailed knowledge of the composition and evolution of emissions from measurements or modeling studies alone. In an attempt to increase understanding, this project simulates the short-term, near- and far-field evolution of aircraft exhaust aerosol and contrail particles and gases with two computer models: GATOR-GCMOM and an LES model. Together, these two models simulate phenomena spanning a spatial range from millimeters to thousands of kilometers. Detailed microphysical processes in the models are validated and improved with field measurements from NASA's ACCESS-2 campaign, so that the models may provide more credible estimates of impacts on climate and atmospheric composition when used at the regional and global scale.

The Alternative Fuel Effects on Contrails and Cruise Emissions (ACCESS-2) field experiment measured a number of aviation exhaust parameters during flight that are useful for studying the chemical and physical evolution of exhaust gases. Ambient and aircraft engine data from ACCESS-2 are used to initialize model simulations and compare results with measured parameters. Model simulations with GATOR-GCMOM simulate the evolution of aerosol and contrail particle size distributions for comparison with data and with Aerodyne model results (obtained in a parallel study). The high fidelity LES simulations are run to develop a deeper understanding of the dynamics of the evolution of contrails and provide parameters for plume spreading and shearing to GATOR-GCMOM. Results are obtained following the analysis of data from six aircraft flights.

Approach

The Alternative Fuel Effects on Contrails and Cruise Emissions (ACCESS-2) field experiment involved 8 flights performed in May 2014, designed to measure the aircraft exhaust composition and contrail characteristics as a NASA DC-8 source

aircraft burned (1) high sulfur JP-8, and (2) a 50/50 blend of low sulfur JP-8 and a HEFA (hydro-processed esters and fatty acids) biofuel produced from camelina plant oil. The flights were in the 10-11 km altitude range, typical of commercial cruise flight conditions. Sampling of contrails was performed in situ in the national air space (NAS) within the first seconds to minutes of exhaust emission. Statistics were gathered on aerosol/ice emission indices (e.g., grams of ice per kg fuel) from flights using the different fuels. Model simulations are initialized with ambient conditions (temperature, pressure, location, and relative humidity) to match those of the ACCESS 2 campaign.

GATOR-GCMOM is a Reynolds-Averaged Navier-Stokes (RANS) model that treats the microphysical evolution of aerosol size and composition within a subgrid contrail plume. The second model used in this study is a large-eddy simulation (LES) model with a detailed three-dimensional dynamical model. Near-field simulations on the order of several seconds are run with both models, while GATOR-GCMOM simulations continue to capture far-field results.

LES Model

Model Description

Variable	Description
$\boldsymbol{u} = u\boldsymbol{i}+v\boldsymbol{j}+w\boldsymbol{k}$	Filtered air velocity vector
p'	Pressure fluctuation
ρ', ρ_0	Density fluctuation, mean ambient density
$\boldsymbol{G}$	Gravitational acceleration vector
v	Kinematic viscosity of air
θ', θ_0	Potential temperature fluctuation, Reference potential temperature

Table 1: Variable names and descriptions

The LES model to be used for this study is CDP-IF2, an incompressible turbulent flow solver, with Boussinesq approximation for buoyancy effects and Euler-Lagrangian treatment for ice-microphysics [Naiman et al., 2011]. Potential temperature and water vapor concentration are treated as Eulerian fields. The model treats the emissions of aerosols, which are tracked for the primary purpose of simulating contrail development. Water vapor deposition on aerosol particle nuclei is based on local supersaturation. The model treats multiple ice crystal-habits [Inamdar et al., 2013]. It has been used for process studies of persistent aircraft contrails [Naiman et al., 2011; Inamdar et al., 2013] and has supported the development of a subgrid-plume model [Naiman et al., 2010, 2011] for use with global circulation models.

The large eddy simulation (LES) model is described in detail by Naiman [2011]. The following description is taken from Naiman [2011], Naiman et al. [2011], and Inamdar et al. [2013, 2014]. The computational domain for the simulations is stationary with respect to the ground, so the computation represents a temporal simulation. Facing the aircraft, the coordinate system is positioned with the x-axis extending from the left wingtip to the right wingtip of the aircraft, the y-axis pointing opposite gravity, and the z-axis pointing opposite the flight direction.

The large eddy simulation solves the incompressible Navier-Stokes equations with a Boussinesq approximation for buoyancy forces,

$$\nabla . \boldsymbol{u} = 0$$

$$\frac{D\boldsymbol{u}}{Dt} = -\frac{\nabla p'}{\rho_0} + \frac{\rho' \boldsymbol{g}}{\rho_0} + \upsilon \nabla^2 \boldsymbol{u} + \nabla . \boldsymbol{\tau}^{sgs}$$

The subgrid scale stress tensor, $\boldsymbol{\tau}^{sgs}$, is modeled. The Boussinesq approximation gives the equation of state,

$$\frac{\rho'}{\rho_0} = -\frac{\theta'}{\theta_0}$$

Coupled scalar transport equations are solved for potential temperature: θ, water vapor density: Y, and a passive scalar: $\boldsymbol{\varphi}$,

$$\frac{D\theta'}{Dt} = -\frac{d\theta_y}{dy}v + \kappa\nabla^2\theta' + \nabla.\boldsymbol{q}^{sgs,\theta} + \omega_T$$
$$\frac{DY}{Dt} = -\frac{dY}{dy}v + D_v\nabla^2 Y' + \nabla.\boldsymbol{q}^{sgs,Y} + \omega_Y$$
$$\frac{D\varphi'}{Dt} = D_v\nabla^2\varphi' + \nabla.\boldsymbol{q}^{sgs,\varphi}$$

where κ is the thermal diffusivity of air and D_v is the diffusivity of water vapor in air. The passive scalar is tracked to mark engine exhaust. Temperature and water vapor density are prescribed to vary linearly with altitude, so the vertical gradients $d\vartheta_v/dy$ and dY_v/dy are constants. The subgrid scale stress tensors, $\mathbf{q}^{sgs}$, are modeled for each scalar variable. The source terms ω_T and ω_Y couple ice microphysics to the vapor phase through mass exchange of water and latent heat release by ice sublimation/deposition. The terms are related, $\rho_0 C_P \omega_T = -\omega_Y L$, where C_p is the specific heat of air and L is the latent heat of sublimation of ice. The source term ω_Y is calculated in the ice microphysics model described below.

The contrail ice in the simulation is modeled using a Lagrangian tracking approach. The exchange of mass between the Eulerian gas phase and the Lagrangian solid phase is modeled as a deposition/sublimation process. In addition to the conservative mass exchange of water vapor and ice, the heat transfer due to latent heat of sublimation is also modeled through an energy source term in the gas phase. The energy released by this process is applied to the gas phase temperature equation; the solid phase is assumed to be in thermal equilibrium with the gas phase; this is a reasonable assumption given insignificant slip and sedimentation up to 20 min. of time. Contrail particles are assumed to be nonvolatile ice nuclei of a prescribed effective radius that are fully activated for ice deposition and are initially coated in ice. The initial growth and activation of ice nuclei from jet emission products is a complex process and is not treated here. Re-growth is allowed, but other processes, such as additional nucleation, coagulation, and conductive heat transfer between the solid and gas phases are not modeled.

The ice deposition and sublimation calculation is based on a diffusional model. Growth rates are calculated based on the water vapor density field interpolated to the particle location and integrated over the time step. The source of water vapor, ω_Y, is the mass of water deposited to each particle distributed over the local volume from which the water vapor is sourced, ΔV,

$$\omega_Y = \frac{1}{\Delta V}\frac{dm_p}{dt} = \frac{1}{\Delta V}2\pi\rho_p r_p \frac{dr_p{}^2}{dt} N_\mathrm{p}$$

where r_p is the effective spherical radius of the non-spherical ice particle (i.e. radius of a spherical particle of the same mass) and N_p is the number of ice particles represented by each computational particle.

The full equations of motion for spherical particles are complex, but can be simplified for the case of small Stokes number. The Stokes number, St = τ_p/t_0, characterizes the ratio of the particle response time, τ_p, to the characteristic flow time scale, t_0. For small Stokes numbers, particles follow the carrier fluid path lines, so their location, $\boldsymbol{x}_p$, can be advanced in time,

$$\frac{d\boldsymbol{x}_p}{dt} = \boldsymbol{u}(\boldsymbol{x}_p, t)$$

This formulation neglects forces on the particles such as drag and gravitational settling, which become more important for larger Stokes numbers. Over the first twenty minutes of simulation time, a posteriori analysis shows that the maximum Stokes number reached was below 2×10^{-4}, well within the regime of small Stokes number. Sub-grid scale velocity fluctuations are also neglected, since the fluid velocity, u, is the LES filtered velocity.

NASA Data Analysis

Data collected by both the DC-8 and the trailing Falcon were provided for measurements made on 8 separate days. The data collected by NASA on these 8 days – May 7th, 8th, 9th, 10th, 22nd, 27th, 29th and 30th – was collated to observe the inter-day variability in ambient conditions. The following filters were applied to the data:

1. Eliminate all incomplete measurements (i.e. those containing NANs, -99s, -999s)
2. Eliminate all measurements below 10 km altitude
3. Eliminate measurements corresponding to a contrail age of less than 1s

As Figures. 1b and 1c suggest, the local pressure and temperature profiles did not vary significantly between the measurement days. The measured ambient super-saturation w.r.t ice, however, is seen to have a large spread, indicating a large variation in RHi along the flight direction. As the LES model simulates the temporal evolution of a contrail in a stationary ambient, and as the contrail evolution is sensitive to RHi, best estimates of RHi values that span the measured contrail conditions are necessary for the 3-D LES simulations. Thus, data points are clustered (shown in Figure 1a) such that points within a cluster are statistically indistinguishable up to 95% confidence – i.e at a given altitude, the pressure, temperature and RHi in these clusters can be considered almost the same with 95% confidence.

Comparison of LES Simulations and NASA Measurements

It is clear from the data that most contrails evaporated rapidly because of subsaturated ambient air, indicated by the low RHi values (<100%) for most clusters. The highest 2 RHi clusters, however, are seen to sustain a contrail for up to a couple of minutes. These correspond to the measurements made on May 27th and 29th, with the longest-lasting contrail on the 29th. Another point of consideration for the LES model is the inclusion of the impact of fuel sulfur content (FSC). It is known that higher FSC affects jet exhaust by significantly increasing the fine size aerosols. Thus, the LES model incorporates the impact of sulfur by modifying the initialization of contrail particles to include additional fine-size particles. It is observed that the smaller sizes do not impact the integrated quantities of interest, as they do not grow due to inhibition by the Kelvin effect. Kelvin effect refers to the increase in actual vapor pressure due to an increase in curvature of the smaller particles' surface, resulting in preferential evaporation of smaller particles or growth of larger particles.

Finally, in Table 2, we present a comparison of the LES model results and observed data for May 29th. The values of particle concentrations as predicted by the LES are within the margins of error of the observed data. This is promising as it indicates that the LES model is capable of capturing the observed trends in contrail evolution even in subsaturated conditions.

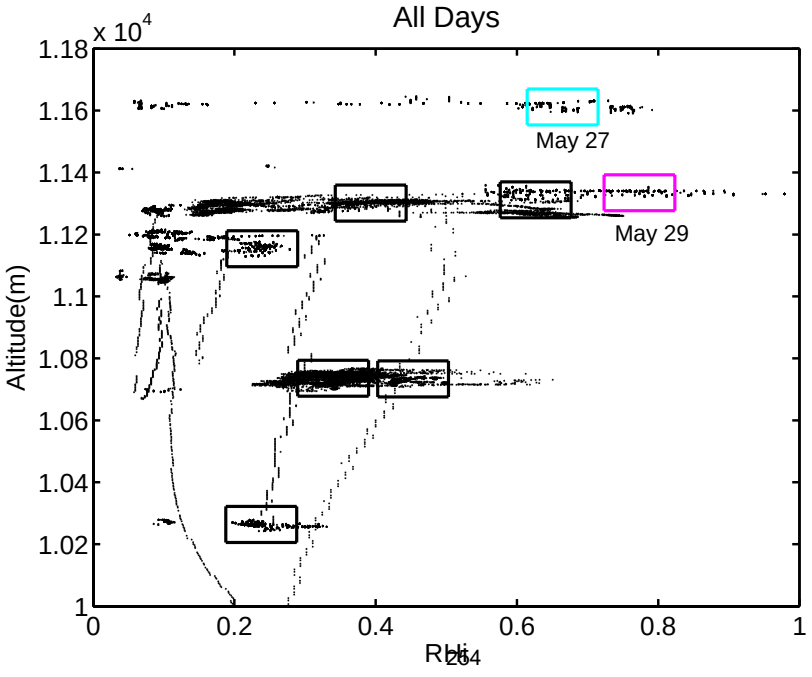

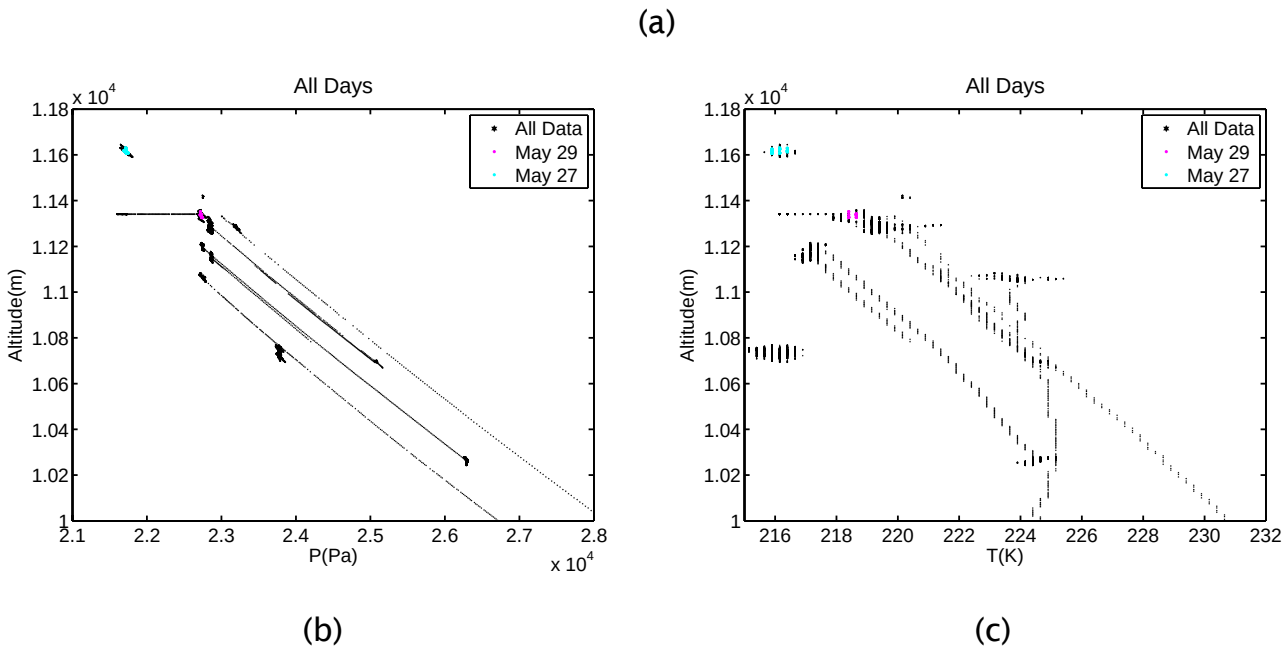

Figure 1: Analysis of Collated Observational Data: a) Altitude (m) vs. RHi (%); b) Altitude vs. Pressure (Pa); and c) Altitude vs. Temperature (K).

Temperature	Pressure	Stratification	RHi
218 K	227 hPa	-7.2 K/km	77.30%
		Particle Conc. (#/cm^3)	
		NASA Data	LES Data
	30	53.15 ± 19.53	41.37
	130	25.23 ± 6.3	19.03

Table 2: Comparison of bulk LES results with Data for May 29th

Discrepancies between different LES models

Numerically observed sensitivities of particle survival rates, mean size and mean optical extinction to parameters such as EI_{soot} and ice supersaturation(RHi) reported in the literature [Picot et al., 2015; Unterstrasser, 2014; Naiman et al., 2011] have discrepancies that can be large. Unterstrasser [2014] observes 40% to 70% survival rates for RHi ranging from 120% to 140% and 50% to 90% survival rates for a reduction in EI_{soot} by a factor of 10. In Picot et al. [2015] a change in RHi from 110% to 130% increases survival rate from 65% to near 100% while Naiman et al. [2011] see negligible sensitivity of survival rates to RHi ranging from 110% to 130% and an increase of survival rate from 20% to 90% due to a decrease in EI_{soot} by a

factor of 10. In Inamdar et al. [2013] and Lewellen et al. [2014], neglecting the Kelvin effect has a dramatic order-of-magnitude impact on particle survival rates for both young and aged contrails.

We address the important question of whether the observed discrepancies are due to modeling assumptions and differences in simulation initializations. In particular, we examine the impact of changing the Kelvin correction factor that raises the apparent vapor saturation pressure over a curved ice surface relative to a flat one, for a given temperature, T , as follows:

$$p_{sat}^{kelvin} = p_{sat}^{0} \exp\left(\frac{a_k}{r_p}\right) \quad | \quad a_k = \frac{2\sigma M_{H2O}}{RT\rho_p}$$

where r_p is the radius of curvature of the surface, σ is the ice-vapor surface tension, M_{H_2O} is the molecular mass of water, R is the universal gas constant, and ρ_p is the density of ice.

Exclusion of jet exhaust enthalpy is a common modeling assumption [Unterstrasser, 2014] as it is expected to not have any persistent impact. Keeping in mind that several in-situ measurements provide data for young contrails and that Unterstrasser [2014] observes a delayed onset of particle loss as compared to Naiman et al. [2011] and Inamdar et al. [2013], it is necessary to examine the impact of this assumption on the LES of young contrails.
The following cases were run to address the above mentioned issues:

Cases	Description	Legend
B0	$EI_{soot} = 10^{15}$, RHi = 130%, a_k = f(T)	solid black
B1	$EI_{soot} = 10^{15}$, RHi = 110%, a_k = f(T)	dashed black
B2	$EI_{soot} = 10^{15}$, RHi = 130%, $a_k = 10^{-9}$m	solid blue
B3	$EI_{soot} = 10^{15}$, RHi = 110%, $a_k = 10^{-9}$m	dashed blue
B4	$EI_{soot} = 10^{15}$, RHi = 130%, a_k = 0 m	solid red
B5	$EI_{soot} = 10^{15}$, RHi = 110%, a_k = 0m	dashed red
L0	$EI_{soot} = 10^{14}$, RHi = 130%, a_k = f(T)	solid green
L1	$EI_{soot} = 10^{14}$, RHi = 110%, a_k = f(T)	dashed green
L2	$EI_{soot} = 10^{14}$, RHi = 130%, $a_k = 10^{-9}$m	solid cyan
L3	$EI_{soot} = 10^{14}$, RHi = 110%, $a_k = 10^{-9}$m	dashed cyan
U0	Same as B0, but no jet exhaust enthalpy	solid magenta
U1	Same as B1, but no jet exhaust enthalpy	dashed magenta

Table 3: LES cases for sensitivity to Kelvin Effect

We observe that the cases with low EI_{soot} are indifferent to the Kelvin effect as lower EI_{soot} results in larger ice particles at our simulation initialization and the Kelvin correction affects smaller particles (typically < 0.1 μm). In Fig. 2 we have shown the particle survival rate and mean optical depth for cases with high EI_{soot}.

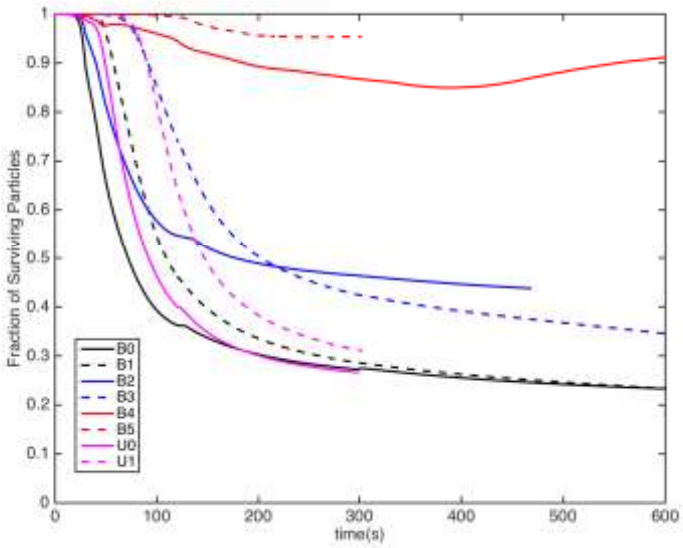

a)

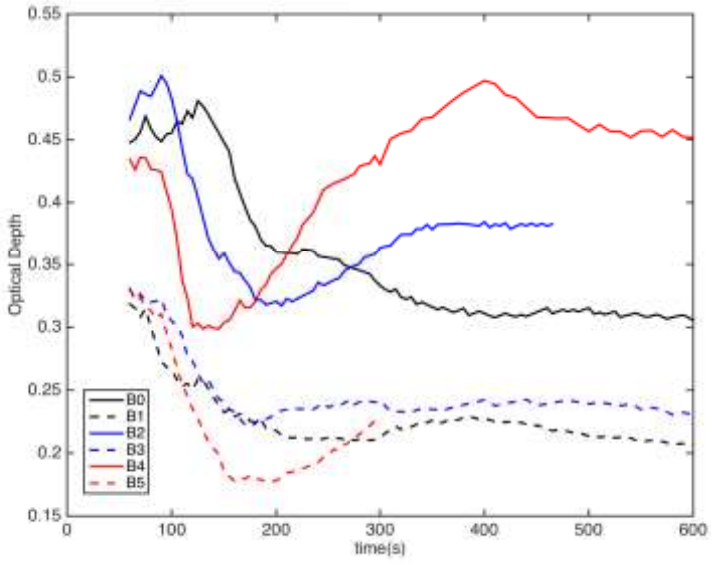

b)

Figure 2: (a) Particle Survival Rate (b) Mean Optical Depth

We can thus conclude the following:

1. The discrepancies in particle survival rates and sensitivities to RHi observed in LES of early contrails using different modeling approaches are primarily due to the different treatment of the Kelvin effect.
2. Particle survival rate and optical depth are the most sensitive to the treatment of the Kelvin effect for high EI_{soot}. This sensitivity is reduced to negligible by lowering the EI_{soot} by a factor of 10.

These results have been submitted to *Atmospheric Chemistry and Physics* [Inamdar et al., 2016, in review]. Results from all LES simulations performed so far are being compiled into a two-part paper [Inamdar et. al., 2016 (b,c)]. As a step towards this, our efforts at developing a reduced order ODE model for contrails up to the vortex phase has been presented [Inamdar et. al., 2016a] at this year's AIAA conference.

GATOR-GCMOM Simulations

GATOR-GCMOM is a one-way nested, online gas-aerosol transport, radiation, general-circulation, mesoscale, and ocean model [Jacobson et al., 2011, 2012, 2013; Whitt et al., 2011]. It is a RANS model that treats gas photochemistry, spectral radiative transfer, size- and composition-resolved aerosol and cloud microphysics and chemistry, dynamical meteorology, and ocean and soil processes. Gas, aerosol, meteorological, and radiative parameters have been evaluated against SCAQS, SARMAP, AERONET, IMPROVE, U.S. EPA monitoring, CARB monitoring, OMI satellite, MODIS satellite, AIRS satellite, and other data.

With respect to aircraft, GATOR-GCMOM treats the subgrid evolution of aircraft exhaust from individual flights with an analytical subgrid plume model (SPM) [Naiman et al., 2010, 2011; Cameron et al., 2013] coupled with a size-and-composition-resolved aerosol and contrail module [Jacobson et al., 2011]. The model also treats subgrid gas chemistry. Emissions from individual flights worldwide are obtained from the 2006 chorded Volpe emission inventory [Wilkerson et al., 2010].

GATOR-GCMOM model simulations are initialized by adding aircraft emissions to a subgrid-scale plume that expands over time, gradually entraining ambient air. Emissions include black carbon (BC), primary organic matter (POM), and sulfate [S (VI)] particulate matter, as well as gaseous water vapor (H_20), CO, CO_2, speciated total hydrocarbons (THCs), NO_x, and SO_2. Figure 3 shows the change in plume volume due to ambient wind shear and diffusion. At each 1-second time step, coagulation, condensation/evaporation, deposition/sublimation, plume expansion, and contrail dilution is solved as in Jacobson et al. [2011]. To more closely match ACCESS 2 measurements, the baseline scenario is run with parameters given in Table 4. The sensitivity of contrail ice and aerosol size distribution to changes in ambient relative humidity, fuel sulfur content, and black carbon emission index is explored below.

Table 4: Baseline scenario parameters for GATOR-GCMOM

Temperature	216.65 K	**Time Step**	1 second
Pressure	218.4 hPa	**# Vertical layers**	89
Altitude	10.7 km	**# Aerosol size bins**	100
RH-liquid, RH-ice*,+	45%, 76.9%	**Initial plume x-section**	7.5 m x 7.5 m
Fuel sulfur content*	600 ppmm		
BC emissions Factor*	0.03 g-BC/kg-fuel		

*Varied in sensitivity scenarios; + RH-liq=40% for Figures 12-14

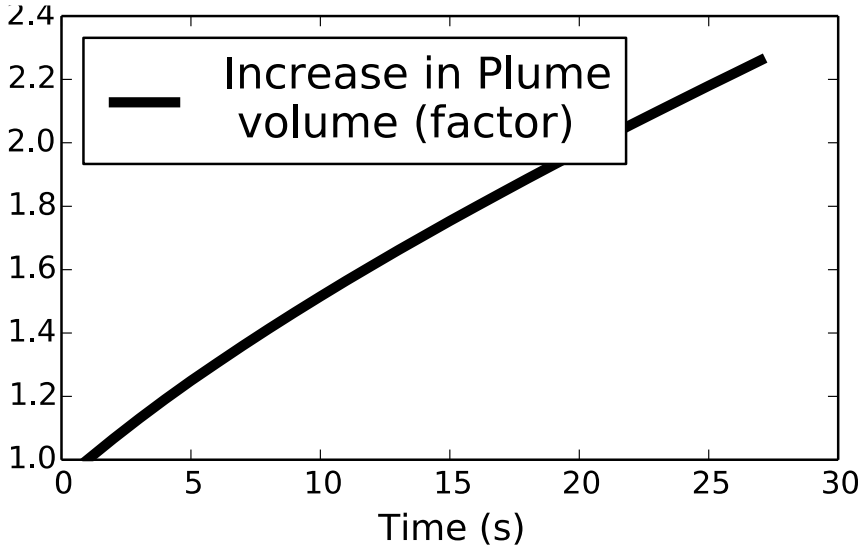

Figure 3: Change in plume volume over the lifetime of the 30-s simulation using GATOR-GCMOM

Baseline Scenario Results

Conditions for the baseline scenario yield aerosol size distributions shown in Figure 4. The contrail aerosols are initialized with a fossil fuel combustion aerosol size distribution shown in yellow ("t=0s") in Figure 4. After the first time step, particles with diameter ~0.03 to 0.2 μm coagulate to form larger particles, which then compete with smaller aerosols for available water vapor. After ~6 seconds, the uptake of all excess water vapor is complete, and RHi within the plume decreases such that evaporation begins (RHi < 100%). Figure 5 shows the change in contrail ice mass concentration as the entrainment of dry, ambient air outweighs the addition of vapor from exhaust. After 30 seconds, the in-plume ice concentration continues to decrease due to the low ambient relative humidity. The Kelvin effect, a result of surface tension on aerosols that increases the saturation vapor pressure over a curved surface relative to a flat surface, is displayed in Figure 4. The Kelvin effect allows water to evaporate more easily from smaller particles than larger particles. As a result, the smallest particles do not grow, and the largest particles scavenge water from the mid-size particles. After 30 seconds, the number concentration is bimodal, with peaks near 0.01 and ~1 μm.

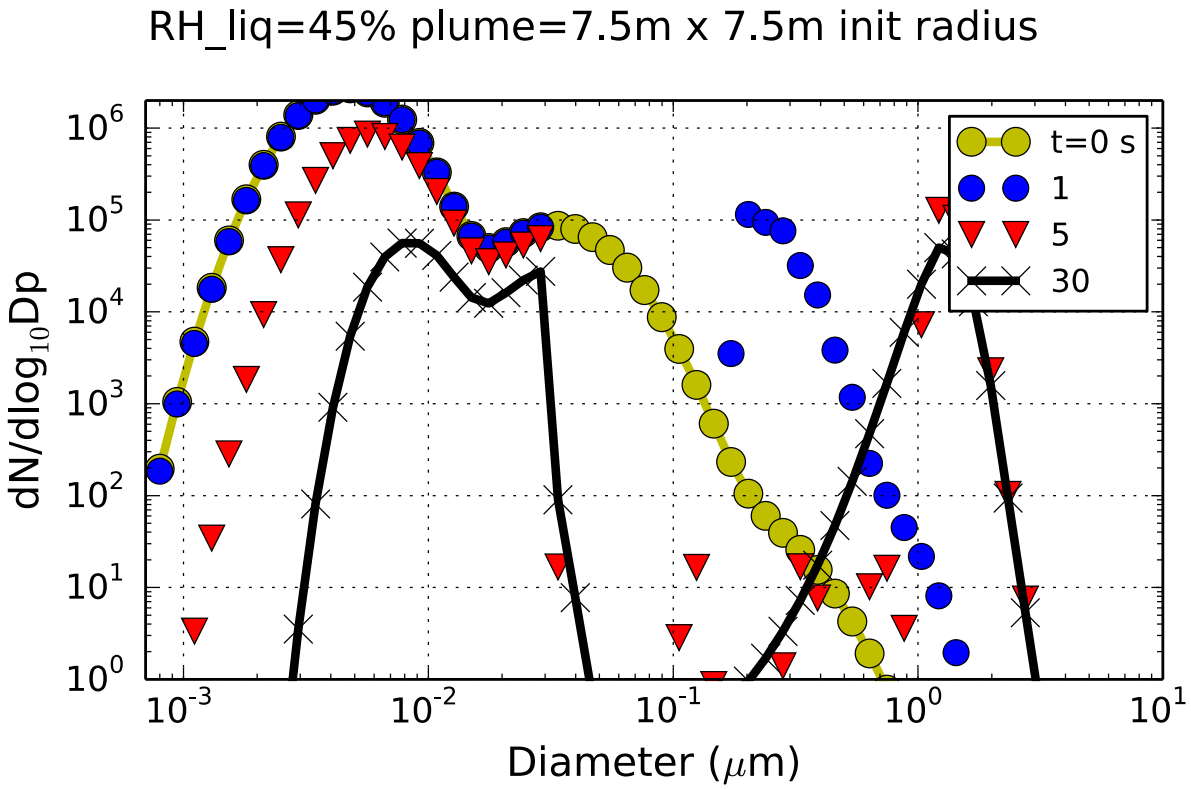

Figure 4: The base case aerosol size distribution (N = #/cm^3) at initialization (0 s) and after 1, 5, and 30 seconds using GATOR-GCMOM. Aerosol composition includes black carbon (BC), primary organic matter (POM), sulfate [S (VI)], and water vapor (H_20).

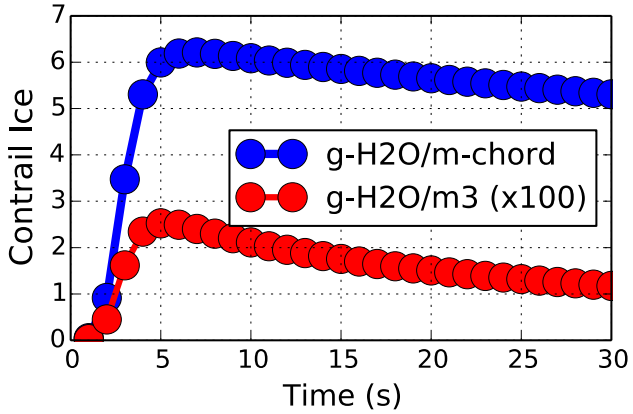

Figure 5: Change in contrail ice concentration (red: g/m^3) and ice concentration per meter of plume chord length (blue, g/m) using GATOR-GCMOM. Values in red are multiplied by 100 for scale.

Sensitivity to Relative Humidity

Figures 6 and 7 show the aerosol size distributions for simulations that vary ambient relative humidity on a logarithmic (left) and linear (right) scale after 23 simulation seconds. As in the baseline case, there is a decrease in small particles from coagulation after initialization, and a decrease in particles around ~0.1 μm from the Kelvin effect. As expected, simulations

with relative humidity below the baseline value of 45% show a more rapid loss of ice content, while simulations with higher humidity demonstrate more ice content (Figure 7). Beyond ~60% RH-liquid, volatile particles become saturated and there is no discernible difference from increasing humidity, shown by the overlapping yellow, orange, and red lines.

Sensitivity to Black Carbon Emissions

Figures 8 and 9 show the effects of black carbon emission indices on contrail development. A baseline value of 0.03 g-BC/kg-fuel ("100% Base" case) is representative of Jet-A fuel and the 50% value corresponds to a 50/50 Jet-A/HEFA biofuel blend. The results show that BC has a noticeable effect on the contrail size distributions, but does not significantly affect total ice content after several seconds. In general, a higher BC EI resulted in fewer smaller aerosols, an increase in larger aerosols, and a slight increase in contrail ice.

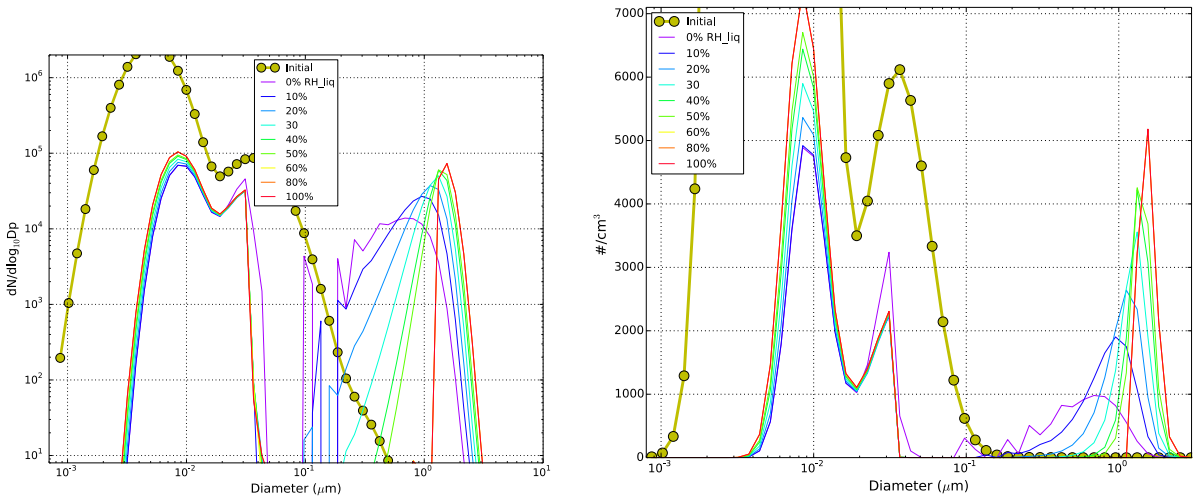

Figure 6: Aerosol size distribution after 23 seconds for simulations with varying ambient relative humidity (RH-liquid) using GATOR-GCMOM. Number concentration (N = #/cm^3) is normalized by size bin diameter (Dp) in the left figure.

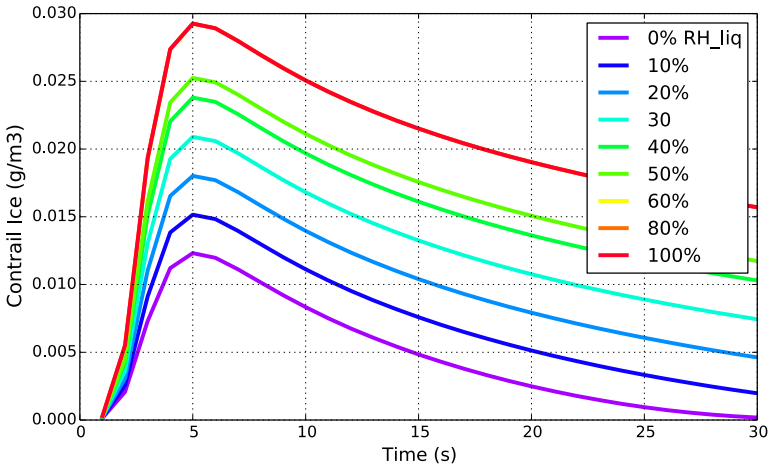

Figure 7: Contrail ice concentration for simulations that vary ambient relative humidity w.r.t. liquid using GATOR-GCMOM. Above 60% RH-liq, activated aerosols are saturated and additional increases in RH do not increase total ice content, shown by overlapping yellow, orange, and red lines.

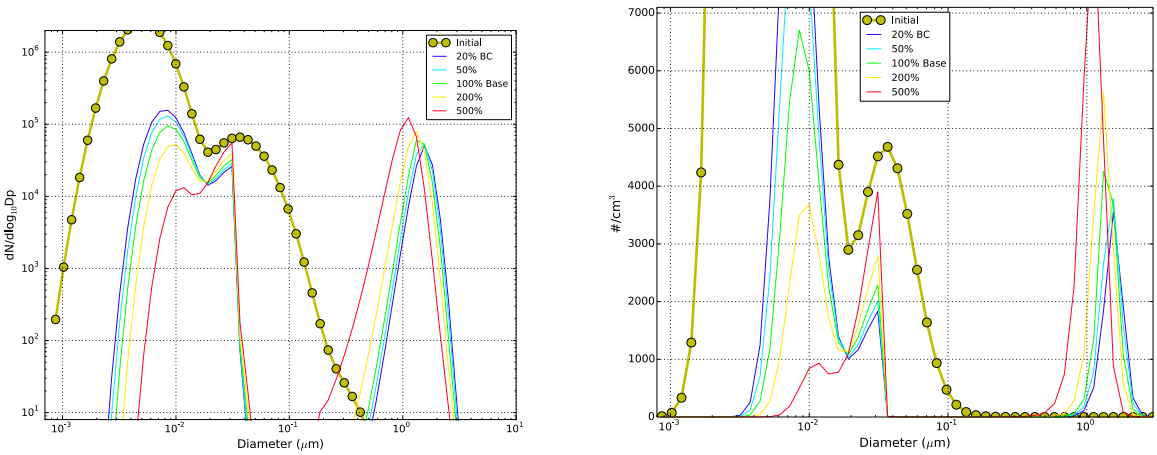

Figure 8: Aerosol size distribution after 23 seconds for simulations using GATOR-GCMOM that vary the BC emission index. Number concentration (#/cm^3) is normalized by size bin diameter (Dp) in the left figure.

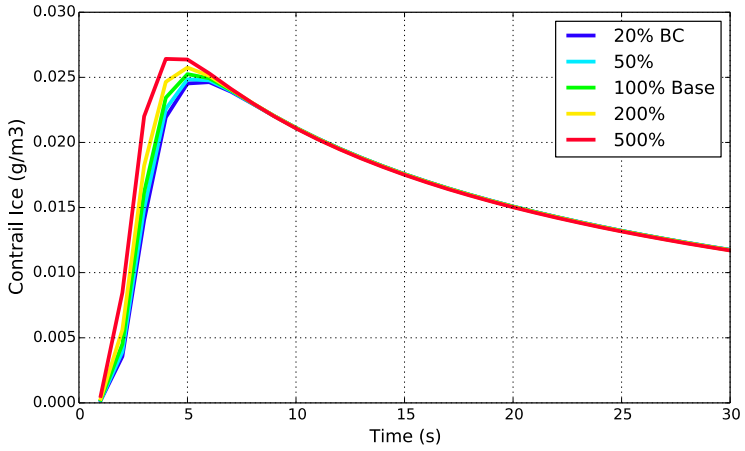

Figure 9: Contrail ice concentration for simulations using GATOR-GCMOM that vary the BC emissions index. An increase in BC results in more initial contrail ice, but the differences diminish after a few seconds.

Sensitivity to Fuel Sulfur Content

Figures 10 and 11 demonstrate the effects of fuel sulfur content (FSC) on aerosol size distribution and ice content after 23 seconds. As with the BC simulation, an increase in FSC showed an initial slight increase in ice content, a decrease in the number concentration of very small aerosols, and an increase in the number of larger aerosols. The baseline FSC is 600 ppmm. A 50/50 Jet-A/HEFA blend has a FSC ranging from ~10-20 ppmm, corresponding to the purple and blue lines in the figures below.

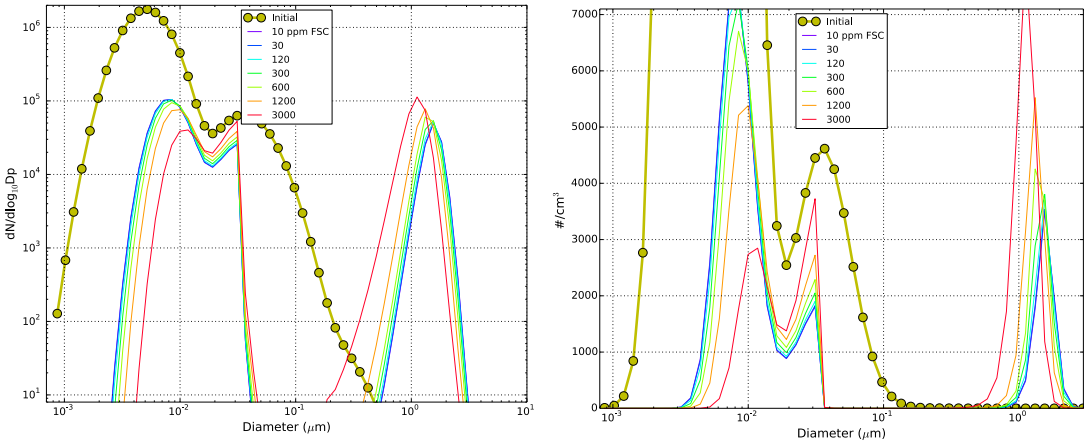

Figure 10: Aerosol size distribution after 23 seconds for simulations using GATOR-GCMOM that vary the fuel sulfur content. Number concentration (#/cm^3) is normalized by size bin in the left figure. The base case uses a FSC of 600 ppmm.

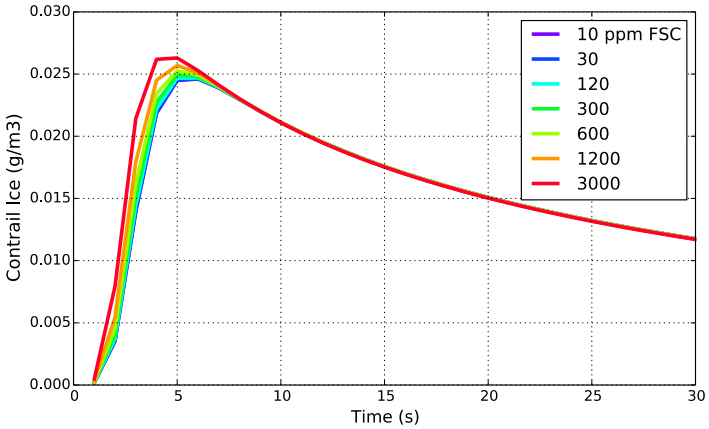

Figure 11: Contrail ice concentration for simulations using GATOR-GCMOM that vary the fuel sulfur content (ppmm). An increase in FSC results in more initial contrail ice, but the differences diminish with time.

Comparison of Model Results with Measurements

Figure 12 shows a comparison of the baseline scenario with contrail measurements taken from the ACCESS 2 campaign on May 29, 2014. This flight was chosen for analysis as it had the longest-lasting contrail, with plume measurements of up to 2 minutes. The size distributions, extracted from 4 instruments (CAS: Cloud and aerosol spectrometer, CIP: Cloud imaging probe, CDP: cloud droplet probe, and UHSAS: Ultra-High Sensitivity Aerosol Spectrometer) are filtered such that all missing data is removed and measurements were taken above 9km altitude. Furthermore, at different time segments, different instruments were directly in the exhaust, and so measurements for the other instruments were discarded. Finally, to further filter ambient data, only data that met at least 1 of the following 3 criteria were used: CO > 117 ppbv, $CO_{2,a}$ > 400 ppmv, and $CO_{2,b}$ > 420 ppmv, where $CO_{2,a}$ is the carbon dioxide mixing ratio taken from the Los Gatos CRD instrument, and $CO_{2,b}$ is the CO_2 mixing ratio measured on the CAS pylon. The age of the plume measurements is determined by the separation distance of the source (DC-8) and chase (NASA HU-25 Falcon) aircraft, and the Mach number of the DC-8. The resulting measurements, separated by age, are shown in the 9 panels of Figure 12. The baseline model size distributions at t=0, 1, 5, 10, 30, 60, 90, 120, 150, and 180 seconds are also shown in panels with data of the same age. For this GATOR-GCMOM simulations, relative humidity (liquid) is 40%.

As shown in Figure 12, the GATOR-GCMOM normalized number concentrations peak at aerosol diameters of 0.01, 0.03, and 1 micron after ~60 seconds. The threshold for the lowest measurable aerosol diameter (UHSAS instrument) is .06 microns, so the smaller GATOR-GCMOM peaks are undetectable. The CAS and CDP probes, however, both show peak number concentrations for aerosols ~1 micron in diameter, with those peak number concentrations close to the modeled GATOR-GCMOM peaks. The maximum CDP number concentrations near ~1um and GATOR-GCMOM results align quite well after 60 seconds (panels 6-9).

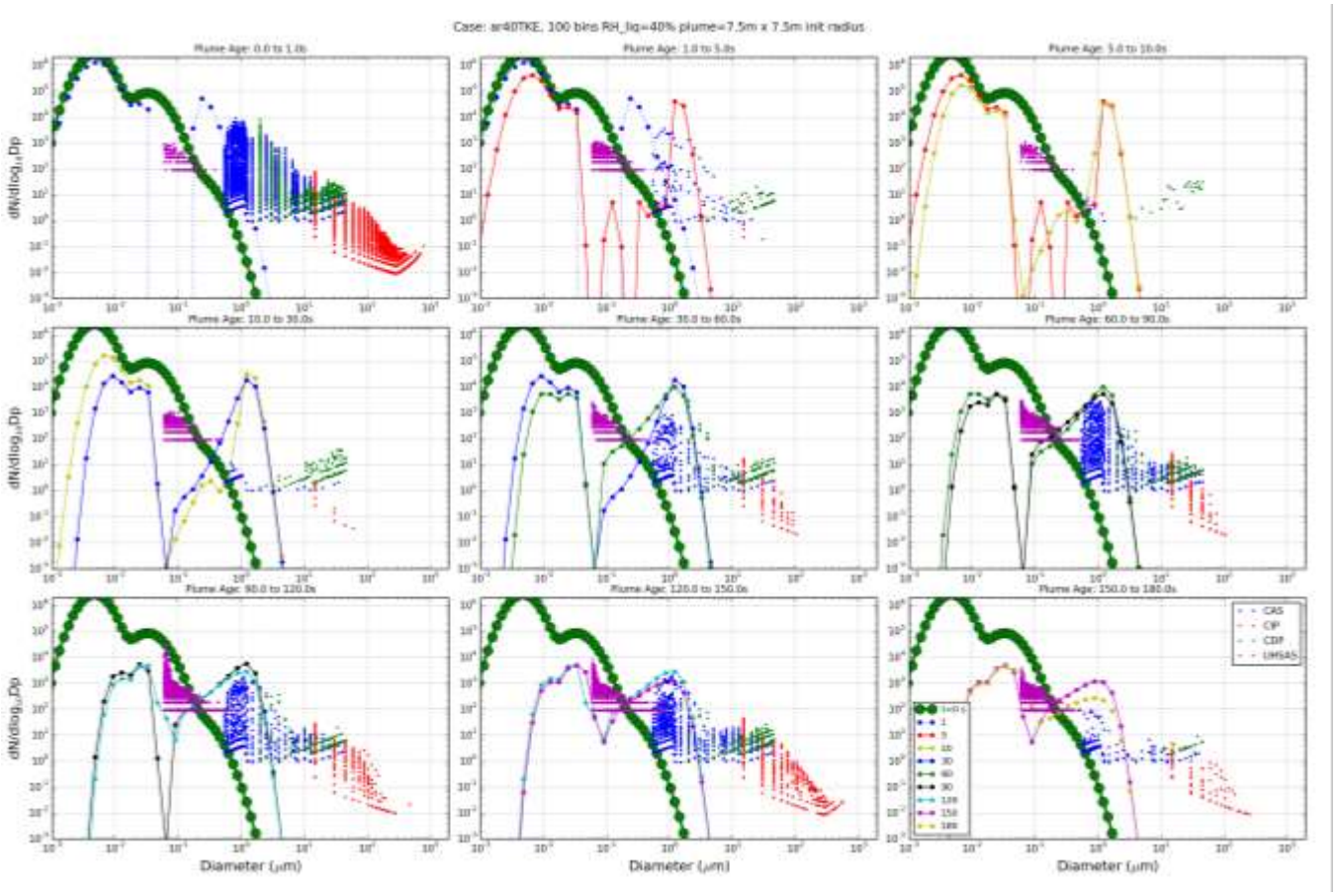

Figure 12: Measured contrail size distributions for the May 29, 2014 ACCESS 2 flight, filtered and separated by plume age. GATOR-GCMOM model results at t=0, 1, 5, 10, 30, 60, 90, 120, 150, and 180s are also shown in panels with data of the same age.

Comparison of GATOR-GCMOM and Aerodyne model results

Figures 13 and 14 show a comparison of model results from the baseline GATOR-GCMOM simulations at 40% (Fig. 13) and 80% (Fig. 14) ambient relative humidity with the Aerodyne simulations also at 40% and 80% RH. The initial distributions for both models are shown in all panels in green circles (GATOR-GCMOM) and red triangles (Aerodyne). The models have quite different initial size distributions, though both show contrail growth within a few seconds, as exhaust vapor raises the in-plume RHi. Both models show peak contrail sizes at or near 1 micron.

In the sub-saturated 40% RH scenario, the smaller aerosols in GATOR-GCMOM coagulate, reducing the number concentrations for smaller size bins within a few seconds. The Aerodyne model shows little change in the small (<.06 μm) size bins, and while initial in-plume supersaturation causes growth of the larger aerosols, the subsequent dehydration as the plume entrains drier ambient air causes the larger contrail particles to return to their initial size distribution (Figure 13, panel 8.) The GATOR-GCMOM distribution, on the other hand, does not return to the original distribution, despite also showing growth and evaporation from the change in plume relative humidity. This is a result of the coagulation of smaller particles into larger ones, that do not break apart after evaporation and thus maintain the larger distribution (Figure 13, panel 9).

In the super-saturated 80% RH scenario, both models show the growth of larger size bins as water freezes onto exhaust aerosols. Both models show number concentration peaks for larger particles in the 1-4 μm diameter range. Both models

also show an inhibition of growth of smaller particles beyond ~.03 μm as a result of the Kelvin effect. After ~115 seconds, both models show similar qualitative size distributions with peaks at similar locations, though the magnitude of the distributions vary (Figure 14, panel 8.) Again as in Figure 13, coagulation and growth of the smaller particles in GATOR-GCMOM results in a decrease in number concentration for those smaller particles.

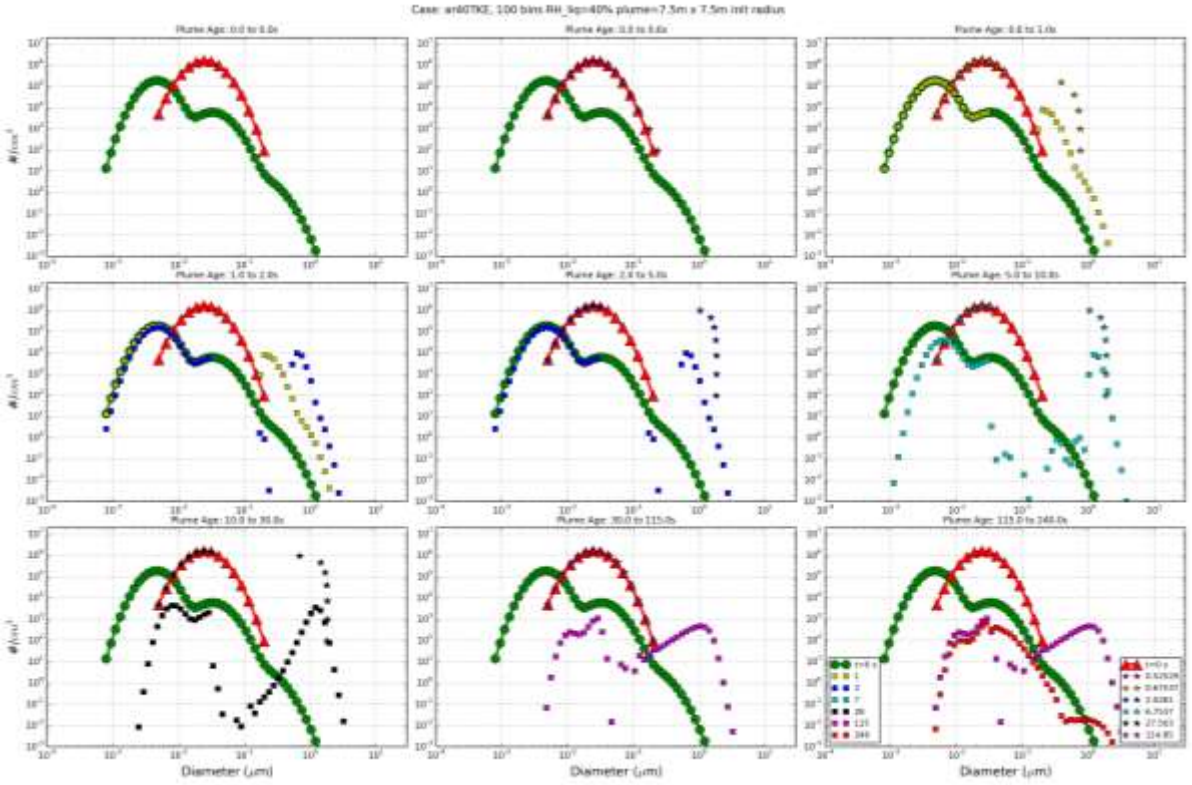

Figure 13: Comparison of GATOR-GCMOM (squares) and Aerodyne (stars) modeled number concentrations (#/cm^3) at 40% ambient relative humidity. Initial distributions for GATOR-GCMOM (green circles) and Aerodyne (red triangles) are also shown in each panel.

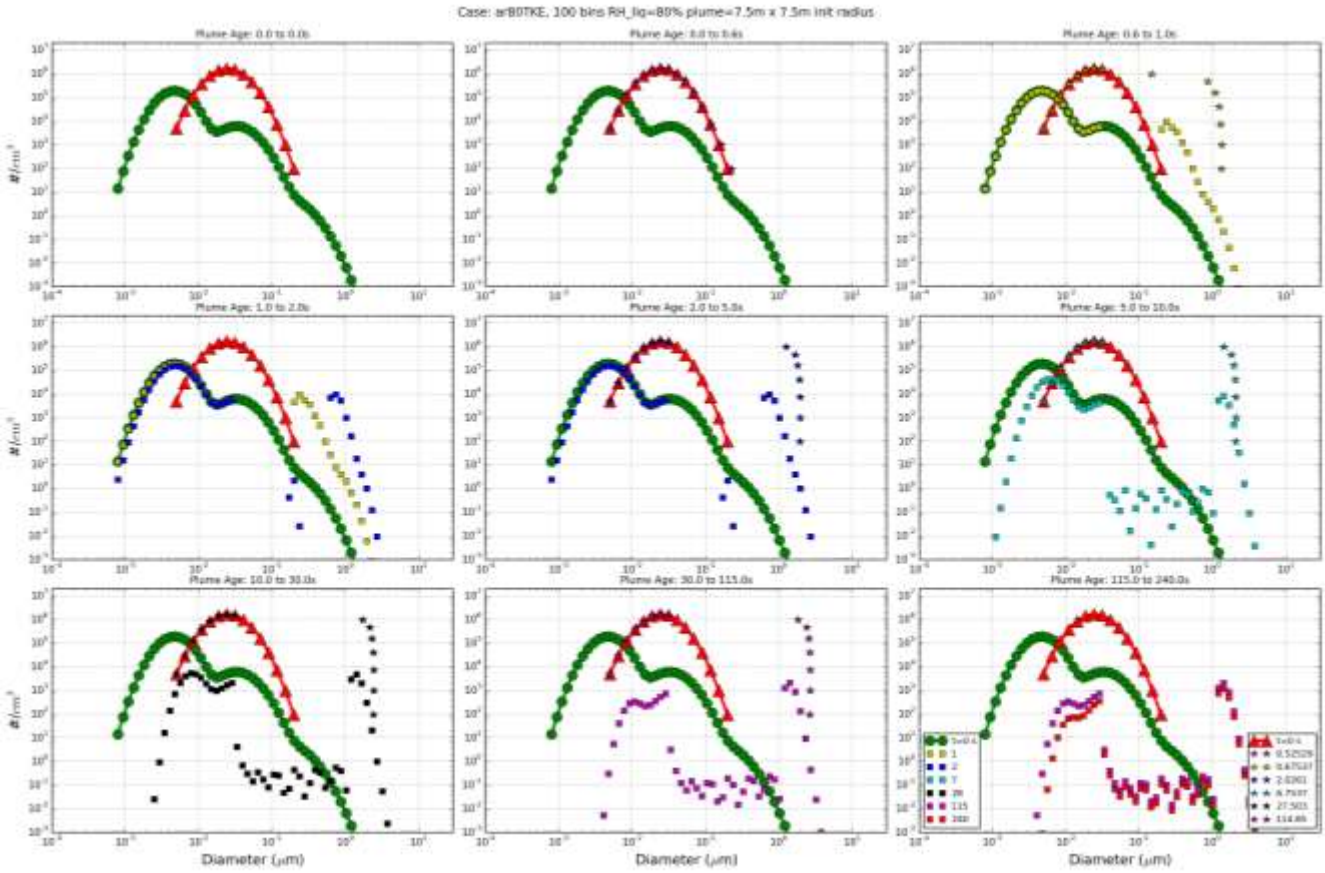

Figure 14: Comparison of GATOR-GCMOM (squares) and Aerodyne (stars) modeled number concentrations (#/cm^3) at 80% ambient relative humidity. Initial distributions for GATOR-GCMOM (green circles) and Aerodyne (red triangles) are also shown in each panel.

Future Research Directions

The present work helps illuminate the effects of alternative aviation fuels on contrail properties. However, additional analysis and comparison with measured data sets are required before firm conclusions on such effects can be made. At present, the available contrail size distribution data shows large measured contrail particles that may not be realistic. As data becomes available, it may be beneficial to reevaluate model results for comparison with more thoroughly filtered contrail measurements, including: (1) volatile and non-volatile aerosol number, mass, and composition, and (2) ice particle number and size. Datasets from partner institutions (DLR and Transport Canada) also involved in ACCESS-II measurement campaign may provide additional measurements from both the ACCESS 2 campaign, as well as the older CONCERT campaign that includes far-field (~10-20 minute) measurements. In particular, the completed 20-minute supersaturated LES and GATOR-GCMOM cases may be compared with the measured aged contrails from the CONCERT campaign for longer-lived contrail modeling.

References

Cameron, M.A., M.Z. Jacobson, A.D. Naiman, and S.K. Lele, Effects of plume-scale versus grid-scale treatment of aircraft exhaust photochemistry, *Geophys. Res. Lett., 40*, 5815-5820, 2013.

Inamdar A.R., Lele S.K., Jacobson M.Z., A Probabilistic Ice Habit Model for LES of Contrails, *5th Atmos. & Space Env. Conference*, AIAA control number 1586391, 2013.

Inamdar A. R., Lele S. K., and Jacobson M. Z., LES of Contrails With Ice Habit Treatment Using the Fickian-Distribution Model. ASME 4th Joint US-European Fluids Engineering Division Summer Meeting, 2014.

Inamdar A. R., Lele S. K., and Jacobson M. Z., Reduced Order Modeling of Contrails: Jet Induction and Vortex Phases, AIAA Conference, 2016a.

Inamdar A. R., Naiman A.D., Lele S. K., and Jacobson M.Z., Sensitivity of Particle Loss to the Kelvin Effect in Young Contrails, Atmospheric Chemistry and Physics Discussions, in review, 2016b.

Inamdar A. R., Naiman A.D., Lele S. K., and Jacobson M.Z., Sensitivity of Early Persistent Contrails to Aircraft Type, Ambient Conditions and Microphysical Modeling, Part I: LES Results, Atmospheric Chemistry and Physics, in progress, 2016b.

Inamdar A. R., Naiman A.D., Lele S. K., and Jacobson M.Z., Sensitivity of Early Persistent Contrails to Aircraft Type, Ambient Conditions and Microphysical Modeling, Part II: ODE Model Results, Atmospheric Chemistry and Physics, in progress, 2016c.

Jacobson, M.Z., J.T. Wilkerson, A.D. Naiman, and S.K. Lele, The effects of aircraft on climate and pollution. Part I: Numerical methods for treating the subgrid evolution of discrete size- and composition-resolved contrails from all commercial flights worldwide, J. Comp. Phys., 230, 5115-5132, doi:10.1016/j.jcp.2011.03.031, 2011, http://www.stanford.edu/group/efmh/jacobson/Articles/VIII/aircraftflights.html.

Jacobson, M.Z., J.T. Wilkerson, S. Balasubramanian, W.W. Cooper, Jr., and N. Mohleji, The effects of rerouting aircraft around the Arctic Circle on Arctic and global climate, *Climatic Change*, 115, 709-724, doi:10.1007/s10584-012-0462-0, 2012.

Jacobson, M.Z., J.T. Wilkerson, A.D. Naiman, and S.K. Lele, The effects of aircraft on climate and pollution. Part II: 20-year impacts of exhaust from all commercial aircraft worldwide treated individually at the subgrid scale, *Faraday Discussions*, *165,* 369-382*,* doi:10.1039/C3FD00034F, 2013, http://www.stanford.edu/group/efmh/jacobson/Articles/VIII/aircraftflights.html.

Lewellen, D.C., Meza, O., and Huebsch, W.W., Persistent Contrails and Contrail Cirrus. Part I: Large-Eddy Simulations from Inception to Demise, Journal of the Atmospheric Sciences, 71, 4399-4419, 2014.

Naiman, A.D., S.K. Lele, J.T. Wilkerson, and M.Z. Jacobson, Parameterization of subgrid aircraft emission plumes for use in large-scale atmospheric simulations, *Atmos. Chem. Phys.*, 10, 2551-2560, 2010.

Naiman, A.D., S.K. Lele, and M.Z. Jacobson, Large eddy simulations of contrail development: Sensitivity to initial and ambient conditions over first twenty minutes, *J. Geophys. Res.*, *116*, D21208, doi:10.1029/2011JD015806, 2011.

Naiman, A.D., Modeling Aircraft Contrails and Emission Plumes for Contrail Impacts, Ph.D. Dissertation, Stanford University, 2011.

Picot, J., Paoli, R., Thouron, O., Cariolle, D., Large-eddy Simulations of Contrail Evolution in the Vortex Phase and its Interaction with Atmospheric Turbulence, Atmospheric Chemistry and Physics, 15, 7369-7389, 2015.

Unterstrasser, S., Large-eddy Simulation Study of Contrail Microphysics and Geometry During the Vortex Phase and Consequences on Contrail-to-Cirrus Transition, Journal of Geophysical Research: Atmospheres, 119, 7537-7555, 2014.

Whitt, D.B., J.T. Wilkerson, M.Z. Jacobson, A.D. Naiman, and S.K. Lele, Vertical mixing of commercial aviation emissions from cruise altitude to the surface, *Journal of Geophysical Research.*, *116*, D14109, doi:1029/2010JD015532, 2011, www.stanford.edu/group/efmh/jacobson/Articles/VIII/aircraftflights.html.

Wilkerson, J.T., M.Z. Jacobson, A. Malwitz, S. Balasubramanian, R. Wayson, G. Fleming, A.D. Naiman, and S.K. Lele, Analysis of emission data from global commercial aviation: 2004 and 2006, *Atmos. Chem. Phys., 10*, 6391-6408, 2010, www.stanford.edu/group/efmh/jacobson/Articles/VIII/aircraftflights.html.

Project 014 Analysis to Support the Development of an Aircraft CO2 Standard

Georgia Institute of Technology
Massachusetts Institute of Technology
Booz Allen Hamilton

Project Lead Investigator

Co-lead by all participants listed below.

University Participants/Companies/Organizations

Georgia Institute of Technology (GT)

- P.I.(s): Prof. Dimitri Mavris, Dr. Michelle R. Kirby (Co-PI)
- FAA Award Number: 13-C-AJFE-GIT-003, Amendment 003
- Period of Performance: July 1, 2014 to January 31, 2016

Massachusetts Institute of Technology (MIT)

- P.I.(s): Prof. R. John Hansman
- FAA Award Number: P.O. DTRT5714P80095
- Period of Performance: Sept. 16, 2014 to Feb. 29, 2016

Booz Allen Hamilton (BAH)

- P.I.(s): Dr. Philippe Bonnefoy
- FAA Award Number: DTFAWA-14-D-00013
- Period of Performance: January 1st 2015 to February 2016

Project Funding Level

GT
Funded amount is $500,000 for the period of performance of July 1, 2014 to January 31, 2016. The Georgia Institute of Technology has agreed to a total of $500,000 in matching funds. This total includes salaries for the project director, research engineers, graduate research assistants and computing, financial and administrative support. The institute has also agreed to provide equipment funds as well as tuition remission for the students paid for by state funds.

BAH
FAA Award Number: DTFAWA-14-D-00013and DTRT57-10-D-30015
Period of Performance: September 2014 to February 2016
Project Funding Level: $363,900 FAA funding.

MIT
DOT Volpe TSC Award Number: P.O. DTRT5714P80095
Period of Performance: Sept. 16, 2014 to Feb. 29, 2016
Project Funding Level: $147,385.55 FAA funding and no matching funds. No source of match is required for this contract.

Investigation Team

GT
Prof. Dimitri Mavris, Dr. Michelle Kirby, Dr. Don Lim, Dr. Yongchang Li, Robert Moss (Graduate Student), Fatma Karagoz (Graduate Student)
MIT

Prof R. John Hansman (PI). Dr. Brian Yutko (I), Edward Mugica (Graduate Student), Morrisa Brenner (Graduate Student)
BAH:
Dr. Philippe Bonnefoy, Dominic McConnachie

Project Overview

The Federal Aviation Administration's Office of Environment and Energy (FAA/AEE) is working with the International Civil Aviation Organization's (ICAO) Committee on Aviation Environmental Protection (CAEP) to establish an international aircraft carbon dioxide (CO2) standard, which is a combination of a regulatory level and a certification requirement. The research team has been instrumental in the progress made to date within CAEP. The research team will utilize prior efforts to conduct a shadow cost benefit and cost effectiveness analysis of the 10 stringency options that have been established by CAEP in order to provide sound scientific information and insight to the FAA decision-making process.

Objectives

The objective of ASCENT Project 14 is to conduct analyses on the CO2 standard to shadow those being done internationally, in order to provide sound scientific information to the decision-making process. In particular:

- Continue support of CAEP CO2 standard setting process through the expected decision at the CAEP/10 meeting in Feb 2016
- Inform U.S. policy makers with analytical information for the CO2 standard setting process
- Provide a preliminary analysis of the CO2 cost-benefit analysis ahead of the CAEP cost-effectiveness assessment to ensure that U.S. policy makers are well informed of the expected outcomes and potential issues
- Address any emerging issues associated with various stakeholders in the process either in a quantitative or qualitative manner

Research Approach

- Conduct extensive cost benefit analysis using the full FAA Tool Suite, in order to inform the U.S. position for the development of an aircraft CO2 standard which will result in technology responses with the greatest environmental benefits while being technically feasible and economically viable
- Provide quantitative and methodological support of CO2 Standard Main Analysis modelling process
- Conduct sensitivity analyses in order to inform decision makers of potential outcomes under different scenarios and assumptions using the FAA Tool Suite, quantitative and qualitative research methods
- Actively engaging stakeholders using a data driven collaborative approach

Recent Accomplishment #1: Cost Benefit Analysis

ASCENT Project 14 team is conducting extensive cost benefit analysis using the full FAA Tool Suite, as depicted below, in order to inform the U.S. position for the development of an aircraft CO2 standard which will result in technology responses with the greatest environmental benefits while being technically feasible and economically viable.

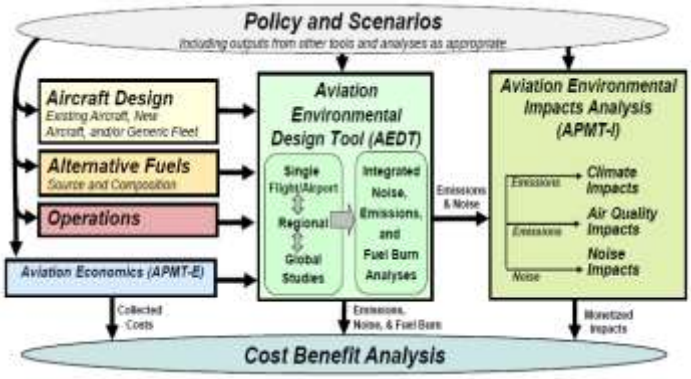

Figure 1: Depiction of FAA Tool Suite

Recent Accomplishment #2: CO2 Main Analysis Support

Research team has provided quantitative and methodological support of CO2 Standard Main Analysis modelling process, which is depicted below.

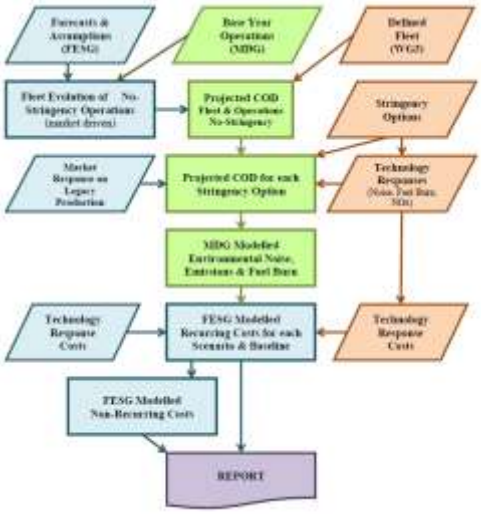

Figure 2: Illustration of the CO2 Standard Main Analysis

Recent Accomplishment #3: Sensitivity Analyses

The ASCENT Project 14 team is conducting sensitivity analyses in order to inform decision makers of potential outcomes under different scenarios and assumptions using the FAA Tool Suite, quantitative and qualitative research methods. A notional example of the sensitivity analysis is depicted below.

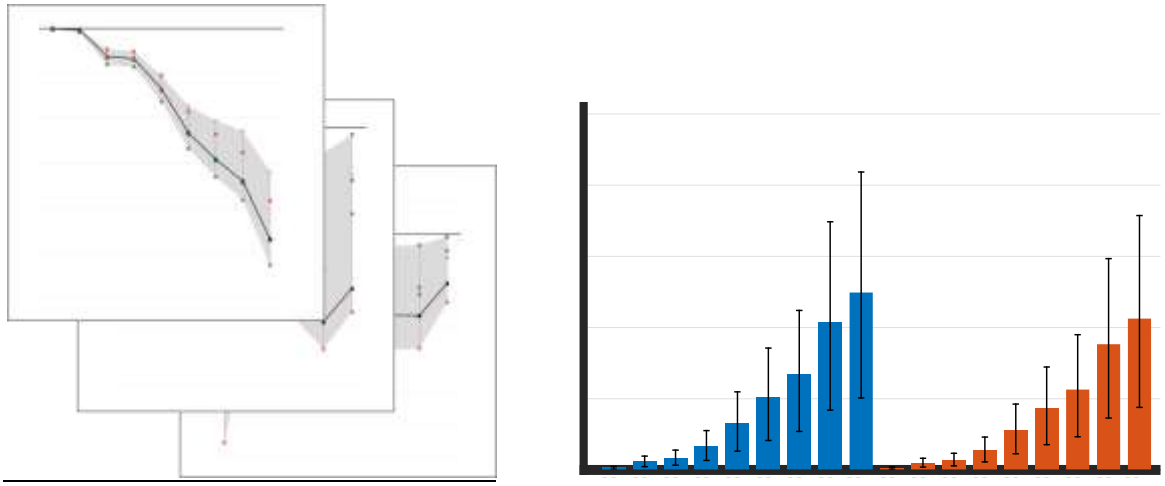

Figure 3: Illustration of sensitivity analyses

Recent Accomplishment #4: Stakeholder Analysis

ASCENT Project 14 team is actively engaging stakeholders using a data driven collaborative approach by quantifying the potential impact of the various CO2 Standard options on forecast fleet evolution, airline and manufacturer economic metrics, and interdependencies using the FAA Tool Suite

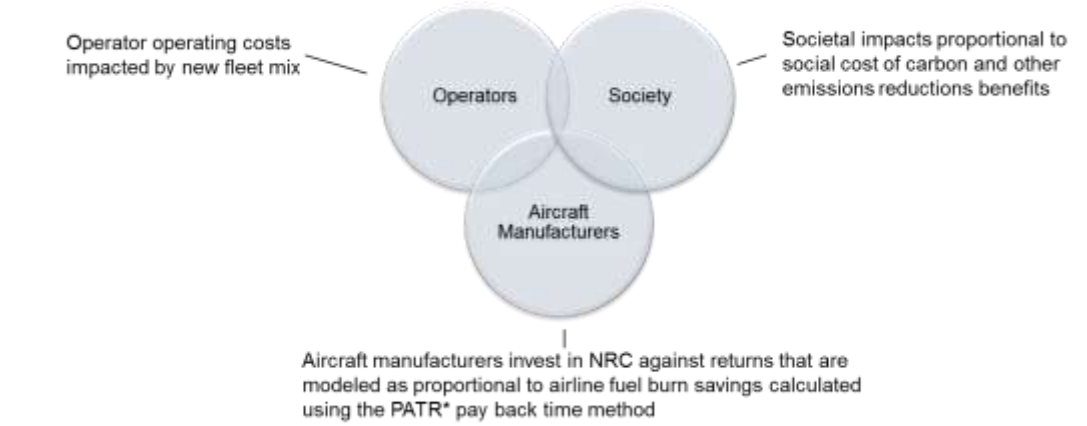

Figure 4: Illustration of Stakeholder Analysis

Recent Accomplishment #5: Green House Gas (GHG) Modeling in FAA's AEDT using Direct Transformation Approach

ASCENT Project 14 has been investigating how to perform GHG modeling in AEDT 2b. As a result, a direct transformation approach has been developed that can directly manipulating the database to create a GHG modeling study in AEDT for any size of schedule data generated from the APMT-E outputs. This approach used an empty AEDT study DB and developed SQL scripts to populate the data tables of the Study DB required to run AEDT analysis. To test this process, the 629 operation schedules given as part of BADA3 vs BADA4 comparison study in October 2014 were used as a test study. The direct transformation approach was successfully conducted on the test study, and the results generated by this approach were compared with the results produced by Volpe. It shows that most of the results have a good agreement with the results produced by Volpe, and for a small portion the flights (from 2 of 9 OD pairs), AEDT does not generate right results. The team is working with AEDT support team to resolve this inconsistency and will give the updates once it is accomplished.

Recent Accomplishment #6: Connecting CO2 Stringency Options

The ASCENT Project 14 team has developed a tool which can help the CAEP members to connect CO2 stringency options. Some of the CAEP Member States, including the United States, have proposed different SO lines for aeroplane types below and above the 60t MTOM kink point. If different SOs are selected, it would be necessary to agree on a method to join the SO lines. However, there are various methods that can be used to connect SOs, and it is recognized that no method is perfect or better than the other. The research team developed guiding principles that the connecting methods should meet.

The first guiding principal is to minimize market distortions. Considerations should be given to the magnitude of the impacts by the connecting method on the CO2 main analysis results. Depending on the selection of the SOs, some connecting methods may not have any impacts on aeroplane types (e.g. due to gaps or lack of aeroplane types) in the MV-MTOM space. Other connecting methods, however, may impact aeroplane types (e.g., fail, or imply a different technology response) and slightly perturb the CO2ma results from CAEP MDG/FESG.

The second guiding principle is to minimize impacts to aeroplane types above 60t MTOM. The connection of SOs should strive to avoid changing the regulatory level of the aeroplane type above 60t since the majority of the CO2 reduction benefits come from the aeroplane types above 60t. Therefore, perturbation of the SO lines below 60t due to a connecting method is likely to have fewer impacts on the CO2ma results than perturbation of the lines above 60t.

The third guiding principle is to avoid separating aeroplane type families. This principle address the concerns that, to the extent possible, avoid connecting SOs such that existing aeroplane type families are separated by a line between stringency options. Since this could create significant differences in margins to regulatory levels across aeroplane types within the same family (i.e., technology level) and could result in unintended consequences.

A few connecting methods were investigated and a decision support tool was developed to implement these methods, as shown in Figure 5. There are three methods implemented in this decision support tool, including plateau, fanning and plateau shift methods. The tool can allow the user to choose which two SOs to connect below and above 60t MTOM. In addition, the user can adjust the MTOM at left or right hand kink for different method. With these inputs (green cells in Figure 5) defined, the tool can interactively illustrate the blended SO line (red line). And it can also automatically filter out the aeroplane which are impacted by the blended SO, that is the aeroplane whose margin(s) to the SO line change after connecting. By using this tool, the user can effectively make decision on selecting the method which adhere to the guiding principles for connecting different SOs.

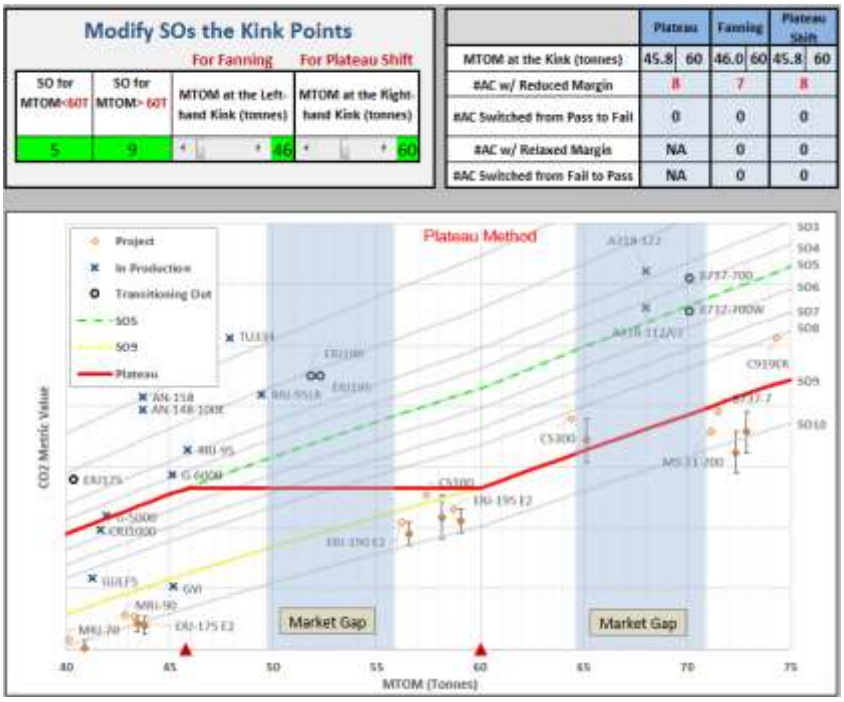

Figure 5: Decision Support Tool for Connecting SOs

Milestone(s)

- A14 supported U.S. policy maker to reach agreement with other CAPE members on the carbon standards for commercial aircraft at CAEP meeting
- A14 supported U.S. policy makers leading up to the July 2015 Steering Group Meeting in Montreal, Canada
- A14 is completing an extensive cost benefit analysis in order to inform the U.S. position for the development of an aircraft CO2 standard
- A14 to inform U.S. policy makers leading up to Feb 2016 CAEP CO2 standard decision
- Provide materials to support MDG/FESG and WG3 meetings during October 2015

Major Accomplishments

- The U.S. and 22 other countries reached agreement on the first-ever global carbon standards for commercial aircraft
- CAEP consensus on a functional CO2 Standard metric
- Systematic analysis process utilizing the FAA environmental tool suite
- Technical and data driven input into CAEP process
- Cost benefit analysis to inform U.S. policy makers and FAA team
- Future fleet evolution studies for CAEP and NextGen

Publications

CAEP Reports

- Guidance on Connecting CO2 Stringency Options (CAEP 10 IPXX Connecting SOs)
- COST-BENEFIT ANALYSIS… (CAEPx_SGx_IPxx_Cost-Benefit Analysis of CAEP10 CO2 Stringency Options)
- CO2 main analysis: Cost… (CAEPSG.201x.WPx.en_FESG-MDG)
- INVESTIGATION OF PRICE… (IP0x_MDG-FESG-STG-0x)
- POST-PROCESS IMPLEMENTATION OF PRICE… (IP0x_MDG-FESG-STG)
- CO2 MAIN ANALYSIS… (CAEPSG.201x.WP.x.3.en_MDG-FESG)
- CO2MAIN ANALYSIS: FUEL PRICE… (IP0x_MDG-FESG-STG-0x)
- CO2MAIN ANALYSIS: FUEL PRICE… (WP0x_MDG-FESG-STG-0x)
- Technology review… (CAEPx_WGx_CO2_WP0x)
- CO2 MAIN ANALYSIS: FRAMEWORK… (CAEPx_WGx_CO2-x_IP0x)
- CO2 MAIN ANALYSIS: FRAMEWORK… (presentation)

Outreach Efforts

- Participation at ICAO CAEP meeting in Montreal Canada, February 2016
- Participation at ICAO CAEP Steering Group 10 in Montreal Canada, July 2015
- Participation in ICAO CAEP MDG/FESG Meetings
  - Savannah, Georgia (January 2015)
  - Cologne, Germany (April 2015)
- Participation in ICAO CAEP WG3 Meetings
  - Belfast, United Kingdom
  - Washington D.C., U.S.A.
- Extensive interaction with Volpe
- Extensive support of interaction with Stakeholders
  - Manufacturers, Operators, NGOs, EPA
- Within ASCENT
  - Collaboration with ASCENT Projects 20, 21, and 24A on environmental impact modeling to assess value of the standard
  - Collaboration with ASCENT Projects 11A and 11B on fleet modeling
  - Collaborating with Volpe on the GHG modeling in AEDT2b

Awards

None

Student Involvement

Graduate students have been involved in all aspects of this research and have been key members of the team.

GT: Robert Moss (M.S. April 2015, employed), Fatma Karagoz (M.S. April 2015, transitioned to another project)
MIT: Edward Mugica (M.S. May 2015, employed), Morrisa Brenner (estimated: M.S. ’17, PhD ’20)
BAH: None

Plans for Next Period

None. Project is completed.

Project 015 Aircraft Operations Environmental Assessment: Cruise Altitude and Speed Optimization (CASO)

Massachusetts Institute of Technology

Project Lead Investigator

R. John Hansman
T. Wilson Professor of Aeronautics & Astronautics
Department of Aeronautics & Astronautics
MIT
Room 33-303
77 Massachusetts Ave
Cambridge, MA 02139
617-253-2271
rjhans@mit.edu

University Participants

MIT

- P.I.(s): Prof. R. John Hansman
- FAA Award Number: Lincoln Laboratory P.O. 7000213564
- Period of Performance: September 1, 2012 to June 30, 2017
- Task(s):
    1. Identify operations with high fuel reduction potential from CASO
    2. Present results and discuss operational considerations with stakeholders
    3. Develop set of recommended operating procedures to improve fuel performance in domestic operations through cruise altitude and speed optimization
    4. Extend analysis to specific long-haul operations
    5. Explore potential applications for CASO in NextGen concepts
    6. Support Lincoln Labs on refinements to Delayed Deceleration Approach analysis

Project Funding Level

Project Funding Level: MIT is performing as a subcontractor under Lincoln Laboratory which received FAA funding for this project. The MIT subcontract Award Value is $329,724.08 of which $313,196.18 has been released to MIT, and $18,527.90 is identified as Future Funding. No matching funds are required for this contract.

Investigation Team

Prof R. John Hansman (PI)
Luke Jensen (Graduate Student)
Clement Li (Graduate Student)
Henry Tran (Graduate Student)
Sarah Folse (Graduate Student)

Project Overview

This purpose of this project is to examine the potential fuel burn benefits of altitude and speed optimization in the cruise phase of flight for domestic operations in the United States and certain long-haul operations. In addition, the project aims to identify practical and implementable applications for CASO in NextGen concepts (cockpit, ATC, or dispatch).

Airlines can achieve cost reductions and mitigate environmental impact by making small modifications to the cruise phase operating condition. With coordination between air traffic controllers, pilots, and airline dispatchers, the efficiency of air transport activities can be improved. The first phase of this project built off prior work in this area to establish best-case benefits from cruise optimization. High-benefit operations and implementation considerations within the NAS were identified. In order to achieve these objectives, cruise-phase fuel burn estimation software was developed using publicly-available radar tracks and weather data. This estimator was used to examine over 200,000 flights from 2012 and 2015 for optimization potential, with additional follow-on analysis of more recent data from domestic and international operations.

The fuel efficiency of an aircraft at any point along its flight path is a function of weight, altitude, speed, wind, temperature, and other second-order effects. At a fixed weight, there exists a combination of speed and altitude at which instantaneous fuel efficiency is maximized, as shown in **Figure 1** for a typical widebody long-range airliner. For a full flight, this becomes an optimal sequence of speeds and altitudes to minimize fuel consumption [3]. The speed and altitude at which aircraft are actually flown may differ from this optimal point for a variety of operational and practical reasons. Integrated fuel consumption depends on effective trajectory planning in speed and altitude as well as in lateral flight path. Several examples in the literature demonstrate potential techniques and applications for single-flight trajectory optimization in lateral, vertical, and temporal dimensions (e.g. [4]–[11]). This project aims to perform retrospective analysis using single-flight optimization methods and develop potential operational applications.

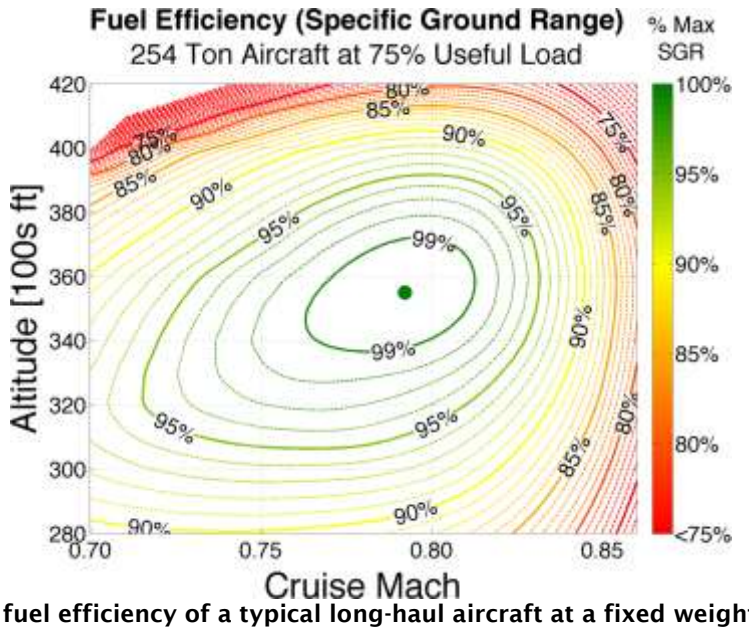

Figure 1. Instantaneous fuel efficiency of a typical long-haul aircraft at a fixed weight (calm winds, standard atmosphere)

This effort has recently focused on the development of a prototype decision support tool (DST) for use in pilot tactical enroute planning decisions. This DST incorporates feedback from multiple stakeholders including pilots, air traffic controllers, and airline dispatchers to provide timely and pertinent data to pilots pertaining to optimal altitudes and speeds, altitude planning, weather, and path change scenario testing. The DST prototype interface is shown in Figure 2**Error! Reference source not found.**. Next steps include further development, user refinement and testing of this tool as a means to realize benefits from CASO in an operational setting.

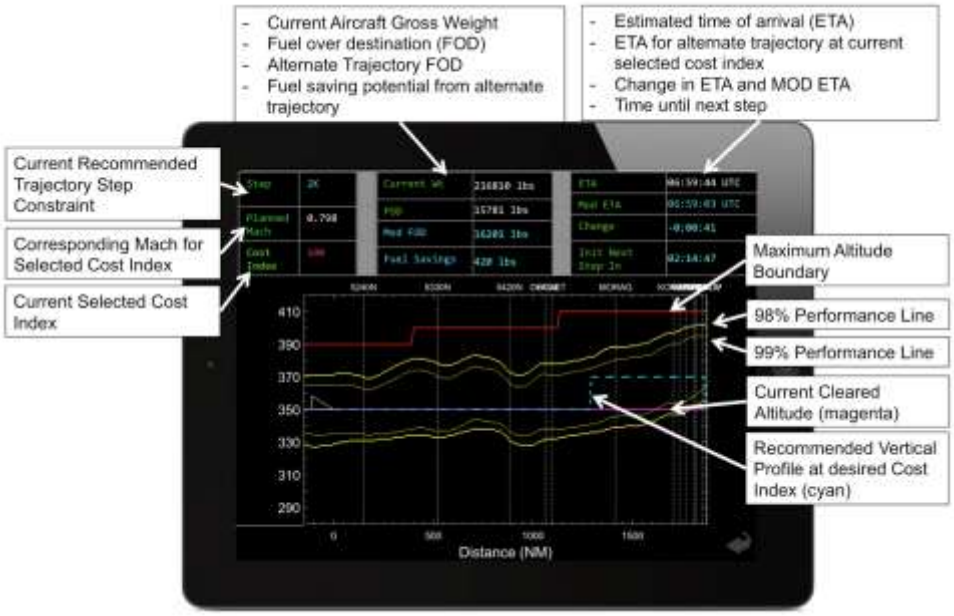

Figure 2. Prototype interface for a tablet-based CASO Decision Support Tool

Task Progress and Plans

Task 1: Identify operations with high fuel reduction potential from CASO
Based on the distribution of benefits evident in the first part of this project, it was clear that some types of operations (i.e. airlines, aircraft types, and routes) had larger benefit potential from CASO implementation than others. Therefore, one objective of this phase of the project is to characterize current operations by type and identify particularly high-benefit candidates for cruise phase optimization. Potential drivers for off-optimal flight conditions, such as airspace congestion or weather impacts, can be investigated at this stage to inform discussions with stakeholders. This task has involved data analysis of cruise fuel saving potential decomposed by airline, aircraft type, origin and destination, and ATC sector. Results based on 2011 and 2015 data showed reduced fuel saving potential from speed optimization in 2015 than in 2011 but more from altitude optimization. A second analysis approach has also identified flights with fuel saving potential because they arrived at their destination early relative to the scheduled time. These flights had the potential to slow down to a more fuel efficient speed without impacting the airline schedule in any way.

Task 2: Present results and discuss operational considerations with stakeholders (airlines and air traffic controllers)
In order to implement CASO concepts in operational contexts, it is necessary to understand system efficiency drivers from the airline and ATC perspectives. Therefore, an objective of this research is to meet with airline operational departments, dispatchers, pilots, and air traffic controllers to discuss the cruise efficiency analysis results generated under Task 1. Based on these meetings, the reasons for particular airline-specific or type-specific results can be understood and incorporated into implementation suggestions. Opportunities for improvement in meaningful, short-term operational contexts can be identified based on these meetings. This task is consisting of a series of in-person and/or remote meetings where results from relevant CASO analysis is being presented in a manner tailored to the specific stakeholder to communicate the opportunity and gather feedback on operational barriers. Results of the analysis have been presented to a number of airlines over the past year, In particular, consultations with Delta Airlines and United Airlines are on-going. This task also entails communicating key findings in technical publications and discussions with other sponsor-recommended groups.

Task 3: Develop set of recommended operating procedures to improve fuel performance in domestic operations through cruise altitude and speed optimization

Based on analysis of historical flight records and discussions with airlines, operational procedures to improve cruise-phase altitude and speed efficiency are being proposed. Areas of potential application include flight planning, tactical altitude and speed assignment, and cockpit procedures. This objective may include development of cockpit and/or controller decision support tools, efficiency evaluation algorithms, or other tools that can be integrated within the existing air transportation infrastructure based on stakeholder input. One particular implementation opportunity being pursued includes utilizing Electronic Flight Bag (EFB) technologies. These could provide improved situational awareness to pilots of current cruise status and potentially more efficient cruise altitude and speed options which could be requested from ATC. EFB display concepts for this use have been developed, and a web survey to elicit input from pilots on EFB functionality has been conducted. Next steps include further development, user refinement and testing of this tool as a means to realize benefits from CASO in an operational setting.

Task 4: Extend analysis to specific long-haul operations
The initial phase of this project focused on domestic US analysis. International and long-haul operations consume a larger amount of fuel in cruise, on an absolute and percentage basis, than short-haul small-gauge flights. Therefore, the environmental and economic impact of fuel burn reduction for these operations may be significant. The analysis framework has been expanded to incorporate data sets other than the FAA flight records and domestic NOAA weather models used in the early stages of the project. Analysis of the cruise altitude and speed efficiency of the North Atlantic Tracks have been conducted under this task based for 4033 flights over 12 days from 2014-2015. It was found that operation at optimal altitude and speed led to a 2.83% fuel reduction potential in average, and 1.24% reduction with optimal altitude alone. These compare to 3.7% from combined altitude and speed optimization and 1.96% from altitude optimization alone in domestic operations.

Task 5: Explore potential applications for CASO in NextGen concepts
Fuel benefits from CASO exist in both current and future operations. This project has potential applications to several concepts in the NextGen ATM framework. Specifically, optimal speed and altitude allocation can be applied to Time-based flow management (TBFM) and four-dimensional trajectory based operations (4DTBO). For example, many flights currently fly faster than their fuel-optimal speed only to incur delay when nearing the destination airport. One concept of operations which could be explored under this task involves using a 4D-TBO procedure which imposes a Required time of Arrival (RTA) at the arrival TRACON with sufficient lead-time to allow operators to plan departure times and/or flight speeds at nearer to the fuel-optimal point while still achieving the same wheels-ON time. With effective information sharing and technology infrastructure, efficiency can play a role in congestion management. The priority level of this was reduced by the sponsor and as such no detailed analysis of these opportunity areas has been conducted.

Major Accomplishments

- Met with technical pilot groups from multiple airlines (United, American, Southwest, Jetblue, Lufthansa).
- Completed retrospective data analysis of nearly 500,000 domestic US and long haul flights on the North Atlantic Tracks.
- Extended CASO domestic analysis to include 2015 data.
- Developed prototype interface for tablet-based cockpit decision support tool.
- Developed online human-in-the-loop (HITL) interface survey for airline pilots, obtained preliminary feedback.

Publications

Folse, S., Tran, H., Jensen, L., & Hansman, R. J. (2016). Cruise Altitude and Speed Optimization Implemented in a Pilot Decision Support Tool. In 16th AIAA Aviation Technology, Integration, and Operations Conference (p. 4211).

Jensen, L., Tran, H., & Hansman, J. R. (2015). Cruise Fuel Reduction Potential from Altitude and Speed Optimization in Global Airline Operations. In Eleventh USA/Europe Air Traffic Management Research and Development Seminar (ATM2015), Lisbon, Portugal.

Jensen, L., Hansman, R. J., Venuti, J., & Reynolds, T. (2014). Commercial airline altitude optimization strategies for reduced cruise fuel consumption. In 14th AIAA Aviation Technology, Integration, and Operations Conference (p. 3006).

Jensen, L., Hansman, R. J., Venuti, J. C., & Reynolds, T. (2013). Commercial airline speed optimization strategies for reduced cruise fuel consumption. In 2013 Aviation Technology, Integration, and Operations Conference (p. 4289).

Outreach Efforts

Meetings with Delta, United, American, and Jetblue technical groups (fuel efficiency, flight planning, and pilots). Additional outreach with USAF Air Mobility Command regarding potential military applications of CASO concepts.

Awards

Luke Jensen selected ASCENT 2014 Student of the Year.

Student Involvement

Graduate students have been involved in all aspects of this research and have been the key implementers.

References

[1] R. Kar, P. A. Bonnefoy, and R. J. Hansman, "Dynamics Of Implementation Of Mitigating Measures To Reduce CO2 Emissions From Commercial Aviation," 2010.

[2] K. B. Marais, T. G. Reynolds, P. Uday, D. Muller, J. Lovegren, J.-M. Dumont, and R. J. Hansman, "Evaluation of potential near-term operational changes to mitigate environmental impacts of aviation," *Proc. Inst. Mech. Eng. Part G J. Aerosp. Eng.*, Jul. 2012.

[3] H. H. Hurt Jr., *Aerodynamics for Naval Aviators*, no. January. Navair, 1965.

[4] J. T. Betts, "Survey of Numerical Methods for Trajectory Optimization," *Journal of Guidance, Control, and Dynamics*, vol. 21. pp. 193–207, 1998.

[5] G. Huang, Y. Lu, and Y. Nan, "A survey of numerical algorithms for trajectory optimization of flight vehicles," *Sci. China Technol. Sci.*, vol. 55, pp. 2538–2560, 2012.

[6] D. M. Pargett and M. D. Ardema, "Flight Path Optimization at Constant Altitude," *Journal of Guidance, Control, and Dynamics*, vol. 30. pp. 1197–1201, 2007.

[7] A. Filippone, "Cruise altitude flexibility of jet transport aircraft," *Aerosp. Sci. Technol.*, vol. 14, pp. 283–294, 2010.
[8] D. Rivas, O. Lopez-Garcia, S. Esteban, and E. Gallo, "An analysis of maximum range cruise including wind effects," *Aerosp. Sci. Technol.*, vol. 14, pp. 38–48, 2010.

[9] L. Delgado and X. Prats, "Fuel consumption assessment for speed variation concepts during the cruise phase," in *Conference on Air Traffic Management (ATM) Economics*, 2009.

[10] L. Delgado and X. Prats, "En Route Speed Reduction Concept for Absorbing Air Traffic Flow Management Delays," *J. Aircr.*, vol. 49, no. 1, pp. 214–224, Jan. 2012.

[11] E. T. Turgut, M. Cavcar, O. Usanmaz, A. O. Canarslanlar, T. Dogeroglu, K. Armutlu, and O. D. Yay, "Fuel flow analysis for the cruise phase of commercial aircraft on domestic routes," *Aerosp. Sci. Technol.*, vol. 37, pp. 1–9, 2014.

Project 016 Airport Surface Movement Optimization

Massachusetts Institute of Technology
Massachusetts Institute of Technology Lincoln Laboratory

Project Lead Investigator

Hamsa Balakrishnan
Associate Professor
Aeronautics and Astronautics
Massachusetts Institute of Technology
77 Massachusetts Ave, 33-328, Cambridge, MA 02139
(617) 253 6101
hamsa@mit.edu

University Participants

MIT Lincoln Laboratory

- Tom Reynolds
- FAA Award Number: IA # DTFAWA-11-X-80007, FAA Task # 18
- Period of Performance: 1 April 2015 to 31 May 2016
- Task(s):
    1. Site adaptation to different airports
    2. Analysis of the impacts of departure metering in different operating environments
    3. Identification and evaluation of barriers to implementation
    4. Design of implementation protocols and field-testing at selection of study airports
    5. Coordination with Advances Surface Management Programs

MIT

- Hamsa Balakrishnan
- Lincoln subcontract number: Purchase Order 7000332744
- Period of Performance: 1 September 2015 to 31 August 2016
    6. See tasking above

Project Funding Level

$100,000

Investigation Team

Hamsa Balakrishnan (PI -- MIT), Tom Reynolds (PI – MIT Lincoln Laboratory), Patrick McFarlane (graduate student researcher, MIT), Sandeep Badrinath (graduate student researcher, MIT), Melanie Sandberg (associate staff, MIT Lincoln Laboratory).

Project Overview

Aircraft taxiing on the surface contribute significantly to fuel burn and emissions at airports. The quantities of fuel burned as well as different pollutants such as carbon dioxide, hydrocarbons, nitrogen oxides, sulfur oxides and particulate matter are proportional to the taxi times of aircraft, in combination with other factors such as the throttle settings, number of engines that are powered, and pilot and airline decisions regarding engine shutdowns during delays. Domestic flights in the United States in 2008 emitted about 6.6 million US tons of CO_2, 49,000 US tons of CO, 8,800 US tons of NOx, and

4,400 US tons of HC taxiing out for takeoff; almost half of these emissions occurred at the 20 most congested airports in the country. Similar trends have been noted at major airports in Europe, where it is estimated that aircraft spend 10-30% of their flight time taxiing, and that a short/medium range A320 expends as much as 5-10% of its fuel on the ground. The purpose of the Airport Surface Movement Optimization study is to show that a significant portion of these impacts can be reduced through "technologically-lightweight" operational measures to limit airport surface congestion.

A simple airport congestion control strategy would be a pushback policy aimed at reducing congestion on the ground that would consider the situation on the airport surface (also called the state). The N-control strategy is one such approach, and was first considered in the Departure Planner project. Several variants of this policy have been studied since in literature. The policy is effectively a simple threshold heuristic: if the total number of departing aircraft on the ground exceeds a certain threshold, further pushbacks are stopped until the number of aircraft on the ground drops below the threshold. In our early analysis we discovered that this form of discrete, on-off control strategy was difficult to implement in practice, and could also be overly reactive, potentially leading to instability. By contrast, the pushback rate control strategy that we have developed and tested at Boston Logan International airport (BOS) does not stop pushbacks once the surface is in a congested state, instead it regulates the rate at which aircraft pushback from their gates during high departure demand periods so that the airport does not reach undesirably high congested states. This document summarizes the Phase 2 efforts, including site selection criteria and developing techniques for characterizing airport surface operations, in order to enable the adaptation of a given congestion management approach to different airports, and the comprehensive evaluation of implementations.

As part of this project, MIT undertook an initial assessment of the applicability and potential benefits of "light-weight" airport-wide surface management control concepts involving minimal levels of automation to complement other Federal Aviation Administration (FAA) surface congestion management programs. It involved defining and modeling surface management control schemes, implementing them in a field demonstration at Boston Logan International airport, and evaluating performance in terms of impacts on taxi time, fuel burn and environmental emissions. During 15 four-hour tests conducted during the summers of 2010 and 2011, fuel use was reduced by an estimated 23-25 US tons (6,600-7,300 US gallons), while carbon dioxide emissions were reduced by an estimated 71-79 US tons. These savings were achieved with average gate-holds of just 4.7 min, and savings of 114-128 lb of fuel per gate-held flight. In addition to these savings achieved during field trials, many important lessons were learned regarding operational implementation of surface management techniques in both nominal and off-nominal conditions.

Most prior research (including this project to date) has focused on demonstrations of a proposed congestion management approach at a particular airport, and not on the adaptation of a particular approach to a range of airport operating environments. The current focus of this project addresses the challenges involved with adapting any class of surface congestion management approaches to different airports. Data and case studies from New York's LaGuardia Airport and Philadelphia International Airport are used to illustrate the diversity in operating environments. In particular, the MIT team has developed techniques for characterizing airport surface operations using site surveys and operational data. These characterizations are used for the adaptation of a given congestion management approach to different airports, and for the comprehensive evaluation of implementations.

Integration of Departure Metering Concepts into Surface Capabilities

Objective(s)

The objectives of this project are to conduct an initial assessment of the applicability and potential benefits of relatively easy-to-implement airport-wide surface management control concepts involving minimal levels of automation and procedural modifications, to complement other FAA surface congestion management programs. Phase 1 involved defining and modeling surface management control schemes, implementing them in a field demonstration at Boston Logan International airport, and evaluating performance in terms of impacts on taxi time, fuel burn and environmental emissions. Phase 2, conducted during FY14 and 15, is exploring adaptation of the approach to other airport locations with very different operating characteristics to help understand and inform requirements for more general deployment in future FAA decision support tools.

Research Approach

Framework for adapting approaches to different operating environments

This study has identified the overall process for designing a congestion management approach illustrated in Figure 1. The main steps involved in this process are: (1) Airport Selection, where an airport with surface congestion problems are identified; (2) Airport Characterization, where the details of the operation relevant to surface congestion management at an airport are identified; (3) Algorithm Development, where specific surface congestion management approaches are created; (4) Implementation Design, where the protocols of the execution of the algorithms are developed for the airport; and (5) Operational Testing and Performance Evaluation, where the approach is tested and evaluated in the operational setting.

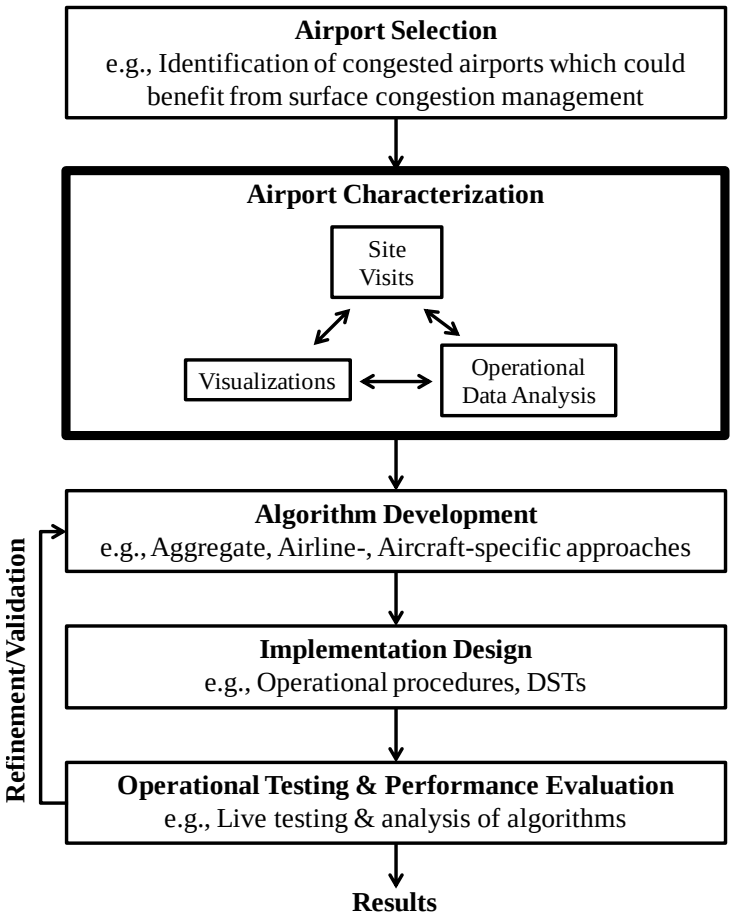

Figure 1. Overall design process for a congestion management approach.

The airport selection step resulted in an analysis focus on LGA and PHL airports during Phase 2 activities.

Framework for incorporating departure metering into Surface CDM

Figure 2 presents a schematic of the S-CDM concept of operations, with a particular emphasis on the data elements required, and the outputs.

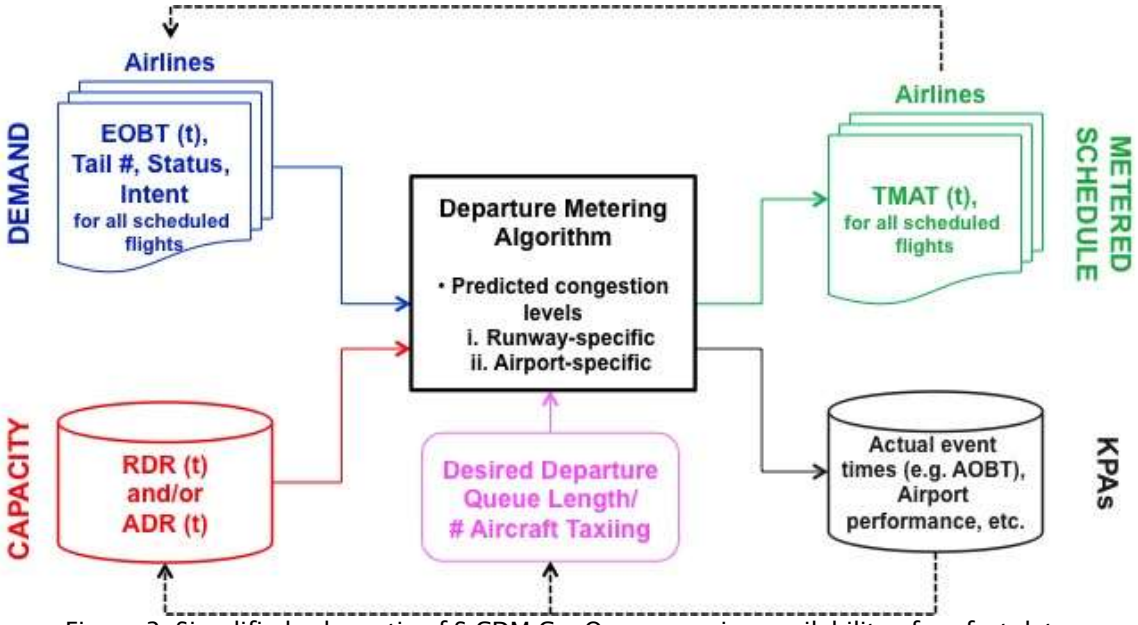

Figure 2. Simplified schematic of S-CDM ConOps, assuming availability of perfect data.

In prior work, research team has developed and validated data-driven algorithms for determining the appropriate values of the desired departure queue length and the number of aircraft taxiing (the quantities shown in magenta), given tactical (i.e., 15-minutes ahead) estimates of the demand and operating conditions. The algorithms account for the variability/uncertainty in throughput (RDR/ADR) over the next 15-minute period.

Departure metering using Pushback Rate Control strategies

Two classes of Pushback Rate Control (PRC) strategies were developed and analyzed: (1) An N-Control policy, and (2) a more advanced dynamic programming based policy. N-control aims to maintain departing traffic around an acceptable value N_{ctrl} based on empirical analysis of the relationship between departure throughput and active traffic, while dynamic programming seeks to minimize a cost function that penalizes both long queues and runway starvation by calculating the probability of the airport being in a certain state at some future time. Both approaches use predictions of the departure throughput in a time-window of interest by considering the runway configuration, weather conditions, and arrival demand using regression trees. Information on downstream restrictions is used for more accurate predictions of the operational throughput of an airport by leveraging the Route Availability Planning Tool (RAPT), an automated decision support tool that identifies departure routes that will be impacted by convective weather. Archived RAPT data can be used to predict the impact of route availability on the capacity of the airport. Regression trees are used to predict the departure throughput of LGA in each 15-minute interval as a function of arrival rate and a "RAPT value", which is used to measure the level of route blockage in the departure airspace.

N-Control based PRC: The N-Control policy considers the runway configuration, meteorological conditions, demand and RAPT forecast in a 15-minute period in order to determine the suggested pushback rate for that time period. A schematic of this process is shown in Figure 3.

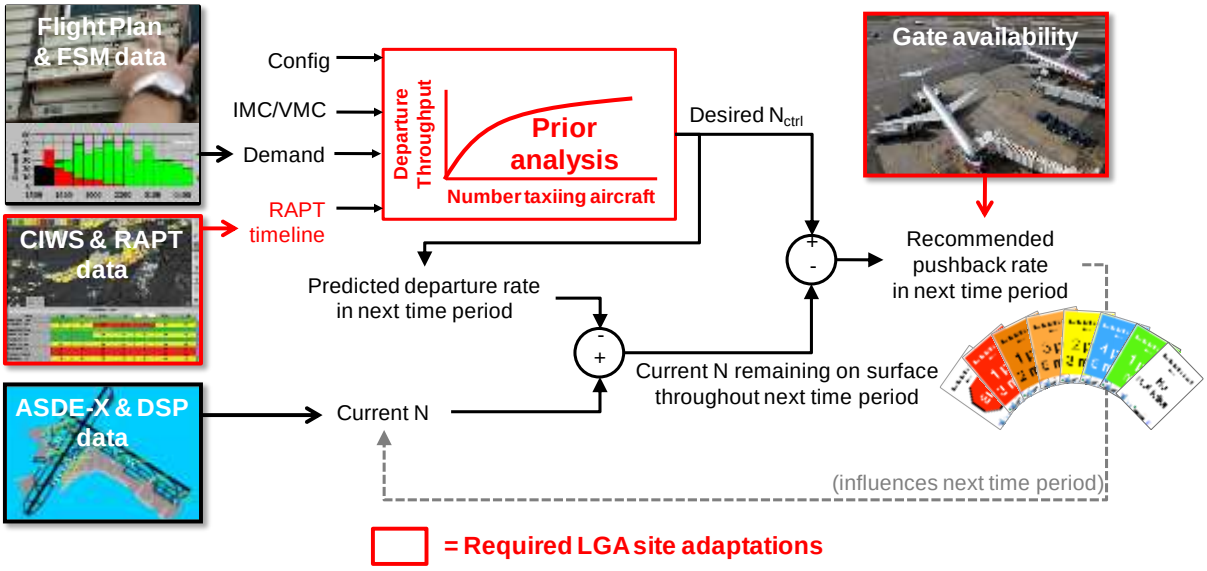

Figure 3. Adaptation of N-control to derive a PRC policy for LGA.

Dynamic Programming based PRC: Dynamic programming can be used to determine PRC policies that control the departure pushback rate by minimizing a cost function that penalizes long runway queues and low runway utilization. For each time-window (say, 15 min) and given the current state of the system, a queuing model is used to predict the state of the system at the end of that time-window. A prediction of the departure throughput of the airport for that time-window (which in turn depends on the arrival rate of the airport) is required in order to predict the state of the airport. The dynamic program then determines an optimal pushback rate for the duration of the time-window. The dynamic programming policy has the benefit that it accommodates probabilistic predictions of throughput. Figure 4 illustrates such a policy derived for LGA.

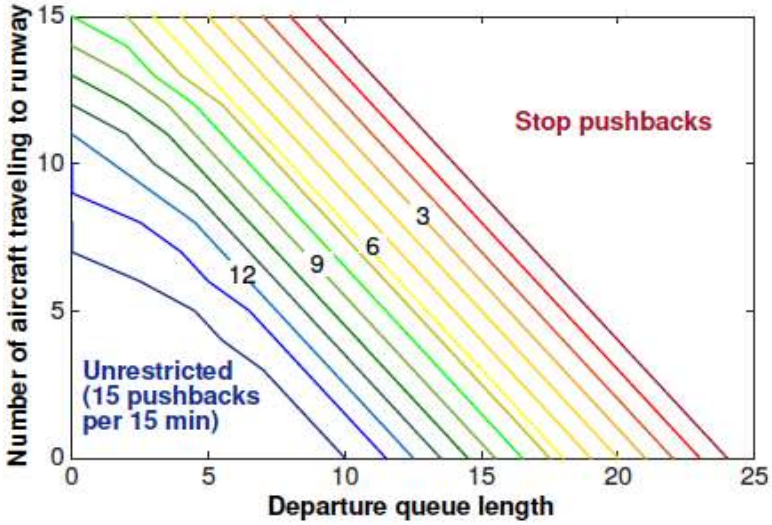

Figure 4. Dynamic programming based pushback rate policy for a time-window of 15 min.

The dynamic programming policy contrasts with the N-control policy in the following manner. N-control uses a simple equation to maintain departure surface traffic at a predetermined level based on empirical data. Dynamic programming models the runway service time to get a probability distribution of the state of the airport at some point in the future. With this, and a cost of queuing and runway utilization function, dynamic programming finds the departure pushback rate that minimizes costs. While N-control predicts that the state of the airport surface will evolve in a certain manner, dynamic

programming considers all of the potential states of the airport and the departure pushback rate accounts for the uncertainty in the evolution of the state of the airport. From this perspective, the dynamic programming approach, while more complex than the N-Control based approach, is a more robust policy. In addition, while N-control is only in effect during times of significant congestion ($N > N_{ctrl}$), the dynamic programming policy is always in effect. As a result, the dynamic programming based approach remedies even smaller (temporary) imbalances between throughput and demand, and results in greater taxi-out time reductions.

Time windows and time horizons

The PRC policies, N-control and dynamic programming, both generate a pushback rate for departures valid for a given time window. Historically, this time window has been set to 15 minutes, but varying this time window can lead to advantages and disadvantages. Also, a pushback rate can be calculated for earlier time windows in the future by changing the time horizon of the policy. Changing the time window or time horizon allows an airport or airline to tailor the PRC policy to specific needs and requirements. Consequently, stakeholders need to be aware of how varying these parameter values can affect the performance of PRC policies. Figure 5 illustrates the difference between time windows and time horizons.

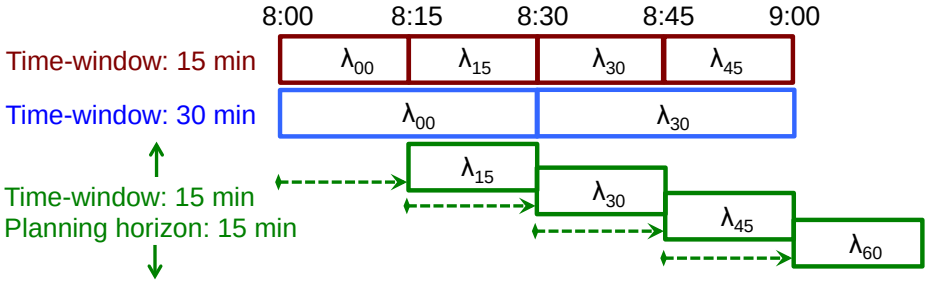

Figure 5. Visualization of time windows and time horizons.

PRC policies calculate a pushback rate for departing aircraft that is valid for a certain time window. This time window impacts some performance characteristics of the policy. The length of this time window is a tradeoff between accuracy, ease of implementation, and value added to operators (airlines and air traffic controllers). For accuracy, the policies become less accurate as the length of the time window increases. Because the PRC policies calculate the pushback rate at the beginning of the time window based on the state of the airport surface, a longer time window means that the pushback rate is valid (recommended) for a longer period of time. As time gets farther away from the beginning of the window, the state of the airport surface changes relative to what was expected at the start of the time window, resulting in a decrease in metering performance.

The time horizon is the number of time windows before a given time window that a departure rate is calculated. The time horizon length variation has similar tradeoffs to those associated with time window length variation. Extending time windows or horizons reduces operator workload resulting from the policy, but prediction and data accuracy also decrease. Shortening time windows or horizons increases accuracy, but operator workload also increases due to short planning horizons.

Impact of uncertainty

The uncertainty associated with the throughput prediction increases if either the time window increases (say, to 30 min instead of 15 min), or if the time horizon increases (for example, planning for the time-windows that begin 15- or 30-min later instead of just at the current time). On the demand-side, arrival rate predictions may not be accurate, which will in turn increase the uncertainty associated with the predicted departure throughput. Similarly, departure demand may vary and aircraft may not push back at the times recommended by the pushback rate.

Departure demand (EOBT) uncertainty

Both N-control and dynamic programming rely on departure demand being ready for pushback in a given time window, as expected when determining the pushback rate. In the S-CDM context, this translates to an accurate knowledge of the

Earliest Off-Block Times (EOBTs). If the available departures are less than the pushback rate, the departure surface traffic may fall below acceptable levels. If there are many available departures during a time of low congestion, those departures may cause congestion in the future. As such, PRC policies need to handle variability in departure demand. Such variability is modeled in simulations of LGA operations by assuming that the perturbations in the EOBT are drawn from a normal distribution with a mean of the published EOBT and a standard deviation of 3.5 minutes. The assumption of a standard deviation of 3.5 minutes ensures that two standard deviations from the expected EOBT approximately encompasses a 15-minute time window.

Arrival rate uncertainty

The number of arrivals landing at an airport in a given time window is also uncertain. The scheduled arrival time of an aircraft changes due to many of the reasons that affect the scheduled departure time, including weather and congestion. Instead of scheduled arrival times, a tool called the Flight Status Monitor (FSM) forecasts the number of arrivals that will be ready to land for time windows into the future. The FAA's Airport Arrival Demand Chart (AADC) is used as a surrogate for the arrival rate predictions from the FSM. Figure 6 shows an example of the AADC predictions for LGA.

Figure 6. Airport Arrival Demand Chart for LGA on 3/12/2015. The bars indicate how many aircraft will be approaching LGA for landing during each 15-minute time window.

With this information, the predicted arrivals for the next 15, 30, and 60 minutes can be extracted. If the predicted number of arrivals is above the capacity, the predicted arrivals is set to the capacity. The prediction accuracy analysis that follows establishes the perturbations for the variable arrival rate analysis. The AADC data was gathered over a four-month period from January-April 2015. Figure 7 shows the distribution of the difference between AADC arrival predictions and the actual arrivals for 15-minute windows.

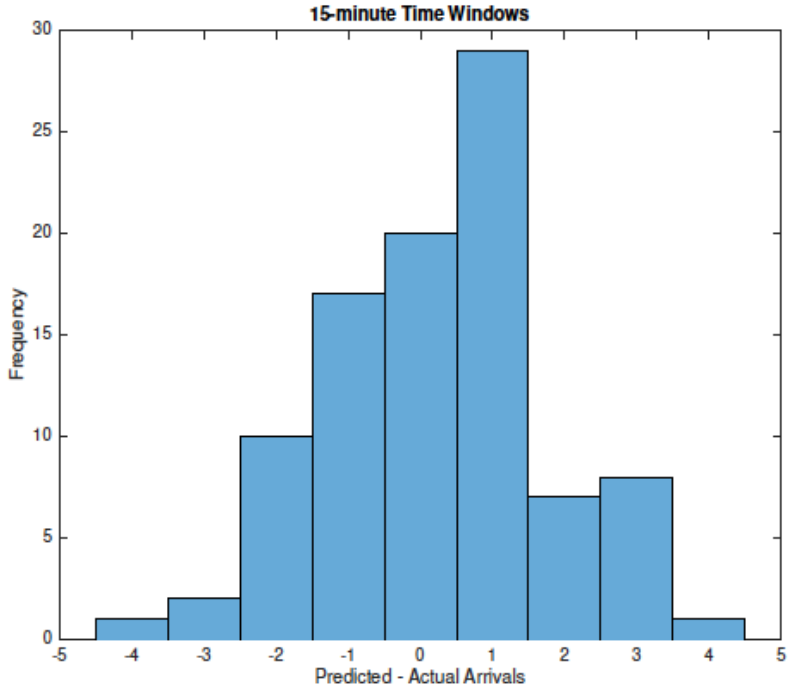

Figure 7. Predicted minus actual arrivals at LGA for the next 15-minute window.

Simulations of departure metering under uncertainty

Input data

The data required for the simulation are extracted from multiple sources. The ASPM dataset provides flight-specific metrics such as pushback time, wheels off time, and wheels on time. Gate and terminal assignments allow for the calculation of unimpeded taxi-out times, and allow the policy to monitor gate conflicts. The simulations resolve all gate conflicts by clearing a departure to pushback (if its EOBT has passed) as soon as an arrival assigned to that gate has landed. The last dataset contains the weather data, RAPT, described previously. The simulations consider July and August 2013.

Each simulation contains both a baseline case and two metering cases. The baseline case simulates the airport operations by releasing departures from their gates on a First-Come-First-Served (FCFS) basis based on their EOBTs (assumed to be the scheduled departure times with the appropriate perturbation). The metering cases simulate the airport operations using the N-Control and dynamic programming policies. The benefits of departure metering include the taxi-out time reduction, which is the difference between the taxi-out times in the baseline case and metering case. Taxi-out time reduction contrasts with gate holding time, which is the length of time an aircraft is held at a gate beyond the scheduled departure time due to the departure metering policy. Although aircraft still belong to the virtual queue with engines off, occupying the gate for longer periods of time causes more gate conflicts, and extended gate holding times after boarding can inconvenience passengers.

Simulation results

The results of the simulations are presented below. For each departure metering strategy, the plots show the resulting reduction in taxi-out time, namely, the difference between the baseline taxi-out time and the one under the metering policy. As mentioned earlier, comparing the results of the N-control and the dynamic programming based policy simulations highlights some of the differences between the algorithms. The absolute benefits of the dynamic programming policy are therefore much greater than the benefits of the N-control policy. However, this does not immediately indicate that dynamic programming is the better policy. Because the dynamic programming algorithm relies on an infinite horizon solution, the dynamic programming algorithm controls departures at all times, not just during times of congestion like the N-control policy. Therefore, the dynamic programming algorithm meters many more flights than the N-control algorithm. As a result, taxi-out time reductions are expected to be greater under the dynamic programming based policy.

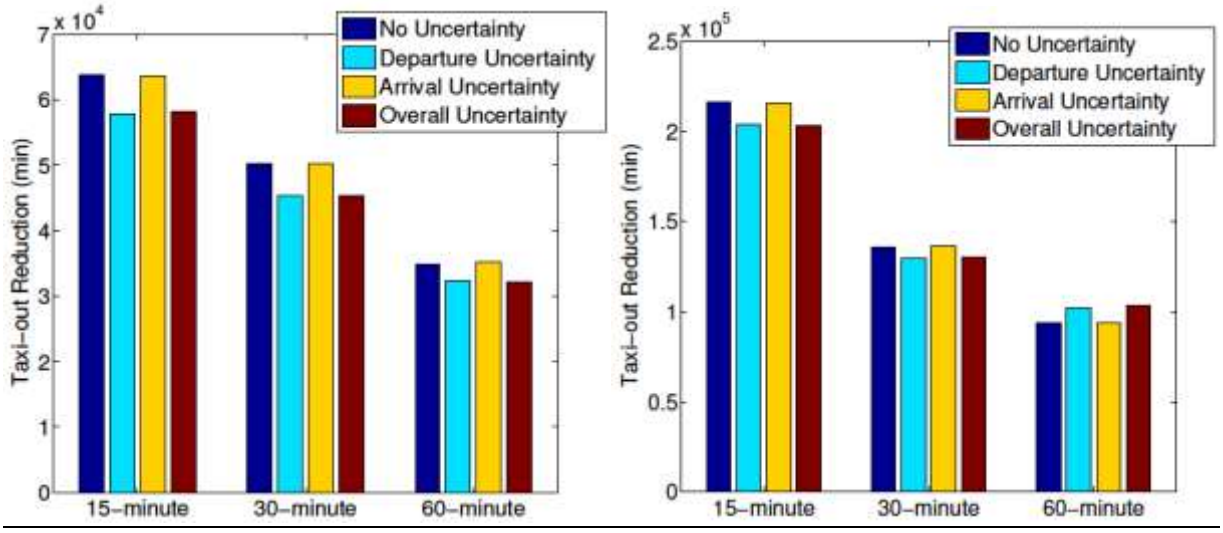

Figure 8. Total taxi-out reduction for the LGA time window simulations, under (left) N-Control, and (b) dynamic programming. Note that the y-axis scales are different in the two plots.

Influence of time window length: Three time windows are investigated: 15-, 30- and 60-minutes. Figure 8 shows the taxi-out time reductions under (left) N-Control, and (right) dynamic programming based PRC. As expected, it shows that the taxi-out time reduction relative to the baseline under the N-control policy (for a time window of 15 min, and no further advance time horizon) is significantly more under the dynamic programming based policy than the N-control policy, for all three values of time window. The results show that the benefits decrease as the time window increases, since a single pushback rate is selected for the entire time window, even if the departure demand fluctuates within it. As a result, the 30-minute time window simulation has 79% of the taxi-out time reduction of the 15-minute time window simulation, while the 60-minute time window simulation has 55% of the taxi-out time reduction of the 15-minute time window simulation. However, even the longer time-windows exhibit considerable benefits, nearly 100,000 min with a 60 min time window over the two month period, using a dynamic programming based pushback rate control policy.
The results show that the EOBT (departure demand) uncertainty has a larger effect on taxi-out reduction than does the arrival rate uncertainty. The overall uncertainty (both EOBT and arrival rate uncertainty) analysis results virtually match the EOBT uncertainty-alone analysis results for all time window lengths. While the 15-minute and 30-minute time window simulations have a decrease in taxi-out reduction due to the EOBT uncertainty, the 60-minute time window simulation has a slight increase in taxi-out reduction. This increase may be due to the spreading out of the departure demand through perturbations, which could result in more flights being metered than initially planned.
Influence of time horizon length: Three time windows were investigated, each with a time window of 15-min. They corresponded to no look ahead (i.e., the pushback rate is determined only for the immediately next 15-minute period), 1 time window look ahead (i.e., a pushback rate was determined for the 15-minute interval that was 15-30 minutes from the current time), and a 3 time window look ahead (i.e., a pushback rate was determined for the 15-minute interval that was 45-60 minutes from the current time). These results, shown in Figure 8, are similar to the results for time window variation shown in Figure 9.

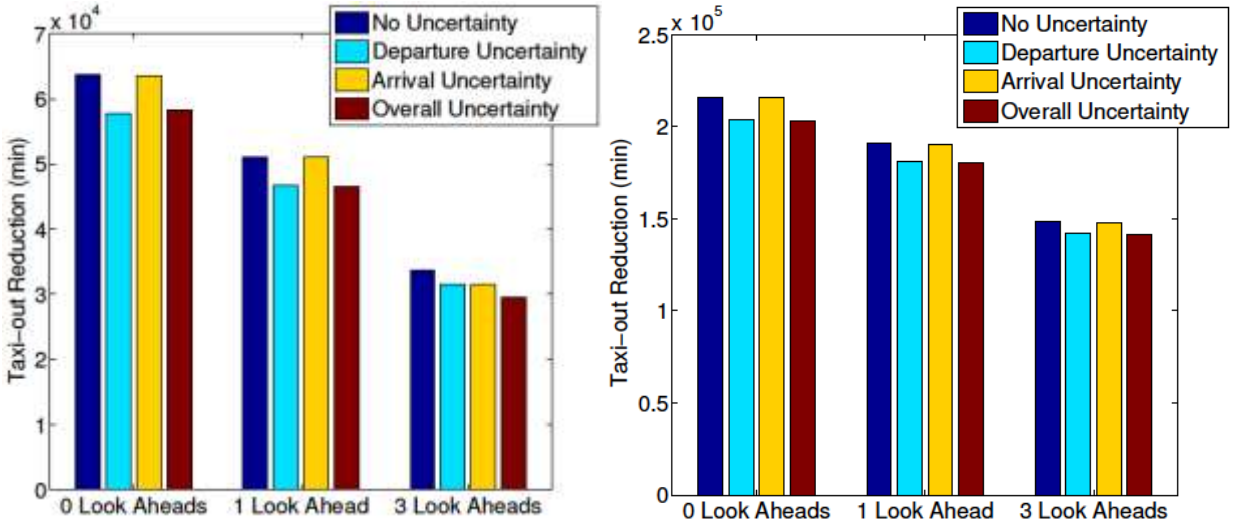

Figure 9. Total taxi-out reduction for the LGA time horizon simulations, under (left) N-Control, and (b) dynamic programming. Note that the y-axis scales are different in the two plots.

The results show that the departure schedule uncertainty has a larger effect on policy benefits than does the arrival rate uncertainty. For both N-control and dynamic programming, the departure schedule uncertainty has less of a negative influence on the results as the time window length increases. In fact, for the 60-minute time window dynamic programming simulation, the departure schedule uncertainty slightly increases the taxi-out reduction. For the time horizon simulations, the influence of each uncertainty remains proportional to the policy benefits with no uncertainty. The arrival rate uncertainty has very little effect on taxi-out reduction for any simulation.

Next Steps and Timeline

Ongoing work consists largely of further refining the proposed framework to support the integration of departure metering with NextGen surface management capabilities. Pursuant to the recent FAA decision to address the RTCA NextGen Integrated Working Group (NIWG) surface team departure metering recommendation with a field demonstration by NASA at Charlotte (CLT) Douglas airport, the research team has been extending the methodologies to CLT, in order to support the ATD-2 demonstration. The team had previously analyzed CLT as part of the site selection task for Phase 2, and also investigated the impacts of the new runway at CLT that became operational in 2011. In particular, discussions with the NASA benefits analysis team lead for the CLT activity has highlighted strong interest in getting a better understanding of departure metering benefits estimates, particularly with the Spot and Runway Departure Advisor (SARDA) algorithm coupled into an S-CDM-compliant architecture, and the framework proposed in this research can enable that. NASA is also concerned with the impact to benefits of uncertainties (e.g., in EOBTs, in departure sequencing times, in gaps in the airspace, etc.) as a function of different look ahead times, similar to the analysis presented in this document.
As the capability is being refined, the team is also coordinating with the TFDM program office and the Surface Operations Office to ensure maximum impact from the N-Control activities. TFDM will be the FAA's primary acquisition program to deliver surface capabilities. The results of these studies were briefed to the TFDM Investment Analysis Team (IAT) to assist with the validation of potential benefits from their departure metering capability.

Milestone(s)

- Site selection [Complete]
- Framework to adapt departure metering concepts to different operating environments [Complete]
- Protocol design for LGA and refinement (multiple) [Complete]
- Initial stakeholder engagement [Complete]
- Modeling and simulation of departure metering at LGA [Complete]
- Modeling and simulation of departure metering at PHL [Complete]

- Engagement/coordination with TFDM benefits analysis [Ongoing]
- Investigation of benefits of incorporation of S-CDM data elements (e.g. EOBT) [Ongoing]
- Identification of most appropriate departure metering algorithm for different airports and operating conditions and levels of uncertainty/ data accuracy (CLT adaptation) [Ongoing]
- Coordination with Advanced Surface Management Programs [Ongoing]

Publications

Peer-reviewed conference publications:
P. McFarlane and H. Balakrishnan. "Optimal Control of Airport Pushbacks in the Presence of Uncertainties," American Control Conference, July 2016.

Outreach Efforts

N/A

Student Involvement

Patrick McFarlane. Modeling and simulation of PHL operations as well as uncertainty analysis. Graduated with Masters degree in February 2016 and currently employed at MITRE.

Sandeep Badrinath, currently a graduate student at MIT. Analysis and control of queuing network models of airport operations.

Plans for Next Period

Task 1: Investigate effect on departure metering algorithms/benefits of incorporation of S-CDM data elements (e.g., EOBT, gate information, etc)

Task 2: Investigate most appropriate departure metering algorithm for different types of airports and operating conditions. Focus on CLT ramp operations.

Task 3: Determine what metrics should be collected to assess and refine strategic and tactical departure metering performance.

Task 4: Coordination with Advanced Surface Management Programs (S-CDM and TFDM)

Project 017 Pilot Study on Aircraft Noise and Sleep Disturbance

University of Pennsylvania

Project Lead Investigator

Mathias Basner
Associate Professor of Sleep and Chronobiology
Department of Psychiatry
University of Pennsylvania
1019 Blockley Hall, 423 Guardian Dr.
Philadelphia, PA 19104-6021
215-573-5866
basner@mail.med.upenn.edu

University Participants

University of Pennsylvania

- P.I.: Mathias Basner, Associate Professor
- FAA Award Number: 13-C-AJE-UPENN-003
- Period of Performance: October 1, 2015 to September 30, 2016
- Task(s):
  (1) Philadelphia Sleep Study: Data analysis
  (2) Second Pilot Sleep Study: Data acquisition

Project Funding Level

The funding amount for this period was $343,498.00. The cost sharing requirement for this project was met by our international collaborators at the German Aerospace Center (DLR).

Investigation Team

- Principal Investigator: Mathias Basner
- Co-Investigator: Sarah McGuire
- Research Assistants: Anjana Kallarackal, Maryam Witte

Project Overview

The long-term goal of this line of research is to derive exposure-response relationships for aircraft noise-induced sleep disturbance that are representative of the exposed U.S. population. As studies will have to investigate samples around multiple airports it will not be possible to use polysomnography (i.e., simultaneous recording of the electroencephalogram, electromyogram, and electrooculogram) to monitor sleep, as this method requires trained personnel at the measurement site in the evening and in the morning and is thus too costly. An alternative methodology of using a single channel electrocardiogram (ECG) and actigraphy to monitor sleep has been examined. This methodology allows the investigation of larger subject samples at lower cost as individuals can be taught how to apply the electrodes themselves. Also unlike polysomnography, awakenings can be identified automatically. As part of previous research, an algorithm for identifying EEG arousals (Basner, Griefahn, Müller et al., 2007) based on increases in heart rate was refined in order to only identify those arousals greater than or equal to 15 seconds in duration, which is the most agreed upon indicator of noise-induced sleep disturbance. High agreement between EEG visually scored arousals and arousals identified using the refined ECG based algorithm was obtained. The methodology of using ECG and actigraphy to monitor sleep has been implemented in two pilot field studies to evaluate the quality of data that can be obtained for unattended physiological and noise measurements. Based on lessons learned, the study protocol is being refined in order to inform the design and cost of a potential multi-airport study on the effects of noise on sleep.

Task1- Philadelphia Sleep Study: Data analysis

University of Pennsylvania

Objectives

(1) Evaluate the completeness and quality of data obtained through unattended sleep measurements.
(2) Compare the degree of sleep fragmentation, subjective sleep ratings, and subjective health ratings between participants that lived near the airport and those that lived in a control region.
(3) Develop models relating awakenings to indoor noise levels and compare results to models derived from similar studies conducted by DLR in Germany.
(4) Further refine study protocol and methodology based on lessons learned.

Research Approach

A pilot sleep study was conducted around Philadelphia International Airport. This airport was selected as it was in close proximity to the study team and had relevant amounts of nighttime air traffic. Measurements took place between July 2014 and July 2015. Forty participants who lived near the airport and 40 participants from a control region in Philadelphia County were enrolled in the study. Participants were recruited primarily through mailed flyers. Each participant completed 3 nights/4 days of unattended measurements. Staff went to the participant's home on the first day of the study to explain the protocol and setup the equipment and after the third night to collect the equipment. Baseline sleep and health characteristics were obtained subjectively on the first day. Each night participants completed ECG and actigraphy measurement with concurrent indoor noise recordings. Each morning participants completed blood pressure measurements and self-report assessments of their previous night's sleep. The methodology, analysis, and results are described in detail in a separate ASCENT project report.

There were several limitations of the Philadelpia sleep study methodology. First, while the target enrollment of the study was met, the response rate was low with 3700 flyers mailed. This low response rate could affect the generalizability of the results. One potential reason for the low response rate could be that individuals were reluctant to allow unknown staff members enter their homes to setup the equipment. Another limitation was the methodological expense as trained staff was in the field 2 to 4 days per week. These limitations have been addressed in the refined methodology implemented in the second pilot sleep study.

Task 2 - Second Pilot Sleep Study: Data acquisition

University of Pennsylvania

Objectives

(1) Complete acquisition of survey and acoustical and physiological data
(2) Refine and to the extent possible, automatize the methodology to identify aircraft noise events and maximum sound pressure levels in complex acoustical signals
(3) Inform the design and cost of a potential multiple airport study based on lessons learned

Research Approach

Based on lessons learned in the Philadelphia Sleep study, the methodology has been refined and a second pilot study is being conducted to evaluate its feasibility. The airport for this study was selected in consultation with the FAA and has relevant amounts of nighttime air traffic and a sufficient population to sample from. To determine the sample regions around the airport, L_{Night} noise contours were provided by the FAA. Additionally we calculated L_{Night} contours for 84 weekdays based on flight track data. For the study we have 10 sampling regions, 5 east and west of the airport of the following noise categories: < 40 dB (control region), 40-45 dB, 45-50 dB, 50-55 dB, and > 55 dB L_{Night}.

To recruit participants for the study a brief survey is mailed to randomly selected households within each of the 10 sampling frames. The primary purpose of the survey is determining the eligibility of individuals to take part in an in-home sleep study. The survey contains questions on the individual's health, sleep, and noise sensitivity. For completing the survey participants receive an Amazon gift card. The amount of the gift card is$2.00, $5.00, or $10.00 which is randomly assigned. The purpose of varying the gift card amount is to examine the difference in response rate received. The target number of completed surveys is 200 per 5dB noise category.

In the survey, participants indicate their interest in taking part in the in-home sleep study which consists of 5 nights of unattended ECG and actigraphy measurements and indoor sound recordings. The equipment is mailed to the participant's homes and instruction manuals and videos on how to setup and use the equipment are provided. Mailing the equipment eliminates the need for staff in the field which significantly reduces the study cost. In addition, by mailing the equipment the response rate may increase as staff does not enter the participant's homes. The target enrollment for the in-home study is 40 per 5 dB noise category. The outcomes for this study are to determine the response rates for both the mail and in-home study, assess the feasibility of mailing equipment, and evaluate the quality of data that can be obtained.

Data collection is ongoing.

Milestones

The following are milestones that were achieved during the past 12 months:
(1) Data analysis for the Philadelphia Sleep Study was completed 8/2016
(2) Data collection for the second pilot sleep study began 9/2016.

Major Accomplishments

Task 1: The primary objective of the Philadelphia Sleep Study was to evaluate the feasibility of conducting a study with unattended acoustical and physiological measurements. For this study 79 out of 80 participants enrolled completed the measurements, and all but 1 completed all three nights of the study. In addition, for all measurements there was less than 10% of data loss. This result suggests that participants are able to follow protocol and complete unattended measurements.

Task 2: All preparations for the study were completed during the last period including; preparing the survey, purchasing and testing physiological and noise measurement equipment, and obtaining addresses. As part of the preparations, low cost sound recording equipment was identified, which includes a class 1 microphone and small recorder. The identification of this noise monitoring equipment has reduced the methodological cost and enabled more sites to be studied concurrently.

Publications

ASCENT Project Report

Basner M, McGuire S, and Witte M. Pilot sleep study near Philadelphia International Airport: ASCENT Project 17 Report, 2016.

Conference Proceedings

McGuire S, Witte M, and Basner M. Evaluation and refinement of a methodology for examining the effects of aircraft noise on sleep in communities in the US. Internoise, Hamburg, Germany, 2016.

Outreach Efforts

None

Awards

None

Student Involvement

None

Plans for Next Period

Task 1: We will continue to compare the results from the Philadelphia Sleep Study to the results from German field studies conducted around Cologne-Bonn and Frankfurt Airport and publish the findings as part of continued collaboration with colleagues at the German Aerospace Center (DLR).

Task 2: Concurrently with the data collection, we will analyze the sound recordings. For this analysis we will refine and automatize the methodology of identifying aircraft noise events and maximum sound pressure levels in the recordings. The identification of aircraft noise events can be challenging based on indoor sound measurements only due to masking of other noise events (e.g., air conditioning system, snoring). A methodology will be developed that automatically identifies aircraft noise events based on flight track data provided by FAA and estimates indoor noise levels based on outdoor noise predictions and an established relationship of outdoor/indoor noise attenuation in cases were the aircraft noise event is masked by other noise sources.

References

Basner M, Griefahn B, Müller U, Plath G, Samel A. An ECG-based algorithm for the automatic identification of autonomic activations associated with cortical arousal. Sleep 2007; 30(10):1349-61.

Project 018 Modeling Airport-Related Air Pollutant Concentrations and Health Impacts

Boston University School of Public Health

Project Lead Investigator

Jonathan I. Levy
Professor and Associate Chair
Department of Environmental Health
Boston University School of Public Health
715 Albany St. T4W, Boston, MA 02118
617-638-4663
jonlevy@bu.edu

University Participants

Boston University School of Public Health

- P.I.(s): Jonathan I. Levy, Professor and Associate Chair
- FAA Award Number: 13-C-AJFE-BU, Amendment 5
- Period of Performance: October 1, 2015 – September 30, 2016
- Task(s):
    1. Apply the health damage functions (all airports) and spatial pollutant concentration surfaces (directly modeled airports) to evaluate hypothetical policy scenarios.
    2. Compare aviation-related health impacts as well as damage functions with those from other important source sectors.
    3. Identify UFP concentration datasets that could be used to determine the magnitude and spatial extent of contributions from arriving aircraft in a near-airport setting.
    4. Apply multivariable regression modeling techniques to quantify the contribution of aircraft arrivals and other source activity with measured UFP concentrations.

Project Funding Level

$150,000. Matching funds provided by carry forward from funding from the North American Insulation Manufacturers Association, with 75:25 cost share waiver.

Investigation Team

Principal Investigator: Jonathan I. Levy, Sc.D. (Professor of Environmental Health, Department of Environmental Health, Boston University School of Public Health). Dr. Levy is the Boston University PI of ASCENT. He has primary responsibility for the execution of the project and contributes to manuscripts and reports produced.

Post-doctoral researcher: Stefani Penn, MS, PhD. Dr. Penn led the analytical efforts to develop the individual airport health damage function model, as part of her dissertation work, including the effort to design individual airport atmospheric modeling runs and to estimate health damage functions.

Graduate Student: Lindsay Underhill, MS. Ms. Underhill leads the analytical efforts involving application of the health damage function models (Tasks 1 and 2).

Graduate Student: Chloe Kim, MPH. Ms. Kim leads the analytical efforts involving identification of UFP monitoring datasets and statistical analyses of those data (Tasks 3 and 4).

Research Assistant: May Woo. Ms. Woo supported data management and other analytical efforts across the project.

Project Overview

The overall objective of this research is to develop tools that will enable quantification of airport-specific health impacts from aircraft emissions at selected airports, working collaboratively with air quality modeling efforts under other ASCENT projects. Our primary objective within this funding year was to apply previously-developed health damage function models for policy and comparative analyses. In addition, there has been increasing interest in the question of whether aircraft emissions, and in particular arrival emissions, can contribute significantly to ultrafine particulate matter (UFP) concentrations at appreciable distances from the airport. Our objective within the current funding year was to identify and work with an existing near-airport dataset and apply advanced regression modeling techniques to isolate the contribution of aircraft emissions, specifically examining the magnitude associated with arrival flight paths. This work will enhance the interpretability of the dispersion model-based work and will provide additional insight about individual airport contributions to exposures and health risks.

Task 1 - Apply the health damage functions (all airports) and spatial pollutant concentration surfaces (directly modeled airports) to evaluate hypothetical policy scenarios.

Boston University School of Public Health

Objective(s)

To demonstrate the utility of our individual airport health damage function modeling approach, we proposed to apply our previously-generated estimates of health risks per unit emissions to a series of hypothetical policy scenarios. We proposed to work closely with FAA and other stakeholders to determine realistic scenarios, including some that have been evaluated using other modeling approaches, which would allow us to do model intercomparisons and general quality assurance checks. Along with the defined scenarios, we proposed to conduct a series of “what if” analyses meant to determine the importance of the individual airport insights. Because of the importance and sensitivity of this work, we proposed to present both our hypothetical policy scenarios and set of “what if” analyses to FAA and the ASCENT advisory board, gathering feedback before conducting the analyses.

Research Approach

Given regression models developed previously as part of Project 18, explaining variability in health risks per unit emissions across airports and pollutants, we developed statistical code to calculate health damage functions for all airports in the US (both directly modeled by Project 18 and others), and to rapidly estimate the national health impacts of alternative emissions scenarios. In December 2015, we were given four emissions scenarios to model by FAA: 1. Use of ultra-low sulfur fuel: sulfur emissions reduced by 97.5% nationally; 2. Use of 50% blended fuel: 50% primary elemental carbon emissions, 50% sulfur emissions; 3. Implementation of ULS fuel along the East Coast (~50% reduction in sulfur emissions for airports in the eastern seaboard states); 4. Implementation of ULS fuel along the West Coast (~50% reduction in sulfur emissions for airports in CA, OR, WA). Those analyses were completed and presented at the spring 2016 ASCENT meeting, but we were subsequently told by FAA to discontinue this task, given a lack of consensus at FAA on the most appropriate scenarios to model.

Milestone(s)

We proposed to identify defined policy scenarios by 12/31/15 (Task 1.1), to apply the health damage functions to evaluate policy scenarios by 4/30/16 (Task 1.2), and to complete the policy analysis manuscript by 9/30/16 (Task 1.3). Tasks 1.1 and 1.2 were completed by the due dates, but Task 1.3 was not completed per FAA guidance to discontinue the work.

Major Accomplishments

As this task was discontinued per FAA request, no major accomplishments are provided.

Publications

None

Outreach Efforts
None

Awards
None

Student Involvement
Individual airport health damage function modeling was led by Stefani Penn as a doctoral student (graduated 9/15), and the policy scenario modeling work was led by Lindsay Underhill as a doctoral student.

Plans for Next Period
None, as the work was discontinued per FAA request.

Task 2 - Compare aviation-related health impacts as well as damage functions with those from other important source sectors.
Boston University School of Public Health

Objective(s)
For any analyses of the health effects of aviation emissions, it is important to be able to place the output in context. Aviation is a relatively small contributor to ambient air pollution in most locations, so it is valuable to consider how other source sectors contribute. However, while multiple previous studies have done these comparisons, no studies to date have compared health damage functions (health impacts normalized by emission rate) across source sectors using comparable modeling techniques. This type of comparison will provide multiple useful insights, including whether aviation sources are more like ground-level sources (e.g., residential combustion, road traffic) or sources with elevated stack heights (e.g., power plants) from a public health perspective, and the extent to which the geographic patterns of where airports are located influence the damage functions relative to other source sectors.

Research Approach
For each of the three source sectors (power plants, residential combustion sources, and aviation), health damage functions were derived using identical versions of CMAQ-DDM using the same meteorological year and other basic assumptions. Briefly, we used CMAQ v 4.7.1 instrumented with DDM in three dimensions. We modeled power plants as state aggregates, allocating each power plant to a 36 x 36 km grid cell. Residential combustion sources were modeled as low-level area sources, aggregated to county level for apportionment to grid cells by state. Airports were modeled individually, for the subset of 66 airports included in the modeling platform, using chorded aircraft LTO emissions derived from AEDT. Because modeling the full year was computationally intensive, we selected two months (January and July) to provide bi-seasonal representation, using all-source emissions and meteorology from 2005. To provide initial background conditions, a spin-up period of 11 days prior to each month was simulated. Whole-month sensitivity values from January and July were averaged to represent annual estimated contributions to ambient $PM_{2.5}$ and O_3 concentrations. Values are reported as 24-hour averages for $PM_{2.5}$ constituents and 8-hour maximum values for O_3 for consistency with current regulatory policies.

Due to the computationally intensive nature of CMAQ-DDM, it was not practical to construct separate runs for each source sector and source-state. To maximize efficiency, we incorporated 1-3 states or airports into a single DDM run, and we developed algorithms to separate the concentration impacts from each state or airport. Briefly, we applied image separation techniques using MATLAB 8.1.0, R2013a (MathWorks, Natick, MA). We developed a region-growing algorithm to determine regions of concentrations attributable to each source-state for each emitted precursor / ambient pollutant relationship within each model run and season. This algorithm allowed for both positive and negative sensitivities to be included within regions, and ensured that within a run, a smaller state's region could capture the extent of its health impacts. Quality assurance (QA) analyses were performed, including analysis of total health impact and health damage function distributions for resultant health values, as well as visual inspection of concentration surfaces. For runs that did not meet QA criteria, we re-ran CMAQ-DDM for individual states in isolation. This process allowed determination of

emissions impacts from individual source-states within a CMAQ-run group. The image segmentation algorithm is described in detail in Penn et al. 2016.

The resultant ambient pollutant concentrations (for $PM_{2.5}$ and O_3) were then linked with population and mortality rate data from the Centers for Disease Control and Prevention (CDC). Concentration-response functions associating ambient pollutant concentrations with health effects were derived from the epidemiological literature. To associate premature mortalities with $PM_{2.5}$ concentrations, we applied a central estimate concentration-response function of a 1% increase in mortality associated with every 1 $\mu g/m^3$ increase in annual average $PM_{2.5}$ concentration. To associate premature mortalities with O_3 concentrations, we applied a central estimate concentration-response function of a 0.4% increase in daily mortality per 10 ppb increase in daily 8-hour maximum O_3 concentrations, based on major multi-city and meta-analysis studies that evaluated health impacts across the year.

Health damage functions (HDFs) were calculated as mortality risk per thousand tons of emitted pollutants. HDFs were developed by source sector and source state for several precursor pollutants, including primary elemental carbon (PEC), primary organic carbon (POC), and primary sulfate (PSO4) as primary $PM_{2.5}$ precursors; nitrogen oxides (NOx), sulfur dioxide (SO_2), and volatile organic compounds (VOCs) as secondary $PM_{2.5}$ precursors; and NOx and VOCs as O_3 precursors. To compare HDFs across source sectors, we focused on a subset of states with sufficiently robust values. Exclusion criteria included states with very low emissions for at least one of the source sectors or states where a majority of total aviation emissions was not modeled directly, to ensure robust health damage functions that are representative of the state as a whole. For the remaining 21 states, we first visually compared HDFs across pollutants, sources, states, and seasons to examine potential drivers of variability. We then formalized the comparisons by developing explanatory variables related to downwind population patterns and meteorology. While developing formal regression models to explain variability was beyond the scope of the work and not needed given the applications, we examined explanatory variables individually and in combination.

Milestone(s)

We proposed to complete the manuscript comparing health damage functions across source sectors by 6/30/16 (Task 2). This task was not completed by the projected date, in part because of the multiple redirections of effort related to Task 1, which was ultimately discontinued per FAA request. The core datasets have been compiled and the final comparative analyses are in progress, and we anticipate the manuscript being completed in the first quarter of 2017.

Major Accomplishments

As seen in Figure 18.1, HDFs were successfully derived and were shown to vary by pollutant precursor, source sector, state, and season. Overall, the range of HDFs for primary $PM_{2.5}$ from aviation is lower than those from power plants and residential combustion in January, but the distributions are similar in July. However, aviation HDFs are not consistently lower than the other sectors, and in a few cases, they are higher than HDFs from other sectors. For example, in January, the HDF for California is higher for aviation compared to residential combustion, but lower for aviation compared to power plants. This is likely attributable to a complex combination of source locations relative to population patterns and emissions/plume characteristics.

We examined the variability of pollutant-, sector-, and season-specific HDF values between states to potentially identify factors contributing to regional differences. In line with our expectation that population would be a key driver of HDF variability for primary $PM_{2.5}$ precursors, we found that the highest HDF values tend to be from states with a relatively greater potential for population exposure to source emissions (i.e. high population density downwind). To develop a more refined sense of the influence of population patterns, we developed metrics that reflected the emissions-weighted average population within various distances from sources, taking account of meteorological trends.

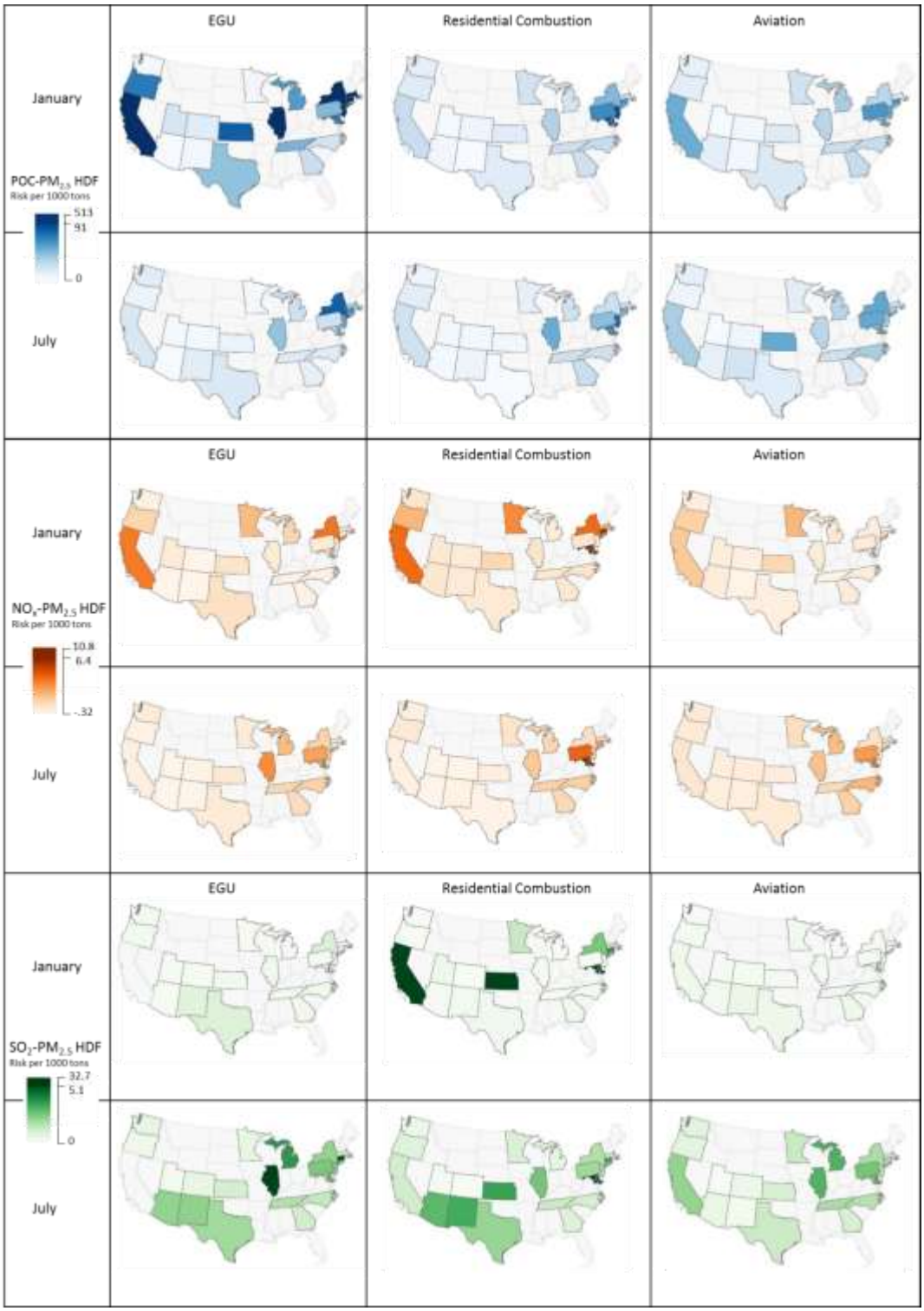

Figure 18.1. HDF variability by source sector, season, and $PM_{2.5}$ precursor pollutant, including POC in blue (top), NO_x in orange (middle), and SO_2 in green (bottom). The comparative analysis is focused on states with sufficient emissions from each sector and excluded states are represented in gray.

Figure 18.2 provides an illustration of the importance of more spatially refined analyses to facilitate interpretation of values. We present the relative proximity of POC emissions from aviation to high population areas within northwestern and northeastern states in the US. In general, the HDF values for the selected northwestern states are lower than those from the northeastern states. In both regions, emissions are clustered around areas with high population density; however, the northeast tends to have more densely populated areas surrounding and downwind of areas of high emissions.

Figure 18.2. Relationship between population density and (2a) primary organic carbon (POC) emissions in January from aviation in the northwestern US and (2b) POC emissions in January from the aviation sector in the northeastern US. Total emissions per 36 x 36 km grid cell is represented by red graduated symbols, with larger symbols indicating higher emissions. Population density is represented by grayscale shading, with darker shading indicating higher population density.

As anticipated, HDF patterns for secondarily formed pollutants are less easily explained by population patterns, given the influence of meteorology and background concentrations on $PM_{2.5}$ and O_3 formation. In ongoing analyses, we are developing refined estimates of downwind populations at various distances and of background concentrations of key pollutants, to inform future comparative analyses.

Publications

Penn SL, Arunachalam S, Woody M, Heiger-Bernays W, Tripodis Y, Levy JI. Estimating state-specific contributions to PM2.5- and O3-related health burden from residential combustion and electricity generating unit emissions in the United States. Environ Health Perspect, in press.

Penn SL, Boone ST, Harvey BC, Heiger-Bernays W, Tripodis Y, Arunachalam S, Levy JI. Modeling variability in air pollution-related health damages from individual airport emissions. Under review.

Underhill LJ, Penn SL, Boone S, Arunachalam S, Woo M, Levy JI. A comparative analysis of health damage functions across pollutants, source sectors, and geographic locations. Presented at the International Society for Exposure Science Annual Meeting, October 2016.

Outreach Efforts

Presentation at ASCENT meetings and academic conferences.

Awards

None

Student Involvement

Individual airport health damage function modeling was led by Stefani Penn as a doctoral student (graduated 9/15), and the comparative analysis work was led by Lindsay Underhill as a doctoral student.

Plans for Next Period
We plan to complete the formal comparative analyses and the corresponding manuscript in the first quarter of 2017.

Task 3 - Identify UFP concentration datasets that could be used to determine the magnitude and spatial extent of contributions from arriving aircraft in a near-airport setting.
Boston University School of Public Health

Objective(s)
As an initial step in constructing models of the contribution of aircraft arrivals to UFP concentrations, we needed to identify a candidate dataset for secondary analysis. While fully addressing all relevant research questions is challenging using field data not collected with the primary objective of aviation source apportionment, multiple pre-existing datasets would allow us to gain important insights and better determine the appropriate scope and scale of future efforts. Our objective was therefore to contact investigators, conduct sufficient preliminary analyses, and execute data use agreements to allow for statistical analyses to be conducted by our research team.

Research Approach
Not applicable – see Task 4 for analytical approaches for these data.

Milestone(s)
We proposed to identify the UFP concentration dataset and execute a data use agreement by 12/31/15 (Task 3), and this was completed in a timely fashion, with slight delays related to maternity leave for the doctoral student working on the project.

Major Accomplishments
We reviewed recent publications and available data and determined that the most appropriate candidate for secondary data analysis would be the CAFEH study conducted in the Boston area (http://sites.tufts.edu/cafeh/). The study had extensive fixed-site and mobile monitoring data including UFP across multiple neighborhoods that are both along flight paths and further away from flight paths. After meeting with lead investigators from CAFEH, we determined that real-time UFP monitoring data from a single fixed site at the Boston Globe would be ideal for our initial analysis (Figure 18.3). The site is directly underneath arrival flight paths and is generally upwind from major highways and other sources of UFP, so it would provide the cleanest natural experiment, without the analytical challenges related to mobile monitoring data collected in close proximity to traffic sources.

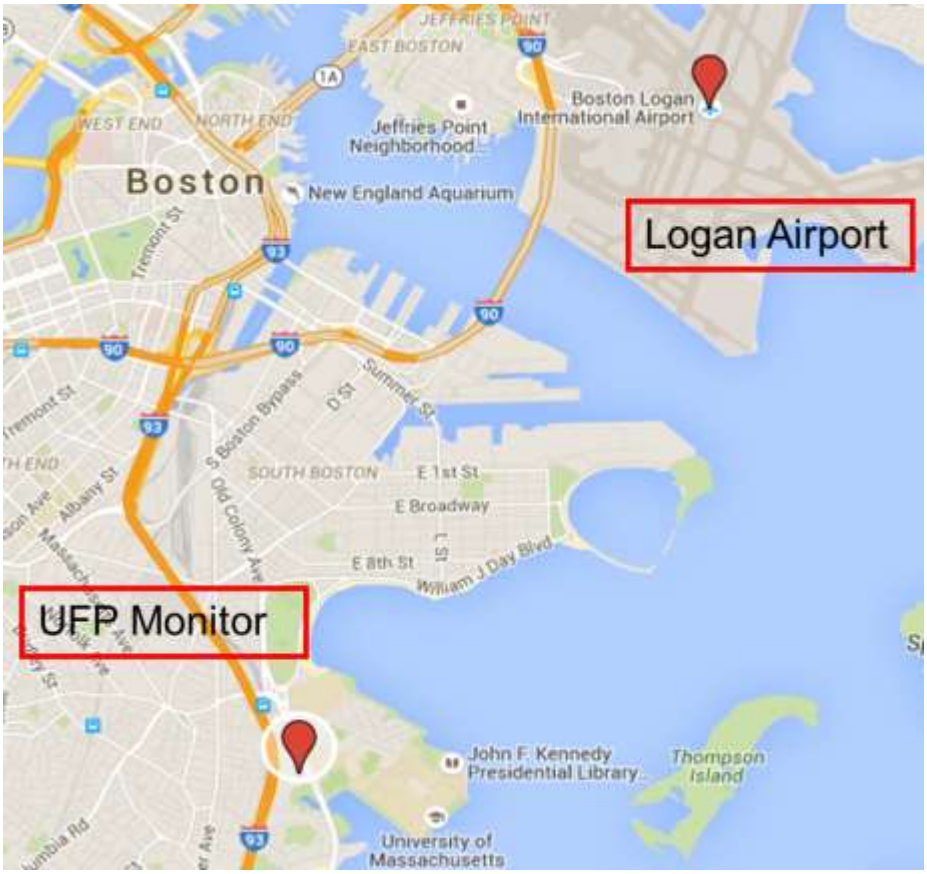

Figure 18.3. Location of UFP monitor relative to Logan Airport and major highways.

Publications
Not applicable – see Task 4.

Outreach Efforts
Not applicable – see Task 4.

Awards
Not applicable – see Task 4.

Student Involvement
The effort to identify an appropriate dataset was led by Chloe Kim, a doctoral student at BUSPH.

Plans for Next Period
None, as the task was completed and all analyses of the data are described under Task 4.

Task 4 - Apply multivariable regression modeling techniques to quantify the contribution of aircraft arrivals and other source activity with measured UFP concentrations.

Boston University School of Public Health

Objective(s)

With the dataset identified in Task 3, our objective was to conduct a series of statistical analyses aimed at quantifying the contribution of aircraft arrivals to UFP concentrations at the identified monitoring site underneath an arrival flight path. This involved using regression models to predict measured UFP concentrations as a function of real-time flight activity, meteorology, and other related variables. The objective was to use a regression modeling structure that accounted for the anticipated lag between when the flight was overhead and when the plume would reach the monitoring site, while also capturing autocorrelation in the real-time measurements. In addition, we proposed to conduct a series of data visualizations and exploratory analyses to identify the prevailing meteorological conditions that led to elevated concentrations.

Research Approach

Four different datasets – flight activity data, UFP concentration data, wind data, and temperature data – were collected and merged by their date-time stamp. PDARS/ASDE-X data (flight activity data) were provided by the FAA at 1-second resolution capturing all non-military arrival aircrafts to runway 4L and 4R at Boston Logan International Airport. Real-time UFP concentrations were collected from CAFEH investigators using a TSI 3775 Condensation Particle Counter between March 9, 2011 and May 31, 2011 at 1-second resolution at the Boston Globe building, which is located ~7 km south of the airport and underneath the flight arrival path to 4L/4R. Meteorological data were collected at 1-minute resolution at Boston Logan International Airport by the National Climatic Data Center.

We determined aircraft position at each observed second by its latitude and longitude in relation to the UFP monitor location. We then constructed multiple dummy variables to indicate the presence of aircraft at each time point within defined grid cells; by incorporating all of these spatial variables into the regression model, we were able to capture potential time lags between emissions and exposure. Multivariable regression models were developed using log-transformed UFP concentrations as the outcome variable and aircraft presence/absence at defined locations as the predictors, adjusting for wind speed, temperature, time of day, and day of week for each given wind direction (by 30˚ sections).

Milestone(s)

We proposed to complete statistical analyses of UFP concentrations and aircraft arrivals (Task 4.1) by 6/30/16 and to complete the related manuscript (Task 4.2) by 9/30/16. The tasks were delayed slightly because of the maternity leave of the doctoral student leading the analysis, as well as because of the statistical complexity and interpretability challenges inherent in real-time air pollution and flight activity data. The core regression models have been constructed and a manuscript is in progress, and we anticipate the manuscript being completed in the first quarter of 2017.

Major Accomplishments

First examining the distribution of UFP concentrations by wind direction (Figure 18.4), we see elevated concentrations with winds from the west (210-300 degrees), consistent with the proximity of the monitor to I-93, a major north-south highway located < 50 meters due west of the monitor. There also appears to be a secondary peak between 0 and 60 degrees, consistent with an aircraft influence related to 4L/4R.

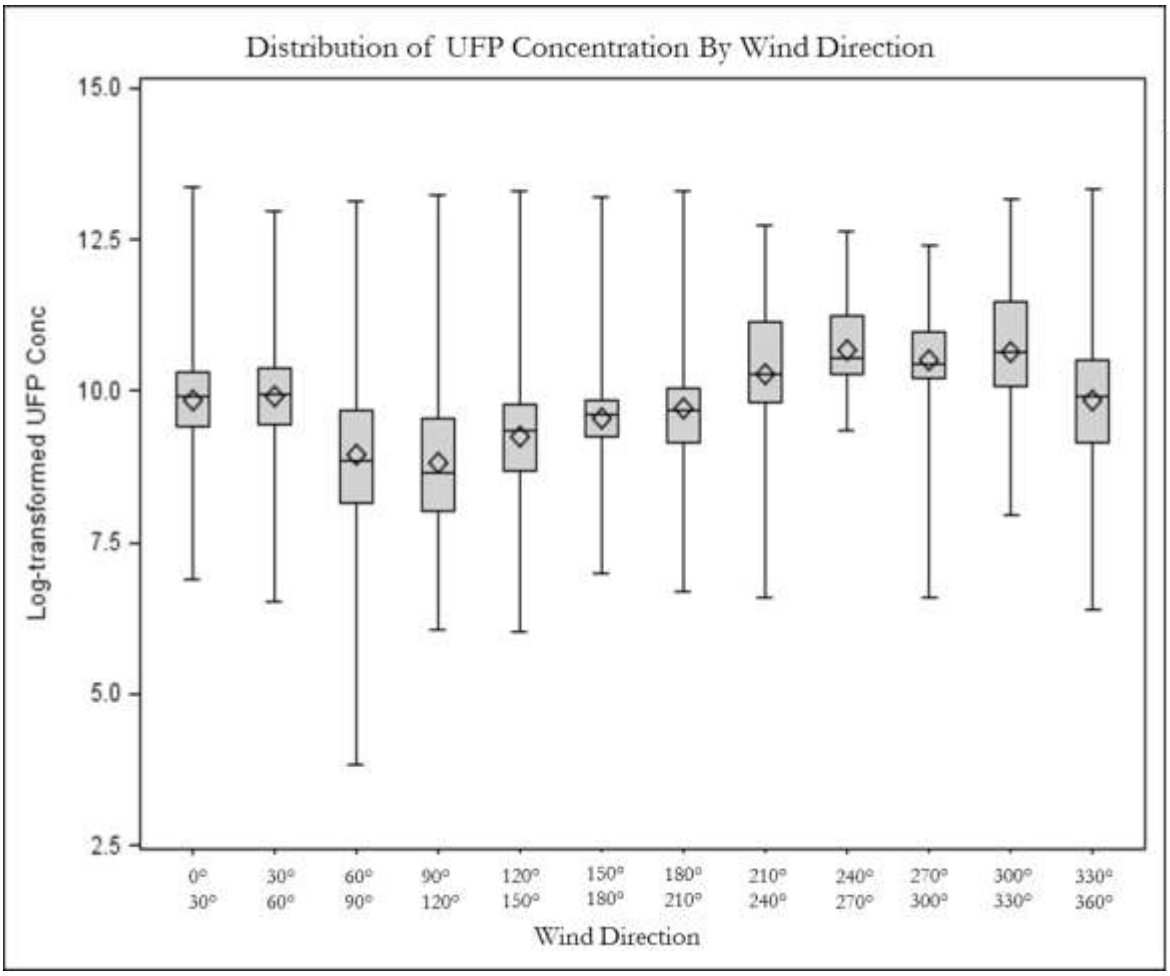

Figure 18.,4. UFP concentrations at the Boston Globe site as a function of wind direction.

Our analyses also suggested that the impact of aircraft arrivals on ambient UFP concentrations may not be limited to areas directly underneath the flight path, given that plumes of descending aircraft travel in a highly complex manner that is not yet well understood. As an illustration, we mapped UFP concentrations of two example flights. Within Figure 18.5, the spatial patterns of UFP measurements reflect the geographic locations of aircraft during the second in which fixed-site UFP concentrations were measured at the Boston Globe site. In other words, the concentrations represented at a given point in space do not reflect concentrations measured in that location, but rather concentrations at the fixed site when the aircraft was at the designated location. For both flights, there were two segments of elevated UFP concentrations. One happens close to the monitor, when the aircraft are relatively lower, suggesting a relatively short lag between emissions and increased concentrations. A second elevation happens further away from the monitor when the aircraft are relatively higher, with the influence of wind speed and direction suggesting an influence earlier in the flight trajectory. When wind speed is slower (left of Figure 18.5), there is a lingering effect of the aircraft for some time (~3 min) over a larger area, while when wind speed is faster (right of Figure 18.5), the longer-distance effect of the aircraft is higher but disappears more quickly (~1 min).

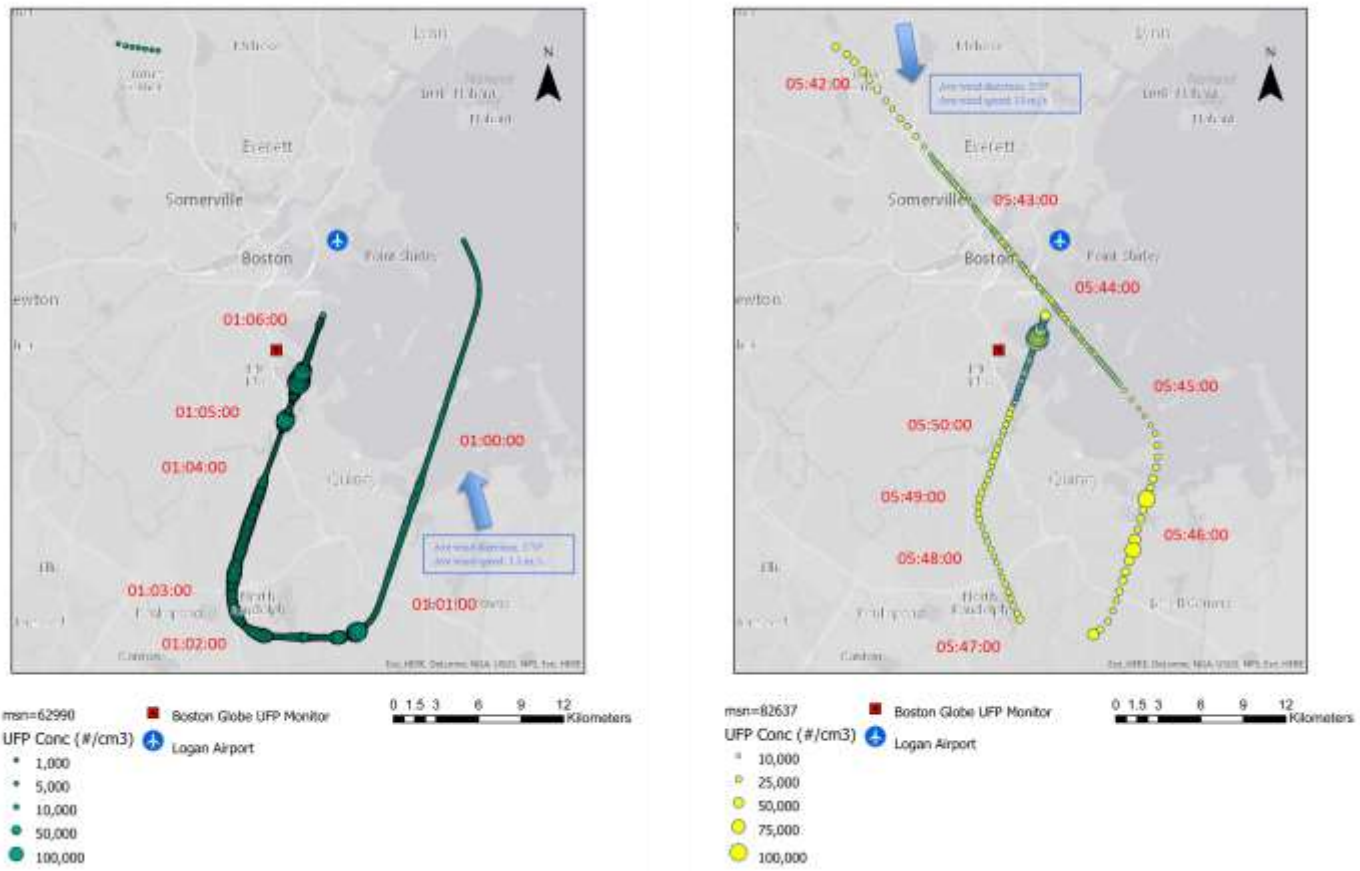

Figure 18.5. UFP concentrations at the Boston Globe site for two sample flight trajectories. Measurements in space represent concentrations measured at the fixed site during the second in which the aircraft was in a given location.

Within our regression models, we identified geographic hot spots under specific wind conditions (Figure 18.6). Since the models did not include time lags and the spatial covariates were intended to capture lags between emissions and ground-level impact, the hot spots likely reflect the effects of aircraft arrivals at earlier locations in their trajectories. As anticipated, the locations of hotspots vary widely depending on the wind direction. However, the consistent pattern is that the greatest increases in UFP concentrations were observed when aircraft were farther from the monitor. Given distance, elevation, and prevailing winds, this likely reflects times earlier in the flight trajectory when the monitor would be downwind of the plume (i.e., Figure 18.5). These results suggest that the impacts of aircraft arrivals on ambient UFP concentrations may not be limited to areas directly underneath the flight path. Given the elevation of the aircraft above the monitoring site, the point of average maximal impact appears to be a considerable distance from the flight path.

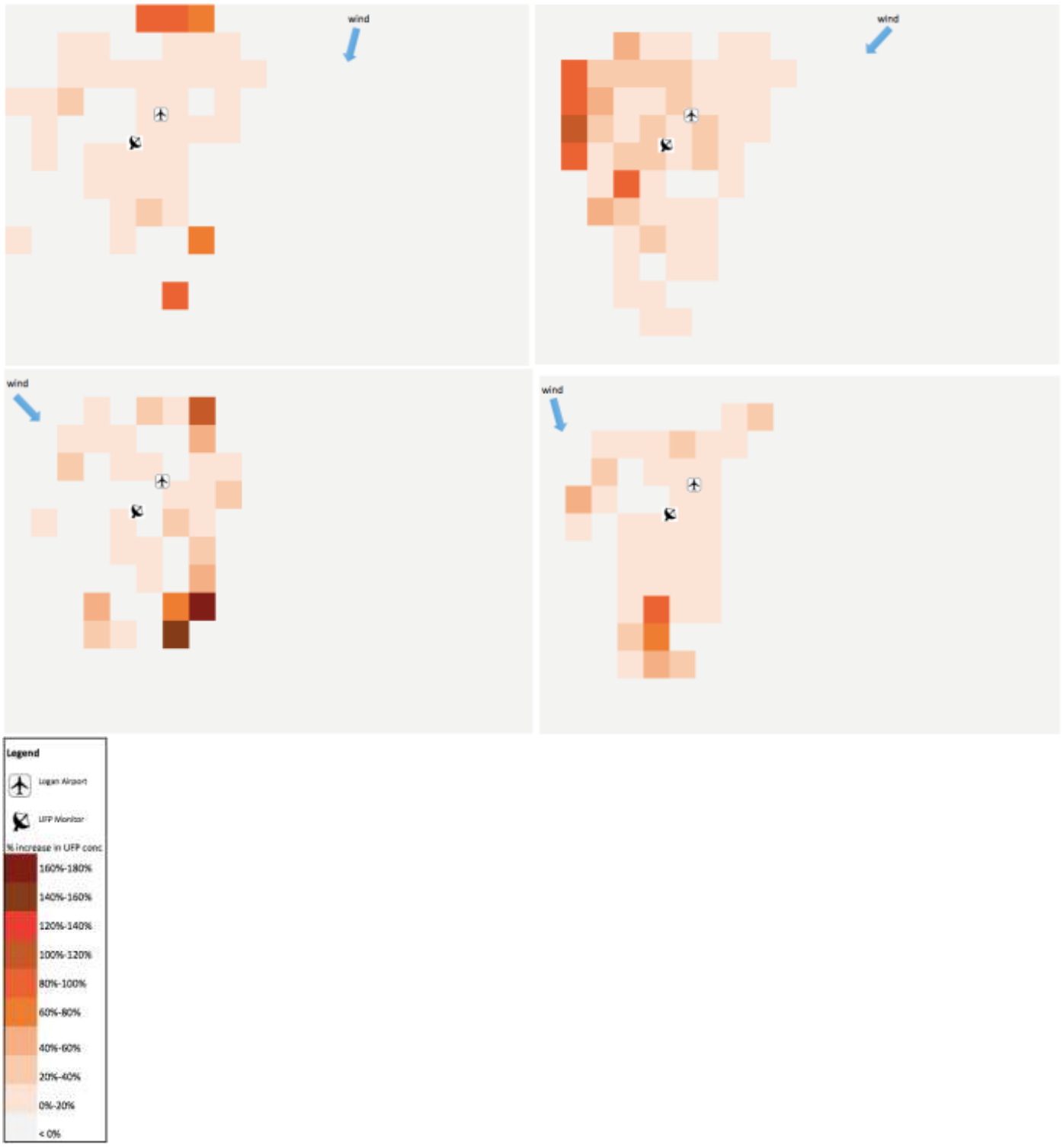

Figure 18.6. Heat-map displaying aircraft locations associated with increased UFP concentrations under four different wind directions, derived from multivariable regression models.

Publications
Kim CS, Tripodis Y, Levy JI. Magnitude and spatial patterns of ultrafine particulate matter associated with aircraft arrivals near Boston Logan Airport. Presented at the International Society for Exposure Science Annual Meeting, October 2016.

Outreach Efforts
Presentation at ASCENT meetings and academic conferences.

Awards
None

Student Involvement
The work was led by Chloe Kim as a doctoral student.

Plans for Next Period
We plan to complete the final statistical analyses and the corresponding manuscript in the first quarter of 2017. We also plan to use the modeling results to support site selection for our forthcoming UFP monitoring campaign.

ASCENT 019 Development of Aviation Air Quality Tools for Airshed-Specific Impact Assessment: Air Quality Modeling

University of North Carolina at Chapel Hill

Project Lead Investigator

Saravanan Arunachalam, Ph.D.
Research Associate Professor
Institute for the Environment
University of North Carolina at Chapel Hill
100 Europa Drive, Suite 490
Chapel Hill, NC 27517
919-966-2126
sarav@email.unc.edu

University Participants

University of North Carolina at Chapel Hill

- PI: Saravanan Arunachalam, Research Associate Professor
- FAA Award Number: 13-C-AJFE-UNC Amendments 1 - 5
- Period of Performance: September 13, 2013 – December 31, 2016
- Task(s):
  1. Develop and Assess Efficacy of Multiple Emissions Scenarios using the APMT-Impacts Air Quality Modeling Platform for year-over-year analysis to achieve Air Quality (and Health) Goals under FAA's Policy Initiatives
  2. Extend current prototype modeling for CMAQ-DDM-3D to compute Airport-specific Sensitivities for the year 2005, and explore possibilities to extrapolate for a future year
  3. Assess PM Size Distribution Impacts of Aircraft Emissions
  4. Assess impacts of coupled models on Aviation-related AQ Impacts
  5. Develop High Fidelity Weather for Global Inventories using AEDT

Project Funding Level

$369,966

Matching funds from
A) Los Angeles World Airport Authority (LAWA)
B) North American Insulation Manufacturers Association (NAIMA).

Investigation Team

Prof. Saravanan Arunachalam (UNC) (Principal Investigator) [Tasks 1-5]
Dr. Jared Bowden (UNC) (Co-Investigator) [Tasks 1, 4, 5]
Dr. Mohammad Omary (UNC) (Co-Investigator) [Tasks 1, 4]
Dr. Moniruzzaman Chowdhury (Co-Investigator) [Task 4]
Dr. Jiaoyan Huang (UNC) (Co-Investigator) [Task 3]
Ms. Pradeepa Vennam (UNC) (Graduate Research Assistant) [Tasks 1-4]
Mr. Calvin Arter (UNC) (Graduate Research Assistant) [Task 2]

Project Overview

With aviation forecasted to grow steadily in upcoming years,[1] a variety of aviation environmental policies will be required to meet emissions reduction goals in aviation-related air quality and health impacts, and tools will be needed to rapidly assess the implications of alternative policies in the context of an evolving population and atmosphere. In addition, tools are required to understand the implications of global aviation emissions, in the context of the International Civil Aviation Organization (ICAO)'s Committee on Aviation Environmental Protection (CAEP).

The overall objective of this project is to continue to develop and subsequently implement tools to allow for assessment of year-over-year changes in significant health outcomes, both within the US and globally. These tools are intended to be acceptable to FAA (in the context of Destination 2025) or to other decision-makers, while providing outputs quickly enough to allow for a variety of "what if" analyses and other investigations. While the tools for use within and outside the US (for CAEP) need not be identical, a number of attributes would be ideal to include in both:

- Enable the assessment of premature mortality and morbidity risk due to aviation-attributable $PM_{2.5}$, ozone, and any other pollutants determined to contribute to significant health impacts from aviation emissions;
- Capture airport-specific health impacts at a regional and local scale;
- Account for the impact of non-LTO and LTO emissions, including separation of effects;
- Allow for the assessment of a wide range of aircraft emissions scenarios, including differential growth rates and emissions indices;
- Account for changes in non-aviation emissions and allow for assessing sensitivity to meteorology;
- Provide domestic and global results;
- Have quantified uncertainties and quantified differences from EPA practices, which are to be minimized where scientifically appropriate; and
- Be computationally efficient such that tools can be used in time-sensitive rapid turnaround contexts and for uncertainty quantification.

The overall scope of work is being conducted amongst three collaborating universities – Boston University (BU), Massachusetts Institute of Technology (MIT) and the University of North Carolina at Chapel Hill (UNC). However, while the reporting is being done under three separate projects (ASCENT 18, 19 and 20) by each collaborating university, the project is performed as a coordinated effort with extensive interactions among the three institutions. The components led by the University of North Carolina at Chapel Hill's Institute for the Environment (UNC-IE) included detailed modeling of air quality using the Community Multiscale Air Quality (CMAQ) model. UNC-IE is collaborating with BU to develop health risk estimates on a national scale using CMAQ outputs, and with MIT for inter-comparing against nested GEOS-Chem model applications within the US and to further compare/contrast the forward sensitivity versus the inverse sensitivity (such as adjoint) techniques for source attribution. Our efforts for this project build directly on previous efforts within Project 16 of PARTNER, including detailed air quality modeling and analyses using CMAQ at multiple scales for multiple current and future year scenarios, health risk projection work that successfully characterizes the influence of time-varying emissions, background concentrations, and population patterns on the public health impacts of aviation emissions under a notional future emissions scenario for 2025. Under Project 16, we started to develop a new state-of-the-art base year modeling platform for the US using the latest version of models (CMAQ, WRF, SMOKE) and emissions datasets (AEDT, NEI), and tools (MERRA-2-WRF, CAM-2-CMAQ) to downscale from GCMs being used in Aviation Climate Change Research Initiative (ACCRI).

In this project, we are performing research on multiple fronts during the stated period of performance:

1. Develop and assess efficacy of multiple emissions scenarios using the APMT-Impacts Air Quality Modeling Platform for year-over-year modeling to achieve air quality (and health) goals under FAA's Policy Initiatives
2. Extend current prototype modeling for CMAQ-DDM-3D to compute higher order sensitivity coefficients
3. Assess PM size distribution impacts of aircraft emissions on ambient air quality

[1] Boeing Commercial Airplane Market Analysis, 2010.

4. Assess impacts of meteorology-chemistry coupled models and the feedback processes on Aviation-related AQ Impacts
5. Develop High Fidelity Weather for Global Inventories using AEDT

Task 1: Develop and Assess Efficacy of Multiple Emissions Scenarios using the APMT-Impacts Air Quality Modeling Platform for Year-over-year Analysis to Achieve Air Quality (and Health) Goals under FAA's Policy Initiatives

University of North Carolina at Chapel Hill

Objective(s)

The objective of this task is to develop a multi-year WRF-SMOKE-CMAQ modeling platform to assess the past, present and future year US-wide aviation impacts on air quality. This platform helps to address the aspirational goal of FAA to reduce aviation emissions contribution to significant air quality and health impacts in future years.

Research Approach

We reported WRF-SMOKE-CMAQ modeling framework development and model predictions for annual years 2005 and 2010 in last year's annual report. This year, we worked on few additional tasks to improve the future CMAQ modeling framework for air quality and health assessment studies. Figure 1.1 shows the modeling framework that UNC has been developing. While initially the years identified were 2005, 2010 and 2018, recently FAA has recommended that we model 2011 and 2015 moving forward.

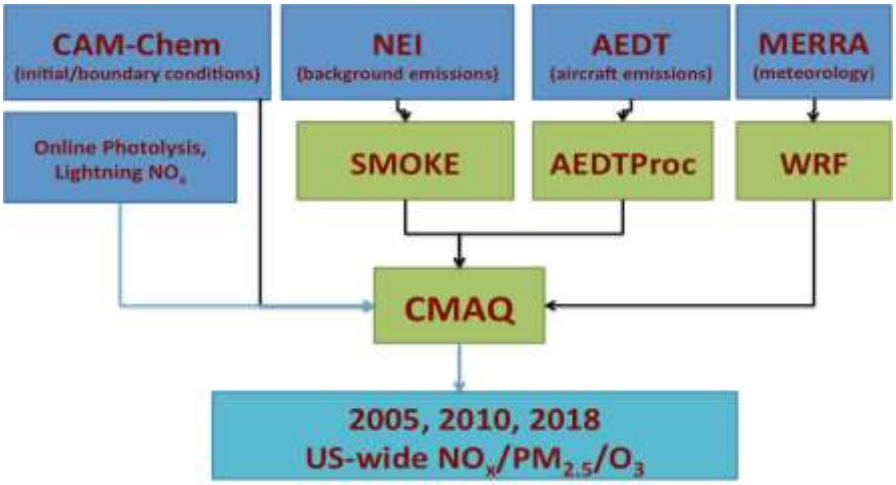

Figure 1.1: Flowchart representing the modeling methodology platform.

CMAQ-DDM v4.7.1 Results: We completed 2005 annual year all-airports CMAQ-DDM (direct decoupled method) model simulations and provided annual and quarterly average results to Boston university (BU) for health studies. Figure 1.2 shows the domain wide $PM_{2.5}$ and O_3 aviation-attributable concentrations from CMAQ-DDM model outputs. Here we compared pseudo two-month average contributions with four annual quarters (P1: JFM, P2: AMJ, P3: JAS, P4: OND months) and annual averages to understand the differences in various temporal averaging. This exercise will also explain if it is necessary to conduct annual simulations or the pseudo two-month simulations are sufficient to estimate the annual aviation-attributable perturbations. The results indicate that in the case of $PM_{2.5}$ the monthly and quarterly averages are comparable to annual average whereas in the case of O_3, due to non-linear chemistry, we observed high seasonal differences (summer contributions were higher than winter), which are averaged with the annual average. Therefore in the case of O_3, it is important to conduct a full annual model simulation to capture the annual seasonal trend.

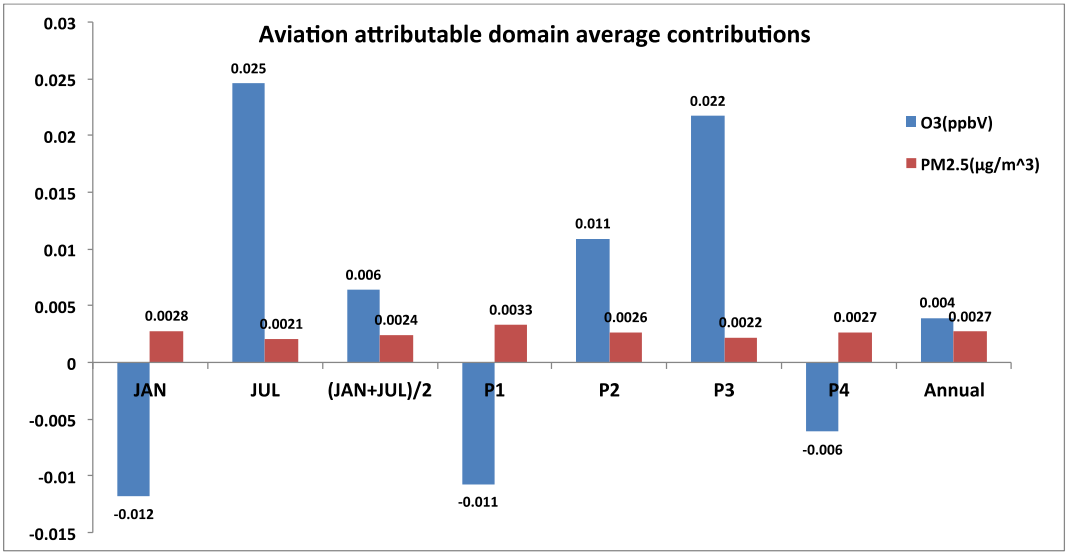

Figure 1.2: Aviation attributable domain average contributions of O_3 (blue) and $PM_{2.5}$ (red) for January, July, pseudo two-month (JAN+JUL/2), quarterly (P1, P2, P3, P4) and annual time periods.

Meteorological Inputs: In support of the High Fidelity Weather task, we migrated to drive WRF with inputs from NASA's Modern-Era Retrospective Analysis for Research and Applications reanalysis data (MERRA) (Rienecker et al., 2011). We completed downscaling MERRA with WRF for the year 2013 and 2015 is in progress.

Boundary conditions for future CMAQ modeling: In this task we generated downscaled dynamical boundary conditions for CMAQ model from global model CAM-Chem modeling scenarios provided by UIUC under ACCRI project. The 2005 and 2050 scenarios are described in Table 1.1 which indicates the emission modifications that went into future year 2050 modeling. We generated 2005, 2050 boundary conditions and compared them for four quarters in the modeling period, as shown in Figure 1.2. In the case of O_3 at the surface (as represented in Figure 1.3), the 2050 boundary concentrations are lower than in 2005, whereas in upper model layers (not shown here) 2050 concentrations are higher than 2005. Therefore, for future modeling, these downscaled boundary conditions can be utilized as inputs to run a regional scale CMAQ model for both present and future year scenarios. In addition, we also explored another option to use a hemispheric CMAQ application to generate boundary conditions for regional CMAQ, which should also be considered for future work.

Table 1.1: 2005 and 2050 ACCRI modeling scenarios for CAM-Chem global model

Scenarios	Emissions Description
2005 sens	2005 all sources + aviation
2050 SC1	2050 all sources + aviation (technology improvement, reduction in NOx emissions)
2050 Alt	2050 all sources + aviation (alternative fuel, zero sulfur emissions and 50% reduction in BC emissions)

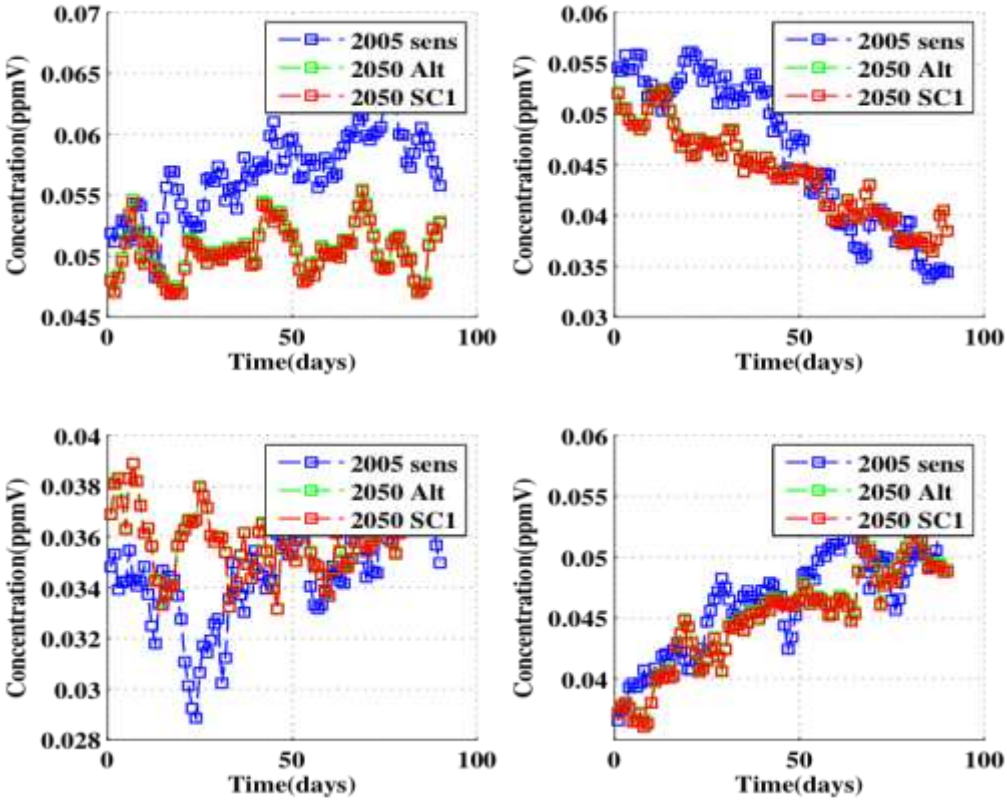

Figure 1.3: Layer 1 (model surface layer) daily average boundary conditions of Ozone for four quarters P1 (JFM, top left), P2 (AMJ, top right), P3 (JAS, bottom left) and P4 (OND, bottom right) in annual year.

Airport-based emissions: We analyzed airport-based emissions from raw AEDT segment data to understand the contribution from top airports in U.S. This data was performed in support of BU's health assessment study, so we provided airport specific annual, as well as monthly, fuel burn and emissions information. We calculated all U.S. airport total fuel burn and emissions for year 2005 and estimated the total contribution from the top 66, 100, 150, 200 and 300 airports relative to all U.S. airports fuel burn, as shown in Table 1.2. It appears that the top 300 airports cover ~97% of the U.S. aviation fuel burn. The highest fuel burn percentage is shown at the ATL airport, contributing ~5.2% to the total U.S. airport fuel burn, followed by ORD (~ 5.1%), LAX (~4%), DFW (~4%) and JFK (~3.5%). This information can be very helpful in future airport-specific DDM modeling work to make decisions regarding the number of airports that need to be considered for first and second aviation emissions-related sensitivities.

Table 1.2: Airports grouping and their respective Fuel Burn percentage

Airports	Fuel Burn (%)
DDM – 66 airports work	77%
Top 66 airports	84%
Top 100	89%
Top 150	94%
Top 200	95%
Top 300	97%

AEDT testing: This year we received sample recent years of AEDT segment and flight data a few different times (early 2016 and again during end of 2016). We tested our tool each time and reported the issues to FAA. Finally last month, we

received recent years' raw AEDT (2010, 2015) annual segment and flight data. The initial single day testing was completed and presently we are processing month-long gridded data with our AEDTProc processing tool (Baek et al., 2012). Once we complete this phase of testing, we are ready to generate annual flight gridded emission inputs for multiple annual years.

Milestone(s)

April 2016 - Completed generating boundary conditions for CMAQ platform using CAM-Chem global model outputs from model ensemble ACCRI project for 2005 and 2050 scenarios.
July 2016 - Generated 2005 airport-by-airport based fuel burn percentages and provided the top airports emissions that contribute to 97% of U.S. fuel burn.
December 2016 - Tested and processed new 2010 and 2015 AEDT raw segment data using our AEDTProc gridding tool to generate CMAQ domain specific gridded emission inputs.

Major Accomplishments

The different study areas conducted in task 1 provide us the information necessary for various NAS-wide modeling future work decisions. The tools tested and the data generated in this task will be used in the remaining all other DDM, coupled WRF-CMAQ and particulate matter size distribution tasks under this project.

Publications

None

Outreach Efforts

None

Awards

None

Student Involvement

Pradeepa Vennam conducted most of the work under this task and graduated this semester with her PhD.

Plans for Next Period

NAS-wide modeling platform possible updates:

For the next phase of modeling, we are planning to update and change several modeling specifications and data inputs. Below are the details for some possible updates to improve the NAS-wide modeling platform to perform year-by-year simulations.

1) MERRA2: New reanalysis of MERRA2 meteorology data (data available from 1978-recent) is released with recent updates to MERRA, which showed improvement in seasonal mean climate, re-evaporation of frozen precipitation and cloud condensate (Molod et al., 2015; Bosilovich et al., 2015).
2) CMAQv5.1: EPA released new CMAQ version 5.1 (Bash et al., 2015) with important updates (ACM2 scheme (vertical velocity calculation) modification, potential vorticity update, SOA updates). We will use this version or CMAQ v5.2 Beta, which is expected to be finalized in spring 2017 for next phase of modeling.
3) Boundary conditions: Generate downscaled boundary conditions from hemispheric CMAQ to drive regional CMAQ. This approach maintains the consistency in chemical and physical processes used between the regional scale model and boundary conditions. Hemispheric model based tools were already developed for some of our other projects that can be utilized and applied here. We strongly recommend the benefits of using hemispheric boundary conditions based on availability instead of different global model boundary conditions.
4) Domain resolution: In recent years, EPA started to use 12-km grid resolution for most of their policy related modeling tasks and CMAQ testing purposes. So upgrading to 12-km model grid resolution from 36-km in our modeling work will better capture the fine-scale impacts near the airports and will be consistent to other regulatory modeling protocols.

5) Background emissions: Update background emissions for all sources to the latest NEI emissions (2014 or 2011) from the EPA.

References

Baek, B. H., Arunachalam, S., Woody, M., Vennam, L. P., Omary, M., Binkowski, F., and Fleming, G.: A new interface to model global commercial aircraft emissions from the FAA Aviation Environmental Design Tool (AEDT) in air quality models, Annual CMAS Conference, Chapel Hill, NC, USA, 15–17 October, 2012.

Molod, A., Takacs, L., Suarez, M., & Bacmeister, J. (2015). Development of the GEOS-5 atmospheric general circulation model: evolution from MERRA to MERRA2. *Geoscientific Model Development*, *8*(5), 1339-1356.

Bash, J., K. Fahey, AND H. Foroutan. CMAQv5.1 RELEASE NOTES. U.S. Environmental Protection Agency, Washington, DC, 2015.

Bosilovich, M., Akella, S., Coy, L., Cullather, R., Draper, C., Gelaro, R., Kovach, R., Liu, Q., Molod, A., Norris, P., Wargan, K., Chao, W., Reichle, R., Takacs, L., Vikhliaev, Y., Bloom, S., Collow, A., Firth, S., Labow, G., Partyka, G., Pawson, S., Reale, O., Schubert, S. D., and Suarez, M.: MERRA-2: Initial evaluation of the climate, NASA Tech. Rep. Series on Global Modeling and Data Assimilation, NASA/TM – 2015 - 104606, Vol. 43, 2015.

Rienecker, M. M., Suarez, M. J., Gelaro, R., Todling, R., Bacmeister, J., Liu, E., … Woollen, J. (2011). MERRA: NASA's modern-era retrospective analysis for research and applications. *Journal of Climate*, *24*(14), 3624–3648. http://doi.org/10.1175/JCLI-D-11-00015.1.

Task 2: Develop 2nd Order Sensitivities with CMAQ-DDM

University of North Carolina at Chapel Hill

Objective(s)

The objective of this task is to implement and explore second order Decoupled Direct Method (DDM) sensitivity coefficient calculations with LTO emissions from aircraft across the United States. This will be done with the Community Multiscale Air Quality Model (CMAQ) version 5.0.2.

Research Approach

Introduction

Air quality models are used to estimate concentrations of pollutants in the atmosphere. We aim to use air quality models to estimate concentrations of pollutants from aircraft emissions in order to model the impact of aircraft emissions on human health for populations in the vicinity of airports.

Sensitivity analysis tools are often used within the air quality modeling framework to evaluate impacts due to changing input parameters in the model such as emission rates, initial conditions, or boundary conditions. These become important for utilizing models as a way to guide emission reduction policies. Sensitivity tools have been limited to finite difference and regression-based methods that often become computationally intractable and are often unable to describe *ad hoc* analyses. Furthermore, to calculate pollutant concentration sensitivities to LTO emissions, we use the Decoupled Direct Method (DDM) in CMAQ. DDM methods calculate sensitivity coefficients in a single model run (Russell, 2005; Zhang et al., 2012), allowing for *ad hoc* analyses from changing multiple input parameters at a time. And perhaps most importantly, the use of DDM allows for the inline calculation of both first and higher order sensitivity coefficients, which become important for pollutant species that may not be linearly dependent on certain precursors. First order sensitivity calculations will yield information about the change in species concentrations with respect to varying one input parameter. In our case, these calculations will only describe linear changes of concentrations with respect to increasing or decreasing emissions from aircraft. However, some changes in species, such as secondary organic aerosols, do not linearly change with increasing or decreasing precursor emissions and higher order sensitivity coefficients can capture the non-linear change in species concentrations.

Methodology

Higher order DDM was implemented in CMAQ version 5.0.2. DDM becomes an ideal choice for describing aircraft (airport) emissions since the relatively small quantity of emissions emitted by each source can lead to numerical noise with other sensitivity methods that require multiple model runs for each varied parameter (Napelenok, Cohan, Hu, & Russell, 2006). CMAQ-DDM first and second order runs were performed for all airports (~2100 airports) in the continental United States (CONUS) in January and July of 2005. Ten day spin-up simulations were performed prior to the start of each month (December and June, respectively). Six precursor species groups (NO_x, SO_2, VOCs, PSO_4, PEC and POC) were designated as sensitivity input parameters. First and second order sensitivities of O_3 and $PM_{2.5}$ to the emissions of these six precursors were calculated.

Flight segment data from AEDT (Roof & Fleming, 2007; Wilkerson et al., 2010) were processed into gridded emission rate files using AEDTProc (Baek, B.H., Arunachalam, S., Woody, M., Vennam, L.P., Omary, M., Binkowski, F., Fleming, 2012). Landing and takeoff operations were considered by capping full-flight aircraft emissions at 3,000 feet. Our domain covered the continental United States with 36x36 km horizontal grid resolution and thirty-four time-varying pressure-based vertical layers (LTO constrained to the first 17 layers around 3,000 feet or 914 meters).

Other background anthropogenic emission sources were obtained from EPA's National Emissions Inventories (NEI-2005) and 2005 boundary conditions were derived from global CAM-chem simulations (Lamarque et al., 2012). Meteorology conditions for 2005 were obtained from the Weather Research and Forecasting model (WRF) (Skamarock et al., 2008), with outputs downscaled from NASA's Modern-Era Retrospective Analysis for Research and Applications data (MERRA) (Rienecker et al., 2011).

Results

A key milestone of the overall work of this project has been the successful implementation of HDDM with CMAQ version 5.0.2. Prior studies (Boone, n.d.) only looked at first order DDM sensitivity coefficient calculations with CMAQ version 4.7.1. By utilizing a more up to date version of the model, we hope to utilize more accurate chemical mechanisms and science modules. Model evaluation will be performed by comparing CMAQ HDDM sensitivity coefficient output with CMAQ Brute Force sensitivity calculations. We will also compare CMAQ HDDM concentration outputs to observed data using the Atmospheric Model Evaluation Tool (AMET). Preliminary model runs have been performed, calculating the sensitivity of O_3 to first order changes in NO_x emissions, first order changes in VOC emissions, and second order changes to NO_x and VOC emissions ($\frac{dC_{O_3}}{dE_{NO_x}dE_{VOC}}$). We also calculated the sensitivity of Nitrate aerosols, Sulfate aerosols, and total $PM_{2.5}$ to first order changes in NO_x emissions, first order changes in SO_2 emissions, and second order changes to NO_x and SO_2 emissions.

Figures 2-1 through 2-3 show spatial plots of the calculated sensitivity coefficients in our domain for the months of January (left figures) and July (right figures) for first order changes to O_3 concentrations with respect to NO_x emissions (Fig. 2-1) and VOC emissions (Fig. 2-2), and second order changes to O_3 concentrations with respect to NO_x emissions and VOC emissions (Fig. 2-3). Figures 2-4 through 2-6 show spatial plots of the calculated sensitivity coefficients in our domain for the months of January (left figures) and July (right figures) for first order changes to $PM_{2.5}$ concentrations with respect to NO_x emissions (Fig. 2-4) and SO_2 emissions (Fig. 2-5), and second order changes to $PM_{2.5}$ concentrations with respect to NO_x emissions and SO_2 emissions (Fig. 2-6). Figure 2-7 shows linear regression plots comparing DDM-generated sensitivities and brute force deltas.

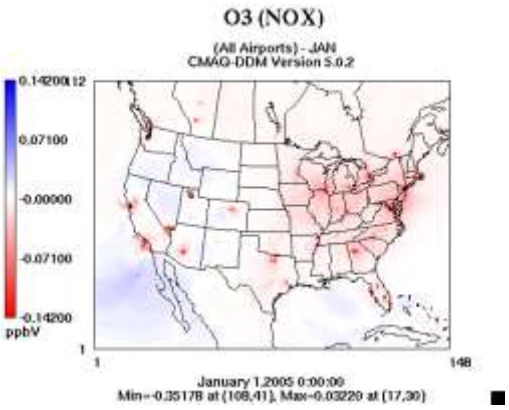

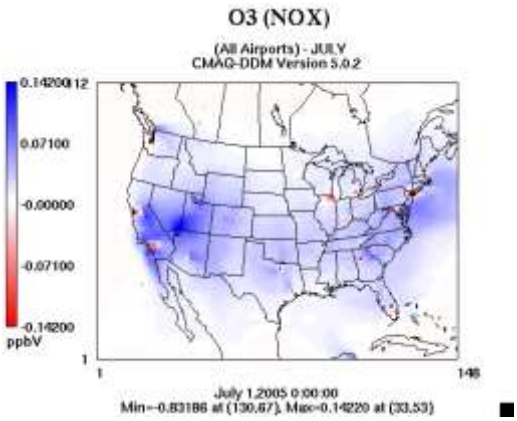

Figure 2-1: First order sensitivity coefficient calculations of O_3 sensitivities to NO_x for January (Left) and July (Right)

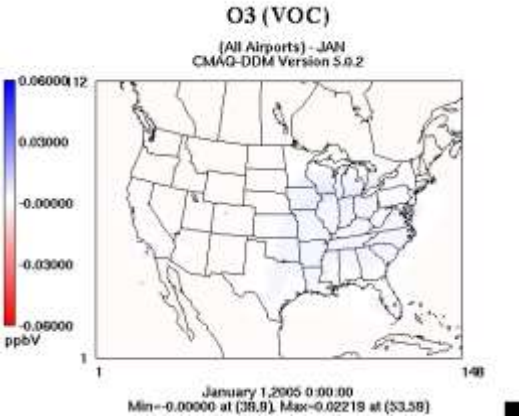

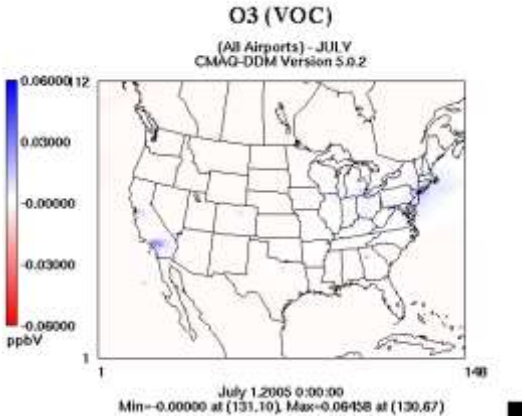

Figure 2-2: First order sensitivity coefficient calculations of O_3 sensitivities to VOCs for January (Left) and July (Right)

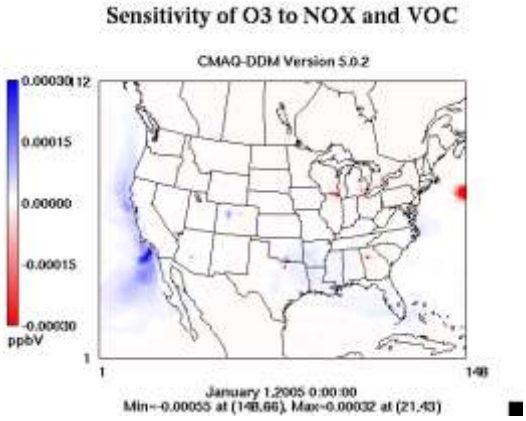

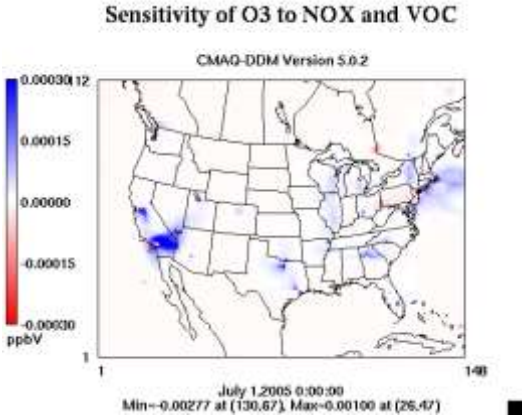

Figure 2-3: Second order sensitivity coefficient calculations of O_3 sensitivities to NO_x and VOCs for January (Left) and July (Right)

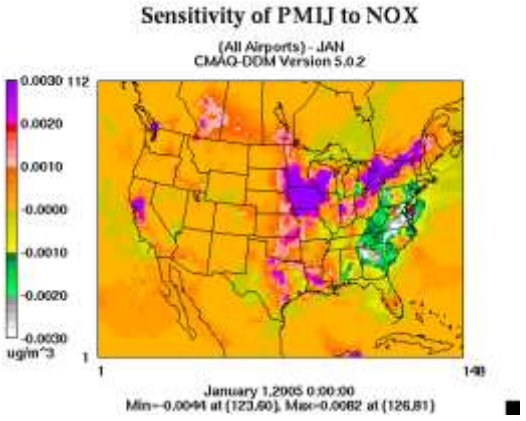

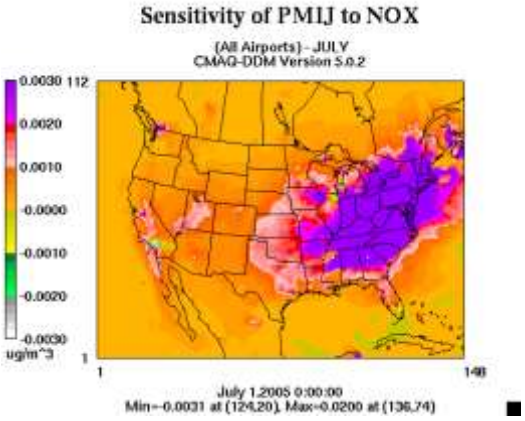

Figure 2-4: First order sensitivity coefficient calculations of $PM_{2.5}$ sensitivities to NO_x for January (Left) and July (Right)

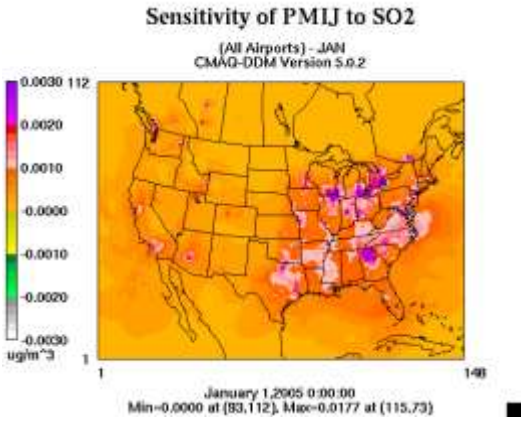

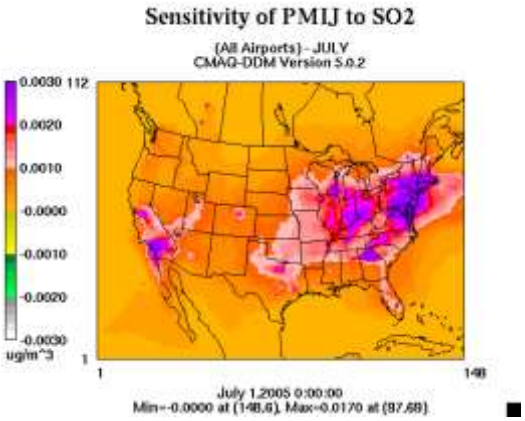

Figure 2-5: First order sensitivity coefficient calculations of $PM_{2.5}$ sensitivities to SO_2 for January (Left) and July (Right)

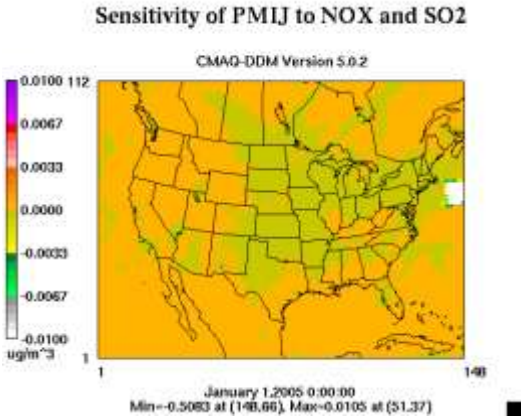

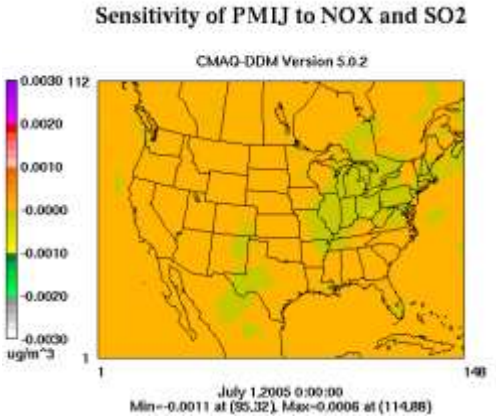

Figure 2-6: Second order sensitivity coefficient calculations of $PM_{2.5}$ sensitivities to NO_x and SO_2 for January (Left) and July (Right)

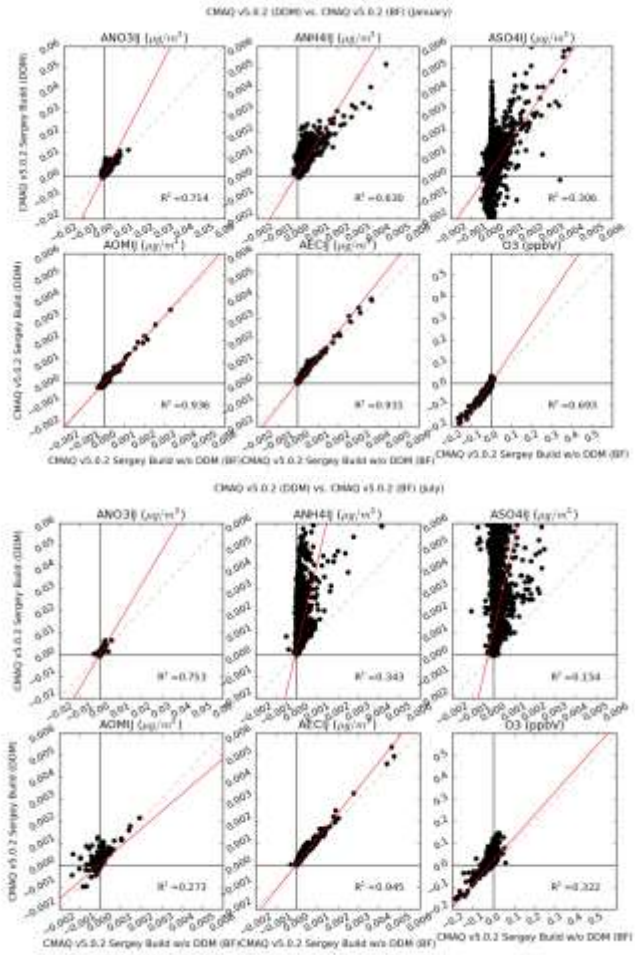

Figure 2-7: Comparison of DDM-generated sensitivities and brute force deltas for January (Top) and July (Bottom). Model setups between the two runs differ by the build used, and we anticipate better performance with consistent builds across setups.

Milestone(s)

December 2016 – First implementation of CMAQ-HDDM for aircraft emissions for test simulation period

Major Accomplishments

We have successfully implemented and tested higher order sensitivity in CMAQ v5.0.2 for aircraft emissions. With continued testing and evaluation, we will be able to assess the potential non-linearities in second order sensitivities that were not captured with first order sensitivities that have been the focus of this project to date. We will thus be able to better inform emission reduction policies with regards to mitigating air quality (and health) impacts around key airsheds of the nation.

Publications

None

Outreach Efforts

None

Awards
None

Student Involvement
Calvin Arter is a 1st year Ph.D. student who started work on this project in summer 2016.

Plans for Next Period
Next steps will include detailed analyses of the results with regards to constructing an emissions reductions policy. FAA has provided us with a draft set of policy options to use as illustration of applying the DDM-based sensitivity outputs. We plan to utilize these results to answer for e.g., how many airports would be needed in a clean air region to bring that area from attainment to nonattainment for NAAQS of O_3 and $PM_{2.5}$. We can also look to analyze how air pollutant concentrations may change if ultra-low sulfur jet fuel was used across the United States. We also hope to expand our sensitivity matrix to include additional sensitivities to precursors and utilize the second order DDM sensitivity coefficient calculations to accurately observe nonlinear dependence of secondarily formed inorganic aerosols on their precursors. This work will eventually be performed with an updated modeling framework for the year 2011, with all inputs (meteorology, background and aircraft emissions) and modeling framework updated.

References

Baek, B.H., Arunachalam, S., Woody, M., Vennam, L.P., Omary, M., Binkowski, F., Fleming, G. (2012). A New Interface to Model Global Commercial Aircraft Emissions from the FAA Aviation Environmental Design Tool (AEDT) in Air Quality Models.

Boone, S. (n.d.). Calculation of Sensitivity Coefficients for Individual Airport Emissions in the Continental U . S . using CMAQ-DDM / PM, (x).

Lamarque, J. F., Emmons, L. K., Hess, P. G., Kinnison, D. E., Tilmes, S., Vitt, F., … Tyndall, G. K. (2012). CAM-chem: Description and evaluation of interactive atmospheric chemistry in the Community Earth System Model. *Geoscientific Model Development*, *5*(2), 369–411. http://doi.org/10.5194/gmd-5-369-2012

Napelenok, S. L., Cohan, D. S., Hu, Y., & Russell, A. G. (2006). Decoupled direct 3D sensitivity analysis for particulate matter (DDM-3D / PM), *40*, 6112–6121. http://doi.org/10.1016/j.atmosenv.2006.05.039.

Rienecker, M. M., Suarez, M. J., Gelaro, R., Todling, R., Bacmeister, J., Liu, E., … Woollen, J. (2011). MERRA: NASA's modern-era retrospective analysis for research and applications. *Journal of Climate*, *24*(14), 3624–3648. http://doi.org/10.1175/JCLI-D-11-00015.1.

Roof, C., & Fleming, G. G. (2007). Aviation Environmental Design Tool (AEDT). *22nd Annual UC Symposium on Aviation Noise and Air Quality*, (March), 1–30.

Russell, A. G. (2005). Nonlinear Response of Ozone to Emissions : Source Apportionment and Sensitivity Analysis, *39*(17), 6739–6748.

Skamarock, W. C., Klemp, J. B., Dudhi, J., Gill, D. O., Barker, D. M., Duda, M. G., … Powers, J. G. (2008). A Description of the Advanced Research WRF Version 3. *Technical Report*, (June), 113. http://doi.org/10.5065/D6DZ069T.

Wilkerson, J. T., Jacobson, M. Z., Malwitz, A., Balasubramanian, S., Wayson, R., Fleming, G., … Lele, S. K. (2010). Analysis of emission data from global commercial aviation: 2004 and 2006. *Atmospheric Chemistry and Physics*, *10*(13), 6391–6408. http://doi.org/10.5194/acp-10-6391-2010.

Zhang, W., Capps, S. L., Hu, Y., Nenes, A., Napelenok, S. L., & Russell, A. G. (2012). Model Development Development of the high-order decoupled direct method in three dimensions for particulate matter : enabling advanced sensitivity analysis in air quality models, 355–368. http://doi.org/10.5194/gmd-5-355-2012.

Task 3: Assess PM Size Distribution Impacts of Aircraft Emissions
University of North Carolina at Chapel Hill

Objective(s)

To enhance representation of particle size distribution of aircraft emissions in the Community Multiscale Air Quality (CMAQ) Model.

To understand impacts on CMAQ chemical and physical processes due to changes in particle size distribution of aircraft emissions.

To investigate ultrafine particle (UFP, < 0.1 μm) number concentrations contributed from commercial aircraft landing and take-off (LTO) operations in the U.S.

Research Approach

Introduction

The CMAQ model has been used to understand ground-level air quality impacted by aircraft emissions since 2011 with various model configurations (Woody et al., 2011; Rissman et al., 2013; Woody and Arunachalam, 2013). These studies stated that fine particulate matter ($PM_{2.5}$) mass concentrations impacted by LTO in the contiguous United States (CONUS) domain were relatively minor (up to 0.232 μg m^{-3} near Atlanta airport using plume in grid model) compared to ambient $PM_{2.5}$ level. However, recent field measurements found significant UFP number concentrations increases due to LTO near several U.S. and European airports (Hudda et al., 2016; Hudda and Fruin, 2016; Keuken et al., 2015; Stafoggia et al., 2016). Therefore, the main goal of Task 3 is to understand the impact on UFP number concentrations near airports from LTO using CMAQ.

Default CMAQ considers that all PM are emitted mostly in accumulation mode (size: 0.1-2.5 μm) for all anthropogenic emission sectors (Nolte et al., 2015). However, previous studies based on aircraft measurement campaigns reported PM emitted from aircrafts should be in UFP size range (0.02-0.05 μm) (Kinsey et al., 2010; Petzold et al., 1999). Our first goal in this task was to add a new module which can read aircraft emissions and assign PM size distribution separately from all non-aircraft emissions. The second goal of this task was to apply this new configuration of CMAQ to understand impacts on ground-level $PM_{2.5}$ mass and UFP number concentrations from LTO emissions.

Our hypothesis is that, using the new approach, particle size distribution from aircraft emissions can be better represented than in a traditional CMAQ configuration, and that this will impact PM number concentrations due to aircraft emissions.

Methodology

CMAQ v5.0.2 was used in this study to simulate ground-level PM mass and number concentrations impacted by aircraft emissions. Particles emitted from all emission sources are lumped together and assigned as 0.1 and 99.9% in Aitken (similar to UFP) and accumulation modes, respectively, in default CMAQ v5.0.2. In this study, aircraft and non-aircraft emissions files were generated, separately. A new module was developed to read emissions from aircraft and non-aircraft separately, and assign a reasonable particle size distribution to aircraft emissions based on species (black carbon, organic carbon, and sulfate). We investigated six different configurations for PM emissions from aircraft during two months (January and July 2005) to understand the influences from various particle size distributions for aircrafts. One of these configurations was selected for annual simulation (Table 3.1, New Method), since large amounts of small particle (< 0.005 μm) would skew particle size distribution in ambient air. Three scenarios were simulated to estimate contribution of aircrafts with different particle size configurations to PM mass and number (Table 3.1) for 2005. In this study, only LTO emissions in North America were considered, which were generated from AEDT (Wilkerson et al., 2010). Background emissions were generated based on the National Emission Inventory 2005 (EPA, 2007). The Weather Research and Forecasting model was used to create 2005 meteorological data for CMAQ (Skamarock et al., 2008). Boundary and initial conditions of CAMQ were downscaled from CAM-Chem global model (Lamarque et al., 2012).

Results

Number concentrations of UFP at major airports in North America were simulated by CMAQ with the new module increased 1.2 to 5.1 times (Table 3.2) due to LTO emissions. These numbers are in the range of those reported by recent field studies (Hudda et al., 2016; Hudda and Fruin, 2016). Hudda et al. (2016) and Hudda and Fruin (2016) reported significant increases of UFP number concentrations due to LTO at LAX and BOS at 10km and 6km, respectively. However, CMAQ UFP number concentrations were calculated based on a 36x36 km^2 grid size; therefore, the following equation was used to adjust the spatial effects:

$$C_{adj} = C_{measured} \times \frac{d^2}{36^2}$$

Here, d is the distance from sampling sites to airports. After spatial adjustment of these measurements, UFP number concentrations contributed by LTO at both airports were similar to the numbers reported by new CMAQ simulations.

In downwind areas, aircraft-attributable nitrate was enhanced by high surface areas of aerosols. Because of large amount emissions of NO_x from LTO in the downwind areas of airports, when free ammonia was available ammonium nitrate could be formed. This has been discussed in detail in Woody et al. (2011). New CMAQ simulations even increased surface areas of PM, and nitrate is a semi-volatile species which can partition on PM surfaces, depending on temperature. High surface areas of PM enhanced nitrate concentrations in the new method compared to the traditional approach for treating size distribution in CMAQ. Overall, at the top three airports in North America, number concentration increased dramatically, and its peak shifted to smaller particle diameter. However, only minor changes were observed in surface and volume concentrations (Figure 3.1).

Milestone(s)

Apr, 2016 - Completed developing and testing of new module to treat aircraft emissions with different size distribution
Aug, 2016 - Completed CMAQ model simulations using new module for annual 2005 period

Major Accomplishments

1. Quantified the effect of using new aircraft emissions size distribution information on modeled number concentration
2. Compared model results with recent field measurement campaigns, and seeing comparable results, determined the need to look at UFP from aircraft in increased detail

Publications

Huang, J., L.P. Vennam, F.S. Binkowski, B. Murphy and S. Arunachalam (2016). Impacts on Ambient Particulate Matter by Changing Particle Size Distribution from Emissions Using the Community Air Quality Model (CMAQ): A Case Study of Commercial Aircraft emissions from Landing and Take-off, CMAS, 2016, Chapel Hill, NC.

Outreach Efforts

Research findings were presented in a podium presentation at the 15th Annual CMAS conference held on October 24-26, 2016, at Chapel Hill, NC.

In addition, the UNC PI explored aspects of this work with international researchers at the *FORUM-AE Air Quality workshop* held in Amsterdam, the Netherlands in April 2016, and at the *Harmonisation within Atmospheric Dispersion Modelling for Regulatory Purposes* (HARMO) in Budapest in May 2016.

Awards

None

Student Involvement

Pradeepa Vennam, Ph. D. student, helped generating the emissions files and initial/boundary conditions for CMAQ simulations and reviewed the data.

Plans for Next Period

Understand negative sulfate mass concentrations at major airports due to change of particle size distribution of aircraft emissions in CMAQ.
Compare CMAQ simulated UFP number concentrations at more airports (not LAX and BOS), if field data are available.
Finalize and submit manuscript.

References

EPA, 2007. 2005 National Emission Inventory [WWW Document]. URL http://www.epa.gov/ttn/chief/net/2005inventory.html.
Hudda, N., Fruin, S.A., 2016. International Airport Impacts to Air Quality: Size and Related Properties of Large Increases in

Ultrafine Particle Number Concentrations. *Environ. Sci. Technol.* 50, 3362–3370. doi:10.1021/acs.est.5b05313.
Hudda, N., Simon, M.C., Zamore, W., Brugge, D., Durant, J.L., 2016. Aviation Emissions Impact Ambient Ultrafine Particle Concentrations in the Greater Boston Area. *Environ. Sci. Technol.* 50, 8514–8521. doi:10.1021/acs.est.6b01815.
Keuken, M.P., Moerman, M., Zandveld, P., Henzing, J.S., Hoek, G., 2015. Total and size-resolved particle number and black carbon concentrations in urban areas near Schiphol airport (the Netherlands). *Atmos. Environ.* 104, 132–142. doi:10.1016/j.atmosenv.2015.01.015.
Kinsey, J.S., Dong, Y., Williams, D.C., Logan, R., 2010. Physical characterization of the fine particle emissions from commercial aircraft engines during the Aircraft Particle Emissions eXperiment (APEX) 1e3. *Atmos. Environ.* 44, 2147–2156. doi:10.1016/j.atmosenv.2010.02.010.
Lamarque, J.F., Emmons, L.K., Hess, P.G., Kinnison, D.E., Tilmes, S., Vitt, F., Heald, C.L., Holland, E.A., Lauritzen, P.H., Neu, J., Orlando, J.J., Rasch, P.J., Tyndall, G.K., 2012. CAM-chem: Description and evaluation of interactive atmospheric chemistry in the Community Earth System Model. *Geosci. Model Dev.* 5, 369–411. doi:10.5194/gmd-5-369-2012.
Nolte, C.G., Appel, K.W., Kelly, J.T., Bhave, P. V., Fahey, K.M., Collett, J.L., Zhang, L., Young, J.O., 2015. Evaluation of the Community Multiscale Air Quality (CMAQ) model v5.0 against size-resolved measurements of inorganic particle composition across sites in North America. Geosci. Model Dev. 8, 2877–2892. doi:10.5194/gmd-8-2877-2015
Petzold, A., Spelheuer, @bullet A D /, Brock, C.A., Schr, F., @bullet, S., 1999. In situ observations and model calculations of black carbon emission by aircraft at cruise altitude. *J. Geophys. Res.* 104181, 171–22. doi:10.1029/1999JD900460.
Rissman, J., Arunachalam, S., Woody, M., West, J.J., Bendor, T., Binkowski, F.S., 2013. A plume-in-grid approach to characterize air quality impacts of aircraft emissions at the Hartsfield–Jackson Atlanta International Airport. *Atmos. Chem. Phys* 13, 9285–9302. doi:10.5194/acp-13-9285-2013.
Skamarock, W.C., Klemp, J.B., Dudhi, J., Gill, D.O., Barker, D.M., Duda, M.G., Huang, X.-Y., Wang, W., Powers, J.G., 2008. A Description of the Advanced Research WRF Version 3. Tech. Rep. 113. doi:10.5065/D6DZ069T.
Stafoggia, M., Cattani, G., Forastiere, F., Di Menno di Bucchianico, A., Gaeta, A., Ancona, C., 2016. Particle number concentrations near the Rome-Ciampino city airport. *Atmos. Environ.* 147, 264–273. doi:10.1016/j.atmosenv.2016.09.062.
Wilkerson, J.T., Jacobson, M.Z., Malwitz, A., Balasubramanian, S., Wayson, R., Fleming, G., Naiman, A.D., Lele, S.K., 2010. Analysis of emission data from global commercial aviation: 2004 and 2006. *Atmos. Chem. Phys. Atmos. Chem. Phys.* 10, 6391–6408. doi:10.5194/acp-10-6391-2010.
Woody, M., Haeng, B., Adelman, Z., Omary, M., Fat, Y., West, J.J., Arunachalam, S., 2011. An assessment of Aviation ' s contribution to current and future fine particulate matter in the United States. *Atmos. Environ.* 45, 3424–3433. doi:10.1016/j.atmosenv.2011.03.041.
Woody, M.C., Arunachalam, S., 2013. Secondary organic aerosol produced from aircraft emissions at the Atlanta Airport: An advanced diagnostic investigation using process analysis. *Atmos. Environ.* 79, 101–109. doi:10.1016/j.atmosenv.2013.06.007.

Table 3.1: Configurations of CMAQ particle size distribution from emission in annual simulations, nvPM: black carbon, vPM: organic carbon and sulfate

	Emission split factor	GMD (nm)	GSD	Emission data
Background (bkgd)	EC/OC/NCOM Aitken: 0.1 Accumulation: 99.9 OTHER Aitken: 0 Accumulation: 1	EC/OC/NCOM Aitken: 30 Accumulation: 300 OTHER Accumulation: 300	EC/OC/NCOM Aitken: 1.7 Accumulation: 2.0 OTHER Accumulation: 2.0	All emissions without aircraft emissions
Traditional method	nvPM Aitken: 0.1 Accumulation: 99.9 vPM Aitken: 0.1 Accumulation: 99.9	nvPM Aitken: 30 Accumulation: 300 vPM Aitken: 30 Accumulation: 300	nvPM Aitken: 1.7 Accumulation: 2.0 vPM Aitken: 1.7 Accumulation: 2.0	All emissions and aircraft emissions in separate files
New method	nvPM Aitken: 91.8 Accumulation: 8.2 vPM Aitken: 91.8 Accumulation: 8.2	nvPM Aitken: 40 Accumulation: 150 vPM Aitken: 20 Accumulation: 150	nvPM Aitken: 1.6 Accumulation: 1.87 vPM Aitken: 1.5 Accumulation: 1.87	All emissions and aircraft emissions in separate files

Table 3.2: Ultrafine particle concentrations (10^9 number/m^3) at top 10 airports (by fuel burn, 2005 AEDT) in North America, and Boston airport.

	Traditional method	New method	Background	New - background	Measured LTO impact without spatial correction[1]	Measured LTO impact with spatial correction[2]	Ratio (new/bkgd)
ATL	1.8	3.0	1.8	1.2			1.7
ORD	2.2	3.0	2.2	0.8			1.4
LAX	0.4	2.0	0.4	1.6	28-100	2.2-7.7	5.1
DFW	0.6	1.3	0.6	0.7			2.2
JFK	2.4	3.6	2.4	1.2			1.5
EWR	3.0	3.5	3.0	0.5			1.2
IAH	0.6	1.1	0.6	0.5			1.9
DTW	2.8	3.5	2.8	0.6			1.3
MSP	2.1	2.5	2.1	0.4			1.2
MIA	0.4	0.8	0.4	0.4			2.0
BOS	1.9	2.2	1.9	0.3	10-20	0.28-0.56	1.2

1: data directly from Hudda et al., 2016 and Hudda and Fruin, 2016
2: correct the spatial effects from 10 and 6 km to 36 km grid size, respectively.

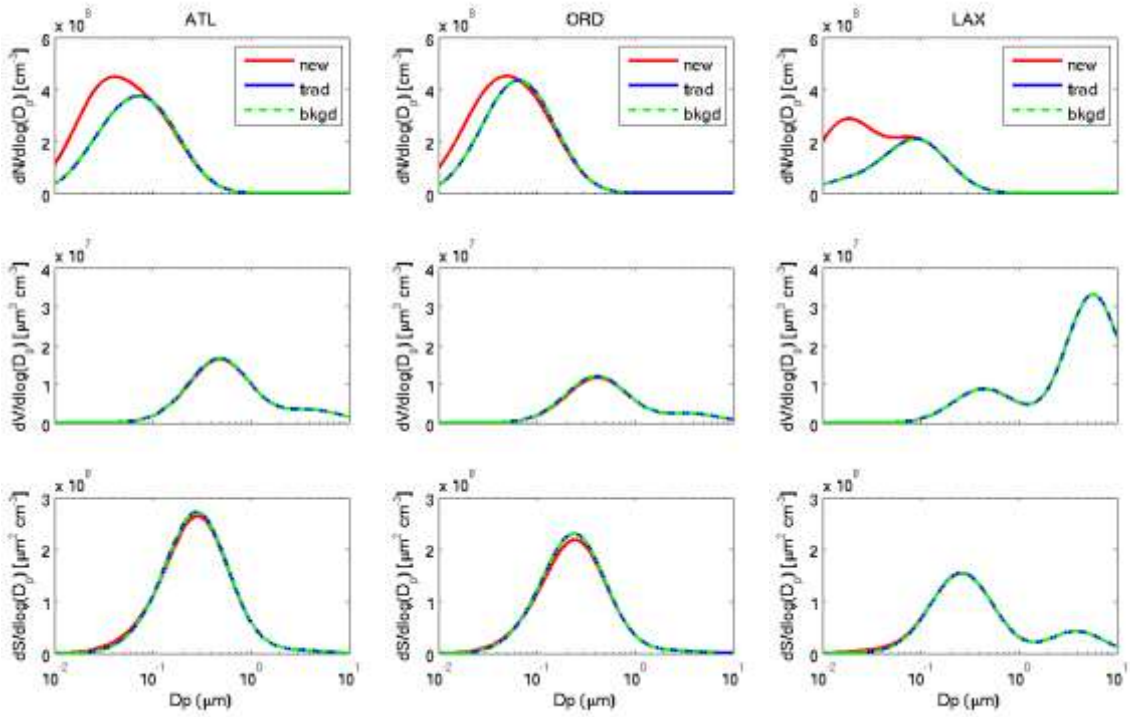

Figure 3.1 – Particle size distribution of ambient particles (annual average) at ATL (left), ORD (middle), and LAX(right), new and trad represent new and traditional CMAQ approaches, respectively. Bkgd is the background scenario.

Task 4: Assess impacts of coupled models on Aviation-related AQ Impacts

University of North Carolina at Chapel Hill

Objective(s)

The objective of task-4 was to study the effect of particulate matter's (PM's) radiative feedback effects on estimating the aircraft's landing and take-off (LTO) emission attributable change in surface ozone (O_3) and PM having a size less than 2.5 micron ($PM_{2.5}$) concentrations and to quantify the aircraft's LTO emission attributable change in some meteorological variables by the WRF-CMAQ coupled meteorology-chemistry transport model.

Research Approach

Introduction

Aircraft LTO emissions contribute to 75 (Levy et al., 2012) to 210 (Brunelle-Yeung et al., 2014) premature deaths in the US. Aircraft LTO emissions cause mortality even as far as 300 km away from a major airport through increases in secondary ammonium nitrate and sulfate (Arunachalam et al., 2011). Aviation emissions also affect global radiative forcing (RF) (global warming or cooling) through greenhouse gases such as CO_2, H_2O, primary and secondary PM and cloud particle interaction (Jacobson et al. 2013, Brasseur et al. 2016). Although all these RF effects are mainly caused by the aircraft emissions during cruise mode, it is also important to know how much RF is affected by the aircraft LTO emitted PM at the surface layers.

Aircraft-emitted PM scatters and absorbs radiation from the sun, which changes temperature, wind speed, relative humidity and planetary boundary layer (PBL) height in the atmosphere. The changes also affect atmospheric pollutant formation chemistry, which causes PM concentration change. This change in PM concentration in the atmosphere then effects meteorology. The process is called aerosol feedback. The aerosol feedback effects are neglected in traditional air quality

models (where meteorology is used as input and not affected by chemistry) which cannot simulate real atmospheric pollutant concentration. An online coupled meteorology-chemistry model such as WRF-CMAQ (Wong et al., 2012) can simulate this aerosol feedback effects in estimating aircraft LTO emission attributable change in surface layer O_3 and $PM_{2.5}$ concentrations and also quantifying how much RF is attributed at the surface by the aircraft's LTO-emitted PM. Note that prior to this study, all aviation-attributable air quality impacts research for local-to-regional scale air quality under PARTNER and ASCENT only used CMAQ without this key atmospheric process (feedback of chemistry on meteorology).

Method

The change in O_3, $PM_{2.5}$ and some important meteorological variables such as temperature at 2 m (T2), short-wave radiation (SWR) at surface and PBL height by the commercial aviation's LTO emission in the continental US are determined by coupled WRF-CMAQ model (Wong et al., 2012) runs for with- and-without LTO emissions for both with- and-without aerosol feedback (the four sensitivity simulation cases are shown in Table 4-1). Deduction of the values of output variables of case 1 from case 3 gives the aviation's LTO emission-attributable change when aerosol feedback was not considered. Deduction of values of output variables of case 2 from case 4 gives the aviation's LTO emission-attributable change when aerosol feedback is considered.

Table 4-1. Four sensitivity simulation cases.

Case number	Case description
1	Without LTO emissions (non-aviation emission only) without aerosol feedback
2	Without LTO emissions (non-aviation emission only) with aerosol feedback
3	With LTO emissions (non-aviation emission +LTO emission) without aerosol feedback
4	With LTO emissions (non-aviation emission +LTO emission) with aerosol feedback

The present study is focused on a 1-year simulation period in 2005 in the continental US, with a 36-km horizontal grid with 34 vertical sigma layers with top of the layer at 50 hPa. WRF model configurations include ACM2 PBL scheme (Pleim 2007), Morrison cloud microphysics scheme (Morrison et al., 2009), Pleim-Xiu land surface model (Pleim and Xiu 1995; Xiu and Pleim 2001), KF2 cumulus cloud parameterization (Kain 2004), USGS 24 land use and RRTMG radiation model (Iacono et al. 2008). The CMAQ configuration includes Carbon Bond 05 gas chemistry (Whitten et al. 2010; Yarwood and Rao 2005) and AER06 aerosol chemistry (Appel et al. 2013).

Input meteorological data for WRF were processed and downscaled from the NASA MERRA data (MERRA 2016; Rienecker et al. 2011). The CMAQ boundary conditions data were taken from CAM-Chem global model outputs. Aircraft LTO emission data were produced by the Federal Aviation Administration, Environmental Design Tool (AEDT) (FAA-AEDT, 2016). Non aircraft emission data were processed by the Sparse Matrix Operator Kernel Emissions (SMOKE) model (SMOKE 2016) using the U.S. EPA, National Emission Inventory for 2005 (EPA 2016).

Results

Aerosol feedback effects in aircraft LTO emission-attributable change in O_3 are shown in Figure 4-1. With feedback, both positive and negative O_3 perturbation were found in almost all of the 48 states in January 2005 (Fig. 4-1d), in July 2005 (Fig. 4-1e), and in the 2005 annual average (Fig 4-1f) caused by the T2 change (shown in Fig. 4-3a,b,c) and PBL changes (shown in Fig. 4-3g,h,i), but without feedback, in most states, it was positive in the west and negative in east in January (Fig. 4-1a), positive almost everywhere in July (Fig. 4-1b) and positive near the airport and negative or zero far away from airports in the annual average (Fig. 4-1c). Perturbation of domain average values for with-feedback for all 12 months and for annual average were found to be different than that without feedback which is not presented in this report, but will be presented in the manuscript (under development).

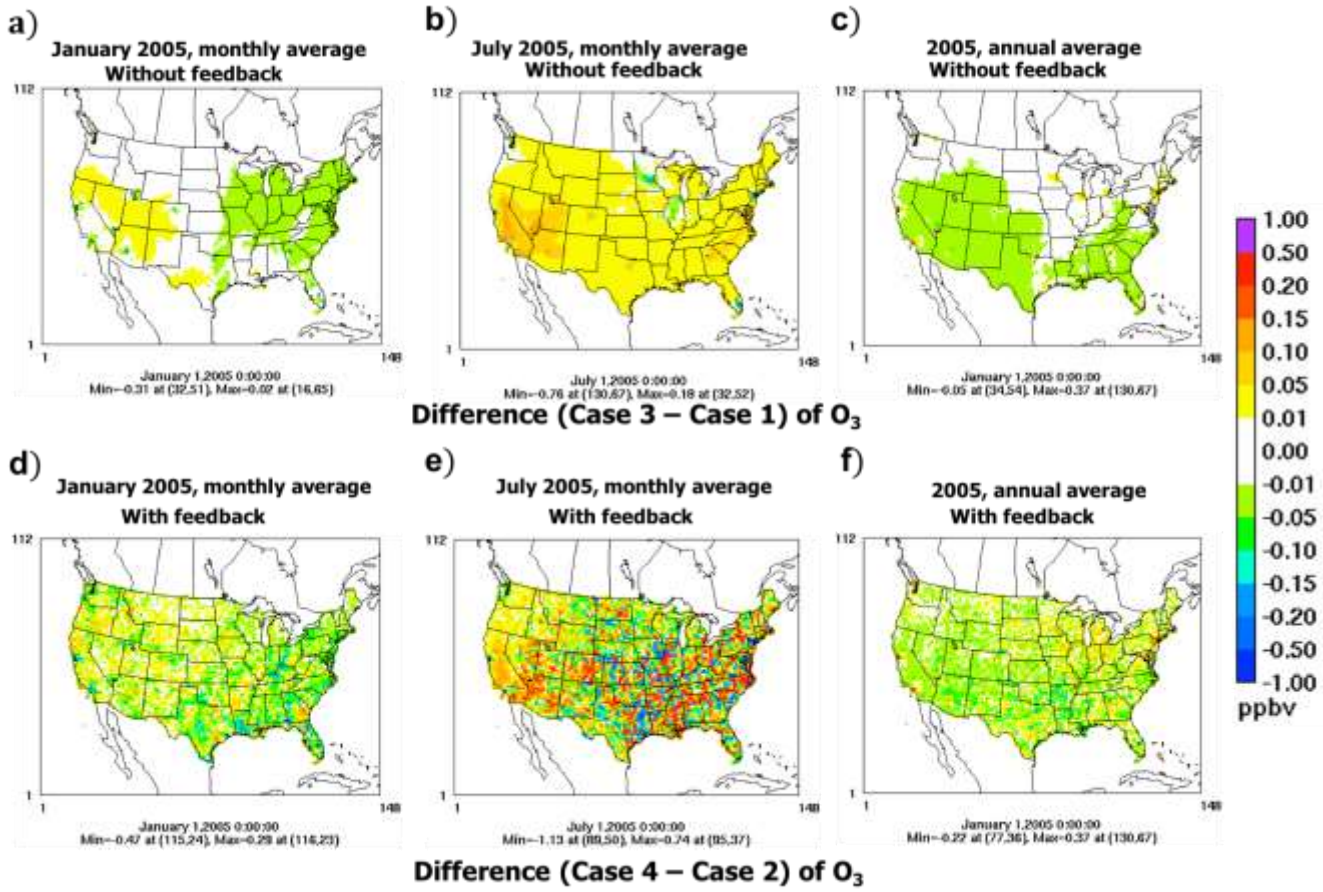

Figure 4-1: Effects of aircraft's LTO emission on surface layer O_3 without feedback (top row): a) monthly average, January 2005, b) monthly average, July 2005 and c) annual average, 2005 and with feedback (bottom row): d) monthly average, January 2005, e) monthly average, July 2005 and f) annual average, 2005 predicted by the coupled WRF-CMAQ model.

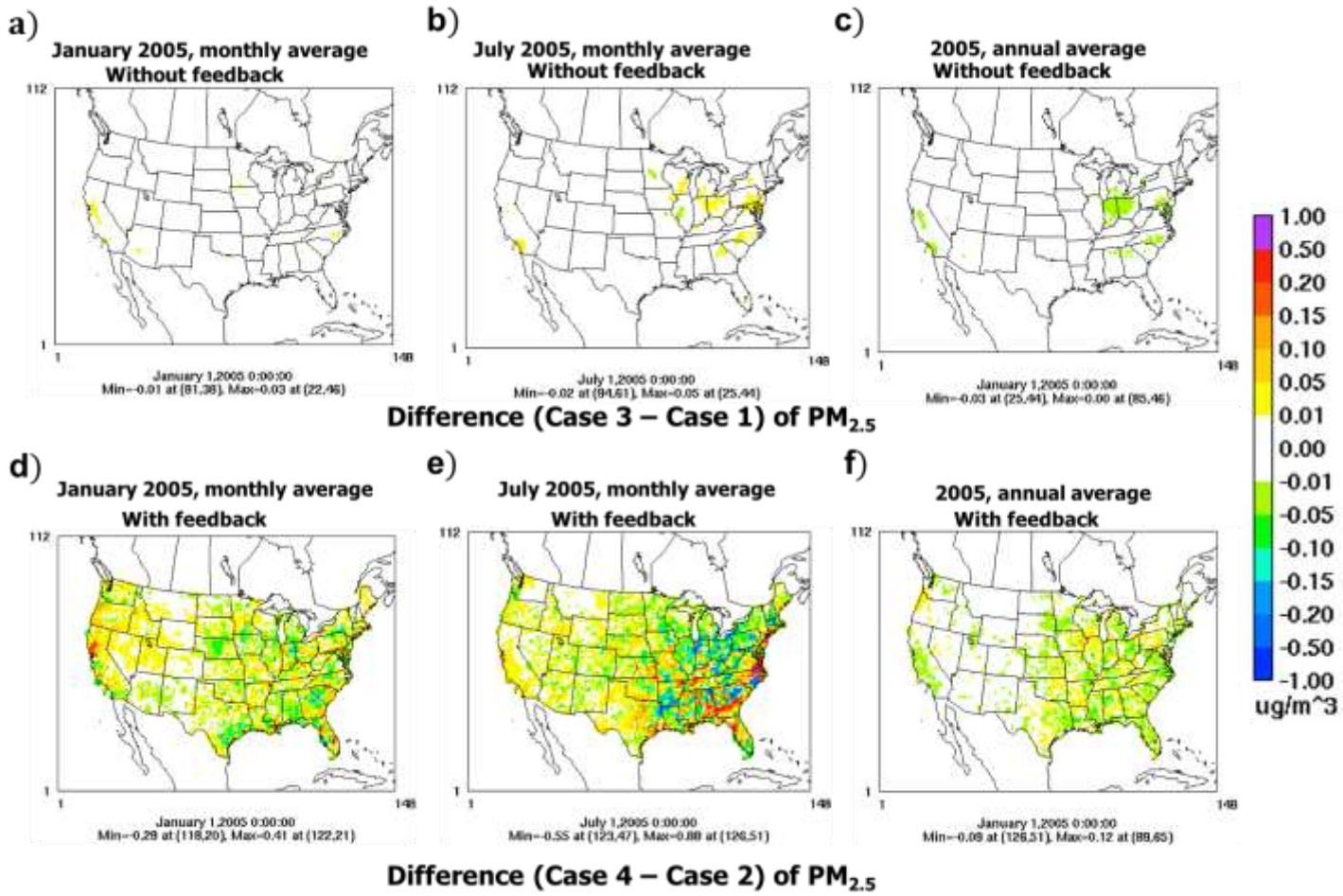

Figure 4-2: Effects of aircraft's LTO emission on surface layer $PM_{2.5}$ without feedback (top row): a) monthly average, January 2005, b) monthly average, July 2005 and c) annual average, 2005 and with feedback (bottom row): d) monthly average, January 2005, e) monthly average, July 2005 and f) annual average, 2005 predicted by the coupled WRF-CMAQ model.

The spatial $PM_{2.5}$ perturbations are shown in Fig. 4-2. With feedback, both positive and negative $PM_{2.5}$ perturbations were found in a majority of the states in January (Fig. 4-2d), in July 2005 (Fig. 4-2e), and in annual average (Fig 4-2f) caused by the T2 change (shown in Fig. 4-3a,b,c) and PBL changes (shown in Fig. 4-3g,h,i) in nearby grids but without feedback, in most states, it was either positive or negative or no change both in January (Fig. 4-2a), in July 2005 (Fig. 4-2b) and in the annual average (Fig. 4-2c). Perturbation of domain average values for with feedback for all 12 months and for annual average were different than that without feedback, which is not presented in this report, but will be presented in the final manuscript (under preparation).

One advantage of using the coupled WRF-CMAQ model is that it gives aviation LTO emission attributable perturbation of meteorological variables T2 (shown in Fig. 4-3a,b,c), SWR (shown in Fig. 4-3d,e,f) and PBL (shown in Fig. 4-3g,h,i) caused by PM radiative feedback. T2 perturbation is more in July (shown in Fig. 4-3b) than in January (shown in Fig. 4-3a) and both positive and negative perturbation occurs in adjacent grid-cells, which cancel each other when spatial summation is done for domain average (not shown in this report). SWR also shows similar perturbation which is higher in July (shown in Fig. 4-3e) than in January (shown in Fig. 4-3d) and also both positive and negative perturbation occurs in nearby grid-cells. Perturbation for SWR for annual average is smaller (shown in Fig. 4-3f) than in July (shown in Fig. 4-3e). PBL height affects dilution and dispersion of pollutants and also cloud formation. PBL is changed with the change in T2 caused by the change of short-wave radiation reaching the surface caused by aerosol's radiative effects. PBL height perturbation by aerosol

feedback effects also shows that perturbation is higher in July (shown in Fig. 4-3h) than in January (shown in Fig. 4-3g) and both positive and negative perturbation occurs in nearby grid-cells which cancel each other when spatial summation is done for the domain average (not shown in this report).

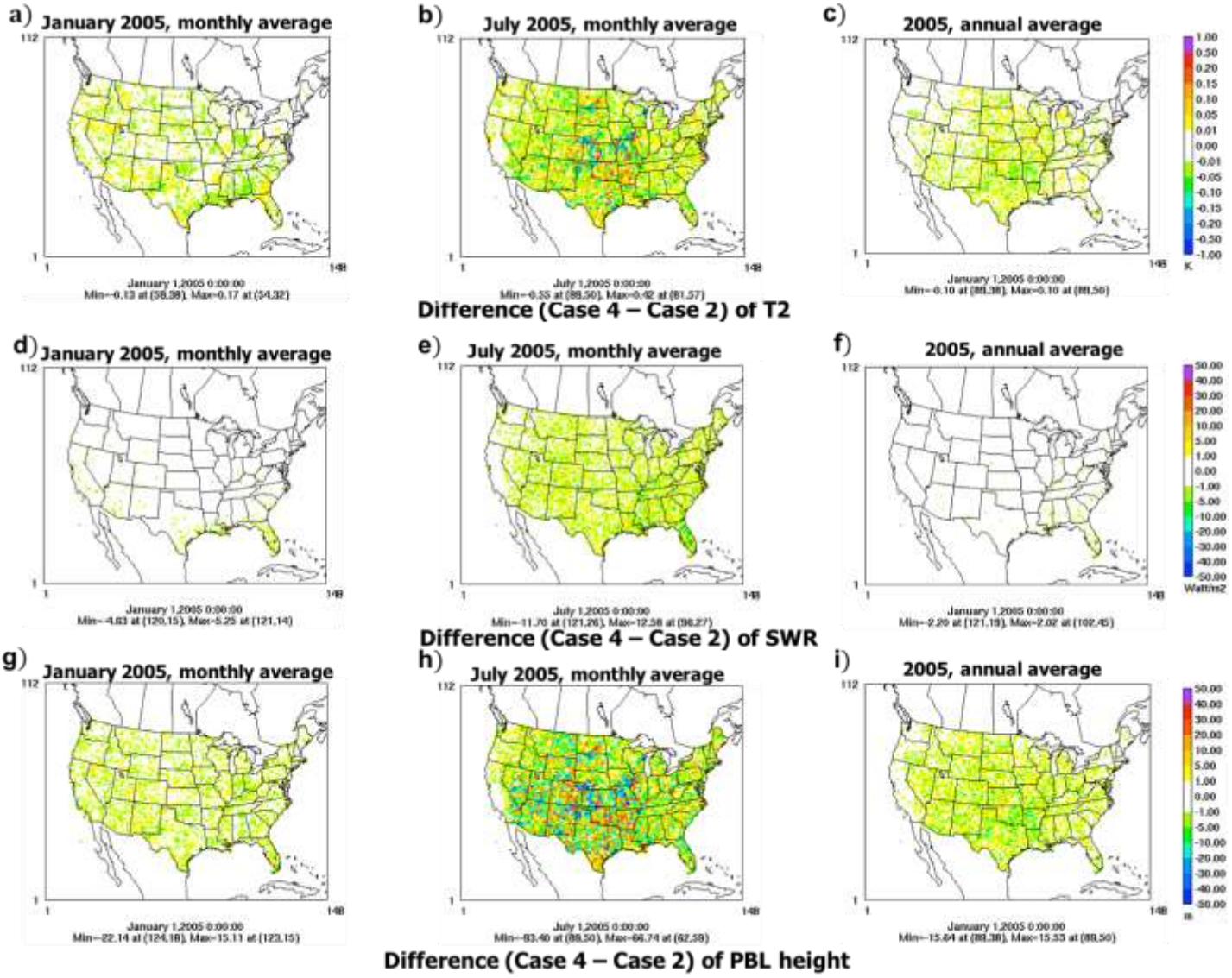

Figure 4-3: Effects of aircraft's LTO emission on temperature at 2 m (T2) (top row): a) monthly average, January 2005, b) monthly average, July 2005 and c) annual average, 2005, short-wave radiation(SWR) (middle row): d) monthly average, January 2005, e) monthly average, July, 2005 and f) annual average, 2005 and planetary boundary layer (PBL) height (bottom row): g) monthly average, January 2005, h) monthly average, July, 2005, and i) annual average, 2005 predicted by the coupled WRF-CMAQ model.

References

1. Appel, K. Wyat, Robert C. Gilliam, Neil Davis, Alexis Zubrow, and Steven C. Howard. "Overview of the Atmospheric Model Evaluation Tool (AMET) v1.1 for Evaluating Meteorological and Air Quality Models." Environmental Modelling and Software 26, no. 4 (2011): 434–43. doi:10.1016/j.envsoft.2010.09.007.

2. Arunachalam, Saravanan, Wang Binyu, Neil Davis, Bok Haeng Baek, and Jonathan I. Levy. "Effect of Chemistry-Transport Model Scale and Resolution on Population Exposure to PM2.5 from Aircraft Emissions during Landing and Takeoff." Atmospheric Environment 45 (2011): 3294–3300. doi:10.1016/j.atmosenv.2011.03.029.
3. Brasseur, Guy P., Mohan Gupta, Bruce E. Anderson, Sathya Balasubramanian, Steven Barrett, David Duda, Greg Fleming, et al. "Impact of Aviation on Climate: FAA's Aviation Climate Change Research Initiative (ACCRI) Phase II." Bulletin of the American Meteorological Society 97, no. 4 (2016): 561–83. doi:10.1175/BAMS-D-13-00089.1.
4. Brunelle-Yeung, Elza, Tudor Masek, Julien J. Rojo, Jonathan I. Levy, Saravanan Arunachalam, Sondra M. Miller, Steven R H Barrett, Stephen R. Kuhn, and Ian A. Waitz. "Assessing the Impact of Aviation Environmental Policies on Public Health." Transport Policy 34 (2014): 21–28. doi:10.1016/j.tranpol.2014.02.015.
5. EPA, US. "National Emission Inventory for 2005," 2016. https://www.epa.gov/air-emissions-inventories.
6. FAA-AEDT. "Aviation Environmental Design Tool (AEDT) Version 2 B Beta 9 Installation Guide." Washington, DC, 2016. https://aedt.faa.gov/Documents/UserGuide.pdf.
7. Iacono, Michael J., Jennifer S. Delamere, Eli J. Mlawer, Mark W. Shephard, Shepard A. Clough, and William D. Collins. "Radiative Forcing by Long-Lived Greenhouse Gases: Calculations with the AER Radiative Transfer Models." Journal of Geophysical Research Atmospheres 113, no. 13 (2008): 2–9. doi:10.1029/2008JD009944.
8. Jacobson, M. Z., J. T. Wilkerson, A. D. Naiman, and S. K. Lele. "The Effects of Aircraft on Climate and Pollution. Part II: 20-Year Impacts of Exhaust from All Commercial Aircraft Worldwide Treated Individually at the Subgrid Scale M." Faraday Discussion 165 (2013): 369. doi:10.1016/j.jcp.2011.03.031.
9. Kain, John S. "The Kain–Fritsch Convective Parameterization: An Update." Journal of Applied Meteorology 43, no. 1 (2004): 170–81. doi:10.1175/1520-0450(2004)043.
10. Lee, H., S. C. Olsen, D. J. Wuebbles, and D. Youn. "Impacts of Aircraft Emissions on the Air Quality near the Ground." Atmospheric Chemistry and Physics 13, no. 11 (2013): 5505–22. doi:10.5194/acp-13-5505-2013.
11. Levy, Jonathan I., Matthew Woody, Bok Haeng Baek, Uma Shankar, and Saravanan Arunachalam. "Current and Future Particulate-Matter-Related Mortality Risks in the United States from Aviation Emissions During Landing and Takeoff." Risk Analysis 32, no. 2 (2012): 237–49. doi:10.1111/j.1539-6924.2011.01660.x.
12. MERRA. "NASA Modern Era Reanalysis for Research and Applications (MERRA," 2016. http://disc.sci.gsfc.nasa.gov/mdisc/.
13. Morrison, H., G. Thomson, and V. Tatarskii. "Impact of Cloud Microphysics on the Development of Trailing Stratiform Precipitation in a Simulated Squall Line: Comparison of One- and Two-Moment Schemes." Monthly Weather Review 137, no. 3 (2009): 991–1007. doi:10.1175/2008MWR2556.1.
14. Pleim, Jonathan E. "A Combined Local and Nonlocal Closure Model for the Atmospheric Boundary Layer. Part II: Application and Evaluation in a Mesoscale Meteorological Model." Journal of Applied Meteorology and Climatology 46, no. 9 (2007): 1396–1409. doi:10.1175/JAM2534.1.
15. Pleim, Jonathan E., and Aijun Xiu. "Development and Testing of a Surface Flux and Planetary Boundary Layer Model for Application in Mesoscale Models." Journal of Applied Meteorology, 1995. doi:10.1175/1520-0450-34.1.16.
16. Rienecker, Michele M, Max J Suarez, Ronald Gelaro, Ricardo Todling, Julio Bacmeister, Emily Liu, Siegfried D Bosilovich, Michael G Schubert, et al. "MERRA: NASA's Modern-Era Retrospective Analysis for Research and Applications." Journal of Climate 24, no. 14 (2011): 3624–48.
17. SMOKE. "SMOKE: Spare Matrix Operator Kernel Emissions (SMOKE) Model," 2016. https://www.cmascenter.org/smoke/. Accessed December 12, 2016.
18. Whitten, Gary Z., Gookyoung Heo, Yosuke Kimura, Elena McDonald-Buller, David T. Allen, William P L Carter, and Greg Yarwood. "A New Condensed Toluene Mechanism for Carbon Bond: CB05-TU." Atmospheric Environment 44, no. 40 (2010): 5346–55. doi:10.1016/j.atmosenv.2009.12.029.
19. Wong, D. C., J. Pleim, R. Mathur, F. Binkowski, T. Otte, R. Gilliam, G. Pouliot, A. Xiu, J. O. Young, and D. Kang. "WRF-CMAQ Two-Way Coupled System with Aerosol Feedback: Software Development and Preliminary Results." Geoscientific Model Development 5, no. 2 (2012): 299–312. doi:10.5194/gmd-5-299-2012.
20. Yarwood, Greg, and Sunja Rao. "UPDATES TO THE CARBON BOND CHEMICAL MECHANISM: CB05." Novato, CA, 2005. http://www.camx.com/publ/pdfs/cb05_final_report_120805.pdf.

Milestone(s)

July 2016: Simulation of January 2005 with 11-day spin-up completed
August 2016: Simulation of July 2005 with 11-day spin-up completed
October 2016: Simulation of entire 2005 year with 6-month spin-up completed
December 2016: Post processing, data analysis and model evaluation have been completed

Major Accomplishments

1. Quantified the effects of aerosol feedback in estimating the aircraft LTO emission attributable change in surface O_3 and $PM_{2.5}$ in CONUS grid for entire year of 2005 which was missing in the output of traditional uncoupled air quality model where meteorology is used as input to CTM, and is not changed by chemistry.
2. Quantified the aircraft LTO emission-attributable change to meteorology in CONUS grid for entire year for 2005 which was missing in the output of traditional uncoupled meteorology model.

Publications

Moniruzzaman, C. G., Bowden, J., Arunachalam, 2016. Effects of aerosol feedback on aircraft-attributable surface O3 and PM2. 5 concentrations using the two-way coupled WRF-CMAQ modeling system. Presentation at the 15th Annual CMAS Conference, October 24-26, 2016 Chapel Hill, NC, available online at: https://www.cmascenter.org/conference/2016/slides/monir_effects_aerosol_2016.pdf.

Outreach Efforts

Research findings were presented in a poster session at the 15th Annual CMAS conference held on October 24-26, 2016, at Chapel Hill, NC.

Awards

None

Student Involvement

Pradeepa Vennam, a PhD student, provided the CMAQ emissions, initial and boundary conditions files and post processing scripts and helped in numerous steps of the research.

Plans for Next Period

Effects of aerosol feedback on estimating aircraft's cruise emissions' contribution to both vertical profile of O_3, $PM_{2.5}$, temperature and also the surface O_3 and $PM_{2.5}$ and surface temperature will be quantified by the coupled WRF-CMAQ model for northern hemisphere domain. 80% aviation black carbon (BC) emission occurs during climb and cruise (non LTO) operation (Lee et al. 2013) and it will be interesting to see aerosol feedback effects in estimating cruise emission effects on both surface air quality and meteorology and their vertical profile.

APPENDIX A

Additional results

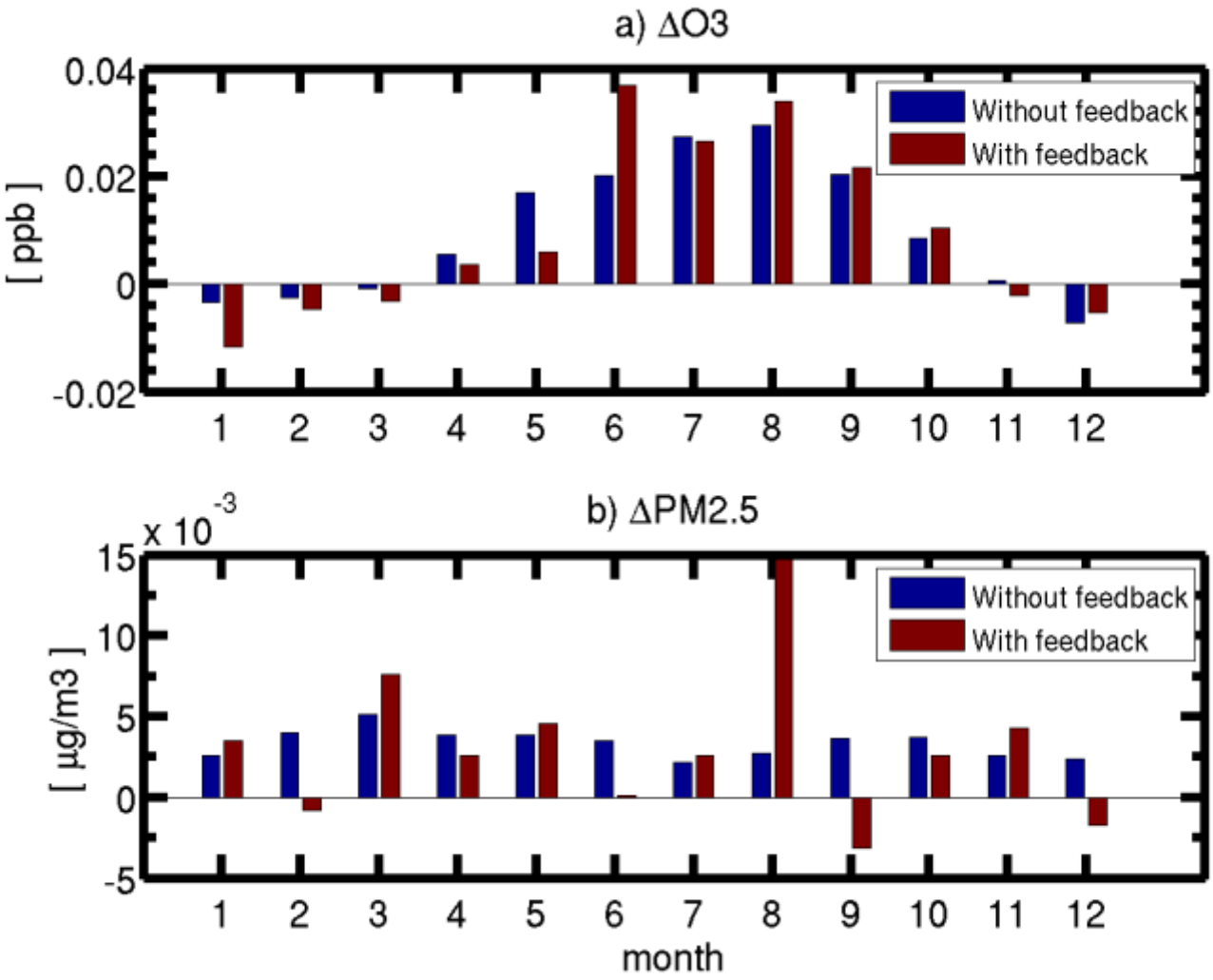

Figure 4-A1: Effects of aircraft's LTO emission on domain average of monthly average of surface a) O_3 and b) $PM_{2.5}$ for without feedback and with feedback in 2005.

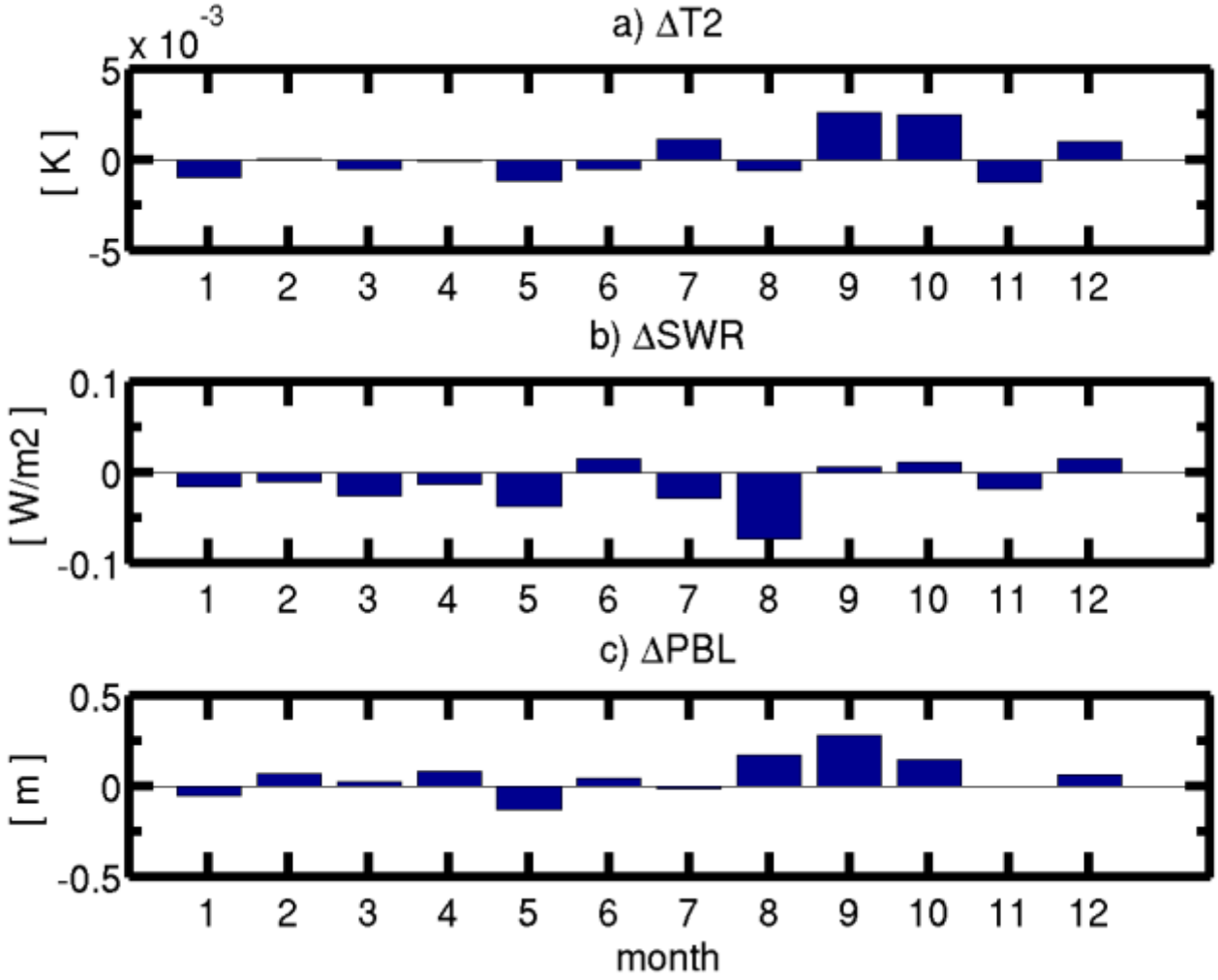

Figure 4-A2: Effects of aircraft's LTO emission (Case 4 – Case 2) on domain average of monthly average of a) temperature at 2 m (T2) b) short-wave radiation (SWR) at surface and c) planetary boundary layer (PBL) height in 2005 with aerosol feedback.

Task 5: Support for High Fidelity Weather

University of North Carolina at Chapel Hill

Objective(s)

Provide support to FAA (ATAC and Volpe Center) in processing high fidelity weather for AEDT.

Research Approach

In this task, UNC assisted FAA contractors ATAC and Volpe Center in the identification, acquisition and implementation of high fidelity weather data from global scale datasets for use in the Aviation Environmental Design Tool (AEDT) for developing aviation emissions inventories. Specifically, UNC worked with ATAC and U.S. DOT's Volpe Center for implementing the Modern Era Retrospective Analyses for Research and Applications (MERRA)[2] (Rienecker et al., 2011) dataset to derive meteorological fields in AEDT's calculations. Prior to this, UNC reviewed all available datasets with global coverage and recommended that MERRA be the choice of data for driving AEDT with high fidelity weather. Once we learned that NASA was in the process of migrating from MERRA to MERRA-2 (Bosilovich et al., 2015), we recommended that FAA move to MERRA-2, and we will continue to engage with NASA developers as necessary and assist both ATAC and Volpe in developing and implementing the prototype tool for use in AEDT. UNC's assistance to the FAA contractors included the following:

a) Identifying appropriate datasets

b) Developing scripts for data downloads from NASA servers

c) Assist with QA of AEDT processing, and troubleshooting as necessary

d) Assist with evaluation of results

At the end of this performance period, we collaborated with ATAC in preparing a joint final report covering the process for creating high fidelity weather full flight environmental analyses for global inventories using AEDT, using both great circle routes and radar flight tracks as input. This report included a description of the optimal high fidelity weather data sources for this purpose, instructions on how to use the optimal weather data within AEDT, validation of its use using Cockpit Flight Data Record (CFDR) data, and issues and recommendations of high fidelity weather usage in AEDT 2b. This report did not cover actual AEDT enhancement implementation in the form of software development, but identified multiple issues, and provided suggestions for improvements. The summary of the issues is provided below, and the reader is referred to the actual final report for further details.

1. Database-related issues
    a. UTC Time
    b. Inconsistent Runway Effective & Expiration Dates
    c. Unusable Airports through Importation
    d. Runway ends with null elevations
    e. Null airport weather
2. Performance module issues fixed in AEDT 2b
    a. Track distance disagreements
    b. Weather reading altitude in the FPPM
    c. Weather reading times in the FPPM
    d. Incorrect Location for Controlled-Point Weather Readings
    e. Altitude AFE in ANP Thrust Equations
3. Outstanding Performance Module Issues
    a. Fuel Burn in the Terminal Area
    b. Sampling Rate of High-fidelity Weather
    c. General Airspeed to Groundspeed Conversion
    d. Inconsistent High-fidelity Weather Sampling Rates
    e. Wind Perpendicular to Airplane Course
    f. Enroute Groundspeed/True-Airspeed Conversions
    g. Modeling Failures Due to Extreme Weather Conditions

[2] http://gmao.gsfc.nasa.gov/merra/

4. Weather Module Issues
    a. International Dateline
    b. Minimum Amount of Weather Data
    c. Peculiar Interpretation of MERRA Time Data
    d. Missing Values in MERRA Data
    e. Negative Latitudes
    f. Single Day Limit
    g. Specific Humidity
    h. MERRA Version 2

Milestone(s)
September 2016 - Research Approach for Hi-Fi Weather in AEDT, with ATAC

Major Accomplishments
Completed prototyping an approach for use of MERRA in AEDT and developed a report that summarizes various issues that need to be resolved, with our recommendations.

Publications
None

Outreach Efforts
Multiple presentations to FAA and Volpe Center during this performance period

Awards
None

Student Involvement
None

Plans for Next Period
We will continue working with Volpe to migrate from MERRA to MERRA-2, and also with the implementation of BADA4 in AEDT. In addition, we will also assist Volpe in processing WRF data directly in AEDT (instead of MERRA or MERRA-2). This will assist in additional consistency in meteorological fields for regional-scale air quality applications.

References
ATAC and University of North Carolina at Chapel Hill (2016). Final High Fidelity Weather Report, prepared for the Federal Aviation Administration Office of Environment and Energy, September 2016.

Bosilovich, M., Akella, S., Coy, L., Cullather , R., Draper, C., Gelaro, R., Kovach, R., Liu , Q., Molod, A., Norris, P., Wargan, K., Chao, W., Reichle, R., Takacs, L., Vikhliaev, Y., Bloom, S., Collow, A., Firth, S., Labow, G., Partyka, G., Pawson, S., Reale, O., Schubert, S. D., and Suarez, M.: MERRA-2: Initial evaluation of the climate, NASA Tech. Rep. Series on Global Modeling and Data Assimilation, NASA/TM – 2015 - 104606, Vol. 43, 2015.

Rienecker, M. M., Suarez, M. J., Gelaro, R., Todling, R., Bacmeister, J., Liu, E., … Woollen, J. (2011). MERRA: NASA's modern-era retrospective analysis for research and applications. *Journal of Climate*, *24*(14), 3624–3648. http://doi.org/10.1175/JCLI-D-11-00015.1.

Project 020 Development of NAS wide and Global Rapid Aviation Air Quality Tools

Massachusetts Institute of Technology

Project Lead Investigator

Prof. Steven R.H. Barrett
Associate Professor of Aeronautics and Astronautics
Department of Aeronautics & Astronautics
Massachusetts Institute of Technology
77 Massachusetts Ave.
(617) 452-2550
sbarrett@mit.edu

University Participants

MIT
P.I.: Steven Barrett, Associate Professor of Aeronautics and Astronautics

- FAA Award Number: 13-C-AJFE-MIT, Amendment Nos. 007, 018, and 025.
- Period of Performance: August 19, 2014 to August 31, 2017. (reporting with the exception of funding levels and cost share only for period from October 1, 2015 to September 30, 2016)
- Tasks:
    1. Update and extend the global GEOS-Chem adjoint tool to include global ozone impacts calculations
    2. Calculate and analyze second-order sensitivities
    3. Provide assistance to FAA as needed

Project Funding Level

$550,000 FAA funding and $50,000 Transport Canada funding, with $550,000 matching funds. Sources of match are that same $50,000 Transport Canada funding which constitutes both sponsoring funds and matching funds, plus approximately $146,000 from MIT, and 3rd party in-kind contributions of $114,000 from Byogy Renewables, Inc. and $240,000 from Oliver Wyman Group.

Investigation Team (all MIT)

Principal Investigator: Prof. Steven Barrett
Co-Investigator: Dr. Raymond L. Speth
Co-Investigator: Dr. Robert Malina
Graduate students: Irene Dedoussi, Guillaume Chossiere

Project Overview

The aim of this project is to develop tools that enable the rapid assessment of the health impacts of aviation emissions. The focus of the project is on aviation-attributable $PM_{2.5}$ and ozone at the NAS-wide and global scales. These tools should allow for rapid policy analysis and scenario comparison. The adjoint method, which the tools are based on, provides a computationally efficient way of calculating the sensitivities of an objective function with respect to multiple model inputs. The project enhances the existing tools in terms of the domains and impacts covered, and in terms of uncertainty

quantification. The enhanced tools support the FAA in its strategic vision to reduce the significant health impacts of aviation emissions, and allow for detailed and quantified policy analyses.

Tasks and Plans for Next Period

Current Period

- **Task 1:** Update and extend the global GEOS-Chem adjoint tool to include global ozone impacts calculations
- **Task 2:** Calculate and analyze second-order sensitivities
- **Task 3:** Provide assistance to FAA as needed

Next Period

- **Task 1:** Extend second-order sensitivities to future years
- **Task 2:** Evaluate sources of uncertainty within the tool
- **Task 3:** Extend North American nested grid focused to represent Canadian impacts
- **Task 4:** Develop nested grids for Europe and southeast Asia

Objectives

The aim of the project is to enhance the capabilities of the existing rapid assessment tool. The main objectives of this cycle are aligned with the aforementioned tasks. Specifically:

1. To expand the scope of the current policy tool to include the global health impacts of aviation-attributable ozone. This will complement the existing PM capability and provide more extensive quantification.
2. To provide understanding about how the change in the background concentrations affects the values of the sensitivities. This will eventually allow us to assess more accurately the impacts of future policy scenarios.
3. To apply the tool to support policy analysis as requested by the FAA.

Research Approach

Sensitivity calculations

The first task for this period of performance consisted in extending the adjoint tool to include the calculation of global ozone impacts caused by aviation emissions at the global level. This capability complements the PM capability and allows for more extensive analysis. As was already the case previously, the global rapid assessment tool will allow to distinguish LTO from non-LTO impacts and capture differential scenarios. This also allows the study of transport of cruise emissions between regions in the global domain as per Koo et al. 2013. The spatial domain that is covered by this extended tool is shown below (Figure 1).

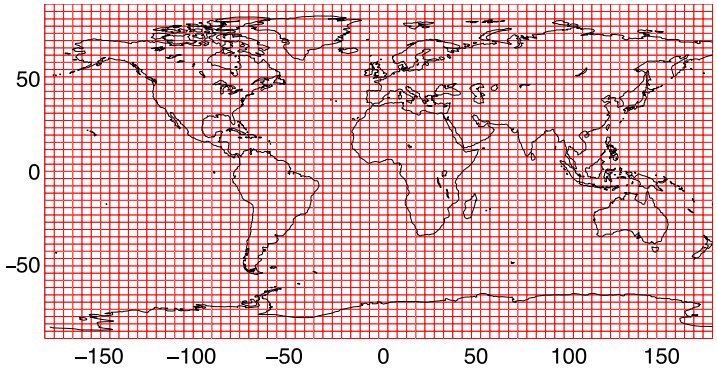

Figure 1: GEOS-Chem global 4°×5° grid

Before completing this task, we updated the version of the GEOS-Chem model that we are using, in order to produce up-to-date results. The aviation emissions inventory that are used in our calculations also needed to be updated, and we have been in contact with VOLPE to obtain and validate the new inventory data.

Given that the ozone Concentration Response Function (CRF), unlike the one for $PM_{2.5}$, is non-linear, the adjoint model needed to be modified to be able to capture global ozone impacts. The forward GEOS-Chem was used to select the portion of the day when O_3 contributes to the health impacts.

The calculation of the ozone impacts of aviation emissions required a careful definition of the metric used to measure exposure. On that front, we collaborated with the ASCENT 18 project contributors. Jon Levy and his team suggested an appropriate metric for ozone exposure, and helped us with the choice of the concentration-response function to be used. The one that was chosen ensures consistency with previous FAA work.

Once these data were obtained and the model properly updated and validated, we needed to implement the calculation of the ozone impacts in the code, test our implementation, and finally run the model to obtain sensitivities. The computational process that we use can be summarized as follows (Figure 2).

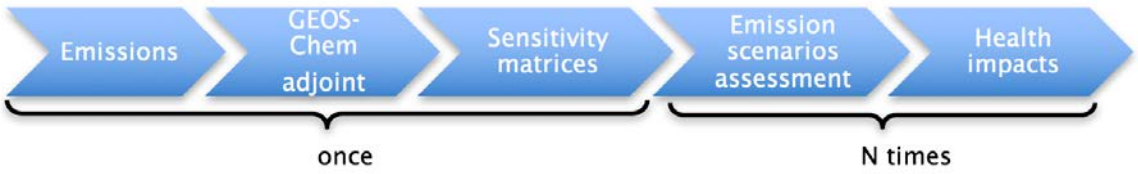

Figure 2: Computational workflow

The sensitivities calculated allow us to quantify the speciated, temporal, and spatial origins of the population exposure to aviation-attributable ozone. Specifically, they measure how much the emissions in each grid cell contribute to the total population exposure to ozone and to the resulting health impacts. This allows us to identify the LTO impacts and differentiate them from non-LTO impacts, as well as to calculate what percentage of the total aviation impacts originates from each aviation emissions species. The sensitivities also provide information about the temporal aspect of emissions and can be used to identify seasonality effect. These effects were shown to be important in the case of $PM_{2.5}$ impacts. For instance, SO_2 emissions over the summer months (April to September) are approximately twice as impactful in terms of $PM_{2.5}$ exposure as those over the winter months (October to March). This implies that the benefit of sulfur emissions control (e.g. using alternative fuels, or low sulfur jet fuel) over the summer is twice as high as that of the winter.

The 3D sensitivities matrices can be used to assess the impacts of different emissions scenarios. The health impacts associated with a specific emissions scenario are given by the inner matrix multiplication of the sensitivity matrix with the emissions matrix as shown in Figure 4 below. This computation is of negligible computational cost, compared to the 3D Chemical Transport Model (CTM) tools that have been conventionally used until now in assessing air quality impacts of different emissions. This is the main benefit of the adjoint approach.

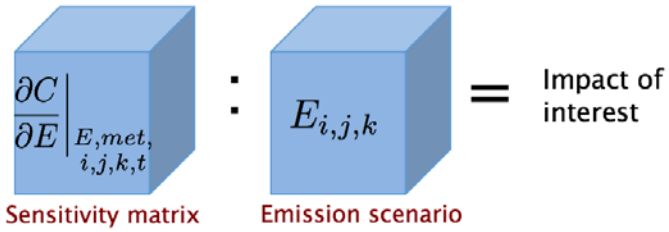

Figure 3: Application of sensitivities

In addition to the ozone work, we conducted preliminary research in order to eventually extend our modeling capacities to the fine resolution South-East Asian and European domains (0.5°×0.667°). Besides the nested North American domain, which is functional and already transitioned to the FAA, the development of the two other geographical domains is underway too. We identified the code development and modifications that need to be performed, and investigated the emissions inventories and other inputs to be used.

Application of the sensitivities to the ICAO CAEP 10 CO_2 standard

The rapid air quality policy assessment tool was for the first time applied in the ICAO CAEP CO_2 standard work, where multiple scenarios were analyzed and compared. The ASCENT 20 team supported the ASCENT 14 team in interpreting the results and compiling the Information Paper that was presented at the CAEP meeting.

FAA training

In the context of supporting the FAA in using the policy assessment tools, MIT organized and performed a series of trainings, one of which was on the adjoint air quality tool for the global and nested NA domains. The training consisted of two parts: an information session (performed remotely on Oct 27th 2015) and a hands-on training (performed at the FAA office on Oct 29th 2015). The information session aimed to present the motivation behind this (global and nested NA) tool, and to provide an overview of the application of the tool. It was aimed for people who are going to run or interpret the tool, and for people who are going to manage projects that involve the use of this adjoint tool. The broader capabilities and limitations of the tool and some of the future work aspects were also mentioned. This WebEx presentation has been recorded and transferred to the FAA in order to assist with future training later on and/or serve as a reference for how to use the tool. The hands-on training involved the application of the tool to a set of sample inputs, and the transfer of the tool (code and examples) to the FAA server/workstations.

2nd-order sensitivities

We also investigated how the adjoint sensitivities, that the tool is based on, depend on the background concentrations (and thereby the level of background emissions. This is of interest as, in particular in the US, there have been significant anthropogenic emissions reductions over the past 15 years, as shown in Figure 4. The aim of this part of the project is to capture the impacts of the change in background emissions to the GEOS-Chem adjoint particulate matter ($PM_{2.5}$) sensitivity values. In order to calculate this impact, we are calculated the sensitivities for a different year, specifically 2011, taking into account changes in background emissions and meteorology. By comparing the 2011 sensitivities with the sensitivities of 2006 (that we already have), we were able to quantify the impacts that the changing atmospheric composition has on the atmospheric response to emissions (i.e. the adjoint sensitivities).

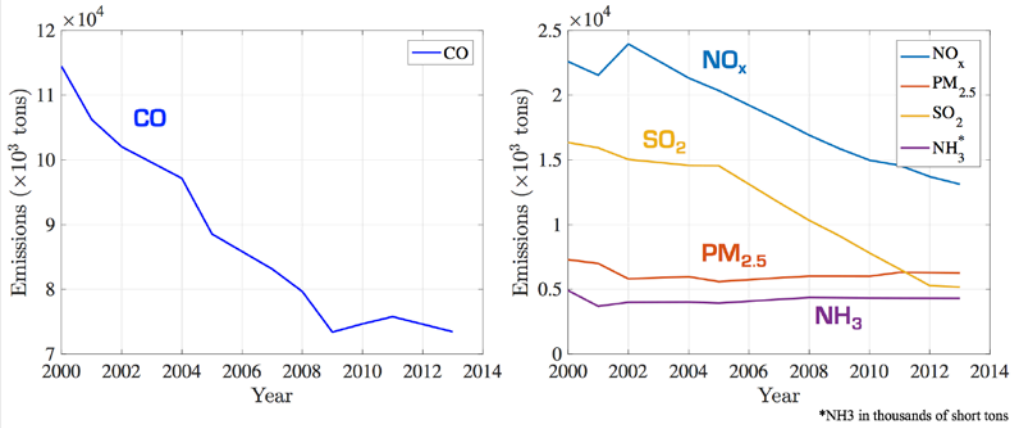

Figure 4: Anthropogenic emissions reductions in the US [USA EPA 2016]

The major findings are presented in figures 5 and 6 below. We find that the sensitivities to NO_x emissions increase between 2006 and 2011. In addition, we find that the sensitivities to SO_2 emissions decrease between 2006 and 2011, with some

increases in the coasts. The sensitivity changes are the superposition of a variety of phenomena, including the changing emissions (in particular those of SO_2 and NO_x), meteorology and population.

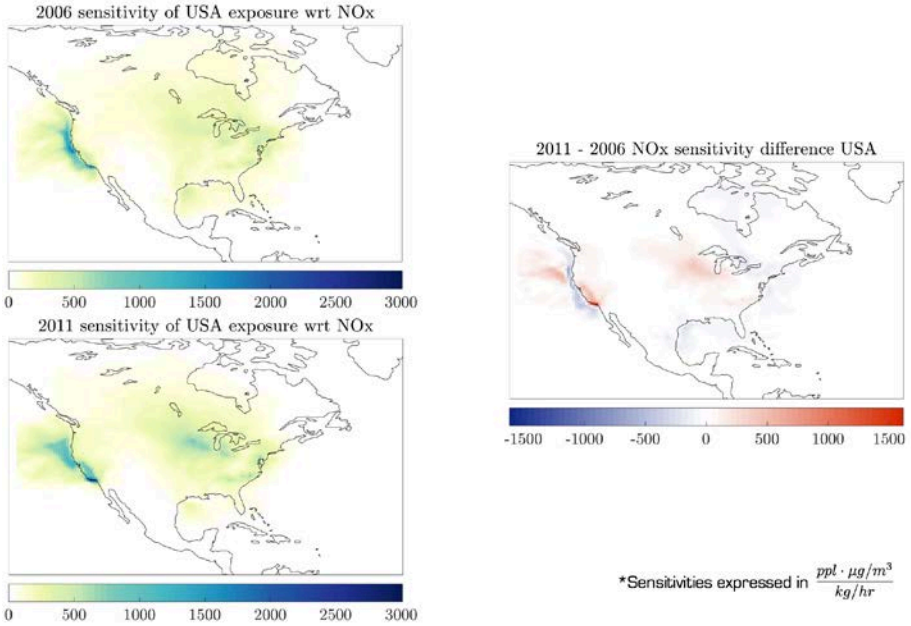

Figure 5: Sensitivity of US population exposure to $PM_{2.5}$ with respect to a unit of near-surface NO_x emissions for 2006, 2011 and the difference between the two

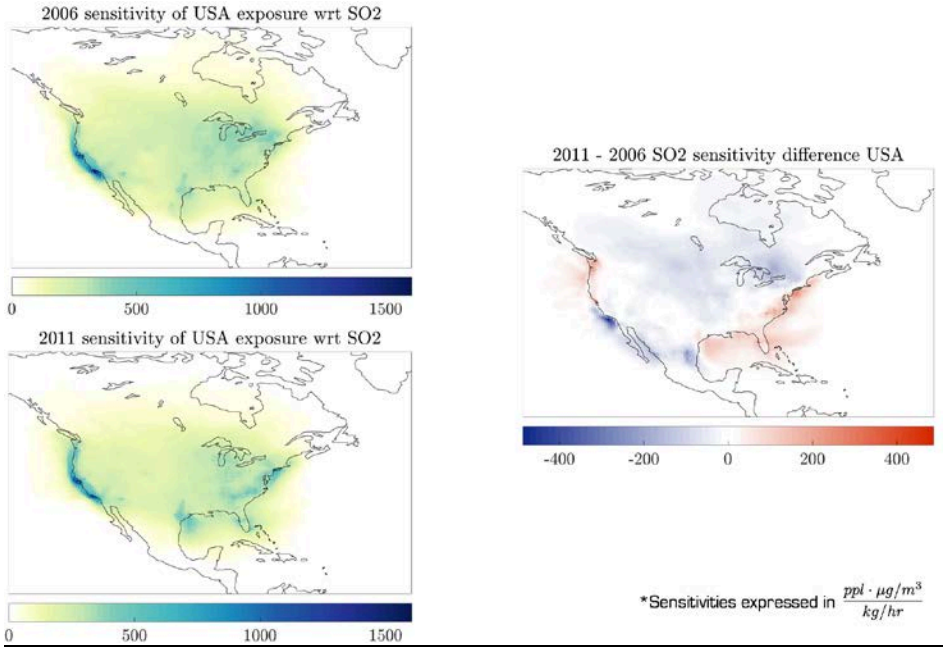

Figure 6: Sensitivity of US population exposure to $PM_{2.5}$ with respect to a unit of near-surface SO_2 emissions for 2006, 2011 and the difference between the two

Milestones

- *Add the ozone capability to the adjoint air quality tool, and make this available for use outside MIT:* The ozone sensitivity calculation methodology was developed and tested during this reporting period. The model update and data collection from various sources are in progress under the next period of work.
- *Provide FAA with a briefing on the progress regarding the non-US nested domains (in project month 12)*: This was accomplished on schedule.
- *Brief FAA on second order sensitivities progress:* The FAA is aware of the progress made regarding the sensitivities work.
- *CO_2 work:* Contributed to the ICAO CAEP Information Paper on the cost-benefit analysis of the ICAO CO_2 stringency options
- *Training:* We performed a series of training to the FAA on using the adjoint air quality tool and interpreting results. The training material and recordings were also passed to the FAA.

Major Accomplishments

During this period of performance, we conducted a complete update of our model and the input data used to compute sensitivities, in order to produce up-to-date results.
In addition, we quantified the impacts of the changing atmospheric composition on the adjoint sensitivities, thus allowing us to gain understanding of how the sensitivities are affected from the reductions of other anthropogenic combustion emissions sources (e.g. road transportation, power plants, etc.).
The tool was for the first time applied on a real-world policy assessment, and was used to quantify the air quality impacts of the CO_2 standard stringency options. The FAA was also trained on using the model and interpreting the outputs.

References

Koo, Jamin, Qiqi Wang, Daven K. Henze, Ian A. Waitz, and Steven R. H. Barrett. 2013. "Spatial Sensitivities of Human Health Risk to Intercontinental and High-Altitude Pollution." *Atmospheric Environment* 71 (June): 140–147. doi:10.1016/j.atmosenv.2013.01.025. http://linkinghub.elsevier.com/retrieve/pii/S1352231013000502.

USA EPA, 2016. Air Pollutant Emissions Trends Data. URL: https://www.epa.gov/air-emissions-inventories/air-pollutant-emissions-trends-data.

Publications

Brenner, M.; Yutko, B.; Wolfe, P.; Dedoussi. I. US cost-benefit analysis of ICAO CO_2 standard stringency options. ICAO CAEP Information paper to inform CO_2 standard work. 12/14/2015.

Outreach Efforts

Include descriptions of any and all oral presentations, electronic communications, conference presentations, or other forms of outreach.

Awards

None

Student Involvement

Irene Dedoussi is a PhD candidate in the Department of Aeronautics and Astronautics at MIT. Guillaume Chossiere is a Master's student in the Department of Aeronautics and Astronautics at MIT. Both of them are involved in this project.

Plans for Next Period

Over the next period of this project (2016-2017), we aim to analyze and improve the robustness of the GEOS-Chem Adjoint rapid policy assessment tool, as well as to further expand the capabilities of the tool, particularly with regard to spatial scope.

First, work completed thus far on second-order sensitivities between 2006 and 2011 will be extended to future years (e.g. to 2018 by using the EPA's National Emissions Inventory forecast). This will allow quantification of future changes in sensitivities to aviation emissions due to future changes in background emissions. Inclusion of these sensitivities in the tool will improve its future policy scenario assessment capability, as they enable the tool to account for the second-order effect of changes in background emissions to future aviation impacts. Furthermore, second-order sensitivities will also be used to estimate uncertainty propagation from background emissions inventories (e.g. for ammonia) to the aviation impacts computed by this tool, as well as to estimate the impact of meteorological changes to the computed aviation impacts as a first step in investigating coupling between climate and air quality.

Second, an in-depth evaluation of sources of uncertainty in the tool will be conducted through comparison of adjoint sensitivity results against forward model results with perturbed emissions as well as through tool inter-comparisons of the forward model against CMAQ. Comparisons will also be made with observational data from the EPA Air Quality System (AQS) to quantify this tool's biases in over- or under-predicting concentrations of certain pollutant species. These biases are a representation of the tool's inherent uncertainty. Once quantified, the biases can be factored in to the uncertainty calculation for the tool's aviation impact results, broadening their scope to include the model's inherent uncertainty.

Third, the tool will be extended to capture Canadian air quality and health impacts at fine resolution. This will be done by using the tool's built-in nested NA grid, which has so far been used to compute US impacts, but also extends over most of Canada, and by redefining the objective functions to be the Canadian population's exposure to $PM_{2.5}$ and O_3. The computed sensitivities of this redefined objective function can be used to attribute Canadian air quality and health impacts to species, locations, and times of emissions, as is done currently for the US.

Fourth, the tool will be extended to function with GEOS-Chem's built-in nested grids for the EU (Europe) and SEA (Southeast Asia) regions. While the adjoint model for the EU grid has yet to be developed, progress has already been made on setting up the SEA adjoint model with the relevant regional meteorological and emissions data. The coarse ($4^\circ \times 5^\circ$) global model will be used to obtain boundary conditions for these nested regional models. The nested forward models will first be validated through comparison with both global grid forward model results and observational data. The nested adjoint models can then be validated against their respective forward models. Adding these nested regional grids will greatly expand the tool's global policy assessment capability in terms of $PM_{2.5}$ and O_3 impacts to the same level as is currently done nationally for the US.

The enhanced tool will enable the assessment of the aviation-attributable $PM_{2.5}$ and O_3 impacts in a rapid manner, appropriate for policy scenario assessment. This tool will be capable of capturing both the LTO and non-LTO impacts, for either a subdomain or the whole of the domain, thus enabling the study of exchange of pollution between different regions. Since the adjoint sensitivities give spatial and temporal information about the sources that lead to the aggregated impacts, differential growth scenarios can be assessed as well. The second order sensitivities analyses will enable the estimation of the aviation impacts for given changes in the background emissions or meteorology, and the model uncertainty analysis will be to provide estimates of the potential biases in the calculations.

We will continue to collaborate with the research teams that will be continuing ASCENT projects 18 and 19 to maintain consistency between assumptions and inventories in the rapid assessment tools, health impacts assessments and airport-specific analyses, as we have successfully done in the past with the groups of Prof. Levy at Boston University and Prof. Arunachalam at University of North Carolina. We will also continue to assist the teams (e.g. currently ASCENT 48 for the non-volatile PM standard work and ASCENT 39 for the assessment of naphthalene removal from jet fuel) who are either applying or require contributions from the adjoint tool for air quality analyses.

ASCENT 021 Improving Climate Policy Analysis Tools

Massachusetts Institute of Technology

Project Lead Investigator

Steven R. H. Barrett
Associate Professor of Aeronautics and Astronautics
Department of Aeronautics and Astronautics
Massachusetts Institute of Technology
77 Massachusetts Avenue
Cambridge, MA 02139
+1 (617) 452-2550
sbarrett@mit.edu

University Participants

Massachusetts Institute of Technology

- P.I.: Steven R. H. Barrett
- FAA Award Number: 13-C-AJFE-MIT, Amendment Nos. 004, 017, and 024
- Period of Performance: Aug. 1, 2014 to Aug. 31, 2017 (reporting with the exception of funding levels and cost share for October 1, 2015 to September 30, 2016 only)
- Tasks:
    1. Preparation of APMT-Impacts Climate Version 24 development
    2. Investigation of contrail and contrail-cirrus in aviation climate models
    3. Support FAA analyses of national and global policies with relation to climate change and environmental impacts
    4. Support knowledge transfer

Project Funding Level

$450,000 FAA funding and $450,000 matching funds. Sources of match are approximately $120,000 from MIT, plus 3rd party in-kind contributions of $114,000 from Byogy Renewables, Inc. and $216,000 from Oliver Wyman Group.

Investigation Team

Dr. Steven R. H. Barrett, Principal Investigator
Dr. Robert Malina, Project Management and Alternative Fuel Expert
Dr. Raymond Speth
Dr. Florian Allroggen, since October 2016
Dr. Philip Wolfe, Tasks 1, 3 and 4
Lawrence Wong, Task 2
Carla Grobler, Task 1, since September 2016

Project Overview

The objective of ASCENT Project 2014-21 is to facilitate continued development of climate policy analysis tools that will enable climate impact assessments for different policy scenarios at global, zonal and regional scales and will enable FAA to address its strategic vision on sustainable aviation growth. Following this overall objective, the particular objectives of ASCENT 2014-21 are (1) to continue the development of a reduced-order climate model for policy analysis consistent with the latest literature and scientific understanding; and (2) to support FAA analyses of national and global policies as they relate to climate change and environmental impacts.

In the current reporting period, these objectives have been addressed through (i) preparing the development of the version 24 code of APMT-Impacts Climate to replace APMT-Impacts Climate version 23; (ii) investigating the role of contrail and contrail-cirrus in aviation climate models through exploring the physical and chemical mechanisms of contrail formation and aviation-induced cloudiness; (iii) supporting FAA analyses of national and global policies, such as the preparation of the aircraft CO_2 standard for the ICAO CAEP/10 meeting in February 2016; and (iv) facilitating knowledge transfer to FAA-AEE and other research groups.

Task 1 – Preparation of APMT-Impacts Climate Version 24 development

Massachusetts Institute of Technology

Objectives

The ASCENT 21 work aimed at preparing the development of APMT-Impacts Climate Version 24 to replace the year-2015 operational version. This work is needed to reflect the most recent scientific consensus in APMT-Impacts Climate. The main objectives under Task 1 are threefold.

1.1 FAA's Aviation Climate Change Research Initiative (ACCRI) Phase II has identified significant climate responses from tropospheric nitrate impacts and stratospheric water vapor impacts (Lee et al., 2009). Version 24 is prepared to assess the impacts of these forcers and the uncertainties linked to these impacts.

1.2 After evaluating APMT-Impacts Climate with the Office of Management and Budget (OMB), APMT-Impacts Climate is supposed to be amended to produce output which is consistent with the results from the Interagency Working Group (IAWG)'s Social Cost of Carbon (SCC).

1.3 For APMT-Impacts Climate Version 24, other metrics and distributions such as atmospheric CO_2 concentrations, climate sensitivity distributions, and measures of inflation will be updated to reflect the most recent scientific consensus in the model.

Research Approach and Accomplishments

To effectively model aviation's impact on the environment for policy analyses, fast, efficient, and robust tools are needed. Therefore, the APMT-Impacts Climate Model was developed as a reduced-order model to probabilistically project aviation's impact on climate using both physical and monetary impact metrics. The APMT-Impacts Climate Module adopts the impulse response approach (Hasselmann et al., 1997; Sausen and Schumann, 2000; Shine et al., 2005). The effects modeled include long-lived CO_2, the intermediate-lived impact of NO_x on methane (NO_x-CH_4) and its associated primary mode interaction on ozone (NO_x-O_3 long), the short-lived effects of NO_x on ozone (NO_x-O_3 short), the production of aviation induced cloudiness, sulfates, soot, and H_2O. A detailed description of past versions of APMT-Impacts Climate can be found in Marais et al. (2010), Mahashabde et al. (2011) and Wolfe (2012).

APMT-Impacts Climate is supposed to provide estimates of radiative forcing, temperature change, and climate damages from all aviation short-lived climate forcers for which there is appropriate scientific consensus. Following Lee et al. (2009), these forcers should include black carbon, tropospheric water vapor, short-lived ozone production from NO_x, longer-lived methane and ozone destruction from NO_x feedbacks, sulfates, and direct production of aviation-induced cloudiness. As long-term (long-lived) ozone change is already incorporated in APMT-Impacts Climate and indirect effects of soot and sulfate are discussed through aviation-induced cloudiness, the impacts of aviation nitrates, stratospheric water vapor, and aviation black carbon have been identified to be included in APMT-Impacts Climate Version 24.

Based on feedback from the OMB, the ASCENT 21 team has included the IAWG's Social Cost of Carbon (SCC) into APMT-Impacts Climate. In doing so, the standard APMT-Impacts Climate output routinely allows for direct comparison of its results to the SCC results. To account for aviation's non-CO_2 climate impacts, further steps towards computing derived ratios have been initiated. These metrics provide an estimate for the ratio of non-CO_2 to CO_2 impacts for different endpoint metrics such as Global Warming Potential (GWP), Integrated Temperature Potential or Net Present Value of damages.

In order to reflect the most recent scientific consensus in APMT-Impacts Climate, further updates to APMT-Impacts Climate have been identified. For example, climate sensitivity distributions as discussed by Roe and Baker (2007) will be considered to improve consistency with computation of the IAWG SCC values. Furthermore, predicted data, such as atmospheric CO_2 concentrations and measures of inflation will be updated.

Milestones

The first milestone surpassed this year under Task 1 of ASCENT-2014-21 was to prepare a draft of the Requirements Document for the Development of APMT-Impacts Climate Version 24. This milestone was achieved in February 2016. FAA-AEE has provided feedback to this document during the year. The planned development of APMT-Impacts Climate Version

24 has not been completed due to pending final approval of the document. A drafted framework version for use by the developers has been prepared and will continue to be revised as the Requirements Document is finalized.

For the other milestones under Task 1, including model evaluation and inter-comparisons, FAA and LAE have agreed to replace this work with model outreach for APMT-Impacts Climate and with running APMT-Impacts Climate for the evaluation of a potential CO_2 standard. In particular, this included briefings of the OMB for evaluating APMT-Impacts Climate, which has further informed the requirements for developing APMT-Impacts Climate Version 24. These additional milestones, which had not been included into the proposal, have been accomplished as agreed between FAA and LAE.

Publications

Reports

Wolfe, P., Barrett, S. R. H., Wong, L. M. K., Jacob, S. D. (2016). Requirements Document for Future Iterations of the Aviation Environmental Portfolio Management Tool – Impacts Climate Model, Laboratory of Aviation and the Environment

Peer-reviewed literature

Brasseur, et al. (2016). Impact of Aviation on Climate: FAA's Aviation Climate Change Research Initiative (ACCRI) Phase II. BAMS. 2016.

Outreach Efforts

- ASCENT advisory board presentation/poster (Fall 2015, Spring 2016, and Fall 2016)
- AGU Conference: Aviation Panel Attendance (Fall 2015)
- Office of Management and Budget Briefing (Winter 2015/2016)

Student Involvement

Under Task 1, *Dr. Philip Wolfe* has focused his work on scoping the development of APMT-Impacts Climate Version 24. Philip Wolfe graduated in September 2015 and accepted a post-doctoral research position through the MIT Department of Aeronautics and Astronautics.

Carla Grobler (Ph.D. Student, MIT) has started working on APMT-Impacts Climate in September 2016. Her primary work focuses on APMT-Impacts Climate Version 24 development and validation, and on applying the model for analyzing derived ratios and for conducting policy analyses.

Plans for Next Period

In the next year, we will further enhance FAA's capabilities to perform rapid environmental policy assessment by developing APMT-Impacts Climate Version 24, and by performing verification and validation of the new model. Furthermore, we will perform code sensitivity and uncertainty analyses, capturing multiple years of model development since the last sensitivity analysis.

Second, we will develop and validate a supplemental module that would replicate models used in US Regulatory Impact Assessments. Under the guidance of the OMB, the IAWG has promulgated guidance for incorporating external costs of direct CO_2 and methane emissions in domestic Regulatory Impact Analyses. As part of APMT-Impacts Climate v24 updates, estimates of social damages from CO_2 emissions using IAWG numbers will permanently be included in the APMT-Impacts Climate outputs. To further account for the non-CO2 impacts, we will compute derived ratios which provide an estimate for the ratio of aviation's non-CO_2 to CO_2 climate impacts.

Task 2 – Investigation of contrail and contrail-cirrus in aviation climate models

Massachusetts Institute of Technology

Objectives

Aviation-induced contrail and contrail-cirrus, referred to as aviation-induced cloudiness (AIC), has been found to potentially be the largest radiative forcing impact of aviation (Lee et al., 2009; Burkhardt and Kärcher, 2011). At the same time, AIC is one of the most uncertain environmental impacts of aviation (Burkhardt et al., 2011). Recent work from ACCRI Phase II has better constrained the current climate-related uncertainty from aviation-induced cloudiness. However, further work is needed to understand the role of AIC on the climate, and the impact of modeling assumptions on temperature and damage

projections. The objective of this research is to explore the physical and chemical mechanisms of contrail formation and aviation-induced cloudiness. This leads to threefold objectives for ASCENT 21 under Task 2.

2.1 Apply and support the extension of a 3D contrail model, which has been used for the US and, more recently, for the global domain, as a tool to facilitate the development of a reduced-order contrail model
2.2 Support the extension of the contrail model, e.g. the development of a novel computation scheme for sub-grid variation in ice supersaturation
2.3 Explore published satellite contrail observations data to use the data for validation of the contrail code

Research Approach and Accomplishments

Under the ASCENT Project 21 project, the ASCENT 21 team has investigated the significance of contrail and contrail-cirrus to aviation climate models. More specifically, the Contrail Evolution and Radiation Model (CERM), a physically realistic 3D model of dynamical and microphysical processes from the jet phase at contrail formation to the diffusion phase as contrail-cirrus (Caiazzo, 2015), has been applied to explore the physical and chemical mechanisms of contrail formation and aviation-induced cloudiness.

In particular, the ASCENT 21 team has been trained to use CERM and supported the extension of CERM from the US domain to the global domain. This model, once validated, will be used to facilitate the development of a reduced-order model to estimate climate impacts from global contrail and contrail-cirrus in the future. Furthermore, the ASCENT 21 team has supported the development of a novel computation scheme to assess sub-grid variation in ice supersaturation in CERM. This novel scheme uses a fine set of reanalyzed meteorological data coupled with a probability density function approach to estimate the proportion of a cell that is expected to be supersaturated and to drive contrail formation and growth.

Lastly, to validate the contrail code and to further constrain the uncertainty of contrail- and contrail-cirrus-induced climate impacts, a comparison of contrail coverage, and microphysical properties between CERM-modeled results and satellite observation for the northern hemisphere was initiated. The work has been aiming to develop an extensive comparison study between observed and simulated contrails in the northern hemisphere.

Milestones

Under Task 2 of ASCENT-2014-21, the research team delivered a comprehensive status update on modelling aviation cloudiness and contrails in Spring 2016.

Publications

Peer-reviewed literature

Brasseur, et al. (2016). Impact of Aviation on Climate: FAA's Aviation Climate Change Research Initiative (ACCRI) Phase II. BAMS. 2016.

Outreach Efforts

ASCENT advisory board presentation (Spring 2016)

Student Involvement

Lawrence Wong (Ph.D. Student, MIT) has led research on contrail and aviation-induced cirrus for ASCENT Project 21. His research is in exploring the physical and chemical mechanisms of contrail formation and aviation-induced cloudiness in the present and under future conditions.

Plans for Next Period

We will continue investigating the role of contrail and contrail-cirrus in aviation climate models. We will improve modeling of climate impacts of contrails and aviation-induced cirrus in CERM, focusing on the validation of CERM with satellite observation data and improving our understanding of non-linearities in contrail formation. The latter analyses are highly significant since, for instance, the growth of aviation in high traffic corridors may lead to saturation and newer engine technology changes the critical temperature for contrail formation. Ultimately, this work will allow for more robust assessments of the climate impact from contrails and contrail-cirrus in a reduced-order model such APMT-Impacts Climate.

Task 3 – Support FAA analyses of national and global policies with relation to climate change and environmental impacts

Massachusetts Institute of Technology

Objectives

APMT-Impacts Climate has become a powerful rapid assessment tool for aviation climate impact assessments at the FAA. Thus, it is routinely used for analyses of national and global policies affecting aviation, such as for analyses in preparation of the ICAO CAEP/8, and ICAO-CAEP/9 meetings. In the current reporting period, the ASCENT 21 project has supported policy analyses for negotiating a potential CO_2 standard in preparation of the ICAO CAEP/10 meeting in February 2016.

Research Approach and Accomplishments

The APMT-Impacts Climate tool has been adapted and applied for conducting impact assessments of aviation-related policies. For example, Mahashabde et al. (2011) used the APMT-Impacts Climate tool to study the impacts and social costs of a NO_x emissions standard and Wolfe et al. (2014) applied APMT-Impacts Climate to investigate the distribution of aviation environmental costs. The results were included as technical appendices to US Information Papers at ICAO-CAEP meetings (CAEP/8 and CAEP/9).

As part of this year's work on ASCENT 21, the team provided modeling and technical support to the CAEP analysis of a CO_2 standard for CAEP/10, particularly in modeling short-lived climate forcers, in developing scientific and economic lenses, and in investigating climate-noise trade-offs and co-benefits. Furthermore, the ASCENT 21 team has supported the analysis of a CO_2 standard through usability updates to APMT-Impacts and setting up more than 100 policy scenario runs of APMT-Impacts Climate and Noise. The results have been presented as part of two US Information Papers at the 10th meeting of ICAO CAEP and has been presented to the Office of Management and Budget.

Milestones

Under Task 3 of ASCENT 2014-21, no milestones had been planned. However, FAA and LAE have agreed to replace milestones on APMT-Impacts Climate model evaluation and inter-comparisons with model outreach and with running APMT-Impacts Climate for the evaluation of a potential CO_2 standard. Besides briefings of the OMB for evaluating APMT-Impacts Climate (see Task 1), the ASCENT 21 team has been asked to support the ASCENT 14 team, which needed to apply APMT-Impacts Climate and Noise for the analysis of a CO_2 standard in preparation of the CAEP/10 meeting. These additional milestones have been accomplished as agreed between FAA and LAE

Publications

Reports

Brenner, M., Yutko, B., Wolfe, P., Dedoussi. I., et al. (2015): US cost-benefit analysis of ICAO CO_2 standard stringency options. ICAO CAEP Information paper.

Outreach Efforts

- AGU Conference: Aviation Panel Attendance (Fall 2015)
- Office of Management and Budget Briefing (Winter 2015/2016)
- ICAO CAEP Meeting: The climate code methodology and current valuation techniques were presented as part of a review of cost-benefit tools (Spring 2016)

Student Involvement

Under Task 3, Dr. Philip Wolfe provided input to the Policy Assessments.

Plans for Next Period

We will continue to support FAA analyses of national and global policies as they relate to climate change and environmental impacts. ICAO CAEP is currently considering the introduction of a nvPM-emission standard for international aviation, for which air quality impacts will be a definite cost/benefit driver, and for which there may be trade-offs or co-benefits in climate. Efforts will be required from the ASCENT 21 team to assist with the application of the tool in the CAEP nvPM standard evaluation, to ensure that the input and outputs are handled correctly, the assumptions are clearly stated, that assumptions on nvPM emissions are aligned with air quality tools, and that the outputs are correctly interpreted.

Task 4 – Support knowledge transfer

Massachusetts Institute of Technology

Objectives

Through transferring APMT-Impacts Climate knowledge to FAA and other research groups, the application of a standardized assessment tool for aviation's climate impacts is encouraged.

Research Approach and Accomplishments

Transferring APMT-Impacts Climate knowledge to FAA and other research groups has been regarded as an enabler for the application of APMT-Impacts Climate for policy analyses. In the current year, knowledge transfer was conducted on the basis of the training modules developed for FAA knowledge transfer. With UIUC, climate code capabilities were taught for future code review; new researchers on the ASCENT 21 project were trained; and ASCENT 48 researchers were coached to apply APMT-Impacts Climate for assessing a potential nvPM aircraft engine standard.

Milestones

Training has been provided to researchers as needed, including the following sessions:

- FAA Tools Training on APMT-Impacts Climate (Fall 2015)
- Tools Training for UIUC to teach and review Climate Code Capabilities (Spring 2016)
- Tools Training for new ASCENT 21 researchers (Fall 2016)
- Tools Training for ASCENT 48 researchers to teach APMT-I Climate Capabilities for policy analysis (Fall 2016)

Student Involvement

Dr. Philip Wolfe has used his multi-year APMT-Impacts Climate experience from being the primary developer of the code for the knowledge transfer.

Plans for Next Period

The ASCENT 21 team will provide APMT-Impacts Climate Coaching as requested. In addition, once the Version 24 code is validated, the team will transfer operational capabilities to FAA-AEE.

References

Burkhardt, U., and Karcher, B. (2011). Global radiative forcing from contrail cirrus. *Nature Clim. Change* 1, 54-58.

Caiazzo, F. (2015). Non-CO_2 Environmental Impacts of Transportation Fuel Use and Production. PhD Thesis, Massachusetts Institute of Technology.

Dorbian C.S, Wolfe P.J, Waitz, I.A. (2011). Estimating the climate and air quality benefits of aviation fuel and emissions reductions. *Atmospheric Environment* 45, 2750–2759

Hasselmann, Klaus, et al. (1997). Sensitivity study of optimal CO_2 emission paths using a simplified structural integrated assessment model (SIAM). *Climatic Change* 37, 345-386.

Lee, David S., et al.(2009). Aviation and global climate change in the 21st century. *Atmospheric Environment* 43, 3520-3537.

Mahashabde, Anuja, et al. (2011). Assessing the environmental impacts of aircraft noise and emissions. *Progress in Aerospace Sciences* 47, 15-52.

Marais, Karen, et al. (2008). Assessing the impact of aviation on climate. *Meteorologische Zeitschrift* 17, 157-172.

Roe, G. H., Baker, M. B. (2007). Why is climate sensitivity so unpredictable? *Science* 318, 629-632.

Sausen, R., Schumann, U. (2000). Estimates of the Climate Response to Aircraft CO_2 and NO_x Emissions Scenarios. *Climatic Change* 44, 27-58.

Shine, Keith P., et al. (2005). Alternatives to the global warming potential for comparing climate impacts of emissions of greenhouse gases. *Climatic Change* 68, 281-302.

Wolfe, P. (2012). Aviation environmental policy effects on national-and regional-scale air quality, noise, and climate impacts. Diss. Massachusetts Institute of Technology, 2012.

Wolfe, P., et al. (2014). Near-airport distribution of the environmental costs of aviation. *Transport Policy* 34, 102-108.

Project 022 Evaluation of FAA Climate Tools: APMT

University of Illinois at Urbana-Champaign

Project Lead Investigator

Dr. Donald Wuebbles (Dr. Robert Rauber acting as Principal Investigator while Dr. Wuebbles is on special assignment with the National Science Foundation and the Office of Science and Technology Policy of the Executive Office of the President)
Dept. of Atmospheric Sciences
University of Illinois
105 S. Gregory Street
Urbana, IL 61801
Tel: 217-244-1568
Fax: 217-244-4393
Email: wuebbles@illinois.edu

University Participants

University of Illinois at Urbana-Champaign
P.I.(s): Dr. Donald Wuebbles

- Period of Performance: December 15, 2015 to December 15, 2016
- Task(s):
    1. Evaluate version 23 of APMT
    2. Provide Feedback on plans for APMT version 24
    3. Complete journal articles with Stanford and NCAR based on prior FAA supported modeling studies

Project Funding Level

Support from the FAA over this time period was almost $38,900, with an additional $18,900 in matching support, including about $10,000 from the University of Illinois, but also as in kind support from Reading University.

Investigation Team

Dr. Donald Wuebbles: project oversight
Dr. Arezoo Khodayari (post doc; most recently on subcontract) and Jun Zhang (graduate student): analyses of APMT and 3-D atmospheric climate-chemistry modeling analyses

Project Overview

The primary objective of this project is to evaluate the capabilities of the APMT-I model, particularly the Climate module, to ensure this FAA policy analysis tool uses the current state of climate science. Regional climate impacts of aviation will also be evaluated when available. In 2016, we also completed several journal papers based on prior work.

Task 1: APMT-I Climate Evaluation and Review of Requirements Document

University of Illinois at Urbana-Champaign

Objective(s)

In this project, we act as a resource to FAA for analyses relating to metrics and to model development and evaluation of FAA modeling tools and datasets, with special emphasis on testing the Aviation Environmental Portfolio Tool (APMT) model and the further development and evaluation of its climate component to ensure that the underlying physics of the model is addressed properly. A specific focus of this project is on analyses of zonal and regional effects of aviation on climate and testing the resulting incorporation of such effects within APMT. As such, we want to make sure the APMT linking of

aviation emissions with climate impacts and the representation of the various components of the cause-effect chain (i.e., from emissions to climate effect) properly represents the state-of-the science.

Research Approach

We have focused on evaluating the climate component of the Aviation Environmental Portfolio Tool (APMT) for three main aspects of the model, mainly its treatment of carbon dioxide and the carbon cycle, short-lived species, and NOx-related impacts. The project evaluates the APMT components relative to state-of-the-art modeling that fully considers the physics and chemistry important to the various processes. Our aim is to ensure that the physics and chemistry underlying the treatments in APMT are addressed properly.

Milestone(s)

Milestone	Milestone reached
Evaluation of the newly developed APMT version 23.	Report to the FAA by June 30, 2016
Feedback on plans for APMT version 24	Report to the FAA by December 15, 2016

Major Accomplishments

Most relevant to this project is a special report (Zhang and Wuebbles, Evaluation of FAA Climate Tools: APMT, June 2016) sent to the FAA. This report evaluates the climate component of the current version of the Aviation Environmental Portfolio Tool (APMT) for three main aspects of the model, mainly its treatment of carbon dioxide and the carbon cycle, short-lived species, and NOx-related impacts. Our aim is to ensure that the physics and chemistry underlying the treatments in APMT are addressed properly based on our and others published modeling studies. Our major findings include the following. Small changes are needed in the carbon cycle treatment to assure accuracy relative to current carbon cycle models. The indirect effect of aerosols and the stratospheric water vapor induced by methane oxidation should be included in the short-lived species. Furthermore, the method used to calculate the radiative forcing (RF) of short-lived ozone should be revised. The radiative forcing of nitrates should be added to the NOx-related emissions effects. As a result of making these changes, APMT should be better able to link the various components of aviation emissions with climate impacts relative to the findings from ACCRI.

Publications

Zhang and Wuebbles, Evaluation of FAA Climate Tools: APMT. Report for the FAA, June 2016

Outreach Efforts

ASCENT Advisory Committee Meeting – September 27-28, 2016 (Presentation)
Tools/Analysis Coordination Meeting – November 22, 2016 (Presentation)
Bi-weekly meeting with project manager Daniel Jacob

Awards

None

Student Involvement

Graduate Student: Jun Zhang
Ms. Zhang is responsible for the analyses and modeling studies within the project, and leading the initial preparation of the project reports.

Plans for Next Period

1. Based on existing published papers and reports, plus our own global modeling studies, evaluate APMT version 24 when it becomes available.
2. Using the CESM chemistry-climate model, update our earlier analyses of regional effects from aviation based on latitude bands.

3. Evaluate the GTP concept for aviation that is being developed by the CICERO research team,
4. As in our past projects with the FAA, we will also continue to act as a resource for the FAA in questions and issues associated with atmospheric chemistry, composition, and climate. This scope of work may be modified as necessary through the consultation with the FAA Program Managers.

Each of these studies should result in a report to the FAA and possibly resulting journal papers.

Task 2: Three-dimensional atmospheric climate-chemistry modeling studies for aviation effects on climate and air quality

University of Illinois at Urbana-Champaign

Objective(s)

The aim in this work was to further evaluate the much more complex 3-D chemistry-climate model to further our understanding of the chemistry and climate effects from aviation emissions. As part of this effort we used CAM5-Chem, the atmospheric component of Community Earth System Model (CESM), and did a series of studies to evaluate aviation impact both on surface air quality in 2006 and on climate in 2050.

Research Approach

We have completed the studies modeling of aviation effects on global atmospheric composition and on climate we did with FAA support that were published as FAA reports and have now been rewritten and updated for journal publication.

Milestone(s)

Completed journal papers referenced below.

Major Accomplishments

We have contributed to the journal paper led by Andrew Gettleman investigating the effects of aviation cruise emissions on climate in 2050. The study found that a growth in the climate impact of aviation by 2050, including positive radiative forcing from contrails up to ~80mWm^{-2} and enhanced upper tropospheric and lower stratospheric ozone (O3), due to nitrogen oxide (NOx) emissions of ~60mWm^{-2}. Changes in methane (CH4) forcing resulting from changes in the CH4 lifetime induced by aviation are estimated at -25mWm^{-2} in 2050.
We have also contributed to a report lead by Mark Jacobson investigating the effects of aviation cruise emissions on air quality. This study found that all models (Three-dimensional chemical-transport models (CTMs) and Climate Response Models (CRMs)) show increases in near-surface ozone (0.4 to 1.9% globally), perturbations in the Northern Hemisphere that are highest in winter (when ambient ozone levels are lower and potentially of not as much concern to human health compared to the higher ozone in the summer months).
We are also revising a paper for journal publication that expands the understanding the sensitivity of aviation emissions on ozone to levels of background lightning effects on nitrogen oxides.

Publications

Cameron, M. A., M. Z. Jacobson, S. R. H. Barrett, H. Bian, C. C. Chen, S. D. Eastham, A. Gettelman, A. Khodayari, Q. Liang, D. Phoenix, H. B. Selkirk, N. Unger, D. J. Wuebbles, and X. Yue, 2016: Inter-comparative study of effects of aircraft on surface air quality. *J. Geophys. Res.*, submitted.

Gettelman, A., C.-C. Chen, M. Z. Jacobson, M. A. Cameron, D. J. Wuebbles, and A. Khodayari, 2016: Coupled chemistry-climate effects from 2050 projected aviation emissions. *Atmos. Chem. Phys.*, submitted.

Khodayari, A., D. Phoenix, and D. J. Wuebbles, 2016: Sensitivity of NOx emissions from lightning on the production of aviation-induced ozone. *J. Geophys. Res.*, being revised.

Outreach Efforts

Results presented at various meetings in 2015, but none in 2016.

Awards

None

Student Involvement

Former post-doc Arezoo Khodayari has been responsible for the analyses and modeling studies within the project, and leading the initial preparation of our portions of the project reports.

Plans for Next Period

Project largely completed except for further revisions to the papers towards journal publication.

Project 023 Analytical Approach for Quantifying Noise from Advanced Operational Procedures

Massachusetts Institute of Technology

Project Lead Investigator

R. John Hansman
T. Wilson Professor of Aeronautics & Astronautics
Department of Aeronautics & Astronautics
MIT
Room 33-303
77 Massachusetts Ave
Cambridge, MA 02139
617-253-2271
rjhans@mit.edu

University Participants

MIT

- P.I.(s): R. John Hansman
- FAA Award Number: 13-C-AJFE-MIT, Amendment Nos. 008, 015, and 022
- Period of Performance: Nov. 1, 2014 to Aug. 31, 2017
- Task(s):
    1. Identify candidate arrival or departure procedures or procedure modifications with noise reduction potential and present analytical framework
    2. Select at least 3 procedures and complete analyses of environmental improvement potential for candidate arrival or departure procedures or procedure modifications with noise reduction potential
    3. Review initial research outcomes and determine next steps for FAA assessment of candidate arrival or departure procedures or procedure modifications with noise reduction potential
    4. Identify, evaluate, and document implementation barriers (pilot workload, controller workload, safety, among other considerations) for proposed procedures. Evaluate and document feasibility of an enhanced NAS-wide air traffic evaluation framework
    5. Repeat process for additional procedures
    6. Final Report on potential air traffic procedural changes at BOS to address noise concerns and the feasibility of an enhanced NAS-wide air traffic procedural framework for assessing implications of proposed operational procedures on fuel burn, noise and environmental justice populations without detriment to safety

Project Funding Level

Project Funding Level: $360,000 FAA funding and $360,000 matching funds. Sources of match are approximately $80,000 from MIT and $280,000 from Massachusetts Port Authority.

Investigation Team

Prof R. John Hansman (PI)
Dr. Brian Yutko (Co-I)
Dr. Greg O'Neill (Postdoc)
Luke Jensen (Graduate Student)

Morrisa Brenner (Graduate Student)
Jacqueline Thomas (Graduate Student)
Cal Brooks (Graduate Student)
Sandro Salguerio (Graduate Student)
Clement Li (Graduate Student)

Project Overview

The objective of the first phase of the research has been the development of an analytical approach for evaluating the noise impacts of advanced operating procedures. Older generations of jet engines produced significantly more noise than current-generation products. The assumption that jet noise dominates aerodynamic sources may have been reasonable in previous environmental impact studies. However, for new advanced approach and departure procedures, aerodynamic noise reduction may contribute strongly to environmental benefits. For example, in a delayed deceleration approach (DDA), deployment of landing gear and high-lift devices can be delayed until later stages in an approach, reducing aerodynamic noise. This effect is not captured using current noise-power-distance (NPD) noise calculation tools now in common use throughout the aerospace industry. This illustrates a gap in noise analysis capability for advanced operational procedures.

The second phase of this research is to use and refine the analytical approach by developing both generic and specific RNAV-RNP procedures which offer the potential to reduce community noise impact.

Task Progress and Plans

Task 1: Identify candidate arrival or departure procedures or procedure modifications with noise reduction potential and present analytical framework.
This task is in progress and a generic set of procedure modification shave been identified.

Task 2: Select at least 3 procedures and complete analyses of environmental improvement potential for candidate arrival or departure procedures or procedure modifications with noise reduction potential.
This task in in progress. Complaint data has been correlated with current procedures at BOS in detail and at DCA. Final selection of target procedures is pending additional input from community groups and ATO.

Task 3: Review initial research outcomes and determine next steps for FAA assessment of candidate arrival or departure procedures or procedure modifications with noise reduction potential.
This task is pending results of Task 2.

Task 4: Identify, evaluate, and document implementation barriers (pilot workload, controller workload, safety, among other considerations) for proposed procedures. Evaluate and document feasibility of an enhanced NAS-wide air traffic evaluation framework.
This task is pending results of Task 2.

Task 6: Repeat process for additional procedures
This task is pending.

Task 7: Final Report on potential air traffic procedural changes at BOS to address noise concerns and the feasibility of an enhanced NAS-wide air traffic procedural framework for assessing implications of proposed operational procedures on fuel burn, noise and environmental justice populations without detriment to safety.
This task is pending.

Major Accomplishments

Have developed and demonstrated TASOPT and ANOPP connection and modeled several aircraft types with good agreement with certification data. Have demonstrated the tool overall design tool on analysis of procedures at BOS, DCA, JFK and LGB. Currently working with MASSPORT on developing new class of low noise RNAV/RNP procedures for BOS,

Publications
None

Outreach Efforts
Briefed the Administrator and the Management Advisory Committee.
Briefed ATA Technical Pilots Working Groups
NPR Appearance to Discuss Modeling Efforts in Boston

Awards
None

Student Involvement
Graduate students have been involved in all aspects of this research and have been the key implementers.

Project 024(B) PM Emission Database Compilation, Analysis and Predictive Assessment

The Pennsylvania State University, GE U.S. Aviation

University Participants

Penn State University

- P.I.(s): Randy L. Vander Wal, Professor, Energy and Mineral Engineering, Materials Science and Engineering
- FAA Award Number: Grant 11712482, Amendment No. 13-C-AJFE-PSU-008
- Period of Performance: Aug. 18th, 2014, Sept. 30th, 2016
- Task(s):
    1. Develop Database. Include mass and number nvPM emission data for fuels, engine, measurement method(s) and engine conditions.
    2. a) Compare current ground nvPM predictive methods to measured values from NASA campaigns. b) Compare current cruise scaling approximation to measured cruise values from NASA's ACCESS.
    3. Correct current engine condition predictive methods using proprietary GE cycle deck data.
    4. Compare current methods using accurate engine condition inputs.
    5. Formulate new predictive relationships for nvPM with engine thrust level.
    6. Evaluate whether a universal relation or separate ones are required for Jet-A and alternative fuels.

Project Funding Level

FAA funding: $149,975

GE Aviation is the Industrial Partner supplying matching funds, level $150,000, with $1,724,895 available to the FAA COE AJFE ASCENT program, administered through Washington State University.

Investigation Team

Professor Randy L. Vander Wal, Penn State EME Dept., with responsibilities for project management, reports, interfacing with FAA program manager, and mentoring the graduate student supported on this project.
Mr. Joseph P. Abrahamson, Graduate student. Responsibilities include data assembly, analysis and predictive relation assessment, as integral towards completion of a Ph.D. program.

Project Overview

Relationships between fuel components, engine operating conditions and emissions are necessary to understanding their formation and achieving mitigation. Present synthetic paraffinic kerosene (SPK) aviation fuels differ from petroleum derived aviation kerosene by their high paraffin (~ 53% n-paraffin, 47%, iso-paraffin, FT Shell), napthene content (~ 87% cycloparaffin, 12%, iso-paraffin, FT Sasol), but most notably absence of aromatics (< 0.5%) and negligible organo-sulfur compounds. Future alternative may have substantially higher cycloparaffin content while hydrotreated depolymerized cellulosic (HDCJ) fuel may even (re)-introduce aromatics, adding to composition variability and need for understanding emissions from varied components and their mixtures.

With the emerging use of alternative fuels and varied compositions markedly change non-volatile PM (nvPM) emissions. Number density and mass changes are found, and hence emission index (EI). These measures in particular are relevant to potential regulations. These quantities can vary with engine power, and are strongly dependent upon fuel components, namely paraffin, naphthene and aromatic content. The value of these studies is that assembling data across platforms, fuels and measurement methods will build a comprehensive picture of PM emissions dependence upon components, engine type, power level and minor fuel species such as sulfur.

Objective(s)

Nonvolatile PM emissions from aircraft engines are primarily comprised of soot particles formed in the engine combustor. The amount of soot formed within a specific combustor design can change by more than an order of magnitude as engine thrust increases from idle to takeoff, due to increasing combustor pressure, temperature, and fuel-air ratio. In order to understand the influence of fuel properties on nvPM emissions from a specific engine, it is important to separate fuel effects from changes in emissions due to differences in combustor operating conditions, which are affected by engine thrust level, ambient conditions, altitude, flight Mach number, and engine deterioration.

Research Approach

Emerging use of alternative fuels markedly change non-volatile PM (nvPM) emissions. Number density and mass changes are found, with emission index (EI) being the most uncertain given its derivation by smoke number. These measures in particular are relevant to future regulations. These quantities can vary with engine power, and are strongly dependent upon fuel components, namely paraffin, naphthene and aromatic content.

In light of this situation emissions data from the FAA CLEEN program, NASA-led ACCESS campaigns, and related NASA Aviation Particle Emission Experiment (APEX) I, and Alternative Aviation Fuel(s) Experiment (AAFEX) I & II campaigns has been collected. These campaigns and tests investigated alternative fuels, varied fuel components and assessed the role and aromatics. To-date there is no comparison(s) between these studies or compilation of results into a unified database. The value of these studies is that assembling data across a range of studies, conducted using one engine class, representative of rich-dome style combustors, platforms, fuels and measurement methods will build a comprehensive picture of PM emissions dependence upon fuel composition and engine thrust at ground and cruise.

Previous studies have used simplified relationships to estimate emissions as a function of engine operating conditions. A more detailed two-step process is planned to correct for these effects in this proposed study. GE Aviation has detailed proprietary analytical models for each GE and CFMI engine type to predict pressures and temperatures throughout the engine as a function of thrust and inlet conditions. The first step in the proposed study is to use this type of model to calculate combustor inlet pressure, temperature, and fuel-air ratio at operating points where nvPM emissions have been measured, and re-evaluate current predictive methods using correct engine operating conditions. By comparison to ground and cruise nvPM emission data, deficiencies in current formulations can be identified and new predictive relations can be developed. With relations benchmarked against measurements, and confidence in engine operating conditions, measured nvPM from alternative fuels may be used to guide parameter formulation in these new predictive relations so as to expand their applicability to alternative fuels. Thereafter these relations will be assessed by comparison to nvPM test data from other engines as from NASA studies and the FAA CLEEN programs.

Milestone(s)

Milestones accomplished during this period of performance include the following.

1. Database development for nvPM mass, number emission data for fuels, engine thrust across field campaigns.
2. Compared GE Aviation cycle deck calculations at ground and cruise conditions, matching test point conditions in the NASA field campaigns.
3. Evaluation of current predictive methods to ground and cruise measurements using accurate engine operating conditions.
4. Formulated new predictive relationships for nvPM with engine thrust level.
5. Developed a universal relation as a predictive tool for estimating nvPM from Jet-A and alternative fuels.

Major Accomplishments (as excepted from ES&T 2016 submission)

IMPROVED METHOD (ImFOX)

1. Improved Engine Condition Relations. In this section engine conditions required as inputs for the improved FOX (ImFOX) expression are more accurately provided in the form of predictive relations based on proprietary cycle deck calculations for a common RQL combustor. Aerosol emissions from the NASA campaigns: Aircraft Particle Emissions eXperiments (APEX-I)[28,29], Alternative Aviation Fuel Experiments I and II (AAFEX-1, AAFEX-II)[30,31], Alternative-Fuel Effects on Contrails & Cruise EmiSSions I and II (ACCESS-I, ACCESS-II)[9] are from a Douglas DC-8 aircraft equipped with four CFM56-2C turbo fan engines. Although, this engine is an older design it is a high-bypass engine and serves as the basis for the whole engine family employed by thousands of commercial and military aircraft worldwide. The EI_{BC} curves from five of the six RQL style combustors tested during APEX-III[32-34] followed a common curve[35], with upturns both at low (idle) and high (take-

off) thrust levels. (The exception was the Rolls-Royce engine RB211-535E4-B with 40,100 lbs. maximum thrust, which has a BC emission profile peaking at 65% of the maximum thrust and deceased emissions thereafter.) Therefore, it appears the relationships developed here are considered applicable for a majority of rich-burn, quick-quench, lean-burn (RQL) style combustors. Only a select few engine conditions are addressed in this section. This is intentional as the goal is to simplify the calculations needed to predict EI_{BC}. For the relations developed here, the only needed input is the fuel flow rate from which all other engine conditions as input for the ImFOX expression can be calculated. For an extended study on conditions especially at cruise altitude the interested reader is referred to reference 1.

Air-to-Fuel Ratio, AFR. The first condition investigated is AFR, it should be mentioned that AFRs found here are those at the back of the combustor, typically referred to as plane-4, and are not the AFRs in the primary zone or the quench zone. The current method, equation 5, has been widely accepted. This is partially because an engine manufacture had released nominal AFR values at 7, 30, 85, and 100 thrust settings.[15] Those values were linearly fit to derive the current predictive AFR expression. However, after comparing values using this relation to engine cycle deck data it was evident that the current method results in over prediction of AFR. Two separate equations are needed to accurately calculate AFR. One for ground and another for cruise, equations 10 and 11 respectively.

$$AFR_{grd} = 71 - 35.8\left(\frac{\dot{m}_f}{\dot{m}_{f,max}}\right)$$

[10]

$$AFR_{cru} = 55.4 - 30.8\left(\frac{\dot{m}_f}{\dot{m}_{f,max}}\right)$$

[11]

As seen from the two AFR equations, at a matching thrust level AFR will be lower at cruise than at ground. This is sensible considering the decreased air density at altitude.

Flame Temperature, T_{fl}. Flame temperature is arguably the most important variable as it appears in both exponential terms in both the FOX and the Döpelheuer and Lecht scaling relation. Several T_{fl} predictive methods have been developed in addition to the one currently used in the FOX expression, equation 7. The common practice is to predict a T_{fl} using a linear relationship to T_3. Whereas equation 7 assumes that 90 % of the incoming sensible heat from the hot air leaving the compressor, T_3, adds to a stoichiometric adiabatic flame temperature of 2120 K. A common alternative flame temperature predictor for an RQL style combustor based on T_3 is given in equation 12.[36]

$T_{fl}[K] = 0.6T_3 + 1800$
[12]

This method assumes that 60 % of the initial air temperature is converted to flame temperature and that the flame temperature without this addition is that of a fuel rich flame at 1800 K. Considering that the primary zone of an RQL combustor runs fuel rich for flame stabilization, equation 12 is a more realistic flame temperature predictor to determine the primary zone flame temperature. However, the only variable in either flame temperature predictor is T_3 and since the AFR is a function of thrust the second term should also be variable with relation to AFR, and hence thrust (given flame temperature dependence upon stoichiometry, or AFR). However, since this localized AFR as a function of thrust is proprietary and not readily determined we have elected to use the temperature at the back of the combustor (T_4) in place of primary zone flame temperature. Using T_4 for the flame temperature is logical considering that the AFR being used is also from the back of the combustor as a global average of the processes occurring in the formation and oxidation regions of the combustor. Additionally, T_4 is readily calculated by the engine cycle deck, yielding equation 13.

$T_4[K] = 490 + 42{,}266FAR$
[13]

There is a strong correlation between T_3 and T_4, the Pearson r correlation value is 0.966. However, as seen in equation 13 it was not selected in the T_4 relation because there is a much stronger correlation between T_4 and fuel-air-ratio (FAR), Pearson r value of 0.995, but more importantly for the fact that an explicit AFR dependence accounts for the expected dependence of T_{fl} upon stoichiometry. Additionally, T_3 is an engine specific parameter that may not be readily available in all cases. Equation 13 accurately predicts T_4 at both ground and cruise. Given the success of this semi-empirical T_4 calculation based on FAR, a thermodynamic basis was evaluated for rationalization of this empirical result. The thermodynamic Air Standard

Brayton Cycle is applied to a jet engine in the SI. The thermodynamic Brayton Cycle equates T_4 to exhaust gas temperature (EGT) squared divided by temperature ambient. The NASA campaigns (APEX I-III, AAFEX I & II, and ACCESS I & II) documented both EGT and ambient temperature. Values of T_4 found using the thermodynamic Brayton Cycle compared to values predicted using equation 13 were slightly higher (~10%), likely because the Brayton Cycle is treated as an idealized adiabatic system. While either relation can be used to find T_4, the benefit of equation 13 is that only the FAR is needed and equations 10 and 11 provide accurate FAR relations for both ground and cruise respectively.

2. Improved EI_{BC} Predictive Relations.

The model we have developed uses the FOX[19] as the starting point. The FOX is a kinetically balanced relation predicting EI_{BC} by subtracting the rate of soot formation from the rate of soot oxidation. Each global process is represented by a single-step Arrhenius rate. The activation energy (E_a) value in the oxidation step is the well accepted value first proposed by Lee et al.[37] Given the success of this value, no modification to the oxidation step was made, outside of correcting AFR and substituting T_{fl} with T_4. The formation activation energy is that reported by Hall et al.[39] and is their inception E_a based on the formation of polyaromatic hydrocarbons (PAHs). The pre-exponential frequency factor (also referred to as formation constant) is a function of two and three member PAH concentrations, reflecting their role as BC building block molecules. Using a formation constant value of 356 Settler et al.[19] achieve a coefficient of determination, R^2, value of 0.8 when fitting to the APEX campaign data. The limitation of this approach is that it does not account for alternative fuels. A different formation constant would be necessary for each fuel composition. By combining the ImFOX with the ASAF relation developed by Speth et al.[20] determination of BC emissions from alternative fuels is possible. However, ASAF does not consider cycloalkanes known to have a higher sooting index[26,39] than that of paraffinic compounds found predominantly in alternative fuels. Therefore, an alternative approach was developed using hydrogen content. Formulation and results from pairing the ImFOX with ASAF are given in the SI.

H-ImFOX. As previously mentioned, the pre-exponential frequency factor is a function of two and three member PAH concentration, which in turn is a function of PAH building block molecule concentrations; acetylene, benzene, phenyl radical, and hydrogen. Since there is no practical way to determine these molecular concentrations this pre-exponential factor (also referred to as a formation constant) is fit to C_{BC} data and given in equation 14.

$$A_{form} = 1013 - 4802\left(\frac{\dot{m}f}{\dot{m}f,max}\right) + 7730\left(\frac{\dot{m}f}{\dot{m}f,max}\right)^2 - 3776\left(\frac{\dot{m}f}{\dot{m}f,max}\right)^3 \quad [14]$$

There is a complex dependence, 3rd order, between thrust and the formation constant. This is sensible considering that PAH building block molecule concentrations will vary with thrust. High-resolution transmission electron microscopy and X-ray photoelectron spectroscopy have been used to demonstrate how the macro, micro, and nano-structure of BC from commercial aircraft vary across thrust settings.[35,40] Black carbon nanostructure can reflect the formation conditions, i.e. species and temperature, of BC.[35] As reported by Vander Wal et al.[35] BC emissions vary from amorphous at low power (idle) to graphitic at high power (take off). This observation supports the need for the formation constant to have a complex dependence on thrust. Black carbon is not an equilibrium product of combustion.[36] Thus, it is difficult to predict its rate of formation and final concentration from kinetics or thermodynamics alone. In practice, the rate of soot formation is strongly impacted by the physical processes of atomization and fuel-air mixing as these processes control the equivalence ratio and resulting flame temperature.[36] This fuel air mixing is captured by the thrust dependent A_{from} term given in equation 14. This mixing effect is the same across all fuels: conventional, blended, and neat SPK. Therefore, equation 14 developed here for conventional fuel can be used to represent the mixing (combustor) effect across all fuels and a separate fuel term can be added to account for fuel effects, specifically decreasing EI_{BC} with increasing hydrogen mass content. The new predictive expression is accordingly termed the H-ImFOX, and given in eqn. 15.

$$C_{BC}\left[\frac{mg}{m^3}\right] = \dot{m}_f \times e^{(13.6-H)}\left(A_{form} \times e^{(-6390/T_4)} - A_{ox} \times AFR \times e^{(-19778/T_4)}\right) \quad [15]$$

The H in equation 15 represents hydrogen mass percent and as seen in equation 15 BC emission decays exponentially with increasing hydrogen content. This trend was observed across the previously mentioned NASA campaigns.[9] The H-ImFOX will hereafter be referred to as just the ImFOX as the new hydrogen fuel term is universally applied across all fuels and therefore, equation 15 is the ImFOX. A strong correlation between hydrogen content and BC reduction was recently observed during the Aircraft Particulate Regulatory Instrumentation Demonstration Experiment (A-PRIDE) 7. It was demonstrated by Brem et al.[41] that BC emissions from conventional fuels vary due to a range of aromatic content and concluded that emissions are best predicted based on hydrogen mass content. Additionally, Lobo et al.[42] recently reported similar findings by varying the ratio of SPK blending components with conventional fuel.

The hydrogen dependent fuel effect developed here based on ground data applies equally well at cruise as the BC emission trend with hydrogen content is the same at both ground and cruise altitude. However, EI_{BC} measured at cruise during the recent ACCESS-II campaign was 264 % higher than ground based measurements when averaged across all observed powers. This is likely due to the decreased AFR at cruise brought on by the reduced air density. The lower AFR or higher equivalence ratio at cruise will give rise to more fuel rich pockets and higher concentrations of BC precursor molecular species. Accordingly, different A_{form} relations are necessary for ground and cruise. During cruise operation thrust settings are typically higher than 30 %, therefore, cruise EI_{BC} emission profiles do not possess the commonly observed emission curve with upturns both at low (idle) and high (take-off) thrust levels as measured from ground campaigns. From the limited cruise altitude BC measurements, the EI_{BC} increases linearly with thrust, hence complex formation constants, like derived for ground based emissions, are not necessary. A complex expression for cruise A_{form} may ultimately be needed, however, the limited range of thrust values at cruise do not provide justification for such, instead the simplest expression (a constant) was chosen and found adequate by quality of fit. A constant A_{form} cruise value of 295 captures the observed linear trend of increasing EI_{BC} with increased thrust at cruise.

References

28. Wey, C. C.; Anderson, B. E.; Hudgins, C.; Wey, C.; Li-Jones, X.; Winstead, E.; Thornhill, L. K.; Lobo, P.; Hagen, D.; Whitefield, P.; Yevington, P. E.; Herndon, S. C.; Onasch, T. B.; Miake-Lye, P. C.; Wormhoudt, J.; Knighton, W. B.; Howard, R.; Bryant, D.; Corporan, E.; Moses, C.; Holve, D.; Dodds, D. *Aircraft Particle Emissions eXperiment (APEX)*; ARL-TR-3903; NASA Langley Research Center: Hampton, VA, 2006

29. Wey, C. C.; Anderson, B. E.; Wey, C.; Miake-Lye, R. C.; Whitefield, P.; Howard, R. Overview of aircraft particle emissions experiment. *J. Propul. Power* **2007**, *23*, 898-905.

30. Anderson, B.; Beyersdorf, A.; Hudgins, C.; Plant, J.; Thornhill, K.; Winstead, E.; Ziemba, L.; Howard, R.; Corporan, E.; Miake-Lye, R. *Alternative aviation fuel experiment (AAFEX)*; NASA Langley Research Center: Hampton, VA, 2011

31. Beyersdorf, A. J.; Timko, M. T.; Ziemba, L. D.; Bulzan, D.; Corporan, E.; Herndon, S. C.; Howard, R.; Miake-Lye, R.; Thornhill, K. L.; Winstead, E.; Wey, C.; Yu, Z.; Anderson, B. E. Reductions in aircraft particulate emissions due to the use of Fischer-Tropsch fuels. *Atmos. Chem. Phys.* **2014**, *14*, 11-23.

9. Moore, R.; Shook, M.; Beyersdorf, A.; Corr, C.; Herndon, S.; Knighton, W.; Miake-Lye, R.; Winstead, S.; Yu, Z.; Ziemba, L.; Anderson, B. Influence of Jet Fuel Composition on Aircraft Engine Emissions: A synthesis of aerosol emissions data from the NASA APEX, AAFEX, and ACCESS missions. *Energy Fuels* **2015,** *29,* 2591-2600.

32. Kinsey, J. S. *Characterization of emissions from commercial aircraft engines during the Aircraft Particle Emissions eXperiment (APEX) 1 to 3*; EPA-600/R-09/130; Environmental Protection Agency: Washington DC, 2009.

33. Kinsey, J. S.; Dong, Y.; Williams, D. C.; Logan, R. Physical characterization of the fine particle
Emissions form commercial aircraft engines during the Aircraft Particle Emissions eXperiment (APEX) 1-3. *Atmos. Environ.* **2010**, *44*, 2147-256.

34. Dong, Y.; Williams, D. C.; Logan, R. Chemical characterization of the fine particle emissions form commercial aircraft engines during the Aircraft Particle Emissions eXperiment (APEX) 1 to 3. *Environ. Sci. Technol.* **2011**, *45*, 3415-3421.

35. Vander Wal, R. L.; Bryg, V. M.; Huang, C.-H. Aircraft engine particulate matter: Macro- mico- and nanostructure by HRTEM and chemistry by XPS. *Combust. Flame* **2014**, *161*, 602-611.

15. Wayson, R. L.; Fleming, G. G.; Lovinelli, R. Methodology to estimate particulate matter emissions from certified commercial aircraft engines. *J. Air Waste Manage. Assoc.* **2009**, *59*, 91-100.

36. Arthur H. Lefebvre; Dilip R. Ballal *Gas Turbine Combustion: Alternative Fuels and Emissions*; 3rd ed.; CRC Press, 2010; p. 72.

37. Lee, K.B; Thring, M.W; Beer, J.M. On the rate of combustion of soot in a laminar soot flame. *Combust. Flame* **1962,** *6,* 137–145.

19. Stettler, M. E. J.; Boise, A. M.; Petzold, A.; Barrett, S. R. H. Global civil aviation black carbon emissions. *Environ. Sci. Technol.* **2013a**, *47*, 10397-10404.

38. R.J. Hall, M.D. Smooke, M.B. Colket, in Physical and Chemical Aspects of Combustion: A Tribute to Irvine Glassman, F.L. Dryer and R.F. Sawyer (Ed.), Gordon & Breach, 1997, p. 201.

19. Stettler, M. E. J.; Boise, A. M.; Petzold, A.; Barrett, S. R. H. Global civil aviation black carbon emissions. *Environ. Sci. Technol.* **2013a**, *47*, 10397-10404.

20. Speth, R. L.; Rojo, C.; Malina, R.; Barrett, S. R. H. Black carbon emissions reductions form combustion of alternative fuels. *Atmos. Environ.* **2015**, *105*, 37-42.

26. Yang, Y.; Boehman, A. L.; Santoro, R. J. A study of jet fuel sooting tendency using the threshold sooting index (TSI) model. *Combust. Flame* **2007**, 149 (1−2), 191−205.

39. Mensch, A.; Santoro, R. J.; Litzinger, T. A.; Lee, Y.-Y. Sooting characteristics of surrogates for jet fuel. *Combust. Flame* **2010**, *157*, 1097-1105.

40. Huang, C.-H.; Vander Wal, R. L. Effect of soot structure evolution from commercial jet engine burning petroleum based JP-8 and synthetic HRJ and FT fuels. *Energy Fuels* **2013**, *27*, 4946-4958.

41. Brem, B. T.; Durdina, L.; Siegerist, F.; Beyerle, P.; Bruderer, K.; Rindlisbacher, T.; Rocci-Denis, S.; Andac, M. G.; Zelina, J.; Penanhoat, O.; Wang, J. Effects of fuel aromatic content on nonvolatile particulate emissions of an in-production aircraft gas turbine. *Environ. Sci. Technol.* **2015**, *49*, 13149-13157.

42. Lobo, P.; Christie, S.; Khandelwal, B.; Blakey, S. G.; Raper, D. W. Evaluation of Non-volatile Particulate Matter Emission Characteristics of an Aircraft Auxiliary Power Unit with Varying Alternative Jet Fuel Blend Ratios. *Energy Fuels* **2015**, *29*, 7705-7711.

Publications & Presentations

1. Publications

1. Abrahamson, J. P., Zelina, J., Andac, G., and Vander Wal, R. L., Aviation black carbon mass predictive model for alternative and traditional fuels at ground and cruise.
FAA Hartman paper (Best paper of the year award). 2016.
Available at: https://ascent.aero/competition/
and
https://ascent.aero/wp-content/uploads/sites/192/2015/12/Hartman_CH_7-20-16JPA.pdf

2. Abrahamson, J. P., Zelina, J., Andac, M. G., & Vander Wal, R. L. (2016). Predictive Model Development for Aviation Black Carbon Mass Emissions from Alternative and Conventional Fuels at Ground and Cruise. *Environmental Science & Technology*, *(submitted).*

2. Presentations

Invited
1. Vander Wal, R. L., Abrahamson, J. P., Jet Engine nvPM Emissions: Status of Predictive Relations. Session 10: Fuel Composition Effects Upon Emissions. Aviation Emissions Characterization Roadmap. 14th Annual Meeting, National Academy of Sciences, Washington, D.C. May 24th – 26th, 2016.

Invited – Student of The Year Award

2. Abrahamson, J. P., and Vander Wal, R. L., nvPM Emissions Database Compilation, Analysis and Predictive Assessment. Project 24B. FAA ASCENT 5th Advisory Board Meeting. FAA Center of Excellence for Alternative Jet Fuels & Environment (FAA COE AJFE). Alexandria, VA April 26th-27thth, 2016.

3. Vander Wal, R. L., Abrahamson, J. P., PM Database Compilation, Analysis and Predictive Assessments. Project 24B Report. 5th Advisory Board Meeting. FAA Center of Excellence for Alternative Jet Fuels & Environment (FAA COE AJFE). Alexandria, VA April 26th-27thth, 2016.

4. Abrahamson, J. P., Vander Wal, R. L., (2016). Gas turbine nvPM formation and oxidation semi-empirical model for commercial aviation. Paper # 138IC-0025. Topic: Internal Combustion and Gas Turbine Engines. 2016 Spring Technical Meeting, Eastern States Section of the Combustion Institute, Princeton University, Princeton, NJ March 13-16th, 2016.

5. Abrahamson, J. P., and Vander Wal, R. L., Retooling Predictive Relations for non-volatile PM by Comparison to Measurements. Session: Quantifying Aviation Impacts on Air Quality and Climate. The annual American Geophysical Union (AGU) Annual Fall Meeting, Dec. 14th – 18th, 2015. San Francisco, CA.

6. Abrahamson, J. P., and Vander Wal, R. L., nvPM Emissions Database Compilation, Analysis and Predictive Assessment. Project 25B. FAA ASCENT Contractor's Meeting. Seattle WA, Oct. 13-15th, 2015.

7. Abrahamson, J. P., and Vander Wal, R. L., nvPM Emissions Database Compilation, Analysis and Predictive Assessment. Project 25B. FAA External Tools Meeting, Seattle WA, Oct. 20th, 2015.

Outreach Efforts

Informal discussions with GE US Aviation regarding the nature of nvPM from next generation lean-burn engines and potential differences relative to nvPM from RQL combustor designs.

Awards

Joseph P. Abrahamson – Energy and Mineral Engineering Dept. Penn State University
Joseph P. Abrahamson has received the FAA Center of Excellence Student of the Year (SOY) Award. Nationally competed, it is sponsored by the Department of Transportation, Council of University Transportation Centers and corporate affiliates. Joseph has also won the FAA ASCENT Joseph A. Hartman Student Paper Competition – a peer-reviewed process to select the best paper with focus on the environmental impact of the aviation industry. Joseph is presently a graduate student in The John and Willie Leone Family Department of Energy and Mineral Engineering at Penn State, pursuing his Ph.D. under the guidance of Professor Randy L. Vander Wal.

Student Involvement

The current graduate student, Joseph P. Abrahamson, is conducting data assembly, analysis and predictive relation assessment, towards partial fulfillment of his Ph.D. program in EME, with Fuel Science option.

Plans for Next Period

The tasks and milestones for this project were completed July 31st, 2016.

Project 025: National Jet Fuels Combustion Program, Area #1 Shock Tube and Flow Reactor Studies of the Kinetics of Jet Fuels

Stanford University

Project Lead Investigator

Ronald K Hanson
Woodard Professor
Mechanical Engineering Department
Stanford University
452 Escondido Mall
650-723-6850
rkhanson@stanford.edu

University Participants

Stanford University

- P.I.s: Prof. Ronald K Hanson, Prof. C Thomas Bowman
- FAA Award Number: 13-C-AJFE-SU-008
- Period of Performance: 11/05/2015 to 11/30/2016
- Task: Area #1 – Chemical Kinetics Combustion Experiments

Project Funding Level

$285,000 from FAA with 1-1 matching funding of $285,000 from Stanford University. Includes $10,000 for travel to meetings.

Investigation Team

Prof. Ronald K Hanson, Principal Investigator, Research Direction
Prof. C Thomas Bowman, Co-Principal Investigator, Research Direction
Dr. David F Davidson, Senior Research Engineer, Research Management
Dr. Kun Wang, Post-Doctoral Research Associate, Research Assistant
Jiankun Shao, Graduate Student, Research Assistant
Tom C Parise, Graduate Student, Research Assistant
Sarah Johnson, Graduate Student, Research Assistant

Project Overview

Provide shock tube/laser absorption and flow reactor experiments for a fundamental kinetics database for jet fuels. Experiments are expected to continue to reveal the sensitivity of combustion properties to fuel composition for the ultimate use in simplifying the alternative fuel certification process.

Task: Area #1 – Chemical Kinetics Combustion Experiments

Stanford University

Objectives

Experiments provide an extensive fundamental kinetics database for selected jet fuels. These data are used as critical input for Area #2 that seeks to develop a new hybrid and detailed kinetics model for jet fuels (HyChem). These experiments continue to reveal the sensitivity of combustion properties to variations in fuel composition for ultimate use

in simplifying the alternative fuel certification process. The team works in close collaboration with Prof. Hai Wang, also of Stanford University, the PI for area #2, who uses the data acquired in our experiments. The data provided will also ensure that the combustion models developed in Area #4 - Combustion Model Development and Validation to model the extinction and ignition processes controlling lean blowout, cold ignition and high altitude relight, are chemically accurate.

Research Approach

The development, refinement and validation of detailed reaction mechanisms describing the pyrolysis and oxidation of fuels require experimental data as targets for kinetics models. Experimentally, the best way to provide these targets at high temperatures and pressures is with shock tube/laser absorption experiments and flow reactor experiments, conducted over a wide range of pressure, temperature, and fuel and oxidizer composition.

Reflected shock wave experiments provide a test environment that does not introduce additional fluid mechanics, turbulence, or heat transfer effects to the target phenomena. This allows isolation of the target phenomena (ignition delay times and species concentration time-histories) in a quiescent high-temperature, high-pressure environment that is very well characterized and hence amenable to modeling. Recent work in our laboratory to develop the Constrained Reaction Volume (CRV) methodology provides an additional tool to provide shock tube data under constant-pressure constraints when needed, to significantly simplify the gasdynamic/thermodymamic models needed to properly simulate reactive reflected shock wave data.

The strength in the Stanford shock tube approach comes with the implementation of laser diagnostics that enable the simultaneous measurement of species time-histories. Using laser absorption, we are able to provide quantitative time-histories during fuel pyrolysis and oxidation of the fuel, including transient radicals (e.g., OH, CH3), stable intermediates (e.g., CH4, C2H4, iso-butene and aromatics), combustion products (including CO, CO2, and H2O), and temperature.

In combination with the shock tube experiments, the Stanford Variable Pressure Flow Reactor is used to provide concentration profile data for important stable intermediate and product species (see Flow Reactor Section) during fuel pyrolysis and oxidation for temperatures ranging from 900 - 1200K, for pressures up to 5 bar, and for residence times from 5 - 100 msec. These species provide critical constraints on the development of the HyChem detailed kinetic models of Prof. Hai Wang.

The range of conditions accessible in the flow reactor partially overlap those achievable in the shock tube so that the combination of shock tube and flow reactor experiments provides a comprehensive species data set over a wide range of experimental conditions that is essential for kinetic model development and validation as well as for model reduction to a size needed for implementation in the Area #4 - Combustion Model Development and Evaluation. To our knowledge, our laboratory is the only one worldwide with this combined capability.

Measurements of the pyrolysis and oxidation systems of real fuels, rather than of surrogates or solvent surrogates, provide a direct link to actual fuel behavior. The combination of high-quality shock tube and flow reactor measurements combined with the HyChem kinetic model based on real fuel decomposition products proposed by Prof. Hai Wang is meeting the FAA program objectives.

Shock Tube Experiments

Stanford has the largest and best-equipped shock tube laboratory in the U.S., perhaps in the world, with five shock tubes: three large-diameter (10, 14 and 15 cm I.D.) high-purity shock tubes (see Fig. 1a); one heated high-pressure shock tube (5 cm I.D., capable of achieving 500+ atm); and 10 cm I.D. expansion tube for generating supersonic flows. Additionally, we have unique capability for species measurements using laser absorption (see Fig. 1b) developed over the past 30 years. In these experiments, temperatures from below 500 K to above 3000 K, and pressure from sub-atmospheric (0.2 atm) to 10-500+ atmospheres can be achieved in different carrier gases, such as argon or air, with demonstrated test times up to and exceeding 50 ms at low temperatures.

Three primary types of shock tube experiments are performed.

The first primary shock tube experiments are species concentration time-history measurements obtained during fuel pyrolysis. These data are used to place strong constraints on the reaction mechanism and the individual reaction rates and pathways. Laser absorption techniques, many pioneered at Stanford, are used to measure these species time-histories. The following species time-histories measurements have been acquired and used in the development of the HyChem

model: fuel at a wavelength of 3.39 microns, and the stable fuel decomposition products: ethylene, methane, and iso-butene, at wavelengths of 10.53, 3.1754 and 11.3 microns respectively. We also are able to measure the transient radical OH (in the UV at 306 nm), the combustion products CO, CO2 and H2O (in the IR at 2.7, 4.6 and 2.5 microns, respectively) as well as other product species.

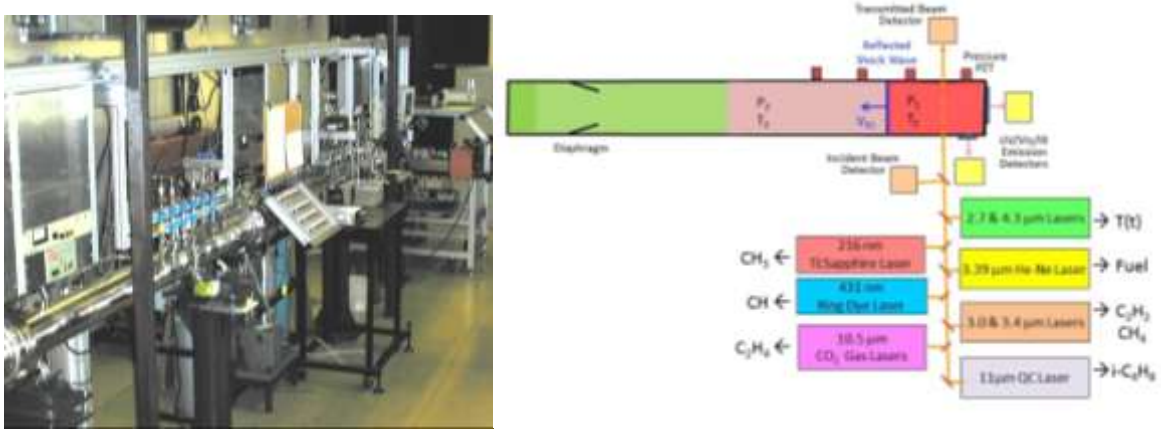

Figure 1a: Stanford 15 cm diameter shock tube. Figure 1b: Schematic of shock tube/laser absorption setup. Simultaneous measurement of multiple species time-histories and temperature with microsecond time resolution are enabled using this arrangement. Only a partial list of accessible species is indicated.

During this year of the program, using shock tube/laser absorption methods we acquired fuel, ethylene, propene, and isobutene time-histories for an investigation of several blends of FAA fuel A-2 and test fuel C-1. These pyrolysis product yield data were directly applicable to the development of the HyChem Fuel X model by Prof. Hai Wang. Representative data and HyChem simulations are shown in Figures 2a, b, and c.

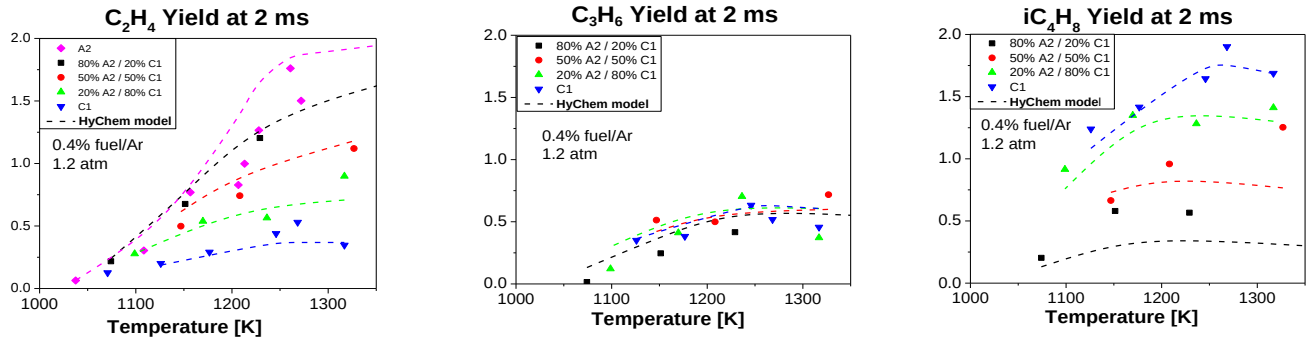

Figure 2a, b, &c: C2H4 C3H6 and iC4H8 yields acquired during the pyrolysis of blends of FAA fuels A1 & C1.

Stanford Variable Pressure Flow Reactor

A schematic diagram of the Stanford Variable Pressure Flow Reactor is shown in Fig. 3a. The facility comprises a quartz reactor tube housed in a stainless steel pressure vessel. A premixed laminar burner provides high-temperature vitiated air and this air is mixed with fuel vapor prior to entering the reactor tube. Electrical resistance heaters surrounding the reactor tube provide for nearly adiabatic reactor conditions. Gas samples are extracted by a cooled translating probe which also is used to measure gas temperature.

A variety of on-line analyzers, including a four-column gas chromatograph and a new spectrometer, obtained using AFOSR funds, are available to measure multiple stable species profiles simultaneously over reaction time scales up to 50 ms. Species that can be measured with these analyzers includes C1 - C12 alkanes, C2 - C8 alkenes, cycloalkanes, allenes,

aromatics, including benzene, toluene, and naphthalene, C1 - C3 aldehydes, H2, CO, CO2, and O2. Many of these species are not currently accessible in proposed shock tube experiments.

During this year of the program, using GC analysis we acquired a wide variety of fuel time-histories during the investigation of several blends of FAA fuel A-2 and test fuel C-1. Representative data and HyChem simulations for iso-butene and ethylene are shown in Figures 3b and c. As with the shock tube data above, these pyrolysis product yield data were directly applicable to the development of the HyChem Fuel X model by Prof. Hai Wang.

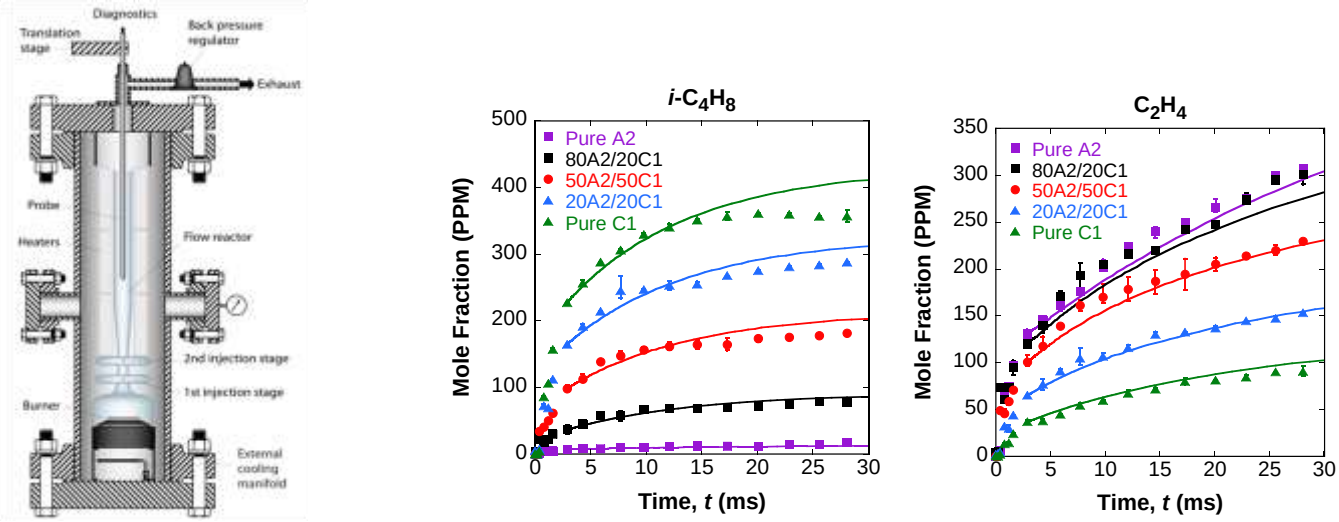

Fig. 3a: Stanford Variable Pressure Flow Reactor. Figure 3b: Species profiles during oxidative pyrolysis of A-2/C-1 fuel blends at 1 atm, ϕ=1 and initial temperature of 1030K.

Milestone(s)

Major Milestones included regular reporting of experimental results and analysis at monthly meetings for both the Testing Working Group and the Steering Working Group, as well as reporting at FAA Quarterly meetings.

Major Accomplishments

During this second year of this program, using shock tube/laser absorption methods we acquired fuel, ethylene, and methane, propene, and iso-butene time-histories for blends of FAA A2 & C1 fuels during pyrolysis and partial oxidation. In flow reactor experiments this set of species from the shock tube data were extended using gas chromatography measurements. These pyrolysis product yield data are directly applicable to the development of the HyChem model by Prof. Hai Wang.

Publications

Published Conference Proceedings and Archival Papers

D. F. Davidson, J. Shao T. Parise, R. K. Hanson, "Shock Tube Measurements of Jet and Rocket Fuel Ignition Delay Times," AIAA SciTech Meeting Grapevine TX, Jan. 2017, in press.

D. F. Davidson, A. Tugestke, Y. Zhu, S. Wang, R. K. Hanson, "Species Time-History Measurements during Jet Fuel Pyrolysis," 30th International Symposium on Shock Waves, Tel Aviv, Israel, November 2016, in press.

D. F. Davidson, Y. Zhu, J. Shao, R. K. Hanson, "Ignition Delay Time Correlations for Distillate Fuels," Fuel 187 26-32 (2017).

T. Parise, D. F. Davidson, R. K. Hanson, "Shock Tube/Laser Absorption Measurements of the Pyrolysis of a Bimodal Test Fuel," Proceedings of the Combustion Institute 36 1-8 (2016).

D. F. Davidson, Y. Zhu, S. Wang, T. Parise, R. Sur, R. K. Hanson, "Shock Tube Measurements of Jet and Rocket Fuels," AIAA Sci. & Tech. Forum, San Diego, Jan. 2016.

Outreach Efforts
Presentations at the AIAA Sci. & Tech. Forum, San Diego, Jan. 2016.
Upcoming presentation at AIAA SciTech Meeting Grapevine TX, Jan. 2017.

Awards
None

Student Involvement
Graduate students are actively involved in the acquisition and analysis of all experimental data.

Plans for Next Period
Advances in the HyChem model development based on the experimental and theoretical work so far indicate that there are several important issues that should be addressed as the model is further developed and validated.

First it is necessary to evaluate the assumptions and range of validity of the HyChem and Fuel X modeling approaches. Studies will be performed to establish temperature and pressure boundaries for the validity of the HyChem modeling approach. Current in-house validation of the model is based on a small set of ignition delay time and flow reactor experiments over limited ranges of pressure, temperature, equivalence ratio, and fuel concentration. Direct testing over a wider range of test conditions, using both shock tubes and flow reactors, can provide a first-order limits of the applicability of the HyChem model. Further measurements are also planned to investigate a wide range of distillate jet fuels to evaluate the behavior of the Fuel X assumptions.

Second, an effort will be made to update the foundational fuel chemistry, paying particular attention to the i-C4H8 sub-mechanism.

Finally, we plan to seek relationships between the measured ignition delay time (IDT) and speciation data and lean blow out (LBO), high altitude relight, and other engine characteristics.

Project 026 Hybrid Approach to Chemical Kinetics Model Development and Evaluation

Stanford University

Project Lead Investigator

Hai Wang
Professor
Mechanical Engineering
Stanford University
Building 520, Room 202, 452 Escondido Mall, Stanford, CA 94305-3032
650-497-0433
haiwang@stanford.edu

University Participants

Stanford University

- P.I.: Hai Wang
- FAA Award Number: 13-C-AJFE-SU-006
- Period of Performance: October 1, 2015 to November 30, 2015
- Overall Task(s):
    1. To develop reduced order reaction models, in close coordination with other areas on conditions and required types of data needed for model development and validation, to capture most important combustion properties of three Category A reference jet fuels and selected category C fuels, including pyrolysis intermediate distributions, ignition delay, flame extinction and flame speed.
    2. To understand the dependency of model parameters on fuel composition and chemical properties (DCN, aromatics, H/C, MW, etc.).

Project Funding Level

Funding from FAA: $200,000
Matching funding: $140,000 (Stanford University), $60,000 (United Technologies Research Center, in-kind)

Investigation Team

Single PI project

Project Overview

The study is designed to satisfy the objective of Area #2 of National Jet Fuels Combustion Program (NJFCP)– Chemical Kinetics Model Development and Evaluation. The overall objective is to providing validated kinetic models for the combustion of the three reference jet fuels ranging in their performance from the best to the worst case. During the course of the program, it was determined that kinetic models are also needed for two Cat C fuels to meet the overall NJFCP objectives. In all cases, the reaction models are validated to ensure that they can predict combustion phenomena of relevance to extinction and ignition processes controlling lean blowout, cold ignition and high altitude relight.

The work is to be carried our in close coordination with Profs. Ronald K. Hanson and C. Thomas Bowman, also of Stanford University, who carry out research in Area #1 of NJFCP – Chemical Kinetics Combustion Experiments. Coordination with Area #4 is also necessary to reduce the reaction model to a target size of < ~ 35 species. During the current reporting period, we have partially address questions surrounding Task 2. Results of Task 1 has been reported in the 2015 report.

Task 2 – Dependency of Model Parameters on Fuel Properties

Stanford University

Objective(s)

Understand the dependency of model parameters on fuel composition and chemical properties (DCN, aromatics, H/C, MW, etc.).

Research Approach

The dependency of model parameters on fuel composition and chemical properties is understood primarily through experimentation, aided with interpretation by kinetic modeling.

Comparisons

Experimental and modeling results show very little dependency of the reaction model parameters on the fuel composition or properties among all Cat A fuels and the C5 fuel. The C1 fuel, on the other hand, exhibits notably different pyrolysis behaviors. Rather than ethylene and methane being the dominant pyrolysis products, the C1 fuel produces predominantly propene and isobutene, both of which tend to have smaller reactivity towards oxidation than ethylene. Indeed, the laminar flame speed of the C1 fuel was computed to be about a few cm/s smaller than those of the Cat A fuels. The ignition delay time shows mixed behaviors. As shown in Figure 1, the ignition delay time of the C1 fuel is larger than that of the three Cat A fuels in a dilute, 4%O_2-Ar mixture, but the trend is seen to be opposite in the air mixture. Analysis of the computational results shows that the ignition delay time is impacted by two factors. The production of isobutene and propene from the pyrolysis of the C1 fuel leads to a longer induction time of radical buildup and thermal runaway, whereas the pyrolysis rate of the C1 fuel is larger than those of the Cat A fuels. It is the competition of these two processes that lead to the behaviors of switched overall reactivity, as seen in Figure 8.

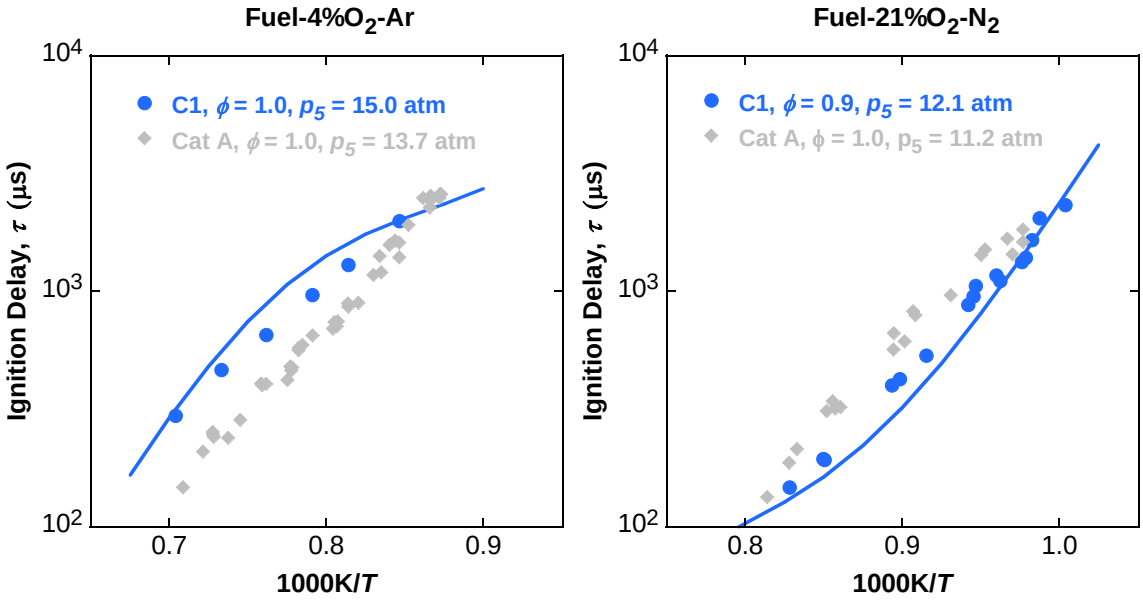

Figure 1. Comparison of the ignition delay times of the C1 and Cat A fuels in 4%O_2-Ar (left panel) and in air (right panel). The symbols are experimental data and the lines are computed results.

Milestone(s)

All milestones have been accomplished. These include the reaction models that can be reduced to less than 35 species for all three Cat A reference fuels and two Cat C fuels and an understanding of the fuel effects on intermediate formation and its effect on basic combustion properties of different jet fuels.

Major Accomplishments

The hybrid modeling approach is shown to be critical to obtaining the predictive capability for five multicomponent real fuels. The resulting models have shown to yield satisfactory results when reduced to about 30 species (by T.-F. Lu). They are used by modelers in Area #4 in their CFD simulations. The models also help us to understand the causes for the different combustion behaviors of different fuels.

Publications

Nothing to report.

Outreach Efforts

Nothing to report.

Awards

Nothing to report.

Student Involvement

One student (Ray Xu) and one postdoctoral fellow (Dongping Chen) worked on the project. They gained useful experience through the project effort.

Project 027 (A) National Jet Fuels Combustion Program – Area #3: Advanced Combustion Tests (Year II)

Georgia Institute of Technology
Oregon State University
University of Illinois

*this report covers portion of University of Illinois

Project Lead Investigator

Tonghun Lee
Associate Professor
Mechanical Science & Engineering
University of Illinois at Urbana-Champaign
1206 W. Green St.
Urbana IL 61801
517-290-8005
tonghun@illinois.edu

University Participants

University of Illinois at Urbana-Champaign

- P.I.(s): Tonghun Lee, Associate Professor
- FAA Award Number: 13-C-AJFE-UI-013
- Period of Performance: 12/1/2015 to 12/31/2017
- Task(s):
    1. Optimize and apply laser diagnostics for application in the Referee Combustor (AFRL).
    2. Optimize and apply laser diagnostics for ignition experiments at Georgia Tech.

Project Funding Level

Funding Level: $120K
Cost Share: In-kind academic time of the PI, cost share contribution from NRC-Canada.

Investigation Team

- Eric Mayhew (Graduate Student, University of Illinois at Urbana-Champaign): Execution of laser and optical diagnostics at ARFL.
- Rajavasanth Rajasegar (Graduate Student, University of Illinois at Urbana-Champaign): Optimization of laser diagnostics strategy.
- Brendan McGann (Graduate Student, University of Illinois at Urbana-Champaign): Execution of laser and optical diagnostics at GATech.

Project Overview

The objective of this proposal is to support the advanced laser and optical diagnostics in the referee rig combustor (AFRAL) and area #3 (Advanced Combustion Tests) of the FAA COE ASCENT's combustion program. The diagnostics effort will strive to meet two critical targets. The first is to optimize diagnostics that has enough fidelity to discern the combustion characteristics of candidate jet fuels in their respective testing conditions (support fuel screening). The second goal is to organize and analyze the data in a structured way that allows partners in the combustion program to refine and validate their numerical models. The success of this program will substantially accelerate the efforts of the FAA and the OEMs to certify alternative, fit for purpose fuels.

Task 1 – Optimize and apply laser and optical diagnostics to characterize fuel spray and fluid mechanics in advanced combustor tests at the referee combustor

University of Illinois at Urbana-Champaign

Objective(s)

The objectives in this proposal are to work with AFRL in their referee rig experiments and achieve the following goals:

- Design and set up laser diagnostic and optical diagnostics for referee rig measurements.
- Implement phase Doppler anemometry to determine fuel spray characteristics, including droplet diameters and velocities.
- Implement high-repetition rate Schlieren imaging to examine flow structures.

Research Approach

Diagnostics Optimization and Setup

A 2D PDPA system was used to characterize the fuel droplets during combustion, measuring diameter and two components of velocity. The 2D PDPA (Dantec 112mm fiber PDPA) measures the frequency of the Doppler burst signal to determine velocity (one component from each pair of beam wavelengths) and the phase difference between two Doppler bursts to calculate the droplet diameter. An argon-ion laser (Ion Laser Technology), which produces a continuous laser beam with wavelengths ranging from 457 nm to 514.5 nm, is directed into a transmitter where the beam is split up by wavelength and coupled into optical fibers. Four beams, two at 488 nm and two at 514.5 nm (about 4 mW of power per beam), are focused by a 500mm focal length lens on the PDPA transmitter head and directed into the combustion chamber. The transmitter head and receiver head, with an 800mm focal length lens, are mounted on traverses placed on either side of the combustor. The traverses, fitted with encoders, are linked and controlled via a LabVIEW code. Data is collected using BSA Flow Software, and the data is written to text files.

Milestone(s)

Include a description of any and all milestones reached in this research according to previously indicated timelines.

Milestones from Each Period

Proposed (3 Month): At the 3 month mark, we will conclude the analysis of the experimental setup and should be close to finishing the design of the laser and diagnostics setup.
Achieved: Design of the laser setup was completed and implementation of a PDPA system on a mock referee combustor setup was conducted at the University of Illinois. Preparations to deploy PDPA system were completed.

Proposed (6 Month): At the 6 month mark, we should be finished the droplet characterization testing campaign experimental set out in Task 1 of the proposal.
Achieved: Four-week droplet characterization testing campaign is completed. Initial analysis of the droplet data has been conducted.

Proposed (9 Month): At the 9 month mark, we should have completed initial analysis of the data collected during the test campaign and distributed summary data sets to modeling and other spray teams. Preparations for Schlieren imaging to examine combustor fluid mechanics should be completed.
Achieved: First test run at GATech for simultaneous PLIF and PIV successfully complete and results analyzed. Laser and optical setup successfully implemented and tested. Identified key problems such as fuel PLIF. Main measurement campaign set for last quarter.

Proposed (12 Month): At the 12 month mark, we should have completed the Schlieren imaging test campaign and completed initial analysis of the imaging data.
Achieved: Schlieren imaging completed, and initial analysis of averaged images shows dilution jet bending.

Major Accomplishments

The main accomplishment of year 2 in this project was that we were able to set up and implement PDPA measurements to obtain fuel droplet diameters and velocities in the referee rig in combusting cases. We analyzed and distributed the data to the modeling teams to provide validation information for the fuel spray characteristics.

Fuel Droplet Characterization

Droplet axial and radial velocity distributions, SMD distributions, and data collection rates for the fuels studied are presented. For A-2 at ϕ = 0.096, data collection rate is shown in Figure 1 as a function of y-position at various axial locations. The origin is taken to be the intersection of the centerline of the injector and the downstream face of the heat shield. Positive z-position is taken to be positive downstream (flowing out of the combustor) and y-position is taken to be positive up (towards the top of the combustor). The axes and basic referee rig geometry is shown in Figure 2 for reference. The data rate is a good indicator of where the spray is located and can be used to calculate and report spray angles. The low data collection rate near the centerline verifies that the fuel injection is a hollow cone.

It is unsurprising that the width of each side of the spray increases with increasing distance downstream, and the overall width of the spray increases until it spans nearly the full height of the combustor (109 mm) by 35 mm downstream. At 35 mm downstream, the data collection rates are greatly diminished, which can be explained by further spread of the spray as well as evaporation due to combustion.

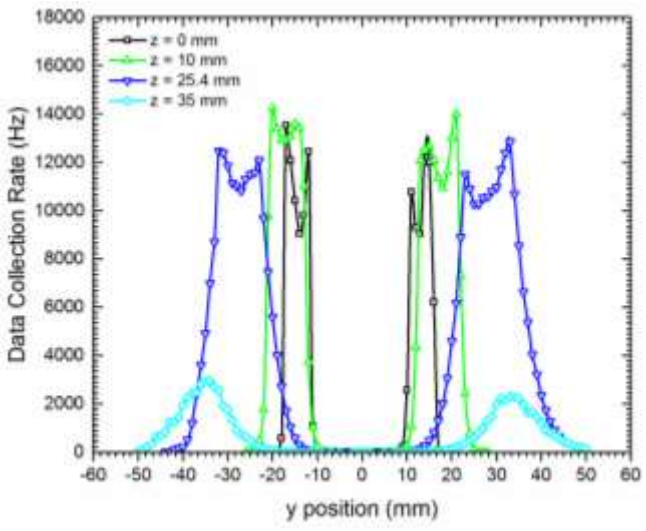

Figure 1. A-2 data collection rate. *Data collection rate versus y-position at various axial locations for A-2 at φ=0.096*

A. Comparison of Fuel Droplet Diameters

SMD is calculated at each position where diameter data is collected, and Figure 3a shows the SMD versus y-position 0 mm, 5 mm, and 10 mm downstream of the deflector plate for each fuel tested. SMDs are only reported at locations where more than 1000 droplets were measured. Figures 3b, 3c, and 3d show normalized histograms of the droplet diameters 10 mm, 15 mm, and 20 mm above the centerline at each axial location shown. The differences in SMD between the fuels are seen in the diameter histograms as a larger fraction of large droplets.

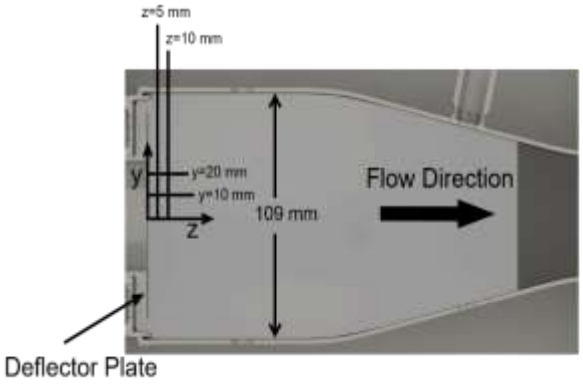

Figure 2. Cutaway of the single cup referee combustor. *The origin is taken to be at the intersection of centerline of the combustor with the front plane of the deflector plate as marked.*

As seen in Figure 3a, just downstream of the deflector plate (z = 0 mm), C-1 has a higher SMD than either A-2 or C-5, between 10 and 35 microns greater at y positions more than 12 mm above the centerline. This can be seen in Figure 3b, as C-1 has relatively few droplets with a diameter less than 20 microns compared with A-2 and C-5 at the same y positions. This seems to indicate that C-1 is either still undergoing fuel droplet breakup or that C-1 experiences less upstream evaporation compared to A-2 and C-5. At 5 mm downstream of the deflector plate, the A-2 and C-5 fuels have very similar SMDs at all measurement points where enough droplets were collected. The maximum difference between the SMDs for those two fuels is about 8 microns, occurring at y = 15 mm. The histograms in Figure 3c and 3d explain this difference;

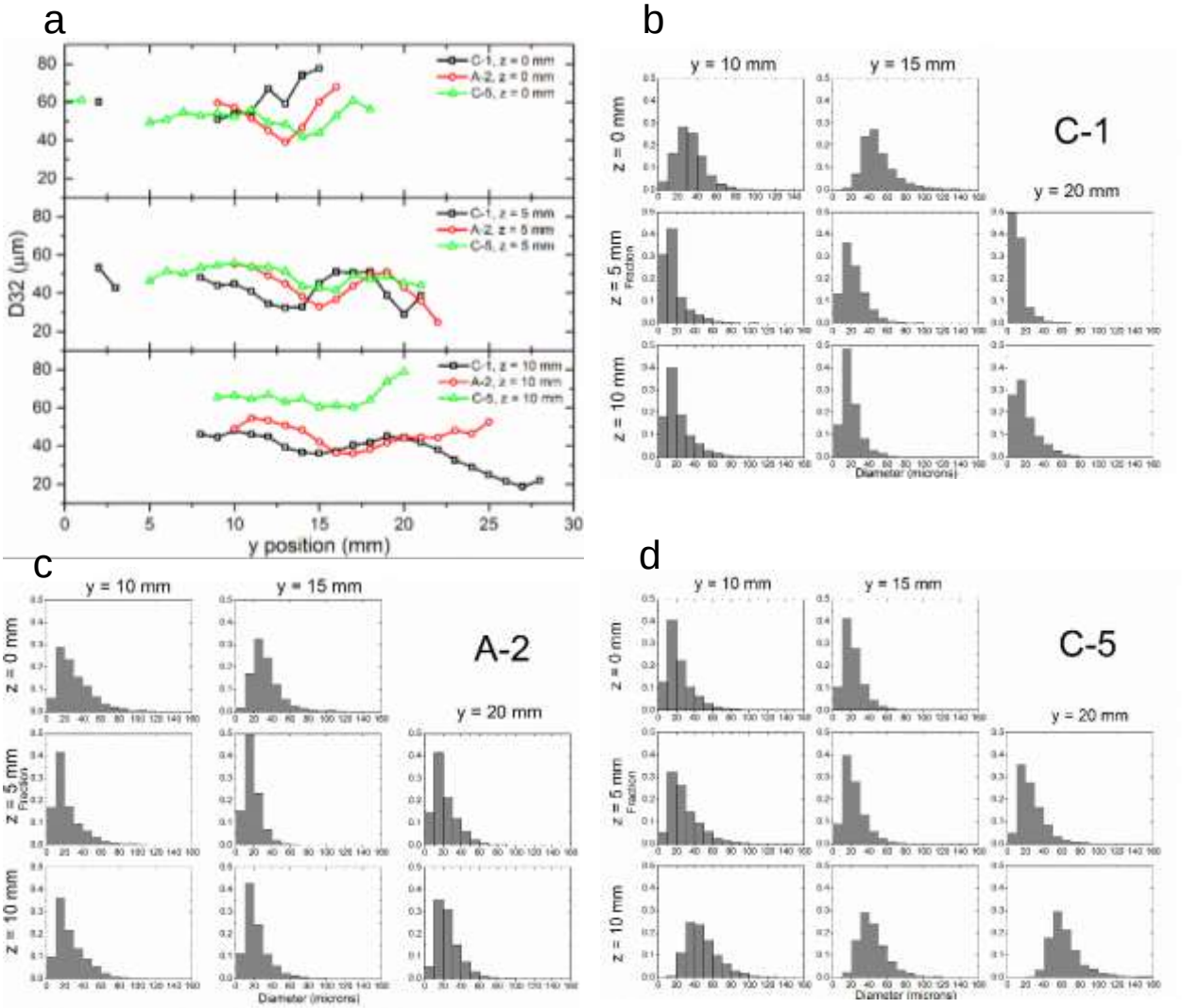

Figure 3. Sauter mean diameter and representative diameter histograms *a) Sauter mean diameter plotted versus y position for each fuel 0 mm, 5 mm, and 10 mm downstream of the deflector plate for comparison with b) C1 diameter histograms, c) A2 diameter histograms and d) C5 diameter histograms at y = 10 mm, 15mm, and 20 mm*

about 65 percent of the A-2 fuel droplets have diameters smaller than 20 microns while less than 50 percent of C-5 fuel droplets have diameters smaller than 20 microns. A-2 also has fewer than 4 percent of droplets with diameters larger than 40 microns while C-5 has about 10 percent of droplets with diameters larger than 40 microns. The C-1 fuel droplets have similar SMDs to A-2 and C-5 at y positions greater than 12 mm above the centerline, but below 12 mm, the SMDs of C-1 are 10 to 15 microns smaller than those of A-2 or C-5. It is also notable that the maximum C-1 SMD has dropped by about 25 microns, bringing it in line with the SMDs of A-2 and C-5.

At 10 mm downstream of the deflector plate, C-1 and A-2 have similar SMD profiles, with a maximum difference of about 11 microns from y = 10 mm up to 22 mm. The profiles diverge at y positions above 22 mm, with the A-2 SMDs increasing slightly, while the C-1 SMDs slowly decrease with increasing y position until it hits a minimum of 20 microns at 27 mm above the combustor centerline. The C-5 fuel droplets at 10 mm downstream of the deflector plate show a marked decrease in the fraction of droplets smaller than 20 microns in diameter as seen in the last row of Figure 3b). Less than 3 percent of C-5 fuel droplets measured 10 mm downstream of the deflector plate (at y = 5, 10, 15 mm) have diameter smaller than 20 microns. At those same locations, at least 40 percent of A-2 and at least 57 percent of C-1 fuel droplets are smaller than 20 microns in diameter. The result of this absence of small C-5 fuel droplets is an SMD that is 12 to 37 microns greater than the corresponding C-1 or A-2 SMD. This indicates that small C-5 fuel droplets have almost completely evaporated between 5 mm and 10 mm downstream of the deflector plate. The small droplets are expected to evaporate first because they have a larger surface area to volume ratio than larger droplets. The evaporation of the small C-5 droplets before those of C-1 and A-2 is consistent with C-5's flat boiling curve (0 to 95 percent distillation between 155˚C and 165˚C) [7]. The C-1 (0 to 95 percent distillation between 175˚C and 246˚C) and A-2 (0 to 95 percent distillation between 160˚C and 255˚C) fuels boil over a much wider range of temperatures[7].

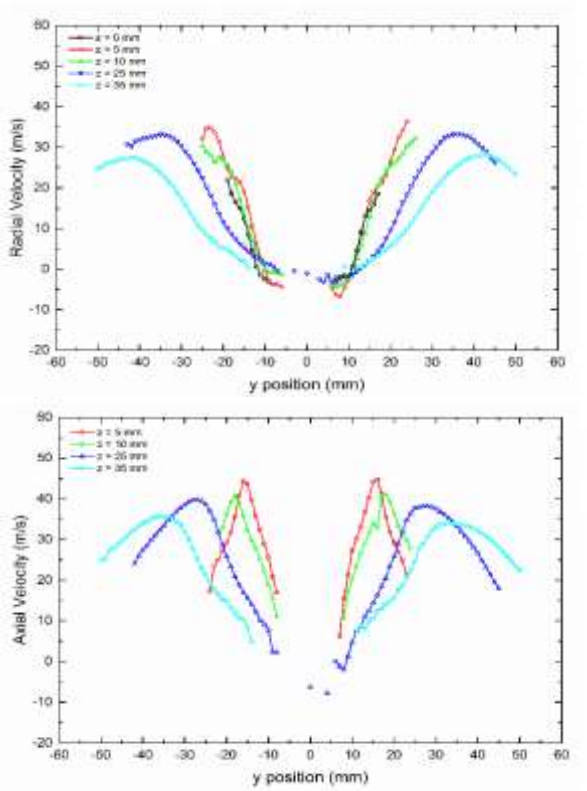

Figure 4. A-2 fuel droplet mean radial and axial velocity. *Mean radial velocity plotted against y position (top) and mean axial velocity plotted against y position (bottom) at various distances from the deflector plate*

B. Droplet Velocities

Figure 4 shows the A-2 fuel droplet mean axial and radial velocity distributions versus y-position at various axial locations. Both the axial and radial velocity distributions are symmetric about the centerline, and the distributions broaden with increasing downstream location. One interesting feature present in both the axial and radial velocity distributions is the near zero or slightly negative velocities along the centerline. This indicates the presence of an inner recirculation zone, but very few droplets are present in the center as indicated by the low data collection rates near the centerline. As seen in Figure 4, the mean radial velocity profiles at 0 mm, 5 mm, and 10 mm downstream of the deflector plate are very similar to each other. At 25 mm and 35 mm downstream of the deflector plate, the radial velocity profiles broaden and the maximum droplet velocities decrease. The axial velocity profiles at 5 mm and 10 mm for A-2 exhibit a sharp peak that roughly corresponds with the center of the spray as marked by the data collection rate. As with the radial velocity, the axial velocity profiles broaden and have a lower maximum value further downstream (25 mm and 35 mm).

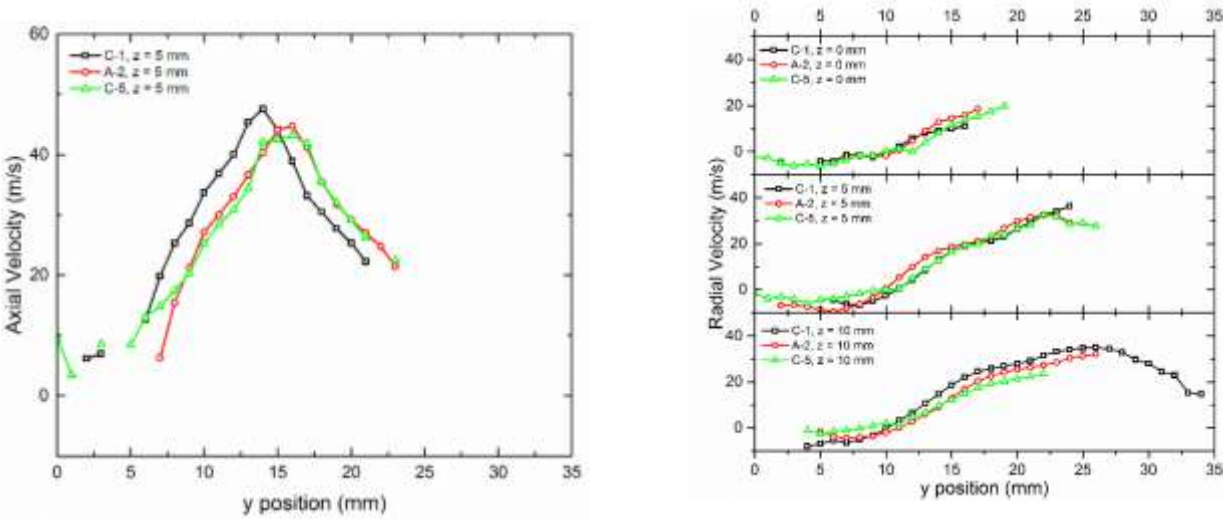

Figure 5. Axial and radial velocity profiles. *a) Axial velocity plotted versus y position for each fuel 5 mm downstream of the deflector plate and b) radial velocity plotted as a function of y position at 0 mm, 5 mm, and 10 mm downstream of the deflector plate for each fuel*

A comparison of fuel droplet radial velocity for the different fuels is shown on the left in Figure 5 at 0 mm, 5 mm, and 10 mm downstream of the deflector plate, and a comparison of fuel droplet axial velocity at 5mm is shown on the right in Figure 5. The radial velocity profiles for each fuel have a great deal of similarity across the fuels at each downstream position shown. Figure 5 also shows the axial velocity profile 5 mm downstream of the deflector plate. The C-1 axial velocity profile is slightly different from C-5 and A-2, reaching its peak about 2 mm inside of the peaks for C-5 and A-2.

Publications
None (in progress to AIAA Sci Tech)

Outreach Efforts
None

Awards
None

Task 2 – Optimize and apply laser and optical diagnostics for application in the advanced ignition tests at Georgia Institute of Technology and Army Research Laboratory
University of Illinois at Urbana-Champaign

Objective(s)
The objectives in this proposal are to work with Georgia Tech in their advanced ignition experiments and achieve the following two goals:
- Evaluate the experimental ignition testing setup and operating conditions for laser and optical diagnostics
- Design and set up laser and optical diagnostics for use in ignition experiments at Georgia Institute of Technology
- Design and construction of high altitude ignition combustor for ARL experiments.

Research Approach
Diagnostics Optimization and Setup on Georgia Tech Atmospheric Ignition Rig

The main goal here is the development of 2D diagnostics using Planar Laser Induced Fluorescence (PLIF), Schlieren, and OH* chemiluminescence to understand the ignition development at the boundaries and flame dynamics in the GATech atmospheric ignition rig. The goal will be to apply simultaneous measurements from high speed PLIF, Schlieren, and chemiluminescence. For each of the imaging sets, we will look to obtain spatially resolved data. We will configure and set up the laser and optical diagnostics equipment around the ignition rig at GATech. For the high speed PLIF measurements, we pumped a high speed dye laser (Credo, Sirah) with a high speed diode pumped Nd:YAG (Edgewave) for generation of the UV light. The PLIF, Schlieren, and chemiluminescence imaging will be 10 kHz. Energy per laser pulse at these conditions may be small (200 μJ/pulse) and light collection from the PLIF will be enhanced using a f/2.8 UV lens.

Design of High Altitude Relight Combustor

The primary goal here is to design and build a combustor that replicates the key geometry and flow features of the referee rig, while allowing three-sided optical access to conduct laser and optical diagnostics. The primary features from the referee rig that have been maintained include: overall combustor interior size, primary dilution jet hole placement, swirler geometry, and injector geometry.

Milestones from Each Period

Proposed (3 Month): At the 3 month mark, we will have identified the key features that are important in the design of the rig. Preliminary designs will have been shared with the OEMs for feedback.
Achieved: Two rounds of preliminary designs have been completed, and key features have been identified.

Proposed (6 Month): At the 6 month mark, we should be have finalized the design and sent the drawings to the machine shop for construction.
Achieved: The designs have been finalized and drawings sent to the machine shop. Materials for the rig have been ordered.

Proposed (9 Month): At the 9 month mark, we should have the main body of the high altitude relight rig constructed and windows for the rig purchased.
Achieved: The main body of the rig has been machined and assembled.

Proposed (12 Month): At the 12 month mark, we should have obtained the swirler and injector and made any modifications to the rig to ensure that they fit into the main body.
Achieved: The swirler and injector have been retrieved from Wright-Patterson Air Force Base. Preparations have been made to transport the rig to ARL.

Major Accomplishments

The main accomplishments of year 2 in this task was that we transported and set up the laser system around the ignition rig at GATech for the execution of simultaneous PLIF, Schlieren, and OH chemiluminescence imaging. The high altitude relight combustor was also completed and has been prepared to ship to ARL. The model and the finished body of the combustor are shown in Figure 6.

Georgia Tech Ignition Experiments

The primary effort on the ignition experiments was transporting the Edgewave Nd:YAG high repetition rate laser to Georgia Tech. The laser was coupled to the Sirah Credo Dye Laser, as shown in Figure 6 (left), and both lasers were tuned to optimize laser power and beam profile. Optics to form and steer the laser sheet in through the top of the combustor, as shown in Figure 6 (right). The primary ignition testing campaign was carried out by Georgia Tech personnel.

Figure 6. *Edgewave pump laser (left) and dye laser with sheet forming optics, and the ignition rig*

High Altitude Relight Combustor

Design and fabrication of a high altitude relight rig, replicating the key geometry and flow features of the referee rig has been completed. The model and completed body of the chamber are shown in Figure 7. Windows, made of UV-grade fused silica, have been ordered to prepare for UV laser and optical diagnostics. A metal 3D printed swirler and a pressure atomizing fuel injector, ones identical to those in the referee rig, were obtained from AFRL to use in the combustor. Construction of the main body of the combustor, as shown in Figure 7, was completed in September, and the swirler/injector combination was obtained from AFRL in November.

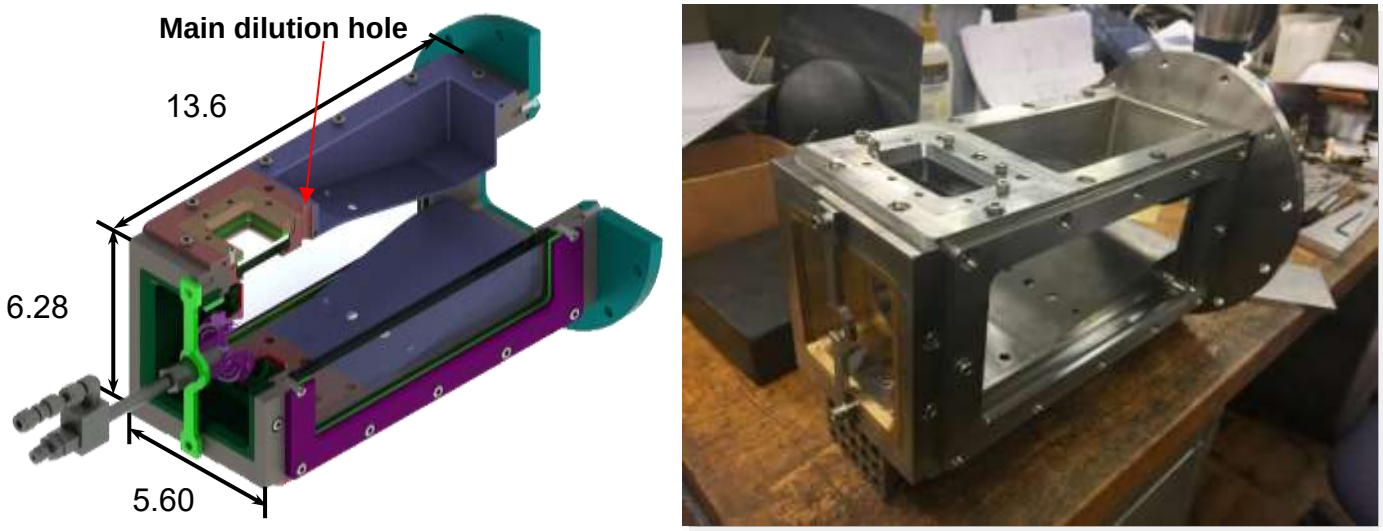

Figure 7. High altitude relight combustor model (left) and completed rig (right). *The high altitude relight combustor replicates the key geometry and flow features of the referee rig, including dilution jet hole placement, overall size, swirler geometry, and injector geometry.*

Publications
None

Outreach Efforts
None

Awards
None

Student Involvement
Three graduate students (listed above) have participated in this project on a rotational basis to address various aspects of the project. Two students executed (Brendan McGann and Eric Mayhew) set up and executed the PDPA measurements outlined in Task 1. Two students (Brendan McGann and Eric Mayhew) made trips to GATech to transport and couple the Edgewave Nd:YAG pump laser to the dye laser for use in the PLIF imaging. In addition, they assisted in the setup of the optics as well as participating in the initial phase of the measurements. The Edgewave as well as other optical and imaging equipment was taken down to GATech for testing. Rajavasanth designed and fabricated the high altitude relight chamber.

Plans for Next Period
In year III of the NJFCP, the main focus of our efforts will be execute high altitude ignition experiments at the Army Research laboratory. The test conditions will be worked out with OEM input and the work will also be coordinated with the ongoing ignition work at GATech. We will continue to support AFRL in any diagnostics efforts required in the referee rig combustor. Looking into the future, we anticipate either PIV or LDV measurements will be required in the referee combustor to measure velocity information. We have already designed the required hardware for this effort and will look for an opportunity to implement them with support from AFRL.

References
none

Project 027(B) National Jet Fuels Combustion Program – Area #3: Advanced Combustion Tests (Year II)

Georgia Institute of Technology
Oregon State University
University of Illinois at Urbana-Champaign

Project Lead Investigator

Tim Lieuwen
Professor
Aerospace Engineering
Georgia Institute of Technology
270 Ferst Drive, G3363 (M/C 0150)
Atlanta, GA 30332-0150
404-894-3041
tim.lieuwen@ae.gatech.edu

University Participants

Georgia Institute of Technology

- P.I.(s):
  - Professor Tim Lieuwen
  - Professor Jerry Seitzman
  - Professor Wenting Sun
- FAA Award Number: 13-C-AJFE-GIT-008
- Period of Performance: 12/1/2015 to 11/30/2016
- Task(s):
  1. Task 1. Blowoff
  2. Task 2. Ignition

Oregon State University

- P.I.(s): David Blunck
- FAA Award Number: 13-C-AJFE-OSU-02
- Period of Performance: 12/1/2015 to 11/30/2016
- Tasks:
  3. Task 3. Turbulent Flame Speed

University of Illinois at Urbana-Champaign

- P.I.(s): Tonghun Lee, Associate Professor
- FAA Award Number: 13-C-AJFE-UI-013
- Period of Performance: 12/1/2015 to 12/31/2017
- Task(s):
  4. Optimize and apply laser diagnostics for application in the Referee Combustor (AFRL).
  5. Optimize and apply laser diagnostics for ignition experiments at Georgia Tech.

Project Funding Level

Georgia Institute of Technology
FAA Funding: $340,000
Cost Share: $340,000 provided by Georgia Institute of Technology

Oregon State University
FAA Funding: $80,000
Cost Share: $80,000 provided by Oregon State University

University of Illinois at Urbana-Champaign
FAA Funding: $120K
Cost Share: In-kind academic time of the PI, cost share contribution from NRC-Canada.

Investigation Team

Tim Lieuwen (Georgia Institute of Technology): Principal Investigator. Professor Lieuwen is the PI overseeing all tasks, and is manager of Task 1. Blowoff
Jerry Seitzman (Georgia Institute of Technology): Co-Principal Investigator. Professor Seitzman is the manager of Task 2. Ignition
David Blunck (Oregon State University): Co-Principal Investigator. Professor Blunck is the manager of Task 3. Turbulent Flame Speed
Fred Dryer: Co-Principal Investigator. Professor Dryer is acting as an expert consultant on alternative jet fuel chemistry
Wenting Sun (Georgia Institute of Technology): Co-Principal Investigator. Professor Sun is acting as an internal expert consultant on kinetic mechanisms
Tonghun Lee (University of Illinois Champaign): Co-Principal Investigator. Professor Lee is the lead diagnostic expert.
Bobby Noble (Georgia Institute of Technology): Research Engineer. Mr. Noble is responsible for designing and maintaining experimental facilities, as well as experimental operations and management & safety of graduates students.
Benjamin Emerson (Georgia Institute of Technology): Research Engineer. Dr. Emerson is responsible for designing and maintaining experimental facilities, as well as experimental operations and management & safety of graduates students. He is also acting as the administrative coordinator for all three tasks.
David Wu (Georgia Institute of Technology): Research Engineer. Mr. Wu is responsible for designing and maintaining experimental facilities, as well as experimental operations and management & safety of graduates students.
Brandon Sforzo (Georgia Institute of Technology): Postdoctoral Fellow. Dr. Sforzo is the lead experimentalist in Task 2. Ignition
Glenda Duncan (Georgia Institute of Technology): Administrative Staff. Mrs. Duncan provides administrative support.
Tiwanna Williams (Georgia Institute of Technology): Administrative Staff. Mrs. Williams provides administrative support.
Seth Hutchins (Georgia Institute of Technology): Lab Coordinator. Mr. Hutchins maintains the core lab facilities and provides technician services.
Machine Shop Staff (Georgia Institute of Technology). The Aerospace Engineering machine shop provides machining services for experimental facility maintenance/construction
Nick Rock (Georgia Institute of Technology): Graduate Student. Mr. Rock is the lead rig operator in Task 1. Blowoff
Ianko Chterev (Georgia Institute of Technology): Graduate Student. Mr. Chterev is the lead diagnostitian in Task 1. Blowoff
Hanna Eck (Georgia Institute of Technology): Graduate Student. Ms. Eck is the lead data analyst in Task 1. Blowoff
Sheng Wei (Georgia Institute of Technology): Graduate Student. Mr. Wei is a research assistant under Task 2. Ignition
Aaron Fillo (Oregon State University): Graduate Student. Mr. Fillo was the lead grad experimentalist in Task 3. Turbulent Flame Speed
Jonathan Bonebrake (Oregon State University): Graduate Student. Mr. Bonebrake is the lead grad experimentalist in Task 3. Turbulent Flame Speed
Eric Mayhew (Graduate Student, University of Illinois at Urbana-Champaign): Execution of laser and optical diagnostics at ARFL.
Rajavasanth Rajasegar (Graduate Student, University of Illinois at Urbana-Champaign): Optimization of laser diagnostics strategy.
Brendan McGann (Graduate Student, University of Illinois at Urbana-Champaign): Execution of laser and optical diagnostics at GATech.

Project Overview

The objective of this activity is to provide advanced combustion testing support to the FAA's alternative jet fuels program. We are performing advanced combustion testing to accomplish two goals. The first goal is to screen candidate jet fuels for sensitivities of their burning properties to fuel physical and chemical properties. The second goal is to provide empirical data to combustion modeling partners to facilitate the refinement and validation of their models, which aim to develop predictive capability for fuel composition sensitivities. The success of this program will substantially accelerate the efforts of the FAA and the OEMs to certify alternative, fit for purpose fuels.

In the second year of the program, we repeated testing of A1, A2, A3, C1, C2, C3, C4, C5, and n-dodecane fuels. Additionally, we tested blends of A2/C1 and A2/C5, and two surrogate fuels known as S1 and S2. For this second year, we had proposed three tasks that address the most critical challenges associated with advanced combustion model development and differentiating differences in fuel chemistries:

(1) Task 1: flame stabilization, extinction, and blowoff in high shear flows
(2) Task 2: forced ignition
(3) Task 3: turbulent flame speed

As detailed in their respective sections, these tasks have been developed toward supporting the overall program goals culminating in referee rig capabilities, as well as acquiring data to differentiate potentially subtle fuel effects that can be used for model validation. Each task has a strong focus on supporting model development and evaluating fuels, and a strong connection to understanding engine operational limits. They were designed toward addressing critical gaps associated with both objectives of the larger program, namely an improved combustor rig evaluation process for ASTM D4054 and validated models for combustor evaluation. This second year extended the first year's work with repeatability datasets, datasets at new conditions, new detailed data to support modeling teams, and improved physical understanding.

Advanced combustion tests, which couple chemical kinetic processes with complex fluid mechanic and/or atomization/evaporation processes, are a critical link in the path from fundamental knowledge to prediction of how fuel composition impacts engine operation. The investigators and the consultant have extensive experience in this field, including developing surrogate mixtures for Jet-A, characterizing changes in pollutants when alternative and conventional jet fuels are burned, and having successfully completed and transitioned similar approaches for synthesis gas fuels and for natural gas fuels.

From a diagnostics standpoint, the objective of this work is to support the advanced laser and optical diagnostics in the referee rig combustor (AFRAL) and area #3 (Advanced Combustion Tests) of the FAA COE ASCENT's combustion program. The diagnostics effort will strive to meet two critical targets. The first is to optimize diagnostics that has enough fidelity to discern the combustion characteristics of candidate jet fuels in their respective testing conditions (support fuel screening). The second goal is to organize and analyze the data in a structured way that allows partners in the combustion program to refine and validate their numerical models. The success of this program will substantially accelerate the efforts of the FAA and the OEMs to certify alternative, fit for purpose fuels.

Task 1. Blowoff

Georgia Institute of Technology

Objective(s)

The objectives of this task were to measure detailed operational data near the blowoff limits of a swirl combustor that mimics OEM hardware. The proposed combustor, used in year 1 of this program, was a swirl-stabilized spray combustor, which was configured similarly to the referee rig, but without dome cooling and liner-cooling flows. The benefits of this task were threefold. The first benefit of this task was the measurement of detailed boundary conditions and validation data that are critical to a successful modeling effort. These measurements were selected collaboratively with our modeling partner at United Technologies Research Corp (UTRC), in order to support their refinement and validation cycle. The second benefit of this task was exploratory refinement of detailed diagnostics and best practices. The third benefit of this task was the capability to rapidly measure a wealth of screening data, in order to extend the existing datasets to new conditions, and also to obtain repeatability data.

Research Approach

The research approach consisted of four major activities: collaborative selection of test conditions, screening data acquisition, detailed data acquisition, and data analysis. The selection of test conditions was conducted collaboratively

within a blowout subcommittee. The subcommittee converged on a test plan consisting of screening fuels at a pressure of 2 atmospheres, and three different preheat temperatures: 300 K, 450 K, and 600 K. The screening was to be performed on as many fuels as possible from year 1, as well as three blends of A2/C1 and two new surrogate fuels known as S1 and S2. The detailed diagnostic tests were to be conducted at 300 K of preheat and 2 atmospheres of pressure. These measurements were to obtain spatio-temporally resolved velocity fields, liquid fuel maps, and [OH] maps, with all three of these measurements synchronized together. These measurements were to be obtained for the A2, C1, and C5 fuels. Additionally, efforts would be made to capture a blowout event with the A2 fuel with as much of these high speed diagnostics as possible. For year 2 of task 1, the detailed diagnostics would be supported by AFRL and Spectral Energies, LLC.

The data analysis task operated on both the screening data and the detailed diagnostic data. Analysis of the screening data was conducted to assess repeatability and to correlate fuel performance trends with various fuel properties. The labor-intensive analysis of the detailed data converted the raw data into meaningful velocity fields, fuel maps, and [OH] maps, and delivered these data to UTRC for support and validation of computational models. Much of this analysis has been performed during the second year, and further analysis is proposed for year 3.

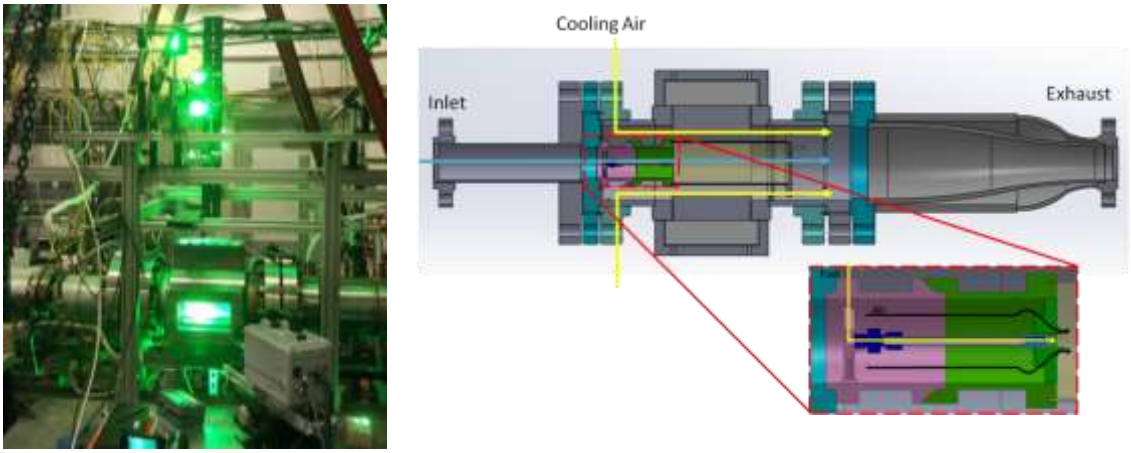

Figure 1. High shear swirl combustor, showing a) pressure vessel instrumented for high speed stereo PIV and OH PLIF, and b) a cross section with generic swirler holder/injector for illustrative purposes

Milestone(s)

1. **Measurements of inflow and boundary conditions.** This has been completed for all planned case and has been delivered to the modeling partners upon request.
2. **Measurement of lean blowout equivalence ratio, mapped over full screening test matrix (screening data).** This has been completed for all planned cases and has been disseminated to the community via the KSN.
3. **Summary of best diagnostic practices.** This has been completed and is being disseminated to the community through a series of publications.
4. **Final data analysis.** This has been completed to the extent that it was planned for year 2. The results have been transmitted directly to modeling groups as needed, and key findings have been disseminated to the community via the KSN and publications. Further analysis is in progress and will continue in year 3.

Major Accomplishments

1. To date, we have built a screening dataset consisting of several thousand blowoff measurements.
2. By building on the technique that we developed in year 1, we have obtained first of its kind quality detailed diagnostic combustion system measurements (see examples in Figure 2 and Figure 3).
3. We have delivered important boundary condition data to the modeling group at UTRC, and we have also delivered data that they have used to demonstrate an impressive level of validation.

4. We have demonstrated that blowoff tends to correlate with physical properties of the fuel at low temperatures and with poor atomization quality, and that it tends to correlate with other properties (e.g. chemical properties) at higher temperatures and with better atomization, which has been a key hypothesis since the start of the program. Some sample correlations are shown in Figure 2.

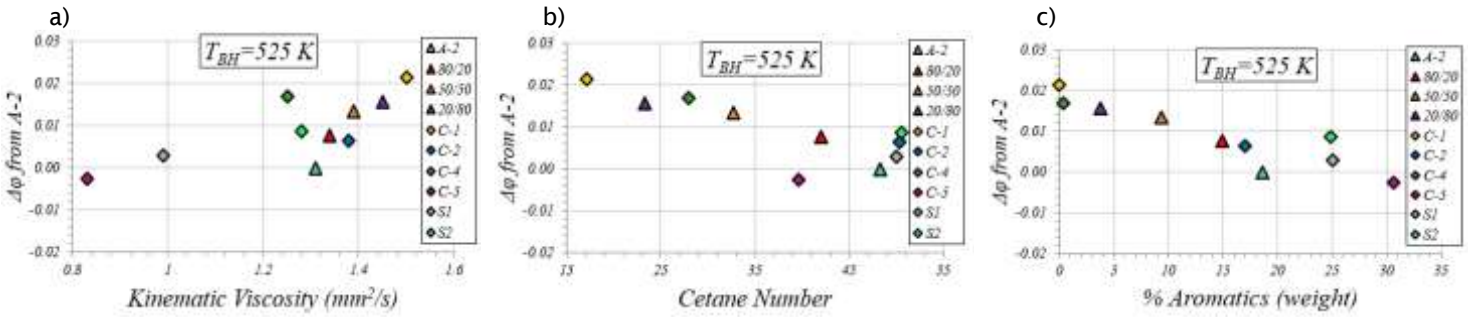

Figure 2. Sample of year 2 screening data at 450 K preheat, 2 atm pressure, showing correlation to a) kinematic viscosity, b) cetane number, and c) % aromatics

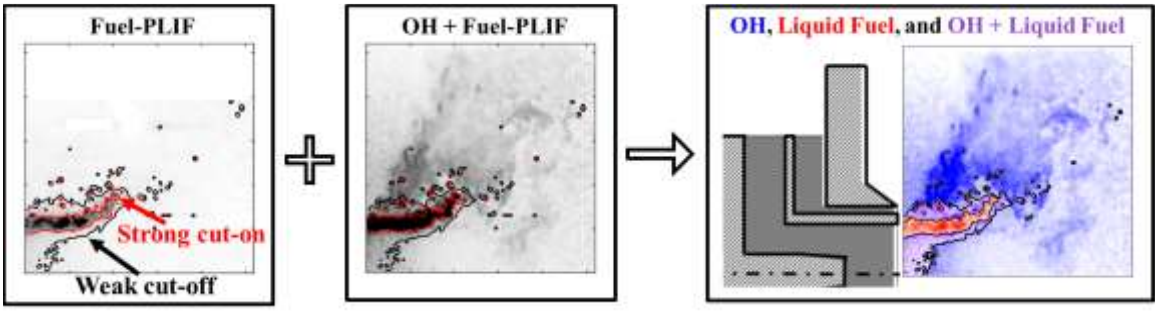

Figure 3. Sample of detailed diagnostic data, showing improved data quality since the first year and new analysis techniques.

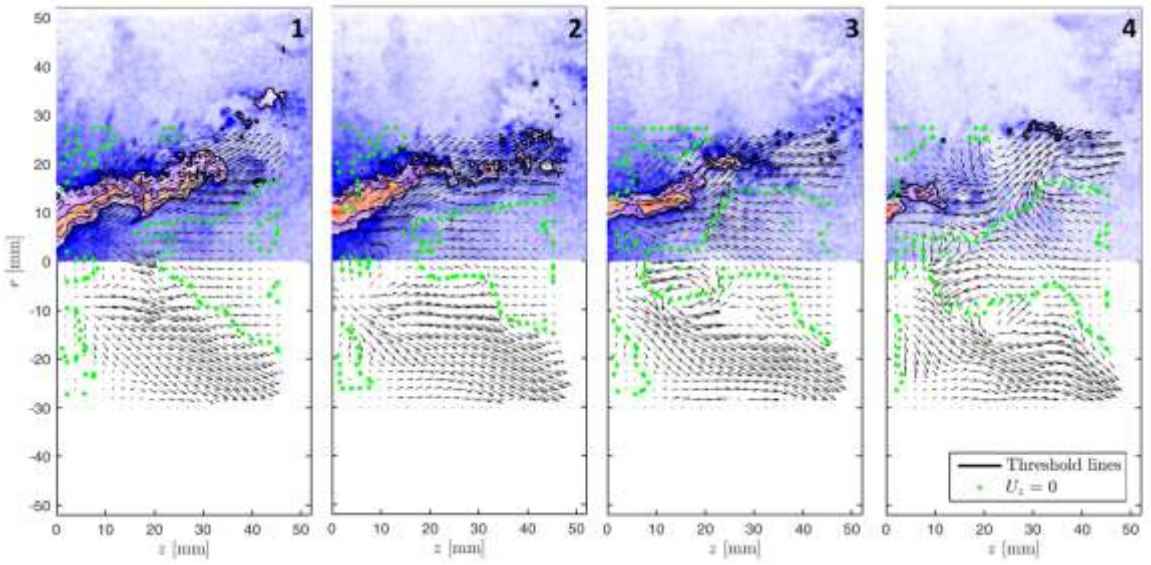

Figure 4. Film-strip of processed detailed diagnostic data, showing OH-PLIF (blue), fuel-PLIF (red), mixture of fuel and OH (purple), and in-plane velocity field (black). Green line indicates contour of zero in/out of plane velocity.

Publications

Rock, N., Chterev, I., Smith, T., Ek, H., Emerson, B., Noble, D., Seitzman, J. and Lieuwen, T., 2016, June. Reacting Pressurized Spray Combustor Dynamics: Part 1—Fuel Sensitivities and Blowoff Characterization. In *ASME Turbo Expo 2016: Turbomachinery Technical Conference and Exposition* (pp. V04AT04A021-V04AT04A021). American Society of Mechanical Engineers.

Chterev, I., Rock, N., Ek, H., Smith, T., Emerson, B., Noble, D.R., Mayhew, E., Lee, T., Jiang, N., Roy, S. and Seitzman, J.M., 2016, June. Reacting Pressurized Spray Combustor Dynamics: Part 2—High Speed Planar Measurements. In *ASME Turbo Expo 2016: Turbomachinery Technical Conference and Exposition* (pp. V04AT04A020-V04AT04A020). American Society of Mechanical Engineers.

Outreach Efforts

We are preparing to present a paper at the 2017 AIAA SciTech conference, we are writing a paper for the 2017 ASME Turbo Expo.

Awards

The ASCENT community nominated Nick Rock for the DOT student of the year award, which is currently awaiting judgement.

Student Involvement

- Nick Rock has been actively involved in the Task 1 experimental effort for both years. Nick was the PhD student responsible for operating the experimental facility. He led the screening measurements and operated the facility for the detailed diagnostic efforts, and has also performed the analysis of the screening data.
- Ianko Chterev was also actively involved in both years of the Task 1 experimental effort. His primary responsibility was the design of experimental procedures and support of detailed diagnostic measurements.
- Hanna Eck was involved in the Task 1 effort as a data analysist. Hanna has been responsible for processing and analyzing the large volume of detailed data produced by the PIV, PLIF, and Mie scattering measurements.

Plans for Next Period

The work plan for the third year will reflect progress from the first two years. The work plan begins with detailed analysis of the PIV, spray, and OH PLIF data acquired in year 2, using the lessons learned during year 2 analysis of the year 1 data. This will elucidate the detailed physics that require the intersection of long analysis time (since this activity has begun in year 2) and high quality (i.e. year 2) data. While this type of analysis has been out of the focus of the first two years, it will be critical at the close of the program as the modeling groups try to determine if the dominant physics of their simulations are matching the dominant physics in the rig (such insight serves beyond the end of the program too, as success of the program will launch a train of modeling activity amongst OEMs). Additionally, the year 3 data analysis will incorporate basic processing of the year 3 datasets to produce velocity vector fields and [OH] fields and transmit these to the modelers. The plan will also execute additional detailed diagnostic campaigns, to be designed in close collaboration with Tonghun Lee, UTRC, Area 4, and OEMs. Finally, the work plan will include additional screening as needed by the program. Screening conditions will be selected from program-wide collaboration, particularly with the OEMs, Area 1, AFRL, and Area 6. Collaboration with Area 6 will ensure overlap at one or more nominal pressure and temperature conditions (as in year 1), while leveraging their sub-atmospheric/low temperature capability and our high pressure/high temperature capability to search for coupled fuel/pressure/temperature trends. For example, between the two teams, we can perform screening over a broad range of pressures to confidently answer the question: "How does pressure couple with fuel composition to influence flame shape and blowoff?" While the key figure of merit and primary focus of this task is blowoff, the detailed diagnostics will help complement the blowoff work by studying fuel effects on flame shape over a range of pressures, as flame shape has important influences on combustor operational characteristics. This type of flame shape screening has only recently become a possibility with the year 2 discovery of a new flame shape at higher preheat temperatures.

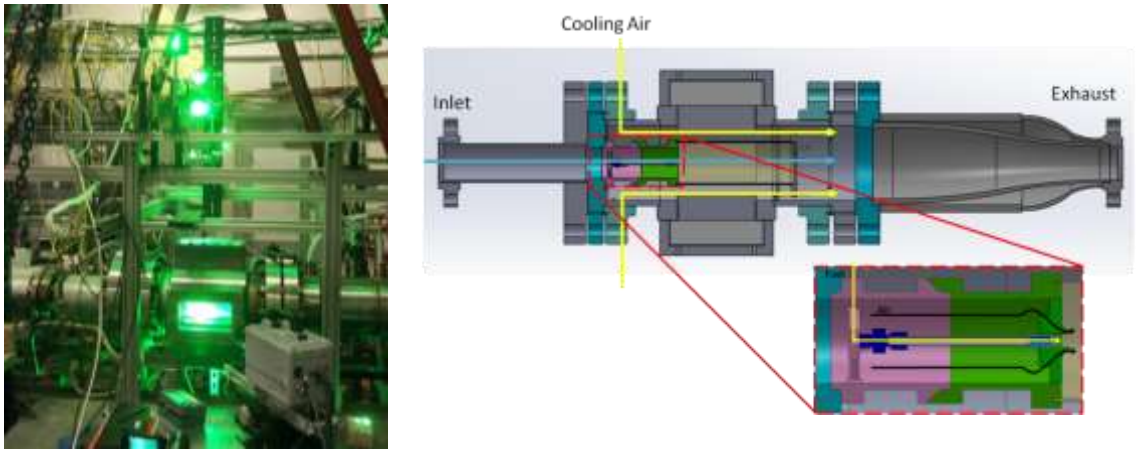

Figure 5. High shear swirl combustor, showing a) pressure vessel instrumented for high speed stereo PIV and OH PLIF, and b) a cross section with generic swirler holder/injector for illustrative purposes

Task 2. Ignition

Georgia Institute of Technology

Objective(s)

This task has two objectives. These objectives focus on the ignition figure of merit in an atmospheric pressure, preheated, pre-vaporized, liquid fueled rig. The rig simulates the ignition environment of an aircraft combustor by implementing an OEM igniter and by establishing an air film flow that separates the igniter from the flammable mixture. The first objective is to measure and demonstrate the sensitivity of the ignition probability to fuel composition, for a range of conventional jet fuels as well as fuels with varying physical and kinetic properties. The second objective is to measure

detailed data that could be used by modelers in subsequent years of the program. A third, tangential objective of this task is to elucidate the fundamental physics that drive the observed fuel sensitivities.

Research Approach

The second year of the ignition task has been divided into three focus areas: screening studies for ignition of prevaporized fuels, reduced-order modeling of prevaporized ignition to examine fuel effects, and development of expanded capabilities for ignititon of two-phase (non-prevaporized) flow. The prevaporized experiments focused on ignition probability measurements of the down selected fuels: A-2, C-1, and C-5, and blends of these three parent fuels. These prevaporized experiments entail preheating of the test facility with 480K air flow and prevaporizing fuel into a 470K carrier air stream that is then injected into upper (fueled) flow of the stratified facility.

The goal of these experiments continues to be evaluation of fuel chemistry influence on the forced ignition process in a realistic non-premixed configuration, with the additional question in year two of the effect of fuel blending compared to neat fuels. The first tests in year 2 examined the neat fuels, looking at repeatability – including comparisons to results from year 1. Example results show good day-to-day repeatability (Figure 6a), and contain the previously observed trend of increasing ignition probability with increasing equivalence ratio. However, the magnitude of the ignition probability for all the fuels is lower than the results found in year 1 (Figure 6b). Because the relative ignition probability of the C3 and C1 fuels is nearly the same for both data sets (~3 at an equivalence ratio of 0.76), the hypothesis for this difference is either aging of the igniter or changes in the fuel distribution and uniformity within the flow; these possibilities are currently being examined. Preliminary results from the fuel blends have been acquired, and additional data will be acquired.

Numerical efforts have also continued for gaseous phase simulations to develop a reduced-order model for the entraining kernel. Ignition development simulations were conducted using chemical mechanisms developed and provided by Area 2 (Stanford). Ignition kernel evolution with A-2 fuel chemistry compared to C-1 chemistry has shown contradictory trends to experimental ranking of the ignition probability performance. Up to this point, Area 2 chemistry models have been validated by experimental autoignition results provided by Area 1. The important chemical pathways involved in these autoignition experiments may differ from forced ignition, and could be the cause of some evolutionary characteristic. Specifically, flame chemistry in forced ignition occurs at much hotter temperatures (>4000K) and at leaner conditions than those tested in the autoignition experiments. This has led to discussion with Area 2 on the development of the chemical models and what modificaitons may need to be implemented for forced ignition modeling.

Finally in year 2, we have designed, fabricated and made preliminary tests of a liquid spray modification to the facility, and designed a fuel chilling system to achieve fuel temperature down to approximately -30°C. The fuel is cooled by passing it through a simple immersion heat exchanger placed in a phase change bath to provide temperature control and an expendable heat sink. The heat transfer bath fluid is a propylene-glycol solution, with a freezing point tuned to achieve the desired liquid fuel temperature, and the bath is cooled by a replaceable dry ice pack.

Adaptation of the numerical model (Figure 8a) to incorporate two phase physics is also part of the effort in year two. The gaseous reactor model relies on a perfectly stirred reactor set of physics, coupled with an air plasma chemical mechanism for the initial unfueled reactions and the appropriate fuel chemical mechanism for the kernel-fuel interaction. The addition of a new liquid droplet sub-model (Figure 8b) to the reactor network serves as the gaseous fuel source term. Additionally, the evaporation of the fuel transfers thermal energy away from the kernel. This work continues to be developed and will lead to simulations that incorporate the different chemical mechanisms provided by Area 2 and the physical fuel properties supplied by the program.

Milestone(s)

- **Rig modification completion.** This milestone was completed early in the year when we began testing liquid sprays.
- **Post-process year 2 detailed data.** This has been completed.
- **Ignition measurement data.** This has been completed for several fuels, and is under way for additional fuels that the program has asked us to test.
- **Final data analysis.** This is underway as new data become available.
- **Final data archiving.** Data are uploaded to the KSN as they become available and are processed.

Major Accomplishments

This task has produced three major accomplishments, which are detailed here.

- The first major accomplishment is extension of the fuel screening ignition dataset. This extension includes repeatability data (see example in Figure 6) as well as new tests with liquid spray.

- High speed OH PLIF imaging (see example sequence in Figure 7) has been performed to help visualize the time-resolved physics of the evolving ignition kernel and eventual propagating flame front.
- The reduced order ignition model has been further developed (shown in Figure 8), and has helped inform the chemical kinetics modeling team as well as elucidate some of the fuel sensitivities observed in ignition.

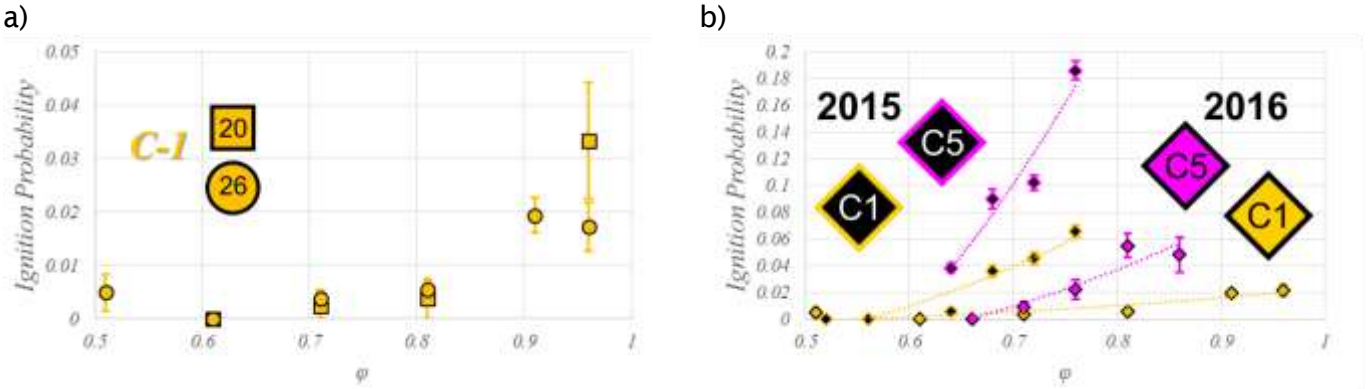

Figure 6. Example of repeatability results for forced ignition testing of igntion, showing a) day-to-day repeatability for current tests (numbers correspond to the day of the month they were taken), and b) repeatability check between 2015 and 2016 data

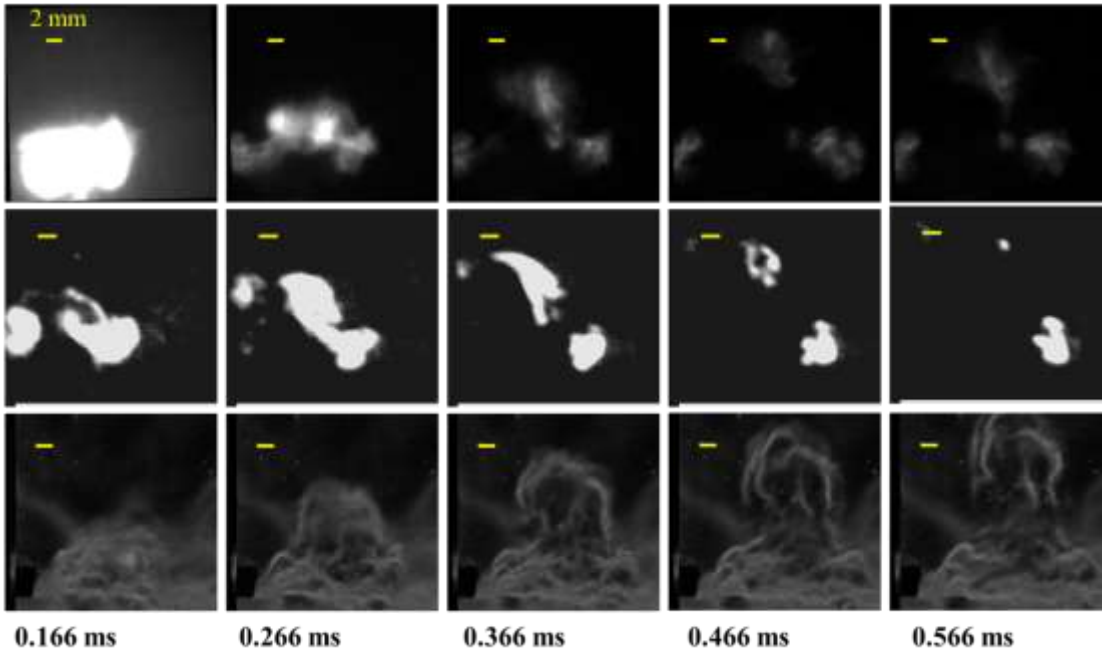

Figure 7. Top row) emission imaging, middle row) OH PLIF imaging, bottom row) Shclieren imaging of an evolving ignition kernel.

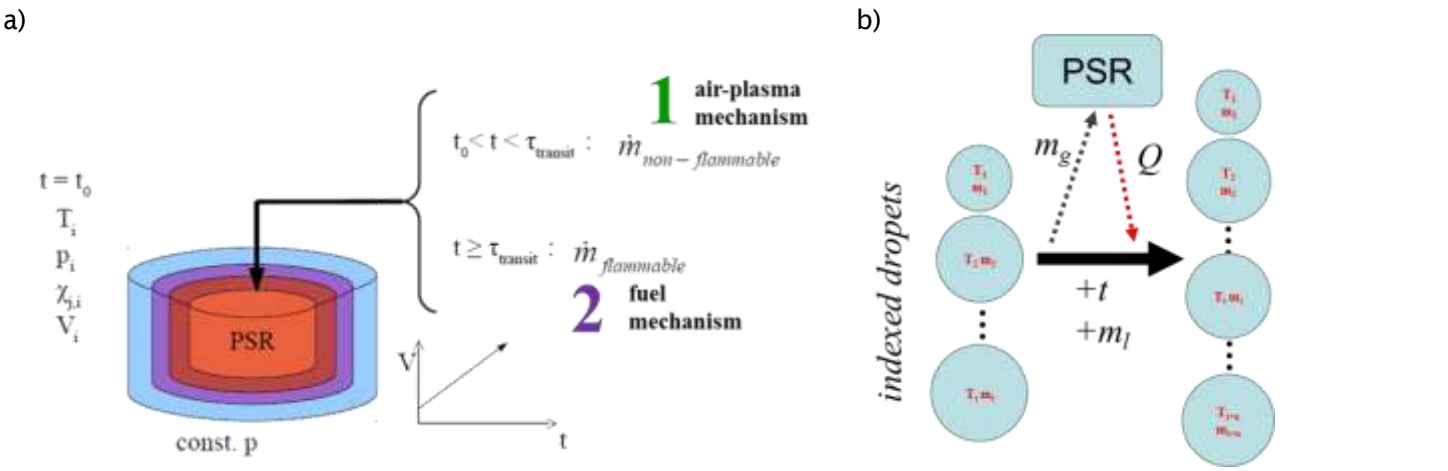

Figure 8. Reduced order ignition model development, showing a) the conceptual model, comprised of a perfectly stirred reactor growing in volume at constant pressure as mass is added, operating on a 1-air plasma chemical mechanism and then 2-a fuel mechanism, and c) the droplet evaporation sub-model which will include two-phase physics into the numerical scheme.

Publications

Sforzo, B., Dao, H., Wei, S. and Seitzman, J., 2017. Liquid Fuel Composition Effects on Forced, Nonpremixed Ignition. *Journal of Engineering for Gas Turbines and Power*, *139*(3), p.031509.

Outreach Efforts

We presented a poster at the UTSR workshop, and we are writing one conference paper to be presented at the ASME Turbo Expo 2017 conference.

Awards

None

Student Involvement

- Hong Dao was actively involved in the Task 2 experimental effort, prior to graduating in May 2015. Hoang was the student responsible for adapting the ignition facility for vaporized jet fuel and collecting ignition probability measurements.
- Sheng Wei has been actively involved in the Task 2 detailed diagnostic effort. Sheng supported the ignition probability measurement collection and was the primary student responsible in collecting schlieren and chemiliuminescence data. Sheng is also the lead student involved in modeling efforts.
- Edwin Goh has been actively involved in the Task 2 modeling efforts. Edwin has been responsible for adapting the model code to accommodate the jet fuel mechanisms and has collected and analyzed the majority of sensitivity studies
- Hee Yong "Bill" Jeon has been involved in the Task 2 modeling effort. Bill has supported the execution of many simulations for sensitivity studies and aided in reduction of the resulting data.

Plans for Next Period

The objectives of this task are threefold. First, the ignition task aims to measure the spark ignition probability of various fuels under experimentally repeatable, engine-relevant, and readily modellable conditions. Secondly, this task will provide detailed data that can help elucidate the physical mechanisms behind (successful) forced ignition. Thirdly, this task aims to continue the past two years of ignition model development (see Figure 8) which offers an additional capability

that can predict fuel sensitivities; this objective is closely coupled to detailed experimental measurements. The benefits of this task are: it can quickly determine the forced ignition response over a wide range of conditions and fuels; it can clearly demonstrate fuel sensitivities; it provides feedback to Areas 1 and 2 to enhance the development of relevant jet fuel chemical kinetic mechanisms; and it provides controlled measurements in a facility amenable to modelling.

1.1.1.1 Analysis of detailed diagnostics on pre-vaporized ignition data and 2-phase (year 2) data, including 2-phase model comparisons

Similar to the blowoff task, the ignition task has gathered large quantities (several terabytes) of experimental data in year 1 and 2 with additional measurements planned for the remainder of year 2. Specifically, detailed diagnostics campaigns conducted during year 2 obtained high speed OH PLIF, chemiluminescence, and schlieren measurements which provide vast information about the spatial and temporal evolution of flame chemistry initiation with respect to the ignition kernel. As improved or additional chemical kinetics models become available from Area 2, the experimental results will also be compared to the results of the reduced order modeling to provide evaluation of the mechanisms' ability to capture fuel effects. In addition, this data base will allow OEM's to pursue ignition modeling even beyond the scope of this program.

1.1.1.2 Continuation of detailed measurements of liquid spray ignition and detailed characterization at targeted conditions

Two-phase screening measurements have been conducted during Q4 of year 2. The ignition probability measurements from these experiments will help differentiate the ignition performance sensitivity to physical fuel effects versus fuel chemistry effects. This information will help modelers incorporate the appropriate influences on forced ignition prediction. Furthermore, comparisons between two-phase experiments and results from the two-phase reduced-order model will help elucidate these effects. The year 3 measurements will include low temperature fuel studies using the liquid chilling device developed in year 2. These measurements are important to provide a reference for some of the detrimental effects associated with cold starts and high altitude relight. In addition, year 3 will include detailed diagnostics of the liquid spray ignition events at select conditions. This characterization is important to (future) CFD simulations in order to match boundary conditions to the properties in the combustor for these cold liquid experiments.

1.1.1.3 Liquid spray ignition model comparisons

Similar to the prevaporized work, the spray ignition results will be compared to the results of the reduced order model to provide evaluation of the mechanisms' ability to capture fuel effects and to better understand the effect of fuel physical properties on ignition success. If successful, this reduced order model may be incorporated (possibly as a post-processing option) into OEM CFD models.

1.1.1.4 Fuel aging effects and performance retention screening

Nominally identical fuels delivered in years 1 and 2 will be retested to study of the effects of fuel aging . There have been recommendations that the jet fuel is compositionally stable under ideal storage conditions, though degradation of fuels may be highly dependent on the base compositions of those fuels. Characterizing the performance retention of these fuels can be an important deciding factor if the fuel composition is highly influential.

1.1.1.5 Screening of any new/additional fuels or blends of interest

Just like for the blowoff task, fuel screening is anticipated to be a lower priority activity in the third year than in the first two years. However, the ignition team will accommodate additional screening at new conditions, with new fuels, or at repeat conditions as needed by the program. One likely source for additional screening needs that may arise during year 3 is the fuel-X endeavor. This endeavor may require a larger database of ignition probabilities for fuel blends, in order to test the robustness of (or potentially refine) the blending rules developed during year 2.

Citations

[4] Rosfjord, T., and Cohen, J., 1990, "Air and Spray Patterns Produced by Gas Turbine High-Shear Nozzle/Swirler Assemblies," AIAA 90-0465.

[5] Li, X., Soteriou, M. C., Kim, W., and Cohen, J. M., 2014, "High Fidelity Simulation of the Spray Generated by a Realistic Swirling Flow Injector," Journal of Engineering for Gas Turbines and Power.
[6] Sforzo, B., Kim, J., Jagoda, J., and Seitzman, J., 2014a, "Ignition Probability in a Stratified Turbulent Flow with a Sunken Fire Igniter," GT2014-26667, Proceedings of the ASME/IGTI Turbo Expo.
[7] Chen, Z., and Ju, Y., 2007, "Theoretical Analysis of the Evolution from Ignition Kernel to Flame Ball and Planar Flame," Combustion Theory and Modeling, 11, pp. 427-453.

Task 3. Turbulent Flame Speed

Oregon State University

Objective(s)

This task has three objectives. The first objective is to measure and identify the sensitivity of the turbulent flame speed to fuel composition, for a range of conventional and jet-like fuels at both atmospheric and subatmospheric conditions. The second objective is to build a database of turbulent flame speeds for pre-vaporized jet fuels. A third, tangential objective of this task is to elucidate the fundamental physics that control the observed fuel sensitivities.

Research Approach

Methodology

Turbulent flames are generated using a vaporizer and burner based on designs developed by the Air Force Research Lab and Lieuwen and colleagues. The experimental setup consists of fuel and air metering systems that deliver jet fuel and air to the burner. Fuel is vaporized using a series of heaters, and elevated to a temperature near 200 ºC. The air/fuel mixture is flowed through an adjustable turbulent generator which generates turbulent fluctuations ranging from 10 to 20% of the bulk flow velocity. Turbulence intensity (TI) is independent of bulk flow velocity. A premixed methane pilot flame is used for ignition and to stabilize the Bunsen burner flame.

Data is collected for each jet fuel variant (A2, C1 and C5) over 5,000 ≤ Re ≤ 10,000, 0.75 ≤ Φ ≤1.0, and 10% ≤ TI ≤ 20%. Measurements are taken using a 16-bit intensified charge-coupled device (ICCD) camera with a 1024 x 1024 pixel resolution and a 25 mm, f/4.0, UV camera lens. For each flow condition (Re, Φ, TI), data is collected over a 3 minute period at 2 Hz.

Measurements of turbulent flame speeds at subatmospheric conditions have been enabled by designing and building a pressure vessel with a vacuums system. Figure 12 shows a picture of a representative flame burning in the vessel at subatmospheric conditions. The vessel can currently operate down to 0.6 atm, although lower pressures are anticipated in the future.

Data Analysis

Image processing to determine the average flame sheet from the measurements was completed using the technique developed by Venkateswaran et al. and is summarized here. The line-of-sight images are time-averaged, the background is subtracted, and the image is cropped to include only the flame. The image is then checked for axis-symmetry, straightened, and filtered using a 2-D median filter with a kernel less than 2% of the burner diameter, as seen in Figure 9 (b) and (c). A 3 point Abel deconvolution is applied and the resulting axial distribution of the centerline intensity is fit to a Gaussian curve. The maximum intensity location is determined. This allows the leading edge of the time averaged flame-brush to be determined. This point is the most probable location of the flame brush, and is defined as the $\langle c \rangle = 0.5$ progress variable contour and corresponds to the location of maximum intensity, see Figure 9 (d). The estimated uncertainty in this process is 1%-2% [1].

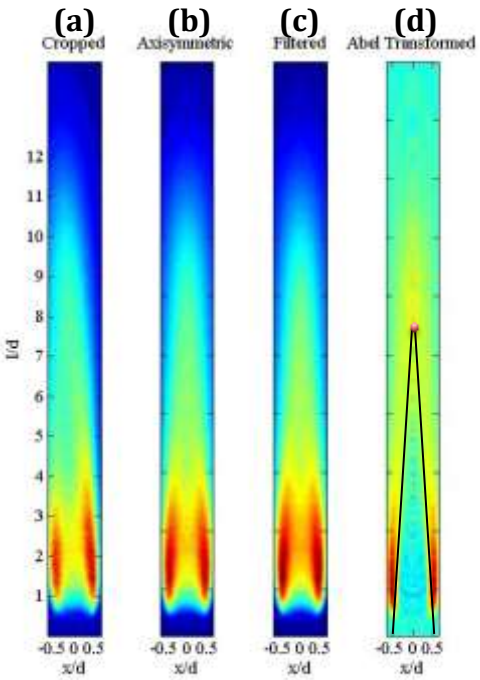

Figure 9. Step-by-step summary of image processing approach:(a) time-averaged, background subtracted and cropped (b) Axisymmetric (c) 2-D median filtered (d) Abel transform with ⟨c⟩=0.5 contour drawn.

Milestone(s)

- Pressure vessel and vacuum system designed and built to enable testing at subatmospheric conditions.
- Measurements of turbulent flame speeds at subatmospheric conditions.

Major Accomplishments

This task has produced two major accomplishments, which are detailed here.

- Additional turbulent flame (consumption) speeds have been measured at atmospheric conditions, with detailed measurements collected for three fuels at varying Reynolds numbers, equivalence ratios, and turbulence conditions. These are some of the only such data in the world reported for these types of fuels. Figure 10 shows representative data at two turbulence conditions. The legend for the data shown in Figure 10 is reported in Figure 11.
- A pressure vessel and vacuum system have been designed, built, and evaluated for operating the Bunsen burner at subatmospheric conditions. Data has been collected for the A2 and C1 fuels at 1 and 0.6 atm. Data collected at the two pressure conditions is reported in Figure 13.

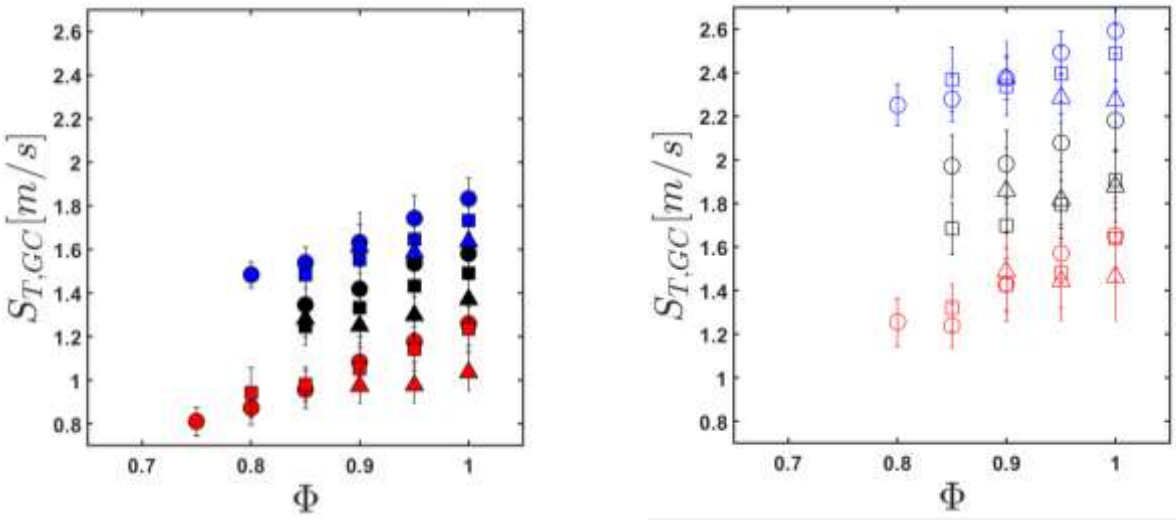

Figure 10. Sample turbulent flame speed data at atmospheric conditions for low (left panel) and high (right panel) turbulence conditions.

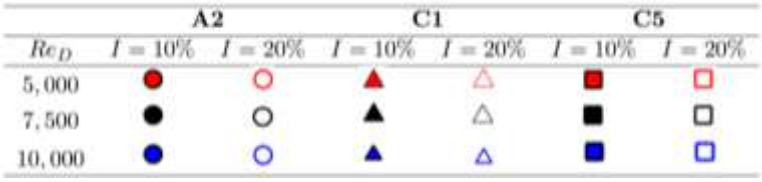

Figure 11. Legend for data shown in Figure 10.

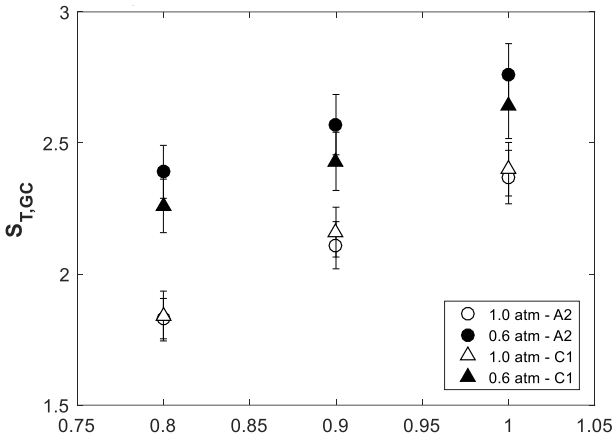

Figure 13. Turbulent consumption speed of C1 and A2 fuels at 1 and 0.6 atm.

Figure 12. Picture of flame operating in pressure vessel at subatmospheric conditions.

Publications

Fillo, Aaron, M.S., Thesis, "The Global Consumption Speeds of Premixed Large- Hydrocarbon Fuel/Air Turbulent Bunsen Flames," Oregon State University.

Plans exists for a peer-reviewed manuscript and multiple conference publications at the US Combustion Meeting in the Spring of 2017.

Outreach Efforts

None

Awards

None

Student Involvement

- Jonathan Bonebrake, a PhD student, has primarily lead efforts to collect and analyze data. He also designed and built the subatmospheric pressure vessel and vacuum system.
- Aaron Fillo, a PhD student, has worked tangentially on this project to analyze results and further investigate scientific phenomena.
- Nathan Schorn, a MS student, has recently started and has transitioned to leading the effort to operate the burner and collect and analyze data.
- Multiple undergraduate students, including underrepresented students have worked with the graduate students to operate the burner and collect data. This has provided a significant opportunity for the students to experience research.

Plans for Next Period

For the third year of this program, we will expand our database of turbulent flame speed measurements at atmospheric and subatmospheric conditions. Moreover, we will collect data for other fuels including a surrogate and fuel-X, as time permits. In addition, we will seek to understand how our results can be used to identify fuel sensitivities for lean blowout and ignition. These tasks should help address critical gaps associated with both objectives of the larger program, namely an improved combustor rig evaluation process for ASTM D4054 and validated models for combustor evaluation. The study will leverage existing facilities and infrastructure that were developed and demonstrated in years 1 and 2 of the current effort.

Two benefits can arise from measuring turbulent flame speeds. First, this work can be useful to help identify chemistry effects of jet fuels that should be captured in the modeling efforts of other groups (Area 4) and OEMs. Second, turbulent flame speed measurements may offer a metric for screening the significance of fuel chemistry of alternative fuels.

Citations

1. Venkateswaran, P., Marshall, A., Shin, D. H., Noble, D., Seitzman, J., and Lieuwen, T. “Measurements and Analysis of Turbulent Consumption Speeds of H2/CO Mixtures” *Combustion and Flame* 158, no. 8 (2011):

Diagnostics Task #1. Optimize and apply laser and optical diagnostics for application in the advanced combustion tests at Georgia Institute of Technology

University of Illinois at Urbana-Champaign

See Project 027 (A) Task 1

Diagnostics Task #2 – Optimize and apply laser and optical diagnostics for application in the advanced ignition tests at Georgia Institute of Technology and Army Research Laboratory

University of Illinois at Urbana-Champaign

See Project 027 (A) Task 2

Project 028 Combustion Model Development and Evaluation. Area #4

Georgia Institute of Technology
University of Connecticut

Project Lead Investigator

Suresh Menon, Professor
School of Aerospace Engineering
Georgia Institute of Technology
270 Ferst Drive, Atlanta, GA 30332-0150
(404)-894-9126
suresh.menon@ae.gatech.edu

University Participants

Georgia Institute of Technology

- P.I.(s): Professor Suresh Menon and Professor Wenting Sun
- FAA Award Number: 13-C-AJFE-GIT-009
- Period of Performance: 12-01-2015 to 11-30-2016
- Task(s):
    - Task 2 (Sun): Only travel funds are provided for this task
    - Task 3 (Menon): Only travel funds are provided for this task

University of Connecticut

- P.I.(s): Professor Tianfeng Lu
- FAA Award Number: 13-C-AJFE-GIT-009
- Period of Performance: 12-01-2015 to 11-30-2016
- Task(s):
    - Task 1 (Lu): Only travel funds are provided for this task

Project Funding Level

$20K from FAA and $20K cost share. Funds are explicitly for travel only.

Investigation Team

List the investigation team and specify the tasks for which they are responsible, their role in the team, and university affiliation. Include graduate students and post-doctoral researchers.

Task 1:

- **Title:** Reduced Kinetic Models with Fuel Sensitivity
- **Lead:** Professor Tianfeng Lu
- **Post Docs & Students:** Yang Gao
- **University Affiliation:** University of Connecticut

Task 2:

- **Title:** Network modeling and kinetics acceleration
- **Lead:** Professor Wenting Sun
- **Post Docs & Students:** Suo Yang

- **University Affiliation:** Georgia Institute of Technology

Task 3:

- **Title:** Large-Eddy simulation of the Referee rig
- **Lead:** Professor Suresh Menon
- **Post Docs & Students:** Dr. Reetesh Ranjan, Achyut Panchal
- **University Affiliation:** Georgia Institute of Technology

Project Overview

For Year 2 FAA support is primarily for travel to attend the mid-year and annual program review (May and Dec). Funds provided are not for research.

Task 1 – Reduced Kinetic Models with Fuel Sensitivity

University of Connecticut

Only travel funds are provided to attend FAA ASCENT and NJFCP program reviews and meetings to present results obtained from the NJFCP project. The Year 1 effort of the NJFCP project was funded by FAA and the Year 2 (2016) research project was funded by a NASA NRA. The FAA sub award to UCONN has been used to cover the following travel expenses:
1. FAA ASCENT program review meeting at Alexandria VA on 4/26/2016. Total cost is $1080.48
2. NJFCP midyear review at UTRC (Hartford Connecticut) from 6/1/2016- 6/3/2016. Total cost is $138.42
3. To present results from the NJFCP project in the 2nd International Workshop on combustion chemistry models of Real Liquid Fuels, at Arlington, VA from 6/5/2016-6/6/2016. Total cost is $421.35
4. NJFCP year 2 review at Rolls-Royce (Indianapolis Indiana) from 12/13/2016-12/16/16. Total direct cost is $1,053.43.

Year 2 total cash cost share from UCONN is $6,864

Task 2 – Network modeling and kinetics acceleration

Georgia Institute of Technology

Only travel funds are provided to attend NJFCP program reviews and other relevant meetings. All research is funded by a NASA NRA. Travel details:
1. midyear review at UTRC (Hartford Connecticut) from May 31 to June 3. Total direct cost is $1,356.3
2. year 2 review at Rolls-Royce (Indianapolis Indiana) from Dec. 12 to Dec. 16. Total direct cost is $1,067.13
3. MACCCR fuel meeting at Argonne national lab (Chicago) from Oct. 17 to Oct. 20. Total direct cost is $1,299.35
4. Jet fuel chemistry workshop at Washington D.C. from June. 6 to June. 7. Total direct cost is $1,185.29

Year 2 total cash cost share from Georgia Institute of Technology is $6,666.

Task 3 – Large-eddy simulations of the Referee rig

Georgia Institute of technology

Travel funds are provided to attend FAA ASCENT and NJFCP program reviews and meetings to present results obtained from the NJFCP project. The Year 2 (2016) research project was funded by a NASA NRA. Travel Expense includes

1. Midyear review at UTRC (Hartford Connecticut) from 6/1/2016- 6/3/2016. Total direct cost is $1510.
2. Year 2 review at Rolls-Royce (Indianapolis Indiana) from 12/13/2016-12/16/16. Total direct cost is $1300
3. Posters for ASCENT meeting: $200

Year 2 total cash cost share from Georgia Institute of Technology is $6,666

Objective(s)

The project's overall goal is to model the sensitivity of lean blow out (LBO) to various alternate fuels. The modeling effort includes three parts: (a) development of efficient reduced kinetics, (b) development of kinetics acceleration techniques and (c) LES studies of spray combustion in the Referee rig under experimental conditions. This work is continued under NASA NRA funding in 2016 but results are directly relevant for this NJFCP program.

Research Approach

All work under NASA NRA is computational in nature and is reported elsewhere.

Milestone(s)

Include a description of any and all milestones reached in this research according to previously indicated timelines.

Major Accomplishments

- New reduced and skeletal kinetics mechanisms were developed for the NJFCP three chosen fuels Cat A2, C1 and C5. These kinetics models have been implemented into LES codes
- Adaptive methods have been developed to speed up kinetics calculations in LES and DNS. These methods are currently being analyzed for relevance to full rig simulations.

Publications

Presentation:
"Model Reduction," Yang Gao, Chao Xu, Tianfeng Lu, Hai Wang, Jacqueline H. Chen, Alexei Poludnendo, Peter Hamlington, 2nd International Workshop on Combustion Chemistry Models of Real Liquid Fuels, Arlington, VA, June 06, 2016.

Publication (refereed):
Yang, S., Ranjan, R., Yang, V., Menon, S., Sun, W., ``Parallel on-the-fly Adaptive Kinetics in Direct Numerical Simulation of Turbulent Premixed Flame," Proceedings of the Combustion Institute, Vol. 36, 2016 (to appear).

Outreach Efforts

None

Awards

None

Student Involvement

Students are still in their PhD graduate programs in both Georgia Tech and UCONN.

Plans for Next Period

Work in the 3rd year is also funded by NASA NRA and not by NJFCP. Travel funds are however, authorized for two meetings in 2017.

Project 029 National Jet Fuels Combustion Program, Area #5: Atomization Test and Models

Purdue University
Stanford University

Project Lead Investigator

Robert P. Lucht
Ralph and Bettye Bailey Distinguished Professor of Combustion
School of Mechanical Engineering
Purdue University
West Lafayette, IN 47907-2088
765-714-6020 (Cell)
Lucht@purdue.edu

Matthias Ihme
Department of Mechanical Engineering
Stanford University, CA 94305-3024
mihme@stanford.edu

University Participants

- P.I.(s): Robert P. Lucht, Jay P. Gore, Carson D. Slabaugh, Paul E. Sojka, and Scott E. Meyer
- FAA Award Number: **COE-2014-29A** , 401321
- Period of Performance: 12/1/2015-11/30/2015
- The experimental tasks to be performed in Year 2 are listed below:

Quarter 1

1. Collaborate with area 4 and 6 groups, and with the Area 5 subcommittee, for development of experimental test matrix for Year 2.
2. Install heat exchangers and cyclone separator for RTS test rig for operation at subatmospheric pressure.
3. Perform extensive characterization of Nozzle B sprays for LBO and other conditions in the RTS test rig using PDPA and high-speed backlit video imaging.
4. Share boundary, initial and operating conditions and resulting experimental data with Ihme and Menon groups.
5. Design system for mixing of liquid and gaseous nitrogen to produce gaseous nitrogen at temperatures down to 230 K.

Quarter 2

1. Exploratory/shakedown testing of the AGTC test rig.
2. Continue extensive characterization of Nozzle B sprays for LBO and other conditions in the RTS test rig using PDPA and high-speed backlit video imaging.
3. Perform characterization of selected Nozzle B spray conditions for LBO conditions in the AGTC test rig using Mie scattering and fuel PLIF imaging.
4. Share boundary, initial and operating conditions and resulting experimental data with Ihme and Menon groups.
5. Fabricate and test system for mixing of liquid and gaseous nitrogen to produce gaseous nitrogen at temperatures down to 230 K.

Quarter 3

1. Perform extensive characterization of Nozzle B sprays for GLO and other conditions in the RTS test rig using PDPA and high-speed backlit video imaging.
2. Perform characterization of selected Nozzle B spray conditions for GLO and other conditions in the AGTC test rig using Mie scattering and fuel PLIF imaging.
3. Install Nozzle A in RTS test rig and perform measurements for selected LBO conditions.
4. Share boundary, initial and operating conditions and resulting experimental data with Ihme and Menon groups.

Quarter 4

1. Continue extensive characterization of Nozzle B sprays for GLO conditions in the RTS test rig using PDPA and high-speed backlit video imaging.
2. Continue characterization of selected Nozzle B spray conditions for GLO and LBO conditions in the AGTC test rig using Mie scattering and fuel PLIF imaging.
3. Install Nozzle A in RTS test rig and perform measurements for selected GLO conditions.
4. Share boundary, initial and operating conditions and resulting experimental data with Ihme and Menon groups.

- P.I.(s): Matthias Ihme
- FAA Award Number: **COE-2014-29B**
- Period of Performance: 12/1/2015-11/30/2016
- The experimental tasks to be performed in Year 2 are listed below:
- The computational modeling tasks to be performed in Year 2 are listed below:
    1. Perform detailed LS/VOF simulations to validate multiphase modeling tools for airblast conditions
    2. Compare simulation results against measurements from PDPA provided by Purdue and UDRI
    3. Analyze correlations for SMD, breakup-length, and droplet distribution using high-fidelity simulation results from LS/VOF computations; identify correlations between droplet distribution and LBO-conditions (coordination with Nader Rizk)
    4. Perform detailed simulations and validation on nozzle A; compare model results with experiments; evaluate effects of different nozzle geometries (nozzle A vs. nozzle B) on ignition and LBO characteristics

Project Funding Level

The funding level from FAA was $250,000 to Purdue University for Year 2. Purdue University provided cost sharing funds in the amount of $250,000.
The funding level from FAA was $40,000 to Stanford University for Year 2. Purdue University provided cost sharing funds in the amount of $40,000.

Investigation Team

PI Dr. Robert Lucht, Bailey Distinguished Professor of Mechanical Engineering is responsible for the oversight of the entire project here at Purdue University. He is also responsible for mentoring one of the graduate students, coordinating activities with Stanford and will work with all parties for appropriate results and reporting as required.

Co-PI Dr. Jay Gore, Reilly Professor of Mechanical works closely with the PI for all deliverables of Purdue University, and also oversees the work performed by one of the graduate students that he is mentoring.

Co-PI Dr. Paul Sojka, Professor of Mechanical Engineering is responsible for mentoring one of the graduate student and is responsible for supervising the PDPA measurements.

Co-PI Scott Meyer, Managing Director of the Maurice J. Zucrow Laboratories is responsible for coordinating facility upgrades and for facility design reviews.

Senior Research Scientist Dr. Sameer V. Naik is responsible for direct supervision of the two graduate students involved in the project.

Graduate students Andrew Bokhart and Daniel Shin are responsible for performing the PDPA measurements and for modifying the RTS test rig for operation at near-lean-blow-out (LBO) conditions.

PI Dr. Matthias Ihme is responsible for the oversight of the computational modeling effort at Stanford University. He is also responsible for supervising the post-doctoral and graduate students at Stanford, coordinating activities with Purdue and UDRI and will work with all parties for appropriate results and reporting as required.

Project Overview

The objectives of this task as stated in the Invitation for ASCENT COE Notice of Intent (COE-2014-29) are to "measure the spray characteristics of the nozzles used in the Referee Combustor used in Area 6 tests and to develop models for characterizing the atomization and vaporization of the reference fuels." We propose a joint experimental and modeling effort to achieve these objectives. The experimental tasks will be performed at Purdue University and the modeling tasks will be performed by Prof. Matthias Ihme's group at Stanford University. The modeling tasks are described in a separate proposal but a specific task will involve rendering of modeling results in the form of measurable and important quantities including liquid surface area density and discrete probability density functions of liquid ligament and drop sizes.

Purdue University has two very capable test rig facilities for measuring spray characteristics over very wide ranges of pressure, inlet air temperature, and fuel temperature. The experimental diagnostics that will be applied will include both well-established diagnostics such as phase Doppler particle anemometry (PDPA) as well as advanced high-frame-rate simultaneous Mie scattering and fuel planar laser-induced fluorescence (PLIF). Recently commercialized and SAE J2715 standards based techniques for liquid surface area density and drop size probability density functions will be utilized by renting patternator equipment from a Purdue Technology Center small business. These tests will help us qualify the nozzles to be installed in the high-pressure rigs. The atomization and spray dynamics of the three reference fuels and referee rig nozzle configurations will be performed in both of our spray rig facilities. These facilities will allow us to test over the entire range of fuel and air temperatures and air pressures of interest. In one of the test rigs we will be able to directly compare reacting and non-reacting flow cases.

The objectives of the computational research are the development and validation of modeling capabilities for the prediction of primary and secondary breakup of liquid fuel under consideration of multicomponent fuel effects. These modeling efforts will be accompanied by validation against measurements from the complementary experimental effort that is conducted at Purdue University.

Task: COE-2014-29A: National Jet Fuels Combustion Program – Area #5: Atomization Tests and Models

Purdue University

Objective(s)

The objectives of this proposal are to visualize and measure the characteristics including drop size distributions, axial, and radial velocity components of the sprays generated by a nozzle being used in the Referee combustor rig in the Area 6 tests and for a nozzle with the design made available by the Pratt & Whitney (P&W) and Georgia Tech teams. The resulting data will be used for the development of spray correlations by consultant Nader Rizk and for the purpose of submodel development for detailed computer simulations being performed by Matthias Ihme (Stanford University), Suresh Menon (Georgia Tech), and Vaidya Sankaran (UTRC). The experimental tasks will be performed at Purdue University and the resulting data will be shared with FAA team members developing modeling, simulations, and engineering correlation based tools. We will develop methods to compare the spray properties under non-reacting flow conditions and those under combustor flow conditions.

The upgraded RTS test facility at Purdue University will be used for measuring spray characteristics over the ranges of pressure, inlet air temperature, and fuel temperature for two different spray nozzles. Our work during the first year and

up to this point in the second year allowed us to identify the challenges associated with making reliable and repeatable spray measurements while keeping the windows of the rig clean. Phase Doppler particle anemometry (PDPA) has emerged as a technique of choice for obtaining fundamental drop size distribution and axial and radial velocity data for comparison with numerical simulations. The atomization and spray dynamics of the three reference fuels and two nozzle configurations will be measured in the Purdue Rules and Tools Spray (RTS) test rig. This facility will be further upgraded to allow us to test over the entire range of fuel and air temperatures and air pressures of interest. We will be able to directly compare reacting and non-reacting spray data by collaborating with the UDRI/AFRL Area 6 team.

The experimental data will support continued development and evaluation of engineering spray correlations including the dependence of Sauter Mean Diameter (SMD), spray cone angle, and particle number density per unit volume on the fuel properties at fuel and air temperatures of interest. The experimental data will provide detailed statistical measurements for comparisons with high-fidelity numerical simulations of mixing and combustion processes. The prediction of the spatial distribution of the liquid fuel and resulting vapors and breakdown components from the liquid fuels critically affects the ignition, flame-stabilization, and pollutant formation processes. The focus during the rest of Year 2 and Year 3 activities will be on obtaining data for extension of long-standing Rizk correlations to include effects of fuel properties and the effects of the non-reacting (RTS rig) and reacting (referee rig) at AFRL and/or the Advanced Gas Turbine Combustor (AGTC) rig at Purdue.

The project objectives are summarized as:

(a) Obtain PDPA data across one plane in the Rules and Tools Spray (RTS) rig operated with the Referee Rig nozzle and the P&W nozzle,

(b) Extend PDPA measurements to obtain data across multiple planes for evaluation of Detailed Combustor Simulations (DeCS) by Suresh Menon, Vaidya Sankaran, and Matthias Ihme,

(c) Obtain PDPA and/or Malvern measurements for selected operating conditions either in the RTS test rig or at atmospheric pressure to provide data for the spray correlation analysis of Nader Rizk,

(d) Perform PDPA measurements for fuel blends including Fuel X and/or another blend designed for testing differences in atomization characteristics to examine the sensitivity of correlations and computations to changes in fuel properties,

(e) Ensure quality of data with repetition tests at Purdue and comparisons with spray measurements at P&W, UDRI/AFRL, and UIUC,

(f) Compare spray data under non-reacting flow conditions of the Rules and Tools Spray test rig with those under reacting flow conditions from the Referee Rig at AFRL and/or the Advanced Gas Turbine Combustor (AGTC) rig at Purdue.

Research Approach

The Purdue University test rig facilities are designed for measuring spray characteristics over very wide ranges of pressure, inlet air temperature, and fuel temperature. An atmospheric pressure spray test rig facility has been extensively used in year 1 of the project to establish the differences in spray properties of the different fuels at multiple fuel temperatures, fuel pressures, and swirler pressure drops. The second facility is the Rules and Tools spray (RTS) test rig which will allow measurements under high and low pressure conditions relevant to the aviation applications and is being reactivated during the last part of year 1 activities and the first part of year 2 activities.

The operating system for the atmospheric pressure spray facility and the instrument positioning and atomization systems have been upgraded over the first year to allow high repeatability for PDPA drop size and velocity measurements. A high speed camera with backlighting has yielded significant insights into the structure of the liquid fuels flowing out of the nozzle with and without the swirling co-flow through the injector. An optical patternator is also used for rapid analysis of spray distribution patterns.

Liquid fuels can be supplied to the test rigs by multiple systems. A facility-integrated system draws fuel from one of two certified flame-shield fuel containments for testing standard aviation fuels as well as other alternative blends. A mobile fuel cart, developed under the combustion rules and tools (CRATCAF) program and redeployed during the first year of the NJFCP program is being utilized for further control of additional injector circuits or for running alternative fuel blends. Both systems were designed with two independently controlled and metered circuits to supply fuel to pilot and main injector channels of the test injector. The mass flow rates of both supplies are measured with Micro Motion Elite® Coriolis flow meters. A nitrogen sparge and blanket ullage system is used to reduce the dissolved oxygen content of the fuel, which is monitored with a sensor just upstream of the fuel control circuits. High pressure gear pumps provide fuel at up to 300 kg/hr, supplied to the control circuits at a 10 MPa regulated line pressure. The mobile fuel cart was built with two onboard heat exchangers and a chilling unit controls the temperature of the fuel over a range of 233 K to 600 K (-40ºF to 600ºF).

Milestone(s)

The major milestones that have accomplished so far during Year 2 of the project are:

1. Modification of the RTS test rig for measurements at near LBO conditions. This was a very significant effort that was complicated by condensation of fuel on the inside of the windows and liquid water or ice on the outside of the windows. The LBO test matrix was developed in coordination with Nader Rizk. The LBO test conditions that were investigated are shown below:

Table 1. of LBO test conditions.

Injector	OP	ΔP/P [%]	Fuel Flow Rate [lbm/hr]	Fuel Temp. [°F]	ΔP_{pilot} [psia]	Vessel Press. [psia]	Vessel Temp. [°F]
100% Pilot	1	2.00	20.00	120	25	30	250
	2	4.00	20.00	120	25	30	250
	3	6.00	20.00	120	25	30	250
	4	2.00	28.28	120	50	30	250
	5	2.00	34.64	120	75	30	250
	6	3.00	20.00	120	25	30	250
	7	3.00	28.28	120	50	30	250
	8	3.00	34.64	120	75	30	250

2. PDPA measurements of A2, C1, and C5 fuels at the test conditions in Table 1. Comparison of our measurements for a non-reacting spray with measurements by UDRI/UIUC for a reacting spray conditions. Sent detailed PDPA data to Dr. Vaidya Sankaran at UTRC for comparison with his spray calculations.
3. High-speed imaging of sprays at LBO conditions to assess spray geometry and aid in the definition of spray angle.
4. Investigated filming on the inner surface of the inner swirler of the nozzle. Established that the pilot spray was impacting this surface.

Major Accomplishments

The work described in this section is a part of the Purdue contributions to the larger FAA-funded effort, the National Jet Fuels Combustion Program (NJFCP). The major objective of the work at Purdue is to perform measurements of spray properties (droplet size, droplet velocity, spray cone angle) for a variety of jet fuels and candidate jet fuels under a wide range of conditions, including lean blowout (LBO), Ground Lift Off (GLO), and high altitude relight (HAR). Representative measurements of spray properties for LBO conditions are presented in the rest of this section. The Purdue Rules and Tools Spray (RTS) test rig is discussed along with modifications needed for the LBO measurements. A generic hybrid air blast injector is used and we have investigated the spray characteristics for three different fuels. The spray data are being used as initial conditions for computational models of the combustion process in a Referee rig developed by the NJFCP team.

Experimental Systems

The rules and tools (RTS) test rig is shown in a photograph in Fig. 1 and in a schematic diagram in Fig. 2. The RTS test rig consists of two major sub-assemblies: a vertically-actuated air-box assembly and an optically-accessible pressure vessel. The air-box assembly houses the injector and (optional) swirler components. This assembly can be operated independently from the pressure vessel for atmospheric-pressure testing utilizing diagnostics requiring unrestricted optical access such as patternation. The injector assembly can be traversed vertically, with precise control, relative to supply manifolds. This design feature supports the application of point diagnostics over a grid of measurement locations with varying distances from the nozzle exit.

Pressure modulation of test conditions is achieved by installing the complete air-box assembly into the pressure vessel. The pressure vessel was originally designed for a study of spray behavior under super-critical conditions and has demonstrated sustained operation at quiescent flow pressures and temperatures up to 4 MPa and 900 K. Optical access is achieved through four windows for high-speed video, Schlieren, Malvern and PDPA measurements. Two of the windows are located on opposite sides of the vessel to achieve a clear line of sight, supporting Schlieren and other line-of-sight measurements. The

other two windows are located 30 degrees from the line of sight optical axis with a 60 degree included angle. A sweeping flow, within the vessel, helps to prevent window fouling by the ejected spray.

A mobile fuel cart, developed under the combustion rules and tools (CRATCAF) program and redeployed during the first year of the NJFCP program is being utilized for further control of additional injector circuits and for running alternative fuel blends. The fuel cart has two independently controlled and metered circuits to supply fuel to pilot and main injector channels of the test injector. The mass flow rates of both supplies are measured with Micro Motion Elite® Coriolis flow meters. A nitrogen sparge and blanket ullage system is used to reduce the dissolved oxygen content of the fuel, which is monitored with a sensor just upstream of the fuel control circuits. High-pressure gear pumps provide fuel at up to 300 kg/hr, supplied to the control circuits at a 10 MPa regulated line pressure. The mobile fuel cart was built with two onboard heat exchangers and a chilling unit to control the temperature of the fuel over a range from 233 K to 600 K (-40˚F to 620˚F).

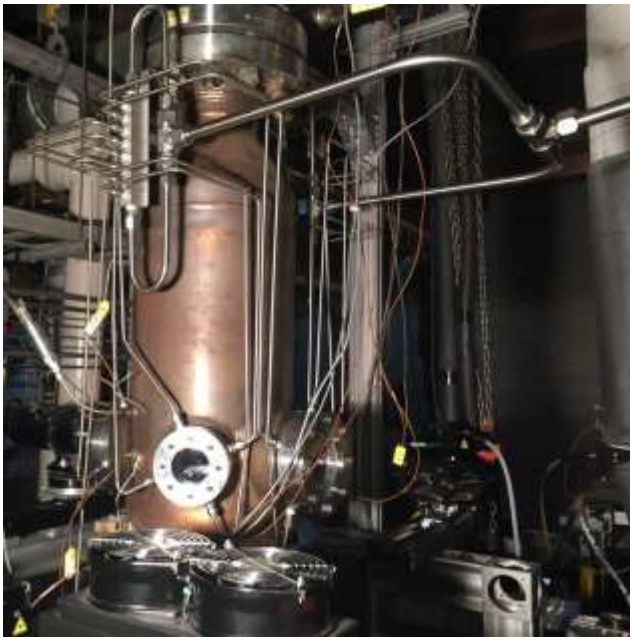

Figure 1. Photograph of the RTS test rig.

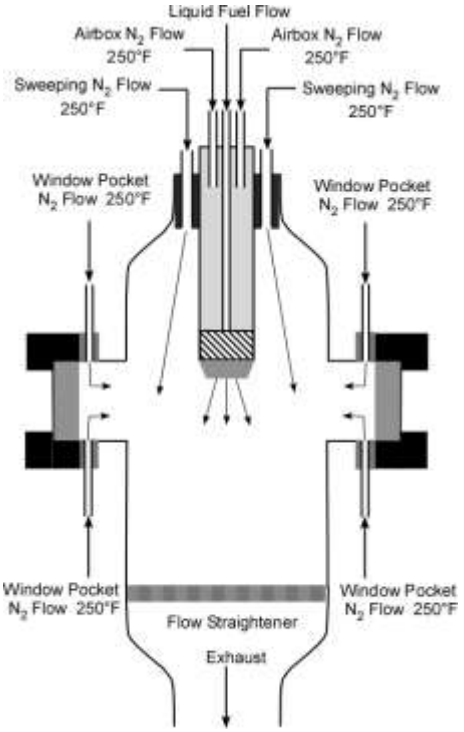

Figure 2. Schematic diagram of the RTS test rig.

We initially tried measurements with a Malvern diffraction particle sizing system in the RTS test rig in collaboration with Andrew Corber from National Research Council (NRC), Canada. For the initial LBO measurements the nitrogen swirler flow was directed to an electric heater, then was mixed into the air box that holds the referee nozzle/swirler assembly. The electric heater is used to heat the air box nitrogen flow so that the temperature is 250˚F at the swirler inlet. For the initial measurements we tried using an unheated sweeping flow of nitrogen. The sweeping flow is intended to keep the fuel droplets from the spray from hitting the windows. However, we observed significant wetting of the inside of the window with fuel, although there were some operating conditions where the fuel on the window was minimal. Moreover, the cold sweeping flow chilled the windows and caused condensation of water vapor on the outside of the windows. Malvern/diffraction measurements are extremely sensitive to window contamination, and we observed artifacts in the acquired data due to window contamination and also due to beam steering resulting from the large temperature difference between the sweeping and the air box nitrogen flows. The sweeping nitrogen flow temperature was about -20˚F as a result of the significant cooling upon expansion from the supply pressure of 6000 psi.

The next step that we took was to install nitrogen purge lines both inside the window in the window flange pocket and then outside the window to flow dry nitrogen over the window surface to prevent condensation of water from the room air. This was not successful, there were some runs where we were able to keep the windows clear but as we tried to increase the chamber pressure to 30 psia and take measurements at LBO conditions significant artifacts in the Malvern measurements occurred, which we now believe are due to beam steering resulting from the temperature gradient between the air box and the sweeping nitrogen flows.

We then decided to heat the sweeping flow by sending it through our natural-gas-fired air heater. This improved the situation but we were still not able to acquire artifact-free Malvern data at LBO conditions, and depending on the particular run conditions we still had problems with fuel condensation on the inside of the window and water condensation on the outside of the window. At this point, the window flange purge flow was unheated and thus entered the pressure vessel at -20°F. To overcome this, we decided to heat the window purge flow. This required a significant plumbing effort. The window purge flow and the sweeping flow are now obtained from the single exit stream from our natural-gas-fired air heater. Heating both the window purge flow and the sweeping flow solved our window contamination problem. At the same time, we decided to switch from Malvern/Sympatec measurement system to a Phase Doppler particle anemometer (PDPA) system allowing simultaneous measurements of drop size distributions, axial, and radial velocity components. As it turns out, it now appears that the PDA measurements are much easier to implement in the RTS test rig than the Malvern measurements.

Experimental Results: PDPA Measurements

We have successfully performed spray measurements in the RTS test rig at LBO conditions using PDPA and high-speed imaging systems for three different fuels (A2, C1, and C5). The LBO operating conditions are at an ambient pressure of 2.07 bars (30 psia), an air box nitrogen temperature of 394 K (250ºF), a pilot fuel temperature of 322 K (120ºF), a pilot fuel mass flow rate of 9.22 kg/hr (2.56 g/s), and a pressure drop of 3% across the swirler. The geometry of the PDPA measurement system is shown in Fig. 3 for negative and positive radial location along a line through the nozzle centerline. Some of the initial measurements are presented in Figs. 4 and 5. All of the data shown were collected at an axial distance of 25.4 mm from the swirler exit plane. Figure 4 shows the measured Sauter Mean Diameter (SMD) for the three fuels for negative radial locations (referring to Fig. 3) and Fig. 5 shows the axial and radial velocities for both positive and negative radial locations for fuel A2. Our work has included analyzing droplet diameter distribution statistics in terms of the probability of occurrence of different drop sizes that lead to the Sauter Mean Diameter (SMD or D_{32}) depicted in Fig. 4. The SMD is biased by the populations representing larger drops because these evaporate at slower rates than the smaller drops as a result of lower surface area to volume ratios.

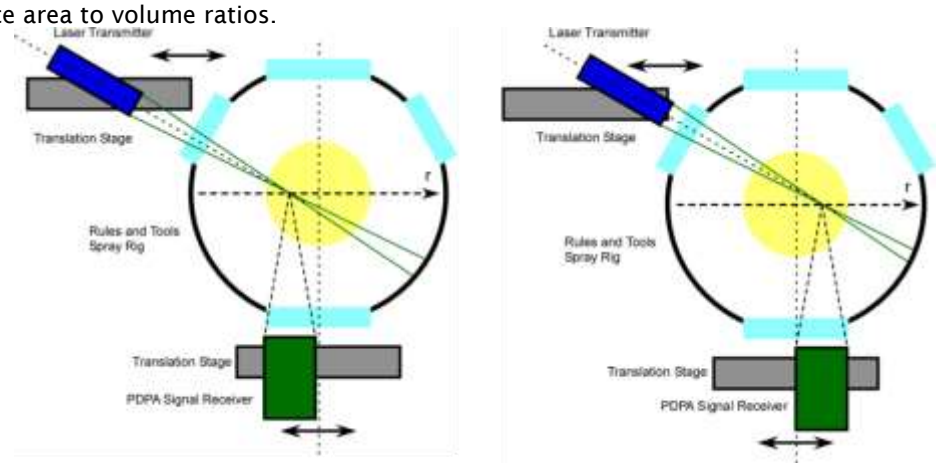

Figure 3. Top view of PDPA measurement geometry.

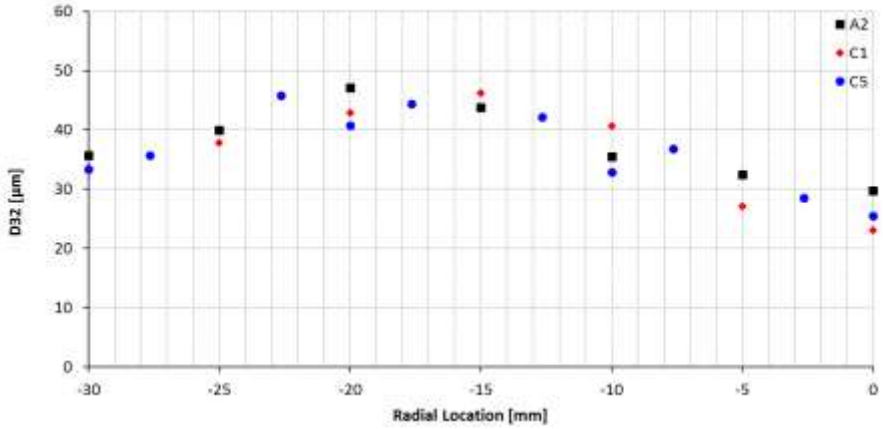

Figure 4. Sauter mean diameter D_{32} as a function of radial position for three different fuels.

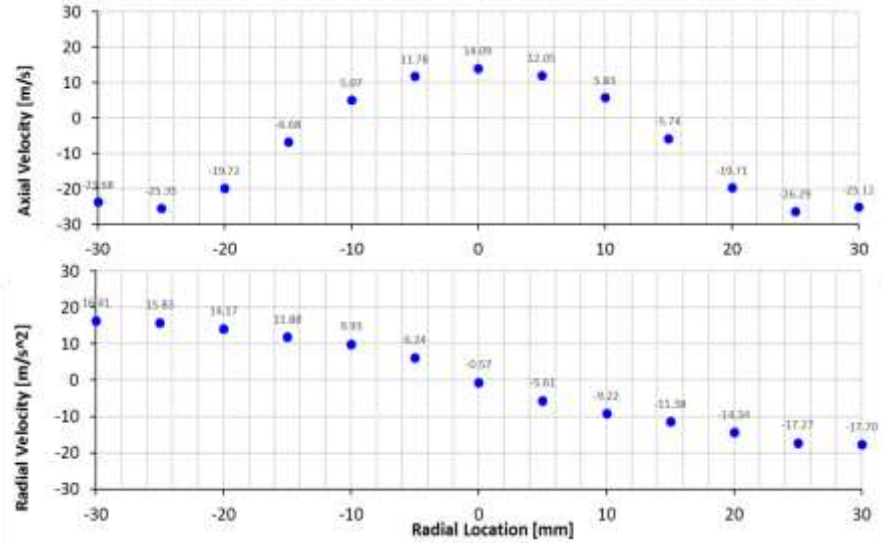

Figure 5. Axial and radial velocities for fuel A2 as a function of radial position. Note the central recirculation zone from -12 mm to +12 mm positive axial velocities (towards the nozzle).

Experimental Results: Spray Geometry

The cone angle is defined in this study as the angle between two straight lines that represent the fuel cone geometry. The lines are drawn from the injector orifice to some specified distance from the nozzle exit so that the edges of the spray cone are determined. The full cone angles 0.5 inches away from the nozzle exit were measured for C-1, C-5, and A-2 with varied differential pressure and fuel flow rate. A simple image processing has been performed on the high speed images in order to determine the spray cone angles. A background image and 5823 high speed spray images were obtained for each test case. These images were averaged and the background was subtracted from the averaged image. Figure 6 shows the average shadowgraph image of an A-2 spray at OP 1 and the modified image after the subtraction of the background.

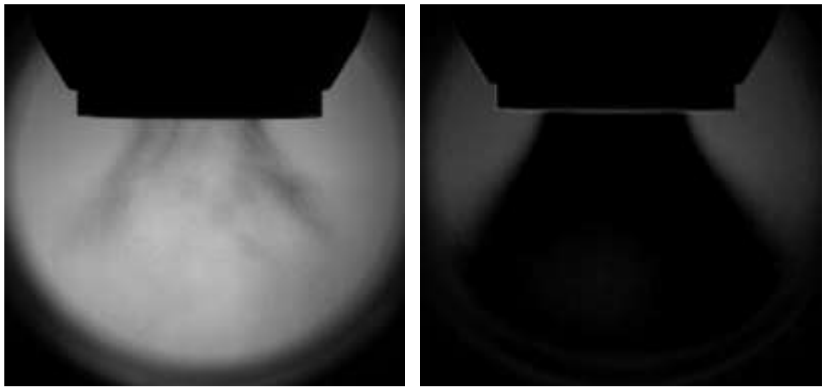

Figure 6. Shadowgraph image of A-2 spray at OP 1 (Left). Spray image with the background subtracted (Right).

In order to define the spray edge from the background subtracted image, the pixels that fit within a specific intensity limit are masked in different colors. The intensity in a grayscale image is a value between 0 to 1. The pixel intensity values near the spray edge were determined to be between 0.025 to 0.043. These intensity limits are divided into three smaller limits and masked in yellow, red, and blue as shown in Figure 7b. By accessing the coordinates of selected pixels along the spray edge, a linear regression fit was applied with the location of the injector orifice fixed within the regression. The location of the injector orifice is marked as a green circle in Fig. 7c and Fig. 7d.

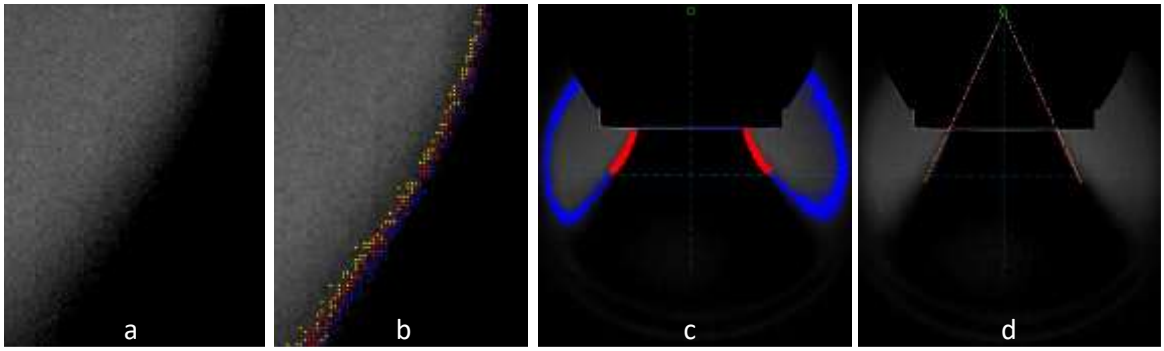

Figure 7. a) Edge of the spray in grayscale image. b) Applied three different masks on the pixels in spray edge. c) Selected masked pixels on the edge of the spray are shown in red. d) Linear regression fit is obtained using the selected pixels and a fixed point at the injector orifice.

The resulting cone angles calculated between the two linear regression lines for each test are shown in Fig. 8 for A-2, C-1, and C-5. The full cone angles obtained from each fuel are between 46.05 ˚ and 49.05˚ with the uncertainty within ±0.33˚ and ±1.65˚. The results show that the effect of pressure drop and fuel flow rate on the cone angles is minimal and the change in cone angles is within the margin of experimental uncertainty. It is also shown that the fuel type has a minimal effect on the cone angles and it is negligible.

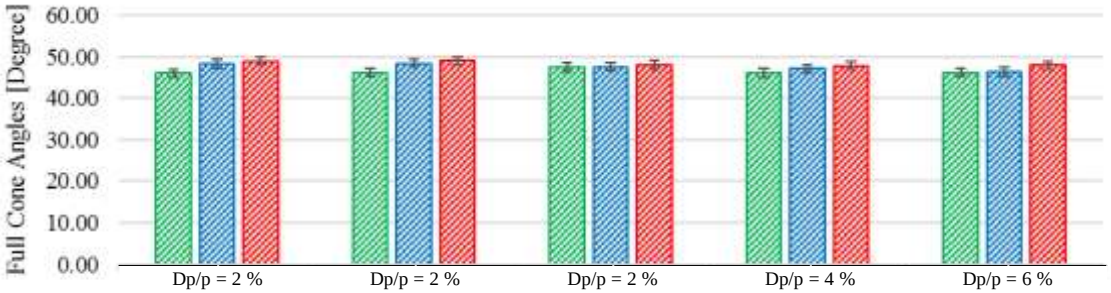

	Dp/p = 2 % FFR = 20 lbm/hr		Dp/p = 2 % FFR = 28.28 lbm/hr		Dp/p = 2 % FFR = 34.64 lbm/hr		Dp/p = 4 % FFR = 20 lbm/hr		Dp/p = 6 % FFR = 20 lbm/hr	
	Cone Angle	Uncertainty	Cone Angle	Uncertainty	Cone Angle	Uncertainty	Cone Angle	Uncertainty	Cone Angle	Uncertainty
C-1	46.05°	±1.16°	46.16°	±0.64°	47.47°	±0.86°	46.11°	±1.65°	46.19°	±1.51°
A-2	48.32°	±0.55°	48.40°	±0.48°	47.60°	±0.41°	47.13°	±0.91°	46.33°	±0.56°
C-5	48.91°	±1.02°	49.05°	±0.76°	48.03°	±0.46°	47.82°	±0.63°	47.95°	±0.33°

Figure 8. Bar graph of full cone angles comparison for A-2, C-1, and C-5 under pressure drop variation and fuel flow rate variation.

Publications

- "Effect of Aviation Fuel Type and Fuel Injection Conditions on Non-Reacting Spray Characteristics of Hybrid Air Blast Fuel Injector," Timo Buschhagen, Robert Z. Zhang, Sameer V. Naik, Carson D. Slabaugh, Scott E. Meyer, Jay P. Gore, and Robert P. Lucht, presented at the 2016 AIAA SciTech Meeting, San Diego, CA, 4-8 January 2016, Paper Number AIAA 2016-1154.
- "Large-Eddy Simulations of Fuel Injection and Atomization of a Hybrid Air-Blast Atomizer," P. C. May, M. B. Nik, S. E. Carbajal, S. Naik, J. P. Gore, R. P. Lucht, and M. Ihme, presented at the 2016 AIAA SciTech Meeting, San Diego, CA, 4-8 January 2016, Paper Number AIAA 2016-1393.
- "Spray Measurements at Elevated Pressures and Temperatures Using Phase Doppler Anemometry," A. J. Bokhart, D. Shin, R. Gejji, T. Buschhagen, S. V. Naik, R. P. Lucht, J. P. Gore, P. E. Sojka, and S. E. Meyer, to be presented at the 2017 AIAA SciTech Meeting, Grapevine, TX, 8-13 January 2017.

Outreach Efforts

- "Effect of Aviation Fuel Type and Fuel Injection Conditions on Non-Reacting Spray Characteristics of Hybrid Air Blast Fuel Injector," Timo Buschhagen, Robert Z. Zhang, Sameer V. Naik, Carson D. Slabaugh, Scott E. Meyer, Jay P. Gore, and Robert P. Lucht, presented at the 2016 AIAA SciTech Meeting, San Diego, CA, 4-8 January 2016
- "Large-Eddy Simulations of Fuel Injection and Atomization of a Hybrid Air-Blast Atomizer," P. C. May, M. B. Nik, S. E. Carbajal, S. Naik, J. P. Gore, R. P. Lucht, and M. Ihme, presented at the 2016 AIAA SciTech Meeting, San Diego, CA, 4-8 January 2016.
- "Spray Measurements at Elevated Pressures and Temperatures Using Phase Doppler Anemometry," A. J. Bokhart, D. Shin, R. Gejji, T. Buschhagen, S. V. Naik, R. P. Lucht, J. P. Gore, P. E. Sojka, and S. E. Meyer, to be presented at the 2017 AIAA SciTech Meeting, Grapevine, TX, 8-13 January 2017.

Awards

None.

Student Involvement

PhD students Andrew Bokhart and Daniel Shin are primarily responsible for performing the PDPA measurements and for modifying the RTS test rig for first LBO and then HAR/GLO measurements. PhD students Timo Buschhagen and Rohan Gejji assist with the project when their expertise is required.

Plans for Next Period

The Year 3 deliverables for Area #5 are as follows:

1. Early in Year 3 we will modify the variable-ambient-pressure RTS test rig (brought back online by us during Year 2) for measurements with chilled fuel and chilled nitrogen swirler flow. We will perform PDPA measurements for low-pressure high-altitude relight (HAR) conditions with fuel temperatures down to -30°F. An ejector will be installed on the RTS rig for sub atmospheric pressure conditions. A heat exchanger for the nitrogen will be installed so that we can run with nitrogen at temperatures below room temperature as well as at temperatures up to 350°F. The RTS spray rig will be suitable for measurements with both heated fuel and chilled fuel. In the RTS spray rig, the diagnostics will include PDPA, Malvern SMD, and high-speed video with backlighting. The RTS test rig will be used for extensive testing guided by a test matrix provided by Nader Rizk for HAR conditions for the selected category A and category C fuels. Ground Lift Off (GLO) measurements will be performed in an atmospheric-pressure spray rig with cold fuel and cold nitrogen for Nozzle B. Measurements will be performed for selected category A and C fuels and the experiments will be guided using a test matrix supplied by Nader Rizk.
2. Spray measurements will be performed near LBO conditions for Configuration 2 in which the main fuel circuit for Nozzle B will be activated. Spray measurements for GLO conditions will also be performed for the Pratt and Whitney swirler/fuel nozzles that are the subject of measurements at LBO conditions in Year 2.
3. We will develop research transition and implementation plan as well as share data and results with other area research teams on a timely basis as applicable and/or as directed by the Steering Committee (Purdue, Stanford, Georgia Tech, and industry partners). We will coordinate closely with Area 6 as their testing capabilities expand in the rest of Year 2. We will share data and get input from Suresh Menon in addition to the input we have been receiving from Matthias Ihme on cases of particular interest and regarding additional measurements needed for characterization of boundary conditions for CFD model validation and calibration.

The tasks to be performed in Year 3 are listed below:

Quarter 1

1. Collaborate with Area 4 and Area 6 members, and with the Area 5 subcommittee, for development of experimental test matrix for Year 3.
2. Install heat exchangers and cyclone separator for Rules and Tools (RTS) test rig for operation at sub-atmospheric pressure.
3. Perform initial spray measurements with Nozzle B for high-altitude relight (HAR) conditions in the RTS test rig and for Ground Lift Off (GLO) conditions in an atmospheric-pressure rig using PDPA and high-speed backlit video imaging.
4. Share boundary, initial, and operating conditions and resulting experimental data with correlations and modeling team (Rizk, Ihme, Menon, and Sankaran).
5. Design a system for mixing of liquid and gaseous nitrogen to produce gaseous nitrogen at temperatures down to 230 K.
6. Perform spray measurements for Nozzle B in Configuration 2 (main fuel circuit activated) near LBO conditions.

Quarter 2

1. Continue extensive characterization of sprays with Nozzle B for HAR conditions in the RTS test rig and for GLO conditions in an atmospheric-pressure rig using Phase Doppler Particle Analyzer (PDPA) and high-speed backlit video imaging.
2. Share boundary, initial, and operating conditions and resulting experimental data with correlations and modeling team (Rizk, Ihme, Menon, and Sankaran).
3. Fabricate and test the system for mixing of liquid and gaseous nitrogen to produce gaseous nitrogen at temperatures down to 230 K.
4. Continue spray measurements for Nozzle B in Configuration 2 (main fuel circuit activated) near LBO conditions.

Quarter 3

1. Continue extensive characterization of sprays with Nozzle B for HAR conditions in the RTS test rig and for GLO conditions in an atmospheric-pressure rig using Phase Doppler Particle Analyzer (PDPA) and high-speed backlit video imaging.
2. Share boundary, initial, and operating conditions and resulting experimental data with correlations and modeling team (Rizk, Ihme, Menon, and Sankaran).
3. Exploratory/shakedown testing of the Advanced Gas Turbine Combustor (AGTC) test rig.
4. Install the P&W swirler and fuel nozzles or another nozzle of interest and perform measurements in the AGTC for selected GLO conditions.

Quarter 4

1. Continue extensive characterization of sprays with Nozzle B for HAR conditions in the RTS test rig and for GLO conditions using Phase Doppler Particle Analyzer (PDPA) and high-speed backlit video imaging.
2. Continue characterization of selected sprays with Nozzle B for LBO conditions in the AGTC test rig using Mie scattering and fuel PLIF imaging.
3. Perform measurements for selected GLO conditions with the P&W swirler and fuel nozzles or another nozzle of interest.
4. Share boundary, initial, and operating conditions and resulting experimental data with correlations and modeling team (Rizk, Ihme, Menon, and Sankaran).

Task: COE-2014-29B: National Jet Fuels Combustion Program – Area #5: Atomization Tests and Models

Stanford University

Objective(s)

The objectives of the computational research are the development and validation of modeling capabilities for the prediction of primary and secondary breakup of liquid fuel under consideration of multicomponent fuel effects. These modeling efforts will be accompanied by validation against measurements from the complementary experimental effort that is conducted at Purdue University.

Research Approach

The objective of this study is to use a LES approach in conjunction with an unstructured Volume-of-Fluid (VoF)/Lagrangian-spray (LSP) framework to conduct high-fidelity simulations of the breakup and atomization processes in a realistic gas-turbine hybrid air blast atomizer. Conditions corresponding to lean blowout are considered in this study to assess the capabilities of the current model under very low liquid Webber number. Simulation results for pilot injection with POSF 10264 Cat-A1 fuel are presented. Fuel droplet statistics are compared to available experimental data measured utilizing phase Doppler particle analyzer (PDPA) systems.

Experimental Setup

Measurements of a Parker-Hannifin hybrid airblast injector that were performed at Purdue University for different aviation fuels and operating conditions. Argon ion laser (488 nm and 514.5 nm) was used with a 400 nm transmitter focal length and a 310 nm receiver focal length. Extinction tomographic measurements using an optical patternator were used to measure the liquid surface area per unit volume. The experimental setup is shown in Figure 9. The hybrid atomizer consists of a low flow number (FN = 4) pressure swirl pilot nozzle and a circuit of five main injectors at a flow number of 15. The hybrid air blast atomizer takes advantage of both the pressure swirl injector at low fuel-flow rates and air blast atomization at high fuel flows. The atomizer has a 90 degree spray angle. The target condition considered in this study is of 100% pilot injection with the PSOF 10264 Cat-A1 fuel at ambient conditions. The fuel pressure drop is 25.4 psi with a mass flow rate of 20.15 lb/hr, and the ambient conditions are 14.7 psi and 60 F. This fuel pressure drop and mass flow rate correspond to the lean blowout conditions where the fuel spray has a very low liquid Webber number.

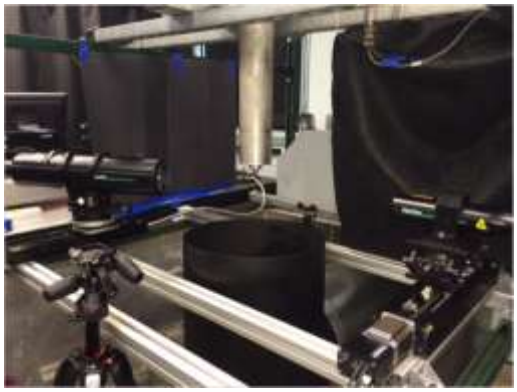

Figure 9: Experimental Setup

Numerical Solver

In this study, a VoF-method coupled with a LSP-framework is adopted. The incompressible Navier-Stokes equations for immiscible, two-phase flows are solved to describe the flow field. Density and viscosity are assumed to be constant within each phase, and can be expressed as a function of the volume of fluid. The Piecewise-Linear Interface Calculation (PLIC) scheme is adopted, which has advantages in conserving the mass and constructing monotone advection schemes. The overall VoF-scheme is geometric and unsplit, enforcing exact mass conservation on unstructured grids. The VoF-method is coupled to the LSP-framework to describe the secondary breakup dynamics, which cannot be fully resolved using available computational resources. The Lagrangian particle method is applicable to droplets with small local Weber numbers in the subsequent breakup and atomization processes. In this manner, the primary breakup and the subsequent atomization can be modeled efficiently. The subgrid stresses in the LES-approach were described using a Vreman model. For the LSP-method, the liquid droplet motion is simulated using the Basset-Boussinesq-Oseen (BBO) equation with shear force, Basset force and added mass neglected. The secondary breakupof Lagrangian particles into smaller drops, which was shown to be important, is modeled by a stochastic breakup model.

Geometry and Mesh Generation

The computational domain is shown in Figure 10 with zoomed view of the near nozzle region. To provide an accurate description of the primary break-up dynamics and cone-angle, a portion of the injector nozzle is included. All the geometry used in the simulation is the same as the geometry provided by Parker-Hannifin. The injector nozzle has three feeding slots, which serve as inlet boundary conditions in the simulation. According to the mass flow rate in the experiments, the inlet velocity at each feeding slot is set to 12.4 m/s. A swirl chamber is located upstream of the discharge orifice. The discharge orifice of the pilot injector has a diameter of D = 1.31 mm, and the feeding slots have diameters of 0.33 mm. The computational domain is described by a cylinder with 300D diameter and 150D height. The geometry of the air-box and the center-cap used to install the injector are also included in the computational domain to have a better description of the recirculation region outside the injector. No-slip boundary conditions are applied to the walls inside the pilot injector, the walls of the air-box, and the upper face of the cylinder. Convective outflow boundary conditions are applied at all other walls of the cylinder.

Results and Discussion

The simulation was first performed without LSP model. Once the flow-field is statistically stationary with regard to the VoF field, the LSP was activated for the modeling of the subsequent secondary breakup and atomization processes. Figure 11 displays representative simulation results for two different view angles. The iso-surface of the VoF-interface is shown in green, displaying the liquid sheet and the liquid ligaments. Lagrangian particles are shown in blue and the size of the particles are scaled by the droplet diameters. It can be seen that the liquid fuel is discharged from the nozzle exit in the form of a conical hollow liquid sheet due to the swirl provided by the atomizer. As the liquid sheet expands, perforations are formed and the liquid sheet deforms into liquid ligaments. At these low Weber number, the main mechanism for the breakup of the liquid fuel spray is the hydrodynamic instability within the liquid sheet rather than external aerodynamic forces. This is also found in the current study that there is little interaction between the liquid sheet and the surrounding air and the turbulence level is low in the velocity field. Finally, the liquid ligaments further break up and disintegrate into fuel droplets, which are represented as Lagrangian particles in the simulation. The operating conditions are representative of

lean blowout conditions. As consequence, the primary breakup of the fuel droplets do not experience a secondary breakup because the shear forces between the fuel droplet and air is so small that the local droplet Weber number is on the order of unity. The numerical simulation qualitatively captures essential features of the breakup and atomization processes for the pilot pressure-swirl atomizer under the conditions considered, demonstrating the capabilities of the current modeling technique.

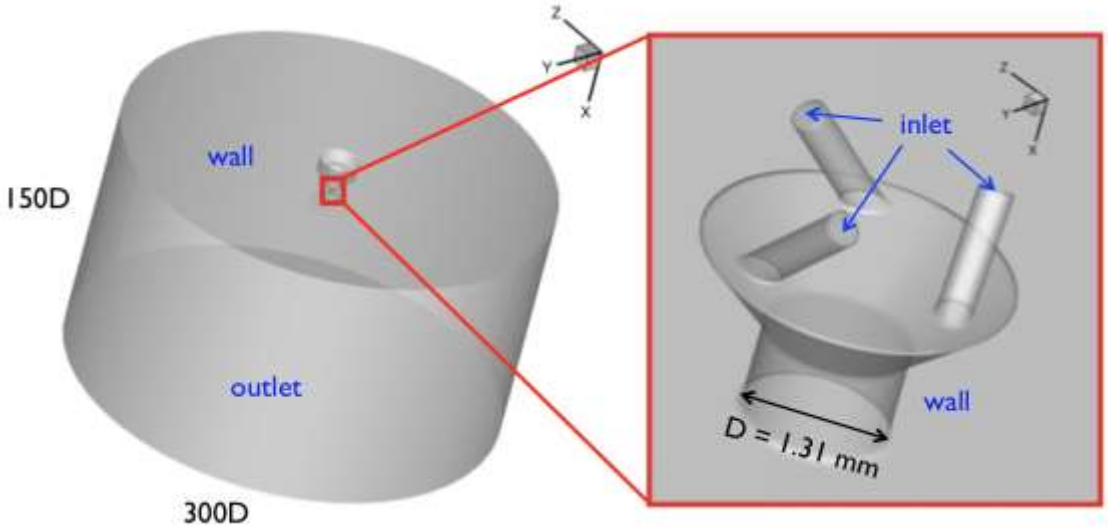

Figure 10: Computation domain and boundary conditions. Left: Shows the whole computational domain and the right gure shows zoom-in view of the injector nozzle region.

Figure 12 shows simulation results and experimental results next to each other for comparison. The instantaneous experimental image was taken from high-speed camera. The simulation results show a VOF iso-surface, augmented with Lagrangian particles scaled by droplet size. From this figure, it can be seen that the spray angle predicted by the numerical simulation is about 90 degree which is in good agreement with experiment. However, the breakup length predicted by the simulation is shorter than the experiment. The early breakup in the simulation is believed to be due to the stringent mesh resolution requirement needed for this low Weber number conditions. The liquid sheet thickness right before breakup can be as thin as 4 μm while the minimum resolution of the computational mesh is about 26 μm. To resolve the thin liquid sheet, typically at least 4-6 grid points are needed. Moreover, the low Weber number condition also yields a long liquid sheet that requires resolution. All these restrictions introduce signifant challenging mesh resolution requirements which are beyond our current available computational resources.

Figure 13 shows the fuel droplet statistics collected from the simulation at the measurement plane which is 20 mm below the nozzle exit. Figure 13(a) shows the droplet size distribution at the measurement plane along with the log-normal and Rosin-Rammler fit to the simulation results. It can be seen that the droplet distribution seems more like a log-normal distribution and has a peak at slightly below 100 μm. Figures 13(b) to 13(d) show simulation results of the droplet SMD and droplet velocities at the measurement plane in comparison with the experimental measurements. The simulation results are averaged in both time and azimuthal direction and then binned at different radial distances to collect the statistics. The correlation for SMD is also shown in Fig. 13(b) for comparison. In the center of hollow cone (radial distance ~ 5 mm), no droplets were found in the simulation due to the short runtime and therefore zero values are plotted in all three figures, while in the experiment droplets were collected by the PDPA system. As can be seen in Fig. 13(b), the simulation results show good agreement in the droplet size with experiment with a slightly underprediction. Both the experiment and simulation show higher SMD compared to the value predicted by the correlation. Results for the droplet axial and radial velocities also show that simulation results are in good agreement with the experimental measurements.

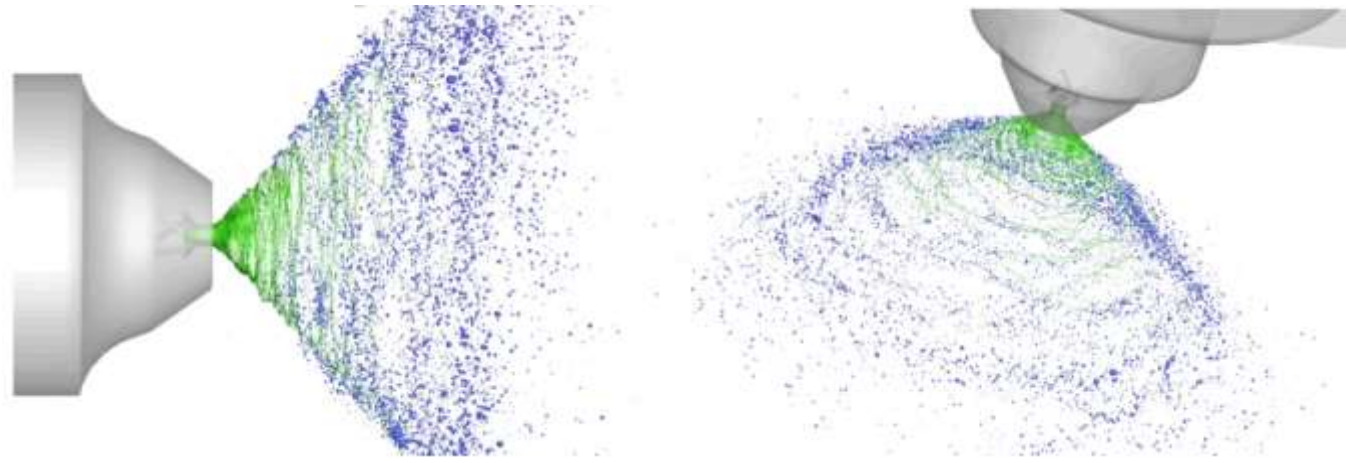

Figure 11: Representative simulation results. The iso-surface of VoF variable = 0:5 is shown in green and the Lagrangian particles is shown as blue spheres whose size is scaled based on the droplet diamter.

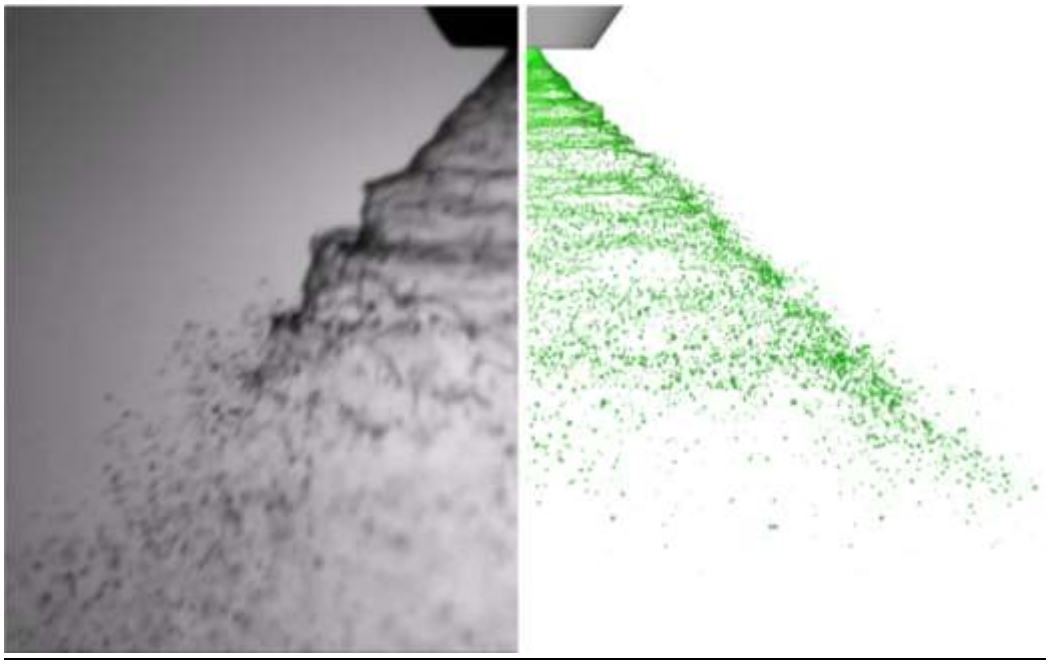

Figure 12: Comparison between numerical simulation and experiment. The image on the left was taken by high-speed camera in the experiment. Simulation results of iso-surface = 0:5 and Lagrangian particles scaled by droplet size are both colored in green shown on the right.

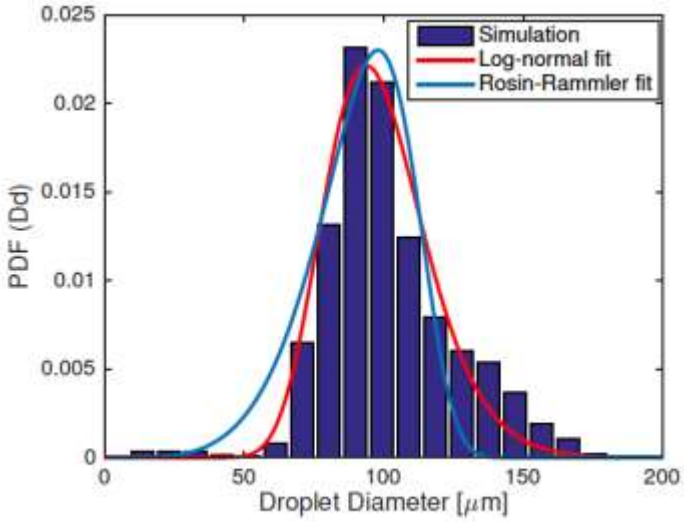

(a) Droplet size distribution.

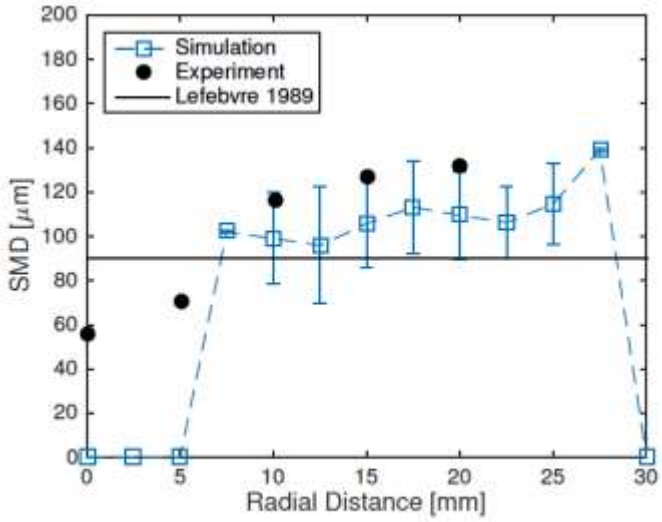

(b) Sauter mean diamter.

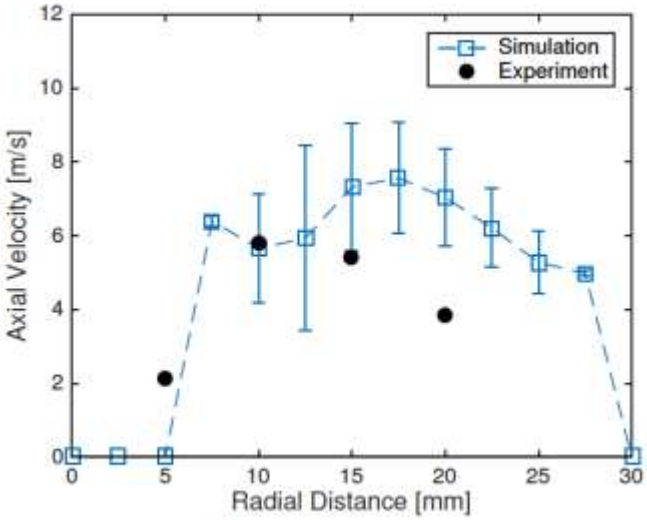

(c) Droplet axial velocity.

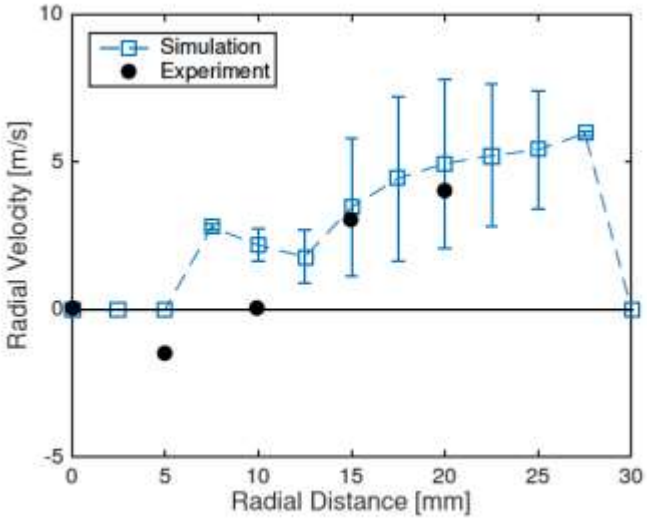

(d) Droplet radial velocity.

Figure 13: Statistics of fuel droplet at measurement plane x = 20 mm downstream the nozzle exit. Log-normal and Rosin-Rammler distributions are used to t the simulation results of the droplet diameters. Simulation results at the measurement plane are averaged in both time and azimuthal direction and then binned at dierent radial locations. One standard deviation is shown for the error bar of the simulation results.

Publications

- "High-Fidelity Simulations of Fuel Injection and Atomization of a Hybrid Air-Blast Atomizer," P. C. Ma, M. B. Nik, S. E. Carbajal, S. Naik, J. P. Gore, R. P. Lucht, and M. Ihme, presented at the 2016 AIAA SciTech Meeting, San Diego, CA, 4-8 January 2016, Paper Number AIAA 2016-1393.
- "Large-Eddy Simulations of Fuel Effect on Gas Turbine Lean Blow-out," L. Esclapez, P. C. Ma, E. Mayhew, R. Xy, S. Stouffer, T. Lee, H. Wang, and M. Ihme, presented at the 2017 AIAA SciTech Meeting, Grapevine, CA, 9-13 January 2017, Paper Number AIAA 2017-1955.
- "The role of preferential evaporation on the ignition of multicomponent fuels in a homogeneous spray/air mixture." Stagni, A., Esclapez, L., Govindaraju, P., Cuoci, A., Faravelli, T., and Ihme, M., Proceedings of the Combustion Institute, 2016, in press.
- "Group contribution method for multicomponent evaluation with application to transportation fuels." Govindaraju, P. B. and Ihme, M., International Journal of Heat and Mass Transfer, 2016, 102, 833-845.

Awards

None.

Student Involvement

PhD students Peter Ma and Pavan Govindaraju and post-doctoral fellow Lucas Esclapez are primarily responsible for the simulations and development of multicomponent evaporation models.

Project 030(A) National Jet Fuels Combustion Program – Area #6: Referee Swirl-Stabilized Combustor Evaluation and Support

Universities

- University of Dayton
- University of Illinois

Industrial Partners

- GE
- Williams International
- Honeywell
- Rolls-Royce
- Pratt & Whitney/United Technologies Research Center
- Parker Hannifin

Federal Agencies

- Air Force research Laboratory
- Air Force Office of Scientific Research
- National Aeronautics and Space Administration
- Defense Logistics Agency - Energy
- NavAir
- Department of Energy
- Army Research Laboratory
- National Institute of Standards and Technology

International Partners

- National Research Council (Canada)
- DLR (Germany)
- University of Sheffield (UK)

ASCENT Committee Member

- CAAFI
- Boeing
- Shell

Project Lead Investigator

Dr. Steve Zabarnick
Division Head, Energy and Environmental Engineering
University of Dayton Research Institute
University of Dayton
300 College Park
Dayton, OH 45469
937- 785-5349
Steven.Zabarnick@udri.udayton.edu

University Participants

University of Dayton

- P.I.: Steve Zabarnick
- Division Head, Energy and Environmental Engineering
  University of Dayton Research Institute
- FAA Award Number: 13-C-AJFE-UD, Amendment 02
- Period of Performance: December 1, 2014 to November 30, 2015
- Task(s):
  1. Referee Swirl-Stabilized Combustor Evaluation and Support.

University of Illinois at Urbana-Champaign

- P.I.: Tonghun Lee
- Associate Professor
  Mechanical Science & Engineering
- FAA Award Number: 11757359
- Period of Performance: December 1, 2014 to November 30, 2015
- Task(s):
  1. Optimize and apply laser diagnostics for application in the Referee Combustor.

Project Funding Level

University of Dayton:
Funding Level: $209,949.00
Cost Share: NRC Canada

University of Illinois at Urbana-Champaign:
Funding Level: $140K
Cost Share: In-kind academic time of the PI, Lab renovation cost by department for diagnostics work

Investigation Team

University of Dayton

Dr. Steve Zabarnick- Team Leader
Dr. Scott Stouffer- Referee Combustor Lead Engineer
Dr. Matt Dewitt- Lead for Emissions
Tyler Hendershott- Referee Combustor Engineer
Jeff Monfort- Graduate Student- Thermo-Acoustics Research Engineer

University of Illinois at Urbana-Champaign

Eric Mayhew -Graduate Student-Execution of laser and optical diagnostics.
Rajavasanth Rajasegar -Graduate Student-Optimization of laser diagnostics strategy.
Stephen Hammack -Graduate Student-Execution of laser and optical diagnostics

Project Overview

This project will develop, conduct, and analyze combustion experiments for alternative jet fuels in the National Jet Fuel Combustion Program's referee combustor.

The effort involves rig testing of combustion parameters as well as implementation of advanced laser and optical measurements in the referee combustor to provide insight into details of the combustion process and provide data for new

predictive combustion models under ASCENT Project 028. The goal of this research is to simplify alternative fuel certification procedures by reducing the need for full-scale engine testing. It is part of the National Jet Fuels Combustion Program and will satisfy Area #6, Referee Swirl-Stabilized Combustor Evaluation and Support.

Task 1: Referee Swirl-Stabilized Combustor Evaluation and Support

University of Dayton

Objective(s)

The main objective of this work is to work with AFRL, the OEM rig committee, and the other team areas of the NJFCP to obtain and interpret the combustor operability for alternative fuels. Specific operational characteristics examined include lean blowout (LBO), combustor stability, and ignition. One of the major purposes of this initial phase was to determine if the facility could be used to determine differences in the operational characteristics between different fuels. In addition to these overall measurements we will also acquire, in cooperation with University of Illinois at Urbana-Champaign, high quality optical diagnostic measurements, which will be passed on to the modeling groups within the NJFCP

Research Approach

Initial Shakedown of the referee combustor rig

The referee combustor is located at the Air Force Research Laboratory (AFRL). The referee combustor is shown in operation in Figure 1. The combustor incorporates many of the features of current state of the art combustor including a realistic swirler and two stage nozzle, dilution holes, and effusion cooling. At the start of the project the referee combustor had just become operational. We worked in collaboration with the OEM rig committee of the NJFCP to identify means for improving the combustor, combustor facility, and test methods for lean blowout tests. As a result of these collaborative efforts many improvements were made to the referee rig including:

1. Improvements in the air temperature, fuel temperature, and back pressure control.
2. Automatic control of fuel ramping rate during LBO experiments.
3. Improvements in light off and flameout detection.
4. Refinements to the dome cooling.

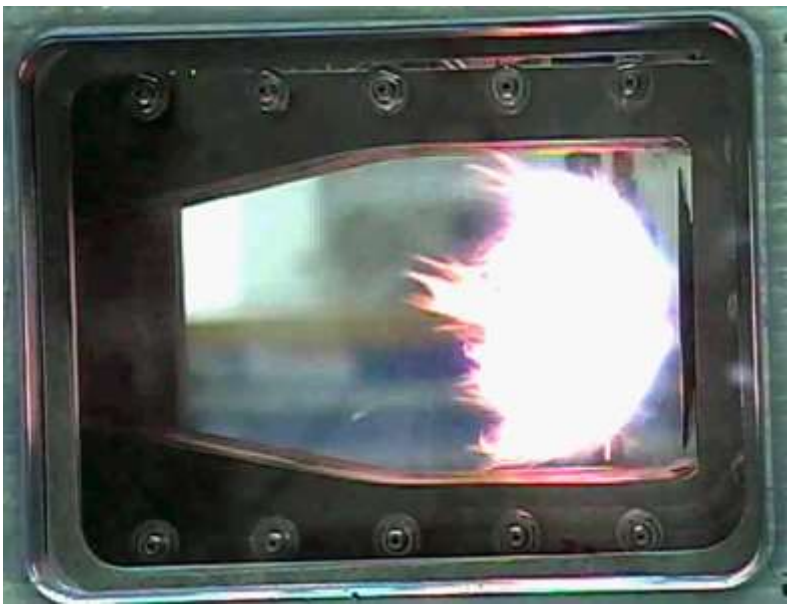

Figure1. Referee combustor during operation.

For the lean blowout experiments a method based on the use of syringe pumps was used to improve the fuel control. Figure 2 shows the fuel flow rate vs time for three successive tests. The close control of fuel flow rate was an essential element of the improvement of the LBO results.

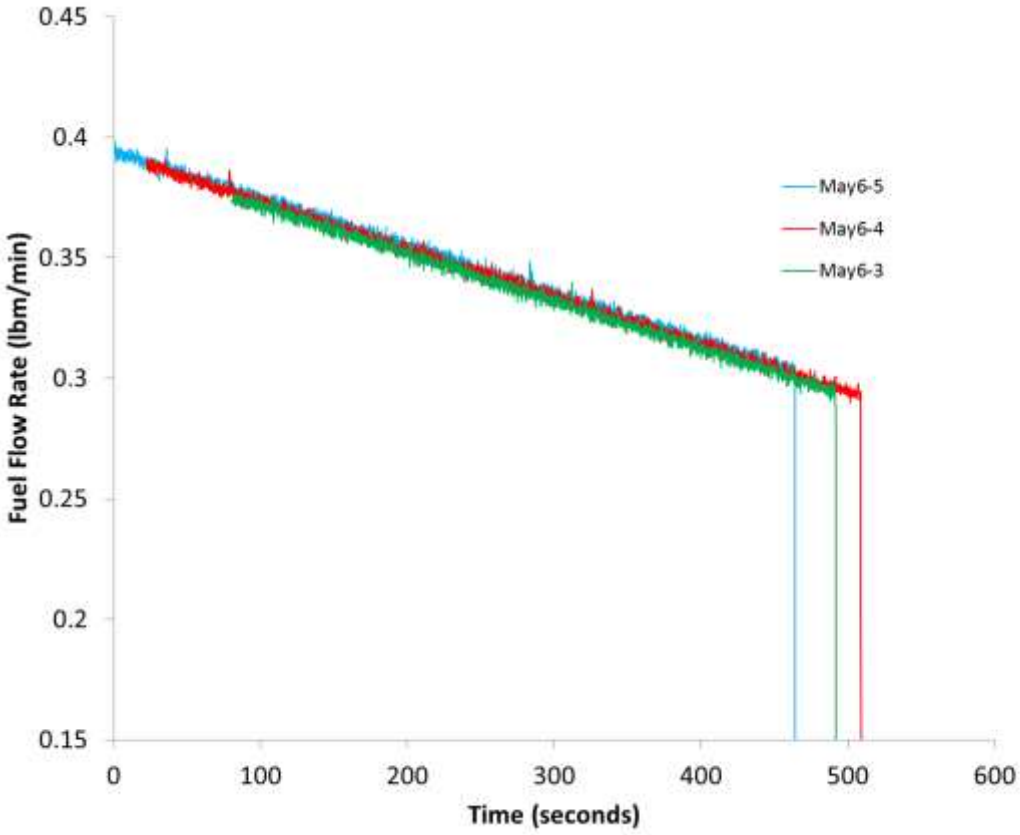

Figure 2. Fuel Ramping Employed during LBO Experiments

During this phase of the experiments we also characterized the acoustic response of the combustor and it was determined that acoustics coupling with the facility was not a factor near lean blowout.

An initial series of LBO experiments was conducted for the fuels. The experiments were showed significant differences in the ignition characteristics of some of the fuels. Differences in the LBO characteristics of the system were not seen during the initial experiments. Further refinements were made on the fuel system which resulted in greatly reduced scatter in the LBO measurements, allowing fuel effects to be seen in the LBO experiments.

We also conducted cold flow experiments of the measurements of the effective areas of the combustor parts (dilution jets, effusion cooling holes, swirler passages), and passed this data onto the modeling groups.

LBO measurements and Optical Diagnostic measurements

With the refinements in the fuel system completed we determined LBO data for the down selected fuels. We also worked with the University of Illinois and the AFRL team to obtain temperature measurements, high speed images, shadowgraph images, and chemiluminescence of the OH*, C_2* and CH^*.

Milestone(s)

Proposed (3 months): During the first quarter we will transition geometry to the modeling teams.

Achieved: The combustor design information transferred to the modeling teams

Proposed (6 months): During the second quarter we will finish the shake-down and characterization experiments for the facility.

Achieved: Initial shakedown experiments were completed with the fuels.

Proposed (9 months): Conduct Lean blowout experiments and begin diagnostics experiments

Achieved: Lean Blowout experiments conducted and optical diagnostics experiments started

Proposed (12 months): Finish initial phase of optical diagnostics experiments

Achieved: In progress to transition all data to modelers.

Major Accomplishments

After refinement of the rig we conducted LBO experiments on the pilot nozzle circuit for the downselected fuels. The shakedown phase of this experiment resulted in improvements in test methods and reduction of data scatter. Figure 3 shows the overall equivalence ratio at lean blowout for the experiment at the experiment at 3%. The results clearly show differences in the lean blowout point between the C-1 and the other three fuels. The results show that the referee rig and combustor is sensitive enough to show fuel effects on LBO.

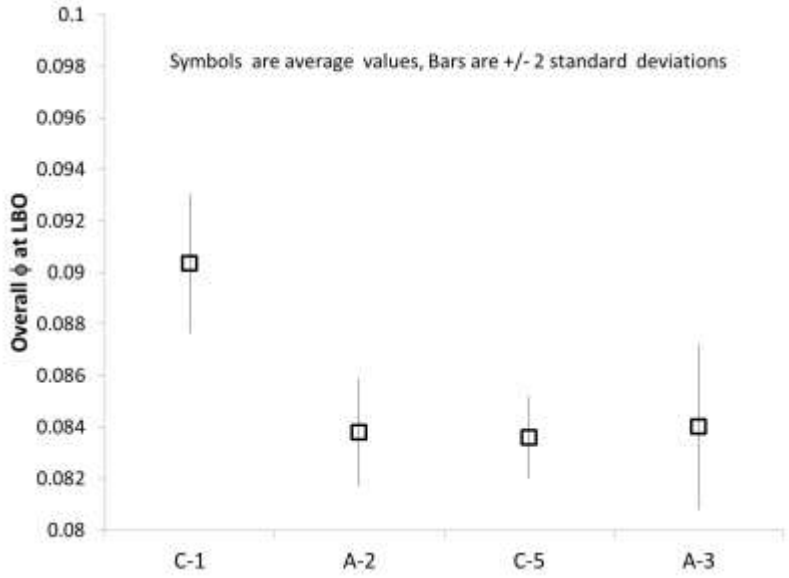

Figure 3. Lean Blowout Data measured at dome ΔP =3%, T_{air} = 250˚F, T_{fuel}= 120˚F

During the LBO measurement campaign we discovered differences in ignition characteristics of the fuels. A detailed ignition experiment was not attempted yet the differences in the ignition characteristics between the different fuels were evident, as shown in Figure 4. Note that the ignition data was acquired at elevated temperatures (Tair = 250°F, Tfuel = 120°F) yet even at these elevated temperatures we see the differences between the different fuels. It is expected that follow on experiments to be conducted at low fuel temperatures will show even more pronounced fuel effects on the ignition characteristics.

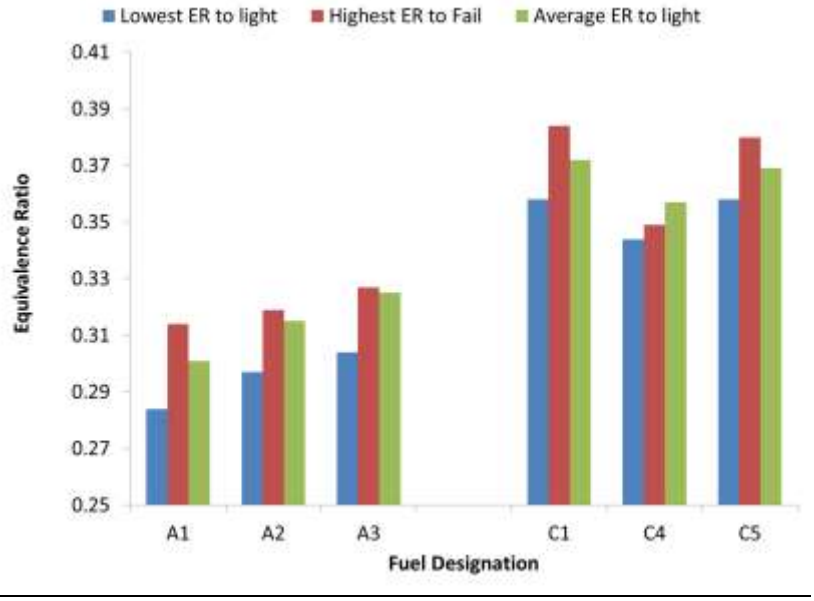

Figure 4. Ignition characteristics measured at T_{air}= 250 F, T_{fuel} = 120 F, P = 2 atm, Dome ΔP = 3%.

Optical experiments were also conducted in cooperation with University of Illinois at Urbana-Champaign, and AFRL. The results from these experiments will be discussed in the next task.

Accomplishments during the last month of the FY 15 money

Work proceeded on the cold fuel system for future cold air cold fuel experiments. We have installed the fuel heat exchanger and anticipate delivery of the fuel chiller in early 2016. We have also performed design work on the cold air capability and high altitude capability. The heat exchangers for the air system have been specified, ordered and received. We also performed preliminary air flow tests on the heat exchangers and have verified that the pressure drop through the air heat exchangers was low enough to accomplish future test objectives. We have also ordered the air chiller and the ejector.

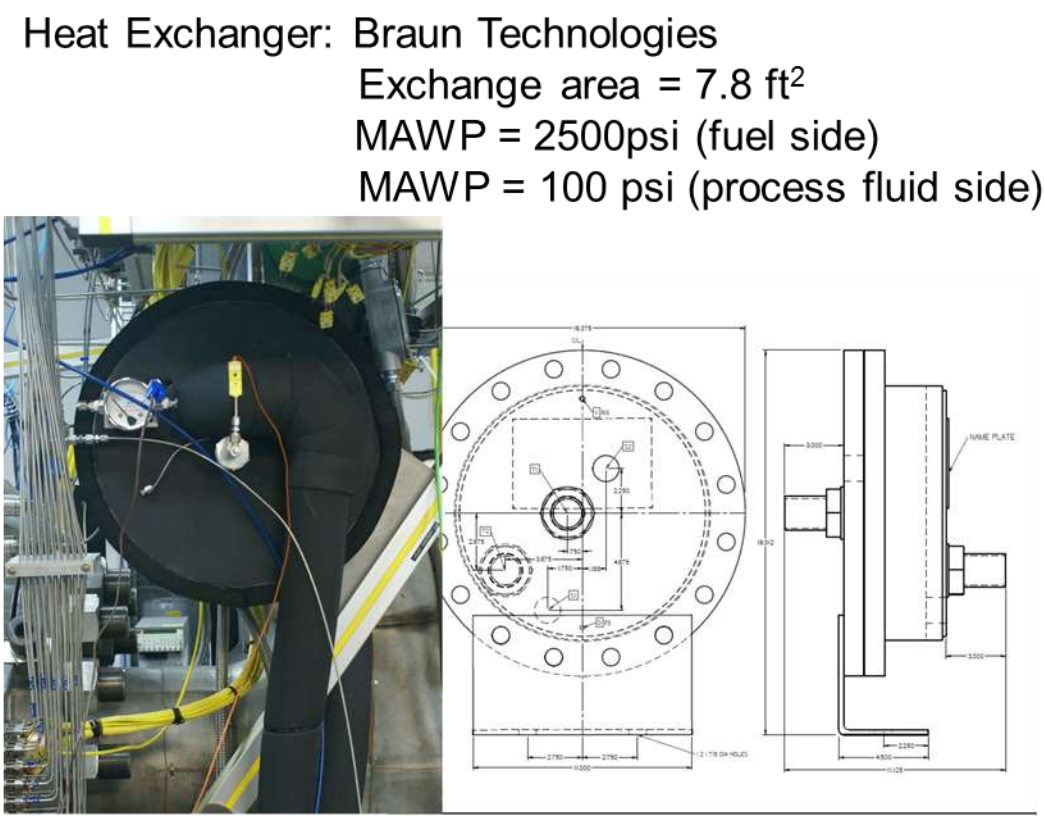

Figure 5. Details of the Fuel Heat Exchanger for Fuel Cooling

In parallel, related work we also started examining the LBO characteristics of other surrogate fuels in the same work and examined the acoustical characteristics of the fuels. Although it was not an objective of the program to explore the thermoacoustic characteristics of the various fuels, it was found that some of the fuels had higher acoustic interactions at lower equivalence ratios. In particular, the C-5 fuel was shown to have a higher acoustic pressure at lower equivalence ratios than A-1 or C-1, as shown in Figure 6.

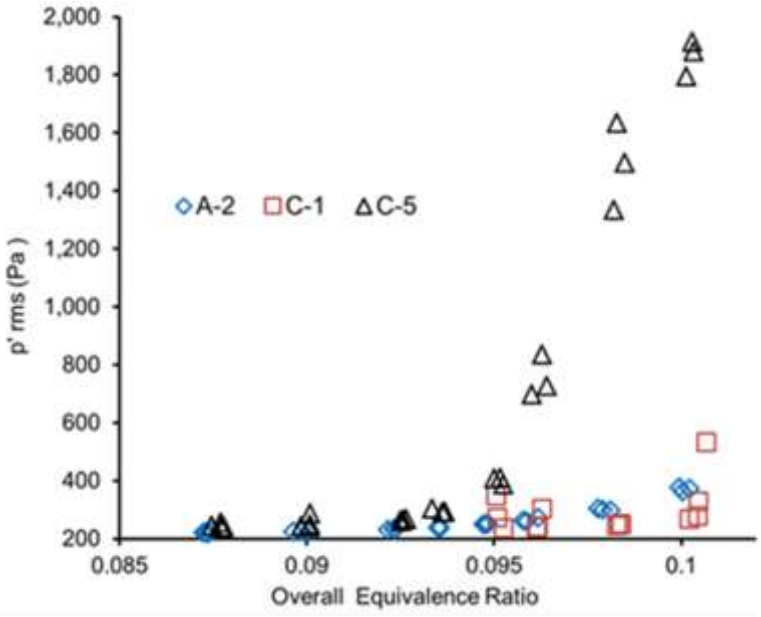

Figure 6. The Acoustic Pressure in the Referee Rig at inlet Conditions of T_{air} = 394 K, T_{fuel} =322 K, P_{comb} = 207kPa, ΔP_{dome} = 3%

Publications
None

Outreach Efforts

Poster Presentation

Edwin Corporan, Scott Stouffer, Tyler Hendershott, Chris Klingshirn, Matt Dewitt, Steve Zabarnick, Craig Neuroth, Dale Shouse, Jacob Diemer, "Initial Studies of Fuel Impacts on Combustor Operability and Emissions at the Air Force Research Laboratory", IASH 2015, the 14TH International Symposium on Stability, Handling, and Use of Liquid Fuels, Charleston, South Carolina USA, 4-8 October 2015

Awards
None

Student Involvement

Jeff Monfort – University of Dayton Ph.D. Candidate
Research – Acoustic analysis of the Referee combustor
Graduated in Aug 2015 with Ph.D. in Mechanical Engineering
Currently employed by University of Dayton

Plans for Next Period

No further FAA funding was received for a second year, but AFRL has funded continued work in this area. Plans for the next year include more refined ignition experiments with cold fuel. We will also be developing the cold air and low pressure (altitude simulation) capability for future experiments. The LBO characteristics of the fuels will also be explored on the main circuit of the nozzle.

Task 1 – Optimize and apply laser and optical diagnostics for application in the Referee Combustor

University of Illinois at Urbana-Champaign

Objective(s)

The main objectives of the work in this proposal are to work with UDRI and AFRL in carrying out diagnostics measurements for the referee combustor. The following tasks will guide this collaboration:

- Identify the operating conditions and key parameters for detection in the referee combustor
- Evaluate and modify the referee combustor at AFRL for laser and optical diagnostics
- Design laser and optical diagnostics setup and assist in the fuel screening process
- Analyze data and pass on data to modeling groups in combustion program

Research Approach

Diagnostics Optimization and Setup

The main goal here is the development of multi-phase high-speed diagnostics using 2D imaging to understand the combustion instabilities at the operational boundaries and flame dynamics. The goal will be to apply selected measurements from PLIF, PIV, and/or chemiluminescence (10 to 50 kHz). Additional high fidelity measurements from AFRL may be integrated with our efforts. In both PLIF and PIV, we will look to target OH and CH radicals in the flame. When required, we may employ high power low repetition PLIF measurements to look at various other flame properties such as nitric oxide generation (226 nm, Nd:YAG pumped dye laser) and/or formaldehyde (355 nm, Nd:YAG laser). For high speed chemiluminescence measurements, we plan to utilized a series of high speed intensified cameras around the referee combustor. For the high PLIF measurements, we plan to first utilize a conventional 10 Hz PLIF laser system and ultimately move to a high speed dye laser (Sirah) pumped by a high speed diode pumped Nd:YAG (Edgewave). AFRL is in possession of a 200 W Edgewave system which may be deployed for the studies. Energy per laser pulse at these conditions maybe small (~30 μJ/pulse) and light collection from the PLIF will be enhanced using a f/1.8 UV lens from Cerco.

Quantification of the LIF Signal and Light Sheet Integration

To ensure that the signal is fully quantified, we set out to build and calibrate a small scale flat flame burner for use in the referee rig. The combustor will be fully calibrated at Illinois using a combination of laser absorption and multi-line nitric oxide LIF thermometry. By calibrating the intensity of the setup with the flat flame combustor, we can assess first order values for concentration of radical concentrations in the flame. One critical issue in the referee combustor is to insert a light sheet into the combustion chamber itself as there as only side windows for detection and no top view or bottom view window for propagation of the laser sheet.

Milestone(s)

Milestones from Each Period

Proposed (3 Month): At the 3 month mark, we will conclude the analysis of the experimental setup and start to modify the optical access of the referee combustor. Simultaneously, we will pursue development of the diagnostics with AFRL.
Achieved: Design of the laser setup complete and fabrication of calibration torch started. Construction on a mockup of the referee combustor begins at Illinois to test out the laser sheet feasibility.

Proposed (6 Month): At the 6 month mark, we should be well into building the experimental setup and modification of the referee combustor for optical access. We should also have made considerable progress in optimization of the CH PLIF strategy in the laboratory as well as commenced in the development of 50 kHz PLIF of OH for deployment in the referee combustor. Preliminary fuel screening measurements using high speed chemiluminescence will be carried out during this phase.
Achieved: CH PLIF is demonstrated at AFRL in a separate lab and is ready for deployment. 50 kHz OH PLIF is also ready for deployment. Measurement plans are pushed back slightly to accommodate for fuel screening in the referee combustor. Design of a multi-species chemiluminescence and shadowgraph setup commences.

Proposed (9 Month): At the 9 month mark, we should have completed the combustor optical access modifications and

also conducted an initial shakedown of the tests. The diagnostics setup should also be completed and tested. We will start to share diagnostics data with other groups, notably 2, 4, and 6.
Achieved: Chemiluminescence measurements of C_2, OH and CH along with shadowgraph measurements of the fuel spray in a cold flow are completed.

Proposed (12 Month): At the 12 month mark, we should have obtained an initial set of data for the 10 Hz OH PLIF. Depending on the progress we may also have some preliminary data set for 10 and/or 50 kHz OH PLIF. We should be fully prepared to implement high speed PLIF measurements for year 2.
Achieved: Data analysis of the chemiluminescence measurements to begin. Test of the light sheet insertion in the referee combustor to begin.

Major Accomplishments

During July 2015, 10 kHz shadowgraph was implemented on the Area 6 referee rig with the primary objective of obtaining the fuel spray cone angle. Shadowgraph images were taken of steady state combustion for each of the C-1, C-5, and A-2 fuels over a range of equivalence ratios. For the C-1 fuel, the equivalence ratios tested were: 0.1, 0.098, 0.096, and 0.095. For the C-5 and A-2 fuels, the equivalence ratios tested were: 0.1, 0.098, 0.096, 0.095, 0.0925, 0.09, and 0.0875. All of the data was taken with an air temperature of 250 °F, fuel temperature of 120 °F, combustor pressure of 30 psia, and a ΔP of 3%. Fuel spray tests were also conducted without combustion over the same range of equivalence ratios; a representative set of shadowgraph images of the fuel spray tests are shown in Figure 1. The images taken are currently being processed to obtain spray cone angle and RMS intensity along the centerline and at the edge of the spray.

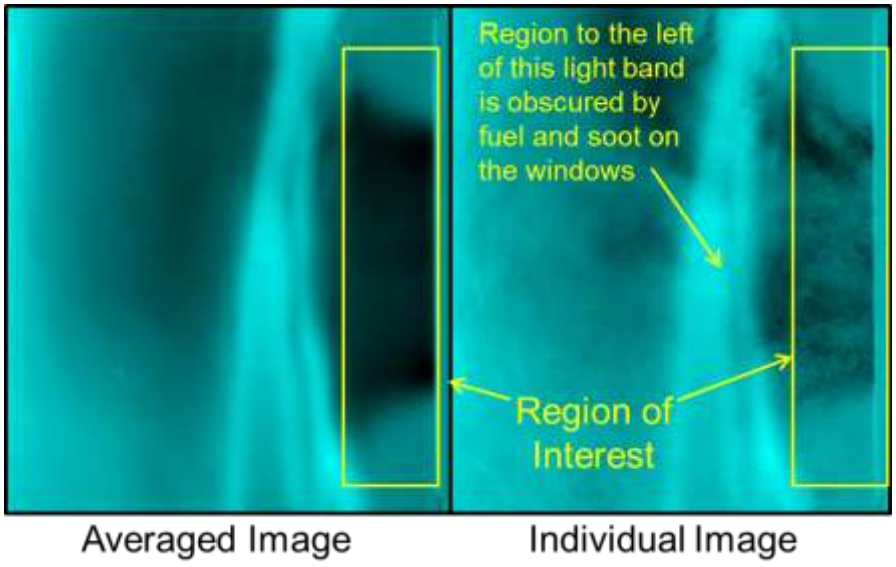

Figure 1 Sample shadowgraph images of an A-2 fuel spray test

During the same measurement campaign, 10 kHz OH*, CH*, and C_2* chemiluminescence images were taken at the same combustion conditions as the shadowgraph images described above. The chemiluminescence was captured using a Photron SA-5 intensified with a LaVision High Speed IRO with a Cerco f/2.8 UV lens. The OH* chemiluminescence was captured by using a Semrock Brightline 320/40 bandpass filter, the CH* chemiluminescence was captured using a Semrock Brightline 427/10 bandpass filter, and the C_2* chemiluminescence was captured using a Semrock Brightline 494/20 bandpass filter. The white vertical stripe shows sooting on the windows of the combustor during these runs, showing the difficulties of running in an actual combustor with real kerosene fuels.

Through discussions in the diagnostics subcommittee, several aspects of the data will be analyzed and transferred over to the modeling groups in the first pass. These include the angle of the spray as shown by the cold shadowgraph images as well as the OH* and CH* chemiluminescence signals. Additionally, we will provide contours of the OH generated in the flame as well as some relative intensities between the various chemiluminescence signals. This type of data will enable the modeling teams to anchor their models and in particular to ensure that the flow characteristics of their

simulations are accurate. All the information will be placed on a grid system so that the PIs can ensure that their computations are to scale. Sample images of OH*, CH* and C_2* are shown in Figure 2.

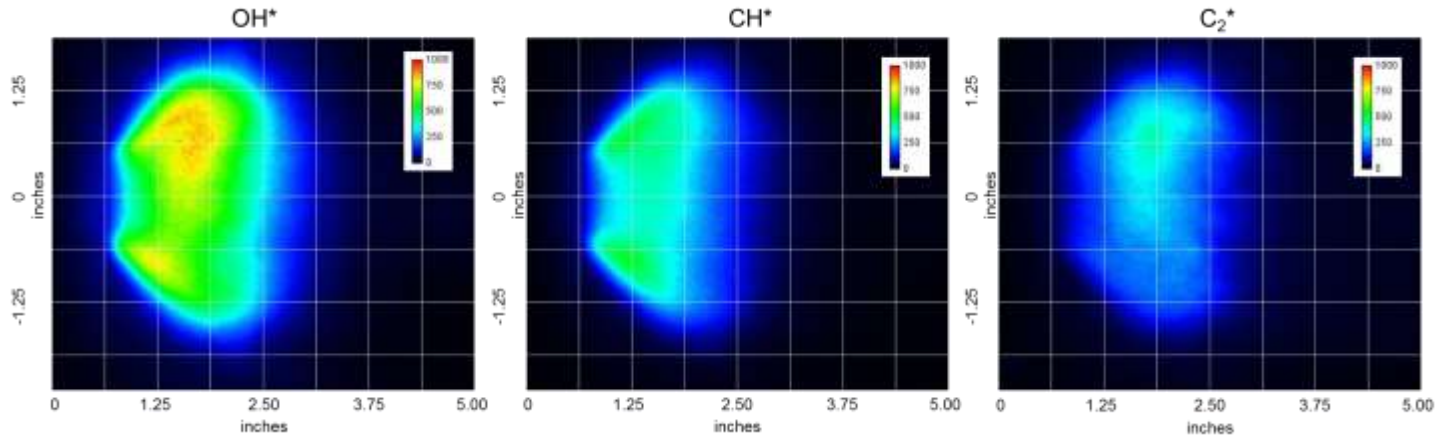

Figure 2 Representative averaged chemiluminescence images of OH*, CH*, and C_2* of the C-5 fuel at an equivalence ratio of 0.096

In addition to the analysis of the data, significant effort was made to develop a method of inserting a laser sheet into the referee combustor using optical engineering. As noted above, the referee combustor does not have top or bottom windows for inserting a laser beam and therefore require creative means for both pitching of the laser sheet into the combustor as well as detection. Several methods were proposed and two are shown in Figure 3. During this year, a mockup SLA of the referee combustor was constructed at Illinois and these light sheet integration methods were tested. They are expected to be integrated into the actual referee combustor in the following years.

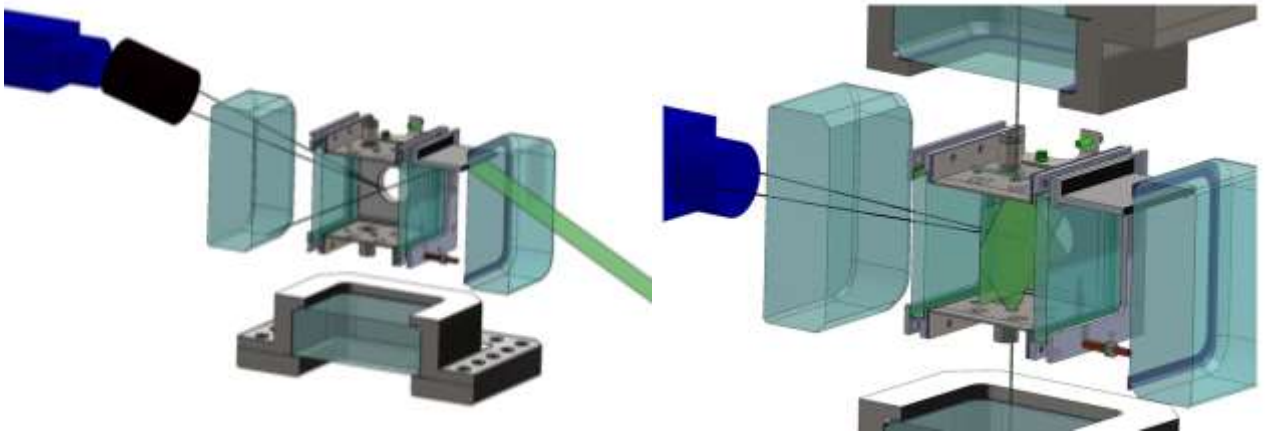

Figure 3 Methods of light sheet integration to the referee combustor. Left side shows a sheimpflug setup coupled with a reflected beam while the right shows the rapid expansion of a single beam.

Publications

None

Outreach Efforts

None

Awards
None

Student Involvement
Three graduate students (listed above) have participated in this project on a rotational basis to address various aspects of the project. Rajavasanth designed and fabricated the calibration burner to be used in the referee combustor, and conducted experiments to determine the actual concentration of radical concentrations in the flame. Two other students (Stephen Hammack and Eric Mayhew) made multiple trips to AFRL to make test measurements in the high shear combustor. This included assisting in the setup of the laser and optics as well as participating in the actual measurements.

Plans for Next Period
In year II of the NJFCP, an effort will be made to fully integrate the laser sheet in the referee combustor. We also expect to continue assisting in their effort to take images in the referee combustor and analyze the data. The high speed laser systems are already at AFRL and will be ready for deployment when we can find a window of run time in the referee combustor. Finally, we will assist with quantification of the referee combustor using the calibration torch built for this project at the University of Illinois.

Project 030(B) National Jet Fuels Combustion Program, Area #6: Referee Swirl-Stabilized Combustor Evaluation/Support

University of Dayton Research Institute
University of Illinois

*this report covers portion of University of Illinois

Project Lead Investigator

Tonghun Lee
Associate Professor
Mechanical Science & Engineering
University of Illinois at Urbana-Champaign
1206 W. Green St.
Urbana IL 61801
517-290-8005
tonghun@illinois.edu

University Participants

University of Illinois at Urbana-Champaign

- P.I.(s): Tonghun Lee, Associate Professor
- FAA Award Number: 13-C-AJFE-UI-004
- Period of Performance: 10/1/2015 to 11/30/2015 (Report for period of 2016 only)
- Task(s):
    1. Optimize and apply laser diagnostics for application in the Referee Combustor.

Project Funding Level

Funding Level: $140K (entire period of 12/1/2014 to 11/30/2015)
Cost Share: In-kind academic time of the PI, Lab Renovation Cost by Department for Diagnostics Work

Investigation Team

- Eric Mayhew (Graduate Student, University of Illinois at Urbana-Champaign): Execution of laser and optical diagnostics at GATech.
- Rajavasanth Rajasegar (Graduate Student, University of Illinois at Urbana-Champaign): Optimization of laser diagnostics strategy.
- Stephen Hammack (Graduate Student, University of Illinois at Urbana-Champaign): Execution of laser and optical diagnostics at GATech.

Project Overview

The goal of this study is to develop, conduct, and analyze advanced laser and optical measurements in the referee combustor (WPAFB, Bldg. 490, RC 152) selected by the ASCENT National Fuel Combustion Program. We will conduct advanced spatially resolved high-speed Planar imaging as well as other advanced diagnostic measurements which can provide insight into the physicochemical response of the combustion process for various alternative fuels. Moreover, the results will provide data for development of new predictive combustion models in ASCENT. Once fully characterized, the standard referee combustor rig can streamline and simplify fuel certification procedures outlined in the ASTM D4054 (Standard Practice for Qualification and Approval of New Aviation Turbine Fuels and Fuel Additives) through minimization of full-scale engine testing.

Task 1 – Analysis of laser and optical diagnostics measurements in the Referee Combustor

University of Illinois at Urbana-Champaign

Objective(s)

The main objectives of the work in this proposal are to work with UDRI and AFRL in carrying out diagnostics measurements for the referee combustor. The following tasks will guide this collaboration:

- Identify the operating conditions and key parameters for detection in the referee combustor
- Design laser and optical diagnostics for chemiluminescence imaging of radicals
- Analyze data and pass on data to modeling groups in combustion program

Research Approach

Diagnostics Optimization and Schlieren Imaging

During October 2017, Schlieren imaging was conducted on the swirl-stabilized referee combustor. We used a standard Z-configuration with a narrowband LED (~440 nm center wavelength, ~20 nm FWHM) focused through an aperture. This wavelength region is chosen to avoid the major chemiluminescence peaks (OH* at ~310 nm, CH* at ~430 nm, and C_2* at ~516.5 nm) and the broadband emission (particularly of A-2). Two 6-inch diameter mirrors collimated and then focused the light onto a knife-edge and then into a Photron SA-Z. Figure 1 shows a picture of the experimental setup with the light source on the near side and the camera on the far side. Imaging of the non-combusting flow was conducted at 2 kHz, and the combusting flow was imaged at 10kHz. The non-combusting imaging is conducted at 3 different swirler pressure drops: 2, 3, and 4.5 percent. The combusting imaging is conducted, where possible (due to lean blowout restrictions) at global equivalence ratios: 0.096 (A-2 and C-1), 0.092 (A-2 and C-1), and 0.086 (A-2 only), all with swirler pressure drop and combustor pressure held constant.

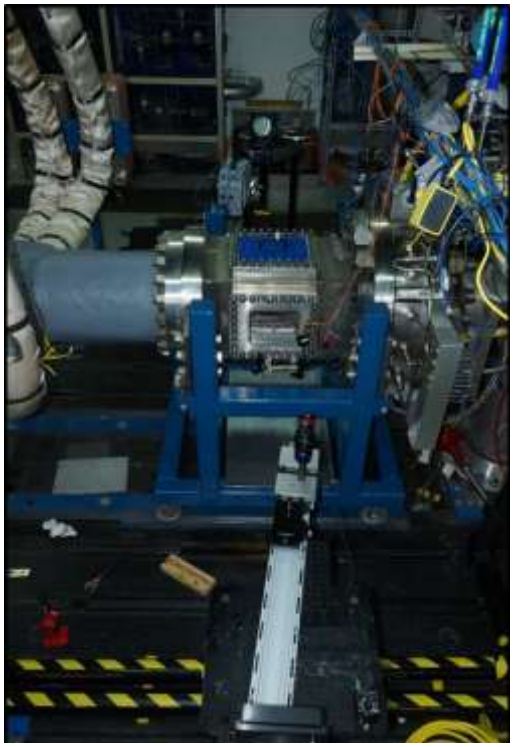

Figure 1: Picture of the Schlieren imaging setup spanning the swirl-stabilized referee combustor at AFRL.

Milestone(s)

Milestones from Each Period

Analysis Period (Final 2 Month): For the final 2 months, we will begin preliminary analysis of the imaging conducted in October.

Achieved: We completed preliminary analysis with averaged images and calculations of the measured dilution jet angles shown below.

Major Accomplishments

In the last, two months we have completed a preliminary analysis of the Schlieren imaging conducted in October. The primary interest of this first analysis was the issue of 1) whether the primary dilution jets bent, 2) by how much, and 3) whether there was significant dilution jet flapping. Schlieren begins to answer these questions as the imaging marks density gradients in the test section; some of the strongest density gradients are due to the relatively cold dilution jets impinging on the main flow. To help answer the first two questions, 3,000 images at each condition are averaged (more than 35,000 images were taken for combusting cases). In the averaged image, the peak count intensity along the dilution jet stream is used to mark the center of the jet at each point moving from the outside of the combustor to the inside of the combustor. A liner regression fit on the points is conducted to obtain the average angle.

As seen in Figure 1 (left), even the non-combusting case shows an average dilution jet bending of about 14˚ on the top half of the combustor and 10˚ on the bottom half of the combustor for a swirler pressure drop of 3 percent. The combusting cases all demonstrated greater dilution jet bending than the non-combusting cases as seen in Figures 2 and 3.

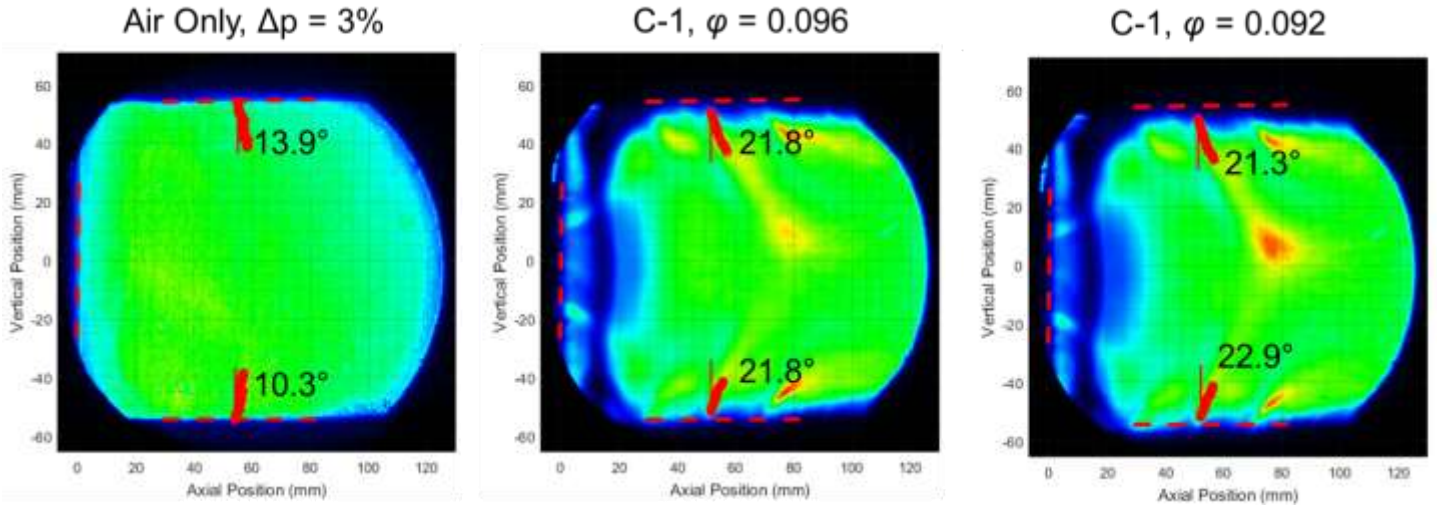

Figure 2: Average of 3,000 instantaneous Schlieren images with the measured dilution angles for air only (left) with a swirler pressure drop of 3 percent, C-1 at a global equivalence ratio of 0.096 (center), and C-1 at a global equivalence ratio of 0.092.

Figures 2 and 3 both show that there is very little variation in the dilution jet angles across equivalence ratios. The averaged images for A-2, shown in Figure 3), reveal that some of the asymmetry seen in OH* images may also be reflected in the dilution jet bending. The larger flame lobe in the lower half of the combustor, as seen in Figure 4, corresponds to greater bending in the lower half for A-2. This effect is the strongest in the φ=0.096 case with a lower bending angle of 24.5˚ and the weakest in the φ=0.086 case with a bending angle of 22˚. Analysis averaging more images to accurately pinpoint these trends is ongoing.

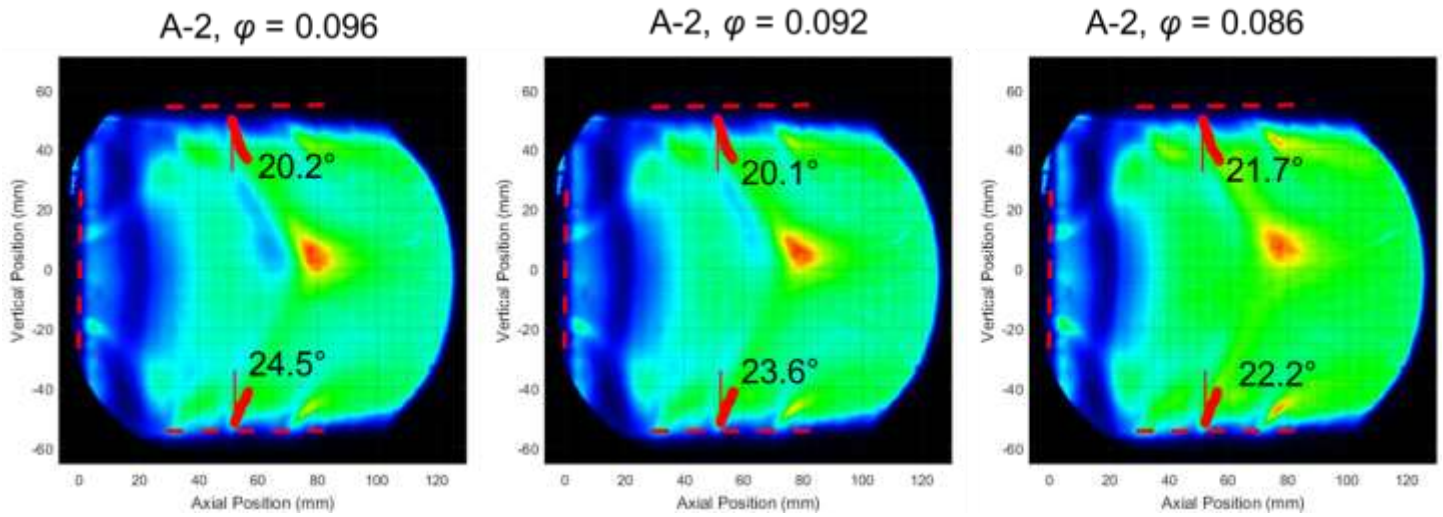

Figure 3: Average of 3,000 instantaneous Schlieren images with the measured dilution angles A-2 at a global equivalence ratio of 0.096 (left), A-2 at a global equivalence ratio of 0.092 (center), and C-1 at a global equivalence ratio of 0.086.

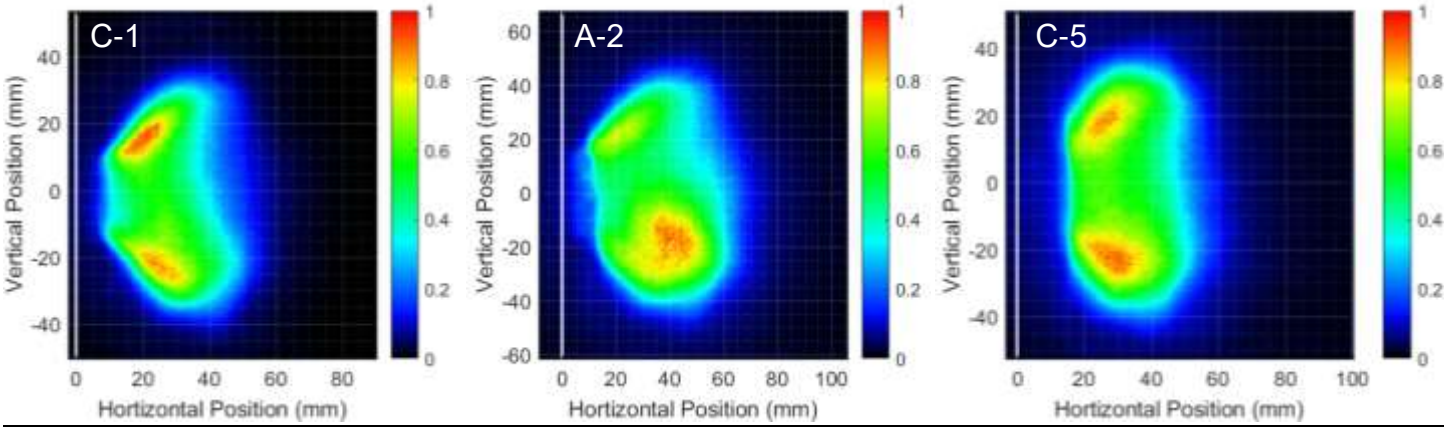

Figure 4: Averaged OH* images of the three down-selected NJFCP fuels at an equivalence ratio of 0.096

The third question of whether the dilutions jets flap has not been analyzed quantitatively, though the 10 kHz Schlieren imaging shows no visual evidence that the jets wave more than 10 degrees. Sample imaging, including the averaged images with calculated dilution jet angles, has been passed along to the modeling teams for comparison with their simulations.

Publications
None

Outreach Efforts
None

Awards
None

Student Involvement
Three graduate students (listed above) have participated in this project on a rotational basis to address various aspects of the project. Rajavasanth designed and fabricated the calibration burner to be used in the referee combustor, and conducted experiments to determine the actual concentration of radical concentrations in the flame. Two other students (Stephen Hammack and Eric Mayhew) made multiple trips to AFRL to make test measurements in the high shear combustor. This included assisting in the setup of the laser and optics as well as participating in the actual measurements.

Plans for Next Period
In year II of the NJFCP, an effort will be made to fully integrate a PDPA system in the referee combustor. We also expect to continue assisting in their effort to take images in the referee combustor and analyze the data. The PDPA systems are already at AFRL and will be ready for deployment when we can find a window of run time in the referee combustor. Finally, we will assist with quantification of the referee combustor using the calibration torch built for this project at the University of Illinois.

Project 031(A) Alternative Jet Fuel Test and Evaluation

University of Dayton Research Institute

Project Lead Investigator

Steven Zabarnick, Ph.D.
Division Head
Energy & Environmental Engineering Division
University of Dayton Research Institute
300 College Park, Dayton, OH 45469-0043
937-255-3549
Steven.Zabarnick@udri.udayton.edu

University Participants

University of Dayton Research Institute

- P.I.(s): Steven Zabarnick, Division Head
- FAA Award Number: 13-C-AJFE-UD
- Period of Performance: April 8, 2015 to March 14, 2016 – Amendment No. 6
- Task(s):
  1. Evaluate candidate alternative fuels for their performance via the ASTM D4054 approval process
- Period of Performance: April 8, 2015 to August 31, 2016 – Amendment No. 7
- Task(s):
  2. Evaluate candidate alternative fuels for their performance via the ASTM D4054 approval process
- Period of Performance: April 8, 2015 to August 31, 2017 – Amendment No. 12
- Task(s):
  3. Evaluate candidate alternative fuels for their performance via the ASTM D4054 approval process

Project Funding Level

Amendment No. 6, $309,885
Amendment No. 7, $ 99,739
Amendment No. 12, $639,928

Cost Share:
LanzaTech $55,801 (2015)
LanzaTech $381,451 (2016)

Investigation Team

Steven Zabarnick, UDRI, PI and overall coordination
Matthew DeWitt, UDRI, low temperature and combustion emissions properties
Richard Striebich, UDRI, fuel chemical analysis and composition
Linda Shafer, UDRI, fuel chemical analysis and composition
John Graham, UDRI, fuel seal swell and materials compatibility
Zachary West, UDRI, fuel properties

Project Overview

Alternative jet fuels offer potential benefits of reducing global environmental impacts, achieving national energy security, and stabilizing fuel costs for the aviation industry. The Federal Aviation Administration is committed to the advancement of “drop in” alternative fuels and has set the aspirational goal of enabling the use of 25 million gallons annually by 2018.

Successful adoption of alternative fuels requires approval for use of the fuel by the aviation community followed by large scale production of a fuel that is cost competitive and meets safety standards of conventional jet fuel. Alternative jet fuels must undergo rigorous testing in order to become qualified for use and incorporated into ASTM International Specifications.

Cost effective and coordinated performance testing capability (in accordance with ASTM D4054) to support evaluation of promising alternative jet fuels is needed. The objective of this project is to provide capability to conduct the necessary work to support alternative jet fuel evaluation of either a) to-be-determined fuel(s) that will be selected in coordination with the FAA, or b) a fuel test and evaluation project with a specific fuel(s) in mind.
The proposed program should provide the following capabilities:

- Identify alternative jet fuels (which may include blends with conventional jet fuel) to be tested and that have the potential to be economically viable and support FAA's NextGen environmental goals.
- Perform engine, component, rig, or laboratory tests, or any combination thereof, to evaluate the performance of an alternative jet fuel in accordance with ASTM International standard practice D4054.
- Identify and conduct unique testing beyond that defined in ASTM International standard practice D4054 necessary to support evaluation of alternative jet fuels for inclusion in ASTM International jet fuel specifications.
- Obtain data for baseline and alternative jet fuels to demonstrate any effects of the alternative jet fuel on aircraft performance, maintenance requirements, and reliability.
- Coordinate effort with activities sponsored by Department of Defense and/or other government parties that may be supporting relevant work.
- Report relevant performance data of the alternative fuels tested including a quantification of the effects of the alternative fuel on aircraft and/or engine performance and on air quality emissions relative to conventional jet fuel. Reported data will be shared with both the FAA (NJFCP) and the broader community (e.g. ASTM International) and with ASCENT COE Program 33 "Alternative Fuels Test Database Library."

Task 1, 2 and 3 - Evaluate Candidate Alternative Fuels for their Performance via the ASTM D4054 Approval Process

University of Dayton Research Institute

Objective(s)

Cost effective and coordinated performance testing capability (in accordance with ASTM D4054) to support evaluation of promising alternative jet fuels is needed. The objective of this project is to provide capability to conduct the necessary work to support alternative jet fuel evaluation of either a) to-be-determined fuel(s) that will be selected in coordination with the FAA, or b) a fuel test and evaluation project with a specific fuel(s) in mind.

Research Approach

The intent of this program is to provide the capability of performing specification and fit-for-purpose (FFP) evaluations of candidate alternative fuels towards providing a pathway forward through the ASTM D4054 approval process. The UDRI team possesses the capability of performing a large of number of these evaluations, and we are prepared to work with other organizations such as SwRI and engine OEM's, as needed, for their unique test capabilities. These include additional engine, APU, component, and rig evaluations. The UDRI testing capabilities cover our efforts at the laboratories of the Fuels Branch of AFRL and at our campus laboratory facilities.

The following are examples of the evaluations that UDRI is able to provide:

Tier I
1. Thermal Stability (Quartz Crystal Microbalance)
2. Freeze Point (ASTM D5972)
3. Distillation (ASTM D 86)
4. Hydrocarbon Range (ASTM D6379 & D2425)
5. Heat of Combustion (ASTM D 4809)
6. Density, API Gravity (ASTM D 4052)
7. Flash Point (ASTM D 93)
8. Aromatics (ASTM D 1319)

Tier II
1. Color, Saybolt (ASTM D 156 or D 6045)
2. Total acid number (ASTM D 3242)
3. Aromatics, (ASTM D 1319 & ASTM D 6379)
4. Sulfur (ASTM D 2622)
5. Sulfur mercaptan (ASTM D 3227)
6. Distillation temperature (ASTM D 86)
7. Flash point (ASTM D 56, D 93, or D 3828)
8. Density (ASTM D 1298 or D 4052)
9. Freezing point (ASTM D 2386, D 5972, D 7153, or d 7154)
10. Viscosity, at -20˚C, (ASTM D 445)
11. Net heat of combustion (ASTM D 4809)
12. Hydrogen content (ASTM D 3343 or D 3701)
13. Smoke point (ASTM D 1322)
14. Naphthalenes (ASTM D 1840)
15. Calculated cetane index (ASTM D 976 or D4737)
16. Copper strip corrosion (ASTM D 130)
17. Existent gum (ASTM D 381)
18. Particulate matter (ASTM D 2276 or D 5452)
19. Filtration time (MIL-DTL-83133F Appendix B)
20. Water reaction interface rating (ASTM D 1094)
21. Electrical conductivity (ASTM D 2624)
22. Standard Test Method for Thermal Oxidation Stability of Aviation Turbine Fuels (ASTM D3241)

Extended Physical and Chemical Characterization
1. Lubricity Evaluation- BOCLE test (ASTM D 5001)
2. Low Temperature Properties – Scanning Brookfield Viscosity
3. Detect, quantify, and/or identify polar species - Analyze as necessary
4. Detect, quantify and/or identify dissolved metals - Analyze as necessary
5. Initial Material Compatibility Evaluation – Perform optical dilatometry and Partition Coefficient Measurements to determine the fuel-effected swell and the fuel solvency in 3 O-ring materials (nitrile, fluorosilicone and fluorocarbon) and up to 2 additional fuel system materials
6. Experimental Thermal Stability Evaluation – Quartz Crystal Microbalance – Measure thermal deposit tendencies and oxidation profile at elevated temperatures
7. Viscosity versus Temperature – (ASTM D 445) determination of the fuels viscosity at 40˚C and -40˚C to assess the fuel's viscosity's variation with temperature

In addition to the above physical and chemical fuel evaluation capabilities, UDRI also has extensive experience in evaluation of microbial growth in petroleum-derived and alternative fuels. These evaluations include standard lab culturing and colony counting methods, as well as advanced techniques such as quantitative polymerase chain reaction (QPCR) and metagenomic sequencing. These methods allow the quantitative measurement of microbial growth rates in candidate alternative fuels in comparison with petroleum fuels.

UDRI also has extensive experience in evaluation of elastomer degradation upon exposure to candidate alternative fuels. Various methods are used to evaluate seal swell and o-ring fixture leakage, including: optical dilatometry, measurement of sealing pressure, fuel partitioning into elastomer, and a pressurized temperature controlled o-ring test device.

UDRI is also able to perform fuel-material compatibility testing using the D4054 procedures for fuel soak testing, post-exposure non-metallic and metal materials tests, and surface and microstructural evaluation. Testing of both 68 "short-list" materials and the complete 255 materials list can be performed.

Milestone(s)

The schedule for this project is dependent upon receipt of alternative fuel candidates for testing. As candidate fuels are received a schedule of testing will be coordinated with the FAA and collaborators. Our existing relationships with these organizations will help expedite this process.

Major Accomplishments
The Phase I Research Report for the LanzaTech/PNNL Ethanol-to-Jet (LT/PNNL ATJ) Synthetic Paraffinic Kerosene Fuels and Blends has been completed and submitted to the OEM's for approval.

Publications
"Evaluation of LanzaTech/PNNL Ethanol-to-Jet (LT/PNNL ATJ) Synthetic Paraffinic Kerosene Fuels and Blends Phase 1 Research Report"

Outreach Efforts
None

Awards
None

Student Involvement
None

Plans for Next Period
Work is beginning on instituting the D4054 Clearinghouse concept. UDRI will subcontract with the relevant engine and aircraft OEM's for Research Report review support and with Southwest Research Institute for assisting with the ASTM process.

Project 031(B) Methods for the Fast Quantification of Oxygenated Compounds in Alternative Jet Fuels

Washington State University

Project Lead Investigator

Manuel Garcia-Perez
Associate Professor
Biological Systems Engineering
Washington State University
LJ Smith, Room 205, PO Box 646120
Pullman, WA 99164-6120
509-335-7758
Email: mgarcia-perez@wsu.edu

University Participants

Washington State University

- P.I.(s): Manuel Garcia-Perez
- FAA Award Number: 13CAJFEWaSU-008
- Period of Performance: July 1st, 2016, to June 30st, 2017
- Task(s):
    1. Literature review
    2. Improving the method for quantification of independent oxygenated compounds in AJFs
    3. Development of methods for the fast quantification of oxygenated compounds in jet fuels

Project Funding Level

Washington State University: Amount of funding from the FAA ($ 50,963), Matching funds ($ 51,130), Source: State Funds to support one graduate student (from Dr. Cavalieri's program) and Dr. Garcia-Perez's salary.

Investigation Team

Yinglei Han (PhD student): Improving the methods for quantification of independent oxygenated compounds in AJFs

Mainali Kalidas (MSc student): Literature review and development of methods for the fast quantification of oxygenated compounds in jet fuels

Manuel Garcia-Perez (Associate Professor): Principal Investigator, project management and reporting

Project Overview

The studies conducted last year show that the chemical compositions of the alternative jet fuels studied (SK and SAK from Virent, Kior, Gevo, Amyris, and ARA; HEFA from UOP; FT from Sasol and Syntroleum) range from fuels comprised of single molecules to fuels with thousands of molecules with a wide range of molecular weights and functionalities. These fuels have contents of trace oxygenated molecules similar to commercial jet fuels, but the types of oxygen groups are fuel dependent. This year we want to continue the work we started last year but focusing on improving the method for the quantification of oxygenated compounds and developing fast detection methods for oxygenated functional groups that can be used during AJF production or at distribution and blending points to control fuel quality.

Tasks

Task 1 Literature review

Washington State University

Objective(s)

To conduct a literature review on the methods for the quantification of oxygenated compounds in alternative jet fuels.

Research Approach

We conducted a literature review on methods for the quantification of oxygenated compounds in alternative jet fuels. The main goal of this task is to review the methods available for the quantification of total functional groups (acids, carbonyl, phenols) and the methods for the quantification of independent compounds in alternative jet fuels. We also reviewed methods that can be potentially used for the quantification of targeted oxygenated compounds in organic matrices.

Milestone(s)

The literature review has been completed and it is now under internal review.

Major Accomplishments

The first draft of the literature review has been completed.

Publications

None

Outreach Efforts

None

Awards

None

Student Involvement

A MSc student (Mainali Kalidas) conducted this literature review.

Plans for Next Period

Prepare a presentation with the main outcomes of this literature review for our first 2017 ASCENT workshop.

Task 2 Improving the method for quantification of independent oxygenated compounds in AJFs

Washington State University

Objective(s)

Validation of Balster's method (Balster et al 2006) for the quantification of oxygenated compounds in AJFs.

Research Approach

In the first year of this project we quantified the content of individual oxygenated compounds by the method described by Balster et al. (2006). The polar molecules were concentrated through Solid phase Extraction (SPE) using a 6 mL Agilent SampliQ silica SPE cartridge. 10 mL sample of jet fuel was analyzed per run. A volume of 12 mL hexane was used to rinse the cartridge and after that 11 mL of methanol eluted to polar species. The samples collected from SPE were then analyzed by GC/MS. Both internal and external standards were used for the analysis. This method was validated with new standards

this year. The main question we want to answer is if all the oxygenated compounds adsorbed on the SPE cartridge were in fact removed with the methanol and to confirm that the quantitative results are reliable.

Milestone(s)
Studies were conducted with several bio-oil methanol ratios, with jet fuels doped with several phenols. In all cases the recovery obtained was close to 100 %, confirming that all the oxygenated compounds retained in the Silica SPE cartridge can be recovered with methanol.

Major Accomplishments
We confirmed that the method proposed by Balster et al (2006) is a reliable quantitative approach for the quantification of polar oxygenated compounds in jet fuel.

Publications
None

Outreach Efforts
None

Awards
None

Student Involvement
Two graduate students (Yinglei Han and Kalidas Mainali) worked on this task.

Plans for Next Period
To prepare the presentation for the first 2017 ASCENT workshop.

Task 3 Development of Methods for the Fast Quantification of Oxygenated Compounds in Jet Fuels
Washington State University

Objective(s)

Develop a method for the fast quantification of oxygenated functional groups in alternative jet fuels

Research Approach

The third task consists on studies to develop methods for the fast quantification of oxygenated functional groups in alternative jet fuels (E411 2012, Christiensen et al. 2011). The goal is to develop fast detection kits that can be used on field conditions. We will focus on the development of kits for the analysis of total carbonyl, total acids, and total phenols by spectroscopic and electrochemical techniques that can be easily miniaturized (Kauffman 1998, Qian et al 2008, Galuszka et al 2013, Novakova and Vickova 2009, Saito et al 2002, Tobiszewski et al 2009).

Milestone(s)

In the last six months we have been developing a strategy to quantify oxygenated compounds that used the extraction of the oxygenated compounds in methanol in a similar way that is done by the method proposed by Balster et al (2006) but after absorbing the polar compound silica cartridge is washed with hexane and to remove the jet fuel non polar molecules left on the cartridge. A washing step with methanol follows to obtain a solution of methanol with jet fuel polar compound in the ppm range. The resulting methanol solution was analyzed by UV-Fluorescence.

Major Accomplishments

A new method based on the analysis of methanol solutions containing jet fuel polar compounds by UV fluorescence has been developed. The appropriate jet fuel/silica/hexane/methanol ratio was determined to ensure a content of polar compounds in the resulting methanol solution below 5 ppm. This low concentration is needed to ensure a linear response of the UV-Fluorescence spectra to the changes in the concentration of poplar compounds. Jet fuel doped with phenolic compounds were tested and the response obtained was in all cases linear. We are currently studying the response of other compounds found in the GC/MS chromatograms of the alternative jet fuel polar compounds.

Publications

None

Outreach Efforts

We are now working on the presentation for the first 2017 ASCENT workshop.

Awards

None

Student Involvement

This task was conducted by our MSc student Mainali Kalidas.

Plans for Next Period

We will conduct studies with other polar compounds found in alternative jet fuels.

References:

Balster, LM., Zabarnick S, Striebich RC, Shafer LM, West ZJ. Analysis of Polar Species in Jet Fuel and Determination of Their Role in Autoxidative Deposit Formation. *Energy & Fuels*, 2006, 2564–71.
Christensen ED, Chupka GM, Luecke J, Smurthwaite T, Alleman TL, Iisa K, Franz JA, Elliott DC, McCormick RL: Analysis of Oxygenated Compounds in Hydrotreated Biomass Fast pyrolysis Oil Distillate Fractions. *Energy Fuels* 2011, 25, 5462-5471
Galuszka A, Migaszewski Z, Namiesnik J: The 12 principles of green analytical chemistry and the SIGNIFICANCE mnemonic of green analytical practices. TrAC *Trends in Analytical Chemisytry*, Vol. 50, 2013, 78-84
E411, ASTM. 2012. "Standard Test Method for Trace Quantities of Carbonyl Compounds with 2 ,4-."
Kauffman RE: Rapid, Potable Voltammetric Techniques for Performing Antiocidant, Total Acid Number (TAN) and Total Base Number (TBN) Measurements. *Lubrication Engineering* 54.1 (1998), 39
Novakova L, Vickova H: A review of current trends and advances in modern bio-analytical methods: Chromatography and sample preparation. *Analytical Chimica Acta*. Vol. 656, Issues 1-2, December 2009, pages 8-35
Qian K, Edwards KE, Deschert GJ, Jaffe SB, Green LA, Olmstead WN: Measuremnt of Total Acid Number (TAN) and TAN Boiling Point Distribution in Petroleum Products by electrospray Ionization Mass Spectrimetry. *Analytical Chem*. 2008, 80 (3), pp. 849-855
Saito Y, Kawazoe M, Imaizumi M, Morishima Y, Nakao K, Hayashida M, Jinno K: Miniaturized Sample Preparation and Separation Methods for Environmental and Drug Analyses. *Analytical Sciences*. Vol. 18 (2002) No 1, pp. 7-17
Tobiszewski M, Mechlinska A, Zygmut B, Namiesnik J: Green analytical in sample preparation for determination of trace organic pollutants. TrAC *Trends in Analytical Chemistry*, Vol. 28, 8, 2009, 943-951

Project 032 Worldwide Life Cycle Analysis (LCA) of Greenhouse Gas (GHG) Emissions from Petroleum Jet Fuel

Massachusetts Institute of Technology (MIT)

Project Lead Investigator

Steven Barrett
Professor
Department of Aeronautics and Astronautics
Massachusetts Institute of Technology
77 Massachusetts Avenue, 33-322, Cambridge, MA 02139
+1 (617) 452-2550
sbarrett@mit.edu

University Participants

Massachusetts Institute of Technology

- P.I.(s): Professor Steven Barrett,
- FAA Award Number: 13-C-AJFE-MIT, Amendment No. 010
- Period of Performance: December 4, 2014 to September 30, 2016 (reporting with the exception of funding levels and cost share only for period from October 1, 2015 to September 30, 2016)
- Task(s):
    1. Preliminary global baseline analysis for 2005 and 2020
    2. Analysis of changes to the baseline in 2050, and assessment of opportunities for reduction in lifecycle GHG emissions
    3. Analysis of world region baseline for recent past and 2020
    4. Final report and data handover

Project Funding Level

$150,000 FAA funding and $150,000 matching funds. Sources of match are approximately $39,000 from MIT, plus 3rd party in-kind contributions of $111,000 from Byogy Renewables, Inc.

Investigation Team

Principal Investigator: Prof. Steven Barrett
Co-Investigator: Dr. Robert Malina, Tasks 1-4
Co-Investigator: Dr. Raymond Speth, Tasks 1-4
Dr. Pooya Azadi, Postdoctoral Associate, Tasks 1-4
Cassandra Rosen, Masters Student, Tasks 2, 4

Project Overview

The total greenhouse gas impact of petroleum-derived fuels includes both direct combustion emissions and the well-to-pump (WTP) emissions associated with extraction, transportation, and refining of crude oil and transportation of refined products. In this project, the WTP life cycle emissions of petroleum-derived jet fuel were quantified. The analysis addressed both temporal and spatial variation in WTP emissions of jet fuel.

Tasks and Plans for Next Period

Task 1: Preliminary global baseline analysis for 2005 and 2020

1.1 Analysis of global portfolio for crude recovery emissions
1.2. Analysis of global transportation emissions developed
1.3 Analysis of global refinery emissions
1.4 Completion of white paper for use at ICAO steering group meeting

Task 2: Analysis of changes to the baseline in 2050, assessment of opportunities for reduction in lifecycle GHG emissions

2.1 Assessment of 2050 emissions baseline for jet fuel from petroleum
2.2 Quantification of opportunities for reduction in lifecycle GHG emissions by lifecycle stage

Task 3: Analysis of world region baseline for recent past and 2020

3.1. Analysis of crude mix profiles by world region
3.2 Analysis of transportation and refinery emission profiles by world region accounting for differences in straight-run and hydroprocessed processing
3.3 Analysis of lifecycle GHG emissions baseline for jet fuel from petroleum by world region
3.4 Refinement of preliminary global baseline using world-region results

Task 4: Final report and data handover

4.1 Completion of white paper on project available for sponsor review
4.2 Data preparation for handover to Argonne National Laboratory for use in GREET model

Plans for next period

Project is complete – publications pending.

Objectives

The main objective of this project was to calculate GHG emissions estimates for petroleum jet fuels for the recent past and for future scenarios in the coming decades. Results were reported globally and broken out by world regions, and the impact of changes in future demand for certain petroleum products and of changes in crude properties were quantified. Opportunities for reductions in GHG emissions along the supply chain were estimated.

Research Approach

Background

To date, only a limited number of analyses of GHG emissions for jet fuel from petroleum sources exist, limited to the United States and generally relying on 2005 data (Skone and Gerdes 2009, Stratton et al. 2012). A recent update to the Greenhouse Gases, Regulated Emissions, and Energy Use in Transportation Model (GREET) developed and maintained by Argonne National Laboratory includes more recent data on refining efficiency from a report by Elgowainy et al. (2014), but is still U.S.-specific, only. Furthermore, existing estimates of lifecycle emissions are limited temporally, with no known projections of short- or long-term future.

To the best of our knowledge, no baseline value for jet fuel from petroleum has been established in other world regions. In Europe, for example, baseline values are calculated for diesel fuels from petroleum, but not for jet fuel (JEC 2014). Moreover, there is no baseline value on a global scale that describes average lifecycle GHG intensity of using jet fuel from petroleum, either for fuel produced now or for scenarios of projected future petroleum-derived jet fuel use. Existing values for jet and diesel that are used in the US and the EU are summarized in Figure 1.

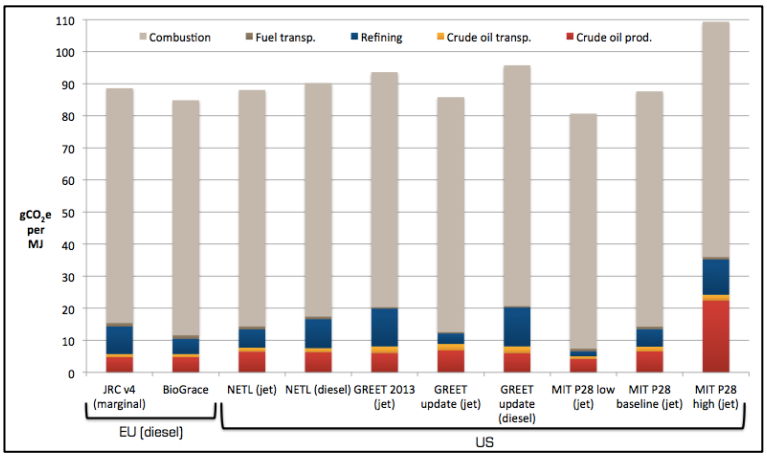

Figure 1: Lifecycle GHG emission values used as baselines in the EU and U.S. (Malina et al. 2014).

This is a particularly important research gap given the ongoing efforts under the Committee on Aviation Environmental Protection (CAEP) of the International Civil Aviation Organization (ICAO) to include alternative fuels into a global system of market-based measures, CORSIA (Carbon Offsetting and Reductions Scheme for International Aviation). Alternative fuels require the existence of a petroleum-centric benchmark for comparison, so that airlines can receive appropriate monetary credits for using these fuels. Moreover, a baseline is required for current work under the Alternative Fuels Task Force (AFTF) of ICAO CAEP to estimate the potential contribution of large-scale alternative jet fuel introduction to mitigating aviation's climate impact by the year 2050.

From a temporal perspective, the crude mix used in refineries changes over time, as do refining and recovery practices and product slates produced. These factors might impact associated lifecycle emissions for jet fuel from petroleum both globally and within specific world regions. For example, the average lifecycle GHG emissions attributable to jet fuel from petroleum in the U.S. are estimated at 85.8 g CO_2e per MJ of jet fuel via the 2015 update to GREET, whereas Skone and Gerdes (2009) reported 88.0 g CO_2e per MJ (Malina et al., 2014). Aside from crude quality and refinery changes, other technological or policy factors may change in the future as well, and need to be considered in future projections.

Methodology

Extraction
For both conventional and unconventional (e.g., oil sands, shale) petroleum-derived jet fuels, we investigated and quantified greenhouse gas emissions in all stages of the petroleum-derived jet fuel lifecycle (crude recovery, feedstock transportation, feedstock-to-fuel conversion, jet fuel transportation, and jet fuel combustion). For the recovery stage, we built upon existing analyses on emission profiles for different representative crude types and recovery practices such as the analyses by Rahman et al. (2014), Bouvart et al. (2013), Garg et al. (2013), Charpentier (2009) and Skone and Gerdes (2009). In the case of missing data for emissions associated with recovery of certain crude types, we approximated them with emissions from crude types with similar recovery practices. For analyses of future emissions, projections of changes in constituent emissions indices and production capacity have also been utilized (Jiang, 2011; Exxon 2015; IEA 2014; Brandt, 2011).

Data on crude mixes used in the different world regions has been obtained from existing analysis mentioned above and by data from the International Energy Agency (IEA, 2014 and 2015) and the Energy Information Administration (EIA, 2015). This data was necessary both for assigning recovery emissions to jet fuel produced in a particular word region, and for estimating refinery emissions. Future crude quality was assessed using global projections (OPEC, 2015 and EIA, 2015).

Refinery
Refinery GHG emissions were based on refinery usage statistics in world regions where this data wass available (i.e. U.S. and Europe), and estimated based on refinery configurations and capacities in other regions. Characteristics of the input crude slate, such as sulfur content and API gravity, have been used to determine process energy requirements and resulting emissions. We used available information to estimate the relative amounts of straight-run and hydroprocessed jet fuel that

are produced by refineries worldwide. We used insights from process-level refinery linear programming (LP) models to estimate the emissions from both the production of straight-run and hydroprocessed jet fuels. As well as, these LP models were used to understand how changes in relative transportation fuel demand affects refinery energy usage and GHG production, and how those changes affect the GHG emissions attributed jet fuel.

For future scenarios where demand for jet fuel may exceed straight-run production capabilities, emissions were estimated for the upgrading processes needed to convert other fractions of the input crude to jet fuel. The ratio for demand amongst different crude products (e.g. jet fuel versus diesel) will also impact refinery operations. Future demand for petroleum fuels has been projected by other agencies, and was used in the 2050 analysis (WEC 2011 and 2013; IEA 2014; IEA 2015).

Transportation
Feedstock and product transportation emissions for each world region were calculated by combining representative transportation distances with emission profiles of representative means of transportations accessible in the GREET and/or SimaPro tools.

Future and Opportunities
Projections for future emissions were created through a scenario-based analysis, similar to that used by the IPCC and others (IPCC, 2010). Scenarios were created in order to conceptualize different potential ways in which the future may unfold. To create these scenarios, first key drivers of emission within the petroleum lifecycle were identified. Once identified, future emissions regarding how these factors change by the year 2050 were collected. This literature data was then be used to create scenarios, such that each scenario was coherent and has consistent assumptions. These scenarios were then assessed using the LCA model so that the lifecycle emissions could be determined.

Opportunities for reducing lifecycle GHG emissions of jet fuel from petroleum were investigated and quantified through sensitivity analyses of different factors. These factors included those utilized in the 2050 scenario construction, as well as additional ones. For example, the emissions intensity of key inputs was varied, such as hydrogen production (ICAO, 2015; ANL, 2005), electricity generation (PSI, 2014; WEC, 2013), and transportation.

Milestone(s)

Due Date	Milestone
May 1st, 2015	MS 1 (related to Task 1): Crude extraction emission's profiles compiled
August 1st, 2015	MS 2 (related to Task 1): Preliminary global baseline results available for FAA discussions
Mid October 2015	MS 3 (related to Task 1): Presentation of preliminary global baseline emissions at CRC Workshop
November 1st, 2015	MS 4 (related to Task 1): White paper available on preliminary global baseline for use at ICAO Steering group meeting
March 1st, 2016	MS 5 (related to Task 2): Preliminary results of GHG emissions baseline for 2050 available for discussion
May 1st, 2016	MS 6 (related to Task 3): World-region specific baseline results available for discussion
June 1st, 2016	MS 7 (related to Task 2): Opportunities for lifecycle GHG reductions for jet fuel from petroleum available for discussion
September 30th, 2016	MS 8 (related to Task 4): White paper on project available for FAA review

Major Accomplishments

Thus far, all milestones of the project have been fulfilled, with MS2 through MS8 completed during the current reporting period. For the 2050 analysis, scenarios have been constructed through the methodology discussed above (Research Approach – Methodology – Future and Opportunities). The key factors identified included: production capacity and emissions indices of conventional and unconventional extraction methods, crude quality (API and sulfur content), hydrogen production, electricity generation, and refinery impacts of varied demand for petroleum products. Relevant literature on these factors was surveyed, so that projections of their values in 2050 could be assessed. This data is summarized below in Table 1:

Table 1: Life cycle inventory data for 2020 and 2050 analysis

Category	Factor	Reference Case: 2020 Analysis	2050 Case: Current Policies	2050 Case: Moderate New Policies	2050 Case: Strong New Policies
Extraction	Tight Oil Emissions Index [g CO_2 / MJ]	MIT 2020 (6.3) Azadi et al, 2016	Medium (6.3) Azadi et al, 2016	Medium (6.3) Azadi et al, 2016	Low (1.8) Jiang et al, 2011
	Tight Oil Production [kbbl / d]	MIT 2020 5.2 (5.2%) Azadi et al, 2016	High 12.2 (9.9%) Exxon, 2015	Medium 5.7 (5.5 %) IEA, 2015	Low 3.5 (5.5%) IEA, 2014
	Heavy Oil Emission Index (1) [g CO_2 / MJ]	MIT 2020 Azadi et al, 2016	MIT 2020 Azadi et al, 2016	MIT 2020 Azadi et al, 2016	Low Brandt, 2011
	Heavy Oil Production [kbbl / d]	MIT 2020 6.0 (6.0 %) Azadi et al, 2016	High 9.6 (7.8%) Exxon, 2015	Medium 8.0 (7.7%) IEA, 2015	Low 4.9 (4.9%) IEA, 2014
	Crude Oil API (2)	MIT 2020 Azadi et al, 2016	Uniform – projected decrease: 0.4 to 1.9 OPEC, 2014 and EIA, 2015		
Utilities	Electricity Generation Emission Index (2) [g CO_2 / MJ]	MIT 2020 PSI, 2014	MIT 2020 PSI, 2014	Medium ("jazz" case) WEC, 2013	Low ("symphony" case) WEC, 2013
	Hydrogen Production Emission Index [g CO_2 / MJ]	MIT 2020 (0.099) Azadi et al, 2016	High (0.099) ICAO, 2015	Medium (0.068) ANL, 2005	Low (0.028) ICAO, 2015
Refinery	Global Middle Distillate Demand [mmbbl / d]	MIT 2020 (35) Azadi et al, 2016	High (66.3) ("freeway" case) WEC, 2011	Medium (44.5) ("jazz" case) WEC, 2013	Low (33.1) ("symphony" case) WEC, 2013
	Global Jet Fuel Demand [mmbbl / d]	MIT 2020 (5.4) Azadi et al, 2016	High (19.5) ("freeway" case) WEC, 2011	Medium (17.0) ("jazz" case) WEC, 2013	Low (10.3) ("symphony" case) WEC, 2013
	Ratio of Jet Fuel to Middle Distillate	0.15	0.29	0.38	0.31
	Crude Sulfur Content (2)	MIT 2020 Azadi et al, 2016	Uniform – projected increase: 0.1 to 1.4 OPEC, 2014 and EIA, 2015		

(1) Values vary with extraction method (e.g. bitumen vs. SCO, in-situ vs. surface)
(2) Values vary by world region or country

This was then used to create three future scenarios. These scenarios focus on actions and policies regarding environmental issues, and how the stringency of these approaches may vary. The lowest level of stringency scenario is Current Policies, for which no new environmental actions are taken in addition to current policies. Moderate New Policies and Strong New Policies build on Current Policies through the addition of more stringent actions or policies. These three scenarios vary on three main axes: the extent to which unconventional resources are restricted (with respect to capacity and emissions), the extent to

which hydrogen and electricity utilities are decarbonized, and the extent to which demand for different petroleum products is abated.

Together, the data for each of these scenarios was utilized in the LCA model. These results, as well as those for the Opportunities for Emissions Reductions are shown below in Figure 2.

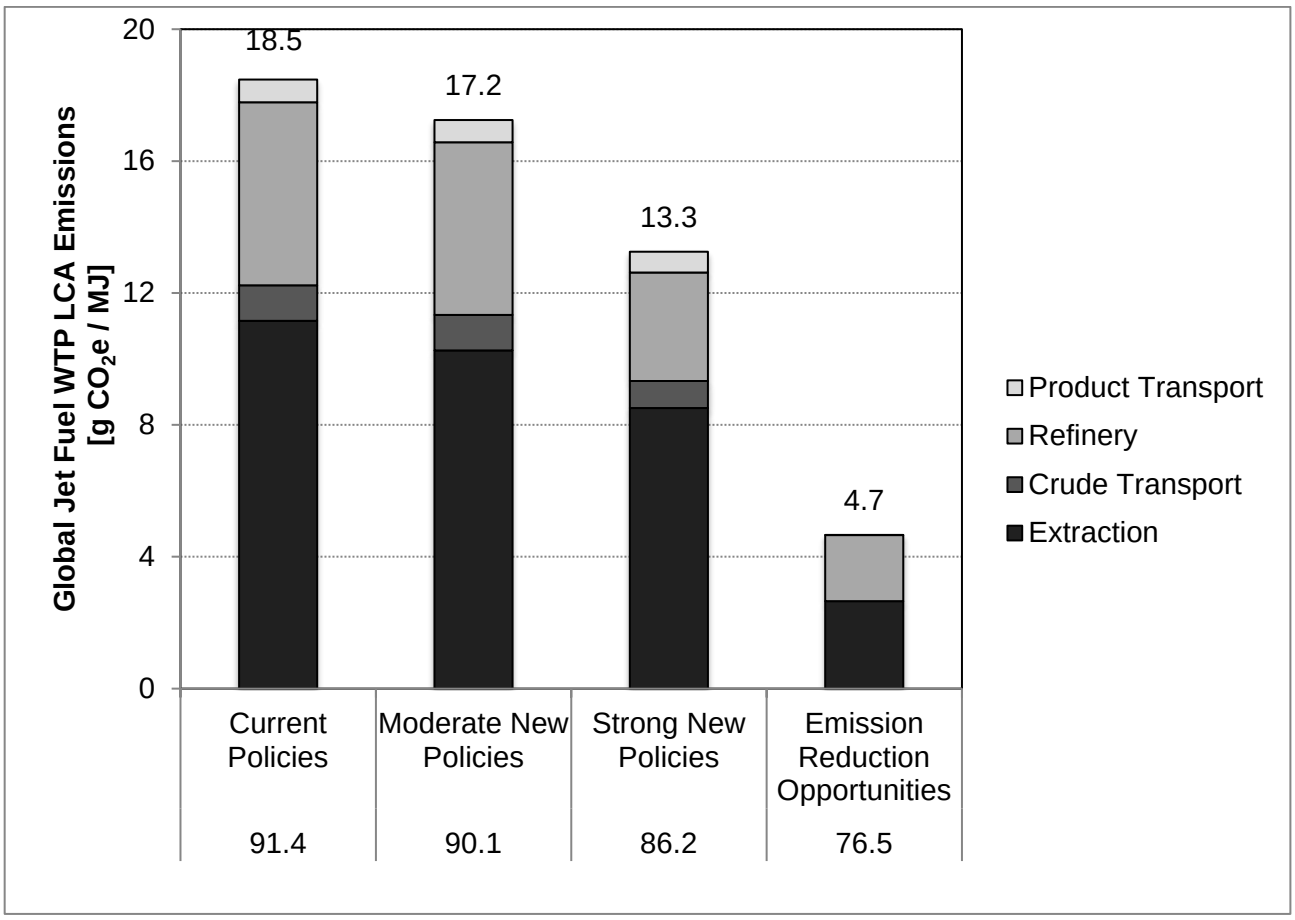

Figure 2: Global lifecycle GHG emission for jet fuel in the year 2050 for three scenarios

The well-to-pump emissions are shown on the y-axis and above the bars in the figure, and the well-to-wake emissions are shown below the x-axis. Compared to the WTP emissions for 2020 of 16 g CO_2e/MJ, the emissions in 2050 may increase by 2.5 or decrease by 2.7. Which scenario path is taken is largely dependent on choices regarding human action and government policy.

Opportunities for emissions reduction were also identified. Additional factors to those considered in the 2050 analysis were examined. These included: venting, flaring, and fugitive gases; emissions intensity of transportation; electrically powered extraction processes; jet fuel composition in relation to combustion emissions. By reducing the aromatic content of jet fuel within the specification range, the combustion CO_2 emissions can be decreased by 1.8 g CO_2e/MJ. Taken together, these various opportunities resulted in WTP lifecycle emissions of 4.7 g CO_2e/MJ, as shown in Figure 2 above. These opportunities can be examined individually, as shown below in Figure 3.

Opportunities such as extraction processes being powered through fossil free methods, or hydrogen being produced with zero emissions, yield the biggest opportunities for reduction, at about 3 g CO_2e/MJ each. Opportunities such as electricity generation with zero emissions, or carbon neutral transportation, yield the smallest opportunities for reduction, at about 1 g CO_2e/MJ. This indicates that some opportunities are able to reduce emissions more than others.

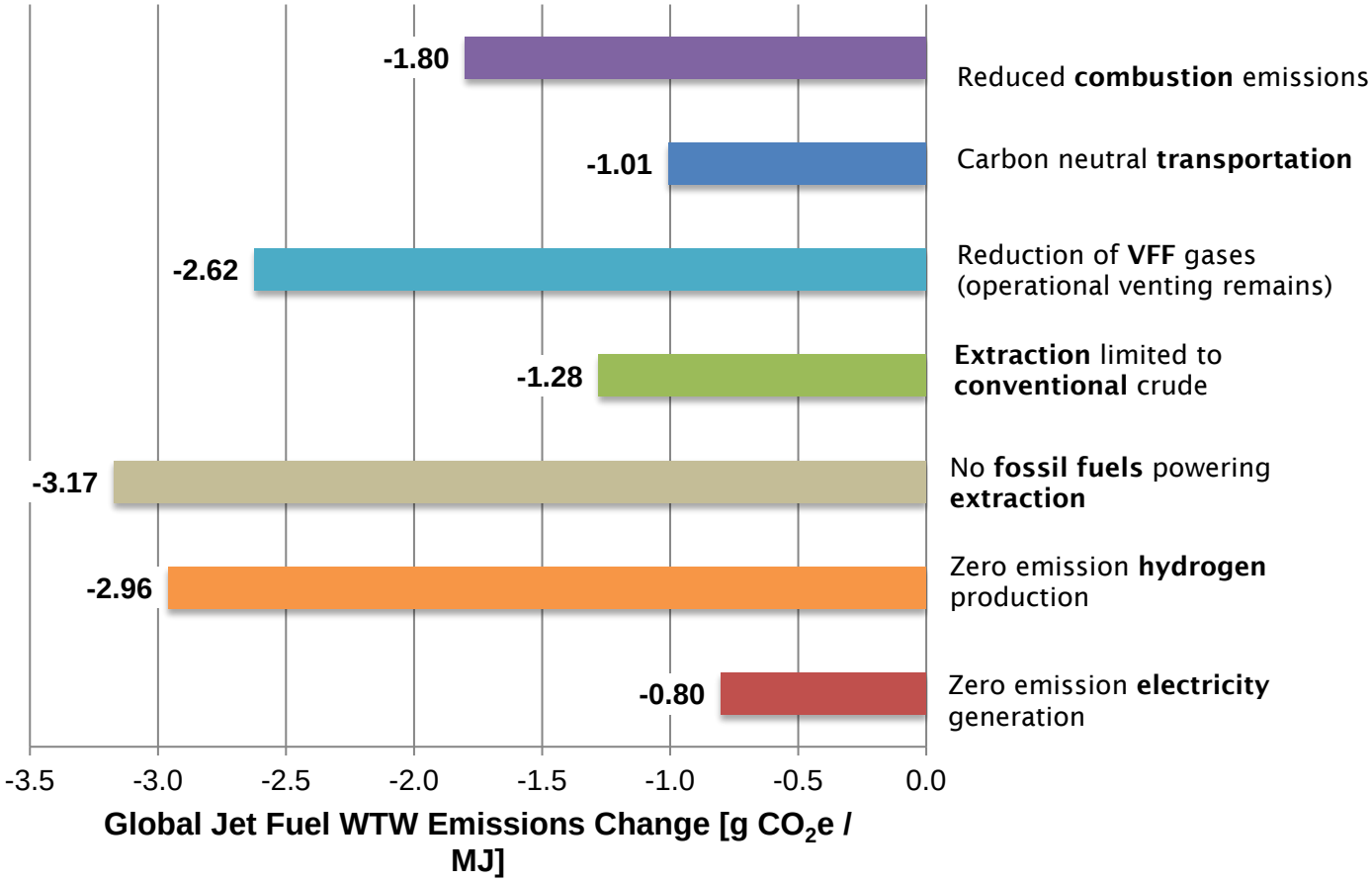

Figure 3: Opportunities for emissions reductions by action type

The remaining 4.7 g CO_2e/MJ emissions in the Opportunities for Emissions Reductions scenario come from extraction and refinery emissions. The 2.7 g CO_2e/MJ from the extraction stage are mainly from non-operational unavoidable venting, as well as land use change and fugitive gases. The 2.0 g CO_2e/MJ from the refinery stage are due to process units powered by refinery fuel gas and catalyst coke.

Overall, the results from 2005 through to 2050 show that lifecycle emissions for petroleum jet fuel tend to increase with time, unless action is taken to reduce them in the future. Depending on the policies implemented within the petroleum industry and beyond, long-term emissions may increase or decrease by about 2.5 g CO_2e/MJ from 2020 levels. If significant reductions are desired, opportunities for emissions reduction have been identified, which can result in a decrease of emissions by 11.3 g CO_2e/MJ from 2020 levels, a 71% reduction.

This work has established a baseline of petroleum jet fuel emissions for various geographical regions in the past, near-term, and long-term future. These values can be used when developing relevant policies. For example, the 2020 global result informed ICAO CAEP in its adoption of the reference values for international jet fuel. In addition, the 2050 global values were used in ICAO CAEP/10 Fuel Production assessment for quantification of GHG emission's benefit of long-term alternative jet fuel market penetration.

Publications

Azadi, P; Speth, R.L.; Malina, R.; Barrett, S.R.H. Worldwide and Regional Greenhouse Gas Emissions of Petroleum-Derived Transportation Fuels. Submitted for publication.

Rosen, C.V.; Speth, R.L.; Malina, R.; Barrett, S.R.H. Scenario-Based Lifecycle Greenhouse Gas Emissions of Petroleum-Derived Transportation Fuels in 2050. In preparation.

Outreach Efforts

- Presentation at CRC Workshop on Life Cycle Analysis of Transportation Fuels (October, 2015)
- Presentation at DOE BETO Alternative Aviation Fuel workshop (September, 2016)
- ASCENT Poster (April, 2016) and Presentation (September, 2016)
- FAA "External Tools Call" (December, 2016)

Awards

Professor Steven Barrett – newly Tenured Associate Professor, Department of Aeronautics and Astronautics, School of Engineering, MIT

Student Involvement

A Masters' Student, Cassandra Rosen, has been involved in this work from September 2015 – September 2016. She has worked on Task 2 and 4. She will be graduating from MIT in June 2017 with a Masters of Science in Technology and Policy.

Plans for Next Period

Project 32 is complete – no further steps are needed for this research. Publications on Project 32 are pending.

References

Argonne National Laboratory, ANL (2005): Hydrogen Demand, Production, and Cost by Region to 2050. ANL/ESD/05-2, Chicago, USA.

Brandt. A. R. (2011): Upstream greenhouse gas (GHG) emissions from Canadian oil sands as a feedstock for European refineries. Stanford University.

Bouvart, F. / Saint-Antonin, V. / Gruson, J. (2013): Well-to-tank carbon impact of fossil fuels, ADEME report PAE02 002 600, Rueil-Malmaison, France.

Charpentier, A. / Bergerson, J. / MacLean, H. (2009): Understanding the Canadian oil sands industry's greenhouse gas emissions. Environmental Research Letters, Vol. 4(1), 014005.

Elgowainy, A. / Han, J. / Cai, H. / Wang, M. / Forman, G. / Divita, V. (2014): Energy Efficiency and Greenhouse Gas Emission Intensity of Petroleum Products at US Refineries. Environmental Science & Technology, in press.

Energy Information Administration, EIA (2015): US Crude Oil Production to 2025: Updated Projection of Crude Types. Washington, DC, USA.

Exxon Mobil (2015): The Outlook for Energy – A View to 2040. Irving, Texas, USA.

Garg A. / Vishwanathan S. / Avashia V (2013): Life cycle greenhouse gas emission assessment of major petroleum oil products for transport and household sectors in India. Energy Policy, Vol. 58, pp. 38-48.

ICAO CAEP (2014): Draft LCA methodology report, Information Paper CAEP-SG/20142-IP/5, Montreal, Canada.

ICAO CAEP (2015): Proposal for methodology to augment existing life-cycle assessments to 2050. Information Paper, Montreal, Canada.

IPCC, Intergovernmental Panel on Climate Change (2010): Workshop on Socio-Economic Scenarios. Workshop Report, Berlin, Germany.

International Energy Agency, IEA (2014 and 2015): World Energy Outlook. Paris, France.

Jiang M. / et al (2011): Life cycle greenhouse gas emissions of Marcellus shale gas. Environmental Research Letters, Vol. 6, pp. 9.

JEC (2014): Well-to-tank report Report Version 4.a, Ispra, Italy.

Malina, R. / Staples M. / Wang, M.: "A quantitative comparison of LC GHG accounting for alternative fuels in the US and EU", Inaugural meeting ICAO CAEP AFTF April 1, 2014, Montreal, Canada.

Organization of the Petroleum Exporting Countries, OPEC (2014): World Oil Outlook. Vienna, Austria.

Paul Scherrer Institute, PSI (2014): Life Cycle Inventories of Electricity Mixes and Grid, V 1.3. Uster, Switzerland.

Rahman, M. /, Canter, C., / Kumar, A. (2014): Greenhouse gas emissions from recovery of various North American conventional crudes. *Energy*, in press.

Skone, T / Gerdes, K (2009): Development of Baseline Data and Analysis of Life Cycle Greenhouse Gas Emissions of Petroleum-Based Fuels, DOE/NETL-2009/1346, National Energy and Technology Laboratory, Pittsburgh, PA.

Stratton, R. / Wong, H. / Hileman, J. (2011): Quantifying variability in life cycle greenhouse gas inventories of alternative middle distillate transportation fuels. Environmental science & technology, Vol. 45(10), pp. 4637-4644.

World Energy Council, WEC (2011): Global Transport Scenarios 2050. London, United Kingdom.

World Energy Council, WEC (2013): World Energy Scenarios: composing energy futures to 2050. London, United Kingdom.

Project 033(A) and Project 033(B) Alternative Fuels Test Database Library (Year II)

University of Dayton Research Institute
University of Illinois

Project Lead Investigator (033(A) - University of Dayton)

Steven Zabarnick
Division Head, Energy & Environmental Engineering
University of Dayton Research Institute
Dayton, OH 45469-0043
937-255-3549
Steven.Zabarnick@udri.udayton.edu

Project Lead Investigator (033(B) - University of Illinois)

Tonghun Lee
Associate Professor
Mechanical Science & Engineering
University of Illinois at Urbana-Champaign
1206 W. Green St.
Urbana IL 61801
517-290-8005
tonghun@illinois.edu

University Participants

University of Illinois at Urbana-Champaign

- P.I.(s): Tonghun Lee, Associate Professor
- FAA Award Number: 13-C-AJFE-UI-009
- Period of Performance: 7/21/2015 to 8/14/2017
- Task(s):
    1. Development of an alternative fuels test database

University of Dayton Research Institute

- P.I.(s): Steven Zabarnick
- FAA Award Number: 13-C-AJFE-UD-012
- Period of Performance: 7/21/2015 to 8/14/2017
- Task(s):
    2. Development of an alternative fuels test database

Project Funding Level

University of Illinois at Urbana-Champaign
Funding Level: $70K
Cost Share: Software license support from Reaction Design (ANSYS)

University of Dayton Research Institute
Funding Level: $30K
Cost Share: Software license support from Reaction Design (ANSYS)

Investigation Team

- Kyungwook Min (Graduate Student, University of Illinois at Urbana-Champaign): Compilation of fuel test data.
- Anna Oldani (Graduate Student, University of Illinois at Urbana-Champaign): Compilation of fuel test data and development of database.

Project Overview

This study seeks to create a comprehensive, foundational database of current and emerging alternative jet fuels by integrating relevant pre-existing jet fuel data into a common archive which can provide guidelines for design and certification of new jet fuels in our future as well as aid federal work including fuel certification. Thus far, the effort has focused on the integration and analysis of pre-existing jet fuel data from various government agencies and individual research groups with oversight from the Federal Aviation Administration (FAA). We hope that the database will one day serve as 'the comprehensive and centralized knowledgebase' shared by the academic, government, and industrial communities in fuels research and policy, possibly facilitated on a cyber-based infrastructure. With ongoing prolific diversification of new jet fuels, this effort to integrate dispersed information is critical in providing the FAA with an overview of the latest developments and to support many other tangential fields of research in government, industry, and academia impacted by integration of new alternative jet fuels.

Task 1 – Development of an Alternative Fuels Test Database

University of Illinois at Urbana-Champaign

Objective(s)

The main objective of this study is to establish a ***foundational database*** of current and newly emerging alternative jet fuels by integrating all relevant pre-existing jet fuel data into a common archive which can provide guidelines for design and certification of new jet fuels in our future as well as aid and shorten fuel certification relevant work. This proposal outlines the year II efforts under this mandate. The vision is to institute a database that can be utilized for the design and optimization of new propulsion and energy systems including development of next-generation engines, fuel delivery systems, as well as pollution mitigation technologies. Furthermore, it can provide data for screening and certification of newly emerging fuels and thereby impacting legislative measures and national policy. In so doing, the goals of this project are as follows:

- Survey current pre-existing data and analyze information
- Prioritize current data and compile into centralized logical structure
- Analyze the obtained information into chronological order and regroup into relevant groups
- Obtain information on detailed test platforms and test conditions
- Develop a controlled web portal for access to the information
- Develop and implement a database/web portal infrastructure and methodology
- Integrate available alternative fuel test data into the database in organized format
- (Future Work) Integrate FAA ASCENT and NJFCP Data

Research Approach

Development Strategy of a Successful Fuels Test Database (Long Term Plan)

- **Phase I:** Integrate Current Pre-Existing Data: Preliminary survey and integration of all pre-existing database and data (including raw data) on jet fuels from universities, national laboratories, government archives, and private industry (i.e., existing database from Sandia, NIST, DoD Labs, ASTM research reports, government technical reports etc. is part of the year I efforts and will be used to initially seed the basic infrastructure of the fuels database proposed in this study). Year II efforts continued to assemble information and annex a prioritized set into the web portal/database. In year II, we focused our efforts on obtaining relevant fuel property specification test data for the certification process.
- **Phase II:** Analysis of Preliminary Data: Conduct comprehensive analysis of the initial data to categorize all relevant physical and chemical characteristics of the fuels and relevant testing conditions. Effort will be made to determine

insufficient areas for further investigation. In year II, we have significantly expanded our efforts to the analysis of information into chronological order and in incorporating detailed test platform and test condition data. An effort will be made to re-categorize the data according to different testing groups and performance. A preliminary effort will be made to vet some of the data according to test conditions as required (future efforts will more fully address vetting and analysis of data).

- **Phase III:** Establish Web Portal/Database Infrastructure and Methodology: A basic web portal has been established during the year I efforts. In year II, based on the analysis of pre-existing data, we will work with national laboratories to establish a flexible and accessible database structure and data access protocols both for retrieval of current data and also for integration of new information in the future. This will be integrated into the web portal. We anticipate increased functionality in the web portal to conduct advanced searches and user feedback on each data item (community based vetting system).
- **Phase III-b:** Integration of FAA ASCENT and NJFCP Data: New data generated from both the FAA ASCENT and the NJFCP will be integrated into the database according to the pre-defined infrastructure. This will be coordinated with Area #7 of the NJFCP program.
- **Phase IV:** Integrate with Current and Future Research: Disseminate and integrate new database to relevant research groups in universities, national laboratories, government, and industry. Formulate partnerships for stewardship, preservation, and continued development of the alternative jet fuel database.
- **Phase V:** Continued Development: Continue development of the database after the initial integration and distribution phase into a more widely distributed community based infrastructure (potentially cyber-based). Link and expand the database to encompass pre-existing data from other countries.

Milestone(s)

Milestones from Each Period

Proposed (3 Month): At the 3 month mark, we will have concluded an exhaustive survey to obtain all fuel relevant data from individual PIs and national laboratories. We will work with the advisory committee and other PIs in the NJFCP and ASCENT to ensure that a comprehensive and complete survey of data has been completed. During this time, we will initiate efforts to start the physical construction of a database and work with web designers and relevant personnel for deployment. Data format for the FAA ASCENT and NJFCP research will also be acquired during this time.
Achieved: Basic survey of the fuels test data has been accomplished and a plan is in place for construction of a web based database. We have discussed the format of a metafile to deal with the data. We have a list of data formats that will become available in the database.

Proposed (6 Month): At the 6 month mark, we should have a preliminary version of a standardized platform with integration of data from all federal, academic, and industrial sources. The focus will be on smooth and logical integration of data, and clear organization of information into subgroups.
Achieved: A preliminary outline of a web-based portal is in place and we have started to analyze the data for integration into the database. The NJFCP has also contributed two quarters of data to be integrated in to the database. We have visited AFRL to discuss how to extract data at AFRL for integration into the database.

Proposed (9 Month): At the 9 month mark, we will assess which data categories are insufficient and seek to further populate these areas with continued data searches. The target is to continue building up the resources available in the database to meet the goal of establishing a comprehensive archive. We will also work during this time to ensure the data provided in the database are correctly categorized and properly accessible for users.
Achieved: We have continued with AFRL site visits to gather data including previously approved fuels and fuels currently undergoing the certification process. We have discussed the procedure for inclusion of NJFCP data into the database to ensure that the data provided is in a final, approved format. The data that has been collected thus far has been checked to assure that it is approved for public release and available in a downloadable format. An effort has been made to transfer any tabulated data contained within PDF resources into corresponding .xlsx files to improve the accessibility for users.

Proposed (12 Month): At the 12 month mark, we will assess ways to move forward with the data collection and archiving and begin to outline potential analysis routes. It is also important during this time to assess the capabilities of the web portal and determine if archiving or search procedures require improvement.
Achieved: The data archiving process has been re-formatted to better accommodate the data that has been acquired. We hope to continue to elicit feedback from users of the web portal in the fuels community on improvements they would like to see implemented with regard to data organization and ease of access. We have incorporated new search algorithms that

allow for expanded searching capabilities to provide the users with more robust search results. Successful tests of these search capabilities make us confident that users are able to access all relevant data when using both the basic and advanced search functions. We have also begun to identify possible targets for a statistical analysis of the data, focusing on relevant specifications crucial early in the certification process.

Proposed (15 Month): At the 15 month mark, we will discuss methods by which the data can be analyzed to provide a statistical analysis of existing jet fuel data to-date. During this time, an effort will be made to further define the goal of analyzing fuel data with regard to key specifications of the fuel certification process. Population of the database will continue with additional visits to AFRL to gather relevant fuel testing data.
Achieved: A preliminary outline has been discussed and developed for utilizing the data collected to provide an overview of the fuel certification process with a focus on the specifications and issues relevant to alternative jet fuels. A sampling of fuels representing the various alternative fuel categories has been selected and will be used to furnish the data needed for the analysis. An AFRL visit provided further fuel test data that has been categorized and is undergoing submission to the database.

Major Accomplishments

The new alternative jet fuels database website homepage is shown in Figure 1 (altjetfuels.web.engr.illinois.edu). The enhanced search features are shown in Figure 2, with the improved search results shown in Figure 3.

Figure 1 Alternative Jet Fuel Test Database site homepage

During year II, several tasks were completed with regard to development of the Alternative Jet Fuels Test Database. The site to house the database, established during year I through the coordinated efforts of members of the University of Illinois, has been further improved and populated with additional relevant jet fuel test data. Improvements to the site were made during year II including the development of basic and advanced search functionalities and enhanced search algorithms to return more robust search results. A screenshot of the homepage of the site is shown in Figure 1, displaying the main features of the site. These features include a general *About* section with information regarding the mission and goals of the database project, funding agencies of the program, a directory of members involved in the work, and links to partner institutions participating in the larger FAA ASCENT database project.

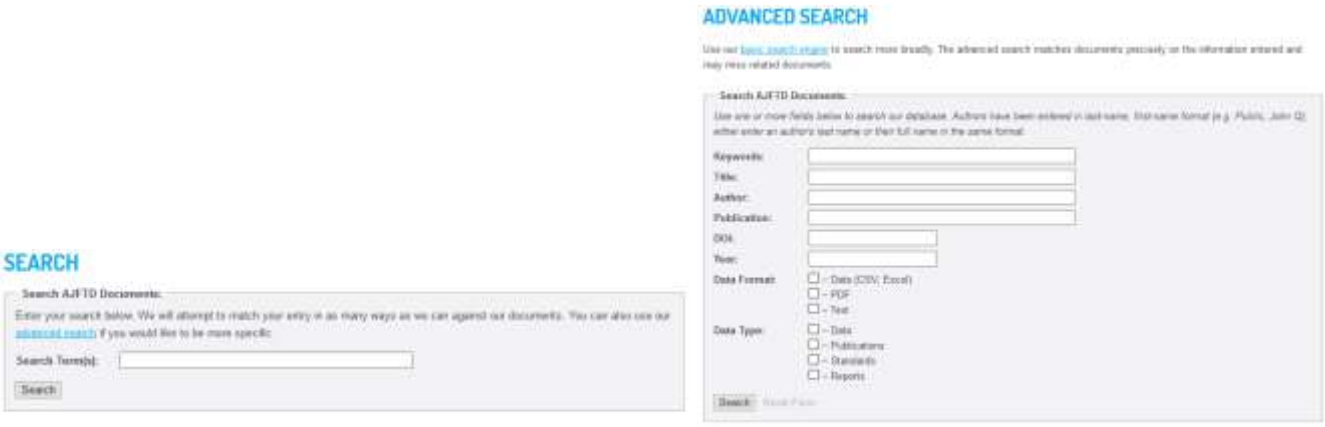

Figure 2 Alternative Jet Fuel Test Database basic (left) and advanced (right) search functions

Users have two methods to access data made available on the site. The first is a search feature where users can select from a basic or advanced search, shown in Figure 2. The advanced search allows users to search by terms of interest including authors, title, DOI, year of publication, data type, and keywords.

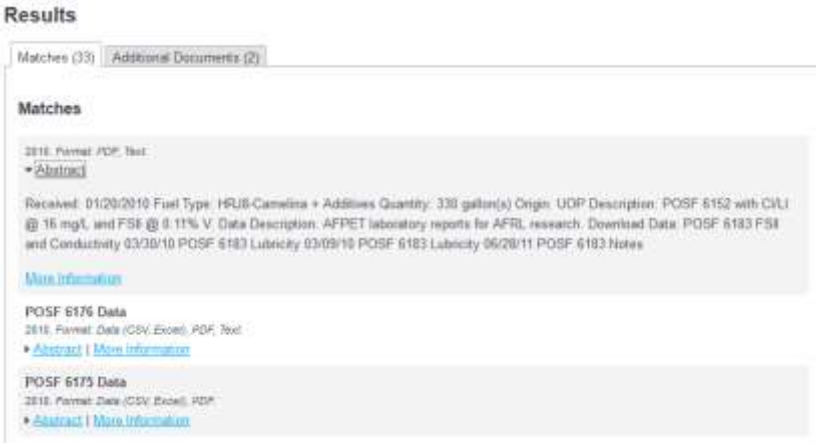

Figure 3 Alternative Jet Fuel Test Database sample search results

The improved search results achieved during year II are shown in Figure 3. Users now see exact metadata matches on the first tab (e.g. if a user searches for "fuel" in the title category, only documents with "fuel" in the title are displayed) with additional documents shown on the second tab (e.g. for the same "fuel" search, documents with "fuel" in additional categories will be displayed).

Data Type	Examples	Sample File Types
Chemical Kinetics Mechanisms	Mechanisms	.TXT, CHEMKIN
Emissions	Emission Test Data	PDF, .XLSX
Testing Results	Shock Tube, Rapid Compression Machine, GC MS	.XLSX, .CSV
Fuel Properties	Lab Analysis Reports	.XLSX, .CSV, PDF
POSF Data	POSF Fuel Specification Testing	PDF, .XLSX
Publications	Production Processes, Reaction Studies, Chemical Kinetics, Economic Analyses, Technical Reports, Fuel Certifications	PDF

Figure 4 Sample data categories

Figure 4 displays a sampling of the current data categorization along with sample file types found under each category. Users are able to download original file formats as well as any tabular data that has been converted into .XLSX files for improved accessibility. The site will also house data from the National Jet Fuel Combustion Program (NJFCP) Areas 1 through 6. Discussions are ongoing as how to best to include data from this multi-group collaborative effort. Once further guidelines have been discussed and approved regarding which data to include, this section of the site will be expanded. The second feature for users to access data is a grouping of data by subject area; users can then follow through a familiar folder sublevel categories to access specific data grouped under various topic areas. This structure is broken down in Figure 5, which shows the various main and sublevel categories of data contained within the database. This structure allows for flexibility as more data is incorporated into the database. It can easily handle adding additional categories as new data is acquired.

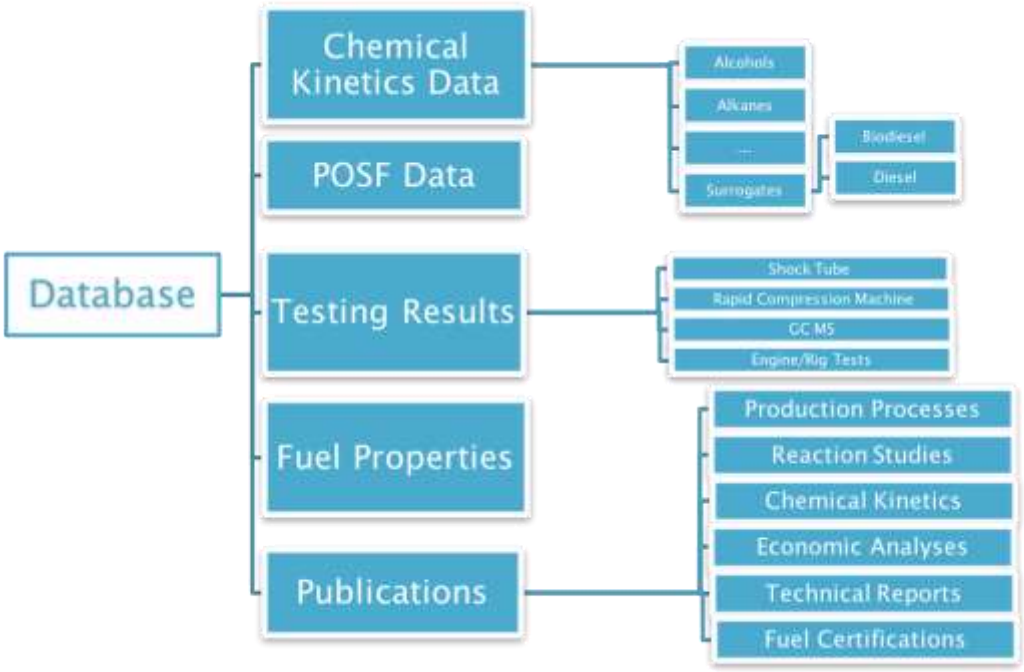

Figure 5 Database structure breakdown

To access any data (in the *Search*, *Database*, and *NJFCP* menu headings), users will first be required to request access, and once the request for access has been approved by site administrators, the user can then register a username and password to login on the site and search through the database. Registered users will also be able to submit data directly to the site. These submissions will be received by the site administrators and posted once the proper classification has been assigned to the data. The site will display general information available to the public only in the *About* and *News* headings. The *News* section highlights recent activity related to the various projects underway in the program and general activity in the alternative jet fuels field. Finally, users will be able to leave comments under the *Contact* section, which will direct all submissions to site administrators. The general sections of the site have been and testing of the search features for sample data submissions has been completed. Data received from AFRL has been populated on the database and data from the NJFCP program areas is currently ongoing discussions for future inclusion once finalized. Data will continue to be uploaded and updated on the site as it is received, with registered users able to submit comments on all available data.

The University of Dayton's contributions to the project primarily involve the identification, collection, and critical review of alternative fuel data and reports. Through UD's on-site work with AFRL, we have access to a wide variety of alternative and petroleum-based fuels data. We have a large amount of expertise in conventional and alternative fuel composition to property relationships which gives us the ability to provide critical evaluation of candidate for inclusion in the database.

Thus we continue to provide access to alternative and conventional fuel data and reports and the expertise to advise on the value of including the numerous identified data into the FAA database.

Publications
None

Outreach Efforts
None

Awards
Anna Oldani (Graduate Student): Society of Women in Engineering (SWE) Award for Research Excellence

Student Involvement
Two graduate students (listed above) have participated in this project on a rotational basis to address various aspects of the project. Their main tasks have been to survey the data, interact with the data source and come up with a strategy to integrate the data into the database. They have also been working to develop the web-based portal for the actual implementation of the web interface.

Plans for Next Period: Start of Analysis
Year III for the database project will be an exciting period which transitions from the database construction and seeding of initial data to analysis and prioritization of the data. Several key efforts are planned and are currently underway. They are:

- Continued refinement of the database (search algorithms, database structure)
- Analysis of data I: determine key correlations between fuel properties and performance properties (i.e., DCN, viscosity, chemical group content, etc.)
- Analysis of data II: analysis of data to support the ASTM General Annex effort of fuel certification which includes a careful study of all relevant data used in the General Annex work to date and determine gaps or improvements as well as additional correlation work to link fuel properties to the overall evaluation
- Inclusion of NJFCP data: put up vetted and organized NJFCP data on the database.

Project 034, National Jet Fuels Combustion Program, Area #7: Overall Integration and Coordination

University of Dayton

Project Lead Investigator

Joshua Heyne
Assistant Professor
Mechanical Engineering
University of Dayton
300 College Park
Dayton, OH 45458
937 229-5319
Jheyne1@udayton.edu

University Participants

University of Dayton

- P.I.(s): Joshua Heyne and Alejandro Briones
- FAA Award Number: 13-C-AJFE-UD (Amendment Nos. 9, 10, &13)
- Period of Performance: September, 18 2015 to December, 31 2017
- Task(s):
    1. Overall NJFCP integration and coordination
    2. Well-Stirred Reactor experiments on LBO and Speciation
    3. Cross-experiment analysis
    4. Common format routine software and model development
    5. Spray modeling of Area 3 (GT P&W pressure atomizer)
    6. Procurement of additional geometries for testing

Project Funding Level

Amendment No. 9: $134,999.00 (September, 18 2015 to February, 28 2017)
Amendment No. 10: $249,330.00 (July, 7 2016 to December, 31 2017)
Amendment No. 13: $386,035.00 (August, 30 2016 to December, 31 2017)

Cost share is provided by GE Aviation ($135,000.00), DLR Germany ($512,924.00), United Technologies Research Center ($150,000.00), and the University of Dayton ($53,887.00) in to form of in-kind research at GE Aviation, DLR Germany, and United Technologies and direct financial support at the University of Dayton.

Investigation Team

- Joshua Heyne (University of Dayton) is the Project Lead Investigator for coordinating all NJFCP teams (both ASCENT and non-ASCENT efforts), Well-Stirred Reactor experiments, procuring additional geometrical configurations, and leading studies across experimental platforms within the NJFCP.
- Alejandro Briones (University of Dayton Research Institute) is the P.I. responsible for leading the common format routine software development.
- Vaidya Sankaran (UTRC) is sub-contracted to conduct the spray modeling of the Area 3 pressure atomizing spray injector.

- Bob Olding (University of Dayton Research Institute) is part of the team managed by Alejandro Briones to develop the common format routine software. Mr. Olding's main task is on Scheme GUI/TUI programing for later use by OEM CFD teams.
- Mike Hanchak (University of Dayton Research Institute) is part of the team managed by Alejandro Briones to develop the common format routine software. Mr. Hanchak's main task is on CFD and combustion programing for later use by OEM CFD teams.
- Robert Stachler (University of Dayton) is a Ph.D. student conducting the Lean Blowout and emissions measurements in the Well-Stirred Reactor.
- Jeremy Carson (University of Dayton) is a Master's student linking experimental results across ASCENT and non-ASCENT teams.
- Sherri Alexander (University of Dayton) is an administrative assistant aiding in the compilation of meeting minutes and setting up teleconference times.
- Scott Stouffer (University of Dayton Research Institute) is aiding in the procurement of additional geometries for NJFCP testing.

Project Overview

In total, the NJFCP is composed of more than two dozen member institutions contributing information and data as diverse as expert advice from gas turbine Original Equipment Manufacturers (OEMs), federal agencies, other ASCENT universities and corroborating experiments at DLR Germany, NRC Canada and other international partners etc. The project is tasked to coordinate and integrate amongst these diverse program stakeholders, academic Principle Investigators (PIs) and etc., cross-analyze results from other NJFCP areas, collect data for modeling and fuel comparison purposes in a Well-Stirred Reactor (WSR), conduct Large Eddy Simulations (LES) of sprays for the Area 3 High Sheer Rig, and procure additional swirler geometries for the NJFCP Areas and Allied Partners while developing interface of NJFCP modeling capabilities with OEM requirements. Work under this program consists of, but is not limited to:

- meetings with member institutions to facilitate the consistency of testing and modeling,
- coordinate timely completion of program milestones,
- documentation of results and procedures,
- creation of documents critical for program process (e.g. fuel down selection criteria)
- solicit and incorporate program feedback from OEMs,
- reporting and presenting on behalf of the NJFCP at meetings and technical conferences,
- integrate the state-of-the-art combustion and spray models into user-defined-functions (UDFs),
- WSR testing of NJFCP Category A, Category C, and Surrogate fuels,
- LES of sprays for A2, C1, and C5 fuels using the Area 3 High Sheer Rig Pratt & Whitney swirler and air blast atomizer,
- and advise the program Steering Committee.

Task 1: Integration and Coordination of NJFCP Teams

University of Dayton

Objective(s)

The objective of this task is to integrate and coordinate all ASCENT and non-ASCENT team efforts via facilitation of meetings, summarizing results, presenting results external to the NJFCP, communicating on a regular basis with the Steering Committee, and other related activities.

Research Approach

The NJFCP is integrated and coordinate via two main techniques: 1) the structural lumping of various teams into 6 Topic areas and 2) routine meeting and discussion both internal and external to individual Topic areas. The Topic areas are distinguished by the dominant physics associated with them (Topics I and IV), the culmination of all relevant combustion physics (Topics II, III, V), and wrapping all work into a singular OEM GUI package (Topic VI). These 6 Topic areas are:

Topic I. Chemical Kinetics: Foundational to any combustion model is a chemical kinetic model and the validation data anchoring modeling predictions.

Topic II. Lean Blow Off (LBO): This Topic covers data, screening, and validation at relevant conditions to statistically and theoretically anticipate fuel property effects on this FOM.

Topic III. Ignition: Similar to the LBO topic, the focus here is experimental screening and validation data for statistical and theoretical predictions.
Topic IV. Sprays: Historically, the dominant effect of fuel FOM behavior has been the spray character of the fuel relative to others. Experimentalists in this Topic area focus on measuring the fuel property effects on spray behavior. In analogy to Topic I, the spray behavior is not a FOM like Topic II and III, although it is critical to bound the physical property effects on combustion behavior relative to other processes, i.e. chemical kinetics.
Topic V. Computational Fluid Dynamics (CFD) Modeling: Complementary to the empirical Topics II, III, and IV, the CFD Modeling Topic focuses on the theoretical prediction of measured data and facilitates the development of theoretical modeling approaches.
Topic VI. User Defined Function (UDF) Development: Once the theoretical modeling approaches matured in Topic V are validated. UDFs are developed for OEM evaluation of fuel performance in proprietary rigs.

These Topic areas meet and coordinate on a regular basis. At minimum, NJFCP wide meetings are held monthly with Topic area meeting occurring on an as needed basis.

Milestone(s)
NJFCP Mid-Year Meeting 2016
NJFCP Year-End Meeting 2016

Major Accomplishments
Presentations at CRC Aviation Meeting, AIAA SciTech Meeting Paper and Presentation, and ASCENT Spring and Fall presentations 2016.

Publications
Peer-Reviewed Journal Publications:
Colket, Meredith B., Joshua S. Heyne, Mark Rumizen, James T. Edwards, Mohan Gupta, William M. Roquemore, Jeffrey P. Moder, Julian M. Tishkoff, and Chiping Li. 2016. “An Overview of the National Jet Fuels Combustion Program.” AIAA Journal.

Published conference proceedings:
Colket, Meredith B., Joshua S. Heyne, Mark Rumizen, James T. Edwards, Mohan Gupta, William M. Roquemore, Jeffrey P. Moder, Julian M. Tishkoff, and Chiping Li. 2016. “An Overview of the National Jet Fuels Combustion Program.” In AIAA SciTech. AIAA SciTech. San Diego, CA: American Institute of Aeronautics and Astronautics. doi:doi:10.2514/6.2016-0177.

Written reports:
None.

Outreach Efforts
Presentations at CRC Aviation Meeting, AIAA SciTech Meeting Paper and Presentation, ASCENT Spring and Fall presentations 2016, and DESS ASME conference.

Awards
Joshua Heyne – SOCHE Faculty Excellence Award

Student Involvement
None.

Plans for Next Period
Continue to perform all relevant coordination and integration related tasks.

Task 2: Testing of NJFCP in a Well-Stirred Reactor
University of Dayton

Objective(s)

We aim to measure the Lean Blowout (LBO) limit and emissions/speciation characteristics for NJFCP fuels within the program.

Research Approach

In response to legislative orders, industrial and governmental organizations are actively pursuing strategies to promote alternative energy fuels in gas turbine combustors, and to reduce pollutant emissions. Emissions tend to be of importance because of the adverse effects they have on air quality, health and the environment. Gaseous emissions of interest include nitrogen oxides (NO and NO_2), sulfur oxides (SO_x), carbon monoxide (CO), carbon dioxide (CO_2) and unburned hydrocarbons (UHC). The International Civil Aviation Organization (ICAO) currently regulates the total amount of UHC among NO_x, CO, and particulate (smoke number) emissions for aircraft, but the concentration of these emissions, whether unburned hydrocarbons or carbon monoxide, etc., have seen to have a local effect on areas around airports or flight lines (Anneken et al. 2014; D. L. Blunck et al. 2015; FAA 2012; Colket et al. 2016). Because of these effects and these initiatives, it is important to understand the emissions footprints of fuels for aviation for not only a sustainable future, but for better aircraft performance towards a carbon neutral future.

The National Jet Fuels Combustion Program (NJFCP) aims in streamlining the alternative jet fuel research and evaluation process, which is a major R&D directive covered in the Federal Alternative Jet Fuels Research and Development Strategy(AJF-IWG 2016; Colket et al. 2016). Use of specialized laboratory scale rigs are used in this program to determine fuel performance of a candidate alternative jet fuel while minimizing the use of multiple combustor rig tests. These rigs evaluate the impact of engine operability Figures of Merit (FOMs) such as lean blow off (LBO, high altitude relight, and cold start. These FOMs chosen indicate a strong impact on aircraft safety or engine hardware and are likely due fuel variation, whether due to the physical or chemical effects of the fuel. Performance and operability are also studied via emissions, combustor fuel coking and effects of temperature through pattern factors, radiation, and flame structure, all of which are secondary FOMs(Colket et al. 2016). It is imperative to investigate and pursue novel strategies and balance the combustor design characteristics with emissions reduction. Understanding performance and emissions with varying fuel composition provides the opportunity for use of potential alternative fuels in legacy and future aircraft and guidance to the quality and quantity of aircraft emissions produced.

Well-Stirred Reactor (WSR) experiments provide a simplified combustion environment to investigate chemical kinetic effects, among other parameters, such as combustion efficiency and LBO in the absence of physical property effects from the fuels. The lean premixed, prevaporized fuel and air mixtures used in these experiments remove physical effects such as droplet injection, evaporation, and atomization in addition to molecular mixing and transient and chemistry interaction of which is seen in typical gas-turbine combustors. With removing these physical effects, we also eliminate the physical complications native to modeling practical diffusion flame combustors such as, multi-dimensional flow, multi-phase fuel, and transient fluid dynamic and chemistry interactions. Use of this fundamental combustor experiment provides insight into LBO and emissions, a primary and secondary FOM in the NJFCP program, respectively, under relevant residence times and temperatures typically seen in practical gas-turbine-combustor environments(Colket et al. 2016).

We report the investigation of emissions and LBO of surrogate, conventional, and alternative fuel mixtures as lean combustion limits are approached in the WSR as funded by the FAA in relation the NJFCP. The WSR has provided considerable knowledge towards understanding lean and rich blow off limits, pollutant and particulate formation, kinetics of gaseous and liquid fuel combustion and combustion stability(D. Blunck et al. 2012; J. Blust, Ballal, and Sturgess 1997; S. D. Stouffer et al. 2005; J. W. Blust, Ballal, and Sturgess 1999; S Stouffer et al. 2002; Manzello et al. 2007; Vijlee 2014; Scott Stouffer et al. 2007; Nenniger et al. 1984; Zelina 1995; Karalus 2013; D. L. Blunck et al. 2015). Knowledge of the emissions and LBO provides the opportunity to investigate the controlling chemical kinetics and relating chemical properties among the fuels. Here we report a statistically significant correlation between LBO, derived cetane number, and radical index, yielding insight to the controlling chemical effects experienced in typical gas turbine combustors near LBO.

I. Experimental Details and Methodology

A. Well-Stirred Reactor

LBO and emissions experiments were performed in the well-stirred reactor (WSR) facility at the Air Force Research Laboratory in Dayton, OH. The toroidal WSR design was derived from the work of Nenniger et al.(Nenniger et al. 1984), Zelina(Zelina 1995), and Stouffer(S Stouffer et al. 2002) and approximates a zero-dimensional perfectly stirred reactor, *i.e.* homogeneous in both space and time. The reactor, shown during operation in Figure 1 a and b, comprises an Inconel jet ring, upper and lower ceramic reactor hemispheres, flow straightener, and exhaust stack. A representative cross section

drawing of the reactor is shown in Figure 1b. Premixed prevaporized fuel and air enter the jet ring through two opposed inlets to ensure equal flow around the reactor.

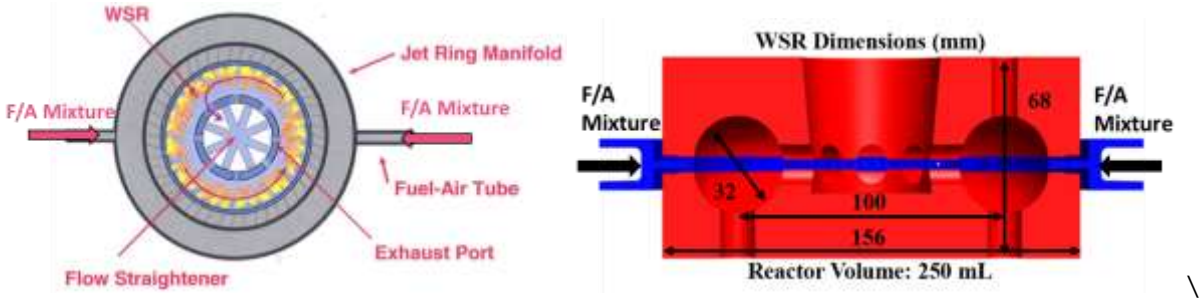

(a) (b)

Figure 1. (a) Cross-section of the WSR, top view(S. D. Stouffer et al. 2005; Scott Stouffer et al. 2007). Premixed, prevaporized fuel and air enters the jet ring via the two opposed inlets. The angled jets (20 degrees from the radius of the torus) inject the mixture into the reactor, where bulk recirculation and flow occurs around the reactor. Burned products exit towards the inner diameter of the toroid through the exhaust ports, the flow straightener, and exhaust stack. (b) Cross-section of the WSR, side view. Fuel an air enter the toroidal reactor through the jet ring in blue.

In the current work, a fused silica reactor (Rescor 750, SiO_2) was utilized and sealed using spring loaded sections.(S Stouffer et al. 2002; D. Blunck et al. 2012) This reactor material was chosen due to its low thermal conductivity, resistance to thermal cracking from fast transients, and reduction in the active cooling necessary around the reactor yielding reduced heat loss. An Inconel jet ring with 48 fuel/air jets at 1mm diameter was sealed between the reactor components. A ceramic paper gasket seal (Cotronics 390, 1/8" thickness) was placed between the upper reactor halve and jet ring while a mica gasket (0.064" thickness) was placed between the jet ring and bottom half to seal the reactor under fuel-lean operating conditions. Figure 1b highlights the construction of the WSR with the ceramic components in red and the jet ring in blue.

The feed jets in the jet ring inject the premixed fuel/air at an angle 20 degrees off the radius of the torus causing the bulk flow to move circumferentially around the reactor(S. D. Stouffer et al. 2005; S Stouffer et al. 2002; Vijlee 2014; Scott Stouffer et al. 2007; Nenniger et al. 1984). The sonic velocity and angle from the jets provides for recirculation zones around the upper and lower half of the toroid in addition to around the toroid. The high rate of continuous mixing between the unburned reactants and burned products is an additional characteristic that separates the WSR from other premixed combustions systems(Briones et al. 2008; D. L. Blunck et al. 2015; D. Blunck et al. 2012; S. D. Stouffer et al. 2005; Scott Stouffer et al. 2007). Previous work using numerical modeling has been performed to show that the WSR operates in the well-stirred turbulent regime(Briones et al. 2008). Products from combustion exit the reactor via 8 radial ports at the toroid inner diameter and through a 5-cm-diameter ceramic stack above the WSR. In this region, recirculation zones and bulk flow are reduced via the use of an alumina flow straightener, rested at the end of the exhaust and base of the stack(D. L. Blunck et al. 2015).

Liquid fuel is delivered to the vaporizer by two syringe pumps (Isco 500 D) operated in continuous flow mode. The piston flow meter accuracy is +/- 0.5%. The liquid fuel passes through a swirler and enters a heat exchanger, where the fuel reaches a temperature of 473 K at the inlet of the vaporizer. Heated fuel is introduced in the vaporizer with 10-20% of the total combustion air via an air-swirled atomizer nozzle containing heated air at 400 K and mass flow of 60 standard liters per minute (slpm). Remaining air at 489 K and mass flow of 440 slpm is added in the vaporizer as a coaxial stream(Scott Stouffer et al. 2007). Prior to entering the vaporizer, the air lines are filtered and monitored along with being controlled using two mass flow controllers, one rated at 1000 slpm and one rated at 75 slpm (Brooks Instruments) (S Stouffer et al. 2002). The accuracy for the mass flow controllers is rated at +/- 1% full scale and a repeatability of 0.25% of the flow rate. The flow controllers were measured and calibrated using sonic nozzles to allow for a more accurate measurement of the air flow rate. Electric, PID-controlled heaters preheat the incoming fuel and air streams. Flow rates of the fuel and air, paired with the temperature control of each, are used to control the incoming fuel-air mixture to the reactor. These flow rates ensure turbulent mixing and sonic velocities from the jets into the reactor (Vijlee 2014). The vaporizer used for the atmospheric WSR has been used in previous tests and was shown to safely and successfully mix the fuel with the air(S. D. Stouffer et al. 2005; Scott Stouffer et al. 2007). This strategy, using premixed and pre-vaporized fuel, eliminated physical complications associated with droplet combustion and established an ideal premixed combustion environment without physical complication.

A fixed custom spark igniter within the reactor initiates combustion. When testing with liquid fuel, the reactor was first brought to a stable thermal condition using a gaseous fuel (usually ethylene). Gaseous fuel flowrate into the WSR was controlled with a series of pressure regulators, to slowly reduce pressure, and mass flow controllers (Brooks Instruments). Introducing gaseous fuel before the liquid fuel allowed the reactor to effectively preheat for prevention of fuel condensation within the small jet ring passages. After operational temperatures were reached, the fuel was transitioned smoothly from the gaseous fuel to the given liquid fuel(Scott Stouffer et al. 2007).

B. Fuels

Four fuels tested in the current work are part of the National Jet Fuels Combustion Program (NJFCP). The NJFCP focus is to streamline the certification process for alternative jet fuels. Here the focus is to study the fundamental fuel kinetics and investigate the impact of alternative fuels on engine operability FOMs relative to reference fuels(Colket et al. 2016), enabling the process to be streamlined. FOMs such as cold start, altitude relight and LBO are key parameters considered in these fuels studies(Colket et al. 2016). The WSR is aimed to focus on the LBO FOM of engine operability in addition to determining the emissions footprint of the fuels in similar gas turbine combustor environments. The test fuels and their properties are shown in Table 1. These test fuels were characterized from the Combustion Rules and Tools for the Characterization of Alternative Fuels (CRATCAF) program and defined previously by OEMs(Colket et al. 2016). The category A fuels are intended to represent current jet fuels over a range of properties seen in current practice. Previous work has shown that flash point, aromatic content, and viscosity are of most impact for combustion behavior(Colket et al. 2016). A-2 and A-3 are fuels which exhibit 'average'/'worst' physical and chemical properties such as flash point, viscosity, aromatics, density, and derived cetane number respectively, giving an expectation envelope for conventional fuel combustion properties as they map to combustion behavior. C-1 and C-5 are alternative test fuels down selected by the NJFCP committee in 2015 from a total of six alt. jet fuel solvents(Colket et al. 2016). These fuel blends were selected to have properties near or exceed the limits acceptable jet fuels (i.e. viscosity, distillation curve, and chemical composition)(Colket et al. 2016). C-1 is composed of highly branched iso-paraffinic molecules with 12 and 16 carbon atoms, which have a low reactivity as exhibited by a derived cetane number of 17.1 (Colket et al. 2016). C-5 is a test fuel composed of two components, an isoparaffinic 10 carbon molecule and 1,3,5 trimethyl-benzene, which results in a flat boiling temperature/distillation curve(Colket et al. 2016). These two test fuels, C-1 and C-5, were intended to investigate effects of low cetane and narrow vaporization range of fuels on these combustor FOMs (Colket et al. 2016).

Table 1. Properties of the NJFCP Fuels Used for Testing in the WSR.

Fuel ID	A-2	A-3	C-1	C-5
POSF	10325	10289	12368	12345
Empirical Formula	$C_{11.4}H_{22.1}$	$C_{11.9}H_{22.6}$	$C_{12.6}H_{27.2}$	$C_{9.7}H_{18.7}$
AMW (g/mole)*	159	166	178	135
H/C Ratio	1.939	1.899	2.159	1.928
Stoichiometric Fuel/Air	0.0685	0.0687	0.0671	0.0686
Heat of Combustion (MJ/kg)	43.3	43	43.9	42.8
Density (g/cc)**	0.803	0.827	0.759	0.770
Derived Cetane Number (DCN)***	48.3	48.8	17.1	39.6

*Average molecular weight (AMW) measured using GCxGC
**Density measured using ASTM 4052, 15°C (kg/L)
***DCN measured using ASTM D5890(Colket et al. 2016)

Additional fuel surrogates were studied to investigate the effects of chemical structure on combustion performance and emissions and compared against current conventional fuels and fuel solvents. The surrogate fuels were chosen from the Strategic Environmental Research and Development Program (SERDP) aimed at studying the science of emissions of alternative fuels. *n*-Dodecane was used as a base fuel, and commonly used as a second generation fuel surrogate,

emulating JP-8 flame speed. This surrogate provides a better representation of the n-alkane content in jet fuels. *m*-Xylene was chosen as an additive to the base surrogate fuel to study the effects of aromatic content, and was chosen as 25% by volume to emulate the aromatic limit of JP-8. Molar carbon for the additive was kept constant to the aromatic content in the *n*-dodecane mixture, establishing a baseline for comparing surrogate performance. This fuel surrogate represents the *iso*-alkane hydrocarbon structure in jet fuels, and typically found in gas-to-liquid and FT fuels. Methylcyclohexane is used as the fuel surrogate for the cycloparaffins found in coal derived fuels. *n*-heptane is a straight chained hydrocarbon that mimics the light hydrocarbons in jet fuel and represents straight chain alkanes for a gasoline fuel surrogate. All surrogate mixtures in this paper were formulated to preserve the same carbon mole fraction as the *m*-xylene additive. Table 2 contains a list of relevant fuel properties pertaining to the WSR. Derived cetane number (DCN) for S-1, S-2, S-4, and S-5 were measured using the same ASTM standard as the NJFCP fuels. The DCN for S-3 was calculated using the summation of the volume fraction of the given fuel multiplied by its corresponding cetane number(Yanowitz et al. 2004).

Table 2. Properties of the Surrogate Fuels Used for Testing in the WSR.

Surrogate Blends	*n*-dodecane (61.8 mol%) / *m*-Xylene (38.2 mol%)	*n*-dodecane (61.8 mol %) / *iso*-Octane (38.2 mol%)	*n*-dodecane	*n*-dodecane (58.6 mol%) / Methyl-cyclohexane (41.4 mol%)	*n*-dodecane (58.6 mol%) / *n*-heptane (41.4 mol%)
Fuel ID	S-1	S-2	S-3	S-4	S-5
Empirical Formula	$C_{10.47}H_{19.9}$	$C_{10.49}H_{22.98}$	$C_{12}H_{26}$	$C_{9.93}H_{21.03}$	$C_{9.93}H_{21.86}$
H/C Ratio	1.900	2.191	2.167	2.118	2.201
Stoichiometric Fuel/air	0.0687	0.0669	0.0670	0.0673	0.0668
MW	145.84	149.12	170.31	140.45	141.28
Density (g/cc)	0.778	0.737	0.750	0.758	0.734
Derived Cetane* Number (DCN)	57.47	60.91	78.5	54.05	67.46

*DCN for S-1, S-2, S-4, S-5 measured using ASTM D5890(Colket et al. 2016)

C. Emissions and Instrumentation

A bare, linear-tracking, custom, type-B thermocouple (0.2mm diameter, platinum – 6% rhodium, platinum – 30% rhodium) without coating was used to measure reactor temperature. Measurements for temperature were taken at 0.25" from the outer wall of the reactor and were not corrected for radiation and other heat losses. Therefore, the gas temperature readings may not be accurate in an absolute sense, yielding lower temperatures than expected, but enable relative comparisons between conditions. The thermocouple location is within the uniform temperature region in the WSR and the temperature can therefore be taken as the average temperature in the reactor. A 0–5 psia pressure transducer was used to monitor the slight pressure increase in the reactor during operation. A maximum pressure of 5.5 kPa above ambient conditions was experienced during testing.

Exhaust samples were extracted using an oil-cooled probe (420 K) through a 1.4-mm-diameter orifice. The samples were passed through the probe which quenches the reactions, similar to quenching in a typical combustor (D. Blunck et al. 2012). The probe rested 5 mm above the wall of the lower toroid and is 90 degrees around the axis of the toroid from the thermocouple. Temperatures of the oil were kept constant at 420K while sampling to minimize condensation in the sampling line.

Gaseous emissions were transported through a heated line containing a pump, filter and oven before entering the Fourier Transform Infrared (FTIR) analyzer. The heated lines and oven were maintained at 420 K by PID controllers. Flow entered and exited the FTIR at a constant temperature of 463K where it was exhausted or sampled via charcoal tubes and gas bags. A sketch of the sampling methodology is shown in Figure 2.

The FTIR system utilized in the current work was a MKS 2030 High Speed (5Hz) gas analyzer with a gas cell path length of 5.11 m and was used to measure the emissions from the WSR. This FTIR system allows major gaseous species to be detected online, while saving the spectra for later detailed investigation. The Gasoline Ethanol method, within the MKS

software package, was employed to analyze the IR spectra and calculate emission concentration values. Measurement accuracy using this FTIR is +/- 2%. Carbon monoxide (CO), carbon dioxide (CO_2), water (H_2O), nitrogen oxide (NO), nitrogen dioxide (NO2), acetylene (C_2H_2), ethylene (C_2H_4), and formaldehyde (CH_2O) are among the many emissions that absorb infrared radiation and can be quantified using the method employed in the FTIR.

Following the FTIR was a valve to capture bag samples and enable offline measurement of C1-C12 species, primarily for C1-C4 hydrocarbons. An Agilent 6890/5973 GC-FID-MS (Gas Chromatography-Flame Ionization Detector-Mass Spectrometry) and Gas Pro Column was utilized to analyze emissions from the extracted samples. Capturing exhaust emissions through charcoal tubes was also employed as a sampling technique to obtain heavy hydrocarbon species, generally above C4 species. Another valve following the FTIR was used to draw these samples. A pump drew 1-liter exhaust emission samples at a rate of 1 liter per minute. Remaining gases pulled through the pump were exhausted through the hood where the WSR operates. Previous work has been performed using this method to extract hydrocarbons from jet-fuel emissions (Anneken et al. 2014). The tube was later extracted with carbon disulfide and the mass of each component was measured using an Agilent 7890 GC-FID and Gas Pro Column.

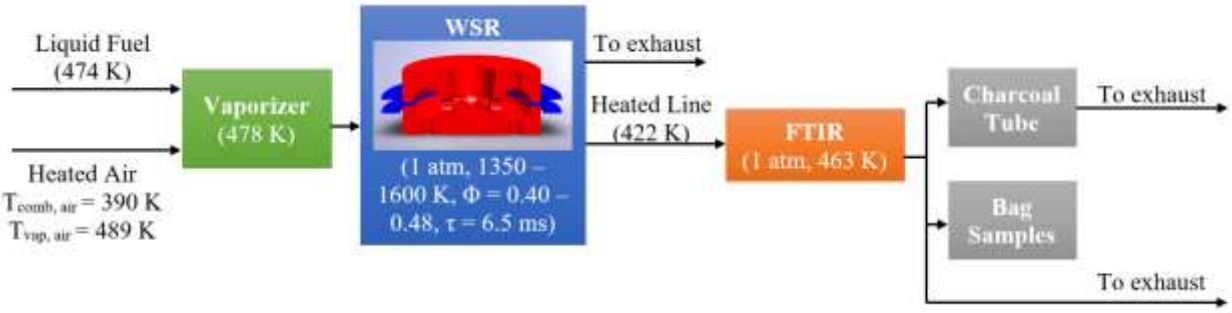

Figure 2. Experimental Schematic for WSR Emission Studies. A heated line takes the sample from the reaction region in the WSR to the FTIR. Charcoal tube and bag samples are taken after the FTIR before being exhausted.

During testing, online concentration measurements of various species were made using an FTIR. Roughly 95% of the carbon containing species were recovered by the FTIR at the higher equivalence ratios, reducing to roughly 92% near LBO as shown in Figure 3. The ~5% carbon deficit can be attributed primarily to FTIR measurement uncertainties. In addition, insufficient quenching during extractive sampling from the WSR can contribute to the uncertainty as sampled could react in the sampling lines and measurements are not representative of the actual combusting environment. The high percent of carbon recovered provides confidence as to the quantitative fidelity of species measured and the relative species concentration between fuels.

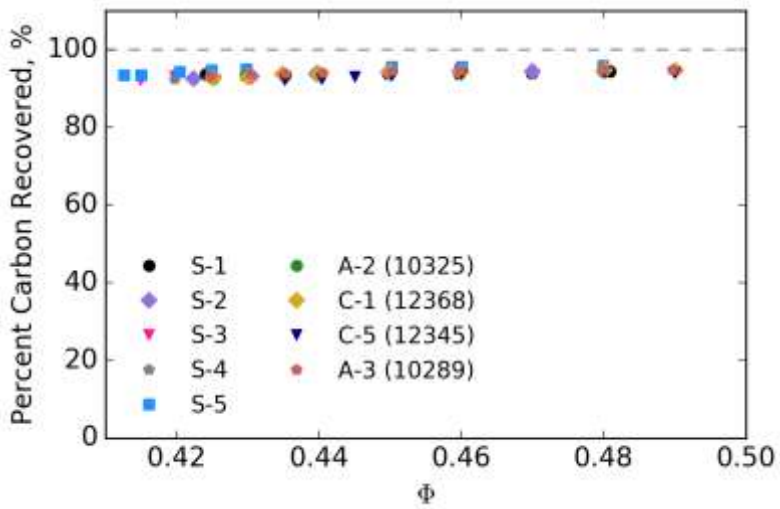

Figure 3. Carbon recovery from the species captured via online FTIR sampling. A decrease in percent carbon recovered is seen as equivalence ratio (Φ) is decreased. This signifies that intermediate species are produced and some are not recovered using this emissions measurement technique. The high percentage of carbon recovered provides confidence that this method captures emissions adequately to yield quantitative results.

II. Experimental Conditions

The equivalence ratio was set by varying fuel flow rate. Each LBO measurement was initiated at an equivalence ratio of >0.48 where formaldehyde levels dropped below the detection limit (≈0 ppm). Equivalence ratios were reduced by keeping air constant and decreasing fuel flow until LBO where the flame extinguished. Heat loss at LBO conditions becomes too large and combustion is unstable and is not sustained. A drop in reactor temperature and change in noise generated by the reactor corresponded to a LBO(Scott Stouffer et al. 2007).

Temperatures at these conditions were well below the maximum operating temperature of the ceramic. This enabled durability for testing with a single build of the reactor and prevented cracking. Premixed fuel and air coming into the jet ring was held at a constant temperature of 460 K, which is in the typical combustor range of 200–900 K (McAllister, Chen, and Fernandez-Pello 2011; Colket et al. 2016). Reactor temperatures during the test varied between 1350 K and 1500 K based on the heat of combustion of each fuel and heat loss from the system. The heat loss from the system was estimated at 5% using the ceramic reactor(J. Blust, Ballal, and Sturgess 1997). The health of the ceramic reactor was monitored by measuring the temperature of the jet ring. When a cracked formed, a large asymmetric temperature profile was observed in the jet ring. Towards leaner conditions, the jet ring temperature profile varied a maximum of approximately 2% (10 K) peak-to-peak, indicating the ceramic reactor remained free from cracks.

Global reacting residence time for the experiments was 6-7 ms. Bulk residence time was calculated using the volume of the reactor, the flow rates of the fuel and air, and the density of the mixture under reacting conditions. Variations in residence time were primarily a result of changes in reactor temperature and fuel mass flow since change in reactor pressure and molecular weight are small(Scott Stouffer et al. 2007). At most points throughout each experiment, the reactor was allowed to reach a thermal steady state and then held at constant flow and thermal conditions for more than 12 minutes. Non-emission data was captured from a running average of approximately 12 seconds every 3 minutes.

FTIR measurements, recorded continuously at 5 Hz, were averaged over the 12 second running average period for each sample, while gas bags and charcoal tubes were taken at the last point of the sampling process for each equivalence ratio. This holistic sampling process captured major and minor species throughout the duration of the experiment, while ensuring steady state conditions for the bag and charcoal tube samples.

For points at or near LBO, the reactor could not be held constant for 12 minutes because of the tendency to blow off. At these near-LBO conditions, a non-steady-state condition between the wall and gas temperatures may be responsible for some scatter in the WSR temperature data. Once blow off occurred, the reactor was re-ignited by reducing air and fuel flow rates. Once steady state conditions were reached at the start of the blow off test, a second test was conducted in a similar fashion. As experienced in previous experiments, hysteresis does exist in approaching LBO if there is insufficient time for the reactor to reach a steady-state temperature at each condition. Leaner conditions can be reached if the reactor walls are

relatively hot, resulting from a rapid decrease in equivalence ratio. If LBO is approached more slowly, the walls have sufficient time to cool to the local gas temperature and, therefore, LBO is experienced at higher equivalence ratios(Vijlee 2014). Increments were small while decreasing the fuel flow, thus reducing the chance for hysteresis. Previous literature showed variance in blow off temperature of +/- 50 K(Vijlee 2014) and uncertainty of blow off equivalence ratio near 2% (D. L. Blunck et al. 2015). Based on the sonic nozzle calibration and the self-consistency between the two or more LBO tests per fuel, the uncertainty in equivalence ratio was estimated as Φ +/- ~0.0025. The primary parameter controlling the uncertainty was the repeatability of the air mass flow controllers based on the operating conditions.

Table 3. Operating conditions using the WSR

Pressure (atm)	**1**
Inlet Temperature (K)	460
Reactor Temperature (K)	1350 – 1600
Bulk Residence Time (ms)	6 – 7
Mass Flow Air (g/min)	600
Equivalence Ratio	0.425 – 0.49

III. Results and Discussion

A. LBO

LBO occurs when the flame cannot be sustained because of either fluid dynamic or chemical processes. In the WSR, LBO is most sensitive to chemical processes associated with heat release, and ideally insensitive to mixing and fluid processes. Experimental results are shown in the figures below for the four NJFCP fuels and the five surrogate mixtures. Figure 4 shows the effect of lowering the fuel flow, hence lowering the equivalence ratio. The reactor trends to decrease linearly with leaner conditions. C-1 shows to have the least resistance to LBO, having the highest Φ at LBO, while the S-3 and S-5 straight chained alkane surrogates trended to have the most resistance to LBO. LBO occurs at the lowest recorded equivalence ratio of roughly 0.414, In contrast, the C-1 fuel exhibits LBO at the highest recorded equivalence ratio.

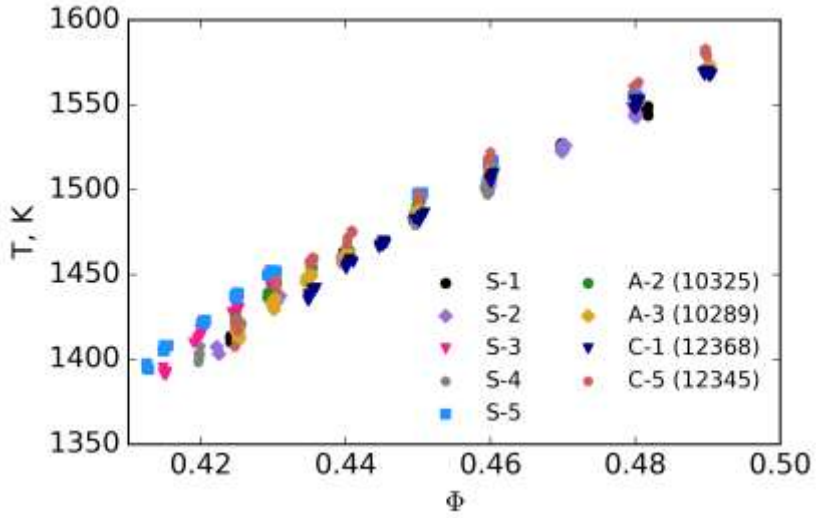

Figure 4. Reactor temperature (K) as a function of Φ for the fuels. Points represent the samples taken at each equivalence ratio tested. As leaner conditions are approached, the reactor temperature lowers linearly to the point where combustion cannot be sustained, corresponding to LBO. C-1 has the least resistance to LBO, having the highest Φ at LBO, while S-3 and S-5, straight chain alkane blends, trended to have the most resistance to LBO.

Since the WSR is operating in a lean, premixed, prevaporized combustion environment, the combustion property targets (CPTs) can be investigated as it relates to LBO. These CPTs, H/C ratio, MW, Threshold Sooting Index (TSI), and derived cetane number (DCN), have shown to sufficiently match combustion behaviors in pre-vaporized environments for petroleum-derived and synthetic jet fuels(Won, Veloo, Santner, Ju, Dryer, et al., n.d.). H/C ratio is used as it relates energy density of a particular fuel, as well as describes the composition and the distribution of radicals produced form combustion processes.(Won, Veloo, Santner, Ju, Dryer, et al., n.d.) LBO is shown below in Figure 5 as a function of H/C ratio. For each fuel, the last sampled condition immediately preceding LBO was averaged for both runs. If LBO occurred during sampling, the mean LBO was calculated using the average of those samples with the previous full sample preceding LBO. The uncertainty bars represent the uncertainty based on the air and mass flow rates. Towards the left of Figure 5, mean LBO was nearly identical at ~0.425. This is a result of the roughly 0.005 (~1%) step size in equivalence ratio, used to obtain stable points for emissions capture near LBO. The mean Φ represents roughly the last point captured for emissions data before blow off occurs. However, based on the given fuels and their LBO conditions, there exists a distribution of fuels which lie outside the bounds of the uncertainty estimated and are statistically significant. Based on the current distribution of data, there doesn't exist a correlation of LBO for the given fuels with varying H/C ratios. Molecular weight was also plotted as a function of Φ for the fuels. This property corresponds to the reactivity of the fuel via the normal and branched alkanes in the fuel and also does not trend to correlate, shown in Figure 6.

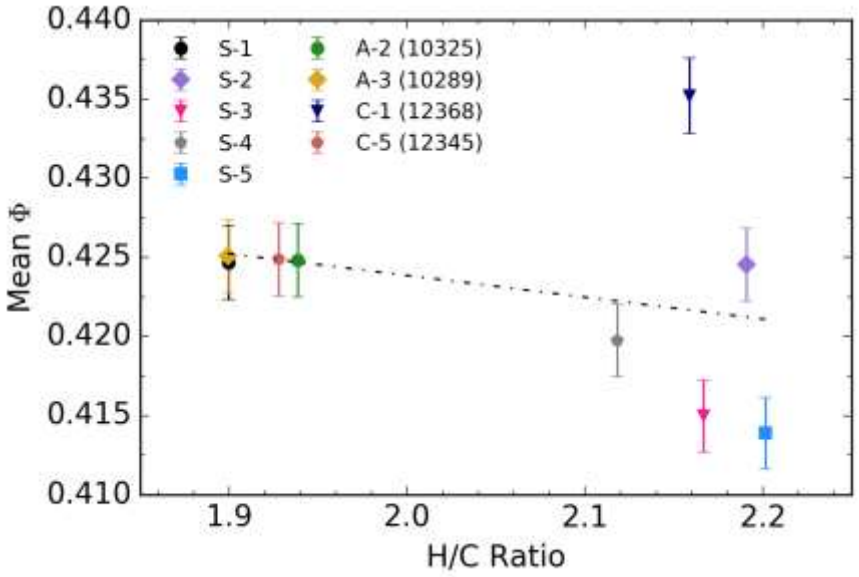

Figure 5. Mean Φ as a function of H/C Ratio. Points represent the average of the data at each equivalence ratio, while the error bars represent the uncertainty of the measured and averaged Φ. (Eq. -0.01374x+0.45134 = y, R^2 = 0.0849).

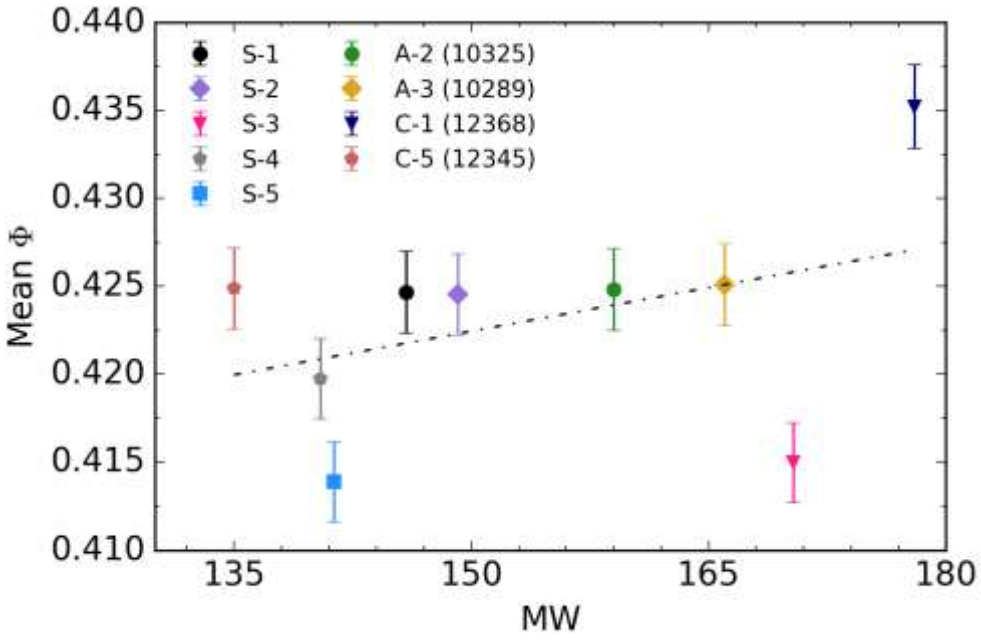

Figure 6. Mean Φ as a function of molecular weight. Points represent the average of the data at each equivalence ratio, while the error bars represent the uncertainty of the measured and averaged Φ. (Eq. 1.652E-04x+0.0.3977 = y, R^2 = 0.1527).

TSI, another CPT, correlates the competition of aromatic molecules and highly-branched alkanes with the radical pool and is important as it describes the sooting tendency of a fuel(Won, Veloo, Santner, Ju, Dryer, et al., n.d.). This correlation of reactivity of a fuel varies inversely with TSI, using this methodology(Won, Veloo, Santner, Ju, Dryer, et al., n.d.). Values were estimated for the given surrogate fuels using linear combination of each mole percent of components by their corresponding TSI.(Mensch 2009) Based on Figure 7 below, there doesn't exist to show a correlation among the TSI and LBO. Although there is no apparent correlation, the effect of aromatic content in S-1 shows to have an effect on increasing the TSI, where further investigation on determining the TSI of the conventional and alternative fuels would be useful.

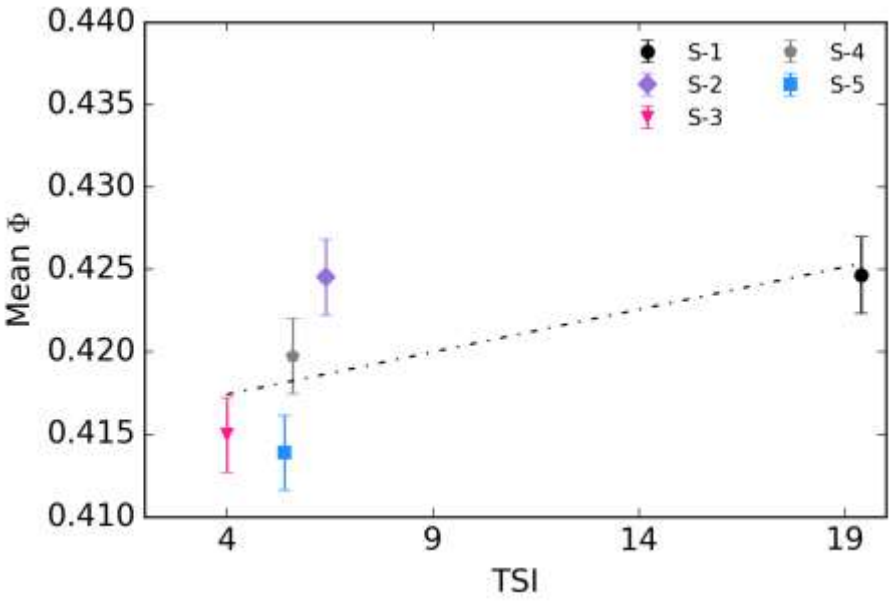

Figure 7. Mean Φ as a function of TSI. Points represent the average of the data at each equivalence ratio, while the error bars represent the uncertainty of the measured and averaged Φ. (Eq. 5.158E-04x+0.41536= y, R^2 = 0.41134).

Figures 8 and 9 display the effects of LBO with DCN and radical index, respectively. Based on the given data set and Figure 8 below, there appears to be a functional dependence on cetane number of the fuel when comparing to LBO. Low derived cetane numbers correspond to a longer ignition delay, which is a potential attribute to the LBO difference seen in the given fuels set. This trend can yield understand towards this parameter and potential implications in gas turbine combustors. Also, the tested data only contains two emissions profiles per fuel, yielding some additional uncertainty.

Radical indices were approximated from literature (Won, Veloo, Santner, Ju, and Dryer, n.d.; Won, Dooley, et al., n.d.). S-1 and S-2 were estimated using the radical indices of the surrogate mixture components multiplied by the corresponding mole percentage. The radical index for *m*-Xylene was approximated between toluene and 135TMB assuming a linear correlation(Won, Dooley, et al., n.d.). S-3 and S-5 mixture was approximated at 1, being of n-paraffinic structure, where A-2 and C-1 were assumed to be similar to JP-8 and IPK, respectively(Won, Veloo, Santner, Ju, and Dryer, n.d.). A-3 was assumed to be of JP8(Won, Veloo, Santner, Ju, and Dryer, n.d.), even though A-3 contains more iso-paraffins. The radical indices for *iso*-octane and JP8 were near identical and used as a rough estimate to investigate potential correlations of LBO with radical index. A radical index for m-xylene was approximated between the values of toluene and 135TMB, assuming a linear relationship between the values. These preliminary approximations show a correlation with LBO as seen in Figure 8. The higher radical index indicates a larger radical pool in which the radicals aid in sustaining combustion, tending to blow out at leaner conditions. Towards the left portion of Figure 6, C-1 trends to blow out at a higher equivalence ratio, where it has the lowest assumed radical index. Behavior experienced in Figure 8 and 9 show a similar trend with LBO and indicate dependence on DCN and on radical index. This knowledge, along with the ability to create surrogates to vary one of the characteristics (DCN or RI), can assist in further understanding the extinction and LBO behavior of a given fuel.

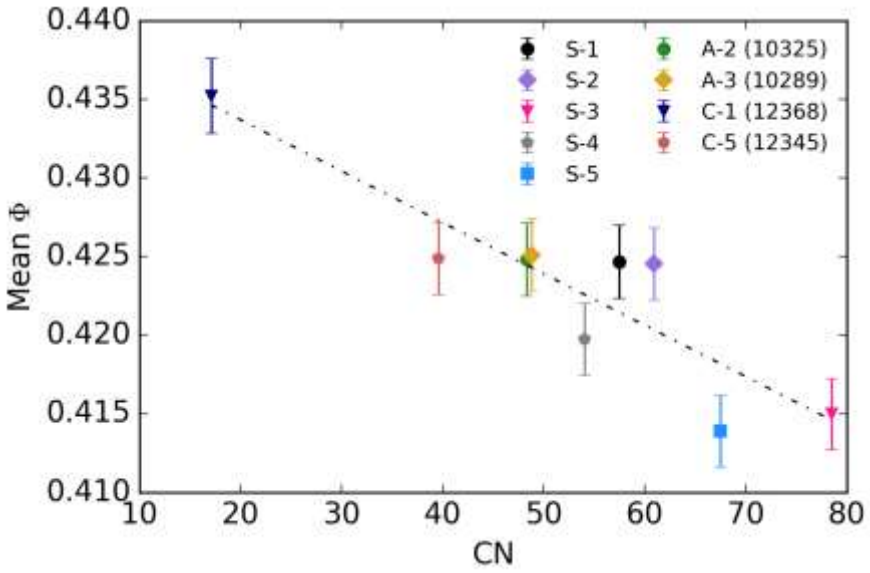

Figure 8. Mean Φ as a function of DCN. Points represent the average of the data at each equivalence ratio, while the error bars represent the uncertainty of the measured and averaged Φ. (Eq. -3.268E-4x+0.44023 = y, R^2 = 0.8097). Percent Difference in Φ from S-5 to C-1 is ~5%.

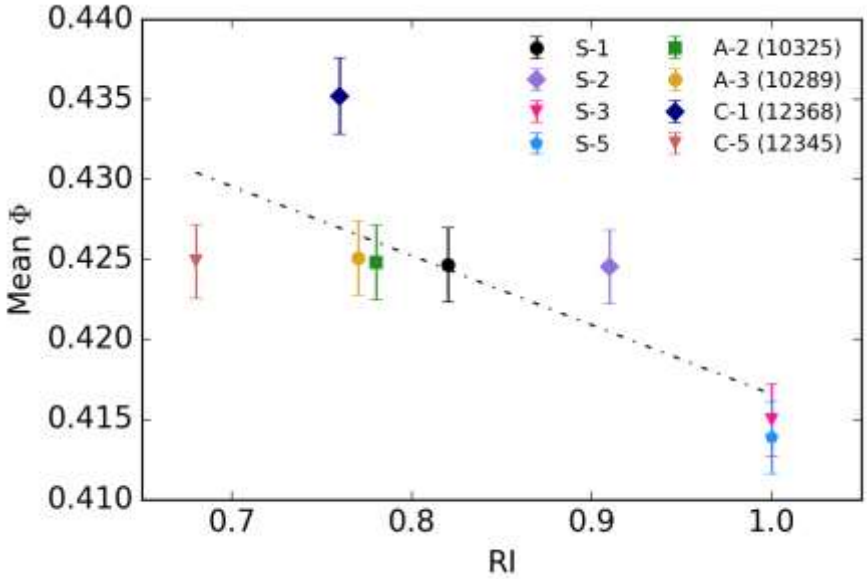

Figure 9. Mean Φ as a function of Radical Index. Points represent the average of the data at each equivalence ratio, while the error bars represent the uncertainty of the measured and averaged Φ. (Eq. -0.04328x+0.4599= y, R^2 = 0.585)

B. Emissions Profile

As described in the previous section, the fuel chemistry can play an important role in LBO. For instance, surrogate fuels may have a similar heat of combustion and derived cetane number, S-1 and S-2, but different radical index, 0.82 and 0.91 respectively. This difference in radical index can be caused by the presence of radical-promoting reactions and/or radical-trapping reactions that occur as a result of the fuel chemistry, in this case aromatic or iso-alkane content. The WSR is

specifically designed to provide relevant information on the effects of fuel chemistry on combustion emissions and stability under conditions similar to those in typical combustors, specifically the primary and secondary zones. This approach enables fuel-specific emissions fingerprints to be generated while approaching LBO. The species produced under these conditions are highly sensitive to the specific fuel chemistry and, therefore, provide a sensitive metric for developing reduced-order chemical mechanisms. These emissions profiles can also be utilized along with the DCN, radical index, H/C ratio, MW, and TSI to determine the chemical property dependencies driving LBO in various experimental arrangements.

Figure 10 shows the major carbon-containing combustion products, as a function of equivalence ratio, produced during testing of the WSR. CO and CO_2 compose approximately 99.9% and 99% of the total carbon count in the sampled emissions at the areas of higher equivalence ratios and towards the leanest conditions, respectively. As the fuel rate decreases to leaner conditions, less CO_2 is produced allowing for intermediate species to be formed as a result of incomplete combustion and thus incomplete conversion to CO_2. As observed in Figure 10(a), CO_2 produced from the C-1 fuel and the S-2 surrogate mixture are similar yet follow a distinctly different curve towards LBO relative to the other fuels, although C-1 LBO occurs at a higher equivalence ratio. In contrast, CO is increased as LBO is approached for all fuels. The two bounding fuels are S-5 which produced the most CO_2 and least CO and C-1 which produced the least CO_2 and most CO for a given equivalence ratio.

Although the carbon deficit in the CO_2 production between C-1 and S-5 was primarily recovered in the form of CO, the total carbon count for the six largest carbon containing species is shown in Figure 11. It is clear that at $\Phi = 0.435$, C-1 produces an order of magnitude more formaldehyde than any other fuel, in addition to increased concentrations of ethylene, acetylene, methane, and isobutene.

Formaldehyde production as a function of equivalence ratio is displayed in Figure 12 for all fuels. This species is particularly important as it is a key intermediate species in the oxidation of hydrocarbons and can significantly shorten the ignition delay time of fuel/air mixtures. Specifically, previous work has shown that many hydrocarbon species can be linearly related to formaldehyde production, regardless of fuel type(D. L. Blunck et al. 2015), although C-1 tends to be the outlier. Methane recorded from the FTIR is seen to exhibit that linear relationship as a function of formaldehyde, as observed in the same figure. For this reason, species production in all subsequent figures is plotted against both equivalence ratio and formaldehyde.

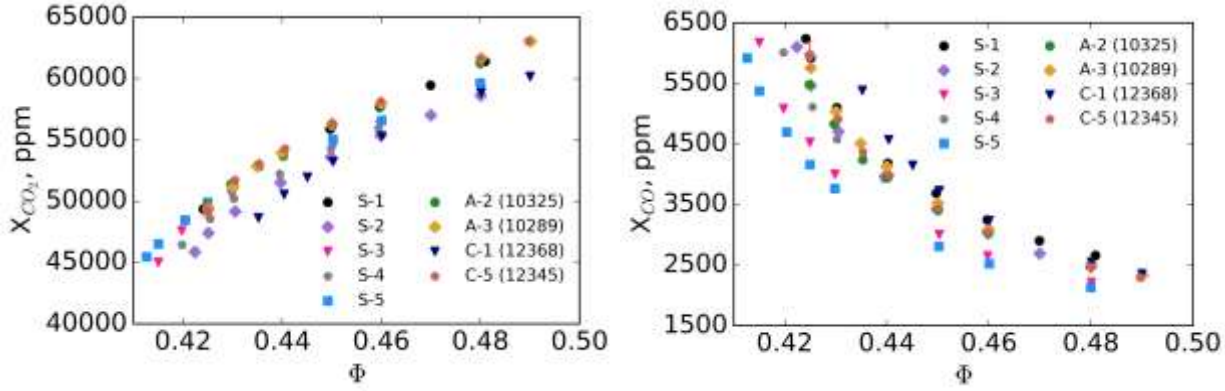

(a) (b)

Figure 10. CO_2 (a) and CO (b) as a function of equivalence ratio (Φ). Points represent the average of the data at each equivalence ratio, while the error bars represent one standard deviation. Trends in decreasing CO_2 and increasing CO while approaching leaner conditions is expected, signifying losses in combustion efficiency towards LBO.

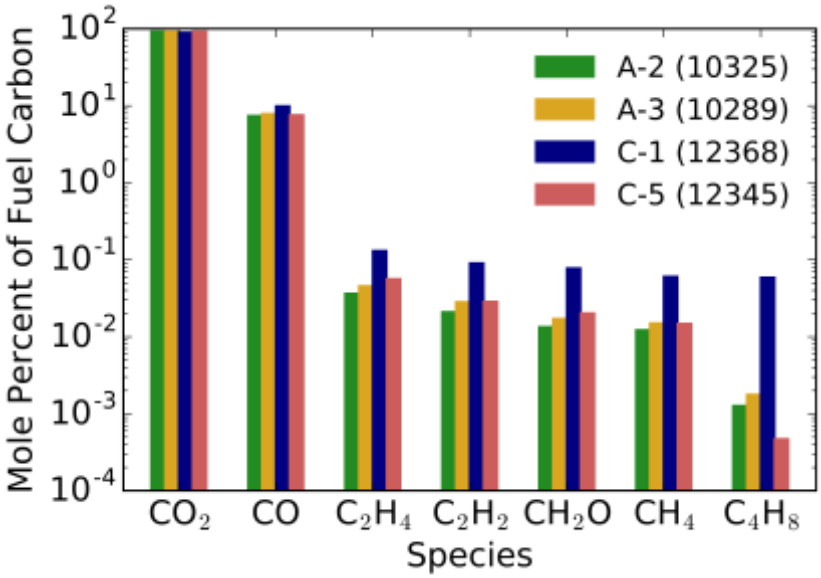

Figure 11. Mole percent of fuel carbon on the given species at Φ = 0.435. C-1 appears to be most distinguished, as it is at the leanest condition before LBO, producing more intermediate species.

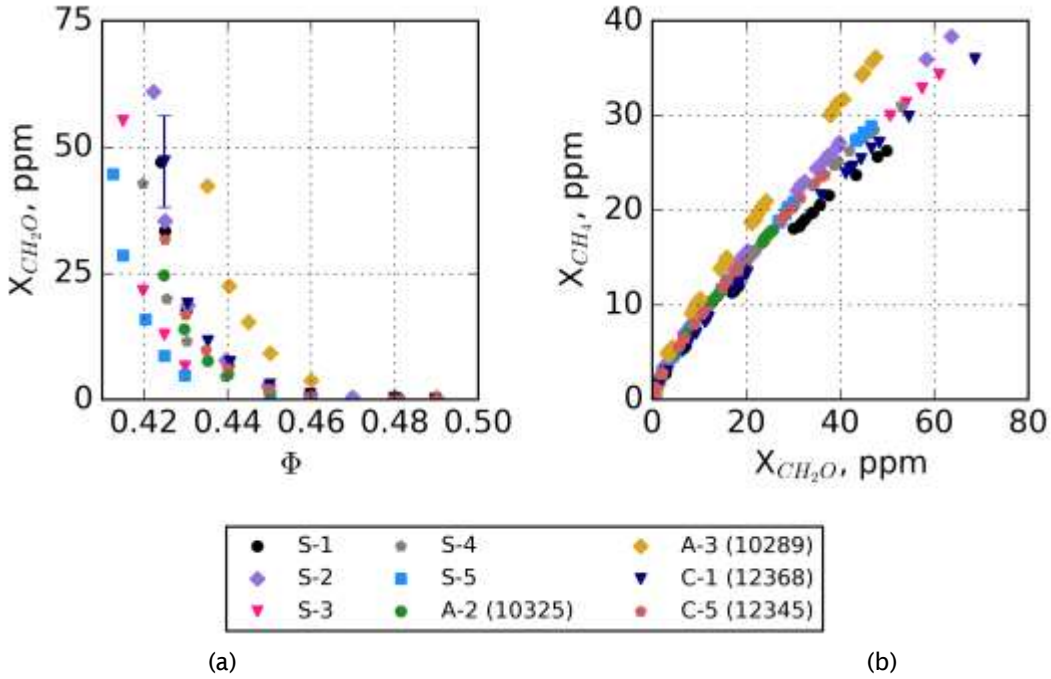

(a) (b)

Figure 12. Formaldehyde (CH_2O) as a function of equivalence ratio (Φ) and methane (CH_4) as a function of formaldehyde production. Points represent the average of the data at each equivalence ratio, while the error bars represent the maximum standard deviation in the reported set.

Figure 13 and 14 displays ethylene and acetylene production towards lean low off conditions using the online FTIR method, respectively.

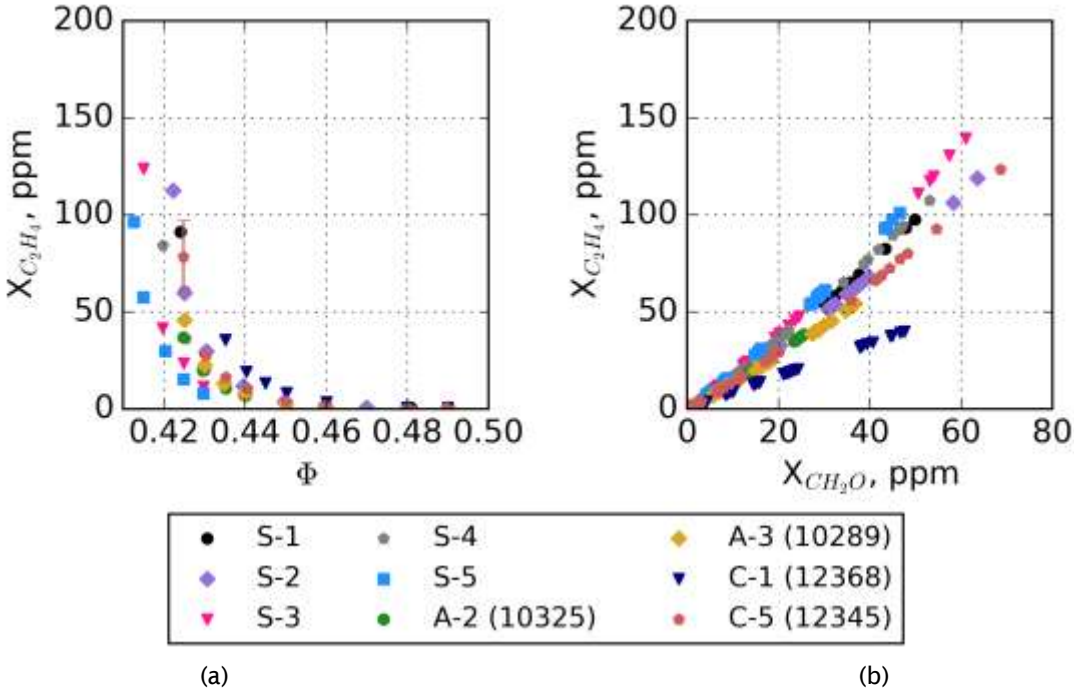

(a) (b)

Figure 13. Ethylene (C_2H_4) as a function of equivalence ratio (Φ) sampled from the FTIR. (a) Points represent the average of the data at each equivalence ratio, while the error bars represent the maximum standard deviation in the reported set. (b) Points represent the all the sampled data as a function of formaldehyde.

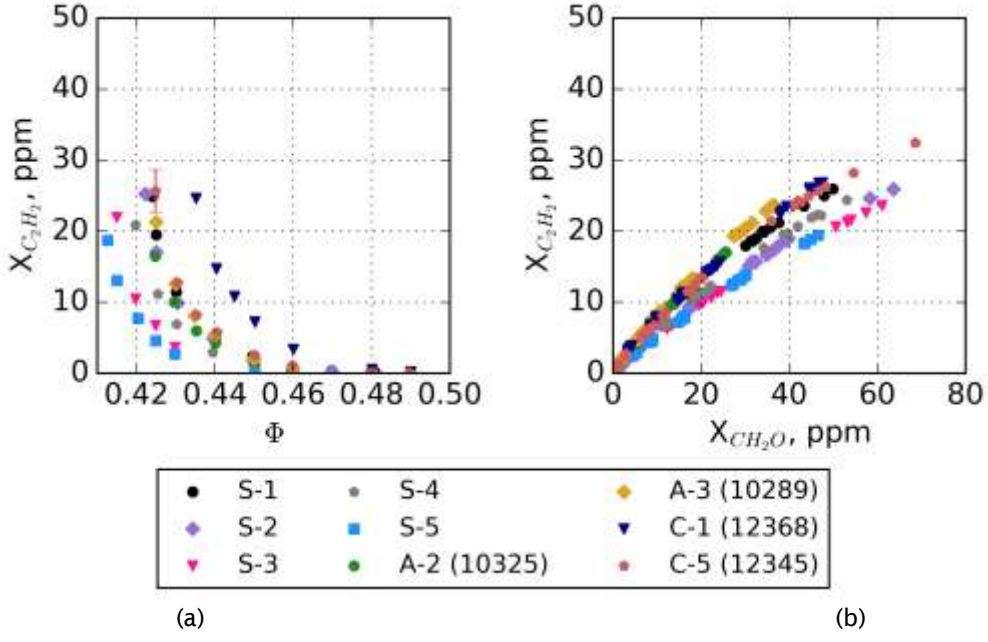

(a) (b)

Figure 14. Acetylene (C_2H_2) as a function of equivalence ratio (Φ) sampled from the FTIR. (a) Points represent the average of the data at each equivalence ratio, while the error bars represent the maximum standard deviation in the reported set. (b) Points represent the all the sampled data as a function of formaldehyde.

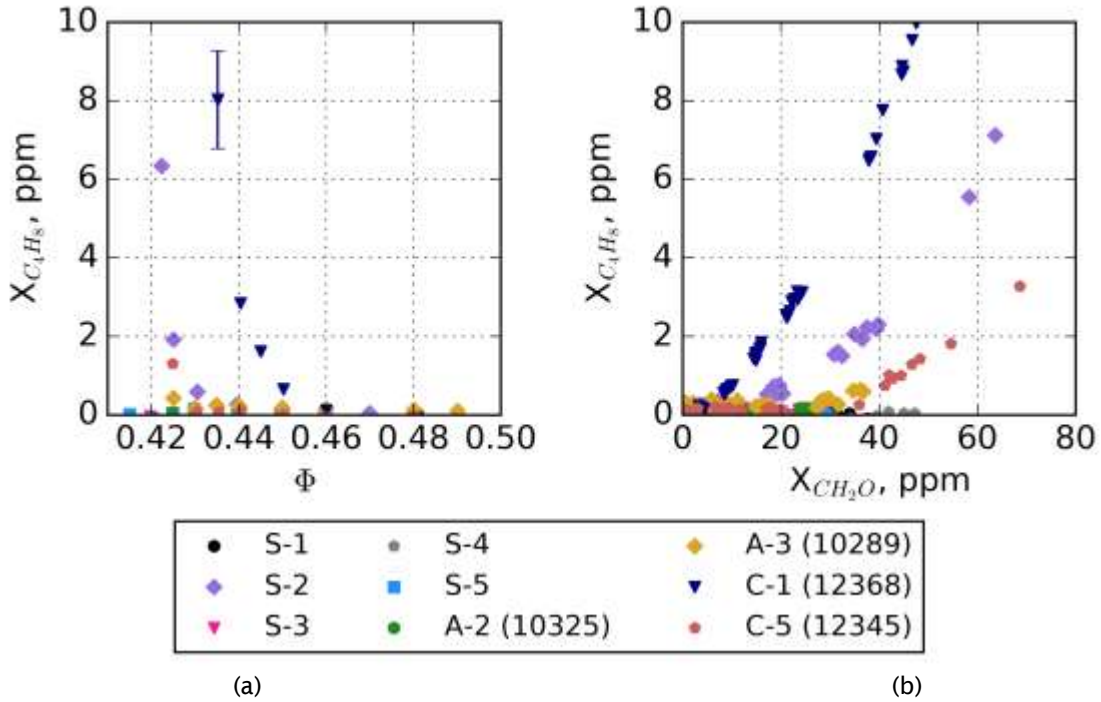

(a) (b)

Figure 15. Isobutene (C_4H_8) as a function of equivalence ratio (Φ) sampled from the FTIR. (a) Points represent the average of the data at each equivalence ratio, while the error bars represent the maximum standard deviation in the reported set. (b) Points represent the all the sampled data as a function of formaldehyde.

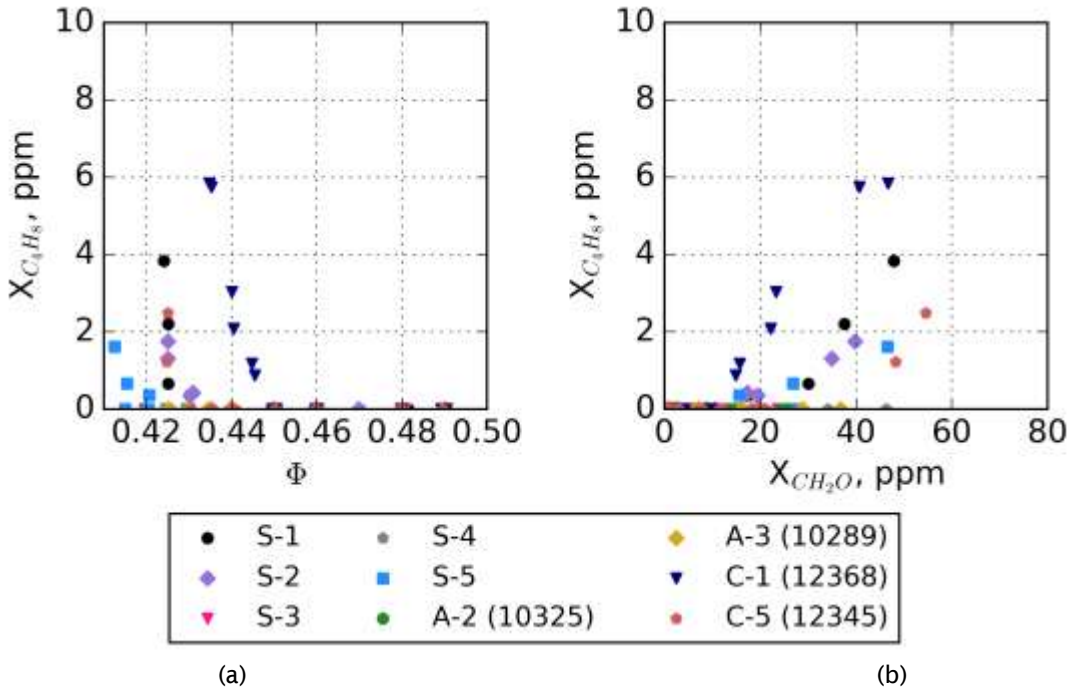

Figure 16. Isobutene (C_4H_8) as a function of equivalence ratio (Φ) from the charcoal tube methodology. (a) Points and samples taken during testing at the end of each condition as a function of equivalence ratio. (b) Points and samples taken during testing at the end of each condition as a function of formaldehyde.

V. Conclusions

A WSR operating under fuel-lean conditions was utilized to measure performance and gaseous emissions characteristics of conventional and alternative aviation fuels. LBO was also explored under the same loading condition to determine the difference in LBO with different fuels. The experiment showed:

1. Recovery of carbon captured is favorable from the FTIR and can provide encouraging results with the current species captured.
2. The C-1 test fuel is least resistant to LBO as the conditions for which it occurs happens at a higher equivalence ratio and at a higher reactor temperature than the other tested fuels.
3. LBO shows a strong correlation with derived cetane number, which describes a need for investigating fuel dependency on combustor design.
4. As conditions approach LBO, intermediate species are produced of which have a correlation between formaldhyde production. These conditions towards LBO signify decreased combustion efficiency as more intermediate species are seen.

Derived cetane number will be investigated in the future to determine if derived cetane number is driving the LBO conditions and emissions towards LBO. A fuel surrogate will be tested, C_{12}/TMB establishing a very similar cetane number, but is comprised of aromatics, to bridge preliminary understanding of derived cetane number and its relation to LBO. Continued analysis will enable investigation of chemical kinetic pathways specific to each fuel, which then establishes an understanding of the chemical effects in a lean, premixed, prevaporized environment, a relevant area of interest for future gas turbine combustor design.

The WSR represents an ideal, premixed, pre-vaporized combustor. It is used to study fuel chemistry effects on emissions and LBO. Thus, we believe the knowledge gained from the fuel effects in our LBO and emissions studies have relevance to current and future combustion systems.

References

AJF-IWG. 2016. "Federal Alternative Jet Fuels Research and Development Strategy." OSTP.

Anneken, David, Richard Striebich, Matthew J. DeWitt, Christopher Klingshirn, and Edwin Corporan. 2014. "Development of Methodologies for Identification and Quantification of Hazardous Air Pollutants from Turbine Engine Emissions." Journal of the Air & Waste Management Association 65 (3): 336–46. doi:10.1080/10962247.2014.991855.

Blunck, D, J Cain, Rc Striebich, Sz Vijlee, Sd Stouffer, and Wm Roquemore. 2012. "Fuel-Rich Combustion Products from a Well-Stirred Reactor Operated Using Traditional and Alternative Fuels." Central States Combustion Meeting, 1–8.

Blunck, David L., Steven Zeppieri, Justin T. Gross, Scott Stouffer, and Meredith B. Colket. 2015. "Hydrocarbon Emissions from a WSR Near Lean Blow-Off." In 53rd AIAA Aerospace Sciences Meeting, 1–12. Kissimmee, FL: American Institute of Aeronautics and Astronautics. doi:10.2514/6.2015-0415.

Blust, J., D. Ballal, and G. Sturgess. 1997. "Emissions Characteristics of Liquid Hydrocarbons in a Well Stirred Reactor." In 33rd AIAA/ASME/SAE/ASEE Joint Propulsion Conference & Exhibit, 1–18. Seattle, WA: AIAA. doi:10.2514/6.1997-2710.

Blust, J. W., D R Ballal, and G J Sturgess. 1999. "Fuel Effects on Lean Blowout and Emissions from a Well-Stirred Reactor." Journal of Propulsion and Power 15 (2): 216–23. doi:10.2514/2.5444.

Briones, AM, B Sekar, J Zelina, R Pawlik, and SD Stouffer. 2008. "Numerical Modeling of Combustion Performance for a Well-Stirred Reactor for Aviation Hydrocarbon Fuels (AIAA-2008-4565)." In 44th AIAA/ASME/SAE/ASEE Joint Propulsion Conference & Exhibit, 1–19. Hartford, CT: AIAA. doi:doi:10.2514/6.2008-4565.

Colket, Meredith B., Joshua S. Heyne, Mark Rumizen, James T. Edwards, Mohan Gupta, William M. Roquemore, Jeffrey P. Moder, Julian M. Tishkoff, and Chiping Li. 2016. "An Overview of the National Jet Fuels Combustion Program." In AIAA SciTech. AIAA SciTech. San Diego, CA: American Institute of Aeronautics and Astronautics. doi:doi:10.2514/6.2016-0177.

FAA. 2012. "U.S. Aviation Greenhouse Gas Emissions Reduction Plan," no. June: 1–16.

Karalus, Megan. 2013. "An Investigation of Lean Blowout of Gaseous Fuel Alternatives to Natural Gas." University of Washington.

Manzello, Samuel L., David B. Lenhert, Ahmet Yozgatligil, Michael T. Donovan, George W. Mulholland, Michael R. Zachariah, and Wing Tsang. 2007. "Soot Particle Size Distributions in a Well-Stirred Reactor/plug Flow Reactor." Proceedings of the Combustion Institute 31 (1): 675–83. doi:10.1016/j.proci.2006.07.013.

McAllister, Sara, Jyh-Yuan Chen, and A. Carlos Fernandez-Pello. 2011. Fundamentals of Combustion Processes. Mechanical Engineering Series. New York, NY: Springer New York. doi:10.1007/978-1-4419-7943-8.

Mensch, Amy. 2009. "A Study on the Sooting Tendency of Jet Fuel Surrogates Using the Threshold Soot Index." M.S. Thesis. The Pennsylvania State University.

Nenniger, J.E., A. Kridiotis, J. Chomiak, J.P. Longwell, and A.F. Sarofim. 1984. "Characterization of a Toroidal Well Stirred Reactor." Twentieth Symposium (International) on Combustion. The Combustion Institute, 473–79.

Stouffer, S, R C Striebich, C W Frayne, and J Zelina. 2002. "Combustion Particulates Mitigation Investigation Using a Well-Stirred Reactor." In 38th AIAA/ASME/SAE/ASEE Joint Propulsion Conference and Exhibit, 1–11. Indianapolis, IN: American Institute of Aeronautics and Astronautics. doi:10.2514/6.2002-3723.

Stouffer, Scott D, Dilip R Ballal, Joseph Zelina, Dale T Shouse, Robert D Hancock, and Hukam C Mongia. 2005. "Development and Combustion Performance of High Pressure WSR and TAPS Combustor." In 43rd AIAA Aerospace Sciences Meeting and Exhibit, 1–9. Reno, NV: American Institute of Aeronautics and Astronautics. doi:10.2514/6.2005-1416.

Stouffer, Scott, Robert Pawlik, Garth Justinger, Joshua Heyne, Joseph Zelina, and Dilip Ballal. 2007. "Combustion Performance and Emissions Characteristics for a Well Stirred Reactor for Low Volatility Hydrocarbon Fuels." In 43rd AIAA/ASME/SAE/ASEE Joint Propulsion Conference and Exhibit, 1–12. Cincinnati, OH: American Institute of Aeronautics and Astronautics. doi:10.2514/6.2007-5663.

Vijlee, Shazib Z. 2014. "Effects of Fuel Composition on Combustion Stability and NOX Emissions for Traditional and Alternative Jet Fuels." University of Washington.

Won, Sang Hee, Stephen Dooley, Frederick L Dryer, and Yiguang Ju. n.d. "Radical Index on Extinction Limits of Diffusion Flames for Large Hydrocabon Fuels." doi:10.2514/6.2011-318.

Won, Sang Hee, Peter S Veloo, Jeffrey Santner, Yiguang Ju, and Frederick L Dryer. n.d. "Comparative Evaluation of Global Combustion Properties of Alternative Jet Fuels." doi:10.2514/6.2013-156.

Won, Sang Hee, Peter S Veloo, Jeffrey Santner, Yiguang Ju, Frederick L Dryer, and Stephen Dooley. n.d. "Characterization of Global Combustion Properties with Simple Fuel Property Measurements for Alternative Jet Fuels." doi:10.2514/6.2014-3469.
Wordland, Justin. 2015. "What to Know About the Historic 'Paris Agreement' on Climate Change." Time.
Yanowitz, J, Ecoengineering M A Ratcliff, R L Mccormick, J D Taylor, and M J Murphy. 2004. "Compendium of Experimental Cetane Numbers."
Zelina, Joseph. 1995. "Combustion Studies in a Well-Stirred Reactor." University of Dayton.

Milestone(s)
Measured LBO, a Figure of Merit in the NJFCP, for 4 fuels. Results are consistent with the more complicated Area 6 Referee Rig.

Major Accomplishments
Reporting LBO equivalence ratios for four NJFCP fuels.

Publications
Peer-reviewed Publications:
None. (One publication is in preparation.)

Conference Proceedings:
Stachler, Robert D., Joshua S. Heyne, Scott D. Stouffer, Joseph D. Miller, and William M. Roquemore. 2017. "Investigation of Combustion Emissions from Conventional and Alternative Aviation Fuels in a Well-Stirred Reactor." In 55th AIAA Aerospace Sciences Meeting. Grapevine, TX: American Institute of Aeronautics and Astronautics.

Written Reports:
None.

Outreach Efforts
Conference presentations:
Stachler, Robert D., Joshua S. Heyne, Scott D. Stouffer, Joseph D. Miller, and William M. Roquemore. 2017. "Investigation of Combustion Emissions from Conventional and Alternative Aviation Fuels in a Well-Stirred Reactor." In 55th AIAA Aerospace Sciences Meeting. Grapevine, TX: American Institute of Aeronautics and Astronautics.
Stachler, Robert D., Joshua S. Heyne, Scott D. Stouffer, Joseph D. Miller, and William M. Roquemore. 2016. "Investigation of Combustion Emissions from Conventional and Alternative Aviation Fuels in a Well-Stirred Reactor." 12th Annual Dayton Engineering Sciences Symposium. Dayton, OH: ASME.

Awards
Joshua Heyne – SOCHE Faculty Excellence Award
Robert Stachler – ASME Outstanding Young Engineer

Student Involvement
Robert Stachler, Ph.D. student, leads this effort.

Plans for Next Period
It is planned to continue with additional LBO tests for the remaining NJFCP fuels (i.e. the remaining category A and C fuels as well as the fuel blends and surrogate blends).

Task 3: Cross-Experiment Analysis
University of Dayton

Objective(s)
The objective of this task is to link low cost fundamental experiments to larger cost more complicated experiments internal to the NJFCP.

Research Approach

Our current approach to linking experiments within the NJFCP via Random Forest Regression Analysis. This regression technique is advantageous for several reasons: 1) it can handle diverse sets of data with both qualitative and quantitively information, 2) it is a relatively unbiased regression technique, 3) the regression is a white-box approach, and 4) the regression can output the relative importance of various fuel and experimental features. More details regarding Random Forest Regression Analysis can be found elsewhere (e.g. (Hastie, Tibshirani, and Friedman 2009)).

Initial Results

We have been able to compile the data from Area 3 and 6 as well as the data from the WSR studies on LBO. Lean Blowout (LBO) is typically defined as the lower limit equivalence ratio that a geometry at a given condition can sustain a flame. This limit is of particular interest in relation to alternative fuel certification, as it represents an engine operability limit. If an aircraft that is designed to operate with conventional Jet-A fails to hold a flame under similar conditions with an alternative fuel, thrust and/or power would be lost to important aircraft functions and potentially pose a safety risk. LBO is identified as a FOM for this reason, and the NJFCP has multiple works documenting LBO results(Chtev et al. 2017; S. D. Stouffer et al. 2017; Stachler et al. 2017; Khandelwal 2017; Sidney, Allison, and Mastorakos 2017; Allison, Sidney, and Mastorakos 2017; Podboy, Chang, and Moder 2017).

During Year 1 and much of Year 2, of the program mainly focused on the screening of NJFCP fuels in each experimental rig. Figure 1 reports a box and whiskers plot illustrating the percent difference between A-2 and the various NJFCP fuels. The results are reported as a percent difference from A-2 as the rigs display diverse ϕs at LBO, i.e. typical (overall) LBO ϕs for the Referee Rig are an order of magnitude more dilute than the Well-Stirred Reactor, since much of the air in an aero combustor is added subsequent to main combustion for liner cooling and dilution. The box and whisker plot shows significant scatter in the data for several fuels and rigs. The scatter in the data are not necessarily indicative of experimental shortcomings but are characteristic of the stochastic nature of limit phenomena and changing semi-controlled experimental conditions in the case of the Georgia Tech (GT) rig, as incremental bulk head temperatures/boundary conditions effect LBO. Finally, most fuels are found to have statistically similar LBO character, i.e. the whiskers overlap across fuels for a given geometrical configuration.

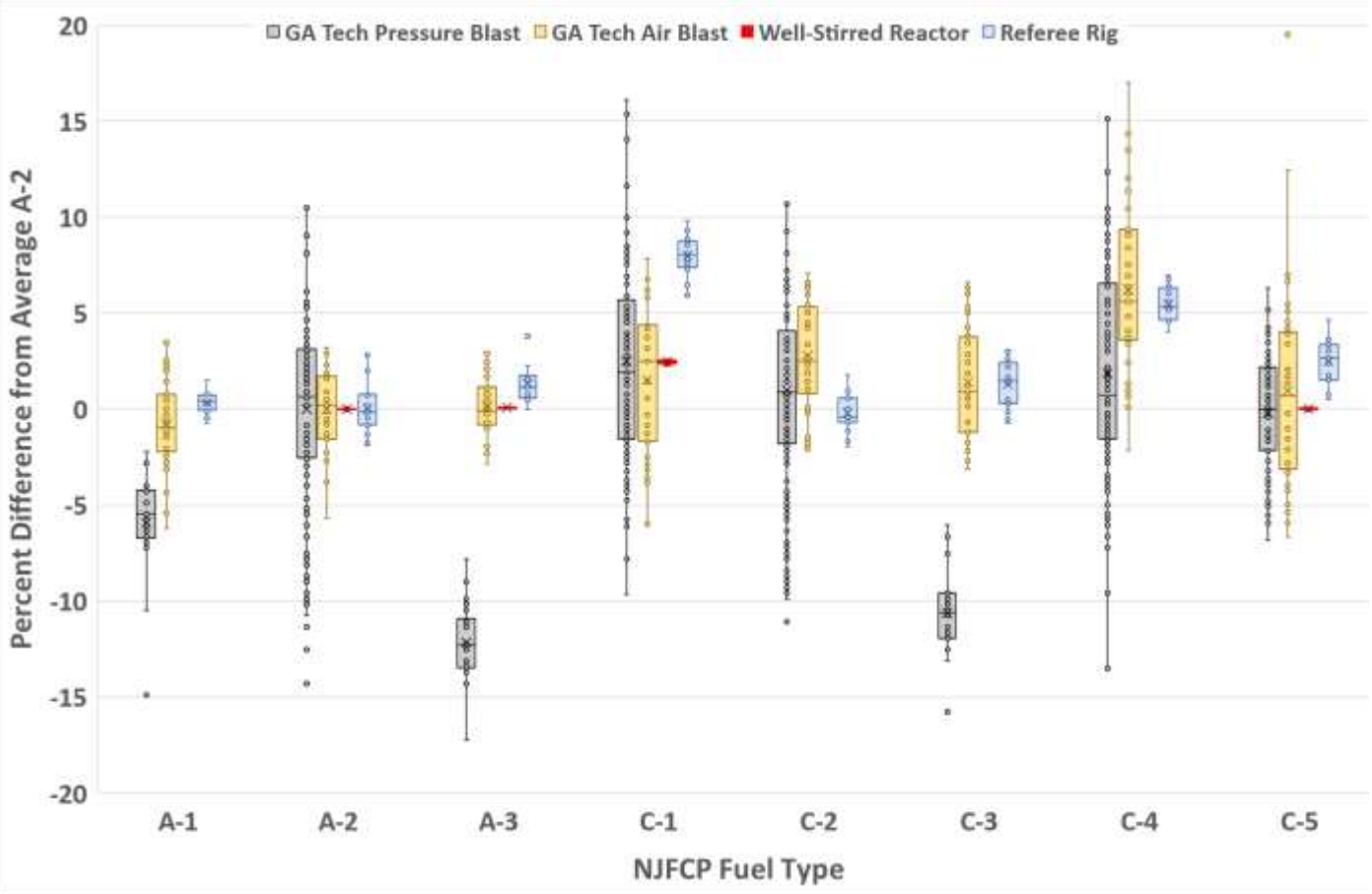

Figure 1: Box plot of percent difference LBO from A-2 for four NJFCP experimental configurations and seven fuels within the program. *The circles represent individual observations, boxes represent the upper and lower 75 and 25 percentiles with the horizontal bar illustrating the median, the 'x' is the mean LBO value, the upper and lower bars are the first and fourth quartiles respectively, and data outside the quartiles are outliers. Experimental repeatability is greater than LBO differences between fuels. Fuel C-1 is observed to blow off at the richest equivalence ratios relative to A-2.*

To further investigate these effects of fuel composition and geometrical variations, data in Figure 1 are further reduced in Figure to eliminate tests with a low bulk head temperature (<550 K) from the GT data sets. From this plot, clear trend variations are observed across the fuels and rigs. The A-3 and C-3 fuels are observed to blow off at richer or equivalent equivalence ratios relative to A-2 for the AB-GT, PA-RR, and PV-WSR (see definitions in caption to Figure 1). However, A-3 and C-3 fuels are observed to blowout at a leaner equivalence ratio for the PA-GT geometrical configuration, implying geometrical configurations alone can switch the direction a fuel performs. Perhaps of greatest interest to the ASTM certification process is when a fuel consistently yields a poor performance vs. A-2 across experimental platforms. This is observed most drastically for the C-1 fuel which showed the most significant difference from A-2 and is observed to blow off at the highest equivalence ratios fuel to blow off. C-4, which is a blend with 40% (by volume) is the 2nd worst performing fuel.

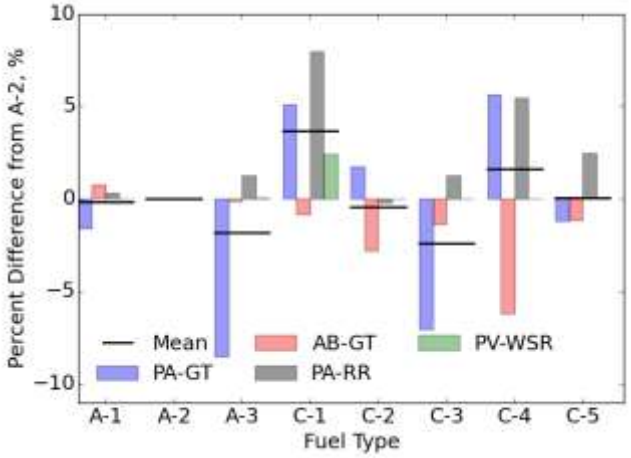

Figure 2: Nominal percent difference for Pressure Atomizer (PA), Air Blast (AB), and Prevaporized (PV) atomization/evaporation configurations using the Georgia Tech (GT), Referee Rig (RR), and Well-Stirred Reactor (WSR) geometries versus A-2. *The solid horizontal black line is the average for all tested fuels. C-1, C-2, and C-4 fuels are observed to be nominally different vs. A-2 for each experimental configuration. A-1, A-3, C-3, and C-5 are observed to blow off at equivalence ratios both leaner and richer than A-2 depending on the geometrical configuration. PA-GT bulk head temperatures are*

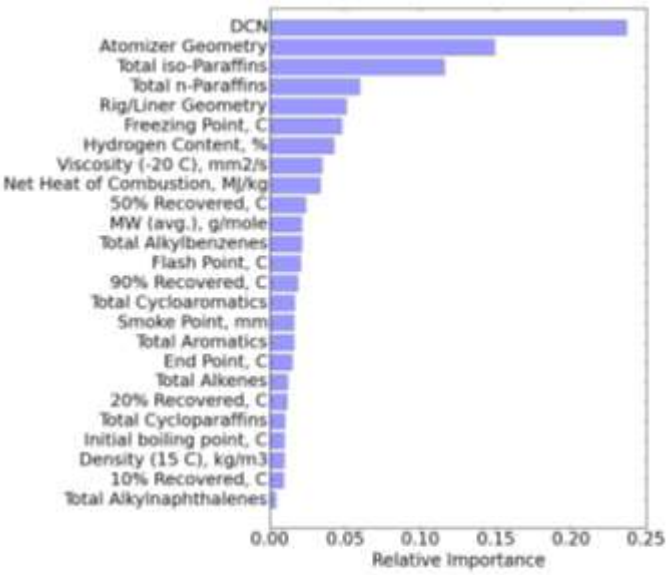

Figure 3: Random Forest relative importance results for LBO in four NJFCP rigs. *The most important feature in predicting LBO relative to A-2 is the DCN, Derived Cetane Number, which is used to evaluate the quality of Diesel fuel. The second and third most important features are the atomizer type and total iso-alkane content of the fuel. The R^2 value for this rearession was better than*

Significant systematic differences are observed across geometries as illustrated with Figure 4, which plots a geometry's root-mean-square (RMS) value across the fuels tested. The RMS value for a geometry is the variance the geometry produces for the variances in the NJFCP fuels. Geometries with relatively high RMS values are more sensitive to fuel variations, and conversely geometries with relatively small RMS values are less fuel sensitive. Figure 4 shows that the greatest fuel sensitivity is observed for the pressure atomized geometries (i.e. the PA-GT and PA-RR configurations). The least fuel-sensitive geometry is observed to be the prevaporized Well-Stirred Reactor with the air-blast atomized configuration between these two other vaporization mechanisms. This observation is consistent across the general consensus in the field that pressure atomized systems are more dependent on fuel physical properties relative to air-blast and prevaporized systems. It is tempting to extrapolate the results in Figure 4 to imply that only 1% of the observed variation is due to chemical property variations with variation due to physical properties. However, this is not necessarily true as a significant fraction of the variance in the more advanced combustion rigs are also a function of the chemical kinetic properties of a fuel as is shown in the regression analysis later for all rigs. To analyze the results collectively, a Random Forest regression analysis is performed on all the LBO data presented in this paper. For the analysis, the average percent difference for each fuel and configuration relative to the LBO ϕ of A-2 at similar conditions is evaluated relative to the chemical and physical properties of each fuel. It should be noted that some of these chemical and physical properties, when unavailable, are estimated via the methods described in Ref. (Bell et al. 2017). The regression results yielded results differing from previous reports and publications, e.g. Ref. (Lefebvre 1983), which implied stronger correlations to physical property effects versus the chemical property effect of DCN observed here. Beyond the reactivity effect of DCN on LBO, there is significant atomizer geometry influence observed on the relative LBO of the fuels. The effect of fuel property effects and the aiding of the development of CFD models will be an area of continued investigation moving into Year 3 of the NJFCP. Finally, it should be noted that these regression techniques are in no way comprehensive in predicting LBO. The predictive capability of the current reported technique returns a R^2 value of approximately 0.85 for test data.

Milestone(s)

Presentation at the NJFCP Year-End Meeting. Contributing to the upcoming AIAA paper and presentation.

Major Accomplishments

We have shown strong evidence that LBO is most strongly predicted by the chemical property DCN across four experimental platforms in the NJFCP. This could potentially

aid in developing blending rules for fuels to proceed through the ASTM approval process.

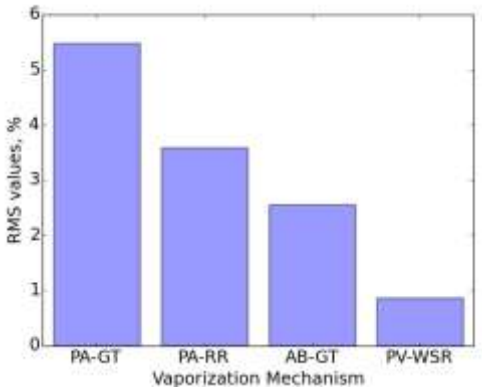

Figure 2: Root-Mean-Square (RMS) values for nominal LBOs across all tested fuels for each experimental configuration. *Greater fuel sensitivity is observered for Pressure Atomizing (PA) configurations relative to Air Blast (AB) and Prevaporized (PV) configurations. These trends are unsurprising given the expectation that PA configurations reflect greater fuel physical property sensitivity relative to AB and in turn PV configurations.*

Publications
Peer-reviewed journal publications:
None.

Published conference proceedings:
None

Written reports:
None.

Outreach Efforts
Oral presentations:
Carson, Jeremy, Joshua S. Heyne, Scott D. Stouffer, and Tyler Hendershott. 2016. "On the Relative Importance of Fuel Properties on LBO Behavior." 12th Annual Dayton Engineering Sciences Symposium. Dayton, OH: ASME.

Electronic communications:
None.

Conference presentations:
None. (One publication and presentation is in preparation.)

Awards
Joshua Heyne – SOCHE Faculty Excellence Award

Student Involvement
Jeremy Carson, a MS student, is the lead for this effort.

Plans for Next Period
We plan to continue our current research technique incorporating greater depth into our results and incorporating additional Figures of Merit, I.e. ignition, into this work.

Task 4: Common Format Routine Software Development

University of Dayton

Objective(s)

We aim to develop a software package in which the OEMs can utilize the state of the art models being developed by the other NJFCP modeling teams.

Research Approach

The culmination of all NJFCP efforts is the delivery of NJFCP CFD models to the engine OEMs who in turn use them to inform the impact of alternative fuels on their proprietary geometries. To deliver these models, so called Common Format Routines (CFRs) need to be developed such that OEMs can utilize the most advanced academic theory and codes for alt. fuel certification. We identified the several key members to support the effort of developing state-of-the-art software which are the core of CFRs for CFD. The team consists of two engineers and a computer scientist (from UDRI) supported by the NJFCP. The commitment time of these members will vary from 100 % when needed to 25 % throughout the year. Two additional engineers from ISSI, Inc. and Engility Corporation provide supplemental support through aligned AFRL funded activities. Initially, the UDF focus is on developing the latest Stanford flamelet-based combustion models, which the team is already familiar with. Simultaneously, UDFs will be generated for other relevant combustion, spray, evaporation and/or turbulent models used in the NJFCP project.

We have developed a schematic of all the required numerical tools that need to be developed to program the Stanford flamelet-based combustion models. These models typically work by generating off-line combustion look-up tables that are accessed during the simulation. The combustion phenomenon is represented by a lower-dimensional manifold. These look-up tables vary from two-dimensional for laminar flames to four-dimensional for turbulent flames. One additional dimension is added for non-adiabatic combustion. We recently developed an optimized table, written in C language, that can effectively perform bilinear (for laminar flows) and trilinear (for turbulent flow) interpolation, in addition to an efficient search algorithm. This algorithm couples with another code that can couple to commercial CFD codes.

The abovementioned tables also necessitate table generators. For these the team, have developed Python scripts that take advantage of CANTERA chemical solver to generate such tables. These python scripts can generate s-curves for the perfectly stirred reactor (PSR), the counter flow diffusion flames and the freely-propagating flames. Note that the diffusion flames are needed for the flamelet-progress variable (FPV) tables whereas the latter is needed for the flamelet-prolongation-intrinsic-lower-dimensional manifold (FPI) tables. Both tables are used by Stanford flamelet models. The PSR s-curve might be useful for ignition problems, but for now it is a by-product of the current efforts to test steady Newton, Newton-Cotes and Broyden solvers as well as a bordering algorithm. The PSR results were validated with those results published in Ref. (Acampora and Marra 2015).

We have identified test cases for implementing the state-of-the-art physical-chemical models. We are currently testing the combustion models in Ref. (Acampora and Marra 2015). We already ran the simulations using a commercial code with flamelet-generated manifolds (FGM), and compared the results with Stanford combustion models. Overall, there is good agreement in terms of mixture fraction, temperature and CO mass fraction between the models when laminar flames are used. Now we are simulating the in-house generated FPI and FPV tables in order to compare their results with Stanford published results (Hao et al. 2015). Subsequently, we will generate tables for the (Filtered Tabulated Chemistry for LES) F-TACLES approach and compare them with the published results in Ref. (Auzillon et al. 2012). Stanford is using F-TACLES to model the referee combustion. Lastly, we developed a Python script that takes the FPI and FPV tables and convolutes them to generate presumed-Beta shaped probability density function (PDF) tables needed for turbulent flames.

Acampora, Luigi, and Francesco S. Marra. 2015. “Numerical Strategies for the Bifurcation Analysis of Perfectly Stirred Reactors with Detailed Combustion Mechanisms.” Computers and Chemical Engineering 82: 273–82.

Auzillon, Pierre, Olivier Gicquel, Nasser Darabiha, Denis Veynante, and Fiorina Benoit. 2012. “A Filtered Tabulated Chemistry Model for LES of Stratified Flames.” Combustion and Flame 159 (8): 2704–17.

Hao, Wu, Yee Chee See, Qing Wang, and Matthias Ihme. 2015. “A Pareto-Efficient Combustion Frame Work with Submodel Assignment for Predicting Complex Flame Configurations.” Combustion and Flame 162 (11): 4208–4230.

Milestone(s)

Nothing to report.

Major Accomplishments

Developing and testing the first Flamlet model developed internally to the team.

Publications

Nothing to report.

Outreach Efforts

None.

Awards
Joshua Heyne – SOCHE Faculty Excellence Award

Student Involvement
None.

Plans for Next Period
We plan to continue our current path with increased OEM participation and input.

Task 5: Spray Modeling of Area 3 Pressure Atomized Spray Injector
University of Dayton

Objective(s)
The objective of this task is to simulate the Area 3 High Sheer Rig pressure blast spray atomizer. Simulations of NJFCP experiments in the Area 3 High Sheer Rig will be done to explore the relative performance of simulations versus experiments and the relative spray and combustor character between the A-2, C-1, and C-5 fuels. These computational results will also illuminate the relative impact of a Pratt & Whitney swirler-injector geometry as compared to the other geometries in the program.

Research Approach
We are aiming to conduct Large Eddy Simulations (LES) of spray combustion in Area 3 Georgia Tech High Shear Rig, rig using Pratt & Whitney air-blast atomizer. The study has the following 3 objectives 1) to demonstrate fuel sensitivity for the identified fuels in a configuration different from the Referee rig combustor, 2) to identify fuel sensitivity at a point near Lean Blow Out conditions and validate with experimental data, and 3) to compare the fuel sensitivity between pressure atomizer and air-blast atomizer in the area 3 tests. These activities will also support the experimental team in definition of the tests and development of procedures for data reduction, interpretation and analysis of experimental and computational model results and their limitations.

Milestone(s)
Nothing to report.

Major Accomplishments
Nothing to report.

Publications
Nothing to report.

Outreach Efforts
Presentation at the NJFCP Year End Meeting 2016.

Awards
Joshua Heyne – SOCHE Faculty Excellence Award

Student Involvement
None.

Plans for Next Period
Execute subcontract to UTRC

Task 6: Procure Additional Geometries for Testing at Various NJFCP Facilities

University of Dayton

Objective(s)

As seen earlier in this report, combustor geometry is an important sensitivity parameter in alt. jet fuel certification. For this reason, the NJFCP is interested in additional geometries for testing and constraining expectations from alt. fuels. Here we will procure these additional geometries for testing at various NJFCP facilities.

Research Approach

We have contacted a vendor capable of manufacturing the necessary hardware.

Milestone(s)

Nothing to report.

Major Accomplishments

Nothing to report.

Publications

Nothing to report.

Outreach Efforts

Nothing to report.

Awards

Joshua Heyne – SOCHE Faculty Excellence Award

Student Involvement

None.

Plans for Next Period

Order and acquire additional geometries from vendors.

Project 035 Airline Flight Data Examination to Improve Flight Performance Modeling

Georgia Institute of Technology
Delta Air Lines, Inc.

Project Lead Investigator

Dr. John-Paul Clarke
Professor
The Daniel Guggenheim School of Aerospace Engineering
Georgia Institute of Technology
270 Ferst Drive, Atlanta. Georgia 30332-0150
404-385-7206
johnpaul@getech.edu

University Participants

Georgia Tech

- P.I.(s): Professor John-Paul Clarke
- FAA Award Number: 13-C-AJFE-GIT Amendment 015
- Period of Performance: July 29, 2015 – August 31, 2016
- Task(s): 1. Airline Flight Data Examination to Improve Flight Performance Modeling

Project Funding Level

FAA: $150,001.00. Matching: $101,121.00 (Georgia Tech); $48,880.00 (Landrum and Brown); Data (Delta Air Lines).

Investigation Team

James Brooks (GT: Data Analysis); Karén Melikov (GT: Analysis Support); Jesse Miers (Delta Air Lines: Subject Matter Expert); Vince Mestre (Landrum and Brown: Subject Matter Expert).

Project Overview

Currently, when modeling either aircraft noise or emissions with the Aviation Environment Design Tool (AEDT), there are simplifications associated with the methodology suggested for determining the aircraft gross takeoff weight [Ref. 1] that can create inaccurate results, along with the inability to model reduced thrust/power departures. The goal of this project is to develop a functional relationship between stage/trip length and weight that can improve the existing guidance provided for weight estimation; and subsequently to determine the percentage of departures that use reduced thrust and the level of reduced thrust that is used for the departure.

Task 1 Airline Flight Data Examination to Improve Flight Performance Modeling

Georgia Tech

Objective(s)

Analyze aircraft departure operating data for two wide-body and two narrow body commercial aircraft to develop a functional relationship between stage/trip length and weight that can replace the existing guidance provided for weight estimation; and potentially determine the percentage of departures that use reduced thrust as well as the level of reduced thrust that is used.

Research Approach

The Air Transportation Laboratory (ATL) at the Georgia Institute of Technology acquired two large independent databases containing operational information with regard to aircraft departures. One is a Flight Planning Database which was used for researching a relationship to improve the estimation of takeoff gross weight. The second is an Aircraft Communications Addressing and Reporting System (ACARS) that was used for researching reduced thrust usage while also serving as a test environment for the takeoff weight estimations. Both contain, among other data, actual departure weight and the departing and destination airports and both were edited to add airport standard elevation, runway length, and Great Circle Distance (GCD). Only the ACARS database contains actual reduced power/thrust used for the departure and the planned trip distance is only available in the Flight Planning Database. This data was used to develop a functional relationship between stage/trip length and weight that can replace the existing guidance provided for weight estimation; and subsequently to determine the percentage of departures that use reduced thrust and the level of reduced thrust that is used.

Takeoff Weight Determination

Although preliminary analysis has shown a strong functional relationship between aircraft weight and Great Circle Distance (GCD) flown there are known issues with using GCD for some specific airport pairs. An additional source of distance flown is the “planned distance” which is contained in the air carrier flight plan. Since one of the factors in determining the total fuel carried is the planned distance, it was anticipated that using this distance could result in a stronger correlation than using the GCD. With regard to modeler access to the planned distance, there are a number of websites that provide flight-tracking information and include the planned distance (i.e., www.Flightaware.com). This research has developed a number of functional relationship using both GCD and Planned Distance along with other parameters that influence aircraft departure gross weight. These results of these relationships have been compared with the existing AEDT Stage Length methodology.

Reduced Thrust (Usage and Level)

The operational database described above is straightforward with respect to the aircraft/engine type and the takeoff weight and amount of reduced thrust used for the departure. While thousands of departures are contained in the database, the task of deriving a relationship to predict the amount

of reduced thrust for any departure of a specific aircraft/engine type is complicated by the way in which the carriers implement the use of reduced thrust.

The performance analysis to certify the maximum reduced thrust that can be used for a departure from a specific runway, at a specific airport, for existing temperature and wind conditions is mandated in the FAA certified Aircraft Flight Manual (AFM). The AFM requirements for performance analysis is the same for each air carrier. What varies between the various air carriers is the presentation of the allowable reduced thrust departure information to the flight crew. The variation is essentially due to the pilot community and their historical views on using something less than maximum thrust available for conducting the critical departure phase of the operation. Although the performance analysis is in compliance with the AFM, as is the performance analysis of any departure, there are those in the pilot community that opt to reduce thrust less than the maximum certified to safely conduct the departure.

The flight crew is presented with takeoff performance information (by the air carrier) for each departure. Based on the agreed information format and the limitations, if any, on the amount of information that can be conveyed, a number of reduced thrust options can be presented. Even in situations where only one reduced thrust option is presented, this single option may be less than the maximum allowable reduced thrust (the existing case for some of the data contained in the ATL operational database).

As a result of the described pilot community reaction there exists a noticeable variation in reduced thrust applied for a given recorded takeoff weight, which complicates the task of developing a relationship describing the level of reduced thrust used. A number of statistical analyses have been performed and assessed with respect to defining the correct strategy for predicting the amount of reduced thrust applied as a function of variables that effect engine thrust. In each strategy, the implementation into the AEDT has been considered with regard to cost and complexity.

Originally, it was planned to work with the airframe manufacturers to provide sufficient data that would support the development of the equation coefficients for aero-profile modeling defined in SAE AIR1845. The interface with the manufacturers was to be the SAE A-21 Committee, but unfortunately, the only meeting scheduled within the research period was cancelled. Communicating directly with one of the manufacturers gave the impression that another course of action may be necessary for future AEDT modelling.

The results of the reduced power/thrust analyses will be presented in both an aggregate as well by individual routes contained in the database.

A total of six departure procedures meeting the requirements contained in AC 91-53A will be provided, three for close-in procedures or NADP1, and three for distant procedures or NADP2. The procedure will specify a takeoff flap setting and a range of operational weights.

The remainder of the report presents the results of the research for the following airframe/engine combinations:

- B757-200/PW2037
- B737-800/CFM56-7B26
- B767-400ER/CF680C2/B8F
- B767-300ER/CF680C2/B6F

Due to the volume of information produced by this report, it will be presented in two sections; Section I, will be the Takeoff Weight Determination and Section II will be the Reduced Thrust (Usage and Level) analysis.

SECTION I

B757-200/PW2037

Takeoff Weight Determination:

Specifics of the Flight Planning Database:

- 45,343 Flights
- 376 Routes Departing 97 Airports
- 7,602 “Tankered” Flights
    - 8102 lbs. Average
    - 691 NM Average Trip
- Added Airport Elevation, Runway Length, and GCD for each Airport/Flight

Multiple linear regressions on the database were conducted in a stepwise method using the following independent variables: runway length, airport elevation, and either GCD or Planned Distance. The regressions were applied to the total database of individual flights and repeated with an “average” database that contained the average data for each route and in the case of Planned Distance, the average planned distance.

The statistical summary of the GCD and Planned Distance regressions are as follows:

B757-200 Planned Distance with All Data:

Model Summary[d]

Model	R	R Square	Adjusted R Square	Std. Error of the Estimate
1	.810[a]	.657	.657	7842.3388878
2	.813[b]	.660	.660	7798.0242986
3	.813[c]	.662	.662	7785.2970748

a. Predictors: (Constant), PLN_DST

b. Predictors: (Constant), PLN_DST, RWYL

c. Predictors: (Constant), PLN_DST, RWYL, ELEV

d. Dependent Variable: GWT

B757-200 Planned Distance with Average/Route Data

Model Summary[c]

Model	R	R Square	Adjusted R Square	Std. Error of the Estimate
1	.909[a]	.826	.825	5900.9364673
2	.910[b]	.828	.827	5874.0057751

a. Predictors: (Constant), AVG_PLND

b. Predictors: (Constant), AVG_PLND, RWYL

c. Dependent Variable: AVG-GWT

B757-200 GCD with All Data

Model Summary[d]

Model	R	R Square	Adjusted R Square	Std. Error of the Estimate
1	.810[a]	.657	.657	7842.1698175
2	.813[b]	.660	.660	7797.8917768
3	.813[c]	.662	.662	7785.1833801

a. Predictors: (Constant), GCD

b. Predictors: (Constant), GCD, RWYL

c. Predictors: (Constant), GCD, RWYL, ELEV

d. Dependent Variable: GWT

B757-200 GCD with Average/Route Data

Model Summary[c]

Model	R	R Square	Adjusted R Square	Std. Error of the Estimate
1	.909[a]	.826	.825	5900.6880141
2	.910[b]	.828	.827	5873.6849681

a. Predictors: (Constant), GCD

b. Predictors: (Constant), GCD, RWYL

c. Dependent Variable: AVG-GWT

As can be seen with the regression model summaries above, the strength of the correlation using GCD is almost identical to using Planned Distance. This result is evident on all regressions made for this research project, the correlation strength using GCD has been equivalent to or slightly better than the correlation using Planned Distance. In addition, the correlation strength has been found to always be improved when regressing Average/Route data.

The regression coefficients for GCD and Average/Route data are as follows:

Coefficients[a]

Model		Unstandardized Coefficients		Standardized Coefficients	t	Sig.
		B	Std. Error	Beta		
1	(Constant)	179794.148	601.772		298.775	.000
	GCD	19.253	.457	.909	42.102	.000
2	(Constant)	175571.496	2090.152		83.999	.000
	GCD	19.188	.456	.906	42.058	.000
	RWYL	.374	.177	.045	2.109	.036

a. Dependent Variable: AVG-GWT

The resulting B757-200 takeoff weight estimation equation is:

$$GWT = 175571.496 + 19.188(GCD) + .374(RUNWAY\ LEN)$$

(Reference Figure 3 below)

Testing of the Takeoff Weight Estimation

The resulting takeoff weight regression equations were compared with data from the ACARS database which has recorded data for 82,646 flights. The resulting data represented 376 routes from 101 airports.

Part of the test procedure was to determine if the presence of "tankered" fuel influenced the takeoff weight estimation. The presence of fuel tankering data in the Flight Plan database raised an issue about whether or not this strategic action would influence the results of the takeoff weight estimation. To resolve the issue, regressions were made using the database with the "tankered" flights removed and the resulting equation tested against the ACARS database. The absolute value of the difference in the estimated weights for the average/route data with both the "untankered" regression and the equation above are plotted in the frequency diagram below.

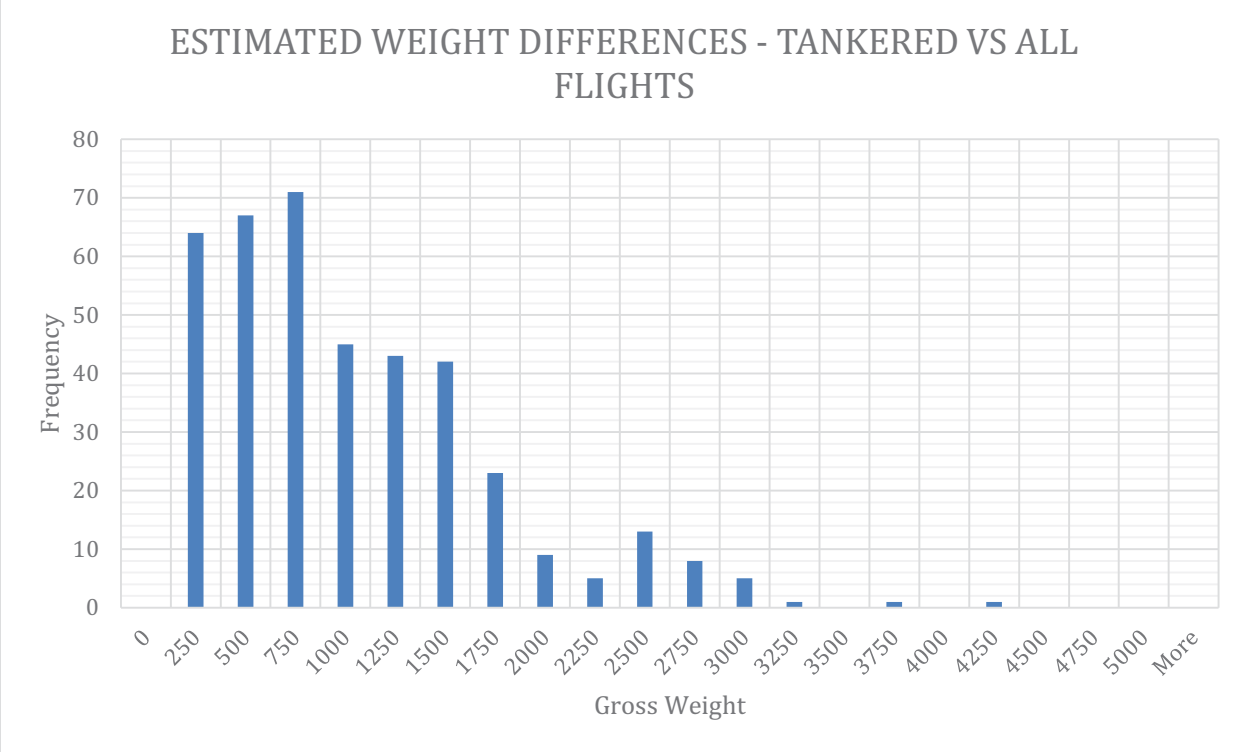

CHART 1

With the majority of the weight differences below 1750 lbs., the difference in the estimated weight between tankered and untankered flights is small compared to the average operating weight for the B757 of 208,000 lbs. and the maximum certified takeoff weight certified of 240,000 lbs. In addition, it would be difficult for a modeler to obtain "tankered" flight information from the air carriers. It should be noted here, that the ACARS data has no information regarding flight fuel loads, so therefore the test database includes all flights.

Test Results

Due to the size of the database, the results are initially presented in graphical form with the reqressed estimated weights plotted against the ACARS data actual recorded weight. The graphical representation also allows additional analysis of the results.

AEDT Stage Length Weights

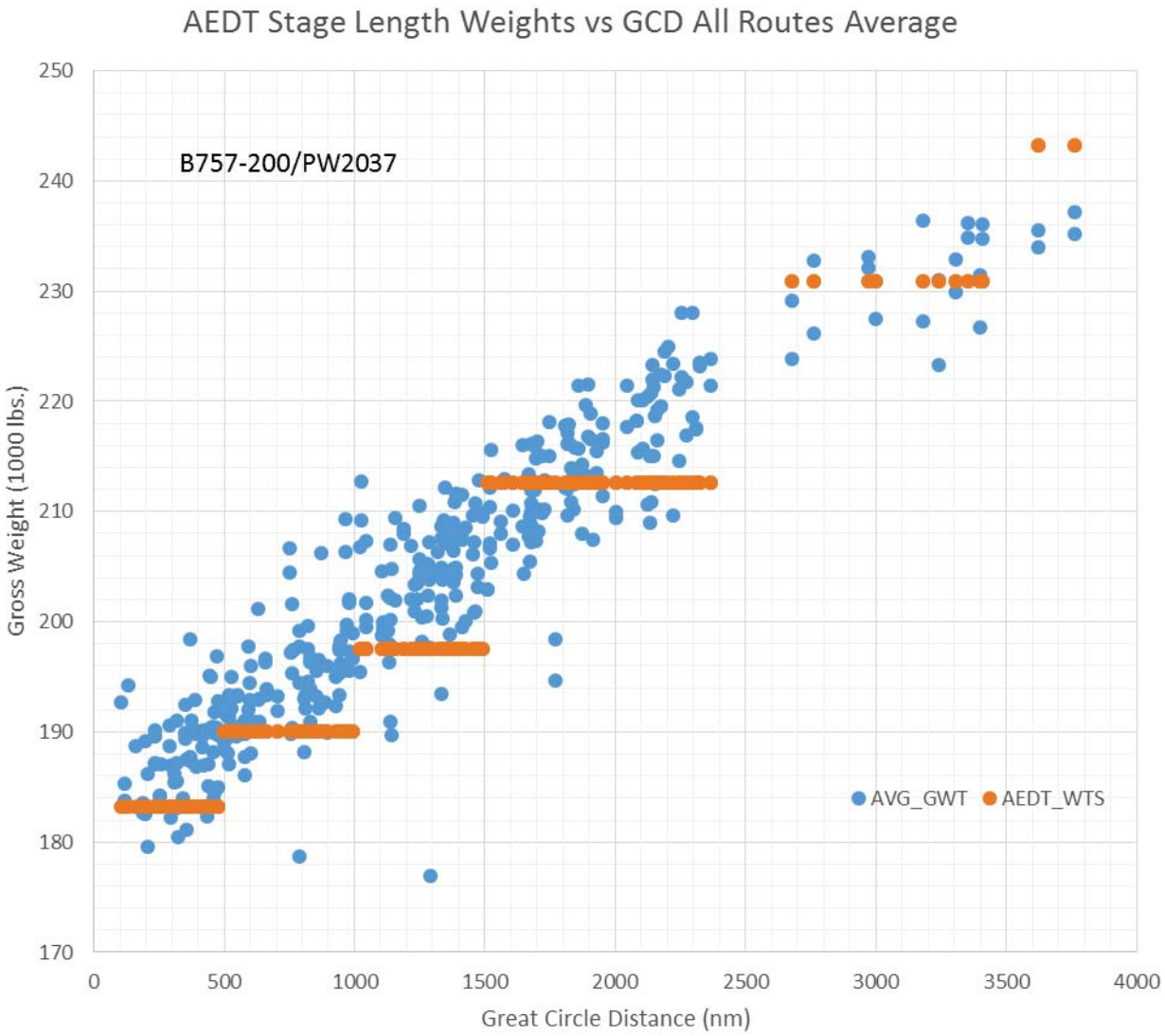

FIGURE 1

Regression Developed Using All Flights

$$GWT = 176599.317 + 18.253(GCD) + .586\,(RUNWAY\ LEN) - .346(ELEV)$$

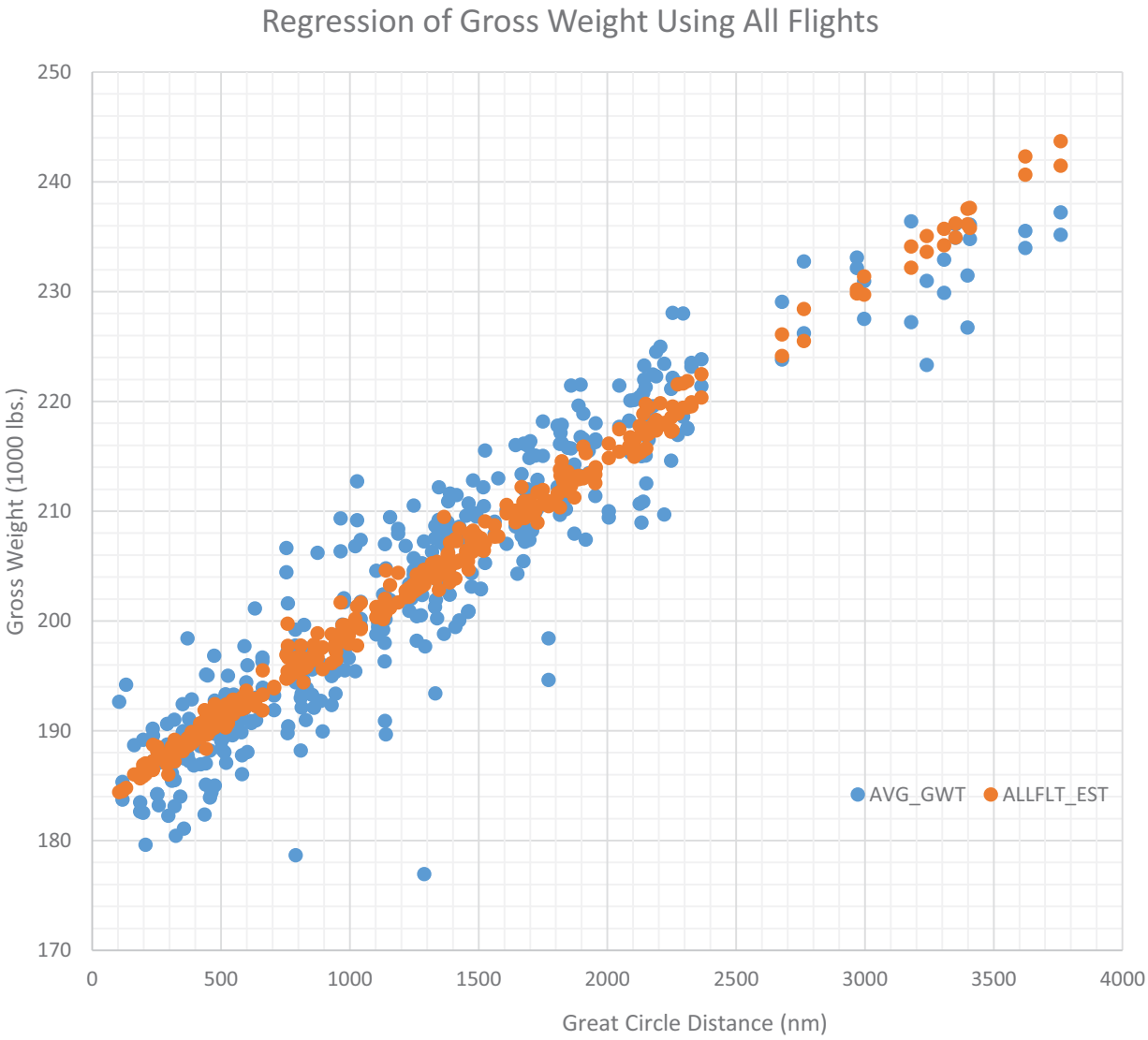

FIGURE 2

Regression Developed Using Average/Route Data of All Flights

$$GWT + 175571.496 + 19.188(GCD) + .374(\text{RUNWAY LEN})$$

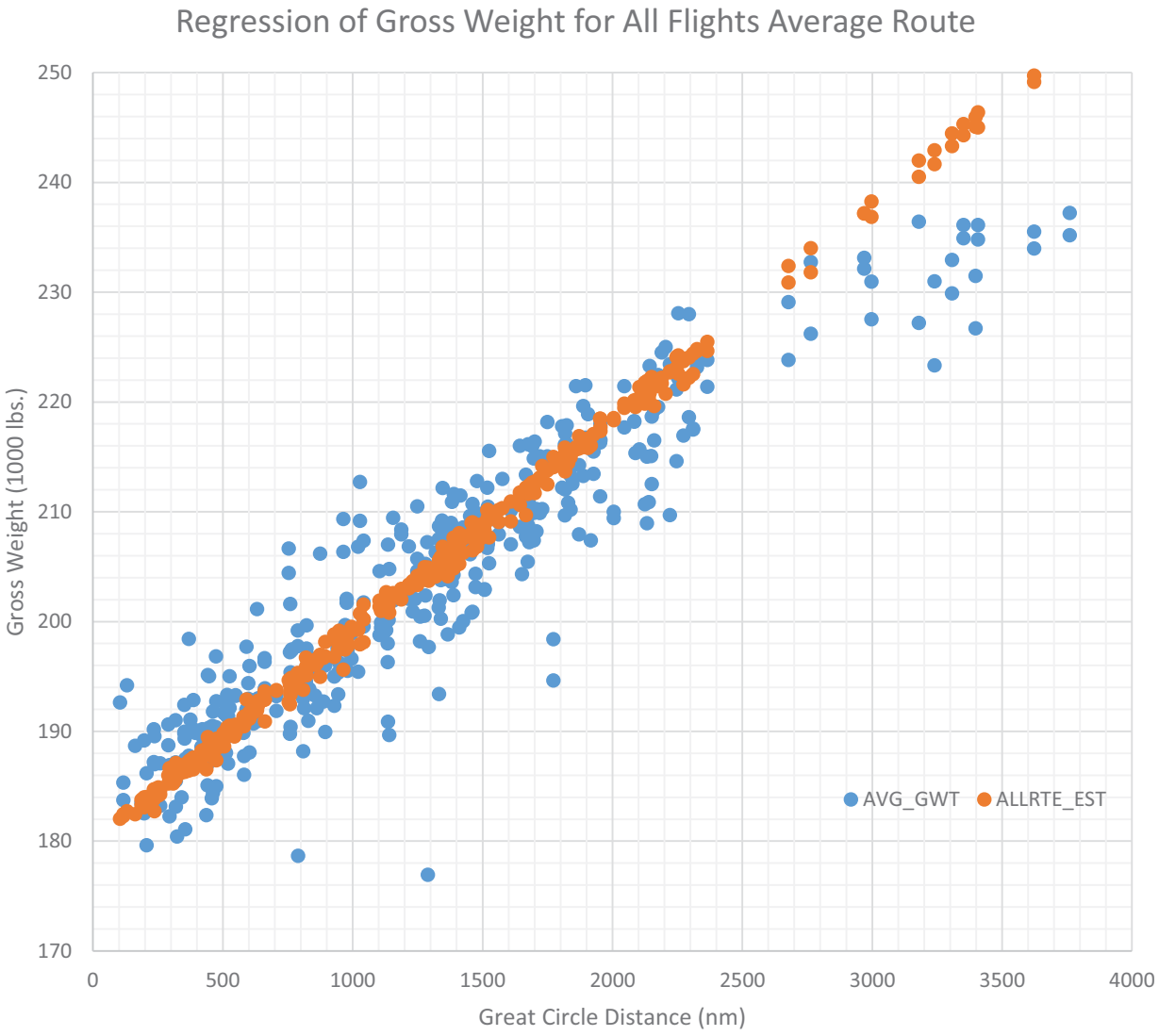

FIGURE 3

The graphical representation of the test results revealed a cluster of flights at distances of more than 3000 nautical miles that were not following the trend of increasing weight with distance even though the recorded weights were still below the maximum certified takeoff weight of 240,000 lbs. A closer examination of these flights revealed they were international flights and at that trip length, were performance or payload limited due to fuel capacity (fuel tanks filled to capacity).

The major air carriers began longer range international flights with the B757 several years ago, so to correctly model the weights associated with all B757 operations, a quadratic regression was developed using the database. The results of this regression are shown in Figure 4.

Quadratic Regression Developed Using Average/Route Data of All Flights

$$GWT = 175381.001 + 27.18(GCD) - .003(GCD)^2$$

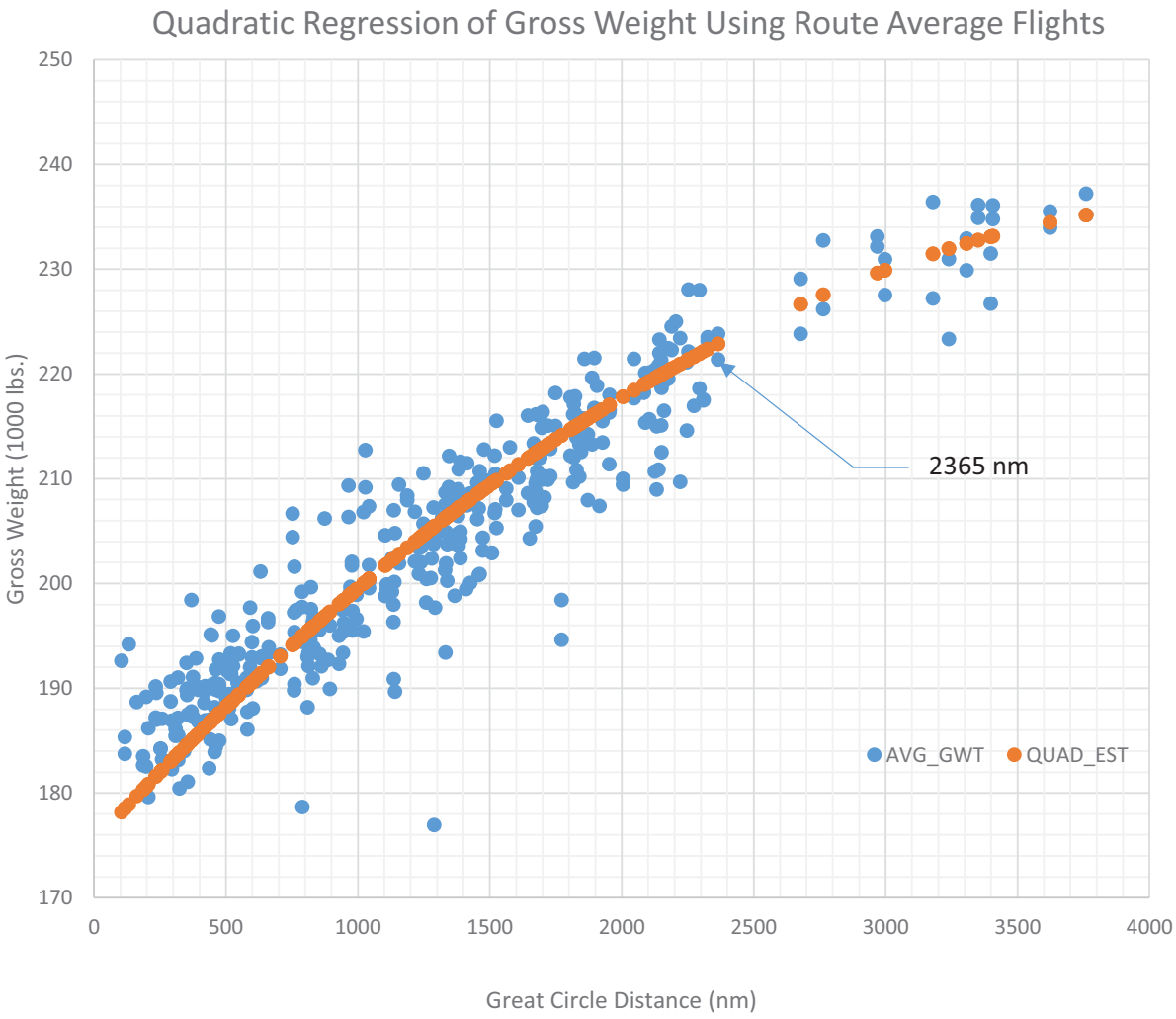

FIGURE 4

B757-200 Takeoff Weight Estimation Final Results

$GWT + 175571.496 + 19.188(GCD) + .374$(RUNWAY LEN) for GCD's < 2365 nm

$GWT = 175381.001 + 27.18(GCD) - .003(GCD)^2$ for GCD's ≥ 2365 nm

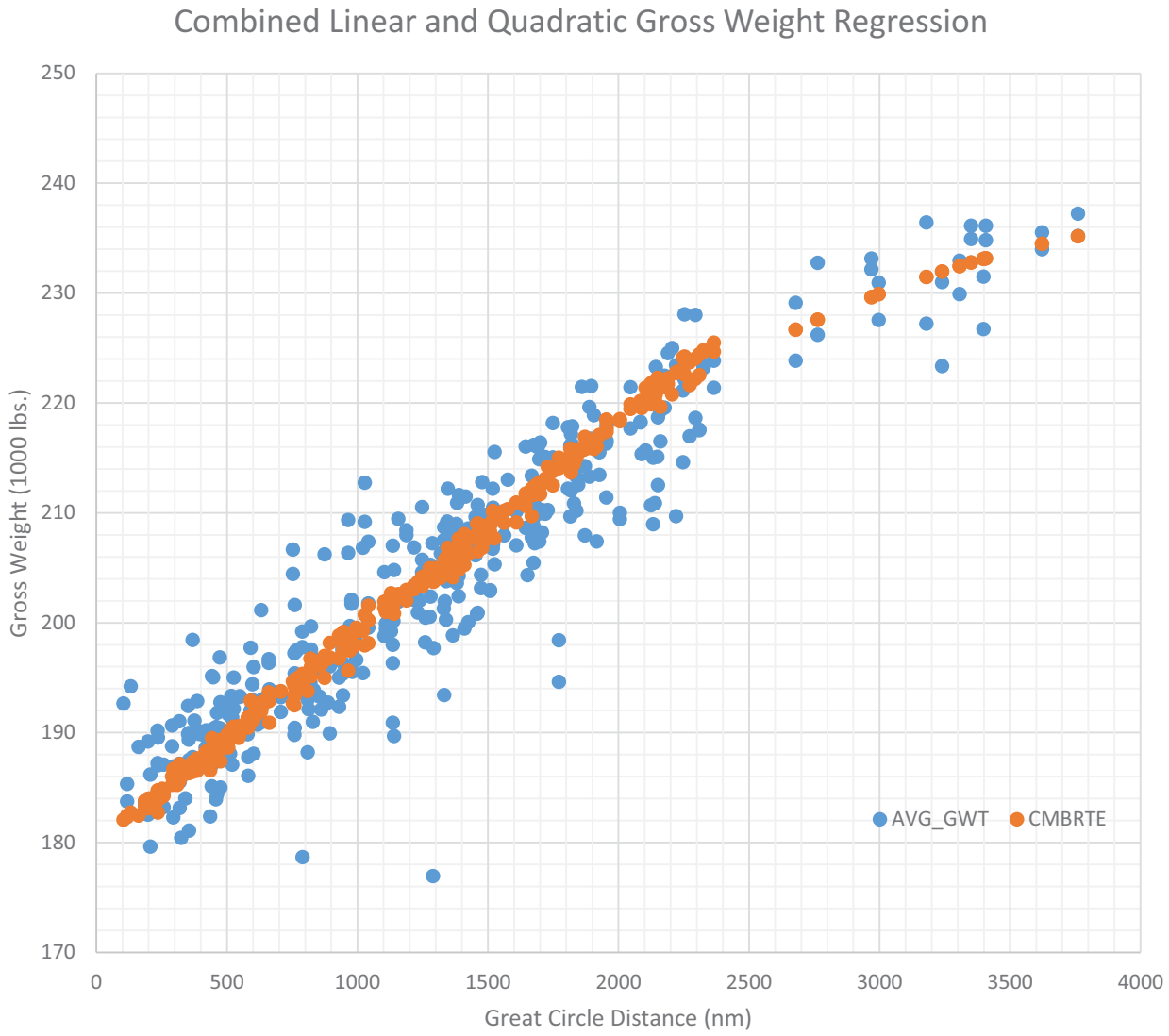

FIGURE 5

The estimated weight, the difference from the actual weight, and the percentage of that difference for both the regression and the current AEDT Stage Length methodology are tabulated in Tables 1 through 4 that follow. The tables represent the average weight for each of the routes contained in the test ACARS database.

The average route tabular data is contained in the following tables, showing the actual weight, and the differences in the regression and AEDT stage length weights.

B757-200 TABULAR RESULTS

APRTS	AVG_GWT	REG_EST	REG_DIF	REG_%DIF	AEDT_EST	AEDT_DIF	AEDT_%DIF	APRTS	AVG_GWT	REG_EST	REG_DIF	REG_%DIF	AEDT_EST	AEDT_DIF	AEDT_%DIF
ABQATL	204.6	201.9	-2692	-1.3%	197.5	-7087	-3.4%	ATLNCA	209.3	198.7	-10645	-5.1%	190	-19348	-9.2%
AGPJFK	227.2	231.5	4258	1.9%	230.9	3690	1.7%	ATLORD	192.1	190.3	-1837	-0.8%	190	-2135	-0.9%
ANCATL	232.2	229.6	-2522	-0.8%	230.9	-1255	-0.2%	ATLPBI	190.4	189.3	-1116	-0.5%	183.2	-7198	-3.7%
ANCMSP	224.5	222.2	-2308	-0.9%	212.6	-11919	-5.2%	ATLPDX	213.3	216.4	3161	1.5%	212.6	-672	-0.3%
ANCSLC	212.6	215.6	3079	1.5%	212.6	49	0.1%	ATLPHL	191.0	191.3	336	0.4%	190	-979	-0.3%
ARNJFK	236.1	233.2	-2951	-1.2%	230.9	-5211	-2.2%	ATLPHX	204.8	206.7	1892	1.0%	197.5	-7274	-3.5%
ATLABQ	198.8	201.4	2582	1.3%	197.5	-1288	-0.6%	ATLPIT	188.2	189.0	766	0.5%	183.2	-5008	-2.6%
ATLANC	233.1	229.6	-3486	-1.5%	230.9	-2220	-0.9%	ATLPNS	187.0	184.7	-2280	-1.2%	183.2	-3814	-2.0%
ATLAUA	209.8	208.8	-992	-0.4%	197.5	-12306	-5.8%	ATLPUJ	204.2	204.2	-83	0.0%	197.5	-6735	-3.3%
ATLAUS	191.9	193.8	1881	1.1%	190	-1871	-0.9%	ATLPVR	203.9	206.2	2282	1.2%	197.5	-6385	-3.1%
ATLBHM	185.3	182.5	-2883	-1.4%	183.2	-2133	-1.0%	ATLRDU	186.1	186.1	0	0.1%	183.2	-2935	-1.4%
ATLBNA	183.5	183.8	274	0.3%	183.2	-300	-0.1%	ATLRIC	188.6	188.2	-385	-0.1%	183.2	-5411	-2.7%
ATLBOG	217.9	215.2	-2680	-1.2%	212.6	-5265	-2.4%	ATLRSW	190.3	188.8	-1544	-0.7%	183.2	-7127	-3.7%
ATLBON	209.1	210.2	1124	0.7%	212.6	3547	1.8%	ATLRTB	200.2	200.2	17	0.1%	197.5	-2682	-1.3%
ATLBOS	197.6	196.0	-1575	-0.7%	190	-7553	-3.7%	ATLSAN	208.6	211.8	3132	1.6%	212.6	3982	2.0%
ATLBSB	234.0	234.5	501	0.3%	243.2	9226	4.0%	ATLSAT	190.4	194.8	4372	2.5%	190	-416	0.0%
ATLBWI	189.0	189.8	771	0.6%	190	953	0.7%	ATLSEA	216.8	216.6	-165	0.0%	212.6	-4151	-1.9%
ATLBZN	200.0	207.5	7501	3.9%	197.5	-2548	-1.2%	ATLSFO	215.7	215.9	148	0.1%	212.6	-3128	-1.4%
ATLCCS	210.7	212.4	1708	0.9%	212.6	1886	0.9%	ATLSJC	210.2	215.5	5301	2.6%	212.6	2409	1.2%
ATLCLT	189.2	184.0	-5193	-2.7%	183.2	-5979	-3.1%	ATLSJD	204.4	208.5	4112	2.3%	197.5	-6857	-3.1%
ATLCUN	197.5	194.9	-2574	-1.3%	190	-7458	-3.7%	ATLSJO	207.4	207.3	-109	0.2%	197.5	-9946	-4.6%
ATLDAB	187.2	186.3	-864	-0.4%	183.2	-3971	-2.0%	ATLSJU	209.2	206.0	-3214	-1.5%	197.5	-11708	-5.5%
ATLDCA	189.7	189.3	-404	-0.1%	183.2	-6524	-3.3%	ATLSKB	205.3	209.5	4167	2.2%	212.6	7300	3.7%
ATLDEN	199.5	200.2	651	0.4%	197.5	-2049	-1.0%	ATLSLC	207.6	206.7	-834	-0.3%	197.5	-10057	-4.8%
ATLDFW	191.0	192.4	1448	0.9%	190	-961	-0.4%	ATLSMF	212.0	215.1	3065	1.5%	212.6	576	0.3%
ATLDTW	192.7	190.1	-2556	-1.2%	190	-2662	-1.3%	ATLSNA	207.8	212.2	4438	2.3%	212.6	4847	2.5%
ATLEGE	189.7	202.1	12401	6.7%	197.5	7821	4.3%	ATLSRQ	190.2	187.6	-2582	-1.2%	183.2	-6994	-3.5%
ATLFLL	191.7	189.9	-1837	-0.8%	190	-1732	-0.7%	ATLSTL	186.9	188.3	1338	0.8%	183.2	-3746	-1.9%
ATLGCM	196.1	197.0	865	0.5%	190	-6111	-3.1%	ATLSTT	204.9	206.9	1909	1.0%	197.5	-7449	-3.5%
ATLGDL	200.5	204.7	4165	2.2%	197.5	-3024	-1.4%	ATLSXM	209.8	208.6	-1261	-0.4%	197.5	-12326	-5.7%
ATLGGT	206.7	194.7	-12004	-5.7%	190	-16658	-8.0%	ATLTPA	190.0	187.0	-2987	-1.5%	183.2	-6766	-3.5%
ATLGUA	208.0	203.0	-4975	-2.2%	197.5	-10457	-4.9%	ATLTUS	200.3	205.9	5648	2.9%	197.5	-2750	-1.3%
ATLHSV	194.2	182.7	-11481	-5.9%	183.2	-11000	-5.6%	ATLUIO	217.7	219.5	1792	0.9%	212.6	-5072	-2.2%
ATLIND	187.3	187.4	151	0.2%	183.2	-4050	-2.0%	ATLUVF	215.0	213.8	-1278	-0.6%	212.6	-2443	-1.1%
ATLJAC	198.8	206.4	7583	3.9%	197.5	-1333	-0.6%	ATLYVR	218.0	217.7	-301	-0.1%	212.6	-5400	-2.4%
ATLJAX	187.2	184.7	-2514	-1.2%	183.2	-4009	-2.0%	AUAATL	209.5	207.5	-1953	-0.9%	197.5	-12000	-5.7%
ATLJFK	196.7	192.9	-3795	-1.9%	190	-6665	-3.3%	AUSATL	193.2	193.7	489	0.3%	190	-3211	-1.6%
ATLLAS	206.7	209.3	2614	1.3%	212.6	5881	2.9%	BHMATL	183.7	182.3	-1433	-0.7%	183.2	-537	-0.2%
ATLLAX	212.0	212.7	662	0.4%	212.6	610	0.4%	BNAATL	182.7	183.3	616	0.4%	183.2	550	0.4%
ATLLGA	193.3	192.9	-437	-0.1%	190	-3345	-1.6%	BOGATL	216.2	215.2	-1000	-0.3%	212.6	-3614	-1.5%
ATLLIR	206.4	206.7	222	0.2%	197.5	-8943	-4.2%	BOGJFK	221.3	221.5	155	0.3%	212.6	-8715	-3.7%
ATLMBJ	199.7	198.8	-847	-0.3%	190	-9684	-4.8%	BOISLC	184.2	184.1	-88	0.1%	183.2	-1035	-0.4%
ATLMCI	188.1	191.8	3679	2.1%	190	1923	1.2%	BONATL	207.9	209.1	1128	0.6%	212.6	4651	2.3%
ATLMCO	189.8	186.9	-2896	-1.4%	183.2	-6636	-3.4%	BOSATL	199.7	195.1	-4543	-2.2%	190	-9658	-4.8%
ATLMEX	201.9	202.4	478	0.4%	197.5	-4409	-2.0%	BOSCDG	231.0	229.9	-1057	-0.4%	230.9	-50	0.1%
ATLMGA	176.9	204.9	27994	16.0%	197.5	20556	11.8%	BOSCUN	202.9	208.3	5378	2.8%	212.6	9700	4.9%
ATLMIA	193.3	190.1	-3202	-1.6%	190	-3328	-1.7%	BOSDTW	193.3	189.9	-3426	-1.7%	190	-3303	-1.6%
ATLMKE	186.1	191.4	5292	3.1%	190	3939	2.3%	BOSJFK	188.7	182.5	-6241	-3.2%	183.2	-5492	-2.8%
ATLMSP	197.8	195.3	-2441	-1.2%	190	-7766	-3.9%	BOSMSP	202.1	198.1	-3980	-1.9%	190	-12069	-5.9%
ATLMSY	198.4	187.3	-11133	-5.3%	183.2	-15219	-7.4%	BOSSLC	210.8	214.4	3604	1.8%	212.6	1767	0.9%
ATLNAS	192.9	192.3	-587	-0.2%	190	-2900	-1.4%	BSBATL	235.5	234.5	-1048	-0.4%	243.2	7676	3.3%

TABLE 1

B757-200 TABULAR RESULTS

APRTS	AVG_GWT	REG_EST	REG_DIF	REG_%DIF	AEDT_EST	AEDT_DIF	AEDT_%DIF
BWIATL	188.4	189.1	746	0.6%	190	1634	1.0%
BWIDTW	181.1	186.3	5228	3.1%	183.2	2117	1.4%
BWIMSP	193.4	195.1	1721	1.1%	190	-3378	-1.6%
BZNATL	208.6	206.3	-2301	-1.0%	197.5	-11079	-5.2%
BZNMSP	201.6	193.5	-8101	-3.9%	190	-11600	-5.6%
CCSATL	207.2	212.1	4861	2.6%	212.6	5378	2.8%
CDGBOS	227.5	229.9	2359	1.1%	230.9	3365	1.5%
CDGPHL	223.3	232.0	8618	4.0%	230.9	7567	3.5%
CDGPIT	226.7	233.1	6380	2.9%	230.9	4181	2.0%
CLTATL	182.5	183.1	558	0.4%	183.2	667	0.5%
CPHJFK	234.9	232.8	-2142	-0.9%	230.9	-4015	-1.7%
CUNATL	197.4	194.5	-2834	-1.4%	190	-7379	-3.7%
CUNBOS	202.9	208.8	5864	3.2%	212.6	9663	5.0%
CUNDTW	202.4	204.4	2052	1.1%	197.5	-4875	-2.3%
CUNMCO	190.7	191.7	991	0.6%	190	-714	-0.3%
CUNSLC	210.0	218.3	8338	4.0%	212.6	2600	1.3%
CVGATL	180.4	186.3	5848	3.6%	183.2	2771	1.9%
CVGLAS	200.8	208.0	7221	3.8%	197.5	-3315	-1.5%
CVGLAX	204.3	211.7	7421	3.8%	212.6	8282	4.2%
CVGSEA	208.2	212.8	4591	2.4%	212.6	4378	2.3%
CVGSLC	200.4	204.2	3792	2.0%	197.5	-2944	-1.4%
DABATL	191.0	185.6	-5414	-2.7%	183.2	-7814	-4.0%
DCAATL	190.0	187.4	-2668	-1.3%	183.2	-6835	-3.5%
DCAMSP	188.2	193.8	5576	3.0%	190	1800	1.0%
DCASLC	207.0	209.1	2099	1.1%	212.6	5572	2.7%
DENATL	201.7	201.5	-194	0.1%	197.5	-4243	-1.9%
DENMSP	197.7	192.9	-4804	-2.3%	190	-7700	-3.8%
DFWATL	193.0	192.8	-234	0.0%	190	-3021	-1.5%
DKRJFK	229.9	232.5	2562	1.2%	230.9	1005	0.5%
DTWATL	191.4	190.0	-1418	-0.6%	190	-1380	-0.6%
DTWBOS	193.2	190.6	-2644	-1.2%	190	-3239	-1.5%
DTWBWI	187.5	186.9	-612	-0.2%	183.2	-4284	-2.1%
DTWCUN	205.3	204.6	-629	-0.3%	197.5	-7750	-3.8%
DTWFLL	197.4	198.9	1504	0.9%	190	-7361	-3.6%
DTWGRR	192.6	182.1	-10580	-5.5%	183.2	-9436	-4.9%
DTWLAS	207.1	209.2	2151	1.1%	212.6	5525	2.7%
DTWLAX	209.9	213.1	3162	1.7%	212.6	2698	1.4%
DTWMCO	193.9	196.0	2143	1.3%	190	-3882	-1.8%
DTWMIA	198.9	199.2	244	0.2%	190	-8909	-4.4%
DTWMKE	186.2	184.0	-2168	-1.0%	183.2	-2982	-1.5%
DTWMSP	190.5	188.9	-1632	-0.7%	183.2	-7300	-3.6%
DTWPBI	193.4	198.2	4799	2.5%	190	-3375	-1.7%
DTWPDX	207.4	212.6	5238	2.6%	212.6	5215	2.6%
DTWPHL	189.9	187.6	-2246	-1.1%	183.2	-6667	-3.4%
DTWPHX	206.1	207.9	1782	0.9%	197.5	-8640	-4.1%
DTWRSW	197.7	198.1	401	0.3%	190	-7735	-3.8%
DTWSAN	209.9	212.7	2751	1.4%	212.6	2671	1.3%
DTWSEA	208.8	212.2	3422	1.7%	212.6	3821	1.9%
DTWSFO	212.2	214.7	2518	1.3%	212.6	404	0.3%
DTWSLC	203.8	204.8	989	0.6%	197.5	-6266	-3.0%
DTWTPA	195.6	196.4	870	0.6%	190	-5577	-2.7%

APRTS	AVG_GWT	REG_EST	REG_DIF	REG_%DIF	AEDT_EST	AEDT_DIF	AEDT_%DIF
DUBJFK	226.2	227.6	1375	0.6%	230.9	4698	2.1%
EGEATL	204.8	200.8	-3983	-1.7%	197.5	-7295	-3.3%
FAIMSP	223.3	221.1	-2164	-0.9%	212.6	-10668	-4.7%
FAISEA	208.7	205.5	-3133	-1.4%	197.5	-11176	-5.2%
FLLATL	191.7	188.6	-3028	-1.5%	190	-1656	-0.8%
FLLDTW	195.5	197.7	2229	1.3%	190	-5513	-2.6%
FLLJFK	192.3	196.8	4418	2.5%	190	-2345	-1.0%
FLLMSP	197.7	203.7	6048	3.3%	197.5	-180	0.1%
GCMATL	206.2	195.0	-11232	-5.4%	190	-16200	-7.8%
GDLATL	204.4	205.0	554	0.4%	197.5	-6909	-3.3%
GDLLAX	207.0	202.3	-4723	-2.2%	197.5	-9500	-4.6%
GEGMSP	206.8	199.3	-7542	-3.6%	197.5	-9319	-4.4%
GEGSLC	192.8	188.8	-3949	-2.0%	183.2	-9550	-4.9%
GGTATL	204.4	192.7	-11776	-5.6%	190	-14433	-6.9%
GGTJFK	209.2	197.9	-11243	-5.2%	197.5	-11676	-5.4%
GGTLAX	217.5	222.5	5041	2.4%	212.6	-4892	-2.2%
GUAATL	208.4	202.0	-6382	-2.9%	197.5	-10895	-5.1%
GUALAX	218.9	215.8	-3072	-1.3%	212.6	-6281	-2.8%
HNLLAX	223.4	222.8	-639	-0.2%	212.6	-10832	-4.8%
HNLSEA	223.2	224.8	1641	0.9%	212.6	-10567	-4.6%
HNLSFO	218.3	220.2	1899	1.0%	212.6	-5665	-2.5%
INDATL	191.1	187.0	-4123	-2.1%	183.2	-7879	-4.1%
JACATL	207.0	204.1	-2861	-1.3%	197.5	-9500	-4.5%
JACMSP	197.2	192.5	-4742	-2.4%	190	-7214	-3.6%
JAXATL	190.2	183.8	-6380	-3.3%	183.2	-6981	-3.6%
JFKAGP	236.4	231.5	-4942	-2.1%	230.9	-5510	-2.3%
JFKARN	234.8	233.2	-1640	-0.6%	230.9	-3900	-1.6%
JFKATL	196.3	193.7	-2668	-1.3%	190	-6331	-3.2%
JFKBOG	215.1	222.2	7153	3.5%	212.6	-2481	-1.0%
JFKCPH	236.1	232.8	-3355	-1.4%	230.9	-5229	-2.2%
JFKDKR	232.9	232.5	-474	-0.1%	230.9	-2031	-0.8%
JFKDTW	195.1	189.5	-5645	-2.8%	183.2	-11925	-6.1%
JFKDUB	232.8	227.6	-5180	-2.2%	230.9	-1857	-0.7%
JFKFLL	195.0	198.8	3824	2.2%	190	-5000	-2.4%
JFKGGT	212.7	200.7	-12003	-5.6%	197.5	-15227	-7.1%
JFKKEF	222.2	224.2	2078	1.1%	212.6	-9551	-4.1%
JFKLAS	211.4	218.5	7077	3.4%	212.6	1204	0.7%
JFKLAX	212.5	222.3	9743	4.7%	212.6	71	0.2%
JFKMCO	194.6	196.7	2138	1.2%	190	-4595	-2.3%
JFKMEX	209.7	215.8	6180	3.1%	212.6	2936	1.5%
JFKMIA	198.3	199.2	836	0.5%	190	-8333	-4.1%
JFKMSP	189.9	198.2	8219	4.5%	190	67	0.2%
JFKPDX	209.0	221.9	12943	6.4%	212.6	3635	1.9%
JFKPHX	207.9	216.9	8955	4.4%	212.6	4656	2.3%
JFKPIT	182.3	186.7	4392	2.6%	183.2	933	0.7%
JFKSAN	210.7	221.8	11091	5.4%	212.6	1918	1.0%
JFKSDQ	208.2	206.8	-1341	-0.5%	197.5	-10667	-5.0%
JFKSEA	215.7	221.4	5694	2.7%	212.6	-3077	-1.3%
JFKSFO	214.6	224.1	9517	4.5%	212.6	-1997	-0.8%
JFKSJU	204.3	207.6	3370	1.7%	197.5	-6762	-3.2%
JFKSLC	210.2	214.2	3932	2.0%	212.6	2358	1.2%

TABLE 2

B757-200 TABULAR RESULTS

APRTS	AVG_GWT	REG_EST	REG_DIF	REG_%DIF	AEDT_EST	AEDT_DIF	AEDT_%DIF
JFKSNN	229.1	226.7	-2433	-1.0%	230.9	1813	0.8%
JFKSSA	237.2	235.2	-2057	-0.8%	243.2	5978	2.5%
JFKSTT	199.5	208.1	8589	4.5%	197.5	-1965	-0.8%
JFKSXM	200.9	209.0	8143	4.3%	197.5	-3389	-1.4%
JNUSEA	194.4	194.0	-384	-0.1%	190	-4426	-2.2%
KEFJFK	228.1	222.6	-5508	-2.3%	212.6	-15471	-6.7%
KOALAX	222.5	221.4	-1017	-0.4%	212.6	-9855	-4.4%
LASATL	212.2	210.1	-2068	-0.9%	212.6	406	0.2%
LASCVG	207.2	209.0	1808	0.9%	197.5	-9667	-4.6%
LASDTW	210.5	210.2	-297	-0.1%	212.6	2138	1.1%
LASJFK	216.3	218.5	2172	1.2%	212.6	-3701	-1.5%
LASMCO	198.4	215.0	16591	8.5%	212.6	14191	7.2%
LASMSP	202.4	202.7	239	0.2%	197.5	-4923	-2.4%
LASSLC	183.1	187.1	3980	2.4%	183.2	60	0.2%
LAXATL	216.0	212.5	-3430	-1.5%	212.6	-3371	-1.5%
LAXDTW	215.1	213.1	-1962	-0.8%	212.6	-2459	-1.1%
LAXGDL	190.9	201.9	11002	6.3%	197.5	6611	4.0%
LAXGGT	217.6	224.4	6846	3.2%	212.6	-4971	-2.2%
LAXGUA	216.6	216.7	87	0.2%	212.6	-3979	-1.7%
LAXHNL	209.7	222.7	13020	6.5%	212.6	2910	1.7%
LAXIND	213.0	210.3	-2666	-1.2%	212.6	-400	-0.2%
LAXJFK	218.7	221.4	2688	1.3%	212.6	-6079	-2.7%
LAXKOA	219.6	221.8	2295	1.1%	212.6	-6952	-3.1%
LAXLIH	217.0	223.7	6753	3.2%	212.6	-4355	-1.9%
LAXMCO	215.5	217.1	1576	0.8%	212.6	-2892	-1.3%
LAXMSP	204.9	205.7	771	0.5%	197.5	-7419	-3.5%
LAXOGG	216.5	221.5	5038	2.4%	212.6	-3902	-1.7%
LAXSEA	196.3	196.0	-288	0.0%	190	-6289	-3.0%
LAXSJO	221.4	225.5	4093	2.0%	212.6	-8780	-3.8%
LAXSLC	189.4	189.9	472	0.3%	190	554	0.4%
LGAATL	193.9	190.9	-3024	-1.5%	190	-3917	-1.9%
LGADTW	182.4	186.6	4182	2.6%	183.2	825	0.8%
LIHLAX	221.7	221.6	-86	0.1%	212.6	-9103	-4.0%
LIRATL	209.0	205.4	-3586	-1.6%	197.5	-11492	-5.4%
MBJATL	199.2	197.5	-1726	-0.8%	190	-9196	-4.6%
MCIATL	196.0	191.2	-4794	-2.3%	190	-5956	-2.9%
MCOATL	192.4	186.8	-5621	-2.8%	183.2	-9217	-4.7%
MCOCUN	190.9	191.9	1025	0.6%	190	-875	-0.4%
MCODTW	196.7	196.0	-713	-0.2%	190	-6738	-3.3%
MCOJFK	194.1	195.8	1743	1.1%	190	-4053	-1.9%
MCOLAS	194.6	214.1	19438	10.2%	212.6	17975	9.4%
MCOLAX	213.5	217.0	3578	1.8%	212.6	-858	-0.3%
MCOMSP	200.2	201.9	1741	1.0%	197.5	-2656	-1.2%
MCOSLC	209.9	212.3	2328	1.2%	212.6	2669	1.3%
MEXATL	209.4	202.6	-6842	-3.2%	197.5	-11944	-5.6%
MEXJFK	216.1	215.3	-862	-0.2%	212.6	-3528	-1.5%
MIAATL	193.1	190.4	-2706	-1.3%	190	-3066	-1.5%
MIADTW	196.6	199.5	2907	1.7%	190	-6625	-3.2%
MIAJFK	196.3	198.6	2361	1.6%	190	-6250	-2.8%
MKEATL	187.8	190.5	2702	1.6%	190	2246	1.4%
MKEDTW	179.6	183.3	3635	2.3%	183.2	3575	2.3%
MKEMSP	183.2	184.3	1044	0.7%	183.2	-14	0.1%
MSPANC	222.3	221.7	-604	-0.2%	212.6	-9694	-4.3%
MSPATL	199.2	194.8	-4396	-2.1%	190	-9204	-4.6%
MSPBOS	201.7	198.4	-3292	-1.6%	190	-11726	-5.7%
MSPBWI	192.1	195.3	3174	1.9%	190	-2114	-0.9%
MSPDCA	193.0	195.2	2211	1.3%	190	-3000	-1.4%
MSPDEN	192.0	191.0	-972	-0.4%	190	-2000	-1.0%
MSPDTW	189.9	188.5	-1383	-0.6%	183.2	-6678	-3.4%
MSPFAI	222.0	220.8	-1192	-0.5%	212.6	-9400	-4.2%
MSPFLL	204.3	204.5	145	0.3%	197.5	-6833	-3.1%
MSPGEG	195.4	199.3	3855	2.0%	197.5	2076	1.1%
MSPJAC	189.8	194.2	4447	2.4%	190	214	0.1%
MSPJFK	196.0	196.8	842	0.7%	190	-6000	-2.8%
MSPLAS	199.2	201.4	2129	1.2%	197.5	-1722	-0.8%
MSPLAX	201.9	205.3	3355	1.8%	197.5	-4429	-2.1%
MSPLGA	192.7	196.7	3993	2.2%	190	-2714	-1.3%
MSPMCI	184.0	186.2	2231	1.3%	183.2	-800	-0.4%
MSPMCO	202.2	201.5	-672	-0.3%	197.5	-4696	-2.3%
MSPMKE	187.1	184.6	-2442	-1.2%	183.2	-3880	-2.0%
MSPORD	188.7	185.3	-3491	-1.8%	183.2	-5543	-2.9%
MSPPDX	202.0	203.5	1417	0.8%	197.5	-4545	-2.2%
MSPPHX	199.4	201.0	1519	0.9%	197.5	-1948	-0.8%
MSPRSW	203.4	203.3	-76	0.0%	197.5	-5884	-2.8%
MSPSAN	201.3	205.2	3952	2.1%	197.5	-3775	-1.7%
MSPSEA	202.1	203.0	937	0.6%	197.5	-4583	-2.2%
MSPSFO	203.6	206.2	2576	1.4%	197.5	-6110	-2.9%
MSPSJO	210.9	220.7	9856	4.9%	212.6	1725	1.0%
MSPSJU	220.1	219.8	-324	0.0%	212.6	-7495	-3.3%
MSPSLC	192.1	196.2	4103	2.4%	190	-2105	-0.8%
MSPTPA	196.3	201.5	5149	2.8%	197.5	1183	0.8%
MSPYVR	205.7	203.6	-2080	-1.0%	197.5	-8214	-3.9%
MSYATL	187.8	186.4	-1342	-0.6%	183.2	-4572	-2.3%
NASATL	201.1	191.9	-9221	-4.6%	190	-11146	-5.5%
NCAATL	206.3	195.6	-10706	-5.2%	190	-16343	-7.9%
OGGLAX	219.3	219.6	357	0.3%	212.6	-6676	-2.9%
OGGSEA	228.0	222.2	-5795	-2.5%	212.6	-15400	-6.7%
ORDATL	195.0	190.5	-4481	-2.2%	190	-5008	-2.5%
ORDMSP	190.6	186.0	-4632	-2.3%	183.2	-7430	-3.8%
PBIATL	196.8	188.4	-8451	-4.2%	183.2	-13639	-6.9%
PBIDTW	195.4	197.4	2068	1.2%	190	-5357	-2.6%
PDXATL	219.6	215.9	-3715	-1.6%	212.6	-7027	-3.1%
PDXDTW	214.9	212.2	-2615	-1.2%	212.6	-2262	-1.0%
PDXJFK	215.0	220.6	5577	2.8%	212.6	-2417	-1.0%
PDXMSP	203.5	203.5	8	0.1%	197.5	-5952	-2.9%
PDXSLC	190.2	190.2	-7	0.1%	190	-189	0.0%
PHLATL	189.9	190.6	751	0.5%	190	141	0.2%
PHLCDG	231.0	232.0	966	0.5%	230.9	-86	0.1%
PHLDTW	186.8	187.1	227	0.3%	183.2	-3633	-1.8%
PHLSLC	205.4	211.6	6181	3.1%	212.6	7160	3.5%
PHXATL	208.3	206.3	-1999	-0.9%	197.5	-10827	-5.1%
PHXDTW	209.6	207.7	-1875	-0.8%	197.5	-12104	-5.7%

TABLE 3

B757-200 TABULAR RESULTS

APRTS	AVG_GWT	REG_EST	REG_DIF	REG_%DIF	AEDT_EST	AEDT_DIF	AEDT_%DIF
PHXJFK	214.3	215.8	1519	0.8%	212.6	-1650	-0.7%
PHXMSP	199.9	201.1	1250	0.7%	197.5	-2397	-1.1%
PHXSLC	185.1	188.3	3238	1.9%	183.2	-1893	-0.9%
PITATL	183.9	188.6	4723	2.8%	183.2	-718	-0.2%
PITCDG	231.5	233.1	1616	0.8%	230.9	-584	-0.2%
PITJFK	186.9	185.5	-1393	-0.5%	183.2	-3726	-1.8%
PNSATL	189.6	182.7	-6838	-3.5%	183.2	-6357	-3.2%
PUJATL	210.5	203.3	-7184	-3.4%	197.5	-13006	-6.1%
PVRATL	207.2	205.3	-1823	-0.8%	197.5	-9660	-4.6%
RDUATL	185.4	185.2	-209	0.0%	183.2	-2249	-1.1%
RICATL	189.6	187.0	-2686	-1.3%	183.2	-6445	-3.3%
RSWATL	195.0	188.6	-6392	-3.2%	183.2	-11829	-6.0%
RSWDTW	197.5	198.1	683	0.5%	190	-7451	-3.6%
RSWMSP	200.9	203.7	2757	1.5%	197.5	-3423	-1.6%
RTBATL	207.4	198.1	-9245	-4.4%	197.5	-9875	-4.7%
SANATL	216.0	210.6	-5381	-2.4%	212.6	-3413	-1.5%
SANDTW	216.4	211.7	-4681	-2.1%	212.6	-3788	-1.7%
SANJFK	220.4	219.9	-541	-0.2%	212.6	-7802	-3.5%
SANMSP	207.5	204.6	-2882	-1.3%	197.5	-10008	-4.8%
SANSLC	190.5	189.5	-1009	-0.4%	190	-534	-0.2%
SATATL	195.4	193.3	-2039	-0.9%	190	-5375	-2.6%
SDQJFK	212.2	205.5	-6669	-2.8%	197.5	-14682	-6.6%
SEAANC	198.2	204.2	5980	3.4%	197.5	-700	0.0%
SEAATL	221.5	216.4	-5122	-2.3%	212.6	-8925	-4.0%
SEACVG	210.2	212.8	2541	1.3%	212.6	2365	1.2%
SEADTW	216.2	212.2	-3990	-1.8%	212.6	-3553	-1.6%
SEAFAI	193.4	205.6	12171	6.5%	197.5	4090	2.3%
SEAHNL	223.5	224.7	1133	0.6%	212.6	-10921	-4.8%
SEAJFK	220.1	220.4	252	0.2%	212.6	-7542	-3.3%
SEAJNU	178.7	195.2	16514	9.5%	190	11333	6.6%
SEALAX	191.0	195.9	4960	2.8%	190	-969	-0.3%
SEAMSP	206.8	203.4	-3485	-1.6%	197.5	-9340	-4.4%
SEAOGG	218.6	224.0	5422	2.6%	212.6	-6018	-2.6%
SEASLC	193.0	191.5	-1458	-0.6%	190	-2955	-1.4%
SFOATL	221.4	215.7	-5759	-2.5%	212.6	-8840	-3.9%
SFODTW	217.8	214.7	-3118	-1.4%	212.6	-5182	-2.3%
SFOHNL	218.2	220.0	1793	0.9%	212.6	-5606	-2.5%
SFOJFK	221.1	223.1	1992	1.0%	212.6	-8535	-3.8%
SFOMSP	208.3	206.5	-1826	-0.8%	197.5	-10835	-5.1%
SFOSLC	191.4	190.0	-1386	-0.6%	190	-1375	-0.6%
SJCATL	213.3	215.0	1689	0.9%	212.6	-683	-0.2%
SJDATL	203.1	207.5	4383	2.2%	197.5	-5633	-2.7%
SJOATL	211.5	206.4	-5085	-2.3%	197.5	-13985	-6.5%
SJOJFK	207.4	216.0	8632	4.4%	212.6	5200	2.7%
SJOLAX	223.8	224.6	806	0.5%	212.6	-11241	-4.9%
SJOMSP	220.8	220.3	-490	-0.2%	212.6	-8200	-3.6%
SJUATL	209.0	205.2	-3725	-1.7%	197.5	-11475	-5.4%
SJUJFK	202.4	206.1	3690	2.1%	197.5	-4904	-2.2%
SJUMSP	215.4	219.5	4195	2.0%	212.6	-2750	-1.2%
SKBATL	215.5	207.7	-7864	-3.6%	212.6	-2938	-1.3%
SLCANC	215.8	215.5	-284	-0.1%	212.6	-3166	-1.4%
SLCATL	210.9	206.6	-4326	-2.0%	197.5	-13404	-6.3%
SLCBOI	184.2	184.9	666	0.5%	183.2	-1030	-0.5%
SLCBOS	213.9	215.2	1222	0.8%	212.6	-1333	-0.4%
SLCCUN	209.4	218.5	9104	4.4%	212.6	3171	1.5%
SLCCVG	204.9	204.2	-663	-0.2%	197.5	-7400	-3.5%
SLCDCA	210.1	210.9	832	0.5%	212.6	2498	1.3%
SLCDTW	207.2	204.8	-2483	-1.1%	197.5	-9738	-4.6%
SLCGEG	185.0	189.2	4175	2.4%	183.2	-1800	-0.9%
SLCJFK	212.9	213.2	384	0.3%	212.6	-252	0.0%
SLCLAS	185.5	186.2	669	0.5%	183.2	-2312	-1.1%
SLCLAX	188.1	189.9	1826	1.1%	190	1941	1.2%
SLCMCO	212.0	212.3	308	0.2%	212.6	650	0.4%
SLCMSP	196.5	196.6	83	0.1%	190	-6498	-3.2%
SLCPDX	190.4	190.6	191	0.2%	190	-365	-0.1%
SLCPHL	209.5	212.2	2634	1.3%	212.6	3053	1.5%
SLCPHX	187.0	188.5	1497	0.9%	183.2	-3825	-1.9%
SLCSAN	189.6	190.5	904	0.6%	190	406	0.3%
SLCSEA	194.4	191.5	-2867	-1.3%	190	-4402	-2.1%
SLCSFO	187.1	190.0	2967	1.6%	190	2929	1.6%
SLCSMF	184.4	188.9	4525	2.5%	183.2	-1200	-0.6%
SMFATL	217.1	213.7	-3468	-1.6%	212.6	-4542	-2.1%
SMFMSP	206.3	204.1	-2187	-1.0%	197.5	-8786	-4.2%
SMFSLC	191.8	187.7	-4145	-2.1%	183.2	-8600	-4.4%
SNAATL	213.4	209.7	-3680	-1.7%	212.6	-770	-0.3%
SNNJFK	223.8	226.7	2825	1.3%	230.9	7071	3.2%
SRQATL	192.9	186.5	-6324	-3.2%	183.2	-9655	-4.9%
SSAJFK	235.2	235.2	-17	0.0%	243.2	8018	3.4%
STLATL	190.2	187.8	-2434	-1.2%	183.2	-7004	-3.6%
STTATL	211.6	204.8	-6780	-3.1%	197.5	-14122	-6.6%
STTJFK	208.0	205.2	-2708	-1.2%	197.5	-10452	-4.9%
SXMATL	212.8	206.8	-5984	-2.7%	197.5	-15298	-7.1%
SXMJFK	210.7	206.5	-4226	-1.9%	197.5	-13214	-6.2%
SXMMSP	225.0	220.8	-4236	-1.8%	212.6	-12400	-5.5%
TPAATL	189.4	186.5	-2893	-1.4%	183.2	-6152	-3.2%
TPADTW	193.3	196.1	2794	1.6%	190	-3278	-1.5%
TPAMSP	198.0	201.5	3465	1.8%	197.5	-500	-0.2%
TUSATL	203.8	205.4	1615	0.8%	197.5	-6262	-3.0%
UIOATL	221.4	219.9	-1577	-0.6%	212.6	-8838	-3.9%
UVFATL	218.2	212.5	-5675	-2.6%	212.6	-5574	-2.5%
YVRATL	216.5	217.4	827	0.4%	212.6	-3938	-1.8%
YVRMSP	204.6	203.8	-781	-0.3%	197.5	-7100	-3.4%

TABLE 4

B767-400ER/CF6-80C2/B8F

Takeoff Weight Determination:

Specifics of the Flight Planning Database:

- 12,138 Flights
- 94 Routes from 28 Departure Airports
- 81 "Tankered" Flights
  - 8187 lbs. Average
  - 3060 NM Average Trip
- Added Airport Elevation, Runway Length, and GCD for each Airport/Flight

As before, multiple linear regressions on the database were conducted in a stepwise method using the independent variables: runway length, airport elevation, and either GCD or Planned Distance. The regressions were applied to the total database of individual flights and repeated with an "average" database that contained the average data for each route and in the case of Planned Distance, the average planned distance.

The statistical summary of the GCD and Planned Distance regressions are as follows:

B767-400ER Planned Distance with All Data:

Model Summary[d]

Model	R	R Square	Adjusted R Square	Std. Error of the Estimate
1	.640[a]	.410	.410	20542.942
2	.642[b]	.412	.412	20513.368
3	.643[c]	.413	.413	20494.976

a. Predictors: (Constant), PL_DIST

b. Predictors: (Constant), PL_DIST, RWYL

c. Predictors: (Constant), PL_DIST, RWYL, ELEV

d. Dependent Variable: ACTWT

B767-400ER Great Circle Distance with All Data:

Model Summary[d]

Model	R	R Square	Adjusted R Square	Std. Error of the Estimate
1	.640[a]	.410	.410	20545.571
2	.642[b]	.412	.412	20516.248
3	.643[c]	.413	.413	20497.507

a. Predictors: (Constant), GCD

b. Predictors: (Constant), GCD, RWYL

c. Predictors: (Constant), GCD, RWYL, ELEV

d. Dependent Variable: ACTWT

B767-400ER Planned Distance with Average Route Data:

Model Summary[b]

Model	R	R Square	Adjusted R Square	Std. Error of the Estimate
1	.930[a]	.865	.863	13.66311234

a. Predictors: (Constant), AVG_PDST

b. Dependent Variable: AVG_GWT

B767-400ER Great Circle Distance with Average Route Data:

Model Summary[b]

Model	R	R Square	Adjusted R Square	Std. Error of the Estimate
1	.930[a]	.865	.863	13.66898455

a. Predictors: (Constant), GCD

b. Dependent Variable: AVG_GWT

Again, there was very little difference in the strength of the correlation using Great Circle Distance or Planned Distance, and the correlation is much better when using average route data versus the total departure data. The stepwise statistical analysis eliminated inputs of runway length and elevation and produced a very acceptable relationship using distance. To remain consistent, GCD will be used.

B767-400ER Takeoff Weight Estimation Final Results

Model Summary[b]

Model	R	R Square	Adjusted R Square	Std. Error of the Estimate
1	.930[a]	.865	.863	13.66898455

a. Predictors: (Constant), GCD

b. Dependent Variable: AVG_GWT

Coefficients[a]

Model		Unstandardized Coefficients		Standardized Coefficients	t	Sig.
		B	Std. Error	Beta		
1	(Constant)	297.966	4.230		70.443	.000
	GCD	.031	.001	.930	24.239	.000

a. Dependent Variable: AVG_GWT

$$GWT = 297.966 + .031(GCD)$$

(See Figure 6 below)

Testing of the Takeoff Weight Estimation

The resulting takeoff weight regression equations were compared with the ACARS database which has recorded data for 10,512 flights. The resulting data represented 56 flights/routes departing 21 airports. The results of the testing are shown in the following figures, and tabulated in Table 5.

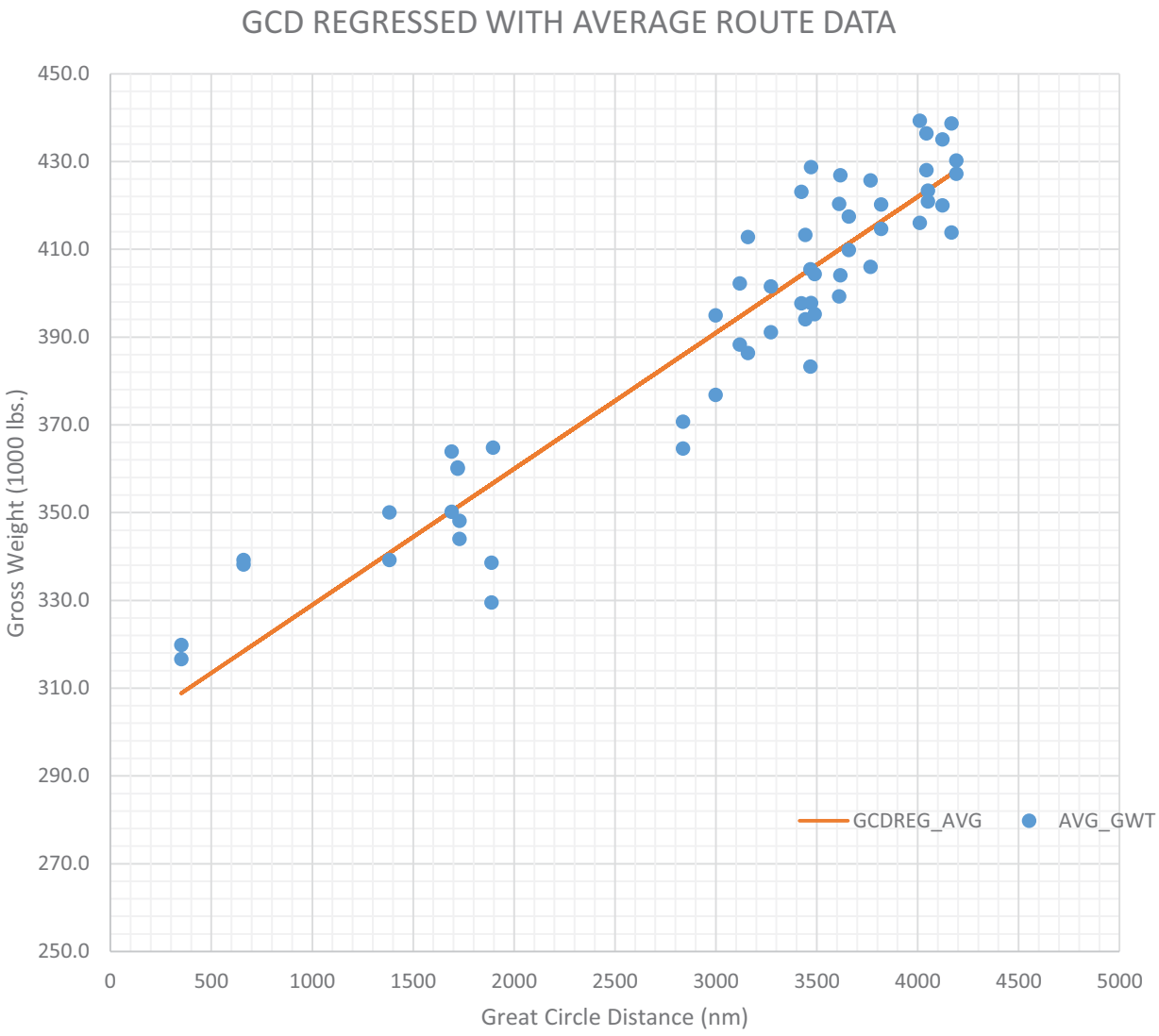
GCD REGRESSED WITH AVERAGE ROUTE DATA
Gross Weight (1000 lbs.)
450.0
430.0
410.0
390.0
370.0
350.0
330.0
310.0
290.0
270.0
250.0
0
500
1000
1500
2000
2500
3000
3500
4000
4500
5000
Great Circle Distance (nm)
GCDREG_AVG
AVG_GWT

FIGURE 6

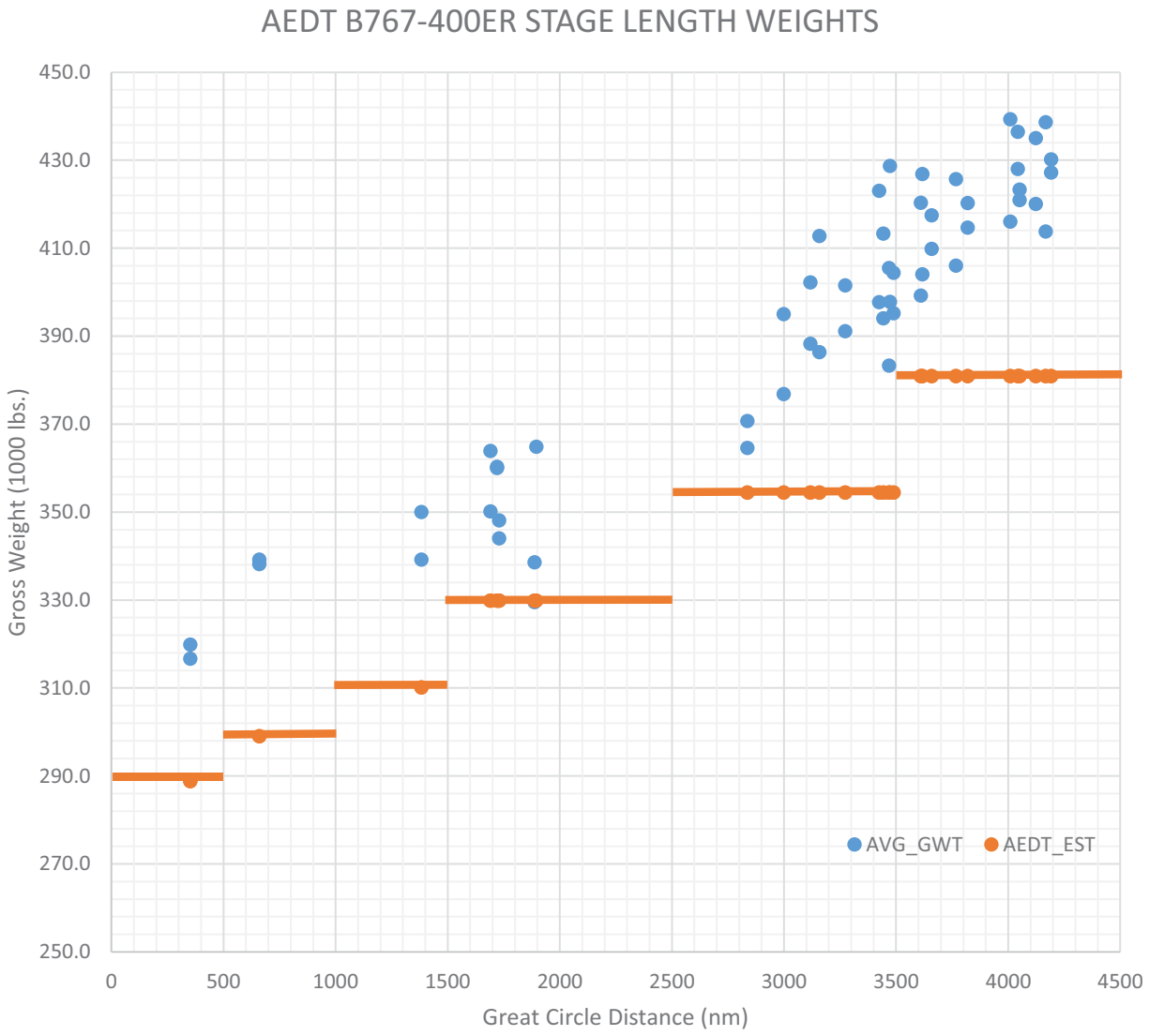

FIGURE 7

The plot for AEDT weights has been augmented by imposing the AEDT weight "step function" over the existing data. It can be clearly seen that the existing AEDT weight tables for the B767-400ER are significantly underestimated.

The average route tabular data is contained in the following tables, showing the actual weight, and the differences in the regression and AEDT stage length weights.

B767-400ER TABULAR RESULTS

APRTS	GWT	REG_GWT	REG_DIF	REG_%DF	AEDT_WT	AEDT_DIF	AEDT_%DF
AMSDTW	423.0	404.1	-18933	-4.5%	354.4	-68616	-16.2%
ATLCDG	414.6	416.4	1719	0.4%	380.9	-33730	-8.1%
ATLFRA	416.0	422.3	6273	1.5%	380.9	-35097	-8.4%
ATLGRU	436.4	423.3	-13094	-3.0%	380.9	-55487	-12.7%
ATLJFK	338.1	318.4	-19689	-5.8%	299.0	-39078	-11.6%
ATLLAX	363.9	350.4	-13470	-3.7%	329.9	-33996	-9.3%
ATLLHR	409.8	411.4	1606	0.4%	380.9	-28883	-7.0%
ATLMAD	406.0	414.7	8753	2.2%	380.9	-25084	-6.2%
ATLMCO	319.8	308.8	-10953	-3.4%	288.8	-30982	-9.7%
ATLMUC	413.8	427.2	13384	3.2%	380.9	-32884	-7.9%
ATLPDX	338.6	356.5	17923	5.3%	329.9	-8710	-2.6%
ATLSEA	364.8	356.7	-8058	-2.2%	329.9	-34939	-9.6%
ATLSLC	350.0	340.8	-9192	-2.6%	310.1	-39875	-11.4%
BOSLHR	364.6	385.9	21350	5.9%	354.4	-10136	-2.8%
CDGATL	420.2	416.4	-3845	-0.9%	380.9	-39294	-9.4%
CDGDTW	413.3	404.7	-8570	-2.1%	354.4	-58842	-14.2%
CDGJFK	412.8	395.9	-16896	-4.1%	354.4	-58333	-14.1%
DTWAMS	397.7	404.1	6443	1.6%	354.4	-43240	-10.9%
DTWCDG	394.1	404.7	10646	2.7%	354.4	-39626	-10.1%
DTWFRA	404.0	410.1	6057	1.5%	380.9	-23130	-5.7%
DTWLAX	360.3	351.3	-8964	-2.5%	329.9	-30389	-8.4%
DTWLHR	391.1	399.4	8358	2.1%	354.4	-36644	-9.4%
FRAATL	439.3	422.3	-17020	-3.9%	380.9	-58390	-13.3%
FRADTW	426.8	410.1	-16717	-3.9%	380.9	-45904	-10.8%
GRUATL	428.0	423.3	-4673	-1.1%	380.9	-47066	-11.0%
GRUJFK	420.0	425.8	5787	1.4%	380.9	-39086	-9.3%
JFKATL	339.2	318.4	-20728	-6.1%	299.0	-40117	-11.8%
JFKCDG	386.3	395.9	9531	2.5%	354.4	-31906	-8.3%
JFKGRU	435.0	425.8	-9194	-2.1%	380.9	-54067	-12.4%
JFKLHR	376.8	390.9	14149	3.8%	354.4	-22359	-5.9%
JFKMAD	388.3	394.6	6355	1.6%	354.4	-33842	-8.7%
JFKMXP	397.8	405.6	7842	2.0%	354.4	-43329	-10.9%
JFKNCE	383.3	405.5	22198	5.8%	354.4	-28849	-7.5%
JFKSLC	348.1	351.6	3491	1.0%	329.9	-18213	-5.2%
JFKSVO	423.3	423.5	241	0.1%	380.9	-42400	-10.0%
JFKVCE	399.2	409.9	10655	2.7%	380.9	-18315	-4.6%
LAXATL	350.1	350.4	244	0.1%	329.9	-20282	-5.8%
LAXDTW	360.0	351.3	-8714	-2.4%	329.9	-30139	-8.4%
LHRATL	417.4	411.4	-6052	-1.4%	380.9	-36541	-8.8%
LHRBOS	370.7	385.9	15222	4.1%	354.4	-16264	-4.4%
LHRDTW	401.5	399.4	-2066	-0.5%	354.4	-47068	-11.7%
LHRJFK	394.9	390.9	-4009	-1.0%	354.4	-40517	-10.3%
LHRMSP	404.4	406.1	1773	0.4%	354.4	-49925	-12.3%
MADATL	425.7	414.7	-10959	-2.6%	380.9	-44796	-10.5%
MADJFK	402.2	394.6	-7539	-1.9%	354.4	-47736	-11.9%
MCOATL	316.6	308.8	-7753	-2.4%	288.8	-27782	-8.8%
MSPLHR	395.2	406.1	10954	2.8%	354.4	-40744	-10.3%
MUCATL	438.6	427.2	-11444	-2.6%	380.9	-57712	-13.2%
MXPJFK	428.7	405.6	-23091	-5.4%	354.4	-74262	-17.3%
NCEJFK	405.4	405.5	45	0.0%	354.4	-51002	-12.6%
NRTPDX	427.2	427.9	720	0.2%	380.9	-46261	-10.8%
PDXATL	329.5	356.5	26994	8.2%	329.9	361	0.1%
PDXNRT	430.2	427.9	-2280	-0.5%	380.9	-49261	-11.5%
SLCATL	339.2	340.8	1641	0.5%	310.1	-29042	-8.6%
SLCJFK	344.0	351.6	7602	2.2%	329.9	-14102	-4.1%
SVOJFK	420.9	423.5	2659	0.6%	380.9	-39982	-9.5%
VCEJFK	420.3	409.9	-10432	-2.5%	380.9	-39402	-9.4%

TABLE 5

B737-800/CFM56-7B26

Takeoff Weight Determination:

Specifics of the Flight Planning Database:

- 33,933 Flights
- 467 Routes Departing 94 Airports
- 4,990 "Tankered" Flights
  - 5960 lbs. Average
  - 704 NM Average Trip
- Added Airport Elevation, Runway Length, and GCD for each Airport/Flight

As with the previous aircraft, multiple linear regressions on the database were conducted in a stepwise method using independent variables: runway length, airport elevation, and either GCD or Planned Distance. The regressions were applied to the total database of individual flights and repeated with an "average" database that contained the average data for each route and in the case of Planned Distance, the average planned distance.

The statistical summary of the GCD and Planned Distance regressions are as follows:

B737-800 Planned Distance with All Flight Data

Model Summary[d]

Model	R	R Square	Adjusted R Square	Std. Error of the Estimate
1	.752[a]	.566	.566	7069.417
2	.755[b]	.570	.570	7036.659
3	.755[c]	.570	.570	7036.198

a. Predictors: (Constant), PLN_DST

b. Predictors: (Constant), PLN_DST, RWYL

c. Predictors: (Constant), PLN_DST, RWYL, ELEV

d. Dependent Variable: ACT_TOGW

B737-800 Planned Distance with Average Route Data

Model Summary[c]

Model	R	R Square	Adjusted R Square	Std. Error of the Estimate
1	.895[a]	.801	.801	4361.5687221
2	.901[b]	.812	.811	4251.5240030

a. Predictors: (Constant), AVG_PLDST

b. Predictors: (Constant), AVG_PLDST, RWYL

c. Dependent Variable: AVG_GWT

B737-800 GCD with All Flight Data

Model Summary[d]

Model	R	R Square	Adjusted R Square	Std. Error of the Estimate
1	.751[a]	.564	.564	7083.650
2	.754[b]	.568	.568	7051.356
3	.754[c]	.569	.569	7049.650

a. Predictors: (Constant), GCD

b. Predictors: (Constant), GCD, RWYL

c. Predictors: (Constant), GCD, RWYL, ELEV

d. Dependent Variable: ACT_TOGW

B737-800 GCD with Average Route Data

Model Summary[c]

Model	R	R Square	Adjusted R Square	Std. Error of the Estimate
1	.895[a]	.801	.801	4361.5687221
2	.901[b]	.812	.811	4251.5240030

a. Predictors: (Constant), AVG_PLDST

b. Predictors: (Constant), AVG_PLDST, RWYL

c. Dependent Variable: AVG_GWT

Again, the correlation for takeoff weight estimate was stronger when using average route data, and when using this dataset, the results using GCD or Planned Distance are nearly identical. As before, GCD is selected to remain consistent.

The regression coefficients for GCD and Average/Route data are as follows:

Coefficients[a]

Model		Unstandardized Coefficients		Standardized Coefficients		
		B	Std. Error	Beta	t	Sig.
1	(Constant)	128007.473	1406.541		91.009	.000
	RWYL	.625	.122	.107	5.124	.000
	ELEV	-.094	.155	-.013	-.606	.545
	GCD	14.880	.346	.886	43.015	.000

a. Dependent Variable: AVG_GWT

The resulting B737-800 takeoff weight estimation equation is:

$$GWT = 128007.473 + .625(RUNWAY\ LEN) - .094(ELEV) + 14.880(GCD)$$

(Reference Figures 9 and 10 below)

Testing of the Takeoff Weight Estimation

The resulting takeoff weight regression equations were compared with the ACARS database which has recorded data for 58,206 flights. The resulting data represented 504 flights/routes departing 104 airports.

As seen in the B757 data, there were a number of "tankered" fuel flights that could have potentially influenced the takeoff weight estimation. To resolve the issue, regressions were made using the database with the "tankered" flights removed and the resulting equation tested against the ACARS database. The absolute value of the difference in the estimated weights for the average/route data with both the "untankered" regression and the equation above are plotted in the frequency diagram below.

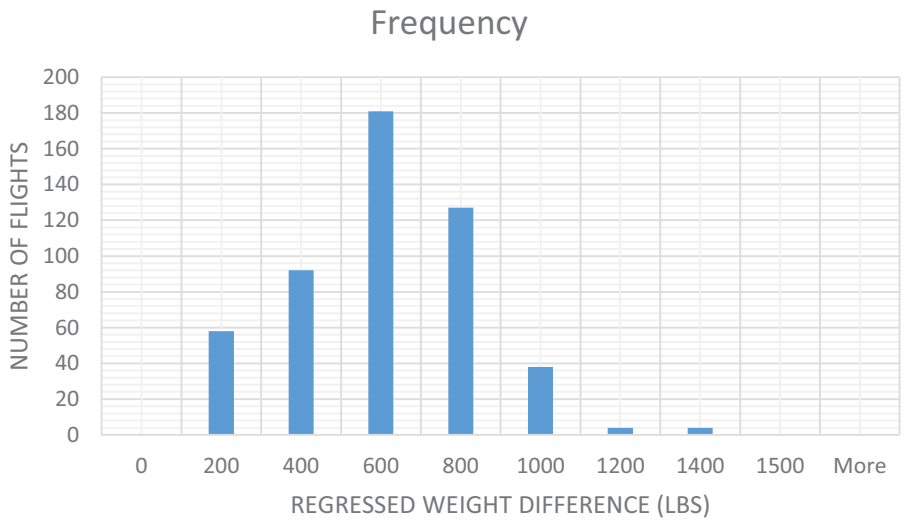

CHART 2

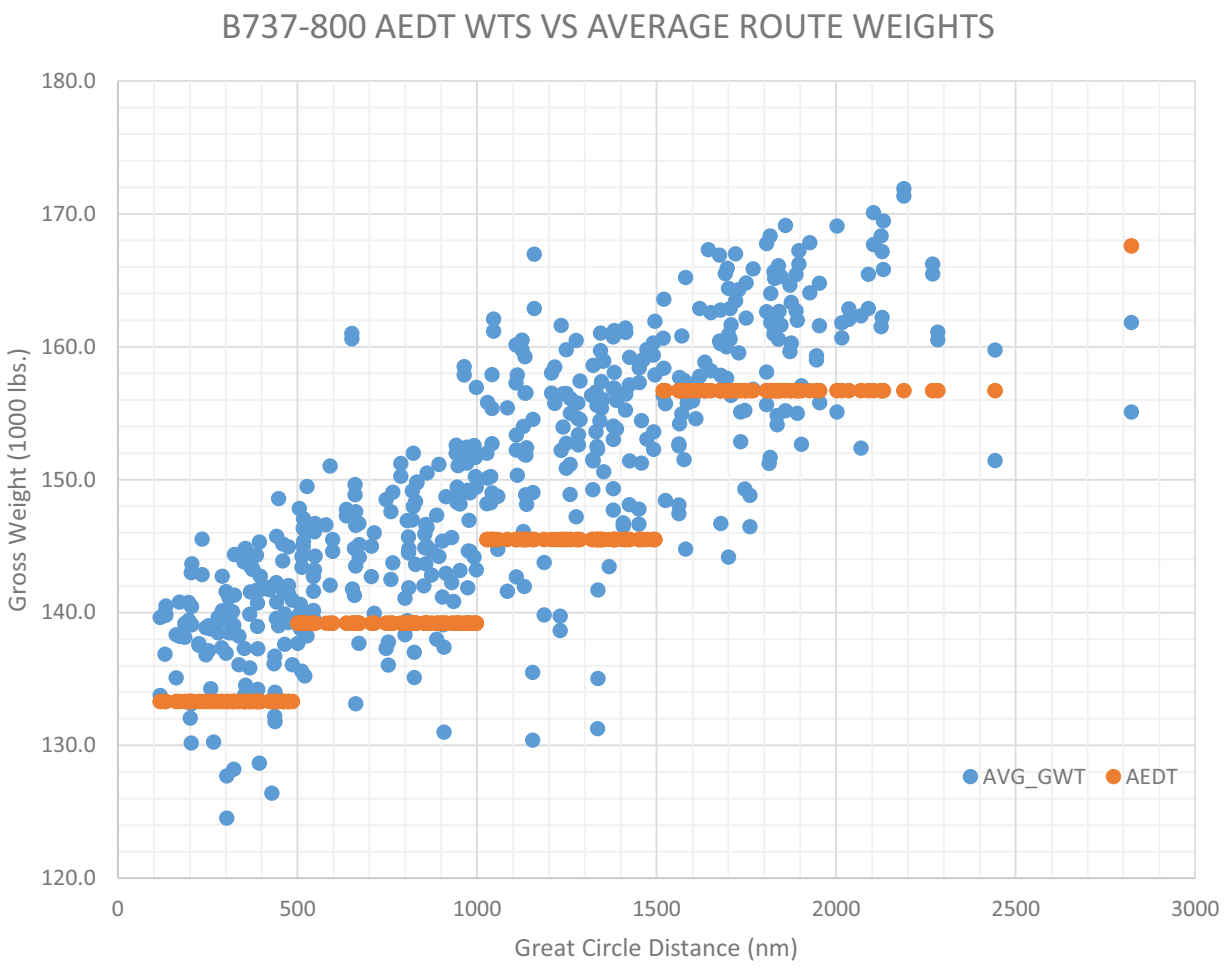
B737-800 AEDT WTS VS AVERAGE ROUTE WEIGHTS
180.0
170.0
160.0
150.0
140.0
130.0
120.0
Gross Weight (1000 lbs.)
0
500
1000
1500
2000
2500
3000
Great Circle Distance (nm)
AVG_GWT
AEDT

FIGURE 8

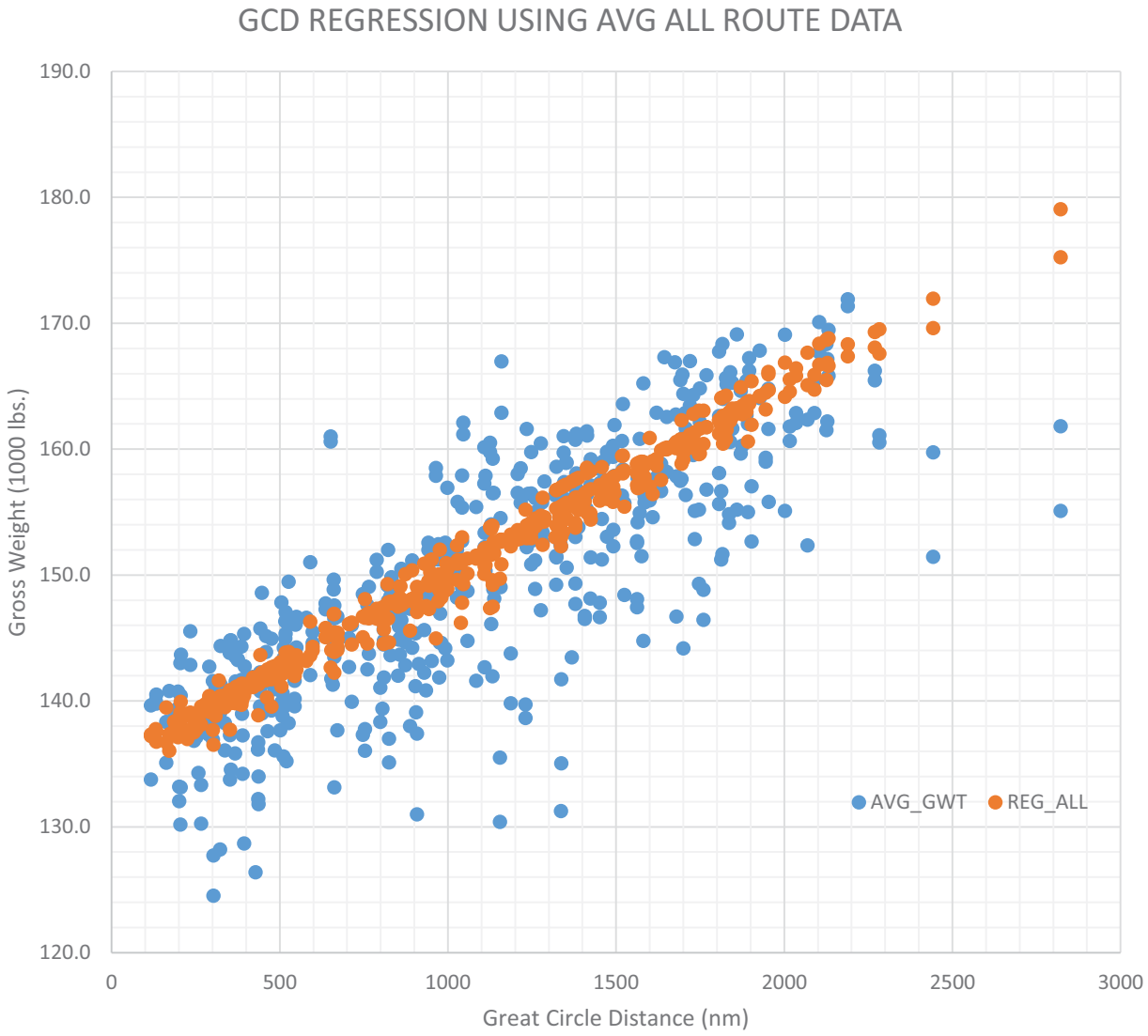

FIGURE 9

Tables 6 through 10 are the tabulated results of comparing the takeoff weight regression with the ACARS database. Shown in the tables are the average route weight, the estimated weight, weight difference and percentage difference of the regressed takeoff weight and the existing AEDT Stage Length Weight.

B737-800 TABULAR RESULTS

APRPTS	AVG_GWT	REG_ALL	REG_DF	%REG_DF	AEDT	AEDT_DF	%AEDT_DF	APRPTS	AVG_GWT	REG_ALL	REG_DF	%REG_DF	AEDT	AEDT_DF	%AEDT_DF
ANCMSP	171.4	168.3	-3025	-1.7%	156.7	-14650	-8.5%	ATLMSY	143.5	141.1	-2388	-1.6%	133.3	-10177	-7.0%
ANCSEA	148.9	154.5	5589	4.3%	145.5	-3398	-1.7%	ATLNCA	157.9	149.9	-7946	-5.0%	139.2	-18689	-11.8%
ANCSLC	165.3	163.2	-2064	-1.2%	156.7	-8586	-5.2%	ATLOMA	146.0	146.2	223	0.4%	139.2	-6800	-4.4%
ANUATL	154.9	157.0	2038	1.8%	156.7	1762	1.6%	ATLORD	149.5	143.4	-6055	-4.0%	139.2	-10280	-6.8%
APAATL	161.2	149.3	-11913	-7.1%	145.5	-15682	-9.4%	ATLPAP	157.9	152.1	-5730	-3.6%	145.5	-12375	-7.8%
APAJFK	148.1	154.9	6768	5.7%	145.5	-2625	-0.7%	ATLPDX	165.4	163.7	-1738	-1.0%	156.7	-8730	-5.2%
ATLANU	160.8	159.0	-1852	-1.0%	156.7	-4113	-2.4%	ATLPHX	160.8	156.1	-4635	-2.8%	145.5	-15253	-9.4%
ATLAPA	162.1	151.2	-10937	-6.5%	145.5	-16600	-10.0%	ATLPTY	161.9	157.8	-4081	-2.4%	145.5	-16425	-10.0%
ATLAUA	159.4	157.8	-1593	-1.0%	145.5	-13878	-8.7%	ATLPUJ	159.8	154.2	-5600	-3.5%	145.5	-14269	-8.9%
ATLAUS	145.0	146.1	1118	1.0%	139.2	-5786	-3.8%	ATLPVR	158.9	155.7	-3212	-1.9%	145.5	-13443	-8.3%
ATLBDA	156.9	150.4	-6487	-4.1%	139.2	-17736	-11.2%	ATLRDU	138.5	140.2	1717	1.5%	133.3	-5180	-3.5%
ATLBDL	137.3	146.7	9406	7.2%	139.2	1892	1.7%	ATLROC	161.0	145.3	-15715	-9.7%	139.2	-21800	-13.5%
ATLBGI	154.1	162.9	8782	6.1%	156.7	2564	2.0%	ATLRSW	148.6	142.2	-6333	-4.2%	133.3	-15283	-10.2%
ATLBHM	139.6	137.3	-2296	-1.6%	133.3	-6335	-4.4%	ATLRTB	157.9	151.1	-6806	-4.3%	145.5	-12409	-7.8%
ATLBNA	139.2	138.4	-813	-0.4%	133.3	-5879	-4.0%	ATLSAL	161.6	154.0	-7640	-4.5%	145.5	-16100	-9.7%
ATLBON	147.4	158.8	11406	8.0%	156.7	9265	6.6%	ATLSAN	167.3	160.1	-7251	-4.3%	156.7	-10613	-6.3%
ATLBOS	152.0	147.8	-4159	-2.7%	139.2	-12789	-8.4%	ATLSAT	147.6	146.9	-693	-0.3%	139.2	-8400	-5.5%
ATLBWI	137.7	143.1	5382	4.2%	139.2	1529	1.4%	ATLSDF	139.6	139.8	129	0.3%	133.3	-6321	-4.3%
ATLBZN	159.2	156.8	-2404	-1.4%	145.5	-13706	-8.5%	ATLSDQ	156.5	153.6	-2961	-1.8%	145.5	-11019	-6.9%
ATLCCS	157.8	160.6	2734	1.9%	156.7	-1148	-0.6%	ATLSEA	167.2	163.8	-3427	-2.0%	156.7	-10538	-6.3%
ATLCHS	137.5	138.9	1407	1.3%	133.3	-4240	-2.8%	ATLSFO	169.1	163.3	-5865	-3.4%	156.7	-12425	-7.3%
ATLCLT	140.8	138.5	-2220	-1.5%	133.3	-7450	-5.2%	ATLSJC	166.1	163.0	-3148	-1.8%	156.7	-9411	-5.6%
ATLCMH	140.7	141.4	668	0.6%	133.3	-7404	-5.1%	ATLSJD	159.8	157.5	-2278	-1.3%	145.5	-14295	-8.8%
ATLCOS	155.8	150.9	-4893	-3.1%	145.5	-10303	-6.5%	ATLSJO	161.1	156.6	-4440	-2.7%	145.5	-15579	-9.6%
ATLCUN	149.1	147.0	-2079	-1.3%	139.2	-9861	-6.5%	ATLSJU	161.0	155.6	-5435	-3.3%	145.5	-15532	-9.6%
ATLCVG	144.4	140.4	-3939	-2.6%	133.3	-11058	-7.6%	ATLSKB	155.7	158.3	2576	2.1%	156.7	986	1.0%
ATLDCA	141.4	142.7	1267	1.0%	133.3	-8100	-5.6%	ATLSLC	161.2	156.2	-5055	-3.0%	145.5	-15718	-9.7%
ATLDEN	155.4	151.1	-4254	-2.7%	145.5	-9857	-6.3%	ATLSLP	160.1	152.1	-8057	-5.0%	145.5	-14643	-9.1%
ATLDFW	147.8	145.1	-2697	-1.8%	139.2	-8560	-5.7%	ATLSMF	164.0	162.7	-1350	-0.8%	156.7	-7300	-4.4%
ATLDSD	158.8	159.9	1075	0.7%	156.7	-2137	-1.3%	ATLSRQ	144.3	141.3	-2980	-1.9%	133.3	-11023	-7.5%
ATLDTW	145.0	143.3	-1681	-1.0%	139.2	-5758	-3.8%	ATLSTL	141.7	141.9	136	0.4%	133.3	-8427	-5.7%
ATLFLL	147.8	143.1	-4716	-3.1%	139.2	-8629	-5.8%	ATLTPA	144.1	140.9	-3290	-2.2%	133.3	-10841	-7.4%
ATLGDL	160.5	154.6	-5885	-3.5%	145.5	-14971	-9.2%	ATLTPP	159.8	172.0	12194	7.7%	156.7	-3057	-1.9%
ATLGSO	130.3	139.6	9307	7.2%	133.3	3050	2.4%	ATLUVF	164.8	161.6	-3193	-1.9%	156.7	-8117	-4.9%
ATLGSP	139.8	137.6	-2212	-1.4%	133.3	-6489	-4.4%	ATLYVR	155.8	164.7	8874	6.3%	156.7	900	1.2%
ATLHSV	136.9	137.5	691	0.7%	133.3	-3557	-2.4%	AUAATL	160.3	155.8	-4462	-2.7%	145.5	-14775	-9.2%
ATLIAD	137.6	142.5	4903	3.8%	133.3	-4300	-2.9%	AUAJFK	157.6	158.8	1219	0.9%	156.7	-930	-0.4%
ATLIND	143.2	141.2	-2057	-1.3%	133.3	-9935	-6.8%	AUSATL	142.7	146.1	3422	2.7%	139.2	-3496	-2.1%
ATLJAX	145.5	139.1	-6445	-4.4%	133.3	-12225	-8.3%	AUSDTW	143.2	150.5	7244	5.5%	139.2	-4019	-2.4%
ATLJFK	149.6	145.4	-4221	-2.7%	139.2	-10440	-6.9%	AUSJFK	149.2	155.3	6046	4.3%	145.5	-3738	-2.2%
ATLLAS	160.7	158.2	-2471	-1.5%	156.7	-3957	-2.4%	BDAATL	149.4	148.9	-546	-0.2%	139.2	-10246	-6.7%
ATLLAX	165.5	160.8	-4732	-2.8%	156.7	-8792	-5.2%	BDABOS	137.7	144.0	6359	4.9%	139.2	1525	1.4%
ATLLGA	146.6	145.4	-1114	-0.7%	139.2	-7363	-4.9%	BDAJFK	133.1	143.9	10773	8.4%	139.2	6074	4.9%
ATLLIR	156.8	156.1	-719	-0.3%	145.5	-11337	-7.0%	BDLATL	148.5	145.1	-3450	-2.2%	139.2	-9300	-6.1%
ATLMBJ	152.4	150.0	-2394	-1.5%	139.2	-13241	-8.6%	BGIATL	154.8	162.2	7353	5.3%	156.7	1867	1.7%
ATLMCO	144.3	140.8	-3429	-2.3%	133.3	-10950	-7.5%	BGIJFK	151.2	161.8	10617	7.8%	156.7	5473	4.4%
ATLMEM	137.3	139.9	2551	2.2%	133.3	-4033	-2.6%	BHMATL	133.8	137.2	3450	2.8%	133.3	-466	-0.1%
ATLMEX	154.5	152.8	-1731	-0.9%	145.5	-9031	-5.6%	BILSLC	136.1	139.5	3414	2.8%	133.3	-2777	-1.8%
ATLMIA	147.1	143.3	-3770	-2.4%	139.2	-7862	-5.2%	BJXLAX	139.8	152.3	12462	9.3%	145.5	5676	4.4%
ATLMSO	157.7	158.9	1179	0.9%	156.7	-992	-0.5%	BNAATL	138.1	137.6	-514	-0.1%	133.3	-4827	-3.2%
ATLMSP	151.2	147.3	-3891	-2.4%	139.2	-12015	-7.8%	BNADTW	141.7	140.7	-991	-0.5%	133.3	-8428	-5.8%

TABLE 6

B737-800 TABULAR RESULTS

APRPTS	AVG_GWT	REG_ALL	REG_DF	%REG_DF	AEDT	AEDT_DF	%AEDT_DF	APRPTS	AVG_GWT	REG_ALL	REG_DF	%REG_DF	AEDT	AEDT_DF	%AEDT_DF
BNALAX	152.5	158.1	5550	3.9%	156.7	4163	3.0%	DFWATL	147.3	145.8	-1488	-0.9%	139.2	-8077	-5.4%
BOIMSP	144.2	148.7	4572	3.4%	139.2	-4976	-3.2%	DFWDTW	146.6	149.1	2456	1.9%	139.2	-7422	-4.8%
BOISLC	137.1	137.7	609	0.7%	133.3	-3828	-2.5%	DFWSLC	145.0	149.1	4089	3.1%	139.2	-5819	-3.7%
BONATL	148.1	157.2	9059	6.7%	156.7	8605	6.4%	DSDATL	156.7	157.6	894	0.6%	156.7	33	0.1%
BOSATL	148.0	146.5	-1434	-0.8%	139.2	-8773	-5.7%	DSDJFK	155.9	157.1	1127	1.2%	156.7	772	1.0%
BOSBDA	146.7	144.3	-2408	-1.5%	139.2	-7500	-5.0%	DTWATL	146.3	143.1	-3203	-2.1%	139.2	-7130	-4.7%
BOSCVG	141.8	144.0	2261	1.8%	139.2	-2563	-1.6%	DTWBNA	142.7	141.3	-1396	-0.8%	133.3	-9437	-6.5%
BOSDTW	144.2	142.5	-1772	-1.0%	139.2	-5048	-3.3%	DTWBOS	146.7	143.6	-3072	-2.0%	139.2	-7490	-5.0%
BOSJFK	138.3	136.7	-1615	-0.8%	133.3	-5033	-3.3%	DTWBWI	134.5	140.7	6188	5.0%	133.3	-1243	-0.5%
BOSLAS	162.3	165.1	2761	2.1%	156.7	-5633	-3.1%	DTWCUN	154.6	154.5	-122	0.0%	145.5	-9117	-5.8%
BOSLAX	166.2	168.1	1840	1.3%	156.7	-9531	-5.6%	DTWDCA	133.8	140.7	6932	5.6%	133.3	-454	0.1%
BOSMCO	141.9	148.8	6927	5.2%	139.2	-2673	-1.6%	DTWDEN	152.0	150.0	-2001	-1.1%	139.2	-12773	-8.2%
BOSMSP	146.9	148.8	1913	1.7%	139.2	-7732	-4.9%	DTWDFW	143.7	148.2	4534	3.3%	139.2	-4467	-3.0%
BOSSLC	165.1	161.5	-3609	-2.1%	156.7	-8432	-5.0%	DTWFLL	144.6	150.0	5425	4.1%	139.2	-5406	-3.4%
BWIATL	139.3	142.0	2719	2.2%	139.2	-93	0.2%	DTWIND	132.0	138.4	6392	5.4%	133.3	1252	1.5%
BWIDTW	144.8	139.8	-4985	-3.3%	133.3	-11525	-7.8%	DTWJFK	140.8	142.0	1248	1.1%	133.3	-7478	-5.1%
BWISLC	162.9	158.7	-4226	-2.5%	156.7	-6189	-3.7%	DTWLAS	163.6	158.1	-5509	-3.3%	156.7	-6876	-4.2%
BZELAX	155.0	160.6	5596	4.0%	156.7	1700	1.4%	DTWLAX	167.0	161.0	-5958	-3.5%	156.7	-10300	-6.1%
BZNATL	151.4	154.4	3001	2.1%	145.5	-5912	-3.8%	DTWLGA	132.2	141.9	9736	7.8%	133.3	1100	1.3%
BZNSLC	136.9	137.7	756	0.7%	133.3	-3632	-2.5%	DTWMCO	149.8	147.8	-1921	-1.2%	139.2	-10550	-6.9%
CCSATL	146.7	160.1	13453	9.6%	156.7	10008	7.3%	DTWMEX	165.2	159.0	-6248	-3.6%	156.7	-8522	-5.0%
CHSATL	137.7	137.0	-676	-0.3%	133.3	-4353	-3.0%	DTWMIA	150.2	150.3	26	0.2%	139.2	-11028	-7.2%
CLTATL	139.4	137.1	-2298	-1.5%	133.3	-6117	-4.3%	DTWMKE	139.1	138.5	-555	-0.4%	133.3	-5769	-4.1%
CMHATL	139.0	140.0	1057	1.0%	133.3	-5668	-3.9%	DTWMSP	145.2	142.3	-2879	-1.9%	133.3	-11858	-8.1%
CMHLAX	155.1	160.1	4958	3.4%	156.7	1605	1.3%	DTWMSY	139.4	147.4	8038	6.4%	139.2	-189	0.5%
CMHMSP	140.2	142.3	2185	1.8%	139.2	-961	-0.5%	DTWORD	130.2	138.5	8302	7.1%	133.3	3118	3.0%
COSATL	150.1	151.2	1064	0.8%	145.5	-4611	-3.0%	DTWPDX	165.9	160.7	-5221	-3.1%	156.7	-9221	-5.5%
CUNATL	143.7	146.6	2811	2.4%	139.2	-4545	-2.8%	DTWPHL	128.7	141.3	12645	10.4%	133.3	4633	4.2%
CUNCVG	141.6	151.3	9712	7.5%	145.5	3900	3.4%	DTWPHX	158.4	157.1	-1357	-0.8%	145.5	-12912	-8.1%
CUNDTW	155.8	154.2	-1561	-1.0%	145.5	-10275	-6.6%	DTWPVR	160.6	160.7	145	0.5%	156.7	-3900	-2.0%
CUNLAX	162.7	162.6	-89	0.0%	156.7	-5959	-3.6%	DTWRDU	136.1	141.9	5788	4.5%	133.3	-2833	-1.8%
CUNMSP	159.0	156.9	-2092	-1.2%	145.5	-13527	-8.4%	DTWRSW	152.6	149.5	-3113	-1.9%	139.2	-13379	-8.6%
CVGATL	141.3	140.2	-1057	-0.6%	133.3	-8002	-5.5%	DTWSAN	164.4	160.7	-3642	-2.2%	156.7	-7687	-4.6%
CVGCUN	155.4	151.6	-3847	-2.4%	145.5	-9900	-6.3%	DTWSEA	166.9	160.4	-6535	-3.9%	156.7	-10208	-6.1%
CVGFLL	141.9	147.5	5609	4.3%	139.2	-2667	-1.5%	DTWSFO	167.8	162.3	-5445	-3.1%	156.7	-11067	-6.5%
CVGLAS	154.5	157.1	2666	2.2%	145.5	-8952	-5.4%	DTWSLC	157.4	154.6	-2826	-1.7%	145.5	-11925	-7.5%
CVGLAX	162.6	160.0	-2568	-1.4%	156.7	-5858	-3.5%	DTWTPA	145.9	148.2	2245	1.8%	139.2	-6711	-4.4%
CVGMCO	144.8	145.2	385	0.4%	139.2	-5629	-3.7%	DTWYVR	162.9	160.8	-2056	-1.2%	156.7	-6175	-3.7%
CVGSEA	161.6	160.8	-823	-0.3%	156.7	-4946	-2.8%	FLLATL	139.9	141.1	1271	1.4%	139.2	-675	0.0%
CVGSFO	165.9	161.7	-4129	-2.5%	156.7	-9175	-5.5%	FLLCVG	144.8	145.7	876	0.9%	139.2	-5608	-3.6%
CVGSLC	156.1	154.2	-1919	-1.0%	145.5	-10591	-6.5%	FLLDTW	149.0	148.2	-786	-0.3%	139.2	-9800	-6.4%
CVGTPA	144.2	145.4	1249	1.1%	139.2	-4974	-3.3%	FLLJFK	142.2	147.5	5211	4.1%	139.2	-3044	-1.7%
CZMMSP	153.6	156.6	2960	2.2%	145.5	-8100	-5.0%	FLLLGA	140.8	147.5	6711	5.2%	139.2	-1633	-0.7%
DCAATL	142.0	139.6	-2485	-1.5%	133.3	-8740	-5.9%	FSDMSP	138.2	136.0	-2158	-1.5%	133.3	-4900	-3.5%
DCADTW	137.3	137.7	439	0.7%	133.3	-3986	-2.6%	GCMJFK	131.3	152.3	21025	16.4%	145.5	14250	11.2%
DCAMSP	145.7	144.5	-1164	-0.6%	139.2	-6490	-4.2%	GDLATL	147.2	154.7	7525	5.7%	145.5	-1700	-0.6%
DCASLC	157.3	156.4	-871	-0.5%	156.7	-600	-0.3%	GDLLAX	151.9	152.6	790	0.7%	145.5	-6352	-4.0%
DENATL	152.7	153.0	295	0.2%	145.5	-7207	-4.7%	GEGSLC	139.3	141.7	2478	2.0%	133.3	-5950	-4.1%
DENDTW	144.6	152.0	7392	5.6%	139.2	-5428	-3.3%	GNDJFK	161.0	160.8	-146	0.2%	156.7	-4260	-2.4%
DENJFK	155.2	158.5	3283	2.2%	145.5	-9739	-6.2%	GSOATL	133.3	138.1	4796	3.8%	133.3	-33	0.2%
DENMSP	142.1	146.3	4237	3.2%	139.2	-2854	-1.8%	GSPATL	140.5	136.8	-3728	-2.6%	133.3	-7200	-5.0%

TABLE 7

B737-800 TABULAR RESULTS

APRPTS	AVG_GWT	REG_ALL	REG_DF	%REG_DF	AEDT	AEDT_DF	%AEDT_DF		APRPTS	AVG_GWT	REG_ALL	REG_DF	%REG_DF	AEDT	AEDT_DF	%AEDT_DF
HSVATL	140.0	137.8	-2227	-1.6%	133.3	-6700	-4.8%		LASDTW	158.4	159.5	1109	0.8%	156.7	-1681	-1.0%
IADATL	139.9	142.1	2176	1.8%	133.3	-6594	-4.5%		LASJFK	161.6	165.9	4338	2.8%	156.7	-4895	-2.9%
INDATL	143.3	140.5	-2800	-1.9%	133.3	-10013	-6.9%		LASLAX	140.4	139.9	-522	-0.1%	133.3	-7144	-4.8%
INDDTW	133.2	137.9	4747	4.2%	133.3	124	0.7%		LASMEM	139.7	155.2	15468	12.1%	145.5	5778	5.1%
INDLAX	157.5	158.4	911	0.9%	156.7	-772	-0.2%		LASMSP	146.1	153.7	7565	5.5%	145.5	-607	-0.2%
INDMSP	131.8	141.4	9635	7.5%	133.3	1500	1.3%		LASRDU	148.8	163.1	14243	10.1%	156.7	7882	5.8%
JAXATL	142.9	137.7	-5117	-3.5%	133.3	-9554	-6.6%		LASSEA	137.8	148.1	10311	8.0%	139.2	1434	1.5%
JFKAPA	157.1	158.3	1140	0.9%	145.5	-11625	-7.2%		LASSLC	140.1	141.6	1569	1.4%	133.3	-6751	-4.5%
JFKATL	148.9	146.9	-1960	-1.1%	139.2	-9657	-6.3%		LAXATL	157.5	160.7	3239	2.3%	156.7	-775	-0.3%
JFKAUA	160.0	162.3	2303	1.6%	156.7	-3294	-1.9%		LAXBJX	143.8	153.2	9440	7.0%	145.5	1725	1.6%
JFKAUS	151.5	156.7	5230	3.7%	145.5	-6017	-3.7%		LAXBNA	152.7	158.8	6107	4.2%	156.7	4011	2.9%
JFKBDA	143.5	146.9	3431	2.6%	139.2	-4296	-2.8%		LAXBOS	165.5	169.3	3846	2.4%	156.7	-8769	-5.2%
JFKBGI	156.7	164.1	7386	4.9%	156.7	33	0.2%		LAXBZE	162.0	163.7	1706	1.2%	156.7	-5300	-3.1%
JFKBOS	135.1	139.5	4395	3.6%	133.3	-1791	-1.0%		LAXCMH	152.9	161.4	8496	5.8%	156.7	3841	2.7%
JFKDEN	161.4	158.1	-3324	-2.0%	145.5	-15925	-9.8%		LAXCUN	161.7	162.9	1243	0.8%	156.7	-5004	-3.0%
JFKDSD	156.2	160.9	4707	3.3%	156.7	524	0.6%		LAXCVG	158.2	160.1	1923	1.3%	156.7	-1497	-0.8%
JFKDTW	145.7	143.7	-2087	-1.3%	133.3	-12439	-8.4%		LAXDTW	163.5	161.1	-2314	-1.3%	156.7	-6760	-4.1%
JFKFLL	145.6	150.9	5262	4.0%	139.2	-6437	-4.0%		LAXGDL	156.5	152.5	-4070	-2.6%	145.5	-11026	-7.0%
JFKGCM	152.3	157.0	4683	3.4%	145.5	-6773	-4.2%		LAXIND	151.5	159.0	7497	5.3%	156.7	5193	3.8%
JFKGND	165.7	164.3	-1391	-0.6%	156.7	-8952	-5.2%		LAXLAS	133.1	138.6	5457	4.7%	133.3	154	0.7%
JFKKIN	143.5	157.4	13977	10.5%	145.5	2045	2.2%		LAXLIR	161.1	169.5	8424	5.5%	156.7	-4400	-2.4%
JFKLAS	164.8	166.1	1346	1.0%	156.7	-8090	-4.8%		LAXMCO	164.1	164.2	168	0.2%	156.7	-7358	-4.4%
JFKLIR	157.1	165.4	8330	5.9%	156.7	-363	0.4%		LAXMEM	146.8	156.5	9737	7.2%	145.5	-1252	-0.4%
JFKMBJ	155.9	157.0	1159	0.9%	145.5	-10385	-6.5%		LAXMIA	162.9	165.8	2966	2.0%	156.7	-6167	-3.6%
JFKMCO	149.2	149.3	124	0.2%	139.2	-9953	-6.5%		LAXMPR	150.2	151.0	766	0.6%	145.5	-4732	-3.1%
JFKMEX	168.3	164.1	-4250	-2.4%	156.7	-11648	-6.8%		LAXMSP	152.5	155.4	2915	2.3%	145.5	-6988	-4.2%
JFKMIA	151.1	151.2	113	0.3%	139.2	-11854	-7.6%		LAXMSY	146.7	157.1	10485	7.7%	145.5	-1158	-0.3%
JFKMSP	151.2	150.4	-777	-0.4%	139.2	-11956	-7.8%		LAXMZT	137.4	149.1	11667	9.1%	139.2	1803	1.9%
JFKMSY	152.0	152.4	357	0.6%	145.5	-6500	-3.9%		LAXPHX	128.2	140.3	12144	10.0%	133.3	5100	4.4%
JFKNAS	148.2	151.2	3088	2.4%	139.2	-8954	-5.8%		LAXPVR	148.7	151.3	2559	2.0%	145.5	-3236	-1.9%
JFKNCA	159.8	153.8	-5946	-3.6%	145.5	-14261	-8.9%		LAXRDU	159.0	164.5	5483	3.6%	156.7	-2311	-1.3%
JFKPAP	158.6	156.8	-1847	-1.0%	145.5	-13109	-8.1%		LAXSAL	161.8	165.6	3748	2.7%	156.7	-5102	-2.8%
JFKPDX	169.5	168.8	-665	-0.3%	156.7	-12764	-7.5%		LAXSEA	143.6	147.9	4258	3.3%	139.2	-4430	-2.8%
JFKPHX	164.6	164.9	283	0.3%	156.7	-7934	-4.7%		LAXSLC	143.4	143.2	-231	0.0%	139.2	-4202	-2.8%
JFKPLS	151.9	153.9	1992	1.6%	145.5	-6428	-3.9%		LAXSLP	167.0	152.8	-14161	-8.2%	145.5	-21459	-12.6%
JFKPUJ	158.9	157.2	-1750	-1.0%	145.5	-13414	-8.4%		LAXTPA	160.3	163.5	3177	2.1%	156.7	-3576	-2.1%
JFKPVR	169.1	166.9	-2226	-1.3%	156.7	-12391	-7.3%		LAXZIH	141.7	155.4	13739	10.4%	145.5	3792	3.4%
JFKSAN	168.3	168.7	351	0.3%	156.7	-11644	-6.8%		LAXZLO	135.5	152.7	17239	13.7%	145.5	10000	8.3%
JFKSAT	149.3	157.6	8273	5.9%	145.5	-3823	-2.2%		LGAATL	147.6	142.2	-5349	-3.4%	139.2	-8382	-5.5%
JFKSDQ	157.4	157.1	-279	0.1%	145.5	-11884	-7.3%		LGADTW	136.7	138.9	2158	1.9%	133.3	-3412	-2.2%
JFKSEA	170.1	168.4	-1710	-0.9%	156.7	-13393	-7.8%		LGAMCO	135.1	144.7	9547	7.5%	139.2	4089	3.4%
JFKSJU	155.9	157.7	1784	1.4%	145.5	-10445	-6.4%		LGAMSP	138.0	145.6	7581	5.5%	139.2	1200	0.9%
JFKSLC	164.3	162.8	-1488	-0.8%	156.7	-7591	-4.5%		LGANCA	156.5	149.2	-7258	-4.6%	145.5	-11000	-7.0%
JFKSTI	153.4	156.2	2778	2.2%	145.5	-7874	-4.7%		LIRATL	154.0	154.1	106	0.4%	145.5	-8536	-5.2%
JFKTPA	144.7	150.1	5399	4.0%	139.2	-5467	-3.6%		LIRJFK	152.7	161.9	9278	6.8%	156.7	4033	3.3%
JFKTPP	161.8	179.1	17236	10.7%	167.6	5769	3.6%		LIRLAX	160.5	167.6	7074	4.7%	156.7	-3822	-2.1%
JFKUVF	155.2	163.1	7856	5.5%	156.7	1500	1.4%		LIRMSP	162.9	164.7	1845	1.6%	156.7	-6175	-3.3%
JFKYVR	167.2	168.7	1588	1.0%	156.7	-10452	-6.2%		MBJATL	151.2	147.9	-3327	-2.1%	139.2	-12042	-7.9%
LASATL	156.3	159.5	3146	2.2%	156.7	386	0.5%		MBJJFK	154.4	153.4	-981	-0.4%	145.5	-8916	-5.6%
LASBOS	152.4	167.7	15297	10.4%	156.7	4338	3.1%		MCISLC	138.3	146.6	8217	6.3%	139.2	867	1.0%
LASCVG	151.2	158.6	7326	5.2%	145.5	-5741	-3.5%		MCOATL	143.8	140.7	-3094	-2.1%	133.3	-10518	-7.3%

TABLE 8

B737-800 TABULAR RESULTS

APRPTS	AVG_GWT	REG_ALL	REG_DF	%REG_DF	AEDT	AEDT_DF	%AEDT_DF	APRPTS	AVG_GWT	REG_ALL	REG_DF	%REG_DF	AEDT	AEDT_DF	%AEDT_DF
MCOBOS	149.2	150.0	795	0.6%	139.2	-10000	-6.6%	MSPSEA	158.5	152.9	-5582	-3.4%	145.5	-12984	-8.1%
MCOCVG	141.3	145.3	3993	3.1%	139.2	-2100	-1.2%	MSPSFO	156.9	155.4	-1518	-0.8%	145.5	-11375	-7.1%
MCODTW	149.8	147.9	-1952	-1.2%	139.2	-10633	-7.0%	MSPSLC	150.5	147.6	-2868	-1.8%	139.2	-11287	-7.4%
MCOJFK	147.0	147.7	731	0.7%	139.2	-7773	-5.1%	MSPSTL	137.3	140.6	3332	2.8%	133.3	-3963	-2.6%
MCOLAX	167.8	164.2	-3648	-2.1%	156.7	-11124	-6.6%	MSPTPA	148.9	151.7	2821	2.1%	145.5	-3375	-2.1%
MCOLGA	137.0	147.8	10778	8.3%	139.2	2200	2.0%	MSPYVR	152.7	153.4	654	0.5%	145.5	-7223	-4.7%
MCOMSP	152.4	152.4	40	0.1%	145.5	-6895	-4.4%	MSYATL	141.6	139.8	-1743	-1.0%	133.3	-8256	-5.6%
MCOSLC	162.8	160.5	-2280	-1.3%	156.7	-6050	-3.6%	MSYDTW	146.9	146.3	-616	-0.3%	139.2	-7717	-5.2%
MDWMSP	124.5	136.5	11996	9.9%	133.3	8762	7.3%	MSYJFK	148.2	149.6	1404	1.1%	145.5	-2700	-1.6%
MEMATL	139.5	139.2	-267	0.0%	133.3	-6178	-4.2%	MSYLAX	147.8	155.9	8121	6.1%	145.5	-2292	-1.0%
MEMLAS	138.6	153.2	14596	11.2%	145.5	6853	5.6%	MSYMSP	145.4	147.8	2392	1.9%	139.2	-6167	-4.0%
MEMLAX	146.5	155.9	9353	6.7%	145.5	-1009	-0.4%	MZTLAX	131.0	147.1	16051	12.9%	139.2	8200	6.9%
MEXATL	149.0	152.6	3603	2.6%	145.5	-3541	-2.2%	NASJFK	143.2	149.3	6101	4.5%	139.2	-3967	-2.5%
MEXDTW	144.8	159.0	14190	10.1%	156.7	11922	8.5%	NCAATL	158.5	145.0	-13529	-8.4%	139.2	-19300	-12.1%
MEXJFK	151.7	162.5	10798	7.1%	156.7	5033	3.3%	NCAJFK	160.5	147.4	-13133	-8.1%	145.5	-15000	-9.2%
MIAATL	145.4	143.8	-1519	-0.9%	139.2	-6154	-4.1%	NCALGA	159.3	147.5	-11764	-7.3%	145.5	-13750	-8.6%
MIADTW	151.7	150.9	-738	-0.3%	139.2	-12486	-8.1%	OAKSLC	135.6	142.2	6597	5.1%	139.2	3612	2.9%
MIAJFK	148.8	150.2	1429	1.2%	139.2	-9604	-6.2%	OMAATL	139.9	144.5	4541	3.4%	139.2	-738	-0.4%
MIALAX	162.1	166.4	4348	2.9%	156.7	-5375	-3.1%	OMAMSP	136.8	137.5	678	0.7%	133.3	-3521	-2.4%
MKEDTW	143.7	137.2	-6430	-4.1%	133.3	-10379	-6.9%	ONTSLC	136.1	142.8	6687	5.1%	133.3	-2771	-1.8%
MKEMSP	138.8	138.0	-743	-0.4%	133.3	-5466	-3.8%	ORDATL	138.2	143.9	5657	4.3%	139.2	960	0.9%
MPRLAX	148.3	146.2	-2046	-1.3%	145.5	-2750	-1.8%	ORDDTW	143.0	139.1	-3895	-2.7%	133.3	-9700	-6.7%
MSOATL	154.2	156.9	2717	1.8%	156.7	2500	1.7%	ORDMSP	140.1	140.4	260	0.5%	133.3	-6825	-4.6%
MSPANC	171.9	167.4	-4525	-2.6%	156.7	-15205	-8.8%	PAPATL	150.3	150.8	444	0.5%	145.5	-4833	-3.0%
MSPATL	150.3	146.5	-3735	-2.4%	139.2	-11067	-7.3%	PAPJFK	151.4	153.9	2507	2.0%	145.5	-5911	-3.5%
MSPAUS	139.1	148.3	9185	6.8%	139.2	112	0.3%	PDXATL	162.7	163.0	264	0.2%	156.7	-6009	-3.6%
MSPBOI	152.6	149.6	-3003	-1.8%	139.2	-13371	-8.6%	PDXDTW	160.4	160.1	-310	-0.1%	156.7	-3741	-2.2%
MSPBOS	151.7	149.3	-2338	-1.4%	139.2	-12483	-8.1%	PDXJFK	165.8	166.6	780	0.5%	156.7	-9124	-5.4%
MSPCMH	139.6	142.9	3319	2.5%	139.2	-383	-0.1%	PDXMSP	154.0	153.3	-637	-0.2%	145.5	-8453	-5.3%
MSPCUN	159.0	156.6	-2453	-1.5%	145.5	-13515	-8.5%	PDXSLC	143.2	143.0	-192	0.1%	139.2	-4011	-2.6%
MSPCZM	152.3	157.0	4723	3.6%	145.5	-6786	-4.0%	PHLATL	146.6	143.2	-3414	-2.3%	139.2	-7400	-5.0%
MSPDCA	144.5	146.8	2360	1.9%	139.2	-5285	-3.4%	PHLDTW	145.3	140.4	-4877	-3.2%	133.3	-12010	-8.1%
MSPDEN	151.0	143.6	-7416	-4.8%	139.2	-11817	-7.7%	PHXATL	153.0	155.6	2590	2.0%	145.5	-7511	-4.6%
MSPDTW	143.9	141.6	-2246	-1.4%	133.3	-10583	-7.2%	PHXDTW	157.3	156.7	-619	-0.3%	145.5	-11807	-7.4%
MSPFSD	140.8	137.4	-3434	-2.3%	133.3	-7486	-5.1%	PHXJFK	159.6	162.9	3282	2.3%	156.7	-2940	-1.6%
MSPIND	134.0	141.3	7310	5.7%	133.3	-700	-0.3%	PHXLAX	139.0	139.9	827	0.8%	133.3	-5745	-3.9%
MSPJFK	144.2	148.1	3888	3.0%	139.2	-5022	-3.2%	PHXMSP	152.2	151.6	-639	-0.3%	145.5	-6722	-4.3%
MSPLAS	154.0	151.6	-2410	-1.5%	145.5	-8516	-5.5%	PHXSLC	142.3	141.6	-618	-0.3%	133.3	-8962	-6.2%
MSPLAX	155.6	154.7	-939	-0.5%	145.5	-10096	-6.4%	PLSJFK	142.0	149.6	7646	5.9%	145.5	3547	3.0%
MSPLGA	147.3	148.0	672	0.6%	139.2	-8133	-5.4%	PTYATL	157.9	156.5	-1395	-0.7%	145.5	-12389	-7.7%
MSPLIR	165.4	165.9	462	0.6%	156.7	-8744	-5.0%	PUJATL	156.5	152.9	-3549	-2.2%	145.5	-10980	-7.0%
MSPMCO	148.1	151.7	3598	2.5%	145.5	-2643	-1.8%	PUJJFK	156.0	154.4	-1582	-0.8%	145.5	-10531	-6.6%
MSPMDW	127.7	139.3	11602	9.3%	133.3	5586	4.6%	PVRATL	150.6	154.5	3895	2.9%	145.5	-5100	-3.1%
MSPMKE	134.3	138.6	4374	3.6%	133.3	-972	-0.4%	PVRDTW	144.2	159.7	15482	11.3%	156.7	12524	9.2%
MSPMSY	141.2	148.2	7066	5.5%	139.2	-1978	-1.0%	PVRJFK	155.1	164.2	9052	6.4%	156.7	1600	1.6%
MSPOMA	138.9	138.5	-402	-0.2%	133.3	-5555	-3.9%	PVRLAX	144.8	150.1	5342	4.2%	145.5	737	1.0%
MSPORD	142.7	139.1	-3611	-2.4%	133.3	-9433	-6.5%	PVRSEA	158.1	161.2	3135	2.1%	156.7	-1400	-0.7%
MSPPDX	156.5	153.2	-3222	-1.9%	145.5	-10965	-6.8%	RDUATL	141.1	138.8	-2301	-1.5%	133.3	-7816	-5.4%
MSPPHX	153.4	151.3	-2050	-1.3%	145.5	-7859	-5.0%	RDULAS	146.5	160.4	13954	9.9%	156.7	10248	7.4%
MSPRDU	142.0	147.5	5485	4.1%	139.2	-2800	-1.8%	RDULAX	159.3	163.2	3847	2.7%	156.7	-2611	-1.3%
MSPSAN	156.6	154.6	-1990	-1.2%	145.5	-11103	-7.0%	RDUMSP	142.7	150.7	8034	5.9%	145.5	2816	2.2%

TABLE 9

B737-800 TABULAR RESULTS

APRPTS	AVG_GWT	REG_ALL	REG_DF	%REG_DF	AEDT	AEDT_DF	%AEDT_DF	APRPTS	AVG_GWT	REG_ALL	REG_DF	%REG_DF	AEDT	AEDT_DF	%AEDT_DF
RDUSLC	155.8	157.8	2032	1.6%	156.7	931	0.9%	SLCDCA	154.6	159.1	4468	3.0%	156.7	2114	1.5%
RNOSLC	135.8	139.9	4108	3.2%	133.3	-2521	-1.7%	SLCDFW	146.5	147.9	1424	1.2%	139.2	-7269	-4.8%
ROCATL	160.6	142.6	-17957	-11.1%	139.2	-21400	-13.2%	SLCDTW	154.5	154.3	-260	-0.1%	145.5	-9022	-5.7%
RSWATL	139.0	142.2	3156	2.5%	133.3	-5700	-3.9%	SLCGEG	144.9	142.2	-2754	-1.8%	133.3	-11633	-7.9%
RSWDTW	152.0	149.5	-2478	-1.6%	139.2	-12800	-8.3%	SLCJFK	159.5	160.8	1309	1.0%	156.7	-2830	-1.6%
RTBATL	149.0	147.8	-1203	-0.7%	145.5	-3500	-2.3%	SLCLAS	138.5	139.9	1371	1.2%	133.3	-5187	-3.5%
SALATL	152.2	152.9	722	1.1%	145.5	-6700	-3.8%	SLCLAX	144.2	142.7	-1492	-0.9%	139.2	-5022	-3.3%
SALLAX	160.7	164.6	3898	2.8%	156.7	-3960	-2.1%	SLCMCI	141.1	147.0	5938	4.4%	139.2	-1863	-1.1%
SANDTW	160.9	159.2	-1742	-1.0%	156.7	-4219	-2.6%	SLCMCO	160.2	160.1	-168	-0.1%	156.7	-3548	-2.2%
SANJFK	161.5	165.5	3994	2.6%	156.7	-4807	-2.9%	SLCMSP	146.4	147.9	1511	1.4%	139.2	-7212	-4.6%
SANMSP	153.6	153.7	92	0.2%	145.5	-8094	-5.2%	SLCOAK	139.5	142.7	3245	2.6%	139.2	-270	0.1%
SANSEA	142.9	147.5	4529	3.4%	139.2	-3738	-2.4%	SLCONT	140.9	142.3	1405	1.3%	133.3	-7623	-5.1%
SANSLC	141.6	142.0	370	0.5%	139.2	-2406	-1.5%	SLCPDX	146.1	143.3	-2818	-1.8%	139.2	-6869	-4.6%
SATATL	142.5	144.6	2056	1.6%	139.2	-3300	-2.2%	SLCPHX	139.6	141.7	2111	1.7%	133.3	-6262	-4.3%
SATJFK	147.7	153.8	6066	4.4%	145.5	-2201	-1.2%	SLCRDU	156.3	158.7	2396	1.6%	156.7	400	0.3%
SATSLC	148.3	147.3	-992	-0.4%	139.2	-9086	-5.9%	SLCRNO	139.9	140.6	704	0.6%	133.3	-6568	-4.6%
SDFATL	138.5	139.5	1075	1.0%	133.3	-5167	-3.5%	SLCSAN	142.7	143.2	500	0.6%	139.2	-3506	-2.2%
SDQATL	158.0	152.8	-5182	-3.2%	145.5	-12519	-7.8%	SLCSAT	149.4	149.2	-286	0.0%	139.2	-10244	-6.7%
SDQJFK	155.4	154.9	-463	0.2%	145.5	-9869	-5.8%	SLCSEA	145.5	144.0	-1476	-0.7%	139.2	-6286	-4.1%
SEAANC	151.2	154.1	2983	2.4%	145.5	-5656	-3.4%	SLCSFO	140.0	142.8	2800	2.4%	139.2	-849	-0.2%
SEAATL	166.2	163.6	-2603	-1.5%	156.7	-9520	-5.7%	SLCSJC	140.6	142.7	2046	1.8%	139.2	-1425	-0.7%
SEACVG	156.3	160.8	4456	3.1%	156.7	351	0.4%	SLCSMF	141.5	142.0	445	0.3%	133.3	-8241	-5.8%
SEADTW	160.4	160.3	-111	0.0%	156.7	-3740	-2.2%	SLPATL	157.3	150.1	-7178	-4.5%	145.5	-11773	-7.4%
SEAJFK	167.7	166.7	-983	-0.5%	156.7	-10996	-6.5%	SLPLAX	162.9	150.9	-12029	-7.1%	145.5	-17382	-10.4%
SEALAS	136.0	146.6	10571	8.4%	139.2	3161	2.9%	SMFATL	161.8	160.4	-1383	-0.8%	156.7	-5118	-3.1%
SEALAX	148.4	147.7	-619	-0.2%	139.2	-9159	-5.9%	SMFMSP	156.3	153.0	-3324	-2.1%	145.5	-10833	-6.9%
SEAMSP	155.7	153.5	-2240	-1.3%	145.5	-10239	-6.5%	SMFSLC	141.8	140.3	-1586	-1.1%	133.3	-8544	-6.0%
SEAPVR	155.6	162.3	6642	4.7%	156.7	1064	1.1%	SRQATL	141.7	139.7	-1992	-1.3%	133.3	-8377	-5.8%
SEASAN	148.7	149.0	267	0.4%	139.2	-9523	-6.2%	STIJFK	152.6	152.4	-215	0.4%	145.5	-7117	-4.1%
SEASLC	144.6	144.3	-306	0.0%	139.2	-5409	-3.5%	STLATL	141.9	141.1	-798	-0.4%	133.3	-8600	-5.9%
SFOATL	155.2	163.1	7896	5.5%	156.7	1510	1.4%	STLMSP	134.2	140.6	6415	5.2%	133.3	-911	-0.2%
SFOCVG	156.8	161.7	4948	3.5%	156.7	-100	0.2%	TPAATL	144.8	140.1	-4653	-3.2%	133.3	-11487	-7.9%
SFODTW	162.6	162.3	-334	-0.1%	156.7	-5932	-3.6%	TPACVG	145.1	144.9	-235	0.1%	139.2	-5915	-3.9%
SFOMSP	156.9	156.0	-909	-0.5%	145.5	-11384	-7.2%	TPADTW	144.9	147.6	2714	2.2%	139.2	-5675	-3.6%
SFOSLC	135.2	143.2	7942	6.4%	139.2	3980	3.4%	TPAJFK	142.8	147.9	5038	3.9%	139.2	-3633	-2.2%
SJCATL	160.6	162.2	1658	1.1%	156.7	-3883	-2.3%	TPALAX	163.3	162.8	-549	-0.2%	156.7	-6630	-3.9%
SJCSLC	138.8	142.4	3650	2.8%	139.2	414	0.5%	TPPATL	151.4	169.6	18166	12.3%	156.7	5257	3.7%
SJDATL	153.0	156.0	2994	2.1%	145.5	-7549	-4.8%	TPPJFK	155.1	175.2	20148	13.2%	167.6	12500	8.3%
SJOATL	156.4	154.9	-1490	-0.7%	145.5	-10930	-6.7%	UVFATL	162.2	159.7	-2505	-1.3%	156.7	-5463	-3.2%
SJUATL	159.7	154.5	-5211	-3.2%	145.5	-14217	-8.9%	UVFJFK	149.3	159.6	10314	7.7%	156.7	7400	5.8%
SJUJFK	153.8	155.2	1345	1.3%	145.5	-8315	-5.0%	YVRDTW	160.6	160.6	-7	0.2%	156.7	-3871	-2.3%
SKBATL	148.4	155.4	7004	4.9%	156.7	8271	5.8%	YVRJFK	162.2	166.9	4661	3.0%	156.7	-5498	-3.3%
SLCABQ	126.4	141.5	15080	12.1%	133.3	6900	5.6%	YVRMSP	150.8	153.8	2914	2.1%	145.5	-5350	-3.4%
SLCANC	161.6	162.6	955	1.1%	156.7	-4925	-2.6%	ZIHLAX	135.0	153.0	17985	14.0%	145.5	10459	8.4%
SLCATL	158.1	155.7	-2402	-1.4%	145.5	-12578	-7.9%	ZLOLAX	130.4	149.7	19302	15.4%	145.5	15100	12.1%
SLCBIL	138.2	140.1	1884	1.7%	133.3	-4942	-3.3%								
SLCBOI	139.0	138.9	-139	0.1%	133.3	-5700	-3.9%								
SLCBOS	161.3	162.3	1062	0.7%	156.7	-4565	-2.8%								
SLCBWI	157.8	159.2	1439	1.0%	156.7	-1078	-0.6%								
SLCBZN	141.6	139.6	-1981	-1.2%	133.3	-8271	-5.6%								
SLCCVG	155.0	153.9	-1144	-0.7%	145.5	-9504	-6.1%								

TABLE 10

B767-300ER/CF680C2/B6F

Takeoff Weight Determination:

Specifics of the Flight Planning Database:

- 15,956 Flights
- 185 Routes Departing 53 Airports
- 179 "Tankered" Flights
  - 12,914lbs. Average
  - 1877 NM Average Trip
- Added Airport Elevation, Runway Length, and GCD for each Airport/Flight

As with the previous aircraft, multiple linear regressions on the database were conducted in a stepwise method using independent variables: runway length, airport elevation, and either GCD or Planned Distance. The regressions were applied to the total database of individual flights and repeated with an "average" database that contained the average data for each route and in the case of Planned Distance, the average planned distance.

The statistical summary of the GCD and Planned Distance regressions are as follows:

B767-300ER Planned Distance with All Flight Data:

Model Summary[c]

Model	R	R Square	Adjusted R Square	Std. Error of the Estimate
1	.834[a]	.695	.695	16320.834
2	.835[b]	.697	.697	16257.502

a. Predictors: (Constant), PLN_DIST

b. Predictors: (Constant), PLN_DIST, RWYL

c. Dependent Variable: ACT_GWT

B767-300ER Great Circle Distance with All Flight Data

Model Summary[c]

Model	R	R Square	Adjusted R Square	Std. Error of the Estimate
1	.824[a]	.680	.680	16721.991
2	.825[b]	.681	.681	16677.780

a. Predictors: (Constant), GCD

b. Predictors: (Constant), GCD, RWYL

c. Dependent Variable: ACT_GWT

B767-300ER Planned Distance with Average Route Data

Model Summary[b]

Model	R	R Square	Adjusted R Square	Std. Error of the Estimate
1	.928[a]	.861	.860	11798.1594128

a. Predictors: (Constant), AVG_PLND

b. Dependent Variable: AVG_GWT

B767-300ER Great Circle Distance with Average Route Data

Model Summary[b]

Model	R	R Square	Adjusted R Square	Std. Error of the Estimate
1	.907[a]	.822	.819	13417.6824909

a. Predictors: (Constant), GCD, RWYL, ELEV

b. Dependent Variable: AVG_GWT

The analysis of this aircraft revealed a number of issues to be addressed. It was the first analysis where the regression with the Planned Distance produced a slightly better correlation with the average route data than did the Great Circle Distance. The Great Circle Distance is a fixed number and can be readily obtained from a number of different sources. The Planned Distance, while also available to the user, can vary with each flight as a result of approved routes and/or changing wind patterns. To effectively use the Planned Distance an "accumulation" of these distances is required.

In an effort to remain consistent with regard to the input required for weight estimation, the absolute differences resulting from both regressions were compared to the ACARS database, and the results are shown in Chart 3 below. The maximum difference of 4000 lbs. on 19 of the 185 routes in the database was considered acceptable for the continued use of the GCD.

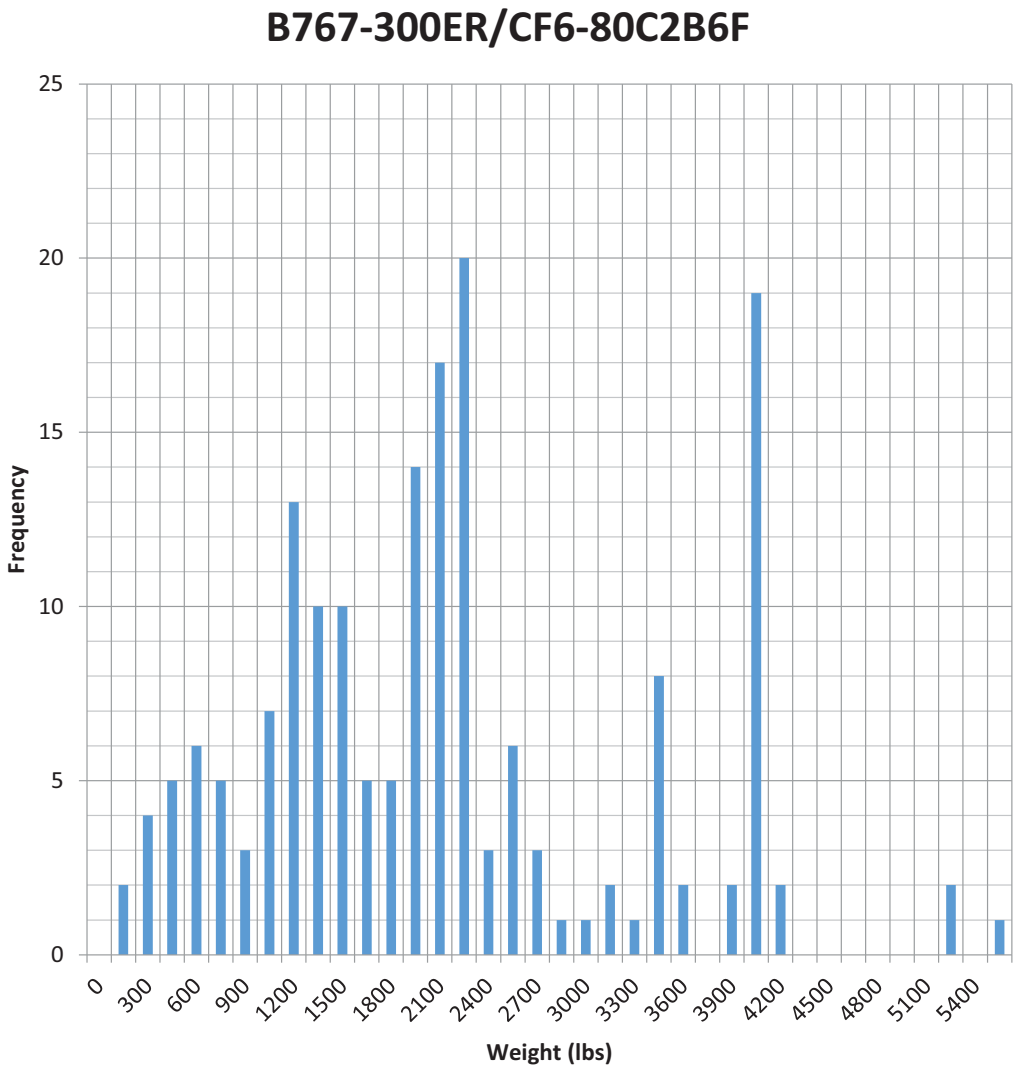

CHART 3

As mentioned, there were other issues requiring attention. The current AEDT Stage Length database does not have weight data for the GE powered B767-300ER. The database only has the PW powered B767-300 and the GE powered B767-400ER. The B767-300ER has a maximum takeoff weight of approximately 55,000 lbs. more than the B767-300 and, depending on variant, a range slightly over 5500 nautical miles. This range is a stage length 8 in the AEDT but there are no stage length 8 weights, the maximum stage length provided is 7; a 4500 to 5500 nautical mile trip.

Maintaining the consistency of using GCD as discussed above, the takeoff weight estimation for the B767-300ER/CF80C2/B6F is:

Model Summary[b]

Model	R	R Square	Adjusted R Square	Std. Error of the Estimate
1	.907[a]	.822	.819	13417.6824909

a. Predictors: (Constant), GCD, RWYL, ELEV

b. Dependent Variable: AVG_GWT

Coefficients[a]

Model		Unstandardized Coefficients		Standardized Coefficients	t	Sig.
		B	Std. Error	Beta		
1	(Constant)	260913.478	10636.292		24.530	.000
	ELEV	.716	1.320	.017	.542	.588
	RWYL	1.247	.816	.048	1.528	.128
	GCD	24.520	.850	.905	28.842	.000

a. Dependent Variable: AVG_GWT

$$GWT = 260913.478 + .716(ELEV) + 1.247(RUNWAY\ LEN) + 24.520(GCD)$$

Figures 10, 11, and 12 below address the issue of the AEDT Stage Length weights discussed and present a graphical representation of the regression. Tabular results comparing the regression and the Average Route data follow in Tables 11 and 12.

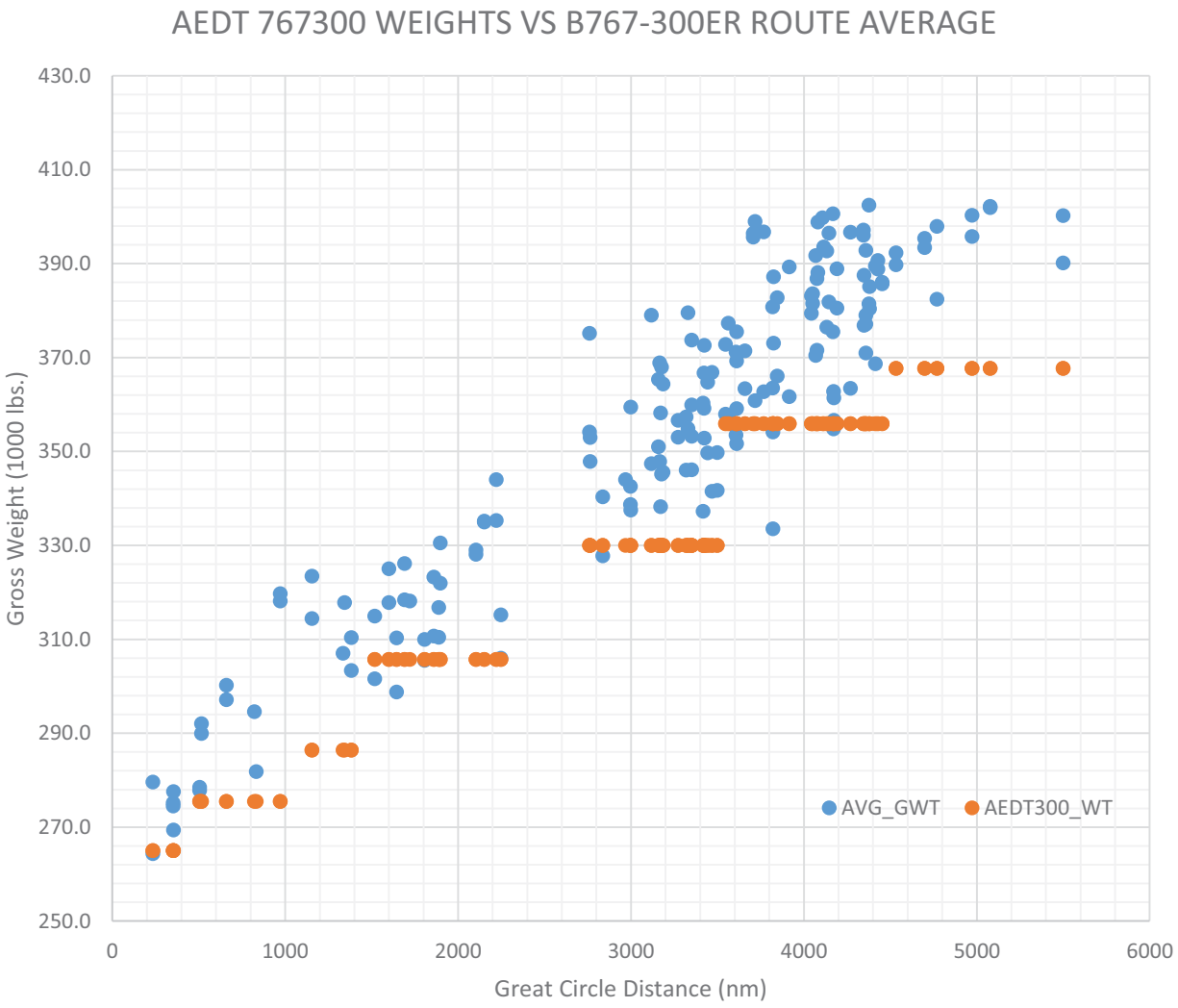

FIGURE 10

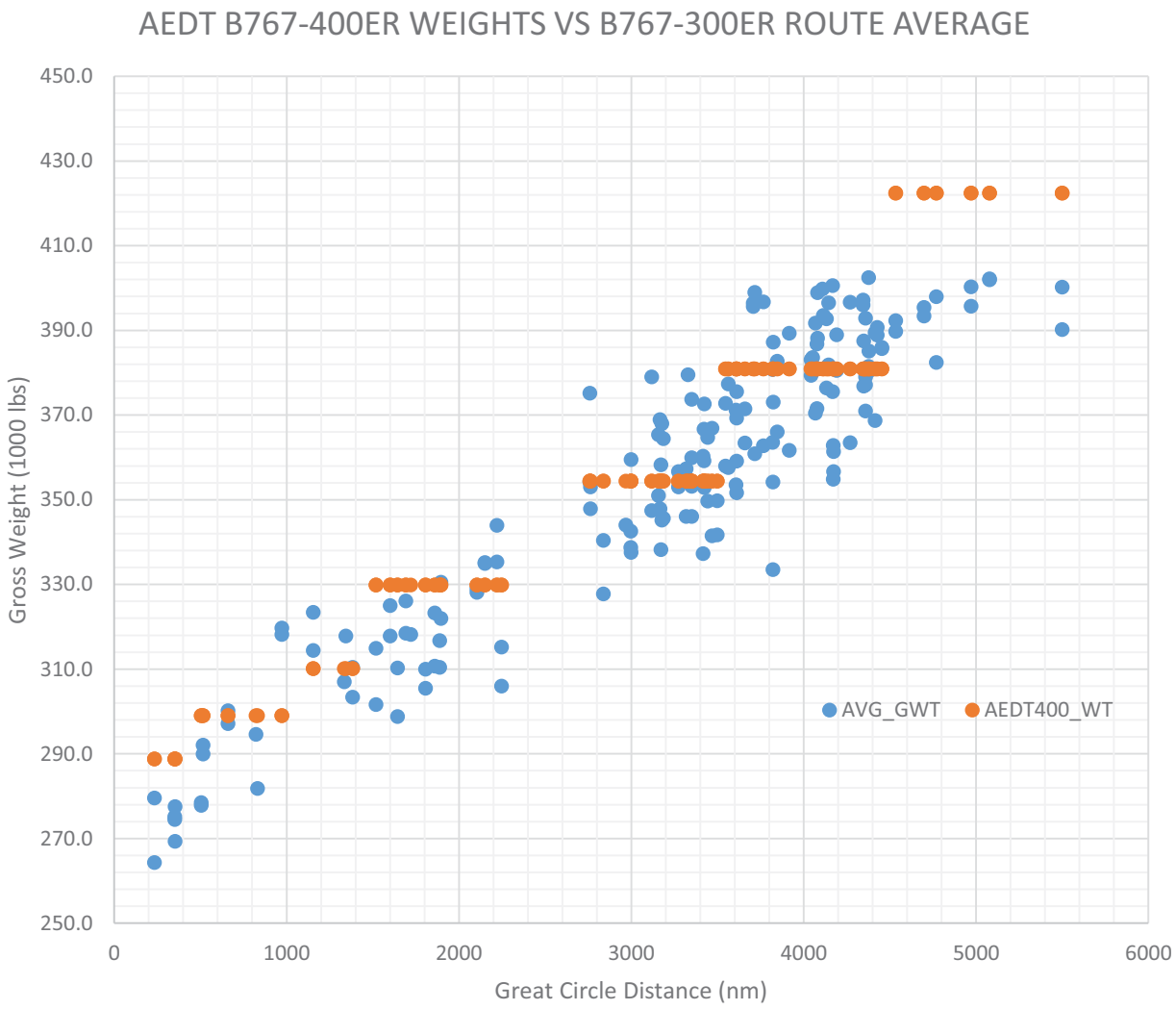
AEDT B767-400ER WEIGHTS VS B767-300ER ROUTE AVERAGE
Gross Weight (1000 lbs)
450.0
430.0
410.0
390.0
370.0
350.0
330.0
310.0
290.0
270.0
250.0
0
1000
2000
3000
4000
5000
6000
Great Circle Distance (nm)
AVG_GWT
AEDT400_WT

FIGURE 11

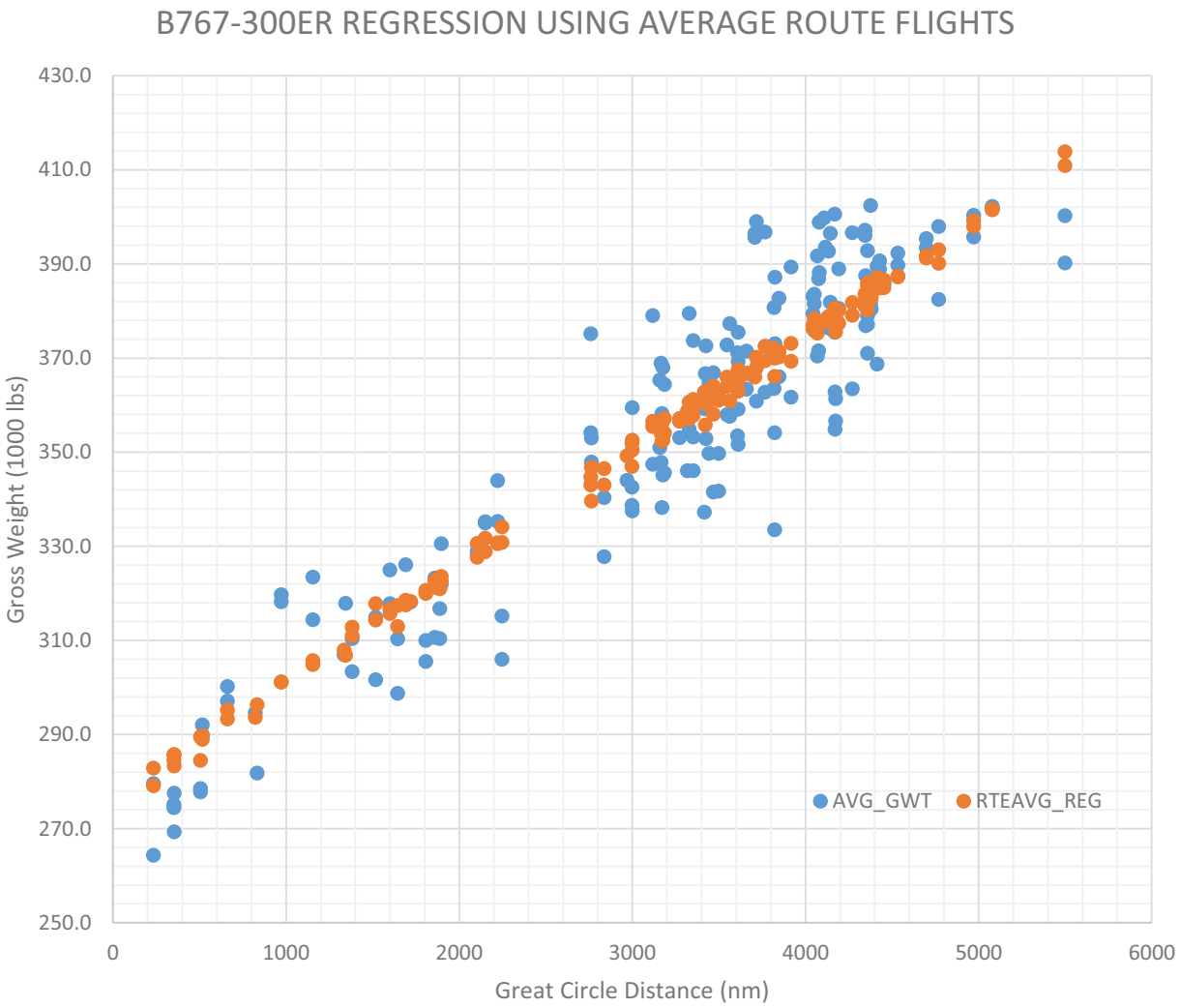
B767-300ER REGRESSION USING AVERAGE ROUTE FLIGHTS
Gross Weight (1000 lbs)
430.0
410.0
390.0
370.0
350.0
330.0
310.0
290.0
270.0
250.0
0
1000
2000
3000
4000
5000
6000
Great Circle Distance (nm)
AVG_GWT
RTEAVG_REG

FIGURE 12

B767-300ER TABULAR RESULTS

ROUTE	AVGWT	REG_WGT	REG_DIF	REG_%	AED_WGT	AED_DIF	AED_%		ROUTE	AVGWT	REG_WGT	REG_DIF	REG_%	AED_WGT	AED_DIF	AED_%
AMSATL	387.2	370.2	-16989	-4.3%	355.9	-31305	-8.0%		CDGDTW	364.8	362.9	-1889	-0.4%	330.0	-34750	-9.4%
AMSBOM	395.7	367.3	-28319	-7.1%	355.9	-39767	-10.0%		CDGEWR	358.2	356.2	-2034	-0.4%	330.0	-28226	-7.8%
AMSDTW	372.6	360.4	-12207	-3.1%	330.0	-42615	-11.3%		CDGJFK	365.3	355.9	-9460	-2.6%	330.0	-35333	-9.6%
AMSEWR	368.0	354.4	-13638	-3.5%	330.0	-37990	-10.2%		CDGORD	371.2	366.9	-4247	-0.8%	355.9	-15254	-3.8%
AMSJFK	368.9	354.1	-14823	-3.9%	330.0	-38905	-10.5%		CDGSEA	379.0	385.3	6312	1.8%	355.9	-23109	-6.0%
AMSPDX	387.5	383.1	-4474	-1.0%	355.9	-31638	-8.1%		CDGSLC	389.5	386.7	-2830	-0.7%	355.9	-33600	-8.6%
ANCATL	344.0	349.2	5209	1.6%	330.0	-14000	-4.0%		CPHJFK	359.9	357.8	-2108	-0.5%	330.0	-29929	-8.2%
ATLAMS	373.1	370.9	-2188	-0.5%	355.9	-17151	-4.5%		CVGCDG	351.7	365.1	13402	4.1%	355.9	4241	1.5%
ATLBRU	366.0	371.4	5353	1.6%	355.9	-10150	-2.7%		DTWAMS	352.9	360.3	7433	2.3%	330.0	-22867	-6.3%
ATLCDG	363.5	370.7	7209	2.1%	355.9	-7631	-2.0%		DTWATL	292.0	289.0	-3048	-0.9%	275.5	-16543	-5.6%
ATLDTW	290.0	289.8	-208	0.1%	275.5	-14459	-4.8%		DTWCDG	349.7	360.8	11051	3.2%	330.0	-19714	-5.6%
ATLDUB	359.2	361.0	1785	0.6%	330.0	-29221	-8.0%		DTWGRU	390.7	384.9	-5797	-1.3%	355.9	-34790	-8.8%
ATLDUS	361.7	373.1	11445	3.3%	355.9	-5774	-1.5%		DTWLHR	353.1	356.6	3538	1.1%	330.0	-23059	-6.4%
ATLEZE	396.0	383.6	-12410	-3.1%	355.9	-40124	-10.1%		DTWSFO	310.0	320.6	10626	3.5%	305.7	-4300	-1.4%
ATLFCO	381.5	384.4	2945	0.8%	355.9	-25553	-6.7%		DUBATL	366.7	355.8	-10917	-2.9%	330.0	-36700	-9.9%
ATLFLL	277.8	289.5	11663	4.2%	275.5	-2318	-0.8%		DUBJFK	353.0	339.6	-13375	-3.7%	330.0	-23000	-6.4%
ATLGIG	393.6	378.0	-15568	-3.9%	355.9	-37667	-9.5%		DUSATL	389.3	369.3	-20009	-5.1%	355.9	-33421	-8.5%
ATLGRU	383.1	376.2	-6880	-1.6%	355.9	-27213	-6.9%		EWRAMS	345.2	352.5	7388	2.3%	330.0	-15155	-4.2%
ATLJAX	279.6	282.8	3236	1.4%	265.0	-14600	-5.0%		EWRCDG	338.2	352.4	14159	4.4%	330.0	-8236	-2.3%
ATLJFK	300.2	293.3	-6915	-2.1%	275.5	-24696	-8.1%		EZEATL	397.2	381.0	-16187	-4.0%	355.9	-41265	-10.3%
ATLLAS	314.9	314.3	-603	0.1%	305.7	-9223	-2.6%		FCOATL	402.4	384.2	-18246	-4.5%	355.9	-46526	-11.5%
ATLLAX	326.1	318.6	-7557	-2.2%	305.7	-20418	-6.2%		FCOJFK	399.0	368.0	-30980	-7.7%	355.9	-43100	-10.8%
ATLLHR	363.4	366.8	3413	1.1%	355.9	-7504	-1.9%		FLLATL	278.5	284.5	6028	2.4%	275.5	-3000	-0.9%
ATLLIM	354.2	344.8	-9385	-2.6%	330.0	-24159	-6.8%		FRAJFK	373.7	359.7	-14037	-3.7%	330.0	-43742	-11.6%
ATLLOS	401.9	401.6	-332	0.0%	367.7	-34243	-8.5%		FUKHNL	333.5	366.1	32569	10.0%	355.9	22387	6.9%
ATLMAD	362.8	369.5	6715	1.9%	355.9	-6850	-1.8%		GIGATL	393.3	378.2	-15093	-3.7%	355.9	-37390	-9.4%
ATLMAN	357.6	364.4	6805	2.0%	355.9	-1734	-0.4%		GRUATL	379.4	376.9	-2447	-0.5%	355.9	-23494	-6.1%
ATLMCO	275.1	285.7	10576	3.9%	265.0	-10129	-3.6%		GRUDTW	388.9	386.4	-2504	-0.5%	355.9	-32967	-8.3%
ATLMUC	375.5	379.3	3784	1.1%	355.9	-19614	-5.1%		HKGNRT	325.0	315.7	-9288	-2.8%	305.7	-19300	-5.9%
ATLMXP	376.4	378.4	1978	0.6%	355.9	-20538	-5.4%		HNDLAX	382.4	390.1	7705	2.1%	367.7	-14734	-3.8%
ATLPDX	316.8	323.4	6627	2.2%	305.7	-11065	-3.4%		HNDSEA	356.6	375.5	18917	5.5%	355.9	-732	0.0%
ATLSAN	310.3	317.4	7115	2.3%	305.7	-4594	-1.4%		HNLFUK	354.2	370.0	15812	4.6%	355.9	1746	0.6%
ATLSCL	388.1	377.1	-11005	-2.8%	355.9	-32245	-8.3%		HNLLAX	335.3	330.7	-4578	-1.3%	305.7	-29613	-8.8%
ATLSEA	330.5	323.6	-6945	-2.0%	305.7	-24834	-7.4%		HNLNGO	349.8	362.0	12280	3.6%	330.0	-19766	-5.5%
ATLSFO	323.2	322.7	-554	0.0%	305.7	-17535	-5.2%		HNLNRT	357.3	357.6	292	0.2%	330.0	-27341	-7.5%
ATLSLC	310.4	311.0	600	0.3%	286.4	-23985	-7.6%		ICNSEA	389.7	387.4	-2306	-0.6%	367.7	-22027	-5.6%
ATLSTR	370.4	376.8	6427	1.8%	355.9	-14519	-3.8%		ISTJFK	392.8	380.2	-12659	-3.2%	355.9	-36946	-9.3%
ATLTPA	277.5	285.8	8209	3.1%	265.0	-12545	-4.4%		JAXATL	264.3	279.1	14809	5.8%	265.0	667	0.5%
ATLVCE	363.5	381.8	18335	5.1%	355.9	-7564	-2.0%		JFKAMS	347.8	356.6	8807	2.6%	330.0	-17841	-5.0%
ATLZRH	371.6	377.0	5476	1.6%	355.9	-15666	-4.1%		JFKATL	297.1	295.2	-1944	-0.6%	275.5	-21645	-7.2%
BCNJFK	379.5	357.1	-22440	-5.8%	330.0	-49522	-13.0%		JFKBCN	354.8	360.6	5803	1.8%	330.0	-24842	-6.9%
BOMAMS	396.4	365.9	-30515	-7.7%	355.9	-40544	-10.2%		JFKBRU	345.6	357.1	11536	3.5%	330.0	-15603	-4.4%
BOSATL	294.6	293.7	-943	-0.1%	275.5	-19100	-6.3%		JFKCDG	351.0	356.5	5452	1.6%	330.0	-21000	-5.9%
BOSCDG	338.7	347.0	8273	2.5%	330.0	-8714	-2.5%		JFKCPH	346.1	361.2	15113	4.4%	330.0	-16071	-4.6%
BOSLHR	327.8	343.1	15263	4.9%	330.0	2198	0.9%		JFKDUB	347.9	346.8	-1100	-0.2%	330.0	-17867	-5.0%
BRUATL	382.7	370.2	-12490	-3.1%	355.9	-26823	-6.9%		JFKFCO	360.8	370.2	9326	2.6%	355.9	-4933	-1.3%
BRUJFK	364.4	354.1	-10340	-2.7%	330.0	-34390	-9.3%		JFKFRA	353.2	361.2	7979	2.4%	330.0	-23206	-6.4%
CDGATL	380.8	372.1	-8683	-2.2%	355.9	-24864	-6.4%		JFKIST	377.1	385.9	8770	2.5%	355.9	-21230	-5.5%
CDGBOS	342.6	351.9	9370	2.8%	330.0	-12556	-3.6%		JFKLAX	335.2	331.8	-3435	-0.9%	305.7	-29495	-8.7%
CDGCVG	369.3	367.0	-2273	-0.5%	355.9	-13354	-3.5%		JFKLHR	337.5	352.6	15023	4.6%	330.0	-7531	-2.1%

TABLE 11

B767-300ER TABULAR RESULTS

ROUTE	AVGWT	REG_WGT	REG_DIF	REG_%	AED_WGT	AED_DIF	AED_%		ROUTE	AVGWT	REG_WGT	REG_DIF	REG_%	AED_WGT	AED_DIF	AED_%
JFKMAD	347.4	355.5	8064	2.5%	330.0	-17407	-4.9%		SANATL	298.8	313.0	14173	4.8%	305.7	6914	2.3%
JFKNCE	341.5	364.1	22553	6.7%	330.0	-11500	-3.3%		SCLATL	398.9	377.6	-21266	-5.2%	355.9	-42981	-10.7%
JFKPRG	358.0	366.0	8040	2.3%	355.9	-2050	-0.5%		SEAATL	321.9	322.6	604	0.3%	305.7	-16250	-4.9%
JFKSEA	329.0	330.6	1608	0.6%	305.7	-23300	-7.0%		SEACDG	371.0	382.9	11956	3.4%	355.9	-15090	-3.9%
JFKSFO	315.2	334.1	18914	6.0%	305.7	-9500	-3.0%		SEAHND	361.4	378.4	17022	5.0%	355.9	-5489	-1.2%
JFKSVO	383.6	378.3	-5242	-1.3%	355.9	-27691	-7.2%		SEAICN	392.3	387.2	-5120	-1.3%	367.7	-24633	-6.3%
JFKTSE	390.2	413.9	23681	6.2%	367.7	-22472	-5.7%		SEAJFK	328.1	327.7	-455	-0.1%	305.7	-22409	-6.8%
JFKVCE	359.1	367.5	8418	2.4%	355.9	-3218	-0.8%		SEAKIX	385.1	383.4	-1697	-0.3%	355.9	-29234	-7.5%
JFKZRH	337.3	362.8	25517	7.8%	330.0	-7261	-2.0%		SEALHR	354.8	378.3	23508	6.8%	355.9	1071	0.5%
KIXSEA	380.4	382.6	2239	0.7%	355.9	-24486	-6.3%		SEANRT	396.5	377.7	-18825	-4.7%	355.9	-40600	-10.2%
LASATL	301.6	317.8	16168	5.4%	305.7	4075	1.4%		SEAPEK	395.4	391.3	-4128	-0.9%	367.7	-27687	-6.9%
LAXATL	318.4	317.5	-898	-0.2%	305.7	-12742	-4.0%		SEAPVG	395.7	398.0	2232	0.7%	367.7	-28046	-7.0%
LAXDTW	318.2	318.3	88	0.1%	305.7	-12467	-3.8%		SFOATL	310.7	321.3	10626	3.5%	305.7	-4982	-1.5%
LAXHND	397.9	393.0	-4929	-1.1%	367.7	-30246	-7.5%		SFODTW	305.5	320.0	14508	4.8%	305.7	200	0.1%
LAXHNL	344.0	330.5	-13439	-3.8%	305.7	-38279	-11.0%		SFOJFK	306.0	330.8	24821	8.2%	305.7	-300	0.0%
LAXJFK	335.0	328.8	-6148	-1.6%	305.7	-29271	-8.6%		SFONRT	385.7	384.9	-754	-0.1%	355.9	-29767	-7.6%
LHRATL	371.5	366.7	-4796	-1.1%	355.9	-15552	-4.0%		SJUATL	317.9	306.8	-11014	-3.1%	286.4	-31457	-9.6%
LHRBOS	340.4	346.5	6137	2.0%	330.0	-10364	-2.8%		SLCATL	303.4	312.8	9408	3.2%	286.4	-16985	-5.5%
LHRDTW	356.6	357.2	555	0.3%	330.0	-26636	-7.3%		SLCCDG	368.7	387.1	18431	5.2%	355.9	-12806	-3.3%
LHRJFK	359.5	350.5	-8993	-2.3%	330.0	-29466	-8.0%		STRATL	391.7	375.3	-16477	-4.2%	355.9	-35836	-9.1%
LHRSEA	362.8	379.2	16394	4.7%	355.9	-6916	-1.8%		SVOJFK	381.5	375.8	-5679	-1.3%	355.9	-25612	-6.6%
LIMATL	375.2	343.0	-32132	-8.5%	330.0	-45150	-12.0%		TPAATL	269.4	283.3	13944	5.4%	265.0	-4364	-1.4%
LOSATL	402.2	401.5	-714	-0.1%	367.7	-34491	-8.5%		TSEJFK	400.2	410.9	10667	2.7%	367.7	-32535	-8.1%
LOSSJU	399.8	377.7	-22108	-5.5%	355.9	-43900	-11.0%		TSEROB	294.3	393.9	99660	34.1%	367.7	73450	25.2%
MADATL	396.8	372.5	-24248	-6.1%	355.9	-40858	-10.3%		VCEATL	396.7	379.1	-17547	-4.4%	355.9	-40767	-10.2%
MADJFK	379.0	356.6	-22438	-5.8%	330.0	-49034	-12.8%		VCEJFK	375.5	362.9	-12563	-3.2%	355.9	-19600	-5.1%
MANATL	377.4	360.9	-16436	-4.3%	355.9	-21452	-5.6%		ZRHATL	386.8	377.0	-9808	-2.5%	355.9	-30917	-7.9%
MCOATL	274.5	284.6	10090	3.9%	265.0	-9469	-3.3%		ZRHJFK	360.3	360.8	521	0.3%	330.0	-30304	-8.3%
MCODTW	281.8	296.4	14553	5.2%	275.5	-6300	-2.2%									
MSPLAX	307.0	307.9	949	0.5%	286.4	-20600	-6.6%									
MUCATL	400.6	380.5	-20052	-5.0%	355.9	-44694	-11.1%									
MXPATL	392.7	378.8	-13902	-3.5%	355.9	-36819	-9.3%									
NCEJFK	366.9	358.1	-8807	-2.0%	330.0	-36875	-9.7%									
NGOHNL	341.7	361.0	19281	5.8%	330.0	-11733	-3.3%									
NRTHKG	317.8	316.6	-1193	-0.3%	305.7	-12100	-3.8%									
NRTHNL	346.0	358.7	12683	3.8%	330.0	-16049	-4.5%									
NRTPDX	380.5	380.1	-383	0.2%	355.9	-24621	-6.2%									
NRTPEK	314.4	305.7	-8722	-2.5%	286.4	-28017	-8.6%									
NRTPVG	318.2	301.2	-16974	-5.1%	275.5	-42682	-13.2%									
NRTSEA	381.8	379.0	-2848	-0.7%	355.9	-25933	-6.8%									
NRTSFO	386.0	386.6	562	0.2%	355.9	-30100	-7.7%									
ORDCDG	353.5	366.1	12571	3.7%	355.9	2400	0.8%									
PDXAMS	376.9	381.3	4398	1.4%	355.9	-20967	-5.4%									
PDXATL	310.4	320.9	10546	3.5%	305.7	-4700	-1.4%									
PDXNRT	388.9	377.4	-11510	-2.9%	355.9	-33025	-8.4%									
PEKNRT	323.4	304.9	-18566	-5.6%	286.4	-37029	-11.4%									
PEKSEA	393.4	391.7	-1654	-0.3%	367.7	-25691	-6.4%									
PRGJFK	372.8	364.0	-8822	-2.3%	355.9	-16900	-4.4%									
PVGNRT	319.7	301.1	-18594	-5.7%	275.5	-44214	-13.8%									
PVGSEA	400.3	399.2	-1113	-0.2%	367.7	-32613	-8.1%									
ROBTSE	275.5	392.5	116957	42.5%	367.7	92162	33.5%									

TABLE 12

SECTION II

REDUCED THRUST (USAGE AND LEVEL)

B757-200/PW2037

Reduced Power/Thrust Determination:

The initial ACARS database contained 91,519 departures, but was reduced, by a number of actions to 85,738 flights. Flights were removed from the database for the following reasons:

- Obvious data recording errors
- Missing essential data (aircraft weight, origin, destination, or de-rate)
- Charter, maintenance, or other non-revenue positioning flights
- An imposed minimum of 5 flights for any city pair (origin and destination)

In addition to the database edits above, there still remained a number of suspect entries for percent reduced thrust/power particularly at very low recorded percentage levels. To circumvent any potential problem with the validity of this data, a decision was made to only consider flights with recorded reduced thrust percentages greater or equal to one as being actual reduced thrust/power departures.

Specifics of the B757-200 ACARS Database:

- 85,738 Flights
- 412 Routes Departing 101 Airports
- 96% of All Departures Used Reduced Thrust/Power
- Average Reduced Thrust/Power was 15.3%

Chart 4 below, is a histogram of the B757-200 reduced thrust percentages, while Tables 13, 14, and 15 provide the average route data of actual weight and reduced thrust/power percentage. There was some concern regarding the increase in frequency at the 2% reduced power level, but the weight distribution shown in Chart 5, shows a step increase in the 220 to 225 thousand pound range. In this weight range, a 2% reduced thrust/power was accepted as correct considering the earlier discussion on pilot acceptance and air carrier implementation of reduced thrust/power takeoffs.

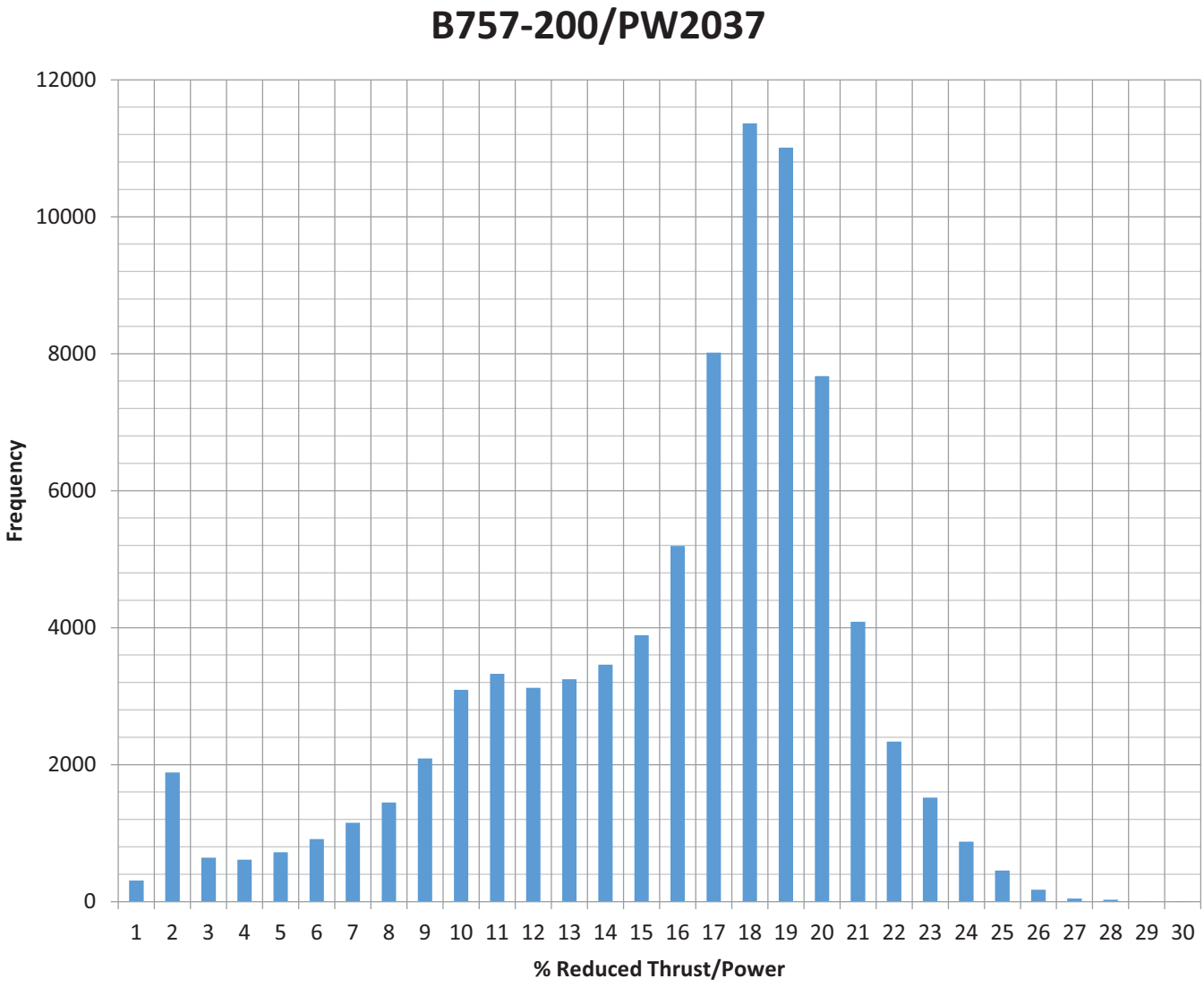
B757-200/PW2037
12000
10000
8000
6000
4000
2000
0
Frequency
1 2 3 4 5 6 7 8 9 10 11 12 13 14 15 16 17 18 19 20 21 22 23 24 25 26 27 28 29 30
% Reduced Thrust/Power

CHART 4

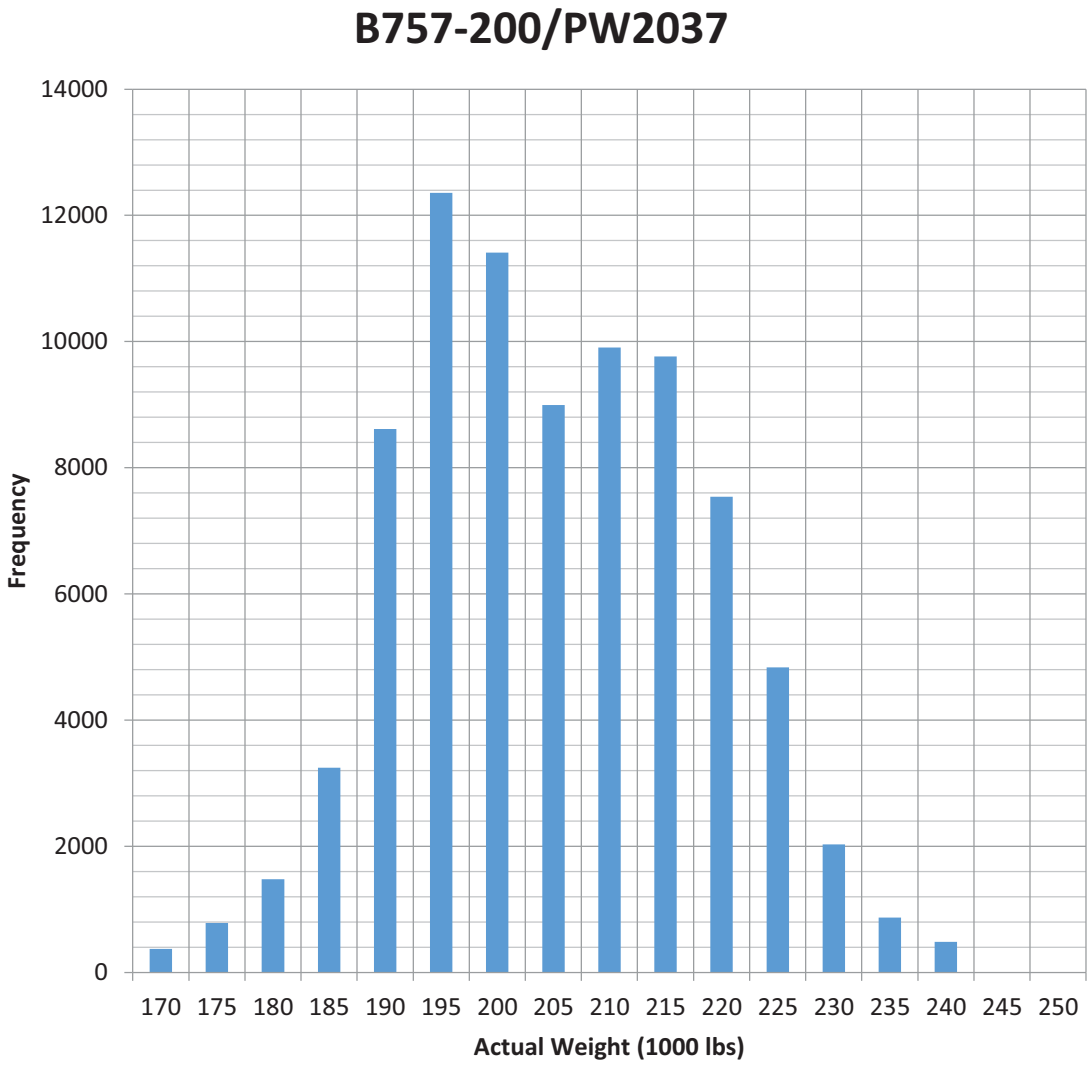
B757-200/PW2037
14000
12000
10000
8000
6000
4000
2000
0
Frequency
170 175 180 185 190 195 200 205 210 215 220 225 230 235 240 245 250
Actual Weight (1000 lbs)

CHART 5

B757-200 AVERAGE ROUTE REDUCED THRUST RESULTS

ROUTE	AVG_WGT	AVG_DRATE		ROUTE	AVG_WGT	AVG_DRATE		ROUTE	AVG_WGT	AVG_DRATE
ABQATL	204.5	15.6		ATLMEX	201.9	9.8		BHMATL	183.7	19.2
AGPJFK	227.2	14.8		ATLMGA	176.9	17.6		BNAATL	182.7	18.5
ANCATL	232.2	6.0		ATLMIA	193.3	18.0		BOGATL	216.2	15.8
ANCMSP	224.5	7.9		ATLMKE	186.1	18.5		BOGJFK	221.3	12.7
ANCSLC	212.6	9.7		ATLMPR	203.5	18.7		BOISLC	184.2	20.2
ARNJFK	236.1	8.1		ATLMSP	197.8	17.0		BONATL	207.9	15.6
ATLABQ	198.8	15.4		ATLMSY	198.4	15.5		BOSATL	199.7	17.8
ATLANC	233.1	5.9		ATLNAS	192.9	19.4		BOSCDG	231.0	11.1
ATLAUA	209.8	6.7		ATLNCA	209.3	8.3		BOSCUN	202.9	16.6
ATLAUS	191.9	18.4		ATLORD	192.1	16.9		BOSDTW	193.3	17.6
ATLBHM	185.3	18.8		ATLPBI	190.4	18.9		BOSJFK	188.7	16.6
ATLBNA	183.5	18.7		ATLPDX	213.3	12.6		BOSMSP	202.1	14.7
ATLBOG	217.9	6.0		ATLPHL	191.0	17.6		BOSSLC	210.8	12.8
ATLBON	209.1	16.2		ATLPHX	204.8	15.9		BRUATL	235.5	10.4
ATLBOS	197.6	13.7		ATLPIT	188.2	18.4		BWIATL	188.4	18.9
ATLBRU	232.5	5.6		ATLPNS	187.0	18.0		BWIDTW	181.1	17.3
ATLBSB	239.5	2.7		ATLPUJ	204.2	18.9		BWIMSP	193.8	17.4
ATLBWI	189.0	18.0		ATLPVR	205.0	17.4		BZNATL	208.6	14.2
ATLBZN	200.0	11.1		ATLRDU	186.1	18.3		BZNMSP	201.6	10.9
ATLCCS	210.7	15.5		ATLRIC	188.6	16.2		CCSATL	207.2	15.5
ATLCLT	189.2	19.0		ATLROC	208.5	7.0		CDGBOS	227.5	9.3
ATLCUN	197.5	19.6		ATLRSW	190.3	18.6		CDGPHL	223.3	11.8
ATLDAB	187.2	18.0		ATLRTB	197.5	12.1		CDGPIT	226.7	11.9
ATLDCA	189.7	16.6		ATLSAN	208.6	8.7		CLTATL	182.5	19.7
ATLDEN	199.5	15.3		ATLSAT	190.4	17.0		CPHJFK	234.9	11.2
ATLDFW	191.2	19.0		ATLSEA	216.8	12.8		CUNATL	197.4	18.3
ATLDTW	192.7	17.6		ATLSFO	215.7	10.5		CUNBOS	202.9	8.9
ATLEGE	189.7	5.1		ATLSJC	210.2	14.1		CUNDTW	202.4	14.7
ATLFLL	191.8	17.8		ATLSJD	204.4	18.0		CUNMCO	190.7	20.7
ATLGCM	196.1	16.8		ATLSJO	205.9	8.2		CUNSLC	210.0	7.6
ATLGDL	200.5	15.0		ATLSJU	209.2	13.1		CVGATL	180.4	17.0
ATLGGT	206.7	7.4		ATLSKB	205.3	13.8		CVGLAS	200.8	16.8
ATLGUA	208.0	7.5		ATLSLC	207.6	14.0		CVGLAX	204.3	16.2
ATLHRO	201.7	9.2		ATLSMF	212.0	11.7		CVGSEA	208.2	15.7
ATLHSV	194.2	16.1		ATLSNA	207.8	3.3		CVGSLC	200.4	18.1
ATLIND	187.3	18.6		ATLSRQ	190.2	17.1		DABATL	191.0	18.4
ATLJAC	198.8	4.3		ATLSTL	186.9	18.3		DCAATL	190.0	18.8
ATLJAX	187.2	18.3		ATLSTT	204.9	3.8		DCAMSP	188.2	19.5
ATLJFK	196.7	16.4		ATLSXM	209.8	4.7		DCASLC	207.0	14.8
ATLLAS	206.7	13.3		ATLTPA	190.0	19.1		DENATL	201.7	15.1
ATLLAX	212.0	14.4		ATLTUS	200.3	16.2		DENMSP	197.7	16.6
ATLLGA	193.3	14.6		ATLUIO	217.7	6.0		DFWATL	193.0	18.2
ATLLIR	206.4	11.2		ATLUVF	215.0	12.0		DKRJFK	229.9	11.0
ATLMBJ	199.7	18.3		ATLYVR	218.0	13.4		DTWATL	191.4	18.2
ATLMCI	188.1	18.3		AUAATL	209.5	15.8		DTWBOS	193.2	14.5
ATLMCO	189.8	18.6		AUSATL	193.2	17.9		DTWBWI	187.5	17.4

TABLE 13

B757-200 AVERAGE ROUTE REDUCED THRUST RESULTS

ROUTE	AVG_WGT	AVG_DRATE		ROUTE	AVG_WGT	AVG_DRATE		ROUTE	AVG_WGT	AVG_DRATE
DTWCUN	205.3	16.9		JFKAGP	236.4	8.2		LAXGUA	216.6	4.7
DTWFLL	197.4	16.5		JFKARN	234.8	8.6		LAXHNL	209.7	13.3
DTWGRR	192.6	18.8		JFKATL	196.3	18.3		LAXIND	213.0	14.3
DTWLAS	207.1	12.9		JFKBOG	215.1	7.2		LAXJFK	218.7	14.5
DTWLAX	209.9	14.1		JFKBOS	181.3	15.7		LAXKOA	219.6	12.8
DTWMCO	193.9	18.7		JFKCPH	236.1	8.4		LAXLIH	217.0	2.9
DTWMIA	198.9	18.2		JFKDKR	232.9	10.8		LAXMCO	215.5	13.4
DTWMKE	186.2	18.6		JFKDTW	195.1	15.4		LAXMSP	204.9	14.8
DTWMSP	190.5	17.8		JFKDUB	232.8	5.4		LAXOGG	216.5	3.8
DTWPBI	193.4	16.9		JFKFLL	195.8	16.4		LAXROC	220.3	4.6
DTWPDX	207.4	15.0		JFKGGT	212.7	4.9		LAXSEA	196.3	17.6
DTWPHL	189.9	18.0		JFKKEF	222.2	11.5		LAXSJO	222.2	5.6
DTWPHX	206.1	16.0		JFKLAS	211.4	11.3		LAXSLC	189.4	19.9
DTWRSW	197.7	18.0		JFKLAX	212.5	15.5		LGAATL	193.9	18.2
DTWSAN	209.9	7.4		JFKMCO	194.6	17.7		LGADTW	182.4	18.4
DTWSEA	208.8	15.6		JFKMEX	209.7	7.9		LGAMSP	182.8	15.2
DTWSFO	212.2	12.1		JFKMIA	198.3	17.8		LIHLAX	221.7	11.1
DTWSLC	203.8	16.1		JFKMSP	189.9	17.8		LIRATL	209.0	15.8
DTWTPA	195.6	16.5		JFKPDX	209.0	14.5		MBJATL	199.2	17.9
DUBJFK	226.2	12.7		JFKPHX	207.9	16.3		MCIATL	196.0	17.2
EGEATL	204.8	16.0		JFKPIT	182.3	19.8		MCOATL	192.4	18.8
FAIMSP	223.3	8.6		JFKROC	198.0	14.9		MCOCUN	190.9	21.1
FAISEA	208.7	14.2		JFKSAN	210.7	8.1		MCODTW	196.7	16.9
FLLATL	191.7	19.0		JFKSDQ	208.2	16.0		MCOJFK	194.1	16.8
FLLDTW	195.5	17.0		JFKSEA	215.7	14.8		MCOLAS	194.6	15.0
FLLJFK	192.3	17.3		JFKSFO	214.6	12.9		MCOLAX	213.5	13.5
FLLMSP	197.7	16.4		JFKSJU	204.3	16.1		MCOMSP	200.2	16.8
GCMATL	206.2	17.5		JFKSLC	210.2	13.9		MCOSLC	209.9	12.7
GDLATL	204.4	14.3		JFKSNN	229.1	10.2		MEXATL	209.4	14.1
GDLLAX	207.0	16.5		JFKSSA	237.2	6.4		MEXJFK	216.1	13.6
GEGMSP	206.8	14.2		JFKSTT	199.5	8.5		MIAATL	193.1	18.6
GEGSLC	192.8	21.4		JFKSXM	200.9	5.8		MIADTW	196.6	17.4
GGTATL	204.4	15.8		JNUSEA	194.4	17.8		MIAJFK	196.3	17.5
GGTJFK	209.2	15.7		KEFJFK	228.1	12.1		MKEATL	187.8	19.7
GGTLAX	217.5	12.8		KOALAX	222.5	11.1		MKEDTW	179.6	18.2
GUAATL	208.4	14.7		LASATL	212.2	12.3		MKEMSP	183.2	18.2
GUALAX	218.9	11.3		LASCVG	207.2	16.0		MPRATL	204.7	15.0
HNLLAX	223.4	8.6		LASDTW	210.5	15.0		MSPANC	222.3	9.0
HNLSEA	223.2	9.5		LASJFK	216.3	13.0		MSPATL	199.2	16.8
HNLSFO	218.3	12.4		LASMCO	198.4	18.8		MSPBOS	201.7	10.8
HROATL	206.1	17.3		LASMSP	202.4	16.6		MSPBWI	192.1	17.5
INDATL	191.1	18.0		LASSLC	183.1	21.1		MSPDCA	193.0	14.1
INDLAX	200.3	14.8		LAXATL	216.0	11.2		MSPDEN	192.0	16.1
JACATL	207.0	14.0		LAXDTW	215.1	13.6		MSPDTW	189.9	17.8
JACMSP	197.2	17.8		LAXGDL	190.9	18.2		MSPFAI	222.0	10.8
JAXATL	190.2	18.7		LAXGGT	217.6	4.6		MSPFLL	204.3	13.2

TABLE 14

B757-200 AVERAGE ROUTE REDUCED THRUST RESULTS

ROUTE	AVG_WGT	AVG_DRATE		ROUTE	AVG_WGT	AVG_DRATE		ROUTE	AVG_WGT	AVG_DRATE
MSPGEG	195.4	20.0		PNSATL	189.6	19.7		SLCATL	210.9	12.8
MSPJAC	189.8	4.5		PUJATL	210.5	15.9		SLCBOI	184.2	19.6
MSPJFK	196.0	18.0		PVRATL	213.6	12.5		SLCBOS	213.9	9.3
MSPLAS	199.2	15.8		RDUATL	185.4	18.6		SLCCUN	209.4	17.1
MSPLAX	201.9	16.7		RICATL	189.6	17.9		SLCCVG	204.9	18.0
MSPLGA	192.7	14.4		ROCATL	208.7	16.6		SLCDCA	210.1	7.3
MSPMCI	184.0	15.5		ROCJFK	207.4	16.2		SLCDTW	207.2	15.6
MSPMCO	202.2	17.2		ROCLAX	221.3	12.6		SLCGEG	185.0	21.6
MSPMKE	187.1	18.0		RSWATL	195.0	18.2		SLCJFK	212.9	14.3
MSPORD	188.7	18.3		RSWDTW	197.5	16.0		SLCLAS	185.5	19.3
MSPPDX	202.0	16.5		RSWMSP	200.9	16.7		SLCLAX	188.1	17.4
MSPPHX	199.4	17.8		RTBATL	208.3	16.1		SLCMCO	212.0	14.7
MSPRSW	203.4	17.7		SANATL	216.0	11.1		SLCMSP	196.5	17.3
MSPSAN	201.3	11.0		SANDTW	216.4	13.6		SLCPDX	190.4	18.0
MSPSEA	202.1	16.9		SANJFK	220.4	12.6		SLCPHL	209.5	15.6
MSPSFO	203.6	15.4		SANMSP	207.5	13.9		SLCPHX	187.0	20.0
MSPSJO	210.9	4.5		SANSLC	190.5	19.0		SLCSAN	189.6	15.9
MSPSJU	220.1	10.3		SATATL	195.4	17.7		SLCSEA	194.4	17.7
MSPSLC	192.1	19.4		SDQJFK	212.2	14.4		SLCSFO	187.1	18.7
MSPTPA	196.3	17.4		SEAANC	198.2	17.7		SLCSMF	184.4	19.8
MSPYVR	205.7	16.6		SEAATL	221.5	9.2		SMFATL	217.1	10.9
MSYATL	187.8	18.6		SEACVG	210.2	16.0		SMFMSP	206.3	15.5
NASATL	201.1	18.6		SEADTW	216.2	13.2		SMFSLC	191.8	19.8
NCAATL	206.3	17.2		SEAFAI	193.4	16.8		SNAATL	213.4	11.8
OGGLAX	219.3	10.4		SEAHNL	223.5	9.3		SNNJFK	223.8	13.3
OGGSEA	228.0	8.3		SEAJFK	220.1	13.6		SRQATL	192.9	18.1
ORDATL	195.0	17.3		SEAJNU	178.7	10.5		SSAJFK	235.2	10.4
ORDMSP	190.6	17.1		SEALAX	191.1	16.9		STLATL	190.2	18.5
PBIATL	196.8	18.5		SEAMSP	206.8	14.0		STLMSP	190.0	20.1
PBIDTW	195.4	16.0		SEAOGG	218.6	2.9		STTATL	211.6	17.4
PDXATL	219.6	9.5		SEASLC	193.0	18.9		STTJFK	208.0	16.5
PDXDTW	214.9	14.3		SFOATL	221.4	8.6		SXMATL	212.8	14.9
PDXJFK	215.0	13.8		SFODTW	217.8	12.6		SXMJFK	210.7	14.6
PDXMSP	203.5	14.9		SFOHNL	218.2	12.9		SXMMSP	225.0	8.6
PDXSLC	190.2	19.8		SFOJFK	221.1	13.8		TPAATL	189.4	18.9
PHLATL	189.9	18.9		SFOMSP	208.3	14.5		TPADTW	193.3	16.8
PHLCDG	231.0	11.4		SFOSLC	191.4	19.3		TPAMSP	198.0	16.6
PHLDTW	186.8	18.6		SJCATL	213.3	12.1		TUSATL	203.8	15.4
PHLSLC	205.4	12.3		SJDATL	203.1	15.9		UIOATL	221.4	14.1
PHXATL	208.4	14.1		SJOATL	214.7	14.3		UVFATL	218.2	13.9
PHXDTW	209.6	14.6		SJOLAX	226.0	11.1		YVRATL	216.5	10.6
PHXJFK	214.3	15.3		SJOMSP	220.8	11.5		YVRMSP	204.6	14.1
PHXMSP	199.9	16.7		SJUATL	209.0	15.7				
PHXSLC	185.1	20.1		SJUJFK	202.4	15.9				
PITATL	183.9	19.3		SJUMSP	215.4	12.5				
PITCDG	231.5	11.2		SKBATL	215.5	14.1				
PITJFK	186.9	17.7		SLCANC	215.8	10.6				

TABLE 15

B767-400ER/CF6-80C2/B8F

Reduced Power/Thrust Determination:

The initial ACARS database contained 11,774 departures, but was reduced, by a number of actions to 11,585 flights. Flights were removed from the database for the following reasons:

- Obvious data recording errors
- Missing essential data (aircraft weight, origin, destination, or de-rate)
- Charter, maintenance, or other non-revenue positioning flights
- An imposed minimum of 5 flights for any city pair (origin and destination)

In addition to the database edits above, there still remained a number of suspect entries for percent reduced thrust/power particularly at very low recorded percentage levels. To circumvent any potential problem with the validity of this data, a decision was made to only consider flights with recorded reduced thrust percentages greater or equal to one as being actual reduced thrust/power departures.

Specifics of the B767-400ER ACARS Database:

- 10,511 Flights
- 57 Routes Departing 21 Airports
- 93.5% of All Departures Used Reduced Thrust/Power
- Average Reduced Thrust/Power was 10.4%

Chart 6 below, is a histogram of the B767-400ER reduced thrust percentages. The explanation for the 2% reduced thrust/power spike is the same as with the B757. The spike is simply more pronounced due to the significant difference in the database size with respect to flights recorded. Chart 6, the weight distribution is also presented to support the explanation.

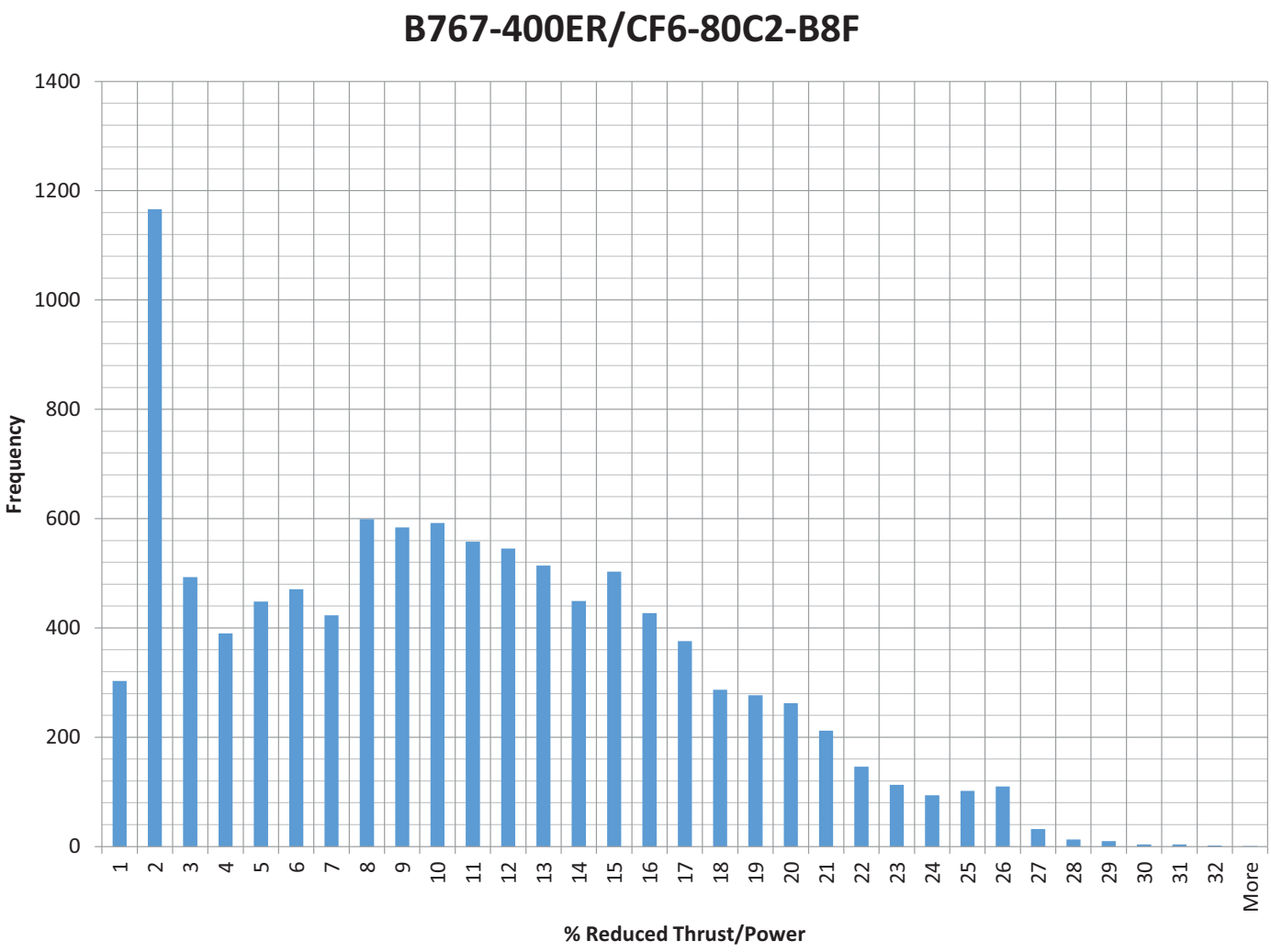
B767-400ER/CF6-80C2-B8F
Frequency
1400
1200
1000
800
600
400
200
0
1
2
3
4
5
6
7
8
9
10
11
12
13
14
15
16
17
18
19
20
21
22
23
24
25
26
27
28
29
30
31
32
More
% Reduced Thrust/Power

CHART 6

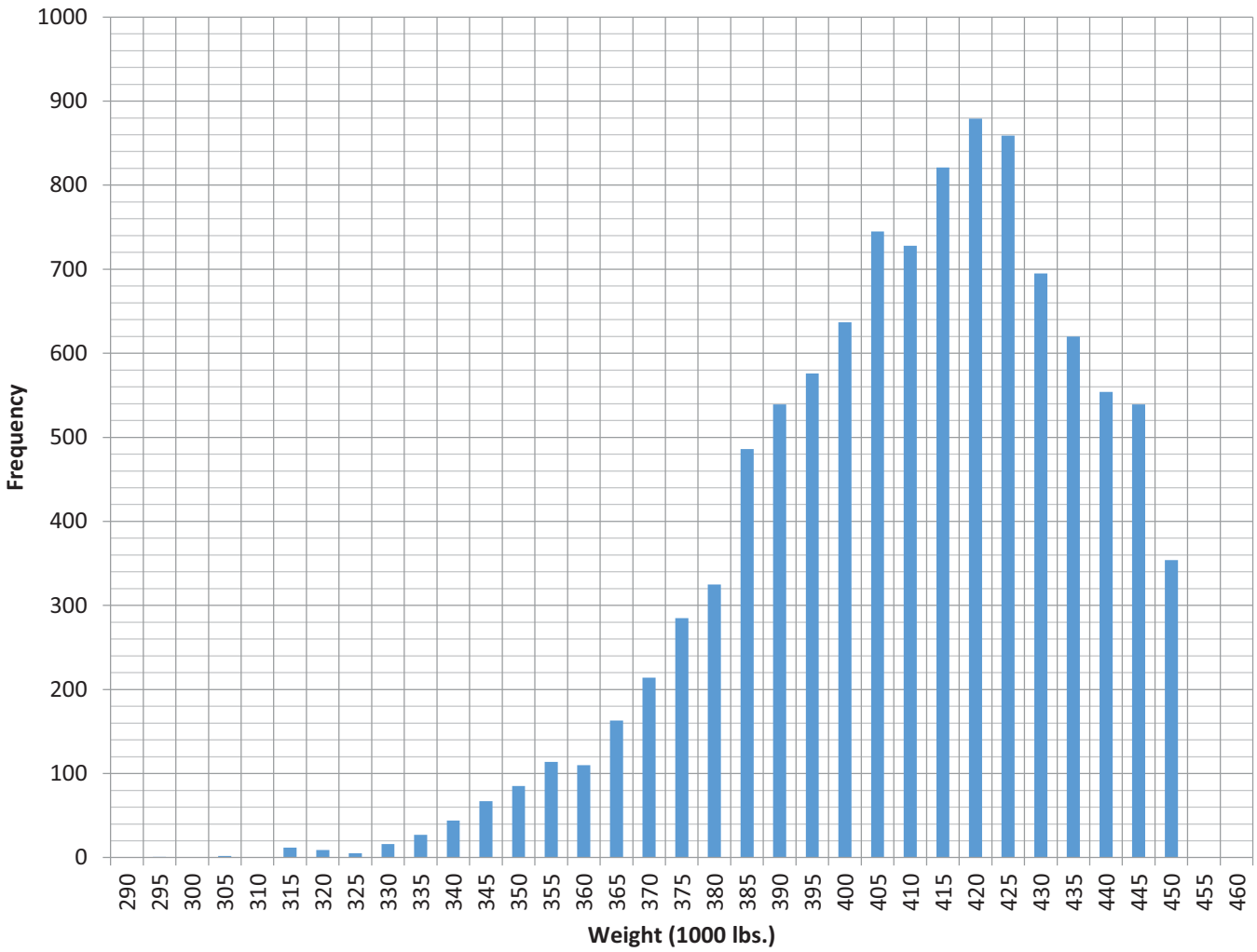
B767-400ER/CF680-C2B8F
Frequency
1000
900
800
700
600
500
400
300
200
100
0
290
295
300
305
310
315
320
325
330
335
340
345
350
355
360
365
370
375
380
385
390
395
400
405
410
415
420
425
430
435
440
445
450
455
460
Weight (1000 lbs.)

CHART 7

B767-400ER AVERAGE ROUTE REDUCED THRUST RESULTS

APRTS	AVG_GWT	AVG_DRATE		APRTS	AVG_GWT	AVG_DRATE
AMSDTW	423.0	4.6%		JFKLHR	376.8	18.7%
ATLCDG	414.6	8.1%		JFKMAD	388.3	15.9%
ATLFRA	416.0	7.1%		JFKMXP	397.8	14.1%
ATLGRU	436.4	2.7%		JFKNCE	383.3	17.5%
ATLJFK	338.1	24.3%		JFKSLC	348.1	22.2%
ATLLAX	363.9	15.8%		JFKSVO	423.3	8.5%
ATLLHR	409.8	8.5%		JFKVCE	399.2	13.8%
ATLMAD	406.0	9.3%		LAXATL	350.1	24.6%
ATLMCO	319.8	27.1%		LAXDTW	360.0	19.7%
ATLMUC	413.8	7.6%		LHRATL	417.4	8.6%
ATLPDX	338.6	22.6%		LHRBOS	370.7	19.1%
ATLSEA	364.8	16.0%		LHRDTW	401.5	12.2%
ATLSLC	350.0	20.7%		LHRJFK	394.9	13.8%
BOSLHR	364.6	11.8%		LHRMSP	404.4	11.6%
CDGATL	420.2	6.2%		MADATL	425.7	8.2%
CDGDTW	413.3	6.9%		MADJFK	402.2	13.7%
CDGJFK	412.8	7.3%		MCOATL	316.6	25.0%
DTWAMS	397.7	11.8%		MSPLHR	395.2	9.1%
DTWCDG	394.1	12.4%		MUCATL	438.6	3.4%
DTWFRA	404.0	10.1%		MXPJFK	428.7	3.4%
DTWLAX	360.3	19.7%		NCEJFK	405.4	7.3%
DTWLHR	391.1	13.3%		NRTPDX	427.2	9.9%
FRAATL	439.3	6.4%		PDXATL	329.5	20.5%
FRADTW	426.8	9.9%		PDXNRT	430.2	3.9%
GRUATL	428.0	6.0%		SLCATL	339.2	18.8%
GRUJFK	420.0	2.5%		SLCJFK	344.0	19.6%
JFKATL	339.2	23.1%		SVOJFK	420.9	8.1%
JFKCDG	386.3	16.5%		VCEJFK	420.3	4.7%
JFKGRU	435.0	5.9%				

TABLE 16

B737-800/CFM56-7B26

Reduced Power/Thrust Determination:

The initial ACARS database was reduced, by a number of actions to 62,326 flights. Flights were removed from the database for the following reasons:

- Obvious data recording errors
- Missing essential data (aircraft weight, origin, destination, or de-rate)
- Charter, maintenance, or other non-revenue positioning flights
- An imposed minimum of 5 flights for any city pair (origin and destination)

In addition to the database edits above, there still remained a number of suspect entries for percent reduced thrust/power particularly at very low recorded percentage levels. To circumvent any potential problem with the validity of this data, a decision was made to only consider flights with recorded reduced thrust percentages greater or equal to one as being actual reduced thrust/power departures.

Specifics of the B737-800 ACARS Database:

- 58,921 Flights
- 504 Routes Departing 105 Airports
- 94.5% of All Departures Used Reduced Thrust/Power
- Average Reduced Thrust/Power was 15.5%

Chart 8 below, is a histogram of the B737-800 reduced thrust percentages. The explanation for the 2% reduced thrust/power spike is the same as with the B757. Chart 9, is the weight frequency or distribution.

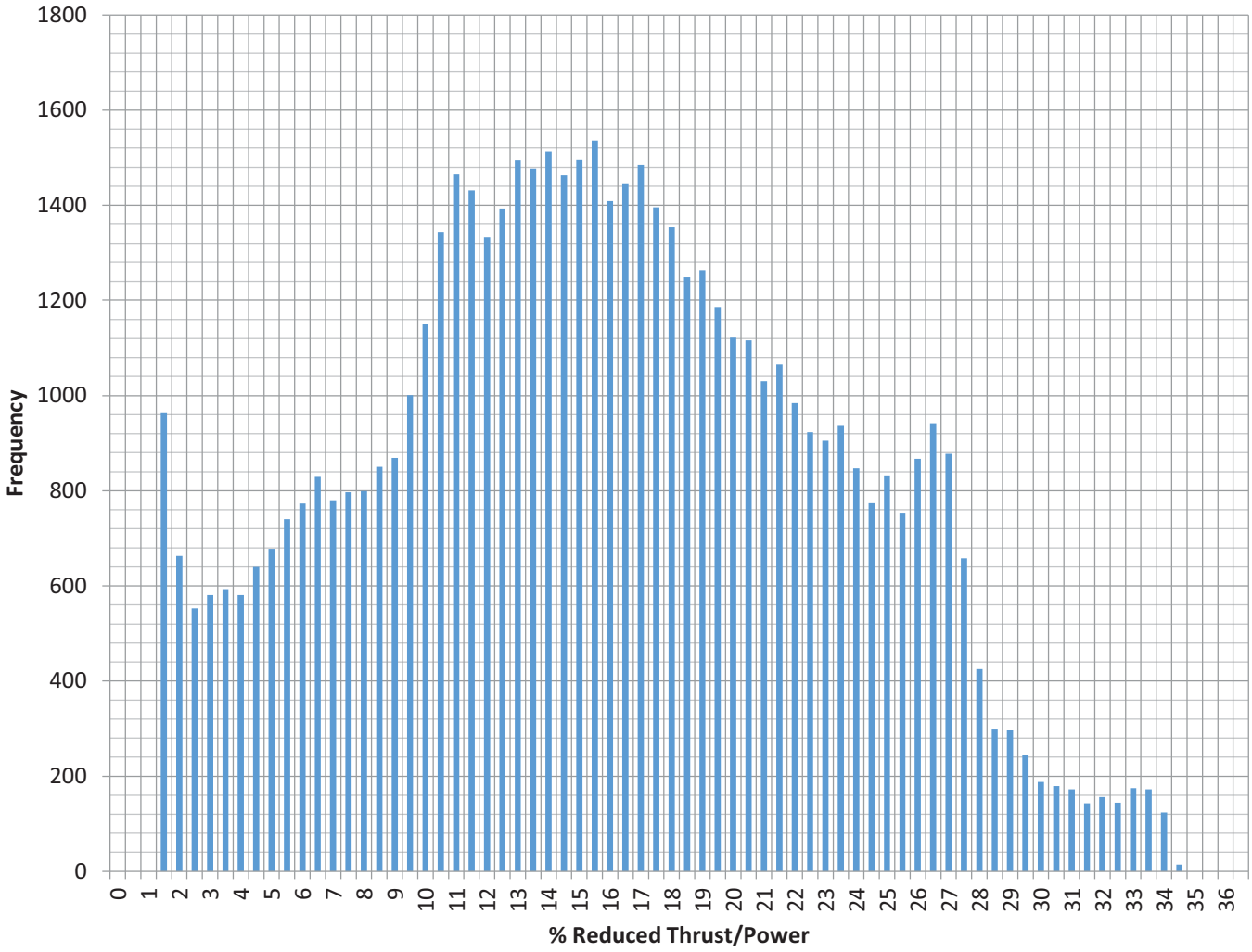
B737-800/CFM56-7B26
Frequency
1800
1600
1400
1200
1000
800
600
400
200
0
0 1 2 3 4 5 6 7 8 9 10 11 12 13 14 15 16 17 18 19 20 21 22 23 24 25 26 27 28 29 30 31 32 33 34 35 36
% Reduced Thrust/Power

CHART 8

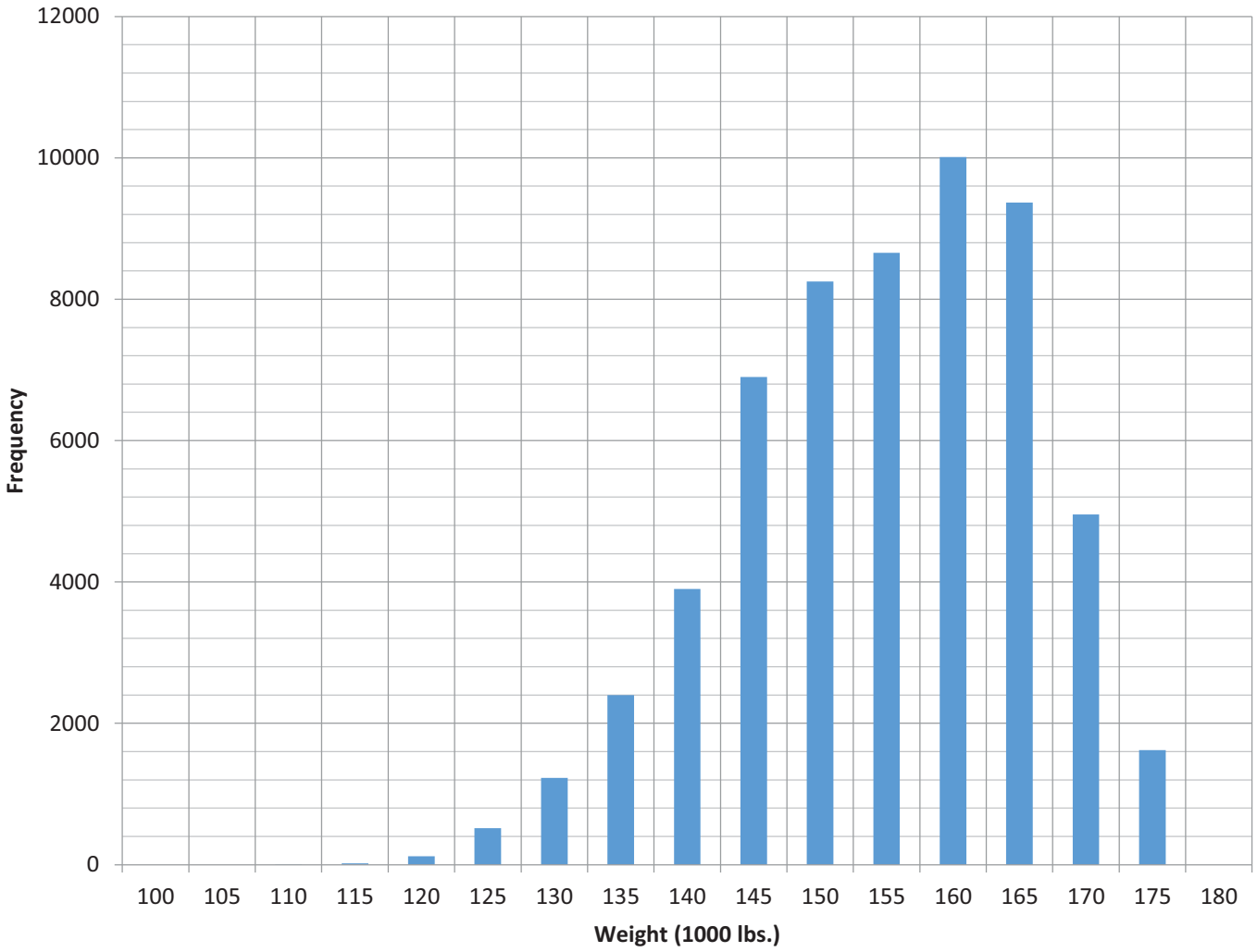
B737-800/CFM56-7B26
12000
10000
8000
6000
4000
2000
0
Frequency
100
105
110
115
120
125
130
135
140
145
150
155
160
165
170
175
180
Weight (1000 lbs.)

CHART 9

B737-800 AVERAGE ROUTE REDUCED THRUST RESULTS

ROUTE	AVG_WT	AVG_%DRATE		ROUTE	AVG_WT	AVG_%DRATE		ROUTE	AVG_WT	AVG_%DRATE
ANCMSP	171.4	4.4		ATLMSY	143.6	21.2		BNALAX	152.5	8.5
ANCSEA	148.9	16.4		ATLNCA	157.9	15.0		BOIMSP	144.2	16.1
ANCSLC	165.3	8.4		ATLOMA	146.0	17.3		BOISLC	137.2	19.7
ANUATL	154.9	15.1		ATLORD	149.5	17.1		BONATL	148.1	19.5
APAATL	161.2	12.0		ATLPAP	157.9	15.1		BOSATL	148.0	11.1
APAJFK	152.0	17.7		ATLPDX	165.4	5.1		BOSBDA	146.7	12.5
ATLANU	160.8	13.9		ATLPHX	160.8	8.6		BOSCVG	141.8	18.4
ATLAPA	162.1	11.7		ATLPTY	161.9	12.5		BOSDTW	144.2	14.2
ATLAUA	159.4	14.8		ATLPUJ	159.8	13.8		BOSJFK	138.3	21.9
ATLAUS	145.1	21.2		ATLPVR	158.9	11.0		BOSLAS	163.3	6.5
ATLBDA	156.9	12.8		ATLRDU	139.9	26.8		BOSLAX	166.5	5.4
ATLBDL	137.3	28.3		ATLROC	161.0	13.0		BOSMCO	142.1	18.0
ATLBGI	154.1	17.6		ATLRSW	148.6	22.5		BOSMSP	146.9	13.7
ATLBHM	140.1	23.8		ATLRTB	157.9	17.4		BOSSLC	165.1	5.5
ATLBNA	139.7	25.6		ATLSAL	161.6	8.8		BWIATL	139.7	26.0
ATLBON	147.4	20.7		ATLSAN	167.3	5.4		BWIDTW	144.8	20.9
ATLBOS	152.0	19.6		ATLSAT	147.6	15.9		BWISLC	162.9	10.3
ATLBWI	137.7	27.4		ATLSDF	139.6	24.8		BZELAX	155.0	15.4
ATLBZN	159.2	9.3		ATLSDQ	156.5	15.8		BZNATL	151.4	2.1
ATLCCS	157.8	14.6		ATLSEA	167.2	4.3		BZNSLC	136.9	11.5
ATLCHS	139.4	26.9		ATLSFO	169.1	3.9		CCSATL	146.7	20.3
ATLCLT	140.8	26.9		ATLSJC	166.1	5.2		CHSATL	137.7	23.0
ATLCMH	140.7	23.0		ATLSJD	159.8	10.2		CLTATL	139.4	27.2
ATLCOS	155.8	11.2		ATLSJO	161.1	13.4		CMHATL	139.2	22.8
ATLCUN	149.1	20.3		ATLSJU	161.2	13.0		CMHLAX	155.2	7.3
ATLCVG	144.4	21.8		ATLSKB	155.7	18.6		CMHMSP	140.2	16.7
ATLDCA	141.5	26.1		ATLSLC	161.4	8.5		COSATL	150.1	3.5
ATLDEN	155.4	11.4		ATLSLP	160.1	10.9		CUNATL	143.7	23.1
ATLDFW	147.8	18.8		ATLSMF	164.0	6.2		CUNCVG	141.6	22.6
ATLDSD	159.0	13.2		ATLSRQ	144.3	25.1		CUNDTW	155.8	17.4
ATLDTW	145.0	20.4		ATLSTL	141.7	24.0		CUNLAX	162.7	14.4
ATLFLL	147.8	21.7		ATLTPA	144.1	24.5		CUNMSP	159.0	15.3
ATLGDL	160.5	10.0		ATLTPP	159.8	13.5		CVGATL	141.7	26.6
ATLGSO	130.9	31.2		ATLUVF	164.8	10.9		CVGCUN	155.4	18.3
ATLGSP	140.9	25.7		ATLYVR	161.0	9.7		CVGFLL	141.9	20.7
ATLHSV	138.8	26.2		AUAATL	160.3	3.3		CVGLAS	155.3	19.2
ATLIAD	139.0	27.4		AUAJFK	157.6	4.9		CVGLAX	162.7	12.4
ATLIND	143.2	22.4		AUSATL	143.0	21.8		CVGMCO	145.1	24.5
ATLJAX	145.5	23.7		AUSDTW	143.2	16.3		CVGSEA	161.9	12.8
ATLJFK	149.7	21.3		AUSJFK	149.3	17.8		CVGSFO	165.9	11.8
ATLLAS	160.7	8.6		BDAATL	149.4	16.0		CVGSLC	156.1	18.8
ATLLAX	165.5	5.5		BDABOS	137.8	22.7		CVGTPA	144.2	25.4
ATLLGA	146.6	23.0		BDAJFK	133.1	22.9		CZMMSP	153.6	8.3
ATLLIR	156.8	15.6		BDLATL	148.5	16.2		DCAATL	142.0	14.5
ATLMBJ	152.4	17.5		BGIATL	154.8	17.6		DCADTW	137.3	14.0
ATLMCO	144.3	24.8		BGIJFK	151.2	19.3		DCAMSP	145.7	8.8
ATLMEM	138.6	25.9		BHMATL	133.8	27.3		DCASLC	157.3	2.2
ATLMEX	154.6	12.1		BILSLC	136.1	17.2		DENATL	152.7	5.4
ATLMIA	147.1	23.2		BJXLAX	139.8	11.4		DENDTW	144.6	10.2
ATLMSO	157.7	10.4		BNAATL	138.7	23.6		DENJFK	155.3	4.5
ATLMSP	151.2	16.5		BNADTW	141.7	15.6		DENMSP	142.1	11.1

TABLE 17

B737-800 AVERAGE ROUTE REDUCED THRUST RESULTS

ROUTE	AVG_WT	AVG_%DRATE		ROUTE	AVG_WT	AVG_%DRATE		ROUTE	AVG_WT	AVG_%DRATE
DFWATL	147.5	21.5		HSVATL	140.0	22.5		LASDTW	158.4	7.4
DFWDTW	146.6	21.6		IADATL	139.9	24.4		LASJFK	161.6	5.7
DFWSLC	145.3	23.6		INDATL	143.3	22.2		LASLAX	140.4	16.8
DSDATL	156.9	18.7		INDDTW	133.2	25.3		LASMEM	139.7	15.3
DSDJFK	155.9	19.3		INDLAX	158.0	14.5		LASMSP	146.2	13.5
DTWATL	146.4	21.4		INDMSP	131.8	27.1		LASRDU	148.8	11.2
DTWBNA	142.7	18.7		JAXATL	143.4	26.8		LASSEA	137.8	17.8
DTWBOS	146.7	19.3		JFKAPA	157.1	17.3		LASSLC	140.2	19.7
DTWBWI	134.5	22.8		JFKATL	149.9	23.3		LAXATL	157.5	18.2
DTWCUN	154.6	12.2		JFKAUA	160.0	14.2		LAXBJX	143.8	21.5
DTWDCA	133.8	23.1		JFKAUS	151.7	22.0		LAXBNA	152.7	16.1
DTWDEN	152.0	17.5		JFKBDA	143.5	23.5		LAXBOS	165.6	9.5
DTWDFW	143.7	23.1		JFKBGI	156.7	15.9		LAXBZE	162.0	11.6
DTWFLL	144.6	22.0		JFKBOS	141.3	27.8		LAXCMH	152.9	16.5
DTWIND	132.8	29.2		JFKDEN	161.4	16.5		LAXCUN	161.7	15.4
DTWJFK	140.8	20.1		JFKDSD	156.2	19.4		LAXCVG	158.2	17.2
DTWLAS	163.6	11.9		JFKDTW	145.7	21.8		LAXDTW	163.5	10.3
DTWLAX	167.0	10.3		JFKFLL	147.1	24.2		LAXGDL	156.5	18.2
DTWLGA	132.2	24.2		JFKGCM	152.3	18.9		LAXIND	151.5	17.1
DTWMCO	149.8	17.8		JFKGND	165.7	11.0		LAXLAS	133.1	24.9
DTWMEX	165.2	9.6		JFKKIN	143.5	20.5		LAXLIR	161.1	12.0
DTWMIA	150.2	17.4		JFKLAS	164.9	14.5		LAXMCO	164.1	10.4
DTWMKE	139.1	24.9		JFKLIR	157.1	16.6		LAXMEM	146.8	19.8
DTWMSP	145.2	24.3		JFKMBJ	155.9	19.0		LAXMIA	163.0	11.2
DTWMSY	139.4	22.4		JFKMCO	149.3	23.6		LAXMPR	150.2	22.7
DTWORD	130.2	25.5		JFKMEX	168.3	9.8		LAXMSP	152.5	16.6
DTWPDX	165.9	11.4		JFKMIA	151.3	22.4		LAXMSY	146.8	24.0
DTWPHL	128.9	28.1		JFKMSP	151.2	19.7		LAXMZT	137.4	23.3
DTWPHX	158.6	16.7		JFKMSY	152.0	19.3		LAXPHX	128.2	26.2
DTWPVR	160.6	13.9		JFKNAS	148.2	21.3		LAXPVR	149.1	23.2
DTWRDU	136.1	22.7		JFKNCA	159.8	15.1		LAXRDU	159.0	13.1
DTWRSW	152.6	13.9		JFKPAP	158.6	17.4		LAXSAL	161.8	11.8
DTWSAN	164.4	11.7		JFKPDX	169.6	9.2		LAXSEA	143.7	24.8
DTWSEA	166.9	10.0		JFKPHX	164.7	14.5		LAXSLC	143.8	26.2
DTWSFO	167.8	9.0		JFKPLS	151.9	18.9		LAXSLP	167.0	9.4
DTWSLC	157.4	15.1		JFKPUJ	158.9	17.9		LAXTPA	160.3	16.3
DTWTPA	145.9	16.9		JFKPVR	169.1	9.5		LAXZIH	141.7	21.5
DTWYVR	162.9	12.6		JFKSAN	168.5	9.7		LAXZLO	135.5	23.5
FLLATL	139.9	22.8		JFKSAT	149.5	20.2		LGAATL	147.6	8.3
FLLCVG	144.8	16.2		JFKSDQ	157.4	18.5		LGADTW	136.7	16.0
FLLDTW	149.0	16.8		JFKSEA	170.3	8.3		LGAMCO	135.1	16.3
FLLJFK	142.3	20.5		JFKSJU	156.1	19.0		LGAMSP	138.0	12.9
FLLLGA	140.8	19.6		JFKSLC	164.3	14.8		LGANCA	156.5	2.8
FSDMSP	138.2	16.2		JFKSTI	153.4	21.0		LIRATL	154.0	12.9
GCMJFK	131.3	20.2		JFKTPA	144.9	25.9		LIRJFK	152.7	13.8
GDLATL	147.2	9.1		JFKTPP	161.8	16.3		LIRLAX	160.5	10.6
GDLLAX	151.9	6.9		JFKUVF	155.2	17.3		LIRMSP	162.9	5.3
GEGSLC	139.3	20.7		JFKYVR	167.2	11.5		MBJATL	151.2	14.2
GNDJFK	161.0	6.7		LASATL	156.3	8.9		MBJJFK	154.4	12.1
GSOATL	134.3	30.1		LASBOS	152.4	10.0		MCISLC	138.3	23.6
GSPATL	140.5	26.9		LASCVG	151.2	12.2		MCOATL	143.8	24.0

TABLE 18

B737-800 AVERAGE ROUTE REDUCED THRUST RESULTS

ROUTE	AVG_WT	AVG_%DRATE		ROUTE	AVG_WT	AVG_%DRATE		ROUTE	AVG_WT	AVG_%DRATE
MCOBOS	150.3	18.5		MSPSEA	158.5	7.3		RDUSLC	157.7	14.2
MCOCVG	141.3	25.5		MSPSFO	156.9	10.9		RNOSLC	135.8	5.7
MCODTW	149.8	21.8		MSPSLC	150.5	17.3		ROCATL	160.6	3.3
MCOJFK	147.8	23.1		MSPSTL	137.3	22.7		RSWATL	139.0	25.5
MCOLAX	167.8	9.0		MSPTPA	148.9	15.2		RSWDTW	152.0	23.0
MCOLGA	141.1	28.5		MSPYVR	152.7	9.2		RTBATL	149.0	6.2
MCOMSP	152.4	20.3		MSYATL	141.6	17.5		SALATL	152.2	16.4
MCOSLC	162.8	11.7		MSYDTW	146.9	9.2		SALLAX	160.7	14.5
MDWMSP	124.5	18.3		MSYJFK	148.2	13.8		SANDTW	160.9	3.6
MEMATL	139.5	26.2		MSYLAX	147.8	13.6		SANJFK	161.5	3.7
MEMLAS	138.6	26.4		MSYMSP	145.4	12.7		SANMSP	153.6	7.7
MEMLAX	146.8	20.6		MZTLAX	131.0	24.1		SANSEA	142.9	14.7
MEXATL	149.2	3.3		NASJFK	143.2	21.7		SANSLC	141.6	15.6
MEXDTW	144.8	4.5		NCAATL	158.5	4.7		SATATL	142.5	15.3
MEXJFK	151.7	2.4		NCAJFK	160.5	3.3		SATJFK	147.7	11.9
MIAATL	145.6	24.4		NCALGA	159.3	4.2		SATSLC	148.3	11.7
MIADTW	151.7	20.7		OAKSLC	137.2	30.0		SDFATL	138.5	19.4
MIAJFK	148.8	18.5		OMAATL	139.9	19.7		SDQATL	158.0	18.3
MIALAX	162.1	11.8		OMAMSP	136.8	22.4		SDQJFK	155.5	19.3
MKEDTW	143.7	14.2		ONTSLC	136.1	25.8		SEAANC	151.2	18.4
MKEMSP	138.8	20.5		ORDATL	138.6	20.8		SEAATL	166.2	10.4
MPRLAX	148.3	21.1		ORDDTW	143.0	23.4		SEACVG	156.3	16.8
MSOATL	154.2	5.2		ORDMSP	140.1	23.3		SEADTW	160.5	14.6
MSPANC	171.9	5.2		PAPATL	150.3	18.8		SEAJFK	167.7	10.8
MSPATL	150.3	19.2		PAPJFK	151.4	14.3		SEALAS	137.1	25.9
MSPAUS	139.1	21.9		PDXATL	162.7	8.4		SEALAX	148.4	20.6
MSPBOI	152.6	16.3		PDXDTW	160.4	11.3		SEAMSP	155.7	16.7
MSPBOS	151.7	10.1		PDXJFK	165.9	7.3		SEAPVR	155.6	17.5
MSPCMH	139.6	21.4		PDXMSP	154.0	14.4		SEASAN	148.7	20.1
MSPCUN	159.0	9.9		PDXSLC	143.2	21.0		SEASLC	144.7	22.9
MSPCZM	152.3	13.3		PHLATL	146.6	24.0		SFOATL	155.2	11.5
MSPDCA	144.5	15.5		PHLDTW	145.3	24.9		SFOCVG	156.8	12.9
MSPDEN	151.0	12.7		PHXATL	153.0	13.1		SFODTW	162.6	7.7
MSPDTW	144.3	22.1		PHXDTW	157.3	10.7		SFOMSP	156.9	10.7
MSPFSD	140.8	24.3		PHXJFK	159.9	10.1		SFOSLC	135.2	22.6
MSPIND	134.0	24.2		PHXLAX	139.0	24.0		SJCATL	160.6	11.9
MSPJFK	144.2	15.9		PHXMSP	152.2	14.0		SJCSLC	140.1	26.5
MSPLAS	154.0	12.9		PHXSLC	142.3	19.2		SJDATL	153.0	15.7
MSPLAX	155.6	13.3		PLSJFK	142.0	21.0		SJOATL	156.4	5.9
MSPLGA	147.3	14.7		PTYATL	157.9	6.8		SJUATL	159.7	8.8
MSPLIR	165.4	8.7		PUJATL	156.6	16.1		SJUJFK	153.9	12.9
MSPMCO	148.1	16.0		PUJJFK	156.0	16.6		SKBATL	148.4	14.0
MSPMDW	127.7	25.8		PVRATL	150.6	19.7		SLCABQ	126.4	22.6
MSPMKE	134.3	22.0		PVRDTW	144.2	21.7		SLCANC	165.4	1.8
MSPMSY	141.2	20.5		PVRJFK	155.1	17.2		SLCATL	158.1	5.5
MSPOMA	138.9	24.5		PVRLAX	144.8	22.1		SLCBIL	138.2	16.6
MSPORD	142.7	20.3		PVRSEA	158.1	15.9		SLCBOI	139.0	15.4
MSPPDX	156.5	8.9		RDUATL	141.4	26.1		SLCBOS	161.3	4.1
MSPPHX	153.4	13.9		RDULAS	146.5	20.0		SLCBWI	157.8	5.5
MSPRDU	142.0	18.1		RDULAX	159.3	12.8		SLCBZN	141.6	14.6
MSPSAN	156.6	11.7		RDUMSP	142.7	22.5		SLCCVG	155.0	6.3

TABLE 19

B737-800 AVERAGE ROUTE REDUCED THRUST RESULTS

ROUTE	AVG_WT	AVG_%DRATE
SLCDCA	154.6	6.6
SLCDFW	146.5	9.5
SLCDTW	154.5	6.4
SLCGEG	144.9	11.2
SLCJFK	159.6	5.2
SLCLAS	138.5	16.8
SLCLAX	144.2	14.1
SLCMCI	141.1	14.6
SLCMCO	160.2	4.8
SLCMSP	146.4	10.8
SLCOAK	139.5	15.8
SLCONT	140.9	14.9
SLCPDX	146.1	11.3
SLCPHX	139.6	13.9
SLCRDU	156.3	4.3
SLCRNO	139.9	16.6
SLCSAN	142.7	13.4
SLCSAT	149.4	9.4
SLCSEA	145.5	11.9
SLCSFO	140.1	14.4
SLCSJC	140.6	16.3
SLCSMF	141.5	12.9
SLPATL	157.3	15.7
SLPLAX	162.9	13.1
SMFATL	161.8	8.6
SMFMSP	156.3	10.5
SMFSLC	141.8	24.1
SRQATL	141.7	20.4
STIJFK	152.7	12.2
STLATL	141.9	19.4
STLMSP	134.2	22.3
TPAATL	144.8	26.1
TPACVG	145.1	25.7
TPADTW	145.0	22.5
TPAJFK	142.8	23.6
TPALAX	163.3	14.0
TPPATL	151.4	11.1
TPPJFK	155.1	10.3
UVFATL	162.2	9.2
UVFJFK	149.3	17.1
YVRDTW	160.6	15.4
YVRJFK	162.2	15.2
YVRMSP	150.8	20.8
ZIHLAX	135.0	21.5
ZLOLAX	130.4	20.1

TABLE 20

B767-300ER/CF680C2-7B26

Reduced Power/Thrust Determination:

The initial ACARS database was reduced, by a number of actions to 12,243 flights. Flights were removed from the database for the following reasons:

- Obvious data recording errors
- Missing essential data (aircraft weight, origin, destination, or de-rate)
- Charter, maintenance, or other non-revenue positioning flights
- An imposed minimum of 5 flights for any city pair (origin and destination)

In addition to the database edits above, there still remained a number of suspect entries for percent reduced thrust/power particularly at very low recorded percentage levels. To circumvent any potential problem with the validity of this data, a decision was made to only consider flights with recorded reduced thrust percentages greater or equal to one as being actual reduced thrust/power departures.

Specifics of the B767-300ER ACARS Database:

- 11,360 Flights
- 179 Routes Departing 61 Airports
- 92.8% of All Departures Used Reduced Thrust/Power
- Average Reduced Thrust/Power was 12.3%

Chart 10 below, is a histogram of the B767-300ER reduced thrust percentages. The explanation for the 2% reduced thrust/power spike is the same as with the B757. Chart 11, is the weight frequency or distribution.

B767-300ER/CF680C2-B6F

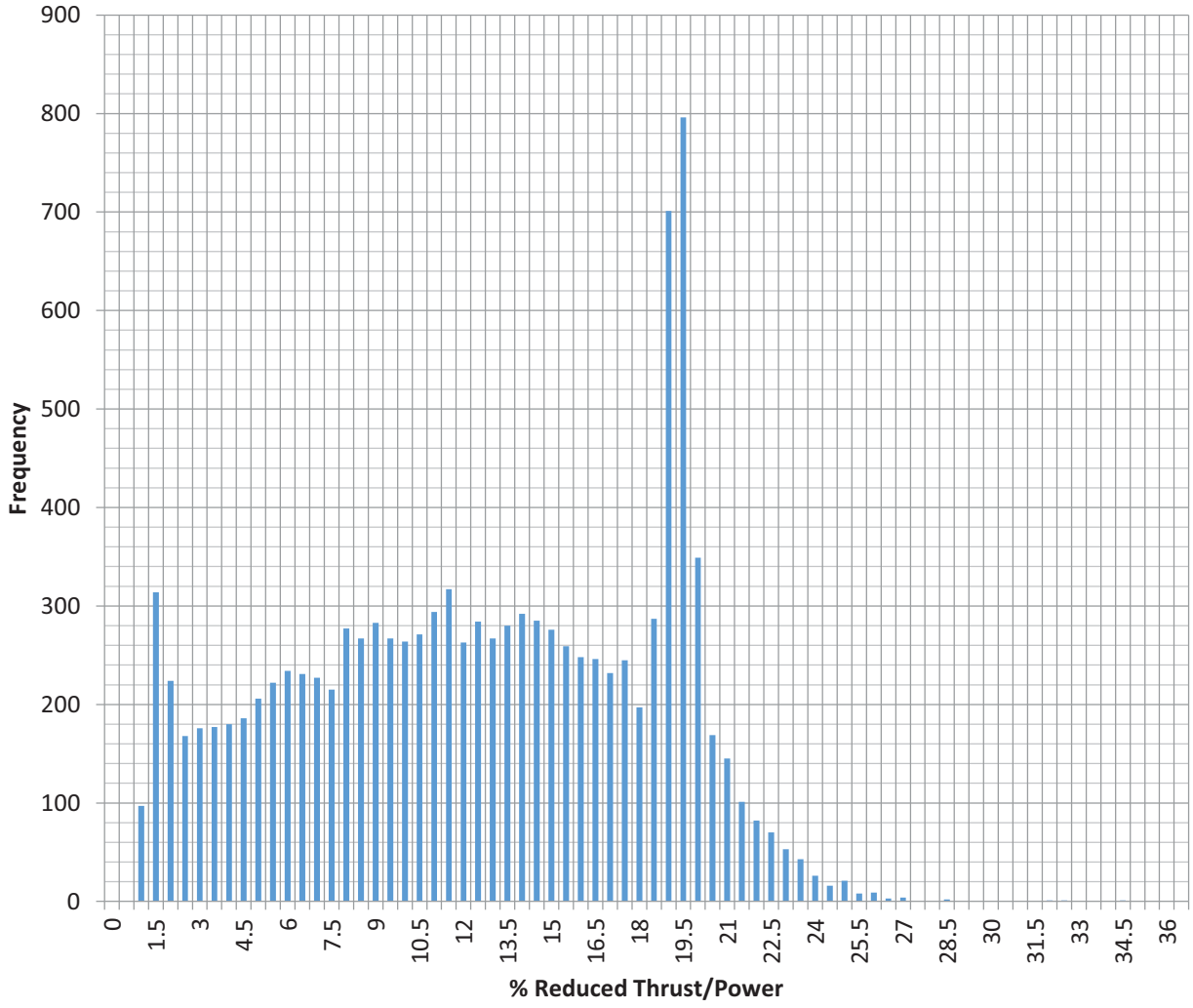

CHART 10

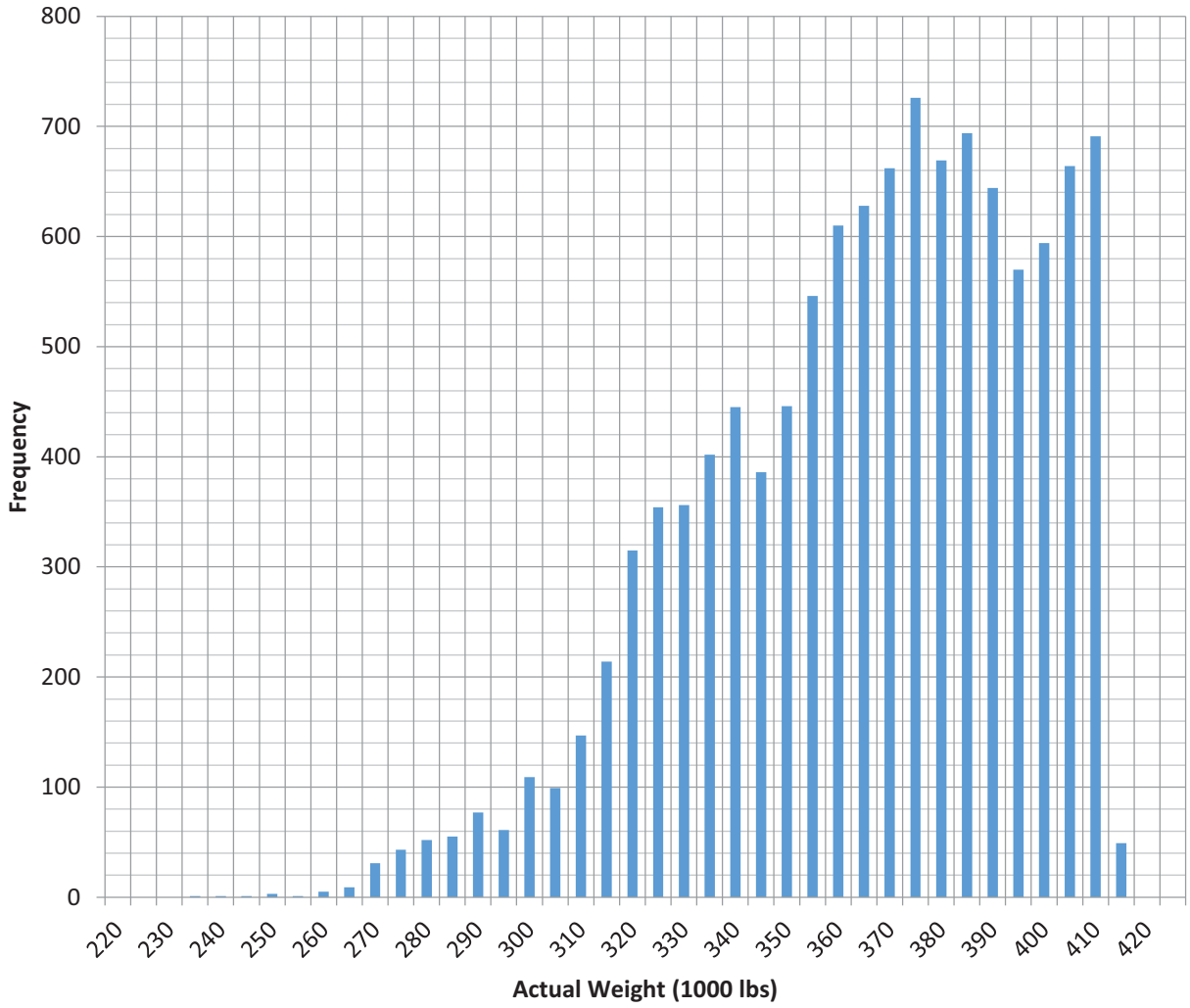
B767-300ER/CF680-C2B6
Frequency
800
700
600
500
400
300
200
100
0
220
230
240
250
260
270
280
290
300
310
320
330
340
350
360
370
380
390
400
410
420
Actual Weight (1000 lbs)

CHART 11

B737-800 AVERAGE ROUTE REDUCED THRUST RESULTS

ROUTE	AVG_WT	AVG_%DRATE		ROUTE	AVG_WT	AVG_%DRATE
AMSATL	388.8	6.9		CDGEWR	359.0	15.7
AMSBOM	396.5	5.9		CDGJFK	365.3	13.3
AMSDTW	372.8	10.8		CDGORD	370.8	12.6
AMSEWR	369.7	12.0		CDGSEA	378.5	11.7
AMSJFK	369.1	12.8		CDGSLC	389.3	9.5
AMSPDX	387.5	5.5		CPHJFK	360.6	14.9
ANCATL	344.0	8.7		CVGCDG	354.1	15.6
ATLAMS	373.3	11.0		DTWAMS	354.7	15.2
ATLBRU	366.5	11.2		DTWATL	292.2	19.7
ATLCDG	363.7	13.3		DTWCDG	351.2	18.1
ATLDTW	290.1	20.3		DTWGRU	390.9	7.5
ATLDUB	359.6	14.2		DTWLHR	353.5	15.8
ATLDUS	360.9	13.3		DTWSFO	310.0	20.7
ATLEZE	396.0	7.4		DUBATL	366.7	6.1
ATLFCO	382.5	9.3		DUBJFK	352.9	9.7
ATLFLL	277.8	21.1		DUSATL	387.1	3.5
ATLGIG	394.5	5.8		EWRAMS	345.7	15.1
ATLGRU	384.4	9.6		EWRCDG	338.7	16.6
ATLJAX	279.6	18.2		EZEATL	396.8	5.3
ATLJFK	300.3	21.1		FCOATL	402.7	7.4
ATLLAS	314.9	19.1		FCOJFK	399.0	7.8
ATLLAX	326.3	17.7		FLLATL	278.5	20.1
ATLLHR	362.8	12.6		FRAJFK	373.5	13.3
ATLLIM	354.2	16.6		FUKHNL	333.5	16.0
ATLLOS	401.9	4.5		GIGATL	394.5	7.4
ATLMAD	363.0	14.1		GRUATL	377.2	6.5
ATLMAN	358.1	14.1		GRUDTW	385.7	4.5
ATLMCO	275.1	19.4		HKGNRT	325.8	20.5
ATLMUC	376.9	9.9		HNDLAX	379.2	3.5
ATLMXP	376.5	9.7		HNDSEA	355.4	8.3
ATLPDX	317.1	18.7		HNLFUK	354.0	18.1
ATLSAN	310.3	19.3		HNLLAX	335.4	20.5
ATLSCL	388.1	8.2		HNLNGO	349.9	18.3
ATLSEA	330.5	17.0		HNLNRT	357.3	17.1
ATLSFO	321.2	18.1		ICNSEA	388.8	10.4
ATLSLC	309.5	19.8		ISTJFK	393.3	4.5
ATLSTR	370.5	10.8		JAXATL	264.3	17.5
ATLTPA	277.5	19.0		JFKAMS	349.1	18.5
ATLVCE	363.5	12.7		JFKATL	297.3	19.8
ATLZRH	371.6	11.2		JFKBCN	354.8	16.9
BCNJFK	379.9	6.3		JFKBRU	346.0	17.9
BOMAMS	396.4	5.1		JFKCDG	351.0	17.7
BOSATL	294.6	18.2		JFKCPH	346.1	19.1
BOSCDG	338.7	12.1		JFKDUB	348.5	17.8
BOSLHR	328.2	13.9		JFKFCO	360.8	15.9
BRUATL	381.2	5.5		JFKFRA	354.5	16.9
BRUJFK	363.2	9.6		JFKIST	377.1	13.2
CDGATL	380.6	11.6		JFKLAX	335.6	19.2
CDGBOS	343.1	18.1		JFKLHR	338.0	18.7
CDGCVG	370.4	13.2		JFKMAD	349.2	16.5
CDGDTW	364.5	14.0		JFKNCE	340.3	20.2

TABLE 21

B737-800 AVERAGE ROUTE REDUCED THRUST RESULTS

ROUTE	AVG_WT	AVG_%DRATE		ROUTE	AVG_WT	AVG_%DRATE
JFKPRG	358.0	17.1		SCLATL	399.0	5.5
JFKSEA	329.3	19.5		SEAATL	322.0	18.9
JFKSFO	315.2	19.3		SEACDG	372.7	12.4
JFKSVO	383.6	11.4		SEAHND	361.8	15.0
JFKTSE	390.3	9.6		SEAICN	392.3	9.5
JFKVCE	359.1	15.8		SEAJFK	328.0	18.7
JFKZRH	337.3	20.6		SEAKIX	385.0	10.6
KIXSEA	380.6	11.4		SEALHR	355.1	16.0
LASATL	301.6	21.7		SEANRT	396.5	2.9
LAXATL	318.4	19.2		SEAPEK	395.8	7.8
LAXDTW	318.2	19.2		SEAPVG	395.7	7.9
LAXHND	397.8	5.0		SFOATL	310.4	20.0
LAXHNL	344.0	16.1		SFODTW	305.5	20.0
LAXJFK	335.6	18.2		SFOJFK	306.0	19.4
LHRATL	371.8	12.3		SFONRT	385.7	7.5
LHRBOS	340.3	17.4		SJUATL	317.9	18.5
LHRDTW	356.6	15.6		SLCATL	302.2	19.1
LHRJFK	360.1	14.6		SLCCDG	369.4	6.8
LHRSEA	363.2	14.5		STRATL	390.2	5.3
LIMATL	375.4	11.3		SVOJFK	381.5	10.0
LOSATL	402.3	7.8		TPAATL	269.4	18.6
LOSSJU	399.8	8.5		TSEJFK	400.2	7.3
MADATL	395.4	6.5		TSEROB	294.3	22.7
MADJFK	379.3	8.4		VCEATL	396.7	6.4
MANATL	377.2	8.2		VCEJFK	374.7	9.9
MCOATL	274.5	20.0		ZRHATL	386.4	7.6
MCODTW	281.8	19.8		ZRHJFK	362.0	12.7
MSPLAX	307.0	19.3				
MUCATL	400.4	5.0				
MXPATL	391.5	4.2				
NCEJFK	364.8	8.8				
NGOHNL	341.7	19.1				
NRTHKG	317.8	18.9				
NRTHNL	346.0	18.9				
NRTPDX	384.2	11.6				
NRTPEK	314.4	18.2				
NRTPVG	319.0	20.5				
NRTSEA	381.8	9.0				
NRTSFO	386.0	11.1				
ORDCDG	353.9	9.5				
PDXAMS	377.5	10.3				
PDXATL	310.0	18.6				
PDXNRT	388.9	7.3				
PEKNRT	323.4	18.8				
PEKSEA	393.2	8.6				
PRGJFK	372.8	8.8				
PVGNRT	319.7	19.8				
PVGSEA	400.4	8.6				
ROBTSE	275.8	18.1				
SANATL	299.1	20.2				

TABLE 22

Departure Profile Impact:

To assess the impact of the weight differences and the use of reduced thrust versus full rated takeoff thrust using the FAA's All Engine Climb Program and the procedures provided in this section:

Weight Impact:
Use the tabular data provided for each aircraft and generate a profile with the AEDT estimated weight and one at either the actual average weight in the table or the weight generated by the suggested regression. Compare the resulting profiles or enter them into the AEDT to produce noise and emission differences.

Reduced Thrust/Power Impact:
Using the tabular data provided for each aircraft generate a profile with the weight shown at both full rated takeoff power and the average percentage of reduced thrust given. As with the weight impact above, compare the resulting profiles or enter them into the AEDT to produce noise and emission differences.

All Engine Climb Departure Procedures:

PROCEDURE 1: CLOSE-IN OR NADP1 (See Notes 3 and 4 below)

1) Takeoff and Climb at V2 + 15 knots to 800' AFE (retracting gear at 400')
2) At 800' AFE, Reduce Power to Maximum Climb
3) Continue Constant Speed Climb to 3000' AFE
4) At 3000' AFE, Reduce Pitch to 10^0-12^0, Accelerate and Retract Flaps per Manufacturer's Flap Speed Schedule. See Note 1 below.
5) Constant Speed Climb at 250 knots (IAS) to 10,000' AFE. See Note 2 below
6) At 10,000' AFE Transition to Normal Enroute Climb.

PROCEDURE 2: DISTANT OR NADP2 (See Notes 3 and 4 below)

1) Takeoff and Climb at V2 + 15 knots to 800' AFE (retracting gear at 400')
2) At 800' AFE, Reduce Power to Maximum Climb While Simultaneously Reducing Pitch to 10^0-12^0, Accelerate and Retract Flaps per Manufacturer's Flap Speed Schedule. See Note 1 below.
3) At Zero Flap or Clean Speed, if Below 3000' AFE, Constant Speed Climb to 3000' AFE. See Note 2 below.
4) At 3000' AFE, Accelerate to 250 knots (IAS)
5) Constant Speed Climb to 10,000' AFE
6) At 10,000' AFE Transition to Normal Enroute Climb.

NOTES:

1. Acceleration segment thrust split 45% Vertical, 55% Horizontal
2. Thrust split 50% Vertical, 50% Horizontal
3. Repeating the above procedures at both 1000' and 1500' AFE will represent the majority of air carrier departure procedures.
4. Takeoff Flap Setting:
    a. B737: Flap 01and 05

b. B757and B767, Flap 05 and 15

Conclusions

Takeoff Weight Determination:

The regressions developed from operational flight planning databases represented a definite improvement in aircraft specific takeoff weight determination. The existing AEDT Stage Length methodology can lead to discrepancies in weight determination which in turn leads to errors in the aircraft departure profile and subsequently errors in the noise and emission levels. Implementation of the regressed equations into the AEDT is not complex and the required information from the user is easily attained from a number of sources.

Reduced Thrust (Level and Usage):

The analysis of the significantly large ACARS databases presented the first known definitive data regarding the air carrier use of reduced thrust/power for departure. The high percentage of use confirms not only that the use of full rated takeoff power is very small but that existing noise and emissions inventories attributed to aircraft departures requires reexamination.

While there may be some discussion of whether one carrier's data is representative of industry practices, it is a fact the maximum certified reduced thrust level for a specific airframe/engine combination is the same for each carrier. As also stated in this report, different levels of use for departure can only result from the choices provided to the flight crew. Since a number of carrier's have reported various options presented to their respective flight crews that, in itself, confirms the comment in this report regarding the pilot community response to reduced thrust/power departures. Simply based on the population size of the ACARS databases used in this research, it would require a large operational database from another carrier which produced a significantly different result to alter the results of this analysis.

References

1. Forsyth, David W.; Gulding, John; DiPardo, Joseph: "Review of Integrated Noise Model (INM) Equations and Processes", NASA/CR-2003-212414 (May 2003)

Project 036 Parametric Uncertainty Assessment for AEDT 2b

Georgia Institute of Technology

Project Lead Investigator

Principal Investigator:
Professor Dimitri N. Mavris
Director
Aerospace Systems Design Laboratory
School of Aerospace Engineering
Georgia Institute of Technology
Phone: (404) 894-1557
Fax: (404) 894-6596
Email: dimitri.mavris@ae.gatech.edu

Co-Principal Investigator:
Dr. Dongwook Lim
Chief, Air Transportation Economics Branch
Aerospace Systems Design Laboratory
School of Aerospace Engineering
Georgia Institute of Technology
Phone: (404) 894-7509
Fax: (404) 894-6596
Email: dongwook.lim@ae.gatech.edu

- FAA Award Number: 13-C-AJFE-GIT, Amendment 019 and Amendment 029
- Period of Performance: May 1, 2016 – April 30, 2017
- Task(s):
    1. Proper Definition of AEDT Input Parameter Uncertainty
    2. Verification and Validation plus Capability Demonstrations
    3. Identification of Important Output to Input Relationships (Optional)
    4. Guidelines for Future Tool Research
- Augmented Task(s):
    1. Use Case A – Inventory Analysis
    2. Use Case B and C– NEPA/CAA Analysis
    3. Use Case D – Part 150 Analysis
    4. Use Case E – Part 1: Air Traffic Airspace and Procedure Analysis

Project Funding Level

According to the original project plan, the funding from the FAA is $175,000 for 12 months. The Georgia Institute of Technology has agreed to a total of $175,000 in matching funds. The project was augmented for the period for 12/1/2016 to 3/31/2017 to add additional tasks. The augmented funding from the FAA is $80,000 for 4 months. The Georgia Institute of Technology has agreed to additional $80,000 in matching funds.

Investigation Team

Prof. Dimitri Mavris, Dr. Michelle Kirby, Dr. Dongwook Lim, Dr. Yongchang Li, Dr. Matthew Levine, Evanthia Kallou (Graduate student), Junghyun Kim (Graduate student), with consultation/support by research staff Dr. Holger Pfaender.

Project Overview

The Federal Aviation Administration's Office of Environment and Energy (FAA/AEE) has developed a comprehensive suite of software tools that allow for a thorough assessment of the environmental effects of aviation, in particular the ability to assess the interdependencies between aviation-related noise and emissions, performance, and cost. At the heart of this tool suite is the high fidelity Aviation Environmental Design Tool (AEDT). AEDT is a software system that models aircraft performance in space and time to estimate fuel consumption, emissions, noise, and air quality consequences. This software has been developed by the FAA Office of Environment and Energy for public release. It is the next generation FAA environmental consequence tool. AEDT satisfies the need to consider the interdependencies between aircraft-related fuel consumption, emissions, and noise. AEDT has been released in two phases. The first version, AEDT 2a, was released in March 2012 [US FAA, 2014]. The second version of AEDT 2b was released in May 2015. AEDT is scheduled to be updated three times in the next 12 months, and ultimately a full new version should be available in the next three to five years.

This uncertainty quantification comprehensively assesses the accuracy, functionality, and capabilities of AEDT during the development process. The major purposes of this effort are to:

- Contribute to the external understanding of AEDT
- Build confidence in AEDT's capability and fidelity (ability to represent reality)
- Help users of AEDT to understand the sensitivities of output response to the variation of input parameters/assumptions
- Identify gaps in functionality
- Identify high-priority areas for further research and development

The uncertainty quantification consists of verification and validation, capability demonstrations, and parametric uncertainty/sensitivity analysis.

Task 1 Design Test Cases to Test the Functionalities and Capabilities of AEDT

Objective(s)

The first step in the UQ effort is to properly define the problem. For each of the AEDT 2b and 2c service pack releases, GT defined the scope of the UQ effort identifying the key changes to the AEDT versions from the previous releases. Depending on the type of updates incorporated, it would be necessary to identify the key sources of uncertainties and the best approach to conduct V&V and parametric uncertainty analysis in Task 2 and Task 3. Depending on the analysis scope of the V&V, Task 3 Parametric UQ can be optional. The outcome of this task is the definition of analysis scope, required tools, required data, V&V method, parametric UQ method, and a list of input parameters to vary and their uncertainty bounds. Due to the dynamic nature of the agile AEDT development process, it is important that the GT team remains flexible in the choice of the V&V approach and the work scope. GT will use the best available methods and data in order to ensure accuracy and functionalities of future AEDT versions based on the discussion with the FAA/AEE.

Research Approach

FAA/AEE's AEDT has been the official environmental consequence modeling tool for US and ICAO CAEP for many years. In order to provide the best possible environmental impacts modeling capabilities, the FAA/AEE continues to develop AEDT by improving existing modeling methods and data and adding new functionalities. The AEDT development team led by Volpe has been exercising the agile development process, as shown in Figure 1, where minor updates are released in a new Sprint version every three weeks. Major updates and/or new functionalities are incorporated as new service packs or feature packs in about a three months cycles (Table 1). An AEDT development cycle includes rigorous testing of all levels of software functionality from the individual modules to the overall system. However, the FAA/AEE seeks a robust uncertainty quantification effort in addition to this test program.

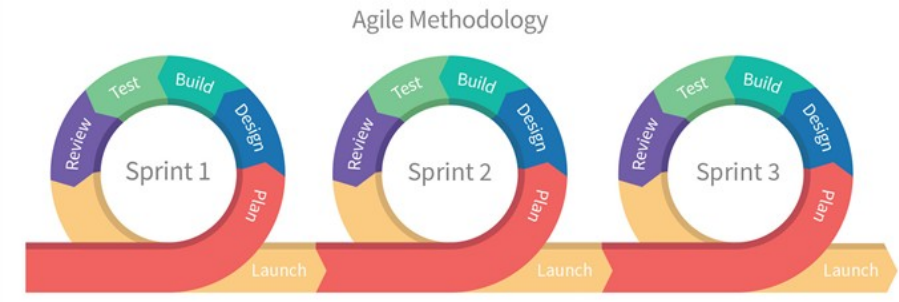

Figure 1: The Agile Methodology [Source: http://www.screenmedia.co.uk]

Table 1: AEDT Development and Public Release Schedule

Dates	Milestones
5/1/2016	Project Start
6/13/2016	AEDT 2b SP3 Release
9/12/2016	AEDT 2c Release
12/5/2016	AEDT 2c SP1 Release
3/13/2017	AEDT 2c SP2 Release
4/30/2017	Project End

For each of the AEDT sprint releases, GT reviewed the AEDT requirement documents and AEDT release notes to identify the key additional features and functionalities that need to be tested. During the period of research period of May 2016 and December 2016, ten versions of AEDT were released including three public releases of AEDT 2b SP3, AEDT 2c, and AEDT 2c SP1, as listed in Table 1.

The main features/capabilities that were added to AEDT during the period include the following:

- Thrust type other (TTO) aircraft emissions
- VALE report
- EDMS2ASIF converter and EDMS to AEDT Importer
- Background emission concentration
- Improved nvPM methods
- Environmental Justice (EJ)
- Time audible (TAUD) noise metrics
- Number Above (NA) noise metrics

GT has either completed or in the process of performing V&V and capability demonstration of the new features listed above. The details on the V&V process are discussed in Task 2.

Task 2 Verification and Validation plus Capability Demonstrations

Objective(s)

In Task 2, GT conducted V&V and capability demonstrations of the newly released AEDT versions. The analysis in this task can take a couple of different approaches depending on the type of updates and data availability. In the past UQ efforts, one of the most important methods of ensuring confidence in the tool capability was to conduct a use case(s) using both legacy tools and the new AEDT release and compare the results. This method would be the most appropriate way whenever a legacy tool has the same or similar functionalities and a validated use case has been modeled in that legacy tool. When the new functionality of AEDT does not exist in the legacy tools, the V&V exercise should use direct comparisons to the results generated by the mathematical algorithms behind the newly added functionality and/or real world data whichever available.

Research Approach

Starting from May 2016, GT has tested all the new AEDT versions released including Sprints from 70 to 79. Sprints 70 – 79 included three public versions of AEDT, namely AEDT 2b SP3, AEDT 2c, and AEDT 2c SP1. GT tested the ten versions of AEDT focusing on new features and capabilities added. Some of the new features/capabilities were minor updates to the GUI, bug fixes, or data updates. Major updates included improved VALE reporting capability, implementation of TTO aircraft fuel burn and emission calculations, implementation of Environmental Justice capability, the addition of TAUD and NA noise metrics, improved nvPM calculations, the addition of background emission concentration, and new features on emission dispersion display.

In order to understand the background of new AEDT features, GT reviewed the relevant documents including the software requirement documents, Database Design Documents (DDD), AEDT sprint release notes, updated technical manual [US FAA, 2012, 2016], user manual [US FAA, 2014,2016], and research papers/reports [Noel, 2010 and 2011; Willcox, 2010; Allaire and Willcox, 2010; EUROCONTROL, 2009]. GT has conducted basic testing of all the new AEDT versions to confirm its functionality. While some of the tests are in progress, the next subsections discuss the current progress and findings in more details.

Thrust Type Other Aircraft Fuel Burn and Emissions

In Sprint 67 of AEDT 2b, the Boeing Fuel Flow Method 2 (BFFM2) for estimating aircraft emissions was applied to ANP airplanes that are designated as having a thrust setting type that is recognized as 'other' by the AEDT 2b Aircraft Performance Module (APM). All thrust type settings besides pounds thrust (THRUST_SET_TYPE = B) are recognized as 'other' by the APM and, prior to Sprint 67, produced a 0 value for all emissions results when flown in AEDT 2b. The ANP airplanes affected by the application of the BFFM2 in sprint 67 map to 192 airframe and engine combinations in the FLEET database, 134 of which can be mapped to EDMS aircraft by airframe model and engine model. For convenience, these aircraft are referred to as Thrust Type Other (TTO) aircraft. This task was focusing on testing if AEDT 2b can produce emission results for TTO aircraft using BFFM2 and validating the emission results against EDMS emission results.

GT obtained the EDMS study 'STUDY_DULLES_TTO' containing a single departure and arrival for each of the TTO aircraft as well as single departure and arrival helicopter operations at Washington Dulles International Airport. In addition, GT obtained the EDMS 5.1.4 program for running the EDMS study. The EDMS study was first exported as a text file and then was used along with the schedule file to create an AEDT 2b study using the EDMS2ASIF converter. It was found that the AEDT study created does not have taxi time specified. The AEDT study was modified to contain taxi time in mode durations matching those of EDMS taxi operations. In addition, it was found that the weather (specifically, temperature) was different for the DULLES airport between AEDT and EDMS. Thus, the temperature in AEDT was modified to match the temperature in EDMS. Then both the AEDT and EDMS studies were run. Table 2 shows the comparison of fuel burn and emission results.

Table 2: Fuel Burn and Emission Comparison between AEDT and EDMS

	Fuel (lb)	CO (lb)	HC (lb)	TOG (lb)	VOC (lb)	NMHC (lb)	NOx (lb)	CO2 (lb)	SOx (lb)	PM 2·5 (lb)	PM 10 (lb)
AEDT	278449.01	9787.76	5909.34	6828.59	6789.81	6826.16	2334.55	878506.61	326.12	76.72	76.72
EDMS	293437.803	10322.885	6213.019	7180.958	7141.346	7179.288	2531.641	925796.212	379.112	319.815	319.815
Diff	-5.11%	-5.18%	-4.89%	-4.91%	-4.92%	-4.92%	-7.79%	-5.11%	-13.98%	-76.01%	-76.01%

Table 2 shows that AEDT underestimates fuel consumption and emissions from the TTO aircraft compared to EDMS. The difference in fuel consumption between AEDT and EDMS is about -5.11%. The difference for the most of other pollutants is under -5%, which is very close to the fuel burn difference. The -7.79% difference for NO_x and -13.98% for SO_x are reasonably close to the fuel consumption difference. One exception is the differences in PM, which is over -76%. To validate the fuel consumption and emission results, GT fully investigated the result differences between AEDT and EDMS by comparing:

- ANP DB coefficients for the TTO aircraft
- Engine DB coefficients for the TTO aircraft
- Fuel burn and emission calculation algorithm (APM and AEM Modules)

The main difference in fuel burn comes from the use of a different version of emission databank (EDB). AEDT (Sprint 78) uses ICAO EDB Issue 22, released on February 5, 2016, while EDMS 5.1.4 uses ICAO EDB Issue 19, issued on April 15, 2013. GT checked the two versions of the EDB and found differences in fuel flow indices and emission indices for many of the TTO aircraft. This explained the differences in fuel burn and emissions including CO, HC, TOG, VOC, NMHC, NOx, CO2 and SOx, except for PM.

For PM calculation, GT investigated the EDMS and AEDT technical manuals and found that AEDT uses FOA 3 adopted by ICAO CAEP while EDMS uses FOA 3a (for US airport), which is a more conservative method modified by the US EPA [CSSI, 2013 and 2014; US FAA, 2016]. FOA 3.0 and 3.0a account for the formation of volatile PM components from fuel sulfur content (FSC) and hydrocarbon (fuel) organics, each component with its own modeling assumptions [Wayson, et.al, 2009; Peck et.al, 2012 and 2013]. FOA 3.0a adds additional computations to account for volatile organic-driven PM from the loss of lubrication oil, for only the takeoff and climb out modes. The contributing modeled species to the volatile PM component are volatile sulfates, fuel organics, and in the case of FOA 3.0a only, lubrication oil. For each of contributing

species, an Emission Index (EI) value is calculated, and all EI values are summed to provide a complete estimation for the volatile PM EI.

Table 3 lists the sulfur factors used by FOA 3 and FOA 3a methods for calculating sulfur PM EI. The table shows that FOA 3a has over twice the sulfur to sulfate conversion rate (ε) than the FOA 3 method has. Table 4 lists the assumptions used to calculate organic PM EIs. As can be seen, the PM EI for volatile organic for FOA 3a is almost 5 times as the one of FOA 3.

Table 3: Sulfur Factors for FOA 3 and FOA 3a Methods

Fuel Chr	FOA3	FOA3a
FSC (g / g)	0.00068	0.00068
ε (%)	0.024	0.05
Ma	96	98

Table 4: Assumption of FOA 3 and FOA 3a for Organic PM EI Calculation

LTO Mode	FOA3 $EI_{PMVol\text{-}orgCFM56}$ (mg/kg fuel) APEX1	FOA3a $EI_{PMVol\text{-}orgCFM56}$ (mg/kg fuel) APEX1	$EI_{HCCFM56}$ (g/kg fuel) ICAO Databank
Takeoff	4.6	(1.2 + 19)	0.04
Climb-out	3.8	(2.9 + 16)	0.05
Approach	4.5	(4.5 + 10)	0.08
Idle	11.3	(11.3 + 25)	1.83

Since the FSC and sulfur to sulfate conversion rate can be customer defined in AEDT, GT then modified these sulfur factors to match the ones in EDMS. After the modification, equivalently AEDT is also using FOA 3a method to calculate the sulfate PM (PMSO). Table 5 shows the PM comparison between AEDT and EDMS before (SFs1) and after (SFs2) matching the sulfur factors. It can be seen that the difference between AEDT and EDMS in PMSO reduced to -5.27% from -60.72%. This -5.27% difference after matching the sulfur factors is mainly attributed to the fuel burn difference of -5.11% as shown in Table 2. Table 5 also shows that EDMS produces about 5 times of organic PM (PMFO) than AEDT does. This is because EDMS used FOA 3a in which a multiplier for calculating PMFO is almost 5 times greater than the one using in FOA 3 method. In addition, there are a large difference in none-volatile PM (nvPM) emissions between AEDT and EDMS. This is due to the different versions of EDB used by AEDT and EDMS. EDMS used an older version of EDB, which does not have smoke numbers (SN) available for many TTO aircraft while AEDT has updated EDB which provides updated SN for the TTO aircraft. Since the nvPM calculations are based on SN, EDMS did not calculate nvPM for those aircraft with missing SN. Based on GT's analysis and investigation for the TTO_DULLES study, it can be concluded that AEDT gives equivalent or improved fuel burn and emissions estimations for the TTO aircraft than EDMS does.

Table 5: PM Comparison between AEDT and EDMS with Different Sulfur Factors

		nvPM Mass (lb)	PMSO (lb)*98/96	PMFO (lb)	PM 2.5 (lb)	PM 10 (lb)
AEDT 2c SP1	SFs 2	1.91	28.96	62.76	93.03	93.03
	SFs 1 (default)	1.91	12.01	62.76	76.68	76.68
EDMS 5.1.4	SFs 2	0.68	30.57	288.60	319.85	319.85
Diff (AEDT w/ SFs 2 VS. EDMS)		180.06%	-5.27%	-78.25%	-70.91%	-70.91%
Diff (AEDT w/ SFs 1 VS. EDMS)		180.06%	-60.72%	-78.25%	-76.03%	-76.03%

VALE Report

The Voluntary Airport Low Emissions (VALE) Program is designed to reduce all sources of airport ground emissions. VALE reduction report shows the net differences in emissions between a baseline and an alternative metric result for a single analysis year. This task was focusing on designing test cases to test the VALE report functionalities and to investigate any issues or gaps found in the testing process. GT used 42 test cases, including 15 newly designed test cases and 27 test cases from Volpe, to thoroughly test the VALE functionalities. The functionalities tested include metric results creation, user input for analysis year, VALE report button, End-of-Life year feature, and emissions value comparison. A few issues were found and reported through TFS. The reported issues were resolved by the AEDT development team. GT confirmed that all the VALE functionalities were currently working properly after the bug fixes.

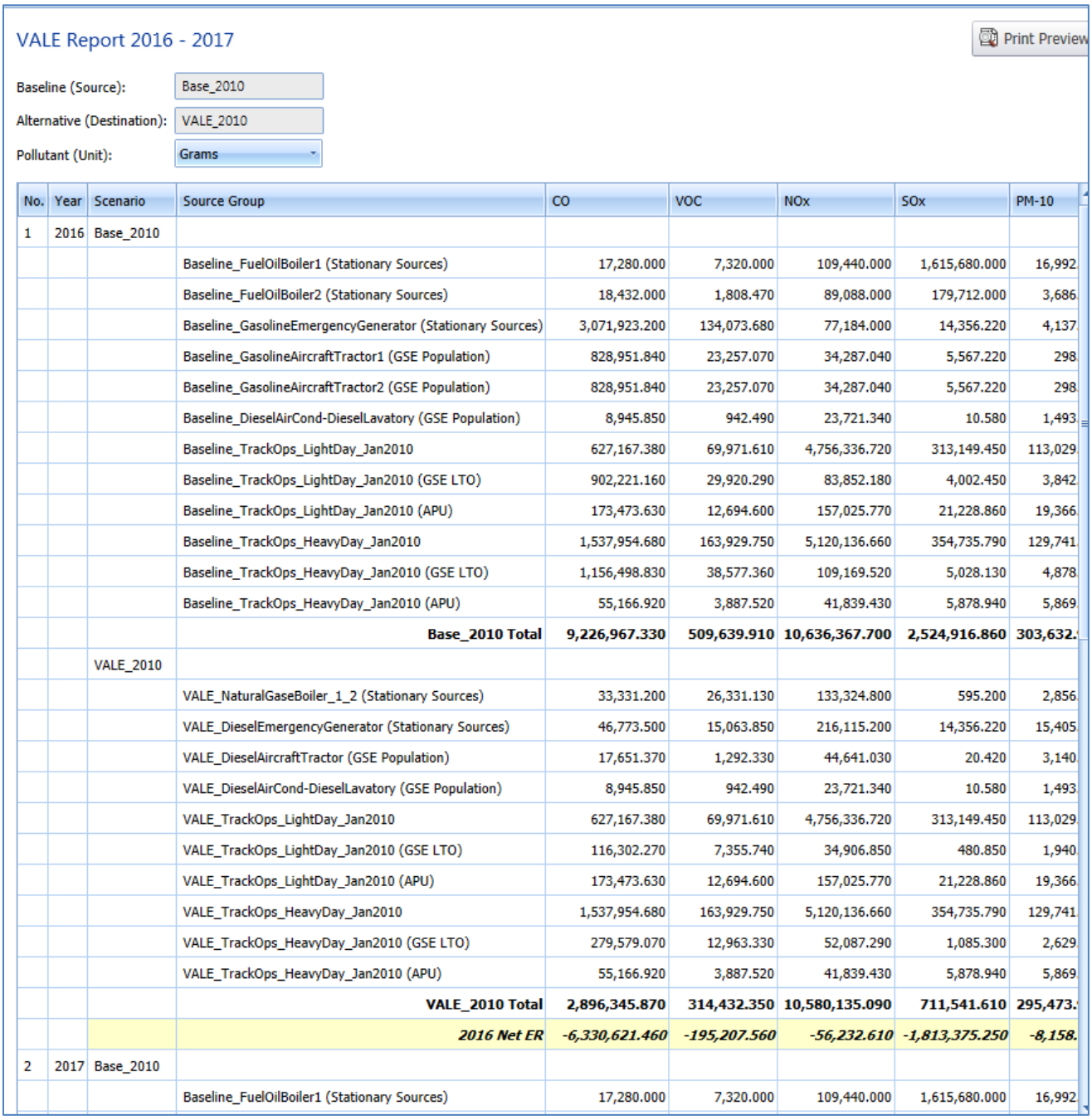

VALE Report 2016 - 2017

Print Preview

Baseline (Source): Base_2010

Alternative (Destination): VALE_2010

Pollutant (Unit): Grams

No.	Year	Scenario	Source Group	CO	VOC	NOx	SOx	PM-10
1	2016	Base_2010						
			Baseline_FuelOilBoiler1 (Stationary Sources)	17,280.000	7,320.000	109,440.000	1,615,680.000	16,992
			Baseline_FuelOilBoiler2 (Stationary Sources)	18,432.000	1,808.470	89,088.000	179,712.000	3,686
			Baseline_GasolineEmergencyGenerator (Stationary Sources)	3,071,923.200	134,073.680	77,184.000	14,356.220	4,137
			Baseline_GasolineAircraftTractor1 (GSE Population)	828,951.840	23,257.070	34,287.040	5,567.220	298
			Baseline_GasolineAircraftTractor2 (GSE Population)	828,951.840	23,257.070	34,287.040	5,567.220	298
			Baseline_DieselAirCond-DieselLavatory (GSE Population)	8,945.850	942.490	23,721.340	10.580	1,493
			Baseline_TrackOps_LightDay_Jan2010	627,167.380	69,971.610	4,756,336.720	313,149.450	113,029
			Baseline_TrackOps_LightDay_Jan2010 (GSE LTO)	902,221.160	29,920.290	83,852.180	4,002.450	3,842
			Baseline_TrackOps_LightDay_Jan2010 (APU)	173,473.630	12,694.600	157,025.770	21,228.860	19,366
			Baseline_TrackOps_HeavyDay_Jan2010	1,537,954.680	163,929.750	5,120,136.660	354,735.790	129,741
			Baseline_TrackOps_HeavyDay_Jan2010 (GSE LTO)	1,156,498.830	38,577.360	109,169.520	5,028.130	4,878
			Baseline_TrackOps_HeavyDay_Jan2010 (APU)	55,166.920	3,887.520	41,839.430	5,878.940	5,869
			Base_2010 Total	**9,226,967.330**	**509,639.910**	**10,636,367.700**	**2,524,916.860**	**303,632.**
		VALE_2010						
			VALE_NaturalGaseBoiler_1_2 (Stationary Sources)	33,331.200	26,331.130	133,324.800	595.200	2,856
			VALE_DieselEmergencyGenerator (Stationary Sources)	46,773.500	15,063.850	216,115.200	14,356.220	15,405
			VALE_DieselAircraftTractor (GSE Population)	17,651.370	1,292.330	44,641.030	20.420	3,140
			VALE_DieselAirCond-DieselLavatory (GSE Population)	8,945.850	942.490	23,721.340	10.580	1,493
			VALE_TrackOps_LightDay_Jan2010	627,167.380	69,971.610	4,756,336.720	313,149.450	113,029
			VALE_TrackOps_LightDay_Jan2010 (GSE LTO)	116,302.270	7,355.740	34,906.850	480.850	1,940
			VALE_TrackOps_LightDay_Jan2010 (APU)	173,473.630	12,694.600	157,025.770	21,228.860	19,366
			VALE_TrackOps_HeavyDay_Jan2010	1,537,954.680	163,929.750	5,120,136.660	354,735.790	129,741
			VALE_TrackOps_HeavyDay_Jan2010 (GSE LTO)	279,579.070	12,963.330	52,087.290	1,085.300	2,629
			VALE_TrackOps_HeavyDay_Jan2010 (APU)	55,166.920	3,887.520	41,839.430	5,878.940	5,869
			VALE_2010 Total	**2,896,345.870**	**314,432.350**	**10,580,135.090**	**711,541.610**	**295,473.**
			2016 Net ER	***-6,330,621.460***	***-195,207.560***	***-56,232.610***	***-1,813,375.250***	***-8,158.***
2	2017	Base_2010						
			Baseline_FuelOilBoiler1 (Stationary Sources)	17,280.000	7,320.000	109,440.000	1,615,680.000	16,992

Figure 2: Example VALE Report

EDMS2ASIF Converter and EDMS Importer

AEDT 2b has the capability of importing studies created with legacy tools such as INM and EDMS. There are two ways to import legacy studies to AEDT: through an external converter tool, which is included with the AEDT installation package or through the built-in importer feature. This task tested the external EDMS2AEDT converter tool and the built-in EDMS importer. As shown in Figure 3, the external EDMS2AEDT converter tool supports importing of EDMS studies by converting the legacy studies into ASIF format first, and then using AEDT to import the converted ASIF to AEDT. On the other hand,

the built-in EDMS importer (can be accessed through Study → Import → EDMS) can directly convert an EDMS study to an AEDT study by following the study import wizard. GT successfully used the EDMS2ASIF converter to convert EDMS studies to ASIF files, and then successfully imported the ASIF files to AEDT to create AEDT studies. In addition, GT successfully used the built-in EDMS importer to import 4 EDMS studies to AEDT. The tests verified that the EDMS importer can handle the EDMS study with inconsistent airport data. One bug was found during the process of importing the study and reported through TFS. GT's conclusion is that EDMS2ASIF converter and EDMS importer are functional and working properly.

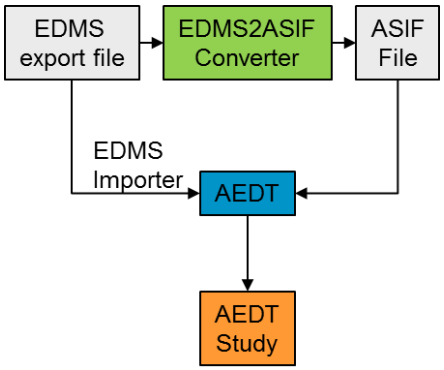

Figure 3: Import EDMS Study through the External EDMS2AEDT Converter or Built-in EDMS Importer

Environmental Justice

One of the key new features added to AEDT 2c is the capability to perform Environmental Justice (EJ) analysis. The EJ capability in AEDT 2c assists identification of potential environment justice populations. According to the *Environmental Desk Reference for Airport Actions* [US FAA, 2016] from the FAA, "Environmental justice analysis considers the potential of Federal actions to cause disproportionate and adverse effects on low-income or minority populations. Environmental justice ensures no low-income or minority population bears a disproportionate burden of effects resulting from Federal actions." In order to use the EJ functionality in AEDT, US Census American Community Survey (ACS) data is required. As of the AEDT 2c release, the ACS data is available for the time period between January 1, 2010 and December 31, 2014. The demographic data is at the Census Block Group level and is approximately 7 GB for the entire US. In AEDT 2c, an EJ analysis is conducted by following the three step work flow: 1) define an EJ boundary, 2) run the EJ analysis, and 3) rerun the EJ analysis by adjusting the analysis thresholds using the EJ analysis pane. AEDT allows the users to define an EJ boundary by either drawing a polygon using the GUI, importing a shapefile, or using pre-computed noise/emission contours.

The EJ capability of AEDT 2c was tested by running four test cases. The first test case used a new AEDT study created from scratch. Two different types of EJ boundaries were created around the San Diego airport. The first boundary was a noise SEL contour that was generated from a study with a single-aisle aircraft departure flight. The second boundary was a user defined polygon around the airport. Test Case 1 showed that the basic functionalities of the AEDT EJ model were working properly. The second and third test cases used DNL contours as EJ boundaries. For Dallas-Forth Worth (KDFW) and Atlanta (KATL) airports, DNL 55, 60, and 65 dB contours were generated for hypothetical future operation schedules using AEDT 2b Feature Pack 1. The DNL contours were exported as shapefiles and then imported into AEDT 2c to use as the EJ boundaries. The tests demonstrated that the shapefiles generated from past AEDT studies could be imported into AEDT 2c and used as EJ boundaries. The EJ analyses were run successfully. Figure 4 shows the EJ test results for the KDFW airport. The Census group blocks that are included in or overlapped with the EJ boundary were colored to indicate whether the block exceeded the poverty rate and/or minority rate thresholds. For example, a Census block shaded blue indicates that both poverty rate and minority rate exceeded the thresholds. Orange color is used to indicate the blocks with high minority and low poverty rate. Yellow is for low minority and high poverty rate. Grey is used when both the thresholds were not exceeded. The thresholds used in this example analysis were 10% for poverty rate and 50% for minority rate, which were set using the GUI in the EJ Analysis pane on the right side of the figure. Users can set the poverty rate and minority rate thresholds using the EJ analysis pane, and then AEDT can almost instantly update the colors for each of the Census blocks. GT confirmed that all of these functionalities associated with EJ capability were working properly.

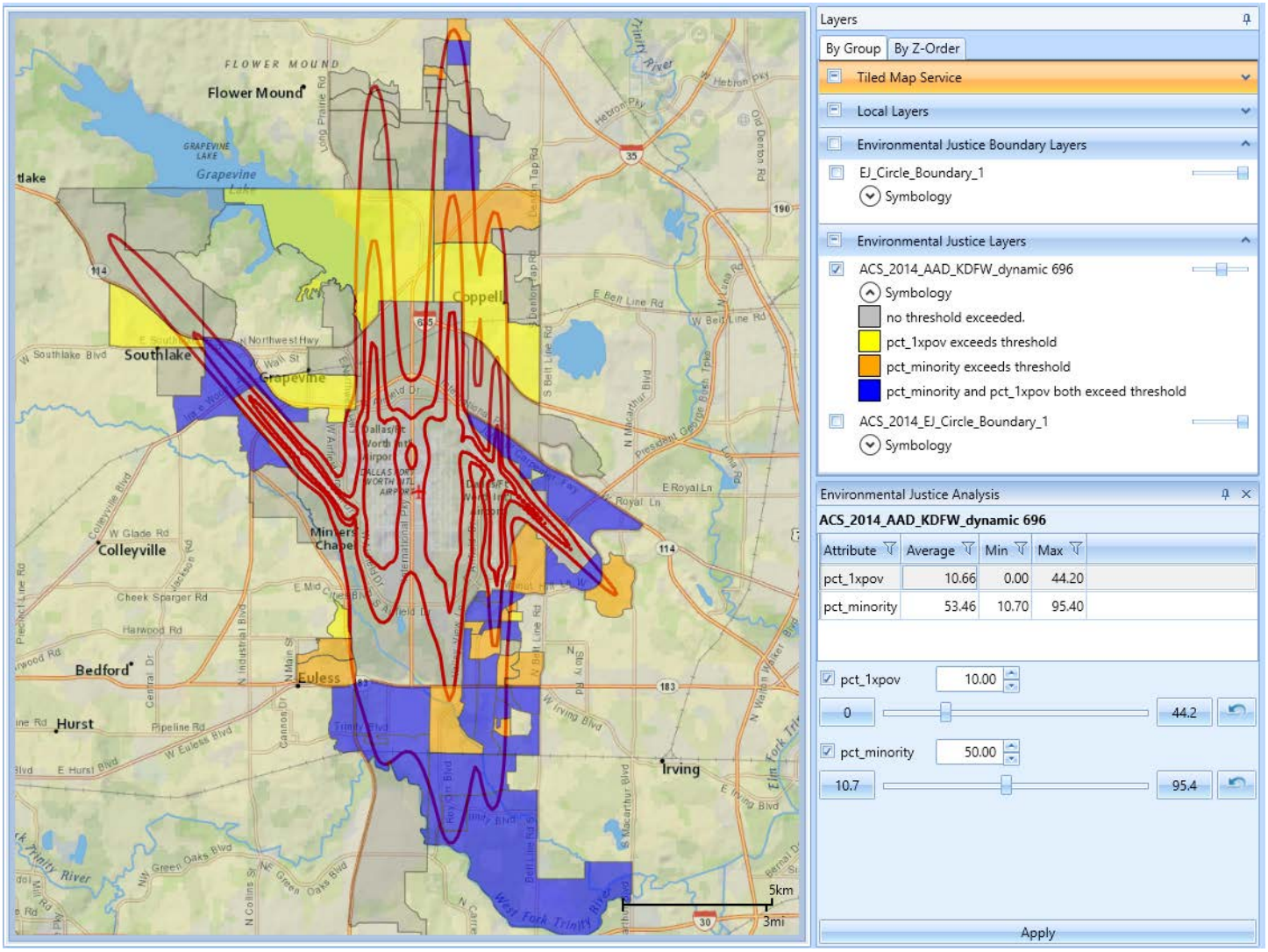

Figure 4: Environmental Justice Analysis Performed Around KDFW for a Sample DNL 55, 60, and 65 dB Contours

Typically, an EJ analysis would be conducted around an airport using either noise or emission related metric results. However, AEDT's EJ functionality is not limit to the vicinity of an airport. Another EJ test was performed to demonstrate that an EJ study can be performed at any location without a metric result. An EJ boundary was created around a random location in Dekalb County, Georgia. A circular EJ boundary with a 6-mile radius was created in AEDT. The EJ analysis was run successfully for the circular boundary and the results are shown in Figure 5. The EJ Layer pane on the right side of the figure explains what the color scheme means. AEDT allows the users to display the Census data for the Census blocks included in the EJ study. It is also possible to export the data into an Excel spreadsheet for further analysis. The data table shown in the bottom of Figure 5 includes the raw ACS data. Users can select a Census Block by clicking a row in the table, and then the boundary of corresponding block on the map gets highlighted. The US Census ACS data include demographic data other than poverty rate and minority rate. AEDT allows the users to change or add demographic parameters and run EJ analyses. This functionality was successfully tested by adding median household income as the third parameter.

A couple of minor bugs on GUI were found and reported through TFS, and were fixed for the subsequent sprint releases. In addition, some potential areas of improvements were identified and reported to the development team as well. Currently, AEDT does not allow the users to change the color scheme for the EJ map. The fixed color scheme works reasonably well when two EJ parameters are used for the analysis. However, when more than two parameters are used, the fixed color

scheme cannot represent all the combinations of potential analysis outcomes. For example, when median household income, poverty rate, and minority rate are used for an EJ analysis, AEDT can use the same color for 1) low median household income, high poverty rate, and high minority rate and 2) high median household income, high poverty rate, and high minority rate. At the moment, it is advised to use two demographic parameters at a time.

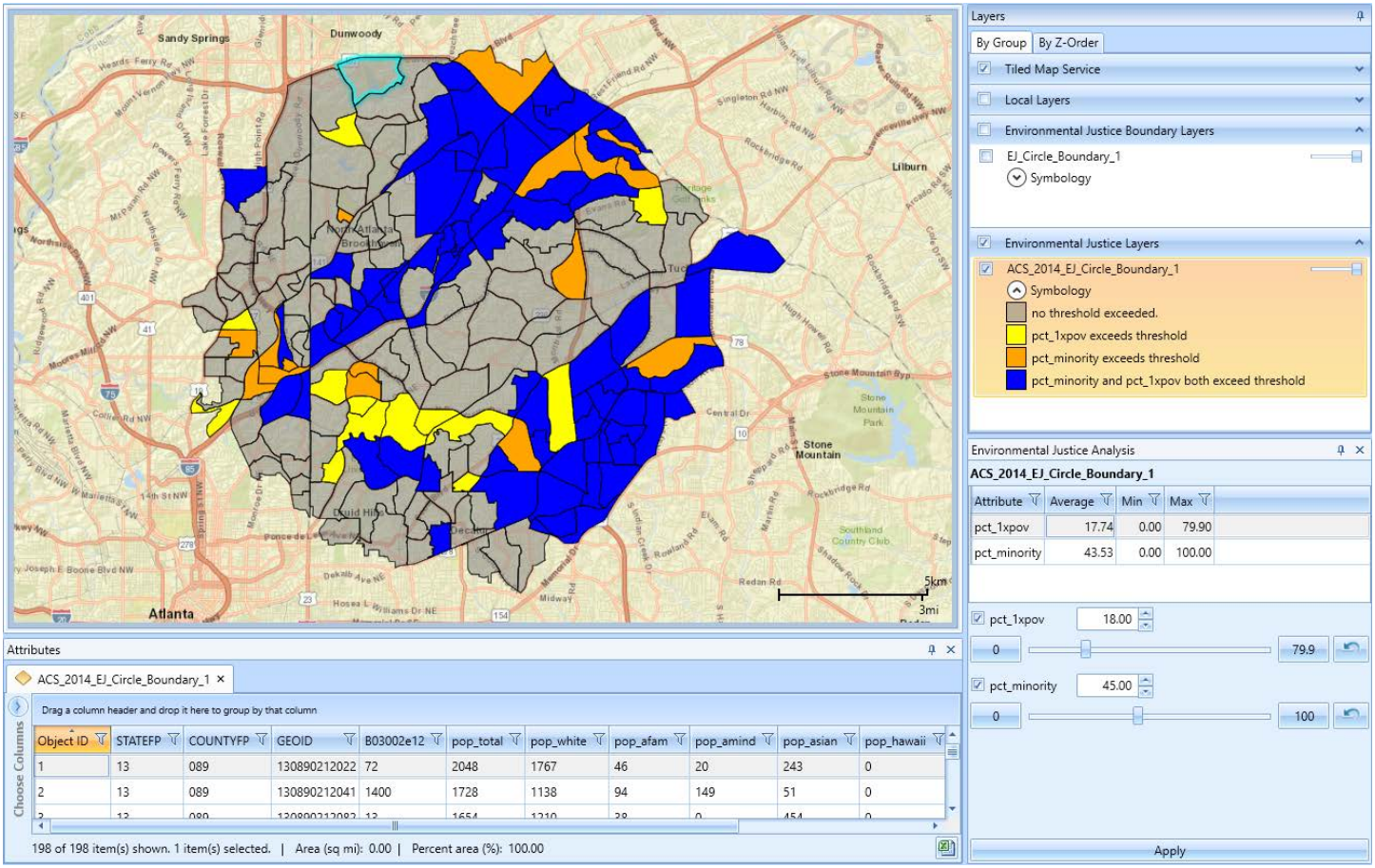

Figure 5: An EJ Analysis Using a Circular EJ Boundary Created in DeKalb Country, Georgia

AEDT allows the users to export the EJ analysis result as a shapefile along with the associated demographic data for the Census blocked included in the shapefile. This functionality was tested by exporting the EJ analysis for KDFW. Then the shapefile was imported into ArcGIS, one of the widely used geographical information system (GIS). When the shapefile was imported, ArcGIS also imported the raw EJ data for the Census Blocks that were included in the EJ analysis. ArcGIS provides various ways to present the EJ data. Figure 6 shows an EJ analysis for KDFW conducted in ArcGIS. The Census block groups were colored by poverty rate. Pie charts represent population size and racial composition of the Census block. AEDT combined with ArcGIS provide very powerful and convenient analytic capability to investigate EJ issues due to environmental impacts from aviation.

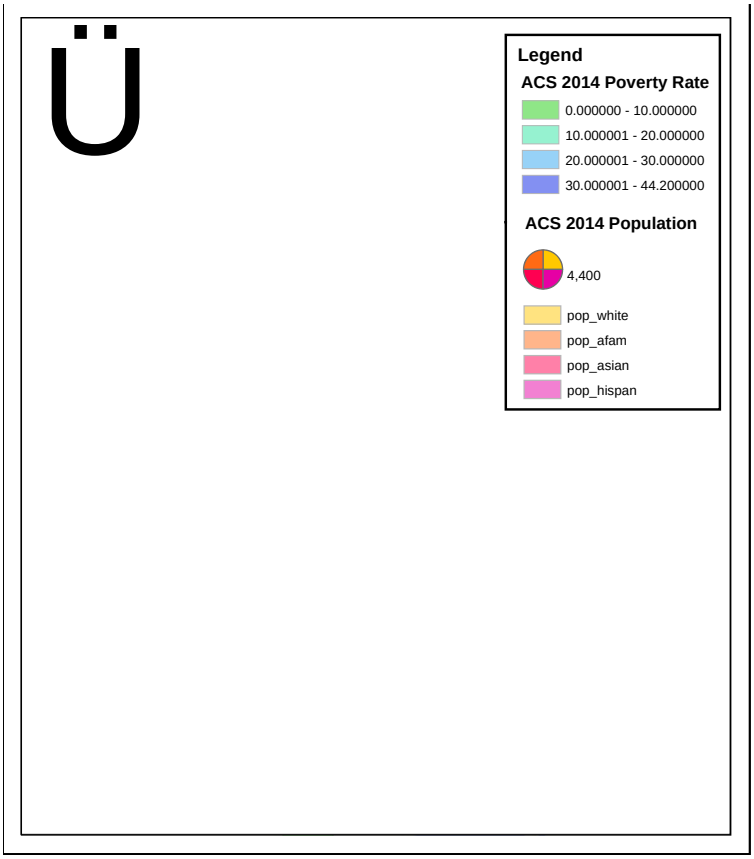

Figure 6: An EJ Analysis for KDFW in ArcGIS Using the Shapefile and Demographic Information Imported from AEDT

Atmospheric Absorption Models

As aircraft noise propagates through the atmosphere, the sound energy dissipates at a rate determined by the atmospheric condition. Relative humidity and air temperature affect the degree of atmospheric absorption most. Figure 7 shows atmospheric attenuation in dB/1000 ft as a function of temperature and relative humidity [Landrum and Brown, 2013]. The figure shows that the degree of atmospheric absorption depends on the frequency of the sound wave. INM and AEDT2a provide two atmospheric absorption models [US FAA, 2014]. The default atmospheric absorption model has been the SAE-AIR-1845. The SAE-AIR-1845 method specifies how the Noise-Power-Distance (NPD) curves are created by normalizing the measured aircraft noise for the standard atmospheric condition. When SAE-AIR-1845 is used as the atmospheric absorption model in INM or AEDT, the NPD curves based on the standard day atmosphere are used without any adjustments. When SAE-ARP-866A model is selected and non-standard, airport specific atmosphere is used, the NPD curves are adjusted to reflect the different atmospheric attenuation rates for the airport atmosphere. The SAE-ARP-866A model adjusts the NPD curves for the non-standard relative humidity and temperature for each of the 1/3rd-octave bands. AEDT 2b implemented an improved atmospheric absorption model based on SAE-ARP-5534, where the NPD curves are adjusted for relative humidity, temperature, and atmospheric pressure.

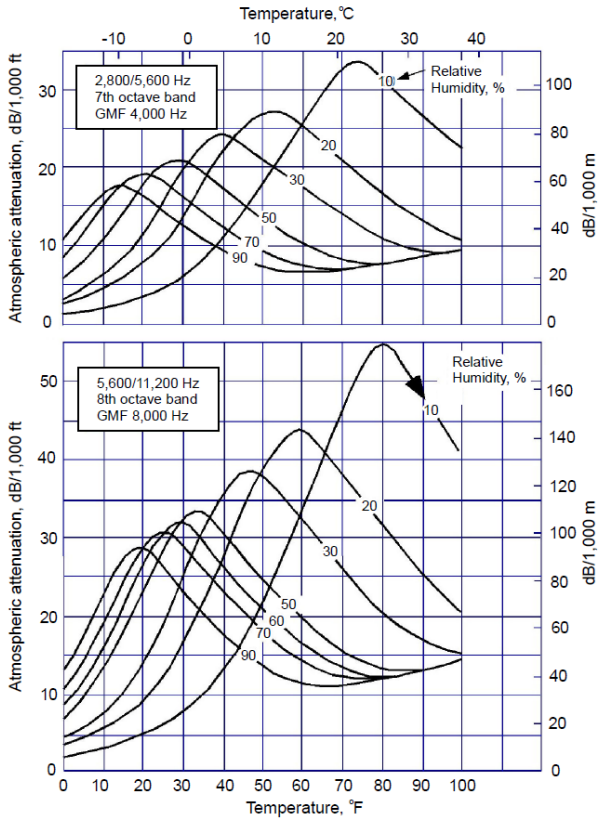

Figure 7: Atmospheric Sound Attenuation Graph

Since airport noise analyses before the release of AEDT 2b were conducted either using SAE-AIR-1845 or SAE-ARP-866A, a sensitivity analysis was conducted to investigate how much noise contours would change based on the selection of an atmospheric absorption model. Sensitivity of noise impacts from atmospheric absorption model was measured in terms of differences in SEL and DNL contour areas. Five different US airports were selected for the study to represent from a small airport with a single runway to medium and large hub airports with complex runway configurations. For the selected five airports, DNL 55, 60, and 65 dB contour areas were calculated for a 2012 average day operations. Table 6 shows the DNL 55, 60, and 65 dB areas for the five studied airports for the three atmospheric absorption models. Based on the results, the SAE-ARP-866A model resulted in greater contour areas than the SAE-AIR-1845 model for all the five airports. Subsequently, the use of SAE-ARP-5543 model resulted in greater contour areas than the SAE-ARP-866A model. For airports Large Hub 2 and 3, the differences between the SAE-ARP-886A/ SAE-ARP-5534 and SAE-AIR-1845were greater for the 55 dB level. For other three airports, the differences due to the different absorption models were close for the three dB levels. Depending on the airport, the use of SAE-ARP-5543 increased the DNL 65 dB contour areas from 7.6% to 16.7% compared to SAE-AIR-1845. Therefore, it is very important to make sure that a consistent absorption model is used when two noise studies are compared. Noise modelers should be very careful comparing past study results from INM or AEDT2a to the updated results from AEDT 2b or AEDT 2c since the atmospheric absorption modes may be different.

Table 6: Comparison of DNL Contour Areas for Different Atmospheric Absorption Models

Airport	DNL (dB)	Contour Areas in Sq Miles				
		SAE-AIR-1845	SAE-ARP-866A		SAE-ARP-5534	
		Area	Area	Diff	Area	Diff
Busy Single Runway	55	19.1	22.0	15.3%	23.0	20.6%
	60	7.4	8.4	14.0%	8.7	18.9%
	65	2.8	3.2	12.4%	3.3	16.0%
Large Hub 1	55	68.7	79.4	15.6%	82.8	20.6%
	60	29.1	33.4	15.0%	35.1	20.8%
	65	12.4	13.9	12.1%	14.4	16.5%
Large Hub 2	55	57.5	74.1	29.0%	80.6	40.2%
	60	21.9	26.5	20.8%	28.3	29.3%
	65	9.5	10.7	12.2%	11.1	16.7%
Large Hub 3	55	25.0	31.4	25.7%	34.2	36.9%
	60	8.0	9.4	17.5%	10.0	25.3%
	65	2.8	3.1	10.4%	3.2	13.8%
Medium Int'l	55	46.6	48.2	3.4%	49.4	6.0%
	60	20.4	21.4	5.0%	22.0	7.8%
	65	8.3	8.7	5.1%	8.9	7.6%

The choice of atmospheric absorption model not only impacts the size of the noise contours area but also affects the contour shape. For airports with single runway with relatively straight flight tracks, the choice of the three absorption models may proportionally scale the noise contours. However, for airports with complex contour shapes due to intersected runways and/or curved flight-tracks, the selection of an absorption model can also impact the shape of the contours. Figure 8 compares the DNL 55, 60, and 65 dB contours for KJFK. The general shapes are similar for the SAE-AIR-1845 and SAE-ARP-5543 models. However, the overall increase in noise levels with the SAE-ARP-5543 model changed the contour shapes. For the SAE-ARP-5543 model as shown at the bottom of the figure, the two DNL 55 dB noise lobes for thesouth-westerly departures were merged.

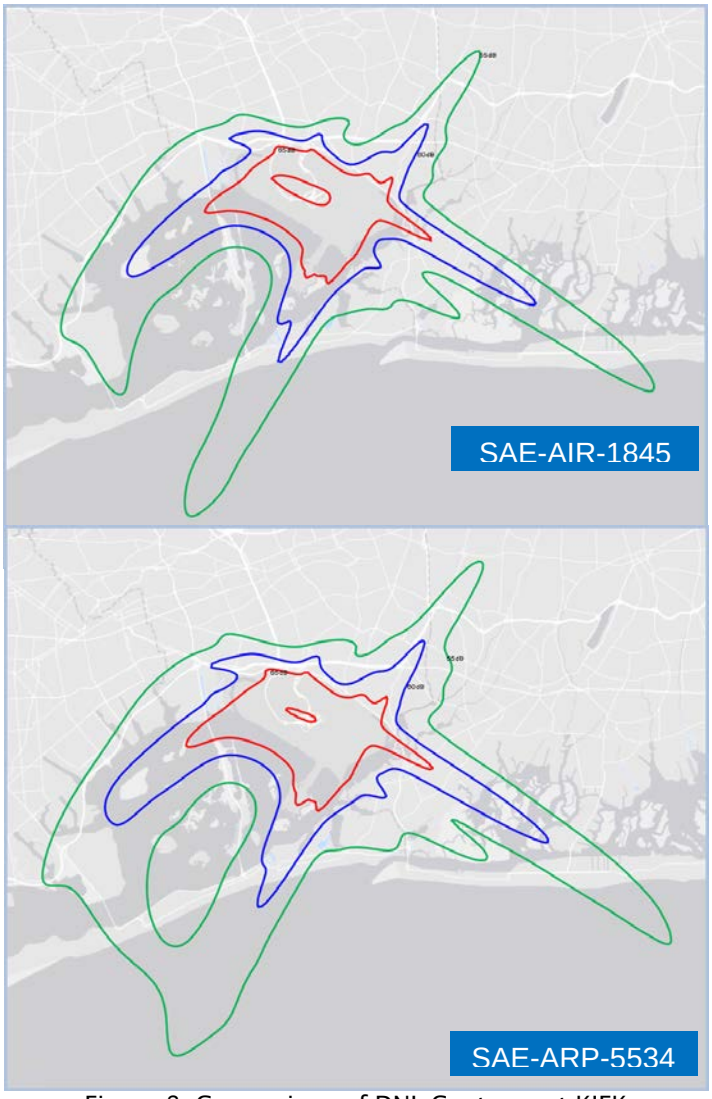

Figure 8: Comparison of DNL Contours at KJFK

Noise Contouring Algorithm

As part of the ASCENT 11b effort, GT conducted noise analysis using AEDT 2b Feature Pack 1 for 38 US airports for three technology scenarios. In some cases, AEDT failed to generate contour plot and/or calculate the areas properly. For theairports in those cases, contour areas were calculated through a MATLAB script developed by GT using the noise reports exported from AEDT. It was found that AEDT and MATLAB showed large differences in contour areas for some cases. GT found out that the issue was that the AEDT contouring algorithm did not properly account for contour holes and islands, and this issue was reported The development team quickly fixed the problem and GT confirmed that the new contouring algorithm worked for all 38 airports. As an example, Figure 9 shows DNL 55, 60, and 65 dB contours for an airport with parallel intersected runways, and the analysis was conducted using AEDT 2b Feature Pack 1 which used the old algorithm. As can be seen from the figure, the 65 dB contour in red appears as a very small island. The contour areas and lengths shown in the table within the figure also indicates disproportionately small 65 dB contour. Figure 10 is the reanalysis of the same study using the new AEDT contouring algorithm after the bug fix. It shows the main 65 dB contour with two contour holes and a small contour island, and the contour lengths and areas in the table are in the right

proportion compared to the 55 and 60 dB contours. GT compared the contour areas calculated using MATLAB code and confirmed that the updated AEDT contouring algorithm worked properly for the 38 US airports used in this investigation.

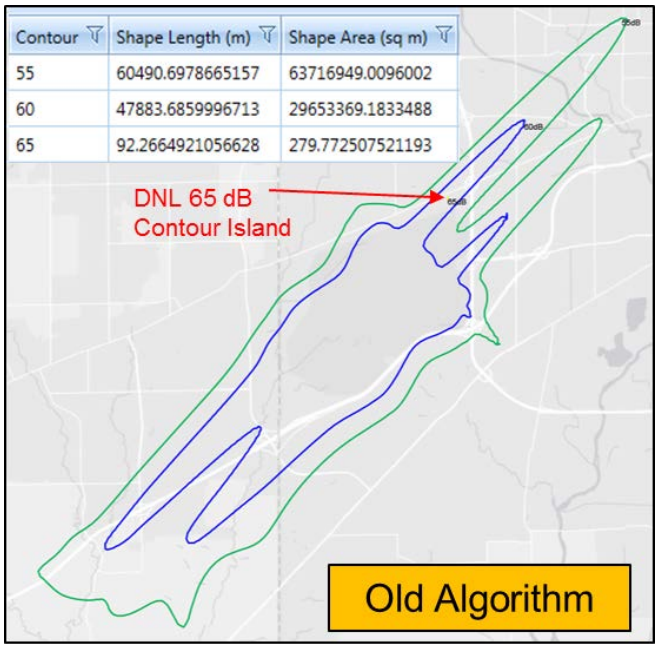

Figure 9: DNL 55, 60, and 65 dB Contours for an Airport Generated in AEDT 2b

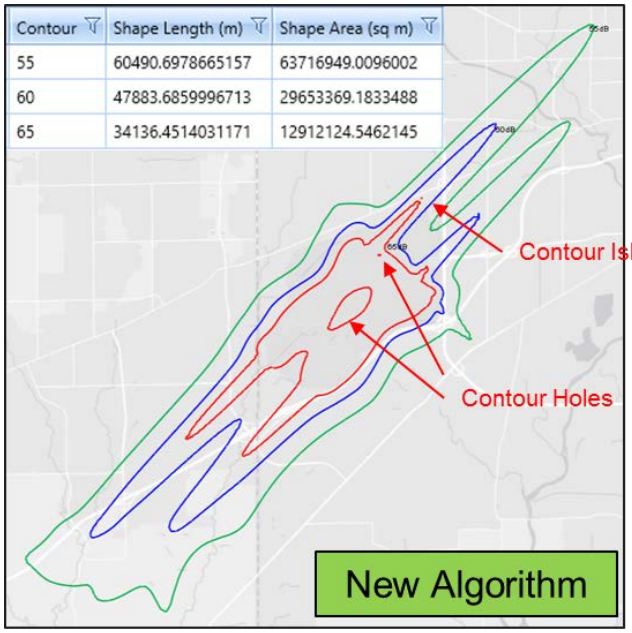

Figure 10: DNL 55, 60, and 65 dB Contours for an Airport Generated in AEDT 2c

Population Exposure Calculation

As part of the ASCENT 11b effort, GT also calculated population exposure in AEDT for 38 US airports. The purpose was to compare noise contour areas and population exposure counts between AEDT and the GREAT tool, which was developed under ASCENT Project 11b. GT identified some issues with population exposure numbers from AEDT. The issue was that for some airports for particular DNL levels and technology scenarios, the population from AEDT was unreasonable small compared to the numbers calculated by GREAT when the contour shapes and sizes were similar. Another issue was that AEDT would fail to calculate population for some airports in a random manner. It would work one day and would not work the next day for the same study. After investigation with the AEDT development team, the first issue was found to be related to the contouring algorithm not properly accounting for the contour islands and holes. AEDT uses two separate geographic processing packages for contour generation and population exposure calculation. The issue was resolved by updating the AEDT GIS module that creates population grids from Census data. The second issue of AEDT's random error with population calculation was related to the caching mechanism, which caused errors when the UTM zones were different. The development team implemented a temporary fix to the problem by disabling the Census caching mechanism. The development team is looking into a permanent fix.

Time Audible Noise Metrics

One of the important enhancements to AEDT 2b SP3 is the addition of Time Audible (TAUD) noise metrics. The four TAUD metrics added to AEDT 2b are TAUD (Time Audible), TAUDP (Time Audible Percent), TAUDSC (Time Audible Statistical Compression), and TAUDPSC (Time Audible Percent Statistical Compression). Audibility or Detectability is the ability for an attentive listener to hear aircraft noise. Audibility depends on both the aircraft sound level ("signal") and the ambient sound level ("noise"). Although DNL is the most widely used noise metric for airport noise analyses, TAUD has been an important metric measuring noise impacts at National Parks.

Using AEDT 2b SP3 and later versions, GT has been testing the TAUD metrics for a study created for the Acadia National Park. At the Acadia National Park, four different types of aircraft operations were created using different types of aircraft. The tests are still in progress, but the preliminary results show that AEDT is calculating TAUD metrics correctly. Figure 11 shows TAUD results from a single-aisle aircraft departure at the KBHB airport near the Acadia National Park. The TAUD results that are shown on the right range from 0 to 3.5 minutes depending on the receptor location. The maximum of 3.5 minutes corresponds to the time duration from the start of take-off roll to the end of climb at 10,000 ft as shown on the trajectory plot. The next steps in TAUD tests include comparing TAUD results between INM 7.0d [Boeker, et.al, 2008; ATAC, 2007] and AEDT for departure, arrival, over-flight, and circuit flights.

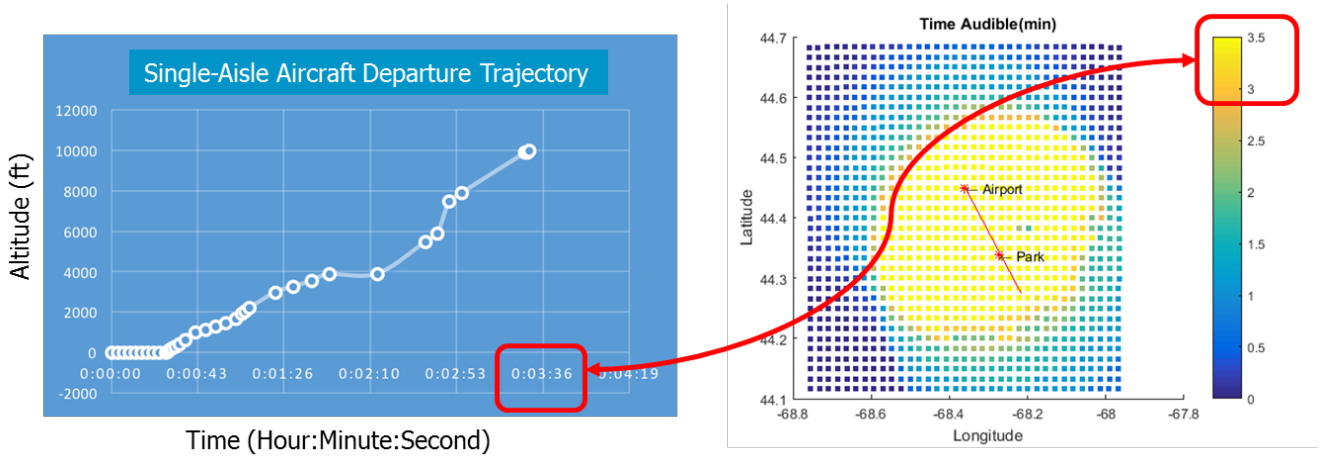

Figure 11: A Single-Aisle Aircraft Departure Trajectory and TAUD Results in Acadia National Park

Milestone(s)

Milestone	Due Date	Estimated Date of Completion	Actual Completion Date	Status	Comments (Problems & Brief Resolution Plan)
A36 Kickoff Meeting	5/3/2016	5/3/2016	5/3/2016	Completed	
Quarterly Report (Aug)	7/31/2016	7/31/2016	7/31/2016	Completed	
ASCENT Meeting	9/27-28/2016	9/27-28/2016	9/27-28/2016	Completed	
Quarterly Report (Nov)	10/31/2016	10/31/2016	10/31/2016	Completed	
Annual Report	1/18/2017	1/18/2017	1/13/2017	Completed	

Major Accomplishments

Starting from May 2016, GT has tested all the new AEDT versions released including Sprints from 70 to 79. Sprints 70 – 79 included three public versions of AEDTs, namely AEDT 2b SP3, AEDT 2c, and AEDT 2c SP1. GT tested the ten versions of AEDT focusing on new features and capabilities added. Some of the new features/capabilities were minor updates to the GUI, bug fixes, or data updates. Major updates included improved VALE reporting capability, implementation of TTO aircraft fuel burn and emission calculations, implementation of Environmental Justice capability, the addition of TAUD and NA noise metrics, improved nvPM calculations, the addition of background emission concentration, and new features on emission dispersion display. In order to understand the background of new AEDT features, GT reviewed all the relevant documents including the software requirement documents, Database Design Document, AEDT sprint release notes, updated technical manual, user manual, and research papers/reports. GT has conducted basic testing of all the new AEDT versions to confirm its functionality. GT identified a number of minor and major bugs and reported them to the FAA and the development team via bi-weekly ASCENT project telecons and weekly AEDT development-leads calls. Through the on-line system named Team Foundation Server (TFS), identified issues and follow-up actions taken by the developers were documented and shared. In addition, GT also reported any potential areas of improvements in AEDT algorithm and user-friendliness.

Publications

None

Outreach Efforts

None

Awards

None

Student Involvement

Evanthia (Eva) Kallou is a second year PhD student who started in fall 2015. As a Graduate Research Assistance, Ms. Kallou has conducted a literature review on UQ methods. Ms. Kallou is being trained on related tools such as EDMS, AEDT Tester, and AEDT2c.

Junghyun (Andy) Kim is a second year PhD student who started in fall 2015. Mr. Kim has conducted a literature review on UQ methods. Mr. Kim is being trained on related tools such as INM, AEDT Tester, and AEDT2c.

Plans for Next Period

GT will continue Task 1 and 2 for new AEDT 2c releases. AEDT 2c SP2 is planned to be released in mid-March 2017. GT will perform Task 1 and 2 for the preliminary versions of AEDT 2c SP2 to identify any issues that need to be addressed by the development team.

Task 1. Proper Definition of AEDT Input Parameter Uncertainty
As discussed above.

Task 2. Verification and Validation plus Capability Demonstrations
As discussed above.

Task 3. Identification of Important Output to Input Relationships (Optional)
This optional task may not be performed for every AEDT service pack releases. Instead, this task will be performed when a major feature is added to the AEDT, and if potential sources of uncertainties remain through the analysis of previous two tasks. The outcome of this task will be the identification of the key input drivers across multiple vehicle types to multiple AEDT metric outputs. This can provide a comprehensive insight to the uncertainty associated with AEDT outputs and the joint-distribution of Fleet DB coefficients. Various uncertainty quantification techniques will be used depending on the metric of interest. This may include, but not limited to the following techniques: Analysis of Variance (ANOVA), Multivariate Analysis of Variance (MANOVA), Monte Carlo Simulation, Copula Techniques, or Global Sensitivity Analysis. The specific techniques will be proposed by GT and reviewed by the FAA for concurrence.

Task 4. Guidelines for Future Tool Research
In this task, each of the prior tasks will culminate into a summary document of the data assumptions, techniques utilized, the resulting observations and findings to help guide the FAA to further research the areas of AEDT development to improve its supporting data structure and algorithms. In addition, the document will build confidence in AEDT's capability and fidelity and help users to understand the sensitivities of output response to the variation of input parameters/assumptions.

Additional Tasks for Next Period

For the work period of 12/1/2016 to 3/31/2017, GT will perform the following additional tasks per the augmented project plan. Building on prior UQ research efforts, GT will coordinate with the FAA/AEE on the details of the specific tests to understand the differences in the use cases between the legacy tools and AEDT2b for the following use cases. In some instances, additional analysis will be conducted; and in other cases, only clarification to the original UQ report will be provided.

Task 1 – Use Case A – Inventory Analysis
For Use Case A, sufficient analysis was conducted in the UQ report. However, the FAA desires a more thorough discussion on the results obtained. As such, GT will add a more detalied discussion. To accomplish this task, GT will need the AEDT study DB utilized for this use case.

Task 2 – Use Case B and C– NEPA/CAA Analysis
The purpose of Use Cases B and C was to provide a capability demonstration of AEDT 2b functionality and a comparison to the Emissions and Dispersion Modeling System (EDMS) at PVD airport. For Use Case B, operational profiles were utilized with AEDT2b Service Pack 2 62.3.43546.1 and EDSM 5.1.4.1. For Use Case C a detailed schedule of aircraft operations was utilized in lieu of operational profiles, and AEDT2b Service Pack 1 62.3.43302.1 and EDSM 5.1.4.1 were used for the analysis. There were a number of discrepancies between AEDT2b and EDMS. GT will conduct the following tasks to enhance the UQ report for both Use Cases:

1. Data analysis by source types and aircraft categories to identify major source of discrepancy
2. Run a single flight study to help investigate the major source that makes the difference
3. Compare flight trajectories to see the differences in APM modules
4. Investigate the causes that lead to the difference between AEDT and EDMS
5. Justify if the difference is reasonable or not

6. Recommend the solutions for improving the results if there is any

To accomplish this task, GT will coordinate with the FAA on the proper version of AEDT2b release to use. The same version will be utilized for both use cases for consistency.

Task 3 – Use Case D – Part 150 Analysis
The purpose of this Use Case was to evaluate the capability of AEDT 2b for performing a Part 150 airport noise analysis and to test other aircraft noise modeling functionality of AEDT 2b. Historically, Part 150 analyses were performed with the legacy Integrated Noise Model (INM) tool. Since a key requirement for AEDT 2b was to sunset INM, Use Case D includes detailed comparisons between INM 7.0d su1 (the final version of INM) and AEDT 2b, to confirm that AEDT 2b performs as expected for Part 150 studies.

In the Phase I of this Use Case, a number of large differences were observed between AEDT2b and INM. Through prior research, GT had identified a contour algorithm bug that could have been the source of discrepancies. As such, GT will redo the noise analysis at the airports with large errors and include ANC, JFK, HNL, and SFO. Additional investigations will be done on the absorption model and the engine installation, and new results will be documented.

For Phase II, the goal was to test the specialized functionality that consists of other noise modeling functionalities that are not always included in Part 150 studies but may be used in specialized noise analyses, for example, atmospheric absorption adjustment over a range of meteorological conditions (SAE-ARP-5534, SAE-ARP-866A). Differences were observed for this Use Case and GT will investigate the source and document the findings. To accomplish this effort, GT will need the AEDT Studies for AIRMOD and UCD.

Task 4 – Use Case E - Part 1: Air Traffic Airspace and Procedure Analysis
The purpose of Use Case E, Part 1, was to test AEDT 2b's capability for performing noise impact, fuel consumption, CO2 production, and emissions calculations to support a NEPA study for an applicable airspace redesign study. This type of NEPA study was conducted as part of this uncertainty quantification effort in order to validate that AEDT 2b has the necessary functionality and capability to perform this type of applicable analysis.

In general, there was good agreement between AEDT2a and 2b. A few differences were observed for LAMAX. GT will investigate the differences and document them.

References

[1] Allaire and Willcox, "Surrogate Modeling for Uncertainty Assessment with Application to Aviation Environmental System Models", *AIAA Journal*, 2010

[2] ATAC Corporation, "Integrated Noise Model (INM) Version 7.0 User's Guide", FAA-AEE-07-04, April 2007

[3] Boeker, Eric; Dinges, Eric; He, Bill; Fleming, Greg; Roof, Christopher; Gerbi, Paul; Rapoza, Amanda; Hemann, Justin; "Integrated Noise Model (INM) Version 7.0 Technical Manual", FAA-AEE-08-01, January 2008

[4] CSSI, Inc., "Emissions and Dispersion Modeling System (EDMS) Version 5", FAA-AEE-07-07, Rev.5, June 2014

[5] CSSI, Inc., "Emissions and Dispersion Modeling System (EDMS) User's Manual", FAA-AEE-07-01, Rev. 10, June 2013

[6] EUROCONTROL, Base of Aircraft Data (BADA) Aircraft Performance Modeling Report, EEC Technical/Scientific Report No. 2009-009, March 2009

[7] Landrum & Brown Team, "Seattle-Tacoma International Airport Part 150 Study", October 2013, URL: http://www.airportsites.net/sea-part150/final.htm, Accessed on 5/1/2016

[8] Noel, George, "AEDT Alpha UQ Report", Volpe, January 2011

[9] Noel, George, "AEDT Uncertainty Quantification", presented in FAA/AEE Tools Review, December 2010

[10] Peck, Jay; Oluwole, Oluwayemisi; Wong, Hsi-Wu; Miake-Lye, Richard; "An algorithm to estimate aircraft cruise black carbon emissions for use in developing a cruise emissions inventory", *Journal of the Air & Waste Management Association*, 63:3, 367-375, 2013

[11] Peck, Jay; Oluwole, Oluwayemisi; Wong, Hsi-Wu; Miake-Lye, Richard; "An Algorithm to Estimate Aircraft Cruise Black Carbon Emissions for Use in Developing a Cruise Emissions Inventory", Aerodyne Research Inc., Black carbon final report, submitted to FAA, June 2012

[12] US FAA, AEDT 2c User Manual, 2016

[13] US FAA, AEDT 2c Technical Manual, 2016

[14] US FAA, Aviation Environmental Design Tool (AEDT) Technical Manual Version 2b Service Pack 3, June 2016

[15] US FAA, *Environmental Desk Reference for Airport Actions*, October 20-7, URL:https://www.faa.gov/airports/environmental/environmental_desk_ref/, Accessed on October 10, 2016

[16] US FAA, *AEDT 2a UQ Report*, 2014

[17] US FAA, *AEDT 2a SP2 UQ Supplemental Report*, 2014

[18] US FAA, Aviation Environmental Design Tool (AEDT) Version 2b Beta 8 User Guide, August 2014

[19] US FAA, Aviation Environmental Design Tool (AEDT) Technical Manual Version 2a, November 2012

[20] Wayson, Roger; Fleming, Gregg G; Iovinelli, Ralph; "Methodology to Estimate Particulate Matter Emissions from Certified Commercial Aircraft Engines", *Journal of the Air & Waste Management Association*, 59:1, 91-100, DOI: 10.3155/1047-3289.59.1.91, 2009

[21] Willcox, "Tools Uncertainty Quantification", presented in FAA/AEE Tools Colloquium, December 2010

Project 037 CLEEN II System Level Assessment

Georgia Institute of Technology

Project Lead Investigator

Dimitri Mavris (PI)
Regents Professor
School of Aerospace Engineering
Georgia Institute of Technology
Mail Stop 0150
Atlanta, GA 30332-0150
Phone: 404-894-1557
Email: dimitri.mavris@ae.gatech.edu

University Participants

Georgia Institute of Technology

- P.I.(s): Dr. Dimitri Mavris (PI), Mr. Christopher Perullo (Co-PI), Dr. Jimmy Tai (Co-PI)
- FAA Award Number: 13-C-AJFE-GIT-013
- Period of Performance: September 1, 2015 –August30th, 2018

Project Funding Level

The project is funded at the following levels: Georgia Institute of Technology ($170,000).

The Georgia Institute of Technology has agreed to a total of $170,000 in matching funds. This total includes salaries for the project director, research engineers, graduate research assistants and computing, financial and administrative support, including meeting arrangements. The institute has also agreed to provide tuition remission for the students paid for by state funds.

Investigation Team

Georgia Institute of Technology
Principal Investigator: Dimitri Mavris
Co-Investigators: Christopher Perullo, Jimmy Tai
Fleet Modeling Technical Lead: Holger Pfaender
Noise Modeling Technical Lead: Greg Busch

Project Overview

Georgia Tech (GT) was previously selected to perform all of the system level assessments for the CLEEN program under PARTNER project 36 and ASCENT project 10. As a result, Georgia Tech has a unique position from both a technical and programmatic standpoint to continue the system level assessments for CLEEN II. From a technical perspective, GT has significantly enhanced the Environmental Design Space (EDS) over the last 5 years to incorporate advanced, adaptive, and operational technologies targeting fuel burn, noise, and emissions. EDS was successfully applied to all CLEEN I contractor technologies including: GE open rotor, TAPS II combustor, FMS-Engine and FMS-Airframe; Pratt & Whitney geared fan; Boeing adaptive trailing edge and CMC nozzle; Honeywell hot section cooling and materials; and Rolls-Royce turbine cooling technologies. GT also gained significant experience in communicating system level modeling requirements to industry engineers and translating the impacts to fleet level fuel burn, noise, and emissions assessments. This broad technical knowledge base covering both detailed aircraft and engine design and high level benefits assessments puts GT in a unique position to assess CLEEN II technologies.

As the ultimate goal of this work is to conduct fleet level assessments for aircraft representative of future 'in-service' systems, GT will create system level EDS models using a combination of both CLEEN II and other public domain N+1 and N+2 technologies. The technology and fleet assumptions setting workshops conducted under ASCENT project 10 will be heavily leveraged for this effort. Non-CLEEN II technologies for consideration along with potential future fleet scenarios will help to bound the impact of CLEEN II on future fleet fuel burn, emissions, and noise.

Long term goals of this project include the vehicle and fleet level assessments of fuel burn, emissions, and noise benefits for the aircraft and engine technologies funded for development under CLEEN II. More specifically, the first period of performance for this work has sought to establish working relationships with each of the chosen CLEEN II contractors to identify system level modeling needs within EDS for each contractor. At the conclusion of this first period of performance, GT has system level modeling roadmaps in place for each contractor along with non-disclosure agreements (NDA) and working timelines to conduct the assessments for each contractor.

More specifically, this year has focused on modelling the technologies of the Aurora D8 Aircraft fuselage with Wing Mounted Engines, GE-FMS Optimal Control technologies, Pratt & Whitney High Pressure Compressor and High Pressure Turbine, Delta Tech Ops / MDS / America's Phenix Leading Edge Protective Coating and GE More Electric Systems and Technologies for Aircraft in the Next Generation, (MESTANG). The modelling efforts are either in progress or in discussions with the OEMs regarding receiving input data.

Modeling and assessment roadmaps have previously been constructed for each CLEEN II contractor. These roadmaps include working schedules for data exchange between GT and each contractor and expected system assessment modeling start and end dates. Roadmaps are broken out by technology and will be used to plan out resources and modeling efforts for the remainder of the CLEEN II program. The roadmaps will also include descriptions of the technology modeling approaches for each CLEEN II technology and whether or not the underlying assessment models (independent of CLEEN II data) are leveraged from prior FAA work, must be newly developed under this work, or are from another effort such as a NASA funded project. GT and the FAA have been working on their prospective modelling tasks. GT has made significant progress for their modelling of the Aurora D8 fuselage. Many discussions between GT and GE-MESTANG as well as Pratt & Whitney are underway regarding initial data for simulating their CLEEN II technologies. Additionally FAA has made progress regarding GE-FMS Optimal Control technologies and as well as the Delta Tech Ops / MDS/ America's Phenix Leading Edge Protective Coating. . Additional information and details on this effort are proprietary and can be obtained through the FAA technical project manager for qualified personnel.

Major Accomplishments

- Modelling activities underway with GT and FAA
- GT has re-signed expired non-disclosure agreements with all CLEEN II contractors
- Modeling roadmaps established for all of the CLEEN II contractors
- Several working meetings with FAA to define modeling roadmaps and tutorials on using EDS to model technology.

Publications

None.

Outreach Efforts

None.

Awards

None

Student Involvement

None yet; students will be involved later in the period of performance once modeling work begins.

Plans for Next Period

Per the modeling roadmaps, GT and the FAA will continue modelling efforts for the Aurora, GE, PW, and Delta technologies. UTAS simulation is expected to start third quarter of 2017.

References

None

Project 038 Rotorcraft Noise Abatement Procedures Development

The Pennsylvania State University
Continuum Dynamics, Inc.
Sikorsky Aircraft Corporation
AHS International

Project Lead Investigator

Kenneth S. Brentner
Professor of Aerospace Engineering]
Department of Aerospace Engineering
The Pennsylvania State University
233 Hammond Building, University Park, PA
(814)865-6433
ksbrentner@psu.edu

University Participants

The Pennsylvania State University

- P.I.: Kenneth S. Brentner, Professor of Aerospace Engineering
- FAA Award Number: 13-C_AJFE-PSU-038, Amendment No. 22
- Period of Performance: August 2015 to July 2017
- Task(s):
  - Year 1:
    1. Selection of helicopters to develop noise abatement procedures
    2. Analyze noise abatement procedures for each of the selected helicopters
    3. Evaluate whether unique noise abatement procedures should be developed for each category
    4. Model noise abatement procedures to demonstrate their advantages
  - Year 2 (Project extension)
    5. Development and evaluation of noise procedure
    6. Analyze noise abatement procedure and plan flight test
    7. Compare flight test data with prediction
    8. Evaluate flight test data

Project Funding Level

Year 1: FAA: $150,000; In-Kind Match: (Continuum Dynamics, Inc.: $75,000 to PSU; Sikorsky Aircraft Corporation: $37,500; AHS International: $37,500); Year 2: FAA: $150,000; In-Kind Match: (Continuum Dynamics, Inc.: $75,000 to PSU; Sikorsky Aircraft Corporation: $37,500; AHS International: $37,500)

Investigation Team

Kenneth S. Brentner, PI, The Pennsylvania State University; acoustics predictions lead on all tasks.
Joseph F. Horn, Co-PI, The Pennsylvania State University; flight simulation lead supporting all tasks

Daniel A Wachspress, Co-PI, Continuum Dynamics, Inc.; responsible for rotor loads and wake integration, and CHARM coupling, primarily involved in tasks 1 and 2.
Willca Villafana, Graduate Research Assistant, The Pennsylvania State University; assisted in development and evaluation of noise prediction procedures, and setup of different helicopter models and comparison of predicted noise for different helicopters, task 1and 2 (graduated and finished work August 2016).
Umberto Saetti, Graduate Research Assistant, The Pennsylvania State University; assisted in setting up the aircraft models in the flight simulator and running the flight simulations to provide data for noise prediction.
Mrunali Botre, Graduate Research Assistant, The Pennsylvania State University; primary responsibility for setting up new aircraft models, developing simulations with new helicopter types, acoustic predictions and development of flight abatement procedures, involved in all tasks. (Started on project August 2016.)
Eric Jacobs, Industrial Partner, Sikorsky Aircraft Corporation; primary responsibility for flight test plan development in task 4, provide feedback on all aspects of project, especially tasks 3 and 4.
Paul Schaaf, Industrial Partner, AHS International; pilot and operator experience, provides guidance on abatement procedure development.

Project Overview

Rotorcraft noise consists of several components including rotor noise, engine noise, gearbox and transmission noise, etc. Rotor noise is typically the dominant component of rotorcraft noise that is heard by the community upon takeoff, landing, and along the flight path of the helicopter. Rotor noise consists of several different noise sources including thickness noise and loading noise (together typically referred to as rotational noise), blade-vortex-interaction (BVI) noise, high-speed-impulsive (HSI) noise, and broadband noise – with each noise source having its own unique directivity pattern around the helicopter. Furthermore, any aerodynamic interaction between rotors, interaction of the airframe wake and a rotor, or unsteady, time-dependent loading generated during maneuvers typically results in significant increases in loading noise. The combination of all the potential rotor noise sources makes prediction of rotorcraft noise quite complex, even though not all of the noise sources are present at any given time in the flight (e.g., BVI noise usually occurs during descent and HSI noise only occurs in high-speed forward flight).
In ASCENT Project 6, "Rotorcraft Noise Abatement Operating Conditions Modeling", the project team coupled a MatLab based flight simulation code with CHARM and PSU-WOPWOP to preform rotorcraft noise predictions. This noise prediction system was used for developing noise abatement procedures through computational and analytical modeling. Although this noise prediction system does not contain engine noise or HSI noise prediction capability, it was thoroughly validated by comparing predicted noise levels for a Bell 430 aircraft with flight test data (Ref. 19) for several observer positions and operating conditions.
OBJECTIVES
The objective of this project is to utilize computational and analytical modeling to develop noise abatement procedures for various helicopters for various phases of flight. An extension of the project also includes predictions to support flight test planning.
The research team will recommend representative helicopters for which noise abatement procedures will be developed. The helicopters will be selected to determine if it is feasible to develop noise abatement procedures for categories of helicopters, (i.e., 2 blade light, 4 blade light, 2 blade medium, etc.) or if aircraft specific design considerations will be required in the development of noise abatement procedures. Noise abatement procedures will be compared to representative baseline operations. Comparisons will be made using various noise metrics (SEL, DNL, EPNL, etc.) along with the acoustic pressure time history and acoustic spectrum plots (which will be used primarily to explain what is impacting the metrics).

Task 1. SELECTION OF HELICOPTERS TO DEVELOP NOISE ABATEMENT PROCEDURES

The Pennsylvania State University

Objective(s)

The objective of this task is to identify several rotorcraft that should be included in the modeling study. These aircraft will consist of helicopters in several categories, including various gross take-off weights, number of main rotor blades, regular vs. quiet tail rotor, etc.

Research Approach

The selection of aircraft for study must be limited, but span a variety of helicopter classes. These aircraft will consist of helicopters in several categories, including various gross take-off weights, number of main rotor blades, regular vs. quiet tail rotor, different generations of similar or the same aircraft from a manufacturer, etc. Some of the aircraft selected should be models that have manufacturer noise abatement procedures described in the HAI Noise Abatement Training CD. Some newer aircraft models that may not have guidelines from the manufactures should also be included (e.g., Sikorsky Aircraft Corporation S-76D). Consideration of which helicopter types have been responsible for the most complaints – and those who have not been associated with complaints – are made in the final selection of 4 to 8 helicopters for the study.

Milestone(s)

Choose the study helicopters to span a range of ages, technology levels, vehicle classes, manufacturers, and weights.

Major Accomplishments

Several aircraft were selected for study. These include 3 generations of the Airbus Helicopters BK 117, EC 145, and H145 (which has a fenestron anti-torque system). To consider different size and number of main rotor blades, the Bell 430, Bell 429, and Bell 206 were selected, along with the Sikorsky S-76C+, S-76D, and S-92. The Bell 206 is an older aircraft with a 2-bladed main rotor that is still in widespread use. The S-76D is a new model of the S-76 which has significant technology upgrades aimed at reducing noise as compared to the S-76C+. The S-92 aircraft was chosen because it is a much heavier helicopter; with maximum take-off weight is more than twice as much as the S-76D. The aircraft are shown in Fig. 1.1. (Note: In the second year of this project, as the FAA/NASA flight test-planning proceeds, it is likely that this list of aircraft will be modified to represent those aircraft that are available for the flight test.

Publications

None

Outreach Efforts

None

Awards

None

Student Involvement

Willca Villafana and Umberto Saetti are the graduate research assistants working on this project. Each of them finished their M.S. degree in Aerospace Engineering at Penn State in August, 2016. They both helped collect data on the various helicopters that were considered for selection.

Plans for Next Period

The selection of aircraft will be modified to represent the aircraft that are available for the FAA/NASA noise test.

References

None

Figure 1.1: Aircraft selected for study in this project. (Note: this list of aircraft will likely be modified to reflect the aircraft available for the FAA/NASA noise abatement flight test.)

Task 2. ANALYZE NOISE ABATEMENT PROCEDURES FOR EACH OF THE SELECTED HELICOPTERS

The Pennsylvania State University

Objective(s)

The objective of this task is to set-up the helicopter models used in this study.

Research Approach

Each of the helicopters selected in task 1 will be modeled in the flight simulation/noise prediction system. Recommended noise abatement procedures will be compared to typical operating procedures. This analysis will evolve throughout the project, i.e., as new procedures are developed for one aircraft, they will be considered for other helicopters with different configurations or weight class. This task will provide the information to assess the effectiveness of noise abatement procedures in general and provide data to investigate if the procedures are generally relevant to helicopters, a particular category of helicopters, or only to a specific helicopter type/model.

Milestone(s)
Flight simulation models set up for the Bell 430, S 76C and BK 117. Noise predictions were made for several flight conditions.

Major Accomplishments
Flight simulation models set up for the Bell 430, S 76C and BK 117. Noise was modeled for level flyover at various speeds and altitudes for these aircraft. Some bugs in the noise prediction system were discovered and fixed. Previous results for steady flight conditions were unaffected, but time-varying flight conditions (e.g., deceleration, etc.) were not correct (and therefore, are not shown. Figure 2.1 shows the PNLT at a microphone directly under the centerline of the aircraft as a function of the position of the aircraft relative to the microphone; i.e., when the aircraft is directly overhead, the distance is zero.

Publications
Saetti, U.; Horn, J. F.; Brentner, K. S.; Villafana, W., and Wachspress, D.A., "Rotorcraft Simulations with Coupled Flight Dynamics, Free Wake, and Acoustics," presented at the AHS Forum, West Palm Beach, FL, May 2016..

Outreach Efforts
None

Awards
None

Student Involvement
Umberto Saetti, graduate assistant at Penn State, was primarily responsible for the flight simulation and loads produced by HeloSim and Charm rotor module. Willca Villafana, also a graduate assistant at Penn State. was responsible for the noise computations with PSU-WOPWOP. Both students completed their M.S. degree in August, 2016.

Plans for Next Period
As the aircraft types are chosen for the FAA/NASA helicopter noise abatement flight test, they will be modelled with this noise prediction system – especially in support of the flight test.

References
None

S76-C+

Bell 430

BK 117

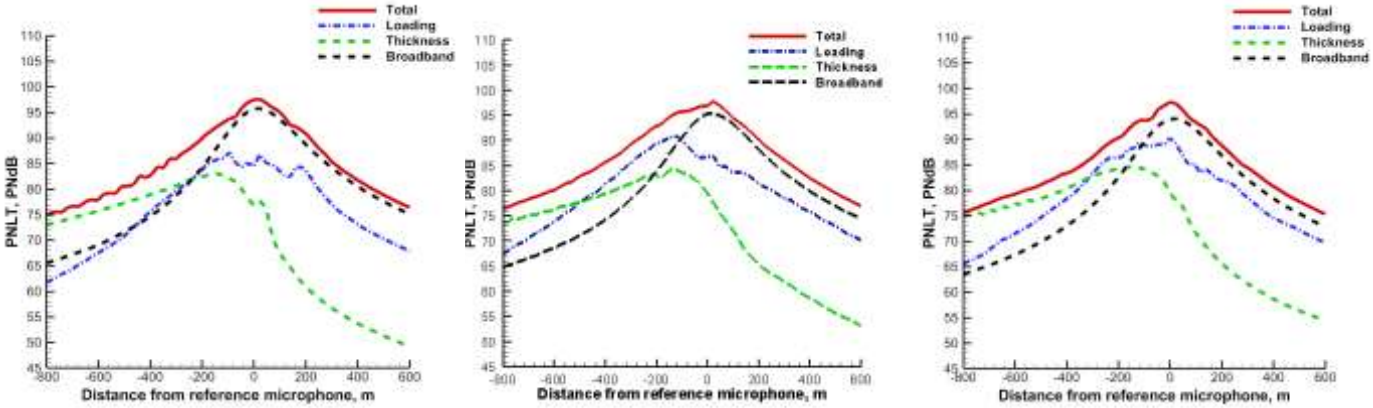

Figure 2.1: Tone-corrected perceived noise level for a level, 90 kts flyover at 500 ft altitude for 3 different helicopters. The various noise sources and the total noise are shown for each aircraft. The figures do not include ground reflection. The weight of the S-76C+ was 11,350 lbs; Bell 430 was 9000 lbs; and the BK 117 weight was 7115 lbs. (these weights are 97% of the helicopter MTOW in each chase).

Task 3. EVALUATE WHETHER UNIQUE NOISE ABATEMENT PROCEDURES SHOULD BE DEVELOPED FOR EACH CATEGORY

The Pennsylvania State University

Objective(s)

An analysis of the results for task 2 will be used to determine to what extent the noise abatement procedures are common across various helicopter categories (weight, number of main rotor blades, tail rotor configuration, etc.)

Research Approach

The analysis will lead to recommendations about whether unique procedures are advantageous for the different helicopter categories or if generalized recommendations are sufficient. Consideration will also be given to individual helicopter models within a category and the differences in the effectiveness of various noise abatement procedures for each helicopter. This task will provide guidance to the FAA, land use planners, and operators about the effectiveness of general noise abatement procedures vs. specific procedures for various helicopter models. It will also provide a basis for future classification and procedure development

Milestone(s)

Evaluation of noise abatement procedures and comparison of results for different helicopter categories.

Major Accomplishments

This task has been delayed due to the error found in the noise prediction system (which has now been fixed), and due to the uncertainty of which aircraft will be used in the flight test.

Publications
None

Outreach Efforts
None

Awards
None

Student Involvement
None

Plans for Next Period
Analysis of the noise for the different aircraft, once the selection and modeling is complete, will be performed for noise abatement procedures.

References
None

Task 4. MODEL NOISE ABATEMENT PROCEDURES TO DEMONSTRATE THEIR ADVANTAGES
The Pennsylvania State University

Objective(s)
Demonstrate the noise abatement procedures in the flight simulation system. Characterize the improvement, both in magnitude and directivity.

Research Approach
Various metrics will be used to evaluate the effectiveness of noise abatement procedures – including metrics like SEL, EPNL, etc. The noise prediction system is able to predict this information on a ground plane to map out the noise directivity and the regions of noise reduction or noise increase. While these results will guide the work in the second and third tasks, in this task the analysis and summary of the benefits will be reported. Results that are more detailed will also be provided. The goal is to demonstrate how effective the noise abatement procedures are in a manner that will be relevant to helicopter pilots, operators, land use planners, and the FAA. A secondary goal is to demonstrate that the noise prediction system is useful to provide guidance for helicopters that do not have the benefit of extensive noise testing to develop noise abatement procedures.

Milestone(s)
Complete noise predictions for all helicopter types and for all baseline and noise abatement procedures; complete evaluation of noise abatement procedures by helicopter category and device recommendations; report effectiveness of various procedures.

Major Accomplishments

In ASCENT Project 6, noise was predicted for the Bell 430 helicopter for a level flight condition (100 kts) at flyover altitudes ranging from 150m to 350m, in 50m increments. This result, shown in Fig. 4.1, demonstrates the powerful impact that distance makes in reducing the noise. When the aircraft is overhead (distance from observer = 0m in the figure), the noise is reduced by approximately 6dB when the distance is doubled (as expected). However, to the side of the flightpath, the noise reduction is not nearly as great because the distance from the observer to the aircraft does not change as much when the helicopter increases its altitude, and can even increase slightly (as shown in Fig. 4.2, especially (b)). The increase on the right side of the aircraft in Fig. 4.2 is not related to distance, but rather a change in the directivity angle that the observer sees when the aircraft is higher. A consideration of where the noise is changing with any abatement procedure will be important.

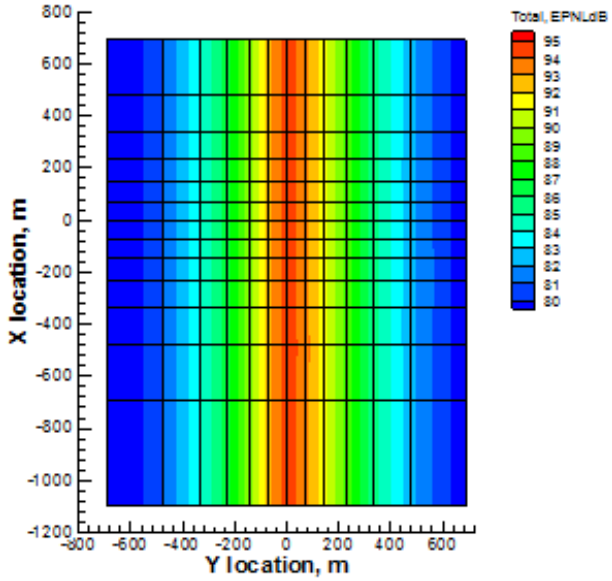

(a) EPNL contours, $V_H = 100$ kts, altitude =150m

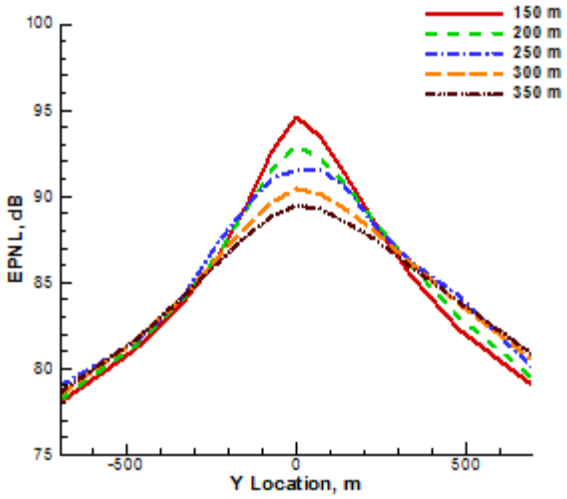

(b) EPNL at $x = 0$ plane, $-700 < y < 700$ m for various altitudes

Figure 4.1 Effective Perceived Noise Levels for Bell 430 helicopter flying at 100 kts at altitudes from 150m to 350 m.

A similar comparison of predicted noise was performed for the Bell 430 operating at forward speeds ranging from 60 kts to 140 kts in level flight at 150m (shown in Fig. 4.3). It is generally understood that flying slower will reduce the noise levels. The physics of the source noise mechanisms (in-plane noise in particular) indeed exhibit this behavior. But when the EPNL is considered, which takes into account the duration of the exposure as well as the level, the levels of EPNL do not change significantly below the helicopter even though the expected trend is seen away from the centerline (see Fig. 3.3). The reason for this is that while the noise level is lower for low speed (e.g., 60 kts), the exposure time is longer. So along the helicopter flight path the EPNL levels are essentially the same for the 60 kts and 140 kts cases. These studies will guide the development of noise abatement procedures in this task.

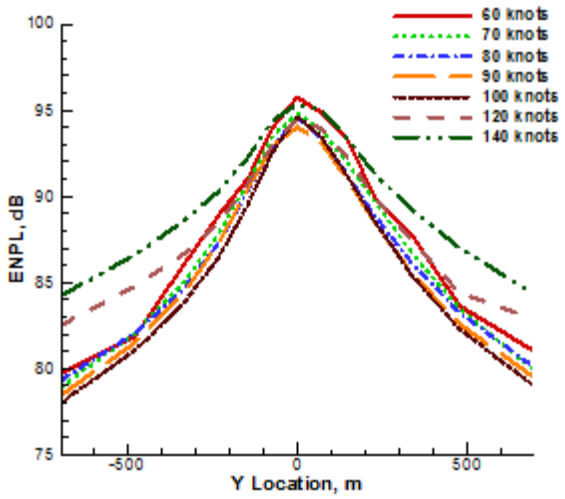

Figure 4.2 EPNL along $x = 0$ plane, $-700 \leq y \leq 700$ m for forward speeds ranging from 60 kts to 140 kts.

Publications
None

Outreach Efforts
None

Awards
None

Student Involvement
None yet.

Plans for Next Period
It is planned to predict the noise for all the flight test aircraft and compare the results for various aircraft.

References
None

Extension (Year 2): Task 5. DEVELOPMENT AND EVALAUTION OF NOISE ABATEMENT PROCEDURES

The Pennsylvania State University

Objective(s)

The object of this task is to continue the development various noise abatement procedures and to determine the noise the procedures common across various helicopter categories (weight, number of main rotor blades, tail rotor configuration, technology generation, etc.). This will help to determine the fidelity required for designing the abatement procedure. The helicopters used for flight test will be used to do the analysis and consequently will design the flight procedure.

Research Approach

For this effort, the noise prediction system developed in ASCENT Project 38 will be used and updated as necessary. The PSU-WOPWOP code will be used for noise prediction, and will be coupled with a MatLab flight simulator and CHARM (Comprehensive Hierarchical Aeromechanics Rotorcraft Model) to form a rotorcraft noise prediction system. Limited validation of the system through comparison with the NASA/Bell flight test has demonstrated that the system is reasonably accurate with very reasonable computational cost. The initial procedure considered is a decelerating decent case, which should reduce or eliminate BVI noise during decent. Other flight procedures will be considered after that, including turns and descending turns – which often occur in urban settings. The noise abatement procedures will be compared to standard procedures through comparison of several different acoustic metrics.

Milestone(s)

Evaluation of noise abatement flight procedures for a variety of helicopter categories.

Major Accomplishments

While evaluating noise prediction of unsteady aircraft motion (like decelerating decent) an error was found in the noise prediction system. This error was related to the reconstruction of the rotor wake in the Charm rotor module that is done to provide high-resolution airloads for the noise prediction. In particular, after the high-resolution airloads were output, the module restores the wake geometry to its original low resolution and then continues the flight simulation until the next time when high-resolution airloads need to be saved. The process of restoration added a small error that accumulated after several reconstruction/restoration cycles. To debug this problem, the code was run multiple times with only reconstruction (no restoration), but the code was run to different times. Once the source of the problem was identified, it was fixed and computations of decelerating flight have now resumed.

Another accomplishment during this task, is related to validation of the noise prediction system. For more direct comparisons with flight test data, a tool was written that takes the acoustic pressure measure in the flight test and puts it into a format that PSU-WOPWOP can read. In this way, noise predictions and flight test data are post processed in exactly the same manner – both using the post processing procedures in PSU-WOPWOP.

The primary accomplishment of this task to date is the simulation of different flight conditions and comparing the noise with flight test data. The validation of the noise prediction system in both level flight and a blade-vortex-interaction flight conditions is a significant achievement for the project. The agreement between the predicted and measured results is quite reasonable for fidelity of these tools and it demonstrates that the tools are able to predict the significant physical noise sources that must be modified to achieve noise abatement. This validation enables the noise prediction system to be used for the other tasks in the project with a degree of confidence. Figure 5.1 shows the prediction for a 95 kts level flight case. The noise components and total noise are shown in terms of OASPL and A-weighted OASPL as a function of the helicopter time (0 sec. is the time with the helicopter is overhead). Note that the flight test data (black line) includes a ground reflection on a hard ground. The noise predictions labeled “Total …. – No Wall” are free-field noise prediction, while the “Total … - Wall in” include the effect of a hard ground; hence, the “wall in” prediction should be compared with the flight test data (Run 273126). In Fig. 5.2, the predicted noise for a 0.05g deceleration along 6 deg. descent is shown. During this flight procedure, the aircraft velocity reduces from 100 kts to approximately 68 kts.

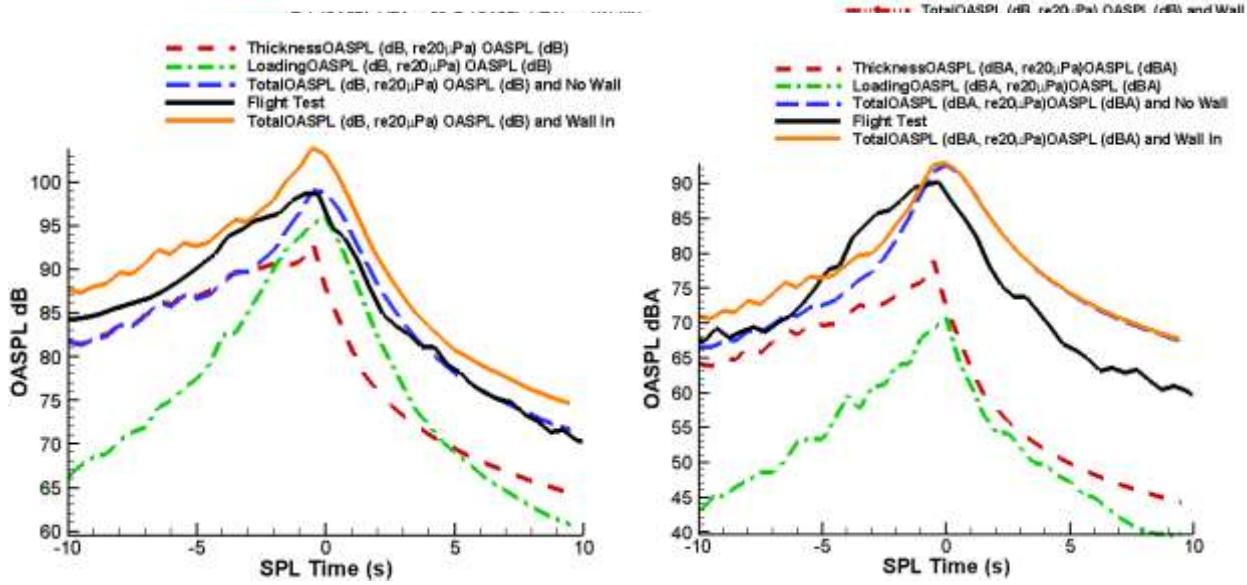

(a) OASPL, dB (b) A-weighted OASPL, dBA

Figure 5.1 OASPL and A-weighted OASPL levels for Bell 430 in 94.7 kts level flight, compared with flight test data (Run 273126).

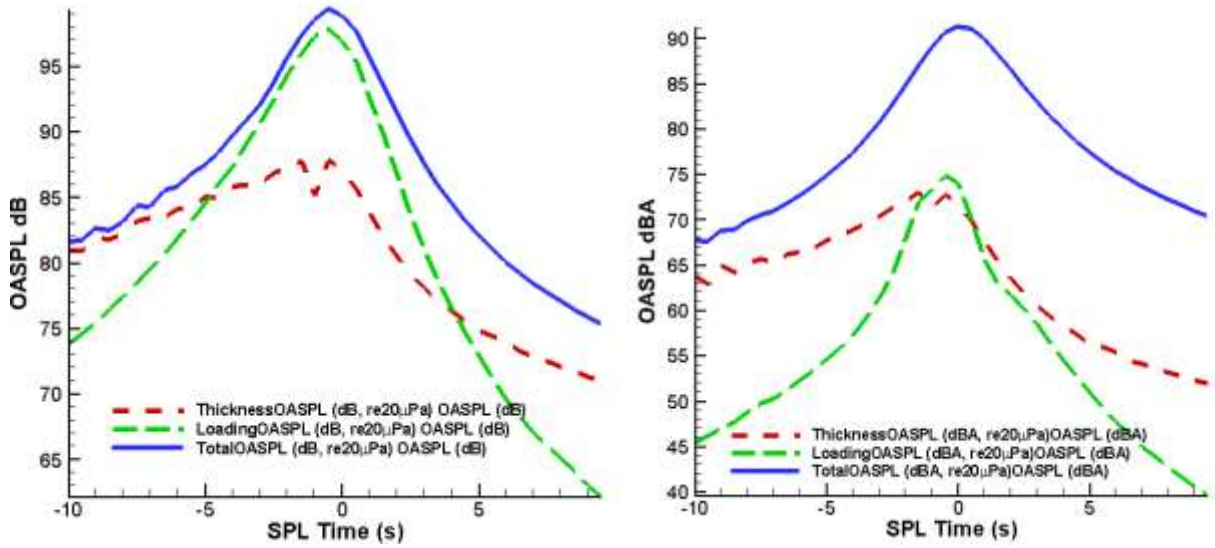

(a) OASPL, dB (b) A-weighted OASPL, dBA

Figure 5.2 OASPL and A-weighted OASPL levels for Bell 430 in deaccelerating descent flight.

Publications

None

Outreach Efforts

None

Awards

None

Student Involvement
Mrunali Botre, graduate assistant currently working toward her Ph.D. at Penn State, performed the acoustic predictions and worked on debugging the problem with the error introduced by the reconstruction/restoration process.

Plans for Next Period
Now that the errors for time-dependent operations have been resolved, the plan is to review several noise abatement procedures – especially those that reduce or eliminate BVI noise. The flight procedures will be examined for one aircraft and then replicated for other aircraft (especially those selected for the upcoming FAA/NASA flight test).

Task 6. ANALYZE NOISE ABATEMENT PROCEDURES IN SUPPORT OF PLANNING OF A POTENTIAL FLIGHT TEST PROGRAM.
The Pennsylvania State University

Objective(s)
This task will develop and analyze of rotorcraft noise abatement flight procedures for the aircraft used in flight test. The procedures will be used to plan flight test and the data will be used to validate the tools.

Research Approach
In support of an anticipated flight test, the helicopters used in the flight test will be modeled and the noise from the anticipated flight procedures (baseline and noise abatement procedures) will be predicted. This predictions will be used to assess if the flight procedure is likely provide sufficient noise abatement to be considered for the flight test, thus minimizing the total number of flight hours while demonstrating maximum noise abatement through various procedures. The noise predictions can also be used to help identify or verify microphone placement for optimal placement of a limited number of microphones (30-45) during the flight test.

Milestone(s)
Computational models for the planned flight test aircraft need to be developed. Then predictions of the planned flight test procedures need to be computed over an area larger than the planned measurement array.

Major Accomplishments
This task is just getting underway.

Publications
None

Outreach Efforts
None

Awards
None

Student Involvement
Mrunali Botre, graduate assistant currently working toward her Ph.D. at Penn State, will lead the noise prediction effort, including development of the flight test aircraft models (with the help of Dan Wachspress and the rest of the team).

Plans for Next Period
The primary noise abatement procedures (or procedure element) for the flight test will be predicted with the noise prediction system. The aircraft models for the anticipated flight test aircraft will be developed.

References
None

Task 7. COMPARE FLIGHT TEST NOISE RESULTS WITH PREDICTED RESULTS FOR THE SAME AIRCRAFT FOR VALIDATION AND ASSESSMENT OF THE NOISE PREDICTION SYSTEM.
The Pennsylvania State University

Objective(s)
The objective is to compare the flight test data with predicted noise levels to validate the effectiveness of the noise abatement procedures.

Research Approach
In this task, it is anticipated that acoustic data from the flight test will be available for comparison with the predicted noise measurement. This comparison will have two primary goals: 1) to assess and validate the effectiveness of the prediction system and to determine the significance of noise sources not currently modeled (i.e., engine noise); and 2) to evaluate and verify the effectiveness of noise abatement flight procedures. If the planned flight test is delayed, the Bell 430 flight test data has a rich set of cases that can be used in the interim for more thorough validation of the noise prediction system. Also some of the maneuvers tested in the Bell 430 flight test may be elemental portions of noise abatement procedures; hence, useful (if the flight test is delayed).

Milestone(s)
Task has not started yet.

Major Accomplishments
None

Publications
None

Outreach Efforts
None

Awards
None

Student Involvement
Mrunali Botre, graduate assistant currently working toward her Ph.D. at Penn State, will support the comparison of predicted results with flight test data.

Plans for Next Period
Comparison will commence for the Bell 430 flight test data that is already available. After (or during) the flight test, comparisons of the predicted results and the flight test data will be performed.

References
None

Task 8. ASSIST IN INITIAL EVALUATION OF FLIGHT TEST DATA TO DETERMINE EFFECTIVENESS OF NOISE ABATEMENT PROCEDURES.

The Pennsylvania State University

Objective(s)

This task will support the flight test team to determine the effectiveness of the noise abatement procedures.

Research Approach

A final task for this extended project is to provide assistance in the initial evaluation of the flight test data and the effectiveness of various noise abatement procedures. This will involve evaluation of the flight test data and examination and comparison of measured and predicted results to help explain any significant unexpected noise measurement. This evaluation can also identify which noise sources are the primary and secondary noise sources involved in a flight procedure and provide understanding about how the noise abatement was achieved (which can lead to generalizing the procedure to other helicopter categories, weights, etc.).

Milestone(s)

None

Major Accomplishments

None

Publications

None

Outreach Efforts

None

Awards

None

Student Involvement

Mrunali Botre, graduate assistant currently working toward her Ph.D. at Penn State, will assist in this effort.

Plans for Next Period

None – this task cannot be performed until the flight test has occurred.

References

None

Project 039 Naphthalene Removal Assessment

Massachusetts Institute of Technology

Project Lead Investigator

Prof. Steven Barrett
Leonardo Associate Professor of Aeronautics and Astronautics
Department of Aeronautics and Astronautics
Massachusetts Institute of Technology
77 Massachusetts Avenue – Bldg 33-322
Cambridge, MA 02139
(617)-452-2550
sbarrett@mit.edu

University Participants

Massachusetts Institute of Technology

- P.I.: Prof. Steven Barrett
- Co-PI: Dr. Raymond Speth
- FAA Award Number: 13-C-AJFE-MIT, Amendment No. 026
- Period of Performance: July 8, 2016 to Aug. 31, 2017 (reporting with the exception of funding levels and cost share only for the period from July 8 1, 2016 to September 30, 2016).
- Task:
    1. Preliminary screening of refinery processes for naphthalene removal

Project Funding Level

$200,000 FAA funding and $200,000 matching funds. Sources of match are approximately $52,000 from MIT, plus 3rd party in-kind contributions of $148,000 from Oliver Wyman Group.

Investigation Team

Prof. Steven Barrett (MIT) serves as principal investigator for the A39 project as head for the Laboratory for Aviation and the Environment. Prof. Barrett coordinates both internal research efforts and maintains communication between investigators in the various MIT research teams mentioned below.

Dr. Raymond Speth (MIT) serves as co-principal investigator for the A39 project. Dr. Speth directly advises student research in the Laboratory for Aviation and the Environment focused on assessment of naphthalene removal refinery options, climate and air quality modelling, and fuel alteration life-cycle analysis. Dr. Speth also coordinates communication with FAA counterparts.

Prof. William Green (MIT) serves as a co-investigator for the A39 project as a head of the Green Research Group. Prof. Green advises student work in the Green Research Group focused on computer-aided chemical kinetic modeling of PAH formation.

Mr. Randall Field (MIT) is the Executive Director of the MIT Energy Initiative, and a co-investigator of the A39 project. Drawing upon his experiences as a business consulting director at Aspen Technology Inc., Mr. Field provides mentorship to student researchers in selection and assessment of naphthalene removal refining option, and process engineering at-large.

Mr. Drew Weibel (MIT) is a graduate student researcher in the Laboratory for Aviation and the Environment. Mr. Weibel is responsible for conducting selection and assessment of naphthalene removal refining options, calculation of refinery process requirements and fuel composition effects from selected processes, relating PAH formation to aircraft PM

emissions, estimating capital and operating costs of naphthalene removal, air quality and climate modelling, and an integrated cost-benefit analysis.

Mr. Max Liu (MIT) is a Ph.D. candidate researcher in the Green Research Group. Mr. Liu is responsible for development and analysis of a chemical kinetic model of PAH formation with fuel-composition effects and developing a relationship between PAH formation and aircraft PM emissions.

Project Overview

Aircraft emissions impact the environment by perturbing the climate and reducing air quality, which leads to adverse health impacts, including increased risk of premature mortality. As a result, understanding how different fuel components can influence pollutant emissions, as well as the resulting impacts and damages to human health and the environment, is of importance to leading future research aims and policy. Recent emissions measurements have shown that removal of naphthalenes, while keeping total aromatic content unchanged, can dramatically reduce emissions of particulate matter. The objective of this research is to determine the benefits, costs, and feasibility of removing naphthalenes from jet fuel, in regards to the refiner, the public, air quality, and the environment. Specific goals of this research include:

- Assessment and selection of candidate refining processes for the removal of naphthalenes from conventional jet fuel, including details of required technology, steady-state costs to the refiner and the public, and changing life-cycle emissions impacts at the refinery.
- Development of a chemical kinetics model to better understand the link between fuel aromatic composition resulting PM emissions due to jet fuel combustion.
- Assessment of the intrinsic climate and air quality impacts associated with naphthalene reduction and/or removal from jet fuel.
- Development of a succinct life-cycle analysis of the relative costs of removing naphthalene from jet fuel and the associated benefits due to avoided premature mortalities and climate damages for a range of possible scenarios.

Task 1: Preliminary Screening of Naphthalene Removal Refining Processes

Massachusetts Institute of Technology

Objective(s)

Naphthalene is present in varying levels in straight-run crude oil distillation cuts used to produce jet fuel, and is currently not targeted for removal in treatments used to meet industry standards. As a result, reducing the naphthalene content in jet fuel entails the introduction of an additional refinery treatment process. The objective of this task is to identify suitable refinery processes that can be used to remove or convert naphthalenes. Once identified, the process will be evaluated through analysis of the associated utility/feedstock inputs and costs of adding each treatment process to the refinery and running it at scale.

Research Approach

In order to screen potential refining processes to be used for naphthalene removal 1) a literature review will be conducted to identify candidate refining processes, 2) the candidate processes will be evaluated against each other, and 3) the trade-off associated with different levels of naphthalene removal will be assessed.

Literature Review

There are a number of processes which could potentially be employed to remove or convert naphthalene's, including selective hydrogenation, liquid-liquid extraction, adsorbents, and reactive distillation. By leveraging existing literature, potential naphthalene removal refining processes will be selected along with the level of technological innovation required (if any). Particular attention will be given to preserving non-naphthalenic aromatics, since reducing the amount of these components would limit the capacity to blend paraffinic alternative jet fuels while still meeting minimum requirements for aromatics.

Process Evaluation

In order to evaluate each candidate process, we will leverage existing literature to estimate the utility (process fuel, electricity, hydrogen, etc.) requirements for each process the effect on the composition of the resulting jet fuel, and the capital costs of new refinery equipment required. We will include the effects of any pre-processing that may be required. We will then compare processes in order to demonstrate the trade-offs associated with naphthalene removal at the refinery.

Removal Severity
As a by-product of analyzing a range of different refining pathways, we will be able to assess the tradeoffs associated with different levels of naphthalene removal. Combined with later work in development of a relationship between jet fuel composition and PAH formation, we will be able to assess the level of severity in which naphthalene's should be removed, in order to optimize costs and benefits.

Milestone(s)

Literature Review
A qualitative literature review was conducted to identify potential refining processes that can remove naphthalene from streams blended to produced jet fuel.

Major Accomplishments

Selection of Potential Naphthalene Removal Refining Processes
A set of candidate refining processes were chosen that could remove naphthalene from jet fuel intermediate streams. The chosen refining processes will be used throughout the remainder of the A39 project to determine the feasibility and associated utilities and costs of naphthalene removal.

Publications

None

Outreach Efforts

A poster describing the motivation and planned approach for this research was presented at the Fall ASCENT Meeting on September 27, 2016 in Washington, DC.

Awards

None

Student Involvement

Drew Weibel, a graduate student in the Laboratory for Aviation and the Environment is working directly with Prof Steven Barrett and Dr. Raymond Speth to conduct the research objectives of Task 1. Mr. Weibel is a 1st year graduate student, and will serve on the research team through the remainder of the A39 project timeline.

Plans for Next Period

Completion of Task 1
The remainder of Task 1 objectives will be met over next period of performance. The end product of task 1 will be the calculated process requirements and fuel composition effects of candidate naphthalene removal refining processes.

Future Work
In addition to Task 1, the effects of naphthalene content on the production of poly-aromatic hydrocarbon (PAH) molecules will be evaluated. A chemical kinetic model of PAH formation with included fuel-composition effects will be developed with Reaction Mechanism Generator (RMG) software. This model will be used along with Cantera, a combustion modeling framework, to compute PAH formation rates in fundamental combustion configurations. Along with existing aircraft engine PM emissions data, this platform will be used to develop scaling relations between PAH formation rates computed from the combustion model, and expected engine-specific PM emissions.

Project 040 Quantifying Uncertainties in Predicting Aircraft Noise in Real-world Scenarios

Pennsylvania State University
Purdue University

Project Lead Investigator

Victor W. Sparrow
Director and Professor of Acoustics
Graduate Program in Acoustics
Penn State
201 Applied Science Bldg.
University Park, PA 16802
+1 (814) 865-6364
vws1@psu.edu

University Participants

Pennsylvania State University

- P.I.: Victor W. Sparrow, Professor of Acoustics
- Co-PI: Philip J. Morris, Boeing/A.D. Welliver Professor of Aerospace Engineering
- FAA Award Number: 13-C-AJFE-PSU, amendment 023.
- Period of Performance: June 28, 2016 to December 31, 2017.
- Task(s):
    1. Assess meteorological and acoustic measurement data sets for noise propagation model validation
    2. Assess influence of aircraft noise sources on uncertainty in noise modeling
    3. Assess overall modeling uncertainty for aircraft noise prediction
    4. Assess usefulness of SILENCE-R dataset

Purdue University

- P.I.(s): Kai Ming Li, Professor of Mechanical Engineering
- FAA Award Number: 13-C-AJFE-PU, amendment 14
- Period of Performance: August 1, 2016 – December 31, 2017
    5. Assess DISCOVER-AQ Acoustics data for model validation
    6. Assess the uncertainty due to the ground effect and source directivity for en-route aircraft

Project Funding Level

FAA funding to Penn State in 2016-2017 is $128K. FAA funding to Purdue in 2016-2017 is $90K.

In-kind cost sharing from Vancouver Airport Authority was recently received for ASCENT Project 5, and additional cost sharing is likely in Project 40. The point of contact for this cost sharing is Mark Cheng, mark_cheng@yvr.ca . Project support is in the form of aircraft noise and trajectory data, meteorology data, and consulting on those datasets.

Additional cost sharing from ANOTEC Engineering, Motril, Spain is likely in the future for ASCENT Project 40 regarding the BANOERAC data set. The point of contact for this cost sharing is Nico van Oosten, nico@anotecengineering.com .

Further cost sharing from National Aviation University of Ukraine (and Airbus) is possible in the future for ASCENT Project 40 regarding the SILENCE-R data set. The point of contact for this cost sharing is Sasha Zaporozhets, zap@nau.edu.ua .

Investigation Team

Penn State

Victor W. Sparrow (PI)
Philip J. Morris (Co-PI)
Graduate Research Assistant Manasi Biwalkar (measurement data sets for noise propagation model validation)

Purdue

Kai Ming Li (PI)
Graduate Research Assistant Yiming Wang (moving source investigation)

Project Overview

To assess the uncertainties in aircraft noise prediction, an integrated approach will be used to understand uncertainties in the aircraft state and resulting noise levels and directivity (source), the atmospheric and meteorological conditions (propagation), and ground impedance and terrain model (receiver). This approach will include all predominant uncertainties between source and receiver. The primary focus in the current year is in validating the propagation uncertainty. In addition, a new collaborative initiative with National Aviation University of Ukraine is underway.

As the tasks in this project all began in late summer 2016, reporting will be provided for tasks 1-4 of Penn State and tasks 5-6 of Purdue collectively instead of separately.

Task 1 "Assess meteorological and acoustic measurement data sets for noise propagation model validation"
Task 2 "Assess influence of aircraft noise sources on uncertainty in noise modeling"
Task 3 "Assess overall modeling uncertainty for aircraft noise prediction"
Task 4 "Assess usefulness of SILENCE-R dataset"

The Pennsylvania State University

Objective(s)

This research seeks to not only to validate current FAA/Volpe noise modeling capabilities by comparing with measurement data, but also to quantify uncertainties of both model prediction and measurement in trying to predict aircraft noise (or patterns or changes) in real world situations, particularly when meteorological conditions over various different time periods may affect prediction output. The research will (1) review and analyze available field measurement data for patterns that are influenced by the (change of) meteorological conditions; (2) identify sets of field data for specific scenarios that contain proper parameters/quality input values to validate the enhanced modeling capabilities; (3) use the enhanced modeling capabilities to understand the patterns identified in the field measurement data that are influenced by the (change of) meteorological conditions and (4) quantify uncertainties in predicting aircraft noise in real-world situations. In addition, a new collaborative initiative on aircraft noise propagation model validation will be begin with National Aviation University, Kiev, Ukraine.

Research Approach

Introduction

It is a challenging task to include the influences of atmospheric conditions and ground properties for the prediction of aircraft noise. However the accuracy of these inputs are critical for the predictions. In the past three years, the research performed by Penn State and Purdue through FAA ASCENT Center research grants has informed FAA regarding the limitations of existing noise tools and helped advance the state-of-the-art in aircraft noise modeling. Appropriate models were enhanced and developed to account for the effects of meteorological conditions, atmospheric absorption, and the Doppler effect due to source motions on the propagation of aircraft noise. Field data obtained from Discover/AQ[1] are currently used to validate these numerical models. At the same time, Penn State and Purdue have also sought support

from Vancouver Airport Authority[2] who has kept a comprehensive set of measured terminal area noise data around the Vancouver Airport. There are plans to use this database, and other databases, to improve the accuracy of the AEDT and quantify the sensitivities in the predicted noise levels due to the variation in atmospheric conditions and ground properties. It is possible that additional data available at National Aviation University of Ukraine may be helpful for the work. In Project 40 Penn State and Purdue will continue their efforts and extend them to quantify noise prediction uncertainties, now beginning to include the effects of the noise source.

Recent work at Penn State in ASCENT Project 5 has shown that the Discover/AQ Acoustics flight tracks can be read into AEDT 2b which will allow for direct comparisons between AEDT 2b noise calculations and the Discover/AQ measured noise data. Also in the last year the meteorological reanalysis data sets have been utilized to determine appropriate sound speed profiles. Profiles can be easily extracted for annual average atmospheric conditions, or for average profiles for shorter time periods. With this important atmospheric input, ray tracing has been used to assess the change in ground contours due to homeogeneous (AEDT 2b) versus linear and polynomial fit sound speed profiles. The new ASCENT Project 40 will take advantage of the new meteorological reanalysis data sets as one tool in the assessment of uncertainty in received sound levels due to aircraft noise.

Survey of available data sets

Almost all of the tasks in Project 40 involve a careful assessment of the available noise datasets that are candidates for validation of existing and future aircraft noise prediction tools. A short summary is available in Table 40.1 .

Table 40.1: Measurement datasets of interest for ASCENT Project 40.

Dataset	Focus	Owner	Potential Cost Share
Discover-AQ	Propeller aircraft	U.S. govt.	N
BANOERAC	Mostly jets en-route	EASA	Y
NINHA	Propeller aircraft en-route	EASA	Y
Vancouver, Canada Airport	Typical aircraft mix at large airport	Vancouver Airport	Y
SILENCE(R)	Airbus A320/A340	Xnoise/Airbus	Y
?			

It is clear that each dataset has its own focus. Ownership and cost share potential are also important regarding the administrative and financial ramifications of using each data set. Some specific information on the five datasets listed is now provided:

- Discover-AQ Acoustics
  Very high quality dataset

Propeller aircraft only
Includes detailed weather

- BANOERAC
  "Background noise level and noise levels from en-route aircraft"
  Owned by EASA, distributed by ANOTEC
  Still unavailable as of December 2016
    Access agreement took much longer than expected
    2nd round of negotiations commenced Summer 2016
    Verbal agreements now completely in place, a signed agreement likely in early 2017.
  Extensive measurements of aircraft at various altitudes (incl. en-route) noise with
  Ground noise data (both 1.2 m mic and inverted ground mic)
  Aircraft slant distance and slant angle data at closest point of approach.
  Full flight trajectory data can be processed (ANOTEC)
  Distant weather data (balloon launches)
- NINHA
  "Noise Impact of aircraft with Novel engine configurations in High Altitude operations"
  Owned by EASA and X-Noise
    Unavailable: They are not yet ready to release to outsiders
  Project completed September 2013

  Extensive noise prediction models in preparation for Counter Rotating Open Rotor (CROR) aircraft
  Measurements with Airbus A440M (large military transport
- Vancouver Airport Authority airport noise
  A non-U.S. airport, but easily accessible
  Fleet mix similar to other large U.S. airports
  Extensive measurements of aircraft terminal-area noise with
    Ground noise data
    Radar tracking data (NAV Canada)
    Local weather data
  Nondisclosure agreements signed between Penn State, Purdue, and Vancouver in June 2016
- SILENCE(R)
  Brought to our attention by Sasha Zaporozhets, National Aviation University, Kiev, Ukraine
  Airbus A320/A340 data
  Just now learning about the unique features of this dataset

The Penn State team began working with the DISCOVER-AQ Acoustics data in the spring of 2016 to gain experience with it. Purdue University is now focusing on that data exclusively, so Penn State is now focused on using the other data sets.

Vancouver Airport Authority Data analysis

At the beginning of ASCENT Project 40 Penn State begin looking at the Vancouver Airport Authority dataset in detail. Figure 40.1 shows an overhead view of the YVR airport and the noise monitors in the surrounding area. The work in Fall of 2016 has centered on understanding the Vancouver acoustics data, meteorology data, and radar data, and the work continues.

Uncertainty in aircraft source models

In order to evaluate aircraft noise propagation methods it is necessary to characterize the noise sources. This includes both the amplitude and the directivity. The latter is particularly important in the determination of the pressure time histories at ground observer locations. The noise directivity generated by a propeller-driven aircraft, as well as the tonal content in the spectra, is very different from those of a jet-powered aircraft. In order to interpret the noise data measured as part of the Discover-AQ Acoustics database, the noise directivity characteristics of a Lockheed P-3B aircraft have been estimated. The aircraft is powered by four Allison T56-A14 engines, each with a four-bladed 4.11 m diameter propeller. The directivity and the effects of forward flight were estimated based on fundamental propeller noise theory. This provided guidance to the modeling effort being undertaken at Purdue University.

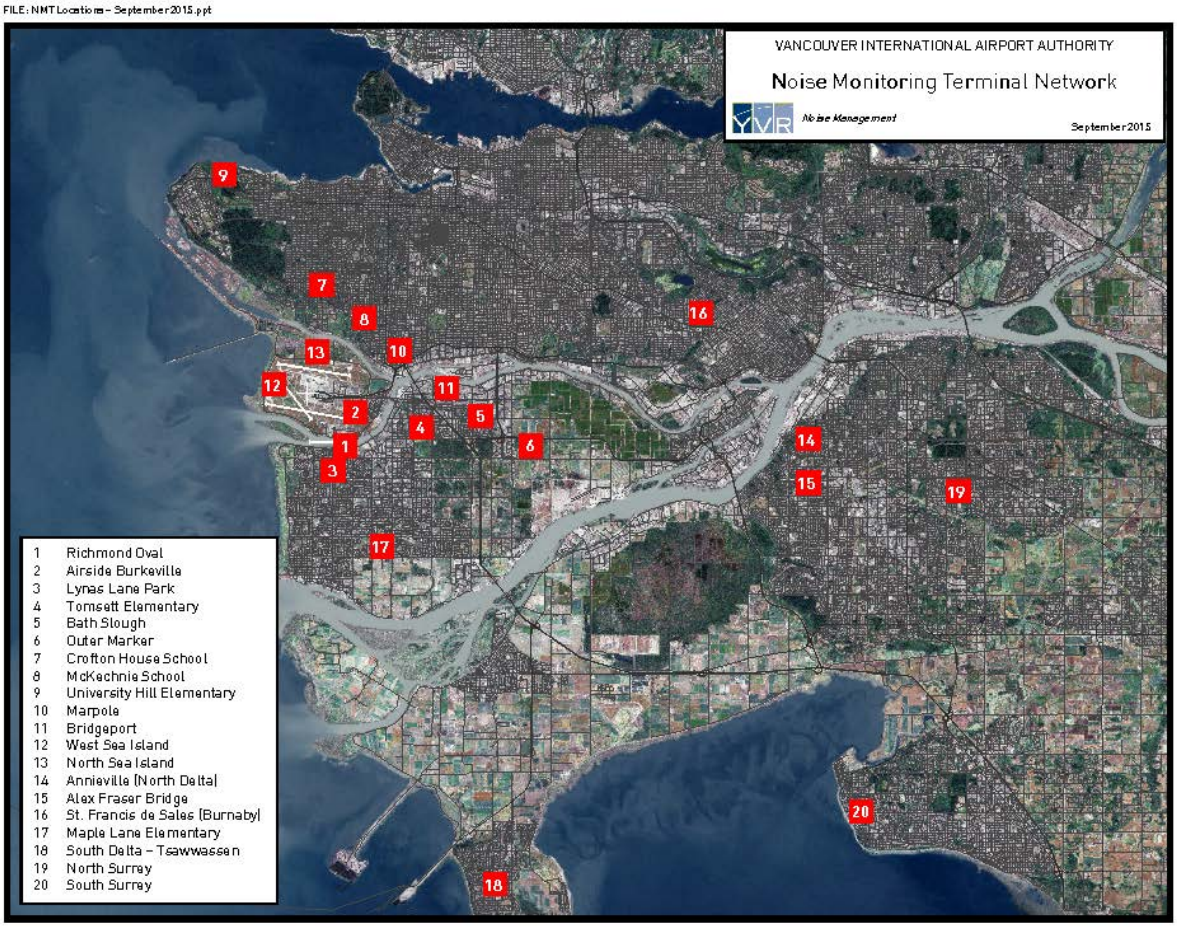

Figure 40.1: Overview of Vancouver International Airport and the surrounding noise monitors.

Milestone(s)
N/A

Major Accomplishments
None. Project started in August 2016.

Publications
None.

Outreach Efforts
None

Awards
None.

Student Involvement
Graduate Research Assistant Manasi Biwalkar has been the primary person working on this task. She is working toward a Summer 2017 graduation with her M.S. in Acoustics.

Plans for Next Period
Continue the work.

References
[1] E. Boeker, *et al.,* "Discover-AQ Acoustics Measurement and Data Report," DOT-VNTSC-FAA-15-09 (2015).
[2] M. Cheng, *et al.,* Vancouver Airport Authority [Private Communication] (2016).
[3] BANOERAC Project final report, Document ID PA074-5-0, ANOTEC Consulting S.L. (2009).
[4] Lopes, L. V. and Burley, C. L., "Design of the Next Generation Aircraft Noise Prediction Program: ANOPP2," AIAA Paper 2011-2854 (2011).
[5] D. K. Wilson, C. L. Pettit, V. E. Ostashev, and S. N Vecherin, "Description and quantification of uncertainty in outdoor sound propagation calculations," J. Acoust. Soc. Am. **136**(3) 1013-1028 (2014).

Task 5 "Assess DISCOVER-AQ Acoustics data for model validation" Task 6 "Assess the uncertainty due to the ground effect and source directivity for en-route aircraft"

Purdue University

Research Approach

FAA's Aviation Environmental Design Tool (AEDT) has now been used by the U.S. Aviation industry for conducting airport noise studies such as FAR part 150 studies and Environmental Impact Statements. In the calculation of lateral attenuation of aircraft noise, AEDT makes use of the standard[4] for modeling the sound absorption by a flat ground. Typically, the ground effect model is based on the well-known Weyl Van der Pol (WVDP) formula:[5]

$$p_{tot}(\vec{r}) = \frac{1}{4\pi}\left[\frac{e^{ik_0R_1}}{R_1} + Q\frac{e^{ik_0R_2}}{R_2}\right], \quad (1)$$

where $\vec{r}$ is the source position, $k_0 = \omega / c_0$ is the reference wavenumber with ω being the angular frequency and c_0 being the sound speed in air. The parameters, R_1 and R_2 correspond to the respective path lengths of the direct and reflected waves. The spherical reflection coefficient, Q, is given by:

$$Q = V_P + (1 - V_P)F(w_\theta) \quad (2)$$

where V_P is the plane wave reflection coefficient and F is the boundary loss factor with a complex argument known as the approximate numerical distance, w_θ. They are defined, respectively, by:

$$V_P = \frac{\cos\theta - \beta}{\cos\theta + \beta}, \quad (3)$$

$$F(w_\theta) = 1 + i\sqrt{\pi}\, w_\theta e^{-w_\theta^2}\,\mathrm{erfc}(-iw_\theta), \quad (4)$$

$$w_\theta = \sqrt{ikR_2/2}(\cos\theta + \beta), \quad (5)$$

where θ is the incidence angle of the reflected wave and $\beta = 1/Z(f)$ is the specific normalized admittance of the ground surface and Z is its characteristic impedance and f is the frequency of the source. In the AEDT model, the Delaney and Bazley model[5] was used to calculate the characteristic impedance of the ground surface where

$$Z(f) = 1 + 9.08(f/\sigma)^{-0.75} + i11.9(f/\sigma)^{-0.73}, \quad (6)$$

and σ is the effective flow resistivity of the ground surface which is expressed in cgs rayls. Typically, AEDT uses 150 cgs rayls for a soft ground and 20,000 cgs rayls for a hard ground. Numerical simulations have suggested that $\beta \to 0$ when σ = 20,000 cgs rayls. In this case, $V_p \to 1$, $F(w_\theta) \to 0$ and $Q \to 1$. Hence, Eq. (1) can be reduced simply to

$$p_{tot}(\vec{r}) = \frac{1}{4\pi}\left[\frac{e^{ik_0R_1}}{R_1} + \frac{e^{ik_0R_2}}{R_2}\right]. \quad (7)$$

In addition, the ground can be treated as a locally reacting one when σ = 150 cgs rayls. Consequently, there is no need to calculate the complex wavenumber (k) of the ground surface as suggested by Fleming et al.[6] As a result, the Delaney and Bazley formula is typically not needed for calculating k in the ground effect model for the prediction of long-range outdoor sound propagation.

In the present project, the Purdue team is examining the uncertainties in the prediction of aircraft noise due to the ground effect. In essence, the ground effect of the measured sound fields is caused by the interference of the direct and reflected waves arriving at the receivers. The intrinsic variability in the predictions depends on a host of factors including the

source/receiver geometry, source frequency, atmospheric turbulence, acoustic characteristics of the ground surface, and, terrain profile.

At the first step, we shall quantify these uncertainties by considering a simple situation with the source placed above a hard ground. The impacts of the source and receiver locations on the accurate prediction of sound fields are investigated. The analysis will focus not only on the narrow band analysis but also on the simulations of one-third octave bands and the integrated A-weighted noise levels of the pass-by noise. In this initial study, we shall investigate the situations for an en-route aircraft or when the source is close to a hard ground modeling the situations of the take-off/landing of an aircraft.

Our next step involves the quantification of uncertainties for the aircraft operating above a locally reacting ground. The computational times can be minimized by assuming a homogeneous atmosphere and Eq. (1) is used in the numerical simulations for predicting the sound fields. The Delaney and Bazley model was used initially because the impedance can be characterized by a single parameter – σ, the effective flow resistivity of the ground surface. A sensitivity analysis can be conducted to investigate the effect of the 'errors' in both σ and the source/receiver geometry on the predicted sound fields. The experimental data (Discover-AQ and Vancouver Airport dataset) will be used to compare with the numerical simulations for quantifying the uncertainties.

In the recent study,[7] Hobbs has examined the possible incorporation of a mixed impedance ground model in AEDT. Hobbs has suggested the use of the National Land Cover Database (NLCD) to derive the information of the ground surface. Basically, NLCD has used satellite imagery (with a 30 m resolution) which provides useful classifications of land cover in the continental U.S. Potentially, this information may be used in conjunction with the National Elevation Data (NED) in AEDT for assessing the ground effects of the aircraft noise. For the current year, we propose to look into the uncertainties introduced by the presence of a mixed impedance ground in the prediction of aircraft noise.

The proposed tasks may lead to a better understanding of the uncertainties due to the ground effect, source/receiver geometry, and their interactions. Insights from the proposed work can be integrated into existing FAA noise modeling tools to handle more realistic propagation effects. Specifically, the Purdue team will focus on (a) the review of the Impact of ground effects, and (b) how the dataset can potentially be used to quantify the uncertainties in predicting noise around airports and the en-route aircraft noise.

The current project aims to quantify the uncertainties in predicting aircraft noise in real-world situations. In the current year, the proposed tasks for the Purdue team can be summarized as follows:

- Study the uncertainties in the predicted noise levels due to the geometric locations of the source and receiver,
- Investigate the 1-parameter ground impedance model on the ground effects of aircraft noise,
- Based on the input from the Penn State team, examine the effect of source directivity for the prediction of noise levels of en-route aircraft.
- Explore the impact of a mixed impedance ground on the uncertainties in the prediction of ground effects of aircraft noise.

Milestone(s)

N/A

Major Accomplishments

None. Project started in August 2016.

Publications

None.

Outreach Efforts

None

Awards

None.

Student Involvement

Graduate Research Assistant Yiming Wang has been the primary person working on this task.

Plans for Next Period

Continue the work.

References

[1] E. Boeker et al. Discover-AQ Acoustics Measurement and Data Report,"DOT-VNTSC-FAA-15-09 (2015).
[2] M. Cheng, *et al.,* Vancouver Airport Authority [Private Communication] (2016).
[3] BANOERAC Project final report, Document ID PA074-5-0, ANOTEC Consulting S.L. (2009).
[4] SAE-AIR-5662 "Method for Predicting Lateral Attenuation of Airplane Noise" (2012).
[5] K. Attenborough, K.M. Li, and K. Horoshenkov. *Predicting Outdoor Sound*. Taylor & Francis, 2007.
[6] C. G. Fleming, J. Burstein, A. S. Rapoza, D. A. Senzig, and J. M. Guilding. "Ground effects in FAA's integrated noise model," Noise Control Engineering Journal **48**, 16-24.
[7] C. Hobbs, Interim Report on ACRP 02-52: Improving AEDT noise modeling of ground surfaces (2016).

Project 041 Identification of Noise Acceptance Onset for Noise Certification Standards of Supersonic Airplanes

The Pennsylvania State University

University Members

Penn State Acoustics Program	Team Lead	Victor W. Sparrow
Penn State Applied Research Laboratory	Co-Principal Investigator	Kathleen K. Hodgdon

Advisory Committee Members

AERION: Jason Matisheck, Peter Sturdza, *et al.*
Boeing: Hao Shen, Bob Welge, *et al.*
Cessna: Kelly Laflin, *et al.*
Gulfstream: Robbie Cowart, Matthew Colmar, Brian Cook, Joe Gavin, *et al.*
Lockheed Martin: John Morgenstern, Tony Pilon, *et al.*
Volpe-The National Transportation Systems Center: Juliet Page, Bob Samiljan, et.al.
Wyle: Kevin Bradley, Chris Hobbs, *et al.*

Project Lead Investigator

Victor W. Sparrow
Director and Professor of Acoustics
Graduate Program in Acoustics
Penn State
201 Applied Science Bldg.
University Park, PA 16802
+1 (814) 865-6364
vws1@psu.edu

University Participants

The Pennsylvania State University

- P.I.: Vic Sparrow, Professor and Director, Graduate Program in Acoustics
- Researcher: Kathleen Hodgdon Research Associate
- FAA Award No.: 13-C-AJFE-PSU Amendment 21
- Period of Performance: June 28, 2016 to December 31, 2017
- Task(s):
  1. Obtaining confidence in signatures, assessing metrics sensitivity, and adjusting for reference day conditions

The Pennsylvania State University

- P.I.: Kathleen Hodgdon Research Associate
- Researcher: John Morgan R&D Engineer
- Researcher: Bernard Kozykowski
- FAA Award No.: 13-C-AJFE-PSU Amendment 25
- Period of Performance: July 21, 2016 to December 31, 2017
- Task(s):
  2. Community Impact and Acoustic Acceptability

Project Funding Level

This project supports the identification of noise acceptance onset for noise certification standards of supersonic through research conducted on multiple tasks at the Penn State University. FAA funding to Penn State in 2016-2017 was $160,000 comprised of $50K to Task 1 and $110K to Task 2. Matching funds are expected to meet cost share on both Tasks.

Investigation Team

For 2016-2017 the investigation team includes:

Penn State
Victor W. Sparrow (Co-PI) (Task 1)
Kathleen K. Hodgdon (Co-PI) (Task 2)
Researcher: John Morgan R&D Engineer (Task 2)
Researcher: Bernard Kozykowski R&D Engineer (Task 2)
ARL Graduate Research Assistant Will Doebler (Task 1: Signatures and metrics investigation)
ARL co-administered PSU Scholarship for Service undergraduate student Mitch Gold (Task 2: Community Monitoring)

Project Overview

FAA participation continues in ICAO CAEP efforts to formulate a new civil, supersonic aircraft sonic boom (noise) certification standard. This research investigates elements related to the potential approval of supersonic flight over land for low boom aircraft. The efforts include investigating certification standards, assessment of community noise impact and methods to assess public acceptability of low boom signatures. The proposed research will support NASA in the collaborative planning and execution of human response studies that gather the data to correlate human annoyance with low level sonic boom noise. As the research progresses, this may involve the support of testing, data acquisition and analyses, of field demonstrations, laboratory experiments or theoretical studies.

Task 1 Obtaining confidence in signatures, assessing metrics sensitivity, and adjusting for reference day conditions

The Pennsylvania State University

Objective

As national aviation authorities move forward to develop noise certification standards for low-boom supersonic airplanes, several research gaps exist in the areas of signature fidelity, metrics, metrics sensitivity to real-world atmospheric effects, adjustments for reference-conditions, etc. Research support is needed by FAA and international partners in these areas to progress toward standards.

The objective of this activity is to continue research at The Pennsylvania State University in the ASCENT COE to complement the sonic boom standards development ongoing within the Committee for Aviation Environmental Protection's (CAEP) Working Group 1 (Noise Technical), Supersonics Standards Task Group (SSTG). This research will ensure that the behavior of the sonic boom metrics considered in the SSTG discussions are well-understood, and account for sonic boom variability effects, to move forward with sonic boom certification and/or rulemaking.

Task 1 in ASCENT Project 41 focuses on several, but not all, research initiatives needed to move forward toward the development of a low-boom supersonic en-route noise certification standard. It addresses neither the important issues of acceptability of low-boom sonic boom nor appropriate metric levels that would eventually become part of a standard. The work proposed here supports CAEP/WG1 in the three areas of:

- obtaining confidence in acoustic signatures,
- assessing metrics sensitivity, and
- adjusting for reference day conditions.

In addition, this project supports the travel of V. Sparrow so that he can serve as co-rapporteur of the CAEP Impacts and Science Group (ISG).

Research Approach

Background

Through the PARTNER and ASCENT Centers of Excellence programs, Penn State has been supporting CAEP/WG1 regarding the development of supersonic aircraft certification standards for 10 years. In recent years the focus has been on understanding the influence of atmospheric turbulence on low-boom waveforms. Work from 2013-2015 showed that both A-weighted sound exposure level and Steven's Mark VII Perceived Loudness (PLdB) metrics were substantially affected by atmospheric turbulence effects [Palmer and Sparrow, 2015]. One can actually hear the differences in the sonic boom waveforms heard 10s of meters away from each other. Thus, the turbulence effect will substantially complicate the data acquisition and signal processing for ground-based measurements to certify supersonic en-route flight. The procedures used to certify subsonic aircraft simply will not work for supersonic en-route noise.

Penn State also aided WG1/SSTG to develop a list of technical terms and definitions for sonic boom, as well as a metrics catalog to enumerate the wide variety of metrics that one could use for sonic boom noise. This development then was the basis for "down-selecting" a limited number of metrics to carry forward for possible use in a standard. [A. Loubeau, *et al.,* (2015)]

In the last year, Penn State's work in ASCENT Project 7 (Part A) has focused on two topics. The first has been to assess the sensitivity of the 5 "finalist" sonic boom metrics to atmospheric turbulence. As was reported to CAEP/WG1 in April 2016, the preliminary result is that B-weighted sound exposure level is the most robust with respect to turbulent distortions, both for N-wave shaped sonic booms and for industry supplied low-boom waveforms. Additional research will be necessary to understand why B-weighted SEL did the best, beating out both PLdB and NASA's Indoor Sonic Boom Annoyance Predictor (ISBAP). The second topic in Project 7, Task 1 has focused on developing signal processing approaches to remove turbulence from ground-measured signatures, described by some as "de-turbing." [Maglieri, *et al.,* 2014] The most recent Penn State work has indicated that to remove turbulent effects it is necessary to estimate a "clean" waveform using predictions or experimental measurements in the absence of turbulence.

Current work

There are several ongoing subtasks in ASCENT Project 41, Task 1. These include assessing the sensitivity of sonic boom metrics to turbulence, developing "de-turb" procedures, and considering the number and placement of ground-based microphones in a certification requirement. Previous work from Project 7 will also be extended to include an evaluation of the role of nonlinearity in obtaining confidence in supersonic signatures, as it relates to reference day-corrections. It is well known that the pressure signature (pressure versus time waveform) distorts substantially during propagation from aircraft to the ground, and one of the key influences on this distortion is acoustic nonlinearity, the fact that higher amplitude portions of the waveform propagate FASTER than lower amplitude portions of the waveform. [Pierce, 1981; Hamilton and Blackstock, 1998] Such acoustical nonlinearities and the resulting shock-induced inaccuracies will be addressed in the context of reference day-corrections. Recent results from other ASCENT projects, such as ASCENT Project 5 (Noise emission and propagation modeling), should be helpful with the task of relating the concepts of "reference day conditions" to future sonic boom certification procedures.

As in previous efforts the Penn State researchers will employ both analytical and computational approaches, supported by field data collected by NASA and others. Industry partners, such as Boeing, Cessna, Gulfstream Aerospace Corporation, Lockheed-Martin Aeronautics, Wyle, and others, will again be asked to provide guidance regarding the project and to provide important supersonic signature predictions that are both absolutely necessary to carry out the research and at the same time provide FAA-required cost sharing. Existing datasets such as those from recent NASA studies (SCAMP, FaINT, WSPR, etc) and NASA studies undertaken this year (SonicBAT and WSPRRR, as they come available) will be utilized.

In addition, work efforts include the support of NASA activities on supersonics and sonic boom research. This may involve the support of testing, data acquisition and analyses, of field demonstrations, laboratory experiments or theoretical studies.

Depropagation does not work for sonic booms

Early work in Project 41 Task 1 has shown that sonic boom propagation cannot be processed with the same de-propagation procedures that are commonly used for subsonic aircraft noise certification. Because of the physics of nonlinear acoustics and the presence of shocks in sonic boom waveforms, very different sonic booms signatures can all result in the same waveform on the ground. This makes the techniques of depropagation impossible for use with sonic booms. The Penn State team reported on this result during an SSTG procedures workshop in July 2016 at NASA Armstrong Flight Research Center, Edwards, CA. Subsequently the information was used in an SSTG and WG1 meeting in Cologne, Germany, and reported on in a CAEP Steering Group Meeting in Washington, DC in December 2016.

Appropriate placement and number of microphones for certification measurements

The Penn State team is making an effort to ascertain how to best make certification measurements in the primary sonic boom carpet. One would like to use as few microphones as possible and know how to locate them to maximum advantage. One possibility would be to minimize the metrics' 90% confidence interval for multiple measurements. Data from NASA's SCAMP program is now being evaluated to assess how removing selected microphones will change the narrowness of the confidence interval for different sonic boom metrics.

Milestone(s)
N/A

Major Accomplishments
It was established that one cannot apply depropagation techniques to sonic boom propagation.

Publications
None.

Outreach Efforts
None.

Awards
V. Sparrow gave the 2016 Rayleigh Lecture to the American Society of Mechanical Engineers (ASME) Noise Control and Acoustics Division on November 15, 2016 at the 2016 International Mechanical Engineering Congress and Exposition in Phoenix, AZ. The title of the talk was "Two approaches to reduce the noise impact of overland civilian supersonic flight."

Student Involvement
William Doebler is the graduate research assistant supported by the Applied Research Laboratory on Project 41 in 2016. He is pursuing his Ph.D. in the Penn State Graduate Program in Acoustics.

Plans for Next Period
Continue the work supporting CAEP WG1, SSTG, and ISG.

References
M. Hamilton and D. Blackstock, *Nonlinear Acoustics* (Academic Press, 1998).
L. Locey and V. Sparrow, “Modeling atmospheric turbulence as a filter for sonic boom propagation,” Noise Control Eng. J. 55(6) 495-503 (2007).
A. Loubeau, *et al*., “A new evaluation of noise metrics for sonic booms using existing data,” in *Recent Developments in Nonlinear Acoustics*, AIP Conf. Proc. 1685 090015 (AIP, 2015).
D. Maglieri, *et al*., *Sonic Boom: Six Decades of Research* (NASA SP-2014-622, 2014), pp. 51-52.
J. Page, C. Hobbs, E. Haering, D. Maglieri, R. Shupe, C. Hunting, J. Giannakis, S. Wiley, F. Houtas, “SCAMP: Focused sonic boom experiment execution and measurement data acquisition,” AIAA paper 2013-0933, 51st AIAA Aerospace Sciences Meeting, Grapevine, TX, January 2013.
J. Palmer and V. Sparrow, “Measured N-wave sonic boom events and sensitivity in sonic boom metrics,” in *Recent Developments in Nonlinear Acoustics*, AIP Conf. Proc. 1685 090012 (AIP, 2015), doi: 10.1063/1.4934478.
A. D. Pierce, *Acoustics* (McGraw Hill, 1981 & Acoustical Society, 1989), Chapter 11.

Task 2 Community Impact and Acoustic Acceptability
The Pennsylvania State University

Objective
This research addresses aspects of the FAA roadmap research question: “What is needed from a standard to reconsider 14 CFR part 91.817, which does not allow for civil supersonic flight over land?” The research supports the standard development process and the identification of noise acceptance onset. The tasks are proposed in support of NASA in the

planning and execution of human response studies, and in the development of protocols, methods and planning for Community Exposure Testing.

Research Approach

The research includes the assessment of community noise impact and methods to assess public acceptability of low boom signatures. The effort will finalize research that was advanced under ASCENT Project 7 and begin new research. The ongoing efforts include the development and testing of low cost noise monitors (LCNM) and the evaluation of social media monitoring (SMM) methods as a means to observe general comments on noise within the field test community. A new task was initiated to conduct a review of differences in perception between urban and suburban/rural environments to better understand the potential impact that masking has on noise field test results for human impact.

Milestone(s)

This research was conducted in support of future NASA sponsored low boom noise community impact field tests. The development and testing of cost effective noise monitors to augment existing field monitors is ongoing. Social media monitoring tools are being investigated, as a means to observe social dynamics and to provide insights into community perceptions of noise impact during the field tests. A literature review was initiated for the background noise masking task. A review of social surveys was initiated and the environmental background noise survey will be considered for implementation during the first WSPRRR community test being conducted with a low boom flight maneuver, most likely in 2018, beyond this project reporting period.

Major Accomplishments

There are several ongoing subtasks in ASCENT Project 7 (Part B) that are being continued in Project 41 in 2016-2017. The continued tasks include finalizing an investigation of Low Cost Noise Monitors (LCNM) and identification of social media monitoring tools. These two tasks will support efforts to gather both objective measurements and subjective observations in test communities. A new task on environmental masking was initiated to understand the potential impact that masking has on noise field test results for human impact, and to develop an associated survey that can be used in future field tests. Accomplishments on each of these tasks follow.

Social Media Monitoring Tools

The monitoring of social media is being explored as a supplemental means to observe the impact of the noise field testing on the community, by observing the publicly available comments that are posted to social media. By monitoring online discussions, researchers have the opportunity to identify concerns within the community related to the proposed or ongoing low boom community field testing. A geographic based search of social media comments during a noise field tests may identify unexpected locations of potential sound channeling due to topography, urban canyons or environmental variability; or community concerns related to the field test. Being made aware of such issues, is valuable in helping to explain secondary influences on the primary data. The observations would be gathered from public domain information only and are not viewed as formal response data.

We are conducting tests of EchoSec, a social media monitoring tool. It appears that we may not have access to archived data from months ago, but we should be able to access “real time” events. We are identifying archived data from sonic booms or Space X booms and comparing findings from new articles to EchoSec searches. Figures 41.1 through 41.3 below compares information on a sonic boom that hit the east coast due to an F-35 that took place on January 28th, 2016. We are comparing content from established media outlets, in this case ABC News, with social media posts using Echosec.com.

Figure 41.1: Hammonton, NJ as the boom source (ABC News) Figure 41.2: Impact of the Noise (ABC News)

"The boom was centered north of Hammontown, NJ, around 1:30 p.m. It was the first of nine booms reported in southern New Jersey and along the Eastern Seaboard to Long Island, New York in the hours following the initial boom, the USGS said." (http://abcnews.go.com/US/jersey-rocked-sonic-boom/story?id=36578433)

Based on the ABC News report we used a data selection of January 28, 2016 to January 29, 2016 to search EchoSec.

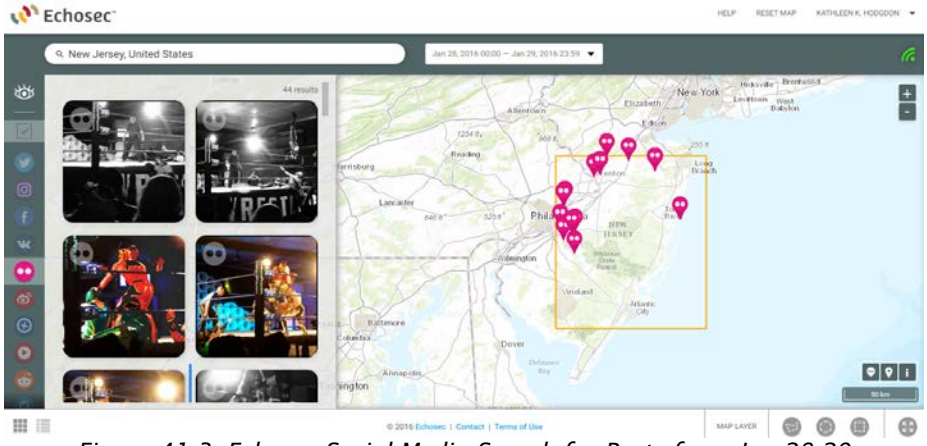

Figure 41.3: Echosec Social Media Search for Posts from Jan 28-29

As depicted in Figure 41.3, the social media application that is appearing is Flickr. As seen along the left side, all other social media sites are greyed out, indicating that the posts we are viewing were on Flickr. There were no available posts within both the selected dates and the geographic location that we specified for Twitter. We are assuming that Twitter will be a valuable social media site, and plan to focus future testing and analysis on Twitter more than Instagram, Reddit, Flickr, or other platforms. The project continues to explore applicability of EchoSec to this effort.

The observations would primarily allow the team to engage the community with targeted news releases or Outreach materials that address issues observed on posts to social media. The observations could also identify if community members have mistaken the impulsive boom noise to be an explosion, prompting the team to issue a media release to alleviate these concerns. While noise monitors will be located across the boom carpet, there is the potential that a combination of wind and terrain could produce a sound channel. The observations may indicate a "noise pocket" that could prompt locating a noise monitor in that area. Monitoring social media provides the opportunity to identify concerns within the community related to the low boom field test.

Low Cost Noise Monitor (LCNM) Instrumentation
The evaluation of LCNM is in progress assessing the applicability of commercial off the shelf (COTS) instrumentation for this effort. Design selection was contingent on the availability of low cost parts. The anticipated cost of components is reflected in the following table.

LCNM Component	Sensor	Cost
Microphones		
Quite Sounds: Rode NT1-A Cardioid Condenser Microphone Recording Package with a Tripod Base Microphone Floor Stand - Black	N/A	$236.00
Loud Sounds: Audio Technica AT2035 Large Diaphragm Condenser Microphone w/Shock Mount, Pop Filter, Mic Cable, and Mic Stand	N/A	$149.00
GPS Sensor		
Adafruit Ultimate GPS Breakout - 66 channel w/10 Hz updates - Version 3	MTK3339	$39.95

Environmental Sensor		
Adafruit BME280 I2C or SPI Temperature Humidity Pressure Sensor	BME280	$19.95
Accelerometer Sensor		
Adafruit Triple-Axis Accelerometer - ±2/4/8g @ 14-bit - MMA8451	MMA8451	$7.95
Single Board Computer		
ELEMENT14 BBONE-BLACK-IND-4G Beaglebone Black Industrial, Sitara ARM Cortex A8 Processor, 512 MB	N/A	$64.00
ELEMENT14 BBONE-GATEWAY-CAPE DEVELOPMENT BOARD, WIRELESS CONNECTIVITY	N/A	$55.00
Banana Pi M3 - BPI-M3 - Octacore A83T ARM Cortex-A7 2GB DDR RAM with WIFI Antenna	N/A	$73.00

Several designs were investigated considering the electrical power considerations, mechanical components, and the electrical data flow and data storage. The design includes two microphone channels that can be set with different dynamic ranges. This affords the ability to capture low level signals with integrity, and affords a second microphone channel set with a higher dynamic range in case there is a focus boom. The design also includes an accelerometer channel, to allow the monitor to have greater applicability for a wider range of noise monitoring projects. The LCNM task will assess the fidelity of lower cost noise monitors to optimize noise measurement requirements and minimize costs in future field tests. PSU researchers are teaming with researchers from Volpe, The National Transportation Systems Center on this effort. The monitor will require the development of software to facilitate the ability to readily download the field data.

Environmental Masking (urban vs suburban/rural) Literature Review and Survey Development
This new task will conduct an initial review of concepts and available literature of noise studies related to the role masking plays on the potential low boom noise impact in differing background noise for urban, suburban or rural noise environments. An undergraduate student will be hired to conduct a literature review and summary. A short list of potentially relevant articles follows.

Potential Reference Citations:

- Kuno, K., Omiya, M., Okumura, Y., Hayashi, A., Mishina, Y., & Oishi, Y. (2000). Criteria for environmental noise based on neutral reaction of inhabitants. Journal of the Acoustical Society of Japan, 21, 349-353.
- Weinstein, N. D. (). Individual differences in reactions to noise: A longitudinal study in a college dormitory. Journal of Applied Psychology, 63, 458-466.
- Sheikh, P. A., & Uhl, C. (2004). Airplane noise: A pervasive disturbance in Pennsylvania Parks, PA. Journal of Sound and Vibration, 274, 411-420.
- Vos, J. (1992). Annoyance Caused by Simultaneous Impulse, Road-Traffic, and Aircraft Sounds: A Quantitative Model. Journal of the Acoustical Society of America, 91, 3330-3345.
- Vos, J. (1998). The Loudness of Impulse and Road-Traffic Sounds in the Presence of Masking Background Noise. ACUSTICA, Vol. 84, 1119-1130

The literature review has just been started. The results of this study should facilitate interpreting noise field test results and masking due to environmental surrounding (community density), and the relevance masking has on low boom noise for such varying background environments.

The planning for an Urban vs. Rural Survey has been started with the PSU Survey Research Center. The survey will include questions identified for the NASA sponsored Waveforms Sonic boom Perception and Response Risk Reduction (WSPRRR) community field test, as well as some specific questions pertaining to the ease of hearing the boom in varying levels of background noise environments. This effort is being initiated now to allow time to develop the survey, to conduct a review

of the survey instrument by both NASA and FAA, and to submit the design for regulatory approvals. The NASA WSPRRR community social survey will most likely be conducted in spring 2018, depending on the NASA field test schedule.

Publications
None

Outreach Efforts
This research task supports NASA activities on supersonics and sonic boom research. The team has provided information to the NASA sponsored Waveforms Sonicboom Perception and Response Risk Reduction (WSPRRR) team. This NASA sponsored team consists of ASCENT Project 41 team members from Penn State, Volpe, Wyle and Gulfstream working with NASA team lead APS to formulate a test plan for future low boom community field tests.

Awards
None

Student Involvement
Mitch Gold is a PSU IST student working on the Social Medial Monitoring task. He is supported through the Federal Cyber Corps Scholarship for Service (SFS) program, which is offered and funded through the National Science Foundation (NSF) and the Department of Homeland Security (DHS). The PSU SFS program is administered through the College of Information Science and Technology and the Applied Research Lab. Because this appointment is funded externally, it does not count as cost share.

ARL has afforded support of a Distinguished Undergraduate Research position to work on the literature review and background research or the Urban vs. Rural survey. This appointment begins in January 2017 with a cost share of approximately 46K per year. The student has not yet been selected.

Plans for Next Period

The SMM effort will finalize evaluations of social media monitoring tools as a means to observe social dynamics in the community. This evaluation of options would identify tools that allow us to observe the social dynamics in the overall community response during a low boom community field test.

The LCNM instrumentation task will finalize aspects related to ongoing development of noise monitoring technology that can be used to supplement existing noise measurement methods for greater quantification of coverage at lower cost and complexity. Such technology could be used as intermediate measures among the standard higher fidelity instrumentation to confirm and interpolate data. Additional software to facilitate the ability to readily download the field data could be developed in the next funding cycle.

The Environmental Masking literature review is applicable to low boom research and other environmental noise research. The development of the Urban vs. Rural Survey will result in a survey for use with the NASA WSPRRR community social survey will most likely be conducted in spring 2018. Additional funds would be required in the next annual funding cycle to implement this survey task in the field and to gather, analyze and correlate the response data with the noise measurements from the community field test.

References
Ruths, D., and J. Pfeffer. "Social Media for Large Studies of Behavior." *Science* 346.6213 (2014): 1063-064. 28 Nov. 2014. Web. 10 Feb. 2015.

Project 042 Acoustical Model of Mach Cut-off Flight

Pennsylvania State University
University of Washington
Georgia Institute of Technology
Volpe National Transportation Systems Center

Project Lead Investigator

Victor W. Sparrow
Director and Professor of Acoustics
Graduate Program in Acoustics
Penn State
201 Applied Science Bldg.
University Park, PA 16802
+1 (814) 865-6364
vws1@psu.edu

University Participants

Pennsylvania State University

- P.I.(s): Dr. Victor W. Sparrow (PI), Dr. Michelle C. Vigeant (Co-PI)
- FAA Award Number: 13-C-AJFE-PSU-020
- Period of Performance: June 28, 2016 - December 31, 2017
- Task(s):
    1. Assess and extend modeling capability for Mach Cut-off events (a.k.a. Task 1A)
    2. Study human perception of Mach Cut-off sounds

University of Washington

- P.I.(s): Dr. Michael Bailey (PI)
- FAA Award Number: 13-C-AJFE-UW-005
- Period of Performance: June 27, 2016 – December 31, 2017
- Task(s):
    3. Determine feasibility for obtaining Mach Cut-off data via scale experiments

Georgia Institute of Technology

- P.I.(s): Dr. Dimitri Mavris (PI), Dr. Jimmy Tai (Co-PI)
- FAA Award Number: 13-C-AJFE-GIT-023
- Period of Performance: June 28, 2016 – August 14, 2017
- Task(s):
    4. Sensitivity Study (a.k.a. Task 1B)
    5. Evaluate technologies to enable Mach cut-off flight

Volpe National Transportation Systems Center (non-University, Interagency Agreement)

- P.I.(s): Juliet Page
- Volpe Project Number: FA5JCT
- Period of Performance: execution date – December 31, 2017
- Task(s):
    6. ASCENT Project 42 support

Project Funding Level

$170K, The Pennsylvania State University

$70K, Georgia Institute of Technology
$15K, University of Washington
$15K, Volpe National Transportation Systems Center

Aerion Corporation is providing cost-share matching funds to Penn State and U. Washington. Our point of contact at Aerion is Jason Matishek, jrmatisheck@aerioncorp.com. Aerion is providing the necessary near-field CFD data and other relevant information to help guide the project team make accurate predictions of the Mach cut-off sonic boom signatures that may be produced by Aerion's future supersonic aircraft.

Investigation Team

Pennsylvania State University
Principal Investigator: Victor W. Sparrow
Co-Investigator: Michelle C. Vigeant
Graduate Research Assistant Zhendong Huang (assessment and extension of Mach cut-off models)
Graduate Research Assistant Nick Ortega (human perception of Mach cut-off sounds)

University of Washington
Principal Investigator: Michael Bailey

Georgia Institute of Technology
Principal Investigator: Dimitri Mavris
Co-Investigator: Jimmy Tai
Research Faculty: Greg Busch
Graduate Research Assistants Ruxandra Duca & Ratheesvar Mohan

Volpe National Transportation Systems Center
Principal Investigator: Juliet Page

Project Overview

ASCENT Project 42 brings together resources to provide preliminary information to the FAA regarding the noise exposure of supersonic aircraft flying under Mach cut-off conditions. Studies in the 1970s showed that Mach cut-off supersonic flight was possible, but there is currently no data establishing the frequency and extent of noise exposures and no guidelines for managing such exposures. Penn State will lead a team of investigators from Penn State, University of Washington, Georgia Tech, and Volpe—each bringing unique contributions to shed light on the Mach cut-off phenomena.

Background for Project 42

Aerion Corporation and many others believe that Mach cut-off supersonic flight is both viable [Plotkin, et al., 2008] and very likely to be acceptable to the public. But there is a lack of data to back up this assertion. Thus, research needs to be conducted to provide a technical basis for rulemaking regarding Mach cut-off operations.

The basic concept of Mach cut-off relies on the fact that the ambient temperature is substantially colder at flight altitudes than on the ground. Hence, the speed of sound is substantially slower at flight altitudes than at the ground. As illustrated in Figure 42.1, it is possible to fly in a range of Mach numbers (perhaps between Mach 1.0 and Mach 1.15) while having the sonic boom noise refract (bend) upwards such that the rays never reach the ground. However, the reader should be aware that this picture is over-simplified since the temperature profile in the atmosphere is never a smooth, linear function as depicted here. For higher Mach numbers, the sonic boom will impact the ground before refracting upward.

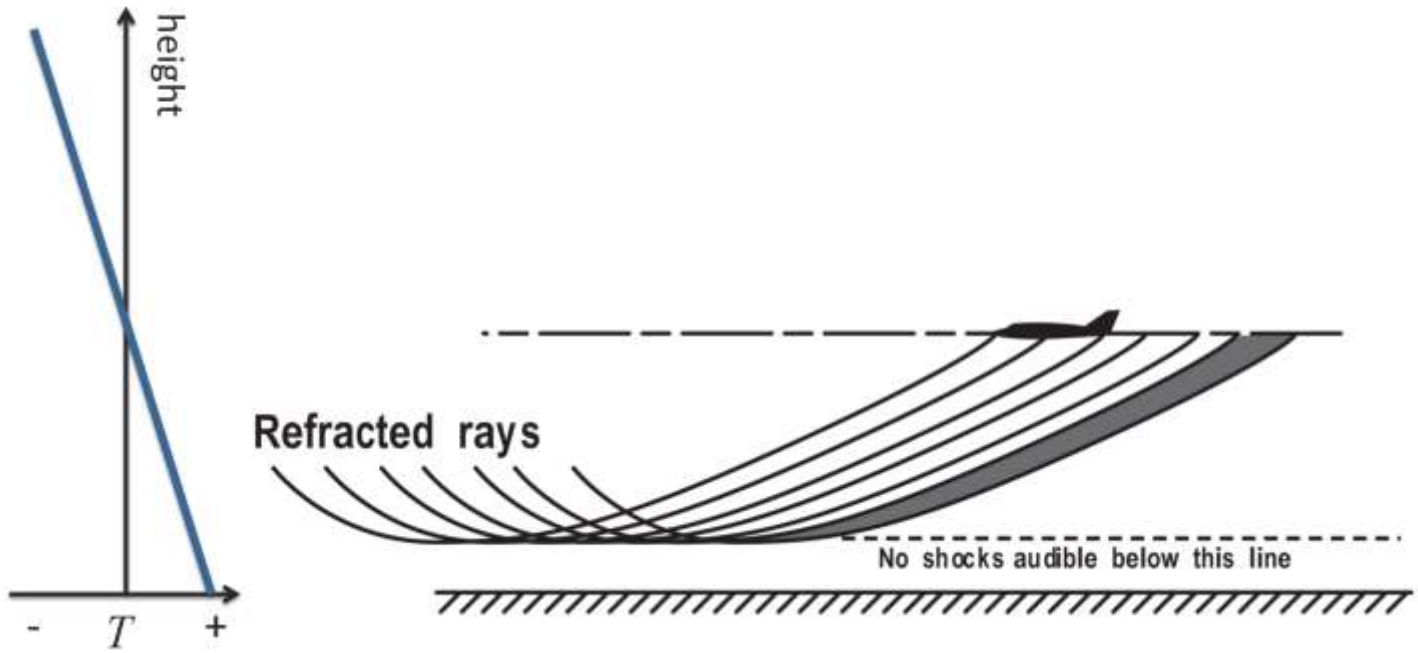

Figure 42.1: Simplified view of Mach cut-off where sonic boom noise does not reach the ground surface. Left: ambient temperature versus height. [Sparrow] Right: aircraft and ray diagram showing refraction of sonic boom [NASA].

Little is known about the noise impact of Mach cut-off operations for future supersonic aircraft. The concept of Mach cut-off was introduced by Lockheed engineers in the mid-1960s [Shurcliff, 1970]. NASA conducted some field experiments in the early 1970s, focusing on other speed regimes of flight, validating some of the Mach cut-off theory for some of the sound field. This research was conducted in Nevada with a 466 m (1,529 ft) tower [Haglund and Kane, 1973]. Then to more directly address the Mach cut-off issue, a theoretical and experimental study was conducted in the mid-1970s with FAA support. The studies estimated altitudes and Mach number regimes to ensure the focus boom does not reach the ground. That field campaign used fighter jets flying out of Langley AFB to a test area in the Atlantic Ocean off Wallops Island, Virginia [Perley, 1977]. Using the available instrumentation, the study concluded that Mach cut-off flight was feasible.

In none of those studies were any recordings made of sufficient quality to assess human response to the Mach cut-off noise. The theoretical studies estimating the altitude and Mach number restrictions for focus boom avoidance assumed a simple atmospheric model (linear sound speed profile), and did not include real-world atmospheric effects. Hence the 1960s-1970s work was very good, but is only a start to determining appropriate flight conditions for routine Mach cut-off supersonic flights over the continental United States.

Task 1A: Assess and Extend Modeling Capabilities for Mach Cut-off Events

Pennsylvania State University

Objectives and Research Approach

For Task 1A, the original propagation theory [Nicholls, 1971] will be retraced for extensibility and to incorporate the operational parameters proposed by Aerion. Ray calculations will be made to assess the back-of-the-envelope predictions for Mach cut-off operations that were known to the FAA in the 1970s. A number of existing tools such as NASA's PCBoom and/or sBOOM prediction codes will be employed to assess the robustness of the theory to realistic atmospheric conditions. Aerion will provide key Computational Fluid Dynamics (CFD) input data to initialize the propagation

predictions for the Mach cut-off noise. Volpe will provide guidance on using near-field CFD solutions as inputs to the boom prediction codes [Plotkin and Page, 2002].

Milestones and Accomplishments

The project just began in August 2016. The Nicholl's theory is being investigated thoroughly and results will be available in Spring 2017.

References

G. Haglund and E. Kane, "Flight test measurements and analysis of sonic boom phenomena near the shock wave extremity," NASA Report CR-2167 (1973).
J. Nicholls, “A note on the calculation of `cut-off’ Mach number,” Meteorological Mag. **100** 33-46 (1971).
R. Perley, “Design and demonstration of a system for routine, boomless, supersonic flights,” FAA Report No. FAA-RD-77-72 (1977).
K. Plotkin and J. Page, "Extrapolation of sonic boom signatures from CFD solutions," AIAA paper 2002-0922, 40th Aerospace Sci. (Reno, NV, January 2002).
K. Plotkin, J. Matisheck, and R. Tracey, "Sonic boom cutoff across the United States," AIAA paper 2008-3033, 14th AIAA/CEAS Aeroacoustics Conf. (Vancouver, BC, Canada, May 2008).
W. Shurcliff, "S/S/T and sonic boom handbook," (Ballentine, 1970), p. 63.

Task 2: Study Human Perception of Mach Cut-off Sounds

Pennsylvania State University

Milestones and Accomplishments

The experimental design of a perceptual study to investigate the subjective response to Mach cut-off sounds is nearly complete. The stimuli for this study will be recordings selected from NASA’s “Farfield Investigation of No-boom Thresholds” (FaINT) field measurements. To select sounds for this subjective listening test, over 400 recording were listened to and categorized based on the perceived quality of the sounds. The listening test has been designed to have two parts: (1) a vocabulary development study, and (2) an annoyance rating study. To this point the vocabulary study has been designed as an exploratory study, where subjects will be asked to provide descriptors of recorded Mach cut-off sounds. Some of these descriptors will be selected for use in the follow up annoyance rating study.

L. Cliatt, *et al.*, "Lateral cutoff analysis and results from NASA's farfield investigation of no-boom thresholds," NASA TM-2016-218850 (2016).

Task 3: Determine Feasibility for Obtaining Mach Cut-off Data Via Scaled Experiments

University of Washington

Objectives and Research Approach

Task 3 is a limited study at the University of Washington to determine the feasibility of laboratory-scale measurements of Mach cut-off. Previous work in Europe [H. Hobaek, *et al.,* 2006] has shown that a refracting medium can be created in a water/ethanol mixture, and ultrasonic waves can be bent in the refracting medium, just like Mach cut-off waves are refracted in the atmosphere. The results of this pilot study will show if such small-scale experiments are possible, as full-scale flight tests are prohibitively expensive. Lab tests with ultrasound can run continuously for hours, and one can easily probe anywhere in the test tank. If viable, it would be very attractive to introduce turbulence into the refractive medium (similar to turbulence in the atmosphere) and evaluate if the turbulence-scattered energy increases the Mach cut-off sound heard on the ground. It was thought by some in the 1970s that turbulent scattering of the focus boom noise down to the

ground would render Mach cut-off operations unacceptable [Shurcliff, 1970]. Future laboratory work could investigate this effect.

The UW team has attended the teleconferences to better understand the Program's efforts and challenges and had monthly internal meetings to begin the planning process. The modification to the proposed design that is under consideration is to not replicate the mixture of fluids as done by Hobaek, but to build a more permanent, fixed, controllable and durable atmospheric analogue from layers of gels. These gels behave very much like fluids with negligible shear wave generation but hold their form. We are also practiced at manipulating what may be more levers to adjust the local speed of sound, attenuation, inhomogeneities, and nonlinearity than with layered fluids alone. NASA is currently funding us to develop similar acoustic phantoms for medical ultrasound training and investigation.

H. Hobaek, *et al.*, "Experiment on finite amplitude sound propagation in a fluid with a strong sound speed gradient," in *Innovations in Nonlinear Acoustics: 17th Intl. Symposium on Nonlinear Acoustics*, Conf. Proc. 838 (American Institute of Physics, 2006).
W. Shurcliff, "S/S/T and sonic boom handbook," (Ballentime, 1970), p. 63.

Task 4 (a.k.a. 1B): Sensitivity Study

Georgia Institute of Technology

Objectives

Georgia Tech's primary task for the ASCENT 42 project is to perform a sensitivity study on the acoustical model for Mach cut-off flight. This task aims to identify the major variables that can impact a supersonic aircraft's ability to fly (and maintain) Mach cut-off and determine the sensitivity of Mach cut-off flight to these variables. This will be determined by assessing both atmospheric variability and flight condition variability. This task will be performed for both a standard vehicle model (the F-18 input model in PCBoom), as well as a model representative of Aerion Corporation's AS2 vehicle. Aerion's vehicle will be assessed using data provided by Aerion under ASCENT 42. The final objective of this task is to determine the sensitivity of Mach cut-off flight to various parameters for Aerion's proposed concept in order to provide insight on the degree of robustness for Mach cut-off flight as it pertains to a supersonic business jet. The hope of this task is to help provide Aerion, the FAA, and the aerospace community at large, a better understanding of how feasible Mach cut-off flight could be and to assist in guiding policy regarding supersonic flight using Mach cut-off.

Research Approach

The research approach for this task is heavily dependent on data, advice, and research to be provided by the other member of the ASCENT 42 team. The final results of this task will be reliant on data from Aerion, advice and guidance from Volpe and NASA, and research performed at Penn State University. The first goal of the research to be performed by Georgia Tech is to understand the mechanics and operating procedures of NASA's PCBoom. This involves running test cases, analyzing results, and understanding the data both given and received from the program. PCBoom will be the primary method in which Georgia Tech will assess the sensitivity of Mach cut-off flight.

The first step in the process is to execute a "preliminary" sensitivity study using PCBoom and the provided F-18 geometry to understand the code and determine if the results make physical sense. This will be done by running the F-18 model through PCBoom at various flight conditions (steady-level flight, acceleration, and a handful of maneuvers) to determine if Georgia Tech has a good handle on the PCBoom settings required to accurately generate results. This model will also be run through various atmospheric conditions as well. The results of this preliminary study will be presented to the ASCENT 42 team to gather their opinions, advice, and suggestions regarding the execution of PCBoom.

After the first step is completed, the AS2 (from Aerion) will be incorporated into PCBoom and a proposed design space of runs will be presented to the ASCENT 42 team. Next, the modeling space that captures the desired combinations of atmospheric and flight conditions will be agreed upon. Since PCBoom, as it currently stands, may encounter numerical error close to Mach cut-off flight, it will be important to incorporate the research being conducted at Penn State University in order to remedy this issue. Georgia Tech will execute a large set of runs through PCBoom to gather the results. An agreed upon metric for assessing the impact of sonic booms, evanescent waves, and Mach cut-off conditions will need to be agreed upon by the ASCENT 42 team and the FAA. Georgia Tech will then present the results of this study to show how sensitive Mach cut-off flight is to both atmospheric and flight conditions.

Milestones

- Research plan for task was completed
- First quarterly report was submitted
- PCBoom 6.7 was received from NASA
- Volpe (Juliet Page) provided instruction on how to use PCBoom
- Initial data from Aerion was received for AS2 at Mach 1.4 undertrack.

Major Accomplishments

Georgia Tech has completed the research plan for this task. Georgia Tech has also acquired both the source code and executable for PCBoom 6.7. This program will be used to perform the sensitivity analysis on the acoustical model provided by Aerion, Volpe, and Penn State University. Georgia Tech has begun learning syntax and operation of PCBoom and has spent a significant amount of time delving into the user's manual to fully understand each component of an input file and the resulting output files generated by the program. Georgia Tech has started an initial study for the sensitivity of Mach cut-off flight on a standard sonic boom signature (F-18 geometry provided with the executable). Georgia Tech has assessed the sensitivity of the resultant boom strength and shape of the F-18 model with variations in atmospheric temperature and humidity as well as various flight Mach numbers. An example of the preliminary results to temperature gradient can be seen in Figure 42.2. It should be noted that these are preliminary results and will change as Georgia Tech becomes more familiar with PCBoom. Georgia Tech has already received valuable guidance from Volpe on how to improve the results generated by PCBoom to account for molecular relaxation and numerical error. These results will mostly likely change at a later date as well, once the model for Mach cut-off flight is received from Penn State University and incorporated into PCBoom. Currently, the immediate goals of this task for the upcoming weeks is to incorporate the suggestions made by Volpe, execute the sensitivity for various wind patterns, assess the sensitivity of the F-18 model to different flight conditions, and incorporate the pressure field data by Aerion into PCBoom.

Figure 42.2: Example of Preliminary PCBoom Sensitivity Runs for F-18 Model

Task 5: Evaluation of Technologies to Facilitate Mach Cut-off Flight

Georgia Institute of Technology

Objectives

The objective of this task is to identify and evaluate technologies that could be utilized to facilitate Mach cut-off flight. This task will primarily focus on nearer-term technologies that could be utilized by supersonic business jets. Most of these potential technologies will be external to the aircraft or technologies that can be placed on an aircraft with minimal to no change in the design. However, Georgia Tech will also investigate more long-term technologies that could be integrated into future aircraft designs and could potentially be applicable to larger supersonic aircraft.

Research Approach

Georgia Tech's research approach in this task is primarily through literature review and solicitation of opinions from experts in the fields of aerospace, policy making, meteorology, and manufacturing. Georgia Tech will perform this task in a phased approach. The first phase is performing an initial literature survey to identify potential technologies that would benefit Mach cut-off flight. Based on the team's initial knowledge and understanding of Mach cut-off flight, the first phase of literature review will target technologies that could make it easier for operators of supersonic business jets to identify or predict atmospheric conditions. These technologies will undergo a cost-benefit type of evaluation to identify both the strengths and potential weakness of each technology. At the time of writing, this first phase has been completed by the Georgia Tech team.

The second phase of this task will be done in concurrence with task 4. This phase will focus on researching more long-term technologies that could be of benefit to Mach cut-off flight. These technologies might impact the design of a supersonic aircraft, or may require additional aircraft capabilities (not available on current aircraft) in order to utilize them to their fullest potential. Some technologies that have been suggested include: active flow control, morphing structures, boom-spikes, etc.

The final phase of this task will be done after the sensitivity study from task 4 has been completed. With the knowledge and insight gained through performing task 4, the ASCENT 42 research team will have a better understanding on how flight conditions and atmospheric conditions impact the capability of a supersonic aircraft to fly at Mach cut-off. This will allow the Georgia Tech team to identify any additional technologies that were overlooked during the initial phases of this task. This phase of research will also identify which technologies have the best potential impact (and least amount of cost), and Georgia Tech will do more research and evaluation of these "big-hitter" technologies, as well as reaching out to subject matter experts to provide opinions on these technologies. The result of this phase will be a portfolio of technologies that will be able to guide investment in technologies to facilitate Mach cut-off flight.

Milestones

- Research plan for task was completed
- First quarterly report was submitted
- Phase 1 of task was performed

Major Accomplishments

After ASCENT 42 project was initiated, Georgia Tech created a research plan for this task. Since Georgia Tech had a period of time before PCBoom was acquired, it was determined that this task would be done in separate phases. The first phase of this task was started soon after the start of the project and has continued until the present (although work on this task has taken a back-seat to task 4 after Georgia Tech received PCBoom). During the first phase of this task, Georgia Tech has identified a number of technologies that could potentially be used or adapted for facilitation of Mach cut-off flight. An example of some of these technologies can be seen in Figure 42.3. Research for phase two of this task will begin in the coming months of the overall ASCENT 42 research effort.

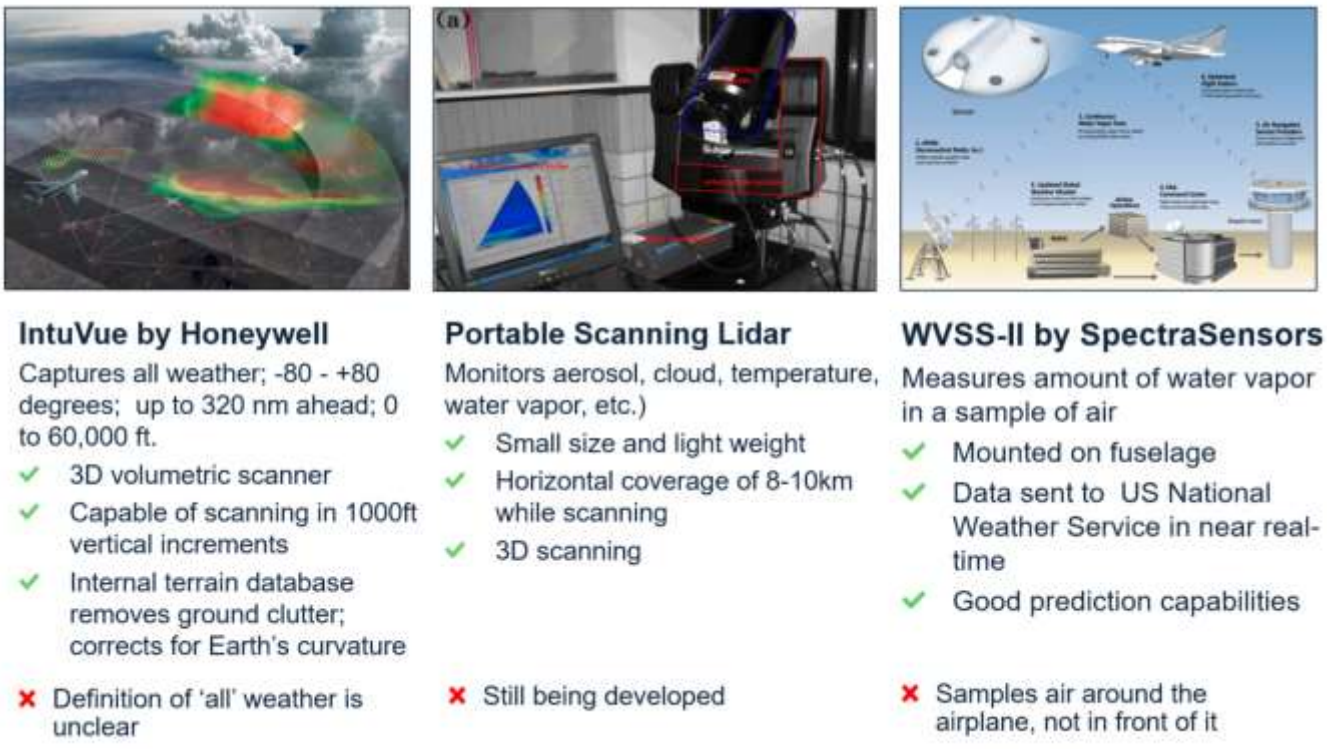

Figure 42.3: Example Technologies from First Phase of Research

Task 6: ASCENT Project 42 Support

Volpe National Transportation Systems Center

Volpe is supporting this project by providing PCBoom modeling expertise, including Mach cut-off and CFD source characteristic as well as specific sonic boom analysis guidance to the ASCENT 42 team.

Major Accomplishments

Volpe has provided initial sonic boom modeling guidance on using suitable CFD-solutions for supersonic aircraft configurations as source inputs to PCBoom. Documentation regarding coordinate system, orientation and CFD pressure extraction protocols has been provided to the ASCENT 42 team. Volpe support included a PCBoom Web based training session for Project 42 participants on November 9th, 2016. This training session was recorded by PSU and has been made available to team members. A set of training briefings, sample input files and test cases were provided to participants and reviewed during the training class.

Examples covered in the PCBoom training class included the following:

- Level flight from an F-18 using the simple Carlson source model
- Assessing Mach and lateral cut-off
- CFD pressure distribution inputs using the NASA LM1021 publicly available dataset
- Burgers loudness propagation applying molecular relaxation

In order to effectively build PCBoom analysis capability amongst team members, Volpe has recommended starting with cruise flight condition analysis and then reducing the Mach number to include acceleration to Mach cut-off conditions. This will lead towards eventual assessment of atmospheric and terrain variability on Mach cut-off using PCBoom.

Volpe has provided some initial guidance to Aerion regarding the development of PCBoom input cylinder formatted data and continues to work with them regarding specific file formatting protocols for PCBoom. Aerion has established an FTP file transfer site and has provided near-field pressure characteristics from CFD for the cruise flight condition. Volpe has assisted with development of cruise pressure input definition PCBoom files based on Aerion's cruise configuration CFD data.

Supporting Information

Publications

N/A. The project began in August 2016.

Outreach Efforts

N/A. The project began in August 2016.

Awards

V. Sparrow gave the 2016 Rayleigh Lecture to the American Society of Mechanical Engineers (ASME) Noise Control and Acoustics Division on November 15, 2016 at the 2016 International Mechanical Engineering Congress and Exposition in Phoenix, AZ. The title of the talk was "Two approaches to reduce the noise impact of overland civilian supersonic flight."

Student Involvement

Penn State: Graduate Research Assistant Zhendong Huang is a key participant in Task 1A. Graduate Research Assistant Nick Ortega is a key participant in Task 2.

Georgia Tech: Ruxandra Duca and Ratheesvar Mohan have both preformed significant work under task 4 and task 5. They are integral parts of the Georgia Tech research team and have worked diligently in researching technologies pertaining to Mach cut-off flight as well as learning how to operate PCBoom and analyze the output/results. Both students attend weekly research meetings and provide deliverables to the Georgia Tech ASCENT 42 research team.

Plans for Next Period

Continue the work described above.

Project 043 Noise Power Distance Re-Evaluation

Georgia Institute of Technology

Project Lead Investigator

Dimitri Mavris (PI)
Regents Professor
School of Aerospace Engineering
Georgia Institute of Technology
Mail Stop 0150
Atlanta, GA 30332-0150
Phone: 404-894-1557
Email: dimitri.mavris@ae.gatech.edu

University Participants

Georgia Institute of Technology

- P.I.(s): Dr. Dimitri Mavris (PI), Mr. Christopher Perullo (Co-PI)
- FAA Award Number: 13-C-AJFE-GIT-021
- Period of Performance: June 28, 2016 – August 14, 2017

Project Funding Level

The project is funded at the following levels: Georgia Institute of Technology ($150,000). Cost share details for each university are below:

The Georgia Institute of Technology has agreed to a total of $150,000 in matching funds. This total includes salaries for the project director, research engineers, graduate research assistants and computing, financial and administrative support, including meeting arrangements. The institute has also agreed to provide tuition remission for the students paid for by state funds.

Investigation Team

Georgia Institute of Technology
Principal Investigator: Dimitri Mavris
Co-Investigator: Christopher Perullo
Research Faculty: Matthew LeVine, Greg Busch, Holger Pfaender, Michelle Kirby
Students: Arturo Santa-Ruiz, Kenneth Decker

Project Overview

The standard technique for evaluating noise from flight procedures is through Noise Power Distance (NPD) relationships. Noise calculations in the Aviation Environmental Design Tool (AEDT) rely on NPD curves derived from aircraft certification data. This dataset reflects representative aircraft families at set power levels and aircraft configurations. Noise levels are obtained as a function of observer distance via spherical spreading through a standard atmosphere. Other correction factors are applied to obtain the desired sound field metrics at the location of the receiver. The current NPD model does not take into account the aircraft configuration (e.g., flap settings) or alternative flight procedures being implemented. This is important as the noise characteristics of an aircraft depend on thrust, aircraft speed and airframe configuration, among other contributing factors such as ambient conditions. The outcome of this research will be a suggested NPD + configuration (NPDC) format that enables more accurate noise prediction due to aircraft configuration and speed changes.

Georgia Tech will leverage domain expertise in aircraft and engine design and analysis to evaluate gaps in the current NPD curve generation and subsequent prediction process as it relates to fleet noise prediction changes from aircraft configuration and approach speed. The team will use EDS physics based modeling capabilities to conduct a sensitivity analysis to identify additional parameters to be included in the NPDC (NPD + Configuration) curve format. The team will also seek out airport noise measurements to assess the increased accuracy of the developed NPDC format.

Task 1: Perform Sensitivity Study on NPD Curve Generation and Prediction

Georgia Institute of Technology

Objectives

The first task involves the identification of parameters for possible inclusion into the NPDC curves that will be generated in Task 2. Georgia Tech will apply its prior expertise in conducting statistical analyses of the impact of vehicle design and operations on fleet noise and NPDs to determine the number of additional dimensions required to sufficiently capture the impact of aircraft configuration and operational changes on vehicle noise. Sensitivities will be performed both at the NPD and SEL contour area levels to properly frame the problem at the fleet/AEDT analysis level.

Research Approach

In order to accomplish these tasks, the research will be broken down into three distinct research phases. The first phase of research is the generation of aircraft Noise-Power-Distance (NPD) curves. At first, these curves will be generated for a single vehicle with various input parameters. The NPD curves for this aircraft will then be analyzed to determine the sensitivity of the magnitudes of the NPD tables to various configuration parameters. The sensitivity analysis will also provide insight on if (and how) interpolation/regression can be used to minimize the number of required NPD generation runs for each vehicle class being investigated. The final research phase of this task is to generate NPD supersets for each vehicle class that can be used in subsequent tasks.

ANOPP NPD Generation

The first phase of research for this task is to generate the vehicle-level NPD curves using non-standard configurations for various vehicle class models. Georgia Tech used the Environmental Design Space (EDS) to generate the aircraft vehicle models. Georgia Tech utilized NASA's Aircraft Noise Prediction Program (ANOPP) to simulate the noise generated and observed by the aircraft. ANOPP has the capability to generate NPD tables (which can be plotted to produce NPD curves) for a specific aircraft model. NPD tables include four noise metrics (as a function of power setting and altitude): sound exposure level (SEL); effective perceived noise level (EPNL); maximum A-weighted sound pressure level (max SPL); and maximum tone-corrected perceived noise level (max PNLT). The input variables in the NPD prediction method include airframe geometry, engine geometry and performance, aerodynamic performance, flight path and configuration parameters.

In this study, Georgia Tech is tasked with assessing configuration specific NPD curves. Due to the fact that AEDT/INM currently requires specific standard settings for NPD generation, ANOPP's NPD prediction module has corresponding pre-set defaults for many of the flight path and configuration parameters. It is necessary to alter ANOPP to account for non-standard configuration settings. This includes flap deployment angle, slat deployment angle, landing gear setting, and flight velocity. Flap/slat deployment angles and landing gear settings are classified as configuration parameters while aircraft flight velocity is a flight path parameter. However, for the sake of simplicity, flight velocity will also be referred to as a configuration parameter in this report. This is required because as the flight velocity changes, the source noise levels will also change drastically—not only at the flight points in the NPD prediction module. Once the parameters to be altered are identified in the ANOPP model, a new set of flight path library files must be generated for each configuration (using a separate ANOPP module). These flight path library files are then leveraged by source prediction and propagation modules that comprise the rest of the ANOPP model to generate NPD curves for the aircraft. This process is repeated for each distinct configuration of the aircraft model used in the sensitivity analysis. The results of the sensitivity analysis will then determine the number of executions of ANOPP are necessary for the NPD superset generation for each vehicle class being assessed.

NPD Sensitivity Analysis

Sensitivity analysis is performed to determine the effect that each configuration parameter has on the sound exposure level (SEL) generated by the vehicle at a given distance. Future revisions will include sensitivity studies of EPNL, Max A-Weighted SPL, and Max PNLT metrics. To perform the sensitivity analysis, ANOPP is used to generate NPD curves for

the 150 passenger class (150pax) vehicle model by sweeping through a range of flap angles, slat angles and speeds for both the gear up and gear down configurations. The 150pax model is used as the baseline vehicle to indicate sensitivity to these factors because the model has gone through extensive calibration and verification in previous studies to emulate the performance a Boeing 737-800. It is important to note that a sensitivity analysis of each vehicle can be time consuming due to program set up and run times; however, the trends are expected to be similar across different vehicle size classes. These results will be used to infer sensitivity of SEL to configuration parameters for other vehicle size classes.
Ultimately, ANOPP data will be used to interpolate noise level with respect to configuration parameters. To avoid extrapolation, the maximum possible ranges of each configuration parameter are considered.

Variable	Min	Baseline	Max	Units
Flap angle	0	15	30	deg
Slat angle	0	10	30	deg
Speed	130	160	200	kts

Table 1. Variable ranges for sensitivity analysis

Table 1 shows the ranges of values considered for each configuration parameter. It is important to note that the flap and slat angle values tested in this study correspond to the actual angles of the devices on the vehicle, not the flap setting that a pilot sets. The mapping of flap setting set by the pilot to the actual flap and slat angle of the vehicle is vehicle dependent and not relevant to the goal of this study, but could be included in future work. Each variable sweep is performed individually with other remaining parameters held fixed at their baseline values. Flap angles are modified in 5 degree increments while speed is varied in ~12 knot increments.

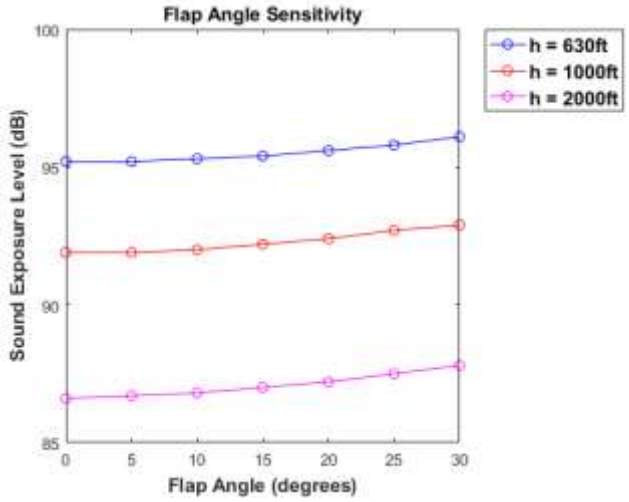

Figure 1. Sound Exposure Level vs. flap angle

Figure 1 shows a sweep of SEL vs. flap angle at various aircraft heights, *h*. Ten different height settings are examined to evaluate the sensitivity of SEL to flap angle (only three were selected for clarity). Flap angle has a significant impact on SEL. Figure 1 shows a portion of the flight envelope at lower altitudes. The sensitivity approaches a 4 dB difference as the flight conditions change to higher altitudes and different thrust settings.

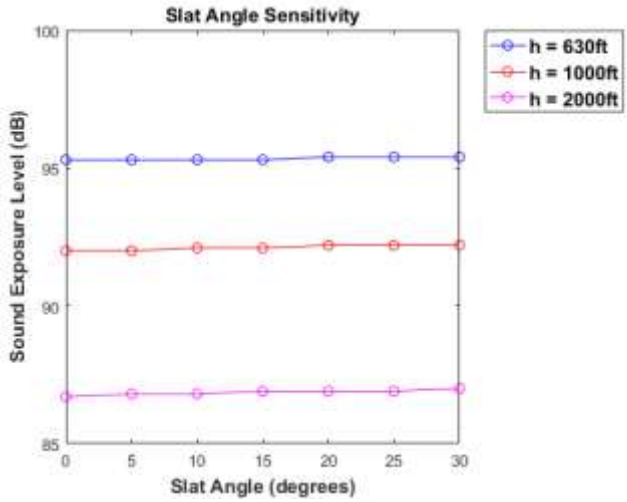

Figure 2. Sound Exposure Level vs. slat angle

Figure 2 shows a sweep of SEL versus slat angles at various aircraft heights. It is observed that slat angle has negligible impact on SEL. The change in SEL over the entire range of flap angles tested is on the order of 0.5 dB, which is likely within modeling uncertainties. The insignificant contribution of slat angle to noise level provides an opportunity to reduce the dimensionality of the problem by removing it as an independent variable. Instead, it is possible to tie the slat angle setting to the flap angle setting. This is also practical because pilots generally do not set slat angles independently of flap angles; they are both tied to flap setting based on a predetermined schedule that is different for each vehicle type. In this study, slat angles are dependent on flap settings. This reduces the number of dimensions that must be interpolated within AEDT while also reducing the number of grid point evaluations needed to accurately obtain the final results.

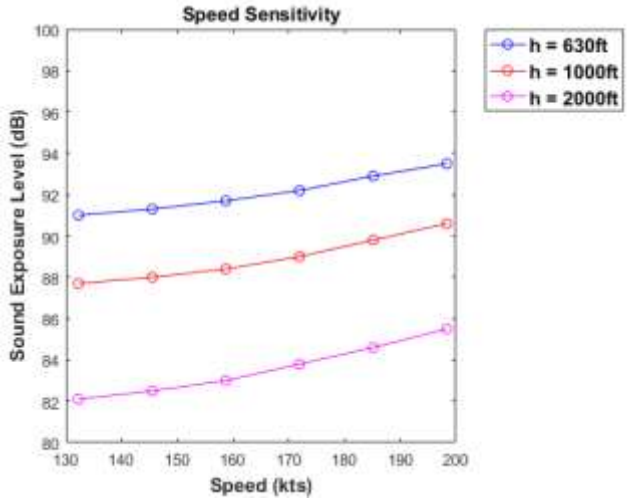

Figure 3. Sound Exposure Level vs. speed

Figure 3 shows the sweeps of SEL vs. speed at various heights. Speed also has a significant effect on SEL, changing it by ~3 dB over the examined ranges. From these sensitivity studies, it is clear that flap angle and speed have significant effects on SEL while slat angle does not. Thus, an interpolation scheme must be developed to include these variables.

NPD Superset Generation

When performing analysis in AEDT, a superset of NPD curves will be imported that includes NPD tables for a range of vehicle configurations. Each vehicle configuration has its own NPD curve that can be used to interpolate noise level based on distance and thrust setting. By considering configuration, multiple dimensions are being added to the noise model, and AEDT must be able to interpolate noise with respect to each of these dimensions. The solution to this problem is to generate a grid of NPD curves, or superset, which contains enough points needed to interpolate with respect to each dimension. These curve fits are then evaluated to interpolate noise level along each dimension. A study is performed to determine the appropriate order of interpolation in each dimension and the appropriate number of points needed to produce these curves.

Since slat angle is tied to flap angle and gear setting is a categorical variable, only flap angle and speed must be analyzed to determine the appropriate interpolation scheme. Due to the run time of each test and the complexity of creating the grid in AEDT, it is desirable to have the fewest number of curves possible in this superset. First, data from the sensitivity analysis will be used to generate polynomial fits at each height. All available data points will be used to generate polynomials curves from first through fourth order based on the least squares method. The R^2 value will be computed at each height to evaluate the quality of the fit. The lowest order that has a good representation of the training data is selected. With the order of the polynomial selected, the number of points used to generate the polynomial is then varied to determine the appropriate grid density. The RMS error at each point is evaluated to determine the quality of each fit. The smallest number of points with which the last additional point provided significant improvement will be selected. Repeating this for both flap angle and speed determines the appropriate density of the superset and the nature of the interpolation scheme in AEDT.

	1st Order	2nd Order	3rd Order	4th Order
R^2	0.9241	0.9805	0.9896	0.9931

Table 2. Correlation coefficient for flap angle curve fits

Table 2 shows the R^2 value of each order curve fit for flap angle. It is shown that significant model improvement occurs from 1st order to 2nd order, but improvement becomes less significant beyond that. For this reason, a second order curve is selected to fit SEL vs flap angle.

Number of Points	3	4	5	6	7
RMS Error (dB)	0.0545	0.0449	0.0406	0.0405	0.0403

Table 3. RMS Error for flap angle curve fits

Table 3 shows the RMS error at each point when fitting flap angle with a 2nd order polynomial at each height. In every case, the RMSE is small enough to be indistinguishable for all practical purposes. As a result, it is possible to fit the 2nd order curves using 3 points, which results in a closed form solution. This eliminates the complexity of having to perform a least squares regression since a closed form solution is available.

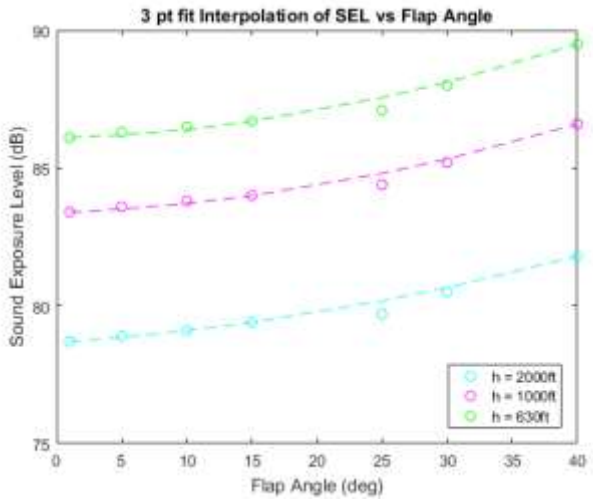

Figure 4. SEL vs. flap angle with 2nd order fit

Figure 4 shows the results of this study at a few example heights. The quality of each fit should be adequate for the purposes of the analysis in AEDT as each fit captures the behavior of SEL with flap angle fairly well.

	1st Order	2nd Order	3rd Order	4th Order
R^2	0.9813	0.999	0.9997	0.9999

Table 4. Correlation coefficient for speed curve fits

Table 4 shows the R^2 value of each order curve fit for flap angle. It is shown that a linear interpolation does an adequate job of capturing the behavior of the data. Consequently, a linear approximation will be used to fit SEL with respect to speed.

	2	3	4	5	6
RMSE (dB)	0.068	0.0453	0.0424	0.0416	0.0416

Table 5. RMS Error for speed curve fits

Table 5 shows RMS error at each point when speed with a linear regression at each height. In every case, the RMSE is small enough to be indistinguishable for all practical purposes. As a result, it is possible to fit the linear approximations using the 2 end points, which results in a closed from solution. This eliminates the complexity of having to perform a least squares regression since a closed form solution is available.

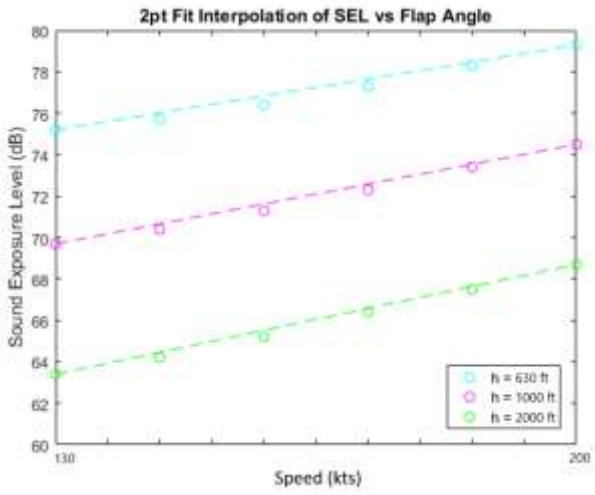

Figure 5. SEL vs. speed with linear approximations

Figure 5 shows the results of this study at a few example distances. The quality of each fit should be adequate for the purposes of the analysis in AEDT as each fit captures the behavior of SEL with flap angle fairly well. Once all relevant NPD data is generated for a given vehicle, it must be compiled into a single XML document to be imported into AEDT. The XML document is generated by EDS and contains relevant data fields and attributes for each vehicle type. Once the new grid of NPD data is incorporated into the XML file, analysis can be performed in AEDT on the full data superset.
In conclusion, dimensions for configuration parameters are to be accounted for in AEDT analysis by importing a superset of NPD relationships that vary in each new dimension. Flap angle is accounted for by importing 3 sets of NPD curves at 3 flap settings at each set of parameters and interpolating between them using parabolic fits. Speed is accounted for by importing two NPD curves for each set of parameters and linearly interpolating between them. Each case will also need to be run for gear up and gear down cases. The result is 12 NPD curves (3 flap settings x 2 speed settings x 2 gear settings) that must be imported into AEDT to fully map the space of configuration parameters.

Run	Gear	Speed (kts)	Flap (deg)
1	Up	130	0
2	Up	130	15
3	Up	130	40
4	Up	190	0
5	Up	190	15
6	Up	190	40
7	Down	130	0
8	Down	130	15
9	Down	130	40
10	Down	190	0
11	Down	190	15
12	Down	190	40

Table 6. NPD superset values for 150 passenger class

Table 6 shows a breakdown of the 12 cases that must be run and imported for this study. It is important to note that while particular values and ranges may change from vehicle to vehicle, it is expected that the same interpolation

method should be valid for each vehicle in the fleet. The 150pax class model provides a valuable case study due to the availability of calibration and verification data from previous studies that can be used to validate the method. Now that the method has been validated, the next step is to apply it to all other vehicles in the fleet.

Milestones

- ANOPP NPD Generation – Completed November 2016
- NPD Sensitivity Analysis – Completed December 2016
- NPD Superset Generation for 150pax Class – Completed December 2016
- NPD Superset Generation for 50pax Class – In Progress
- NPD Superset Generation for 100pax Class – In Progress
- NPD Superset Generation for 210pax Class – In Progress
- NPD Superset Generation for 300pax Class – In Progress
- NPD Superset Generation for 400pax Class – In Progress

Major Accomplishments

- Determined the input parameters to change in the ANOPP model to simulate changes in vehicle configurations and vehicle flight velocity
- Developed an automated method for implementing changes to the desired input parameters to significantly reduce model simulation preparation time
- Generated baseline/reference ANOPP NPD input files for all vehicle classes
- Completed NPD generation set of runs for the 150pax NPD sensitivity study
- Completed analysis of NPD sensitivity study for the 150pax model
- Determined appropriate interpolation methods for SEL for each input parameter
- Generated NPD superset for 150pax model to be used in subsequent tasks

Task 2: NPDC Generation and Sensitivity Study

Georgia Institute of Technology

Objectives

Georgia Tech will use EDS to generate NPDC curves for different aircraft size classes that represent a large portion of the existing fleet. Table 7 lists the EDS vehicles that will be used in the analysis. NPDC curves will be generated for vehicles in each size class to ensure the resulting format is appropriate and representative across the fleet. GT and the FAA will coordinate on the appropriate vehicles of interest to carry forward in the research. EDS and ANOPP will be used to parametrically vary vehicle low-speed configuration, speed, and ambient conditions. The outcome of this parametric study will be a series of NPD curves that represent varying configurations, speeds, and ambient conditions. A sensitivity study will be performed to identify the quantitative impact of changing vehicle characteristics on both the resulting NPD and on the resulting fleet noise. Finally, the results of the sensitivity study will be used to recommend a format for the NPDC tables. The format will include both the additional parameters that should be included (i.e., flap angle, vehicle speed), and the number of additional conditions at which NPD data must be provided (e.g., 3 flap angles and 2 flight speeds). The outcome of Task 2 is a detailed comparison of differences in predicted noise when using the AEDT database NPDs, EDS baseline vehicle NPDs, and the NPDC curves generated in this task.

AIRCRAFT SIZE	EDS REPRESENTATIVE AIRCRAFT
50 pax	CRJ900
100 pax	737-700
150 pax	737-800
210 pax	767-300ER
300 pax	777-200ER
400 pax	747-400

Table 7: Existing EDS baseline vehicles

Research Approach

Including the vehicle's varying low-speed configuration and reference velocity for the complete flight envelope will yield differences in predicted noise. In order to assess these results, representative NPDC curves are required. These curves are acquired through an interpolation of the NPD supersets, which are described in more detail in section 0 of the report. For the first iteration, each superset describes the noise evolution for a combination of the three following parameters: flap and slat setting (1°, 15°, & 40°); aircraft airspeed (133.35 knots & 200 knots); and gear setting (up & down). Furthermore, each individual NPD superset, from the 12 simulated in ANOPP, is composed of 10 NPD curves. A curve describes the uncorrected noise metric for a specified slant distance for increasing thrust settings. Figure 6 depicts a notional NPD supersets library produced in-house.

For the computation of a noise metric, AEDT currently uses a fixed reference speed of 160 knots and flight trajectory information that is discretized into segments. The segment's data can be expanded to include instantaneous reference speed and the vehicle's configuration. By increasing the data used in the acoustic computation algorithm, an interpolated NPD (NPDC) is obtained corresponding to a higher fidelity description of the segmented vehicle parameters. This description is to be propagated in AEDT to appropriately obtain the noise characteristics for the complete flight envelope.

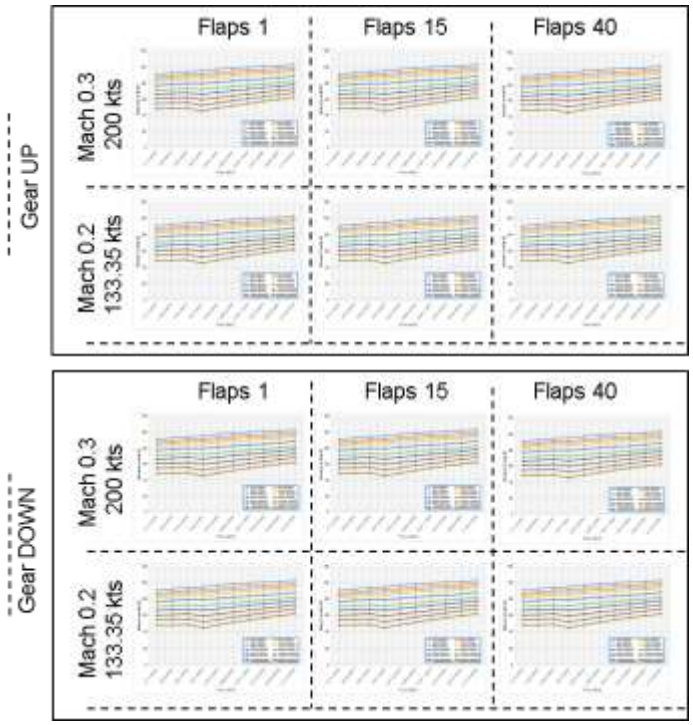

Figure 6. In-house developed NPD supersets library

Potential NPDC Integration Approaches with AEDT

In order to integrate the newly generated noise sources for a given flight profile and configuration, three approaches were initially studied. The first option considered involved running each NPD from the superset one-at-a-time through the AEDT algorithm in order to extract the custom noise metric results describing the flight procedure. This method was discarded due to the prohibitive computational expense incurred for a fleet of vehicles. A normal procedure result is computed on the order of minutes. An analysis including 12 different combinations of a vehicle configuration and reference speed amounts for several hours. Furthermore, by following this process, a more intensive modification of the source code would be required because segment-to-segment information would need to be post-processed. The parameters required to properly assess the noise adjustments would complicate the procedure as each computation would include its native configurations and reference velocities.

A variation to this approach requiring the analysis of all the NPD supersets was deliberated as well. In this case, the custom SEL grid was to be used in the ANGIM tool available to ASDL in order to superimpose the necessary segmented grids to portray the mission. This methodology suffered from the same weaknesses as the aforementioned practice.

Figure 7 further portrays the discarded methods. It is important to note that Figure 7 does not reflect the NPD's currently used. Slat angle and flap angle were found to be correlated in the algorithm and are considered in the same vehicle configuration.

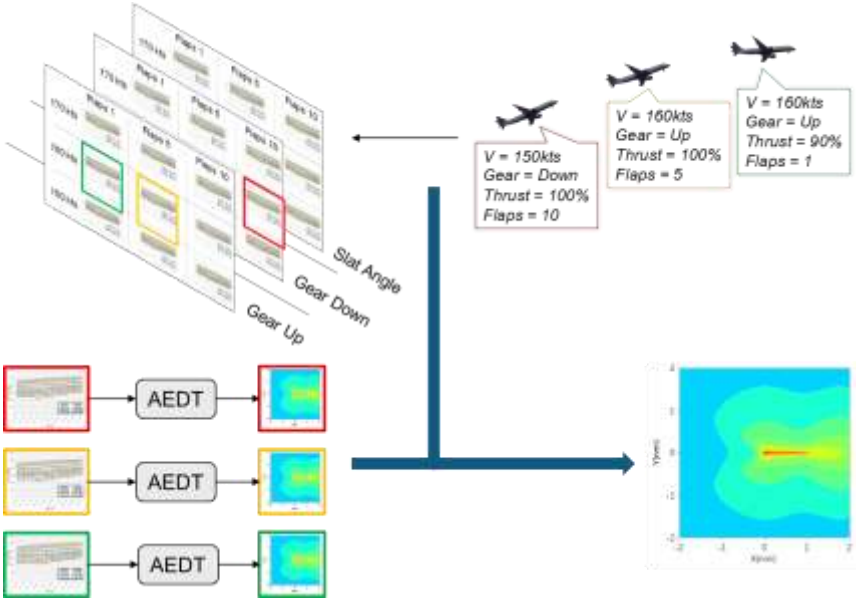

Figure 7. Discarded methods for the integration of the NPD library

The third, and subsequently selected, approach was to assemble a custom NPDC representing the flight procedure input to AEDT. This is performed by obtaining the segment information required to iterate between the NPD sets to create the NPDC curves (Noise-Power-Distance-Configuration). The vehicle object is expanded to include the library of NPD supersets considering flap, slat, and gear configurations. Each of the sets also includes the flap-slat setting, gear setting, and reference velocity data with which the ANOPP simulation was performed. The segment-to-segment part of the acoustic computation process is then expanded to contain an interpolation algorithm for each specific point required within the 12 NPD supersets with 10 NPD curves. The detailed process is explained in section 7.2.3. Using this approach does not increase the computational expense as significantly as the two other solutions considered. The required alterations to AEDT's source code are thought to be minimal due to the potential inclusion of the interpolation algorithm within the segmented information. The parameters describing the mission profile will also be available.

Required AEDT Modifications (Noise Corrections)

Georgia Tech has developed a wrapper (AEDTTester) around the AEDT source code that allows for the automation of reading aircraft definition and flight procedures input files with minimal user interaction. Our focus lies in researching the sensitivity of the acoustic analysis to the expanded data. It is of importance to do so with the least modifications to the AEDT source code as possible, in order to provide the FAA with a relatively simple implementation of the methodology.

As stated in the previous section, the modification to the NPDC curve accounts for both the aircraft configuration in terms of the noise produced due to the different drag characteristics and the speed. The acoustic computation process does not consider the configuration the vehicle is flying in as long as the NPDC curves portray this information; however, this is not the case with regards to the dissimilar reference velocity that was previously used for the creation of the NPD supersets.

The acoustic computation process in AEDT contains two correction algorithms referring to the reference velocity of 160 knots. First, the noise fraction adjustment includes a hard coded number that is 171.92 feet for a sound exposure level (SEL) value or 1,719.2 ft. for an effective perceived noise level (EPNL). The formulation below shows the equations used for the specified adjustment factors. For an arbitrary segment,

$$NF_{ADJ}(dB) = 10 * \log_{10}[F] \qquad F = \left(\frac{1}{\pi}\right)\left[\frac{\alpha_2}{1+\alpha_2^2} + \tan^{-1}\alpha_2 - \frac{\alpha_1}{1+\alpha_1^2} - \tan^{-1}\alpha_1\right]$$

$$\alpha_1 = -\frac{q}{S_L} \qquad \alpha_2 = -\frac{q+L}{S_L}$$

$$S_L = S_0 * 10\text{^}((L_{E,P,d} - L_{Smx,P,d})/10)$$

Where:

- q = relative distance (ft) from segment start point to point P_S
- L = length of segment
- s_0= 171.92 ft for L_{SEL} or 1,719.2 ft. for L_{EPNL}
- $L_{E,P,d}$ = unadjusted interpolated NPD noise exposure level (dB) at 160 knots. This value will reference the NPD interpolated value for the implemented modified velocity.
- $L_{Smx,P,d}$ = unadjusted interpolated NPD maximum noise level (dB) (L_{Amax}, L_{PNTmax})

The s_0 in the AEDT source code is hard coded; nevertheless, after researching the nature of this factor, it was discovered that it comprises the reference velocity utilized in the creation of the NPD. S_0 is to be modified to its physical expression,

$$S_0 = \frac{2}{\pi} V_{ref} t_{ref}.$$

The second correction algorithm that is affected by the alteration of the reference velocity is the duration adjustment. The duration adjustment accounts for the effect of time-varying aircraft speed, with both acceleration and deceleration. The segment aircraft speed is first computed as follows:

$$AS_{seg} = AS_{p1} + \frac{\delta AS}{2}$$

- AS_{p1} : speed (kts) at the start of the flight segment
- δAS: change in speed along the flight segment

The aircraft speed for the segment AS_{seg}, (at the closest point of approach) is included with AS_{ref}, the vehicle's reference speed at which the NPDC was sampled in order to calculate the duration adjustment factor:

$$DUR_{ADJ} = 10 * \log_{10}\left[\frac{AS_{ref}}{AS_{seg}}\right].$$

The flowchart in Figure 8 illustrates the complete acoustic computation process for a single flight segment. It provides an understanding of where these revised correction factors will influence the noise results.

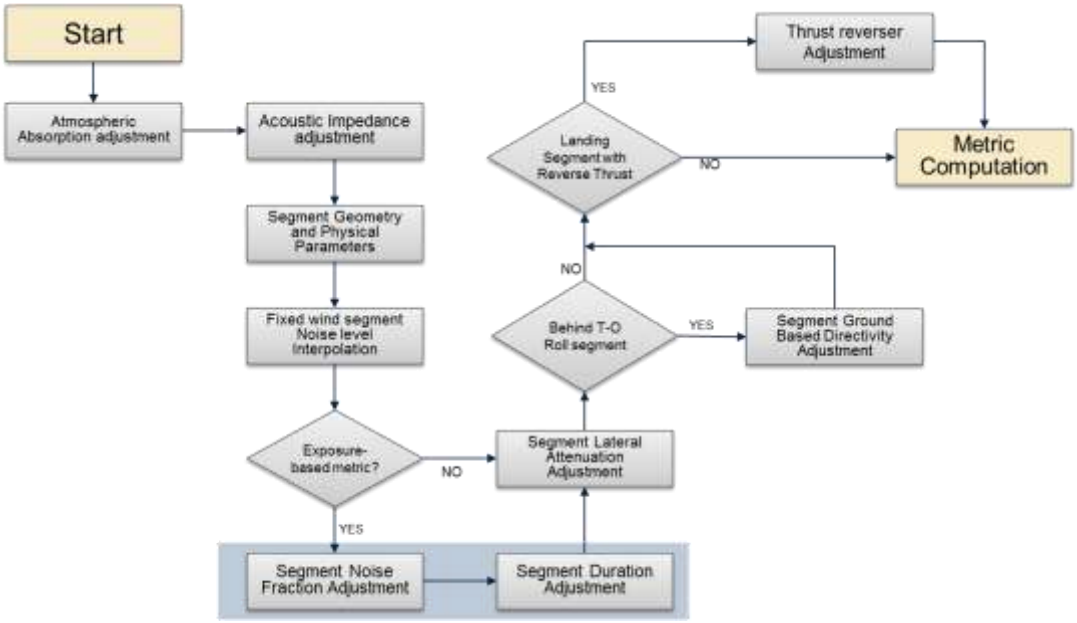

Figure 8. Acoustic computation process in AEDT with the revised noise adjustment factors

Implementation Roadmap

The flight parameters described for each of the NPD curves, including the varying vehicle configuration and speed, are associated with the segment-to-segment information in order to find the appropriate NPDC interpolated values. Consequently, the development of the NPDC is a crucial step in our research efforts. Figure 9 depicts the algorithm procedure and is taken as the baseline to demonstrate the logic behind the NPDC development process.

The first option to include the family of NPD supersets was to directly input the data in the methodology once the algorithm has reached the "Segment Geometry and Physical Parameters" section as seen in Figure 9. All of the required input data from the aircraft and flight procedure readers were obtained at the start of the computation process. It was concluded that an expansion of the vehicle object was preferred as it requires the fewest modifications to the source code. The AEDTTester would otherwise need to be re-called for an appropriate reading of the NPD family superset. This step then leads into modifications in the segment-to-segment calculation, within the main container source algorithm, for the expansion of the object instances and the inclusion of further rules to read the vehicle's parameters.

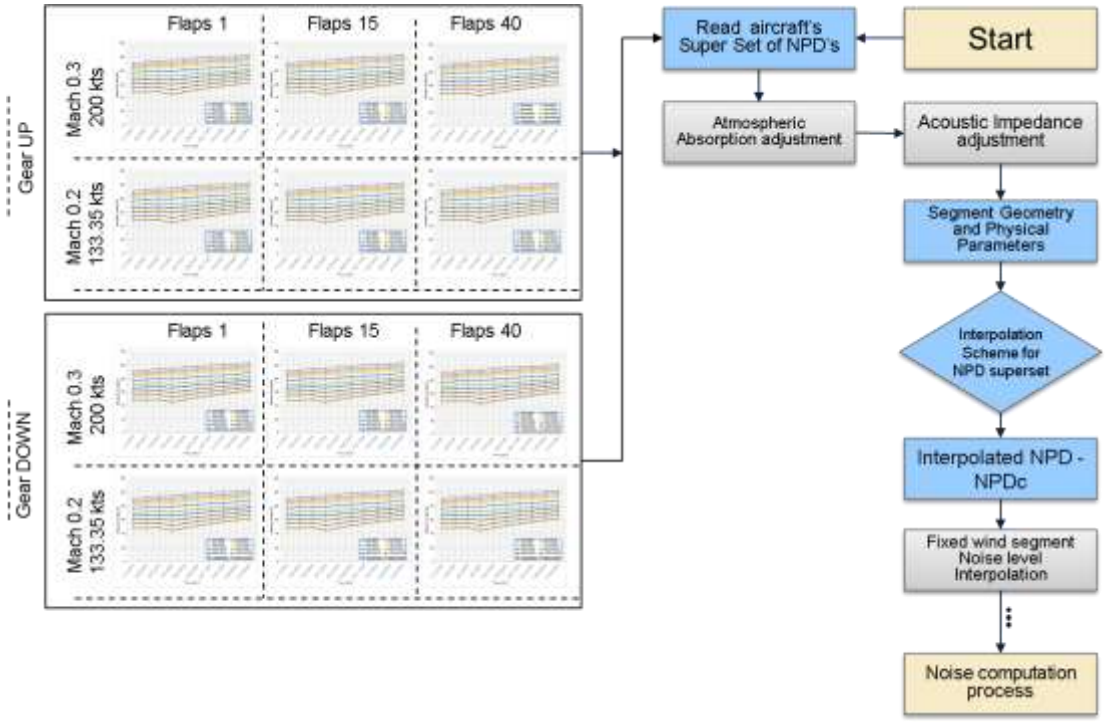

Figure 9. NPDC development process – 1

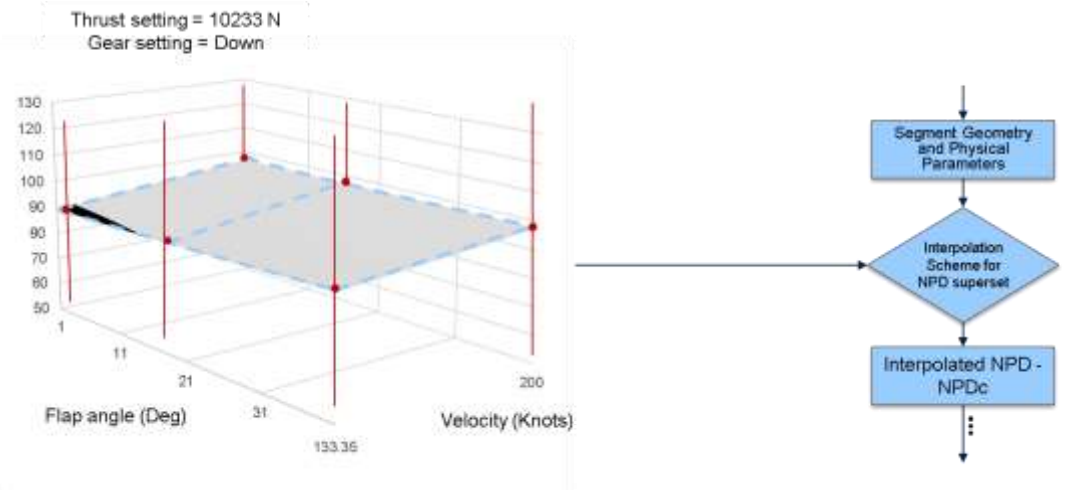

Figure 10. NPDC development process - 2

Major Accomplishments

- Modified the input XML file into the AEDTTester to include 12 NoiseGroup elements with the NPD superset family information
- Modified the schema to accommodate the new format of the input file
- Developed a new class of the noise parameters for the C# method to be able to include noise groups
- Modified the airplane interface for it to include the expanded format
- Modified the Fleet3xAccessAircraftWithLinqObjectsCache for the source code of the AEDT to handle the modifications
- Modified the aircraft XML reader to use the combined noise parameters
- Created a new class including the combined NPD curve long record
- Used it to obtain the reference speed and configuration
- Created a new class for the aircraft combined NPD data to accept the reference values
- In the XML reader, modified the method obtaining the Noise Power Distance Curves to accept the combined NPD curve long records
- Modified the method obtaining the Noise Power Distance Curves to include the combined NPD aircraft data including the three reference velocities
- Changed the airplane interface to account for the combined noise parameters
- Included the references in the noise power distance curve interface
- Modified the thrust interface to make the corrected thrust value available throughout the project
- Developed the interpolation algorithm. Still not applied to the segment-to-segment information

Publications

None, as this project has just started.

Outreach Efforts

None, as this project has just started.

Awards

None.

Student Involvement

Kenneth Decker and Arturo Santa-Ruiz are intimately involved in the day-to-day activities on this research. Kenneth is working on Task 1 and Arturo works on Task 2.

Project 045 Takeoff/Climb Analysis to Support AEDT APM Development

Georgia Institute of Technology

Project Lead Investigator

Prof. Dimitri Mavris
Professor Dimitri N. Mavris
Director
Aerospace Systems Design Laboratory
School of Aerospace Engineering
Georgia Institute of Technology
Phone: (404) 894-1557
Fax: (404) 894-6596
Email: dimitri.mavris@ae.gatech.edu

Dr. Michelle R. Kirby, Co-PI
Chief, Civil Aviation Research Division
Aerospace Systems Design Laboratory
School of Aerospace Engineering
Georgia Institute of Technology
Phone: (404) 385-2780
Fax: (404) 894-6596
Email: michelle.kirby@ae.gatech.edu

University Participants

Georgia Institute of Technology (GT)

- P.I.(s): Prof. Dimitri Mavris, Dr. Michelle R. Kirby (Co-PI)
- FAA Award Number: 13-C-AJFE-GIT, Amendment 020
- Period of Performance: August 15, 2016 to August 14, 2017

Project Funding Level

FAA funded amount is $250,000 for the period of performance of August 15, 2016 to August 14, 2017. The Georgia Institute of Technology has agreed to a total of $250,000 in matching funds. This total includes salaries for the project director, research engineers, graduate research assistants and computing, financial and administrative support. The institute has also agreed to provide equipment funds as well as tuition remission for the students paid for by state funds.

Investigation Team

Prof. Dimitri Mavris, Dr. Michelle Kirby, Dr. Don Lim, Dr. Yongchang Li, Dr. Holger Pfaender, Dr. Matthew Levine, Mr. Chris Perullo, Prof. JP Clarke, and Mr. Jim Brooks. Graduate Students: Vu Ngo and Ameya Behere.

Project Overview

Accurate modeling of aircraft performance is a key factor in estimating aircraft noise, emissions and fuel burn. Within the Aviation Environmental Design Tool (AEDT), many assumptions are made for aircraft performance modeling with respect to aircraft weight and departure procedure coupled with the fact that, typically the aircraft departure is modeled assuming full rated takeoff power/thrust is used. As operations around airports continue to evolve, there is a need to examine those assumptions and to improve the modeling accuracy with flight data. In recent years, flight data has been used more and more in order to enhance models and bring model estimation even closer to reality. Research is needed to build on prior work with a view to develop a robust set of recommendations for improved estimation processes for takeoff weight, reduced thrust takeoffs, and departure profiles within AEDT.

Task 1: Literature Review and AEDT APM Evaluation

Georgia Institute of Technology

Objective(s)

Review the body of existing literature on estimating the takeoff and climb out performance of aircraft using flight data including several ACRP projects 02-41, 02-37, and 02-55 and also ASCENT Project 35 and the AEDT APM.

Research Approach

Using the existing body of work and Georgia Tech's detailed aircraft and engine modeling knowledge, the AEDT APM algorithms will be systematically evaluated to identify areas of improvement in current modeling methods. For all relevant APM assumptions, the team will identify the assumption in question, the validity of the physics behind the APM assumption, suggested improvements, and any issues in data availability or modeling fidelity associated with the suggested improvements. This analysis of APM assumptions will be critical in identifying tuning methods and calibrating AEDT performance to measured flight data.

The objective of ACRP 02-41 was to produce guidance to include the effects of reduced takeoff thrust in their emissions inventory calculations and to develop a Takeoff Thrust-Setting Estimator Tool (TTREAT) based on statistical analyses of extensive takeoff thrust data supplied by airlines. TTREAT was validated based on US Airways data and concluded that the majority of commercial aircraft use approximately a 15% reduced thrust takeoff. This conclusion was similar to the results of ASCENT Project 35.

The objective of ACRP 02-37 was to assess the accuracy of general aviation aircraft SEL noise modeling within INM as compared to measured values. The research team focused on examining performance profiles to help identify causes of error and focused on departures using LJ35, GLF4, and EA50 aircraft, where the error was identified as discrepancies between measure and modeled levels of SEL and also altitude. The observations made were that INM modeling for almost all aircraft types computes departure SEL values higher than the measured levels. Also, the INM departure altitudes for the aircraft are higher than actually occurs. It is likely most error in the INM modeling is caused by significant differences between the standard noise and performance profiles (management of thrust, flaps, speed, climb rates and associated noise-power-distance curves) and actual average practice. The general cause for these discrepancies was the use of maximum thrust departures as standard INM input. Two solutions were proposed to correct the takeoff thrust to provide more realistic results and were based on an assumed temperature method (ATM), where ATM is a process where an aircraft Flight Management System (FMS) is asked to compute the thrust required to safely depart the aircraft from a given runway while demanding a decreased level of engine performance. The two solutions are:

- ATM1:
  - Requires determining the specific thrust levels from manufacturer or operator surveys then creating custom profiles to match these inputs
  - Requires updated Thrust Jet data in order to make reduced thrust departure profiles available as standard INM input.
  - Not a preferred option
- ATM2:
  - First uses the INM's internal computation process to determine the aircraft departure profile at an assumed elevated temperature. The resulting departure data are then converted into a static "profile points" style profile which is then input into the INM and run at the normal or average airfield temperature
  - No radar data, measured sound levels, pilot or manufacturer information is needed
  - Preferred Option

Each method was applied to a set of aircraft and the noise exposure quantified to show a correction of approximately 2.5 dB for a small set of flights within INM, however the recommendations are applicable to AEDT. ATM2 was recommended as the preferred correction approach since ATM1 required manufacturer's input, but is limited to aircraft types that have hi-temperature coefficients. Similar to ACRP 02-41, reduced thrust takeoff was suggested as an improvement in noise exposure to real world flight and would also affect the trajectory of the departure.

The objective of ACRP 02-55 are to develop: (1) standard model aircraft approach and departure profiles that are not currently in AEDT, (2) methods to model customized aircraft approach and departure profiles using AEDT, and (3) technical guidance for selecting appropriate aircraft approach and departure AEDT profiles, including customized profiles, for specific user situations. At present, the results of this study are not public and will be reviewed once available. However,

the objective of modeling departure procedures that are not within AEDT led the GT research team to identify typical departure procedures utilized in real world operations.
FAA AC 91-53A and ICAO PANS OPS Chapter 3 Volume II both contain the minimum safe standards for departure procedures. Both contain the same minimums which are:

1) No thrust cutbacks below 800' AFE and
2) The level of the thrust cutback will not be less than the Airplane Flight Manual (AFM) thrust required to maintain the minimum engine-out climb gradient.

Both documents recommend that all carriers adopt no more than two procedures for each aircraft type; one for noise abatement of communities close to the airport and one for noise abatement of communities far from the airport. Within FAA AC 91-53A, these are defined as the Close-In and the Distant Procedure, which are similar to ICAO Pans Ops NADP1 and NADP 2 defined in CAEP/7 Working Paper 25. Through discussions with Jim Brooks, NAPD1 and NAPD2 most closely resemble real work departure procedures employed by pilots with a suggested variability in the cutback altitude utilized by different airlines of 800', 1000', and 1500' AFE.

The objective of ASCENT Project 35 was to develop a functional relationship between stage/trip length and takeoff weight that can improve the existing guidance provided for weight estimation; and subsequently to determine the percentage of departures that use reduced thrust and the level of reduced thrust that is used for the departure. The project focused on analyzing major US carrier flight data of four engine/airframe combinations, specifically:

- B757-200/PW2037
- B737-800/CFM56-7B26
- B767-400ER/CF680C2/B8F
- B767-300ER/CF680C2/B6F

A series of statistical regressions were conducted to determine the most appropriate functional form to estimate takeoff weight. An example of the results for the B737-800 is depicted in Figure 1 along with the assumption for takeoff weight (TOW) within the AEDT Fleet dB. As evident, the assumed TOW within AEDT is an underestimation of real world operations.

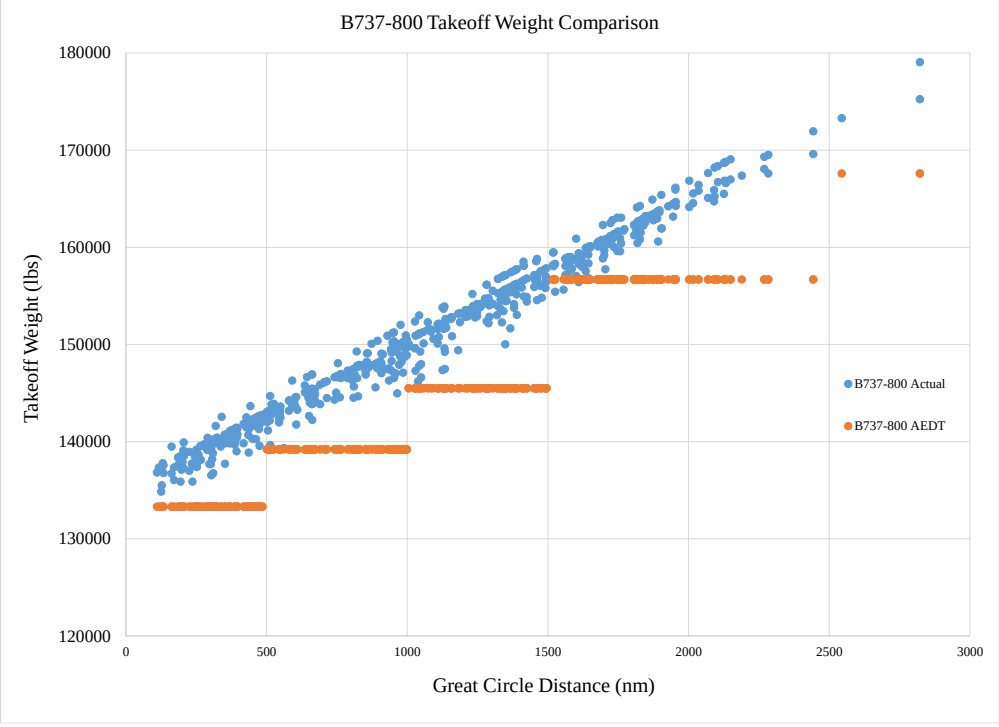

Figure 1. Takeoff Weight Variation with Great Circle Distance

Within AEDT, the manufacturers provide a series of performance and noise coefficients to define their aircraft as guided by BADA and SAE-AIR-1845. SAE-AIR-1845 is the Aircraft Noise and Performance (ANP) database which covers from takeoff and climb performance up to 10,000'. As part of the ANP data, the manufactures provide takeoff weights based on the guidelines in Figure 2 as defined by the AEDT 2b Technical Manual. The two key observations are that a load factor of 65% is assumed and that the TOW within a Stage Length band is constant in lieu of a continual increase with GCD. Based on the results of ASCENT Project 35, real world TOW are higher than the assumptions utilized in AEDT. The main driver for the TOW discrepancies may be the load factor assumption.

Parameter	Planning Rule
Representative Trip Length	Min Range + 0.70*(Max Range – Min Range)
Load Factor	65% Total Payload.
Fuel Load	Fuel Required for Representative Trip Length + ATA Domestic up to 3,000 nmi and International Reserves for trip length > 3,000 nmi. As an example, typical domestics reserves include 5% contingency fuel, 200 nmi alternate landing with 30 minutes of holding.
Cargo	No additional cargo over and above the assumed payload percentage.

Stage number	Trip length (nmi)	Representative Range (nmi)	Weight
1	0-500	350	lb
2	500-1,000	850	lb
3	1,000-1,500	1,350	lb
4	1,500-2,500	2,200	lb
5	2,500-3,500	3,200	lb
6	3,500-4,500	4,200	lb
7	4,500-5,500	5,200	lb
8	5,500-6,500	6,200	lb
9	6,500-7,500	7,200	lb
10	7,500-8,500	8,200	lb
11	>8,500		lb
M	Maximum range at MTOW		lb

Figure 2. ANP Guidance for Takeoff

The load factor assumption of 65% may be a bit low in comparison to historical data. According to the Bureau of Transportation Statistic (BTS), the average load factor, which includes passengers and belly freight, for all carriers and all airports has steadily increased since 2002[1] as depicted in Figure 3. While this data is an aggregate value, BTS does have load factor data at the aircraft level and also for specific air carriers, but is also slightly different than the load factor definition within AEDT. The project 35 results and the BTS data suggest that a further investigation to the load factor assumption should be conducted. Per the FAA project Manager, Booz Allen Hamilton (BAH) is currently conducting an investigation to this assumption. When the results are publically available, the GT research team will review and incorporate the results for the aircraft not included in the Project 35 TOW results.

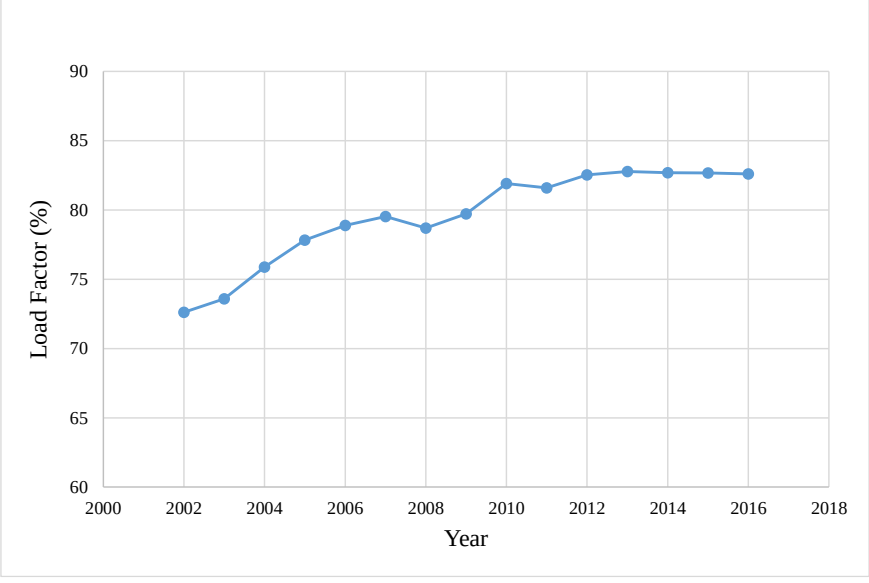

Figure 3. BTS Historical Load Factor

[1] "Load Factor", http://www.transtats.bts.gov/Data_Elements.aspx?Data=5, accessed Dec 20, 2016

In addition to the load factor assumptions associated with the ANP database, the manufacturers are asked, as part of the standard aircraft noise and performance data submittal form, to provide three departure procedures that are used within AEDT. The guidance of the procedures is defined in the AEDT 2b Technical Manual as defined in Figure 4. In many cases, the "Default" procedure is the same as the ICAO B procedure within the AEDT Fleet dB. For each of these procedures, the manufacturer will fill out the performance of their aircraft based on the form depicted in Figure 5.

Default Procedure[xxxi] Modified BBN/AAAI Procedure	ICAO A	ICAO B
Takeoff at MaxToPower (full power) and Climb to 1,000 feet AFE	Takeoff MaxToPower (full power)	Takeoff at MaxToPower (full power)
Pitch over and cutback to climb power. Accelerate to zero flaps retracting flaps on schedule (clean configuration)[xxxii]	Climb at constant speed to 1,500 feet AFE	Climb to 1,000 feet AFE and pitch-over to accelerate at full power to clean configuration
Climb at constant speed to 3,000 feet AFE	Reduce thrust to Climb Power	At Clean Configuration, cutback top climb power
	Climb at constant speed to 3,000 ft AFE	Climb at constant speed to 3,000 ft
Upon achieving 3,000 feet AFE, accelerate to 250 knots[xxxiii]	Accelerate while retracting flaps to Zero (clean configuration)	Upon achieving 3,000 feet AFE, accelerate to 250 kts
	Continue accelerating to 250 knots	
Upon achieving 250 knots, climb to 10,000 feet AFE	Upon achieving 250 knots, climb to 10,000 feet	Upon achieving 250 knots, climb to 10,000 feet

Figure 4. ANP Guidance for Takeoff Departure Procedures Guidance

Stage Number		Procedure Type (Procedural or Points)			Procedure Name	
Segment Type[xxxiv]	Thrust Type[xxxv] (T/C)	Flap Configuration Identifier	Endpoint Altitude (ft AFE)	Rate-of-Climb (ft/min)	Endpoint Speed (KCAS)	Start Thrust[xl] (lb)
Takeoff						lb
Climb			ft			lb
Climb			ft			lb
Accelerate				fpm	kt	lb
Accelerate				fpm	kt	lb
Climb			ft			lb
Climb			ft			lb
Accelerate				fpm	kt	lb
Accelerate				fpm	kt	lb
Climb			10,000			lb

Figure 5. Takeoff Departure Procedures Profile Form

Based on the literature review conducted in Task 1, three elements were identified as the primary drivers for improvement of the APM departure profiles and environmental performance modeling and included the following that will be addressed in the remainder of this project:

- Reduced thrust takeoff of approximately 15%
- Proper takeoff weights as a function of GCD, and
- Proper departure procedure modeling of NADP 1 and 2 versus the existing AEDT STANDARD, ICAO A and ICAO B procedures

The standard procedures typically used in AEDT (and previously in INM) for inventory studies correspond to the sequence of segments first described in SAE-AIR-1845[2]. The ICAO-A and ICAO-B procedures are referenced as "ICAO Noise Abatement Take-off Procedure A and/or Procedure B" in ECAC.CEAC Doc29[3], and an ICAO report[4] from 1982 is cited. This nomenclature is abandoned in the CAEP/7 WP/25 Circular on NADP Noise and Emissions Effects and replaced with NADP1 and NADP2, partially because slight variants on previously defined noise abatement departure procedures were introduced. Georgia Tech investigated the similarities and differences between the ICAO-A and ICAO-B procedures currently in AEDT versus the procedures defined in this working paper. ICAO-A and NADP1 procedures were essentially identical, primarily characterized by delaying acceleration/flap retraction segments until the aircraft clears 3000-ft air-field equivalent altitude. ICAO-B and NADP2 procedures were both characterized by completing acceleration/flap retraction segments before the aircraft attains 3000-ft air-field equivalent altitude with one key difference. ICAO-B procedures perform thrust cutback after the acceleration/flap retraction segments are complete, whereas NADP2 procedures perform thrust cutback before initiating acceleration/flap retraction. In his discussions with Delta pilots, Jim Brooks confirmed that the NADP2 procedure is more consistent with the manner the pilots actually fly the procedures.

Task 2: Statistical Analysis of Flight Data

Georgia Institute of Technology

Objective(s)

Literature review and AEDT APM evaluation conducted in Task 1 will identify the key drivers of variations in takeoff weight and takeoff thrust in real-world day-to-day operations, including energy share profiles or hands on pilot approaches to departures to understand the variability in the takeoff procedures that exists in reality. A quantification of the departure of the APM assumptions to real world operations will be conducted for the key drivers identified in Task 1.

Research Approach

A four step approach was developed to quantify the impact of changing departure assumptions within AEDT and include:

- Conduct a sensitivity study of the APM assumptions with different takeoff weights, thrust, and procedures using EDS generated vehicles and also in AEDT
- Compare both results to high fidelity operational data, when available
- Compare environmental results with existing APM fixed assumptions
- Generate surrogate models of weight, thrust, GCD and procedure variations

The first step was to identify a series of Environmental Design Space (EDS) vehicles to serve as the basis of the sensitivity study. EDS is the key aspect to quantifying the environmental impacts and interdependencies of changing the departure modeling assumptions since the GT researchers can model the physics of the problem directly in a controlled simulation environment. Additionally, EDS has the capability to generate the required AEDT Fleet dB coefficients such that the environmental results may be calculated within the AEDT algorithms. The results of which will form the basis of the suggested APM modeling implementation in Task 3 and 4. GT suggested to the FAA project Manager the following engine/airframe models to use within EDS and AEDT for the parametric sensitivity study, in priority order:

- B737-800 with CFM56-7B27 engines, with winglets
- B767-300ER with CF6-80C2B7F engines
- B777-300ER with GE90-115b
- CRJ-900 with CF34-8C5 engines
- B747-400 with PW4056 engines with reduced emissions combustor or A380-800 with GP7270

Each of the EDS models would be compared to high fidelity performance data, when available, to ensure that the EDS model represents the actual aircraft performance within the fleet. As an example of the comparison to real world data, the aerodynamics for the B737-800 for cruise and low speed are depicted in Figure 6. As evident, the EDS model is a reasonable approximation to the actual B737-800 and can serve as the foundation of the sensitivity study.

[2] "Procedure for the Calculation of Airplane Noise in the Vicinity of Airports", SAE-AIR-1845, prepared by SAE Committee A-21, March 1986.
[3] ECAC.CEAC Doc 29, Report on Standard Method of Computing Noise Contours Around Civil Airports, Vol. 2, 3rd ed., Technical Guide, Dec. 2005.
[4] ICAO, 1982. Procedures for Air Navigation Services-aircraft operations: Volume 1, Flight Procedures, Part V — Noise abatement procedures, pages 5-4 to 5-7. Doc 8168-OPS/611, Volume 1, Amendment 2, 1983.

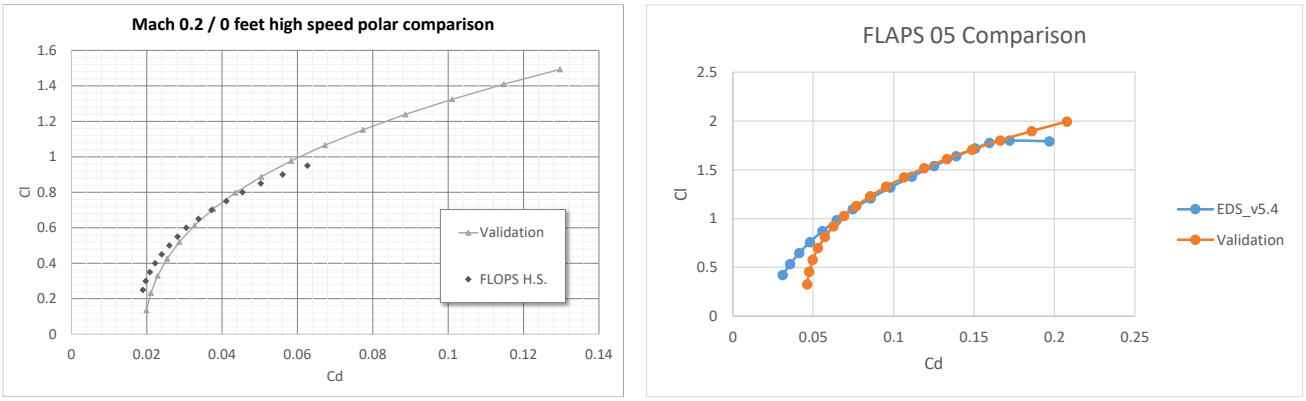

Figure 6. EDS Aerodynamic Comparison to Validation Data

At present, the research team is coordinating with various airlines to obtain actual flight performance data to compare to the EDS representation. From an analytical perspective, a high fidelity performance tool is also being utilized to compare the EDS model results of the sensitivity study. Only preliminary results exist at this time and will be described in future reports. However, the status of the modeling of the NAPD 1 and 2 are described in Task 3.

From an AEDT perspective, GT conducted a simple assessment of the impact of changing the takeoff weight and thrust to gain insight to the environmental impact of the modeling assumptions. The B737-800 model within AEDT was initially investigated with a 5% weight reduction and a15% reduced thrust takeoff (RTT) and to understand the sensitivity to the terminal area performance and noise contour areas. To change the takeoff weight within AEDT, the FLT_ANP_AIRPLANE_PROFILES Table must be modified and a user defined aircraft must be created. The aircraft was flown for a stage length 6 distance for the STANDARD, or Default, and the ICAO A departure procedures and the performance compared. For the 5% TOW reduction, the aircraft could get to a 10,000 ft. (AFE) altitude in a shorter ground track distance for both departure procedures, as depicted in Figure 7. The cutback altitude difference between the two procedures can also be visualized, where the STANDARD procedure cuts back at 1,000 ft. (AFE)and the ICAO A at 1,500 ft. Based on the procedures defined in Figure 4, the flap retraction and the acceleration to a constant speed occur at different altitude resulting in a slightly longer ground track distance for the STANDARD procedure as depicted in the speed and thrust variation in Figure 8 and Figure 9 respectively. The fuel burn is less with the reduced weight, and reduces linearly with flight distance.

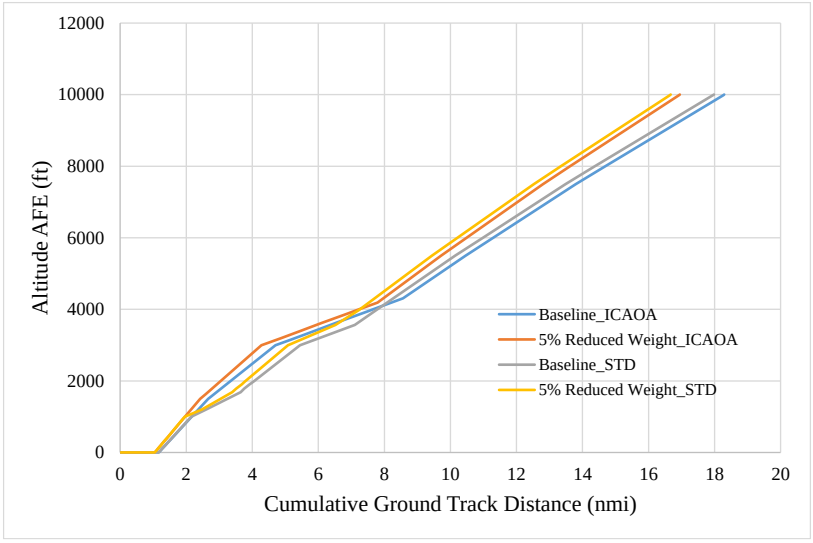

Figure 7. AEDT B737-800 Altitude and Ground Track Variation with -5% TOW Change

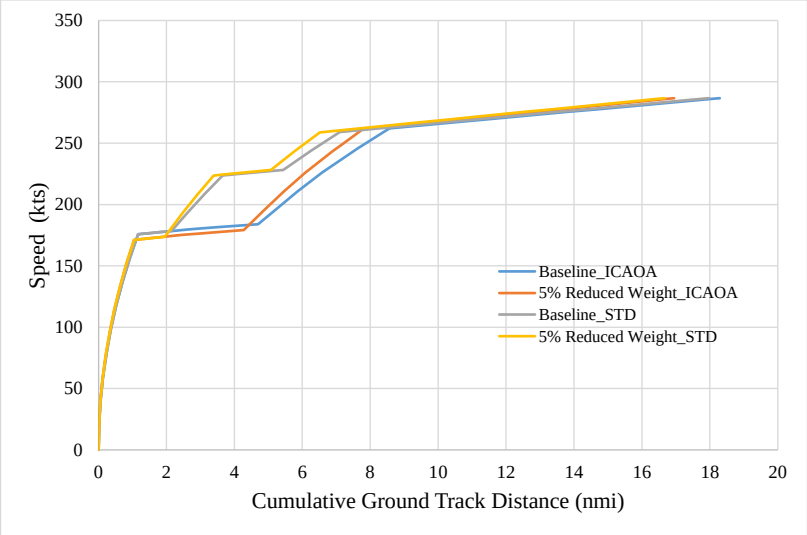

Figure 8. AEDT B737-800 Speed and Ground Track Variation with -5% TOW Change

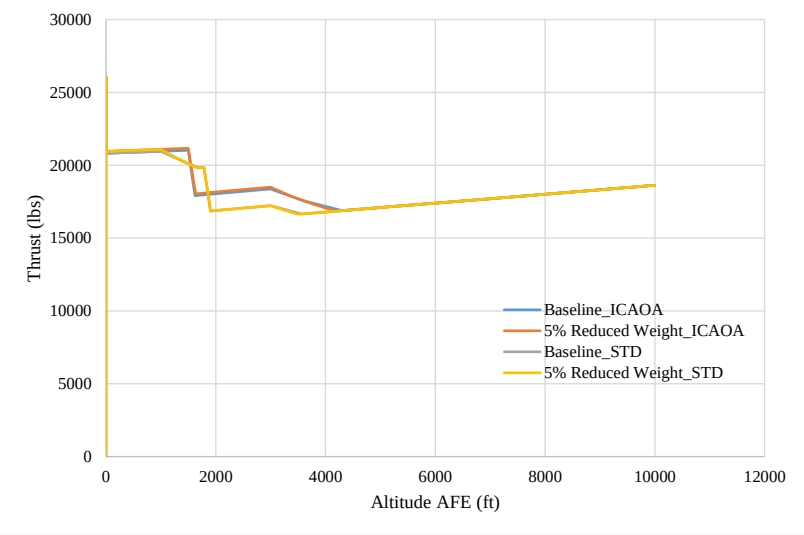

Figure 9. AEDT B737-800 Thrust and Altitude Variation with -5% TOW Change

As expected, the noise contour area is also impacted, as depicted in Figure 10, and for the STANDARD takeoff procedure. The reduced weight contours are highlighted in blue outline. The reduced weight results in a smaller contour length and also total area of approximately a 5% change at different Sound Exposure Levels (SEL) as listed in Table I.

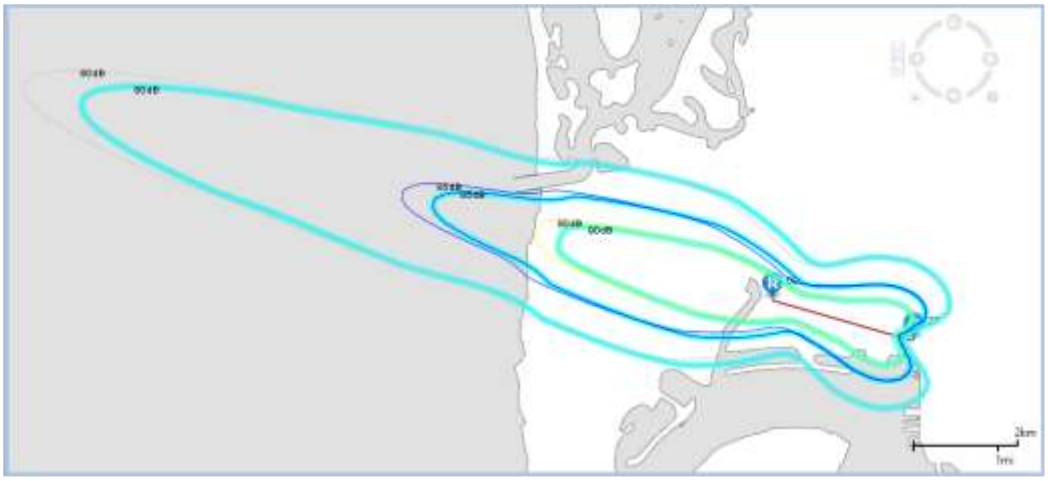

Figure 10. AEDT B737-800 Noise Contour Variation with -5% TOW Change

Table I: SEL Contour Area Changes with 5% TOW Reduction (SEL Metric)

SEL Contour (dB)	Shape Length (m)			Shape Area (nm²)		
	737-800	5% Reduced TOW	Difference	737-800	5% Reduced TOW	Difference
80	41,300	38,787	-6.1%	13.08	12.33	-5.8%
85	23,599	22,303	-5.5%	4.70	4.47	-4.8%
90	16,847	15,951	-5.3%	2.13	2.04	-4.3%

Next, the takeoff thrust impact was investigated. Based on the outcomes of the literature review, a 15% takeoff thrust was assumed. To adjust the takeoff thrust, the ANP coefficients must be modified within the Fleet dB for each of the departure procedure segments. The definition of the existing B737-800 as defined in AEDT is depicted in Figure 11. AEDT calculates jet aircraft corrected net thrust per engine by using a modified version of SAE-AIR-1845 equation:

$$F_n/\delta = E + F^*v + G_A{}^*h + G_B{}^*h^2 + H^*T_C$$

where

F_n/δ Corrected net thrust per engine (lbf);
v Equivalent/calibrated airspeed (kt);
h Pressure altitude (ft) MSL;
T_C Temperature (˚C) at the aircraft; and
E, F, G_A, G_B, H Regression coefficients that depend on power state (max-takeoff or max-climb power) and temperature state (below or above engine breakpoint temperature) (lbf, lbf/kt, lbf/ft, lbf/ft2, lbf/˚C, respectively). Thus, to control the thrust utilized for takeoff, the E coefficient was modified by 15% for both takeoff and climb.

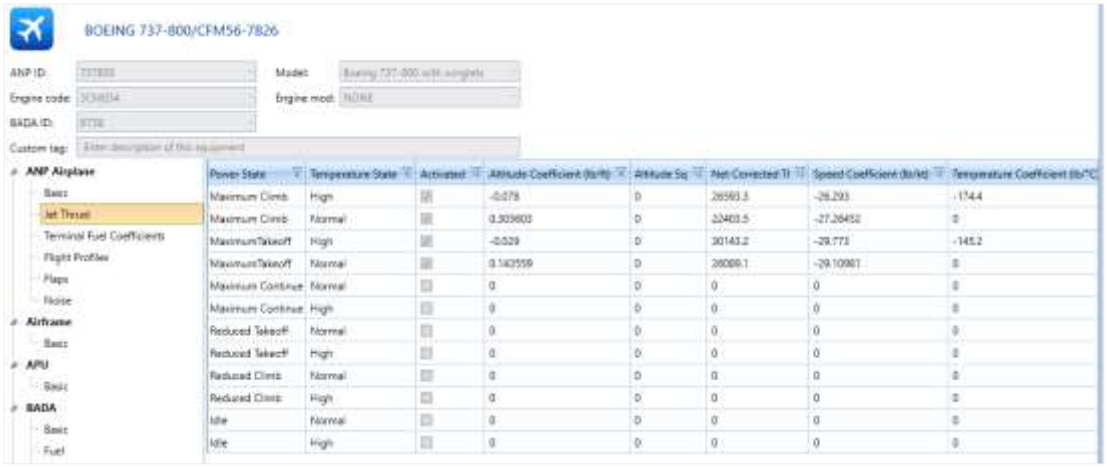

Figure 11. AEDT B737-800 ANP Thrust Coefficients

Only the STANDARD departure procedure was considered for this initial investigation. Similar to the takeoff weight sensitivity, the speed, altitude, and thrust variations were compared based on the maximum takeoff weight for a stage length of 6. For the reduced thrust takeoff, the cumulative ground track distance to reach a 10,000 ft altitude is increased approximately 8 nmi as depicted in Figure 12 and the cutback altitude and the acceleration segment after cut back also requires addition flight time to get to the constant speed climb as shown in Figure 13 and Figure 14, respectively.

From a noise perspective, the reduced thrust takeoff had a much more significant impact on the noise contours as shown in Figure 15. The contour shape and area were significantly reduced except for the 85 dB SEL, which is corresponding to the acceleration stage being delayed in the climb out. Unlike the reduced weight takeoff contours, the change in length and area was not consistent as listed in Table II. The length wasn't changed as much as the width. Thus, the reduced thrust takeoff will lower the lateral propagation.

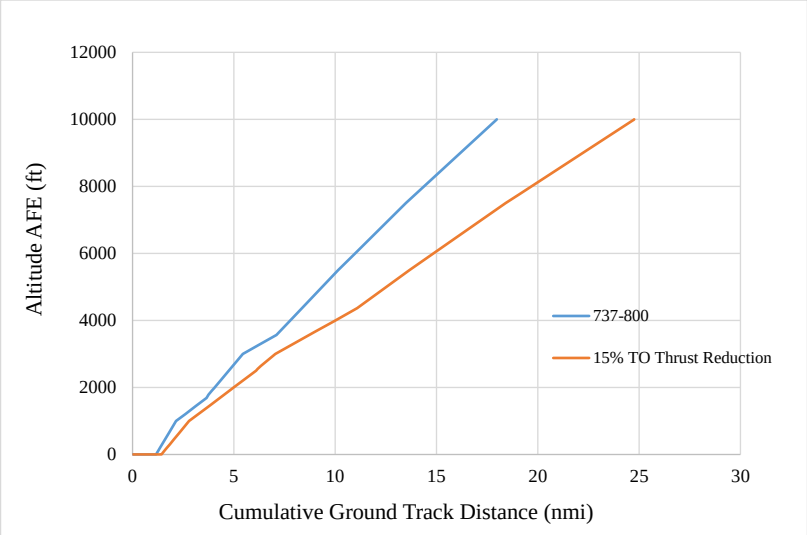

Figure 12. AEDT B737-800 Altitude and Ground Track Variation with 15% Reduced TO Thrust

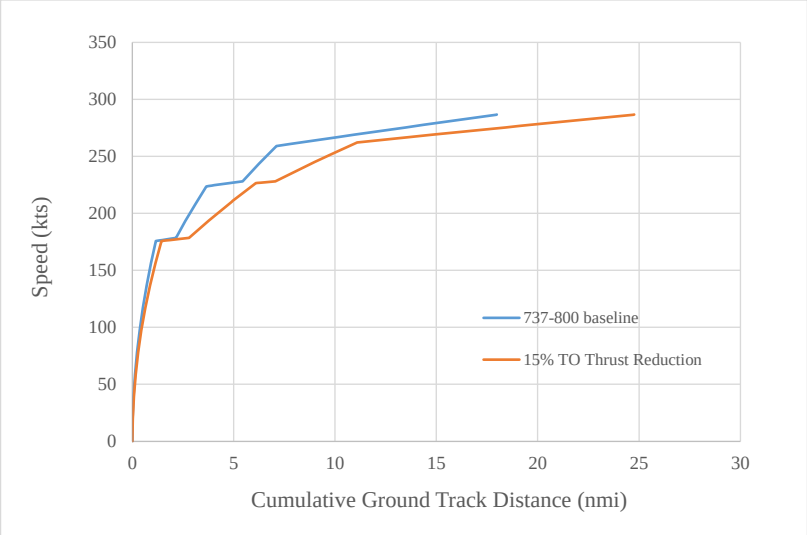

Figure 13. AEDT B737-800 Speed and Ground Track Variation with 15% Reduced TO Thrust

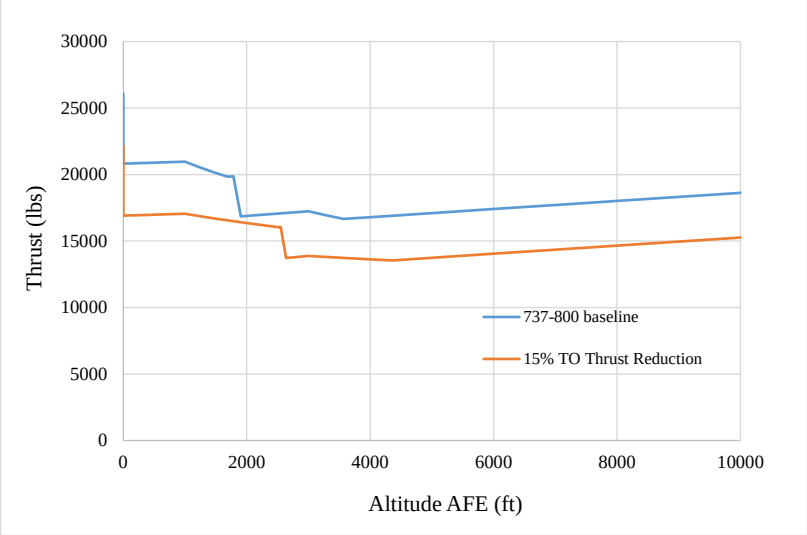

Figure 14. AEDT B737-800 Thrust and Altitude Variation with 15% Reduced TO Thrust

While the notional example procedure shows a 15% reduction in thrust from takeoff all the way up to 10000-ft air field equivalent altitude, these results are only intended as preliminary. In reality, thrust reduction between maximum takeoff thrust and maximum climb thrust are related but not necessarily identical. Based on past experience and prior data analysis, Georgia Tech established the following logic for modeling climb thrust derate relative to takeoff thrust derate:

- If takeoff thrust derate is less than 5%, use maximum climb thrust
- If takeoff derate is between 5% and 15%, derate climb thrust by 10% up to 10000-ft air field equivalent altitude
- If takeoff derate is greater than 15%, derate climb thrust by 20% up to 10000-ft air field equivalent altitude

This logic shall be used in future Georgia Tech modeling of reduced thrust takeoff procedures.

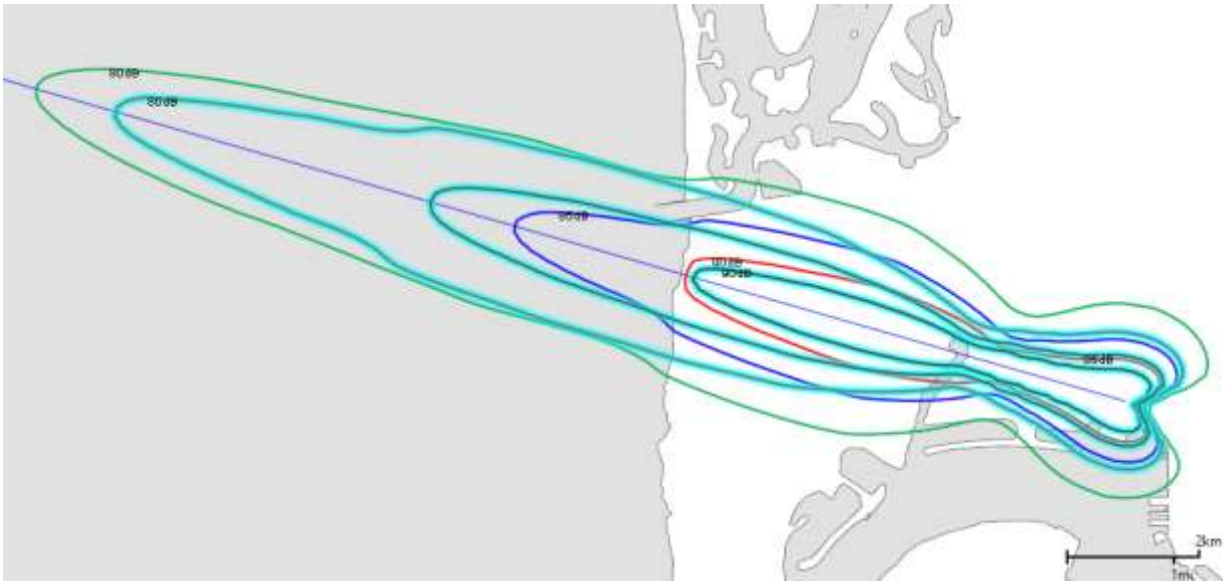

Figure 15. AEDT B737-800 Noise Contour Variation with 15% Reduced TO Thrust

Table II: SEL Contour Area Changes with 15% Reduced TO Thrust

SEL Contour (dB)	Shape Length (m)			Shape Area (nm^2)		
	737-800	5% Reduced TOW	Difference	737-800	5% Reduced TOW	Difference
80	41,301	36,837	-10.8%	13.08	9.23	-29.4%
85	23,599	25,193	6.8%	4.70	3.86	-17.8%
90	16,847	15,769	-6.4%	2.13	1.30	-39.2%

In summary, the initial sensitivity to takeoff weight and thrust has provided valuable insight to the impact of the APM assumptions. Although no definitive conclusions can be drawn, the environmental footprint due to more realistic departure procedures will be significant, especially when coupled together. As the research progresses, the impact to the environmental foot print will be quantified independently and also collectively. However, initial insight from this sensitivity study indicates that thrust will be the larger driver when considering the change in noise area.

From a departure procedure perspective, Georgia Tech (GT) began this task by modeling the Noise Abatement Departure Procedures (NADP) described in CAEP/7-WP/25 by directly changing procedure coefficients in AEDT. The aircraft coefficients and STANDARD procedures for a B737-800 vehicle were extracted from the AEDT Database. No changes were made to weight or thrust assumptions. The primary difference between the STANDARD procedures and the NADP procedures is the thrust cutback altitude. The STANDARD procedure for this vehicle did not cutback thrust from maximum takeoff thrust to maximum climb thrust until the acceleration and flap retraction steps were complete. This procedure specified a cutback altitude of 2040-ft. The NADP procedures feature cutback altitudes as low as 800-ft and no higher than 1500-ft, with cutback thrust always occurring before acceleration/flap retraction steps. For NADP1, the procedures closely align with ICAO-A procedures, with acceleration/flap retraction delayed until the aircraft reaches an altitude of 3000-ft. For NADP2, these acceleration/flap retraction steps begin immediately after flap retraction and the vehicle achieves a clean configuration before reaching an altitude of 3000-ft. NADP2 is similar to ICAO-B procedures, except the latter doesn't cutback thrust until after flap retraction (similar to the STANDARD procedure for this aircraft).

Some preliminary Sound Exposure Level (SEL) contours are shown in Figure 16 for the different noise abatement departure procedures. It should be noted, however, that these procedures only represent estimates from engineering judgment. The

contour comparison is a useful guide to expectations of contour shapes, but the procedures must be dynamically generated to capture impacts of various weight and reduced thrust assumptions. This is primarily a concern for acceleration step, where AEDT specifies climb-rate and a calibrated airspeed where acceleration segments end, each of which varies as thrust or weight is varied. For the contour plots showed in Figure 16 these parameters were only estimated, and an example of these estimates for an accelerated climb step is shown in Figure 17.

Recent modeling efforts have been focused on modifying FLOPS runs in EDS to parametrically generate these parameters for different mission lengths, takeoff weights, and reduced takeoff thrust. Eventually, GT would like to validate these procedures against real FOQA data, but currently this data is unavailable. Instead, GT is validating the FLOPS models against a higher fidelity modeling tool. A subset of mission ranges and departure airport altitudes were chosen to be modeled, as listed in Table III. The “Estimated Weight” column in this table uses departure takeoff weights calculated from ASCENT Project 35 results. It should be noted that all of these weight estimates are higher than the AEDT assumed weight, even when the mission range is shorter than the AEDT representative mission range. SFO and BOS airports were chosen because these airports have altitudes close to sea-level. The stage-length 2 mission was repeated in the opposite direction to see the impact of a higher altitude airport (ATL has an altitude of approximately 1000-ft). DEN airport was also chosen to represent a high altitude airport (DEN has an altitude of approximately 5000-ft). Stage-length 5 and 6 missions are very rare for this vehicle and thus were omitted from this validation study.

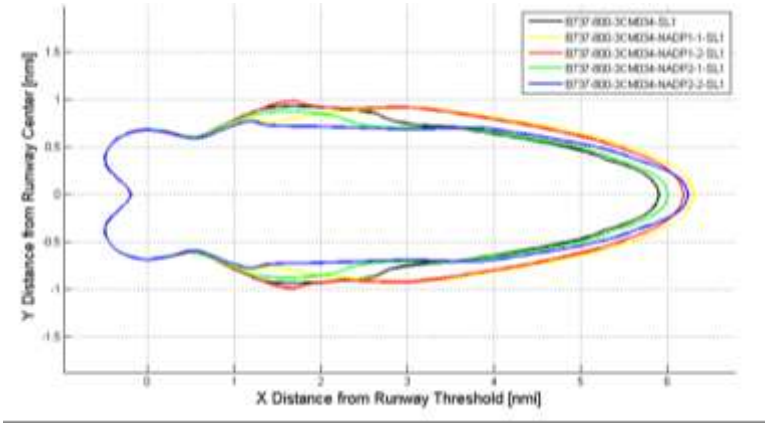

Figure 16. Notional SEL 80dB Contour Comparison for NADP Procedures

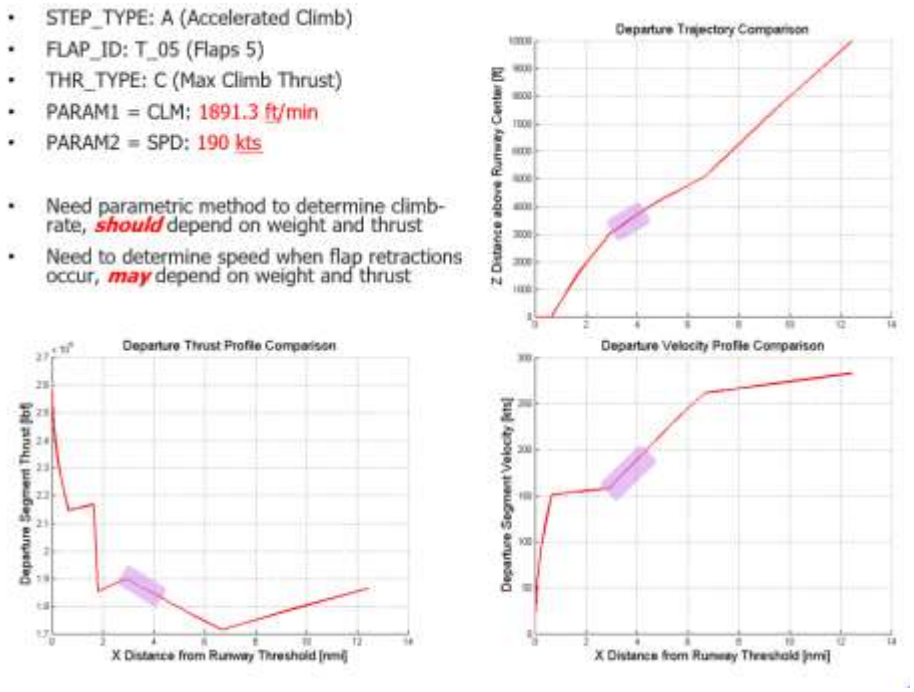

Figure 17. Example of Engineering Estimate for Accelerated Climb Step in AEDT for NADP1 Procedure

Table III: Mission Ranges and Weights to be Modelled for B737-800 Departures

Stage Length	AEDT Representative Mission Range [nm]	AEDT Assumed Weight [lb]	Origin	Destination	Mission Range [nm]	Estimated Weight [lb]
1	350	133300	SFO	SAN	388	141198
2	850	139200	BOS	ATL	822	146539
2	850	139200	ATL	BOS	822	147830
3	1350	145500	DEN	JFK	1413	158522
4	2200	156700	BOS	LAX	2269	168070
5	3200	167600				
6	4200	172300				

After a few iterations comparing FLOPS procedures versus the high-fidelity tool, it was suggested that GT modify FLOPS for the acceleration/flap retraction steps. Previously, GT specified flight path angle which needed to be varied as a function of aircraft weight and thrust, but without much data to determine this relationship. After discussing with Prof. JP Clarke and Jim Brooks, GT instead chose to specify pitch angle (flight path angle plus angle of attack). This approach more closely reflects the manner in which pilots actually fly the procedures, as they typically try to maintain a pitch angle between 10-12 degrees to ensure safe climb rates regardless of aircraft weight. This allows FLOPS to parametrically determine flight path angles and climb rates based on the performance of the aircraft, which makes the method more robust to changing takeoff weight and reduced thrust.

GT changed the method used for modeling reduced thrust. In actual procedures, reduced thrust takeoff is implemented via the Assumed Temperature Method, where the pilot tricks the flight management system into thinking the Outside Ambient Temperature (OAT) is higher than actual OAT. Thus, the engine to operate at lower thrust to protect internal components from excessively high temperatures, as notionally shown in Figure 18. AEDT contains both standard day thrust coefficients to represent the flat-rated curve and high-temperature coefficients for the sloped curve.

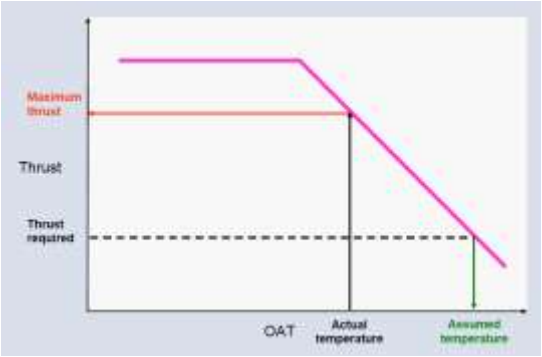

Figure 18. Notional Assumed Temperature Method for Reduced Thrust

FLOPS requires inputting an entire engine deck to calculate thrust levels and fuel flow at different combinations of velocity and altitude. To accomplish the reduced thrust, the engine decks are modified to remove power codes associated with full-rated takeoff thrust. Thrust cutback is accomplished by further removing power codes at cutback altitudes, and thus unique decks are generated for 800-ft, 1000-ft and 1500-ft cutback altitudes, respectively.

Validation efforts for the FLOPS procedures are currently ongoing. Once these procedures are validated, GT will enhance EDS codes to generate these NADP procedures in an automated manner. These procedures will be converted to AEDT procedures, which must also be validated against the high-fidelity tool (and FOQA data if it eventually becomes available). Once these AEDT procedures are validated, SEL contours will be generated with the AAM to quantify the impacts of the increased weight, reduced thrust, and noise abatement departure procedures. GT will look at sensitivities for each of these factors independently as well as the coupled impact of all factors simultaneously.

In summary, initial investigations to the takeoff procedure assumptions have been accomplished and provided initial insights to the environmental impact. GT will continue to investigate various surrogate and/or reduced order modeling techniques to develop mathematical models of takeoff weight and thrust as a function of the key terminal area performance metrics and also the takeoff procedure. For takeoff weight and thrust, GT will provide multiple models that will span the current fleet, which will provide the users different options depending on the data availability. For example, a surrogate model of takeoff weight as a function of great circle distance (GCD) only can be developed for each of the seat classes. Or a model can take much more input parameters including adjustments for each of the aircraft types. For each of the models, associated uncertainty bands will also be analyzed. This research will also quantify the impact to fuel burn, NO_x, and noise at the vehicle and also the fleet level for a TBD fleet scenario.

Task 3: Develop Aircraft State Estimator

Georgia Institute of Technology

Objective(s)

Once GT understands AEDT APM limitations in Task 1 and has a reduced flight dataset resulting from Task 2, work can begin to develop a state estimator for vehicle weight, takeoff thrust, and load factor as a function of ambient conditions and measured profile. Both EDS and AEDT will be tuned using the developed state estimator to predict the state variables. Keeping in mind that simplicity is desired, a methodology will be developed that is capable of tuning AEDT APM aircraft takeoff weights, takeoff thrust, and climb thrust both with and without detailed trajectory data. The methodology will be focused on AEDT APM, however, EDS models will also be tuned to understand how differences in the EDS and AEDT aircraft performance models impact the tuned state estimates.

Research Approach

The challenge of the aircraft state estimator development will be the extension of the focused investigations of a subset of aircraft in Task 2 and how those observations can be extended to the entirety of the aircraft/engine combinations within the AEDT Fleet dB. However, GT has identified that the takeoff weight assumption can be easily adjusted within AEDT based on the results of Project 35 for those 4 aircraft types and also the BAH fuel efficiency metrics investigations, when

available. In instances when aircraft in the AEDT database are not covered by one of these studies, BTS data could be used to approximate takeoff weight assumptions for the remainder of the fleet. It should be noted, a high possibility exists that data may not exist to approximate all aircraft takeoff weights. In this instance, GT will investigate an option of classifying aircraft types and utilizing a broad takeoff weight assumption.

From the thrust perspective, multiple research endeavors have shown that a 15% takeoff thrust reduction is reasonable. However, that assumption should only be applied at takeoff and not at the cutback altitude. A methodology will be developed on how to implement the modification in AEDT based on a subset of the fleet.

The final aspect will be to determine how to implement the modified departure procedure based on an EDS implementation and a comparison to the AEDT procedural definitions. Per the AEDT Technical Manual guidance for the departure procedure defined in Figure 4, it appears the flexibility exists to define any type of procedure, but this must be investigated.

Task 4: Develop APM Enhancement Recommendations

Georgia Institute of Technology

Objective(s)

Each of the prior tasks will culminate into a set of recommendations for enhancements to AEDT in a research report.

Research Approach

Ideally, a simple, straight-forward implementation scheme will be developed that would not rely on Original Equipment Manufacturers (OEMs) to provide new Fleet DB coefficient definitions for BADA3 and BADA4 currently in AEDT2b. As the results of each task are acquired, insight to the most appropriate implementation scheme will evolve and be reviewed with the FAA Project Manager. GT anticipates the following will be generated as a result of this research:

- Report detailing physics and modeling gaps in current AEDT APM algorithms with suggestions for enhancement
- Analysis of flight data and development of statistical correlation between flight data and aircraft state where possible
- Methodology to automatically calibrate aircraft state (thrust, weight) to available data
- Methodology to implement different departure procedures

Milestone(s)

No specific milestones are associated with this project. However, significant progress is being made towards understanding the implications of the APM assumptions for departure.

Major Accomplishments

Significant insight to the impact of the APM assumptions have been obtained through initial sensitivity studies conducted.

SQL scripts written to automate extraction of existing aircraft definitions and modifications to weight and thrust.

Matlab scripts written to automate the departure procedure modeling and visualization of performance.

Identification of sources of data that might provide justification of takeoff weight assumptions with the APM.

Publications

None

Outreach Efforts

Bi-weekly calls with the Project Managers.

Awards

None

Student Involvement

Vu Ngo and Ameya Behere – Graduate Research Assistant, Georgia Institute of Technology

Plans for Next Period

The primary focus for the next period will be Tasks 2 through 4. Task 2 will focus on the implementation of the NAPD procedures within EDS and FLOPS and how that modeling could be extended to the APM. As mentioned previously, validation efforts for the FLOPS NADP procedures are ongoing. Once these procedures are validated, the EDS code will be edited to automatically run these FLOPS NADP procedures and convert them into equivalent AEDT procedures. These procedures will be used in AEDT in conjunction with the acoustics module in order to determine the impacts of weight, thrust, and procedures on SEL noise contours. Currently Georgia Tech is focused on the B737-800, but validation efforts shall be repeated for other vehicles that EDS models. Once this validation is complete, the more detailed sensitivity study of the assumptions will be conducted, which will include one at a time, and also partial derivatives with respect to environmental metrics.

Project 046 Surface Analysis to Support AEDT APM Development

Massachusetts Institute of Technology
MIT Lincoln Laboratory

Project Lead Investigator

Hamsa Balakrishnan
Associate Professor
Aeronautics and Astronautics
Massachusetts Institute of Technology
77 Massachusetts Ave., 33-328
Cambridge, MA 02139
617-253-6101
hamsa@mit.edu

University Participants

MIT

- P.I.(s): Hamsa Balakrishnan
- FAA Award Number: 13-C-AJFE-MIT, Amendment No. 021
- Period of Performance: July 7, 2016 to Aug. 31, 2017
- Task(s):
    1. Assess AEDT aircraft surface performance modeling needs
    2. Develop enhanced aircraft surface performance models
    3. Validate enhanced aircraft surface performance models
    4. Recommend AEDT APM enhancements

Project Funding Level

$75,000 FAA funding and $75,000 matching funds. Source of match is approximately $75,000 all from MIT.

Investigation Team

Prof. Hamsa Balakrishnan, Co-Principal Investigator (MIT)
Dr. Tom Reynolds, Co-Principal Investigator (Lincoln Laboratory, via separate contract)
Yashovardhan Chati (Graduate student)
Sandeep Badrinath (Graduate student)

Project Overview

The taxi phase in the Aviation Environmental Design Tool (AEDT) is currently modeled using default or user-specified taxi times, coupled with engine idle fuel and emissions assumptions from the ICAO Aircraft Engine Emissions Databank. This simplification reduces the accuracy of taxi performance modeling in AEDT. The proposed research aims to enhance the taxi models in AEDT's Aircraft Performance Module (APM) by combining surface surveillance data (from ASDE-X) with statistical models developed using information from Flight Data Recorders.

Task Progress and Plans

Objective(s)

The objective of this research project is to identify and evaluate methods for improving taxi performance modeling in AEDT in order to better reflect actual operations. This objective will be met through the use of surface surveillance (ASDE-X) data, in combination with a comprehensive statistical analysis of Flight Data Recorder (FDR) archives.

Research Approach

Task 1: Assess AEDT aircraft surface performance modeling needs: this includes soliciting input from stakeholders (including FAA AEE sponsors, AEDT developers, users, etc.) and related research (e.g., ACRP studies 02-45 and 02-27) on known gaps and associated needs in current aircraft surface modeling capabilities. In addition, prior research into high fidelity aircraft surface modeling will be assessed and leveraged as appropriate. For example, taxi models resulting in thrust and fuel flow estimates were previously built using Flight Data Recorder (FDR) data. Such aircraft-derived data is the "gold standard" for high fidelity modeling, but its limited availability often results in models with limited applicability.

We conducted a discussion with AEDT developers and users (at the FAA and Volpe) to discuss gaps identified during the literature review and from ACRP studies 02-45 and 02-27. We have also begun familiarizing ourselves with the AEDT APM's current capabilities.

Task 2: Develop enhanced aircraft surface performance models: enhanced aircraft surface performance models will be developed which address needs identified in Task 1. For example, one of the anticipated needs is the development of models which are representative of a wider range of taxi conditions, aircraft types, airports, airlines and weather conditions than current modeling approaches. The research team has access to significant archives of ASDE-X surface surveillance and FDR data covering a wide range of these variables of interest from which improved surface models can be built. For example, ASDE-X data can be used to identify a large range of taxi conditions (e.g., locations, dwell times and speeds between surface events such as engine start, spot, taxiway intersections, runway crossing, departure runway queue, line-up-and-wait, etc.) for a range of major airports, aircraft types, airlines and weather conditions. By correlating to FDR "truth" data, improved thrust and fuel flow models can be developed. This task will also consider the results of prior related studies, such as ACRP 02-45 and 02-27. The research team has good contacts within the stakeholder community to acquire additional FDR data archives if required for this exercise.

We have begun the analysis of ASDE-X data, with an initial focus on CLT airport.

Task 3: Validate enhanced aircraft surface performance models: a subset of the ASDE-X and FDR data archives will be held back from the enhanced model development activity in the previous step so it can be used as independent validation data. For example, fuel burn and thrust profiles based on "new" ASDE-X tracks will be estimated using the enhanced models developed from the previous step and compared to the estimates direct from FDR data. If the differences between the two profiles exceed some appropriate threshold, further refinements to the surface models developed in Task 2 are required (as illustrated by the dashed arrow between steps 3 and 2 in the diagram).

We are in the process of acquiring additional FDR datasets for validation.

Task 4: Recommend AEDT APM enhancements: based on the surface modeling enhancements developed from this process, specific targeted recommendations for AEDT APM improvements for the surface domain will be made.

Awaiting the completion of Tasks 2-3.

Publications

None.

Outreach Efforts

None.

Awards

Yashovardhan Chati. ACRP Graduate Research Award, 2016.

Student Involvement

Graduate students have been involved in all aspects of this research.

Project 048 Analysis to Support the Development of an Engine nvPM Emissions Standard

Massachusetts Institute of Technology

Project Lead Investigator

Steven Barrett
Associate Professor
Department of Aeronautics & Astronautics
Massachusetts Institute of Technology
77 Massachusetts Ave
Building 33-316
Cambridge, MA 02139
617-452-2550
sbarrett@mit.edu

University Participants

Massachusetts Institute of Technology

- P.I.: Prof. Steven Barrett
- Co-PI: Dr. Raymond Speth
- FAA Award Number: 13-C-AJFE-MIT, Amendment No. 027
- Period of Performance: July 8, 2016 to Aug. 31, 2017 (Reporting here with the exception of funding level and cost share only for the period July 8, 2016 to September 30, 2016).
- Tasks:
    - Task 1: Write a detailed scientific background of the APMT-I tools suite
    - Task 2: Map emissions from a short-list of representative engines to all engine/airframe combinations
    - Task 3: Evaluate metrics from the CAEP/WG3/PMTF for evaluating an engine's nvPM performance
    - Task 4: Verify technology response provided by engine manufacturers
    - Task 5: Evaluate proposed fuel sensitivity corrections and ambient conditions corrections
    - Task 6: Evaluate the current nvPM modeling approaches available to CAEP and assess uncertainty contributions

Project Funding Level

$150,000 FAA funding and $150,000 matching funds. Sources of match are approximately $63,000 from MIT, plus 3rd party in-kind contributions of $87,000 from University College London.

Investigation Team (all MIT)

Principal Investigator: Prof. Steven Barrett
Co-Principal Investigator: Dr. Raymond Speth
Co-Investigators: Prof. John Hansman, Dr. Jayant Sabnis, Dr. Brian Yutko
Graduate Students: Akshat Agarwal

Project Overview

This projects aims to provide support to the FAA Office of Environment and Energy (OEE) in developing an emissions standard for non-volatile Particulate Matter (nvPM). The analyses will be further used to inform the International Civil Aviation Organization's Committee on Aviation Environmental Protection (ICAO-CAEP) in developing a global standard for nvPM emissions. The analyses will cover both US NAS-wide and global bases covering the costs and benefits from an economic and environmental (air quality, climate and noise) perspective. The main goals for this project include:

- Writing a scientific overview of the Aviation environmental Portfolio Management Tool's Impact (APMT-I) suite of analysis tools.
- Mapping emissions from a short-list of representative engines to a broader list of engine/airframe combinations.
- Evaluating metrics developed by CAEP Working Group 3 PM Task Force (CAEP/WG3/PMTF) important for evaluating an engine/airframe's nvPM emissions performance.
- Using the initial metrics and stringency options, independently verify the technology response provided by engine manufacturers.
- Evaluating proposed fuel sensitivity corrections and ambient conditions corrections.
- Evaluating the current nvPM modeling approaches available to CAEP, as well as investigating the potential of using number emissions to estimate health impacts. The tools will be further developed to incorporate a number of uncertainties relevant to the nvPM modeling approach.

Task 1 – Write a detailed scientific background of the APMT-I tools suite

Massachusetts Institute of Technology

Objective(s)

This task involves writing a detailed overview of the scientific background and uncertainty estimations used in the noise, air quality and climate models within the APMT-I tools suite.

Research Approach

The APMT-I tools suite consists of models to analyze the noise, air quality and climate impacts of aviation emissions. Each model moves from estimated emissions or noise sources to monetized impacts in order to compare and contrast the various costs and environmental benefits of a particular policy. The papers are written to provide a detailed resource for understanding the scientific background, modeling assumptions and uncertainty analyses used within the APMT-I models. The papers will be written in 4 sections covering each of the APMT-I models (air quality, climate and noise) and an additional section on the advantages of cost-benefit analyses versus the historic use of cost-effectiveness.

Milestone(s)

Draft individual sections for the air quality, climate and noise models have been completed and are being refined in collaboration with FAA project managers. Subsequent aims include writing an overview of cost-benefit analyses and its benefits in comparison with cost-effectiveness. Collating the four sections into a single document is the final step in the process.

Major Accomplishments

None.

Publications

None.

Outreach Efforts

None.

Awards

None.

Student Involvement

Graduate student Akshat Agarwal is primarily responsible for writing the reviews.

Plans for Next Period

Finalize the first full version of the document by January 31, 2017.

Task 2 – Map emissions from a short-list of representative engines to all engine/airframe combinations

Massachusetts Institute of Technology

Objective(s)

The objective of this task is to develop mappings between a short-list of representative engines that were analyzed during the measurement campaign and engine/airframe combinations currently in operation.

Research Approach

A major improvement from historic smoke/PM standards developed by CAEP is the use of a new measurement method to more precisely estimate nvPM emissions from aircraft engines. The measurement campaign will focus on a subset of all available aircraft engines. In order to estimate the emissions from other aircraft engines, a mapping between measured and available engines is required. The mapping will involve analyzing the available data provided by OEMs and map between engines of similar models and configurations as well as mapping to engine/airframe combinations for modeling purposes. Engine/airframe combinations will be provided using a 2012 base using a "growth and replacement" database.

Milestone(s)

Awaiting completion of data use agreements to gain access to the nvPM measurements.

Major Accomplishments

None.

Publications

None.

Outreach Efforts

None.

Awards

None.

Student Involvement

Graduate student Akshat Agarwal is primarily responsible for conducting the mappings.

Plans for Next Period

Develop the mappings upon acceptance of data use agreement.

Task 3 – Evaluate metrics from the CAEP/WG3/PMTG for evaluating an engine's nvPM performance

Massachusetts Institute of Technology

Objective(s)

The third task's objective involves independently evaluating the metrics developed by the PM Task Force of CAEP Working Group 3 (CAEP/WG3/PMTF). The aim is to identify the key issues relevant to describing nvPM emissions performance.

Research Approach
Following on from task 2, metrics must be developed in order to describe the performance of aircraft engines based on nvPM emissions. The metrics will initially be developed by the CAEP/WG3/PMTG and we will suggest alternatives to the FAA and also to CAEP/WG3 in collaboration with FAA management. Alternative metrics will be developed and tested using a data analysis process ensuring they include aircraft and engine properties such as maximum takeoff weight, payload-range capability, cabin floor area, passenger capacity, maximum takeoff thrust, thrust-specific fuel consumption, and nvPM mass and number emissions over the LTO cycle. The metrics will also be considered to satisfy evaluation criteria akin to those used for developing the CO_2 standard. These metrics allowed for differentiation among technology generations to reflect improvements in fundamental design elements and the capabilities of various aircraft/engine architectures.

The metrics are crucial as they may impact the potential of prospective policy and stringency options. Thus, we will also investigate the influence of the metrics on these options. In addition, we will consider the effect of interdependencies with other emissions similar to the tradeoff with efficiency and reducing NO_x emissions. Finally, the role of uncertainties in understanding these interdependencies and how uncertainty is propagated through technology and fleet projections under different metrics and stringencies will also be investigated.

Milestone(s)
None.

Major Accomplishments
None.

Publications
None.

Outreach Efforts
None.

Awards
None.

Student Involvement
Graduate student Akshat Agarwal is primarily responsible for conducting the mappings.

Plans for Next Period
We expect to complete this task by April 30, 2017.

Task 4 – Verify technology response provided by engine manufacturers
Massachusetts Institute of Technology

Objective(s)
The objective of this task is to independently verify the technology response provided by the engine manufacturers and assist the FAA in developing consensus.

Research Approach
For the initial metrics and stringencies developed as part of Task 3, we will independently verify the proposed technology responses suggested by the engine manufacturers.

Milestone(s)
None.

Major Accomplishments
None.

Publications
None.

Outreach Efforts
None.

Awards
None.

Student Involvement
Akshat Agarwal is primarily responsible for conducting the mappings.

Plans for Next Period
We aim to complete this task by May 31, 2017.

Task 5 – Evaluate proposed fuel sensitivity corrections and ambient conditions corrections
Massachusetts Institute of Technology

Objective(s)
The fifth task for this project involves conducting an independent evaluation of the proposed fuel sensitivity corrections and ambient conditions corrections.

Research Approach
nvPM emissions tests are conducted using Jet A fuel, which can vary in its molecular content. We will evaluate the sensitivity of the nvPM emissions to various fuel content factors such as the aromatic or naphthalene content, validating the proposed corrections as well. The emissions tests have also been conducted at sea-level static conditions, however this can vary between tests conducted on different days and at multiple locations. We will evaluate the sensitivity to ambient conditions, validating the proposed corrections as well.

Milestone(s)
None.

Major Accomplishments
None.

Publications
None.

Outreach Efforts
None.

Awards
None.

Student Involvement
Graduate student Akshat Agarwal is primarily responsible for conducting the analyses.

Plans for Next Period
We expect to complete this task before June 30, 2017.

Task 6 – Evaluate the current nvPM modeling approaches available to CAEP and assess uncertainty contributions
Massachusetts Institute of Technology

Objective(s)
The objectives for this task involve assessing the modeling capabilities available to CAEP for estimating the environmental impacts of aviation (air quality, climate and noise) and their potential for incorporating additional measurements available from the new nvPM measurement system. In addition, we aim to include additional uncertainties from the new measurement system that have previously not been included.

Research Approach
In the final task, we not only aim to quantify the environmental impact of an nvPM emissions standard, but also attempt to quantify the various uncertainty contributions due to the new measurement methods. The nvPM emissions tests are conducted at ground level because of their ease in comparison to high-speed, cruise-altitude measurements. However, in order to evaluate the effects of cruise-altitude emissions on other atmospheric processes, e.g. contrail formation, these ground level test data must be mapped to cruise conditions. This has been addressed in historic models such as the FOX model (Stettler et al. 2013a) for nvPM emissions, who used a correlation developed by Dopelheuer and Lecht (1998). In this task, we will evaluate the applicability of these models for the new method of measuring nvPM emissions, quantifying the uncertainty of the measurements.

The next part of this task involves ensuring the advanced nvPM measurement capabilities can be used to model the environmental impacts of an nvPM emissions standard. The new nvPM measurement system allows for the estimation of number emissions. These are important for estimating the health impacts of nvPM exposure and will be incorporated in addition to the mass-based exposure response functions that are currently used. We will also take into account the uncertainties associated with the differential toxicity between the various types of PM species. Finally, we will also incorporate the uncertainties in the climate model due to the direct black carbon warming impact and the warming due to contrails.

These tasks will be done in collaboration with the team at the Pennsylvania State University led by Prof. Randy Vander Wal.

Milestone(s)
None.

Major Accomplishments
None.

Publications
None.

Outreach Efforts
None.

Awards
None.

Student Involvement

Graduate student Akshat Agarwal is primarily responsible for conducting the analyses.

Plans for Next Period

We aim to complete this task by August 31, 2017.

Publications Index

Project 001

Twenty-three graduate students and one undergraduate student were involved with this project.

Publications

- de Carvalho Macedo, I., Andre M. Nassar, Annette L. Cowie, Joaquim E.A. Seabra, Luisa Marelli, Martina Otto, Michael Q. Wang, and Wallace E. Tyner. *Greenhouse Gas Emissions from Bioenergy (chapter 17)*, in *Bioenergy and Sustainability: bridging the gaps*, G.M. Souza, et al., Editors. 2015, Scientific Committee on Problems of the Environment (SCOPE): Paris. p. 582-616.
- Martinkus, N. Rijkhoff, S.A.M., Hoard, S.A., Shi, W., Smith, P., Gaffney, M., & Wolcott, M. (submitted, R&R). Biorefinery Site Selection Using a Stepwise Biogeophysical and Social Analysis Approach. *Biomass and Bioenergy.*
- Rijkhoff, S.A.M., Hoard, S., Gaffney, M., Smith, P. (submitted). Communities Ready for Takeoff: Integrating Social Assets for Biofuel Site-selection Modeling. *Politics and Life Sciences*.
- Smith, P.M., Gaffney, M.J., Shi, W., Hoard, S., Ibarrola Armendariz, I., Mueller, D.W., 2017. Drivers and Barriers to the Adoption and Diffusion of Sustainable Jet Fuel (SFJ) in the U.S. Pacific Northwest. *Journal of Air Transport Management, 58*, 113-124.
- Suresh, p., Malina, R., Staples, M.D., Blazy, D., Pearlson, M.N., Barrett, S.R.H., "Lifecycle greenhouse gas emissions and costs of production of diesel and jet fuel from municipal solid waste," (*in preparation)*
- Taheripour, F., Cui, H., & Tyner, W. E. (2016). An Exploration of Agricultural Land use Change at the Intensive and Extensive Margins: Implications for Biofuels Induced Land Use Change. In Z. Qin, U. Mishra, & A. Hastings (Eds.), *Bioenergy and Land Use Change*: American Geophysical Union (Wiley)
- Zhao, Xin, Guolin Yao, and Wallace E. Tyner. "Quantifying breakeven price distributions in stochastic techno-economic analysis." *Applied Energy* 183 (2016) 318-326.
- Zhao, Xin, Tristin R. Brown, and Wallace E. Tyner. "Stochastic techno-economic evaluation of cellulosic biofuel pathways." *Bioresource Technology* 198 (2015), pp.755-763.

Reports

- P. Suresh, "Environmental and economic assessment of transportation fuels from municipal solid waste," Master of Science thesis, Department of Aeronautics and Astronautics, Massachusetts Institute of Technology, 2016. Available online: http://lae.mit.edu/uploads/LAE_report_series/2016/LAE-2016-002-T.pdf

Presentations

- English, Burton C., Markel, Evan, Rahman, Umama, and Chad Hellwinckel, 2016. Cover Crop Potential as a Feedstock for Aviation Fuel, Webinar Dec. 6, 2016
- English, Burton C., Yu, Edward, Lambert, Dayton, and James Larson, 2016. Determination of the Environmental Impact of Growing Feedstock for Aviation Fuel, Webinar Dec. 12 2016.
- Geleynse, Scott, "Evaluation of Alcohol-to-Jet (ATJ) Conversion Technology for Renewable Jet Fuel," 2016 Annual Meeting for the American Institute of Chemical Engineers in San Francisco. November 16, 2016.
- Geleynse, Scott, "Integration of Renewable Jet Fuel Production with the Pulp Industry through Alcohol Conversion," 2016 Annual Meeting for the American Institute of Chemical Engineers in San Francisco. November 17, 2016.

- Kaiphanliam, Kitana, "Techno-Economic Modeling of Lignin to Vanillic Acid Production," 2016 Annual Meeting for the American Institute of Chemical Engineers in San Francisco. November 17, 2016.
- Martinkus, N., Rijkhoff, S., **Hoard, S.,** Shi, W., Smith, P., M. Gaffney. *A Stepwise Biogeophysical and Social Analysis to Approach Site Selection of Biorefineries,* Northwest Wood Based Biofuels Coproducts Conference, May, Seattle, WA.
- Mueller, D., **Hoard, S.,** Smith, P., Sanders, C., M. Gaffney. *Stakeholder Perceptions of Aviation Biofuels in the PNW,* Northwest Wood Based Biofuels Coproducts Conference, May, Seattle, WA.
- Smith, P., Gaffney, M., Shi, W., **Hoard, S.,** Ibarrola Armendariz, I., D.M. Mueller. *Aviation Fuel Supply Chain Stakeholder Perceptions in the PNW,* Northwest Wood Based Biofuels Coproducts Conference, May, Seattle, WA.
- Subramaniam, Senthil, "Pulp Mill Process Integration and Repurposing for Bio-catalytic Alcohol to Jet Fuel Production" 252nd American Chemical Society, August 20-25, 2016, Philadelphia.
- Tanzil, Abid Houssain, Garcia-Perez, Manuel, Zhang, Xiao, and Michael Wolcott, "Alternative Jet Fuel Production in Integrated Biorefineries Using Existing Dry Corn Mill: Cost Reduction Opportunities."
- Tyner, Wallace, "Stochastic TEA for Aviation Biofuels," DOE Workshop on Aviation Biofuels, Macon, GA.
- Tyner, Wallace, "Aviation Biofuels," NAS Committee.

Project 002

No publications or students to report.

Project 003

No publications or students to report.

Project 004(A)

No publication or student to report.

Project 004(B)

Three graduate students involved.

Publications

- "Improved Method for Estimating Noise Level Reduction of Residential Houses", by R. P. Dougherty, T.L. Robinson, and M. Kurosaka, INTER-NOISE and NOISE-CON Congress and Conference Proceedings, InterNoise15, San Francisco, CA, pp. 2063-2074.

Presentations

- "Research + Industry" Symposium by William E Boeing Department of Aeronautics and Astronautics, Mary Gates Hall, UW, November 21, 2014.

Project 005

Four graduate students involved.

Presentation

- Presentation by Graduate Research Assistant Yiming Wang at Noise Con 2016 at Providence RI.

Project 006

Four graduate students involved.

Publications

- Li, Y.; Brentner, K.S.; Wachspress, D.A.; Horn, J.F.; Saetti, U.; and Sharma, K., "Tools for Development and Analysis of Rotorcraft Noise Abatement," proceedings of AHS "Sustainability 2015" conference, Montreal, Quebec, Canada, Sept 22-24, 2015, 10 pages.

Project 007

Two graduate students involved.

Publications

- J. Palmer and V. Sparrow, "Measured N-wave sonic boom events and sensitivity in sonic boom metrics," in *Recent Developments in Nonlinear Acoustics*, AIP Conf. Proc. **1685** 090012 (AIP, 2015), doi: 10.1063/1.4934478. (This conference publication describes the work performed in 2015 on Project 7 Task 1.)

Project 008

No publications or students to report.

Project 010

Publications

- Lukaczyk, T. W., Wendorff, A. D., Colonno, M., Botero, E., Economon, T. D., Alonso, J. J., Orra, T. H., and Ilario, C., "SUAVE: An Open-Source Environment for Multi-Fidelity Conceptual Vehicle Design," 16th AIAA/ISSMO Multidisciplinary Analysis and Optimization Conference, doi:10.2514/6.2015-3087, June, 2015.

Project 011(A)

Four graduate students involved.

Presentations

- Presentations of Results on Tools Teleconference in March and August.
- Prepared detailed comparisons of every airport in GATBA analysis in Powerpoint file, available upon request.

Project 011(B)

Five graduate students involved.

Project 013

No publications or students to report.

Project 014

Four graduate students involved.

Reports

- Guidance on Connecting CO2 Stringency Options (CAEP 10 IPXX Connecting SOs)
- COST-BENEFIT ANALYSIS… (CAEPx_SGx_IPxx_Cost-Benefit Analysis of CAEP10 CO2 Stringency Options)
- CO2 main analysis: Cost… (CAEPSG.201x.WPx.en_FESG-MDG)
- INVESTIGATION OF PRICE… (IP0x_MDG-FESG-STG-0x)
- POST-PROCESS IMPLEMENTATION OF PRICE… (IP0x_MDG-FESG-STG)
- CO2 MAIN ANALYSIS… (CAEPSG.201x.WP.x.3.en_MDG-FESG)
- CO2MAIN ANALYSIS: FUEL PRICE… (IP0x_MDG-FESG-STG-0x)
- CO2MAIN ANALYSIS: FUEL PRICE… (WP0x_MDG-FESG-STG-0x)
- Technology review… (CAEPx_WGx_CO2_WP0x)
- CO2 MAIN ANALYSIS: FRAMEWORK… (CAEPx_WGx_CO2-x_IP0x)
- CO2 MAIN ANALYSIS: FRAMEWORK… (presentation)

Presentation

- Participation at ICAO CAEP meeting in Montreal Canada, February 2016
- Participation at ICAO CAEP Steering Group 10 in Montreal Canada, July 2015
- Participation in ICAO CAEP MDG/FESG Meetings
    - Savannah, Georgia (January 2015)
    - Cologne, Germany (April 2015)
- Participation in ICAO CAEP WG3 Meetings
    - Belfast, United Kingdom
    - Washington D.C., U.S.A.

Project 015

One graduate student involved.

Publications

- Folse, S., Tran, H., Jensen, L., & Hansman, R. J. (2016). Cruise Altitude and Speed Optimization Implemented in a Pilot Decision Support Tool. In 16th AIAA Aviation Technology, Integration, and Operations Conference (p. 4211).
- Jensen, L., Tran, H., & Hansman, J. R. (2015). Cruise Fuel Reduction Potential from Altitude and Speed Optimization in Global Airline Operations. In Eleventh USA/Europe Air Traffic Management Research and Development Seminar (ATM2015), Lisbon, Portugal.
- Jensen, L., Hansman, R. J., Venuti, J., & Reynolds, T. (2014). Commercial airline altitude optimization strategies for reduced cruise fuel consumption. In 14th AIAA Aviation Technology, Integration, and Operations Conference (p. 3006).
- Jensen, L., Hansman, R. J., Venuti, J. C., & Reynolds, T. (2013). Commercial airline speed optimization strategies for reduced cruise fuel consumption. In 2013 Aviation Technology, Integration, and Operations Conference (p. 4289).

Project 016

Two graduate students involved.

Publications

- P. McFarlane and H. Balakrishnan. "Optimal Control of Airport Pushbacks in the Presence of Uncertainties," American Control Conference, July 2016.

Project 017

Publications

- Basner M, McGuire S, and Witte M. Pilot sleep study near Philadelphia International Airport: ASCENT Project 17 Report, 2016.
- McGuire S, Witte M, and Basner M. Evaluation and refinement of a methodology for examining the effects of aircraft noise on sleep in communities in the US. Internoise, Hamburg, Germany, 2016.

Project 018

Three graduate students involved.

Publications

- Kim CS, Tripodis Y, Levy JI. Magnitude and spatial patterns of ultrafine particulate matter associated with aircraft arrivals near Boston Logan Airport. Presented at the International Society for Exposure Science Annual Meeting, October 2016.
- Penn SL, Arunachalam S, Woody M, Heiger-Bernays W, Tripodis Y, Levy JI. Estimating state-specific contributions to PM2.5- and O3-related health burden from residential combustion and electricity generating unit emissions in the United States. Environ Health Perspect, in press.
- Penn SL, Boone ST, Harvey BC, Heiger-Bernays W, Tripodis Y, Arunachalam S, Levy JI. Modeling variability in air pollution-related health damages from individual airport emissions. Under review.
- Underhill LJ, Penn SL, Boone S, Arunachalam S, Woo M, Levy JI. A comparative analysis of health damage functions across pollutants, source sectors, and geographic locations. Presented at the International Society for Exposure Science Annual Meeting, October 2016.

Project 019

One graduate student involved.

Publications

- Huang, J., L.P. Vennam, F.S. Binkowski, B. Murphy and S. Arunachalam (2016). Impacts on Ambient Particulate Matter by Changing Particle Size Distribution from Emissions Using the Community Air Quality Model (CMAQ): A Case Study of Commercial Aircraft emissions from Landing and Take-off, CMAS, 2016, Chapel Hill, NC.
- Moniruzzaman, C. G., Bowden, J., Arunachalam, 2016. Effects of aerosol feedback on aircraft-attributable surface O3 and PM2. 5 concentrations using the two-way coupled WRF-CMAQ modeling system. Presentation at the 15th Annual CMAS Conference, October 24-26, 2016 Chapel Hill, NC, available online at: https://www.cmascenter.org/conference/2016/slides/monir_effects_aerosol_2016.pdf.

Project 020

One graduate student involved.

Publications

- Brenner, M.; Yutko, B.; Wolfe, P.; Dedoussi. I. US cost-benefit analysis of ICAO CO_2 standard stringency options. ICAO CAEP Information paper to inform CO_2 standard work. 12/14/2015.

Project 021

Three graduate students involved.

Publications

- Brasseur, et al. (2016). Impact of Aviation on Climate: FAA's Aviation Climate Change Research Initiative (ACCRI) Phase II. BAMS. 2016.

Reports

- Brenner, M., Yutko, B., Wolfe, P., Dedoussi. I., et al. (2015): US cost-benefit analysis of ICAO CO_2 standard stringency options. ICAO CAEP Information paper.
- Wolfe, P., Barrett, S. R. H., Wong, L. M. K., Jacob, S. D. (2016). Requirements Document for Future Iterations of the Aviation Environmental Portfolio Management Tool – Impacts Climate Model, Laboratory of Aviation and the Environment

Presentations

- AGU Conference: Aviation Panel Attendance (Fall 2015)
- Office of Management and Budget Briefing (Winter 2015/2016)
- ICAO CAEP Meeting: The climate code methodology and current valuation techniques were presented as part of a review of cost-benefit tools (Spring 2016)

Project 022

Two graduate students involved.

Publications

- Cameron, M. A., M. Z. Jacobson, S. R. H. Barrett, H. Bian, C. C. Chen, S. D. Eastham, A. Gettelman, A. Khodayari, Q. Liang, D. Phoenix, H. B. Selkirk, N. Unger, D. J. Wuebbles, and X. Yue, 2016: Inter-comparative study of effects of aircraft on surface air quality. J. Geophys. Res., submitted.
- Gettelman, A., C.-C. Chen, M. Z. Jacobson, M. A. Cameron, D. J. Wuebbles, and A. Khodayari, 2016: Coupled chemistry-climate effects from 2050 projected aviation emissions. Atmos. Chem. Phys., submitted.
- Khodayari, A., D. Phoenix, and D. J. Wuebbles, 2016: Sensitivity of NOx emissions from lightning on the production of aviation-induced ozone. J. Geophys. Res., being revised.
- Zhang and Wuebbles, Evaluation of FAA Climate Tools: APMT. Report for the FAA, June 2016.

Presentations

- Tools/Analysis Coordination Meeting – November 22, 2016 (Presentation)

Project 023

Presentations

- Briefed the Administrator and the Management Advisory Committee.
- Briefed ATA Technical Pilots Working Groups
- NPR Appearance to Discuss Modeling Efforts in Boston

Project 024

One graduate student involved.

Publications

- Abrahamson, J. P., Zelina, J., Andac, G., and Vander Wal, R. L., Aviation black carbon mass predictive model for alternative and traditional fuels at ground and cruise. FAA Hartman paper (Best paper of the year award). 2016. Available at: https://ascent.aero/competition/ and https://ascent.aero/wp-content/uploads/sites/192/2015/12/Hartman_CH_7-20-16JPA.pdf
- Abrahamson, J. P., Zelina, J., Andac, M. G., & Vander Wal, R. L. (2016). Predictive Model Development for Aviation Black Carbon Mass Emissions from Alternative and Conventional Fuels at Ground and Cruise. Environmental Science & Technology, (submitted).

Presentations

- Abrahamson, J. P., and Vander Wal, R. L., nvPM Emissions Database Compilation, Analysis and Predictive Assessment. Project 24B. FAA ASCENT 5th Advisory Board Meeting. FAA Center of Excellence for Alternative Jet Fuels & Environment (FAA COE AJFE). Alexandria, VA April 26th-27thth, 2016.
- Vander Wal, R. L., Abrahamson, J. P., PM Database Compilation, Analysis and Predictive Assessments. Project 24B Report. 5th Advisory Board Meeting. FAA Center of Excellence for Alternative Jet Fuels & Environment (FAA COE AJFE). Alexandria, VA April 26th-27thth, 2016.
- Abrahamson, J. P., Vander Wal, R. L., (2016). Gas turbine nvPM formation and oxidation semi-empirical model for commercial aviation. Paper # 138IC-0025. Topic: Internal Combustion and Gas Turbine Engines. 2016 Spring Technical Meeting, Eastern States Section of the Combustion Institute, Princeton University, Princeton, NJ March 13-16th, 2016.
- Abrahamson, J. P., and Vander Wal, R. L., Retooling Predictive Relations for non-volatile PM by Comparison to Measurements. Session: Quantifying Aviation Impacts on Air Quality and Climate. The annual American Geophysical Union (AGU) Annual Fall Meeting, Dec. 14th – 18th, 2015. San Francisco, CA.
- Abrahamson, J. P., and Vander Wal, R. L., nvPM Emissions Database Compilation, Analysis and Predictive Assessment. Project 25B. FAA ASCENT Contractor's Meeting. Seattle WA, Oct. 13-15th, 2015.
- Abrahamson, J. P., Vander Wal, R. L., Update on nvPM predictive modeling from conventional and alternative jet fuels. WEBEX seminar hosted by the FAA/VOLPE Int.'l Working Group on Cruise BC Emission and Prediction/Estimation. Sept. 21st, 2016.
- Abrahamson, J. P., and Vander Wal, R. L., nvPM Emissions Database Compilation, Analysis and Predictive Assessment. Project 25B. FAA External Tools Meeting, Seattle WA, Oct. 20th, 2015.
- Vander Wal, R. L. Abrahamson, J. P., ASCENT Project No. 24B, Emissions data analysis for CLEEN, ACCESS and other tests. FAA Center of excellence for alternative jet fuels and environment. Contractor's workshop. Alexandria, VA. Sept. 27th – 28th, 2016.
- Vander Wal, R. L., Abrahamson, J. P., Jet Engine nvPM Emissions: Status of Predictive Relations. Session 10: Fuel Composition Effects Upon Emissions. Aviation Emissions Characterization Roadmap. 14th Annual Meeting, National Academy of Sciences, Washington, D.C. May 24th – 26th, 2016.

Project 025

Publications

- D. F. Davidson, J. Shao T. Parise, R. K. Hanson, "Shock Tube Measurements of Jet and Rocket Fuel Ignition Delay Times," AIAA SciTech Meeting Grapevine TX, Jan. 2017, in press.
- D. F. Davidson, A. Tugestke, Y. Zhu, S. Wang, R. K. Hanson, "Species Time-History Measurements during Jet Fuel Pyrolysis," 30th International Symposium on Shock Waves, Tel Aviv, Israel, November 2016, in press.
- D. F. Davidson, Y. Zhu, J. Shao, R. K. Hanson, "Ignition Delay Time Correlations for Distillate Fuels," Fuel 187 26–32 (2017).
- D. F. Davidson, Y. Zhu, S. Wang, T. Parise, R. Sur, R. K. Hanson, "Shock Tube Measurements of Jet and Rocket Fuels," AIAA Sci. & Tech. Forum, San Diego, Jan. 2016.
- T. Parise, D. F. Davidson, R. K. Hanson, "Shock Tube/Laser Absorption Measurements of the Pyrolysis of a Bimodal Test Fuel," Proceedings of the Combustion Institute 36 1-8 (2016).

Project 026

One graduate student involved.

Project 027

Thirteen graduate students involved.

Publications

- Chterev, I., Rock, N., Ek, H., Smith, T., Emerson, B., Noble, D.R., Mayhew, E., Lee, T., Jiang, N., Roy, S. and Seitzman, J.M., 2016, June. Reacting Pressurized Spray Combustor Dynamics: Part 2—High Speed Planar Measurements. In *ASME Turbo Expo 2016: Turbomachinery Technical Conference and Exposition* (pp. V04AT04A020-V04AT04A020). American Society of Mechanical Engineers.
- Rock, N., Chterev, I., Smith, T., Ek, H., Emerson, B., Noble, D., Seitzman, J. and Lieuwen, T., 2016, June. Reacting Pressurized Spray Combustor Dynamics: Part 1—Fuel Sensitivities and Blowoff Characterization. In *ASME Turbo Expo 2016: Turbomachinery Technical Conference and Exposition* (pp. V04AT04A021-V04AT04A021). American Society of Mechanical Engineers.
- Sforzo, B., Dao, H., Wei, S. and Seitzman, J., 2017. Liquid Fuel Composition Effects on Forced, Nonpremixed Ignition. Journal of Engineering for Gas Turbines and Power, 139(3), p.031509.

Thesis

- Fillo, Aaron, M.S., Thesis, "The Global Consumption Speeds of Premixed Large- Hydrocarbon Fuel/Air Turbulent Bunsen Flames," Oregon State University.

Project 028

Publications

- "Model Reduction," Yang Gao, Chao Xu, Tianfeng Lu, Hai Wang, Jacqueline H. Chen, Alexei Poludnendo, Peter Hamlington, 2nd International Workshop on Combustion Chemistry Models of Real Liquid Fuels, Arlington, VA, June 06, 2016.
- Yang, S., Ranjan, R., Yang, V., Menon, S., Sun, W., ``Parallel on-the-fly Adaptive Kinetics in Direct Numerical Simulation of Turbulent Premixed Flame," Proceedings of the Combustion Institute, Vol. 36, 2016 (to appear).

Project 029

Six graduate students involved.

Publications

- "Effect of Aviation Fuel Type and Fuel Injection Conditions on Non-Reacting Spray Characteristics of Hybrid Air Blast Fuel Injector," Timo Buschhagen, Robert Z. Zhang, Sameer V. Naik, Carson D. Slabaugh, Scott E. Meyer, Jay P. Gore, and Robert P. Lucht, presented at the 2016 AIAA SciTech Meeting, San Diego, CA, 4-8 January 2016, Paper Number AIAA 2016-1154.
- "Large-Eddy Simulations of Fuel Injection and Atomization of a Hybrid Air-Blast Atomizer," P. C. May, M. B. Nik, S. E. Carbajal, S. Naik, J. P. Gore, R. P. Lucht, and M. Ihme, presented at the 2016 AIAA SciTech Meeting, San Diego, CA, 4-8 January 2016, Paper Number AIAA 2016-1393.
- "Spray Measurements at Elevated Pressures and Temperatures Using Phase Doppler Anemometry," A. J. Bokhart, D. Shin, R. Gejji, T. Buschhagen, S. V. Naik, R. P. Lucht, J. P. Gore, P. E. Sojka, and S. E. Meyer, to be presented at the 2017 AIAA SciTech Meeting, Grapevine, TX, 8-13 January 2017.
- "High-Fidelity Simulations of Fuel Injection and Atomization of a Hybrid Air-Blast Atomizer," P. C. Ma, M. B. Nik, S. E. Carbajal, S. Naik, J. P. Gore, R. P. Lucht, and M. Ihme, presented at the 2016 AIAA SciTech Meeting, San Diego, CA, 4-8 January 2016, Paper Number AIAA 2016-1393.
- "Large-Eddy Simulations of Fuel Effect on Gas Turbine Lean Blow-out," L. Esclapez, P. C. Ma, E. Mayhew, R. Xy, S. Stouffer, T. Lee, H. Wang, and M. Ihme, presented at the 2017 AIAA SciTech Meeting, Grapevine, CA, 9-13 January 2017, Paper Number AIAA 2017-1955.
- "The role of preferential evaporation on the ignition of multicomponent fuels in a homogeneous spray/air mixture." Stagni, A., Esclapez, L., Govindaraju, P., Cuoci, A., Faravelli, T., and Ihme, M., Proceedings of the Combustion Institute, 2016, in press.
- "Group contribution method for multicomponent evaluation with application to transportation fuels." Govindaraju, P. B. and Ihme, M., International Journal of Heat and Mass Transfer, 2016, 102, 833-845.

Presentations

- "Effect of Aviation Fuel Type and Fuel Injection Conditions on Non-Reacting Spray Characteristics of Hybrid Air Blast Fuel Injector," Timo Buschhagen, Robert Z. Zhang, Sameer V. Naik, Carson D. Slabaugh, Scott E. Meyer, Jay P. Gore, and Robert P. Lucht, presented at the 2016 AIAA SciTech Meeting, San Diego, CA, 4-8 January 2016
- "Large-Eddy Simulations of Fuel Injection and Atomization of a Hybrid Air-Blast Atomizer," P. C. May, M. B. Nik, S. E. Carbajal, S. Naik, J. P. Gore, R. P. Lucht, and M. Ihme, presented at the 2016 AIAA SciTech Meeting, San Diego, CA, 4-8 January 2016.
- "Spray Measurements at Elevated Pressures and Temperatures Using Phase Doppler Anemometry," A. J. Bokhart, D. Shin, R. Gejji, T. Buschhagen, S. V. Naik, R. P. Lucht, J. P. Gore, P. E. Sojka, and S. E. Meyer, to be presented at the 2017 AIAA SciTech Meeting, Grapevine, TX, 8-13 January 2017.

Project 030(A)

Four graduate students involved.

Presentations

- Edwin Corporan, Scott Stouffer, Tyler Hendershott, Chris Klingshirn, Matt Dewitt, Steve Zabarnick, Craig Neuroth, Dale Shouse, Jacob Diemer, "Initial Studies of Fuel Impacts on Combustor Operability and Emissions at the Air Force Research Laboratory", IASH 2015, the 14TH International Symposium on Stability, Handling, and Use of Liquid Fuels, Charleston, South Carolina USA, 4-8 October 2015

Project 030(B)

Three graduate students involved.

Presentations

- Corporan, Edwin, Stouffer, Scott, Hendershott, Tyler, Klingshirn, Chris, Dewitt, Matt, Zabarnick, Steve, Neuroth, Craig, Shouse, Dale, Diemer, Jacob "Initial Studies of Fuel Impacts on Combustor Operability and Emissions at the Air Force Research Laboratory", IASH 2015, the 14TH International Symposium on Stability, Handling, and Use of Liquid Fuels, Charleston, South Carolina USA, 4-8 October 2015

Project 31(A)

Publications

- "Evaluation of LanzaTech/PNNL Ethanol-to-Jet (LT/PNNL ATJ) Synthetic Paraffinic Kerosene Fuels and Blends Phase 1 Research Report"

Project 031(B)

One graduate student involved.

Project 32

One graduate student involved.

Publications

- Azadi, P; Speth, R.L.; Malina, R.; Barrett, S.R.H. Worldwide and Regional Greenhouse Gas Emissions of Petroleum-Derived Transportation Fuels. Submitted for publication.
- Rosen, C.V.; Speth, R.L.; Malina, R.; Barrett, S.R.H. Scenario-Based Lifecycle Greenhouse Gas Emissions of Petroleum-Derived Transportation Fuels in 2050. In preparation.

Presentations

- Presentation at CRC Workshop on Life Cycle Analysis of Transportation Fuels (October, 2015)
- Presentation at DOE BETO Alternative Aviation Fuel workshop (September, 2016)
- FAA "External Tools Call" (December, 2016)

Project 033(A)

Two graduate students involved.

Project 033(B)

Two graduate students involved.

Project 034

Two graduate students involved.

Publications

- Colket, Meredith B., Joshua S. Heyne, Mark Rumizen, James T. Edwards, Mohan Gupta, William M. Roquemore, Jeffrey P. Moder, Julian M. Tishkoff, and Chiping Li. 2016. "An Overview of the National Jet Fuels Combustion Program." AIAA Journal.
- Colket, Meredith B., Joshua S. Heyne, Mark Rumizen, James T. Edwards, Mohan Gupta, William M. Roquemore, Jeffrey P. Moder, Julian M. Tishkoff, and Chiping Li. 2016. "An Overview of the National Jet Fuels Combustion Program." In AIAA SciTech. AIAA SciTech. San Diego, CA: American Institute of Aeronautics and Astronautics. doi:doi:10.2514/6.2016-0177.
- Stachler, Robert D., Joshua S. Heyne, Scott D. Stouffer, Joseph D. Miller, and William M. Roquemore. 2017. "Investigation of Combustion Emissions from Conventional and Alternative Aviation Fuels in a Well-Stirred Reactor." In 55th AIAA Aerospace Sciences Meeting. Grapevine, TX: American Institute of Aeronautics and Astronautics.

Presentations

- Presentations at CRC Aviation Meeting, AIAA SciTech Meeting Paper and Presentation, ASCENT Spring and Fall presentations 2016, and DESS ASME conference.
- Stachler, Robert D., Joshua S. Heyne, Scott D. Stouffer, Joseph D. Miller, and William M. Roquemore. 2017. "Investigation of Combustion Emissions from Conventional and Alternative Aviation Fuels in a Well-Stirred Reactor." In 55th AIAA Aerospace Sciences Meeting. Grapevine, TX: American Institute of Aeronautics and Astronautics.
- Stachler, Robert D., Joshua S. Heyne, Scott D. Stouffer, Joseph D. Miller, and William M. Roquemore. 2016. "Investigation of Combustion Emissions from Conventional and Alternative Aviation Fuels in a Well-Stirred Reactor." 12th Annual Dayton Engineering Sciences Symposium. Dayton, OH: ASME.
- Carson, Jeremy, Joshua S. Heyne, Scott D. Stouffer, and Tyler Hendershott. 2016. "On the Relative Importance of Fuel Properties on LBO Behavior." 12th Annual Dayton Engineering Sciences Symposium. Dayton, OH: ASME.

Project 035

No publications or students to report.

Project 036

Two graduate students involved.

Project 37

No publications or students to report yet

Project 038

Three graduate students involved.

Project 039

One graduate student involved.

Project 040

One graduate student involved.

Project 041

Two graduate students involved.

Project 042

Three graduate students involved.

Project 043

Two graduate students involved.

Project 045

Two graduate students involved.

Project 046

No publications or students to report yet.

Project 048

One graduate student involved.

Project Funding Allocations by Federal Fiscal Year

Breakout by Project

Project		Funding Based on award date			
		2014	2015	2016	Total
001	Alternative Jet Fuel Supply Chain Analysis	$1,599,943	$1,425,000	$1,498,749	$4,523,692
002	Ambient Conditions Corrections for Non-Volatile PM Emissions Measurements	$2,800,000	$750,000	-$147,766	$3,402,234
003	Cardiovascular Disease and Aircraft Noise Exposure	$200,000	$200,000	$200,000	$600,000
004	Estimate of Noise Level Reduction	$150,000	-	-	$150,000
005	Noise Emission and Propagation Modeling	$212,000	$200,000	-	$412,000
006	Rotorcraft Noise Abatement Operating Conditions Modeling	$250,326	-	-	$250,326
007	Civil, Supersonic Over Flight, Sonic Boom (Noise) Standards Development	$100,000	$200,000	-	$300,000

Project		Funding Based on award date			
		2014	2015	2016	Total
008	Noise Outreach	$30,000	$50,000	$75,000	$155,000
010	Aircraft Technology Modeling and Assessment	$899,979	$200,000	$310,000	$1,409,979
011	Rapid Fleet-wide Environmental Assessment Capability	$600,000	$270,000	$300,000	$1,170,000
012	Aircraft Design and Performance Assessment Tool Enhancement	$90,000	-	-	$90,000
013	Micro-Physical Modeling & Analysis of ACCESS 2 Aviation Exhaust Observations	$200,000	-	-	$200,000
014	Analysis to Support the Development of an Aircraft CO2 Standard	$520,000	-	-	$520,000
017	Pilot Study on Aircraft Noise and Sleep Disturbance	$154,000	$343,498	$266,001	$763,499
018	Health Impacts Quantification for Aviation Air Quality Tools	$150,000	$150,000	$200,000	$500,000
019	Development of Aviation Air Quality Tools for Airport-Specific Impact Assessment: Air Quality Modeling	$320,614	$369,996	-	$690,610

Project		Funding Based on award date			
		2014	2015	2016	Total
020	Development of NAS wide and Global Rapid Aviation Air Quality	$150,000	$200,000	$250,000	$600,000
021	Improving Climate Policy Analysis Tools	$150,000	$150,000	$150,000	$450,000
022	Evaluation of FAA Climate Tools	$150,000	$30,000	$75,000	$255,000
023	Analytical Approach for Quantifying Noise from Advanced Operational Procedures	-	$296,711	$250,000	$546,711
024	Emissions Data Analysis for CLEEN, ACCESS, and Other Recent Tests	$244,975	-	$75,000	$319,975
025	National Jet Fuels Combustion Program – Area #1: Chemical Kinetics Combustion Experiments	-	$615,000	$210,000	$825,000
026	National Jet Fuels Combustion Program – Area #2: Chemical Kinetics Model Development and Evaluation	-	$200,000	-	$200,000
027	National Jet Fuels Combustion Program – Area #3: Advanced Combustion Tests	-	$1,010,000	$580,000	$1,590,000

Project		Funding Based on award date			
		2014	2015	2016	Total
028	National Jet Fuels Combustion Program – Area #4: Combustion Model Development and Evaluation	-	$470,000	$55,000	$525,000
029	National Jet Fuels Combustion Program – Area #5: Atomization Tests and Models	-	$640,000	$360,000	$1,000,000
030	National Jet Fuels Combustion Program – Area #6: Referee Swirl-Stabilized Combustor Evaluation/Support	-	$349,949	-	$349,949
031	Alternative Jet Fuels Test and Evaluation	-	$489,619	$744,891	$1,234,510
032	Worldwide LCA of GHG Emissions from Petroleum Jet Fuel	-	$150,000	-	$150,000
033	Alternative Fuels Test Database Library	-	$199,624	$119,794	$319,418
034	National Jet Fuels Combustion Program – Area #7: Overall Program Integration and Analysis	-	$234,999	$635,365	$870,364

Project		Funding Based on award date			
		2014	2015	2016	Total
035	Airline Flight Data Examination to Improve flight Performance Modeling	-	$150,001	-	$150,001
036	Parametric Uncertainty Assessment for AEDT2b	-	$65,000	$175,000	$240,000
037	CLEEN II Technology Modeling and Assessment	-	$200,000	$150,000	$350,000
038	Rotorcraft Noise Abatement Procedures Development	-	$150,000	$150,000	$300,000
039	Nephthalene Removal Assessment	-	-	$200,000	$200,000
040	Quantifying Uncertainties in Predicting Aircraft Noise in Real-world Situations	-	-	$218,426	$218,426
041	Identification of Noise Acceptance Onset for Noise Certification Standards of Supersonic Airplane	-	-	$160,000	$160,000

Project		Funding Based on award date			
		2014	2015	2016	Total
042	Acoustical Model of Mach Cut-off	-	-	$255,000	$255,000
043	Noise Power Distance Re-Evaluation	-	-	$150,000	$150,000
045	Takeoff/Climb Analysis to Support AEDT APM Development	-	-	$250,000	$250,000
046	Surface Analysis to Support AEDT APM Development	-	-	$75,000	$75,000
048	Analysis to Support the Development of an Engine nvPM Emissions Standards	-	-	$150,000	$150,000

Breakout by University*

	Funding Based on award year				
University	**2013**	**2014**	**2015**	**2016**	**Total**
Boston University	$5,000	$350,000	$350,000	$400,000	$1,105,000
Georgia Institute of Technology	$5,000	$1,660,000	$1,625,001	$1,435,000	$4,575,000
Massachusetts Institute of Technology	$10,000	$1,153,927	$1,179,073	$ 1,855,000	$4,143,927
Missouri University of Science and Technology	$5,000	$2,800,000	$750,000	-$147,766	$3,407,234
Oregon State University	$5,000	-	$160,000	$80,000	$245,000
Pennsylvania State University	$5,000	$862,301	$766,711	$958,426	$2,592,438
Purdue University	$5,000	$389,979	$1,030,000	$763,750	$2,188,729
Stanford University	$5,000	$380,000	$1,155,000	$345,000	$1,885,000
University of Dayton	$5,000	-	$906,196	$1,349,087	$2,260,280
University of Hawaii	$10,000	-	$75,000	$100,000	$185,000

	Funding Based on award year				
University	**2013**	**2014**	**2015**	**2016**	**Total**
University of Illinois	$5,000	$349,943	$553,000	$375,000	$1,282,943
University of North Carolina	$5,000	$320,614	$369,996	-	$695,610
University of Pennsylvania	$5,000	$154,000	$343,498	$266,001	$768,499
University of Tennessee	$5,000	$200,000	$100,000	$100,000	$405,000
University of Washington	$5,000	$60,000	$29,997	$15,000	$109,497
Washington State University	$20,000	$974,228	$864,968	$725,961	$2,585,157

Breakout by State*

	Funding Based on award year				
State	**2013**	**2014**	**2015**	**2016**	**Total**
California	$5,000	$380,000	$1,155,000	$345,000	$1,885,000
Georgia	$5,000	$1,660,000	$1,625,001	$1,435,000	$4,575,000
Hawaii	$10,000	-	$75,000	$100,000	$185,000
Illinois	$5,000	$349,943	$553,000	$375,000	$1,282,943
Indiana	$5,000	$389,979	$1,030,000	$763,750	$2,188,729
Massachusetts	$15,000	$1,503,927	$1,529,073	$2,255,000	$5,303,000
Missouri	$5,000	$2,800,000	$750,000	-$147,766	$3,407,234
North Carolina	$5,000	$320,614	$369,996	-	$695,610
Ohio	$5,000	-	$906,196	$1,349,087	$2,260,280
Oregon	$5,000	-	$160,000	$80,000	$245,000
Pennsylvania	$10,000	$1,016,301	$1,110,209	$1,224,427	$3,360,937
Tennessee	$5,000	$200,000	$100,000	$100,000	$405,000
Washington	$25,000	$1,034,228	$894,965	$740,961	$2,695154

*Totals include administrative funds not associated with specific NFOs.